Scientific and Technical Aerospace Reports

STAR

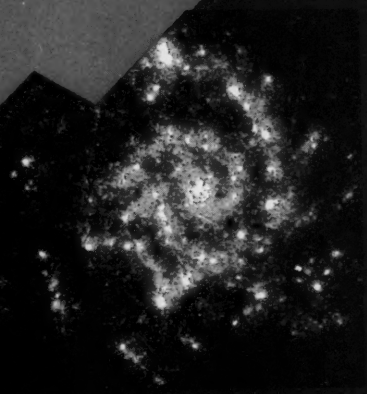

An Abstract Journal

Volume 33, Number 2
February 1995
N95-11698 to N95-13609

The NASA STI Office ... in Profile

Since its founding, NASA has been dedicated to the advancement of aeronautics and space science. The NASA Scientific and Technical Information (STI) Office plays a key part in helping NASA maintain this important role.

The NASA STI Office provides access to the NASA STI Database, the largest collection of aeronautical and space science STI in the world. The Office is also NASA's institutional mechanism for disseminating the results of its research and development activities.

Specialized services that help round out the Office's diverse offerings include creating custom thesauri, translating material to or from 34 foreign languages, building customized databases, organizing and publishing research results ... even providing videos.

For more information about the NASA STI Office, you can:

- **Phone** the NASA Access Help Desk at (301) 621-0390
- **Fax** your question to the NASA Access Help Desk at (301) 621-0134
- **E-mail** your question via the **Internet** to help@sti.nasa.gov
- **Write** to:

NASA Access Help Desk
NASA Center for AeroSpace Information
800 Elkridge Landing Road
Linthicum Heights, MD 21090-2934

Scientific and Technical Aerospace Reports

Scientific and Technical Aerospace Reports (STAR), is published each month as a major product of the NASA Scientific and Technical Information (STI) Office.

Inside this issue you will find:

- **Front Matter** containing a typical citation and abstract sample explaining the standard format, including codes for ordering reports
- **An Abstract Section** containing citations and abstracts of reports and publications that provide comprehensive coverage of worldwide aerospace-related topics including aeronautics and space science technology. *STAR* lists published and publicly available reports entered into the NASA STI Database during the four weeks preceding publication of this issue. These citations and abstracts are listed by subject categories.
- **An Index Section**
  - Subject
  - Personal author
  - Corporate source
  - Contract number
  - Report number
- **An Appendix** containing a guide for ordering cited reports, registering with the NASA STI Office, and using the available products and services. Additionally, price schedules, phone numbers, and addresses are included in this information packed section.

NASA also sponsors the companion journal, *NASA Open Volumes on Aerospace (NOVA)*, which lists abstracts of the open literature on aerospace subjects available worldwide. *NOVA* is for internal NASA use only, available from the NASA Center for AeroSpace Information (CASI).

Entries found in *STAR* are available through the NASA online retrieval service, RECON, and through DIALOG as the Aerospace Database.

The NASA STI Office gathers information through national and international agreements and exchanges and makes this information available to the NASA community and to the public in many forms through various outlets.

For additional information on the NASA STI Office, call the NASA Access Help Desk at (301) 621-0390, or write to:

NASA Center for AeroSpace Information
800 Elkridge Landing Road
Linthicum Heights, Maryland 21090-2934

US ISSN 0036-8741

This publication was prepared by the NASA Center for AeroSpace Information,
800 Elkridge Landing Road, Linthicum Heights, MD 21090-2934, (301) 621-0390.

Volume 33 Number 2 / February 1995

TABLE OF CONTENTS

AERONAUTICS For related information see also *Astronautics.*

01 AERONAUTICS (GENERAL) **229**

02 AERODYNAMICS **229**
Includes aerodynamics of bodies, combinations, wings, rotors, and control surfaces; and internal flow in ducts and turbomachinery. For related information see also *34 Fluid Mechanics and Heat Transfer.*

03 AIR TRANSPORTATION AND SAFETY **234**
Includes passenger and cargo air transport operations; and aircraft accidents. For related information see also *16 Space Transportation* and *85 Urban Technology and Transportation.*

04 AIRCRAFT COMMUNICATIONS AND NAVIGATION **237**
Includes digital and voice communication with aircraft; air navigation systems (satellite and ground based); and air traffic control. For related information see also *17 Space Communications, Spacecraft Communications, Command and Tracking* and *32 Communications and Radar.*

05 AIRCRAFT DESIGN, TESTING AND PERFORMANCE **237**
Includes aircraft simulation technology. For related information see also *18 Spacecraft Design, Testing and Performance* and *39 Structural Mechanics.* For land transportation vehicles see *85 Urban Technology and Transportation.*

06 AIRCRAFT INSTRUMENTATION **242**
Includes cockpit and cabin display devices; and flight instruments. For related information see also *19 Spacecraft Instrumentation* and *35 Instrumentation and Photography.*

07 AIRCRAFT PROPULSION AND POWER **243**
Includes prime propulsion systems and systems components, e.g., gas turbine engines and compressors; and onboard auxiliary power plants for aircraft. For related information see also *20 Spacecraft Propulsion and Power, 28 Propellants and Fuels,* and *44 Energy Production and Conversion.*

08 AIRCRAFT STABILITY AND CONTROL **244**
Includes aircraft handling qualities; piloting; flight controls; and autopilots. For related information see also *05 Aircraft Design, Testing and Performance.*

09 RESEARCH AND SUPPORT FACILITIES (AIR) **245**
Includes airports, hangars and runways; aircraft repair and overhaul facilities; wind tunnels; shock tubes; and aircraft engine test stands. For related information see also *14 Ground Support Systems and Facilities (Space).*

ASTRONAUTICS For related information see also *Aeronautics.*

12 ASTRONAUTICS (GENERAL) **247**
For extraterrestrial exploration see *91 Lunar and Planetary Exploration.*

13 ASTRODYNAMICS **248**
Includes powered and free-flight trajectories; and orbital and launching dynamics.

14 GROUND SUPPORT SYSTEMS AND FACILITIES (SPACE) **248**
Includes launch complexes, research and production facilities; ground support equipment, e.g., mobile transporters; and simulators. For related information see also *09 Research and Support Facilities (Air).*

15 LAUNCH VEHICLES AND SPACE VEHICLES **248**
Includes boosters; operating problems of launch/space vehicle systems; and reusable vehicles. For related information see also *20 Spacecraft Propulsion and Power.*

16 SPACE TRANSPORTATION **249**
Includes passenger and cargo space transportation, e.g., shuttle operations; and space rescue techniques. For related information see also *03 Air Transportation and Safety* and *18 Spacecraft Design, Testing and Performance.* For space suits see *54 Man/System Technology and Life Support.*

17 SPACE COMMUNICATIONS, SPACECRAFT COMMUNICATIONS, COMMAND AND TRACKING....N.A.
Includes telemetry; space communications networks; astronavigation and guidance; and radio blackout. For related information see also *04 Aircraft Communications and Navigation* and *32 Communications and Radar.*

N.A.—No abstracts were assigned to this category for this issue.

18 SPACECRAFT DESIGN, TESTING AND PERFORMANCE **250**
Includes satellites; space platforms; space stations; spacecraft systems and components such as thermal and environmental controls; and attitude controls. For life support systems see *54 Man/System Technology and Life Support.* For related information see also *05 Aircraft Design, Testing and Performance*, *39 Structural Mechanics*, and *16 Space Transportation.*

19 SPACECRAFT INSTRUMENTATION **257**
For related information see also *06 Aircraft Instrumentation* and *35 Instrumentation and Photography.*

20 SPACECRAFT PROPULSION AND POWER **257**
Includes main propulsion systems and components, e.g., rocket engines; and spacecraft auxiliary power sources. For related information see also *07 Aircraft Propulsion and Power*, *28 Propellants and Fuels*, *44 Energy Production and Conversion*, and *15 Launch Vehicles and Space Vehicles.*

CHEMISTRY AND MATERIALS

23 CHEMISTRY AND MATERIALS (GENERAL) **259**

24 COMPOSITE MATERIALS **261**
Includes physical, chemical, and mechanical properties of laminates and other composite materials. For ceramic materials see *27 Nonmetallic Materials.*

25 INORGANIC AND PHYSICAL CHEMISTRY **264**
Includes chemical analysis, e.g., chromatography; combustion theory; electrochemistry; and photochemistry. For related information see also *77 Thermodynamics and Statistical Physics.*

26 METALLIC MATERIALS **269**
Includes physical, chemical, and mechanical properties of metals, e.g., corrosion; and metallurgy.

27 NONMETALLIC MATERIALS **272**
Includes physical, chemical, and mechanical properties of plastics, elastomers, lubricants, polymers, textiles, adhesives, and ceramic materials. For composite materials see *24 Composite Materials.*

28 PROPELLANTS AND FUELS **277**
Includes rocket propellants, igniters and oxidizers; their storage and handling procedures; and aircraft fuels. For related information see also *07 Aircraft Propulsion and Power*, *20 Spacecraft Propulsion and Power*, and *44 Energy Production and Conversion.*

29 MATERIALS PROCESSING **278**
Includes space-based development of products and processes for commercial application. For biological materials see *55 Space Biology:*

ENGINEERING For related information see also *Physics.*

31 ENGINEERING (GENERAL) **279**
Includes vacuum technology; control engineering; display engineering; cryogenics; and fire prevention.

32 COMMUNICATIONS AND RADAR **279**
Includes radar; land and global communications; communications theory; and optical communications. For related information see also *04 Aircraft Communications and Navigation* and *17 Space Communications, Spacecraft Communications, Command and Tracking.* For search and rescue see *03 Air Transportation and Safety,* and *16 Space Transportation.*

33 ELECTRONICS AND ELECTRICAL ENGINEERING **286**
Includes test equipment and maintainability; components, e.g., tunnel diodes and transistors; microminiaturization; and integrated circuitry. For related information see also *60 Computer Operations and Hardware* and *76 Solid-State Physics.*

34 FLUID MECHANICS AND HEAT TRANSFER **289**
Includes boundary layers; hydrodynamics; fluidics; mass transfer and ablation cooling. For related information see also *02 Aerodynamics* and *77 Thermodynamics and Statistical Physics.*

35 INSTRUMENTATION AND PHOTOGRAPHY **295**
Includes remote sensors; measuring instruments and gauges; detectors; cameras and photographic supplies; and holography. For aerial photography see *43 Earth Resources and Remote Sensing.* For related information see also *06 Aircraft Instrumentation* and *19 Spacecraft Instrumentation.*

36 LASERS AND MASERS **297**
Includes parametric amplifiers. For related information see also *76 Solid-State Physics:*

37 MECHANICAL ENGINEERING 299
Includes auxiliary systems (nonpower); machine elements and processes; and mechanical equipment.

38 QUALITY ASSURANCE AND RELIABILITY 308
Includes product sampling procedures and techniques; and quality control.

39 STRUCTURAL MECHANICS 309
Includes structural element design and weight analysis; fatigue; and thermal stress. For applications see *05 Aircraft Design, Testing and Performance* and *18 Spacecraft Design, Testing and Performance.*

GEOSCIENCES For related information see also *Space Sciences.*

42 GEOSCIENCES (GENERAL) 314

43 EARTH RESOURCES AND REMOTE SENSING 314
Includes remote sensing of earth resources by aircraft and spacecraft; photogrammetry; and aerial photography. For instrumentation see *35 Instrumentation and Photography.*

44 ENERGY PRODUCTION AND CONVERSION 317
Includes specific energy conversion systems, e.g., fuel cells; global sources of energy; geophysical conversion; and windpower. For related information see also *07 Aircraft Propulsion and Power, 20 Spacecraft Propulsion and Power,* and *28 Propellants and Fuels.*

45 ENVIRONMENT POLLUTION 318
Includes atmospheric, noise, thermal, and water pollution.

46 GEOPHYSICS 321
Includes aeronomy; upper and lower atmosphere studies; ionospheric and magnetospheric physics; and geomagnetism. For space radiation see *93 Space Radiation.*

47 METEOROLOGY AND CLIMATOLOGY 325
Includes weather forecasting and modification.

48 OCEANOGRAPHY 327
Includes biological, dynamic, and physical oceanography; and marine resources. For related information see also *43 Earth Resources and Remote Sensing.*

LIFE SCIENCES

51 LIFE SCIENCES (GENERAL) 329

52 AEROSPACE MEDICINE 332
Includes physiological factors; biological effects of radiation; and effects of weightlessness on man and animals.

53 BEHAVIORAL SCIENCES 335
Includes psychological factors; individual and group behavior; crew training and evaluation; and psychiatric research.

54 MAN/SYSTEM TECHNOLOGY AND LIFE SUPPORT 337
Includes human engineering; biotechnology; and space suits and protective clothing. For related information see also *16 Space Transportation.*

55 SPACE BIOLOGY 339
Includes exobiology; planetary biology; and extraterrestrial life.

MATHEMATICAL AND COMPUTER SCIENCES

59 MATHEMATICAL AND COMPUTER SCIENCES (GENERAL) 339

60 COMPUTER OPERATIONS AND HARDWARE 340
Includes hardware for computer graphics, firmware, and data processing. For components see *33 Electronics and Electrical Engineering.*

61 COMPUTER PROGRAMMING AND SOFTWARE 341
Includes computer programs, routines, algorithms, and specific applications, e.g., CAD/CAM.

62 COMPUTER SYSTEMS 346
Includes computer networks and special application computer systems.

63 CYBERNETICS **348**
Includes feedback and control theory, artificial intelligence, robotics and expert systems. For related information see also *54 Man/System Technology and Life Support.*

64 NUMERICAL ANALYSIS **351**
Includes iteration, difference equations, and numerical approximation.

65 STATISTICS AND PROBABILITY **353**
Includes data sampling and smoothing; Monte Carlo method; and stochastic processes.

66 SYSTEMS ANALYSIS ..... **N.A.**
Includes mathematical modeling; network analysis; and operations research.

67 THEORETICAL MATHEMATICS **353**
Includes topology and number theory.

PHYSICS For related information see also *Engineering.*

70 PHYSICS (GENERAL) **353**
For precision time and time interval (PTTI) see *35 Instrumentation and Photography*; for geophysics, astrophysics or solar physics see *46 Geophysics, 90 Astrophysics*, or *92 Solar Physics.*

71 ACOUSTICS **355**
Includes sound generation, transmission, and attenuation. For noise pollution see *45 Environment Pollution.*

72 ATOMIC AND MOLECULAR PHYSICS **356**
Includes atomic structure, electron properties, and molecular spectra.

73 NUCLEAR AND HIGH-ENERGY PHYSICS **360**
Includes elementary and nuclear particles; and reactor theory. For space radiation see *93 Space Radiation.*

74 OPTICS **362**
Includes light phenomena and optical devices. For lasers see *36 Lasers and Masers.*

75 PLASMA PHYSICS **364**
Includes magnetohydrodynamics and plasma fusion. For ionospheric plasmas see *46 Geophysics.* For space plasmas see *90 Astrophysics.*

76 SOLID-STATE PHYSICS **371**
Includes superconductivity. For related information see also *33 Electronics and Electrical Engineering* and *36 Lasers and Masers.*

77 THERMODYNAMICS AND STATISTICAL PHYSICS **375**
Includes quantum mechanics; theoretical physics; and Bose and Fermi statistics. For related information see also *25 Inorganic and Physical Chemistry* and *34 Fluid Mechanics and Heat Transfer.*

SOCIAL SCIENCES

80 SOCIAL SCIENCES (GENERAL) **376**
Includes educational matters.

81 ADMINISTRATION AND MANAGEMENT **377**
Includes management planning and research.

82 DOCUMENTATION AND INFORMATION SCIENCE **377**
Includes information management; information storage and retrieval technology; technical writing; graphic arts; and micrography. For computer documentation see *61 Computer Programming and Software.*

83 ECONOMICS AND COST ANALYSIS ..... **N.A.**
Includes cost effectiveness studies.

84 LAW, POLITICAL SCIENCE AND SPACE POLICY **379**
Includes NASA appropriation hearings; aviation law; space law and policy; international law; international cooperation; and patent policy.

85 URBAN TECHNOLOGY AND TRANSPORTATION ..... **N.A.**
Includes applications of space technology to urban problems; technology transfer; technology assessment; and surface and mass transportation. For related information see *03 Air Transportation and Safety, 16 Space Transportation,* and *44 Energy Production and Conversion.*

SPACE SCIENCES For related information see also *Geosciences.*

88 SPACE SCIENCES (GENERAL) ..... **N.A.**

89 ASTRONOMY **379**
Includes radio, gamma-ray, and infrared astronomy; and astrometry.

90 ASTROPHYSICS **381**
Includes cosmology; celestial mechanics; space plasmas; and interstellar and interplanetary gases and dust. For related information see also *75 Plasma Physics.*

91 LUNAR AND PLANETARY EXPLORATION **382**
Includes planetology; and manned and unmanned flights. For spacecraft design or space stations see *18 Spacecraft Design, Testing and Performance.*

92 SOLAR PHYSICS **384**
Includes solar activity, solar flares, solar radiation and sunspots. For related information see also *93 Space Radiation.*

93 SPACE RADIATION **384**
Includes cosmic radiation; and inner and outer earth's radiation belts. For biological effects of radiation see *52 Aerospace Medicine.* For theory see *73 Nuclear and High-Energy Physics.*

GENERAL

Includes aeronautical, astronautical, and space science related histories, biographies, and pertinent reports too broad for categorization; histories or broad overviews of NASA programs.

99 GENERAL **385**

SUBJECT INDEX **I-1**

PERSONAL AUTHOR INDEX **I-83**

CORPORATE SOURCE INDEX **I-93**

CONTRACT NUMBER INDEX **I-107**

REPORT NUMBER INDEX **I-111**

APPENDIX **A-1**

TYPICAL CITATION AND ABSTRACT

NASA SPONSORED — ON MICROFICHE

ACCESSION NUMBER → **N95-10148*#** National Aeronautics and Space Administration. Lewis Research Center, Cleveland, OH. ← CORPORATE SOURCE

TITLE → **EFFECTS OF A FORWARD-SWEPT FRONT ROTOR ON THE FLOWFIELD OF A COUNTERROTATION PROPELLER**

AUTHORS → M. Nallasamy (NYMA, Inc., Brook Park, OH.) and Gary G. Podboy Aug. 1994 19 p Presented at the 30th Joint Propulsion Conference, Indianapolis, IN, 27-29 Jun. 1994; sponsored by AIAA, ASME, SAE, and ASEE ← PUBLICATION DATE

CONTRACT OR GRANT → (Contract NAS3-27186; RTOP 538-03-11)

REPORT NUMBERS → (NASA-TM-106671; E-8994; NAS 1.15:106671; AIAA Paper 94-2694) Avail: CASI HC A03/MF A01; 6 functional color pages ← AVAILABILITY SOURCE AND PRICE CODE

The effects of a forward-swept front rotor on the flowfield of a counterrotation model propeller at takeoff conditions at zero degree angle of attack are studied by solving the unsteady three-dimensional Euler equations. The configuration considered is an uneven blade count counterrotation model with twelve forward-swept blades on the fore rotor and ten aft-swept blades on the aft rotor. The flowfield is compared with that of a reference aft-swept counterrotation geometry and Laser Doppler Velocimeter (LDV) measurements. At the operating conditions considered, the forward-swept blade experiences a higher tip loading and produces a stronger tip vortex compared to the aft-swept blade, consistent with the LDV and acoustic measurements. Neither the solution nor the LDV data indicated the formation of a leading edge vortex. The predicted radial distribution of the circumferentially averaged axial velocity at the measurement station agreed very closely with LDV data, while crossflow velocities showed poor agreement. The discrepancy between prediction and LDV data of tangential and radial velocities is due in part to the insufficient mesh resolution in the region between the rotors and in the tip region to track the tip vortex. The vortex is diffused by the time it arrives at the measurement station. The uneven blade count configuration requires the solution to be carried out for six blade passages of the fore rotor and five passages of the aft rotor, thus making grid refinement prohibitive.

Author

VOLUME 33 NUMBER 2 / February 1995

Scientific and Technical Aerospace Reports

A Monthly Publication of the National Aeronautics and Space Administration

01 AERONAUTICS (GENERAL)

N95-11892 National Academy of Sciences - National Research Council, Washington, DC. Commission on Engineering and Technical Systems.
AERONAUTICS AND SPACE TECHNOLOGY, PAST, PRESENT, AND FUTURE
1994 86 p Proceedings of the 25th Anniversary Symposium of the Aeronautics and Space Engineering Board held 7 May 1993
Copyright Avail: Issuing Activity (The Aeronautics and Space Engineering Board, 2101 Constitution Ave., NW, Washington, DC, 20418)

The topics covered include the following: a national technology strategy; a new role for technology; an Aeronautics and Space Engineering Board (ASEB) historical perspective and lessons learned; a look to the future in aeronautical technologies; setting a course for the future; evolution of technologies for space exploration; space technology as a national resource; and ASEB as advisor to NASA. CASI

N95-12166# National Aerospace Lab., Bangalore (India). Experimental Aerodynamics Div.
EXPERIMENTAL AERODYNAMICS DIVISION Annual Report, 1993
Apr. 1994 83 p
(NAL Proj. EA-9-000)
(NAL-SP-9404) Avail: CASI HC A05/MF A01

This annual report covers research and development activities in experimental aerodynamics carried out at the Indian National Trisonic Aerodynamic Facility. Production was doubled in the course of a year with a total of 1600 blowdowns carried out. The effects of pitot probes, angles of attack, vanes, etc., and their locations on the buzz boundaries of air intakes were systematically studied. The studies indicated that pressure fluctuations downstream of retro rockets could be reduced significantly by proper shaping. Other tests determined control surface effectiveness on a missile model. In the area of flow structure and management, research continued on vortex flows on wings and bodies and aerodynamic drag reduction. In the area of aircraft and missile aerodynamics, the MAHAA code was extended to predict drag characteristics on the aerodynamic configurations at trisonic speeds. CASI

N95-12227*# National Aeronautics and Space Administration. Ames Research Center, Moffett Field, CA.
THE SELECTIVE USE OF FUNCTIONAL OPTICAL VARIABLES IN THE CONTROL OF FORWARD SPEED
Walter W. Johnson and Cynthia A. Awe Sep. 1994 36 p
(RTOP 505-64-36)
(NASA-TM-108849; A-94139; NAS 1.15:108849) Avail: CASI HC A03/MF A01

Previous work on the perception and control of simulated vehicle speed has examined the contributions of optical flow rate (angular visual speed) and texture, or edge rate (frequency of passing terrain objects or markings) on the perception and control of forward speed. However, these studies have not examined the ability to selectively use edge rate or flow rate. The two studies presented here show that this ability is far greater for pilots than non-pilots, as would be expected since pilots must control vehicular speed over a variety of altitudes where flow rates change independently of forward speed. These studies also show that this ability to selectively use these variables is linked to the visual contextual information about the relative validity (linkage with speed) of the two variables. Subjective judgment data also indicated that awareness of altitude and ground texture density did not mediate ground speed awareness. Author

N95-12894* National Aeronautics and Space Administration, Washington, DC.
AERONAUTICAL ENGINEERING: A CONTINUING BIBLIOGRAPHY WITH INDEXES (SUPPLEMENT 309)
Oct. 1994 83 p
(NASA-SP-7037(309); NAS 1.21:7037(309)) Avail: CASI HC A05

This bibliography lists 212 reports, articles, and other documents introduced into the NASA scientific and technical information system in Oct. 1994. Subject coverage includes: design, construction and testing of aircraft and aircraft engines; aircraft components, equipment, and systems; ground support systems; and theoretical and applied aspects of aerodynamics and general fluid dynamics. Author

N95-13166# American Association for Artificial Intelligence, Menlo Park, CA.
THE SECOND WORKSHOP ON PRINCIPLES AND PRACTICE OF CONSTRAINT PROGRAMMING
4 May 1994 290 p Workshop held in Orcas Island, WA, 2-4 May 1994
(AD-A281731) Avail: CASI HC A13/MF A03

This inter-disciplinary meeting focused on constraint programming and constraint-based systems. The contens are divided as such: CSP's (constraint satisfaction problems), User Interfaces, Constraint Logic Programming, Concurrent Constraint Languages, Databases, Artificial Intelligence, and Other Topics. CASI

02 AERODYNAMICS

Includes aerodynamics of bodies, combinations, wings, rotors, and control surfaces; and internal flow in ducts and turbomachinery.

For related information see also *34 Fluid Mechanics and Heat Transfer.*

N95-11710*# National Aeronautics and Space Administration. Marshall Space Flight Center, Huntsville, AL.
A SHADOWGRAPH STUDY OF THE NATIONAL LAUNCH SYSTEM'S 1 1/2 STAGE VEHICLE CONFIGURATION AND HEAVY LIFT LAUNCH VEHICLE CONFIGURATION
Darlene C. Pokora and Anthony M. Springer Washington Aug. 1994 89 p
(NASA-RP-1347; M-755; NAS 1.61:1347) Avail: CASI HC A05/MF A01

A shadowgraph study of the National Launch System's (NLS's) 1 1/2 stage and heavy lift launch vehicle (HLLV) configurations is presented. Shadowgraphs are shown for the range of Mach numbers from Mach 0.6 to 5.0 at various angles-of-attack and roll angles. Since the 1 1/2 stage configuration is generally symmetric, no shadowgraphs of any roll angle are shown for this configuration. The major flow field phenomena over the NLS 1 1/2 stage and HLLV configurations are shown in the shadowgraphs. These shadowgraphs are used in the aerothermodynamic analysis of the external flow conditions the launch vehicle would encounter during the ascent stage of flight. The shadowgraphs presented in this study were obtained from configurations tested in the Marshall Space Flight Center's 14-Inch Trisonic Wind Tunnel during 1992. Author

N95-11766*# MCAT Inst., Moffett Field, CA.
PARALLEL AEROELASTIC COMPUTATIONS FOR WING AND WING-BODY CONFIGURATIONS Annual Report, Jul. 1993 - Jul. 1994
Chansup Byun Jul. 1994 62 p Original contains color illustrations
(Contract NCC2-740)
(NASA-CR-196835; NAS 1.26:196835; MCAT-94-08) Avail: CASI HC A04/MF A01; 6 functional color pages

The objective of this research is to develop computationally efficient methods for solving fluid-structural interaction problems by directly coupling finite difference Euler/Navier-Stokes equations for fluids and finite element dynamics equations for structures on parallel computers. This capability will significantly impact many aerospace projects of national importance such as Advanced Subsonic Civil Transport (ASCT), where the structural stability margin becomes very critical at the transonic region. This research effort will have direct impact on the High Performance Computing and Communication (HPCC) Program of NASA in the area of parallel computing. Derived from text

N95-11807*# Rockwell International Corp., Huntsville, AL. Space Systems Div.
HIGH FREQUENCY FLOW/STRUCTURAL INTERACTION IN DENSE SUBSONIC FLUIDS HANDBOOK Final Report
Baw-Lin Liu and J. M. OFarrell Jul. 1994 217 p
(Contract NAS8-38187)
(NASA-CR-194007; NAS 1.26:194007) Avail: CASI HC A10/MF A03

Prediction of the detailed dynamic behavior of structural elements in rocket propellant feed systems and engines and other such high-energy fluid systems requires precise analysis to assure structural performance. Designs sometimes require placement of bluff bodies in a flow passage. Additionally, there are flexibilities in ducts, liners, and piping systems. A design handbook and iterative data base have been developed for assessing flow/structural interactions as a quick and ready reference to be used as a tool in design and development, to evaluate applicable geometries before problems develop, or to eliminate or minimize problems with existing hardware. Organization of the handbook is by basic geometric shapes for estimating Strouhal numbers, added mass effects, mode shapes for various end constraints, critical onset flow conditions, and possible structural response amplitudes. Emphasis is on dense fluids and high structural loading potentials for fatigue at low subsonic flow speeds where high-frequency excitations are possible. Avoidance and corrective measure illustrations are presented together with analytical curve fits for prediction compiled from a comprehensive data base. Author

N95-11829 Wright Lab., Wright-Patterson AFB, OH.
PRESSURE MEASUREMENTS ON AN F/A-18 TWIN VERTICAL TAIL IN BUFFETING FLOW. VOLUME 3: BUFFET POWER SPECTRAL DENSITIES Final Report, 1 Apr. 1993 - 1 Aug. 1994
Chris Pettit, Dansen Brown, Michael Banford, and Ed Pendleton Aug. 1994 705 p Limited Reproducibility: More than 20% of this document may be affected by microfiche quality
(AF Proj. 2401)
(AD-A281444; WL-TM-94-3066-Vol-3) Avail: CASI HC A99

Buffeting pressure measurements were made on the vertical tail surface of a full scale F/A-18 aircraft model in the National Full Scale Aerodynamics Complex at NASA Ames Research Center. Test variables included aircraft angle-of-attack, aircraft sideslip angle, and dynamic pressure. Accelerometers were used to obtain vertical tail accelerations. Pressure transducers were mounted on the starboard vertical tail. Steady and unsteady pressures were obtained. Unsteady pressure data were reduced to PSD and CSD forms. Both steady and unsteady RMS pressure coefficients are also presented. Volume 1 contains the general description of the model, the test program, and highlights of the reduced data. Volume 2 contains steady and unsteady RMS data. Volume 3 contains unsteady PSD results. Volume 4 contains unsteady CSD results. DTIC

N95-11877*# Research Inst. for Advanced Computer Science, Moffett Field, CA.
OPTIMUM AERODYNAMIC DESIGN VIA BOUNDARY CONTROL
Antony Jameson (Princeton Univ., NJ.) Aug. 1994 35 p Sponsored in part by IBM
(Contracts NAS2-13721; N00014-92-J-1976; AF-AFOSR-0391-91)
(NASA-CR-195882; NAS 1.26:195882; RIACS-TR-94-17) Avail: CASI HC A03/MF A01

These lectures describe the implementation of optimization techniques based on control theory for airfoil and wing design. In previous studies it was shown that control theory could be used to devise an effective optimization procedure for two-dimensional profiles in which the shape is determined by a conformal transformation from a unit circle, and the control is the mapping function. Recently the method has been implemented in an alternative formulation which does not depend on conformal mapping, so that it can more easily be extended to treat general configurations. The method has also been extended to treat the Euler equations, and results are presented for both two and three dimensional cases, including the optimization of a swept wing. Author

N95-11884*# Research Inst. for Advanced Computer Science, Moffett Field, CA.
CONTROL THEORY BASED AIRFOIL DESIGN USING THE EULER EQUATIONS
Antony Jameson (Princeton Univ., NJ.) and James Reuther Sep. 1994 19 p
(Contract NAS2-13721; AF-AFOSR-0391-91)
(NASA-CR-196360; NAS 1.26:196360; RIACS-TR-94-18) Avail: CASI HC A03/MF A01

This paper describes the implementation of optimization techniques based on control theory for airfoil design. In our previous work it was shown that control theory could be employed to devise effective optimization procedures for two-dimensional profiles by using the potential flow equation with either a conformal mapping or a general coordinate system. The goal of our present work is to extend the development to treat the Euler equations in two-dimensions by procedures that can readily be generalized to treat complex shapes in three-dimensions. Therefore, we have developed methods which can address airfoil design through either an analytic mapping or an arbitrary grid perturbation method applied to a finite volume discretization of the Euler equations. Here the control law serves to provide computationally inexpensive gradient information to a standard numerical optimization method. Results are presented for both the inverse problem and drag minimization problem. Author

N95-11898*# National Aeronautics and Space Administration. Hugh L. Dryden Flight Research Facility, Edwards, CA.
WATER TUNNEL FLOW VISUALIZATION STUDY OF A 4.4 PERCENT SCALE X-31 FOREBODY
Brent R. Cobleigh and John DelFrate Washington Sep. 1994 40 p Original contains color illustrations
(RTOP 533-02-00)
(NASA-TM-104276; H-1997; NAS 1.15:104276) Avail: CASI HC A03/MF A01; 22 functional color pages

A water-tunnel test of a 4.4 percent-scale, forebody-only model of the X-31 aircraft with different forebody strakes and nosebooms has been performed in the Flow Visualization Facility at the NASA Dryden Flight Research Center. The focus of the study was to determine the relative effects of the different configurations on the stability and symmetry of the high-angle-of-attack forebody vortex flow field. The clean, noseboom-off configuration resisted the development of asymmetries in the primary vortices through 70 deg angle of attack. The wake of the X-31 flight test noseboom configuration significantly degraded the steadiness of the primary vortex cores and promoted asymmetries. An alternate L-shaped noseboom mounted underneath the forebody had results similar to those seen with the configuration, enabling stable, symmetrical vortices up to 70 deg angle of attack. The addition of strakes near the radome tip along the waterline increased the primary vortex strength while it simultaneously caused the vortex breakdown location co move forward. Forebody strakes did not appear to significantly reduce the asymmetries in the forebody vortex field in the presence of the flight test noseboom. Author

N95-11911*# California Univ., Los Angeles, CA. Dept. of Mechanical, Aerospace and Nuclear Engineering.
AEROELASTIC SIMULATION OF HIGHER HARMONIC CONTROL
Lawson H. Robinson and Peretz P. Friedmann Moffett Field, CA NASA Aug. 1994 301 p
(Grant NAG2-477)

(NASA-CR-4623; A-94118; NAS 1.26:4623) Avail: CASI HC A14/MF A03

This report describes the development of an aeroelastic analysis of a helicopter rotor and its application to the simulation of helicopter vibration reduction through higher harmonic control (HHC). An improved finite-state, time-domain model of unsteady aerodynamics is developed to capture high frequency aerodynamic effects. An improved trim procedure is implemented which accounts for flap, lead-lag, and torsional deformations of the blade. The effect of unsteady aerodynamics is studied and it is found that its impact on blade aeroelastic stability and low frequency response is small, but it has a significant influence on rotor hub vibrations. Several different HHC algorithms are implemented on a hingeless rotor and their effectiveness in reducing hub vibratory shears is compared. All the controllers are found to be quite effective, but very differing HHC inputs are required depending on the aerodynamic model used. Effects of HHC on rotor stability and power requirements are found to be quite small. Simulations of roughly equivalent articulated and hingeless rotors are carried out, and it is found that hingeless rotors can require considerably larger HHC inputs to reduce vibratory shears. This implies that the practical implementation of HHC on hingeless rotors might be considerably more difficult than on articulated rotors. Author

N95-11917*# National Aeronautics and Space Administration. Lewis Research Center, Cleveland, OH.

MODIFICATION OF THE TWO-EQUATION TURBULENCE MODEL IN NPARC TO A CHIEN LOW REYNOLDS NUMBER K-EPSILON FORMULATION

Nicholas J. Georgiadis, Tawit Chitsomboon, and Jiang Zhu Sep. 1994 19 p
(Contract NCC3-233; RTOP 537-02-23)
(NASA-TM-106710; ICOMP-94-20; E-9072; NAS 1.15:106710; CMOTT-94-5) Avail: CASI HC A03/MF A01

This report documents the changes that were made to the two-equation k-epsilon turbulence model in the NPARC (National-PARC) code. The previous model based on the low Reynolds number model of Speziale, was replaced with the low Reynolds number k-epsilon model of Chien. The most significant difference was in the turbulent Prandtl numbers appearing in the diffusion terms of the k and epsilon transport equations. A new inflow boundary condition and stability enhancements were also implemented into the turbulence model within NPARC. The report provides the rationale for making the change to the Chien model, code modifications required, and comparisons of the performances of the new model with the previous k-epsilon model and algebraic models used most often in PARC/NPARC. The comparisons show that the Chien k-epsilon model installed here improves the capability of NPARC to calculate turbulent flows. Author (revised)

N95-11927*# National Aeronautics and Space Administration. Ames Research Center, Moffett Field, CA.

NUMERICAL ANALYSIS OF TANGENTIAL SLOT BLOWING ON A GENERIC CHINED FOREBODY

Roxana M. Agosta Sep. 1994 59 p
(RTOP 505-68-00)
(NASA-TM-108845; A-94125; NAS 1.15:108845) Avail: CASI HC A04/MF A01

A numerical study is performed to investigate the effects of tangential slot blowing on a generic chined forebody. The Reynolds-averaged, thin-layer, Navier-Stokes equations are solved to obtain the high-angle-of-attack viscous flow field about a generic chined forebody. Tangential slot blowing is investigated as a means of forebody flow control to generate side force and yawing moment on the forebody. The effects of jet mass flow ratios, angle of attack, and blowing slot location in the axial and circumferential directions are studied. The computed results are compared with available wind tunnel experimental data. The solutions with and without blowing are also analyzed using helicity density contours, surface flow patterns, and off-surface instantaneous streamlines. The results of this analysis provide details of the flow field about the generic chined forebody, as well as show that tangential slot blowing can be used as a means of forebody flow control to generate side force and yawing moment. Author

N95-11995*# National Aeronautics and Space Administration. Langley Research Center, Hampton, VA.

COMPUTER CODE FOR DETERMINATION OF THERMALLY PERFECT GAS PROPERTIES

David W. Witte and Kenneth E. Tatum Sep. 1994 77 p
(RTOP 505-70-59-03)
(NASA-TP-3447; L-17327; NAS 1.60:3447) Avail: CASI HC A05/MF A01

A set of one-dimensional compressible flow relations for a thermally perfect, calorically imperfect gas is derived for the specific heat c(sub p), expressed as a polynomial function of temperature, and developed into the thermally perfect gas (TPG) computer code. The code produces tables of compressible flow properties similar to those of NACA Rep. 1135. Unlike the tables of NACA Rep. 1135 which are valid only in the calorically perfect temperature regime, the TPG code results are also valid in the thermally perfect calorically imperfect temperature regime which considerably extends the range of temperature application. Accuracy of the TPG code in the calorically perfect temperature regime is verified by comparisons with the tables of NACA Rep. 1135. In the thermally perfect, calorically imperfect temperature regime, the TPG code is validated by comparisons with results obtained from the method of NACA Rep. 1135 for calculating the thermally perfect calorically imperfect compressible flow properties. The temperature limits for application of the TPG code are also examined. The advantage of the TPG code is its applicability to any type of gas (monatomic, diatomic, triatomic, or polyatomic) or any specified mixture thereof, whereas the method of NACA Rep. 1135 is restricted to only diatomic gases. Author (revised)

N95-12176*# National Aeronautics and Space Administration. Langley Research Center, Hampton, VA.

APPLICATION OF TWO PROCEDURES FOR DUAL-POINT DESIGN OF TRANSONIC AIRFOILS

Raymond E. Mineck, Richard L. Campbell, and Dennis O. Allison Sep. 1994 53 p
(RTOP 505-59-54-17)
(NASA-TP-3466; L-17268; NAS 1.60:3466) Avail: CASI HC A04/MF A01

Two dual-point design procedures were developed to reduce the objective function of a baseline airfoil at two design points. The first procedure to develop a redesigned airfoil used a weighted average of the shapes of two intermediate airfoils redesigned at each of the two design points. The second procedure used a weighted average of two pressure distributions obtained from an intermediate airfoil redesigned at each of the two design points. Each procedure was used to design a new airfoil with reduced wave drag at the cruise condition without increasing the wave drag or pitching moment at the climb condition. Two cycles of the airfoil shape-averaging procedure successfully designed a new airfoil that reduced the objective function and satisfied the constraints. One cycle of the target (desired) pressure-averaging procedure was used to design two new airfoils that reduced the objective function and came close to satisfying the constraints. Author

N95-12191*# National Aeronautics and Space Administration. Hugh L. Dryden Flight Research Center, Edwards, CA.

DYNAMIC GROUND EFFECTS FLIGHT TEST OF AN F-15 AIRCRAFT

Stephen Corda (Planning Research Corp., Edwards, CA.), Mark T. Stephenson, Frank W. Burcham, and Robert E. Curry Washington Sep. 1994 28 p
(RTOP 533-02-31)
(NASA-TM-4604; H-1999; NAS 1.15:4604) Avail: CASI HC A03/MF A01

Flight tests to determine the changes in the aerodynamic characteristics of an F-15 aircraft caused by dynamic ground effects are described. Data were obtained for low and high sink rates between 0.7 and 6.5 ft/sec and at two landing approach speeds and flap settings: 150 kn with the flaps down and 170 kn with the flaps up. Simple correlation curves are given for the change in aerodynamic coefficients because of ground effects as a function of sink rate. Ground effects generally caused an increase in the lift, drag, and nose-down pitching movement coefficients. The change in the lift coefficient increased from approximately 0.05 at the high-sink rate to approximately 0.10 at the low-sink rate. The change in the drag coefficient increased from approximately 0 to 0.03 over this decreasing sink rate

range. No significant difference because of the approach configuration was evident for lift and drag; however, a significant difference in pitching movement was observed for the two approach speeds and flap settings. For the 170 kn with the flaps up configuration, the change in the nose-down pitching movement increased from approximately -0.008 to -0.016. For the 150 kn with the flaps down configuration, the change was approximately -0.008 to -0.038. Author

N95-12360*# National Aeronautics and Space Administration. Ames Research Center, Moffett Field, CA.
MEASUREMENTS OF ATMOSPHERIC TURBULENCE EFFECTS ON TAIL ROTOR ACOUSTICS Final Report
Martin J. Hagen (California Polytechnic State Univ., San Luis Obispo, CA.), Gloria K. Yamauchi, David B. Signor, and Marianne Mosher Sep. 1994 81 p
(RTOP 505-59-36)
(NASA-TM-108843; A-94122; NAS 1.15:108843) Avail: CASI HC A05/MF A01

Results from an outdoor hover test of a full-scale Lynx tail rotor are presented. The investigation was designed to further the understanding of the acoustics of an isolated tail rotor hovering out-of-ground effect in atmospheric turbulence, without the effects of the main rotor wake or other helicopter components. Measurements include simultaneous rotor performance, noise, inflow, and far-field atmospheric turbulence. Results with grid-generated inflow turbulence are also presented. The effects of atmospheric turbulence ingestion on rotor noise are quantified. In contradiction to current theories, increasing rotor inflow and rotor thrust were found to increase turbulence ingestion noise. This is the final report of Task 13A--Helicopter Tail Rotor Noise, of the NASA/United Kingdom Defense Research Agency cooperative Aeronautics Research Program. Author

N95-12378*# National Aeronautics and Space Administration. Lewis Research Center, Cleveland, OH.
A NEW ALGORITHM FOR FIVE-HOLE PROBE CALIBRATION, DATA REDUCTION, AND UNCERTAINTY ANALYSIS
Bruce A. Reichert and Bruce J. Wendt Sep. 1994 21 p
(RTOP 505-62-52)
(NASA-TM-106458; E-8319; NAS 1.15:106458) Avail: CASI HC A03/MF A01

A new algorithm for five-hole probe calibration and data reduction using a non-nulling method is developed. The significant features of the algorithm are: (1) two components of the unit vector in the flow direction replace pitch and yaw angles as flow direction variables; and (2) symmetry rules are developed that greatly simplify Taylor's series representations of the calibration data. In data reduction, four pressure coefficients allow total pressure, static pressure, and flow direction to be calculated directly. The new algorithm's simplicity permits an analytical treatment of the propagation of uncertainty in five-hole probe measurement. The objectives of the uncertainty analysis are to quantify uncertainty of five-hole results (e.g., total pressure, static pressure, and flow direction) and determine the dependence of the result uncertainty on the uncertainty of all underlying experimental and calibration measurands. This study outlines a general procedure that other researchers may use to determine five-hole probe result uncertainty and provides guidance to improve measurement technique. The new algorithm is applied to calibrate and reduce data from a rake of five-hole probes. Here, ten individual probes are mounted on a single probe shaft and used simultaneously. Use of this probe is made practical by the simplicity afforded by this algorithm. Author

N95-12389*# MCAT Inst., San Jose, CA.
HIGH SPEED CIVIL TRANSPORT AERODYNAMIC OPTIMIZATION Annual Report, Aug. 1993 - Jul. 1994
James S. Ryan Jul. 1994 6 p Original contains color illustrations
(Contract NCC2-796)
(NASA-CR-196960; NAS 1.26:196960) Avail: CASI HC A02/MF A01; 1 functional colored page

This is a report of work in support of the Computational Aerosciences (CAS) element of the Federal HPCC program. Specifically, CFD and aerodynamic optimization are being performed on parallel computers. The long-range goal of this work is to facilitate teraflops-rate multidisciplinary optimization of aerospace vehicles. This year's work is targeted for application to the High Speed Civil Transport (HSCT), one of four CAS grand challenges identified in the HPCC FY 1995 Blue Book. This vehicle is to be a passenger aircraft, with the promise of cutting overseas flight time by more than half. To meet fuel economy, operational costs, environmental impact, noise production, and range requirements, improved design tools are required, and these tools must eventually integrate optimization, external aerodynamics, propulsion, structures, heat transfer, controls, and perhaps other disciplines. The fundamental goal of this project is to contribute to improved design tools for U.S. industry, and thus to the nation's economic competitiveness. Derived from text

N95-12548 Air Force Inst. of Tech., Wright-Patterson AFB, OH.
MEASUREMENTS OF PRESSURE AND THERMAL WAKES IN A TRANSONIC TURBINE CASCADE M.S. Thesis
Alexis Mezynski Aug. 1994 80 p Limited Reproducibility: More than 20% of this document may be affected by microfiche quality
(AD-A283464; AFIT/CI/CIA-94-118) Avail: CASI HC A05

The effects of freestream turbulence on the total pressure and total temperature in the wake of a cooled transonic turbine cascade with heated flow are presented in this thesis. The experiment was conducted in the Virginia Tech Cascade Wind Tunnel. A dual hot wire aspirating probe was used to make high frequency, unsteady total pressure and temperature measurements. The probe design was modified to be used in a high temperature environment. The flow was heated to temperatures exceeding 140 deg C and the turbine blades were actively cooled using gaseous nitrogen to maintain a gas to blade temperature ratio between 1.3 and 1.4. A turbulence screen was used to change the freestream turbulence from 3.3% to 7.5%. Mean and turbulent total pressure and temperature quantities are presented. The higher freestream turbulence resulted in lower total pressure and total temperature turbulence intensifies in the wakes of the turbine blades. The freestream turbulence level had no measurable effect on the blade losses. DTIC

N95-12578 Institut Franco-Allemand de Recherches, Saint-Louis (France).
SUPERSONIC BASE FLOW INVESTIGATION OVER AXISYMMETRIC AFTERBODIES
C. Berner 1993 13 p Presented at the 5th Conference on Laser Anemometry - Advances and Applications, Veldhoven, Netherlands, 23-27 Aug. 1993 Sponsored by Direction des Recherches, Etudes et Techniques, Paris, France and Centre de Documentation de l'Armement
(PB94-180957; ISL-PU-347/93) Avail: Issuing Activity (National Technical Information Service (NTIS))

Experimental and computational investigations were carried out to study base flows behind afterbodies embedded in a supersonic freestream. Experiments were conducted in a blowdown wind tunnel at a nominal Mach number of 2.06 and for an angle of attack of zero degree. Afterbody models are interchangeable and sting mounted to avoid interference on the base from usual support systems. The experimental study consisted of two axisymmetric afterbodies, a cylindrical afterbody and a tapered afterbody with a conical boattail of 6 degrees and a boattail length of one diameter. Results include flow visualization, static wall pressure distributions and turbulent flow properties obtained by means of a two-dimensional laser Doppler velocimeter (LDV). Computations were carried out using a multi-dimensional Navier-Stokes code based upon a fully implicit, combined finite volume/flux element discretization approach with a standard K-epsilon turbulence model. Computed solutions show some good agreement with experiment as far as concerning the flow field structure, surface and base pressures but show some deficiencies with velocities and shear stress correlations. NTIS

N95-12652# Los Alamos National Lab., NM.
HYPERSONIC GAS-SURFACE ENERGY ACCOMMODATION TEST FACILITY
J. B. Cross, M. A. Hoffbauer, and S. R. Cook 1994 20 p Presented at the 6th AIAA/ASME Thermophysics and Heat Transfer Conference, Colorado Springs, CO, 20-23 Jun. 1994
(Contract W-7405-eng-36)
(DE94-014468; LA-UR-94-2080; CONF-940625-7) Avail: CASI HC A03/MF A01

A test facility is described that determines energy and momentum accommodation coefficients by direct measurement. Momentum

accommodation coefficients are obtained by measuring the force exerted on surfaces by molecular beams using a torsion balance. Energy accommodation coefficients are obtained through the measurement of angular and velocity distributions of the molecules reflected off the scattering surface. Data obtained from the recoil angular and velocity distribution measurements are also used to calculate momentum accommodation coefficients which are then compared to the results obtained from the torsion balance. Results from a torsion balance measurement of 1.5 km/sec N2 scattered from solar cell cover plate material are shown. DOE

N95-12770* National Aeronautics and Space Administration. Langley Research Center, Hampton, VA.

EXPERIMENTAL AERODYNAMIC CHARACTERISTICS OF A GENERIC HYPERSONIC ACCELERATOR CONFIGURATION AT MACH NUMBERS 1.5 AND 2.0

Ira J. Walker (Lockheed Engineering and Sciences Co., Hampton, VA.), Peter F. Covell, and Dana K. Forrest Mar. 1993 124 p Non-standard MF as supplement

(RTOP 505-59-40-10)

(NASA-TM-4413; L-17105; NAS 1.15:4413) Avail: CASI HC A06/MF A02

An experimental investigation of the static longitudinal and lateral-directional aerodynamic characteristics of a generic hypersonic research vehicle was conducted in the Langley Unitary Plan Wind Tunnel (UPWT). A parametric study was performed to determine the interference effects of various model components. Configuration variables included delta and trapezoidal canards; large and small centerline-mounted vertical tails, along with a set of wing-mounted vertical tails; and a set of model noses with different degrees of bluntness. Wing position was varied by changing the longitudinal location and the incidence angle. The test Mach numbers were 1.5 and 2.0 at Reynolds numbers of 1 x 10(exp 6) per foot, 2 x 10(exp 6) per foot, and 4 x 10(exp 6) per foot. Angle of attack was varied from -4 degrees to 27 degrees, and sideslip angle was varied from -8 degrees to 8 degrees. Generally, the effect of Reynolds number did not deviate from conventional trends. The longitudinal stability and lift-curve slope decreased with increasing Mach number. As the wing was shifted rearward, the lift-curve slope decreased and the longitudinal stability increased. Also, the wing-mounted vertical tails resulted in a more longitudinally stable configuration. In general, the lift-drag ratio was not significantly affected by vertical-tail arrangement. The best lateral-directional stability was achieved with the large centerline-mounted tail, although the wing-mounted vertical tails exhibited the most favorable characteristics at the higher angles of attack. Author (revised)

N95-13058*# National Aeronautics and Space Administration. Lewis Research Center, Cleveland, OH.

VALIDATION OF THE RPLUS3D CODE FOR SUPERSONIC INLET APPLICATIONS INVOLVING THREE-DIMENSIONAL SHOCK WAVE-BOUNDARY LAYER INTERACTIONS

Kamlesh Kapoor, Bernhard H. Anderson, and Robert J. Shaw Sep. 1994 17 p Original contains color illustrations

(RTOP 537-02-23)

(NASA-TM-106579; E-8839; NAS 1.15:106579) Avail: CASI HC A03/MF A01; 2 functional color pages

A three-dimensional computational fluid dynamics code, RPLUS3D, which was developed for the reactive propulsive flows of ramjets and scramjets, was validated for glancing shock wave-boundary layer interactions. Both laminar and turbulent flows were studied. A supersonic flow over a wedge mounted on a flat plate was numerically simulated. For the laminar case, the static pressure distribution, velocity vectors, and particle traces on the flat plate were obtained. For turbulent flow, both the Baldwin-Lomax and Chien two-equation turbulent models were used. The static pressure distributions, pitot pressure, and yaw angle profiles were computed. In addition, the velocity vectors and particle traces on the flat plate were also obtained from the computed solution. Overall, the computed results for both laminar and turbulent cases compared very well with the experimentally obtained data. Author

N95-13197*# National Aeronautics and Space Administration. Lewis Research Center, Cleveland, OH.

ROLE OF WIND TUNNELS AND COMPUTER CODES IN THE CERTIFICATION AND QUALIFICATION OF ROTORCRAFT FOR FLIGHT IN FORECAST ICING

Robert J. Flemming (United Technologies Corp., Stratford, CT.), Randall K. Britton (NYMA, Inc., Brook Park, OH.), and Thomas H. Bond Oct. 1994 23 p Presented at the 20th European Rotorcraft Forum, Amsterdam, The Netherlands, 4-7 Oct. 1994; sponsored by the National Aerospace Laboratory NLR

(Contract NAS3-27186; RTOP 505-68-10)

(NASA-TM-106747; E-9159; NAS 1.15:106747) Avail: CASI HC A03/MF A01

The cost and time to certify or qualify a rotorcraft for flight in forecast icing has been a major impediment to the development of ice protection systems for helicopter rotors. Development and flight test programs for those aircraft that have achieved certification or qualification for flight in icing conditions have taken many years, and the costs have been very high. NASA, Sikorsky, and others have been conducting research into alternative means for providing information for the development of ice protection systems, and subsequent flight testing to substantiate the air-worthiness of a rotor ice protection system. Model rotor icing tests conducted in 1989 and 1993 have provided a data base for correlation of codes, and for the validation of wind tunnel icing test techniques. This paper summarizes this research, showing test and correlation trends as functions of cloud liquid water content, rotor lift, flight speed, and ambient temperature. Molds were made of several of the ice formations on the rotor blades. These molds were used to form simulated ice on the rotor blades, and the blades were then tested in a wind tunnel to determine flight performance characteristics. These simulated-ice rotor performance tests are discussed in the paper. The levels of correlation achieved and the role of these tools (codes and wind tunnel tests) in flight test planning, testing, and extension of flight data to the limits of the icing envelope are discussed. The potential application of simulated ice, the NASA LEWICE computer, the Sikorsky Generalized Rotor Performance aerodynamic computer code, and NASA Icing Research Tunnel rotor tests in a rotorcraft certification or qualification program are also discussed. The correlation of these computer codes with tunnel test data is presented, and a procedure or process to use these methods as part of a certification or qualification program is introduced. Author (revised)

N95-13250 Technische Univ., Delft (Netherlands).

STUDIES ON THE FLOW INDUCED BY AN OSCILLATING AIRFOIL IN A UNIFORM STREAM Ph.D. Thesis

Z. Wang 8 Mar. 1994 198 p

(PB94-204450; ISBN-90-6275-963-7) Copyright Avail: Issuing Activity (National Technical Information Service (NTIS))

The thesis is organized into six chapters. Chapter 1 provides an introduction to the problem of oscillating airfoils. In chapter 2 a review of the classical unsteady airfoil theory is given. A survey of viscous flow structure is presented in chapter 3. Experimental studies are described in chapter 4. The experimental study consists of two parts, namely, experimental measurements and numerical calculations based on a panel method which is discussed in detail in chapter 5. Conclusions are summarized in chapter 6. NTIS

N95-11967*# Eloret Corp., Palo Alto, CA.

COMPUTATIONAL FLOW PREDICTIONS FOR HYPERSONIC DRAG DEVICES

Susan A. Tokarcik and Ethiraj Venkatapathy *In* NASA. Ames Research Center, Technical Paper Contest for Women 1992. Space Challenges: Earth and Beyond 1993 p 145-170 (For primary document see N95-11955 02-99)

Avail: CASI HC A03/MF A03

03 AIR TRANSPORTATION AND SAFETY

Includes passenger and cargo air transport operations; and aircraft accidents.

For related information see also *16 Space Transportation* and *85 Urban Technology and Transportation.*

N95-12146# Civil Aeromedical Inst., Oklahoma City, OK.
THE PERFORMANCE OF CHILD RESTRAINT DEVICES IN TRANSPORT AIRPLANE PASSENGER SEATS Final Report
Van Gowdy and Richard DeWeese Sep. 1994 32 p
(DOT/FAA/AM-94/19) Avail: CASI HC A03/MF A01

The performance of child restraint devices (CRD's) in commercial transport airplane passenger seats was evaluated by a dynamic impact test program. Background information on the policies and regulations related to child restraints is summarized. Tests were conducted at the FAA Civil Aeromedical Institute, Six types (CRD's) certified for use in airplanes were tested. Booster seats, forward facing carriers, aft facing carriers, a harness device, a belly belt, and passenger seat lap belts were evaluated. Impact tests were conducted with CRD's installed on airplane passenger seats. The test severity was 16 Gpk with an impact velocity of 44 ft/sec. Effects of multiple row seats, aft row occupant impact loads, and seat back breakover were part of the project protocol. Four child size anthropomorphic test dummies were utilized. The 6-month and 36-month size ATD's defined in 49 CFR Part 572, the 6-month size CRABI ATD, and a 24-month size experimental ATD identified as CAMIX were used in these tests. An experimental device to measure abdominal pressure was evaluated in the CRABI and CAMIX ATD's. Analyses of the data acquired from the tests and observations related to the performance of the CRD's in airplane seats are presented. Author

N95-12499# Southwest Research Inst., San Antonio, TX. Fuels and Lubricants Research Facility.
A STUDY OF AIRCRAFT POST-CRASH FUEL FIRE MITIGATION Interim Report, Jul. 1991 - Feb. 1993
D. W. Naegeli, B. R. Wright, and D. M. Zallen Jun. 1994 38 p
(Contracts DAAK70-87-C-0043; DAAK70-92-C-0059)
(AD-A282208; BFLRF-292) Avail: CASI HC A03/MF A01

Extensive research has been conducted on methods of controlling aircraft post-impact fuel fires. Mechanism studies of hydrocarbon fuel ignition and flame propagation have identified feasible approaches to agent selection and dispersal schemes. Selection of agents is closely controlled by guidelines of the Montreal Protocol Agreements and allowable agent manufacturing as specified by the Environmental Protection Agency. Effectiveness of agents has been determined under a variety of laboratory test conditions. Mass transport of the inerting agent into the vapor above the fuel as well as the environmental conditions in the vapor space play an important role in inerting agent effectiveness. Schemes to control hydrocarbon vapor and to enhance inerting agent effectiveness are discussed. DTIC

N95-12623 Carnegie-Mellon Inst. of Research, Pittsburgh, PA.
DEVELOPMENT OF AN AUTOMATED NONDESTRUCTIVE INSPECTION (ANDI) SYSTEM FOR COMMERCIAL AIRCRAFT, PHASE 1 Final Report, 15 May 1992 - 31 Jan. 1993
C. J. Alberts, W. M. Kaufman, and M. W. Siegel Jun. 1994 50 p
Sponsored by FAA Limited Reproducibility: More than 20% of this document may be affected by microfiche quality
(AD-A283500; DOT/FAA/CT-94/23-Phase-1) Avail: CASI HC A03

This report describes the first phase in the development of a robotic system designed to assist aircraft inspectors by remotely deploying nondestructive inspection (NDI) sensors and acquiring, processing, and storing inspection data. To demonstrate the feasibility of using robots to acquire data, a prototype inspection system was developed. The system comprises a surface-walking robot for sensor deployment and a personal computer for controlling the robot and for processing and displaying the acquired data. The robot can deploy an eddy current sensor on the skin surface, scan a portion of a rivet row, and step to another location to gather more data. In addition, requirements to include video cameras to provide visual images of the surface were specified. The prototype system was tested in a laboratory setting on a simulated aircraft panel. The design of the robot satisfied the mobility and manipulation requirements of the skin inspection application. The eddy current traces displayed on the computer monitor from the robotically deployed eddy current sensor were comparable to those from manually deployed eddy current sensors. Overall, the results of this phase of work indicate that robotic inspection tools designed to assist human inspectors hold great promise. DTIC

N95-13203*# National Aeronautics and Space Administration. Langley Research Center, Hampton, VA.
AIRBORNE WINDSHEAR DETECTION AND WARNING SYSTEMS. FIFTH AND FINAL COMBINED MANUFACTURERS' AND TECHNOLOGISTS' CONFERENCE, PART 2
Victor E. Delnore, comp. (Lockheed Engineering and Sciences Co., Hampton, VA.) Jul. 1994 426 p Conference held in Hampton, VA, 28-30 Sep. 1993; cosponsored by FAA Prepared in cooperation with FAA, Washington, DC
(RTOP 505-64-12-01)
(NASA-CP-10139-Pt-2; NAS 1.55:10139-Pt-2; DOT/FAA/RD-94/14-Pt-2)
Avail: CASI HC A19/MF A04

The Fifth Combined Manufacturers' and Technologists' Airborne Windshear Review Meeting was hosted by the NASA Langley Research Center and the Federal Aviation Administration in Hampton, Virginia, on September 28-30, 1993. The purpose was to report on the highly successful windshear experiments conducted by government, academic institutions, and industry; to transfer the results to regulators, manufacturers, and users; and to set initiatives for future aeronautics technology research. The formal sessions covered recent developments in windshear flight testing, windshear modeling, flight management, and ground-based systems, airborne windshear detection systems, certification and regulatory issues, and development and applications of sensors for wake vortices and for synthetic and enhanced vision systems. This report was compiled to record and make available the technology updates and materials from the conference. For individual titles, see N95-13204 through N95-13215.

N95-13204*# National Aeronautics and Space Administration. Langley Research Center, Hampton, VA.
WINDSHEAR CERTIFICATION DATA BASE FOR FORWARD-LOOK DETECTION SYSTEMS
George F. Switzer (Research Triangle Inst., Hampton, VA.), David A. Hinton, and Fred H. Proctor *In its* Airborne Windshear Detection and Warning Systems. Fifth and Final Combined Manufacturers' and Technologists' Conference, Part 2 Jul. 1994 p 447-461 (For primary document see N95-13203 02-03)
Avail: CASI HC A03/MF A04

Described is an introduction to a comprehensive database that is to be used for certification testing of airborne forward-look windshear detection systems. The database was developed by NASA Langley Research Center, at the request of the Federal Aviation Administration (FAA), to support the industry initiative to certify and produce forward-looking windshear detection equipment. The database contains high-resolution three-dimensional fields for meteorological variables that may be sensed by forward-looking systems. The database is made up of seven case studies that are generated by the Terminal Area Simulation System, a state-of-the-art numerical system for the realistic modeling of windshear phenomena. The selected cases contained in the certification documentation represent a wide spectrum of windshear events. The database will be used with vendor-developed sensor simulation software and vendor-collected ground-clutter data to demonstrate detection performance in a variety of meteorological conditions using NASA/FAA pre-defined path scenarios for each of the certification cases. A brief outline of the contents and sample plots from the database documentation are included. These plots show fields of hazard factor, or F-factor (Bowles 1990), radar reflectivity, and velocity vectors on a horizontal plane overlayed with the applicable certification paths. For the plot of the F-factor field the region of 0.105 and above signify an area of hazardous, performance decreasing windshear, while negative values indicate regions of performance increasing windshear. The values of F-factor are based on 1-Km averaged segments along horizontal flight paths, assuming an air speed of 150 knots (approx. 75 m/s). The database has been released to vendors participating in the certification process. The database and associated document have been transferred to the FAA for archival storage and distribution. Author (revised)

N95-13205*# National Aeronautics and Space Administration. Langley Research Center, Hampton, VA.

CERTIFICATION METHODOLOGY APPLIED TO THE NASA EXPERIMENTAL RADAR SYSTEM

Charles L. Britt (Research Triangle Inst., Hampton, VA.), George F. Switzer (Research Triangle Inst., Hampton, VA.), and Emedio M. Bracalente *In its* Airborne Windshear Detection and Warning Systems. Fifth and Final Combined Manufacturers' and Technologists' Conference, Part 2 Jul. 1994 p 463-488 (For primary document see N95-13203 02-03)

Avail: CASI HC A03/MF A04

The objective of the research is to apply selected FAA certification techniques to the NASA experimental wind shear radar system. Although there is no intent to certify the NASA system, the procedures developed may prove useful to manufacturers that plan to undergo the certification process. The certification methodology for forward-looking wind shear detection radars will require estimation of system performance in several FAA-specified microburst/clutter scenarios as well as the estimation of probabilities of missed and false hazard alerts under general operational conditions. Because of the near-impossibility of obtaining these results experimentally, analytical and simulation approaches must be used. Hazard detection algorithms were developed that derived predictive estimates of aircraft hazard from basic radar measurements of weather reflectivity and radial wind velocity. These algorithms were designed to prevent false alarms due to ground clutter while providing accurate predictions of hazard to the aircraft due to weather. A method of calculation of the probability of missed and false hazard alerts has been developed that takes into account the effect of the various algorithms used in the system and provides estimates of the probability of missed and false alerts per microburst encounter under weather conditions found at Denver, Kansas City, and Orlando. Simulation techniques have been developed that permit the proper merging of radar ground clutter data (obtained from flight tests) with simulated microburst data (obtained from microburst models) to estimate system performance using the microburst/clutter scenarios defined by the FAA.

Author

N95-13206*# Westinghouse Electric Corp., Baltimore, MD. Electronic Systems Group.

CERTIFICATION OF WINDSHEAR PERFORMANCE WITH RTCA CLASS D RADOMES

Bruce D. Mathews, Fran Miller, Kirk Rittenhouse, Lee Barnett, and William Rowe *In* NASA. Langley Research Center, Airborne Windshear Detection and Warning Systems. Fifth and Final Combined Manufacturers' and Technologists' Conference, Part 2 Jul. 1994 p 489-498 (For primary document see N95-13203 02-03)

Avail: CASI HC A02/MF A04

Superposition testing of detection range performance forms a digital signal for input into a simulation of signal and data processing equipment and algorithms to be employed in a sensor system for advanced warning of hazardous windshear. For suitable pulse-Doppler radar, recording of the digital data at the input to the digital signal processor furnishes a realistic operational scenario and environmentally responsive clutter signal including all sidelobe clutter, ground moving target indications (GMTI), and large signal spurious due to mainbeam clutter and/or RFI respective of the urban airport clutter and aircraft scenarios (approach and landing antenna pointing). For linear radar system processes, a signal at the same point in the process from a hazard phenomena may be calculated from models of the scattering phenomena, for example, as represented in fine 3 dimensional reflectivity and velocity grid structures. Superposition testing furnishes a competing signal environment for detection and warning time performance confirmation of phenomena uncontrollable in a natural environment.

Author

N95-13207*# Coherent Technologies, Inc., Boulder, CO.

AIRPORT SURVEILLANCE USING A SOLID STATE COHERENT LIDAR

R. Milton Huffaker and Stephen M. Hannon *In* NASA. Langley Research Center, Airborne Windshear Detection and Warning Systems. Fifth and Final Combined Manufacturers' and Technologists' Conference, Part 2 Jul. 1994 p 499-523 (For primary document see N95-13203 02-03)

Avail: CASI HC A03/MF A04

The utility of solid state coherent LIDAR was assessed in the following application areas: (1) wake vortices; (2) dry and wet microburst windshear; (3) gusts; (4) vertical and general wind profiling; and (5) cloud ceiling. The system performance model described was based on a concept definition, system sizing, measurement planning, and algorithm and graphics display development. Data were collected at the Kennedy Space Center and the National Weather Service site adjacent to Denver's Stapleton Airport.

CASI

N95-13208*# Research Triangle Inst., Hampton, VA.

CHARACTERISTICS OF CIVIL AVIATION ATMOSPHERIC HAZARDS

Robert E. Marshall, J. Montoya, Mark A. Richards, and J. Galliano *In* NASA. Langley Research Center, Airborne Windshear Detection and Warning Systems. Fifth and Final Combined Manufacturers' and Technologists' Conference, Part 2 Jul. 1994 p 545-568 (For primary document see N95-13203 02-03)

Avail: CASI HC A03/MF A04

Clear air turbulence, wake vortices, dry hail, and volcanic ash are hazards to civil aviation that have not been brought to the forefront of public attention by a catastrophic accident. However, these four hazards are responsible for major and minor injuries, emotional trauma, significant aircraft damage, and in route and terminal area inefficiency. Most injuries occur during clear air turbulence. There is significant aircraft damage for any volcanic ash encounter. Rolls induced by wake vortices occur near the ground. Dry hail often appears as an area of weak echo on the weather radar. This paper will present the meteorological, electromagnetic, and spatiotemporal characteristics of each hazard. A description of a typical aircraft encounter with each hazard will be given. Analyzed microwave and millimeter wave sensor systems to detect each hazard will be presented.

Author

N95-13209*# Massachusetts Inst. of Tech., Lexington. Lincoln Lab.

GROUND-BASED WAKE VORTEX MONITORING, PREDICTION, AND ATC INTERFACE

Steven D. Campbell and James E. Evans *In* NASA. Langley Research Center, Airborne Windshear Detection and Warning Systems. Fifth and Final Combined Manufacturers' and Technologists' Conference, Part 2 Jul. 1994 p 569-601 (For primary document see N95-13203 02-03)

(Contract F19628-90-C-002)

Avail: CASI HC A03/MF A04

This talk will discuss three elements of a proposed Wake Vortex Advisory Service: monitoring, prediction and ATC interface. The monitoring element is needed to ensure safety by warning controllers of hazardous wake vortex conditions. Such conditions exist when wake vortices persist in the approach/departure flight paths due to advection or to atmospheric conditions which prevent their decay. The prediction element is needed to provide ATC supervisors with advance warning that wake vortex separation conditions are about to change (i.e., require increased or decreased wake vortex separation). The ATC interface element is needed to provide controllers with adaptive wake vortex separations. The use of these adaptive wake vortex separations would lead to increased airport capacity under most conditions, while maintaining safety under conditions of wake vortex hazard.

Author

N95-13210*# Massachusetts Inst. of Tech., Lexington. Lincoln Lab.

AIRCRAFT WAKE RCS MEASUREMENT c32

William H. Gilson *In* NASA. Langley Research Center, Airborne Windshear Detection and Warning Systems. Fifth and Final Combined Manufacturers' and Technologists' Conference, Part 2 Jul. 1994 p 603-623 Sponsored by Office of Naval Technology (For primary document see N95-13203 02-03)

Avail: CASI HC A03/MF A04

A series of multi-frequency radar measurements of aircraft wakes at altitudes of 5,000 to 25,00 ft. were performed at Kwajalein, R.M.I., in May and June of 1990. Two aircraft were tested, a Learjet 35 and a Lockheed C-5A. The cross-section of the wake of the Learjet was too small for detection at Kwajalein. The wake of the C-5A, although also very small, was detected and measured at VHF, UHF, L-, S-, and C-bands, at distances behind the aircraft ranging from about one hundred meters to tens of kilometers. The data suggest that the mechanism by which aircraft wakes have detectable radar signatures is, contrary to previous expectations, unrelated to engine exhaust but instead due to turbulent mixing by the wake vortices of pre-existing index of refraction gradients in the ambient atmosphere. These measurements were of necessity performed with

extremely powerful and sensitive instrumentation radars, and the wake cross-section is too small for most practical applications. Author

N95-13211*# Coherent Technologies, Inc., Boulder, CO.
WAKE VORTEX DETECTION AT DENVER STAPLETON AIRPORT WITH A PULSED 2-MICRON COHERENT LIDAR
Stephen M. Hannon and J. Alex Thomson *In* NASA. Langley Research Center, Airborne Windshear Detection and Warning Systems. Fifth and Final Combined Manufacturers' and Technologists' Conference, Part 2 Jul. 1994 p 625-650 (For primary document see N95-13203 02-03)
Avail: CASI HC A03/MF A04

This report describes the effort undertaken to relate aircraft wake history to the local environment. This involved the monitoring of the embedded windfield, monitoring of local meteorological parameters, a high-resolution velocity field analysis in vertical scan planes and measurement of the axial velocity signature. A flashlight pumped 2.09 micron solid state coherent laser radar system was used to detect and track wake vortices. Strong wake vortex signatures were measured for moderate to large aircraft at Denver's Stapleton airport and a large vortex database was compiled. CASI

N95-13212*# Martin Marietta Corp., Moorestown, NJ. Government Electronic Systems.
DOPPLER RADAR DETECTION OF VORTEX HAZARD INDICATORS
Jerald D. Nespor, B. Hudson, R. L. Stegall, and Jerome E. Freedman *In* NASA. Langley Research Center, Airborne Windshear Detection and Warning Systems. Fifth and Final Combined Manufacturers' and Technologists' Conference, Part 2 Jul. 1994 p 651-688 (For primary document see N95-13203 02-03)
Avail: CASI HC A03/MF A04

Wake vortex experiments were conducted at White Sands Missile Range, NM using the AN/MPS-39 Multiple Object Tracking Radar (MOTR). The purpose of these experiments was twofold. The first objective was to verify that radar returns from wake vortex are observed for some time after the passage of an aircraft. The second objective was to verify that other vortex hazard indicators such as ambient wind speed and direction could also be detected. The present study addresses the Doppler characteristics of wake vortex and clear air returns based upon measurements employing MOTR, a very sensitive C-Band phased array radar. In this regard, the experiment was conducted so that the spectral characteristics could be determined on a dwell to-dwell basis. Results are presented from measurements of the backscattered power (equivalent structure constant), radial velocity and spectral width when the aircraft flies transverse and axial to the radar beam. The statistics of the backscattered power and spectral width for each case are given. In addition, the scan strategy, experimental test procedure and radar parameters are presented. Author

N95-13213*# Lightwave Atmospherics, Inc., Marblehead, MA.
REMOTE SENSING OF TURBULENCE IN THE CLEAR ATMOSPHERE WITH 2-MICRON LIDARS **c36**
Robert J. Martinson and John H. Flint *In* NASA. Langley Research Center, Airborne Windshear Detection and Warning Systems. Fifth and Final Combined Manufacturers' and Technologists' Conference, Part 2 Jul. 1994 p 689-705 (For primary document see N95-13203 02-03)
(Contract DAAH01-92-C-R097)
Avail: CASI HC A03/MF A04

The development of an eye-safe, airborne LIDAR that exploits the decorrelation of the heterodyne signal to detect clear air turbulence is reported. A one watt average power transmitter is capable of detecting clear air turbulence to over 20 km is subvisual cirrus (an environment highly correlated with instabilities of stratified shear layers). In the absence of subvisual cirrus, a 4 km detection range is maintained. A table depicting the warning time in seconds with respect to the aircraft speed and instrument range (in kilometers) is presented. CASI

N95-13214*# Georgia Tech Research Inst., Atlanta, GA.
EVALUATION OF CANDIDATE MILLIMETER WAVE SENSORS FOR SYNTHETIC VISION **c54**
Neal T. Alexander, Brian H. Hudson, and Jim D. Echard *In* NASA. Langley Research Center, Airborne Windshear Detection and Warning Systems. Fifth and Final Combined Manufacturers' and Technologists' Conference, Part 2 Jul. 1994 p 747-764 (For primary document see N95-13203 02-03)
Avail: CASI HC A03/MF A04

The goal of the Synthetic Vision Technology Demonstration Program was to demonstrate and document the capabilities of current technologies to achieve safe aircraft landing, take off, and ground operation in very low visibility conditions. Two of the major thrusts of the program were (1) sensor evaluation in measured weather conditions on a tower overlooking an unused airfield and (2) flight testing of sensor and pilot performance via a prototype system. The presentation first briefly addresses the overall technology thrusts and goals of the program and provides a summary of MMW sensor tower-test and flight-test data collection efforts. Data analysis and calibration procedures for both the tower tests and flight tests are presented. The remainder of the presentation addresses the MMW sensor flight-test evaluation results, including the processing approach for determination of various performance metrics (e.g., contrast, sharpness, and variability). The variation of the very important contrast metric in adverse weather conditions is described. Design trade-off considerations for Synthetic Vision MMW sensors are presented. Author (revised)

N95-13215*# TRW, Inc., Redondo Beach, CA. Applications Technology Div.
PASSIVE MMW CAMERA FOR LOW VISIBILITY LANDINGS **c35**
Merit Shoucri *In* NASA. Langley Research Center, Airborne Windshear Detection and Warning Systems. Fifth and Final Combined Manufacturers' and Technologists' Conference, Part 2 Jul. 1994 p 765-785 (For primary document see N95-13203 02-03)
Avail: CASI HC A03/MF A04

A passive, millimeter wave imaging sensor for aircraft landing in low or poor visibility conditions is described. The sensor can be incorporated in a camera for future enhanced/synthetic vision systems. Contrast is provided by differences in material reflectivities, temperature, and sky illumination of the scene being imaged. Photographic images of the system's fog penetration capabilities are presented. A combinatorial geometry technique is used to construct the scene geometries. This technique uses eight basic geometric shapes which are used as building blocks for 3-D complex-shaped objects. The building blocks are then combined via union, intersection and exclusion operations to form 3-D scene objects and the combinatorial geometry package determines ray intercepts with scene objects, providing the specific surfaces and propagation distance for the scene. CASI

N95-13247 National Inst. of Standards and Technology, Gaithersburg, MD. BFRL.
EVALUATION OF ALTERNATIVE IN-FLIGHT FIRE SUPPRESSANTS FOR FULL-SCALE TESTING IN SIMULATED AIRCRAFT ENGINE NACELLES AND DRY BAYS
W. L. Grosshandler, R. G. Gann, and W. M. Pitts Apr. 1994 857 p Sponsored by Dept. of AF; Naval Air Systems Command; Army Aviation and Troop Command; and FAA
(PB94-203403; NIST/SP-861) Avail: Issuing Activity (National Technical Information Service (NTIS))

Civilian and military aircraft suppliers and operators are searching for alternatives to the discontinued chemical Halon 1301 (CF_3Br) for protecting aircraft against in-flight fires. This study identifies the best two or three candidates from among a list of twelve fluorocarbons (FC's), hydrofluorocarbons (HFC's), and hydrochlorofluorocarbons (HCFC's) for full-scale testing in the engine nacelle and dry bay simulators at Wright-Patterson Air Force Base. An assessment of the potential for a powder, sodium bicarbonate ($NaHCO_3$), and other realistic gaseous candidates was also requested. The primary recommendations for the dry bay application were FC-218 and HFC-125; partial testing of CF_3I was also recommended. Details of all aspects of the research program and the rationale for making these recommendations are provided in this special publication. NTIS

04 AIRCRAFT COMMUNICATIONS AND NAVIGATION

Includes digital and voice communication with aircraft; air navigation systems (satellite and ground based); and air traffic control.

For related information see also *17 Space Communications, Spacecraft Communications, Command and Tracking* and *Communications and Radar.*

N95-12177# New South Wales Univ., Kensington (Australia). Dept. of Engineering.

PRINCIPLES OF GPS ONE-WAY DATA PROCESSING FOR HIGH PRECISION POSITIONING APPLICATIONS: ALGORITHMS AND SOFTWARE ISSUES Ph.D. Thesis Abstract Only

Pen-Shan Hung 14 Oct. 1993 1 p

Avail: Issuing Activity

The aim of this study was to investigate the—undifferenced GPS data pre-processing and analysis algorithms required for high precision positioning applications. An important component of the project therefore was to extend and test the algorithms in the fourth generation of the UNSW GPS software package. There are several advantages in using the undifferenced data processing mode and these were described. The GPS measurement biases and errors have been summarized. One of the significant biases is that due to the ionosphere. The ionosphere affects the propagation of microwaves that pass through it. For example, during periods of high sunspot activity (unstable ionosphere), irregular changes in carrier phase measurements may reach a level of 1 cycle or more per minute. This affects not only cycle slip detection and repair but also the ambiguity resolution problem. For GPS undifferenced data processing, a simple piecewise polynomial model for the elimination of ionospheric path delay variation relative to the initial epoch is suggested which makes use of L1 and L2 observations. With the above model, a new form of the L5 (or 'wide-lane') observable is developed, which can be regarded as a pseudo-ionosphere-free observation. It has the advantage that the integer nature of the ambiguities is preserved. A three-step algorithm for the detection and repair of cycle slips for the undifferenced observables is also described, and implemented within the software. In the main processing module, the algorithm to eliminate nuisance parameters from observation equations, rather than normal equations, for GPS data processing is implemented. The software is tested on a dataset collected in 1990 during the Bass Strait GPS Tide Gauge Survey campaign. Several combinations of dual- and single-frequency phase data were tried, in combination with different solution strategies for parameters such as the tropospheric zenith delay. Estimated baseline lengths using the ionosphere corrected L1 data showed results consistent with using the L3 (ionosphere elimination) observable at the better then 0.2 ppm level for a network of 400 x 500 km in extent. Other features of the software were also tested, such as the determination of the zenith tropospheric bias and the satellite orbital elements. It has been demonstrated that it is feasible to use undifferenced GPS data for the determination of baselines and satellite orbits. Further testing is required to check that the quality of results obtained from using such algorithms are as good as those obtained using data differencing software, or whether there are other special advantages to using the undifferenced data mode of processing that would lead to its being used more frequently for GPS geodesy applications. Author

N95-12230# New South Wales Univ., Kensington (Australia). School of Engineering.

EFFICIENT AND EFFECTIVE HANDLING OF CYCLE SLIPS IN GLOBAL POSITIONING SYSTEM DATA Ph.D. Thesis Abstract Only

Ching-Mei Chu 1994 1 p

Avail: Issuing Activity

A prerequisite for high precision GPS-based geodesy is the reliable detection and correction of cycle slips in the carrier phase data. Without reliable data editing, further processing of GPS data is compromised. The detection and repair of cycle slips can, however, be a labor intensive and time consuming procedure, particularly if the data is noisy, if there are gaps in the data series and there are many slips on more than one satellite at the same time. In this research, the possibility of performing efficient and effective cycle slip editing of GPS carrier phase signal was studied and a polynomial solution technique was developed. The technique was designed to operate in either a single-station mode or multi-station mode, but was used in the single-station model for most investigations. There are a number of advantages in such a procedure, including: (1) it can be used on site, shortly after data has been collected; and (2) it permits cycle slips to be detected and repaired in the raw one-way data, a significant boon if phase data is to be processed in the undifferenced (as opposed to the double-differenced) mode. Today a number of software packages are available to process GPS observations for high precision, scientific applications. They all provide a number of a different options for data processing. Solutions can therefore differ due to a number of factors, such as the algorithms themselves, the frequencies or frequency combinations used, cutoff angle selected, etc. Often there is no standardised procedure, just precedent, the analyst has a variety of data processing strategies from which to choose reasonable, appropriate, and justifiable alternatives, to obtain the 'best' solutions. Do different solutions and software agree with each other? And how accurate are the results? We used GAMIT, a well established GPS program, to verify the technique of cycle slip editing. The technique has been shown to be capable of editing cycle slips reliably and quickly. Solutions using two processing methods (GAMIT and our own scientific software) were compared. Comparisons were also made between solutions in which cycle slip detection and repair were carried out within two programs. Significant differences were detected between them using two 'clean' data sets. The impact of undetected cycle slips on a GPS network solution has also been studied in this research. The simulation of cycle slip was done to study the effect of leaving undetected cycle slips. The results confirmed that, for the highest precision, all cycle slips must be removed from the data thoroughly before a solution is carried out. Author (revised)

N95-12582# Helsinki Univ. of Technology, Espoo (Finland). Automation Technology Lab.

USING LANDMARKS FOR THE VEHICLE LOCATION MEASUREMENT

H. Yang Feb. 1994 23 p

(PB94-184512; ISBN-951-22-1994-8) Avail: CASI HC A03/MF A01

This paper mainly deals with the position of the ground vehicle as well as finding its heading direction by using landmarks. First, from the geometric theorems, a set of reasoning is given in detail for the formulations that were introduced. Some limited conditions are attached to these formulations for calculating without mistakes in some cases. Some formulations are simplified, and some equations were developed for the special cases. Moreover, on the basis of above, a new method for calculating the position of the vehicle is proposed. In this method, instead of three marks, one angle and only two marks are required for the calculations. The advantage of this method is to use one hardware that measures one angle to reduce 1/3 amount of the landmark. The analyses and experiences show that the new method has advantages in the position calculating accuracy requirement as well as the processing speed. In this paper, an algorithm for recognizing the circle-landmarks is also proposed. Then some errors are analyzed, which give some suggestions to fix camera and landmarks. NTIS

05 AIRCRAFT DESIGN, TESTING AND PERFORMANCE

Includes aircraft simulation technology.

For related information see also *18 Spacecraft Design, Testing and Performance* and *39 Structural Mechanics.* For land transportation vehicles see *85 Urban Technology and Transportation.*

N95-11699*# Arizona State Univ., Tempe, AZ. Dept. of Mechanical and Aerospace Engineering.

THE POTENTIAL OF GENETIC ALGORITHMS FOR CONCEPTUAL DESIGN OF ROTOR SYSTEMS Semiannual Report

William A. Crossley, Valana L. Wells, and David H. Laananen 1993 29 p

(Grant NAG2-882)

(NASA-CR-196813; NAS 1.26:196813) Avail: CASI HC A03/MF A01

The capabilities of genetic algorithms as a non-calculus based, global search method make them potentially useful in the conceptual design of rotor systems. Coupling reasonably simple analysis tools to the genetic algorithm was accomplished, and the resulting program was used to generate designs for rotor systems to match requirements similar to those of both

an existing helicopter and a proposed helicopter design. This provides a comparison with the existing design and also provides insight into the potential of genetic algorithms in design of new rotors. Author

N95-11774 ESDU International Ltd., London (England).
SYMMETRIC STEADY MANOEUVRE LOADS ON RIGID AIRCRAFT OF CLASSICAL CONFIGURATION AT SUBSONIC SPEEDS
Apr. 1994 27 p
(ISSN 0141-3988)
(ESDU-94009; ISBN-0-85679-896-7) Avail: ESDU

ESDU 94009 examines the process of determining the structural strength requirements for an aircraft in steady maneuvering flight. To evaluate the shear force, bending moment and torque across the wing span and along the fuselage requires a knowledge of the mass distribution and of the loading distribution of each surface. The loading depends on the maneuver loads appropriate to the use of the aircraft. To provide the loading information, the aircraft is here treated as a wing-fuselage combination with the tail applying a point load acting at the aerodynamic center of the tailplane. The tail assembly is treated as a point mass. The loading on the wing-body combination is considered as wing lift and pitching movement distributions along the span, taking account of camber, twist, incidence and pitch rate, the carry-over lift on the fuselage and the lift distributions on the fuselage and on the engine nacelles. The spanwise distribution of the chordwise position of the wing-alone aerodynamic center is required together with the centers of lift of the carry-over lift and of the nacelle loading. ESDU 94009 develops the equations for these loading distributions in terms of the component contributions for level flight, a steady pitch-up, and a steady turn. It also discusses sources for the aerodynamic data, in particular the use of ESDU data from the Aerodynamics and Transonic Aerodynamics Sub-series. Author

N95-11793 ESDU International Ltd., London (England).
APPLICATION OF MULTIVARIATE OPTIMISATION TECHNIQUES TO DETERMINATION OF OPTIMUM FLIGHT PATH TRAJECTORIES
May 1994 26 p
(ISSN 0141-4054)
(ESDU-94012; ISBN-0-85679-899-1) Avail: ESDU

ESDU 94012 explains in broad terms the method of optimization used by such techniques and emphasizes that numerical optimization will not locate an absolute minimum but requires the user to set a tolerance on the result, the choice of which is critical. The value of seeking an optimum from two diverse starting points is suggested, and will usually allow any suboptimum located to be eliminated and will enable an assessment to be made of the choice of tolerance. Using results obtained in the work of ESDU 93021 optimizing a complete sortie, the information to be gleaned from exploration around the calculated optimum is illustrated. Also, it is noted that nonoptimum results can be obtained and it is important to assess the trends in the results as an aid to eliminating them, again illustrated with data obtained for ESDU 93021. To use the optimizer, subroutines have to be written, in the case of ESDU 93021 to calculate the segments of the flight profile. Because the optimizer needs gradients to the variables and constraints, the subroutines may have to work in unrealistic areas and any optimal results obtained in such regions must be trapped and discounted. The treatment of finite steps in a variable is considered (in this case cruise height as constrained by air traffic rules). The particular features of the optimizer RQPMIN, developed at the then Royal Aerospace Establishment, are discussed, and the format of its input and output files illustrated. ESDU

N95-11794 ESDU International Ltd., London (England).
EXAMPLES OF FLIGHT PATH OPTIMISATION USING A MULTIVARIATE GRADIENT-SEARCH METHOD. ADDENDUM A: VARIATION OF OPTIMUM FLIGHT PROFILE PARAMETERS WITH RANGE
Jun. 1994 6 p
(ISSN 0141-4054)
(ESDU-94016-Add-A; ISBN-0-85679-903-3) Avail: ESDU

ESDU 94016 gives a further study to that in ESDU 93021 of optimizing a complete sortie. The aircraft is the same as used in ESDU 93021, and fuel required (and hence ramp mass) is minimized for a series of ranges from 150 to 3900 n. miles under the same constraints and assumptions on fuel reserves as were previously used. The profile parameters to vary are climb and descent speed, cruise Mach number, and height at start of cruise, and a cruise-climb was used because those profile parameters showed greater sensitivity than in the more practical level or stepped cruise and so illustrated the effects better. Sketches show the effect of range on the profile flown; the height at start and end of cruise; the Mach number in climb, cruise, and descent; and the ramp mass. The flight profile parameters vary little for ranges exceeding 1000 n. miles when for each range the profile effectively joins at the top of climb the optimum for 3900 n. mile range; below 1000 n. mile range significant changes occur down to 150 n. mile range to retain a cruise segment starting at progressively lower heights. Below 150 n. mile the profile is a simple climb and descent. ESDU

N95-11952* McDonnell-Douglas Aerospace, Saint Louis, MO.
IMPACT OF AGILITY REQUIREMENTS ON CONFIGURATION SYNTHESIS
Patrick J. ONeil, Gregory Nyberg, Robin deTurk, Daniel W. Seal, and Christian E. Grethlein Hampton, VA NASA Sep. 1994 367 p
(Contract NAS1-18763; RTOP 505-68-70-09)
(NASA-CR-4627; NAS 1.26:4627) Avail: Issuing Activity

A configuration design study was performed by McDonnell Douglas Aerospace (MDA) for the NASA Langley Research Center to determine the impact of agility-based requirements on the design of multirole aircraft. Design guidelines and methodologies were developed which can guide the aircraft designer in the selection of aerodynamics, controls, avionics, propulsion, and materials technologies for a given level of both agility and observables requirements. A matrix of nine aircraft was generated to investigate the quantitative effects of agility-based requirements and observables requirements on vehicle design and sizing. This matrix of aircraft indicates the relatively large TOGW penalty associated with high levels of agility when applied to a vehicle with significant observables requirements. However, the matrix also suggests that optimal integration of certain advanced technologies, such as in tailless fighter design synthesis, might have significant advantages over designs incorporating more conventional technologies. Finally, the study identifies the types of technologies required to achieve high agility under different observables requirements and allows some assessment of the current risks associated with these technologies and how future research might be focused toward reducing such risks. Author

N95-12225*# National Aeronautics and Space Administration. Ames Research Center, Moffett Field, CA.
FLIGHT INVESTIGATION OF THE USE OF A NOSE GEAR JUMP STRUT TO REDUCE TAKEOFF GROUND ROLL DISTANCE OF STOL AIRCRAFT
Joseph C. Eppel, Gordon Hardy, and James L. Martin Sep. 1994 44 p
(RTOP 505-59-37)
(NASA-TM-108819; A-94076; NAS 1.15:108819) Avail: CASI HC A03/MF A01

A series of flight tests was conducted to evaluate the reduction of takeoff ground roll distance obtainable from a rapid extension of the nose gear strut. The NASA Quiet Short-haul Research Aircraft (QSRA) used for this investigation is a transport-size short takeoff and landing (STOL) research vehicle with a slightly swept wing that employs the upper surface blowing (USB) concept to attain the high lift levels required for its low speed, short-field performance. Minor modifications to the conventional nose gear assembly and the addition of a high pressure pneumatic system and a control system provided the extendible nose gear, or 'jump strut,' capability. The limited flight test program explored the effects of thrust-to-weight ratio, storage tank initial pressure, and control valve open time duration on the ground roll distance. The data show that the predicted reduction of takeoff ground roll on the order of 10 percent was achieved with the use of the jump strut. Takeoff performance with the jump strut was also found to be essentially independent of the pneumatic supply pressure and was only slightly affected by control valve open time within the range of the parameters examined. Author (revised)

N95-12294*# Michigan Univ., Ann Arbor, MI. Dept. of Aerospace Engineering.
CONCEPTUAL DESIGN OF THE AE481 DEMON REMOTELY PILOTED VEHICLE (RPV)
Chris Hailes, Jill Kolver, Julie Nestor, Mike Patterson, Jan Selow, Pradip

Sagdeo, and Kenneth Katz 1994 44 p
(Contract NASw-4435)
(NASA-CR-197164; NAS 1.26:197164) Avail: CASI HC A03/MF A01

This project report presents a conceptual design for a high speed remotely piloted vehicle (RPV). The AE481 Demon RPV is capable of performing video reconnaissance missions and electronic jamming over hostile territory. The RPV cruises at a speed of Mach 0.8 and an altitude of 300 feet above the ground throughout its mission. It incorporates a rocket assisted takeoff and a parachute-airbag landing. Missions are preprogrammed, but in-flight changes are possible. The Demon is the answer to a military need for a high speed, low altitude RPV. The design methods, onboard systems, and avionics payload are discussed in this conceptual design report along with economic viability. Author

N95-12305*# Embry-Riddle Aeronautical Univ., Daytona Beach, FL.
VIPER CABIN-FUSELAGE STRUCTURAL DESIGN CONCEPT WITH ENGINE INSTALLATION AND WING STRUCTURAL DESIGN
B. Marchesseault, D. Carr, T. McCorkle, C. Stevens, and D. Turner 6 Dec. 1993 77 p
(Contract NASw-4435)
(NASA-CR-197162; NAS 1.26:197162) Avail: CASI HC A05/MF A01

This report describes the process and considerations in designing the cabin, nose, drive shaft, and wing assemblies for the 'Viper' concept aircraft. Interfaces of these assemblies, as well as interfaces with the sections of the aircraft aft of the cabin, are also discussed. The results of the design process are included. The goal of this project is to provide a structural design which complies with FAR 23 requirements regarding occupant safety, emergency landing loads, and maneuvering loads. The design must also address the interfaces of the various systems in the cabin, nose, and wing, including the drive shaft, venting, vacuum, electrical, fuel, and control systems. Interfaces between the cabin assembly and the wing carrythrough and empennage assemblies were required, as well. In the design of the wing assemblies, consistency with the existing cabin design was required. The major areas considered in this report are materials and construction, loading, maintenance, environmental considerations, wing assembly fatigue, and weight. The first three areas are developed separately for the nose, cabin, drive shaft, and wing assemblies, while the last three are discussed for the entire design. For each assembly, loading calculations were performed to determine the proper sizing of major load carrying components. Table 1.0 lists the resulting margins of safety for these key components, along with the types of the loads involved, and the page number upon which they are discussed. Author (revised)

N95-12363*# Purdue Univ., West Lafayette, IN. School of Aeronautics and Astronautics.
DESIGN OF A HIGH CAPACITY LONG RANGE CARGO AIRCRAFT Final Report
Terrence A. Weisshaar 30 Jul. 1994 10 p
(Contract NASw-4435)
(NASA-CR-197176; NAS 1.26:197176) Avail: CASI HC A02/MF A01

This report examines the design of a long range cargo transport to attempt to reduce ton-mile shipping costs and to stimulate the air cargo market. This design effort involves the usual issues but must also include consideration of: airport terminal facilities; cargo loading and unloading; and defeating the 'square-cube' law to design large structures. This report reviews the long range transport design problem and several solutions developed by senior student design teams at Purdue University. The results show that it will be difficult to build large transports unless the infrastructure is changed and unless the basic form of the airplane changes so that aerodynamic and structural efficiencies are employed. Author

N95-12410 Naval Postgraduate School, Monterey, CA.
FLIGHT DYNAMICS OF AN UNMANNED AERIAL VEHICLE M.S. Thesis
Eric J. Watkiss Mar. 1994 94 p Limited Reproducibility: More than 20% of this document may be affected by microfiche quality
(AD-A282259) Avail: Issuing Activity (Defense Technical Information Center (DTIC))

Moments of inertia were experimentally determined and longitudinal and lateral/directional static and dynamic stability and control derivatives were estimated for a fixed wing Unmanned Air Vehicle (UAV). Dynamic responses to various inputs were predicted based upon the estimated derivatives. A divergent spiral mode was revealed, but no particularly hazardous dynamics were predicted. The aircraft was then instrumented with an airspeed indicator, which when combined with the ability to determine elevator deflection through trim setting on the flight control transmitter, allowed for the determination of the aircraft's neutral point through flight test. The neutral point determined experimentally corresponded well to the theoretical neutral point. However, further flight testing with improved instrumentation is planned to raise the confidence level in the neutral point location. Further flight testing will also include dynamic studies in order to refine the estimated stability and control derivatives. DTIC

N95-12530*# Notre Dame Univ., IN. Dept. of Aerospace and Mechanical Engineering.
THE ELITE: A HIGH SPEED, LOW-COST GENERAL AVIATION AIRCRAFT FOR AEROWORLD Final Design Proposal
Amy Rueter, Jonathan Fay, Douglas Staudmeister, Daniel Avis, Tuan Le, and Steven Stem Apr. 1994 144 p Prepared for Universities Space Research Association, Columbia, MD
(Contract NASw-4435)
(NASA-CR-197161; NAS 1.26:197161) Avail: CASI HC A07/MF A02

The Elite is a six passenger, general aviation aircraft targeted at the upper middle class private pilot. The Elite is a low wing, conventional monoplane utilizing rudder, ailerons, and a stabilator. The Elite will create a new class of aircraft in Aeroworld. This class of aircraft will demonstrate a substantial improvement in cruise speed over the current existing commercial fleet of aircraft in Aeroworld. This new class will be capable of servicing all existing airstrips in Aeroworld, including rough and short airways. The drivers of this design were aesthetics, a high cruise speed, and take-off distance. Author (revised)

N95-12609*# Notre Dame Univ., IN. Dept. of Aerospace and Mechanical Engineering.
ICARUS REWAXED: A HIGH SPEED, LOW-COST GENERAL AVIATION AIRCRAFT FOR AEROWORLD
Bryan Farrens, Macy Hueckel, Dan Fulkerson, Matt Barents, Brian Capozzi, and Keri Ramsey Apr. 1994 159 p Prepared for Universities Space Research Association, Columbia, MD
(Contract NASw-4435)
(NASA-CR-197155; NAS 1.26:197155) Avail: CASI HC A08/MF A02

Icarus Rewaxed is a single engine, six passenger, general aviation airplane. With a cruise velocity of 72 ft/s, the Icarus can compete with the performance of any other airplane in its class with an eye on economics and safety. It has a very competitive initial price ($3498.00) and cost per flight ($6.36-8.40). Icarus can serve all airports in Aeroworld with a takeoff distance of 25.4 feet and maximum range of 38,000 feet. It is capable of taking off from an unprepared field with a grass depth of 3 inches. Icarus Rewaxed fills the market need for a high-speed, low cost aircraft. It provides customers with a general aviation craft that can compete in the existing performance market with the added security of an advanced structure. With the use of advanced materials, the maneuvering capability of the Icarus is increased, as it can withstand greater load factors than previous aircraft. Author (revised)

N95-12626*# Kansas Univ., Lawrence, KS. Graduate Design Class.
GEMINI: A LONG-RANGE CARGO TRANSPORT
10 May 1994 151 p Prepared for Universities Space Research Association, Houston, TX
(Contract NASw-4435)
(NASA-CR-197149; NAS 1.26:197149) Avail: CASI HC A08/MF A02

The proposed Gemini, a long-range cargo transport, is designed as a high capacity, dedicated cargo transporter of 8'x8'x20' inter-modal containers, and long-range design. These requirements will result in a design that is larger than any existing aircraft. Due to the size, a conventional configuration would result in an aircraft unable to operate economically at existing airports. It is necessary to design for a minimum possible empty weight, wingspan, and landing gear track. After considering both a single fuselage biplane and a double fuselage biplane configuration, the design team choose the double fuselage biplane configuration. Both of these configuration choices result in a reduced wing root bending moment and subsequently in substantial savings in the wing weight. An overall decrease in the weight of the airplane, its systems, and fuel will be a direct result of the wing weight savings. Author (revised)

N95-12628*# California Polytechnic State Univ., San Luis Obispo, CA.
THE FC-1D: THE PROFITABLE ALTERNATIVE FLYING CIRCUS COMMERCIAL AVIATION GROUP
Victor J. Meza, Jaime Alvarez, Brook Harrington, Michael A. Lujan, David Mitlyng, Andy Saroughian, Alex Silva, and Tim Teale 6 Jun. 1994 110 p Prepared for Universities Space Research Association, Columbia, MD
(Contract NASw-4435)
(NASA-CR-197152; NAS 1.26:197152) Avail: CASI HC A06/MF A02

The FC-1D was designed as an advanced solution for a low cost commercial transport meeting or exceeding all of the 1993/1994 AIAA/Lockheed request for proposal requirements. The driving philosophy behind the design of the FC-1D was the reduction of airline direct operating costs. Every effort was made during the design process to have the customer in mind. The Flying Circus Commercial Aviation Group targeted reductions in drag, fuel consumption, manufacturing costs, and maintenance costs. Flying Circus emphasized cost reduction throughout the entire design program. Drag reduction was achieved by implementation of the aft nacelle wing configuration to reduce cruise drag and increase cruise speeds. To reduce induced drag, rather than increasing the wing span of the FC-1D, spiroids were included in the efficient wing design. Profile and friction drag are reduced by using riblets in place of paint around the fuselage and empennage of the FC-1D. Choosing a single aisle configuration enabled the Flying Circus to optimize the fuselage diameter. Thus, reducing fuselage drag while gaining high structural efficiency. To further reduce fuel consumption a weight reduction program was conducted through the use of composite materials. An additional quality of the FC-1D is its design for low cost manufacturing and assembly. As a result of this design attribute, the FC-1D will have fewer parts which reduces weight as well as maintenance and assembly costs. The FC-1D is affordable and effective, the apex of commercial transport design. Author (revised)

N95-12636*# Embry-Riddle Aeronautical Univ., Daytona Beach, FL.
TRITON 2 (1B)
Michelle L. Clark, A. G. Meiss, Jason R. Neher, and Richard H. Rudolph 3 May 1994 94 p Prepared for Universities Space Research Association, Columbia, MD
(Contract NASw-4435)
(NASA-CR-197188; NAS 1.26:197188) Avail: CASI HC A05/MF A01

The goal of this project was to perform a detailed design analysis on a conceptually designed preliminary flight trainer. The Triton 2 (1B) must meet the current regulations in FAR Part 23. The detailed design process included the tasks of sizing load carrying members, pulleys, bolts, rivets, and fuselage skin for the safety cage, empennage, and control systems. In addition to the regulations in FAR Part 23, the detail design had to meet established minimums for environmental operating conditions and material corrosion resistance. Derived from text

N95-12637*# California Polytechnic State Univ., San Luis Obispo, CA.
THE OFP-6M TRANSPORT JET
Kelly Alexander, Brian Heneghan, Joules Holmes, Bret Hughes, Mark Kettering, Jennifer Wells, and Todd Whelan 3 Jun. 1994 120 p Prepared for Universities Space Research Association, Columbia, MD Original contains color illustrations
(Contract NASw-4435)
(NASA-CR-197159; NAS 1.26:197159) Avail: CASI HC A06/MF A02; 1 functional color page

This report presents a preliminary design of a commercial jet transport that meets the criteria of the Request For Proposal presented by the American Institute of Aeronautics and Astronauts (AIAA). The proposal requires an innovative design of a low cost domestic commercial transport that will reduce operating costs for airline companies while still meeting present and future requirements of the Federal Aviation Regulations for this type of aircraft. Specifications for the design include a mixed class, 153 passenger aircraft, traveling a range of 3000 nm. The intent of the project is to identify factors that reduce cost and to design within the limits of these constraints. The project includes techniques or options that incorporate new technologies but do not override practicality, alternative design approaches, and a comparison between the new design and current aircraft in its class. The OFP-6M is an alternative design approach to the conventional commercial transport jet and is geared towards customer satisfaction through efficiency and reliability. The goals of the OFP-6M transport design are to provide original, sensible, and practical solutions by combining essential preliminary design factors with growing technology. The design focus of the OFP-6M reduces costs by simplifying systems where significant weight or maintenance savings can be achieved, and by integrating advanced technology for improved performance. Key aspects of the OFP-6M design are efficient use of materials like composites, and efficient advanced ducted high bypass turbofan engines. The high bypass engines lower fuel consumption and aid in reducing costs and meeting future noise emission restrictions. Composites are used for most structural components, including flooring and wing box. Although composites are an emerging technology and presently, a high maintenance material, they can be cost effective and an alternative to aluminum structures when correct manufacturing and design strategies are applied. Since, composites are lighter and require less manufacturing of complex parts, they can significantly reduce structural weight. Because of the large 17 ft. diameter, sophisticated aerodynamic considerations were implemented to significantly lower the drag. Supercritical airfoils were chosen with simple control surface design which allows for less maintenance and manufacturing costs. The interior configuration accommodates either all passenger, dual and single class flights or complete cargo. Also, a relaxed conventional stability is integrated with a stability augmentation system. As a result of these design implementations, the OFP-6M bottom line direct operating costs, compare favorably with the Boeing 737 and 757, at 3.49 cents per available seat mile and costs are expected to reduce when improved manufacturing and maintenance methods are implemented. Author (revised)

N95-12638*# Notre Dame Univ., IN. Dept. of Aerospace and Mechanical Engineering.
THE BALSA BULLET: A HIGH SPEED, LOW-COST GENERAL AVIATION AIRCRAFT FOR AEROWORLD Final Design Proposal
Kevin Eastland, Sean Greenwood, Dan Kelly, Chuck Leonard, John Rooff, and Jeff Scherock Apr. 1994 172 p Prepared for Universities Space Research Association, Columbia, MD
(Contract NASw-4435)
(NASA-CR-197165; NAS 1.26:197165) Avail: CASI HC A08/MF A02

The Balsa Bullet is a high speed, low cost six passenger general aviation aircraft. It will cruise at a speed of 55 ft/s with a maximum speed of 75 ft/s for distances in excess of 27000 feet. This range and speed combination provide The Balsa Bullet with the capability to service any two existing airports in Aeroworld in an efficient and timely manner. Overall, three major design drivers have been identified by the design team. The first is to provide a low cost airplane to the Aeroworld market. Maintaining the low cost objective will not simply meet the mission objective, but will also make the Bullet an economically viable option for a wide number of consumers. The Balsa Bullet has a total manufacturing cost of $1000 with a price to the consumer of only $2562. The second major driver is high speed performance. Once again this driver exists not only to meet the mission objective given Long Shot Aeronautics but it provides a desirable feature to the consumer, pride in owning the fastest aircraft in Aeroworld. The third design driver identified is the capability to service any runway in Aeroworld necessitating the ability to takeoff within 28 ft, the length of the shortest runways in Aeroworld. These design drivers provide three great reasons for the general public to purchase a Bullet. Derived from text

N95-12639*# Embry-Riddle Aeronautical Univ., Daytona Beach, FL. Dept. of Aerospace Engineering.
CABIN FUSELAGE STRUCTURAL DESIGN WITH ENGINE INSTALLATION AND CONTROL SYSTEM
Tanapaal Balakrishnan, Mike Bishop, Ilker Gumus, Joel Gussy, and Mike Triggs 3 May 1994 71 p Prepared for Universities Space Research Association, Columbia, MD
(Contract NASw-4435)
(NASA-CR-197173; NAS 1.26:197173) Avail: CASI HC A04/MF A01

Design requirements for the cabin, cabin system, flight controls, engine installation, and wing-fuselage interface that provide adequate interior volume for occupant seating, cabin ingress and egress, and safety are presented. The fuselage structure must be sufficient to meet the loadings specified in the appropriate sections of Federal Aviation Regulation Part 23. The critical structure must provide a safe life of 10(exp 6) load cycles and 10,000 operational mission cycles. The cabin seating and controls must provide adjustment to account for various pilot physiques and to aid in maintenance and operation of the aircraft. Seats and doors shall not bind or lockup

under normal operation. Cabin systems such as heating and ventilation, electrical, lighting, intercom, and avionics must be included in the design. The control system will consist of ailerons, elevator, and rudders. The system must provide required deflections with a combination of push rods, bell cranks, pulleys, and linkages. The system will be free from slack and provide smooth operation without binding. Environmental considerations include variations in temperature and atmospheric pressure, protection against sand, dust, rain, humidity, ice, snow, salt/fog atmosphere, wind and gusts, and shock and vibration. The following design goals were set to meet the requirements of the statement of work: safety, performance, manufacturing and cost. To prevent the engine from penetrating the passenger area in the event of a crash was the primary safety concern. Weight and the fuselage aerodynamics were the primary performance concerns. Commonality and ease of manufacturing were major considerations to reduce cost. Derived from text

N95-12643*# California Polytechnic State Univ., San Luis Obispo, CA.
CENTRAL COAST DESIGNS: THE EIGHTBALL EXPRESS. TAKING OFF WITH CONVENTION, CRUISING WITH IMPROVEMENTS AND LANDING WITH ABSOLUTE SUCCESS
Ryan Edwin Davis, Anne Marie Dawson, Paul Hans Fecht, Roman Zyabash Fry, Robert vantRiet, Dominique Dujale Macabantad, Robert Glenn Miller, Gustavo Perez, Jr., and Timothy Michael Weise 1 Jun. 1994 109 p Prepared for Universities Space Research Association, Columbia, MD Original contains color illustrations
(Contract NASw-4435)
(NASA-CR-197181; NAS 1.26:197181) Avail: CASI HC A06/MF A02; 9 functional color pages

The airline industry is very competitive, resulting in most U.S. and many international airlines being unprofitable. Because of this competition the airlines have been engaging in fare wars (which reduce revenue generated by transporting passengers) while inflation has increased. This situation of course is not developing revenue for the airlines. To revive the airlines to profitability, the difference between revenue received and airline operational cost must be improved. To solve these extreme conditions, the Eightball Express was designed with the main philosophy of developing an aircraft with a low direct operating cost and acquisition cost. Central Coast Designs' (CCD) aircraft utilizes primarily aluminum in the structure to minimize manufacturing cost, supercritical airfoil sections to minimize drag, and fuel efficient engines to minimize fuel burn. Furthermore, the aircraft was designed using Total Quality Management and Integrated Product Development to minimize development and manufacturing costs. Using these primary cost reduction techniques, the Eightball Express was designed to meet the Lockheed/AIAA Request for Proposal (RFP) requirements of a low cost, 153 passenger, 3000 nm. range transport. The Eightball Express is able to takeoff on less than a 7000 ft. runway, cruise at Mach 0.82 at an altitude of 36,000 ft. for a range of 3,000 nm., and lands on a 5,000 ft. runway. It is able to perform this mission at a direct operating cost of 3.51 cents/available seat mile in 1992 dollars while the acquisition cost is only $28 million in 1992 dollars. By utilizing and improving on proven technologies, CCD has produced an efficient low cost commercial transport for the future. Author (revised)

N95-12645*# Universities Space Research Association, Columbia, MD.
LCX: PROPOSAL FOR A LOW-COST COMMERCIAL TRANSPORT
Troy Hartman, Maziar Hayatdavoudi, Joel Hettinga, Matt Hooper, and Phong Nguyen 1994 102 p Original contains color illustrations
(Contract NASw-4435)
(NASA-CR-197186; NAS 1.26:197186) Avail: CASI HC A06/MF A02; 8 functional color pages

The LCX has been developed in response to a request for proposal for an aircraft with 153 passenger capacity and a range of 3000 nautical miles. The goals of the LCX are to provide an aircraft which will achieve the stated mission requirements at the lowest cost possible, both for the manufacturer and the operator. Low cost in this request is defined as short and long term profitability. To achieve this objective, modern technologies attributing to low-cost operation without greatly increasing the cost of manufacturing were employed. These technologies include hybrid laminar flow control and the use of developing new manufacturing processes and philosophies. The LCX will provide a competitive alternative to the use of the Airbus A319/320/321 and the Boeing 737 series of aircraft. The LCX has a maximum weight of 150,000 lb. carried by a wing of 1140 ft(exp 2) and an aspect ratio of 10. The selling price of the LCX is 31 million in 1994 US dollars. Author

N95-12689*# Kansas Univ., Lawrence, KS.
A PRELIMINARY DESIGN PROPOSAL FOR A MARITIME PATROL STRIKE AIRCRAFT: MPS-2000 CONDOR
1994 93 p Prepared for Universities Space Research Association, Columbia, MD
(Contract NASw-4435)
(NASA-CR-197182; NAS 1.26:197182) Avail: CASI HC A05/MF A01

The four member graduate design team assembled to submit a proposal for the 1993/1994 RFP at the University of Kansas has designed a four seat, variable swept wing, twin turbofan aircraft with STOL capabilities. The aircraft is named the MPS-2000 Condor and is capable of carrying air-to-surface or air-to-air weapon systems along with attack and surveillance radar and IRF systems. The aircraft has a cruise range of 800 nautical miles, a loiter of 4 hours, and a dash speed of 500 kts. Derived from text

N95-12695*# Worcester Polytechnic Inst., MA.
DESIGN AND CONSTRUCTION OF A REMOTE PILOTED FLYING WING B.S. Thesis
Alfred J. Costa, Fritz Koopman, Craig Soboleski, Thai-Ba Trieu, Jaime Duquette, Scott Krause, David Susko, and Thuyba Trieu 2 May 1994 187 p Prepared for Universities Space Research Association, Columbia, MD
(Contract NASw-4435)
(NASA-CR-197195; NAS 1.26:197195) Avail: CASI HC A09/MF A02

Currently, there is a need for a high-speed, high-lift civilian transport. Although unconventional, a flying wing could fly at speeds in excess of Mach 2 and still retain the capacity of a 747. The design of the flying wing is inherently unstable since it lacks a fuselage and a horizontal tail. The project goal was to design, construct, fly, and test a remote-piloted scale model flying wing. The project was completed as part of the NASA/USRA Advanced Aeronautics Design Program. These unique restrictions required us to implement several fundamental design changes from last year's Elang configuration including wing sweepback and wingtip endplates. Unique features such as a single ducted fan engine, composite structural materials, and an electrostatic stability system were incorporated. The result is the Banshee '94. Our efforts will aid future projects in design and construction techniques so that a viable flying wing can become an integral part of the aviation industry. Author

N95-12700*# Georgia Inst. of Tech., Atlanta, GA. School of Aerospace Engineering.
INTEGRATED DESIGN AND MANUFACTURING FOR THE HIGH SPEED CIVIL TRANSPORT Final Report
Jae Moon Lee, Anurag Gupta, Craig Mueller, Monica Morrisette, John Dec, Jason Brewer, Kevin Donofrio, Hilton Sturisky, Doug Smick, and Meng Lin An et al Jun. 1994 99 p Prepared for Universities Space Research Association, Columbia, MD Original contains color illustrations
(Contract NASw-4435)
(NASA-CR-197183; NAS 1.26:197183) Avail: CASI HC A05/MF A02; 1 functional color page

In June 1992, the School of Aerospace Engineering at Georgia Tech was awarded a three year NASA University Space Research Association (USRA) Advanced Design Program (ADP) grant to address issues associated with the Integrated Design and Manufacturing of High Speed Civil Transport (HSCT) configurations in its graduate Aerospace Systems Design courses. This report provides an overview of the on-going Georgia Tech initiative to address these design/manufacturing issues during the preliminary design phases of an HSCT concept. The new design methodology presented here has been incorporated in the graduate aerospace design curriculum and is based on the concept of Integrated Product and Process Development (IPPD). The selection of the HSCT as a pilot project was motivated by its potential global transportation payoffs; its technological, environmental, and economic challenges; and its impact on U.S. global competitiveness. This pilot project was the focus of each of the five design courses that form the graduate level aerospace systems design curriculum. This year's main objective was the development of a systematic approach to preliminary design and optimization and its implementation to an HSCT wing/propulsion

configuration. The new methodology, based on the Taguchi Parameter Design Optimization Method (PDOM), was established and was used to carry out a parametric study where various feasible alternative configurations were evaluated. The comparison criterion selected for this evaluation was the economic impact of this aircraft, measured in terms of average yield per revenue passenger mile ($/RPM). Author

N95-12702*# Virginia Polytechnic Inst. and State Univ., Blacksburg, VA. Dept. of Aerospace and Ocean Engineering.
DESIGN OF A VEHICLE BASED SYSTEM TO PREVENT OZONE LOSS Final Report
Matthew D. Talbot, Steven C. Eby, Glen J. Ireland, Michael C. McWithey, Mark S. Schneider, Daniel L. Youngblood, Matt Johnson, and Chris Taylor 1 Jun. 1994 124 p Prepared for Universities Space Research Association, Columbia, MD
(Contract NASw-4435)
(NASA-CR-197199; NAS 1.26:197199) Avail: CASI HC A06/MF A02

This project is designed to be completed over a three year period. Overall project goals are: (1) to understand the processes that contribute to stratospheric ozone loss; (2) to determine the best scheme to prevent ozone loss; and (3) to design a vehicle based system to carry out the prevention scheme. The 1993/1994 design objectives included: (1) to review the results of the 1992/1993 design team, including a reevaluation of the key assumptions used; (2) to develop a matrix of baseline vehicle concepts as candidates for the delivery vehicle; and (3) to develop a selection criteria and perform quantitative trade studies to use in the selection of the specific vehicle concept. Derived from text

N95-12785*# MCAT Inst., San Jose, CA.
DESIGN AND TESTING OF AN OBLIQUE ALL-WING SUPERSONIC TRANSPORT Annual Report
Christopher A. Lee Jul. 1994 5 p
(Contract NCC2-617)
(NASA-CR-196394; NAS 1.26:196394; MCAT-94-09) Avail: CASI HC A01/MF A01

This report describes the preliminary design of an Oblique All-Wing (OAW) supersonic transport and a corresponding wind-tunnel model that was tested in the NASA Ames 9- by 7-Foot supersonic wind tunnel. The main goal was the determination of the cruise performance (lift/drag ratio) of a realistically configured OAW. To achieve an acceptable level of realism, it was necessary to consider many issues of design practicality such as the need for a viable propulsion system, adequate control surfaces, landing gear, provisions for 450 passengers, and fuel to fly 5,000 nautical miles. The aircraft had to be stable, structurally sound, and needed to fit into airports across the world. Support was directed primarily towards integration of the propulsion system, however, there were notable contributions to many aspects of the configuration design, wind tunnel model, and wind tunnel test. Derived from text

N95-12787*# Ohio Aerospace Inst., Brook Park.
OPTIMIZATION OF AEROSPACE STRUCTURES Final Technical Report, 17 Aug. 1990 - 30 Apr. 1993
Theo G. Keith, Jr. and Surya N. Patnaik Aug. 1994 7 p
(Grant NAG3-1203)
(NASA-CR-196763; NAS 1.26:196763) Avail: CASI HC A02/MF A01

Research carried out is grouped under two topics: (1) Design Optimization, and (2) Integrated Force Method of Analysis. Design Optimization Research Topics are singularity alleviation enhances structural optimization methods, computer based design capability extended through substructure synthesis, and optimality criteria provides optimum design for a select class of structural problems. Integrated Force Method of Analysis Research Topics are boundary compatibility formulation improves stress analysis of shell structures. Brief descriptions of the four topics are appended. Author

N95-12831*# Planning Research Corp., Edwards, CA.
STRAIN GAGE SELECTION IN LOADS EQUATIONS USING A GENETIC ALGORITHM
Washington NASA Oct. 1994 21 p
(Contract NAS2-13445)
(NASA-CR-4597; H-1962; NAS 1.26:4597) Avail: CASI HC A03/MF A01

Traditionally, structural loads are measured using strain gages. A loads calibration test must be done before loads can be accurately measured. In one measurement method, a series of point loads is applied to the structure, and loads equations are derived via the least squares curve fitting algorithm using the strain gage responses to the applied point loads. However, many research structures are highly instrumented with strain gages, and the number and selection of gages used in a loads equation can be problematic. This paper presents an improved technique using a genetic algorithm to choose the strain gages used in the loads equations. Also presented are a comparison of the genetic algorithm performance with the current T-value technique and a variant known as the Best Step-down technique. Examples are shown using aerospace vehicle wings of high and low aspect ratio. In addition, a significant limitation in the current methods is revealed. The genetic algorithm arrived at a comparable or superior set of gages with significantly less human effort, and could be applied in instances when the current methods could not. Author

N95-12993*# Universities Space Research Association, Columbia, MD.
CABIN-FUSELAGE-WING STRUCTURAL DESIGN CONCEPT WITH ENGINE INSTALLATION
Scott Ariotti, M. Garner, A. Cepeda, J. Vieira, and D. Bolton 6 Dec. 1993 87 p
(Contract NASw-4435)
(NASA-CR-197172; NAS 1.26:197172) Avail: CASI HC A05/MF A01

The purpose of this project is to provide a fuselage structural assembly and wing structural design that will be able to withstand the given operational parameters and loads provided by Federal Aviation Regulation Part 23 (FAR 23) and the Statement of Work (SOW). The goal is to provide a durable lightweight structure that will transfer the applied loads through the most efficient load path. Areas of producibility and maintainability of the structure will also be addressed. All of the structural members will also meet or exceed the desired loading criteria, along with providing adequate stiffness, reliability, and fatigue life as stated in the SOW. Considerations need to be made for control system routing and cabin heating/ventilation. The goal of the wing structure and carry through structure is also to provide a simple, lightweight structure that will transfer the aerodynamic forces produced by the wing, tailboom, and landing gear. These forces will be channeled through various internal structures sized for the pre-determined loading criteria. Other considerations were to include space for flaps, ailerons, fuel tanks, and electrical and control system routing. The difficulties encountered in the fuselage design include expanding the fuselage cabin to accept a third occupant in a staggered configuration and providing ample volume for their safety. By adding a third person the CG of aircraft will move forward so the engine needs to be moved aft to compensate for the difference in the moment. This required the provisions of a ring frame structure for the new position of the engine mount. The difficulties encountered in the wing structural design include resizing the wing for the increased capacity and weight, and compensating for a large torsion produced by the tail boom by placing a great number of stiffeners inside the boom, which will result in the relocation of the fuel tank. Finally, an adequate carry through structure for the wing and fuselage interface will be designed to effectively transmit loads through the fuselage.
Derived from text

06 AIRCRAFT INSTRUMENTATION

Includes cockpit and cabin display devices; and flight instruments.

For related information see also *19 Spacecraft Instrumentation* and *35 Instrumentation and Photography.*

N95-11913*# Lockheed Engineering and Sciences Co., Houston, TX.
AN AVIONICS SCENARIO AND COMMAND MODEL DESCRIPTION FOR SPACE GENERIC OPEN AVIONICS ARCHITECTURE (SGOAA)
John R. Stovall and Richard B. Wray Houston, TX NASA Jul. 1994 203 p
(Contract NAS9-19100)
(NASA-CR-188330; NAS 1.26:188330; LESC-31195) Avail: CASI HC A10/MF A03

This paper presents a description of a model for a space vehicle operational scenario and the commands for avionics. This model will be used in developing a dynamic architecture simulation model using the

Statemate CASE tool for validation of the Space Generic Open Avionics Architecture (SGOAA). The SGOAA has been proposed as an avionics architecture standard to NASA through its Strategic Avionics Technology Working Group (SATWG) and has been accepted by the Society of Automotive Engineers (SAE) for conversion into an SAE Avionics Standard. This architecture was developed for the Flight Data Systems Division (FDSD) of the NASA Johnson Space Center (JSC) by the Lockheed Engineering and Sciences Company (LESC), Houston, Texas. This SGOAA includes a generic system architecture for the entities in spacecraft avionics, a generic processing external and internal hardware architecture, and a nine class model of interfaces. The SGOAA is both scalable and recursive and can be applied to any hierarchical level of hardware/software processing systems. Derived from text

N95-12591# Wright Lab., Wright-Patterson AFB, OH.
DRAFT STANDARD FOR COLOR ACTIVE MATRIX LIQUID CRYSTAL DISPLAYS (AMLCDs) IN US MILITARY AIRCRAFT. RECOMMENDED BEST PRACTICES Final Report, 1 Apr. 1993 - 1 Jun. 1994
Darrel G. Hopper, William K. Dolezal, Keith Schur, and John W. Liccione Jun. 1994 70 p
(AF Proj. 2003)
(AD-A282950; WL-TR-93-1177) Avail: CASI HC A04/MF A01

This report is written in the format of a military standard as a draft to establish the performance, form, fit, design, and development requirements for a family of color active matrix liquid crystal display (AMLCD) modules to be procured for military airborne cockpit applications. This document provides guidance for the selection, design, and development of AMLCD flat panel displays for use in military aircraft cockpits. Author (DTIC)

N95-13027*# Smith Advanced Technology, Inc., Huntsville, AL.
HLLV AVIONICS REQUIREMENTS STUDY AND ELECTRONIC FILING SYSTEM DATABASE DEVELOPMENT Final Report
30 Jun. 1994 22 p
(Contract NAS8-39215)
(NASA-CR-193993; NAS 1.26:193993) Avail: CASI HC A03/MF A01

This final report provides a summary of achievements and activities performed under Contract NAS8-39215. The contract's objective was to explore a new way of delivering, storing, accessing, and archiving study products and information and to define top level system requirements for Heavy Lift Launch Vehicle (HLLV) avionics that incorporate Vehicle Health Management (VHM). This report includes technical objectives, methods, assumptions, recommendations, sample data, and issues as specified by DPD No. 772, DR-3. The report is organized into two major subsections, one specific to each of the two tasks defined in the Statement of Work: the Index Database Task and the HLLV Avionics Requirements Task. The Index Database Task resulted in the selection and modification of a commercial database software tool to contain the data developed during the HLLV Avionics Requirements Task. All summary information is addressed within each task's section. Author (revised)

07 AIRCRAFT PROPULSION AND POWER

Includes prime propulsion systems and systems components, e.g., gas turbine engines and compressors; and onboard auxilliary power plants for aircraft.

For related information see also *20 Spacecraft Propulsion and Power, 28 Propellants and Fuels,* and *44 Energy Production and Conversion.*

N95-11864*# National Aeronautics and Space Administration. Lewis Research Center, Cleveland, OH.
OBJECT-ORIENTED TECHNOLOGY FOR COMPRESSOR SIMULATION
C. K. Drummond, G. J. Follen, and M. R. Cannon Aug. 1994 23 p Presented at the 30th Joint Propulsion Conference, Indianapolis, IN, 27-29 Jun. 1994; sponsored by AIAA, ASME, SAE, and ASEE
(RTOP 505-68-32)
(NASA-TM-106723; E-9089; NAS 1.15:106723; AIAA Paper 94-3095)
Avail: CASI HC A03/MF A01

An object-oriented basis for interdisciplinary compressor simulation can, in principle, overcome several barriers associated with the traditional structured (procedural) development approach. This paper presents the results of a research effort with the objective to explore the repercussions on design, analysis, and implementation of a compressor model in an object oriented (OO) language, and to examine the ability of the OO system design to accommodate computational fluid dynamics (CFD) code for compressor performance prediction. Three fundamental results are that: (1) the selection of the object oriented language is not the central issue; enhanced (interdisciplinary) analysis capability derives from a broader focus on object-oriented technology; (2) object-oriented designs will produce more effective and reusable computer programs when the technology is applied to issues involving complex system inter-relationships (more so than when addressing the complex physics of an isolated discipline); and (3) the concept of disposable prototypes is effective for exploratory research programs, but this requires organizations to have a commensurate long-term perspective. This work also suggests that interdisciplinary simulation can be effectively accomplished (over several levels of fidelity) with a mixed language treatment (i.e., FORTRAN-C++), reinforcing the notion the OO technology implementation into simulations is a 'journey' in which the syntax can, by design, continuously evolve. Author

N95-11867*# National Aeronautics and Space Administration. Lewis Research Center, Cleveland, OH.
THE DEVELOPMENT OF A HIGHLY RELIABLE POWER MANAGEMENT AND DISTRIBUTION SYSTEM FOR CIVIL TRANSPORT AIRCRAFT
Anthony S. Coleman (NYMA, Inc., Brook Park, OH.) and Irving G. Hansen Aug. 1994 8 p Presented at the 29th Intersociety Energy Conversion Engineering Conference, Monterey, CA, 8-12 Aug. 1994; cosponsored by AIAA, ASME, IEEE, AIChE, ANS, SAE, and ACS
(Contract NAS3-27186; RTOP 538-01-11)
(NASA-TM-106697; E-9058; NAS 1.15:106697; AIAA Paper 94-4107)
Avail: CASI HC A02/MF A01

NASA is pursuing a program in Advanced Subsonic Transport (AST) to develop the technology for a highly reliable Fly-By-Light/Power-By-Wire aircraft. One of the primary objectives of the program is to develop the technology base for confident application of integrated PBW components and systems to transport aircraft to improve operating reliability and efficiency. Technology will be developed so that the present hydraulic and pneumatic systems of the aircraft can be systematically eliminated and replaced by electrical systems. These motor driven actuators would move the aircraft wing surfaces as well as the rudder to provide steering controls for the pilot. Existing aircraft electrical systems are not flight critical and are prone to failure due to Electromagnetic Interference (EMI) (1), ground faults and component failures. In order to successfully implement electromechanical flight control actuation, a Power Management and Distribution (PMAD) System must be designed having a reliability of 1 failure in 10(exp +9) hours, EMI hardening and a fault tolerance architecture to ensure uninterrupted power to all aircraft flight critical systems. The focus of this paper is to analyze, define, and describe technically challenging areas associated with the development of a Power By Wire Aircraft and typical requirements to be established at the box level. The authors will attempt to propose areas of investigation, citing specific military standards and requirements that need to be revised to accommodate the 'More Electric Aircraft Systems'. Author

N95-11890*# National Aeronautics and Space Administration. Lewis Research Center, Cleveland, OH.
STRUCTURE OF A SWIRL-STABILIZED, COMBUSTING SPRAY
Daniel L. Bulzan Aug. 1994 30 p Original contains color illustrations
(RTOP 505-62-12)
(NASA-TM-106724; E-9091; NAS 1.15:106724) Avail: CASI HC A03/MF A01; 1 functional color page

Measurements of the structure of a swirl-stabilized, reacting spray are presented. The configuration consisted of a research air-assist atomizer located in the center surrounded by a coflowing air stream. Both the air assist and coflow streams had swirl imparted to them in the same direction with 45 degree angle swirlers. The fuel and air entered the combustor at ambient temperature and the combustor was operated in an unconfined environment. The gas phase was seeded with aluminum oxide particles in order to obtain velocity measurements. Velocity measurements for the gas phase are reported for both an isothermal, single-phase case without drops and a reacting spray case at axial distances from 2.5 to 350 mm downstream of the nozzle. Both mean and fluctuating values are reported. Heptane fuel was used for all the experiments. Drop size and velocity, and drop

number flux are also reported for five axial distances downstream. Both mean and fluctuating values are reported for the drops. The measurements were performed using a two-component phase/Doppler particle analyzer. Profiles across the entire flowfield where velocities were significant are presented. Mean gas phase temperatures were also measured intrusively using a single pt/pt-13 percent rh thermocouple and are reported at axial distances from 2.5 to 200 mm downstream of the nozzle. Author

N95-11901*# Allison Engine Co., Indianapolis, IN.
INVESTIGATION OF ADVANCED COUNTERROTATION BLADE CONFIGURATION CONCEPTS FOR HIGH SPEED TURBOPROP SYSTEMS. TASK 8: COOLING FLOW/HEAT TRANSFER ANALYSIS Final Report, Feb. 1993 - Jun. 1994
Edward J. Hall, David A. Topp, Nathan J. Heidegger, and Robert A. Delaney Cleveland, OH NASA Sep. 1994 193 p
(Contract NAS3-25270; RTOP 538-03-11)
(NASA-CR-195359; E-9024; NAS 1.26:195359) Avail: CASI HC A09/MF A03

The focus of this task was to validate the ADPAC code for heat transfer calculations. To accomplish this goal, the ADPAC code was modified to allow for a Cartesian coordinate system capability and to add boundary conditions to handle spanwise periodicity and transpiration boundaries. The primary validation case was the film cooled C3X vane. The cooling hole modeling included both a porous region and grid in each discrete hold. Predictions for these models as well as smooth wall compared well with the experimental data. Author

N95-11951*# Allison Engine Co., Indianapolis, IN.
INVESTIGATION OF ADVANCED COUNTERROTATION BLADE CONFIGURATION CONCEPTS FOR HIGH SPEED TURBOPROP SYSTEMS. TASK 8: COOLING FLOW/HEAT TRANSFER ANALYSIS USER'S MANUAL Final Report
Edward J. Hall, David A. Topp, Nathan J. Heidegger, and Robert A. Delaney Cleveland, OH NASA Sep. 1994 362 p
(Contract NAS3-25270; RTOP 538-03-11)
(NASA-CR-195360; E-9025; NAS 1.26:195360) Avail: CASI HC A16/MF A03

The focus of this task was to validate the ADPAC code for heat transfer calculations. To accomplish this goal, the ADPAC code was modified to allow for a Cartesian coordinate system capability and to add boundary conditions to handle spanwise periodicity and transpiration boundaries. This user's manual describes how to use the ADPAC code as developed in Task 5, NAS3-25270, including the modifications made to date in Tasks 7 and 8, NAS3-25270. Author

N95-12860*# National Aeronautics and Space Administration. Langley Research Center, Hampton, VA.
NASA'S HYPERSONIC RESEARCH ENGINE PROJECT: A REVIEW
Earl H. Andrews and Ernest A. Mackley Oct. 1994 57 p
(RTOP 505-70-62-03)
(NASA-TM-107759; NAS 1.15:107759) Avail: CASI HC A04/MF A01

The goals of the NASA Hypersonic Research Engine (HRE) Project, which began in 1964, were to design, develop, and construct a high-performance hypersonic research ramjet/scramjet engine for flight tests of the developed concept over the speed range of Mach 4 to 8. The project was planned to be accomplished in three phases: project definition, research engine development, and flight test using the X-15A-2 research airplane, which was modified to carry hydrogen fuel for the research engine. The project goal of an engine flight test was eliminated when the X-15 program was canceled in 1968. Ground tests of full-scale engine models then became the focus of the project. Two axisymmetric full-scale engine models, having 18-inch-diameter cowls, were fabricated and tested: a structural model and combustion/propulsion model. A brief historical review of the project, with salient features, typical data results, and lessons learned, is presented. An extensive number of documents were generated during the HRE Project and are listed. Author

N95-13289 RAND Corp., Santa Monica, CA.
THE DEVELOPMENT OF THE F100-PW-220 AND F110-GE-100 ENGINES: A CASE STUDY OF RISK ASSESSMENT AND RISK MANAGEMENT
Frank Camm 1993 112 p Limited Reproducibility: More than 20% of this document may be affected by microfiche quality
(AD-A282467; RAND/N-3618-AF) Avail: Issuing Activity (Defense Technical Information Center (DTIC))

The 'Great Engine War' pitted Pratt and Whitney (P&W) and General Electric (GE) against one another to supply engines, the F100-PW-220 and the F110-GE-100, respectively, for the Air Force's new F-15 and F-16 fighters. Known more formally as the Alternate Fighter Engine competition, this acquisition used 'derivative' engines - engines that incorporated small changes in selected parts of existing engines to greatly improve operability, durability, and the operating and support costs of fighter engines. This note examines the exceptionally successful development programs that created these engines and seeks the basis for that success, giving special attention to risk assessment and risk management in the two development programs. This summary briefly reviews the history of the two developments, raises four basic policy issues revealed by our analysis to be important, and then reviews briefly several lessons offered by these developments for the future. Author

08 AIRCRAFT STABILITY AND CONTROL

Includes aircraft handling qualities; piloting; flight controls; and autopilots.

For related information see also *05 Aircraft Design, Testing and Performance.*

N95-11868*# National Aeronautics and Space Administration. Hugh L. Dryden Flight Research Center, Edwards, CA.
EFFECTS OF MASS ON AIRCRAFT SIDEARM CONTROLLER CHARACTERISTICS
Charles A. Wagner Washington Sep. 1994 11 p
(RTOP 505-68-20)
(NASA-TM-104277; H-2014; NAS 1.15:104277) Avail: CASI HC A03/MF A01

When designing a flight simulator, providing a set of low mass variable-characteristic pilot controls can be very difficult. Thus, a strong incentive exists to identify the highest possible mass that will not degrade the validity of a simulation. The NASA Dryden Flight Research Center has conducted a brief flight program to determine the maximum acceptable mass (system inertia) of an aircraft sidearm controller as a function of force gradient. This information is useful for control system design in aircraft as well as development of suitable flight simulator controls. A modified Learjet with a variable-characteristic sidearm controller was used to obtain data. A boundary was defined between mass considered acceptable and mass considered unacceptable to the pilot. This boundary is defined as a function of force gradient over a range of natural frequencies. This investigation is limited to a study of mass-frequency characteristics only. Results of this investigation are presented in this paper. Author

N95-11869*# Lockheed Engineering and Sciences Co., Hampton, VA.
DETERMINING THE ACCURACY OF MAXIMUM LIKELIHOOD PARAMETER ESTIMATES WITH COLORED RESIDUALS
Eugene A. Morelli and Vladislav Klein Sep. 1994 48 p
(Contracts NAS1-19000; NCC1-29; RTOP 505-64-30-01)
(NASA-CR-194893; NAS 1.26:194893) Avail: CASI HC A03/MF A01

An important part of building high fidelity mathematical models based on measured data is calculating the accuracy associated with statistical estimates of the model parameters. Indeed, without some idea of the accuracy of parameter estimates, the estimates themselves have limited value. In this work, an expression based on theoretical analysis was developed to properly compute parameter accuracy measures for maximum likelihood estimates with colored residuals. This result is important because experience from the analysis of measured data reveals that the residuals from maximum likelihood estimation are almost always colored. The calculations involved can be appended to conventional maximum likelihood estimation algorithms. Simulated data runs were used to show that the parameter accuracy measures computed with this technique accurately reflect the quality of the parameter estimates from maximum likelihood estimation without the need for analysis of the output residuals in the frequency domain or heuristically determined multiplication factors. The result is general, although the application studied here is maximum likelihood estimation of aerodynamic model parameters from flight test data. Author

N95-12664*# National Aeronautics and Space Administration. Langley Research Center, Hampton, VA.
FLIGHT TEST OF TAKEOFF PERFORMANCE MONITORING SYSTEM
David B. Middleton, Raghavachari Srivatsan, and Lee H. Person, Jr. May 1994 29 p Original contains color illustrations
(RTOP 505-64-13-04)
(NASA-TP-3403; L-17274; NAS 1.60:3403) Avail: CASI HC A03/MF A01; 8 functional color pages

The Takeoff Performance Monitoring System (TOPMS) is a computer software and hardware graphics system that visually displays current runway position, acceleration performance, engine status, and other situation advisory information to aid pilots in their decision to continue or to abort a takeoff. The system was developed at the Langley Research Center using the fixed-base Transport Systems Research Vehicle (TSRV) simulator. (The TSRV is a highly modified Boeing 737-100 research airplane.) Several versions of the TOPMS displays were evaluated on the TSRV B-737 simulator by more than 40 research, United States Air Force, airline and industry and pilots who rated the system satisfactory and recommended further development and testing. In this study, the TOPMS was flight tested on the TSRV. A total of 55 takeoff and 30 abort situations were investigated at 5 airfields. TOPMS displays were observed on the navigation display screen in the TSRV research flight deck during various nominal and off-nominal situations, including normal takeoffs; reduced-throttle takeoffs; induced-acceleration deficiencies; simulated-engine failures; and several gross-weight, runway-geometry, runway-surface, and ambient conditions. All tests were performed on dry runways. The TOPMS software executed accurately during the flight tests and the displays correctly depicted the various test conditions. Evaluation pilots found the displays easy to monitor and understand. The algorithm provides pretakeoff predictions of the nominal distances that are needed to accelerate the airplane to takeoff speed and to brake it to a stop; these predictions agreed reasonably well with corresponding values measured during several fully executed and aborted takeoffs. The TOPMS is operational and has been retained on the TSRV for general use and demonstration. Author

N95-12763*# National Aeronautics and Space Administration. Lewis Research Center, Cleveland, OH.
PILOTED EVALUATION OF AN INTEGRATED METHODOLOGY FOR PROPULSION AND AIRFRAME CONTROL DESIGN
Michelle M. Bright, Donald L. Simon, Sanjay Garg, Duane L. Mattern, Richard J. Ranaudo, and Dennis P. ODonoghue Sep. 1994 14 p Presented at the Guidance, Navigation and Control Conference, Scottsdale, AZ, 1-3 Aug. 1994; sponsored by AIAA
(Contract NAS3-27186; RTOP 505-62-50)
(NASA-TM-106741; E-9149; NAS 1.15:106741; ARL-TR-519; AIAA Paper 94-3612-CP) Avail: CASI HC A03/MF A01

An integrated methodology for propulsion and airframe control has been developed and evaluated for a Short Take-Off Vertical Landing (STOVL) aircraft using a fixed base flight simulator at NASA Lewis Research Center. For this evaluation the flight simulator is configured for transition flight using a STOVL aircraft model, a full nonlinear turbofan engine model, simulated cockpit and displays, and pilot effectors. The paper provides a brief description of the simulation models, the flight simulation environment, the displays and symbology, the integrated control design, and the piloted tasks used for control design evaluation. In the simulation, the pilots successfully completed typical transition phase tasks such as combined constant deceleration with flight path tracking, and constant acceleration wave-off maneuvers. The pilot comments of the integrated system performance and the display symbology are discussed and analyzed to identify potential areas of improvement. Author

N95-12791*# Maryland Univ., College Park, MD. Dept. of Electrical Engineering.
TECHNIQUES FOR DESIGNING ROTORCRAFT CONTROL SYSTEMS Final Report, 1 Apr. 1992 - 31 Aug. 1994
Gil Yudilevitch and William S. Levine 1994 121 p
(Grant NAG2-794)
(NASA-CR-196192; NAS 1.26:196192) Avail: CASI HC A06/MF A02

Over the last two and a half years we have been demonstrating a new methodology for the design of rotorcraft flight control systems (FCS) to meet handling qualities requirements. This method is based on multicriterion optimization as implemented in the optimization package CONSOL-OPTCAD (C-O). This package has been developed at the Institute for Systems Research (ISR) at the University of Maryland at College Park. This design methodology has been applied to the design of a FCS for the UH-60A helicopter in hover having the ADOCS control structure. The controller parameters have been optimized to meet the ADS-33C specifications. Furthermore, using this approach, an optimal (minimum control energy) controller has been obtained and trade-off studies have been performed. Author

09 RESEARCH AND SUPPORT FACILITIES (AIR)

Includes airports, hangars and runways; aircraft repair and overhaul facilities; wind tunnels; shock tubes; and aircraft engine test stands.

For related information see also *14 Ground Support Systems and Facilities (Space).*

N95-11752# Argonne National Lab., IL.
PARALLEL METHODS FOR THE FLIGHT SIMULATION MODEL
Wei-Zhong Xiong and C. Swietlik 1994 11 p Presented at the ACM/IEEE/SCS Workshop on Parallel and Distributed Simulation, Edinburg, Scotland, 6-8 Jul. 1994
(Contract W-31-109-eng-38)
(DE94-013330; ANL/DIS/CP-81788; CONF-940784-1) Avail: CASI HC A03/MF A01

The Advanced Computer Applications Center (ACAC) has been involved in evaluating advanced parallel architecture computers and the applicability of these machines to computer simulation models. The advanced systems investigated include parallel machines with shared memory and distributed architectures consisting of an eight processor Alliant FX/8, a twenty four processor sor Sequent Symmetry, Cray XMP, IBM RISC 6000 model 550, and the Intel Touchstone eight processor Gamma and 512 processor Delta machines. Since parallelizing a truly efficient application program for the parallel machine is a difficult task, the implementation for these machines in a realistic setting has been largely overlooked. The ACAC has developed considerable expertise in optimizing and parallelizing application models on a collection of advanced multiprocessor systems. One of aspect of such an application model is the Flight Simulation Model, which used a set of differential equations to describe the flight characteristics of a launched missile by means of a trajectory. The Flight Simulation Model was written in the FORTRAN language with approximately 29,000 lines of source code. Depending on the number of trajectories, the computation can require several hours to full day of CPU time on DEC/VAX 8650 system. There is an impetus to reduce the execution time and utilize the advanced parallel architecture computing environment available. ACAC researchers developed a parallel method that allows the Flight Simulation Model to be able to run in parallel on the multiprocessor system. For the benchmark data tested, the parallel Flight Simulation Model implemented on the Alliant FX/8 has achieved nearly linear speedup. In this paper, we describe a parallel method for the Flight Simulation Model. We believe the method presented in this paper provides a general concept for the design of parallel applications. This concept, in most cases, can be adapted to many other sequential application programs. DOE

N95-11789 Naval Facilities Engineering Service Center, Port Hueneme, CA.
MOISTURE INDUCED PRESSURES IN CONCRETE AIRFIELD PAVEMENTS
C. A. Kodres May 1994 105 p Limited Reproducibility: More than 20% of this document may be affected by microfiche quality
(AD-A281974; NFESC-TR-2019-ENV) Avail: Issuing Activity (Defense Technical Information Center (DTIC))

The erosion of military concrete airfield pavements by jet exhausts is an expensive problem expected to get worse. Scaling of pavements is being observed beneath the auxiliary power units (APU's) of F/A-18 and B-1 aircraft. The AV-8B Harrier and future vertical takeoff and landing aircraft will generate a concrete environment much more severe than that generated by the low power APU's. In order to develop pavements impervious to this form of erosion, the failure mechanism must be known. One plausible culprit, suggested by the apparent role of heating, is moisture. To examine this hypothesis, a mathematical model was developed to predict pore pressures caused by water vapor and air migrating through the pores of a

heated section of concrete. The foundation of this model is a constitutive relationship developed to characterize the flow of high velocity, compressible, heated gases through concrete. This relationship equates a nondimensional flow parameter with pressure and temperature ratios across the medium. The key premise is that the resistance to flow through a high resistance porous medium can be modeled with friction coefficients analogous to the method used for simpler geometries. Pore pressures predicted using this model show that moisture in the pores of the cement is unlikely to be the primary cause of material failure in airfield pavements heated by the F/A-1 8 APU. Moisture is a probable cause of failure, however, when the cement is being heated by the exhaust of a Harrier during takeoff and landing.

DTIC

N95-11938*# MCAT Inst., San Jose, CA.

SHOCK-TUNNEL COMBUSTOR TESTING FOR HYPERSONIC VEHICLES Final Report

Mark P. Loomis Jul. 1994 33 p

(Contract NCC2-738)

(NASA-CR-196836; NAS 1.26:196836; MCAT-94-07) Avail: CASI HC A03/MF A01

Proposed configurations for the next generation of transatmospheric vehicles will rely on air breathing propulsion systems during all or part of their mission. At flight Mach numbers greater than about 7 these engines will operate in the supersonic combustion ramjet mode (scramjet). Ground testing of these engine concepts above Mach 8 requires high pressure, high enthalpy facilities such as shock tunnels and expansion tubes. These impulse, or short duration facilities have test times on the order of a millisecond, requiring high speed instrumentation and data systems. One such facility ideally suited for scramjet testing is the NASA-Ames 16-Inch shock tunnel, which over the last two years has completed a series of tests for the NASP (National Aero-Space Plane) program at simulated flight Mach numbers ranging from 12-16. The focus of the experimental programs consisted of a series of classified tests involving a near-full scale hydrogen fueled scramjet combustor model in the semi-free jet method of engine testing whereby the compressed forebody flow ahead of the cowl inlet is reproduced (see appendix A). The AIMHYE-1 (Ames Integrated Modular Hypersonic Engine) test entry for the NASP program was completed in April 1993, while AIMHYE-2 was completed in May 1994. The test entries were regarded as successful, resulting in some of the first data of its kind on the performance of a near full scale scramjet engine at Mach 12-16. The data was distributed to NASP team members for use in design system verification and development. Due to the classified nature of the hardware and data, the data reports resulting from this work are classified and have been published as part of the NASP literature. However, an unclassified AIAA paper resulted from the work and has been included as appendix A. It contains an overview of the test program and a description of some of the important issues. Derived from text

N95-12216# Army Engineer Waterways Experiment Station, Vicksburg, MS. Geotechnical Lab.

MARGINAL AGGREGATES IN FLEXIBLE PAVEMENTS: BACKGROUND SURVEY AND EXPERIMENTAL PLAN Final Report, Oct. 1990 - Jun. 1993

Randy C. Ahlrich and Raymond S. Rollings Aug. 1994 57 p

(Contract DTFA01-90-Z-02069)

(DOT/FAA/CT-94/58; DOT/FAA/RD-93/34) Avail: CASI HC A04/MF A01

The purpose of this study is to evaluate the utilization of substandard or marginal aggregates in flexible pavement construction of airport pavements. This investigation was undertaken to evaluate the effects of using lower quality aggregates such as rounded uncrushed gravels and sands on the rutting of flexible pavements. The scope of this research study included a review of available literature and existing data (Phase 1), a laboratory evaluation organized to determine the effects of marginal aggregates and potential techniques to upgrade these substandard materials (Phase 2), and a field evaluation involving test sections utilizing the most promising techniques (Phase 3). This report provides a review of existing data and literature concerning aggregate properties and their influence on the performance of base course materials and asphalt concrete mixtures. This report also discusses the experimental plan for this research study and provides a discussion and description of the state-of-the-art laboratory testing equipment that is being used to evaluate the engineering properties of the marginal aggregates. A summary and schedule of the remaining work has been included. Author

N95-13200*# Ohio Univ., Athens. Center for Stirling Technology Research.

OSCILLATING-FLOW REGENERATOR TEST RIG Final Report, 1 Apr. 1991 - 26 Sep. 1994

J. G. Wood and D. R. Gedeon 26 Sep. 1994 34 p

(Grant NAG3-1269)

(NASA-CR-196982; NAS 1.26:196982) Avail: CASI HC A03/MF A01

This report summarizes work performed in setting up and performing tests on a regenerator test rig. An earlier status report presented test results, together with heat transfer correlations, for four regenerator samples (two woven screen samples and two felt metal samples). Lessons learned from this testing led to improvements to the experimental setup, mainly instrumentation as well as to the test procedure. Given funding and time constraints for this project it was decided to complete as much testing as possible while the rig was set up and operational, and to forego final data reduction and analysis until later. Additional testing was performed on several of the previously tested samples as well an on five newly fabricated samples. The following report is a summary of the work performed at OU, with many of the final test results included in raw data form.

Author (revised)

N95-13243 National Aerospace Lab., Amsterdam (Netherlands).

MACH NUMBER CONTROL IN THE HIGH SPEED WIND TUNNEL OF NLR [REGELING VAN HET MACH GETAL IN DE HOGE SNELHEIDS TUNNEL VAN HET NLR]

J. F. T. Bos and P. R. Faasse 1992 24 p In DUTCH

(PB94-201670; NLR-TP-92371-U) Avail: Issuing Activity (National Technical Information Service (NTIS))

The High Speed Wind Tunnel (HST) of the National Aerospace Laboratory NLR is one of the major transonic windtunnels and is used for aerodynamic research on scale models. The measurements require the control of the Mach number. Two kinds of controller tasks can be distinguished: keeping the Mach number constant, and realizing a different Mach number. When keeping the Mach number constant, substantial disturbances can occur due to a changing angle of attack of the scale model. In the past a PID controller was implemented to counteract these disturbances. The PID controller was only valid in a limited working range of the HST. Therefore, the Mach control system was extended with gain-scheduling techniques and a kind of path-planner for realizing different Mach numbers. Simulation results show that the controller structure yields satisfactory results. NTIS

N95-13553*# National Aeronautics and Space Administration. Langley Research Center, Hampton, VA.

SIMULTANEOUS THREE-DIMENSIONAL VELOCITY AND MIXING MEASUREMENTS BY USE OF LASER DOPPLER VELOCIMETRY AND FLUORESCENCE PROBES IN A WATER TUNNEL

Dan H. Neuhart (Lockheed Engineering and Sciences Co., Hampton, VA.), David J. Wing, and Uleses C. Henderson, Jr. Sep. 1994 90 p Original contains color illustrations

(RTOP 505-62-30-01)

(NASA-TP-3454; L-17328; NAS 1.60:3454) Avail: CASI HC A05/MF A01; 2 functional color pages

A water tunnel investigation was conducted to demonstrate the capabilities of a laser-based instrument that can measure velocity and fluorescence intensity simultaneously. Fluorescence intensity of an excited fluorescent dye is directly related to concentration level and is used to indicate the extent of mixing in flow. This instrument is a three-dimensional laser Doppler velocimeter (LDV) in combination with a fluorometer for measuring fluorescence intensity variations. This capability allows simultaneous flow measurements of the three orthogonal velocity components and mixing within the same region. Two different flows which were generated by two models were studied: a generic nonaxisymmetric nozzle propulsion simulation model with an auxiliary internal water source that generated a jet flow and an axisymmetric forebody model with a circular sector strake that generated a vortex flow. The off-body flow fields around these models were investigated in the Langley 16- by 24-Inch Water Tunnel. The experimental results were used to calculate 17 quantities that included mean and fluctuating velocities, Reynolds stresses, mean

and fluctuating dye fluorescence intensities (proportional to concentration), and fluctuating velocity and dye concentration correlations. An uncertainty analysis was performed to establish confidence levels in the experimental results. In general, uncertainties in mean velocities varied between 1 and 7 percent of free-stream velocity; uncertainties in fluctuating velocities varied between 1 and 5 percent of reference values. The results show characteristics that are unique to each type of flow. Author (revised)

N95-11960*# Bentley Engineering, Moffett Field, CA.
ARCHITECTURAL DESIGN OF THE SCIENCE COMPLEX AT ELIZABETH CITY STATE UNIVERSITY
Soheila Jahromi *In* NASA. Ames Research Center, Technical Paper Contest for Women 1992. Space Challenges: Earth and Beyond 1993 p 49-67 (For primary document see N95-11955 02-99)
Avail: CASI HC A03/MF A03

N95-11961*# National Aeronautics and Space Administration. Ames Research Center, Moffett Field, CA.
THE BIOLOGICAL FLIGHT RESEARCH FACILITY
Catherine C. Johnson *In its* Technical Paper Contest for Women 1992. Space Challenges: Earth and Beyond 1993 p 69-80 (For primary document see N95-11955 02-99)
Avail: CASI HC A03/MF A03

N95-11965*# National Aeronautics and Space Administration. Ames Research Center, Moffett Field, CA.
THE RHESUS MEASUREMENT SYSTEM: A NEW INSTRUMENT FOR SPACE RESEARCH
Julie E. Schonfeld and John W. Hines *In its* Technical Paper Contest for Women 1992. Space Challenges: Earth and Beyond 1993 p 129-136 (For primary document see N95-11955 02-99)
Avail: CASI HC A02/MF A03

N95-13593*# National Aeronautics and Space Administration. Lewis Research Center, Cleveland, OH.
HIGH TEMPERATURE SEAL TEST RIG
Harold E. Addy, Jr. *In its* Seals Flow Code Development 1993 Jul. 1994 p 131-132 (For primary document see N95-13583 02-37)
Avail: CASI HC A01/MF A03

N95-13601*# General Motors Corp., Lagrange, IL.
HIGH-SPEED SEAL AND BEARING TEST FACILITY
Jean B. Panos *In* NASA. Lewis Research Center, Seals Flow Code Development 1993 235-238 (SEE N95-13583 02-37) Jul. 1994 (For primary document see N95-13583 02-37)
Avail: CASI HC A01/MF A03

12 ASTRONAUTICS (GENERAL)

For extraterrestrial exploration see *91 Lunar and Planetary Exploration.*

N95-12000 Joint Publications Research Service, Arlington, VA.
JPRS REPORT: SCIENCE AND TECHNOLOGY. CENTRAL EURASIA: SPACE
9 Aug. 1994 40 p Transl. into ENGLISH from various Russian articles (JPRS-USP-94-006) Copyright Avail: Issuing Activity

Translated articles cover the following topics: need for long-duration space missions discussed; discovery and observation of hard transient x-ray source GRS; catalog of space gamma bursts recorded with the Phebus Instrument of the Granat Observatory; observations of transient x-ray pulsar GRS 0834-43 in low state by instruments of Rentgen Observatory aboard Mir-Kvant module in November 1992; hypersonic propulsion flight test program; control of a variable-mass spacecraft in problems involving a hard encounter; dynamics of an orbital station with a long truss; background fluxes of ions as a source of upsets of electronics aboard space vehicles; Chelomey Organization's project for proton-launched 'light space plane'; aerospace studies of the earth in the Ukraine (state of the art and prospects); aerospace studies of earth in Ukraine (status and perspectives); statistical textural analysis of radar images produced by the Almaz satellite; horizontal-exchange processes in the near-surface layer of the Black Sea; analysis of the doppler radar method of measuring a field of mesoscale ocean currents from an orbital vehicle; and use of radar images taken from Almaz-1 for identifying varying-contrast geodynamic systems. CASI

N95-12001 Joint Publications Research Service, Arlington, VA.
JPRS REPORT: SCIENCE AND TECHNOLOGY. CENTRAL EURASIA
9 Aug. 1994 130 p Transl. into ENGLISH from various Russian articles (JPRS-UST-94-017) Copyright Avail: Issuing Activity

Translated articles cover the following topics: boronizing laser treatment of titanium alloys; argon-arc welding-on titanium dowels to inserts for aircraft structures made of composite materials; method of reducing level of thermally stressed state of gas turbine engine blades by selecting optimum thickness distribution of ceramic heat shield coating; certifying modern ceramics for mechanical properties; superplastic ceramic: possibilities for application in modeling pressworking manufacturing processes; monitoring strength of ceramics by acoustic emission; physical and mechanical properties of Al2O3 + ZrO2:Y2O3 composite produced by directional crystallization from melt; influence that microalloying with rare earth elements has on resistance of steels to deformation and fracture under alternating elastic-plastic loading; conceptions of constructing information management networks for distributed objects; concept of a document information system based on an object-oriented subject-area model; underground future of rocket technologies; geoinformation approach to organizing automated information systems for regional-local monitoring of atmospheric pollutants; and possibility of using lidar wind sounding in climatic-ecologic monitoring of limited areas. CASI

N95-12880*# National Academy of Sciences - National Research Council, Washington, DC. Commission on Physical Sciences, Mathematics, and Applications.
[ACTIVITIES OF THE SPACE STUDIES BOARD OF THE NATIONAL RESEARCH COUNCIL] Annual Report
1993 61 p
(Contracts NASw-4627; N00173-93-P-6207; NOAA-50-DGNE-1-00138)
(NASA-CR-195738; NAS 1.26:195738) Avail: CASI HC A04/MF A01

This 1993 annual report of the Space Studies Board of the National Research Council chronicles the activities of the board during a year filled with questioning and change in the country's civil space program. The brief accounts contained herein of the activities of the board and of its committees, together with summaries of two major reports and the complete texts of three letter reports, sketch out major space research issues that faced the nation's space scientists and engineers during the year, including scientific prerequisites for the human exploration of space, improving NASA's technology for space science, the space station and prerequisites for the human exploration program, several issues in the space life sciences, and the Advanced X-ray Astrophysics Facility. Derived from text

N95-13196*# National Aeronautics and Space Administration. Langley Research Center, Hampton, VA.
PLANAR RAYLEIGH SCATTERING AND LASER-INDUCED FLUORESCENCE FOR VISUALIZATION OF A HOT, MACH 2 ANNULAR AIR JET
R. Jeffrey Balla Oct. 1994 17 p
(RTOP 505-70-91-01)
(NASA-TM-4576; L-17374; NAS 1.15:4576) Avail: CASI HC A03/MF A01

Planar Rayleigh scattering (PRS) and planar laser-induced fluorescence (PLIF) were used to investigate the vitiated air component of a coaxial hydrogen/vitiated air nonpremixed turbulent jet flame that is ejected at a Mach number of 2. All experiments were performed with a xenon chloride tunable excimer laser. Planar information for both techniques was obtained using laser sheets 6 cm high, 5 cm wide, and 300 micron thick. In this flow field, the effective Rayleigh cross section of the components in the vitiated air was assumed to be independent of composition. Therefore, the PRS technique produced signals which were proportional to total density. When the flow field was assumed to be at a known and uniform pressure, the PRS signal data for the vitiated air could be converted to temperature information. Also, PLIF images were generated by probing the OH molecule. These images contain striation patterns attributed to small localized instantaneous temperature nonuniformities. The results from the PLIF and PRS techniques were used to show that this flow field contains a nongaseous

component, most likely liquid water that can be reduced by increasing the settling chamber wall temperature. Author

13 ASTRODYNAMICS

Includes powered and free-flight trajectories; and orbital and launching dynamics.

N95-12837*# Colorado Univ., Boulder, CO. Dept. of Aerospace Engineering Sciences.
SATELLITE LASER RANGING AND GRAVITY FIELD MODELING ACCURACY Final Report
George W. Rosborough 1990 72 p
(Grant NAG5-760)
(NASA-CR-196057; NAS 1.26:196057) Avail: CASI HC A04/MF A01

Gravitational field mismodeling procedures errors in the estimated orbital motion of near Earth satellites. This effect is studied using a linear perturbation approach following the analysis of Kaula. The perturbations in the orbital position as defined by either orbital elements or Cartesian components are determined. From these perturbations it is possible to ascertain the expected signal due to gravitational mismodeling that would be present in station-to-satellite laser ranging measurements. This expected signal has been estimated for the case of the Lageos satellite and using the predicted uncertainties of the GEM-T1 and GEM-T2 gravity field models. The results indicate that observable signal still exists in the laser range residuals given the current accuracy of the range measurements and the accuracy of the gravity field models. Author

14 GROUND SUPPORT SYSTEMS AND FACILITIES (SPACE)

Includes launch complexes, research and production facilities; ground support equipment, e.g., mobile transporters; and simulators.

For related information see also *09 Research and Support Facilities (Air).*

N95-12474*# National Academy of Sciences - National Research Council, Washington, DC. Committee on Space Facilities.
SPACE FACILITIES: MEETING FUTURE NEEDS FOR RESEARCH, DEVELOPMENT, AND OPERATIONS
1994 35 p
(Contract NASw-4003)
(NASA-CR-194821; NAS 1.26:194821) Copyright Avail: CASI HC A03/MF A01

The National Facilities Study (NFS) represents an interagency effort to develop a comprehensive and integrated long-term plan for world-class aeronautical and space facilities that meet current and projected needs for commercial and government aerospace research and development and space operations. At the request of NASA and the DOD, the National Research Council's Committee on Space Facilities has reviewed the space related findings of the NFS. The inventory of more than 2800 facilities will be an important resource, especially if it continues to be updated and maintained as the NFS report recommends. The data in the inventory provide the basis for a much better understanding of the resources available in the national facilities infrastructure, as well as extensive information on which to base rational decisions about current and future facilities needs. The working groups have used the inventory data and other information to make a set of recommendations that include estimates of cost savings and steps for implementation. While it is natural that the NFS focused on cost reduction and consolidations, such a study is most useful to future planning if it gives equal weight to guiding the direction of future facilities needed to satisfy legitimate national aspirations. Even in the context of cost reduction through facilities closures and consolidations, the study is timid about recognizing and proposing program changes and realignments of roles and missions to capture what could be significant savings and increased effectiveness. The recommendations of the Committee on Space Facilities are driven by the clear need to be more realistic and precise both in recognizing current incentives and disincentives in the aerospace industry and in forecasting future conditions for U.S. space activities. Derived from text

N95-11969*# National Aeronautics and Space Administration. Ames Research Center, Moffett Field, CA.
THE CROP GROWTH RESEARCH CHAMBER
Kimberly Wagenbach *In its* Technical Paper Contest for Women 1992. Space Challenges: Earth and Beyond 1993 p 183-193 (For primary document see N95-11955 02-99)
Avail: CASI HC A03/MF A03

15 LAUNCH VEHICLES AND SPACE VEHICLES

Includes boosters; operating problems of launch/space vehicle systems; and reusable vehicles.

For related information see also *20 Spacecraft Propulsion and Power.*

N95-11870*# National Aeronautics and Space Administration. Marshall Space Flight Center, Huntsville, AL.
ILLUSTRATED STRUCTURAL APPLICATION OF UNIVERSAL FIRST-ORDER RELIABILITY METHOD
V. Verderaime Washington Aug. 1994 41 p
(NASA-TP-3501; M-756; NAS 1.60:3501) Avail: CASI HC A03/MF A01

The general application of the proposed first-order reliability method was achieved through the universal normalization of engineering probability distribution data. The method superimposes prevailing deterministic techniques and practices on the first-order reliability method to surmount deficiencies of the deterministic method and provide benefits of reliability techniques and predictions. A reliability design factor is derived from the reliability criterion to satisfy a specified reliability and is analogous to the deterministic safety factor. Its application is numerically illustrated on several practical structural design and verification cases with interesting results and insights. Two concepts of reliability selection criteria are suggested. Though the method was developed to support affordable structures for access to space, the method should also be applicable for most high-performance air and surface transportation systems. Author

N95-11934*# National Aeronautics and Space Administration. Lyndon B. Johnson Space Center, Houston, TX.
LIQUID FLYBACK BOOSTER PRE-PHASE: A STUDY ASSESSMENT
W. Peterson, W. Ankney, J. Bell, M. Berning, L. Bryant, A. Bufkin, L. Cain, J. Caram, B. Cockrell, and D. Curry et al Sep. 1994 175 p
(NASA-TM-104801; S-778; NAS 1.15:104801) Avail: CASI HC A08/MF A02

The concept of a flyback booster has been around since early in the shuttle program. The original two-stage shuttle concepts used a manned flyback booster. These boosters were eliminated from the program for funding and size reasons. The current shuttle uses two Redesigned Solid Rocket Motors (RSRM's), which are recovered and refurbished after each flight; this is one of the major cost factors of the program. Replacement options have been studied over the past ten years. The conclusion reached by the most recent study is that the liquid flyback booster (LFBB) is the only competitive option from a life-cycle cost perspective. The purpose of this study was to assess the feasibility and practicality of LFBB's. The study provides an expansion of the recommendations made during the aforementioned study. The primary benefits are the potential for enhanced reusability and a reduction of recurring costs. The potential savings in vehicle turnaround could offset the up-front costs. Development of LFBB's requires a commitment to the shuttle program for 20 to 30 years. LFBB's also offer enhanced safety and abort capabilities. Currently, any failure of an RSRM can be considered catastrophic, since there are no intact abort capabilities during the burn of the RSRM's. The performance goal of the LFBB's was to lift a fully loaded orbiter under optimal conditions, so as not to be the limiting factor of the performance capability of the shuttle. In addition, a final benefit is the availability of growth paths for applications other than shuttle. Author (revised)

N95-12531*# Texas Univ., Austin, TX. Dept. of Aerospace Engineering.
CONVERTING THE MINUTEMAN MISSILE INTO A SMALL SATELLITE LAUNCH SYSTEM Final Report
Bill Alexander, Rodolfo Gonzalez, Greg Humble, Gordon MacKay, Rod McHaty, and Vu Pham 24 Nov. 1993 86 p
(Contract NASw-4435)
(NASA-CR-197169; NAS 1.26:197169) Avail: CASI HC A05/MF A01

Due to the Strategic Arms Reduction Talks (START) treaty between the United States and Ex-Soviet Union, 450 Minuteman 2 (MM 2) missiles were recently taken out of service. Minotaur Designs Incorporated (MDI) intends to convert the MM 2 ballistic missile from a nuclear warhead carrier into a small satellite launcher. MDI will perform this conversion by acquiring the Minuteman stages, purchasing currently available control wafers, and designing a new shroud and interfaces for the satellite. MDI is also responsible for properly integrating all systems. Author (revised)

N95-13129* National Aeronautics and Space Administration. Lyndon B. Johnson Space Center, Houston, TX.
WHITE SANDS TEST FACILITY (Videotape)
1994 Videotape: 27 min. 30 sec. playing time, in color, with sound
(NASA-TM-109901; NONP-NASA-VT-94-28237) Avail: CASI VHS A01/BETA A22

This is an overview of the White Sands Test Facility's role in ensuring the safety and reliability of materials and hardware slated for launch aboard the Space Shuttle. Engine firings, orbital flights debris impact tests, and propulsion tests are featured as well as illustrating how they provide flight safety testing for the Johnson Space Center, other NASA centers, and various government agencies. It also contains a historical perspective and highlights of major programs that have been participated in as part of NASA. JSC

16 SPACE TRANSPORTATION

Includes passenger and cargo space transportation, e.g., shuttle operations; and space rescue techniques.

For related information see also *03 Air Transportation and Safety* and *18 Spacecraft Design, Testing and Performance*. For space suits see *54 Man/System Technology and Life Support*.

N95-11703*# National Aeronautics and Space Administration. Lewis Research Center, Cleveland, OH.
A REVOLUTIONARY LUNAR SPACE TRANSPORTATION SYSTEM ARCHITECTURE USING EXTRATERRESTRIAL LOX-AUGMENTED NTR PROPULSION
Stanley K. Borowski, Robert R. Corban, Donald W. Culver, Melvin J. Bulman, and Mel C. McIlwain Aug. 1994 23 p Presented at the 30th Joint Propulsion Conference, Indianapolis, IN, 27-29 Jun. 1994; sponsored by AIAA, ASME, SAE, and ASEE
(NASA-TM-106726; E-9096; NAS 1.15:106726; AIAA Paper 94-3343)
Avail: CASI HC A03/MF A01

The concept of a liquid oxygen (LOX)-augmented nuclear thermal rocket (NTR) engine is introduced, and its potential for revolutionizing lunar space transportation system (LTS) performance using extraterrestrial 'lunar-derived' liquid oxygen (LUNOX) is outlined. The LOX-augmented NTR (LANTR) represents the marriage of conventional liquid hydrogen (LH2)-cooled NTR and airbreathing engine technologies. The large divergent section of the NTR nozzle functions as an 'afterburner' into which oxygen is injected and supersonically combusted with nuclear preheated hydrogen emerging from the NTR's choked sonic throat: 'scramjet propulsion in reverse.' By varying the oxygen-to-fuel mixture ratio (MR), the LANTR concept can provide variable thrust and specific impulse (Isp) capability with a LH2-cooled NTR operating at relatively constant power output. For example, at a MR = 3, the thrust per engine can be increased by a factor of 2.75 while the Isp decreases by only 30 percent. With this thrust augmentation option, smaller, 'easier to develop' NTR's become more acceptable from a mission performance standpoint (e.g., earth escape gravity losses are reduced and perigee propulsion requirements are eliminated). Hydrogen mass and volume is also reduced resulting in smaller space vehicles. An evolutionary NTR-based lunar architecture requiring only Shuttle C and/or 'in-line' shuttle-derived launch vehicles (SDV's) would operate initially in an 'expandable mode' with NTR lunar transfer vehicles (LTV's) delivering 80 percent more payload on piloted missions than their LOX/LH2 chemical propulsion counterparts. With the establishment of LUNOX production facilities on the lunar surface and 'fuel/oxidizer' depot in low lunar orbit (LLO), monopropellant NTR's would be outfitted with an oxygen propellant module, feed system, and afterburner nozzle for 'bipropellant' operation. The LANTR cislunar LTV now transitions to a reusable mode with smaller vehicle and payload doubling benefits on each piloted round trip mission. As the initial lunar outposts grow to centralized bases and settlements with a substantial permanent human presence, a LANTR-powered shuttle capable of 36 to 24 hour 'one-way' trip times to the moon and back becomes possible with initial mass in low earth orbit (IMLEO) requirements of approximately 160 to 240 metric tons, respectively. Author (revised)

N95-12224*# National Aeronautics and Space Administration. John F. Kennedy Space Center, Cocoa Beach, FL.
DEBRIS/ICE/TPS ASSESSMENT AND INTEGRATED PHOTOGRAPHIC ANALYSIS OF SHUTTLE MISSION STS-65 Final Report, period ending 25 Jul. 1994
Gregory N. Katnik, Barry C. Bowen, and J. Bradley Davis Aug. 1994 122 p Original contains color illustrations
(NASA-TM-109205; NAS 1.15:109205) Avail: CASI HC A06/MF A02; 51 functional color pages

A debris/ice/thermal protection system assessment and integrated photographic analysis was conducted for shuttle mission STS-65. Debris inspections of the flight elements and launch pad were performed before and after launch. Icing conditions on the external tank were assessed by the use of computer programs, nomographs, and infrared scanner data during cryogenic loading of the vehicle followed by on-pad visual inspection. High speed photography of the launch was analyzed to identify ice/debris sources and evaluate potential vehicle damage and/or in-flight anomalies. This report documents the ice/debris/thermal protection system conditions and integrated photographic analysis of shuttle mission STS-65, and the resulting effect on the Space Shuttle Program. Author

N95-12510 Naval Postgraduate School, Monterey, CA.
NPS STATE VECTOR ANALYSIS AND RELATIVE MOTION PLOTTING SOFTWARE FOR STS-51 M.S. Thesis
Lee A. Barker Mar. 1994 139 p Limited Reproducibility: More than 20% of this document may be affected by microfiche quality
(AD-A282909) Avail: CASI HC A07

This thesis outlines the objectives, structure, and operation of the software designed to meet requirements set forth by Development Test Objective 700-6 for the space shuttle Discovery mission STS-51. The primary goals were the comparison of state vector information produced by GPS sources and Discovery's inertial navigation computer, and the real-time display of relative position and rendezvous information between Discovery and a retrievable shuttle pallet satellite. In-flight and postflight examination of GPS and inertial state vectors provided the first step in the development of GPS as an on-orbit navigation system. Analysis of the Orbiter and target satellite state vectors produced real-time graphical displays of operationally significant data to the Discovery's flight crew during rendezvous and proximity operations. DTIC

N95-12851# General Accounting Office, Washington, DC. National Security and International Affairs Div.
SPACE SHUTTLE: NASA'S PLANS FOR REPAIRING OR REPLACING A DAMAGED OR DESTROYED ORBITER. REPORT TO THE CHAIRMAN, SUBCOMMITTEE ON INVESTIGATIONS AND OVERSIGHT, COMMITTEE ON SCIENCE, SPACE, AND TECHNOLOGY, HOUSE OF REPRESENTATIVES
Jul. 1994 12 p
(GAO/NSIAD-94-197; B-257409) Avail: CASI HC A03/MF A01; also available from GAO, PO Box 6015, Gaithersburg, MD 20884-6015

This reports the result of an investigation into NASA's current plans in the event that an accident occur that destroys or seriously damages a space shuttle orbiter, NASA's plans for maintaining critical manufacturing skills in the shuttle work force, and NASA facilities that will be essential to maintain the shuttle orbiters over their expected lifetime.

Derived from text

N95-12917 Aerospace Corp., El Segundo, CA. Technology Operations.
INFRARED SPECTRAL MEASUREMENT OF SPACE SHUTTLE GLOW
M. Ahmadjian, D. E. Jennings, M. J. Mumma, F. Espenak, and C. J. Rice
15 Jul. 1994 9 p Limited Reproducibility: More than 20% of this document may be affected by microfiche quality
(Contract F04701-88-C-0089)
(AD-A282883; TR-0091(6940-03)-2; SMC-TR-93-53) Avail: CASI HC A02

The U.S. Air Force and NASA successfully conducted infrared spectral measurements of the space shuttle glow during STS-39. Preliminary analysis indicates that NO, NO+, OH, and CO produce infrared glow during quiescent orbiter conditions. During orbiter thruster firings the glow intensities in the infrared are enhanced by factors of 10X to 100X with significant changes in spectral distribution. These measurements were obtained with the Spacecraft Kinetic Infrared Test (SKIRT) payload which included a cryogenic infrared circular variable filter infrared spectrometer covering the 0.7 to 5.4 micron wavelength region. Approximately 14,000 spectra of shuttle glow, airglow, aurora, and the orbiter environment were obtained during the eight day mission. The STS-39 Space Shuttle Discovery was launched from the NASA Kennedy Space Center on 28 April 1991 into a 57 deg inclination circular orbit at an altitude of 260 km. DTIC

N95-13122* National Aeronautics and Space Administration. Lyndon B. Johnson Space Center, Houston, TX.
FROM UNDERSEA TO OUTER SPACE: THE STS-40 JELLYFISH EXPERIMENT (Videotape)
1994 Videotape: 15 min. playing time, in color, with sound
(NASA-TM-109958; NONP-NASA-VT-94-28236) Avail: CASI VHS A01/BETA A22

This is an educational production featuring 'Ari', animated jellyfish who recounts his journey into space. Jellyfish were flown aboard the shuttle to study the effects of microgravity on living organisms. Topics Ari explores are: microgravity, life sciences, similarities between jellyfish and humans, and the life cycle and anatomy of a jellyfish. JSC

N95-13130* National Aeronautics and Space Administration. Lyndon B. Johnson Space Center, Houston, TX.
STS-65 MISSION HIGHLIGHTS RESOURCE TAPE (Videotape)
1994 Videotape: 57 min. 30 sec. playing time, in color, with sound
(NASA-TM-108589; NONP-NASA-VT-94-28238) Avail: CASI VHS A01/BETA A22

The important visual events of each mission including launch, onboard crew activities, and landing are depicted. JSC

N95-13131* National Aeronautics and Space Administration. Lyndon B. Johnson Space Center, Houston, TX.
STS-68 POST FLIGHT PRESENTATION (Videotape)
1994 Videotape: 47 min. playing time, in color, with sound
(NASA-TM-109959; NONP-NASA-VT-94-28239) Avail: CASI VHS A01/BETA A22

This contains mission footage selected by the STS-68 crew of pre-launch, launch, onboard activities and experiments, Space Radar Laboratory-2 (SRL-2), Get Away Special canisters (GAS cans), Earth views, and landing. Crew members provide descriptive voice-over narration of the scenes. JSC

N95-13132* National Aeronautics and Space Administration. Lyndon B. Johnson Space Center, Houston, TX.
STS-61 MISSION HIGHLIGHTS RESOURCE TAPE (Videotape)
1994 Videotape: 2 hr. 1 min. playing time, in color, with sound
(NASA-TM-109963; NONP-NASA-VT-94-28240) Avail: CASI VHS A01/BETA A22

This contains important visual events including launch, Hubble Space Telescope (HST) capture, repair and re-deployment, onboard activities, earth views, and landing. Also included is the air-to-ground transmission between the crew and Mission Control. JSC

N95-13133* National Aeronautics and Space Administration. Lyndon B. Johnson Space Center, Houston, TX.
MEMORIAL SERVICE FOR THE MISSION 51-L CREW (EDITED) (Videotape)
31 Jan. 1994 Videotape: 27 min. 30 sec. playing time, in color, with sound
(NASA-TM-109900; NONP-NASA-VT-94-28241) Avail: CASI VHS A01/BETA A22

The original memorial service held at NASA JSC for the STS-51L Challenger crew who died onboard the Shuttle is presented. President Ronald Reagan conducts this briefing. JSC

17 SPACE COMM., SPACECRAFT COMM., COMMAND & TRACKING

Includes telemetry; space communications networks; astronavigation and guidance; and radio blackout.

For related information see also *04 Aircraft Communications and Navigation* and *32 Communications and Radar.*

No abstracts in this category.

18 SPACECRAFT DESIGN, TESTING AND PERFORMANCE

Includes satellites; space platforms; space stations; spacecraft systems and components such as thermal and environmental controls; and attitude controls.

For life support systems see *54 Man/System Technology and Life Support.* For related information see also *05 Aircraft Design, Testing and Performance, 39 Structural Mechanics,* and *16 Space Transportation.*

N95-11755# Oak Ridge National Lab., TN.
VULNERABILITY ASSESSMENT OF A SPACE BASED WEAPON PLATFORM ELECTRONICS SYSTEM EXPOSED TO A THERMONUCLEAR WEAPON DETONATION
C. L. Perez (North Carolina Univ., Chapel Hill, NC.) and J. O. Johnson
May 1994 42 p
(Contract DE-AC05-84OR-21400)
(DE94-013415; ORNL/TM-12487) Avail: CASI HC A03/MF A01

The utilization of reconnaissance/surveillance satellite and weapon platform assets in space will subject the sensitive electronic equipment to a variety of natural and man-made radiation environments. These include Van Allen Belt protons and electrons; galactic and solar flare protons; neutrons, gamma rays, and x-rays from fission and fusion weapons; and directed neutral particle beams and lasers. Electronic equipment, including modern integrated circuits, may undergo permanent or transient changes of the electrical properties of the active components when exposed to these sources of radiation. This report summarizes the results of the Monte Carlo Adjoint Shielding code system -- MASH v1.0 calculations designed to estimate the dose to the critical electronics components of an idealized spaced based weapon platform from neutron and gamma-ray radiation emanating from a thermonuclear weapon detonation. The MASH calculations modeled several source/platform geometry configurations, obtaining results for multiple distances and weapon detonation positions relative to the platform. For certain source/platform orientations, the results indicate vulnerabilities to the C3 bay critical components box to radiation damage from a nuclear weapon detonation. Neutron protection factors ranged from 0.7 to 3.4 for the three platform configurations analyzed, and gamma-ray protection factors ranged from approximately 1.5 to 9.8. The results further indicate the source has a direct line-of-sight to the critical components box for certain source/platform orientations, regardless of the number of interceptors present. The merits of utilizing the MASH code system for estimating dose and shielding factors for spaced based assets has been demonstrated. The geometry configuration studied here is greatly simplified compared to those that will be encountered in an actual design. DOE

N95-11767*# Rockwell International Corp., Downey, CA. Space Systems Div.
TEST PLAN. GCPS TASK 7, SUBTASK 7.1: IHM DEVELOPMENT

H. S. Greenberg 2 Sep. 1994 19 p Prepared in cooperation with Northrop Corp., Los Angeles, CA
(Contract NCC1-193)
(NASA-CR-106876; NAS 1.26:196876; SSD940212) Avail: CASI HC A03/MF A01

The overall objective of Task 7 is to identify cost-effective life cycle integrated health management (IHM) approaches for a reusable launch vehicle's primary structure. Acceptable IHM approaches must: eliminate and accommodate faults through robust designs, identify optimum inspection/maintenance periods, automate ground and on-board test and check-out, and accommodate and detect structural faults by providing wide and localized area sensor and test coverage as required. These requirements are elements of our targeted primary structure low cost operations approach using airline-like maintenance by exception philosophies. This development plan will follow an evolutionary path paving the way to the ultimate development of flight-quality production, operations, and vehicle systems. This effort will be focused on maturing the recommended sensor technologies required for localized and wide area health monitoring to a technology readiness level (TRL) of 6 and to establish flight ready system design requirements. The following is a brief list of IHM program objectives: design out faults by analyzing material properties, structural geometry, and load and environment variables and identify failure modes and damage tolerance requirements; design in system robustness while meeting performance objectives (weight limitations) of the reusable launch vehicle primary structure; establish structural integrity margins to preclude the need for test and checkout and predict optimum inspection/maintenance periods through life prediction analysis; identify optimum fault protection system concept definitions combining system robustness and integrity margins established above with cost effective health monitoring technologies; and use coupons, panels, and integrated full scale primary structure test articles to identify, evaluate, and characterize the preferred NDE/NDI/IHM sensor technologies that will be a part of the fault protection system.

Derived from text

N95-11777*# Rockwell International Corp., Downey, CA. Space Systems Div.
REQUIREMENTS REPORT FOR SSTO VERTICAL TAKE-OFF/HORIZONTAL LANDING VEHICLE
H. S. Greenberg 29 Jul. 1994 58 p Prepared in cooperation with Northrop Corp., Los Angeles, CA and Hercules Aerospace Co., Wilmington, DE
(Contracts NCC1-193; NCC2-9003; NCC8-39)
(NASA-CR-196875; NAS 1.26:196875; SSD94D0217; SSTO-REQ-1) Avail: CASI HC A04/MF A01

This document describes the detailed design requirements and design criteria to support Structures/TPS Technology development for SSTO winged vehicle configurations that use vertical take-off and horizontal landing and deliver 25,000 lb payloads to a 220 nm circular orbit at an inclination of 51.6 degrees or 40,000 lb payloads to a 150 nm circular orbit at a 28.5 degree of inclination. This document will be updated on a timely basis as information becomes available throughout the project. Author

N95-11802*# Rockwell International Corp., Downey, CA. Space Systems Div.
TEST PLAN. TASK 5, SUBTASK 5.2: EARLY ON-ORBIT TPSDEBRIS IMPACT TESTS
H. S. Greenberg 29 Jul. 1994 12 p Prepared in cooperation with Hercules, Inc., Wilmington, DE
(Contract NCC8-39)
(NASA-CR-196873; NAS 1.26:196873; SSD94D0221; RHCTS-TP-1) Avail: CASI HC A03/MF A01

The limitation of damage to, and survival of, the cryogenic tankage during the on-orbit stay despite potential impact of orbital debris, may be a significant discriminator in the RHCTS trade studies described in the TA-1 trade study plan (ref. RHCTS-TSP-1) dated July 29, 1994. The objective of this early phase of an overall debris impact test program is to provide the data to support assessment of the relative suitability of integral and non integral tanks. Author

N95-11809*# Rockwell International Corp., Downey, CA. Space Systems Div.
SELECTION PROCESS FOR TRADE STUDY: REUSABLE HYDROGEN COMPOSITE TANK SYSTEM (RHCTS)
H. S. Greenberg 2 Sep. 1994 15 p Prepared in cooperation with Hercules, Inc., Wilmington, DE
(Contract NCC8-39)
(NASA-CR-196874; NAS 1.26:196874; SSD94D0209) Avail: CASI HC A03/MF A01

This document describes the selection process that will be used to identify the most suitable structural configuration option for an SSTO winged vehicle capable of delivering 25,000 lbs to a 220 nm circular orbit at 51.6 degree inclination. The most suitable RHCTS is within this configuration and will be the prototype design for subsequent design and analysis and the basis for the design and fabrication of a scale test article to be subjected to life cycle testing. The selection process for this TA 1 trade study is the same as that for the TA 2 trade study. As the trade study progresses additional insight may result in modifications to the selection criteria within in this process. Such modifications will result in an update of this document as appropriate. Author

N95-11833*# Rockwell International Corp., Downey, CA. Space Science Div.
TEST PLAN. GCPS TASK 4, SUBTASK 4.2 THRUST STRUCTURE DEVELOPMENT
H. S. Greenberg 2 Sep. 1994 170 p Prepared in cooperation with Northrop Corp., Los Angeles, CA
(Contract NCC1-193)
(NASA-CR-196869; NAS 1.26:196869; SSD94D0211) Avail: CASI HC A08/MF A02

The Single Stage To Orbit (SSTO) vehicle is designed to lift off from a vertical position, go into orbit, return to earth for a horizontal landing, and be reusable for the next mission. (NASA baseline only) In order to meet its performance goals, the SSTO relies on light weight structure and the use of 8 tri-propellant engines. These engines are mounted to the thrust structure. This test plan addresses selection of the material for this structure, and the integrity of the design through testing of elements and a full-scale subcomponent. This test plan supports the development of the design for an advanced composite thrust structure for a Single Stage to Orbit manned, heavy launch vehicle. The thrust structure is designed to transmit very high thrust loads from the engines to the rest of the vehicle (see Figure 1). The thrust structure will also be used for primary attachment of the twin vertical tails and possibly act as the aft attach point for the wing. The combination of high loading, high vibration, long service life and high acoustic environments will need to be evaluated by tests. To minimize design risk, a building block approach will be used. We will first screen materials to determine which materials show the most promise for this application. Factors in this screening will be the suitability of these materials for chosen design concepts, particularly concerning specific strength, environmental compatibility and applicability to fabrication processes. Next we will characterize two material systems that will be used in the design; the characterization will allow us to generate preliminary design data that will be used for the analysis. Element testing will be performed to evaluate critical structural locations under load. Final testing on the full scale test article will be performed to verify the design and to demonstrate predictability of the analysis. Additionally, risks associated with fabricating full scale thrust structures will be reduced through testing activities. One of the major concerns that stems from full scale fabrication is the realities of size and the associated complexities of handling, manufacturing, and assembly. The need exists to fabricate, assemble and test—representative joint specimens to achieve—confidence in the design and manufacturing technologies being proposed. Author

N95-11937*# Lockheed Engineering and Sciences Co., Houston, TX.
AN AXISYMMETRIC ANALOG TWO-LAYER CONVECTIVE HEATING PROCEDURE WITH APPLICATION TO THE EVALUATION OF SPACE SHUTTLE ORBITER WING LEADING EDGE AND WINDWARD SURFACE HEATING
K. C. Wang (Lockheed Engineering and Sciences Co., Houston, TX.) Sep. 1994 143 p
(Contract NAS9-17900)
(NASA-CR-188343; NAS 1.26:188343) Avail: CASI HC A07/MF A02

A numerical procedure for predicting the convective heating rate of hypersonic reentry vehicles is described. The procedure, which is based on the axisymmetric analog, consists of obtaining the three-dimensional inviscid flowfield solution; then the surface streamlines and metrics are calculated using the inviscid velocity components on the surface; finally, an axisymmetric boundary layer code or approximate convective heating equations are used to evaluate heating rates. This approach yields heating predictions to general three-dimensional body shapes. The procedure has been applied to the prediction of the wing leading edge heating to the Space Shuttle Orbiter. The numerical results are compared with the results of heat transfer testing (OH66) of an 0.025 scale model of the Space Shuttle Orbiter configuration in the Calspan Hypersonic Shock Tunnel (HST) at Mach 10 and angles of attack of 30 and 40 degrees. Comparisons with STS-5 flight data at Mach 9.15 and angle of attack of 37.4 degrees and STS-2 flight data at Mach 12.86 and angle of attack of 39.7 degrees are also given. Author

N95-11945*# Rockwell International Corp., Downey, CA. Space Systems Div.

TRADE STUDY PLAN FOR REUSABLE HYDROGEN COMPOSITE TANK SYSTEM (RHCTS)

H. S. Greenberg 29 Jul. 1994 25 p Prepared in cooperation with Hercules, Inc., Wilmington, DE

(Contract NCC8-39)

(NASA-CR-196871; NAS 1.26:196871; SSD94D0219; RHCTS-TSP-1)

Avail: CASI HC A03/MF A01

This TA 1 document describes the trade study plan (with support from TA 2) that will identify the most suitable structural configuration for an SSTO winged vehicle capable of delivering 25,000 lbs to a 220 nm circular orbit at 51.6 degree inclination. The analysis uses information derived in the TA 2 study as identified within the study plan. In view of this, for convenience, the TA 2 study plan is included as an appendix to this document. Derived from text

N95-11947*# National Aeronautics and Space Administration. Langley Research Center, Hampton, VA.

MODELLING AND SIMULATION OF SPACE STATION FREEDOM BERTHING DYNAMICS AND CONTROL

Paul A. Cooper, James L. Garrison, Jr., Raymond C. Montgomery, Shih-Chin Wu, Alan E. Stockwell, and Martha E. Demeo Aug. 1994 169 p

(RTOP 233-01-01-01)

(NASA-TM-109151; NAS 1.15:109151) Avail: CASI HC A08/MF A02

A large-angle, flexible, multibody, dynamic modeling capability has been developed to help validate numerical simulations of the dynamic motion and control forces which occur during berthing of Space Station Freedom to the Shuttle Orbiter in the early assembly flights. This paper outlines the dynamics and control of the station, the attached Shuttle Remote Manipulator System, and the orbiter. The simulation tool developed for the analysis is described and the results of two simulations are presented. The first is a simulated maneuver from a gravity-gradient attitude to a torque equilibrium attitude using the station reaction control jets. The second simulation is the berthing of the station to the orbiter with the station control moment gyros actively maintaining an estimated torque equilibrium attitude. The influence of the elastic dynamic behavior of the station and of the Remote Manipulator System on the attitude control of the station/orbiter system during each maneuver was investigated. The flexibility of the station and the arm were found to have only a minor influence on the attitude control of the system during the maneuvers. Author

N95-11948*# National Aeronautics and Space Administration. Marshall Space Flight Center, Huntsville, AL.

INNER MAGNETOSPHERE IMAGER (IMI) SOLAR TERRESTRIAL PROBE CLASS MISSION PRELIMINARY DESIGN STUDY REPORT

M. Hermann and L. Johnson Washington Aug. 1994 26 p

(NASA-TM-108464; NAS 1.15:108464) Avail: CASI HC A03/MF A01

For three decades, magnetospheric field and plasma measurements have been made by diverse instruments flown on spacecraft in many different orbits, widely separated in space and time, and under various solar and magnetospheric conditions. Scientists have used this information to piece together an intricate, yet incomplete view of the magnetosphere. A simultaneous global view, using various light wavelengths and energetic neutral atoms, could reveal exciting new data and help explain complex magnetospheric processes, thus providing us with a clear picture of this region of space. The George C. Marshall Space Flight Center (MSFC) is responsible for defining the IMI mission which will study this region of space. NASA's Space Physics Division of the Office of Space Science placed the IMI third in its queue of Solar Terrestrial Probe missions for launch in the 1990's. A core instrument complement of three images (with the potential addition of one or more mission enhancing instruments) will fly in an elliptical, polar earth orbit with an apogee of 44,600 km and a perigee of 4,800 km. This paper will address the mission objectives, spacecraft design consideration, interim results of the MSFC concept definition study, and future plans. Author

N95-12106*# Smithsonian Astrophysical Observatory, Cambridge, MA.

ANALYTICAL INVESTIGATION OF THE DYNAMICS OF TETHERED CONSTELLATIONS IN EARTH ORBIT, PHASE 2 Final Report, 22 Feb. 1985 - 31 Mar. 1994

Enrico C. Lorenzini, Gordon E. Gullahorn, Mario L. Cosmo, Robert D. Estes, and Mario D. Grossi May 1994 341 p

(Contract NAS8-36606)

(NASA-CR-196509; NAS 1.26:196509) Avail: CASI HC A15/MF A03

This final report covers nine years of research on future tether applications and on the actual flights of the Small Expendable Deployment System (SEDS). Topics covered include: (1) a description of numerical codes used to simulate the orbital and attitude dynamics of tethered systems during station keeping and deployment maneuvers; (2) a comparison of various tethered system simulators; (3) dynamics analysis, conceptual design, potential applications and propagation of disturbances and isolation from noise of a variable gravity/microgravity laboratory tethered to the Space Station; (4) stability of a tethered space centrifuge; (5) various proposed two-dimensional tethered structures for low Earth orbit for use as planar array antennas; (6) tethered high gain antennas; (7) numerical calculation of the electromagnetic wave field on the Earth's surface on an electrodynamically tethered satellite; (8) reentry of tethered capsules; (9) deployment dynamics of SEDS-1; (10) analysis of SEDS-1 flight data; and (11) dynamics and control of SEDS-2. CASI

N95-12165*# Massachusetts Inst. of Tech., Cambridge.

DESIGN OF PASSIVE PIEZOELECTRIC DAMPING FOR SPACE STRUCTURES Final Report Ph.D. Thesis

Nesbitt W. Hagood, IV, Jack B. Aldrich, and Andreas H. vonFlotow Hampton, VA NASA Sep. 1994 104 p

(Contract NAS1-19381; RTOP 590-14-91-52)

(NASA-CR-4625; NAS 1.26:4625) Avail: CASI HC A06/MF A02

Passive damping of structural dynamics using piezoceramic electromechanical energy conversion and passive electrical networks is a relatively recent concept with little implementation experience base. This report describes an implementation case study, starting from conceptual design and technique selection, through detailed component design and testing to simulation on the structure to be damped. About 0.5kg. of piezoelectric material was employed to damp the ASTREX testbed, a 500kg structure. Emphasis was placed upon designing the damping to enable high bandwidth robust feedback control. Resistive piezoelectric shunting provided the necessary broadband damping. The piezoelectric element was incorporated into a mechanically-tuned vibration absorber in order to concentrate damping into the 30 to 40 Hz frequency modes at the rolloff region of the proposed compensator. A prototype of a steel flex-tensional motion amplification device was built and tested. The effective stiffness and damping of the flex-tensional device was experimentally verified. When six of these effective springs are placed in an orthogonal configuration, strain energy is absorbed from all six degrees of freedom of a 90kg. mass. A NASTRAN finite element model of the testbed was modified to include the six-spring damping system. An analytical model was developed for the spring in order to see how the flex-tensional device and piezoelectric dimensions effect the critical stress and strain energy distribution throughout the component. Simulation of the testbed demonstrated the damping levels achievable in the completed system. Author

N95-12175*# Vigyan Research Associates, Inc., Hampton, VA.

A SIMPLE ANALYTICAL AERODYNAMIC MODEL OF LANGLEY WINGED-CONE AEROSPACE PLANE CONCEPT

Bandu N. Pamadi Hampton, VA NASA Oct. 1994 45 p

(Contract NAS1-19341; RTOP 232-01-04-05)
(NASA-CR-194987; NAS 1.26:194987) Avail: CASI HC A03/MF A01

A simple three DOF analytical aerodynamic model of the Langley Winged-Coned Aerospace Plane concept is presented in a form suitable for simulation, trajectory optimization, and guidance and control studies. The analytical model is especially suitable for methods based on variational calculus. Analytical expressions are presented for lift, drag, and pitching moment coefficients from subsonic to hypersonic Mach numbers and angles of attack up to +/- 20 deg. This analytical model has break points at Mach numbers of 1.0, 1.4, 4.0, and 6.0. Across these Mach number break points, the lift, drag, and pitching moment coefficients are made continuous but their derivatives are not. There are no break points in angle of attack. The effect of control surface deflection is not considered. The present analytical model compares well with the APAS calculations and wind tunnel test data for most angles of attack and Mach numbers. Author (revised)

N95-12528# Naval Postgraduate School, Monterey, CA.
PRELIMINARY DIGITAL CONTROL SYSTEM DESIGN FOR THE PETITE AMATEUR NAVY SATELLITE (PANSAT) M.S. Thesis
David L. Leu Mar. 1994 83 p
(AD-A282804) Avail: CASI HC A05/MF A01

The Petite Amateur Navy Satellite (PANSAT) project was initiated to demonstrate the feasibility of a quick reaction, low-cost communications satellite incorporating digital communications and a store and forward memory area for the use of amateur radio operators interested in spread spectrum and packet communications. Designed to operate autonomously and under the guidance of a ground station located at the Naval Postgraduate School (NPS) in Monterey, California, it requires a reliable Digital Control System (DCS) to control operations while processing communications and telemetry. This thesis deals with a preliminary hardware design for the DCS and related subsystems. In addition to the design process, individual components were selected which were deemed suitable for the space environment while operating under project constraints of limited power and a desire to create a system using off-the-shelf devices capable of handling temperature and physical constraints equivalent to MIL-STD-883. Reliability, redundancy, and flexibility were requirements of the DCS design. DTIC

N95-12545 Naval Oceanographic Office, Bay Saint Louis, MS.
INITIAL ANALYSIS AND MODELING RESULTS FROM THE POLAR ORBITING GEOMAGNETIC SURVEY (POGS) SATELLITE
John M. Quinn, Donald L. Shiel, Mario H. Acuna, and John Scheifle Aug. 1993 65 p Limited Reproducibility: More than 20% of this document may be affected by microfiche quality
(AD-A283454; NOO-TR-311) Avail: CASI HC A04

The spatial and temporal character of fully calibrated geomagnetic data collected on selected orbits of the Polar Orbiting Geomagnetic Survey (POGS) satellite mission during the first 6 months of 1991 is analyzed with respect to a preliminary, degree 12 spherical-harmonic magnetic field model derived from selected POGS data collected during January and February 1991. The accuracy of global models derived from these data depends on the vector magnetometer calibrations, thermal corrections, satellite magnetic mapping, and the time synching of the satellite's quartz clock with respect to the satellite's ephemeris, which is referenced to Universal Time (UT) and which is supplied by the Defense Mapping Agency's tracking network (TRANET). The calibration and correction factors applied to the POGS data set are fully documented. Additionally, the current status of the POGS satellite and the corresponding data reduction and distribution efforts along with the current status of subsequent POGS experiments, which are part of the Defense Meteorological Satellite Program (DMSP) Block 5 and Block 6 satellite missions known as DMSP/POGS follow-on experiments, are presented. DTIC

N95-12564*# Maryland Univ., College Park, MD. Dept. of Aerospace Engineering.
ORION: DESIGN OF A SYSTEM FOR ASSURED LOW-COST HUMAN ACCESS TO SPACE
Josh Elvander, Andy Heifetz, Teresa Hunt, and Martin Zhu et al 1994 314 p Prepared for Universities Space Research Association, Columbia, MD
(Contract NASw-4435)
(NASA-CR-197185; NAS 1.26:197185) Avail: CASI HC A14/MF A03

In recent years, Congress and the American people have begun to seriously question the role and importance of future manned spaceflight. This is mainly due to two factors: a decline in technical competition caused by the collapse of communism, and the high costs associated with the Space Shuttle transportation system. With these factors in mind, the ORION system was designed to enable manned spaceflight at a low cost, while maintaining the ability to carry out diverse missions, each with a high degree of flexibility. It is capable of performing satellite servicing missions, supporting a space station via crew rotation and resupply, and delivering satellites into geosynchronous orbit. The components of the system are a primary launch module, an upper stage, and a manned spacecraft capable of dynamic reentry. For satellite servicing and space station resupply missions, the ORION system utilizes three primary modules, an upper stage, and the spacecraft, which is delivered to low earth orbit and used to rendezvous, transfer materials, and make repairs. For launching a geosynchronous satellite, one primary module and an upper stage are used to deliver the satellite, along with an apogee kick motor, into orbit. The system is designed with reusability and modularity in mind in an attempt to lower cost. Author

N95-12632*# Spectrolab, Inc., Sylmar, CA.
RINGSAT
Dowdy, Guthrie, Kuykendall, Martyn, Okano, Niedermeier, and Williams May 1994 59 p
(Contract NASw-4435)
(NASA-CR-197167; NAS 1.26:197167) Avail: CASI HC A04/MF A01

Radio frequency interference (RFI) presents a serious problem to naval communications. Unauthorized transmissions on the same frequencies that FLTSAT or LEASAT use cause a loss of one or more transponders on a satellite. The problem is not correctable until the emitter is located and turned off, or until it runs off on its own. The present geolocation system cannot deal with the RFI problem adequately. This causes the Navy to lose operational capability and money. The proposed Radio Frequency Interference Navy Geolocation Satellite (RINGSAT) would locate the source of the interference within 3 hours, an outstanding improvement over current equipment. Furthermore, RINGSAT can be built quickly, at minimal cost, and can be used concurrently for other military missions. Currently, geolocation to identify the RFI is done at Naval Space Command. Using single satellite doppler, time delay of arrival, and frequency delay of arrival techniques, it is possible to locate the interfering emitter. However, for the first quarter of fiscal year 1993, about 50 different channels used by the Navy were nonoperational for over 500 hours. Almost 30 percent of the interference occurrences lasted for over 12 hours. In only one quarter of the cases was the interference turned off in less than two—hours either by our detection or on its own. Derived from text

N95-12661*# Alaska Univ., Fairbanks, AK. School of Engineering.
POWERSAT: A TECHNOLOGY DEMONSTRATION OF A SOLAR POWER SATELLITE
Douglas L. Sigler, ed., John Riedman, Jon Duracinski, Joe Edwards, Garry Brown, Ron Webb, Mike Platzke, Xiaolin Yuan, Pete Rogers, and Afsar Khan 1994 93 p Prepared for Universities Space Research Association, Columbia, MD
(Contract NASw-4435)
(NASA-CR-197210; NAS 1.26:197210) Avail: CASI HC A05/MF A01

PowerSat is a preliminary design strategy for microwave wireless power transfer of solar energy. Solar power satellites convert solar power into microwave energy and use wireless power transmission to transfer the power to the Earth's surface. The PowerSat project will show how new developments in inflatable technology can be used to deploy solar panels and phased array antennas. Author

N95-12663*# California Univ., Los Angeles, CA. School of Engineering and Applied Science.
SPACE HARDWARE DESIGNS, VOLUME 1 Final Report
Rudolf X. Meyer, Richard Cribbs, Mark Honda, Christina Ma, and Christopher Robson 1994 11 p Prepared for Universities Space Research Association, Columbia, MD Original contains color illustrations
(Contract NASw-4435)
(NASA-CR-197209; NAS 1.26:197209) Avail: CASI HC A03/MF A01; 2 functional color pages

The design of a solar sail space vehicle with a novel sail deployment mechanism is described. The sail is triangular in shape and is deployed

and stabilized by three miniature spacecraft, one at each corner of the triangle. A concept demonstrator for a spherical microrover for the exploration of a planetary surface is described. Lastly, laboratory experiments have been conducted to study the migration of thin oil films on metal surfaces in the presence of a thermal gradient. Author (revised)

N95-12696*# West Virginia Univ., Morgantown, VA. Dept. of Mechanical and Aerospace Engineering.
CONCEPTUAL DESIGN OF AN ORBITAL DEBRIS DEFENSE SYSTEM
Erik Bedillion, Gary Blevins, Brian Bohs, David Bragg, Christopher Brown, Jose Casanova, David Cribbs, Richard Demko, Brian Henry, and Kelly James et al 1994 64 p Prepared for Universities Space Research Association, Columbia, MD
(Contract NASw-4435)
(NASA-CR-197211; NAS 1.26:197211) Avail: CASI HC A04/MF A01

Man made orbital debris has become a serious problem. Currently NORAD tracks over 7000 objects in orbit and less than 10 percent of these are active payloads. Common estimates are that the amount of debris will increase at a rate of 10 percent per year. Impacts of space debris with operational payloads or vehicles is a serious risk to human safety and mission success. For example, the impact of a 0.2 mm diameter paint fleck with the Space Shuttle Challenger window created a 2 mm wide by 0.6 mm deep pit. The cost to replace the window was over $50,000. A conceptual design for a Orbital Debris Defense System (ODDS) is presented which considers a wide range of debris sizes, orbits and velocities. Two vehicles were designed to collect and remove space debris. The first would attach a re-entry package to de-orbit very large debris, e.g. inactive satellites and spent upper stages that tend to break up and form small debris. This vehicle was designed to contain several re-entry packages, and be refueled and resupplied with more re-entry packages as needed. The second vehicle was designed to rendezvous with and capture debris ranging from 10 cm to 2 m. Due to tracking limitations, no technically feasible method for collecting debris below 10 cm in size could be devised; it must be accomplished through international regulations which reduce the accumulation of space debris. Author (revised)

N95-12698*# Universities Space Research Association, Columbia, MD.
ASPOD MODIFICATIONS OF 1993-1994 Final Report
Jennifer J. Jackson, ed., Paul W. Fogarty, Matthew Muller, Thomas A. Martucci, III, Daniel Williams, and David A. Rowney 1994 270 p
(Contract NASw-4435)
(NASA-CR-197204; NAS 1.26:197204) Avail: CASI HC A12/MF A03

ASPOD, Autonomous Space Processors for Orbital Debris, provides a unique way of collecting the space debris that has built up over the past 37 years. For the past several years, ASPOD has gone through several different modifications. This year's concentrations were on the solar cutting array, the solar tracker, the earth based main frame/tilt table, the controls for the two robotic arms, and accurate autocad drawings of ASPOD. This final report contains the reports written by the students who worked on the ASPOD project this year. Author

N95-12737*# Massachusetts Inst. of Tech., Cambridge.
PROJECT FREEBIRD: AN ORBITAL TRANSFER VEHICLE
Carlos A. Aneses, Ryan L. Blanchette, David M. Brann, Mario J. Campos, Lisa E. Cohen, Daniel J. Corcoran, III, James F. Cox, Trevor J. Curtis, Deborah A. Douglass, and Catherine L. Downard et al 1994 338 p Prepared for Universities Space Research Association, Columbia, MD
(Contract NASw-4435)
(NASA-CR-197201; NAS 1.26:197201) Avail: CASI HC A15/MF A03

Freebird is a space-based orbital transfer vehicle designed to repair and deorbit orbital assets. Freebird is based at International Space Station Alpha (ISSA) at an inclination of 51.6 deg and is capable of three types of missions: crewed and teleoperated LEO missions, and extended robotic missions. In a crewed local configuration, the vehicle can visit inclinations between 30.8 deg and 72.4 deg at altitudes close to 390 km. Adding extra fuel tanks extends this range of inclination up to 84.9 deg and down to 18.3 deg. Furthermore, removing the crew module, using the vehicle in a teleoperated manner, and operating with extra fuel tanks allows missions to polar and geosynchronous orbits. To allow for mission flexibility, the vehicle was designed in a semimodular configuration. The major system components include a crew module, a 'smart box' (which contains command, communications, guidance, and navigation equipment), a propulsion pack, extra fuel tanks, and a vehicle storage facility (VSF) for storage purposes. To minimize risk as well as development time and cost, the vehicle was designed using only proven technology or technology which is expected to be flight-qualified in time for the intended launch date of 2002. And, because Freebird carries crew and operates near the space station, it must meet or exceed the NASA reliability standard of 0.994, as well as other standard requirements for such vehicles. The Freebird program was conceived and designed as a way to provide important and currently unavailable satellite repair and replacement services of a value equal to or exceeding operational costs. Author

N95-12765*# Texas Univ., Austin, TX. Dept. of Aerospace Engineering.
MINUTEMAN 2 LAUNCHED SMALL SATELLITE Final Report
Sunny Chan, Kriss Hinders, Trent Martin, Shandy McMillian, Brad Sharp, and Greg Vajdos 6 May 1994 73 p Prepared for Universities Space Research Association, Columbia, MD
(Contract NASw-4435)
(NASA-CR-197203; NAS 1.26:197203) Avail: CASI HC A04/MF A01

The goal of LEOSat Industries' Spring 1994 project was to design a small satellite that has a strong technology demonstration or scientific justification and incorporates a high level of student involvement. The satellite is to be launched into low earth orbit by the converted Minuteman 2 satellite launcher designed by Minotaur Designs, Inc. in 1993. The launch vehicle shroud was modified to a height of 90 inches, a diameter of 48 inches at the bottom and 35 inches at the top for a total volume of 85 cubic feet. The maximum allowable mass of the payload is about 1100 lb., depending on the launch site, orbit altitude, and inclination. The satellite designed by LEOSat Industries is TerraSat, a remote-sensing satellite that will provide information for use in space-based earth studies. It will consist of infrared and ultraviolet/visible sensors similar to the SDI-developed sensors being tested on Clementine. The sensors will be mounted on the Defense Systems, Inc. Standard Satellite-1 spacecraft bus. LEOSat has planned for two satellites orbiting the Earth with trajectories similar to that of LANDSAT 5. The semi-major axis is 7080 kilometers, the eccentricity is 0, and the inclination is 98.2 degrees. The estimated mass of TerraSat is 145 kilograms and the estimated volume is 1.8 cubic meters. The estimated cost of TerraSat is $13.7 million. The projected length of time from assembly of the sensors to launch of the spacecraft is 13 months. Author

N95-12766*# Stanford Univ., CA. Guidance and Control Lab.
PRECISION TETHERED SATELLITE ATTITUDE CONTROL Ph.D. Thesis
Robert J. Kline-Schoder Mar. 1990 143 p
(Contract NCC2-389)
(NASA-CR-196950; NAS 1.26:196950) Copyright Avail: CASI HC A07/MF A02

Tethered spacecraft possess unique dynamic characteristics which make them advantageous for certain classes of experiments. One use for which tethers are particularly well suited is to provide an isolated platform for spaceborne observatories. The advantages of tethering a pointing platform 1 or 2 km from a space shuttle or space station are that, compared to placing the observatory on the parent spacecraft, vibrational disturbances are attenuated and contamination is eliminated. In practice, all satellites have some requirement on the attitude control of the spacecraft, and tethered satellites are no exception. It has previously been shown that conventional means of performing attitude control for tethered satellites are insufficient for any mission with pointing requirements more stringent than about 1 deg. This is due mainly to the relatively large force applied by the tether to the spacecraft. A particularly effective method of implementing attitude control for tethered satellites is to use this tether tension force to generate control torques by moving the tether attach point relative to the subsatellite center of mass. A demonstration of this attitude control technique on an astrophysical pointing platform has been proposed for a space shuttle flight test project and is referred to as the Kinetic Isolation Tether Experiment (KITE). Author (revised)

N95-12790*# Maryland Univ., College Park, MD. Dept. of Aerospace Engineering.
MOOSE: MANNED ON-ORBIT SERVICING EQUIPMENT
J. Budinoff, ed., N. Leontsinis, ed., J. Lane, ed., R. Singh, ed., K. Angelone, C. Boswell, I. Chamberlain, M. Concha, M. Corrodo, and O. Custodio et al 1993 415 p

(Contract NASw-4435)
(NASA-CR-197151; NAS 1.26:197151) Avail: CASI HC A18/MF A04

The ability to service satellites has thus far been limited to low earth orbit platforms within reach of the Space Shuttle. Other orbits, such as geosynchronous orbits containing high-value spacecraft have not been attainable by a servicing vehicle. The useful life of a satellite can be extended by replacing spent propellant and damaged orbital replacement units, forestalling the need for eventual replacement. This growing need for satellite on-orbits servicing can be met by the Manned On-Orbit Servicing Equipment (MOOSE). Missions requiring orbit transfer capability, precision manipulation and maneuvering, and man-in-the-loop control can be accomplished using MOOSE. MOOSE is a flexible, reusable, single operator, aerobraking spacecraft designed to refuel, repair, and service orbiting spacecraft. MOOSE will be deployed from Space Station Freedom, (SSF), where it will be stored, resupplied, and refurbished. Author (revised)

N95-12838*# National Aeronautics and Space Administration. Langley Research Center, Hampton, VA.

HYPERSONIC VEHICLE MODEL AND CONTROL LAW DEVELOPMENT USING H(INFINITY) AND MICRON SYNTHESIS

Irene M. Gregory, Rajiv S. Chowdhry, John D. McMinn, and John D. Shaughnessy Oct. 1994 43 p
(RTOP 505-70-64-01)
(NASA-TM-4562; L-17217; NAS 1.15:4562) Avail: CASI HC A03/MF A01

The control system design for a Single Stage To Orbit (SSTO) air breathing vehicle will be central to a successful mission because a precise ascent trajectory will preserve narrow payload margins. The air breathing propulsion system requires the vehicle to fly roughly halfway around the Earth through atmospheric turbulence. The turbulence, the high sensitivity of the propulsion system to inlet flow conditions, the relatively large uncertainty of the parameters characterizing the vehicle, and continuous acceleration make the problem especially challenging. Adequate stability margins must be provided without sacrificing payload mass since payload margins are critical. Therefore, a multivariable control theory capable of explicitly including both uncertainty and performance is needed. The H(infinity) controller in general provides good robustness but can result in conservative solutions for practical problems involving structured uncertainty. Structured singular value mu framework for analysis and synthesis is potentially much less conservative and hence more appropriate for problems with tight margins. An SSTO control system requires: highly accurate tracking of velocity and altitude commands while limiting angle-of-attack oscillations, minimized control power usage, and a stabilized vehicle when atmospheric turbulence and system uncertainty are present. The controller designs using H(infinity) and mu-synthesis procedures were compared. An integrated flight/propulsion dynamic mathematical model of a conical accelerator vehicle was linearized as the vehicle accelerated through Mach 8. Vehicle acceleration through the selected flight condition gives rise to parametric variation that was modeled as a structured uncertainty. The mu-analysis approach was used in the frequency domain to conduct controller analysis and was confirmed by time history plots. Results demonstrate the inherent advantages of the mu framework for this class of problems.
Author (revised)

N95-12858*# National Aeronautics and Space Administration. Goddard Space Flight Center, Greenbelt, MD.

SPACECRAFT ATTITUDE DETERMINATION ACCURACY FROM MISSION EXPERIENCE

D. Brasoveanu (Computer Sciences Corp., Lanham, MD.), J. Hashmall (Computer Sciences Corp., Lanham, MD.), and D. Baker Oct. 1994 96 p
(RTOP 550-00-00)
(NASA-TM-104613; Rept-95B00001; NAS 1.15:104613) Avail: CASI HC A05/MF A01

This document presents a compilation of the attitude accuracy attained by a number of satellites that have been supported by the Flight Dynamics Facility (FDF) at Goddard Space Flight Center (GSFC). It starts with a general description of the factors that influence spacecraft attitude accuracy. After brief descriptions of the missions supported, it presents the attitude accuracy results for currently active and older missions, including both three-axis stabilized and spin-stabilized spacecraft. The attitude accuracy results are grouped by the sensor pair used to determine the attitudes. A supplementary section is also included, containing the results of theoretical computations of the effects of variation of sensor accuracy on overall attitude accuracy. Author

N95-12879*# National Academy of Sciences - National Research Council, Washington, DC. Subcommittee on Spacecraft Maximum Allowable Concentrations.

SPACECRAFT MAXIMUM ALLOWABLE CONCENTRATIONS FOR SELECTED AIRBORNE CONTAMINANTS, VOLUME 1

1994 226 p
(Grant NAGw-2239)
(NASA-CR-196446; NAS 1.26:196446) Copyright Avail: CASI HC A11/MF A03

As part of its efforts to promote safe conditions aboard spacecraft, NASA requested the National Research Council (NRC) to develop guidelines for establishing spacecraft maximum allowable concentrations (SMAC's) for contaminants, and to review SMAC's for various spacecraft contaminants to determine whether NASA's recommended exposure limits are consistent with the guidelines recommended by the subcommittee. In response to NASA's request, the NRC organized the Subcommittee on Guidelines for Developing Spacecraft Maximum Allowable Concentrations for Space Station Contaminants within the Committee on Toxicology (COT). In the first phase of its work, the subcommittee developed the criteria and methods for preparing SMAC's for spacecraft contaminants. The subcommittee's report, entitled Guidelines for Developing Spacecraft Maximum Allowable Concentrations for Space Station Contaminants, was published in 1992. The executive summary of that report is reprinted as Appendix A of this volume. In the second phase of the study, the Subcommittee on Spacecraft Maximum Allowable Concentrations reviewed reports prepared by NASA scientists and contractors recommending SMAC's for 35 spacecraft contaminants. The subcommittee sought to determine whether the SMAC reports were consistent with the 1992 guidelines. Appendix B of this volume contains the first 11 SMAC reports that have been reviewed for their application of the guidelines developed in the first phase of this activity and approved by the subcommittee. Derived from text

N95-12921 Naval Postgraduate School, Monterey, CA.

LIFETIME AND REENTRY PREDICTION FOR THE PETITE AMATEUR NAVY SATELLITE (PANSAT) M.S. Thesis

Daniel J. Cuff 16 Jun. 1994 80 p Limited Reproducibility: More than 20% of this document may be affected by microfiche quality
(AD-A283366) Avail: CASI HC A05

The Naval Postgraduate School (NPS) is developing a small satellite for digital communications in the amateur frequency band. The Petite Amateur Navy Satellite (PANSAT) will primarily act as an orbiting spread-spectrum communications laboratory, possesses neither an attitude control nor a propulsion system, and is designed to 'tumble' along its orbital path once it is released from the launch vehicle which is scheduled to be the space shuttle. An explanation of the many variables and assumptions affecting PANSAT is provided as insight for the lifetime and reentry predictions. Using a conservative approach, results from combining altitudes and inclinations from expected space shuttle missions, solar flux and magnetic indices from three different sources, and the use of an orbital propagator program, LIFETIME 4.1, which was developed by Aerospace Corporation, attest that the minimum 2 year lifetime requirement for PANSAT will be met by nine shuttle missions between July 1996 and December 1997. A reentry analysis concluded that PANSAT will experience sufficient aerodynamic forces to cause structural failure and breakup during atmospheric reentry. DTIC

N95-13006*# Duke Univ., Durham, NC. Dept. of Mechanical Engineering and Materials Science.

A MAGNETIC SHIELD/DUAL PURPOSE MISSION Final Report, 1993 - 1994

Seth Watkins, Jamil Albertelli, R. Braden Copeland, Eric Correll, Chris Dales, Dana Davis, Nechole Davis, Rob Duck, Sandi Feaster, and Patrick Grant et al Jul. 1994 26 p Prepared for Universities Space Research Association, Columbia, MD
(Contract NASw-4435)
(NASA-CR-197192; NAS 1.26:197192) Avail: CASI HC A03/MF A01

The objective of this work is to design, build, and fly a dual-purpose payload whose function is to produce a large volume, low intensity magnetic

field and to test the concept of using such a magnetic field to protect manned spacecraft against particle radiation. An additional mission objective is to study the effect of this moving field on upper atmosphere plasmas. Both mission objectives appear to be capable of being tested using the same superconducting coil. The potential benefits of this magnetic shield concept apply directly to both earth-orbital and interplanetary missions. This payload would be a first step in assessing the true potential of large volume magnetic fields in the U.S. space program. Either converted launch systems or piggyback payload opportunities may be appropriate for this mission. The use of superconducting coils for magnetic shielding against solar flare radiation during manned interplanetary missions has long been contemplated and was considered in detail in the years preceding the Apollo mission. With the advent of new superconductors, it has now become realistic to reconsider this concept for a Mars mission. Even in near-earth orbits, large volume magnetic fields produced using conventional metallic superconductors allow novel plasma physics experiments to be contemplated. Both deployed field-coil and non-deployed field-coil shielding arrangements have been investigated, with the latter being most suitable for an initial test payload in a polar orbit. Author

N95-13138# Amptek, Inc., Bedford, MA.
DETAILED COMPONENT DESIGN FOR A COMPACT ENVIRONMENTAL ANOMALY SENSOR (CEASE)
John O. McGarity, Alan C. Huber, John A. Pantazis, David J. Sperry, and Hugh Anderson 25 Mar. 1994 74 p
(Contract F19628-90-C-0159)
(AD-A283144; PL-TR-94-2132; AD-E202116; SR-3) Avail: CASI HC A04/MF A01

The outer space environment experienced by a modern, electronically sophisticated spacecraft can be very hostile due to interaction between its complex, sensitive electronics systems and the naturally occuring energetic particle population indigenous to the solar system. The Compact Environmental Anomaly Sensor (CEASE) is being developed as a small, low-power device to monitor space 'weather' and provide autonomous warnings of conditions that may cause operational anomalies in a host spacecraft. CEASE uses a two-element solid-state telescope and two radiation dosimeters to sample critical energetic particle fluxes and uses a sophisticated real-time processing program that can forecast hazardous environmental conditions before they effect the spacecraft. The spacecraft, in turn, can reprioritize its operations, inhibit any anomaly sensitive operations such as attitude adjustments, or take any other prudent action suggested by the potential of erratic conditions. The CEASE instrument is forecast to be packaged as a 4 inch cube weighing 2 pounds and dissipating a maximum of 2 watts. DTIC

N95-13194*# National Aeronautics and Space Administration. Lewis Research Center, Cleveland, OH.
EVALUATION OF WIRING CONSTRUCTIONS FOR SPACE APPLICATIONS
Ahmad N. Hammoud (NYMA, Inc., Brook Park, OH.), Mark W. Stavnes (NYMA, Inc., Brook Park, OH.), John E. Dickman, Linda A. Burkhardt, Lynn M. Woodford, James R. Ide, and Ed Muegge Oct. 1994 6 p Presented at the 1994 International Symposium on Electrical Insulation, Pittsburgh, PA, 5-8 Jun. 1994; sponsored by the IEEE Dielectrics and Electrical Insulation Society
(Contracts NAS1-18580; NAS3-25266; NAS3-27186; RTOP 323-57-4A)
(NASA-TM-106735; E-9129; NAS 1.15:106735) Avail: CASI HC A02/MF A01

A NASA Office of Safety and Mission Assurance (OS&MA) program to develop lightweight, reliable, and safe wiring insulations for aerospace applications is being performed by the NASA Lewis Research Center (LeRC). As part of this effort, a new wiring construction utilizing high strength PTFE (poly tetrafluoroethylene) as the insulation has been tested and compared with the existing military standard polyimide-based MIL-W-81381 wire construction. Electrical properties which were investigated included ac corona inception and extinction voltages (sea level and 60,000 feet), time/current to smoke, and wire fusing time. The two constructions were also characterized in terms of their mechanical properties of flexural strength, abrasion resistance (23 C and 150 C), and dynamic cut-through (23 C and 200 C). The results obtained in this testing effort are presented and discussed in this paper. Author

N95-13195*# Lockheed Missiles and Space Co., Sunnyvale, CA.
DEVELOPMENT OF THE CSI PHASE-3 EVOLUTIONARY MODEL TESTBED
M. J. Gronet, D. A. Davis, and M. K. Tan Oct. 1994 119 p
(Contract NAS1-19241; RTOP 233-01-01-07)
(NASA-CR-4630; LMSC/P086632; NAS 1.26:4630) Avail: CASI HC A06/MF A02

This report documents the development effort for the reconfiguration of the Controls-Structures Integration (CSI) Evolutionary Model (CEM) Phase-2 testbed into the CEM Phase-3 configuration. This step responds to the need to develop and test CSI technologies associated with typical planned earth science and remote sensing platforms. The primary objective of the CEM Phase-3 ground testbed is to simulate the overall on-orbit dynamic behavior of the EOS AM-1 spacecraft. Key elements of the objective include approximating the low-frequency appendage dynamic interaction of EOS AM-1, allowing for the changeout of components, and simulating the free-free on-orbit environment using an advanced suspension system. The fundamentals of appendage dynamic interaction are reviewed. A new version of the multiple scaling method is used to design the testbed to have the full-scale geometry and dynamics of the EOS AM-1 spacecraft, but at one-tenth the weight. The testbed design is discussed, along with the testing of the solar array, high gain antenna, and strut components. Analytical performance comparisons show that the CEM Phase-3 testbed simulates the EOS AM-1 spacecraft with good fidelity for the important parameters of interest. Author

N95-13232# Martin Marietta Space Systems, Inc., Denver, CO. Astronautics Group.
CRYOGENIC ON-ORBIT LIQUID DEPOT STORAGE, ACQUISITION, AND TRANSFER SATELLITE (COLD-SAT) FEASIBILITY STUDY Final Report, Feb. 1988 - Jun. 1990
William J. Bailey, Stephen P. Weiner, Douglas H. Beekman, Mark F. Dennis, and Timothy A. Martin Jun. 1990 299 p
(Contract NAS3-25063; RTOP 506-48-21)
(NASA-CR-185247; NAS 1.26:185247; MCR-90-1307) Avail: CASI HC A13/MF A03

The Cryogenic On-Orbit Liquid Depot Storage, Acquisition, and Transfer Satellite (COLD-SAT) is an experimental spacecraft launched from an expendable launch vehicle which is designed to investigate the systems and technologies required for efficient, effective, and reliable management of cryogenic fluid in the reduced gravity space environment. The COLD-SAT program will provide the necessary data base and provide low-g proving of fluid and thermal models of cryogenic storage, transfer, and resupply concepts and processes. A conceptual approach was developed and an overview of the results of the 24 month COLD-SAT Phase A feasibility is described which includes: (1) a definition of the technology needs and the accompanying experimental 3 month baseline mission; (2) a description of the experiment subsystem, major features and rationale for satisfaction of primary and secondary experiment requirements using liquid hydrogen as the test fluid; and (3) a presentation of the conceptual design of the COLD-SAT spacecraft subsystems which support the on-orbit experiment with emphasis on areas of greatest challenge. Author

N95-13236*# National Aeronautics and Space Administration. Lewis Research Center, Cleveland, OH.
SPACE STATION FREEDOM PROPULSION ACTIVITIES
David A. Spera, ed. Apr. 1990 22 p
(NASA-TM-108604; NAS 1.15:108604; DAAP-LEW-146939) Avail: CASI HC A03/MF A01

The technical highlights and accomplishments made at NASA LeRC in the development of the Space Station Freedom (SSF) propulsion system are discussed. The objectives are as follows: develop and characterize resistojet-thruster components and assemblies; develop and characterize hydrogen-oxygen thruster components; and conduct system trade studies. The research projects primarily characterize propulsion performance and life. Other tests include environmental impacts, such as exhaust gas profiles and electromagnetic interference. The technical activities that are highlighted are being conducted at LeRC within the Aerospace Technology and Space Station Freedom directorates. These activities include the following: derivation of design analysis models; trade studies of design options; propulsion system impact studies; and component testing for characterization and design verification. Author

N95-13581*# Utah State Univ., Logan, UT.
SolSTUS: SOLAR SOURCE THERMAL UPPER STAGE
1994 44 p Prepared for Universities Space Research Association, Columbia, MD
(Contract NASw-4435)
(NASA-CR-197179; NAS 1.26:197179) Avail: CASI HC A03/MF A01

This paper was written by members of the Utah State University (USU) Space Systems Design class, fall quarter 1993. The class is funded by NASA and administered by the University Space Research Association (USRA). The focus of the class is to give students some experience in design of space systems and as a source of original ideas for NASA. This paper is a summary of the work done by members of the Space Systems Design class during the opening phase of the course. The class was divided into groups to work on different areas of the Solar Thermal Rocket (STR) booster in order to produce a design reference mission that would identify the key design issues. The design reference mission focused upon a small satellite mission to Mars. There are several critical components in a Solar Thermal Rocket. STR's produce a very low thrust, but have a high specific impulse, meaning that they take longer to reach the desired orbit, but use a lot less fuel in doing it. The complexity of the rocket is discussed in this paper. Some of the more critical design problems discussed are: (1) the structural and optical complexity of collecting and focusing sunlight onto a specific point, (2) long term storage of fuel (liquid hydrogen), (3) attitude control while thrusting in an elliptical orbit and orienting the mirrors to collect sunlight, and (4) power and communications for the rocket and it's internal systems. The design reference mission discussed here is a very general mission to Mars. A first order trajectory design has been done and a possible basic science payload for Mars has been suggested. This paper summarizes the design reference mission (DRM) formulated by the USU students during fall quarter and identifies major design challenges that will confront the design team during the next two quarters here at USU. Author (revised)

19 SPACECRAFT INSTRUMENTATION

For related information see also *06 Aircraft Instrumentation* and *35 Instrumentation and Photography.*

N95-11805*# Michigan Univ., Ann Arbor, MI. Space Physics Research Lab.
PIONEER VENUS ORBITER ELECTRON TEMPERATURE PROBE Final Report
Larry H. Brace Sep. 1994 10 p
(Grant NAG2-644)
(NASA-CR-196844; NAS 1.26:196844) Avail: CASI HC A02/MF A01

This document lists the scientific accomplishments of the Orbiter Electron Temperature Probe (OETP) group. The OETP instrument was fabricated in 1976, integrated into the PVO spacecraft in 1977, and placed in orbit about Venus in December 1978. The instrument operated flawlessly for nearly 14 years until PVO was lost as it entered the Venusian atmosphere in October 1992. The OETP group worked closely with other PVO investigators to examine the Venus ionosphere and its interactions with the solar wind. After the mission was completed we continued to work with the scientist selected for the Venus Data Analysis Program (VDAP), and this is currently leading to additional publications. Derived from text

20 SPACECRAFT PROPULSION AND POWER

Includes main propulsion systems and components, e.g., rocket engines; and spacecraft auxilliary power sources.

For related information see also *07 Aircraft Propulsion and Power, 28 Propellants and Fuels, 44 Energy Production and Conversion,* and *15 Launch Vehicles and Space Vehicles.*

N95-11782# Los Alamos National Lab., NM.
NUCLEAR ROCKETS: HIGH-PERFORMANCE PROPULSION FOR MARS
C. W. Watson May 1994 28 p
(Contract W-7405-eng-36)
(DE94-013642; LA-12784-MS) Avail: CASI HC A03/MF A01

A new impetus to manned Mars exploration was introduced by President Bush in his Space Exploration Initiative. This has led, in turn, to a renewed interest in high-thrust nuclear thermal rocket propulsion (NTP). The purpose of this report is to give a brief tutorial introduction to NTP and provide a basic understanding of some of the technical issues in the realization of an operational NTP engine. Fundamental physical principles are outlined from which a variety of qualitative advantages of NTP over chemical propulsion systems derive, and quantitative performance comparisons are presented for illustrative Mars missions. Key technologies are described for a representative solid-core heat-exchanger class of engine, based on the extensive development work in the Rover and NERVA nuclear rocket programs (1955 to 1973). The most driving technology, fuel development, is discussed in some detail for these systems. Essential highlights are presented for the 19 full-scale reactor and engine tests performed in these programs. On the basis of these tests, the practicality of graphite-based nuclear rocket engines was established. Finally, several higher-performance advanced concepts are discussed. These have received considerable attention, but have not, as yet, developed enough credibility to receive large-scale development. DOE

N95-11823*# Rockwell International Corp., Downey, CA.
INTEGRATED PROPULSION TECHNOLOGY DEMONSTRATOR. PROGRAM PLAN
15 Aug. 1994 91 p
(Contract NCC1-193)
(NASA-CR-196870; NAS 1.26:196870; SSD94D0207) Avail: CASI HC A05/MF A01

NASA and Rockwell have embarked on a cooperative agreement to define, develop, fabricate, and operate an integrated propulsion technology demonstrator (IPTD) for the purpose of validating design, process, and technology improvements of launch vehicle propulsion systems. This program, a result of NRA8-11, Task Area 1 A, is jointly funded by both NASA and Rockwell and is sponsored by the Reusable Launch Vehicle office at NASA Marshall Space flight Center. This program plan provides to the joint NASA/Rockwell integrated propulsion technology demonstrator (IPTD) team a description of the activities within tasks / sub tasks and associated schedules required to successfully achieve program objectives. This document also defines the cost elements and manpower allocations for each sub task for purpose of program control. This plan is updated periodically by developing greater depth of direction for outyear tasks as the program matures. Updating is accomplished by adding revisions to existing pages or attaching page revisions to this plan. In either case, revisions will be identified by appropriate highlighting of the change, or specifying a revision page through the use of footnotes on the bottom right of each change page. Authorization for the change is provided by the principal investigators to maintain control of this program plan document and IPTD program activities. Author

N95-11919*# NYMA, Inc., Brook Park, OH. Engineering Services Div.
STATIONARY PLASMA THRUSTER ION VELOCITY DISTRIBUTION Final Report
David H. Manzella Aug. 1994 13 p Presented at the 30th Joint Propulsion Conference, Indianapolis, IN, 27-29 Jun. 1994; sponsored by AIAA, ASME, SAE, and ASEE Original contains color illustrations
(Contract NAS3-27186; RTOP 506-42-31)
(NASA-CR-195379; E-9094; NAS 1.26:195379; AIAA Paper 94-3141)
Avail: CASI HC A03/MF A01; 1 functional color page

A nonintrusive velocity diagnostic based on laser induced fluorescence of the 5d4F(5/2)-6p4D(5/2) singly ionized xenon transition was used to interrogate the exhaust of a 1.5 kW Stationary Plasma Thruster (SPT). A detailed map of plume velocity vectors was obtained using a simplified, cost-effective, nonintrusive, semiconductor laser based scheme. Circumferential velocities on the order of 250 m/s were measured which implied induced momentum torques of approximately 5 x 10(exp -2) N-cm. Axial and radial velocities were evaluated one mm downstream of the cathode at several locations across the width of the annular acceleration channel. Radial velocities varied linearly with radial distance. A maximum radial velocity of 7500 m/s was measured 8 mm from the center of the channel. Axial velocities as large as 16,500 m/s were measured. Author

N95-12507# Air Force Office of Scientific Research, Bolling AFB, Washington, DC.
AFOSR CONTRACTORS MEETING IN PROPULSION

M. A. Birkan and J. M. Tishkoff 13 Jul. 1994 311 p Meeting held in Lake Tahoe, NV, 8-10 Jun. 1994
(AF Proj. 2308)
(AD-A282729; AFOSR-TR-94-0463) Avail: CASI HC A14/MF A03

Abstracts are given for research in airbreathing combustion, rocket propulsion, and diagnostics in reacting media supported by the Air Force Office of Scientific Research. DTIC

N95-12604*# Michigan Univ., Ann Arbor, MI. Dept. of Aerospace Engineering.
ATHENA: ADVANCED AIR LAUNCHED SPACE BOOSTER
Corey G. Booker, John Ziemer, John Plonka, Scott Henderson, Paul Copioli, Charles Reese, Christopher Ullman, Jeremy Frank, Alan Breslauer, and Hristos Patonis et al Jun. 1994 251 p Prepared for Universities Space Research Association, Columbia, MD
(Contract NASw-4435)
(NASA-CR-197148; NAS 1.26:197148) Avail: CASI HC A12/MF A03

The infrastructure for routine, reliable, and inexpensive access of space is a goal that has been actively pursued over the past 50 years, but has yet not been realized. Current launch systems utilize ground launching facilities which require the booster vehicle to plow up through the dense lower atmosphere before reaching space. An air launched system on the other hand has the advantage of being launched from a carrier aircraft above this dense portion of the atmosphere and hence can be smaller and lighter compared to its ground based counterpart. The goal of last year's Aerospace Engineering Course 483 (AE 483) was to design a 227,272 kg (500,000 lb.) air launched space booster which would beat the customer's launch cost on existing launch vehicles by at least 50 percent. While the cost analysis conducted by the class showed that this goal could be met, the cost and size of the carrier aircraft make it appear dubious that any private company would be willing to invest in such a project. To avoid this potential pitfall, this year's AE 483 class was to design as large an air launched space booster as possible which can be launched from an existing or modification to an existing aircraft. An initial estimate of the weight of the booster is 136,363 kg (300,000 lb.) to 159,091 kg (350,000 lb.). Derived from text

N95-12622*# NYMA, Inc., Brook Park, OH. Engineering Services Div.
STATUS OF HOLLOW CATHODE HEATER DEVELOPMENT FOR THE SPACE STATION PLASMA CONTACTOR Final Report
George C. Soulas Jul. 1994 17 p Presented at the 30th Propulsion Conference, Indianapolis, IN, 27-29 Jun. 1994; cosponsored by AIAA, ASME, SAE, and ASEE
(Contract NAS3-25266; RTOP 474-46-10)
(NASA-CR-195364; E-9030; AIAA Paper 94-3309; NAS 1.26:195364)
Avail: CASI HC A03/MF A01

A hollow cathode-based plasma contactor has been selected for use on the Space Station. During the operation of the plasma contactor, the hollow cathode heater will endure approximately 12000 thermal cycles. Since a hollow cathode heater failure would result in a plasma contactor failure, a hollow cathode heater development program was established to produce a reliable heater. The development program includes the heater design, process documents for both heater fabrication and assembly, and heater testing. The heater design was a modification of a sheathed ion thruster cathode heater. Heater tests included testing of the heater unit alone and plasma contactor and ion thruster testing. To date, eight heaters have been or are being processed through heater unit testing, two through plasma contactor testing and three through ion thruster testing, all using direct current power supplies. Comparisons of data from heater unit performance tests before cyclic testing, plasma contactor tests, and ion thruster tests at the ignition input current level show the average deviation of input power and tube temperature near the cathode tip to be +/-0.9 W and +/- 21 C, respectively. Heater unit testing included cyclic testing to evaluate reliability under thermal cycling. The first heater, although damaged during assembly, completed 5985 ignition cycles before failing. Four additional heaters successfully completed 6300, 6300, 700, and 700 cycles. Heater unit testing is currently ongoing for three heaters which have to date accumulated greater than 7250, greater than 5500, and greater than 5500 cycles, respectively. Author

N95-12630*# Vanderbilt Univ., Nashville, TN. Dept. of Mechanical Engineering.
[VARIOUS ADVANCED DESIGN PROJECTS PROMOTING ENGINEERING EDUCATION] Final Report
1994 135 p Prepared for Universities Space Research Association, Columbia, MD Original contains color illustrations
(Contract NASw-4435)
(NASA-CR-197170; NAS 1.26:197170) Avail: CASI HC A07/MF A02; 6 functional color pages

The Universities Space Research Association (USRA) Advanced Design Program (ADP) program promotes engineering education in the field of design by presenting students with challenging design projects drawn from actual NASA interests. In doing so, the program yields two very positive results. Firstly, the students gain a valuable experience that will prepare them for design problems with which they will be faced in their professional careers. Secondly, NASA is able to use the work done by students as an additional resource in meeting its own design objectives. The 1994 projects include: Universal Test Facility; Automated Protein Crystal Growth Facility; Stiffening of the ACES Deployable Space Boom; Launch System Design for Access to Space; LH2 Fuel Tank Design for SSTO Vehicle; and Feed System Design for a Reduced Pressure Tank. CASI

N95-12750*# National Aeronautics and Space Administration. Lewis Research Center, Cleveland, OH.
RECYCLE REQUIREMENTS FOR NASA'S 30 cm XENON ION THRUSTER
Luis R. Pinero and Vincent K. Rawlin Sep. 1994 13 p Presented at the 30th Joint Propulsion Conference, Indianapolis, IN, 27-29 Jun. 1994; sponsored by AIAA, SAE, ASME, and ASEE
(RTOP 232-02-02)
(NASA-TM-106668; E-9151; NAS 1.15:106668) Avail: CASI HC A03/MF A01

Electrical breakdowns have been observed during ion thruster operation. These breakdowns, or arcs, can be caused by several conditions. In flight systems, the power processing unit must be designed to handle these faults autonomously. This has a strong impact on power processor requirements and must be understood fully for the power processing unit being designed for the NASA Solar Electric Propulsion Technology Application Readiness program. In this study, fault conditions were investigated using a NASA 30 cm ion thruster and a power console. Power processing unit output specifications were defined based on the breakdown phenomena identified and characterized. Author

N95-12819*# Martin Marietta Corp., Denver, CO. Astronautics Group.
SPACE STATION MODULE POWER MANAGEMENT AND DISTRIBUTION SYSTEM (SSM/PMAD) Final Report
William Miller, comp., Daniel Britt, comp., Michael Elges, comp., and Chris Myers, comp. May 1994 591 p
(Contract NAS8-36433)
(NASA-CR-193991; NAS 1.26:193991; MCR-94-1315) Avail: CASI HC A25/MF A06

This report provides an overview of the Space Station Module Power Management and Distribution (SSM/PMAD) testbed system and describes recent enhancements to that system. Four tasks made up the original contract: (1) common module power management and distribution system automation plan definition; (2) definition of hardware and software elements of automation; (3) design, implementation and delivery of the hardware and software making up the SSM/PMAD system; and (4) definition and development of the host breadboard computer environment. Additions and/or enhancements to the SSM/PMAD test bed that have occurred since July 1990 are reported. These include: (1) rehosting the MAESTRO scheduler; (2) reorganization of the automation software internals; (3) a more robust communications package; (4) the activity editor to the MAESTRO scheduler; (5) rehosting the LPLMS to execute under KNOMAD; implementation of intermediate levels of autonomy; (6) completion of the KNOMAD knowledge management facility; (7) significant improvement of the user interface; (8) soft and incipient fault handling design; (9) intermediate levels of autonomy, and (10) switch maintenance. CASI

N95-12885 Naval Postgraduate School, Monterey, CA.
INVESTIGATION OF THE EFFECTS OF SOLID ROCKET MOTOR PROPELLANT COMPOSITION ON PLUME SIGNATURE M.S. Thesis

Clay J. Snaza 16 Jun. 1994 65 p Limited Reproducibility: More than 20% of this document may be affected by microfiche quality
(AD-A283365) Avail: CASI HC A04

Three propellants with aluminum/silicon weight percentages of 18/0%, 13.5/4.5%, and 12/6% were fired in a subscale motor to determine if the plume infrared signature could be reduced without a significant loss in specific impulse. Spectral measurements from 2.5 to 5.5 micrometers and thermal measurements from 3.5 to 5.0 micrometers were made. Plume particle size measurements showed that only particles with small diameters (less than 1.93 micrometers) were present with any significant volume. Replacing a portion of the aluminum in a highly metallized solid propellant with silicon was found to eliminate the Al2O3 in favor of SiO2 and Al6SiO13, without any change in particulate mass concentration or any large change in particle size distribution. These particulates were found to have significantly lower absorptivity than Al2O3. An additional investigation was conducted to determine the particle size distribution at the nozzle entrance. Malvern ensemble scattering, phase-Doppler single particle scattering, and laser transmittance measurements made through windows in the combustion chamber at the nozzle entrance indicated that large particles were present (to 250 micrometers). However, most of the mass of the particles was contained in particles with diameters smaller than 5 micrometers. Approximate calculations made with the measured data showed that if 100 micrometer particles are present with the smoke (particles with diameters less than 2 micrometers) they could account for only approximately 10% of the article volume. DTIC

N95-13237*# General Dynamics Corp., San Diego, CA. Space Systems Div.
CRYOGENIC ON-ORBIT LIQUID DEPOT STORAGE, ACQUISITION, AND TRANSFER SATELLITE (COLD-SAT) Feasibility Study Final Report, Mar. 1988 - Feb. 1990
John R. Schuster, Edwin J. Russ, and Joseph P. Wachter Jul. 1990 413 p
(Contract NAS3-25062)
(NASA-CR-185249; NAS 1.26:185249) Avail: CASI HC A18/MF A04

The Cryogenic On-Orbit Liquid Depot Storage, Acquisition, and Transfer Satellite (COLD-SAT) will perform subcritical liquid hydrogen handling experiments under low gravity conditions to provide engineering data for future space transportation missions. Comprising the four Class 1 enabling experiments are tank press control, tank chilldown, tank no-vent fill, and liquid acquisition device fill/refill. The nine Class 2 enhancing experiments are tanker thermal performance, pressurization, low-gravity setting and outflow, liquid acquisition device performance, transfer line chilldown, outflow subcooling, low-gravity vented fill, fluid dumping, and advanced instrumentation. Consisting of an experiment module mated to a spacecraft bus, COLD-SAT will be placed in an initial 1300 km circular orbit by an Atlas commercial launch vehicle, and will perform experiments in a semi-autonomous mode for a period of up to six months. The three-axis controlled spacecraft bus provides electric power, control and data management, communications, and attitude control along with propulsive acceleration levels ranging from 10(exp -6) to 10(exp -4) g. It is desired to understand the effects that low acceleration levels might have on the heat and mass transfer processes involved in some of the experiments. The experiment module contains the three liquid hydrogen tanks, valves, pressurization and pumping equipment, and instrumentation. Within the highly insulated tanks are specialized fluid management equipment that might be used in future space transportation systems. At launch all the liquid hydrogen for the experiments is contained in the largest tank, which has helium-purged insulation to prevent cryo-pumping of air on the launch pad. The tank is loaded by the hydrogen tanking system used for the Centaur upper stage of the Atlas. After reaching orbit the two smaller tanks become receivers for fluid transfers, and when tanked, become the vessels for performing many of the experiments. Author

N95-13347*# National Aeronautics and Space Administration. Lewis Research Center, Cleveland, OH.
A LOW-EROSION STARTING TECHNIQUE FOR HIGH-PERFORMANCE ARCJETS
John M. Sankovic and Francis M. Curran Sep. 1994 17 p Presented at the 30th Joint Propulsion Conference, Indianapolis, IN, 27-29 Jun. 1994; sponsored by AIAA, ASME, SAE, and ASEE
(RTOP 506-42-31)
(NASA-TM-106627; E-8921; NAS 1.15:106627) Avail: CASI HC A03/MF A01

The NASA arcjet program is currently sponsoring development of high specific impulse thrusters for next generation geosynchronous communications satellites (2 kW-class) and low-power arcjets for power limited spacecraft (approx. 0.5 kW-class). Performance goals in both of these efforts will require up to 1000 starts at propellant mass flow rates significantly below those used in state-of-the-art arcjet thruster systems (i.e., high specific power levels). Reductions in mass flow rate can lead to damaging modes of operation, particularly at thruster ignition. During the starting sequence, the gas dynamic force due to low propellant flow is often insufficient to rapidly push the arc anode attachment to its steady-state position in the diverging section of the nozzle. This paper describes the development and demonstration of a technique which provides for non-damaging starts at low steady-state flow rates. The technique employs a brief propellant pressure pulse at ignition to increase gas dynamic forces during the critical ignition/transition phase of operation. Starting characteristics obtained using both pressure-pulsed and conventional starting techniques were compared across a wide range of propellant flow rates. The pressure-pulsed starting technique provided reliable starts at mass flow rates down to 21 mg/s, typically required for 700 s specific impulse level operation of 2 kW thrusters. Following the comparison, a 600 start test was performed across a wide flow rate range. Post-test inspection showed minimal erosion of critical arcjet anode/nozzle surfaces. Author

23 CHEMISTRY AND MATERIALS (GENERAL)

N95-11844 Cornell Univ., Ithaca, NY.
AMINE CATALYZED INTRAMOLECULAR IMIDIZATION OF ALKYL AND ARYL PHTHALAMATES, KINETICS AND MECHANISM IN DEUTERATED CHLOROFORM
Man-Kit Leung and Jean M. Frechet 30 Jun. 1994 28 p Limited Reproducibility: More than 20% of this document may be affected by microfiche quality
(Contract N00014-91-J-1338)
(AD-A281741; TR-18) Avail: CASI HC A03

The kinetics of the amine catalyzed intramolecular imidization of alkyl and phenyl phthalamates with a variety of amines were measured in deuterated chloroform at 40.1 deg C. An overall second-order kinetic rate law, rate = k sub overall (amine)(phthalamate), was obtained from our experiments. Although pre-association between the amides and the amines through hydrogen bonding interaction was suggested by proton NMR spectroscopy, the catalytic ability of amines was found to be related to their basicity rather than to their hydrogen-bonding ability or nucleophilicity. This observation implies the involvement of proton transfer from the amide to the amine in the critical transition state. In addition, by changing the leaving group from phenoxy to n-butoxy group, the reaction rate constants decrease by a factor of 30 to 70. On the basis of these kinetic results, we propose that the intramolecular imidization proceeds through an amine assisted cyclization to a zwitterionic intermediate, followed by the expulsion of the alkoxy or phenoxy group to provide phthalimide and the corresponding alcohol. DTIC

N95-11891*# Vanderbilt Univ., Nashville, TN. Center for the Space Processing of Engineering Materials.
[RESEARCH ACTIVITIES OF THE CENTER FOR THE SPACE PROCESSING OF ENGINEERING MATERIALS] Final Technical Report, 15 Sep. 1985 - 31 Mar. 1993
J. L. Davidson 1994 4 p
(Grant NAGw-810)
(NASA-CR-196484; NAS 1.26:196484) Avail: CASI HC A01/MF A01

A bibliography is provided of materials presentations and publications resulting from NAGW-810. CASI

N95-12551 Defence Research Establishment Ottawa, Ottawa (Ontario).
NOVEL ACTIVATED CARBON IMPREGNANTS CONSISTING OF TRANSITION METAL COMPLEXES. PART 1: BACKGROUND, SYNTHESES AND CHARACTERIZATIONS

S. H. Liang, J. M. Whalen, R. L. Cooperstock, and B. O. Patrick Dec. 1993 81 p Limited Reproducibility: More than 20% of this document may be affected by microfiche quality
(AD-A282583; DREO-1197-Pt-1) Avail: CASI HC A05

In the search for novel impregnants for activated carbon to enhance its chemical activity, a variety of organometallic complexes containing transition metals which may be used as impregnants have been synthesized. Copper, chromium, cobalt and silver are the transition metals employed. The ligands studied included triethylenediamine (TEDA), quinuclidine (QUIN), acetylacetonate (acac) and its fluoro-derivative, hexafluoroacetylacetonate (hfac), and some cyclic dienes such as 1,5-cyclooctadiene (1,5-COD). In all, three classes of organometallic complexes were studied. The first class consisted of metal salts using TEDA (or QUIN) as ligands. The second class consisted of transition metals using acetylacetone, and TEDA (or QUIN) as ligands. The last class consisted of transition metals, using acetylacetonate and cyclic dienes as ligands. In this report, the synthetic routes and the characterization of these organometallic complexes obtained by various spectroscopic techniques are detailed. DTIC

N95-12613 Edgewood Research Development and Engineering Center, Aberdeen Proving Ground, MD.
PHENOXYTHIOCARBONYLATION AND DEOXYGENATION OF ARYL TRIFLUOROMETHYL CARBINOLS Final Report, Oct. 1992 - Jun. 1993
Fu-Lian Hsu, Frederic J. Berg, Xiaoyan Zhang, Seoung-Soo Hong, and Duane D. Miller Apr. 1994 17 p Limited Reproducibility: More than 20% of this document may be affected by microfiche quality
(DA Proj. 1O1-61102-A-71-A)
(AD-A280519; ERDEC-TR-153) Avail: CASI HC A03

Methods for the selective replacement of the OH group by H are very useful in organic transformations and the preparation of biologically active compounds. The most commonly used method for deoxygenation is the catalytic reduction under acidic conditions. However, deoxygenation does not take place when CF3 is attached at the benzylic carbon. This could be due to the electron-withdrawing property of CF3, which destabilizes the carbonium ion intermediate. Thus, free radical reactions were selected for reductive cleavage of the C-0 Bond. The thiocarbonylation of secondary alcohols and tertiary alcohols carrying an imidazole moiety at the 4-position, followed by the homolytic deoxygenation, yields the deoxygenated products in good yield. DTIC

N95-12662*# National Aeronautics and Space Administration. Lewis Research Center, Cleveland, OH.
ROOM-TEMPERATURE SYNTHESIS OF CuInQ2 (Q = S OR Se) IN NON-AQUEOUS SOLUTION USING AN ORGANOINDIUM REAGENT
Aloysius F. Hepp, Maria T. Andras, Christopher C. Landry, and Andrew R. Barron Jul. 1994 8 p Presented at the Fall Meeting, Boston, MA, 29 Nov. - 3 Dec. 1993; sponsored by Materials Research Society
(Grant NGT-50942; RTOP 233-01-0A)
(NASA-TM-106557; E-8717; NAS 1.15:106557) Avail: CASI HC A02/MF A01

We have discovered a novel two-phase synthesis of CuInSe2 at 25 deg C from Cu2Se and (C5H5)3In in 4-methylpyridine (4-MePy). An analogous reaction to produce CuInS2 must be run at 140 deg C in refluxing 4-MePy in the presence of 2-mercaptopyridine. Microscopy of CuInSe2 produced at 25 deg C shows it to be platelet-shaped crystallites with an approximate particle size of 10 microns, less than 2 percent C and H, with a small amount of unidentified crystalline impurity. Our results demonstrate that it is possible to produce from solution a material that is ordinarily synthesized in bulk or films at much higher temperatures or using extraneous reagents and/or electrons. Author

N95-12692*# National Aeronautics and Space Administration. Lewis Research Center, Cleveland, OH.
ONE-STEP SYNTHESIS OF DITHIOCARBAMATES FROM METAL POWDERS
Aloysius F. Hepp, David G. Hehemann, Stan A. Duraj, Eric B. Clark, William E. Eckles, and Phillip E. Fanwick Jul. 1994 8 p Presented at the Fall Meeting, Boston, MA, 29 Nov. - 3 Dec. 1993; sponsored by the Materials Research Society
(Contracts NCC3-318; NCC3-162; NCC3-246; RTOP 233-01-0A)
(NASA-TM-106558; E-8718; NAS 1.15:106558) Avail: CASI HC A02/MF A01

Neutral metal dithiocarbamate complexes (M(NR2CS2)X) are well-known precursors to metal sulfides, a class of materials with numerous technological applications. We are involved in a research effort to prepare new precursors to metal sulfides using simple, reproducible synthetic procedures. We describe the results of our synthetic and characterization studies for M = Fe, Co, Ni, Cu. and In. For example, treatment of metallic indium with tetramethylthiuram disulfide (tmtd) in 4-methylpyridine (4-Mepy) at 25 deg C produces a new homoleptic indium (III) dithiocarbamate, In(N(CH3)2CS2)3(I), in yields of over 60 percent. The indium (III) dithiocarbamate was characterized by X-ray crystallography; (I) exists in the solid state as discrete distorted-octahedral molecules. Compound (I) crystallizes in the P1bar (No. 2) space group with lattice parameters: a = 9.282(1) A, b = 10.081(1) A, c = 12.502 A, alpha = 73.91(1) deg, beta = 70.21(1) deg, gamma = 85.8(1)deg, and Z = 2. X-ray diffraction and mass spectral data were used to characterize the products of the analogous reactions with Fe, Co, Ni, and Cu. We discuss both use of dithiocarbamates as precursors and our approach to their preparation. Author

N95-12693*# National Aeronautics and Space Administration. Lewis Research Center, Cleveland, OH.
SYNTHESIS AND DECOMPOSITION OF A NOVEL CARBOXYLATE PRECURSOR TO INDIUM OXIDE
Aloysius F. Hepp, Maria T. Andras, Stan A. Duraj, Eric B. Clark, David G. Hehemann, Daniel A. Scheiman, and Phillip E. Fanwick Jul. 1994 8 p Presented at the Fall Meeting, Boston, MA, 29 Nov. - 3 Dec. 1993; sponsored by the Materials Research Society
(Contracts NCC3-162; NCC3-318; NAS3-25266; NCC3-246; RTOP 233-01-0A)
(NASA-TM-106555; E-8715; NAS 1.15:106555) Avail: CASI HC A02/MF A01

Reaction of metallic indium with benzoyl peroxide in 4-1 methylpyridine (4-Mepy) at 25 C produces an eight-coordinate mononuclear indium(III) benzoate, In(eta(sup 2)-O2CC6H5)3(4-Mepy)2 4H2O (I), in yields of up to 60 percent. The indium(III) benzoate was fully characterized by elemental analysis, spectroscopy, and X-ray crystallography; (I) exists in the crystalline state as discrete eight-coordinate molecules; the coordination sphere around the central indium atom is best described as pseudo-square pyramidal. Thermogravimetric analysis of (I) and X-ray diffraction powder studies on the resulting pyrolysate demonstrate that this new benzoate is an inorganic precursor to indium oxide. Decomposition of (I) occurs first by loss of 4-methylpyridine ligands (100 deg-200 deg C), then loss of benzoates with formation of In2O3 at 450 C. We discuss both use of carboxylates as precursors and our approach to their preparation. Author

N95-12764*# National Aeronautics and Space Administration. Lewis Research Center, Cleveland, OH.
HIGH TEMPERATURE SOLID LUBRICANT MATERIALS FOR HEAVY DUTY AND ADVANCED HEAT ENGINES
C. DellaCorte and J. C. Wood Sep. 1994 20 p Presented at the 1994 Fall Technical Conference, LaFayette, IN, 2-5 Oct. 1994; sponsored by the International Combustion Engine Division of the ASME Sponsored by NASA. Lewis Research Center
(Contract DE-AI01-91CE-50306; RTOP 778-34-2A; RTOP 505-63-5A)
(NASA-TM-106570; E-8798; NAS 1.15:106570; DOE/NASA/50306-5)
Avail: CASI HC A03/MF A01

Advanced engine designs incorporate higher mechanical and thermal loading to achieve efficiency improvements. This approach often leads to higher operating temperatures of critical sliding elements (e.g. piston ring/cylinder wall contacts and valve guides) which compromise the use of conventional and even advanced synthetic liquid lubricants. For these applications solid lubricants must be considered. Several novel solid lubricant composites and coatings designated PS/PM200 have been employed to dry and marginally oil lubricated contacts in advanced heat engines. These applications include cylinder kits of heavy duty diesels, and high temperature Stirling engines, sidewall seals of rotary engines, and various exhaust valve and exhaust component applications. This paper describes the tribological and thermophysical properties of these tribomaterials and reviews the results of applying them to engine applications. Other potential tribological materials and applications are also discussed with particular emphasis on heavy duty and advanced heat engines. Author

N95-12783*# National Aeronautics and Space Administration. Lewis Research Center, Cleveland, OH.
FERRIC CHLORIDE GRAPHITE INTERCALATION COMPOUNDS PREPARED FROM GRAPHITE FLUORIDE
Ching-Cheh Hung Oct. 1994 16 p Presented at the 21st Biennial Conference on Carbon, Buffalo, NY, 13-18 Jun. 1993; sponsored by American Carbon Society
(RTOP 506-41-41)
(NASA-TM-106447; E-8299-1; NAS 1.15:106447) Avail: CASI HC A03/MF A01

The reaction between graphite fluoride and ferric chloride was observed in the temperature range of 300 to 400 C. The graphite fluorides used for this reaction have an sp3 electronic structure and are electrical insulators. They can be made by fluorinating either carbon fibers or powder having various degrees of graphitization. Reaction is fast and spontaneous and can occur in the presence of air. The ferric chloride does not have to be predried. The products have an sp2 electronic structure and are electrical conductors. They contain first stage FeCl3 intercalated graphite. Some of the products contain FeCl2*2H2O, others contain FeF3 in concentrations that depend on the intercalation condition. The graphite intercalated compounds (GIC) deintercalated slowly in air at room temperature, but deintercalated quickly and completely at 370 C. Deintercalation is accompanied by the disappearing of iron halides and the formation of rust (hematite) distributed unevenly on the fiber surface. When heated to 400 C in pure N2 (99.99 vol %), this new GIC deintercalates without losing its molecular structure. However, when the compounds are heated to 800 C in quartz tube, they lost most of its halogen atoms and formed iron oxides (other than hematite), distributed evenly in or on the fiber. This iron-oxide-covered fiber may be useful in making carbon-fiber/ceramic-matrix composites with strong bonding at the fiber-ceramic interface. Author

N95-13151 Department of the Navy, Washington, DC.
SYNTHETIC METHOD FOR ETHYNYLATION OF AROMATIC COMPOUNDS Patent
Thomas DiBerardino, inventor (to Navy), Patricia M. Lutz, inventor (to Navy), and Barbara F. Howell, inventor (to Navy) 14 Jun. 1994 5 p Filed 14 Jun. 1993
(AD-D016398; US-Patent-5,321,165; US-Patent-Appl-SN-075933; US-Patent-Class-568/437) Avail: US Patent and Trademark Office

A method of producing an ethynyl aromatic aldehyde comprises reacting a protected copper acetylide salt with a halogen substituted aromatic compound to produce a protected ethynyl aromatic aldehyde. The protected ethynyl aromatic aldehyde may be deprotected to yield an acetylene terminated aromatic aldehyde which is useful for making acetylenic Schiff's base monomers and conductive polymers thereof DTIC

24 COMPOSITE MATERIALS

Includes physical, chemical, and mechanical properties of laminates and other composite materials.

For ceramic materials see *27 Nonmetallic Materials*.

N95-11700*# Virginia Polytechnic Inst. and State Univ., Blacksburg, VA. Dept. of Mechanical Engineering.
OPTIMAL EXPERIMENTAL DESIGNS FOR THE ESTIMATION OF THERMAL PROPERTIES OF COMPOSITE MATERIALS Annual Report
Elaine P. Scott and Deborah A. Moncman 5 May 1994 216 p
(Grant NAG1-1507)
(NASA-CR-196792; NAS 1.26:196792) Avail: CASI HC A10/MF A03

Reliable estimation of thermal properties is extremely important in the utilization of new advanced materials, such as composite materials. The accuracy of these estimates can be increased if the experiments are designed carefully. The objectives of this study are to design optimal experiments to be used in the prediction of these thermal properties and to then utilize these designs in the development of an estimation procedure to determine the effective thermal properties (thermal conductivity and volumetric heat capacity). The experiments were optimized by choosing experimental parameters that maximize the temperature derivatives with respect to all of the unknown thermal properties. This procedure has the effect of minimizing the confidence intervals of the resulting thermal property estimates. Both one-dimensional and two-dimensional experimental designs were optimized. A heat flux boundary condition is required in both analyses for the simultaneous estimation of the thermal properties. For the one-dimensional experiment, the parameters optimized were the heating time of the applied heat flux, the temperature sensor location, and the experimental time. In addition to these parameters, the optimal location of the heat flux was also determined for the two-dimensional experiments. Utilizing the optimal one-dimensional experiment, the effective thermal conductivity perpendicular to the fibers and the effective volumetric heat capacity were then estimated for an IM7-Bismaleimide composite material. The estimation procedure used is based on the minimization of a least squares function which incorporates both calculated and measured temperatures and allows for the parameters to be estimated simultaneously. Author

N95-11803*# Rockwell International Corp., Downey, CA. Space Systems Div.
SELECTION PROCESS FOR TRADE STUDY: GRAPHITE COMPOSITE PRIMARY STRUCTURE (GCPS)
H. S. Greenberg 2 Sep. 1994 16 p Prepared in cooperation with Grumman Aerospace Corp., Bethpage, NY
(Contract NCC1-193)
(NASA-CR-196866; NAS 1.26:196866; SSD94D0210) Avail: CASI HC A03/MF A01

This TA 2 document describes the selection process that will be used to identify the most suitable structural configuration for an SSTO winged vehicle capable of delivering 25,000 lbs to a 220 nm circular orbit at 51.6 degree inclination. The most suitable unpressurized graphite composite structures and material selections is within this configuration and will be the prototype design for subsequent design and analysis and the basis for the design and fabrication of payload bay, wing, and thrust structure full scale test articles representing segments of the prototype structures. The selection process for this TA 2 trade study is the same as that for the TA 1 trade study. As the trade study progresses additional insight may result in modifications to the selection criteria within this process. Such modifications will result in an update of this document as appropriate.
Author

N95-11816*# National Aeronautics and Space Administration. Marshall Space Flight Center, Huntsville, AL.
DAMAGE TOLERANCE OF CANDIDATE THERMOSET COMPOSITES FOR USE ON SINGLE STAGE TO ORBIT VEHICLES
A. T. Nettles, D. Lance, and A. Hodge Washington Sep. 1994 50 p
(NASA-TP-3506; M-758; NAS 1.60:3506) Avail: CASI HC A03/MF A01

Four fiber/resin systems were compared for resistance to damage and damage tolerance. One toughened epoxy and three toughened bismaleimide (BMI) resins were used, all with IM7 carbon fiber reinforcement. A statistical design of experiments technique was used to evaluate the effects of impact energy, specimen thickness, and impactor diameter on the damage area, as computed by C-scans, and residual compression-after-impact (CAI) strength. Results showed that two of the BMI systems sustained relatively large damage zones yet had an excellent retention of CAI strength.
Author (revised)

N95-11834*# Rockwell International Corp., Downey, CA. Space Systems Div.
TRADE STUDY PLAN FOR GRAPHITE COMPOSITE PRIMARY STRUCTURE (GCPS)
H. S. Greenberg 29 Jul. 1994 26 p Prepared in cooperation with Grumman Aerospace Corp., Bethpage, NY
(Contract NCC1-193)
(NASA-CR-196868; NAS 1.26:196868; SSD94D0222; GCPS-TSP-1) Avail: CASI HC A03/MF A01

This TA 2 document (with support from TA 1) describes the trade study plan that will identify the most suitable structural configuration for an SSTO winged vehicle capable of delivering 25,000 lbs to a 220 nm circular orbit at 51.6 degree inclination For this most suitable configuration the structural attachment of the wing, and the most suitable GCPS composite materials for intertank, wing, tail and thrust structure are identified. This trade study analysis uses extensive information derived in the TA 1 trade study plan and is identified within the study plan. In view of this, for convenience, the TA 1 study plan is included as an appendix to this document. Author

N95-11835*# Rockwell International Corp., Downey, CA. Space Systems Div.

TEST PLANS. LIGHTWEIGHT DURABLE TPS: TASKS 1,2,4,5, AND 6

H. S. Greenberg and Tina Tu 29 Jul. 1994 222 p

(Contract NCC2-9003)

(NASA-CR-196867; NAS 1.26:196867; LDTPS-TP-1; SSD94D0218) Avail: CASI HC A10/MF A03

The objective of this task is to develop the fluted core flexible blankets, also referred to as the Tailorable Advanced Blanket Insulation (TABI), to a technology readiness level (TRL) of 6. This task is one of the six tasks under TA 3, Lightweight Durable TPS study, of the Single Stage to Orbit (SSTO) program. The purpose of this task is to develop a durable and low maintenance flexible TPS blanket material to be implemented on the SSTO vehicle. Author

N95-11854# New Orleans Univ., LA.

ARMY RESEARCH OFFICE WORKSHOP ON DYNAMIC RESPONSE OF COMPOSITE STRUCTURES Final Report, 1 Feb. - 30 Sep. 1993

David Hui Apr. 1994 94 p Workshop held in New Orleans, LA, 30 Aug. - 1 Sep. 1993

(Contract DAAH04-93-G-0052)

(AD-A281471; ARO-30904.1-EG-CF) Avail: CASI HC A05/MF A01

The purpose of the workshop was to: (1) assess the state of the art in the modeling and analysis of modern composite structures that are relevant to the Army's need to improve the design and operation of land vehicles, helicopters, weapon systems, etc; and (2) identify new opportunities for relevant research. The special areas of interest were crashworthiness of composite structures, composite helicopter rotor blade dynamics, stability and control, smart composite structures, etc. The workshop contained six keynote and distinguished lectures and 34 lectures for a total of 40 paper presentations. The regular sessions include (1) vibration of composite structures, (2) smart structures, (3) impact of composite structures, (4) damage and failure, (5) design of composite structures, and (6) structural mechanics. DTIC

N95-11926*# Analytical Services and Materials, Inc., Hampton, VA.

FAILURE ANALYSIS OF WOVEN AND BRAIDED FABRIC REINFORCED COMPOSITES Final Report

Rajiv A. Naik Sep. 1994 48 p Presented at the NASA/DOE Advanced Composites Technology (ACT) Conference, Seattle, WA, 22-26 Aug. 1994

(Contract NAS1-19708; RTOP 510-02-12-09)

(NASA-CR-194981; NAS 1.26:194981) Avail: CASI HC A03/MF A01

A general purpose micromechanics analysis that discretely models the yarn architecture within the textile repeating unit cell was developed to predict overall, three dimensional, thermal and mechanical properties, damage initiation and progression, and strength. This analytical technique was implemented in a user-friendly, personal computer-based, menu-driven code called Textile Composite Analysis for Design (TEXCAD). TEXCAD was used to analyze plain weave and 2x2, 2-D triaxial braided composites. The calculated tension, compression, and shear strengths correlated well with available test data for both woven and braided composites. Parametric studies were performed on both woven and braided architectures to investigate the effects of parameters such as yarn size, yarn spacing, yarn crimp, braid angle, and overall fiber volume fraction on the strength properties of the textile composite. Author

N95-12357*# National Aeronautics and Space Administration. Langley Research Center, Hampton, VA.

TEN-YEAR GROUND EXPOSURE OF COMPOSITE MATERIALS USED ON THE BELL MODEL 206L HELICOPTER FLIGHT SERVICE PROGRAM

Donald J. Baker Sep. 1994 57 p Sponsored by NASA. Langley Research Center and Army Research Lab., Adelphi, MD

(DA Proj. 1L1-62211-A-47-AB; RTOP 532-05-37-03)

(NASA-TP-3468; L-17341; ARL-TR-480; NAS 1.60:3468) Avail: CASI HC A04/MF A01

Residual strength results are presented for four composite material systems that have been exposed for up to 10 years to the environment at five different locations on the North American continent. The exposure locations are near where the Bell Model 206L helicopters, which participated in a flight service program sponsored by NASA Langley Research Center and the U.S. Army, were flying in daily commercial service. The composite material systems are (1) Kevlar-49 fabric/F-185 epoxy; (2) Kevlar-49 fabric/LRF-277 epoxy; (3) Kevlar-49 fabric/CE-306 epoxy; and (4) T-300 graphite/E-788 epoxy. Six replicates of each material were removed and tested after 1, 3, 5, 7, and 10 years of exposure. The average baseline strength was determined from testing six as-fabricated specimens. More than 1700 specimens have been tested. All specimens that were tested to determine their strength were painted with a polyurethane paint. Each set of specimens also included an unpainted panel for observing the weathering effects on the composite materials. A statistically based procedure has been used to determine the strength value above which at least 90 percent of the population is expected to fall with a 95-percent confidence level. The computed compression strengths are 80 to 90 percent of the baseline (no-exposure) strengths. The resulting compression strengths are approximately 8 percent below the population mean strengths. The computed short-beam-shear strengths are 83 to 92 percent of the baseline (no-exposure) strengths. The computed tension strength of all materials is 93 to 97 percent of the baseline (no-exposure) strengths. Author

N95-12396 University of Southern Mississippi, Hattiesburg, MS. Dept. of Polymer Science.

TOWARDS TAILORED INTERPHASE FORMATION UTILIZING SURFACE-ACTIVE BENZYLSULFONIUM SALTS AS CATIONIC INITIATORS Technical Report, 1 Jun. 1993 - 31 May 1994

John A. McGowen and Lon J. Mathias 15 Jul. 1994 3 p Limited Reproducibility: More than 20% of this document may be affected by microfiche quality

(Contract N00014-89-J-1225)

(AD-A282511; TR-69) Avail: Issuing Activity (Defense Technical Information Center (DTIC))

The bonding between reinforcement and matrix in a composite involves a microscopic interphase region that is generally composed of a polymer network formed by multilayer buildup of a coupling agent attached to the surface of the fiber into which the matrix can propagate and bond. The main purpose of the interphase is to provide a structural lattice that will allow for good energy transfer from the matrix to the reinforcement. The interphase plays a dominant role in the fracture toughness properties of composites and in their response to aqueous and corrosive environments. Being able to develop tailored interphases will allow control of composite properties to optimize strength, modulus, and toughness. DTIC

N95-12404 Rochester Univ., NY. Dept. of Chemical Engineering.

ENHANCEMENT OF LUMINESCENCE IN POLYMER NANOCOMPOSITES

Samson A. Jenekhe and John A. Osaheni 13 Jul. 1994 18 p Limited Reproducibility: More than 20% of this document may be affected by microfiche quality

(Contract N00014-94-1-0540)

(AD-A282539; TR-3) Avail: Issuing Activity (Defense Technical Information Center (DTIC))

The effect of supramolecular structure and morphology on the solid state luminescence of polymers is explored through a rod-coil co-polymer system, poly(benzobisthiazole-1, 4-phenylene co-benzobisthiazole decamethylene), which forms nanocomposites at compositions below 50 mol% rods. The composition dependence of the photoluminescence quantum efficiency exhibited a sharp change corresponding to a change in supramolecular structure of the copolymers. The photoluminescence quantum efficiency of the polymer nanocomposites was as high as 37% which represents over sixfold enhancement compared to the corresponding 'bulk' conjugated polymer. These results have implications for the fundamental understanding of the origin of luminescence quenching in conjugated polymers and they also suggest that control of supramolecular structure and morphology is key to efficient solid state luminescence in polymers. Author (DTIC)

N95-12793*# Boeing Defense and Space Group, Philadelphia, PA. Helicopters Div.

TEST METHODS FOR TEXTILE COMPOSITES Final Report

Pierre J. Minguet, Mark J. Fedro, and Christian K. Gunther Hampton, VA NASA Jul. 1994 226 p

(Contract NAS1-19247; RTOP 510-02-12-09)

(NASA-CR-4609; NAS 1.26:4609) Avail: CASI HC A11/MF A03

Various test methods commonly used for measuring properties of tape laminate composites were evaluated to determine their suitability for the

testing of textile composites. Three different types of textile composites were utilized in this investigation: two-dimensional (2-D) triaxial braids, stitched uniweave fabric, and three-dimensional (3-D) interlock woven fabric. Four 2-D braid architectures, five stitched laminates, and six 3-D woven architectures were tested. All preforms used AS4 fibers and were resin-transfer-molded with Shell RSL-1895 epoxy resin. Ten categories of material properties were investigated: tension, open-hole tension, compression, open-hole compression, in-plane shear, filled-hole tension, bolt bearing, interlaminar tension, interlaminar shear, and interlaminar fracture toughness. Different test methods and specimen sizes were considered for each category of test. Strength and stiffness properties obtained with each of these methods are documented in this report for all the material systems mentioned above. Author (revised)

N95-12813*# National Aeronautics and Space Administration. Lewis Research Center, Cleveland, OH.

TENSILE CREEP AND STRESS-RUPTURE BEHAVIOR OF POLYMER DERIVED SiC FIBERS

H. M. Yun (Cleveland State Univ., OH.), J. C. Goldsby, and J. A. DiCarlo Aug. 1994 14 p Presented at the 96th Annual Meeting and Exposition, Indianapolis, IN, 24-28 Apr. 1994; sponsored by the American Ceramic Society

(RTOP 537-04-20)

(NASA-TM-106692; E-9047; NAS 1.15:106692) Avail: CASI HC A03/MF A01

Tensile creep and stress-rupture studies were conducted on polymer derived Nicalon, Hi-Nicalon, and SiC/BN-coated Nicalon SiC fibers. Test conditions were temperatures from 1200 to 1400 C, stresses from 100 to 1600 MPa, stress application times up to 200 hours, and air, argon, and vacuum test environments. For all fibers, creep occurred predominantly in the primary stage. Hi-Nicalon had much higher 0.2 and 1 percent creep strengths than as-produced as well as-coated Nicalon fibers. The stress-rupture strength of Hi-Nicalon up to 100 hours was also higher than that of the coated and as-produced Nicalon fibers. SiC/BN coating on Nicalon increased only the short-term low-temperature rupture strength. Limited testing in argon and vacuum suggests that for all fiber types, creep and rupture resistances are reduced in comparison to the results in air. Possible mechanisms for the observed behavior are discussed. Author (revised)

N95-12833 Fairfax Materials Research, Inc., Alexandria, VA.

COMPUTER MODELLING OF CYCLIC DEFORMATION OF HIGH-TEMPERATURE MATERIALS Technical Progress Report, 1 Mar. - 31 May 1994

M. S. Duesbery 31 May 1994 9 p Limited Reproducibility: More than 20% of this document may be affected by microfiche quality

(Contract N00014-91-C-0067)

(AD-A282457) Avail: Issuing Activity (Defense Technical Information Center (DTIC))

Current methods of lifetime assessment leave much to be desired. Typically, the expected life of a full-scale component exposed to a complex environment is based upon empirical interpretations of measurements performed on microscopic samples in controlled laboratory conditions. Extrapolation to the service component is accomplished by scaling laws which, if used at all, are empirical; little or no attention is paid to synergistic interactions between the different components of the real environment. With the increasingly hostile conditions which must be faced in modern aerospace applications, improvement in lifetime estimation is mandated by both cost and safety considerations. This program aims at improving current methods of lifetime assessment by building in the characteristics of the micro-mechanisms known to be responsible for damage and failure. The broad approach entails the integration and, where necessary, augmentation of the micro-scale research results currently available in the literature into a macro-scale model with predictive capability. In more detail, the program will develop a set of hierarchically structured models at different length scales, from atomic to macroscopic, at each level taking as parametric input the results of the model at the next smaller scale. DTIC

N95-12862# Pacific Northwest Lab., Richland, WA.

THE EFFECT OF IRRADIATION ON THE STABILITY AND PROPERTIES OF MONOLITHIC SILICON CARBIDE AND SiC(f)/SiC COMPOSITES UP TO 25 DPA

G. W. Hollenberg, C. H. Henager, Jr., G. E. Youngblood, D. J. Trimble, and S. A. Simonson Apr. 1994 46 p Presented at the 96th Annual Meeting of the American Ceramic Society, Indianapolis, 24-28 Apr. 1994

(Contract DE-AC06-76RL-01830)

(DE94-014568; PNL-SA-23607; CONF-940416-19) Avail: CASI HC A03/MF A01

Stability and properties of monolithic and SiC(sub f)/SiC composites were measured before and after irradiation in a fast neutron spectrum up to 25 dpa between 500 and 1500 C. Dimensional changes were relatively consistent with previous investigations. Strength and modulus of SiC(sub f)/SiC composites decreased after irradiation as a result of fiber/matrix decoupling. For some composites, uniform elongation was not significantly degraded by irradiation. Thermal conductivity also decreased after irradiation at low temperatures because of the introduction of lattice defects as phonon scattering sites. Retention of properties under the severe conditions of 25 dpa and 800 C suggests that a composite tailored for neutron damage resistance can be developed. DOE

N95-12883 Martin Marietta Labs., Baltimore, MD.

THIN-FILM MODEL STUDIES OF INTERFACIAL REACTIONS IN INTERMETALLIC MATRIX COMPOSITES Final Report, 1 Jun. 1991 - 30 May 1994

M. Nathan and J. S. Ahearn Aug. 1994 39 p Limited Reproducibility: More than 20% of this document may be affected by microfiche quality

(Contract N00014-91-C-0168)

(AD-A283360; MML-TR-94-12) Avail: Issuing Activity (Defense Technical Information Center (DTIC))

This study strongly suggests that the likelihood of nanoscale interfacial reactions in stable systems is greater than anticipated. This finding appears to contradict existing evidence of BULK nonreactivity in most of these systems (except TiAl/TiC). There may be a number of reasons for this apparent contradiction between bulk and thin-film results. For example, the resolution of the techniques used in bulk studies may be too poor to detect nanometer-scale reaction products; the reactions may be self-limiting, with the product phase becoming an efficient diffusion barrier preventing further layer growth. Thin films may differ chemically from bulk, affecting the reactivity, although comparisons of TiAl (film) reactions with thin Al2O3 films and with sapphire show that if anything, the sapphire is more reactive. We suggest however that the existence of nanoscale reactions at supposedly stable interfaces should be considered the norm, rather than the exception, particularly at the high temperatures of IMC preparation or use. DTIC

N95-13082*# NYMA, Inc., Brook Park, OH. Engineering Services Div.

THERMOMECHANICAL FATIGUE DAMAGE/FAILURE MECHANISMS IN SCS-6/TIMETAL 21S (0/90)s COMPOSITE Final Report

Michael G. Castelli Cleveland, OH NASA Jun. 1994 20 p

(Contract NAS3-27186; RTOP 763-22-41)

(NASA-CR-191115; E-8940; NAS 1.26:191115) Avail: CASI HC A03/MF A01

The thermomechanical fatigue (TMF) deformation, damage, and life behaviors of SCS6/Timetal 21S (0/90)s were investigated under zero-tension conditions. In-phase (IP) and out-of-phase (OP) loadings were investigated with a temperature cycle from 150 to 650 deg C. An advanced TMF test technique was used to quantify mechanically damage progression. The technique incorporated explicit measurements of the macroscopic (1) isothermal static moduli at the temperature extremes of the TMF cycle and (2) coefficient of thermal expansion (CTE) as functions of the TMF cycles. The importance of thermal property degradation and its relevance to accurate post-test data analysis and interpretation is briefly addressed. Extensive fractography and metallography were conducted on specimens from failed and interrupted tests to characterize the extent of damage at the microstructure level. Fatigue life results indicated trends analogous to those established for similar unidirectional(0) reinforced titanium matrix composite systems. High stress IP and mid to low stress OP loading conditions were life-limiting in comparison to maximum temperature isothermal conditions. Dominant damage mechanisms changed with cycle type. Damage resulting from IP TMF conditions produced measurable decreases in static moduli but only minimal changes in the CTE. Metallography on interrupted and failed specimens revealed extensive (0) fiber cracking with sparse matrix damage. No surface initiated matrix cracks were present. Comparable OP TMF conditions initiated environment enhanced surface cracking and matrix cracking initiated at (90) fiber/matrix

(F/M) interfaces. Notable static moduli and CTE degradations were measured. Fractography and metallography revealed that the transverse cracks originating from the surface and (90) F/M interfaces tended to converge and coalesce at the (0) fibers. Author

N95-13193*# National Aeronautics and Space Administration. Lewis Research Center, Cleveland, OH.
MICROMECHANICS ANALYSIS CODE (MAC). USER GUIDE: VERSION 1.0
T. E. Wilt (Akron Univ., OH.) and S. M. Arnold Oct. 1994 70 p
(RTOP 505-63-12)
(NASA-TM-106706; E-9068; NAS 1.15:106706) Avail: CASI HC A04/MF A01

The ability to accurately predict the thermomechanical deformation response of advanced composite materials continues to play an important role in the development of these strategic materials. Analytical models that predict the effective behavior of composites are used not only by engineers performing structural analysis of large-scale composite components but also by material scientists in developing new material systems. For an analytical model to fulfill these two distinct functions it must be based on a micromechanics approach which utilizes physically based deformation and life constitutive models and allows one to generate the average (macro) response of a composite material given the properties of the individual consituents and their geometric arrangement. Here the user guide for the recently developed, computationally efficient and comprehensive micromechanics analysis code, MAC, who's predictive capability rests entirely upon the fully analytical generalized method of cells, GMC, micromechanics model is described. MAC is a versatile form of research software that 'drives' the double or triple ply periodic micromechanics constitutive models based upon GMC. MAC enhances the basic capabilities of GMC by providing a modular framework wherein (1) various thermal, mechanical (stress or strain control), and thermomechanical load histories can be imposed; (2) different integration algorithms may be selected; (3) a variety of constituent constitutive models may be utilized and/or implemented; and (4) a variety of fiber architectures may be easily accessed through their corresponding representative volume elements. Author (revised)

N95-13298 University of Southern Mississippi, Hattiesburg, MS. Dept. of Polymer Science.
GLASS REINFORCED-DIALLYLBISPHENOL/MALEIMIDE COMPOSITES WITH MODIFIED INTERPHASES Technical Report, 1 Jun. 1993 - 31 May 1994
Raj A. Sundar and Lon J. Mathias 15 Jul. 1994 5 p Limited Reproducibility: More than 20% of this document may be affected by microfiche quality
(Contract N00014-89-J-1225)
(AD-A282496; TR-66) Avail: Issuing Activity (Defense Technical Information Center (DTIC))

A silane coupling agent, based on the reaction between gamma amino propyl triethoxysilane (APS) and maleic anhydride (MA), was prepared. The coupling agent, maleamido propylsilane (MAPS), was chemisorbed onto E-glass cloth. TGA analysis of the treated glass cloth showed 0.8% weight loss (silane loading), when heated to 700 C in an air atmosphere. The treated glass cloths were used in the fabrication of composite laminates having approximately 60 +/- 1 wt% glass reinforcement, with the matrix being a thermosetting system based on diallylbisphenol (DAP)/bismaleimide (BMI). DMTA analysis of the cured composite laminates showed unexpected 10-20 GPA increased in the modulus and a 30-40 C increase in the Tg for the treated versus untreated glass cloths. Author (DTIC)

N95-13533# Lawrence Livermore National Lab., Livermore, CA.
NUMERICAL SIMULATIONS OF CREEP IN DUCTILE-PHASE TOUGHENED INTERMETALLIC MATRIX COMPOSITES
G. A. Henshall and M. J. Strum Apr. 1994 6 p Presented at the 3rd Intermetallic Matrix Composites, San Francisco, CA, 4-6 Apr. 1994
(Contract W-7405-eng-48)
(DE94-014744; UCRL-JC-116440; CONF-9404182-1) Avail: CASI HC A02/MF A01

Analytical and finite element method (FEM) simulations of creep in idealized ductile-phase toughened intermetallic composites are described. For these strong-matrix materials, the two types of analyses predict similar time-independent composite creep rates if each phase individually exhibits only steady-state creep. The composite creep rate becomes increasingly higher than that of the monolithic intermetallic as the stress exponent of the intermetallic and the volume fraction and creep rate of the ductile phase increase. FEM analysis shows that the shape of the ductile phase does not affect the creep rate but may affect the internal stress and strain distributions, and thus damage accumulation rates. If primary creep occurs in one or both of the individual phases, the composite also exhibits primary creep. In this case, there can be significant deviations in the creep curves computed by the analytical and FEM models. The model predictions are compared with data for the Nb5Si3/Nb system. DOE

25 INORGANIC AND PHYSICAL CHEMISTRY

Includes chemical analysis, e.g., chromatography; combustion theory; electrochemistry; and photochemistry.

For related information see also *77 Thermodynamics and Statistical Physics.*.

N95-11735# Oak Ridge National Lab., TN.
TRIPLE SORBENT THERMAL DESORPTION/GAS CHROMATOGRAPHY/MASS SPECTROMETRY DETERMINATION OF VAPOR PHASE ORGANIC CONTAMINANTS
C. Y. Ma, J. T. Skeen, A. B. Dindal, C. E. Higgins, and R. A. Jenkins May 1994 13 p Presented at the Measurement of Toxic and Related Air Pollutants, Durham, NC, 3-6 May 1994
(Contract DE-AC05-84OR-21400)
(DE94-013634; CONF-9405167-1) Avail: CASI HC A03/MF A01

A thermal desorption/ps chromatography/mass spectrometry (TD/GC/MS) has been evaluated for the determination of volatile organic compounds (VOCS) in vapor phase samples using Carbosieve S-III/Carbotrap/Carotrap C triple sorbent traps (TST) similar to those available from a commercial source. The analysis was carried out with a Hewlett-Packard 5985A or 5995 GC/MS system with a modified injector to adapt an inhouse manufactured short-path desorber for transferring desorbate directly onto a cryofocusing loop for subsequent GC/MS analysis. Vapor phase standards generated from twenty six compounds were used for method validation, including alkanes, alkyl alcohols, alkyl ketones, and alkyl nitrites, a group of representative compounds that have previously been identified in a target airborne matrix. The method was validated based on the satisfactory results in terms of reproducibility, recovery rate, stability, and linearity. A relative, standard deviation of 0.55 to 24.3 percent was obtained for the entire TD process (generation of gas phase standards, spiking the standards on and desorbing from TST) over a concentration range of 20 to 500 ng/trap. Linear correlation coefficients for the calibration curves as determined ranged from 0.81 to 0.99 and limits of detection ranged from 3 to 76 ng. For a majority of standards, recoveries of greater than 90 percent were observed. For three selected standards spiked on TSTS, minimal loss (10 to 22 percent) was observed after storing the spiked in, a 4 deg C refrigerator for 29 days. The only chromatographable artifact observed was a 5 percent conversion of isopropanol to acetone. The validated method been successfully applied, to the determination of VOC's collected from various emission sources in a diversified concentration range. DOE

N95-11756# Sandia National Labs., Albuquerque, NM.
COMPARISON OF THE KAMELEON FIRE MODEL TO LARGE-SCALE OPEN POOL FIRE DATA
V. F. Nicolette, L. A. Gritzo, J. Holen, and B. F. Magnussen 1994 19 p Presented at the 4th International Symposium on Fire Safety Science, Ottawa, Ontario, 13-17 Jun. 1994
(Contract DE-AC04-94AL-85000)
(DE94-013441; SAND-93-2416C; CONF-940668-3) Avail: CASI HC A03/MF A01

A comparison of the KAMELEON fire model to large-scale open pool fire experimental data is presented. The model was used to calculate large-scale JP-4 pool fires with and without wind, and with and without large objects in the fire. The effect of wind and large objects on the fire environment is clearly seen. For the pool fire calculations without any object in the fire, excellent agreement is seen in the location of the oxygen-starved region near the pool center. Calculated flame temperatures are about 200-300 K higher than measured. This results in higher heat

fluxes back to the fuel pool and higher fuel evaporation rates (by a factor of 2). Fuel concentrations at lower elevations and peak soot concentrations are in good agreement with data. For pool fire calculations with objects, similar trends in the fire environment are observed. Excellent agreement is seen in the distribution of the heat flux around a cylindrical calorimeter in a rectangular pool with wind effects. The magnitude of the calculated heat flux to the object is high by a factor of 2 relative to the test data, due to the higher temperatures calculated. For the case of a large flat plate adjacent to a circular pool, excellent qualitative agreement is seen in the predicted and measured flame shapes as a function of wind. DOE

N95-11775 ESDU International Ltd., London (England).
THERMOPHYSICAL PROPERTIES OF MtBE (METHYL TERTBUTYL ETHER)
May 1994 17 p
(ISSN 0141-4062)
(ESDU-94010; ISBN-0-85679-897-5) Avail: ESDU

ESDU 94010 gives equations obtained from a critical evaluation of experimental data in the literature for the variation along the saturation line with temperature, for both the liquid and the vapor, of: density, enthalpy, heat capacity at constant pressure, dynamic viscosity and thermal conductivity. Also given are equations for the variation with temperature along the saturation line of the vapor pressure, latent heat of vaporization and surface tension, together with equations for the variation with temperature for the ideal gas of specific heat capacity at constant pressure, enthalpy, dynamic viscosity and thermal conductivity. Results on the saturation line evaluated in SI units using the equations are tabulated at 10 K intervals and at 10 degree Celsius intervals from the melting point to the critical point, or as close to it as possible for some properties. Results for the ideal gas evaluated also in SI units using the equations are also tabulated at 20 K and at 20 degree Celsius intervals from the melting point to 1000 K. In the absence of experimental values some of these results involve extrapolation and they are indicated in the tables. Conversion factors to facilitate use of the data in British units are included. Author

N95-11790# Lawrence Livermore National Lab., Livermore, CA.
MSW TO HYDROGEN
A. D. Pasternak, J. H. Richardson, R. S. Rogers, C. B. Thorsness, H. Wallman, G. N. Richter, and J. K. Wolfenbarger 19 Apr. 1994 18 p Presented at the Hydrogen Program Review Meeting, Livermore, CA, 18-21 Apr. 1994
(Contract W-7405-eng-48)
(DE94-014741; UCRL-JC-116421; CONF-9404170-2) Avail: CASI HC A03/MF A01

LLNL and Texaco are cooperatively developing a physical and chemical treatment method for the preparation and conversion of municipal solid waste (MSW) to hydrogen by gasification and purification. The laboratory focus will be on pretreatment of MSW waste in order to prepare a slurry of suitable viscosity and heating value to allow efficient and economical gasification and hydrogen production. Initial pretreatment approaches include (1) hydrothermal processing at saturated conditions around 300 C with or without chemical/pH modification and (2) mild dry pyrolysis with subsequent incorporation into an appropriate slurry. Initial experiments will be performed with newspaper, a major constituent of MSW, prior to actual work with progressively more representative MSW samples. Overall system modeling with special attention to energy efficiency and waste water handling of the pretreatment process will provide overall guidance to critical scale-up parameters. Incorporation of additional feed stock elements (e.g., heavy oil) will be evaluated subject to the heating value, viscosity, and economics of the MSW optimal slurry for hydrogen production. Ultimate scale-up of the optimized process will provide sufficient material for demonstration in the Texaco pilot facility; additional long term objectives include more detailed economic analysis of the process as a function of technical parameters and development of a measure/control system to ensure slagging ash for variable MSW feed stocks. Details of the overall project plan and initial experimental and modeling results are presented. DOE

N95-11795 ESDU International Ltd., London (England).
THERMAL CONDUCTIVITY OF GASEOUS OXYGENATED ALIPHATIC HYDROCARBONS. ALCOHOLS, ALDEHYDES, KETONES AND ETHERS
May 1994 55 p
(ISSN 0141-4062)
(ESDU-94018; ISBN-0-85679-905-X) Avail: ESDU

ESDU 94018 uses a third-order polynomial in reduced temperature to correlate data extracted from the literature for 14 alcohols, 7 aldehydes, 6 ketones, and 16 ethers. The range is from the boiling point to at least 1.2 times critical temperature (Tc), except for pentyl, hexyl, and heptyl alcohols, heptan-4-one, and dihexyl and diheptyl ethers for which it is to 1.1 Tc, and for octyl, nonyl, and decyl alcohols for which it is to just over Tc. Association occurs near the boiling point for the lower alcohols and acetone, and data on the effect of that are included. The coefficients of the equation are given for each compound, and the equation is used to tabulate thermal conductivity in SI units at both 20 K and 20 C intervals. The sources of data used for each compound are listed and values that involve extrapolation of the available data are indicated. The likely accuracy of the values quoted is discussed and the effect of pressure on thermal conductivity is briefly considered. ESDU

N95-11796 Institut Franco-Allemand de Recherches, Saint-Louis (France).
SHOCK TUBE INVESTIGATIONS OF COMBUSTION PHENOMENA IN SUPERSONIC FLOWS
G. Smeets 1993 21 p Sponsored by Direction des Recherches, Etudes et Techniques, Paris, France and Centre de Documentation de l'Armement
(PB94-175262) Avail: Issuing Activity (National Technical Information Service (NTIS))

A survey is given of recent combustion dynamics research using shock tubes. There are three different fields where phenomena in supersonic gas flows resulting from chemical heat release are of particular interest: (1) combustion in an external flow field for lift and thrust generation on hypersonic vehicles, for drag reduction, or for piloting hypervelocity projectiles; (2) scramjet combustor: detailed information on the supersonic combustion can be obtained with 'direct connect' shock tube experiments; and (3) ram acceleration of projectiles in a tube by self-synchronized ignition of a combustible gas mixture. The ignition and combustion processes in the flow field around the high-speed projectile can be studied in an expansion tube. NTIS

N95-11827 Office of Naval Research, Arlington, VA.
NAVAL RESEARCH REVIEWS, VOLUME 46, FEBRUARY 1994
Feb. 1994 43 p Limited Reproducibility: More than 20% of this document may be affected by microfiche quality
(AD-A281435) Avail: CASI HC A03

The following topics are discussed: (1) crystal and molecular structure of p,p'-dimethoxybenzophenone by the direct probability method; (2) crystal structure of (Leu1) zervamicin, a membrane ion-channel peptide; (3) implications for gating mechanisms; (4) internal motion and molecular structure studies by electron diffraction; and (5) an application of the symbolic additiona method to the structure of L-arginine dihydrate. DTIC

N95-11685# Instituto de Pesquisas Espaciais, Sao Paulo (Brazil).
REVIEW OF PULSE IGNITION [REVISAO DA COMBUSTAO PULSANTE]
Lourdes Junko Momma, Victor Racy Abdalla, and Joao Andrade deCarvalho, Jr. Jun. 1994 56 p In PORTUGESE
(INPE-5569-PUD/063) Avail: CASI HC A04/MF A01

In this work, a critical review of the field of pulse ignition is undertaken, from its origins to the present time. In addition, the basic principles of pulse ignition systems are established, indicating various practical applications. The work concludes by presenting the advantages and disadvantages of pulse ignition. Author

N95-12107*# Wake Forest Univ., Winston-Salem, NC. Dept. of Chemistry.
QUANTUM CHEMICAL STUDY OF METHANE OXIDATION SPECIES
Final Report, Jun. 1981 - Dec. 1993
Charles F. Jackels 1993 10 p
(Contract NCC1-55)
(NASA-CR-196158; NAS 1.26:196158) Avail: CASI HC A02/MF A01

The research funded by this project has focused on quantum chemical investigations of molecular species thought to be important in the chemistry of the earth's upper and lower atmospheres. The body of this report contains brief discussions of the results of the several phases of this

investigation. In many instances these results have been presented at scientific meetings and/or published in refereed journals. Those bibliographic references are given. In addition to the study of specific chemical systems, there were several phases during the course of this investigation where much of the effort went into the development and modification of computer codes necessary to carry out these calculations on the wide range of computer equipment used during this study. This type of code maintenance and development work did not generally result in publications and presentations, but a brief review is given. Derived from text

N95-12128 ESDU International Ltd., London (England).
VAPOUR PRESSURES AND CRITICAL POINTS OF LIQUIDS. POLYCYCLIC PHENYL AND CYCLOHEXYL COMPOUNDS
Jan. 1994 48 p
(ISSN 0141-4062)
(ESDU-94001; ISBN-0-85679-888-6) Avail: ESDU

ESDU 94001 presents vapor pressure data for 21 compounds. The data were obtained by a critical evaluation of experimental results in the literature. The data available were limited but using a correlation previously developed for the alkanes that relates the second differential of the Wagner vapor pressure equation to the difference between the ideal gas and liquid heat capacities extrapolation was possible. The Wagner equation was used over a temperature range from close to the melting point to the critical point, although for some compounds the correlation was stopped at about 0.9 of the critical temperature. The coefficients of the equation are given and two tables of vapor pressure calculated using them are included; in SI units at 5 K intervals (although at low temperatures a 10 K interval is used for the first four values) and in mm of mercury or atmospheres (for the higher values) at 5 C intervals. A table also gives the saturation temperature at various specified pressures and indicates the possible uncertainty in the calculated values. An Antoine equation is given fitting the Wagner equation values between 2 and 200 kPa with an rms deviation of less than 0.05 percent. The sources of data for each compound are also listed. Density data for the compounds (except 4-methylbiphenyl) appear in ESDU 94002, and the choice of critical point values gave the best correlations for both vapor pressure and density. ESDU

N95-12129 ESDU International Ltd., London (England).
ORTHOBARIC DENSITIES AND MOLAR VOLUMES OF LIQUIDS. POLYCYCLIC PHENYL AND CYCLOHEXYL COMPOUNDS
Jan. 1994 46 p
(ISSN 0141-4062)
(ESDU-94002; ISBN-0-85679-889-4) Avail: ESDU

ESDU 94002 tabulates density and molar volume for 20 compounds in units of kg/cu m and cu cm/mol respectively from near the melting point to about 0.9 of the critical point (although for some compounds the data go up to the critical point). The temperature interval is usually 5 K, although for a few compounds it is varied to keep the increments in density small. The critical density was calculated using the Rackett and Riedel equations and values of the critical pressure and temperature adjusted until predictions from the two equations were in agreement. The choice of values was also influenced by achieving an optimum correlation for the vapor pressure data provided for these compounds in ESDU 94001. Experimental data for density for each compound were taken from sources in the literature, but were limited to medium reduced temperatures and so were fitted for each compound by the correlation obtained for the alkanes. The equation used relates log reduced density to a polynomial function of reduced temperature. Values for the coefficients in the equation are tabulated for each compound together with estimates of the accuracy of the predictions using them as a list of the sources of data used. Values at the critical point are also given together with normal boiling and melting points. ESDU

N95-12302# Instituto de Pesquisas Espaciais, Sao Jose dos Campos (Brazil).
STUDY OF A VORTICAL/AXIAL TYPE FLAMEHOLDERS WITH VARIABLE ANGLE BLADES M.S. Thesis [ESTUDO DE UM RETENTOR DE CHAMA DO TIPO VORTICAL/AXIAL COM PAS DE ANGULO VARIAVEL]
Wilson deFreitasMuniz Dec. 1993 91 p In PORTUGESE
(INPE-5558-TDI/538) Avail: CASI HC A05/MF A01

This work describes a theoretical model of an axial swirler with a diameter smaller or equal than the secondary air duct. The swirler was installed downstream of the duct. The present model contributes to the understanding of this flameholder set-up. Experimental results have shown easy flame control concerning its dynamic aspects and dimensions, providing greater flexibility to the combustion chamber optimization process. The use of Image Processing and Treatment techniques has confirmed the feasibility of flame control. The experimental results have also shown that the flame is fully stable when the axial swirler is used for large swirl numbers.
Author

N95-12514# Pennsylvania State Univ., University Park, PA. Dept. of Chemistry.
NANOMETER SCALE PHASE SEPARATION IN MIXED COMPOSITION SELF-ASSEMBLED MONOLAYERS
S. J. Stranick, S. V. Atre, A. N. Parikh, M. C. Wood, and D. L. Allara 14 Jul. 1994 17 p
(Contract N00014-91-J-1630)
(AD-A282671; TR-18) Avail: CASI HC A03/MF A01

Mixed composition monolayers of similar n-alkanethiols on Au(111) are formed by self-assembly. While the average surface composition of these films accurately reflects the composition of the deposition solution, scanning tunneling microscopy and secondary ion mass spectroscopy measurements show that the films phase separate on the nanometer scale. Scanning tunneling microscopy has been used to follow molecular motions within these films. We discuss our observations in terms of the formation and stability of the phase segregated domains, and their potential importance in nanoscale applications. DTIC

N95-12539# Woods Hole Oceanographic Inst., MA.
ACQUISITION OF A GAS SOURCE MASS SPECTROMETER FOR PALEOCLIMATOLOGY AND PALEOCEANOGRAPHY RESEARCH Final Report
William B. Curry 21 Jul. 1994 5 p
(Contract N00014-92-J-1301)
(AD-A282634) Avail: CASI HC A01/MF A01

The purpose of this award was to partially fund the acquisition of a high-sensitivity, automated mass spectrometer system dedicated to the analysis of carbonate samples. The acquisition was jointly funded by this award, by an award from the National Sciences Foundation Division of Ocean Sciences, and by supporting funds from the Woods Hole Oceanographic Institution. We purchased a Finnigan MAT252 mass spectrometer with an automated carbonate device known as the 'Kiel device'. The instrument was delivered in December 1992. It was installed in March 1993 and met factory specifications within three weeks. Routine operational use of the system began in March 1993. DTIC

N95-12549# Naval Air Warfare Center, Warminster, PA. Air Vehicle and Crew Systems Technology Dept.
HYDROGEN DESULFURIZATION OF NICKEL: THERMODYNAMICS AND KINETICS Final Report, 1 Jan. - 27 Oct. 1993
William E. Frazier, Thu-Ha T. Mickel, and Bruce A. Pregger 1 Nov. 1993 28 p
(AD-A282581; NAWCADWAR-93074-60) Avail: CASI HC A03/MF A01

The presence of minute amounts of sulfur (10ppm) in nickel-base superalloys has been associated with reduced oxidation resistance and the premature spallation of protective coatings. Removal of sulfur by annealing these alloys in a hydrogen atmosphere has been successfully attempted by several researchers. This paper examines the fundamental thermodynamics and kinetics governing hydrogen desulfurization of elemental nickel. Limiting conditions for successful desulfurization are delineated. Assuming that the diffusion of sulfur is the rate limiting process of desulfurization, the effectiveness as well as time associated with hydrogen desulfurization is explored. DTIC

N95-12584# Helsinki Univ. of Technology, Espoo (Finland). Lab. of Chemical Engineering.
CHEMICAL ENGINEERING SEMINAR 1993
M. Hurme 1993 145 p Seminar held in Espoo, Finland, 11-12 May 1993
(PB94-184538; ISBN-951-22-1777-5) Avail: CASI HC A07/MF A02

The aim of the seminar was to create a forum for Finnish chemical engineering professionals and to acquaint them with the new process engineering developments. The seminar was organized now for the first

time and succeeded well with about 100 participants. The first part of the seminar discussed process simulation including steady state and dynamic simulation, expert systems and computer aided tools for information management. The topic of the second day was separation process engineering including biological gas purification, sterile air filtration and liquid filtration by different methods. The seminar also included quite an extensive exhibition of process engineering oriented computer programs and an evening banquet. NTIS

N95-12585# Helsinki Univ. of Technology, Espoo (Finland). Lab. of Physical Chemistry and Electrochemistry.
MICROEMULSIONS AS REACTION MEDIA: LITERATURE REVIEW
R. Lindberg 22 Dec. 1993 84 p See also AD-A156046 and AD-A156060
(PB94-184553) Avail: CASI HC A05/MF A01

Microemulsion catalysis represents an alternative to phase transfer catalysis and other techniques for reaction of water insoluble organic substrates with water soluble reagents. A microemulsion can physically catalyse or inhibit chemical reactions by solubilization, compartmentalization and concentration of reactants and products. It can solubilize a wide variety of compounds simultaneously. Microemulsions are used widely in domestics and industrial applications ranging from detergency to cosmetics, pharmaceuticals and tertiary oil recovery as well as media for chemical reactions. Many reactions of interest occur too fast to be accessible by normal techniques, however it is well known, that micelle and microemulsion solutions can have a profound effect on reaction rates for organic and inorganic reactions. Very interesting examples of techniques evolving from research on processes in inverse microemulsions are particle synthesis and polymerization. NTIS

N95-12762# Cornell Univ., Ithaca, NY. School of Applied and Engineering Physics.
PROGRESS ON RESONANCE IONIZATION DETECTION OF COMBUSTION RADICALS
T. A. Cool 1994 7 p
(Contract DE-FG02-86ER-13508)
(DE94-015339; DOE/ER-13508/8) Avail: CASI HC A02/MF A01

Selective laser ionization techniques are used in our laboratory for the measurement of concentration profiles of radical intermediates in the combustion of chlorinated hydrocarbon flames. A new ultra sensitive detection technique, made possible with the advent of tunable VUV laser sources, enables the selective near-threshold photoionization of all radical intermediates in premixed hydrocarbon and chlorinated hydrocarbon flames. The progress made on the following three separate experiments during the past year is briefly described in this report: Flame Radical Concentration Measurements with VUV Spectroscopy; observation of hyperfine quantum beats in cyanogen; and the spectroscopy of the ClCO radical. DOE

N95-12778# California Univ., Berkeley, CA. Dept. of Mechanical Engineering.
FIRE PROPAGATION IN CONCURRENT FLOWS Final Progress Report, 1 Sep. 1992 - 31 Aug. 1993
A. C. Fernandez-Pello ,Jun. 1994 68 p See also PB91-157206 Prepared for National Inst. of Standards and Technology, Gaithersburg, MD
(Grant NIST-60NANB1D1174)
(PB94-193844; NIST/GCR-94/644) Avail: CASI HC A04/MF A01

A research program has being conducted to study the mechanisms controlling the spread of flames in an oxidizing gas flow moving in the direction of flame propagation. During this reporting period research has been conducted to study the effect of the oxidizer flow characteristics on the concurrent flame spread over thick PMMA sheets. The parameters varied in the experiments are the oxidizer flow velocity, turbulence intensity and oxygen concentration, and the geometrical orientation (floor and ceiling). Their effect on the flame spread process is studied by measuring the rate of flame spread, flame length, surface heat flux, products of combustion and soot. The results of the experiments show that the combined effect of flow velocity, turbulence intensity, and oxygen concentration has a complex influence on the flame spread process. At low flow velocity, the flame spread rate increases monotonically with turbulence intensity. At high flow velocity, however, the flame spread rate increases with flow turbulence at low turbulence intensities, but it decreases at high turbulence intensity values. The effect is more pronounced at high oxygen concentration. These trends appear to be due to a strong influence of the turbulence intensity on the flame temperature and length, and on that heat flux from the flame to the solid fuel. Turbulence enhances mixing, which increases the flame temperature and then the heat flux. NTIS

N95-12807# New Mexico Univ., Albuquerque, NM. Dept. of Chemistry.
HYDROLYSIS AND CONDENSATION OF TIN (4) ALKOXIDE COMPOUNDS: THE CONTROL OF STRUCTURAL EVOLUTION Annual Report, Apr. 1993 - Jun. 1994
M. J. Hampden-Smith 3 Jun. 1994 19 p
(Contract F49620-93-1-0197)
(AD-A282789; AFOSR-94-0447TR) Avail: CASI HC A03/MF A01

We are investigating the mechanism of ester elimination reactions between metal alkoxide compounds and metal carboxylate compounds as a method to form metal-oxo clusters in a controlled fashion. We anticipate that the fundamental insight gained will result in a better understanding of methods to control the evolution of microstructure in metal oxide ceramics. Two parts of our preliminary experiments are reported here. Part 1 describes a series of proton (1H) NMR magnetization transfer experiments utilized to measure the kinetic parameters of alcohol interchange between the homoleptic metal alkoxide, Sn(O-t-Bu)4, and t-butanol, its parent alcohol. These data suggest that the metal center, even in sterically encumbered metal alkoxide compounds such as Sn(O-t-Bu)4, are sufficiently coordinately and electronically unsaturated to react with bulky alcohols. These observations must be taken into account when conducting sol-gel type hydrolysis and condensation reactions. In part 2, the alkoxide Sn(O-t-Bu)4 and carboxylate Me3Si(OAc) are used in a detailed study of the ester elimination process. We report time dependent 170 NMR spectra of the ester elimination reaction of the two from which a plausible associative transition state can be described. DTIC

N95-12836# Edgewood Arsenal, Aberdeen Proving Ground, MD. Research Development and Engineering Center.
EFFECTS OF SAMPLE FORMULATION ON THE ANALYSIS OF HEAVY METALS BY X-RAY FLUORESCENCE Final Report, Jul. - Aug. 1993
Sandra J. Steele and William E. White May 1994 23 p
(Contract DAAL03-91-C-0034)
(AD-A282733; ERDEC-TR-162) Avail: CASI HC A03/MF A01

A key area of research in environmental studies is the identification and analysis of metals in soil. Methods of testing soil samples have, in the past, involved much time in the laboratory setting. This report describes the use of an x-ray fluorescence spectrometer (X-MET 840) that can be used in the field, and a method of creating standard samples for its calibration. The method was developed to decrease the time factor involved in calibrating the X-MET 840 and testing soil samples for heavy metal contaminants. Analysis by x-ray fluorescence has many advantages because of the ease of operation and portability of instrumentation. This report describes the effect of pelletizing samples upon reproducibility of analysis. DTIC

N95-12852# California Univ., Berkeley, CA.
BACKDRAFT PHENOMENA Ph.D. Thesis
C. M. Fleischmann Jun. 1994 237 p Prepared for National Inst. of Standards and Technology, Gaithersburg, MD
(Grant NIST-60NANB0D1042)
(PB94-193927; NIST/GCR-94/646) Copyright Avail: CASI HC A11/MF A03

The purpose of this project was to develop a fundamental physical understanding of backdraft phenomena. The research was divided into three phases: exploratory simulations, gravity current modeling, and quantitative backdraft experiments. The primary goal of the first phase was to safely simulate a backdraft in the laboratory. A half-residential-scale compartment was built to conduct exploratory experiments. The initial experiments concluded with a scenario describing the fundamental physics of backdrafts. The importance of the gravity current which enters the compartment after opening was identified. In the second phase, the gravity current speed and the extent of its mixed region was investigated in a series of scaled salt water experiments. The scaled compartment (0.3m x 0.15m x 0.15m) was fitted with a variety of end openings; full, slot, door, and window. Video and photo data indicate that the mixing layer which rides on the gravity current in the full opening case, expands to occupy

nearly the entire current in the partial opening cases. The Froude number and nondimensional head height are independent of beta and are in good agreement with numerical simulations and special limits from the literature. In the final phase, 28 backdraft experiments were conducted in a 1.2m by 1.2m by 2.4m compartment. NTIS

N95-13084*# Alabama Univ., Huntsville, AL.
ANALYSIS FOR Be-7 AND Be-10 ON LDEF MATERIALS AND THEIR SOURCES Final Report
John C. Gregory Jul. 1994 6 p
(Contract NAS8-38609)
(NASA-CR-193989; NAS 1.26:193989) Copyright Avail: CASI HC A02/MF A01

Work has continued on the search for 10Be on metals other than aluminum flown on LDEF. Much time-consuming extractive chemistry has been performed at Rutgers University on turnings obtained from the ends of two stainless steel trunnions from LDEF and prepared samples will be run on the University of Pennsylvania accelerator mass spectrometer. We have continued to investigate our discovery of naturally-occurring 10Be contamination in bauxite and industrial aluminum from different sources. Measurements of 10Be in ores from three different sites, and from four different samples of commercial aluminum have been made. Author

N95-13180 Emory Univ., Atlanta, GA.
LASER SPECTROSCOPY OF GdO: LIGAND FIELD ASSIGNMENTS OF 4f7(8S)6p REVERSING 4f7(8)6s TRANSITIONS
Leonid A. Kaledin, Matthew G. Erickson, and Michael C. Heaven 1994 13 p Submitted for publication Limited Reproducibility: More than 20% of this document may be affected by microfiche quality
(AF Proj. 2303)
(AD-A282827; AFOSR-94-0438TR) Avail: CASI HC A03

Wavelength-resolved fluorescence excitation techniques have been used to record three electronic transitions of GdO at a resolution of 0.03/cm1. Previous analyses of two bands have been extended with some corrections to the assignments of low-J lines. Improved molecular constants were obtained for the X9(sigma)- and a7(sigma)- states that correlate with Gd2+(4f7(8S)6s)02-. A large difference between the spin-orbit coupling constants for X9(Sigma)-(Lambda = -0.10353/cm) and a7(Sigma)-(Lambda = 0.64712/cm) was noted. This difference was ascribed to the fact that the X state is almost pure f7(8S), whereas the a state has partial f7(6P) character. Analysis of the state required off-diagonal matrix elements of the spin-orbit interaction, evaluated using sixth-order degenerate perturbation theory, for treatment of non-rotating molecule spin-orbit intervals. In principle, these elements are needed to describe Sigma states of septet and higher multiplicity. Energy intervals reflecting the structure Gd2+(4f7(8S)6p)02- were recognized among the excited states of GdO. Overall, the results were consistent with ligand field theory models for the excited states of lanthanide oxide (LnO) molecules DTIC

N95-13251# Yale Univ., New Haven, CT. Dept. of Chemical Engineering.
FUNDAMENTAL AND EXPERIMENTAL STUDIES ON THE CATALYTIC COMBUSTION OF METHANE Annual Report, 1 Jul. 1992 - 31 Dec. 1993
L. D. Pfefferle and M. D. Smooke 1994 74 p See also PB94-112661
(Contract GRI-5091-260-2206)
(PB94-205895; GRI-94/0118) Avail: CASI HC A04/MF A01

The overall objective of this project is to obtain and use fundamental experimental data on surface reactivity to model real catalytic combustors. This objective is being approached by focusing on two experimental areas: (1) the effect of surface reactivity on heat and mass transfer and (2) the characterization of the surface reactivity of natural gas on supported metal catalysts. Modeling work focuses on the development of a full 2-D transport model with detailed chemistry to describe systems where a fully developed boundary layer is not achieved and exploring possible simplified models for incorporation into turbulent reacting flow codes. The different components of the project are interrelated in that the experimental objective is to provide both chemical and transport boundary conditions for the model. NTIS

N95-13288 California Univ., Irvine, CA. Dept. of Chemistry.
ELECTROCHEMICAL DEPOSITION OF METAL NANO-DISK STRUCTURES USING THE SCANNING TUNNELING MICROSCOPE Interim Report, May 1993 - Jun. 1994
W. Li, T. Duong, J. A. Virtanen, and R. M. Penner 13 Jul. 1994 12 p Limited Reproducibility: More than 20% of this document may be affected by microfiche quality
(Contract N00014-93-1-0757)
(AD-A282464; TR-1) Avail: Issuing Activity (Defense Technical Information Center (DTIC))

Silver nanodisk structures were electrochemically deposited on graphite surfaces using a scanning tunneling microscope (STM). The deposition of metal occurs via a two-step mechanism involving the fast (2-5 microsec) formation of a 7 A-deep pit in the graphite surface, followed by nucleation and diffusion limited electrochemical deposition at this pit. An electrolysis time of 50 microsec produces diffusion-limited nanostructure dimensions of approximately 200-400 A in diameter and 20-50 A in height. Silver nanodisk structures are stable in dilute aqueous solutions containing Ag(+) at small (approximately 20 mV) sample-negative imaging biases, but are unstable with respect to dissolution at sample positive biases or when immersed in a pure water ambient (irrespective of the applied bias). The mechanism of discharge of a nanometer-scale battery consisting of copper anodes and silver cathodes is examined. DTIC

N95-13372# Optical Society of America, Washington, DC.
SUMMARIES OF PAPERS PRESENTED AT THE HIGH RESOLUTION SPECTROSCOPY TOPICAL MEETING. TECHNICAL DIGEST SERIES. VOLUME 1: POST CONFERENCE EDITION Final Report, 10 Dec. 1992 - 14 Jan. 1994
Jarus W. Quinn May 1994 210 p Meeting held in Salt Lake City, UT, 18-21 Jan. 1993
(Contract DAAH04-93-G-0056)
(AD-A281261; ARO-31111.1-PH-CF) Avail: CASI HC A10/MF A03

The postconference edition of the High Resolution Spectroscopy conference contains summaries of the papers presented at the meeting. The sessions at the conference included double resonance techniques, intra- and inter-molecular interactions, sub-Doppler techniques, condensed phase spectroscopy laboratory astrophysics, and atoms and radicals. DTIC

N95-13531# Atomic Energy of Canada Ltd., Chalk River (Ontario). Nuclear Labs.
CRYOCOL: A COMPUTER PROGRAM TO CALCULATE THE CRYOGENIC DISTILLATION OF HYDROGEN ISOTOPES
S. R. Douglas Feb. 1993 13 p
(DE94-622012; AECL-10830) Avail: CASI HC A03/MF A01 (US Sales Only)

This report describes the computer model and mathematical method coded into the AECL Research computer program CRYOCOL. The purpose of CRYOCOL is to calculate the separation of hydrogen isotopes by cryogenic distillation. DOE

N95-13549 Washington Univ., Seattle, WA.
HYDROGEN BONDING AND MOLECULAR ORIENTATION IN WATER/FLUORINE ADLAYERS ON SILVER(110)
A. Krasnopoler, A. L. Johnson, and E. M. Stuve 11 Jul. 1994 30 p Limited Reproducibility: More than 20% of this document may be affected by microfiche quality
(Contract N00014-91-J-1909)
(AD-A282652; TR-3) Avail: Issuing Activity (Defense Technical Information Center (DTIC))

The orientation and hydrogen bonding interactions of water coadsorbed with atomic fluorine on Ag(110) were examined with high resolution electron energy loss spectroscopy (HREELS) and time-of-flight measurements of electron stimulated desorption ion angular distribution (TOF-ESDIAD). Water exhibits four stabilized adsorption states in the presence of fluorine, identified as the B, A1, A2, and A3 states in order of their decreasing desorption temperatures. The B state interacts with fluorine through one hydrogen bond with the other hydrogen remaining free as evidenced by an O-H stretching frequency of 3700/cm. Water molecules in the A1 state interact through two strong hydrogen bonds in a ratio of one water molecule per fluorine atom and cause a (2x1) to (1x2) surface phase transition of fluorine.

Surprisingly, TOF-ESDIAD measurements detected no H+ emission from either the B or A1 states indicating that all hydrogens are either pointed towards the surface or far enough away from the surface normal to escape detection by ESDIA-D. Instead, emission of only high mass ions (O+/OH+/H2O+/F+) occurs in two beams along the 110 direction for the B state and along the 001 direction for the combined B + A1 states. The A2 and A3 states of water hydrogen bond to the B and A1 states and exhibit vibrational spectra that approach that of ice, although the interaction with fluorine remains sufficiently strong to impart measurable spectral differences. DTIC

26 METALLIC MATERIALS

Includes physical, chemical, and mechanical properties of metals, e.g., corrosion; and metallurgy.

N95-11738# California Univ., Santa Barbara, CA. Dept. of Chemical and Nuclear Engineering.

STUDIES OF LOW TEMPERATURE, LOW FLUX RADIATION EMBRITTLEMENT OF NUCLEAR REACTOR STRUCTURAL MATERIALS

G. R. Odette and G. E. Lucas 1 Jun. 1993 66 p

(Contract DE-FG02-89ER-12895)

(DE94-013710; DOE/ER-12895/T1) Avail: CASI HC A04/MF A01

There are several existing research programs which have components pertinent to the issue of low flux/low temperature embrittlement; in particular, examination of the Shippingport shield tank which has been exposed to low flux and relatively low temperature is being performed by ANL, and evaluation of low temperature embrittlement in A508 and A533B steels in support of the HTGR is currently being performed by ORNL. However, these programs are not specifically directed at the broader issue of low flux/low temperature embrittlement in a range of structural steels. Hence, the authors coordinated their effort with these programs so that their investigations were complementary to existing programs, and they focused on a set of materials which expand the data base developed in these programs. In particular, the authors have investigated embrittlement phenomena in steels that are similar to those used in support structure. DOE

N95-11785# Sandia National Labs., Albuquerque, NM.

A NOVEL LEAD-FREE SOLDER REPLACEMENT

Ning-Cheng Lee (Indium Corp. of America, Utica, NY.), J. A. Slattery (Indium Corp. of America, Utica, NY.), J. R. Sovinsky (Indium Corp. of America, Utica, NY.), I. Artaki (Bell Telephone Labs., Inc., Princeton, NJ.), and P. T. Vianco 1994 10 p Presented at the Surface Mount International Meeting, San Jose, CA, 28 Aug. - 1 Sep. 1994

(Contract DE-AC04-94AL-85000)

(DE94-013782; SAND-94-1542C; CONF-9408109-1) Avail: CASI HC A02/MF A01

Environmental and toxicity concerns related to the use of lead have initiated the search for acceptable, alternate joining materials for electronics assembly. This paper describes a novel lead-free solder designed as a 'drop in' replacement for common tin/lead eutectic solder. The physical and mechanical properties of this solder are discussed in comparison to tin/lead eutectic solder. The performance of this solder when used for electronics assembly is discussed and compared to other common solders. Fatigue testing results are reported for thermal cycling electronics assemblies soldered with this lead-free composition. The paper concludes with a discussion on indium metal availability, supply, and price. DOE

N95-11897# Oak Ridge National Lab., TN.

CERTAIN ASPECTS OF THE MELTING, CASTING AND WELDING OF NI3AI ALLOYS

M. L. Santella and V. K. Sikka 1994 20 p Presented at the 2nd Advanced Joining Technologies for New Materials, Cocoa Beach, FL, 2-4 Mar. 1994

(Contract DE-AC05-84OR-21400)

(DE94-013628; CONF-940367-3) Avail: CASI HC A03/MF A01

Two alloys under development for castings are IC221M, (nominal composition Ni-8Al-7.7Cr-1.4Mo-1.7Zr wt percent), and IC396M (nominal composition Ni-8Al-7.7Cr-3Mo-0.85Zr wt percent). These alloys can be melted and cast using the techniques normally used for Ni-based materials. Oxidation of the liquid alloys can be controlled by vacuum processing or inert gas cover during processing. The liquid alloys can react with silica and zircon sands during casting, but this can be controlled through the use of appropriate mold washes like carbon-based materials. Welding studies showed that these alloys are susceptible to solidification cracking in weld fusion zones; the cracks are generally associated with occurrence of Ni-Ni5Zr eutectic in interdendritic regions of the weld. Amount of eutectic in the weld microstructures increases with Zr concentration in weld filler metal. Weld filler metal Zr concentrations of 3 wt percent and higher prevented solidification cracking of weld deposits on the base casting alloys; This is consistent with accepted phenomonological theory of this process. A weld filler metal with a composition of Ni-8Al-7.7Cr-1.5Mo-3.0Zr wt percent was prepared and used to gas tungsten arc weld together 15-mm-thick plates of the IC221M alloy. This weldment was free of cracks. Weldment tensile specimens were machined from the plate and tested at 21, 800, and 900 C. Weldment yield strength at elevated temperatures was higher than room temperature and nearly comparable with that of the base IC221M alloy. Evaluation of the cast Ni3Al alloys for furnace furniture, turbocharger rotors, and manufacturing tooling is also briefly discussed. DOE

N95-11915*# National Aeronautics and Space Administration. Langley Research Center, Hampton, VA.

MODELING AND LIFE PREDICTION METHODOLOGY FOR TITANIUM MATRIX COMPOSITES SUBJECTED TO MISSION PROFILES

M. Mirdamadi (Analytical Services and Materials, Inc., Hampton, VA.) and W. S. Johnson Aug. 1994 37 p

(RTOP 505-63-50-04)

(NASA-TM-109148; NAS 1.15:109148) Avail: CASI HC A03/MF A01

Titanium matrix composites (TMC) are being evaluated as structural materials for elevated temperature applications in future generation hypersonic vehicles. In such applications, TMC components are subjected to complex thermomechanical loading profiles at various elevated temperatures. Therefore, thermomechanical fatigue (TMF) testing, using a simulated mission profile, is essential for evaluation and development of life prediction methodologies. The objective of the research presented in this paper was to evaluate the TMF response of the (0/90)2s SCS-6/Timetal-21S subjected to a generic hypersonic flight profile and its portions with a temperature ranging from -130 C to 816 C. It was found that the composite modulus, prior to rapid degradation, had consistent values for all the profiles tested. A micromechanics based analysis was used to predict the stress-strain response of the laminate and of the constituents in each ply during thermomechanical loading conditions by using only constituent properties as input. The fiber was modeled as elastic with transverse orthotropic and temperature dependent properties. The matrix was modeled using a thermoviscoplastic constitutive relation. In the analysis, the composite modulus degradation was assumed to result from matrix cracking and was modeled by reducing the matrix modulus. Fatigue lives of the composite subjected to the complex generic hypersonic flight profile were well correlated using the predicted stress in 0 degree fibers. Author

N95-11933*# Virginia Univ., Charlottesville, VA.

COMPUTER MODELING THE FATIGUE CRACK GROWTH RATE BEHAVIOR OF METALS IN CORROSIVE ENVIRONMENTS Final Report

Edward Richey, III, Allen W. Wilson, Jonathan M. Pope, and Richard P. Gangloff Sep. 1994 174 p

(Grant NAG1-745; RTOP 538-02-10-01)

(NASA-CR-194982; NAS 1.26:194982) Avail: CASI HC A08/MF A02

The emphasis of the second phase of this research project has been to develop a single computer program that would establish the foundation to incorporate deleterious environmental effects on fatigue crack propagation laws into NASA FLAGRO. The program was the result of team research projects conducted by three undergraduates in the Department of Mechanical and Aerospace Engineering at University of Virginia. Known methods to interpolate and potentially extrapolate environmental fatigue crack propagation (FCP) data were emphasized, including linear superposition and empirical curve-fitting descriptions of fatigue crack growth rate (da/dN) versus applied or effective stress intensity range (delta K). This program contains elements that were extracted from the NASA FLAGRO source code, particularly library data on material fatigue and fracture properties, as well as the Forman equations for calculations on fatigue crack growth rate versus stress intensity relationships, including the effect of crack closure. The program was written in Fortran and is executed by entering MENU

from the DOS prompt on an IBM-compatible personal computer. The user can then select one of the following three options that resulted from each undergraduate project. The projects are as follows: Digitization of Crack Growth Rate Data, Interpolation Modeling of Environmental FCP Data, and Linear Superposition Modeling of Environmental FCP Data. Example calculations demonstrating each element of the program are presented in several appendices to this report. CASI

N95-12104*# National Aeronautics and Space Administration. Lewis Research Center, Cleveland, OH.
GROWTH OF Au ON Ni(110): A BFS MODELLING OF SURFACE ALLOY PHASES
Guillermo Bozzolo (Analex Corp., Brook Park, OH.), Rodrigo Ibanez-Meier, and John Ferrante Sep. 1994 27 p
(Contract NAS3-25776; RTOP 505-90-53)
(NASA-TM-106732; E-9108; NAS 1.15:106732) Avail: CASI HC A03/MF A01

Recent experiments using scanning tunneling microscopy show evidence for the formation of surface alloys of otherwise immiscible metals. Such is the case for Au deposited in Ni(11), where experiments by Pleth Nielsen et al. indicate that at low Au coverage (less than 0.5 ML), Au atoms replace Ni atoms in the surface layer forming a surface alloy while the Ni atoms form islands on the surface. In this work, we present results of a theoretical modeling of this phenomenon using the recently developed BFS method for alloys. We provide results of an extensive analysis of the growth process which strongly support the conclusions drawn from the experiment; at very low coverages, there is tendency for dimer formation on the overlayer, which later exchange positions with Ni atoms in the surface layer, thus accounting for the large number of substituted dimers. Ni island formations as well as other alternative short range order patterns are discussed. Author

N95-12148*# Aerospace Corp., El Segundo, CA. Electronics Technology Center.
SCREEN TEST FOR CADMIUM AND NICKEL PLATES AS DEVELOPED AND USED WITHIN THE AEROSPACE CORPORATION
A. H. Phan and A. H. Zimmerman 15 Aug. 1994 18 p Sponsored by NASA. Marshall Space Flight Center
(NASA-CR-196961; NAS 1.26:196961; ATR-94(8010)-3) Avail: CASI HC A03/MF A01

A new procedure described here was recently developed to quantify loading uniformity of nickel and cadmium plates and to screen finished electrodes prior to cell assembly. The technique utilizes the initial solubility rates of the active material in a standard chemical deloading solution at fixed conditions. The method can provide a reproducible indication of plate loading uniformity in situations where high surface loading limits the free flow of deloading solution into the internal porosity of the sinter plate. A preliminary study indicates that 'good' cell performance is associated with higher deloading rates. Author

N95-12372# Pacific Northwest Lab., Richland, WA.
EFFECT OF PRE-WELDING HEAT-TREATMENTS ON WELDING A TWO-PHASE NI3AI ALLOY
Hua-Xin Li (Associated Western Universities, Inc., Salt Lake City, UT.) and R. H. Jones May 1994 21 p Presented at the International Conference on High-Temperature Intermetallics, San Diego, CA, 16-19 May 1994
(Contract DE-AC06-76RL-01830)
(DE94-014409; PNL-SA-22934; CONF-940598-2) Avail: CASI HC A03/MF A01

Autogenous gas-tungsten arc welding was performed on a two-phase Ni3Al alloy. Plates 3 mm thick were subjected to three pre-welding heat treatments (PWHT): as-cast, annealed at 1100 C for 23 h (HT1), and HT1 plus 1120 C/30 min/air cool (HT2). As-cast alloy was characterized by dendrites with many eutectic cells located at dendrite boundaries (DB's). The eutectic cells were destroyed by HT1. However, HT2 made no further changes on microstructure. Energy dispersive x-ray spectroscopy (EDX) revealed that the DB's of as-cast alloy were enriched with Zr. The Zr enrichment at DB's was increased further by HT1 and HT2. No solidification crack visible to the unaided eye was found in either fusion zone (FZ) or heat-affected zone (HAZ) due to welding. The FZ consisted of columnar grains with a eutectic structure along the boundaries. The eutectic structure was enriched with Zr and contained many microcracks and some Zr-rich phases. Micro-solidification cracks were occasionally found along boundaries in FZ. The alloy was sensitive to liquation cracks that occurred along DB's in the HAZ. While PWHT had no effect on the characteristics of the FZ, PWHT had a notable effect on the severity of liquation cracking. The average crack numbers per 5 cm weldment were 12 for as-cast, 14 for HT1, and 17 for HT2. The role of Zr-inducing solidification cracks in FZ and liquation cracks in HAZ is discussed. DOE

N95-12401 Army Armament Research, Development and Engineering Center, Watervliet, NY. Benet Lab.
YIELD-BEFORE-BREAK FRACTURE MECHANICS ANALYSIS OF HIGH STRENGTH STEEL PRESSURE VEHICLES Final Report
John H. Underwood, Richard A. Farrara, and Michael J. Audino May 1994 25 p Limited Reproducibility: More than 20% of this document may be affected by microfiche quality
(AD-A282518; ARCCB-TR-94017) Avail: CASI HC A03

Case study examples of fracture mechanics testing and analysis of Ni-Cr-Mo high strength steel cannon tubes are presented. The testing and analysis include significant plastic deformation accompanying fracture, which often occurs when high pressure is applied to high toughness steel pressure vessels. The analysis is based on a comparison of the size of the Irwin crack-tip plastic zone with the remaining ligament of the tube in the critical fatigue crack area that cause final failure. The results of the study show that the type of final failure can be predicted as either a relatively safe yield-before-break failure or a less safe running-crack type of failure for a variety of material, configuration, and loading conditions. DTIC

N95-12543 Texas Univ., Austin, TX.
FIRST PRINCIPLES INVESTIGATION OF THE Ir-Zr-Nb TERNARY SYSTEM M.S. Thesis
Gregory A. Miller May 1994 46 p Limited Reproducibility: More than 20% of this document may be affected by microfiche quality
(Contract N00014-90-J-1185)
(AD-A282644) Avail: CASI HC A03

Alloy design could benefit greatly from a systematic approach that combines current empirical practices with the predictive capabilities of computer modeling such as first principles based methods. At this point in time, realization of such an aid to alloy design requires the investigation of alloying systems based on first principles approaches to determine ultimate limitations and gauge the merits of this type of predictive method. The following study begins an investigation of the Ir-Zr-Nb ternary system based on combining first principles total energy calculations with a statistical mechanics description of solids. The Ir-Zr-Nb ternary system was initially chosen for the two highly ordered binary systems, Ir-Zr and Ir-Nb, and, more specifically, for coordinating with experimental work on the Ir(3)Zr(1-x)Nb(x) system. The two main contributions of this study include compiling a database of first principles data for fcc- and bcc-based compounds for the Ir-Zr-Nb ternary system, and calculating the Ir-Zr-Nb fcc metastable ternary phase diagram. DTIC

N95-12546 Pratt and Whitney Aircraft, West Palm Beach, FL. Government Engines and Space Propulsion.
FATIGUE IN SINGLE CRYSTAL NICKEL SUPERALLOYS Progress Report, 16 Feb. - 15 May 1994
Daniel P. DeLuca and Charles Annis 15 May 1994 12 p Limited Reproducibility: More than 20% of this document may be affected by microfiche quality
(Contract N00014-91-C-0124)
(AD-A283459; PW/GESP-FR21998-23) Avail: CASI HC A03

This program investigates the seemingly unusual behavior of single crystal airfoil materials. The fatigue initiation processes in single crystal (SC) materials are significantly more complicated and involved than fatigue initiation and subsequent behavior of a (single) macrocrack in conventional, isotropic, materials. To understand these differences is the major goal of this project. DTIC

N95-12630*# Southern Research Inst., Birmingham, AL.
CGF CARTRIDGE DEVELOPMENT, VOLUME 1 Final Report, Nov. 1990 - Dec. 1992
Carl A. Dixon Mar. 1993 234 p
(Contract NAS8-39026)

(NASA-CR-196508; NAS 1.26:196508; SRI-MME-93-261-7244.02-Vol-1) Avail: CASI HC A11/MF A03

This report is a summary of SRI's efforts in Crystal Growth Furnace cartridge developments. It includes: evaluation of molybdenum, TZM, and WC-103 as cartridge materials; a survey of oxidation resistant coatings; chemical compatibility studies of cadmium-zinc-telluride and gallium-arsenide with TZM and WC-103; a survey of future cartridge materials; and suggested improvements in ampoule design. Author

N95-12895# Colorado School of Mines, Golden, CO. Center for Welding and Joining Research.

NOVEL CONCEPTS IN WELD SCIENCE: ROLE OF GRADIENTS AND COMPOSITE STRUCTURE

D. K. Matlock and D. L. Olson Mar. 1994 23 p

(Contract DE-FG02-87ER-45308)

(DE94-015482; DOE/ER-45308/7; MT-CWR-094-013) Avail: CASI HC A03/MF A01

The effects of compositional and microstructural gradients on weld metal and simulated weld metal properties were evaluated in this multi-part study. The results obtained on single phase solid solution systems were used as a basis for a fundamental study of the effects of compositional gradients on crack growth, both at low temperatures in fatigue and at high temperatures during creep. Methods to physically simulate gradients in weld metals with roll bonded laminate composites were applied to analyses of ferrite-austenite and ferrite-sigma-austenite multiphase systems. Finally, results of the physical simulation analyses were utilized to predict the effects of weld process parameters on weld metal properties. DOE

N95-12925 Defence Metallurgical Research Lab., Hyderabad (India).

SYMPOSIUM ON STRUCTURAL INTERMETALLICS: PERSPECTIVES ON SCIENCE AND TECHNOLOGY, VOLUME 1

6 Feb. 1994 191 p Symposium held in Hyderabad, India, 5-6 Feb. 1994 Limited Reproducibility: More than 20% of this document may be affected by microfiche quality

(AD-A283378) Avail: Issuing Activity (Defense Technical Information Center (DTIC))

A two day symposium on 'Structural Intermetallics: Perspectives on Science and Technology' was held at the Defence Metallurgical Research Laboratory, Hyderabad, India, on February 5 and 6, 1994. The Symposium was organized by the Metal Group of the Materials Research Society of India and cosponsored by the Asian Office of Aerospace Research and Development, US Air Force. C.V. Sundaram, Chairman, Metals Group of the Materials Research Society of India, noted in his introductory remarks that the progress towards the development of intermetallics to application has been 'exasperatingly' slow. Robert Cahn of the University of Cambridge, UK, in a keynote lecture provided a historical perspective on early research on 'weakly ordered' alloys and examples of more recent work on 'strongly ordered' compounds. DTIC

N95-13140# Naval Research Lab., Washington, DC.

ORIGIN OF OPTICAL ANISOTROPY IN STRAINED In(x)Ga(1-x)As/InP AND In(y)Al(1-y)As/InP HETEROSTRUCTURES

B. R. Bennett, J. A. delAlamo, M. T. Sinn, F. Peiro, A. Cornet, and D. E. Aspnes 10 Oct. 1993 32 p

(AD-A283152) Avail: CASI HC A03/MF A01

Optical anisotropy in mismatched In(x)Ga(1-x)As/InP and In(y)Al(1-y)As/InP heterostructures has been investigated by variable azimuthal angle ellipsometry and reflectance difference spectroscopy. The two approaches are shown to yield strongly correlated results. A comparison to high resolution x-ray diffraction, transmission electron microscopy, and atomic force microscopy studies indicates that large optical anisotropies are associated with surface roughening that results from three dimensional growth. Our findings demonstrate that fast and nondestructive measurements of optical anisotropy can provide important information about the growth mode and crystalline quality of strained epitaxial layers. DTIC

N95-13411 Technische Univ., Delft (Netherlands).

KINETICS AND CHARACTERIZATION OF TUNGSTEN CVD PROCESSES Ph.D. Thesis

J. A. M. Ammerlaan 28 Feb. 1994 183 p

(PB94-206901; ISBN-90-6275-961-0) Copyright Avail: Issuing Activity (National Techical Information Service (NTIS))

The present thesis comprises the results of experimental and theoretical studies of different tungsten chemical vapor deposition (CVD) processes. It focuses on two aspects of basic research. The first part deals with the kinetics and mechanism of currently employed WF6-based processes, using H2 and SiH4 as reducing agents. An account of investigations in the field of alternative, fluorine-free tungsten precursors, is given in the second part. NTIS

N95-13543# Northwestern Univ., Evanston, IL. Dept. of Materials Science and Engineering.

ATOMIC STRUCTURES AND COMPOSITIONS OF INTERNAL INTERFACES

D. N. Seidman and K. L. Merkle 14 Jun. 1994 13 p

(Contract DE-FG02-89ER-45403)

(DE94-013594; DOE/ER-45403/5) Avail: CASI HC A03/MF A01

An atomic scale study was made of the Ag/CdO(222) heterophase interface produced by internal oxidation of a Ag(Cd) alloy, using HREM (High Resolution Electron Microscopy) and atom-probe field-ion microscopy (APFIM). A study was commenced of interfacial segregation at metal/metal oxide interfaces; the system being studied is the Cu(Ag)/MgO(222) heterophase interface, where Ag is the segregating species. A study was made of the necessary conditions to measure the oxygen content in MgO precipitates produced by internal oxidation of Cu(Mg) alloys, using APFIM. We are also studying solute-atom segregation at grain boundaries in Ni-Pd alloys via computer simulations and combined APFIM/TEM. DOE

N95-13544# Sandia National Labs., Albuquerque, NM.

DESCRIPTION OF A HIGH TEMPERATURE QUENCHING FURNACE FOR THE STUDY OF THE DIRECTIONAL SOLIDIFICATION OF NICKEL-BASE SUPERALLOYS

D. T. Schmale, J. B. Kelley, and B. K. Damkroger Jun. 1994 27 p

(Contract DE-AC04-94AL-85000)

(DE94-013812; SAND-94-0663) Avail: CASI HC A03/MF A01

A high temperature resistance furnace has been modified for the study of directional solidification of nickel-base superalloys such as alloys 718 and 625. The furnace will be used to study segregation and solidification phenomena that occur in consumable-electrode melting processes such as vacuum arc remelting and electro-slag remelting. The system consists of a water cooled high temperature furnace (maximum temperature approximately 2900 C), roughing vacuum, system, cooling system, cooled hearth, molten metal quenching bath, and a mechanism to lower the hearth from the furnace into the molten metal bath. The lowering mechanism is actuated by a digital stopping motor with a programmable controller. The specimen (1.9 cm dia x 14 cm long) is melted and contained within an alumina tube (2.54 cm dia x 15.24 cm long) which is seated on a copper hearth cooled with approximately 13 C water. Directional solidification can then be accomplished by decreasing the furnace temperature while holding the specimen in position, maintaining the temperature gradient in the furnace and lowering the specimen at a controlled rate or a combination of both. At any point the specimen can be lowered rapidly into the 70 C molten metal bath to quench the specimen, preserve the solidification structure, and minimize solid state diffusion, enhancing the ability to study the localized solidification conditions. DOE

N95-13554# Michigan Univ., Ann Arbor, MI.

SYNCHROTRON STUDIES OF NARROW BAND MATERIALS

1994 4 p

(Contract DE-FG02-90ER-45416)

(DE94-013698; DOE/ER-45416/4) Avail: CASI HC A01/MF A01

This progress report is divided into: (1) activity (beamtime, data analysis, lab studies); (2) model Fermi liquids and non-Fermi liquids- TiTe2 -further ARPES and lineshape analysis, TiS2 ARPES, K(0.3)MoO3 and Li(0.9)Mo6O17 ARPES); (3) insulator to metal transitions (early transition metal oxides, Fe3O4, La(2-x)Sr(x)CuO4 ARPES); (4) rare earth and actinide materials UCu(1-x)Pd(x)5, UPt(1-x)Pd(x)3, CeAl3 and CeSi2 resonant photoemission, CeFe2/CeRh3B2/CeCo2/CeCo5 x-ray magnetic circular dichroism; and (5) technique oriented resonant photoemission studies-resonant ARPES in TiTe 2, resonant photoemission at 2p edge in TiTe2. DOE

27 NONMETALLIC MATERIALS

Includes physical, chemical, and mechanical properties of plastics, elastomers, lubricants, polymers, textiles, adhesives, and ceramic materials.

For composite materials see *24 Composite Materials.*

N95-11733# Oak Ridge National Lab., TN.
STUDIES OF POSITRON INDUCED LUMINESCENCE FROM POLYMERS
J. Xu, L. D. Hulett, Jr., T. A. Lewis, and N. H. Tolk 1994 5 p Presented at the 10th International Conference on Positron Annihilation, Beijing, China, 23-29 May 1994
(Contract DE-AC05-84OR-21400)
(DE94-013622; CONF-9405170-2) Avail: CASI HC A01/MF A01

Light emission from polymers (anthracene dissolved in polystyrene) induced by low-energy positrons and electrons has been studied. Results indicate a clear difference between optical emissions under positron and electron bombardment. The positron-induced luminescence spectrum is believed to be generated by both collisional and annihilation processes. DOE

N95-11736# Oak Ridge National Lab., TN.
SURFACE ROUGHNESS CHARACTERIZATION OF VARIOUS CERAMIC FIBERS USING AFM AND LOW VOLTAGE SEM
K. L. More, E. Lara-Curzio, and R. A. Lowden 1994 3 p Presented at the Microscopy Society of America and Microbeam Analysis Society Joint Meeting, New Orleans, LA, 31 Jul. - 5 Aug. 1994
(Contract DE-AC05-84OR-21400)
(DE94-013635; CONF-940753-21) Avail: CASI HC A01/MF A01

Effect of interfacial properties in fiber-reinforced ceramic matrix composites is critical to overall mechanical behavior of the composite. In this study, the surfaces of several ceramic fibers (Nicalon SiC, Nextel aluminosilicate) were studied qualitatively using a FEG SEM at low voltages and quantitatively using AFM. Nicalon fibers had a Ra (arithmetic mean of absolute values of departure of roughness profile from mean line) of 3.4 nm over several line scans, 3.9 nm from area analysis. Nextel fibers, which are oval, are slightly rougher than Nicalon and have an average Ra of 4.8 nm from several line profiles. Grooves ran the entire length of the Nextel fibers. DOE

N95-11781# Research Management Consultants, Inc., Washington, DC.
COMPOSITES (CFCCs) FOR LOW COST ENERGY AND CLEANER ENVIRONMENT
Feb. 1994 20 p
(Contracts DE-AC05-84OR-21400; DE-AC01-91CE-40956)
(DE94-013601; DOE/OR-2002; ORNL/M-3326) Avail: CASI HC A03/MF A01

For many industrial applications, materials are desired which combine light weight, high temperature strength, and stability in corrosive environments. Among competing materials, ceramics are noteworthy candidates for such applications. The use of ceramics is often constrained, however, by brittleness; i.e., low toughness. Ceramic composites are being developed to overcome this limitation. With recent advances in ceramic fiber technology, it is possible to design a composite material based on continuous ceramic fibers embedded in a ceramic matrix. The use of ceramic composites in industrial applications will result in reduced fuel consumption, but will also prevent airborne pollution (principally NO, SO(x), CO2, and particulates), and economically benefit the end user through energy and environmental savings and increased competitiveness. Industry will also benefit through increased productivity and consumers will benefit through lower energy and environmental costs and a cleaner environment. The development and use of CFCC's could become an important factor in the international competitiveness of U.S. industry. CFCC's will be a critical enabling material in the design and engineering of advanced components, systems, and processes. If CFCC technology is developed outside the United States, domestic users of these materials may be forced to rely on foreign suppliers of the products fabricated from CFCC's, as well as the materials themselves. Foreign countries, including Japan and France, have embarked on government-supported CFCC development efforts. With the market for CFCC products expected to be a $10 billion dollar market by 2010, CFCC development will be important for the competitiveness of U.S. industry and for retaining and creating jobs for U.S. citizens. This document summarizes the potential energy, environmental, and economic benefits that CFCC's will have for the U.S. economy and particularly for the industrial sector. DOE

N95-11832 Pennsylvania State Univ., University Park, PA. Dept. of Chemistry.
THE SYNTHESIS AND STRUCTURE OF POLYPHOSPHAZENES Final Report, 1 May 1991 - 30 Apr. 1994
Harry R. Allcock 21 Jun. 1994 6 p Limited Reproducibility: More than 20% of this document may be affected by microfiche quality
(Contract DAAL03-91-G-0124)
(AD-A281723; ARO-28711.21-CH) Avail: CASI HC A02

A substantial number of new polymer systems have been synthesized and developed to make use of the valuable properties imparted by inorganic elements incorporated into a macromolecular structure. The new polymers range from solvent-resistant elastomers to non-burning materials, and species that form excellent membranes and structural materials. The work has led also to the development of a system for understanding the relationship between polymer structure and useful property combinations in ways that should assist the rapid evolution of new polymers needed for specific specialized applications. Author (DTIC)

N95-11847 Helsinki Univ. of Technology, Espoo (Finland). Lab. of Material Physics.
TUNING THROUGH THE CRITICAL REGIME OF THE METAL-INSULATOR-TRANSITION IN CONDUCTING POLYMERS BY PRESSURE AND MAGNETIC FIELD
R. M. K. Vaekiparta, C. O. Yoon, Y. Cao, D. Moses, and A. J. Heeger 1993 16 p Prepared in cooperation with California Univ., Santa Barbara, CA Limited Reproducibility: More than 20% of this document may be affected by microfiche quality
(PB94-179165; TKK-F-A716) Avail: CASI HC A03

In the critical regime of the disorder-induced metal insulator (M-I) transition, the temperature dependence of conductivity follows a power law, and the reduced activation energy function, W, is temperature independent. The authors have observed charge transport in the critical regime for four conducting polymer systems: potassium doped polyacetylene (CH)x, iodine doped polyacetylene, phosphorous hexafluoride (PF6(-)) doped polypyrrole (PPy), and camphor sulphonic acid (CSA) doped polyaniline (PANI). It is shown that the electrical properties of conducting polymers can be tuned through the disorder-induced critical regime of M-I transition into metallic or insulating regimes and magnetic field, respectively. NTIS

N95-11852# Massachusetts Univ., Amherst, MA. Dept. of Polymer Science and Engineering.
SYNTHESIS, STRUCTURE AND PROPERTIES OF SEGMENTED POLYMERS CONTAINING MESOGENS Final Report, 22 Apr. 1991 - 21 Apr. 1994
Richard J. Farris, Shaw L. Hsu, and William J. MacKnight Jun. 1994 6 p
(Contract DAAL03-91-G-0127)
(AD-A281419; ARO-28314.10-CH) Avail: CASI HC A02/MF A01

The purpose of the research carried out under Contract Number DAAL-03-9IG-0127 was to determine the phase behavior and to explore the conditions for thermodynamic stability in polyurethanes containing mesogens. The work involved both segmented polyurethanes with the mesogens residing in the hard segments, and model nonsegmented polyurethanes containing mesogenic groups. In addition, molecular simulation techniques were brought to bear upon the problem of the structure of the mesogen containing polyurethanes and the phase diagram of segmented polyurethanes with hard segments containing rigid (diacetylene) moieties. The research was a cooperative venture among three members of the Polymer Science and Engineering Department at the University of Massachusetts. R.J. Farris studied the thermodynamics of deformation and the processing of the polyurethanes to produce high degrees of orientation in both films and fibers. S.L. Hsu concentrated on molecular characterization using vibrational spectroscopy. He also was largely responsible for the molecular simulation efforts. W.J. MacKnight conducted the synthesis, characterization, mechanical and thermal properties, and morphology studies. DTIC

N95-12008 University of Southern Mississippi, Hattiesburg, MS. Dept. of Polymer Science.
NOVEL THERMOOXIDATIVELY STABLE POLY(ETHER-IMIDE-BENZOXAZOLE) AND POLY(ESTER-IMIDE-BENZOXAZOLE) Technical Report, 1 Jun. 1993 - 31 May 1994
Raj A. Sundar and Lon J. Mathias 15 Jul. 1994 53 p Limited Reproducibility: More than 20% of this document may be affected by microfiche quality
(Contract N00014-89-J-1225)
(AD-A282381; TR-72) Avail: CASI HC A04

4-Hydroxy-5-nitrophthalimides were produced via nucleophilic aromatic substitution (NAS) of 4,5-dichloro phthalimide substituents by potassium nitrite. The use of a N-phenylphthalimide having a protected 4'-hydroxyl group allows concurrent deprotection and nitro reduction to amine to give the 4-hydroxy-5-amino-N-(4' hydroxyphenyl) phthalimide. This key intermediate is the precursor to a poly(ether-imide-benzoxazole), and is the condensable monomer for a poly(ester-imide-benzoxazole). Benzoxazole monomer formation via condensation with p-fluorobenzoyl chloride afforded 2-(4'-fluorophenyl)- 5,6,-N-(4'(-hydroxyphenyl)imide) benzoxazole, which was polymerized under NAS condiditons to produce a poly(ether-imide-benzoxazole) having an endothermic transition at 454 C with weight retention of 90% at 500 C in both air and nitrogen. Solution polycondensation of the 4-hydroxy-5-amino- N-(4'-hydroxyphenyl) phthalimide monomer with isophthaloyl chloride afforded a poly(ester-amide-imide) which was isolated and thermally cyclodehydrated in the solid state under vacuum to give a poly(ester-imide-benzoxazole) having 95% weight retention at 500 C in both air and nitrogen, with no detectable DSC transitions up to 500 C. DTIC

N95-12131# Army Engineer Waterways Experiment Station, Vicksburg, MS. Geotechnical Lab.
ADDITIVES IN BITUMINOUS MATERIALS AND FUEL-RESISTANT SEALERS Final Report, Oct. 1990 - Jul. 1993
Gary L. Anderton and Laurand H. Lewandowski Aug. 1994 117 p
(Contract DTFA01-90-Z-02069)
(DOT/FAA/CT-94/78; DOT/FAA/RD-93/30) Avail: CASI HC A06/MF A02

This report provides a matrix of information on the current state-of-the-art of commercially available additives for bituminous materials and fuel-resistant sealers. Included in this report is a brief history of these types of additives, the results of an airport field survey, descriptions of seven airport site visits, and detailed discussions of a series of laboratory tests used to physically and chemically characterize these additives. A literature search was conducted throughout the study in order to provide the latest information on each reported additive. The information gained from the literature search, field survey, site visits, and laboratory analyses was used to develop an additives database containing information profiles of each additive. The database is presented in hard copy as an appendix of this report, and is also presents in a user-friendly computerized database as a supplement to this report. Author

N95-12397 University of Southern Mississippi, Hattiesburg, MS. Dept. of Polymer Science.
SYNTHESIS AND SOLID-STATE NMR CHARACTERIZATION OF 13C- AND 15N-LABELLED N-METHYLPHTHALIMIDE: A MODEL COMPOUND FOR STUDYING POLYIMIDES Technical Report, 1 Jun. 1993 - 31 May 1994
William L. Jarrett, Lon J. Mathias, and C. G. Johnson 15 Jul. 1994 3 p Limited Reproducibility: More than 20% of this document may be affected by microfiche quality
(Contract N00014-89-J-1225)
(AD-A282510; TR-68) Avail: Issuing Activity (Defense Technical Information Center (DTIC))

The Gabriel method allows preparation of imide derivatives from methyl iodide in good yields. The 1H T(sub 1)'s were approximately 65-78 s for all protons, including the aromatic protons. 13C CP/MAS NMR spectra of the model N-methylphthalimides showed multiplet peaks for the aromatic carbons which may be due to differences in crystal packing. However, the 15N spectra show a single peak for imides 2 and 3. A procedure has been developed for incorporating 15N and 13C isotopic labeling into N-methylphthalimide, a model imide. From solid-state 15N NMR spectroscopic methods the values and orientation of the delta shift tensor with respect to the N-CH3 bond as well as the N-CH3 bond length have been determined. DTIC

N95-12399 University of Southern Mississippi, Hattiesburg, MS. Dept. of Polymer Science.
SYNTHESIS AND CHARACTERIZATION OF THIANTHRENE-BASED POLYAMIDES Technical Report, 1 Jun. 1993 - 31 May 1994
Randy A. Johnson and Lon J. Mathias 15 Jul. 1994 31 p Limited Reproducibility: More than 20% of this document may be affected by microfiche quality
(Contract N00014-89-J-1225)
(AD-A282512; TR-73) Avail: Issuing Activity (Defense Technical Information Center (DTIC))

Thianthrene-2,7- and -2,8-dicarboxylic acids plus a synthetic intermediate, 4,4'-thiobis (3-chlorobenzoic acid), have been synthesized in good yields via nucleophilic aromatic substitution of Na2S on N,N-dimethyl -3,4-dichlorobenzamide. New aromatic polyamides having inherent viscosities of 1.29 to 2.39 dL/g were prepared by the direct polycondensation reaction of the dicarboxylic acids with 4,4'-oxydianiline and 1,4-phenylenediamine in N-methyl 2-pyrrolidinone using triphenyl phosphite and pyridine. The fused-ring thianthrene-based polyamides were more soluble than analogous poly(thioether amide)s. Polymer films were cast from either DMF or DMAc/LiCl solutions and analyzed by FTIR and NMR. All prepared aramids displayed good thermal stability by DSC and TGA. Author (DTIC)

N95-12400 University of Southern Mississippi, Hattiesburg, MS. Dept. of Polymer Science.
MULTIFUNCTIONAL ACRYLIC ETHER MONOMERS, THEIR POLYMERS, AND POLYMERIZABLE EPOXIDE DERIVATIVES FROM SIMPLE ALPHA-SUBSTITUTION OF ALKYL ACRYLATES Technical Report, 1 Jun. 1993 - 31 May 1994
Robert D. Johnson, Lon J. Mathias, and Thomas H. Barclay 15 Jul. 1994 3 p Limited Reproducibility: More than 20% of this document may be affected by microfiche quality
(Contract N00014-89-J-1225)
(AD-A282513; TR-67) Avail: Issuing Activity (Defense Technical Information Center (DTIC))

Our group has been exploring the synthesis of 1,1-disubstituted monomers and their polymers obtained via the DABCO catalyzed hydroxy-methylation of alkyl acrylates. Previous work in this area has involved complicated or low yield syntheses. We are using a simple, clean synthetic technique using paraformaldehyde and neat substrate to produce alkyl alpha(hydroxymethyl)acrylates, albeit in yields of only 25-30%. Conversion of the hydroxymethyl group with thionyl chloride gives a reactive allyl chloride which allows a wide range of ether forming reactions to be applied. The ether linkage is inherently more stable than the ester linkage and is much more flexible. DTIC

N95-12403 Ibis Associates, Inc., Wellesley, MA.
ANALYSIS OF COST: COMBUSTION FLAME CVD DIAMOND DEPOSITION Quarterly Report No. 2
1994 19 p Limited Reproducibility: More than 20% of this document may be affected by microfiche quality
(Contract N00014-93-C-2044)
(AD-A282527) Avail: Issuing Activity (Defense Technical Information Center (DTIC))

IBIS Associates has improved its predictive spreadsheet model of combustion flame chemical vapor deposition (CVD) diamond film fabrication. This report explains the improvements on the combustion flame deposition theory, and shows preliminary results of the economics of this CVD diamond process. The changes to the model include the incorporation of thermal conductivity as an input to the model, allowing the user to specify the thermal properties of the diamond being formed. Also, the deposition theory in the model has been streamlined with the assistance of diamond deposition experts. Numerous inputs have been eliminated in this process, making the model easier to use. For this report and the results contained herein, it is assumed that the transport theory model which predicts growth rates in the CVD diamond technical cost model closely predicts actual growth rates for the combustion flame technology and that the input values for variables such as the gas flow rate and substrate diameter are physically achievable. DTIC

N95-12407# Rochester Univ., NY. Dept. of Chemical Engineering.
ELECTRONIC ENERGY TRANSFER IN NEW POLYMER NANOCOMPOSITE ASSEMBLIES
S. A. Jenekhe and C.-J. Yang 13 Jul. 1994 39 p
(Contract N00014-94-1-0540)
(AD-A282233; TR-4) Avail: CASI HC A03/MF A01

New light-harvesting thin film supramolecular assemblies, consisting of rod-coil polymer nanocomposites as the light-absorbing energy donors and a randomly dispersed conjugated rigid-rod polymer as the energy acceptor, have been prepared and shown to exhibit efficiency for singlet electronic energy transfer as high as 93 percent. The film thickness dependence of energy-transfer efficiency allowed us to determine the contributions of Forster and radiative mechanisms to energy transfer in the polymer nanocomposite assemblies. The Forster energy transfer efficiency was found to increase with increasing acceptor concentration, reaching an asymptotic maximum of 48 percent at approximately 3 percent. On the other hand, radiative transfer diminished to an insignificant contribution at low acceptor concentration (less than 1 mol percent). The Forster energy transfer efficiency varied significantly with the length of the flexible coil segment which regulates the supramolecular structure of the photoactive nanocomposite energy donor. The average intersite distance between donor and acceptor chromophores was measured spectroscopically to be in the range of 10 to 25 A with corresponding Forster radii of 19-23 A in the three series of supramolecular donor/acceptor assemblies investigated, depending on the acceptor concentration. The present results on novel light-harvesting polymer nanocomposite assemblies represent the successful supramolecular regulation of efficient electronic energy transfer in thin films and hence are promising for exploring optoelectronic applications. DTIC

N95-12417# California Univ., Irvine, CA. Dept. of Chemistry.
SELF ASSEMBLY OF N-ALKANETHIOLATE MONOLAYERS ON SILVER NANO-STRUCTURES: DETERMINATION OF THE APPARENT THICKNESS OF THE MONOLAYER BY SCANNING TUNNELING MICROSCOPY
Weinjie Li, Jorma A. Virtanen, and Reginald M. Penner 12 Jul. 1994 24 p
(Contract N00014-93-1-0757)
(AD-A282322; TR-2) Avail: CASI HC A03/MF A01

The STM is employed to monitor the effect of adsorption of an n-alkanethiolate monolayer, from an aqueous solution of the thiol, on the apparent topography of nanoscopic silver adsorption sites. Silver nano-disk structures were electrochemically deposited on graphite surfaces using the STM. The topography of these adsorption sites was then determined in-situ by STM imaging prior to the exposure of the nano-structure to an aqueous solution of an n-alkane thiol. The apparent thickness of the self-assembled monolayer (SAM), estimated from the difference in the nano-structure height measured before and after adsorption of the monolayer, increased linearly with the alkyl chain length for five n-alkane thiols (i.e., CnH(2n+1)SH) having even numbered chain lengths from n=10 to 18. For SAMs of tetradecane thiol, hexadecane thiol, and octadecane thiol, the average height increments equaled the expected all-trans chain length of these molecules indicating that little penetration of the STM tip into the surface of the monolayer occurs during the STM imaging experiment. DTIC

N95-12419# University of Southern Mississippi, Hattiesburg, MS. Dept. of Polymer Science.
THIANTHRENE-BASED POLY(BENZOXAZOLE)S Technical Report, 1 Jun. 1993 - 31 May 1994
R. A. Johnson and L. J. Mathias 15 Jul. 1994 5 p
(Contract N00014-89-J-1225)
(AD-A282326; TR-65) Avail: CASI HC A01/MF A01

Poly(benzoxazole)s (PBO's) are a class of rigid-rod polymers that are known to have good thermal stability, high mechanical properties, and environmental resistance. Processing of PBO's is difficult since they have low solubility, high glass transition temperatures, and decompose before their melting points. This study is focused on improving the processibility of poly(benzoxazole)s by increasing their solubility while maintaining good thermal stability. With this goal in mind, we synthesized thianthrene-based PBO's from thianthrene-2,7- and 2,8-dicarbonyl chlorides with commercially available bis-o-aminophenols. Polymers were prepared in poly(phosphoric acid) at 90-200 deg C. Transparent PBO films were casted from polymerization solutions and m-cresol depending on solubility. Thermal analysis has shown 10 percent weight loss in air at greater than 500 deg C. DMA has shown good mechanical properties with a transition greater than 400 deg C for polymer I-HAB. DTIC

N95-12420# Clark Univ., Worcester, MA.
ADHEREND SURFACE EFFECTS ON EPOXY CURE BY NMR Final Report, Sep. 1991 - Sep. 1993
Paul T. Inglefield 11 May 1994 12 p
(Contract DAAL03-91-G-0333)
(AD-A282165; ARO-28795.1-CH) Avail: CASI HC A03/MF A01

A solid state NMR investigation is undertaken to characterize at the molecular level the structure and dynamic nature of epoxy resin systems cured in the presence of an active surface intended to represent an adherend surface. Comparison is made with the cure reaction in the bulk phase in the absence of a surface. This comparison focuses both on the different products and different kinetics which result from the presence of an active surface. The major system considered is that based on the diglycidyl ether of bisphenol A cured with primary amines, in particular 4,4' diaminodiphenyl sulfone. Aluminum oxide is used as a high surface area model of aluminum adherend surfaces. The NMR experiments utilize line narrowing techniques to yield resolved spectra of the solid materials. 13C and 15N NMR are used to identify the structures, with various relaxation experiments being employed to aid in the assignments and to characterize the mobility of the cured resin. This represents a new and powerful probe of surface adhesion and the understanding achieved can hopefully yield benefit in terms of improved understanding of adhesive joint performance. DTIC

N95-12424# Massachusetts Univ., Lowell, MA. Dept. of Chemistry.
DESIGN, SYNTHESIS AND CHARACTERIZATION OF NOVEL NONLINEAR OPTICAL POLYMERS
Sukant Tripathy 31 May 1994 31 p
(Contract N00014-90-J-1148)
(AD-A282201) Avail: CASI HC A03/MF A01

The principal focus of the project is to develop new materials chemistry based on molecular level design and solid state chemistry. The goals have been to develop electroactive polymers with novel electronic, optical and nonlinear optical properties. Second and third order nonlinear optical materials have been developed based on conjugated macromolecules and asymmetric anharmonic molecular electronic dipolar oscillators. In this multidisciplinary research effort, starting from the first principle, polymeric systems have been developed with stable large nonlinear optical coefficients, ultrathin electroactive redox monolayers, molecular superlattices, and others. Sol-gel chemistry, photochemical crosslinking and photopolymerization have been employed as engineering tools in materials fabrication and to elicit new phenomenon. DTIC

N95-12520# Connecticut Univ., Storrs, CT. Inst. of Materials Science.
UV AND FLUORESCENCE STUDIES FOR VINYL POLYMERIZATION Technical Report, Jun. 1993 - May 1994
Y. S. Kim and C. S. Sugn 1 Jun. 1994 4 p
(Contract N00014-89-J-1145)
(AD-A281187; TR-41) Avail: CASI HC A01/MF A01

Polymerizations of styrene and methyl methacrylate (MMA) in bulk as well as in solutions were followed by UV-visible and fluorescence spectroscopies as potential on-line monitoring techniques. For the solution polymerization of styrene, the monomer conversion obtained by UV and fluorescence measurements could be correlated with IR results at three different temperatures: 65, 70, and 75 C. From the initial slope at each temperature, the activation energy of about 6 Kcal/mol was determined. For MMA solution polymerization, UV of MMA and fluorescence of styrene laced as an extrinsic sensor were monitored. The monomer conversion of this reaction could be obtained by measuring fluorescence intensity of styrene through the correlation curve. Bulk polymerization of styrene was in-situ monitored by using fluorescence fiber-optic cable. The fluorescence intensity of styrene in bulk became significant only after 80% monomer conversion because of self-quenching effect. Bulk polymerization of MMA was followed by UV reflection technique. The initial peak at 225 nm was gradually shifted to the shorter wavelength with polymerization, which is not observable in UV transmission absorption spectra. Also, the percent reflectance increased with reaction. Based on these results, this technique shows a promising future as an on-line monitoring tool. DTIC

N95-12536# Purdue Univ., West Lafayette, IN. Dept. of Physics.
THEORY OF COMPLEX DEFECTS ON DNA POLYMER CHAIN Final Report, 31 Mar. 1991 - 1 Apr. 1994
L. L. VanZandt 18 Jul. 1994 6 p
(Contract N00014-91-S-1703)
(AD-A282619) Avail: CASI HC A02/MF A01

A theoretical/computational study of vibrational states of long chain polymeric DNA of nearly perfect translational symmetry but containing isolated damage, substitutions, or defects of other sorts, is presented. A new, closed form, computational algorithm is developed for such systems and applied to certain simple example cases. A computationally modest scheme for estimating relative intensities of Raman scattered lines is developed and applied to simple molecules, preparatory to application to DNA polymer. DTIC

N95-12537 Rochester Univ., NY. Dept. of Chemical Engineering.
PHOTOGENERATION OF CHARGE CARRIERS IN BILAYER ASSEMBLIES OF CONJUGATED RIGID-ROD POLYMERS
Samson A. Jenekhe, John A. Osaheni, and Jerry Perlstein 8 Jul. 1994 51 p Limited Reproducibility: More than 20% of this document may be affected by microfiche quality
(Contract N00014-94-1-0540)
(AD-A282625; TR-2) Avail: CASI HC A04

The quantum yield and the mechanism of photogeneration of charge carriers are investigated in bilayer assemblies consisting of a pi-conjugated rigid-rod polymer layer and a triarylamine doped polycarbonate layer. The electric field dependent quantum efficiency of photocarrier generation, Phi(E), in the bilayers containing a series of conjugated polybenzobisazoles was measured by photoinduced discharge and was found to be in the range of 10(exp -3) to 10(exp -2) at low fields (less than 10(exp 4) V/cm) and as high as 0.12 - 0.32 at approximately 10(exp 6) V/cm. The Phi(E) data were qualitatively in accord with Onsager's three-dimensional model for ion-pair dissociation. Transient (ps) absorption spectroscopy of single layer thin films of the polymers showed that the primary photoexcitations were excitons. However, picosecond photoinduced absorption and photoluminescence experiments on the bilayers revealed photoinduced electron transfer and exciplex formation at the bilayer interface. Thus photocarrier generation on photoexcitation of the conjugated rigid-rod polymers in the bilayer occurs by photoinduced electron transfer, forming intermolecular exciplexes which dissociate efficiently in electric field. This mechanistic picture of charge carrier photogeneration provided a satisfactory account for the observed field dependent quantum yields in the series of bilayer assemblies. DTIC

N95-12586# Clemson Univ., SC. Dept. of Ceramic Engineering.
INTELLIGENT PROCESSING OF FERROELECTRIC THIN FILMS Annual Report, 2 Jul. 1993 - 31 May 1994
Gene Haertling, Eric Skaar, Raj Singh, Feiling Wang, and David Dausch 31 May 1994 246 p
(Contract N00014-91-J-1508)
(AD-A282833) Avail: CASI HC A11/MF A03

The work described in this report covers the third year of a four-year program involving intelligent processing of ferroelectric thin films and bulk materials. It is presented in eight parts dealing with automation, powder electrooptic behavior of thin films and published work. In regard to process automation and intelligence, the fluid flow pattern for the batching system has been thoroughly assessed. The data show that the gravity flow of solutions through the system is sufficient for batching into a central vessel. In addition to the resistance probe, an LVDT will be linked directly to the computer through analog ports and will provide the necessary feedback to batch solutions more reliably. DTIC

N95-12600# Swedish Inst. for Materials Testing, Boras (Sweden).
VAMAS ROUND ROBIN ON FRACTOGRAPHY OF CERAMICS. SWEDISH RESULTS
L. Carlsson 1993 31 p
(PB94-180155; SP-RAPP-1993:38) Avail: CASI HC A03/MF A01

Fractography is an important tool for determining the failure-causing flaw in a brittle ceramic component or test specimen. In a first step towards standardization, U.S. Army Materials Technology Laboratory in cooperation with the National Institute of Standards and Technology has arranged a VAMAS Round Robin, where the participants should use Military Handbook MIL-HDBK-790 to characterize flaws with respect to origin and location in advanced ceramics. The exercise consisted of three topics: evaluation of machining damage from given SEM micrographs, characterization of flaws in six test bars which were fractured, and breaking and characterization of our own specimens. The recommended procedures and the given determination for identifying the flaws were applied in the exercise. The results show that the handbook is a useful tool for fractographic work and should be used as a base for standardization in the field. In this report the fractographic results from the Swedish laboratory, Swedish National Testing and Research Institute, are summarized. NTIS

N95-12773 Carnegie-Mellon Univ., Pittsburgh, PA. Dept. of Chemistry.
THERMAL POLYMERIZATION OF STYRENE IN THE PRESENCE OF STABLE RADICALS AND INHIBITORS
Daniela Mardare and Krzysztof Matyjaszewski 30 Jun. 1994 4 p Limited Reproducibility: More than 20% of this document may be affected by microfiche quality
(Contract N00014-94-1-0101)
(AD-A280926; TR-20) Avail: CASI HC A01

Thermal polymerization of styrene in the presence of several radical scavengers and inhibitors was investigated. Rates, molecular weights and polydispersities depend on the nature of the scavenger, on its concentration and reaction temperature. In the best controlled systems, molecular weights up to M sub n approx. 10,000 and polydispersities M sub w/M sub n approx. 1.2 were observed. It is proposed that in addition to the reversible activation by the homolytic cleavage of the 'dormant' (P-R) species, degenerative chain transfer reactions may be involved. DTIC

N95-12945# Allied-Signal Aerospace Co., Kansas City, MO.
ELIMINATION OF INTERNAL CONTAMINATION ON SEMICONDUCTOR DEVICES (PROTECTIVE COATINGS)
T. Castillo Jul. 1994 15 p
(Contract DE-AC04-76DP-00613)
(DE94-015868; KCP-613-5433) Avail: CASI HC A03/MF A01

Characterization results are described of epoxy and gel coatings that were applied to leadless chip carriers (LCC) and TO-46 semiconductor packages. Samples included silicon dioxide, liquid epoxy, epoxy, RTV silicon, and silicon gel; and a standard test sequence was followed. Test results and coating application feasibility for semiconductor packages and military applications are discussed. DOE

N95-13060# Michigan Univ., Ann Arbor, MI.
THE STRUCTURAL BASIS FOR FATIGUE FAILURE INITIATION IN GLASSY POLYMERS
A. F. Yee 1993 16 p
(Contract DE-FG02-88ER-45366)
(DE94-015415; DOE/ER-45366/6) Avail: CASI HC A03/MF A01

In this period efforts were devoted to studying the microstructural elements characterizing fatigue failure initiation, their evolution as a function of fatigue history, and role of external variables. Materials studied include polycarbonate (PC) and its derivatives with different relaxation behaviors, and epoxies with different cross-link densities. The majority of the studies were devoted to PC. Techniques used included mechanical testing, volumetry, density, DSC, x-ray scattering, positron annihilation, TEM, etc. Results suggest that craze initiation starts with expansion of 'elementary' voids; that fatigue failure initiation in bulk, amorphous PC is generation of stable voids or 'proto-crazes'; that sizes of initial voids are generally in the range of tens of nanometers; that growth of proto- crazes into mature crazes occurs through expansion of voids and generation of new ones perpendicular to fatigue stress; and that fatigue craze initiation in bulk, amorphous PC even at below T(sub g) may involve disentanglement of polymer chains. DOE

N95-13175 Department of the Navy, Washington, DC.
CERAMIC COMPOSITES WITH CERAMIC FIBERS Patent Application
Todd Jessen, inventor (to Navy) 7 Jan. 1994 18 p Limited Reproducibility: More than 20% of this document may be affected by microfiche quality
(AD-D016315; US-Patent-Appl-SN-179013; Navy-Case-75639) Avail: CASI HC A03

A preferred composite which is useful at temperatures in excess of about 1000 deg C comprises a ceramic matrix and 40-60% on volume basis of coated and uncoated fibers embedded in the matrix generally

parallel to each other and in a controlled arrangement. The matrix is selected from the group consisting essentially of silicon nitride, silicon carbide and zirconium titanate. The fibers are silicon carbide fibers 5-20 microns thick. The coating on the coated fibers is boron nitride 0.1-0.3 microns thick. A cross-section of the composite contains about one half, on volume basis, of uncoated fibers in one band extending from one side edge of the cross-section to the opposite side edge. The composite has unexpectedly improved strength and/or toughness compared to a composite composed of only coated or only uncoated fibers. DTIC

N95-13179 Department of the Navy, Washington, DC.
PHOSPHAZENE-CONTAINING AMINE AS CURING AGENT FOR PHTHALONITRILE-BASE POLYMER Patent
Teddy M. Keller, inventor (to Navy) 19 Apr. 1994 6 p Filed 19 Feb. 1993
(AD-D016375; US-Patent-5,304,625; US-Patent-Appl-SN-019956; US-Patent-Class-528-168) Avail: US Patent and Trademark Office

Phosphazene-containing amines having at least one amine or substituted amine moiety reactive with nitrile groups of the phthalonitrile monomers or oligomeric resins are useful curing agents for phthalonitriles. Typically, the phosphazene-containing amines are useful as curing agents in the present invention have the formula: wherein each of X(1-6) is a hydrogen, an unsubstituted amine group, or an amine group substituted with C(1)-C(12) alkyl groups or aromatic groups, at least one of X(1-6) includes an amine group, and each of R'(1-6) is an alkyl, aromatic, or alkyl-substituted aromatic moiety, or a linear polymer of the phosphazene-based amine monomer. The curing agents enhance the speed of cure and also add flame retardancy to the cured polymers. DTIC

N95-13184# Sandia National Labs., Albuquerque, NM.
CERAMIC MANUFACTURING: OPTIMIZING A MULTIVARIABLE SYSTEM
M. J. Readey 1994 16 p Presented at the 96th Annual Meeting of the American Ceramic Society, Indianapolis, IN, 24-28 Apr. 1994
(Contract DE-AC04-94AL-85000)
(DE94-015016; SAND-94-1305C; CONF-940416-20) Avail: CASI HC A03/MF A01

Ceramics offer significant performance advantages over other engineering materials in a great number of applications such as turbocharger rotors and wear components. However, to realize their full market potential, ceramics must become more cost competitive. One way to achieve such competitiveness is to maximize manufacturing yield via process optimization. One simple optimization strategy involves maximizing yield by decreasing product variability (e.g., by operating in a regime that is inherently process tolerant). This paper extends this concept to the simultaneous optimization of many material characteristics, which is more typical of the requirements of a real ceramic manufacturing operation. DOE

N95-13191# Instituto de Pesquisas Espaciais, Sao Jose dos Campos (Brazil).
CeO2-ZrO2 POWDER SYNTHESIS BY WAY OF ALCOHOL DEHYDRATION OF AQUEOUS SALT SOLUTIONS [SINTESE DE POS DE CEO2-ZRO2 POR DESIDRATACAO DE SOLUCOES DE SULFATOS DE ALCOOIS]
Maria doCarmo deAndradeNono Feb. 1993 9 p In PORTUGESE
(INPE-5484-PRE/1783) Avail: CASI HC A02/MF A01

The powder synthesis from aqueous salt solutions via alcohol dehydration is a very attractive method of removing solvent (liquid-liquid extraction) for the preparation of Y-PSZ ceramics. A method for the preparation of CeO2-ZrO2 powder is reported. It involves the powder synthesis by precipitation from an aqueous solution of Y and Zr sulphates in ethanol and isopropanol followed by calcination. The powder characteristics and their relations with the green compaction and densification by sintering are shown and discussed. It is observed that the ethanol gives powders with the best compaction and sintering behavior. Author (revised)

N95-13244 Selskapet for Industriell og Teknisk Forskning, Trondheim (Norway). Corrosion Center.
ACCELERATED TESTING OF COATINGS FOR PROTECTION AGAINST ATMOSPHERIC CORROSION
U. Steinsmo 10 Jan. 1994 84 p
(PB94-202579; STF24-A94508) Avail: Issuing Activity (National Technical Information Service (NTIS))

The intention of this project has been to increase the validity of results obtained during accelerated testing of paint films. The often observed lack of correlation between results of accelerated artificial corrosion tests of corrosion protective paint films and their performance under natural conditions is a growing matter of interest and concern. The introduction of new high quality, environmental friendly paint systems are made difficult by the lack of satisfactory test methods to assess the performance of these new systems. Natural weathering tests is not an alternative because of the long exposure time necessary. NTIS

N95-13284# Technische Univ., Delft (Netherlands).
CVD TECHNIQUES FOR THE SYNTHESIS OR MODIFICATION OF POROUS CERAMICS Ph.D. Thesis
J. P. Dekker 14 Mar. 1994 176 p
(PB94-206836) Avail: CASI HC A09/MF A02

Chemical Vapor Deposition (CVD) has been recognized as an important production method for thin films. In CVD gaseous reactants are introduced into a reactor in which they react to form a solid on a surface. This technology is widely used in the processing of micro-electronic devices. The CVD process for the densification of a porous preform to make up a matrix material is referred to as Chemical Vapor Infiltration (CVI). In particle Precipitation aided CVD (PP-CVD) an aerosol is formed, and the particles are precipitated on a substrate by introducing an external force for particle deposition. This thesis deals with the high temperature chemistry of the formation of titanium nitride and titanium diboride in CVD, CVI, and PP-CVD. It gives a concise presentation of the experimental work on high temperature chemistry of these CVD techniques. NTIS

N95-13296 University of Southern Mississippi, Hattiesburg, MS. Dept. of Polymer Science.
ALL-HYDROCARBON COMPOSITE RESINS BASED ON CYCLOPENTADIENE Technical Report, 1 Jun. 1993 - 31 May 1994
Gregory J. Tregre, Lon J. Mathias, and Jeno Muthiah 15 Jul. 1994 3 p
Limited Reproducibility: More than 20% of this document may be affected by microfiche quality
(Contract N00014-89-J-1225)
(AD-A282495; TR-70) Avail: Issuing Activity (Defense Technical Information Center (DTIC))

Currently available resins for normal and demanding composite applications often suffer from swelling and/or degradation caused by polar organic solvents and hot, wet environments. One possible means of overcoming these disadvantages is to use all-hydrocarbon matrices that inherently limit interaction and penetration by both organic solvents and water. Polybutadiene is an example of a resin whose inherent hydrophobicity provides excellent hot-wet stability and long term resistance to moisture and saline environments; its use in composites has been limited, however, because of poor physical properties at ambient temperature. We have developed an alternative, inexpensive resin based on multiply-substituted cyclopentadienes. DTIC

N95-13367# Connecticut Univ., Storrs, CT. Inst. of Materials Science.
CHARACTERIZATION OF THE ONE STEP POLYIMIDE SYNTHESIS Technical Report, Jun. 1993 - May 1994
G. Jen, S. J. Huang, and C. S. Sung 1 Jun. 1994 4 p
(Contract N00014-89-J-1145)
(AD-A281216; TR-35-ONR) Avail: CASI HC A01/MF A01

The one step high temperature reaction of 3,3',4,4'-benzophenone tetracarboxylic dianhydride (BTDA) and 1,5-naphthyl diamine (DAN) in m-cresol was investigated using UV-visible, fluorescence, and infrared spectroscopy. Results have shown that UV-visible can be used to monitor the wavelength shift from the diamine to the polyamic acid to the polyimide. Deconvolution of the spectra at various reaction times revealed the composition of amic acid and imide, which were also in good agreement with the infrared analysis. Fluorescence spectroscopy utilized the fluorescence nature of the diamine to probe the reactivity of the species during the reaction. Early complexation of the diamine was evidenced by the absence of fluorescence emission due to DAN, which then appeared later in time to a maximum of 9.4%. Upon further reaction, DAN is consumed completely, as evidenced by the gradual decline in emission. Investigation of this reaction in NMP with only 10% m-cresol at lower temperatures

revealed that the apparent rate constants of amic acid formation was actually slower than the controls, 100% NMP as determined by infrared. However, these laced systems did induce imidization at the lower temperatures. DTIC

N95-13508*# Georgia Inst. of Tech., Atlanta, GA. School of Mechanical Engineering.
GLASS MICROSPHERE LUBRICATION
Michelle Geiger, Henry Goode, Sean OHanlon, Stuart Pieloch, Cindy Sorrells, and Chris Willette [1991] 85 p Prepared for Universities Space Research Association, Columbia, MD
(Contract NASw-4435)
(NASA-CR-197157; NAS 1.26:197157) Avail: CASI HC A05/MF A01

The harsh lunar environment eliminated the consideration of most lubricants used on earth. Considering that the majority of the surface of the moon consists of sand, the elements that make up this mixture were analyzed. According to previous space missions, a large portion of the moon's surface is made up of fine grained crystalline rock, about 0.02 to 0.05 mm in size. These fine grained particles can be divided into four groups: lunar rock fragments, glasses, agglutinates (rock particles, crystals, or glasses), and fragments of meteorite material (rare). Analysis of the soil obtained from the missions has given chemical compositions of its materials. It is about 53 to 63 percent oxygen, 16 to 22 percent silicon, 10 to 16 percent sulfur, 5 to 9 percent aluminum, and has lesser amounts of magnesium, carbon, and sodium. To be self-supporting, the lubricant must utilize one or more of the above elements. Considering that the element must be easy to extract and readily manipulated, silicon or glass was the most logical choice. Being a ceramic, glass has a high strength and excellent resistance to temperature. The glass would also not contaminate the environment as it comes directly from it. If sand entered a bearing lubricated with grease, the lubricant would eventually fail and the shaft would bind, causing damage to the system. In a bearing lubricated with a solid glass lubricant, sand would be ground up and have little effect on the system. The next issue was what shape to form the glass in. Solid glass spheres was the only logical choice. The strength of the glass and its endurance would be optimal in this form. To behave as an effective lubricant, the diameter of the spheres would have to be very small, on the order of hundreds of microns or less. This would allow smaller clearances between the bearing and the shaft, and less material would be needed. The production of glass microspheres was divided into two parts, production and sorting. Production includes the manufacturing of the microspheres, while sorting entails deciphering the good microspheres from the bad ones. Each process is discussed in detail. Derived from text

N95-13530# National Inst. of Standards and Technology, Gaithersburg, MD. Ceramics Div.
EQUIPMENT FOR INVESTIGATION OF CRYOGENIC COMPACTION OF NANOSIZE SILICON NITRIDE POWDERS
W. Chen, G. J. Piermarini, S. J. Dapkunas, S. G. Malghan, and A. Pechenik 1993 11 p
(Contract DE-AI05-92OR-22041)
(DE94-013593; DOE/OR-22041/T1) Avail: CASI HC A03/MF A01

This paper describes a highly-specialized system for studies of time-dependent compaction of nanosize silicon nitride powders under a variety of atmospheres and at temperatures ranging from 77 to 1,000 K. The system incorporates a screw-driven press (10 ton capacity) with a piston-cylinder type die and can produce decylindrical powder compacts, 3 mm in diameter and approximately 1 mm in thickness, using pressures up to 3 GPa. The system is computer-controlled and permits accurate measurements of the sample volume, and, after appropriate calibration, can determine the rate and degree of densification of the compacting powder as pressure is applied. Frictional forces between the piston and the die are measured during the compaction process. For calibration of the system, powders with known volume-change accompanied by phase transition under pressure were studied, and good agreement with published results was demonstrated. Several Si3N4 samples have been compacted and sintered at 1,300 to 1,600 C. A maximum random packing density of 64% has been obtained using liquid nitrogen as a lubricant medium at pressures lower than 2.5 GPa. Both green samples and samples sintered at temperatures to 1,500 C exhibited visual transparency under visible light. DOE

N95-13535# Academy of Sciences of the Ukraine, Kharkov. Fiziko-Teknicheskij Inst.
STRUCTURE-PHASE STATE OF THICK AMORPHOUS AND MICROCRYSTALLINE CHROMIUM-CARBON FILMS DEPOSITED BY ION-PLASMA SPUTTERING
A. S. Bakaj, S. N. Sleptsov, I. G. Marchenko, and A. N. Sleptsov 1993 7 p
(DE94-624236; KFTI-93-35) Avail: CASI HC A02/MF A01 (US Sales Only)

The structure-phase state of Cr:C films prepared by reactive evaporation with arc discharge was studied. The nonequilibrium structure and phase diagram of the system in the carbon concentration range 0...35 at.% and at temperatures 300...1100 K was obtained. The temperature-concentration diagram of Cr:C films microhardness is presented. DOE

N95-11968*# National Aeronautics and Space Administration. Ames Research Center, Moffett Field, CA.
TEST MODEL DESIGNS FOR ADVANCED REFRACTORY CERAMIC MATERIALS
Huy Kim Tran *In its* Technical Paper Contest for Women 1992. Space Challenges: Earth and Beyond 1993 p 171-182 (For primary document see N95-11955 02-99)
Avail: CASI HC A03/MF A03

28 PROPELLANTS AND FUELS

Includes rocket propellants, igniters, and oxidizers; their storage and handling procedures; and aircraft fuels.

For related information see also *07 Aircraft Propulsion and Power, 20 Spacecraft Propulsion and Power,* and *44 Energy Production and Conversion.*

N95-12729 California Univ., Irvine, CA. Dept. of Chemistry.
ADVANCED CRYOGENIC PROPELLANTS Annual Research Report, 15 Apr. 1993 - 14 Apr. 1994
V. A. Apkarian, R. B. Gerber, K. C. Janda, J. Rutledge, and P. Taborek 14 Apr. 1994 25 p Limited Reproducibility: More than 20% of this document may be affected by microfiche quality
(Contract F49620-93-1-0251)
(AD-A282451; AFOSR-94-0430TR) Avail: Issuing Activity (Defense Technical Information Center (DTIC))

Molecular photodynamics in cryogenic solids are pursued in an effort to characterize the many-body interactions and dynamics that will control the possibilities of preparing, stabilizing, and subsequently using doped solid H2 as a propellant. While many of the experiments carried out involve inert rare gases, the photophysics sought in these experiments and theoretical developments form the fundamentals that transcend the specific host. In this class of issues are: (a) how to describe the interactions of open shell atoms, which by definition will be the nature of dopants in propellants; (b) development of a basic understanding for the relation between pair potentials and free energy, which controls diffusion kinetics of dopants in compressible solids; (c) to develop time resolved experimental tools to interrogate these in detail; (d) finally, we have carried out studies in one of the candidate systems, namely O doped solid D2. Aspects of this work have already been published. A list of the 1993-1994 publications from our group is included, all of this work has resulted either from the URI or the earlier funded AF contract on HEDM from the Phillips Laboratory. DTIC

N95-12822*# Washington Univ., Seattle, WA. Dept. of Aeronautics and Astronautics.
PROJECT GENESIS: MARS IN SITU PROPELLANT TECHNOLOGY DEMONSTRATOR MISSION Final Report
Francisco Garcia Acosta, Scott Anderson, Jason Andrews, Matt Deger, Matt Hedman, Jared Kipp, Takahisa Kobayashi, Mohrli Marcelo, Karen Mark, and Mark Matheson et al 31 Jul. 1994 250 p Prepared for Universities Space Research Association, Columbia, MD
(Contract NASw-4435)
(NASA-CR-197166; NAS 1.26:197166) Avail: CASI HC A11/MF A03

Project Genesis is a low cost, near-term, unmanned Mars mission, whose primary purpose is to demonstrate in situ resource utilization (ISRU)

technology. The essence of the mission is to use indigenously produced fuel and oxidizer to propel a ballistic hopper. The Mars Landing Vehicle/Hopper (MLVH) has an Earth launch mass of 625 kg and is launched aboard a Delta 117925 launch vehicle into a conjunction class transfer orbit to Mars. Upon reaching its target, the vehicle performs an aerocapture maneuver and enters an elliptical orbit about Mars. Equipped with a ground penetrating radar, the MLVH searches for subsurface water ice deposits while in orbit for several weeks. A deorbit burn is then performed to bring the MLVH into the Martian atmosphere for landing. Following aerobraking and parachute deployment, the vehicle retrofires to a soft landing on Mars. Once on the surface, the MLVH begins to acquire scientific data and to manufacture methane and oxygen via the Sabatier process. This results in a fuel-rich O2/CH4 mass ratio of 2, which yields a sufficiently high specific impulse (335 sec) that no additional oxygen need be manufactured, thus greatly simplifying the design of the propellant production plant. During a period of 153 days the MLVH produces and stores enough fuel and oxidizer to make a 30 km ballistic hop to a different site of scientific interest. At this new location the MLVH resumes collecting surface and atmospheric data with the onboard instrumentation. Thus, the MLVH is able to provide a wealth of scientific data which would otherwise require two separate missions or separate vehicles, while proving a new and valuable technology that will facilitate future unmanned and manned exploration of Mars. Total mission cost, including the Delta launch vehicle, is estimated to be $200 million. Author

N95-12857*# National Aeronautics and Space Administration. Marshall Space Flight Center, Huntsville, AL.
STS PROPELLANT DENSIFICATION FEASIBILITY STUDY DATA BOOK
M. M. Fazah Washington Sep. 1994 62 p
(NASA-TM-108467; NAS 1.15:108467) Avail: CASI HC A04/MF A01

The feasibility of using densification or subcooling with respect to standard temperature propellants on the Space Transportation System (STS) in order to achieve a payload gain is discussed in this report. The objective is to determine the magnitude of the payload gain and to identify any system impacts to the space shuttle on either flight systems or ground systems. Results show that a payload benefit can be obtained by subcooling the liquid hydrogen (LH2) from a nominal temperature of 36.4 R to 28.5 R and by subcooling the liquid oxygen (LO2) from a nominal temperature of 164 R to either 132.1 R or 141.4 R. When the propellants are subcooled to 28.5 R and 132.1 R for the LH2 and LO2, respectively, a maximum payload gain of 7,324 lb can be achieved, and when the propellants are subcooled to 28.5 R and 141.5 R for the LH2 and LO2, respectively, a maximum payload gain of 6,841 lb can be achieved. If the LH2 is subcooled to 28.5 R while the LH2 and LO2 remains at the nominal conditions, a maximum payload gain of 1,303 lb can be achieved. Author

N95-13435# Technische Univ., Delft (Netherlands).
INFLUENCE OF ADDITIVES ON STRUCTURE AND THERMAL STABILITY OF AMMONIUM NITRATE Ph.D. Thesis
C. A. vanDriel 7 Feb. 1994 99 p
(PB94-206943; ISBN-90-9006833-3) Avail: CASI HC A05/MF A02

Ammonium nitrate (AN), NH4NO3, is an important base chemical for the production of mainly fertilizers and explosives. AN exists in at least six polymorphic crystal phases, from which five are stable at atmospheric pressure. The transition between the phases 3 and 4, which occurs upon temperature fluctuations around 32 C, causes a decrease of the mechanical quality of AN products, which may finally lead to pulverization. The resistance of AN granules to deterioration of the mechanical quality due to the 3-4 phase transition is called thermal stability. The thermal stability of AN products can be improved by the application of additives. For fertilizer products with a high nitrogen content (more than 94 wt percent AN) often specific inorganic salts are applied, like Mg(NO3)2 or Al2(SO4)3 or mixtures of such salts. NTIS

29 MATERIALS PROCESSING

Includes space-based development of products and processes for commercial applications.

For biological materials see *55 Space Biology*.

N95-11759*# Alabama Univ., Huntsville, AL. Materials Processing Lab.
GROUND BASED RESEARCH IN MICROGRAVITY MATERIALS PROCESSING Annual Progress Report
Gary L. Workman and Tom Rathz 15 Aug. 1994 20 p
(Contract NCC8-19)
(NASA-CR-196815; NAS 1.26:196815) Avail: CASI HC A03/MF A01

The core activities performed during this time period have been concerned with tracking the TEMPEST experiments on the shuttle with drops of Zr, Ni, and Nb alloys. In particular a lot of Zr drops are being made to better define the recalescence characteristics of that system so that accurate comparisons of the drop tube results with Tempest can be made. A new liner, with minimal reflectivity characteristics, has been inserted into the drop tube in order to improve the recalescence measurements of the falling drops. The first installation to make the geometric measurements to ensure a proper fit has been made. The stovepipe sections are currently in the shop at MSFC being painted with low reflectivity black paint. Work has also continued on setting up the MEL apparatus obtained from Oak Ridge in the down stairs laboratory at the Drop Tube Facilities. Some ground-based experiments on the same metals as are being processed on TEMPEST are planned for the MEL. The flight schedules for the KC-135 experiments are still to be determined in the near future.

Derived from text

N95-12701*# Mitre Corp., Bedford, MA.
GASCAN 2 PAYLOAD INTEGRATION
Henry B. Brown, Jr., Jared G. Buzby, Barbara J. Doyle, and Benedict C. Wibisono 2 May 1994 174 p Prepared in cooperation with Universities Space Research Association, Columbia, MD
(Contract NASw-4435)
(NASA-CR-197200; NAS 1.26:197200) Avail: CASI HC A08/MF A02

This MQP is an ongoing part of the NASA Advanced Space Design Program which examines the integration of the WPI/MITRE Get Away Special Canister (GASCan 2). GASCan 2 contains the Ionospheric Properties and Propagation, Micro-Gravity Ignition, and Rotational Fluid Flow experiments, as well as the integrated support structure. The objectives this year were to finalize the power supply system, connections for experiments, mechanical design of the IPPE's antenna, and to update the structural and vibrational analysis of the integrated support structure.

Author

N95-12703*# National Aeronautics and Space Administration. Lewis Research Center, Cleveland, OH.
AN EXAMINATION OF ANTICIPATED g-JITTER ON SPACE STATION AND ITS EFFECTS ON MATERIALS PROCESSES
Emily S. Nelson Sep. 1994 119 p
(RTOP 412-00-00)
(NASA-TM-103775; E-6042; NAS 1.15:103775) Avail: CASI HC A06/MF A02

This study is concerned with the effects of g-jitter, the residual acceleration aboard spacecraft, on selected classes of materials processes. In particular, the anticipated acceleration environment aboard Space Station Freedom (SSF) and its potential effects are analyzed, but the topic is covered with a sufficient level of generality as to apply to other processes and to other vehicles as well. Some of the key findings of this study include: The present acceleration specifications for SSF are inadequate to assure a quality level low-g environment. The local g vector orientation is an extremely sensitive parameter for certain key processes, but can not be controlled to within the desired tolerance. Therefore, less emphasis should be placed upon achieving a tight control of SSF attitude, but more emphasis should be focused on reducing the overall level of the g-jitter magnitude. Melt-based crystal growth may not be successfully processed in the relatively noisy environment of a large inhabited space structure. Growth from vapor or from solution appears more favorable. A smaller space structure and/or a free flyer can provide better alternatives in terms of g-jitter considerations. A high priority (including budgetary) should be given to coordinated efforts among researchers, SSF designers, and

equipment contractors, to develop practical experiment-specific sensitivity requirements. Combined focused numerical simulations and experiments with well-resolved acceleration measurements should be vigorously pursued for developing reliable experiment-specific sensitivity data. Appendices provide an extensive cross-referenced bibliography, a discussion of the merits offered by g-jitter analysis techniques, as well as definitions of relevant nondimensional quantities and a brief description of available accelerometry hardware. Author

N95-12752*# Alabama Univ., Huntsville, AL. Materials Processing Lab.
PHASE A DESIGN STUDY OF MICROGRAVITY FLUORIDE FIBER PULLER Final Report
Gary L. Workman, Guy A. Smith, and Susan Kosten 31 Aug. 1994 60 p
(Contract NAS8-38609)
(NASA-CR-196513; NAS 1.26:196513) Avail: CASI HC A04/MF A01

Improved transmission properties for fluoride fibers due to space processing has great potential for commercial benefits. Phase A design study will determine conceptual feasibility and provide initial definition of the technical requirements and design issues for space. Author

N95-13202*# Stanford Univ., CA. Center for Materials Research.
PROTEIN CRYSTAL GROWTH IN LOW GRAVITY Final Technical Report, 1 Jun. 1992 - 31 May 1994
Robert S. Feigelson 1994 31 p Original contains color illustrations
(Grant NAG8-920)
(NASA-CR-196980; NAS 1.26:196980; CMR-94-4; SPO-10544) Avail: CASI HC A03/MF A01; 5 functional color pages

This research involved (1) using the Atomic Force Microscope (AFM) in a study on the growth of lysozyme crystals and (2) refinement of the design of the Thermonucleator which controls the supersaturation required for the nucleation and growth of protein crystals separately. AFM studies of the (110) tetragonal face confirmed that lysozyme crystals grow by step propagation. There appears to be very little step pile up in the growth regimes which we studied. The step height was measured at = 54A which was equal to the (110) interpane spacing. The AFM images showed areas of step retardation and the formation of pits. These defects ranged in size from 0.1 to 0.4 mu. The source of these defects was not determined. The redesign of the Thermonucleator produced an instrument based on thermoelectric technology which is both easier to use and more amenable to use in a mu g environment. The use of thermoelectric technology resulted in a considerable size reduction which will allow for the design of a multi-unit growth apparatus. The performance of the new apparatus was demonstrated to be the same as the original design. Author (revised)

31 ENGINEERING (GENERAL)

Includes vacuum technology; control engineering; display engineering; cryogenics; and fire prevention.

N95-11907# National Inst. of Standards and Technology, Gaithersburg, MD. Metric Program.
FEDERAL METRIC PROGRESS IN 1993
G. P. Carver Apr. 1994 15 p See also PB89-114490
(PB94-196029; NISTIR-5413) Avail: CASI HC A03/MF A01

During 1993, cooperation among the federal agencies on interagency issues led to more uniform metric transition approaches. Individually, agencies made significant progress in implementing metric use in their programs. However, the amount of progress by different agencies also show significant variation. Cooperative progress included: Acquisition Guidelines; Functional subcommittees; Strategic Approach; Public Affairs; Metric Transition Plan Revision; Expanded Agency-Industry cooperation; and Federal Standard 376. NTIS

N95-12772 Utah Univ., Salt Lake City, UT. Dept. of Physics.
HIGH FREQUENCY THERMOACOUSTIC REFRIGERATOR Annual Summary Report, 2 Sep. 1993 - 31 May 1994
Orest Symko 16 Jun. 1994 14 p Limited Reproducibility: More than 20% of this document may be affected by microfiche quality
(Contract N00014-93-J-1126)
(AD-A280925; Rept-01) Avail: CASI HC A03

A small thermoacoustic refrigerator was developed for operation at 5 kHz. Its main components are a piezoelectric driver of the bimorph type, a cotton wool stack, a 1/2-wave resonator (operated at its 3rd harmonic), and photolithographically processed copper heat exchangers. Tests with air at 1 atmosphere as the working gas produced a temperature difference Delta T across the stack of 32 deg C in 4 seconds for an acoustic power input level of 160 dB. The refrigerator did not have thermal insulation. Improved performance is expected with pressurized helium gas and helium-xenon mixtures. The performance of this refrigerator and its small size make it attractive for applications in high speed electronics and possibly IR detectors. DTIC

N95-12942# Oak Ridge National Lab., TN.
ADVANCED INDUSTRIAL MATERIALS PROGRAM
F. Stooksbury, comp. Jun. 1994 438 p
(Contract DE-AC05-84OR-21400)
(DE94-015528; ORNL/TM-12763) Avail: CASI HC A19/MF A04

The mission of the Advanced Industrial Materials (AIM) program is to commercialize new/improved materials and materials processing methods that will improve energy efficiency, productivity, and competitiveness. Program investigators in the DOE national laboratories are working with about 100 companies, including 15 partners in CRDA's. Work is being done on intermetallic alloys, ceramic composites, metal composites, polymers, engineered porous materials, and surface modification. The program supports other efforts in the Office of Industrial Technologies to assist the energy-consuming process industries. The aim of the AIM program is to bring materials from basic research to industrial application to strengthen the competitive position of US industry and save energy. DOE

N95-13053# Advanced Mechanical Technology, Inc., Newton, MA.
DIESEL-FIRED SELF-PUMPING WATER HEATER Final Report, Apr. - Nov. 1993
Joseph Gertsmann Jul. 1994 58 p
(Contract DAAK60-93-C-0035)
(AD-A283063; Natick-TR-94/025) Avail: CASI HC A04/MF A01

The object of this project was to study the feasibility of pumping and heating water by sustained oscillatory vaporization and condensation in a fired heat exchanger. Portable field liquid fueled water heaters would facilitate heating water for sanitation, personal hygiene, food service, laundry, equipment maintenance, and decontamination presently available only from larger, less portable, motorized pumping units. The technical tasks consisted of: development of an analytical model, operation of proof-of-principal prototypes, and determination of the thermal and mechanical relationships to evaluate operating range and control characteristics. Four successive pump models were analyzed and tested. The final analytical model gave reasonable agreement with the experimental results, indicating that the actual pumping effect was an order of magnitude lower than originally anticipated. It was concluded that a thermally-activated self pumping water heater based on the proposed principle is not feasible. DTIC

32 COMMUNICATIONS AND RADAR

Includes radar; land and global communications; communications theory; and optical communications.

For related information see also *04 Aircraft Communications and Navigation* and *17 Space Communications, Spacecraft Communications, Command and Tracking.* For search and rescue see *03 Air Transportation and Safety,* and *16 Space Transportation.*

N95-11707*# Michigan Univ., Ann Arbor, MI. Radiation Lab.
INVESTIGATION OF FINITE ELEMENT: ABC METHODS FOR ELECTROMAGNETIC FIELD SIMULATION Ph.D. Thesis
A. Chatterjee, John L. Volakis, and J. Nguyen Sep. 1994 161 p
(Grant NAG2-866)
(NASA-CR-196837; NAS 1.26:196837; UMICH-031155-2-T) Avail: CASI HC A08/MF A02

The mechanics of wave propagation in the presence of obstacles is of great interest in many branches of engineering and applied mathematics like electromagnetics, fluid dynamics, geophysics, seismology, etc. Such problems can be broadly classified into two categories: the bounded domain

or the closed problem and the unbounded domain or the open problem. Analytical techniques have been derived for the simpler problems; however, the need to model complicated geometrical features, complex material coatings and fillings, and to adapt the model to changing design parameters have inevitably tilted the balance in favor of numerical techniques. The modeling of closed problems presents difficulties primarily in proper meshing of the interior region. However, problems in unbounded domains pose a unique challenge to computation, since the exterior region is inappropriate for direct implementation of numerical techniques. A large number of solutions have been proposed but only a few have stood the test of time and experiment. The goal of this thesis is to develop an efficient and reliable partial differential equation technique to model large three dimensional scattering problems in electromagnetics. Derived from text

N95-11760*# Georgia Inst. of Tech., Atlanta, GA. School of Electrical and Computer Engineering.

AN ACOUSTIC CHARGE TRANSPORT IMAGER FOR HIGH DEFINITION TELEVISION APPLICATIONS Semiannual Report No. 1, FY 1994

W. D. Hunt, K. F. Brennan, and C. J. Summers Apr. 1994 132 p

(Grant NAGw-2753)

(NASA-CR-196806; NAS 1.26:196806) Avail: CASI HC A07/MF A02

The primary goal of this research is to develop a solid-state television (HDTV) imager chip operating at a frame rate of about 170 frames/sec at 2 Megapixels/frame. This imager will offer an order of magnitude improvements in speed over CCD designs and will allow for monolithic imagers operating from the IR to UV. The technical approach of the project focuses on the development of the three basic components of the imager and their subsequent integration. The camera chip can be divided into three distinct functions: (1) image capture via an array of avalanche photodiodes (APD's); (2) charge collection, storage, and overflow control via a charge transfer transistor device (CTD); and (3) charge readout via an array of acoustic charge transport (ACT) channels. The use of APD's allows for front end gain at low noise and low operating voltages while the ACT readout enables concomitant high speed and high charge transfer efficiency. Currently work is progressing towards the optimization of each of these component devices. In addition to the development of each of the three distinct components, work towards their integration and manufacturability is also progressing. The component designs are considered not only to meet individual specifications but to provide overall system level performance suitable for HDTV operation upon integration. The ultimate manufacturability and reliability of the chip constrains the design as well. The progress made during this period is described in detail.

Derived from text

N95-11800# Helsinki Univ. of Technology, Espoo (Finland). Lab. of Space Technology.

AIRSAR SOFTWARE: COMPUTER PROGRAMS FOR PREPROCESSING OF JPL COMPRESSED POLARIMETRIC SAR DATA

T. Tares Feb. 1993 155 p

(ISSN 0786-8154)

(PB94-179116; ISBN-951-22-1782-1) Avail: CASI HC A08/MF A02

In July, 1991, a test site located in the Harz Mountains was overflown by the three-frequency (P-, L-, and C-band) polarimetric synthetic aperture radar of NASA/JPL. The test site, the size of which is 12 x 25 km squared, covers a high level region of mainly spruce forests between Bad Harzburg and Braunlage, including the Brocken massive and extended wet areas west of it. The study site is an accepted test site for the SIR-C/X-SAR mission in 1994. The study objectives are to investigate the forest information content of multipolarizational AIRSAR data on different forest stand parameters such as: forest types, age classes, and crown density. Special studies were initiated in order to get information on storm damage areas and status of deforestation and regeneration of the partly severely damaged forest stands. As reference data are used Landsat TM data, digital elevation model, color infrared airphotos, and ground registrations. In this paper, a newly developed computer software for preprocessing of AIRSAR data is presented. With its help, it is possible to make radar images using any given polarization state, to show the pexel and polarization statistics for areas of any shape, to compute polarization response diagrams (polarization signatures), and to do polarization optimization, the results of which can be used to study the possibilities of discrimination of different forest and land cover types, in order to give base for classification approaches.

NTIS

N95-11804*# Virginia Polytechnic Inst., Blacksburg, VA. Systems Engineering Design Lab.

SYSTEMS ENGINEERING TECHNOLOGY FOR NETWORKS Final Report, 16 May 1993 - 31 Jan. 1994

31 Jan. 1994 44 p Prepared in cooperation with Howard Univ., Washington, DC

(Grant NAG5-995)

(NASA-CR-196853; NAS 1.26:196853) Avail: CASI HC A03/MF A01

The report summarizes research pursued within the Systems Engineering Design Laboratory at Virginia Polytechnic Institute and State University between May 16, 1993 and January 31, 1994. The project was proposed in cooperation with the Computational Science and Engineering Research Center at Howard University. Its purpose was to investigate emerging systems engineering tools and their applicability in analyzing the NASA Network Control Center (NCC) on the basis of metrics and measures.

Derived from text

N95-11821 National Defence Research Establishment, Linkoeping (Sweden). Huvudavdelning foer Informationsteknologi.

BURST TRANSMISSION IN THE HF BAND: A SYSTEM ANALYSIS AND PROPOSAL FOR IMPROVEMENT [SYSTEM FOER SNABBSAENDNING INOM KORTVAGSBANDET: ANALYS OCH FOERSLAG TILL FOERBAETTRINGAR]

M. Albinsson Dec. 1993 68 p In SWEDISH

(PB94-190733; FOA-C-30742-3.5) Avail: Issuing Activity (National Technical Information Service (NTIS))

The Swedish national defense uses a portable system for burst transmission in the HF band, consisting of radio Ra 195 and burst transmission unit DART 301. The burst transmission unit receives and sends alphanumeric characters. The signals contain no error correcting code and use traditional modulation methods. The purpose of this work is to analyze the improvements obtained by replacing DART 301 by an alternative burst transmission unit with more efficient modulation and coding methods. The work was performed by means of computer simulations and literature studies. To carry out the simulations, the authors used a discrete channel model that is based on the Gilbert-Elliott-model. The present binary FSK system was simulated and compared with Reed-Solomon coded M-ary FSK. The report presents the results from the simulations, and give a possible implementation of an alternative burst transmission unit. The results show that a system with 8-FSK modulation and an RS(7,3) correcting code, roughly yields an SNR-gain of 23 dB for 1 percent message error probability, compared to the present system. NTIS

N95-11904 Geophysical Survey Systems, Inc., North Salem, NH.

DEVELOPMENT OF GROUND-PENETRATING RADAR EQUIPMENT FOR DETECTING PAVEMENT CONDITION FOR PREVENTIVE MAINTENANCE

S. S. Smith and T. Scuillion Oct. 1993 188 p Prepared in cooperation with Texas A&M Univ., College Station, TX Limited Reproducibility: More than 20% of this document may be affected by microfiche quality

(Contract DOT-SHRP-H-104A)

(PB94-189537; SHRP-H-672) Avail: CASI HC A09

The report documents the development of a ground penetrating radar (GPR) system for locating potential maintenance problems in highway pavements. The report illustrates how GPR has the potential to detect four defects in pavements: stripping in an asphalt layer; moisture in base layer; voids or loss of support under rigid pavements; and overlay delamination. NTIS

N95-11943 Naval Command, Control and Ocean Surveillance Center, San Diego, CA. RDT and E Div.

ULTRAWIDEBAND SHIPBOARD ELECTROOPTIC ELECTROMAGNETIC ENVIRONMENT MONITORING Interim Report, Oct. 1992 - Oct. 1993

S. Pappert, M. Berry, S. Hart, R. Orazi, and L. Koyama May 1994 28 p Limited Reproducibility: More than 20% of this document may be affected by microfiche quality

(AD-A282369; NRAD-TR-1646) Avail: CASI HC A03

The objectives are to: (1) design, construct, package, test, and evaluate the best available wideband photonic electromagnetic field probe for shipboard electromagnetic environment (EME) monitoring; (2) develop engineering solutions to problems encountered in Phase 1 testing of a first-generation breadboarded sensor and investigate and develop alternative

sensor configurations that can lead to improved system performance; and (3) develop requirements and a test plan for the shipboard testing of a 2-MHz to 18-GHz prototype system. DTIC

N95-12010*# New Mexico State Univ., Las Cruces, NM. Dept. of Electrical and Computer Engineering.

ADVANCED S-BAND STUDIES USING THE TDRSS COMMUNICATIONS SATELLITE Final Report, Dec. 1992 - Jun. 1994

Jeffrey D. Jenkins, William P. Osborne, and Yiping Fan 23 Aug. 1994 80 p

(Grants NAG5-2142; NAG5-2141)

(NASA-CR-196931; NAS 1.26:196931) Avail: CASI HC A05/MF A01

This report will describe the design, implementation, and results of a propagation experiment which used TDRSS to transmit spread signals at S-Band to an instrumented mobile receiver. The results consist of fade measurements and distribution functions in 21 environments across the Continental United States (CONUS). From these distribution functions, some idea may be gained about what system designers should expect for excess path loss in many mobile environments. Some of these results may be compared against similar measurements made with narrowband beacon measurements. Such comparisons provide insight into what gains the spread signaling system may or may not have in multipath and shadowing environments. Author

N95-12368# Helsinki Univ. of Technology, Espoo (Finland). Lab. of Telecommunications Technology.

BUFFER SIZE AND SWITCHING CAPACITY STUDY IN PACKET SWITCHES OF BROADBAND ISDN

J. Ma and K. Rahko 8 Nov. 1993 8 p Presented at the Conference on Computer, Communication, Control and Power Enginerring (TENCON 1993), Peking, China, 19-21 Oct. 1993

(PB94-179421; ISBN-951-22-1850-X) Avail: CASI HC A02/MF A01

The paper investigates packet loss probabilities of two alternative two-stage output-buffered switches. The performance of these switches can be improved as the switching capacity per output and buffers size increase. Two traffic models, uniform random traffic and bursty traffic, are considered here. The effects of bursty traffic can degrade switch performance significantly. Especially, the packet loss increases significantly in the buffer when mean burst length increases. In addition, the effect of the bursty traffic on the switching capacity can be ignored. The paper also compares requirement of the buffer size and switching capacity of the two switches. NTIS

N95-12374*# Kansas Univ., Lawrence, KS. Dept. of Electrical Engineering and Computer Science.

THE DESIGN AND DEVELOPMENT OF SIGNAL-PROCESSING ALGORITHMS FOR AN AIRBORNE X-BAND DOPPLER WEATHER RADAR Final Technical Report

Shaun R. Nicholson Sep. 1994 126 p Original contains color illustrations

(Grant NGT-30202)

(NASA-CR-196888; NAS 1.26:196888; RSL-TR-10540-1) Avail: CASI HC A07/MF A02; 2 functional color pages

Improved measurements of precipitation will aid our understanding of the role of latent heating on global circulations. Spaceborne meteorological sensors such as the planned precipitation radar and microwave radiometers on the Tropical Rainfall Measurement Mission (TRMM) provide for the first time a comprehensive means of making these global measurements. Pre-TRMM activities include development of precipitation algorithms using existing satellite data, computer simulations, and measurements from limited aircraft campaigns. Since the TRMM radar will be the first spaceborne precipitation radar, there is limited experience with such measurements, and only recently have airborne radars become available that can attempt to address the issue of the limitations of a spaceborne radar. There are many questions regarding how much attenuation occurs in various cloud types and the effect of cloud vertical motions on the estimation of precipitation rates. The EDOP program being developed by NASA GSFC will provide data useful for testing both rain-retrieval algorithms and the importance of vertical motions on the rain measurements. The purpose of this report is to describe the design and development of real-time embedded parallel algorithms used by EDOP to extract reflectivity and Doppler products (velocity, spectrum width, and signal-to-noise ratio) as the first step in the aforementioned goals. Author

N95-12382*# Michigan Univ., Ann Arbor, MI. Dept. of Electrical Engineering and Computer Science.

ANALYSIS OF CYLINDRICAL WRAP-AROUND AND DOUBLY CONFORMAL PATCH ANTENNAS BY WAY OF THE FINITE ELEMENT-ARTIFICIAL ABSORBER METHOD Final Report

J. L. Volakis, L. C. Kempel, R. Sliva, H. T. G. Wang, and A. G. Woo 30 Sep. 1994 68 p

(Contract NCA2-839)

(NASA-CR-195211; UMICH-031173-3-T; NAS 1.26:195211) Avail: CASI HC A04/MF A01

The goal of this project was to develop analysis codes for computing the scattering and radiation of antennas on cylindrically and doubly conformal platforms. The finite element-boundary integral (FE-BI) method has been shown to accurately model the scattering and radiation of cavity-backed patch antennas. Unfortunately extension of this rigorous technique to coated or doubly curved platforms is cumbersome and inefficient. An alternative approximate approach is to employ an absorbing boundary condition (ABC) for terminating the finite element mesh thus avoiding use of a Green's function. A FE-ABC method is used to calculate the radar cross section (RCS) and radiation pattern of a cavity-backed patch antenna which is recessed within a metallic surface. It is shown that this approach is accurate for RCS and antenna pattern calculations with an ABC surface displaced as little as 0.3 lambda from the cavity aperture. These patch antennas may have a dielectric overlay which may also be modeled with this technique. Derived from text

N95-12402 Naval Research Lab., Washington, DC.

MILLIMETER-WAVE RADIOMETRIC UTILITY STUDY Report, Oct. 1991 - Jul. 1993

James P. Hollinger, Steven R. Highley, and Glenn D. Sandlin 22 Jun. 1994 67 p Limited Reproducibility: More than 20% of this document may be affected by microfiche quality

(AD-A282524; NRL/FR/7210-94-9727) Avail: Issuing Activity (Defense Technical Information Center (DTIC))

The purpose of this task is two-fold. The general purpose is to provide an introductory discussion of passive millimeter-wave radiometry and its value to remote sensing, illustrated by examples of imagery. The imagery of relatively high resolution has been acquired at various frequencies from aircraft, and the imagery of lower resolution (12.5 km), also important in intelligence gathering, has been acquired by the 85.5 GHz channel of the DMSP-SSM/I (F8). Examples of military, man-made, and environmental targets illustrate the all-weather capability of passive millimeter-wave systems and the types of signatures received. The meteorological subjects-particularly the millimeter-wave characteristics of tropical cyclones, frontal systems, and clouds-have become the basis of additional environmental work at NRL (to be published later under separate cover). The more specific purpose in this report is to study the utility of passive millimeter-wave imaging from space enhanced with systems that provide surface resolutions of 100-400 m and operate at 90 GHz. The utility, including limitations, of this system for target detection, surveillance, and environmental monitoring is discussed. DTIC

N95-12408# Naval Postgraduate School, Monterey, CA.

MAGNETIC FIELD GENERATION IN SHOCK WAVES M.S. Thesis

John P. Carter Jun. 1994 121 p

(AD-A282234) Avail: CASI HC A06/MF A02

Laser produced plasma jets interacting with a background plasma have been used to study magnetic field generation in shock waves. Shock heating produces axial electron temperature and density gradients which are perpendicular to the radial temperature and density gradients. Electron heat transport and ion diffusion, in the radial direction, occur at different rates. This combination of nonparallel temperature and density gradients generate a magnetic field in the azimuthal direction. Simulations corroborate the experimental observation that magnetic fields are generated when a supersonic plasma jet interacts with a background plasma. Magnetic flux generated by this mechanism requires no initial field, which is in contrast to the dynamo mechanism which does require an initial seed field. Specific applications analyzed in this thesis include interplanetary shocks and nuclear

EMP effects in the MHD domain. It may be assumed that shock generated magnetic fields are also of importance under astrophysical conditions.
DTIC

N95-12412 Air Force Inst. of Tech., Wright-Patterson AFB, OH.
MODELING AND IMPLEMENTATION OF A PACKET ROUTING SWITCH FOR SATELLITE COMMUNICATIONS M.S. Thesis
Daniel S. Kaye 16 Aug. 1993 74 p Limited Reproducibility: More than 20% of this document may be affected by microfiche quality
(AD-A282262; AFIT/CI/CIA-94-022) Avail: CASI HC A04

The principal component needed to model a satellite communications network node is a high-speed packet routing switch. The design and testing of routing switches utilizing Transputer networks has been examined extensively in the literature. One such implementation by Khan and Ward made use of cooperating processes scheduled by the Transtech Genesys operating system. The performance of this system was unacceptable with problems attributed to packet duplication and process contention. In this report, we examine an alternate approach using cooperating occam processes without the overhead associated with an operating system. The routing switch permits dynamic updates to its routing tables from a host computer. Library functions are provided to host processes to offer this service. However, accommodating these updates influences the design of the underlying Transputer network. Allowances must be made not only for expedient routing of messages within the Transputer network but also for rapid and efficient routing table updates within the Transputer network. Results discussed in this report reflect the design and performance of the routing switch. Throughput efficiency under a variety of test conditions is also provided. DTIC

N95-12416# RAND Corp., Santa Monica, CA.
TACTICAL SATELLITE ORBITAL SIMULATION AND REQUIREMENTS STUDY
E. Bedrosian, E. Cesar, J. Clark, G. Huth, and K. Poehlmann 1993 72 p
(Contract MDA903-91-C-0006)
(AD-A282314; RAND/N-3568-A) Avail: CASI HC A04/MF A01

This note documents the results of a preliminary analysis of space communications requirements that employs scenarios for military operations in three widely separated geographical areas in which U.S. contingency operations could occur. The objectives of this research are to: (1) Assess communications requirements that were not met by military resources for Desert Shield/Desert Storm and other recent operations and might not be met without additional military resources in potential future contingencies, including a hypothetical contingency in the Southern Hemisphere; and (2) Determine how military satellites could be used to overcome shortfalls between requirements and existing or planned military communication systems. DTIC

N95-12493 Ohio State Univ., Columbus. Electroscience Lab.
WIDEBAND ELECTROMAGNETIC SCATTERING PROGRAM. FOURIER-BASED RADAR IMAGING TECHNIQUES Interim Report, 1 May 1992 - 1 May 1993
B. L. Chan, J. D. Young, and R. C. Rudduck Sep. 1993 104 p Limited Reproducibility: More than 20% of this document may be affected by microfiche quality
(Contract F33615-91-C-1729)
(AD-A282540; ESL-724733-2; WL-TR-93-1133) Avail: Issuing Activity (Defense Technical Information Center (DTIC))

This report describes the implementation of Fourier based radar imaging algorithms in a computer program. In particular, the algorithms are derived for wide bandwidth and for specific geometries. These geometries are often measured by radar cross section measurement systems such as compact ranges and near field linear synthetic aperture radar systems. The limitations of different implementations of the algorithms are presented. Imaging results from radar measurements are also presented for an F-4 fighter aircraft, an M35 truck (1/16 scale model), and a forest. DTIC

N95-12496# New Mexico Univ., Albuquerque, NM. Dept. of Mathematics and Statistics.
LIGHT BEAM AND PULSE PROPAGATION IN NONLINEAR DIELECTRICS Final Report, 1 Oct. 1990 - 30 Sep. 1993
Alejandro Aceves 30 Sep. 1993 6 p
(Grant AF-AFOSR-0009-91)
(AD-A282548; AFOSR-94-0465TR) Avail: CASI HC A02/MF A01

Currently, one of the major achievements in this project has been in (1) a proposal to use arrays as a way to amplify and shorten pulses, by means of collapse-type mechanisms; in (2) the characterization of three distinct types of nonlinear modes, where that corresponding to the most localized in energy distribution along the array, shows very stable features, including an absence of mode-mode interaction, which make them excellent candidates of information carriers. Some of these results are to appear in two Optics Letters publications. DTIC

N95-12513 Army Research Lab., Adelphi, MD.
TWO-TONE TEST METHOD FOR DETERMINING FREQUENCY-DOMAIN TRANSFER FUNCTIONS Report, Oct. 1992 - Sep. 1993
Vincent J. Ellis Aug. 1994 24 p Limited Reproducibility: More than 20% of this document may be affected by microfiche quality
(AD-A283452; ARL-TR-461) Avail: CASI HC A03

A method has been developed and used to nonintrusively interrogate electronic systems to determine their characteristic response to electromagnetic energy. The method involves subjecting the system under test to two continuous wave signal sources of different frequencies, f(sub h) and (f sub l) and measuring the difference frequency, Delta(f) (that is, (f sub h) -(f sub l)), emitted from the system under test. The difference frequency created by the mixing action of nonlinear electronic components within the system is a relative indication of the system's response to (f sub h), (f sub l). If the two source signals (f sub h) and flare incremented by the same frequency step size, Delta(f) remains constant in frequency and can be measured for each (f sub h), (f sub l) value. The compilation of amplitude measures of Delta(f), normalized by the corresponding amplitude measures of (f sub h), (f sub l), provides a relative measure of the frequency-domain transfer function of the system under test. Although the present method provides only relative data, the economic benefits of using this method make it a viable alternative to high-tech, high-cost approaches. The method provides more than coupling data, since the measurement of Delta (f) is indicative of not only the relative coupling efficiency of the signal source (f sub h), (f sub l) into the system, but also the relative response of the nonlinear circuit component(s) that mix the source signals. The present method is performed with the test equipment totally isolated from the system under test. Without the need for probes at circuit nodes, less time and effort are expended and the integrity of the system is not violated by instrumentation. DTIC

N95-12521# Rome Lab., Griffiss AFB, NY.
MONOPULSE TRACKER OPERATING CHARACTERISTICS MEASUREMENT ERROR PERFORMANCE FOR AZIMUTH TRACKING Report, May - Jul. 1993
Scott Bolen Jun. 1994 18 p
(AF Proj. 4506)
(AD-A281188; RL-TR-94-52) Avail: CASI HC A03/MF A01

This paper derives the operating characteristics for a monopulse radar tracker as a function of probability of detection and probability of false alarm. Measurement error performance is developed for azimuth tracking in an amplitude comparison monopulse system. A set of receiver operating characteristics is also presented to demonstrate how to determine the detection threshold in the signal processing system to minimize tracking errors for a given signal-to-noise ratio. DTIC

N95-12547 Army Research Lab., Adelphi, MD.
TARGET RECOGNITION IN ULTRA-WIDEBAND SAR IMAGERY Final Report, Jan. - Jul. 1993
Vincent Sabio Aug. 1994 93 p Limited Reproducibility: More than 20% of this document may be affected by microfiche quality
(AD-A283462; ARL-TR-378) Avail: CASI HC A05

Ultra-wideband (UWB) synthetic-aperture radar (SAR) images (with greater than 95-percent bandwidth occupancy) provide the potential for recognition of targets embedded in foliage; recognition methods in these applications are based on wideband resonant signatures of the targets. Currently, resonance-extraction techniques hinge on contemporary adaptations of Prony's method; this method, however, has poor performance in the presence of noise and is very computationally intensive. A form of resonance analysis is proposed that applies linear-transform methods. Both

the Fourier basis and two multiresolution bases, the Haar wavelet and the Gaussian basis, were employed in the analysis. Target declaration confidences were established by simple correlation of the two sets of spectral coefficients: one set from the transformed data, and the other from a synthetic template generated from both prediction and empirical observation. This permits a fast, efficient scheme for recognition of target resonance effects in wideband imagery. Five UWB images from the Army Research Laboratory's UWB SAR instrumentation system were analyzed through the use of canonical targets (dipoles) of differing dimension and orientation. Results are presented and summarized for each of the targets and transform methods employed in the analysis. DTIC

N95-12550 SRI International Corp., Menlo Park, CA.
PASP PLUS TRANSIENT PULSE MONITOR (TPM): PREFLIGHT CHARACTERIZATION REPORT Scientific Report No. 1
Richard C. Adamo, Kathy L. Giori, and David R. Dana Jan. 1994 42 p Limited Reproducibility: More than 20% of this document may be affected by microfiche quality
(Contract F19628-93-K-0014)
(AD-A282582; SRI-4651; PL-TR-94-2131) Avail: CASI HC A03

The Transient Pulse Monitor (TPM), part of the PASP Plus experiment aboard the APEX spacecraft, is designed to detect and characterize electromagnetic transient signals produced by electrostatic discharges on the solar array test modules. However, as a result of the way in which the TPM electric-field sensors are installed on the APEX spacecraft, certain additional information is required to properly analyze and interpret mission data relating to the locations of discharges that may occur. The purpose of the TPM E-Field Sensor Response Characterization Test was to perform a series of preflight measurements on the as-installed sensor/payload configuration. The measurements were made to determine the relative combined responses of the entire set of E-field sensors to electromagnetic signals originating at selected locations on the deployed panel and payload shelf. These data will then be used, during the data analysis phase of the PASP Plus program, to help determine the actual discharge locations. This report describes the TPM E-Field Sensor Response Characterization Test results, and, based upon these results, the development and testing of preliminary flight data analysis techniques and software prior to launch. DTIC

N95-12580# Helsinki Univ. of Technology, Espoo (Finland). Electromagnetics Lab.
PLANE-WAVE REFLECTION FROM UNIAXIAL CHIRAL INTERFACE AND ITS APPLICATION TO POLARIZATION TRANSFORMATION
I. V. Lindell and A. H. Sihvola Feb. 1994 22 p
(PB94-184496; ISBN-951-22-2005-9) Avail: CASI HC A03/MF A01

Plane-wave reflection and transmission in a planar interface between air and axially chiral uniaxial medium whose axis is parallel to the interface is considered in the present study. By finding the reflection dyadic and its eigensolutions we demonstrate that, by dimensioning the uniaxial medium in a proper way, it is possible to make a reflection-transforming reflecting surface. The surface is able to transform the incident linear polarization into any other polarization with chosen axial ratio and handedness and the reflected polarization can be continuously adjusted by rotating the surface around its normal direction. The reflected power is seen to be independent of the polarization of the reflected wave. NTIS

N95-12581# Helsinki Univ. of Technology, Espoo (Finland). Electromagnetics Lab.
SINGULARITY OF THE GREEN DYADICS FOR BI-ISOTROPIC
I. V. Lindell and A. H. Sihvola Mar. 1994 8 p See also PB92-142140
(PB94-184504; ISBN-951-22-2020-2) Avail: CASI HC A02/MF A01

Singularity of the Green dyadic for the general bi-isotropic medium is constructed through decomposition of the bi-isotropic problem in two simple isotropic problems. It is seen that, in contrast to the isotropic medium case, the singularity cannot be written in terms of a simple delta function term but it involves a second term containing the derivative of the delta function as well. NTIS

N95-12592# Naval Postgraduate School, Monterey, CA.
INVESTIGATION OF SPECTRAL-BASED TECHNIQUES FOR CLASSIFICATION OF WIDEBAND TRANSIENT SIGNALS IN ADDITIVE WHITE GAUSSIAN NOISE M.S. Thesis
David A. DeRieux Mar. 1994 163 p
(AD-A282954) Avail: CASI HC A08/MF A02

Spectral-based classification schemes designed to separate various wideband transient signals in added noise have been identified and their performances compared along with those obtained using a back-propagation neural network implementation. The spectral-based measures used include: the normalized cross-correlation coefficient; the modified normalized cross-correlation coefficient, and the divergence and the Bhattacharyya distance. Noise was added to the signals to create signal to noise ratios of 0 dB to -20 dB. Results show that as noise levels increase, the modified normalized cross-correlation coefficient spectral measure remains the most robust scheme. DTIC

N95-12595 Helsinki Univ. of Technology, Espoo (Finland). Electromagnetics Lab.
PROCEEDINGS OF BIANISOTROPICS 1993: SEMINAR ON ELECTRODYNAMICS OF CHIRAL AND BIANISOTROPIC MEDIA
A. Sihvola, S. Tretyakov, and I. Semchenko Dec. 1993 125 p Seminar held in Gomel, Russia, 12-14 Oct. 1993 Limited Reproducibility: More than 20% of this document may be affected by microfiche quality
(PB94-179314; ISBN-951-22-1892-5) Avail: CASI HC A06

The international seminar Bianisotropics '93 was held at the University of Gomel in southeastern Belarus in 12 - 14 October 1993. The topic of the meeting was the electromagnetics of complex materials, as, for example chiral, nonreciprocal, gyrotropic, and anisotropic media. The proceedings contain written reports of the presentations in Bianisotropics '93 as well as contact information of the participants of the seminar. NTIS

N95-12601# Naval Postgraduate School, Monterey, CA.
THE EFFECT OF RICIAN FADING AND PARTIAL-BAND INTERFERENCE ON NOISE-NORMALIZED FAST FREQUENCY-HOPPED MFSK RECEIVERS M.S. Thesis
Melody Kragh Mar. 1994 70 p
(AD-A282805) Avail: CASI HC A04/MF A01

The performance of an M-ary orthogonal frequency-shift keying (MFSK) communication system employing fast frequency-hopped spread spectrum waveforms transmitted over a frequency-nonselective, slowly fading channel with partial-band interference is analyzed. A procedure referred to as noise-normalization combining is employed by the system receiver to minimize partial-band interference effects. Each hop is assumed to fade independently. The partial-band interference is modeled as a Gaussian process. Both the signal and the partial-band interference are assumed to be affected by the fading channel which is modeled as Rician. The effect of fading of the partial-band interference on worst-case receiver performance is relatively minor. When there is no signal fading or when the signal fading is Rician, then the counter-intuitive result of poorer receiver performance when the partial-band interference experiences fading is obtained. This effect is most pronounced when the signal does not fade and the partial-band interference experiences Rayleigh fading. DTIC

N95-12644*# Pennsylvania State Univ., University Park, PA. Dept. of Aerospace Engineering.
PROJECT ECHO: ELECTRONIC COMMUNICATIONS FROM HALO ORBIT
Jason Borrelli, Bryan Cooley, Marcy Debole, Lance Hrivnak, Kenneth Nielsen, Gary Sangmeister, and Matthew Wolfe 1994 157 p Prepared for Universities Space Research Association, Columbia, MD
(Contract NASw-4435)
(NASA-CR-197190; NAS 1.26:197190) Avail: CASI HC A08/MF A02

The design of a communications relay to provide constant access between the Earth and the far side of the Moon is presented. Placement of the relay in a halo orbit about the L2 Earth-Moon Lagrange point allows the satellite to maintain constant simultaneous communication between Earth and scientific payloads on the far side of the Moon. The requirements of NASA's Discovery-class missions adopted and modified for this design are: total project cost should not exceed $150 million excluding launch costs, launch must be provided by Delta-class vehicle, and the satellite should maintain an operational lifetime of 10 to 15 years. The spacecraft will follow a transfer trajectory to the L2 point, after launch by a Delta II 7925 vehicle in 1999. Low-level thrust is used for injection into a stationkeeping-free halo orbit once the spacecraft reaches the L2 point.

The shape of this halo orbit is highly elliptical with the maximum excursion from the L2 point being 35000 km. A spun section and despun section connected through a bearing and power transfer assembly (BAPTA) compose the structure of the spacecraft. Communications equipment is placed on the despun section to provide for a stationary dual parabolic offset-feed array antenna system. The dual system is necessary to provide communications coverage during portions of maximum excursion on the halo orbit. Transmissions to the NASA Deep Space Network 34 m antenna include six channels (color video, two voice, scientific data from lunar payloads, satellite housekeeping and telemetry and uplinked commands) using the S- and X-bands. Four radioisotope thermoelectric generators (RTG's) provide a total of 1360 W to power onboard systems and any two of the four Hughes 13 cm ion thrusters at once. Output of the ion thrusters is approximately 17.8 mN each with xenon as the propellant. Presence of torques generated by solar pressure on the antenna dish require the addition of a 'skirt' extending from the spun section of the satellite for balance. Total mass of the satellite is approximately 900 kg at a cost of $130 million FY99. Author (revised)

N95-12646 Department of the Navy, Washington, DC.
METHOD OF PHASED MAGNITUDE CORRELATION USING BINARY SEQUENCES Patent
Michael Pender, inventor (to Navy) and Donald Tom, inventor (to Navy) 1 Feb. 1994 19 p Filed 26 Feb. 1993
(AD-D016397; US-Patent-5,283,586; US-Patent-Appl-SN-023440; US-Patent-Class-342-189) Avail: US Patent and Trademark Office

A method for allowing a correlation function to be applied to binary codes of length 3 to length 255 is presented. A user may specify the desired length of the binary codes for correlation processing, whether the binary code is to use a phase sidelobe level as the threshold or a sidelobe amplitude as the threshold. The user will also be asked to specify the threshold as well as an in phase coefficient referred to as beta and in out of phase coefficient referred to as a alpha. When the user has specified the parameters for correlation processing of the binary code length selected by the user, the program of the present invention will process the binary codes eliminating allomorphic forms of the codes from correlation and then display the results to the user. DTIC

N95-12674*# National Aeronautics and Space Administration. Lewis Research Center, Cleveland, OH.
MICROFABRICATED HYDROGEN SENSOR TECHNOLOGY FOR AEROSPACE AND COMMERCIAL APPLICATIONS
Gary W. Hunter, R. L. Bickford, E. D. Jansa, D. B. Makel, C. C. Liu, Q. H. Wu, and W. T. Powers Aug. 1994 14 p Presented at the NASA/SPIE Symposium, San Diego, CA, 24-29 Jul. 1994
(Contract NAS8-39029; NAG3-1149; RTOP 232-01-0B)
(NASA-TM-106703; E-9065; NAS 1.15:106703) Avail: CASI HC A03/MF A01

Leaks on the Space Shuttle while on the Launch Pad have generated interest in hydrogen leak monitoring technology. An effective leak monitoring system requires reliable hydrogen sensors, hardware, and software to monitor the sensors. The system should process the sensor outputs and provide real-time leak monitoring information to the operator. This paper discusses the progress in developing such a complete leak monitoring system. Advanced microfabricated hydrogen sensors are being fabricated at Case Western Reserve University (CWRU) and tested at NASA Lewis Research Center (LeRC) and Gencorp Aerojet (Aerojet). Changes in the hydrogen concentrations are detected using a PdAg on silicon Schottky diode structure. Sensor temperature control is achieved with a temperature sensor and heater fabricated onto the sensor chip. Results of the characterization of these sensors are presented. These sensors can detect low concentrations of hydrogen in inert environments with high sensitivity and quick response time. Aerojet is developing the hardware and software for a multipoint leak monitoring system designed to provide leak source and magnitude information in real time. The monitoring system processes data from the hydrogen sensors and presents the operator with a visual indication of the leak location and magnitude. Work has commenced on integrating the NASA LeRC-CWRU hydrogen sensors with the Aerojet designed monitoring system. Although the leak monitoring system was designed for hydrogen propulsion systems, the possible applications of this monitoring system are wide ranged. Possible commercialization of the system will also be discussed. Author

N95-12834 Naval Postgraduate School, Monterey, CA. Dept. of Electrical and Computer Engineering.
EFFICIENT PARABOLIC EQUATION SOLUTION OF RADIOWAVE PROPAGATION IN AN INHOMOGENEOUS ATMOSPHERE AND OVER IRREGULAR TERRAIN: FORMULATION
Ramakrishna Janaswamy Jun. 1994 37 p Limited Reproducibility: More than 20% of this document may be affected by microfiche quality
(AD-A282648; NPS-EC-94-004) Avail: Issuing Activity (Defense Technical Information Center (DTIC))

Formulation is given for efficient parabolic equation solution of radiowave propagation in inhomogeneous atmosphere and over irregular terrain. Both standard and wide angle parabolic equation derivations are presented. Impedance boundary conditions are used to characterize the ground. A tropospheric boundary condition based on the exact solution of Schroedinger equation in a quarter plane is derived. To permit efficient modeling of the irregular boundary, the parabolic equation together with the boundary conditions is transformed into a numerically generated curvilinear coordinate system. Finally, formulation is presented for a finite difference solution using Crank-Nicolson implicit scheme. DTIC

N95-12856*# Ohio State Univ., Columbus. Dept. of Electrical Engineering.
ELECTROMAGNETIC ON-AIRCRAFT ANTENNA RADIATION IN THE PRESENCE OF COMPOSITE PLATES
S. H-T. Kan and R. G. Rojas Jul. 1994 83 p
(Grant NAG1-1058)
(NASA-CR-196126; Rept-722792-5; NAS 1.26:196126) Avail: CASI HC A05/MF A01

The UTD-based NEWAIR3 code is modified such that it can model modern aircraft by composite plates. One good model of conductor-backed composites is the impedance boundary condition where the composites are replaced by surfaces with complex impedances. This impedance-plate model is then used to model the composite plates in the NEWAIR3 code. In most applications, the aircraft distorts the desired radiation pattern of the antenna. However, test examples conducted in this report have shown that the undesired scattered fields are minimized if the right impedance values are chosen for the surface impedance plates. Author

N95-12896*# Martin Marietta Corp., Denver, CO.
EXPERIMENTAL EVALUATION OF SHAPE MEMORY ALLOY ACTUATION TECHNIQUE IN ADAPTIVE ANTENNA DESIGN CONCEPTS Final Report
W. Neill Kefauver and Bernie F. Carpenter Hampton, VA NASA Sep. 1994 65 p Original contains color illustrations
(Contract NAS1-18455; RTOP 233-01-03-22)
(NASA-CR-194983; NAS 1.26:194983) Avail: CASI HC A04/MF A01; 19 functional color pages

Creation of an antenna system that could autonomously adapt contours of reflecting surfaces to compensate for structural loads induced by a variable environment would maximize performance of space-based communication systems. Design of such a system requires the comprehensive development and integration of advanced actuator, sensor, and control technologies. As an initial step in this process, a test has been performed to assess the use of a shape memory alloy as a potential actuation technique. For this test, an existing, offset, cassegrain antenna system was retrofit with a subreflector equipped with shape memory alloy actuators for surface contour control. The impacts that the actuators had on both the subreflector contour and the antenna system patterns were measured. The results of this study indicate the potential for using shape memory alloy actuation techniques to adaptively control antenna performance; both variations in gain and beam steering capabilities were demonstrated. Future development effort is required to evolve this potential into a useful technology for satellite applications. Author

N95-12920 Naval Postgraduate School, Monterey, CA.
LESSONS LEARNED FROM EXPERIMENTS CONDUCTED ON RADAR DATA MANAGEMENT SYSTEMS M.S. Thesis
Mark W. Pierce Jun. 1994 145 p Limited Reproducibility: More than 20% of this document may be affected by microfiche quality
(AD-A282896) Avail: CASI HC A07

The thesis provides lessons learned from experiments conducted by the 11th Air Force to verify the capabilities of two vendor-produced Radar

Data Management Systems (RDMS). The first part of the thesis provides background information explaining the impetus for such experiments and why a lessons learned approach was taken. The experimental plan and the final report from the PACAF experiments are analyzed using evaluation tools taught in the C3 curriculum at the Naval Postgraduate School. The lessons learned from the mistakes made during these experiments are applied to produce a revised experimental plan. A lessons learned section follows the analysis. This section discusses specific lessons learned from the 11th Air Force experiments as well as more general lessons learned by the author. The thesis concludes with two chapters that provide overall conclusions and a summary, and recommendations for future work that can be accomplished in the area of radar data management. DTIC

N95-12924 Kansas Univ. Center for Research, Inc., Lawrence, KS.
PART A: A DATA ACQUISITION/CONTROLLER SYSTEM. PART B: SUPPLEMENT TO A DATA ACQUISITION/CONTROLLER SYSTEM Final Report
Fitratullah Khan and Marcelo Cavalcanti May 1994 86 p Limited Reproducibility: More than 20% of this document may be affected by microfiche quality
(Contract N00014-89-J-3221)
(AD-A283373) Avail: CASI HC A05

A data acquisition/controller system was required for gathering data simultaneously from different radars located spatially apart. Problems encountered in the earlier generation of data acquisition systems were to be alleviated. One of the major problems was the corruption of weak signals by noise on long analog signal cables. Some evidence of video display being another source of noise was also found. Another goal was to reduce the amount of cable going from radar sites to the operator's computer. DTIC

N95-13057# Argonne National Lab., IL.
A HITCHHIKER'S GUIDE TO MICROSCOPY AND MICROANALYSIS USING TELECOMMUNICATIONS, EMAIL AND THE INTERNET
N. J. Zaluzec Mar. 1994 3 p Presented at the Microscopy Society of America and Microbeam Analysis Society Joint Meeting, New Orleans, LA, 31 Jul. - 5 Aug. 1994
(Contract 2-31-109-eng-38)
(DE94-013299; ANL/MSD/CP-82371; CONF-940753-20) Avail: CASI HC A01/MF A01

The Information SuperHighway, Email, The Internet, FTP, BBS, and Modems are all buzz words which are becoming more and more routine in our daily life. Confusing terminology? Hopefully, it won't be in a few minutes, all you need is to have a handle on a few basic concepts and terms and you will be on-line with the rest of the telecommunication experts. These terms all refer to some type or aspect of tools associated with a range of computer-based communication software and hardware. They are in fact far less complex than the instruments we use on a day to day basis as microscopist's and microanalyst's. The key is for each of us to know what each is and how to make use of the wealth of information which they can make available to us for the asking. Basically all of these items relate to mechanisms and protocols by which we as scientists can easily exchange information rapidly and efficiently to colleagues in the office, down the hall, or half-way around the world using computers and various communications media. The purpose of this tutorial/paper is to outline and demonstrate the basic ideas of some of the major information systems available to all of us today. For the sake of simplicity, we will break this presentation down into two distinct (but as we shall see later, connected) areas: telecommunications over conventional phone lines, and telecommunications by computer networks. DOE

N95-13343# Academy of Sciences of the Ukraine, Kharkov. Fiziko-Tekhnicheskij Inst.
STIMULATED SCATTERING OF A SLOW ELECTROMAGNETIC WAVE EXCITED BY THE RELATIVISTIC ELECTRON BEAM
V. V. Ognivenko 1993 4 p
(DE94-625049; KFTI-93-34) Avail: CASI HC A01/MF A01 (US Sales Only)

A theory is presented offering two-stage stimulated scattering of a slow electromagnetic wave excited by a relativistic electron beam under conditions of the anomalous Doppler effect in an axial guide magnetic field. DOE

N95-13371# Colorado Univ., Boulder, CO. Dept. of Electrical and Computer Engineering.
AN INVESTIGATION OF THE CHANNEL CROSSTALK IN OPTICAL HETERODYNE CONTROLLED PHASED ARRAY RADARS Annual Report, 1 Jun. 1993 - 31 May 1994
Alan R. Mickelson 21 Jun. 1994 8 p
(Contract N00014-92-J-1190)
(AD-A281227) Avail: CASI HC A02/MF A01

The principal objective of this project is to investigate problems associated with achieving the drive/read-out system complexity necessary to control a phased array antenna with optical heterodyne techniques. In particular, this work concentrates on multichannel microwave optical conversion. The approach has been to study the problems associated with device arrays of single sideband modulators that would be necessary to control the amplitudes and phases of all signals delivered to a phased array front end. Our approach remains focused on increasing the complexity of control by modulating only a small number of optical channels which can then be locked to a previously locked active antenna array. This approach is also enabling a better understanding of the accuracy and validity of our computer aided analysis and is also allowing a greater range of device complexity to be analyzed. DTIC

N95-13405 Technische Univ., Delft (Netherlands).
TRELLIS-BASED SOURCE AND CHANNEL CODING Ph.D. Thesis
R. J. vanderVleuten 29 Mar. 1994 161 p
(PB94-204443; ISBN-90-5326-013-7) Copyright Avail: Issuing Activity (National Technical Information Service (NTIS))

This thesis concerns the efficient transmission of digital data, such as digitized sounds or images, from a source to its destination. To make the best use of the limited capacity of the source-destination channel, a source coder is used to delete the less significant information. To correct the occurring transmission errors, a channel coder is used. Efficient techniques for source and channel coding, based on trellises, are respectively investigated in Part 1 and Part 2 of this thesis. NTIS

N95-13558 DELAB, Trondheim (Norway).
PROVOKING AND MEASURING CELL LOSSES IN ATM SYSTEMS BY IMPORTANCE SAMPLING, CONTROL VARIABLES AND LOAD CYCLES
P. E. Heegaard and B. E. Helvik 17 Dec. 1993 126 p
(PB94-202520; STF40-A93148) Avail: Issuing Activity (National Technical Information Service (NTIS))

The paper introduces an accelerated measurement technique for Asynchronous Transfer Mode (ATM) systems. It requires no control of the target system. It only relies on the ability to be given continuous feedback of the target system response. The approach is therefore applicable to measurements of real systems, as well as simulators. Unbiased estimates of the cell loss are obtained by combining two variance reduction techniques. The total observation period is divided into measurement periods defined by load cycles. A number of options has been investigated by simulation. NTIS

N95-13559 DELAB, Trondheim (Norway).
200 MHz CHANNEL SOUNDER, OPEN DESCRIPTION
O. Trandem 21 Jan. 1994 53 p
(PB94-202538; STF40-A94015) Avail: Issuing Activity (National Technical Information Service (NTIS))

The channel sounder is built to make complex impulse response (CIR) measurements on broad band radio channels, e.g., indoor communication and wireless subscriber networks, or broadband CDMA (Code Division Multiple Access) mobile networks. Equipment is made, which can do channel impulse response (CIR) measurements with resolution variable from 5 to 160 ns, and impulse response lengths from 64 to 8192 samples. The equipment consists of a transmitter and a receiver, where the transmitter sends a continuous signal, a repetitive chirp, and the receiver analyzes this signal. Interface is at an IF frequency of 1350 MHz. The computed CIR's can be sent via GPIB to a PC, for storing, and further processing. The receiver is also controlled by this PC. Sampling is synchronously on two IF inputs. The receiver can average a number of segments on the input signals, to enhance the signal to noise ratio. It can also do delay-doppler processing, on many consecutive input segments. Receiver dynamic range is -70 - +10 dBm. Instant dynamic range is from 30 to 60 dB, depending on impulse response length. NTIS

N95-13577 DELAB, Trondheim (Norway).
LINEAR APPROXIMATIONS OF DELAYS IN BUFFERS RECEIVING CORRELATED ATM CELL STREAMS
P. R. Hokstad and B. E. Helvik 21 Dec. 1993 29 p See also PB93-162618 and PB93-170660
(PB94-207099; STF40-A93158) Avail: Issuing Activity (National Technical Information Service (NTIS))

In the Asynchronous Transfer Mode (ATM) based Broadband Integrated Services Digital Network (B-ISDN) it is necessary to have a good insight into how the cell streams from various types of sources interact and modify each other and thereby introduce a cross influence of the network performance (NP) quality of service (QoS). Insight into this interaction is necessary for a proper dimensioning of networks and network elements. Since the cell streams have very complex stochastic properties, e.g. a large and irregular autocorrelation, an exact analysis is in the general case out of the question. The report presents an approximation where the number of cells in a buffer is expressed as a linear combination of the numbers of arrivals to the buffer up to that slot. Various approximating models of this type are discussed, and models are presented using the 'shift operator'. The linear expressions are fitted so that certain relations of the exact model will be satisfied. On this basis, an approach for deriving the correlation between the waiting times in two subsequent buffers is also outlined.
NTIS

N95-13210*# Massachusetts Inst. of Tech., Lexington. Lincoln Lab.
AIRCRAFT WAKE RCS MEASUREMENT
William H. Gilson *In* NASA. Langley Research Center, Airborne Windshear Detection and Warning Systems. Fifth and Final Combined Manufacturers' and Technologists' Conference, Part 2 Jul. 1994 p 603-623 Sponsored by Office of Naval Technology (For primary document see N95-13203 02-03)
Avail: CASI HC A03/MF A04

33 ELECTRONICS AND ELECTRICAL ENGINEERING

Includes test equipment and maintainability; components, e.g., tunnel diodes and transistors; microminiaturization; and integrated circuitry.

For related information see also *60 Computer Operations and Hardware* and *76 Solid-State Physics.*

N95-11751# Pacific Northwest Lab., Richland, WA.
POWER SYSTEM APPLICATIONS FOR PASC CONVERTER SYSTEMS
M. K. Donnelly and R. M. Johnson Apr. 1994 7 p Presented at the Institute of Electrical and Electronics Engineers/Power Engineering Society (IEEE/PES) T/D Conference, Chicago, IL, 10-15 Apr. 1994
(Contract DE-AC06-76RL-01830)
(DE94-013329; PNL-SA-23362; CONF-9404175-1) Avail: CASI HC A02/MF A01

This paper shows, using computer EMTP simulations, some preliminary results of applying pulse amplitude synthesis and control (PASC) technology to single-source level voltage converter system. The method can be applied to any single terminal pair source with appropriate modifications in power extraction interface and computer control program to match source and load impedance characteristics. The PASC realization as discussed here employs banks of transformers, one bank per phase, in which the primaries are connected in parallel through a switch matrix to the dc source. Two opposite polarity primaries per transformer are pulsed alternatively in time to produce an oscillatory sinusoidal output waveform. PASC conversion system capabilities to produce both leading and lagging power factor power output in single-phase and three-phase (Delta) or Y configurations are illustrated. EMTP simulations are used to demonstrate the converter capabilities. Also included are discussions regarding harmonics and potential control strategies to adapt the converter to an application or to minimize harmonics. DOE

N95-11860 Minnesota Univ., Minneapolis, MN. Dept. of Electrical Engineering.
DEVELOPMENT OF NANOSTRUCTURE FABRICATION TECHNOLOGY AND NEW ELECTRON-QUANTUM WAVE DEVICES Final Report, 1 Apr. 1990 - 31 Mar. 1993
Stephen Y. Chou 15 Feb. 1994 21 p Limited Reproducibility: More than 20% of this document may be affected by microfiche quality
(Contract DAAL03-90-G-0058)
(AD-A281724; ARO-27578.7-EL) Avail: CASI HC A03

Under the three-year grant, we have investigated and developed various nanofabrication technologies including construction of an ultra-high resolution electron beam lithography system, sub-20 nm electron beam lithography techniques, etching of sub-40 nm silicon pillars and ridges; fabricated various nanoscale transistors including a number of new device structures; studied quantum effects and single electron effects; designed, fabricated, and investigated ultra-fast metal-semiconductor-metal photodetectors with the record speeds on various of semiconductors, including low-temperature GaAs with 510 GHz bandwidth, bulk GaAs with 300 GHz, and bulk Si with 75 GHz. Author (DTIC)

N95-12009 Spire Corp., Bedford, MA.
SILICON-BASED BLUE LIGHT EMITTING DIODE Report, 1 Nov. - 31 Dec. 1993
31 Dec. 1993 11 p Limited Reproducibility: More than 20% of this document may be affected by microfiche quality
(Contract N00014-93-C-0176)
(AD-A282382) Avail: Issuing Activity (Defense Technical Information Center (DTIC))

The overall goal of this program is to fabricate stable green/blue electroluminescent devices based on nanostructures of Si alloyed with group IV (such as carbon and germanium). During the past two years, optically excited visible-light emission from electrochemically etched anodized silicon has provided researchers with the possibility of fabricating a red-to-orange LED based on porous Si. A few groups have used semitransparent gold as a solid state contact to porous Si to form Schottky diodes. Spire, under a SDIO funded SBIR program, has demonstrated a light-emitting device consisting of a heterojunction between electrochemically etched p-type porous Si and n-type transparent indium tin oxide (ITO). The use of ITO or other wide-bandgap semiconductors which are transparent to visible light has potential applications for visible LED's and display panels. DTIC

N95-12421 North Carolina Agricultural and Technical State Univ., Greensboro, NC. Dept. of Electrical Engineering.
SELF-CHECKING STATE MACHINE REALIZATIONS IN CMOS Report, 1 Apr. - 30 Jun. 1994
P. K. Lala 30 Jun. 1994 3 p Limited Reproducibility: More than 20% of this document may be affected by microfiche quality
(Contract N00014-94-1-0462)
(AD-A282177) Avail: Issuing Activity (Defense Technical Information Center (DTIC))

In this reporting period, we have studied the currently available techniques for designing totally self-check checkers for m-out-of-n codes. Such codes can be used for state assignment in self-checking state machines. The major advantage of m-out-of-n codes is that they can detect single and unidirectional multibit errors in the encoded information bits. Thus, if a circuit is designed such that its output forms an m-out-of-n code, any fault in the circuit which creates a single bit error or unidirectional multibit error at the output can be detected on-line. On-line error detection, also known as self-checking, can be accomplished by using a checker to monitor the circuit output. The output of the checker is 01 or 10 if there is no fault in the circuit under test or in the checker itself, otherwise the output will be 00 or 11. DTIC

N95-12494 Texas Technological Univ., Lubbock, TX.
LOCALLY CONNECTED ADAPTIVE GABOR FILTER FOR REAL-TIME MOTION COMPENSATION Progress Report No. 3, 20 Apr. - 19 Jul. 1994
Hau Li 19 Jul. 1994 5 p Limited Reproducibility: More than 20% of this document may be affected by microfiche quality
(Contract N00014-94-1-0077)
(AD-A282544) Avail: CASI HC A01

Software has been developed to implement the Gabor motion detection algorithm. This software consists of utility functions, algorithm modules, and test pattern generators for the experiments and verification of the spatial and temporal selectivity. Based on the theoretical analysis, the optical flow was computed for several artificially generated test patterns. These test patterns are designed to test the concept of spatial and orientation selectivity. The patterns were generated by using virtual reality technique based on three-dimensional computer graphics. In addition to the algorithm development and verification, we have also started work on the design and verification of the electronics basic building blocks for the VLSI implementation. This early start of the hardware design concurrent with the algorithm analysis and verification will further ensure the quality of the work in both hardware and software. In order to benchmark the VLSI chips, a hardware prototype board is under design and construction. This board will be used to compare the performance of digital approach vs. analog approach, analog approach based on the standard off-the-shelf components vs. analog customer-design VLSI approach. DTIC

N95-12509# Naval Undersea Warfare Center, New London, CT.
MODELING OF SPLIT-CORE TRANSFORMERS FOR POWER TRANSMISSION
Dwayne M. Servidio and Anthony B. Bruno 23 Jun. 1994 10 p Presented at the International Magnetics Conference, Stockholm, Sweden, 13-16 Apr. 1993
(AD-A282782; NUWC-NPT-TD-10557) Avail: CASI HC A02/MF A01

This paper was presented in poster format at the International Magnetics Conference in Stockholm, Sweden, 13-16 April 1993. It describes how the magnetic vector potential finite element method is used to predict the performance of a pot-core transformer for power transmission across a variable air gap. Performance predictions computed by the model include mutual and leakage inductance for various air gaps between 1 and 9 mm. Magnetic flux density external to the pot-core was also computed as a function of air gap. The predicted performance was then compared with measurements taken on a prototype core. Experimental and numerical results were shown to be in good agreement. DTIC

N95-12525# Army Research Lab., Fort Monmouth, NJ.
FREQUENCY DOUBLER (FROM 4.7 TO 9.4 GHz) USING A DIODE Technical Report, Feb. 1992 - May 1993
Jeffrey Himmel Jul. 1994 86 p
(AD-A282784; ARL-TR-72) Avail: CASI HC A05/MF A01

This report discusses the design, fabrication and testing of a harmonic generator which has an input frequency of 4.7 GHz and an output frequency of 9.4 GHz. A diode was used as the nonlinear device to produce the harmonics. The designed bandwidth of the output signal was 10 percent of the output frequency, with power optimized at 9.4 GHz. DTIC

N95-12795*# Swales and Associates, Beltsville, MD.
STEPPER MOTOR
Cornelis deKramer 31 Aug. 1994 46 p
(Contract NAS5-32650; RTOP 722-20-00)
(NASA-CR-189373; NAS 1.26:189373; SAI-026) Avail: CASI HC A03/MF A01

The purpose of this document is to describe the more commonly used permanent magnet stepper motors for spaceflight. It will discuss the mechanical and electrical aspects of the devices, their torque behavior, those parameters which need to be controlled and measured, and test methods to be employed. It will also discuss torque margins, compare these to the existing margin requirements, and determine the applicability of these requirements. Finally it will attempt to generate a set of requirements which will be used in any stepper motor procurement and will fully characterize the stepper motor behavior in a consistent and repeatable fashion. Derived from text

N95-12863# Sandia National Labs., Albuquerque, NM.
MODELING OF TRANSFORMERS USING CIRCUIT SIMULATORS
W. E. Archer, M. F. Deveney, and R. L. Nagel 1994 18 p Presented at the Electrical Manufacturing and Coil Winding Conference, Chicago, IL, 27 Sep. 1994
(Contract DE-AC04-94AL-85000)
(DE94-014656; SAND-94-1715C; CONF-9409166-1) Avail: CASI HC A03/MF A01

Transformers of two different designs, an unencapsulated pot core and an encapsulated toroidal core, have been modeled for circuit analysis with circuit simulation tools. We selected MicroSim's PSPICE and Anology's SABER as the simulation tools and used experimental BH Loop and network analyzer measurements to generate the needed input data. The models are compared for accuracy and convergence using the circuit simulators. Results are presented which demonstrate the effects on circuit performance from magnetic core losses, eddy currents, and mechanical stress on the magnetic cores. DOE

N95-12865# Sandia National Labs., Albuquerque, NM.
INFLUENCE OF ELECTRODE GEOMETRY ON THE HIGH-FIELD CHARACTERISTICS OF PHOTOCONDUCTIVE SILICON WAFERS
V. P. Madangarli (South Carolina Univ., Columbia, SC.), G. Gradinaru (South Carolina Univ., Columbia, SC.), G. Korony (South Carolina Univ., Columbia, SC.), T. S. Sudarshan (South Carolina Univ., Columbia, SC.), G. M. Loubriel, and F. J. Zutavern 1994 13 p Presented at the 21st International Power Modulator Symposium, Costa Mesa, CA, 28-30 Jun. 1994
(Contract DE-AC04-94AL-85000)
(DE94-014660; SAND-94-1227C; CONF-940678-2) Avail: CASI HC A03/MF A01

A series of experiments were conducted to study the influence of electrode geometry on the prebreakdown (and breakdown) characteristics of high resistivity (rho greater than 30 k(Omega)-cm), p-type Si wafers under quasi-uniform and non-uniform electric field configurations. In the quasi-uniform field configuration, the 1-mm thick Si wafer was mounted between the slots of two plane parallel stainless steel disc electrodes (parallel), while the non-uniform field was obtained by mounting the wafer between two pillar-type electrodes with a hemispherical tip (pillar). The main objective of the above investigation was to verify if the uniform field configuration under a parallel system has a positive influence by reducing the field enhancement at the contact region, as opposed to the definite field enhancement present in the case of the non-uniform pillar system. Also, it was proposed to study the effect of the contact profile on the field distribution over the wafer surface and hence its influence on the high-field performance of the Si wafers. DOE

N95-12881 Notre Dame Univ., IN. Dept. of Electrical Engineering.
QUANTUM CELLULAR AUTOMATA Annual Report, 1 Jul. 1993 - 30 Jun. 1994
Wolfgang Porod, Craig S. Lent, and Gary H. Bernstein 30 Jun. 1994 22 p Limited Reproducibility: More than 20% of this document may be affected by microfiche quality
(Contract N00014-93-1-1084)
(AD-A283351) Avail: CASI HC A03

The Notre Dame group has developed a new paradigm for ultra-dense and ultra-fast information processing in nanoelectronic systems. These Quantum Cellular Automata (QCA's) are the first concrete proposal for a technology based on arrays of coupled quantum dots. The basic building block of these cellular arrays is the Notre Dame Logic Cell, as it has been called in the literature. The phenomenon of Coulomb exclusion, which is a synergistic interplay of quantum confinement and Coulomb interaction, leads to a bistable behavior of each cell which makes possible their use in large-scale cellular arrays. The physical interaction between neighboring cells has been exploited to implement logic functions. New functionality may be achieved in this fashion, and the Notre Dame group invented a versatile majority logic gate. In a series of papers, the feasibility of QCA wires, wire crossing, inverters, and Boolean logic gates was demonstrated. A major finding is that all logic functions may be integrated in a hierarchial fashion which allows the design of complicated QCA structures. The most complicated system which was simulated to date is a one-bit full adder consisting of some 200 cells. In addition to exploring these new concepts, efforts are under way to physically realize such structures both in semiconductor and metal systems. Extensive modeling work of semiconductor quantum dot structures has helped identify optimum design parameters for QCA experimental implementations. DTIC

N95-12918 Rome Lab., Griffiss AFB, NY.
DIGITAL FILTER DESIGNS THAT ARE FREE OF LIMIT CYCLES Report, Feb. - Apr. 1993
Scott M. Bolen Jun. 1994 23 p Limited Reproducibility: More than

20% of this document may be affected by microfiche quality
(AF Proj. 4506)
(AD-A282885; RL-TR-94-54) Avail: CASI HC A03

Finite word-length adders and quantizing methods used to construct digital filters can cause nonlinearities to occur in the closed-loop filter system. Such nonlinearities can degrade system performance in what is known as a limit cycle behavior of the output. Overflow oscillations are limit cycles that are induced by the repeated overflow of finite word-length adders used in filter realizations. It is possible to construct digital filters that are free of overflow oscillations. Nonlinear analysis techniques can be used to derive conditions to govern digital filter designs that will be free of overflow oscillations. This paper will formulate a general theorem to ensure that nth order digital filters will be free of overflow oscillations. An implementation of digital filters with two's complement arithmetic adders is included to demonstrate the result of the analysis. DTIC

N95-13052# University Coll., Cork (Ireland). National Microelectronics Research Centre.
WOCSDICE 1994: EUROPEAN WORKSHOP ON COMPOUND SEMICONDUCTOR DEVICES AND INTEGRATED CIRCUITS
1 Jun. 1994 109 p Workshop held in Kinsale, Ireland, 29 May - 1 Jun. 1994
(Contract N68171-94-M-5608)
(AD-A283062; R/D-7290-EE-02) Avail: CASI HC A06/MF A02

Contents of the workshop are broken down into the following categories: materials and characterization; modeling/simulation; transistors; optoelectronic integrated circuits (OEICs); two terminal devices; integrated devices; and optical devices. DTIC

N95-13153 Department of the Navy, Washington, DC.
5-VOLT LOW LEVEL SERIAL TRANSCEIVER Patent
Trung H. Tran, inventor (to Navy) 28 Jun. 1994 4 p Filed 31 Mar. 1992
(AD-D016399; US-Patent-5,325,395; US-Patent-Appl-SN-861411; US-Patent-Class-375-7) Avail: US Patent and Trademark Office

A transceiver has a transmitter portion using active comparators coupled to a single low level positive bias source to enable low powered drain transmit and receive conversion of TTL input signals to LLS (low level serial) data output signals for a coaxial data transmission cable. The transceiver also provides a constant impedance for a coaxial or triaxial transmission cable during active transmission periods, standby periods and power-off periods to provide a cost effective method to transmit and receive data. DTIC

N95-13164 Army Research Lab., Fort Monmouth, NJ. Electronics and Power Sources Directorate.
PROCEEDINGS OF THE 36TH POWER SOURCES CONFERENCE
9 Jun. 1994 447 p Conference held in Cherry Hill, NJ, 6-9 Jun. 1994 Limited Reproducibility: More than 20% of this document may be affected by microfiche quality
(AD-A281443) Avail: CASI HC A19

The contents are divided into the following sessions: Capacitors, Primary Aqueous Batteries, Rechargeable Lithium Batteries I, Fuel Cells, Rechargeable Lithium Batteries II, Metal/Air Batteries, Photovoltaic/Thermophotovoltaic Energy Conversion, Military Applications/Dual Use, Rechargeable Aqueous Batteries I, Lithium/Polymer Batteries, Rechargeable Aqueous Batteries II, High-Temperature/Thermal Batteries, Primary Lithium Batteries I, Thermal Batteries, and Primary Lithium Batteries II. CASI

N95-13174 Department of the Navy, Washington, DC.
SEMICONDUCTOR PHOTODETECTOR DEVICE Patent Application
T. F. Carruthers, inventor (to Navy) 31 Mar. 1994 23 p Limited Reproducibility: More than 20% of this document may be affected by microfiche quality
(AD-D016314; US-Patent-Appl-SN-221330; Navy-Case-74809) Avail: CASI HC A03

A semiconductor photodetector which employs a multilayer structure for controlling speed, efficiency and noise is presented. A light-absorbing low band gap semiconductor emitter layer produces photogenerated charge upon absorption of light. A semiconductor collector layer collects the photogenerated charge. A semiconductor barrier layer between the light absorbing layer and the collector layer selectively blocks substantially all but photogenerated charge. A base layer may be optionally employed between the barrier layer and the collector layer for gating the current flow and controlling wavelength sensitivity. DTIC

N95-13181 Department of the Navy, Washington, DC.
SILICON CARBIDE AND SICALN HETEROJUNCTION BIPOLAR TRANSISTOR STRUCTURES Patent
Max N. Yoder, inventor (to Navy) 5 Jul. 1994 10 p Filed 29 Jul. 1992
(AD-D016403; US-Patent-5,326,992; US-Patent-Appl-SN-921151; US-Patent-Class-257-77) Avail: US Patent and Trademark Office

A heterojunction bipolar transistor (HBT) structure is configured so that the heterojunction between hexagonal and cubic materials is electrically active. A first embodiment of the HBT structure comprises both hexagonal and cubic silicon carbide (SiC). The emitter region is fabricated from the higher bandgap hexagonal SiC appropriately doped. The base and collector regions are grown using the lower bandgap cubic SiC. A second embodiment of the HBT structure comprises both a solid solution of SiC material such as an alloy of silicon carbon aluminum nitrogen (SiCAlN) grown upon a substrate of hexagonal SiC. The emitter region can be placed either on the top or bottom of the second embodiment of the HBT structure. Also, the bandgap between the emitter and base regions of the second embodiment can be varied by controlling the mole fraction ratio between the constituent parts of the SiCAlN, i.e., between the SiC and the AlN. DTIC

N95-13231*# Texas Instruments, Inc., Dallas. Central Research Labs.
Ku-BAND HIGH EFFICIENCY GaAs MMIC POWER AMPLIFIERS Interim Report
H. Q. Tserng, L. C. Witkowski, M. Wurtele, and Paul Saunier May 1988 63 p
(Contract NAS3-25076; RTOP 506-44-20)
(NASA-CR-182156; NAS 1.26:182156) Avail: CASI HC A04/MF A01

The development of Ku-band high efficiency GaAs MMIC power amplifiers is examined. Three amplifier modules operating over the 13 to 15 GHz frequency range are to be developed. The first MMIC is a 1 W variable power amplifier (VPA) with 35 percent efficiency. On-chip digital gain control is to be provided. The second MMIC is a medium power amplifier (MPA) with an output power goal of 1 W and 40 percent power-added efficiency. The third MMIC is a high power amplifier (HPA) with 4 W output power goal and 40 percent power-added efficiency. An output power of 0.36 W/mm with 49 percent efficiency was obtained on an ion implanted single gate MESFET at 15 GHz. On a dual gate MESFET, an output power of 0.42 W/mm with 27 percent efficiency was obtained. A mask set was designed that includes single stage, two stage, and three stage single gate amplifiers. A single stage 600 micron amplifier produced 0.4 W/mm output power with 40 percent efficiency at 14 GHz. A four stage dual gate amplifier generated 500 mW of output power with 20 dB gain at 17 GHz. A four-bit digital-to-analog converter was designed and fabricated which has an output swing of -3 V to +/- 1 V. Author

N95-13252 Technische Univ., Delft (Netherlands).
INTEGRATED SENSOR BUS Ph.D. Thesis
M. J. Rutka 22 Mar. 1994 152 p
(PB94-206810; ISBN-90-6275-966-1) Copyright Avail: Issuing Activity (National Technical Information Service (NTIS))

In this thesis an integrated sensor bus interface is presented. The proposed bus offers a number of interface procedures to enhance the system flexibility. It enables a 13-bit data exchange per message frame, automatic addressing, device clearing and resetting, and handling of service-request and polling procedures. Chapter 1 provides an overview of the existing data transmission technologies. It presents the most popular digital buses along with their application fields. Also other research activities on sensor buses are described. Chapter 2 deals with the requirements which have to be imposed on the desired sensor bus. It shows both communication and compatibility requirements. Chapter 3 introduces the proposed sensor bus. It presents the interface structure together with implemented bus procedures. The detailed description of the proposed sensor bus protocol is given in Chapter 4. It is divided into two parts; a logical layer description (i.e., sensor bus protocol) and a physical layer description (i.e., transmission medium and electrical characteristics). Chapter

5 deals with the compatibility issue. It investigates differences between typical processes used for sensors and digital circuits. Chapter 6 shows the design of a sensor bus interface prototype. In Chapter 7 the performance of the fabricated interface is discussed. NTIS

N95-13276# Academy of Sciences of the Ukraine, Kiev. Inst. Teoreticheskoj Fiziki.
THE DISSIPATIVE MECHANISM OF PINNING OF A SUPERCONDUCTING CURRENT
E. N. Ermakov 1994 11 p
(DE94-623252; ITP-93-67) Avail: CASI HC A03/MF A01 (US Sales Only)

The dissipation that causes pinning of a superconducting current is proposed. In the basis of this mechanism there lies a supposition that lowest energy excitation of Cooper's pairs is due to the space movement of pairs. Based on the phenomenological superfluidity criteria it is shown that the only mechanism of pairing leading to the nondissipative movement of pairs is the one that is caused by the interaction with the lowest energy thermal excitations in crystal. In the case of acoustic phonons we have the theory similar to BCS theory. However, in this case the existence of a current without loss is possible only if we take into account the distortion of Fermi sphere by a current. This condition leads to many singularities observed in high-temperature superconductors. DOE

N95-13291 RAND Corp., Santa Monica, CA.
MILITARY APPLICATIONS OF MICROELECTROMECHANICAL SYSTEMS
Keith W. Brendley and Randall Steeb 1993 64 p Limited Reproducibility: More than 20% of this document may be affected by microfiche quality
(AD-A282470) Avail: Issuing Activity (Defense Technical Information Center (DTIC))

Microelectromechanical systems (MEMS) or, more broadly, micro-engineered systems are essentially small devices on the scale of a few millimeters or less. They are often made using variations on techniques used in fabricating electronics; silicon is etched to create very fine, often very flat, structures. However, instead of transistors and diodes, small motors, gears, and sensors are made. Other techniques such as deep x-ray (synchrotron) lithography, electric discharge machining, and acoustic laser etching are also employed, often to create three-dimensional structures. These and other techniques are touched upon in the body of this report. DTIC

N95-13300 Westinghouse Electric Corp., Pittsburgh, PA.
PROCESSING, FABRICATION, AND DEMONSTRATION OF HTS INTEGRATED MICROWAVE CIRCUITS Status Report No. 11, 1 Feb. - 24 Apr. 1994
G. R. Wagner 24 Apr. 1994 14 p Limited Reproducibility: More than 20% of this document may be affected by microfiche quality
(Contract N00014-91-C-0112)
(AD-A282505) Avail: Issuing Activity (Defense Technical Information Center (DTIC))

An EW receiver analysis is currently underway to establish, quantitatively, the benefits of the high temperature superconductor (HTS) components being developed in this program. The switched filterbank, the static filterbank, and the delay lines as well as cooled semiconductor components are all being considered as part of this study. Derived from text

N95-13344*# Michigan Technological Univ., Houghton, MI. Dept. of Chemistry.
RAMAN STRUCTURAL STUDIES OF THE NICKEL ELECTRODE Final Report, 20 Feb. 1984 - 31 Oct. 1991
Bahne C. Cornilsen 7 Sep. 1994 33 p
(Grant NAG3-519)
(NASA-CR-196331; NAS 1.26:196331) Avail: CASI HC A03/MF A01

The objectives of this investigation have been to define the structures of charged active mass, discharged active mass, and related precursor materials (alpha-phases), with the purpose of better understanding the chemical and electrochemical reactions, including failure mechanisms and cobalt incorporation, so that the nickel electrode may be improved. Although our primary tool has been Raman spectroscopy, the structural conclusions drawn from the Raman data have been supported and augmented by three other analysis methods: infrared spectroscopy, powder X-ray Diffraction (XRD), and x-ray absorption spectroscopy (in particular EXAFS, Extended X-ray Absorption Fine Structure spectroscopy). Derived from text

N95-13368# North Carolina Univ., Raleigh, NC. Dept. of Materials Science and Engineering.
PSEUDOMORPHIC SEMICONDUCTING HETEROSTRUCTURES FROM COMBINATIONS OF AlN, GaN AND SELECTED SiC POLYTYPES: THEORETICAL ADVANCEMENT AND ITS COORDINATION WITH EXPERIMENTAL STUDIES OF NUCLEATION, GROWTH, CHARACTERIZATION AND DEVICE DEVELOPMENT Semiannual Technical Report, 1 Jan. - 30 Jun. 1994
R. F. Davis, S. Kern, K. Linthicum, S. Roberson, and S. Tanaka Jun. 1994 35 p
(Contract N00014-90-J-1427)
(AD-A281218) Avail: CASI HC A03/MF A01

AlN films with essentially atomically flat surfaces, indicative of two-dimensional growth, have been deposited on on-axis 6H-SiC(0001) surfaces at 1050 C via plasma-assisted gas source MBE. Island features, the coalescence of which caused defects and influenced film quality, were observed on the vicinal surface. SiC/AlN pseudomorphic multilayers with abrupt interfaces and AlN(x)SiC(1-x) solid solutions have been deposited using a similar technique and substrate. The use of on-axis substrates resulted in superior structures. High AlN solid solutions have been achieved; however, they were polycrystalline. Chemical interdiffusion between 6-H SiC wafers and deposited single crystal AlN thick films between 1800 and 1950 C was not observed via parallel electron energy loss microscopy and Auger depth profiles to within 15 A of the interface. Pseudomorphic GaN/AlGaN double heterostructures with abrupt interfaces have also been produced using GSMBE. The purpose is for UV light emitting diodes. A supersonic jet deposition system has been designed and commissioned for the growth of III-V nitride films. DTIC

34 FLUID MECHANICS AND HEAT TRANSFER

Includes boundary layers; hydrodynamics; fluidics; mass transfer; and ablation cooling.

For related information see also *02 Aerodynamics* and *77 Thermodynamics and Statistical Physics.*

N95-11705*# State Univ. of New York, Buffalo, NY. Dept. of Mechanical and Aerospace Engineering.
LES, DNS AND RANS FOR THE ANALYSIS OF HIGH-SPEED TURBULENT REACTING FLOWS Annual Report, 1 Sep. 1993 - 1 Sep. 1994
Peyman Givi, Dale B. Taulbee, Virgil Adumitroaie, George J. Sabini, and Geoffrey S. Shieh 1 Sep. 1994 126 p
(Grant NAG1-1122)
(NASA-CR-196822; NAS 1.26:196822) Avail: CASI HC A07/MF A02

The purpose of this research is to continue our efforts in advancing the state of knowledge in large eddy simulation (LES), direct numerical simulation (DNS), and Reynolds averaged Navier Stokes (RANS) methods for the computational analysis of high-speed reacting turbulent flows. In the second phase of this work, covering the period 1 Sep. 1993 - 1 Sep. 1994, we have focused our efforts on two research problems: (1) developments of 'algebraic' moment closures for statistical descriptions of nonpremixed reacting systems, and (2) assessments of the Dirichlet frequency in presumed scalar probability density function (PDF) methods in stochastic description of turbulent reacting flows. This report provides a complete description of our efforts during this past year as supported by the NASA Langley Research Center under Grant NAG1-1122. Author

N95-11709*# University of Central Florida, Orlando, FL. Dept. of Mechanical and Aerospace Engineering.
LASER DOPPLER VELOCIMETER MEASUREMENTS OF BOUNDARY LAYER VELOCITY AND TURBULENT INTENSITIES IN MACH 2.5 FLOW Final Report
Jesse Sewell and Larry Chew 1994 33 p
(Grant NAG1-1402)
(NASA-CR-196861; NAS 1.26:196861) Avail: CASI HC A03/MF A01

In recent years, the interest in developing a high-speed civil transport has increased. This has led to an increase in research activity on compressible supersonic flows, in particular the boundary layer. The structure of subsonic boundary layers has been extensively documented using conditional sampling techniques which exploit the knowledge of both u and v velocities. Researchers using these techniques have been able to explore some of the complex three-dimensional motions which are responsible for Reynolds stress production and transport in the boundary layer. As interest in turbulent structure has grown to include supersonic flows, a need for simultaneous multicomponent velocity measurements in these flows has developed. The success of conditional analysis in determining the characteristics of coherent motions and structures in the boundary layer relies on accurate, simultaneous measurement of two instantaneous velocity components. Author

N95-11749# Kiev Univ. (USSR). Inst. Teoreticheskoj Fiziki.
RELATIVISTIC THEORY OF SUPERFLUIDITY WITH TWO CONDENSATES
S. J. Vilchinskij and P. Yi. Fomyin 1993 21 p
(DE94-624073; ITF-93-24) Avail: CASI HC A03/MF A01 (US Sales Only)

A phenomenological derivation of the equations of relativistic theory of superfluidity of systems with two types of condensates in a non-dissipative approximation is given. Three-velocity relativistic thermodynamics and hydrodynamics are derived from the condition of consistency energy-momentum conservation laws generalized charge, entropy and equations for superfluid velocities. The questions about tripling of number of hydrodynamical theorems and possible types of vortices in such systems are considered. Equations which describe propagation of first, second and fourth sound in the system are derived, and expressions for their velocities are obtained. DOE

N95-11753# Argonne National Lab., IL.
SLOSHING ANALYSIS OF TANKS CONTAINING MULTIPLE FLUID LAYERS
R. A. Uras and Yu Tang 1994 10 p Presented at the 5th US National Conference on Earthquake Engineering, Chicago, IL, 10-14 Jul. 1994
(Contract W-31-109-eng-38)
(DE94-013333; ANL/RE/CP-80865; CONF-940752-3) Avail: CASI HC A02/MF A01

The effect of liquid density changes in high level radioactive liquid waste storage tanks is studied. The density variations with the liquid depth is modeled by layers of piecewise constant densities. A computational formulation based on the finite element method is presented. The computer code FLUSTR-ANL has been modified for the analysis of the sloshing response under seismic excitation. DOE

N95-11812*# Institute for Computer Applications in Science and Engineering, Hampton, VA.
ON THE INTERACTION OF JET NOISE WITH A NEARBY FLEXIBLE STRUCTURE Final Report
J. L. McGreevy (National Aeronautics and Space Administration. Langley Research Center, Hampton, VA.), A. Bayliss (Northwestern Univ., Evanston, IL.), and L. Maestrello (National Aeronautics and Space Administration. Langley Research Center, Hampton, VA.) Jun. 1994 29 p Submitted for publication
(Contract NAS1-19480; RTOP 505-90-52-01)
(NASA-CR-194934; NAS 1.26:194934; ICASE-94-48) Avail: CASI HC A03/MF A01

The model of the interaction of the noise from a spreading subsonic jet with a panel-stringer assembly is studied numerically in two dimensions. The radiation resulting from this flow/acoustic/structure coupling is computed and analyzed in both the time and frequency domains. The jet is initially excited by a pulse-like source inserted into the flow field. The pulse triggers instabilities associated with the inviscid instability of the jet mean flow shear layer. These instabilities in turn generate sound which provides the primary loading for the panels. The resulting structural vibration and radiation depends strongly on their placement relative to the jet/nozzle configuration. Results are obtained for the panel responses as well as the transmitted and incident pressure. The effect of the panels is to act as a narrow filter, converting the relatively broad band forcing, heavily influenced by jet instabilities, into radiation concentrated in narrow spectral bands. Author

N95-11840# Rocky Research Corp., Boulder City, NV.
HEAT TRANSFER ADDITIVES FOR ADSORPTION COOLING SYSTEM FLUIDS, PHASE 2 Annual Report, Dec. - Nov. 1993
T. Chandler Nov. 1993 55 p
(Contract GRI-5089-260-1908)
(PB94-187135; GRI-94/0052-Phase-2) Avail: CASI HC A04/MF A01

The objectives of the project are the following: to increase the available information on heat and mass transfer additives used in liquid-vapor absorption equipment so that meaningful analysis of additive function is possible; to analyze the experimental results with respect to various postulated heat and mass transfer mechanisms; to develop reasonable alternate hypotheses for mechanisms that are consistent with known data; to dismiss those which exhibit no significant impact; and to note and refine those that have a major influence. NTIS

N95-11859# Weston (Roy F.), Inc., West Chester, PA.
SUPERCRITICAL FLUID (SCF) TECHNOLOGIES: ASSESSMENT OF APPLICABILITY TO INSTALLATION RESTORATION PROCESSES Final Report
Mar. 1994 111 p
(Contract DACA31-91-D-0079)
(AD-A281504; SFIM-AEC-TS-CR-93127) Avail: CASI HC A06/MF A02

USAEC has conducted an evaluation of supercritical fluid (SCF) technologies for their applicability to treatment of explosives, chlorinated hydrocarbons, and metals in soils, water, and/or waste sludge media. Off-specification explosives and propellants that have traditionally been open burned or openly detonated were also examined. Supercritical fluids are substances which have been heated and compressed to above their critical temperatures and pressures and which possess unique transport and mass transfer properties. Supercritical fluid extraction (SFE) uses the solvating properties of supercritical fluids to extract one or more organic components from a mixture into a supercritical solvent (commonly CO2). The concentrated extract stream may then be recycled, reclaimed, or destroyed by other methods. DTIC

N95-11874*# Research Inst. for Advanced Computer Science, Moffett Field, CA.
ANALYSIS AND DESIGN OF NUMERICAL SCHEMES FOR GAS DYNAMICS. 2: ARTIFICIAL DIFFUSION AND DISCRETE SHOCK STRUCTURE
Antony Jameson (Princeton Univ., NJ.) Aug. 1994 32 p Sponsored in part by IBM
(Contracts NAS2-13721; N00014-92-J-1796; AF-AFOSR-0391-91)
(NASA-CR-196476; NAS 1.26:196476; RIACS-TR-94-16) Avail: CASI HC A03/MF A01

The effect of artificial diffusion on discrete shock structures is examined for a family of schemes which includes scalar diffusion, convective upwind and split pressure (CUSP) schemes, and upwind schemes with characteristics splitting. The analysis leads to conditions on the diffusive flux such that stationary discrete shocks can contain a single interior point. The simplest formulation which meets these conditions is a CUSP scheme in which the coefficients of the pressure differences is fully determined by the coefficient of convective diffusion. It is also shown how both the characteristic and CUSP schemes can be modified to preserve constant stagnation enthalpy in steady flow, leading to four variants, the E and H-characteristic schemes, and the E and H-CUSP schemes. Numerical results are presented which confirm the properties of these schemes. Author

N95-11875*# Research Inst. for Advanced Computer Science, Moffett Field, CA.
ANALYSIS AND DESIGN OF NUMERICAL SCHEMES FOR GAS DYNAMICS 1: ARTIFICIAL DIFFUSION, UPWIND BIASING, LIMITERS AND THEIR EFFECT ON ACCURACY AND MULTIGRID CONVERGENCE
Antony Jameson (Princeton Univ., NJ.) Aug. 1994 42 p Sponsored in part by IBM
(Contracts NAS2-13721; N00014-92-J-1796; AF-AFOSR-0391-91)
(NASA-CR-196477; NAS 1.26:196477; RIACS-TR-94-15) Avail: CASI HC A03/MF A01

The theory of non-oscillatory scalar schemes is developed in this

paper in terms of the local extremum diminishing (LED) principle that maxima should not increase and minima should not decrease. This principle can be used for multi-dimensional problems on both structured and unstructured meshes, while it is equivalent to the total variation diminishing (TVD) principle for one-dimensional problems. A new formulation of symmetric limited positive (SLIP) schemes is presented, which can be generalized to produce schemes with arbitrary high order of accuracy in regions where the solution contains no extrema, and which can also be implemented on multi-dimensional unstructured meshes. Systems of equations lead to waves traveling with distinct speeds and possibly in opposite directions. Alternative treatments using characteristic splitting and scalar diffusive fluxes are examined, together with modification of the scalar diffusion through the addition of pressure differences to the momentum equations to produce full upwinding in supersonic flow. This convective upwind and split pressure (CUSP) scheme exhibits very rapid convergence in multigrid calculations of transonic flow, and provides excellent shock resolution at very high Mach numbers. Author

N95-11888*# Toledo Univ., OH.

USER'S MANUAL FOR THE NASA LEWIS ICE ACCRETION/HEAT TRANSFER PREDICTION CODE WITH ELECTROTHERMAL DEICER INPUT Final Report

Konstanty C. Masiulaniec and William B. Wright Washington NASA Jul. 1994 160 p Sponsored by the FAA

(Contract NAS3-25517; NAG3-72; RTOP 505-68-10)

(NASA-CR-4530; E-7680; NAS 1.26:4530; DOT/FAA/CT-TN92/33) Avail: CASI HC A08/MF A02

A version of LEWICE has been developed that incorporates a recently developed electrothermal deicer code, developed at the University of Toledo by William B. Wright. This was accomplished, in essence, by replacing a subroutine in LEWICE, called EBAL, which balanced the energies at the ice surface, with a subroutine called UTICE. UTICE performs this same energy balance, as well as handles all the time-timperature transients below the ice surface, for all of the layers of a composite blade as well as the ice layer itself. This new addition is set up in such a fashion that a user may specify any number of heaters, any heater chordwise length, and any heater gap desired. The heaters may be fired in unison, or they may be cycled with periods independent of each other. The heater intensity may also be varied. In addition, the user may specify any number of layers and thicknesses depthwise into the blade. Thus, the new addition has maximum flexibility in modeling virtually any electrothermal deicer installed into any airfoil. It should be noted that the model simulates both shedding and runback. With the runback capability, it can simulate the anti-icing mode of heater performance, as well as detect icing downstream of the heaters due to runback in unprotected portions of the airfoil. This version of LEWICE can be run in three modes. In mode 1, no conduction heat transfer is modeled (which would be equivalent to the original version of LEWICE). In mode 2, all heat transfer is considered due to conduction but no heaters are firing. In mode 3, conduction heat transfer where the heaters are engaged is modeled, with subsequent ice shedding. When run in the first mode, there is virtually identical agreement with the original version of LEWICE in the prediction of accreted ice shapes. The code may be run in the second mode to determine the effects of conduction on the ice accretion process. Author

N95-11929*# Institute for Computer Applications in Science and Engineering, Hampton, VA.

SCALE DISPARITY AND SPECTRAL TRANSFER IN ANISOTROPIC NUMERICAL TURBULENCE Final Report

Ye Zhou, P. K. Yeung, and James G. Brasseur Aug. 1994 36 p Submitted for publication

(Contracts NAS1-19480; RTOP 505-90-52-01; AF-AFOSR-0113-90; N00014-92-J-1417; DAAL03-92-G-0117; NSF CTS-93-07973)

(NASA-CR-194956; NAS 1.26:194956; ICASE-94-64) Avail: CASI HC A03/MF A01

To study the effect of cancellations within long-range interactions on local isotropy at the small scales, we calculate explicitly the degree of cancellation in distant interactions in the simulations of Yeung & Brasseur and Yeung, Brasseur & Wang using the single scale disparity parameter 's' developed by Zhou. In the simulations, initially isotropic simulated turbulence was subjected to coherent anisotropic forcing at the large scales and the smallest scales were found to become anisotropic as a consequence of direct large-small scale couplings. We find that the marginally distant interactions in the simulation do not cancel out under summation and that the development of small-scale anisotropy is indeed a direct consequence of the distant triadic group, as argued by Yeung, et. al. A reduction of anisotropy at later times occurs as a result of the isotropizing influences of more local energy-cascading triadic interactions. Nevertheless, the local-to-nonlocal triadic group persists as an isotropizing influence at later times. We find that, whereas long-range interactions, in general, contribute little to net energy transfer into or out of a high wavenumber shell k, the anisotropic transfer of component energy within the shell increases with increasing scale separations. These results are consistent with results by Zhou, and Brasseur & Wei, and suggest that the anisotropizing influences of long range interactions should persist to higher Reynolds numbers. The residual effect of the forced distant group in this low-Reynolds number simulation is found to be forward cascading, on average. Author (revised)

N95-11930*# Institute for Computer Applications in Science and Engineering, Hampton, VA.

MODELING JETS IN CROSS FLOW Final Report

A. O. Demuren (Old Dominion Univ., Norfolk, VA.) Aug. 1994 37 p Submitted for publication

(Contract NAS1-19480; RTOP 505-90-52-01)

(NASA-CR-194965; NAS 1.26:194965; ICASE-94-71) Avail: CASI HC A03/MF A01

Various approaches to the modeling of jets in cross flow are reviewed. These are grouped into four classes, namely: empirical models, integral models, perturbation models, and numerical models. Empirical models depend largely on the correlation of experimental data and are mostly useful for first-order estimates of global properties such as jet trajectory and velocity and temperature decay rates. Integral models are based on some ordinary-differential form of the conservation laws, but require substantial empirical calibration. They allow more details of the flow field to be obtained; simpler versions have to assume similarity of velocity and temperature profiles, but more sophisticated ones can actually calculate these profiles. Perturbation models require little empirical input, but the need for small parameters to ensure convergent expansions limits their application to either the near-field or the far-field. Therefore, they are mostly useful for the study of flow physics. Numerical models are based on conservation laws in partial-differential form. They require little empirical input and have the widest range of applicability. They also require the most computational resources. Although many qualitative and quantitative features of jets in cross flow have been predicted with numerical models, many issues affecting accuracy such as grid resolution and turbulence model are not completely resolved. Author

N95-11935*# National Aeronautics and Space Administration. Lewis Research Center, Cleveland, OH.

METHODS OF ENSURING REALIZABILITY FOR NON-REALIZABLE SECOND ORDER CLOSURES

Tsan-Hsing Shih and Aamir Shabbir Aug. 1994 15 p

(Contract NCC3-233; RTOP 505-90-5K)

(NASA-TM-106681; E-9028; ICOMP-94-14; NAS 1.15:106681; CMOTT-94-7) Avail: CASI HC A03/MF A01

Several methods of ensuring realizability for nonrealizable second order closure models are discussed. The well known isotropization of production (IP) model and the Launder, Reece, and Rodi (LRR) model are particularly studied for their wide application in engineering calculations. Ensuring realizability for these models will extend their applicability to more critical flow situations and reduce the numerical difficulties caused by the nonrealizability of the original models. Different methods of ensuring realizability are tested for several extreme flow situations. The suggested realizability modifications not only make the models realizable but also maintain the performance of the original models for realistic flows. The methods discussed in this paper can be straightforwardly applied to other nonrealizable models. Author

N95-11936*# National Aeronautics and Space Administration. Langley Research Center, Hampton, VA.

PREDICTING RADIATIVE HEAT TRANSFER IN THERMOCHEMICAL NONEQUILIBRIUM FLOW FIELDS. THEORY AND USER'S MANUAL FOR THE LORAN CODE

Lin Hartung Chambers Sep. 1994 73 p

(RTOP 506-40-91-01)
(NASA-TM-4564; L-17372; NAS 1.15:4564) Avail: CASI HC A04/MF A01

The theory for radiation emission, absorption, and transfer in a thermochemical nonequilibrium flow is presented. The expressions developed reduce correctly to the limit at equilibrium. To implement the theory in a practical computer code, some approximations are used, particularly the smearing of molecular radiation. Details of these approximations are presented and helpful information is included concerning the use of the computer code. This user's manual should benefit both occasional users of the Langley Optimized Radiative Nonequilibrium (LORAN) code and those who wish to use it to experiment with improved models or properties. Author

N95-11939# Cambridge Univ., Cambridge (England). Dept. of Engineering.
CONCENTRATION FLUCTUATION MODELS: A COMPARATIVE STUDY
T. S. Panwar, I. R. Cowan, and R. E. Britter May 1994 42 p Sponsored by British Council and IIT Delhi
(ISSN 0309-7293)
(CUED/A-AERO/TR-24) Avail: CASI HC A03/MF A01

Four concentration fluctuation models are considered: Gifford's (1959) meandering plume model; Chatwin & Sullivan's (1990) model; Wilson's (Bara et al., 1992) model; and the UKADMS (Carruthers et al., 1992) model. These are described in brief, and comments made upon their ease of application to practical plume dispersion problems (e.g. the number of problem-specific empirical model parameters required). The stratified turbulent boundary layer (DNS) simulations of Cowan (1994) are described, and a concentration data-set extracted for use in evaluating the performance of the four models. Interest is mainly in the ability of the models to accurately predict the concentration fluctuation levels from the mean concentration data. However, the concentration probability density function is also studied briefly. Author

N95-11953*# National Aeronautics and Space Administration. Lewis Research Center, Cleveland, OH.
A NEW REYNOLDS STRESS ALGEBRAIC EQUATION MODEL
Tsan-Hsing Shih, Jiang Zhu, and John L. Lumley Aug. 1994 30 p
(Contract NCC3-233; RTOP 505-90-5K)
(NASA-TM-106644; ICOMP-94-15; E-8949; NAS 1.15:106644; CMOTT-94-8) Avail: CASI HC A03/MF A01

A general turbulent constitutive relation is directly applied to propose a new Reynolds stress algebraic equation model. In the development of this model, the constraints based on rapid distortion theory and realizability (i.e. the positivity of the normal Reynolds stresses and the Schwarz' inequality between turbulent velocity correlations) are imposed. Model coefficients are calibrated using well-studied basic flows such as homogeneous shear flow and the surface flow in the inertial sublayer. The performance of this model is then tested in complex turbulent flows including the separated flow over a backward-facing step and the flow in a confined jet. The calculation results are encouraging and point to the success of the present model in modeling turbulent flows with complex geometries.
Author (revised)

N95-11992*# Pennsylvania State Univ., University Park, PA. Dept. of Mechanical Engineering.
HYPERSONIC TURBULENT BOUNDARY-LAYER AND FREE SHEAR DATABASE (Diskette Supplement)
Gary S. Settles and Lori J. Dodson Apr. 1993 113 p Diskette supplement: two 3.5-inch DSHD diskettes using MS-DOS high density format
(Grant NAG2-565; RTOP 763-21-31)
(NASA-CR-177610; A-93065; NAS 1.26:177610;
NONP-NASA-Suppl-DK-94-5100) Avail: CASI SET A09 (HC,DK)

A critical assessment and compilation of data are presented on attached hypersonic turbulent boundary layers in pressure gradients and compressible turbulent mixing layers. Extensive searches were conducted to identify candidate experiments, which were subjected to a rigorous set of acceptance criteria. Accepted datasets are both tabulated and provided in machine-readable form. The purpose of this database effort is to make existing high quality data available in detailed form for the turbulence-modeling and computational fluid dynamics communities. While significant recent data were found on the subject of compressible turbulent mixing, the available boundary-layer/pressure-gradient experiments are all older ones of which no acceptable data were found at hypersonic Mach numbers. Author

N95-11999*# Alabama Univ., Huntsville, AL. Dept. of Mechanical and Aerospace Engineering.
[FDNS CODE TO PREDICT WALL HEAT FLUXES OR WALL TEMPERATURES IN ROCKET NOZZLES] Final Report
Gerald R. Karr 4 Nov. 1993 48 p
(Grant NAG8-212)
(NASA-CR-196925; NAS 1.26:196925) Avail: CASI HC A03/MF A01

This report summarizes the findings on the NASA contract NAG8-212, Task No. 3. The overall project consists of three tasks, all of which have been successfully completed. In addition, some supporting supplemental work, not required by the contract, has been performed and is documented herein. Task 1 involved the modification of the wall functions in the code FDNS to use a Reynolds Analogy-based method. Task 2 involved the verification of the code against experimentally available data. The data chosen for comparison was from an experiment involving the injection of helium from a wall jet. Results obtained in completing this task also show the sensitivity of the FDNS code to unknown conditions at the injection slot. Task 3 required computation of the flow of hot exhaust gases through the P&W 40K subscale nozzle. Computations were performed both with and without film coolant injection. The FDNS program tends to overpredict heat fluxes, but, with suitable modeling of backside cooling, may give reasonable wall temperature predictions. For film cooling in the P&W 40K calorimeter subscale nozzle, the average wall temperature is reduced from 1750 R to about 1050 R by the film cooling. The average wall heat flux is reduced by a factor of three. Author (revised)

N95-12105*# High Technology Corp., Hampton, VA.
EFFECT OF NONZERO SURFACE ADMITTANCE ON RECEPTIVITY AND STABILITY OF COMPRESSIBLE BOUNDARY LAYER
Meelan Choudhari Hampton, VA NASA Aug. 1994 24 p
(Contract NAS1-20059; RTOP 505-59-50-01)
(NASA-CR-4621; NAS 1.26:4621) Avail: CASI HC A03/MF A01

The effect of small-amplitude short-scale variations in surface admittance on the acoustic receptivity and stability of two-dimensional compressible boundary layers is examined. In the linearized limit, the two problems are shown to be related both physically and mathematically. This connection between the two problems is used, in conjunction with some previously reported receptivity results, to infer the modification of stability properties due to surface permeability. Numerical calculations are carried out for a self-similar flat-plate boundary layer at subsonic and low supersonic speeds. Variations in mean suction velocity at the perforated admittance surface can also induce receptivity to an acoustic wave. For a subsonic boundary layer, the dependence of admittance-induced receptivity on the acoustic-wave orientation is significantly different from that of the receptivity produced via mean suction variation. The admittance-induced receptivity is generally independent of the angle of acoustic incidence, except in a relatively narrow range of upstream-traveling waves for which the receptivity becomes weaker. However, this range of angles is precisely that for which the suction-induced receptivity tends to be large. At supersonic Mach numbers, the admittance-induced receptivity to slow acoustic models is relatively weaker than that in the case of the fast acoustic modes. We also find that purely real values for the surface admittance tend to have a destabilizing effect on the evolution of an instability wave over a slightly permeable surface. The limits on the validity of the linearized approximation are also assessed in one specific case. Author

N95-12228*# Tennessee Univ. Space Inst., Tullahoma, TN. Center for Space Transportation and Applied Research.
A WALL INTERFERENCE ASSESSMENT AND CORRECTION SYSTEM Final Report, Jun. 1991 - Jun. 1994
C. F. Lo Jun. 1994 10 p
(Grant NAG2-733)
(NASA-CR-196940; NAS 1.26:196940) Avail: CASI HC A02/MF A01

A wall signature method has been selected to be adapted for the Ames 12-ft Wind Tunnel WIAC system. This uses limited measurements of the static pressure at the wall, in conjunction with the solid wall boundary condition, to determine the strength and distribution of singularities

representing the test article. The singularities are used to estimate wall interference at the model location. The development and implementation of a working prototype will be completed, delivered and documented with a software manual. Author (revised)

N95-12380*# National Aeronautics and Space Administration. Lewis Research Center, Cleveland, OH.

BOUNDARY CONDITIONS FOR UNSTEADY COMPRESSIBLE FLOWS

S. I. Hariharan and D. K. Johnson Sep. 1994 28 p

(Contracts NCC3-233; NCC3-104; NSF DMS-89-21189; RTOP 505-90-5K)

(NASA-TM-106737; ICOMP-94-22; E-9138; NAS 1.15:106737) Avail: CASI HC A03/MF A01

This paper explores solutions to the spherically symmetric Euler equations. Motivated by the work of Hagstrom and Hariharan and Geer and Pope, we modeled the effect of a pulsating sphere in a compressible medium. The literature available on this suggests that an accurate numerical solution requires artificial boundary conditions which simulate the propagation of nonlinear waves in open domains. Until recently, the boundary conditions available were in general linear and based on nonreflection. Exceptions to this are the nonlinear nonreflective conditions of Thompson, and the nonlinear reflective conditions of Hagstrom and Hariharan. The former are based on the rate of change of the incoming characteristics; the latter rely on asymptotic analysis and the method of characteristics and account for the coupling of incoming and outgoing characteristics. Furthermore, Hagstrom and Hariharan have shown that, in a test situation in which the flow would reach a steady state over a long time, Thompson's method could lead to an incorrect steady state. The current study considers periodic flows and includes all possible types and techniques of boundary conditions. The technique recommended by Hagstrom and Hariharan proved superior to all others considered and matched the results of asymptotic methods that are valid for low subsonic Mach numbers. Author

N95-12387*# Auburn Univ., AL. Dept. of Aerospace Engineering.

DEVELOPMENT OF NONINTRUSIVE, SCATTER-INDEPENDENT TECHNIQUES FOR MEASUREMENT OF LIQUID DENSITY INSIDE DENSE SPRAYS Interim Report

Roy Hartfield 22 Sep. 1994 7 p

(Grant NAG8-1017)

(NASA-CR-196413; NAS 1.26:196413) Avail: CASI HC A02/MF A01

A nonintrusive optical technique for measuring the liquid density in sprays used to simulate LOX injector flows is under development. This manuscript is a report on work toward that development which is currently in progress. The technique is a scatter-independent, absorption-based approach which depends on the numerical inversion of a collection of absorption profiles. For the case in which visible radiation passes through liquid-gas interfaces so numerous in sprays, substantial reductions and alterations in the signal result from scattering even in the absence of absorption. To avoid these problems, X-Rays will be used as the absorbed radiation. The experimental process is simulated by integrating the absorption spectrum for a known distribution, adding instrument noise to this 'measurement', creating a projection from the 'measurement', filtering the projection, inverting the projection, and comparing the results with the original prescribed distribution. Author

N95-12409# Naval Surface Warfare Center, Silver Spring, MD.

NUMERICAL COMPUTATIONS WITH ABAQUS/EXPLICIT, DYNA3D, AND DYSMAS/L Final Report

Minos Moussouros 1 Apr. 1994 66 p

(AD-A282249; NSWCDD/TR-93/272) Avail: CASI HC A04/MF A01

The purpose of this study is to report two types of numerical experiments. First, a structural problem was modeled using the ABAQUS/Explicit, DYNA3D, and DYSMAS/L computer programs. The problem consisted of the classic problem of Witmer; i.e., an explosive detasheet was tested on a cylindrical panel and the permanent set deflection was measured and compared with the three numerical predictions. Secondly, the problem of a water column impacting on a series of flat or curved, rigid or flexible panels was modeled using the DYNA3D computer program. Due to the lack of experimental data, the calculations were compared to limited Eulerian computer program (CTH) results. DTIC

N95-12422 Colorado Univ., Boulder, CO. Dept. of Aerospace Engineering Sciences.

NUMERICAL SIMULATION OF PARTICLE-WAVE INTERACTION ON BOUNDARY LAYERS Final Report

Sedat Biringen and E. M. Saiki 19 Jul. 1994 43 p Limited Reproducibility: More than 20% of this document may be affected by microfiche quality

(Contract N00014-91-J-1086)

(AD-A282184) Avail: Issuing Activity (Defense Technical Information Center (DTIC))

This research program involves a computational study of the effects of disturbances generated from a moving particle on boundary layer transition. The practical importance of this problem stems from the fact that as an underwater vehicle moves through a particulate environment, particles enter the boundary layer and produce local disturbances. These disturbances may act as a bypass mechanism to transition and turbulence by interacting with boundary layer instabilities. The objective of this research is to study the basic mechanisms of the particle interaction and its effect on transition in the boundary layer. For this purpose, a direct numerical simulation is undertaken and the spherical particle is represented by a forcing function in the Navier Stokes equations. Results reveal good agreement with experimental studies. The report is presented in two parts. The first part concerns a general overview of the work accomplished and the second part summarizes our recent efforts on the modeling of steady/unsteady flow over a cylinder. Author (DTIC)

N95-12619*# Lockheed Engineering and Sciences Co., Hampton, VA. Langley Program Office.

AN IMPLEMENTATION OF A CHEMICAL AND THERMAL NONEQUILIBRIUM FLOW SOLVER ON UNSTRUCTURED MESHES AND APPLICATION TO BLUNT BODIES

Ramadas K. Prabhu NASA Aug. 1994 52 p

(Contract NAS1-19000; RTOP 232-01-04-06)

(NASA-CR-194967; NAS 1.26:194967) Avail: CASI HC A04/MF A01

This paper presents a nonequilibrium flow solver, implementation of the algorithm on unstructured meshes, and application to hypersonic flow past blunt bodies. Air is modeled as a mixture of five chemical species, namely O2, N2, O, NO, and N, having two temperatures namely translational and vibrational. The solution algorithm is a cell centered, point implicit upwind scheme that employs Roe's flux difference splitting technique. Implementation of this algorithm on unstructured meshes is described. The computer code is applied to solve Mach 15 flow with and without a Type IV shock interference on a cylindrical body of 2.5mm radius representing a cowl lip. Adaptively generated meshes are employed, and the meshes are refined several times until the solution exhibits detailed flow features and surface pressure and heat flux distributions. Effects of a catalytic wall on surface heat flux distribution are studied. For the Mach 15 Type IV shock interference flow, present results showed a peak heat flux of 544 MW/m2 for a fully catalytic wall and 431 MW/m(exp 2) for a noncatalytic wall. Some of the results are compared with available computational data.

Author

N95-12859*# Joint Inst. for Advancement of Flight Sciences, Hampton, VA.

COMPUTATION OF TURBULENT BOUNDARY LAYERS EMPLOYING THE DEFECT WALL-FUNCTION METHOD M.S. Thesis

Douglas L. Brown Hampton, VA NASA Sep. 1994 129 p

(Contract NCC1-24; RTOP 505-70-62-01)

(NASA-CR-4629; NAS 1.26:4629) Avail: CASI HC A07/MF A02

In order to decrease overall computational time requirements of spatially-marching parabolized Navier-Stokes finite-difference computer code when applied to turbulent fluid flow, a wall-function methodology, originally proposed by R. Barnwell, was implemented. This numerical effort increases computational speed and calculates reasonably accurate wall shear stress spatial distributions and boundary-layer profiles. Since the wall shear stress is analytically determined from the wall-function model, the computational grid near the wall is not required to spatially resolve the laminar-viscous sublayer. Consequently, a substantially increased computational integration step size is achieved resulting in a considerable decrease in net computational time. This wall-function technique is demonstrated for adiabatic flat plate test cases from Mach 2 to Mach 8. These test cases are analytically verified employing: (1) Eckert reference method solutions, (2) experimental turbulent boundary-layer data of Mabey, and (3) finite-difference

computational code solutions with fully resolved laminar-viscous sublayers. Additionally, results have been obtained for two pressure-gradient cases: (1) an adiabatic expansion corner and (2) an adiabatic compression corner. Author

N95-13075# Pacific Northwest Lab., Richland, WA.
SCALING FLUID CONTENT-PRESSURE RELATIONS OF DIFFERENT FLUID SYSTEMS IN POROUS MEDIA
R. J. Lenhard Apr. 1994 18 p Presented at the 1994 Hydrology Days, Fort Collins, CO, 5-9 Apr. 1994
(Contract DE-AC06-76RL-01830)
(DE94-013349; PNL-SA-23878; CONF-9404180-1) Avail: CASI HC A03/MF A01

Two-fluid-phase relations among fluid saturations (S) and pressures (P) have historically been used to predict S-P relations for three-fluid-phase systems consisting of a gas, nonaqueous phase liquid (NAPL), and water, because measurements of three-phase S-P relations are complex. Two-phase S-P relations of air-NAPL systems are generally used to predict the behavior between total-liquid saturations of three-phase systems and air-NAPL capillary pressures. Two-phase S-P relations of NAPL-water systems are generally used to predict the behavior between water saturations of three-phase systems and NAPL-water capillary pressures. Because S-P measurements are very time-consuming, investigators have attempted to scale S-P relations so that fewer measurements would be required. A S-P scaling technique is discussed in this paper, and methods to predict the scaling factors are evaluated. DOE

N95-13156# California Univ., Berkeley. Lawrence Berkeley Lab, CA.
AN INVESTIGATION OF THE VORTEX METHOD Ph.D. Thesis
D. W. Pryor, Jr. May 1994 160 p
(Contract DE-AC03-76SF-00098)
(DE94-014931; LBL-35707) Avail: CASI HC A08/MF A02

The vortex method is a numerical scheme for solving the vorticity transport equation. Chorin introduced modern vortex methods. The vortex method is a Lagrangian, grid free method which has less intrinsic diffusion than many grid schemes. It is adaptive in the sense that elements are needed only where the vorticity is non-zero. Our description of vortex methods begins with the point vortex method of Rosenhead for two dimensional inviscid flow, and builds upon it to eventually cover the case of three dimensional slightly viscous flow with boundaries. This section gives an introduction to the fundamentals of the vortex method. This is done in order to give a basic impression of the previous work and its line of development, as well as develop some notation and concepts which will be used later. The purpose here is not to give a full review of vortex methods or the contributions made by all the researchers in the field. Please refer to the excellent review papers in Sethian and Gustafson, chapters 1 Sethian, 2 Hald, 3 Sethian, 8 Chorin provide a solid introduction to vortex methods, including convergence theory, application in two dimensions and connection to statistical mechanics and polymers. Much of the information in this review is taken from those chapters, Chorin and Marsden and Batchelor, the chapters are also useful for their extensive bibliographies. DOE

N95-13201*# Old Dominion Univ., Norfolk, VA. Dept. of Mechanical Engineering.
METHODOLOGY FOR SENSITIVITY ANALYSIS, APPROXIMATE ANALYSIS, AND DESIGN OPTIMIZATION IN CFD FOR MULTIDISCIPLINARY APPLICATIONS Progress Report, 1 Feb. 1993 - 31 Aug. 1994
Arthur C. Taylor, III and Gene W. Hou Sep. 1994 53 p Presented at the 5th AIAA/USAF/NASA/OAI Multidisciplinary Design and Optimization Conference, Panama City, FL, Sep. 1994 Submitted for publication
(Grant NAG1-1265)
(NASA-CR-196981; NAS 1.26:196981; AIAA Paper 94-4262) Avail: CASI HC A04/MF A01

The straightforward automatic-differentiation and the hand-differentiated incremental iterative methods are interwoven to produce a hybrid scheme that captures some of the strengths of each strategy. With this compromise, discrete aerodynamic sensitivity derivatives are calculated with the efficient incremental iterative solution algorithm of the original flow code. Moreover, the principal advantage of automatic differentiation is retained (i.e., all complicated source code for the derivative calculations is constructed quickly with accuracy). The basic equations for second-order sensitivity derivatives are presented; four methods are compared. Each scheme requires that large systems are solved first for the first-order derivatives and, in all but one method, for the first-order adjoint variables. Of these latter three schemes, two require no solutions of large systems thereafter. For the other two for which additional systems are solved, the equations and solution procedures are analogous to those for the first order derivatives. From a practical viewpoint, implementation of the second-order methods is feasible only with software tools such as automatic differentiation, because of the extreme complexity and large number of terms. First- and second-order sensitivities are calculated accurately for two airfoil problems, including a turbulent flow example; both geometric-shape and flow-condition design variables are considered. Several methods are tested; results are compared on the basis of accuracy, computational time, and computer memory. For first-order derivatives, the hybrid incremental iterative scheme obtained with automatic differentiation is competitive with the best hand-differentiated method; for six independent variables, it is at least two to four times faster than central finite differences and requires only 60 percent more memory than the original code; the performance is expected to improve further in the future. Author

N95-13233*# Ball Aerospace Systems Div., Boulder, CO.
FEASIBILITY STUDY FOR A CRYOGENIC ON-ORBIT LIQUID DEPOT-STORAGE, ACQUISITION AND TRANSFER (COLD-SAT) SATELLITE Final Report, Feb. 1988 - Mar. 1990
S. C. Rybak, G. S. Willen, W. H. Follett, G. J. Hanna, E. C. Cady, E. DiStefano, and J. S. Meserole Aug. 1990 292 p
(Contract NAS3-25054)
(NASA-CR-185248; NAS 1.26:185248) Avail: CASI HC A13/MF A03

This feasibility study presents the conceptual design of a spacecraft for performing a series of cryogenic fluid management flight experiments. This spacecraft, the Cryogenic On-Orbit Liquid Depot-Storage, Acquisition, and Transfer (COLD-SAT) satellite, will use liquid hydrogen as the test fluid, be launched on a Delta expendable launch vehicle, and conduct a series of experiments over a two to three month period. These experiments will investigate the physics of subcritical cryogens in the low gravity space environment to characterize their behavior and to correlate the data with analytical and numerical models of in-space cryogenic fluid management systems. Primary technologies addressed by COLD-SAT are: (1) pressure control; (2) chilldown; (3) no-vent fill; (4) liquid acquisition device fill; (5) pressurization; (6) low-g fill and drain; (7) liquid acquisition device expulsion; (8) line chilldown; (9) thermodynamic state control; and (10) fluid dumping. Author

N95-13234*# Ball Corp., Boulder, CO.
FEASIBILITY STUDY FOR THE CRYOGENIC ORBITAL NITROGEN EXPERIMENT (CONE) Final Report, Feb. 1990 - Jun. 1991
R. S. Bell, M. A. Crouch, G. J. Hanna, E. C. Cady, and J. S. Meserole Jul. 1991 212 p
(Contract NAS3-25054; RTOP 593-21-21)
(NASA-CR-187231; NAS 1.26:187231) Avail: CASI HC A10/MF A03

An improved understanding of low gravity subcritical cryogenic fluid behavior is critical for the continued development of space based systems. Although early experimental programs provided some fundamental understanding of zero gravity cryogenic fluid behavior, more extensive flight data are required to design space based cryogenic liquid storage and transfer systems with confidence. As NASA's mission concepts evolve, the demand for optimized in-space cryogenic systems is increasing. Cryogenic Orbital Nitrogen Experiment (CONE) is an attached shuttle payload experiment designed to address major technological issues associated with on-orbit storage and supply of cryogenic liquids. During its 7 day mission, CONE will conduct experiments and technology demonstrations in active and passive pressure control, stratification and mixing, liquid delivery and expulsion efficiency, and pressurant bottle recharge. These experiments, conducted with liquid nitrogen as the test fluid, will substantially extend the existing low gravity fluid data base and will provide future system designers with vital performance data from an orbital environment. Author

N95-13249 Technische Univ., Delft (Netherlands). Ship Hydromechanics Lab.
NUMERICAL TIME DEPENDENT SHEET CAVITATION SIMULATIONS USING A HIGHER ORDER PANEL METHOD Ph.D. Thesis

H. J. deKoningGans 15 Mar. 1994 252 p
(PB94-204435; ISBN-90-6275-965-3) Copyright Avail: Issuing Activity (National Technical Information Service (NTIS))

This thesis deals with sheet cavitation. The investigation is aimed at profile design with respect to cavitation control. At present it is possible to predict the shape of cavities on an arbitrary two-dimensional profile in stationary flows. To compute the flow around an arbitrary profile, a higher order three-dimensional panel method program has been developed. The main algorithm used in this program is based on a special case of Green's theorem, called 'de Morino formulation'. This computer program (flow program) can calculate the potential on the body and the velocities at the surface of the body or in the flow field. A theoretical method is developed for time simulation of unsteady sheet cavitation. Numerical simulations of the flow around profiles and of cavitation have been carried out. The numerical results of the panel methods have been compared with other calculations of the two-dimensional flow around profiles and of three-dimensional flow around a sphere and a wing. Simulations of the growth of sheet cavitation on a foil have also been carried out. The conclusion is that higher order panel methods are more accurate than the zero order methods. Further refinement of the Kutta condition is required, however. NTIS

N95-13550*# National Aeronautics and Space Administration. Lewis Research Center, Cleveland, OH.
NUMERICAL SIMULATIONS OF DROP COLLISIONS
M. R. H. Nobari (Michigan Univ., Ann Arbor, MI.) and G. Tryggvason Oct. 1994 12 p Presented at the 32nd Aerospace Sciences Meeting and Exhibit, Reno, NV, 10-13 Jan. 1994; sponsored by AIAA
(Contract NCC3-233; RTOP 505-90-5K)
(NASA-TM-106751; ICOMP-94-23; E-9167; NAS 1.15:106751; AIAA Paper 94-0835) Avail: CASI HC A03/MF A01

Three-dimensional simulations of the off-axis collisions of two drops are presented. The full Navier-Stokes equations are solved by a Front-Tracking/Finite-Difference method that allows a fully deformable fluid interface and the inclusion of surface tension. The drops are accelerated towards each other by a body force that is turned off before the drops collide. Depending on whether the interface between the drops is ruptured or not, the drops either bounce or coalesce. For drops that coalesce, the impact parameter, which measures how far the drops are off the symmetry line, determines the eventual outcome of the collision. For low impact parameters, the drops coalesce permanently, but for higher impact parameters, a grazing collision, where the drops coalesce and then stretch apart again is observed. The results are in agreement with experimental observations. Author

N95-11957*# National Aeronautics and Space Administration. Ames Research Center, Moffett Field, CA.
THE DEVELOPMENT AND APPLICATION OF THE SELF-ADAPTIVE GRID CODE, SAGE
Carol B. Davies *In its* Technical Paper Contest for Women 1992. Space Challenges: Earth and Beyond 1993 p 5-20 (For primary document see N95-11955 02-99)
Avail: CASI HC A03/MF A03

N95-11971*# Eloret Corp., Palo Alto, CA.
INTERFEROGRAMS, SCHLIEREN, AND SHADOWGRAPHS CONSTRUCTED FROM REAL- AND IDEAL-GAS, TWO- AND THREE-DIMENSIONAL COMPUTED FLOWFIELDS
Leslie A. Yates *In* NASA. Ames Research Center, Technical Paper Contest for Women 1992. Space Challenges: Earth and Beyond 1993 p 207-218 See also N93-21356 (For primary document see N95-11955 02-99)
(Contract NCC2-583)
Avail: CASI HC A03/MF A03

35 INSTRUMENTATION AND PHOTOGRAPHY

Includes remote sensors; measuring instruments and gages; detectors; cameras and photographic supplies; and holography.

For aerial photography see *43 Earth Resources and Remote Sensing*. For related information see also *06 Aircraft Instrumentation*, and *19 Spacecraft Instrumentation*.

N95-11780# Brookhaven National Lab., Upton, NY.
FABRICATION OF LARGE AREA SI CYLINDRICAL DRIFT DETECTORS
Wei Chen, H. W. Kraner, Zheng Li, P. Rehak, and F. Hess Apr. 1994 8 p Presented at the 1993 IEEE Nuclear Science Symposium and Medical Imaging Conference, San Francisco, CA, 2-5 Nov. 1993 Revised
(Contract DE-AC02-76CH-00016)
(DE94-013534; BNL-49016-Rev; CONF-931107-1) Avail: CASI HC A02/MF A01

The processing of an advanced silicon detector, a large area cylindrical drift detector (CDD), was carried out in the BNL Instrumentation Division Fabrication Facility. The double-sided planar process technique was developed for the fabrication of the CDD. Important improvements of the double-sided planar process in this fabrication include the introduction of an Al implantation protection mask and implantation of boron through an 1000 angstrom oxide layer in the step of opening the p-window. Another important aspect of the design of the CDD is the structure called 'river,' which allows the current generated on the Si-SiO2 interface to 'flow' into the guard anode, and thus minimize the leakage current at the signal anode. The test result showed that for the best detector most of the signal anodes have leakage currents of about 0.3 nA/cm(exp 2). DOE

N95-11896*# MCAT Inst., San Jose, CA.
A HIGH-PERFORMANCE CONSTANT-TEMPERATURE HOT-WIRE ANEMOMETER
Jonathan H. Watmuff Moffett Field, CA NASA Aug. 1994 86 p
(Contract NCC2-698)
(NASA-CR-177645; A-94126; NAS 1.26:177645) Avail: CASI HC A05/MF A01

A high-performance constant-temperature hot-wire anemometer has been designed based on a system theory analysis that can be extended to arbitrary order. A motivating factor behind the design was to achieve the highest possible frequency response while ensuring overall system stability. Based on these considerations, the design of the circuit and the selection of components is discussed in depth. Basic operating instructions are included in an operator's guide. The analysis is used to identify operating modes, observed in all anemometers, that are misleading in the sense that the operator can be deceived by interpreting an erroneous frequency response. Unlike other anemometers, this instrument provides front panel access to all the circuit parameters which affect system stability and frequency response. Instructions are given on how to identify and avoid these rather subtle and undesirable operating modes by appropriate adjustment of the controls. Details, such as fabrication drawings and a parts list, are provided to enable others to construct the instrument. Author (revised)

N95-11996*# Pratt and Whitney Aircraft, West Palm Beach, FL.
HIGH TEMPERATURE STRAIN GAGE TECHNOLOGY FOR GAS TURBINE ENGINES Final Report
Edward J. Fichtel and Amos D. McDaniel Aug. 1994 26 p
(Contract NAS3-25952)
(NASA-CR-191177; NAS 1.26:191177) Avail: CASI HC A03/MF A01

This report summarizes the results of a six month study that addressed specific issues to transfer the Pd-13Cr static strain sensor to a gas turbine engine environment. The application issues that were addressed include: (1) evaluation of a miniature, variable potentiometer for use as the ballast resistor, in conjunction with a conventional strain gage signal conditioning unit; (2) evaluation of a metal sheathed, platinum conductor leadwire assembly for use with the three-wire sensor; and (3) subjecting the sensor to dynamic strain cyclic testing to determine fatigue characteristics. Results indicate a useful static strain gage system at all temperature levels up to 1350 F. The fatigue characteristics also appear to be very promising, indicating a potential use in dynamic strain measurement applications. The procedure, set-up, and data for all tests are presented in this report. This

report also discusses the specific strain gage installation technique for the Pd-13Cr gage because of its potential impact on the quality of the output data. Author

N95-12111# Polish Academy of Sciences, Warsaw (Poland). Inst. of Physical Acoustics.
A LABORATORY VACUUM APPARATUS FOR MAGNETRON SPUTTERING OF THIN Z ZnO PIEZOELECTRIC FILMS, MAGNETRON SPUTTERING [PROZNIOWE STANOWISKO LABORATORYJNE DO ROZPYLANIA MAGNETRONOWEGO CIENKICH WARSTW PIEZOELEKTRYCZNYCH Z ZNO. ROZPYLANIE MAGNETRONOWE]
Wojciech Ciecwierz 1992 20 p
(ISSN 0208-5658)
Avail: CASI HC A03/MF A01

This article discusses methods for producing thin metallic and non-conductive films with a special emphasis on magnetron sputtering. The author describes the design of prospective and completed planar magnetron guns at the Institute of Physical Acoustics of the Institute of Basic Problems of Technology of the Polish Academy of Sciences and the electrical characteristics of these guns in depositing metallic films, and their technical characteristics. Author

N95-12748*# National Aeronautics and Space Administration. Lewis Research Center, Cleveland, OH.
DEFOCUS MEASUREMENT USING A LIQUID CRYSTAL POINT DIFFRACTION INTERFEROMETER
Carolyn R. Mercer and Katherine Creath Aug. 1994 7 p Presented at the Optical Fabrication and Testing Workshop, Rochester, NY, 6-9 Jun. 1994; sponsored by the Optical Society of America
(RTOP 505-62-50)
(NASA-TM-106687; E-9043; NAS 1.15:106687) Avail: CASI HC A02/MF A01

A liquid crystal PDI is demonstrated by measuring the defocus change between two positions of the interferometer. Errors caused by average intensity variations are discussed. Author

N95-12869# Lawrence Livermore National Lab., Livermore, CA.
STUDY OF MAGNETIC RECORDING MEDIA ON GLASS SUBSTRATES
S. Duan (Seagate Magnetics, Fremont, CA.), Bing Zhang (Seagate Magnetics, Fremont, CA.), Chuan Gao (Seagate Magnetics, Fremont, CA.), G. C. Rauch (Seagate Magnetics, Fremont, CA.), J. L. Pressesky (Seagate Magnetics, Fremont, CA.), and A. Schwartz 31 Mar. 1994 10 p Presented at the 6th Joint Conference on Magnetism and Magnetic Materials, Albuquerque, NM, 20-23 Jun. 1994
(Contract W-7405-eng-48)
(DE94-014740; UCRL-JC-116424; CONF-940629-8) Avail: CASI HC A02/MF A01

Magnetic media deposited on glass substrates with metal seedlayer, Cr underlayer and CoCrPtTa alloy were studied. Within each group of samples, although the bulk magnetic properties were made to be similar, the media noise differed significantly; a microstructural study indicated that the grain sizes of the magnetic layers were similar. An X-ray diffraction study indicated that the magnetic layer was mostly (10.0) textured, with some (00.2) and (10.1) oriented grains also present. A correlation was observed between stronger CoCrPtTa (00.2) diffraction peak and lower media noise; the Cr(200) peak in the lower noise media was also much weaker. The different crystallographic texture is likely promoted by the surface condition of the seedlayer; larger number of (00.2) grains within the mostly (10.0) textured magnetic layer may result in zig-zag transitions with less cross track correlation length, which would result in lower media noise. DOE

N95-13158# California Univ., Berkeley. Lawrence Berkeley Lab, CA.
SIMULATING THE ENERGY PERFORMANCE OF HOLOGRAPHIC GLAZINGS
K. Papamichael, L. Beltran, R. Furler, E. S. Lee, S. Selkowitz, and M. Rubin May 1994 9 p Presented at the SPIE 13: International Symposium on Optical Materials Technology for Energy Efficiency and Solar Energy Conversion, Freiburg, Germany, 18-22 Apr. 1994 Revised
(Contract DE-AC03-76SF-00098)
(DE94-014969; LBL-35382-Rev; CONF-9404167-1-Rev) Avail: CASI HC A02/MF A01

The light diffraction properties of holographic diffractive structures present an opportunity to improve the daylight performance in side-lit office spaces by redirecting and reflecting sunlight off the ceiling, providing adequate daylight illumination up to 9 m from the window wall. Prior studies of prototypical holographic glazings, installed above conventional windows, have shown increased daylight levels over a deeper perimeter area than clear glass, for selected sun positions. In this study, we report on the simulation of the energy performance of prototypical holographic glazings assuming a commercial office building, in the inland Los Angeles climate. The simulation of the energy performance involved determination of both luminous and thermal performance. Since the optical complexity of holographic glazings prevented the use of conventional algorithms for the simulation of their luminous performance, we used a new method that combines experimentally determined directional workplane illuminance coefficients with computer-based analytical routines to determine a comprehensive set of daylight factors for many sun positions. These daylight factors were then used within the DOE-2.1D energy simulation program to determine hourly daylight and energy performance over the course of an entire year for four window orientations. Since the prototypical holographic diffractive structures considered were applied on single pane clear glass, we also simulated the performance of hypothetical glazings, assuming the daylight performance of the prototype holographic glazings and the thermal performance of double-pane and low-e glazings. Our analyses show that these prototypical holographic glazings did not save significant electric energy or reduce peak electricity demand compared to conventional energy-efficient window systems, mainly because of their low diffraction efficiency. Finally, we address design and implementation issues towards potential performance improvement. DOE

N95-13165# Texas Univ., Austin, TX. Dept. of Mechanical Engineering.
COMPREHENSIVE AND CRITICAL LITERATURE REVIEW ON INSITU MICRO-SENSORS FOR APPLICATION IN TRIBOLOGY Final Report
Frederick F. Ling, Ning Wang, and S. F. Murray Apr. 1994 143 p
(Contract N00014-93-1-0674)
(AD-A281646) Avail: CASI HC A07/MF A02

Two filters have been invoked in this survey of literature on sensors: (1) only those which might have relevance, direct or potential, to machinery condition sensing are included; (2) only those which might lend themselves to, presently or potentially, fiber-optical mode of information transmission are included. 190 records were selected to review from the 28,000 found using the University of Texas at Austin's U-Search and the Engineering Index, augmented by several commercial data bases, under LITERATURE ON SENSORS. Throughout, a sensor or transducer is understood to be a device that provides a usable output in response to a specific measurand; it is understood that such devices are called different names in different fields. This project has a highly restricted scope. The goal of the project concerns chemical as well as physical sensors of micro-dimension pertaining to lubricated contacts as to abrasive wear, friction, corrosive wear, cracks, micro-partile analysis, identification of surface film formation, load, miro-particle detection, position, speed, surface damage, and temperature. A research need analysis was proposed in anticipation of the aforementioned fact that few sensors in this context would be in-situ, let alone being of micro-dimension. Derived from text

N95-13171# Fermi National Accelerator Lab., Batavia, IL.
GASEOUS DETECTORS OF ULTRAVIOLET AND VISIBLE PHOTONS
V. Peskov, A. Borovik-Romanov, and T. Volynshikova Jun. 1994 15 p Presented at the 8th Symposium on Radiation Measurements and Applications, Ann Arbor, MI, 16-19 May 1994
(Contract DE-AC02-76CH-03000)
(DE94-014990; FNAL/C-94/140; CONF-940524-12) Avail: CASI HC A03/MF A01

We describe simple methods of manufacturing in a laboratory gaseous detectors of visible photons with GaAs(Cs) and SbCs photocathodes and Ti getters. Covered by CsI protective layers they are robust enough to be stable under ordinary experimental conditions. First attempts to use these detectors for crystal scintillator and fiber readout are presented. DOE

N95-13287# Fermi National Accelerator Lab., Batavia, IL.
DEVELOPMENT OF RADIATION HARD SCINTILLATORS
F. Markley, M. Davidson, J. Keller, G. Foster, A. Pla-Dalmau, J. Harmon, E. Biagtan, G. Schueneman, V. Senchishin, and H. Gustfason et al Nov.

1993 10 p
(Contract DE-AC02-76CH-03000)
(DE94-013204; FNAL-TM-1867) Avail: CASI HC A02/MF A01

The authors have demonstrated that the radiation stability of scintillators made from styrene polymer is very much improved by compounding with pentaphenyl trimethyl trisiloxane (DC 705 vacuum pump oil). The resulting scintillators are softer than desired, so they decided to make the scintillators directly from monomer where the base resin could be easily crosslinked to improve the mechanical properties. They can now demonstrate that scintillators made directly from the monomer, using both styrene and 4-methyl styrene, are also much more radiation resistant when modified with DC705 oil. In fact, they retain from 92% to 95% of their original light output after gamma irradiation to 10 Mrads in nitrogen with air annealing. When these scintillators made directly from monomer are compared with scintillators of the same composition made from polymer the latter have much higher light outputs. They commonly reach 83% while those made from monomer give only 50% to 60% relative to the reference, BC408. When oil modified scintillators using both p-terphenyl and tetra phenyl butadiene are compared with identical scintillators except that they use 3 hydroxy-flavone as the only luminophore the radiation stability is the same. However the 3HF system gives only 30% as much light as BC408 instead of 83% when both are measured with a green extended Phillips XP2081B phototube.
DOE

N95-13537# China Nuclear Information Centre, Beijing (China).
ALIGNMENT AND EXPERIMENT OF THE HL-1 X RAY BENT-CRYSTAL SPECTROMETER
Jiefu Chen (Southwest Inst. of Physics, Sichuan, China.), Chengji Yuan (Southwest Inst. of Physics, Sichuan, China.), Shuxun Zhang (Southwest Inst. of Physics, Sichuan, China.), Jie Lu (Southwest Inst. of Physics, Sichuan, China.), Gaoying Yie (Southwest Inst. of Physics, Sichuan, China.), and Li Zhang (Southwest Inst. of Physics, Sichuan, China.) Apr. 1993 12 p In CHINESE
(DE94-624719; CNIC-00709; SIP-0057) Avail: CASI HC A03/MF A01 (US Sales Only)

An X-ray bent-crystal spectrometer, which is developed by Southwestern Institute of Physics, has been aligned, experimented on with the HL-1 Tokamak device, and has been used to acquire experimental spectrum data. This spectrometer has time resolution function and is a high through-put and high resolution Bragg crystal spectrometer with a Johann configuration. It uses a large quartz lamina, its effective area is 11 x 5 sq cm, with a radius of curvature of 377 cm as the dispersion elernent. The detector is a large size (10 x 10 sq cm) one-dimensional resolving multiwire proportional counter, and the spectral resolving power is R (approx equal) 18000. Under the injection of Ar into hydrogen plasma, the He-like Ar ion satellite spectra at certain wavelength ranges are obtained. The central ion temperature has been given out from the Doppler broadening of He-like Ar x VII 3.9457 angstrom resonance line. This shows the success of spectrometer developed. The experimental results and further improvement of this spectrometer are discussed.
DOE

N95-13215*# TRW, Inc., Redondo Beach, CA. Applications Technology Div.
PASSIVE MMW CAMERA FOR LOW VISIBILITY LANDINGS
Merit Shoucri *In* NASA. Langley Research Center, Airborne Windshear Detection and Warning Systems. Fifth and Final Combined Manufacturers' and Technologists' Conference, Part 2 Jul. 1994 p 765-785 (For primary document see N95-13203 02-03)
Avail: CASI HC A03/MF A04

36 LASERS AND MASERS

Includes parametric amplifiers.
For related information see also *76 Solid-State Physics.*

N95-11940 Air Force Inst. of Tech., Wright-Patterson AFB, OH.
MODE-LOCKING A LONGITUDINALLY PUMPED LOW PRESSURE ATOMIC IODINE LASER M.S. Thesis
Kenneth S. Gurley Jul. 1994 78 p Limited Reproducibility: More than 20% of this document may be affected by microfiche quality
(AD-A282363; AFIT/CI/CIA-94-052) Avail: CASI HC A05

This paper describes the process leading up to and including the mode locking of a gain switched, photolytic iodine laser of low pressures less than 30 Torr. First, prior to mode locking, the laser is characterized via output energy, pulse shape cavity buildup time, and transverse and longitudinal mode structures. Second, the gain on the strongest transition line is measured two ways: directly with a narrowed source of tunable 1.3 mm coherent light from a solid state diode laser and indirectly using energy absorption arguments and gain probe dimensions. Finally, the laser is mode locked through active intracavity modulation with an acousto-optic modulator. Experimental data of minimum pulse width versus pressure are analyzed in detail.
DTIC

N95-12375# National Academy of Sciences - National Research Council, Washington, DC. Commission on Physical Sciences, Mathematics, and Applications.
FREE ELECTRON LASERS AND OTHER ADVANCED SOURCES OF LIGHT: SCIENTIFIC RESEARCH OPPORTUNITIES
1994 65 p
(Contracts DE-FG05-89ER-14032; N00014-89-J-1728)
Copyright Avail: CASI HC A04/MF A01

The free electron laser uses a beam of relativistic electrons passing through a periodic, transverse magnetic field to produce coherent radiation. The advantages of these devices are: A resonance condition that involves the energy of the electron beam, the strength of the magnetic field, and the periodicity of the magnet determines the wavelength of the radiation. Because one medium, the electrons, provides the gain in all spectral regions, adjusting either the beam energy or the field strength tunes the wavelength easily and rapidly over a wide range. Waste energy leaves the medium as kinetic energy of the electrons at nearly the speed of light. Moreover, the lasting medium consists only of electrons in a vacuum, and it does not have the material damage or thermal lensing problems associated with ordinary lasers. Therefore, free electron lasers can achieve very high peak powers. The main disadvantages of the free electron laser are its size and cost. Because the free electron laser requires an electron accelerator with its associated shielding, it has not been a device that could be placed in an individual investigator's laboratory and be operated and maintained by graduate students whose primary expertise is in other areas of science. Because free electron lasers are currently used only in central facilities, their use in scientific research involves both the cost of the device, and the cost and inconvenience of maintaining a facility. Unlike synchrotrons, free electron lasers serve one user, or at most a few users, at any one time. The required electron beam energy increases with decreasing wavelength, and the cost and size of the accelerator as well as the cost and size of the magnetic structure increase with decreasing wavelength. In addition to energy requirements, the electron beam must meet other requirements for emittance, energy spread, and peak current that become more stringent at shorter wavelengths. The shortest wavelength reached by existing free electron lasers is 240 nm, but most scientific uses of free electron lasers have been in the infrared. There are alternative methods proposed for generating radiation, such as plasma sources, high-order harmonic generation, and Compton backscattering sources. Some of these use terawatt laboratory lasers, which are themselves costly devices, and interest in these other sources is confined to the vacuum ultraviolet and x-ray regions for which the cost of free electron lasers is highest. Although the same physical principles govern the design of free elctron lasers in all wavelength regions, the costs and benefits are a strong function of wavelength. Therefore, this report is organized by spectral region, and the committee's findings and recommendations are very different in the different wavelength regions. However, research and development aimed at improving free electron lasers in a specific wavelength region may be important to the improvement of free electron lasers in all wavelength regions.
Author (revised)

N95-12751 Maryland Univ., College Park, MD. Dept. of Electrical Engineering.
WAVELENGTH-ENCODED PROCESSING IN SEMICONDUCTOR LASERS Final Report
M. Dagenais Jun. 1994 142 p Limited Reproducibility: More than 20% of this document may be affected by microfiche quality
(Grant AF-AFOSR-0132-91)
(AD-A282649; AFOSR-94-0457TR) Avail: CASI HC A07

It was the goal of this proposal to study the process of wavelength

conversion and wavelength encoded processing in semiconductor laser types of devices. In particular, we report on: (1) the implementation of Boolean logic using wavelength encoded inputs; (2) the use of frequency modulation to control the transmission of a Fabry-Perot laser; (3) nonlinear spectral filtering of a multi-wavelength signal; (4) wavelength-conversion and logic operation based on bistable diode laser amplifiers, including a study of crosstalk, switching power, bit-error-rates, and demonstration of an optically controllable space-switch; (5) wavelength-conversion by a T-gate device; (6) wavelength conversion using four-wave mixing in a Fabry-Perot edge-emitting and vertical cavity surface emitting laser; and (7) high-speed polarization switching in vertical-cavity lasers. DTIC

N95-12761# Lawrence Livermore National Lab., Livermore, CA.
EXPERIMENTAL AND THEORETICAL STUDY OF NEON-LIKE SELENIUM X-RAY LASER SPECTRAL LINE PROFILES Ph.D. Thesis
J. A. Koch Oct. 1993 222 p
(Contract W-7405-eng-48)
(DE94-015327; UCRL-LR-116938) Avail: CASI HC A10/MF A03

Laser action at soft x-ray wavelengths was first demonstrated in 1985 at Lawrence Livermore National Laboratory. These experiments used two superimposed, line-focused beams of the Novette visible-light laser to heat and explode a thin foil of selenium. The resulting cylindrical expanding selenium plasma had sufficiently high electron temperatures and electron densities to produce population inversions between various 3p and 3s levels in the neon-like ionization state of selenium, predominantly through electron collisional excitation from the closed-shell Ne-like ground state to the upper laser level. This led to the observation of amplification on several lines near 200 (Angstrom), the brightest of which was at 206.38 (Angstrom). Laser spectral line profiles were assumed to be dominated by Doppler broadening, based on calculated densities and ion temperatures, but prior to this work the line widths had not been measured. The primary purpose of this research is to investigate the applicability of the Doppler-broadening assumption for the intrinsic line width and for the saturation behavior of the 206.4 (Angstrom) Ne-like Se x-ray laser. The major component of this work is a series of high-resolution spectroscopic measurements of the 206.4 (Angstrom) laser line width from Se amplifiers of varying lengths. Shorter amplifiers provide data on the small-signal line width, while the longest amplifiers have sufficient gain to saturate some laser transitions, including the 206.4 (Angstrom) line, and thus provide data on the saturated line width of this laser. Laser line transfer models are also investigated and developed which predict the amplified line width of Doppler broadened, lifetime broadened and Voigt-profile lasers. Experimental data and the modeling results support the conclusion that an inhomogeneous Doppler broadening model is inadequate for describing the intrinsic line width and the effects of amplification on the line profile of this laser. DOE

N95-12779 Department of the Navy, Washington, DC.
METHOD FOR LASER-ASSISTED ETCHING OF III-V AND II-VI SEMICONDUCTOR COMPOUNDS USING CHLOROFLUOROCARBON AMBIENTS Patent
Stephen D. Russell, inventor (to Navy), Douglas A. Sexton, inventor (to Navy), and Richard J. Orazi, inventor (to Navy) 10 May 1994 23 p Filed 21 Jan. 1992
(AD-D016385; US-Patent-5,310,989; US-Patent-Appl-SN-831830; US-Patent-Class-219-121.68) Avail: US Patent and Trademark Office

An etching process allows a selective single-step patterning of III-V or II-VI semiconductor compound devices such as GaAs and InP or CdS and ZnSe in a noncorrosive environment. The etching relies on a maskless laser-assisted technique in a gaseous chlorofluorocarbon ambient, such as gaseous dichlorodifluoromethane and chloropentafluoroethane. Laser-assisted photothermal chemical etching reactions on the III-V or II-VI semiconductor compounds occur in these ambients when the incident fluence from an excimer laser at 248 nm exceeds the melt threshold. This provides a means for thin membrane formation in III-V or II-VI semiconductor compounds, rapid etches and processing of packaged devices or partially fabricated dies. The reduction in processing steps as compared to conventional wet chemical etches provides improvements in yield, reliability and cost. DTIC

N95-12780 Department of the Navy, Washington, DC.
METHOD OF LASER PROCESSING FERROELECTRIC MATERIALS Patent
Stephen D. Russell, inventor (to Navy) and Douglas A. Sexton, inventor (to Navy) 10 May 1994 12 p Filed 3 Jun. 1991
(AD-D016386; US-Patent-5,310,990; US-Patent-Appl-SN-709671; US-Patent-Class-219-121.69) Avail: US Patent and Trademark Office

Processing methods transform ferroelectric precursor films into a desired crystalline structure without adversely heating nearby materials and circuitry such as those found associated with lead zirconate titanate films. The thin film sample is placed within an appropriate chamber, where a suitable ambient is in contact with the thin film sample. The ambient may be air, oxygen or any other ambient which is known in the art to be appropriate for annealing ferroelectric materials. In this regard annealing in air can do without the processing chamber. The process for annealing relies upon continuous wave (CW) laser annealing, pulse UV annealing with or without a laser and various combinations of thermal pretreatment and processing to allow solid state diffusion in accordance with parameters appropriate for a particular application. Methods of laser patterning thin film ferroelectrics without adversely damaging adjacent or underlying layers, e.g. electrodes, are also disclosed. DTIC

N95-12868# Lawrence Livermore National Lab., Livermore, CA.
THE FUTURE OF DIODE PUMPED SOLID STATE LASERS AND THEIR APPLICABILITY TO THE AUTOMOTIVE INDUSTRY
R. Solarz, R. Beach, and L. Hackel et al Mar. 1994 9 p Presented at the Automotive Laser Applications Workshop, Dearborn, MI, 7-8 Mar. 1994
(Contract W-7405-eng-48)
(DE94-014736; UCRL-JC-116773; CONF-9403138-1) Avail: CASI HC A02/MF A01

The largest commercial application of high power lasers is for cutting and welding. Their ability to increase productivity by introducing processing flexibility and integrated automation into the fabrication process is well demonstrated. This paper addresses the potential importance of recent developments in laser technology to further impact their use within the automotive industry. The laser technology we will concentrate upon is diode laser technology and diode-pumped solid-state laser technology. We will review present device performance and cost and make projections for the future in these areas. Semiconductor laser arrays have matured dramatically over the last several years. They are lasers of unparalleled efficiency (greater than 50%), reliability (greater than 10,000 hours of continuous operation), and offer the potential of dramatic cost reductions (less than a dollar per watt). They can be used directly in many applications or can be used to pump solid-state lasers. When used as solid-state laser pump arrays, they simultaneously improve overall laser efficiency, reduce size, and improve reliability. DOE

N95-12951*# City Coll. of the City Univ. of New York, NY. Inst. for Ultrafast Spectroscopy and Lasers.
TETRAVALENT CHROMIUM (Cr(4+)) AS LASER-ACTIVE ION FOR TUNABLE SOLID-STATE LASERS Final Report, 1 Nov. 1991 - 31 Oct. 1993
A. Seas, V. Petricevic, and Robert R. Alfano 31 Oct. 1993 64 p
(Grant NAG1-1346)
(NASA-CR-196481; NAS 1.26:196481) Avail: CASI HC A04/MF A01

Major accomplishments under NASA grant NAG-1-1346 are summarized. (1) numerical modeling of the four mirror astigmatically compensated, Z-fold cavity was performed and several design parameters to be used for the construction of a femtosecond forsterite laser were revealed by simulation. (2) femtosecond pulses from a continuous wave mode-locked chromium doped forsterite laser were generated. The forsterite laser was actively mode-locked using an acousto-optic modulator operating at 78 MHz with two Brewster high dispersion glass prisms for intra-cavity chirp compensation. Transform-limited sub-100-fs pulses were routinely generated in the TEM(sub 00) mode with 85 mW of continuous power tunable over 1230-1280 nm. The shortest pulses of 60-fs pulsewidth were measured. (3) Self-mode-locked operation of the Cr:forsterite laser was achieved. Synchronous pumping was used to mode lock the forsterite laser resulting in picosecond pulses, which in turn provided the starting mechanism for self-mode-locking. The pulses generated had an FWHM of 105 fs and were tunable between 1230-1270 nm. (4) Numerical calculations indicated that the pair of SF 14 prisms used in the cavity compensated for quadratic phase but introduced a large cubic phase term. Further calculations of other optical glasses indicated that a pair of SFN 64 prisms can introduce the same amount of

quadratic phase as SF 14 prisms but introduce a smaller cubic phase. When the SF 14 prisms were replaced by SFN 64 prisms the pulsewidth was reduced to 50 fs. Great improvement was observed in the stability of the self mode-locked forsterite laser and in the ease of achieving mode locking. Using the same experimental arrangement and a new forsterite crystal with improved FOM the pulse width was reduced to 36 fs.

Author (revised)

N95-13076# Oak Ridge National Lab., TN.
THE LASER AND ITS APPLICATIONS ON ENVIRONMENT AND BIOTECHNOLOGY RESEARCH
C. H. Chen, S. L. Allman, R. C. Phillips, W. R. Garrett, and K. Tang 1994 5 p Presented at the Chinese American Academic and Professional Association in the Southeastern United States Meeting, Atlanta, GA, 10-12 Jun. 1994
(Contract DE-AC05-84OR-21400)
(DE94-013831; CONF-9406185-1) Avail: CASI HC A01/MF A01

During the past few years, researchers at ORNL have developed the following new instruments involving the use of a laser for environmental and biotechnology research: (1) a single atom detector; (2) a rare gas atom counter; (3) a biopolymer mass spectrometer; and (4) a vacuum ultraviolet (VUV) ionizer mass spectrometer. Their basic principles and applications are briefly described. DOE

N95-13080# Los Alamos National Lab., NM.
LOADS FOR PULSED POWER CYLINDRICAL IMPLOSION EXPERIMENTS
W. E. Anderson, E. V. Armijo, B. L. Barthell, J. J. Bartos, H. Bush, L. R. Foreman, F. P. Garcia, P. L. Gobby, V. M. Gomez, and V. A. Gurule et al 1994 7 p Presented at the American Nuclear Society Meeting, La Grange Park, IL, 19-24 Jun. 1994
(Contract W-7405-eng-36)
(DE94-014429; LA-UR-94-2107; CONF-9406197-1) Avail: CASI HC A02/MF A01

Pulse power can be used to generate high energy density conditions in convergent hollow cylindrical geometry through the use of appropriate electrode configuration and cylindrical loads. Cylindrically symmetric experiments are conducted with the Pegasus-H inductive store, capacitor energized pulse power facility at Los Alamos using both precision machined cylindrical liner loads and low mass vapor deposited cylindrical foil loads. The liner experiments investigate solid density hydrodynamic topics. Foil loads vaporize from Joule heating to generate an imploding cylindrical plasma which can be used to simulate some fluxes associated with fusion energy processes. Similar experiments are conducted with 'Procyon' inductive store pulse power assemblies energized by explosively driven magnetic flux compression. DOE

N95-13139# Naval Research Lab., Washington, DC.
A COMPARISON OF TWO SITES FOR THE PURPOSE OF SATELLITE LASER RANGING
Anne E. Clement 27 Jul. 1994 25 p
(AD-A283149; NRL/MR/8120-94-7604) Avail: CASI HC A03/MF A01

The efficacy of satellite laser ranging off of enhanced and unenhanced satellites for the purposes of precise positioning and orbital determination is compared for two configurations. This report is not a tutorial in laser ranging but does present and define the laser link equation and all key parameters. Results from field tests conducted using the NRL laser ranging system installed at Malabar, Florida, are compared with predicted returns if the NRL system were installed at the USAF 3.5 meter facility in Albuquerque, New Mexico. It was found that 33.4 dB of increased system sensitivity is possible when ranging from the New Mexico site. In the field tests, it was found that unenhanced target acquisition and subsequent glint location could not be determined from the Malabar configuration. However, the question of precise positioning of unenhanced targets could be reopened from the New Mexico site due to the potential increase in return signal strength. DTIC

N95-13246 Selskapet for Industriell og Teknisk Forskning, Trondheim (Norway). Div. of Applied Thermodynamics.
LASER BASED COMBUSTION LABORATORY AT NTH/SINTEF APPLIED THERMODYNAMICS
F. Tichy and T. Bjoerge 17 Dec. 1993 40 p
(PB94-202603; STF15-A93105) Avail: Issuing Activity (National Technical Information Service (NTIS))

During the SPUNG-program, a laser based laboratory has been built up at NTH/SINTEF Applied Thermodynamics by the funding from that program. The laser based laboratory consists of a Nd:YAG laser and an image intensifier electronic camera system. There are numerous different laser based techniques that can be used, using the laser based laboratory, but we have concentrated on laser induced fluorescence (LIF). By shaping the laser beam into a flat plane, 2D imaging of combustion radicals (OH, CH) and emission species (NO) are possible. This can give valuable information about flame structure, flame stabilization, turbulence scales and so on, but at the time being not quantitative concentrations. NTIS

N95-13294 Spectra Diode Labs., San Jose, CA.
DIODE-PUMPED MICRO-LASER ARRAYS Final Report, 30 Sep. 1993 - 18 Feb. 1994
R. Waarts 1 Jun. 1994 42 p Limited Reproducibility: More than 20% of this document may be affected by microfiche quality
(Contract MDA972-92-C-0047; ARPA Order 8778)
(AD-A282494) Avail: Issuing Activity (Defense Technical Information Center (DTIC))

In this work SDL investigated the operation of 2-D high power microlaser arrays based on novel monolithic surface-emitting laser diode arrays coupled to Yb:YAG and Er:YSGG microlaser crystals. The experimental demonstrations include: (1) 200 mW, q-CW single Yb:YAG microlaser; (2) 930 mW CW linear, 12-element Er:YSGG microlaser; (3) 130 W q-CW 2-D surface-emitting laser diode array at 970 nm; and (4) 600 mW, q-CW from an 18-element 3-D Er:YSGG microlaser array. The experiments performed at SDL under this contract demonstrate the suitability of monolithic 2-D laser diode arrays for pumping solids state lasers. In addition, the experiments show the flexibility of the microlaser concept. Using different pump wavelengths in combination with different microlasers a wide output wavelength range from 1 micron to 3 micron is demonstrated. Finally, the microlaser array is shown to be scalable by exploiting one and two dimensional laser diode pump arrays. DTIC

N95-13534# Lawrence Livermore National Lab., Livermore, CA.
LASER PHYSICS OF Nd(EXP 3+)-DOPED PHOSPHATE GLASSES
S. A. Payne, C. Bibeau, and J. S. Hayden Mar. 1994 8 p Presented at the European Quantum Electronics Conference 1994, Amsterdam, Netherlands, 28 Aug. - 2 Sep. 1994
(Contract W-7405-eng-48)
(DE94-015141; UCRL-JC-116742; CONF-940871-2) Avail: CASI HC A02/MF A01

New data and analysis regarding the four fundamental processes that impact the laser performance of Nd-doped glasses will be discussed, including concentration quenching, Auger upconversion, the (exp 4)I(exp 11/2) lower level lifetime, and hole-burning. DOE

N95-13213*# Lightwave Atmospherics, Inc., Marblehead, MA.
REMOTE SENSING OF TURBULENCE IN THE CLEAR ATMOSPHERE WITH 2-MICRON LIDARS
Robert J. Martinson and John H. Flint *In* NASA. Langley Research Center, Airborne Windshear Detection and Warning Systems. Fifth and Final Combined Manufacturers' and Technologists' Conference, Part 2 Jul. 1994 p 689-705 (For primary document see N95-13203 02-03)
(Contract DAAH01-92-C-R097)
Avail: CASI HC A03/MF A04

37 MECHANICAL ENGINEERING

Includes auxiliary systems (nonpower); machine elements and processes; and mechanical equipment.

N95-11701*# Alabama Univ., Tuscaloosa, AL. Dept. of Electrical Engineering.
DESIGN AND APPLICATION OF ELECTROMECHANICAL ACTUATORS FOR DEEP SPACE MISSIONS Annual Progress Report No. 2, 16 Aug. 1993 - 15 A ug. 1994
Tim A. Haskew and John Wander Aug. 1994 70 p

(Grant NAG8-240)
(NASA-CR-196791; NAS 1.26:196791; BER-612-163) Avail: CASI HC A04/MF A01

This progress report documents research and development efforts performed from August 16, 1993 through August 15, 1994 on NASA Grant NAG8-240, 'Design and Application of Electromechanical Actuators for Deep Space Missions.' Since the submission of our last progress report in February 1994, our efforts have been almost entirely focused on final construction of the test stand and experiment design. Hence, this report is dedicated solely to these topics. However, updates on our research personnel and our health monitoring and fault management efforts are provided in this summary. Following this executive summary are two report sections. The first is devoted to the motor drive being constructed for the test stand. The thrust of the next section is the mechanical and hydraulic design and construction based on the planned experimental requirements. Following both major sections are three appendices. Author

N95-11729 Automated Precision, Inc., Gaithersburg, MD.
DEVELOPMENT OF A SPINDLE THERMAL ERROR CHARACTERIZATION AND COMPENSATION SENSOR SYSTEM FOR MACHINING CENTER ACCURACY ENHANCEMENT Final Technical Report, Apr. 1991 - Mar. 1993
K. C. Lau Dec. 1993 41 p Limited Reproducibility: More than 20% of this document may be affected by microfiche quality
(Contract F33615-91-C-5709)
(AD-A280891; WL-TR-93-8034) Avail: Issuing Activity (Defense Technical Information Center (DTIC))

Automated Precision Incorporated under contract with Wright Laboratory's Manufacturing Technology Directorate has developed a low cost, real-time, sensor/computer based, high performance spindle thermal modeling and compensation system for production computer numeric control (CNC) machining centers. This sensor based system is designed to measure spindle thermal error which, when corrected, improves precision machining accuracy. DTIC

N95-11889*# Akron Univ., OH.
TLIFE: A PROGRAM FOR SPUR, HELICAL AND SPIRAL BEVEL TRANSMISSION LIFE AND RELIABILITY MODELING Final Report
M. Savage, M. G. Prasanna, and K. L. Rubadeux Cleveland, OH NASA Aug. 1994 184 p
(Grant NAG3-1047; RTOP 505-62-36; DA Proj. 1L1-62211-A-47-A)
(NASA-CR-4622; E-9073; NAS 1.26:4622; ARL-TR-506) Avail: CASI HC A09/MF A02

This report describes a computer program, 'TLIFE', which models the service life of a transmission. The program is written in ANSI standard Fortran 77 and has an executable size of about 157 K bytes for use on a personal computer running DOS. It can also be compiled and executed in UNIX. The computer program can analyze any one of eleven unit transmissions either singly or in a series combination of up to twenty-five unit transmissions. Metric or English unit calculations are performed with the same routines using consistent input data and a units flag. Primary outputs are the dynamic capacity of the transmission and the mean lives of the transmission and of the sum of its components. The program uses a modular approach to separate the load analyses from the system life calculations. The program and its input and output data files are described herein. Three examples illustrate its use. A development of the theory behind the analysis in the program is included after the examples. Author

N95-12377*# National Aeronautics and Space Administration. Lewis Research Center, Cleveland, OH.
ANALYTICAL AND EXPERIMENTAL VIBRATION ANALYSIS OF A FAULTY GEAR SYSTEM
F. K. Choy (Akron Univ., OH.), M. J. Braun, V. Polyshchuk, J. J. Zakrajsek, D. P. Townsend, and R. F. Handschuh Oct. 1994 19 p Presented at the 1994 Fall Technical Workshop, St. Louis, MO, 24-26 Oct. 1994; sponsored by the American Gear Manufacturers' Association
(DA Proj. 1L1-62211-A-47-A; RTOP 505-62-36)
(NASA-TM-106689; E-9045; NAS 1.15:106689; ARL-TR-574) Avail: CASI HC A03/MF A01

A comprehensive analytical procedure was developed for predicting faults in gear transmission systems under normal operating conditions. A gear tooth fault model is developed to simulate the effects of pitting and wear on the vibration signal under normal operating conditions. The model uses changes in the gear mesh stiffness to simulate the effects of gear tooth faults. The overall dynamics of the gear transmission system is evaluated by coupling the dynamics of each individual gear-rotor system through gear mesh forces generated between each gear-rotor system and the bearing forces generated between the rotor and the gearbox structure. The predicted results were compared with experimental results obtained from a spiral bevel gear fatigue test rig at NASA Lewis Research Center. The Wigner-Ville distribution (WVD) was used to give a comprehensive comparison of the predicted and experimental results. The WVD method applied to the experimental results were also compared to other fault detection techniques to verify the WVD's ability to detect the pitting damage, and to determine its relative performance. Overall results show good correlation between the experimental vibration data of the damaged test gear and the predicted vibration from the model with simulated gear tooth pitting damage. Results also verified that the WVD method can successfully detect and locate gear tooth wear and pitting damage. Author

N95-12394# Carnegie-Mellon Univ., Pittsburgh, PA. Robotics Inst.
ESSENTIAL KINEMATICS FOR AUTONOMOUS VEHICLES Technical Report
Alonzo Kelly 2 May 1994 48 p
(Contracts DACA76-89-C-0014; DAAE07-90-C-RO59)
(AD-A282456; CMU-RI-TR-94-14) Avail: CASI HC A03/MF A01

A short tutorial on Homogeneous Transforms is presented covering the triple interpretation of a homogeneous transform as an operator, a coordinate frame, and a coordinate transform. The operator transform duality is derived and its use in the Denavit Hartenberg convention is explained. Forward, inverse, and differential kinematics are derived for a simple manipulator to illustrate concepts. A standard set of coordinate frames is proposed for wheeled mobile robots. It is shown that the RPY transform serves the same purpose as the DH matrix in this case. It serves to interface with vehicle position estimation systems of all kinds, to control and model pan/tilt mechanisms and stabilized platforms, and to model the rigid transforms from place to place on the vehicle. Forward and inverse kinematics and the Euler angle rate to the angular velocity transform are derived for the RPY transform. Projective kinematics for ideal video cameras and laser rangefinders, and the imaging Jacobian relating world space and image space is derived. Finally, the kinematics of the Ackerman steer vehicle is presented for reference purposes. This report is both a tutorial and a reference for the transforms used in the RANGER vehicle controller. It is both because the models keep evolving and it was necessary to provide the tools, mechanisms, and discipline required to continue the evolution. DTIC

N95-12505# Carnegie-Mellon Univ., Pittsburgh, PA. Robotics Inst.
MINIMAL FIXTURING OF FRICTIONLESS ASSEMBLIES: COMPLEXITY AND ALGORITHMS
David Baraff, Raju Mattikalli, and Pradeep Khosla Apr. 1994 46 p
(AD-A282724; CMU-RI-TR-94-08) Avail: CASI HC A03/MF A01

In many assembly tasks, it is necessary to insure the stability of a subcollection of contacting object. To achieve stability, it is often necessary to introduce fixture elements (also called fingers in some work) to help hold objects in place. In this paper, the complexity of stabilizing multiple contacting bodies with the fewest number of fixture elements possible is considered. Standard fixture elements of the type explored in previous single-object grasping work are considered, along with two generalized fixture element variants. The types of stability considered are: (1) form-closure (complete immobility of the assembly); (2) stability with respect to a specific external force and torque on each body; and (3) stability in the neighborhood of a specific external force and torque on each body. The major result is that for most of the combinations of fixture element varieties, and types of stability considered, achieving an optimal solution (that is, finding a smallest set of fixture elements yielding stability) is NP-hard. However, for many fixturing problems it seems likely that suboptimal, yet acceptably small solutions can be found in polynomial time, and some candidate algorithms are presented. DTIC

N95-12526# Carnegie-Mellon Univ., Pittsburgh, PA. Robotics Inst.
ACTUABILITY OF UNDERACTUATED MANIPULATORS
Christopher Lee and Yangsheng Xu Jun. 1994 25 p
(AD-A282788; CMU-RI-TR-94-13) Avail: CASI HC A03/MF A01

In this paper we study underactuated manipulator systems, which are composed of both active and passive joints. The study of underactuated systems is interesting for a variety of applications including space robots, hyperredundant robots, and mobile robots. When one or more joints in a normal manipulator system fail, control techniques for the resulting underactuated system can make use of dynamic coupling within the system for position control. In this paper, we define a performance measure for the motion of these underactuated manipulator systems. We call this performance measure actuability. Actuability is a measure of the ability of the actuators in a robot manipulator to cause acceleration of the end-effector. Based on this concept, we develop sensitivity analysis of the system's performance with respect to geometric and dynamics parameters of the robot. This investigation is significant for the design and control of an underactuated robot system. DTIC

N95-12532*# Kansas State Univ., Manhattan, KS. Dept. of Mechanical Engineering.

HUMAN-LIKE ROBOTS FOR SPACE AND HAZARDOUS ENVIRONMENTS

1994 194 p Prepared for Universities Space Research Association, Columbia, MD

(Contract NASw-4435)

(NASA-CR-197171; NAS 1.26:197171) Avail: CASI HC A09/MF A03

The three year goal for the Kansas State USRA/NASA Senior Design team is to design and build a walking autonomous robotic rover. The rover should be capable of crossing rough terrain, traversing human made obstacles (such as stairs and doors), and moving through human and robot occupied spaces without collision. The rover is also to evidence considerable decision making ability, navigation, and path planning skills. Derived from text

N95-12554*# Georgia Inst. of Tech., Atlanta, GA. School of Mechanical Engineering.

MARS EQUIPMENT TRANSPORT SYSTEM Final Project Report

Cindy Sorrells, Michelle Geiger, Sean OHanlon, Stuart Pieloch, and Nick Brogan 8 Dec. 1993 90 p Prepared for Universities Space Research Association, Columbia, MD

(Contract NASw-4435)

(NASA-CR-197158; NAS 1.26:197158) Avail: CASI HC A05/MF A01

Mechanical Engineering Senior Design Project 1 (ME4182) is a part of the NASA/University Advanced Design Program. Under this program, NASA allocates money and resources to students to be used in design work for a specified topic. The current topic is the exploration and colonization of Mars. The specific area in which we are to work is the transportation of the modules in which astronauts will live while on Mars. NASA is concerned about the weight of the module transferring system, as the shipping cost to Mars is quite expensive. NASA has specified that the weight of the system is to be minimized in order to reduce the shipping costs. Derived from text

N95-12579# Southwest Research Inst., San Antonio, TX. Engine, Fuel, and Vehicle Research Div.

OPEN-CHAMBER COMBUSTION STUDY Topical Report, June 1991 - August 1992

D. P. Meyers and R. C. Meyer Apr. 1994 247 p

(Contract GRI-5086-293-1848)

(PB94-184090; SWRI-3178-4.3; GRI-93/0133) Avail: CASI HC A11/MF A03

The test program was undertaken to research trade-offs between engine design and operational parameters on open-chamber, premixed spark-ignited gas engines, with a primary focus on combustion effects. This included combustion chamber designs which are conceptually diametrically opposed -- a high squish design typical of diesel engines and a virtually quiescent design. The reader should note that these data are somewhat abstract compared to conventional engines, because the Labeco test engine has exceptionally high friction and the lean-burn data were run unboosted. NTIS

N95-12587# Carnegie-Mellon Univ., Pittsburgh, PA. Robotics Inst.

ROBUST CONTROL OF UNDERACTUATED MANIPULATORS: ANALYSIS AND IMPLEMENTATION

Marcel Bergerman and Yangsheng Xu May 1994 27 p

(AD-A282836; CMU-RI-TR-94-12) Avail: CASI HC A03/MF A01

Underactuated manipulators are robot manipulators composed of both active and passive joints. The advantages of using such systems reside in the fact that they weigh less and consume less energy than their fully-actuated counterparts, thus being useful for applications such as space robotics. Another interest resides in the reliability or fault-tolerant design of fully-actuated manipulators. If any of the joint actuators of such a device fails, an entire operation may have to be aborted because of the loss of one or more degrees of freedom. The methodology proposed in this paper uses the dynamic coupling between the passive joints and the active joints, and controls the active ones in order to bring the passive joint angles to a desired set-point. Therefore, the control law and the performance of the system are completely dependent on the dynamic model. Since it is difficult to obtain the exact dynamic model of the system in general, considerable position errors and even instability can result in some cases. In this paper, we propose a variable structure controller to provide the system with the robustness necessary to perform tasks regardless of the modelling errors. Case studies are provided as a means of illustration. DTIC

N95-12621*# National Aeronautics and Space Administration. Lewis Research Center, Cleveland, OH.

ANALYSIS OF THE EFFECTS OF SURFACE PITTING AND WEAR ON THE VIBRATIONS OF A GEAR TRANSMISSION SYSTEM

F. K. Choy (Akron Univ., OH.), V. Polyshchuk (Akron Univ., OH.), J. J. Zakrajsek, R. F. Handschuh, and D. P. Townsend Jul. 1994 10 p Presented at the AUSTRIB 1994, Perth, Australia, 5-8 Dec. 1994; sponsored by the Institution of Engineers Prepared in cooperation with Army Research Lab., Cleveland, OH

(RTOP 505-62-36; DA Proj. 1L1-62211-A-47-A)

(NASA-TM-106678; E-9014; NAS 1.15:106678; ARL-TR-520) Avail: CASI HC A02/MF A01

A comprehensive procedure to simulate and analyze the vibrations in a gear transmission system with surface pitting, 'wear' and partial tooth fracture of the gear teeth is presented. An analytical model was developed where the effects of surface pitting and wear of the gear tooth were simulated by phase and magnitude changes in the gear mesh stiffness. Changes in the gear mesh stiffness were incorporated into each gear-shaft model during the global dynamic simulation of the system. The overall dynamics of the system were evaluated by solving for the transient dynamics of each shaft system simultaneously with the vibration of the gearbox structure. In order to reduce the number of degrees-of-freedom in the system, a modal synthesis procedure was used in the global transient dynamic analysis of the overall transmission system. An FFT procedure was used to transform the averaged time signal into the frequency domain for signature analysis. In addition, the Wigner-Ville distribution was also introduced to examine the gear vibration in the joint time frequency domain for vibration pattern recognition. Experimental results obtained from a gear fatigue test rig at NASA Lewis Research Center were used to evaluate the analytical model. Author

N95-12625*# Georgia Inst. of Tech., Atlanta, GA. School of Mechanical Engineering.

EXTERNAL DEVICE TO INCREMENTALLY SKID THE HABITAT (E-DISH)

J. W. Brazell, Steve Introne, Lisa Bedell, Ben Credle, Graham Holp, Siao Ly, and Terry Tait [1994] 76 p Prepared for Universities Space Research Association, Columbia, MD

(Contract NASw-4435)

(NASA-CR-197147; NAS 1.26:197147) Avail: CASI HC A05/MF A01

A Mars habitat transport system was designed as part of the NASA Mars exploration program. The transport system, the External Device to Incrementally Skid the Habitat (E - DISH), will be used to transport Mars habitats from their landing sites to the colony base and will be detached after unloading. The system requirements for Mars were calculated and scaled for model purposes. Specific model materials are commonly found and recommendations for materials for the Mars design are included. Author (revised)

N95-12627*# Texas Univ., Austin, TX.
PROPOSAL FOR THE DESIGN OF A ZERO GRAVITY TOOL STORAGE DEVICE
Sue Stuckwisch, Carlos A. Carrion, Lee Phillips, Julia Laughlin, and Jason Francois 1 Apr. 1994 44 p Prepared for Universities Space Research Association, Columbia, MD
(Contract NASw-4435)
(NASA-CR-197150; NAS 1.26:197150) Avail: CASI HC A03/MF A01

Astronauts frequently use a variety of hand tools during space missions, especially on repair missions. A toolbox is needed to allow storage and retrieval of tools with minimal difficulties. The toolbox must contain tools during launch, landing, and on-orbit operations. The toolbox will be used in the Shuttle Bay and therefore must withstand the hazardous space environment. The three main functions of the toolbox in space are: to protect the tools from the space environment and from damaging one another, to allow for quick, one-handed access to the tools; and to minimize the heat transfer between the astronaut's hand and the tools. This proposal explores the primary design issues associated with the design of the toolbox. Included are the customer and design specifications, global and refined function structures, possible solution principles, concept variants, and finally design recommendations. Author

N95-12640*# Universities Space Research Association, Columbia, MD.
INTRODUCTION TO MAGNETIC BEARINGS
Lori Skowronski and Anne Bisese 5 Apr. 1993 23 p
(Contract NASw-4435)
(NASA-CR-197187; NAS 1.26:197187) Avail: CASI HC A03/MF A01

Multi-axis suspension has several advantages over single axis system, in that it provides control of an object with precision in two or three orthogonal axes. In this report, we discuss the primary use of magnetic-bearing suspension and it's relevance to what was formally known as NASA's Annular Suspension and Pointing System (ASPS). This system is an experimental pointing system with applications for the space shuttle and the space station programs. The objectives behind this magnetic suspension research project are to provide insight to the use of the ASPS configuration, to control the solar panels of the space station. This is important to maintain the correct position of the panels in relation to the sun and orbiting space station for the continuous supply of solar energy. Since the panels are suspended, they can be aligned with minimum outside interference. The approach of using magnetic suspension technology guarantees mechanical isolation since there are no contacting surfaces. This isolation reduces vibration transmission and mechanical wear which in turn extends the life of the payload and of the carrier. It should be noted that ASPS has a high pointing accuracy along the line of 0.01 arc-second. This research will be done in a laboratory setting by incorporating five bearing stations and one motion control station. We will attempt to suspend an object of dead weight similar to that of a solar panel. The long term applications may include deep-space navigation, fire control in weapon systems, and an improved mass transit system. Author

N95-12648# National Renewable Energy Lab., Golden, CO.
EFFECTS OF PISTON SURFACE TREATMENTS ON PERFORMANCE AND EMISSIONS OF A METHANOL-FUELED, DIRECT INJECTION, STRATIFIED CHARGE ENGINE
B. West (Oak Ridge National Lab., TN.) and J. B. Green (Oak Ridge National Lab., TN.) Jul. 1994 14 p
(Contract DE-AC36-83CH-10093)
(DE94-011851; NREL/TP-425-6161) Avail: CASI HC A03/MF A01

The purpose of this study was to investigate the effects of thermal barrier coatings and/or surface treatments on the performance and emissions of a methanol-fueled, direct-injection, stratified-charge (DISC) engine. A Ricardo Hydra Mark III engine was used for this work and in previous experiments at Oak Ridge National Laboratory (ORNL). The primary focus of the study was to examine the effects of various piston insert surface treatments on hydrocarbon (HC) and oxides of nitrogen (NO(x)) emissions. Previous studies have shown that engines of this class have a tendency to perform poorly at low loads and have high unburned fuel emissions. A blank aluminum piston was modified to employ removable piston bowl inserts. Four different inserts were tested in the experiment: aluminum, stainless steel with a 1.27-mm (0.050-in.) air gap (to act as a thermal barrier), and two stainless steel/air-gap inserts with coatings. Two stainless steel inserts were dimensionally modified to account for the coating thickness (1.27-mm) and coated identically with partially stabilized zirconia (PSZ). One of the coated inserts then had an additional seal-coat applied. The coated inserts were otherwise identical to the stainless steel/air-gap insert (i.e., they employed the same 1.27-mm air gap). Thermal barrier coatings were employed in an attempt to increase combustion chamber surface temperatures, thereby reducing wall quenching and promoting more complete combustion of the fuel in the quench zone. The seal-coat was applied to the zirconia to reduce the surface porosity; previous research suggested that despite the possibly higher surface temperatures obtainable with a ceramic coating, the high surface area of a plasma-sprayed coating may actually allow fuel to adhere to the surface and increase the unburned fuel emissions and fuel consumption. DOE

N95-12666*# Old Dominion Univ., Norfolk, VA.
ANNULAR SUSPENSION AND POINTING SYSTEM WITH CONTROLLED DC ELECTROMAGNETS
Josephine Lynn Vu and Kwok Hung Tam 22 Apr. 1993 51 p Prepared for Universities Space Research Association, Columbia, MD
(Contract NASw-4435)
(NASA-CR-197206; NAS 1.26:197206) Avail: CASI HC A04/MF A01

The Annular Suspension and Pointing System (ASPS) developed by the Flight System division of Sperry Corporation is a six-degree of freedom payload pointing system designed for use with the space shuttle. This magnetic suspension and pointing system provides precise controlled pointing in six-degrees of freedom, isolation of payload-carrier disturbances, and end mount controlled pointing. Those are great advantages over the traditional mechanical joints for space applications. In this design, we first analyzed the assumed model of the single degree ASPS bearing actuator and obtained the plant dynamics equations. By linearizing the plant dynamics equations, we designed the cascade and feedback compensators such that a stable and satisfied result was obtained. The specified feedback compensator was computer simulated with the nonlinearized plant dynamics equations. The results indicated that an unstable output occurred. In other words, the designed feedback compensator failed. The failure of the design is due to the Taylor's series expansion not converging. Derived from text

N95-12668*# Universities Space Research Association, Columbia, MD.
MARS METHANE ENGINE Final Report
Hung Bui, Chris Coletta, and Alain DeBois 21 Apr. 1994 47 p
(Contract NASw-4435)
(NASA-CR-197205; NAS 1.26:197205) Avail: CASI HC A03/MF A01

The feasibility of an internal combustion engine operating on a mixture of methane, carbon dioxide, and oxygen has been verified by previous design groups for the Mars Methane Engine Project. Preliminary stoichiometric calculations examined the theoretical fuel-air ratios needed for the combustion of methane. Installation of a computer data acquisition system along with various ancillary components will enable the performance of the engine, running on the described methane mixture, to be optimized with respect to minimizing excess fuel. Theoretical calculations for stoichiometric combustion of methane-oxygen-carbon dioxide mixtures yielded a ratio of 1:2:4.79 for a methane-oxygen-carbon dioxide mixture. Empirical data shows the values to be closer to 1:2.33:3.69 for optimum operation. Author

N95-12690*# Idaho Univ., Moscow, ID. Dept. of Mechanical Engineering.
A LUNAR/MARTIAN ANCHOR EMPLACEMENT SYSTEM
Dustin Clinton, Andrew Holt, Erik Jantz, Teresa Kaufman, James Martin, and Reed Weber 1993 96 p Prepared for Universities Space Research Association, Columbia, MD
(Contract NASw-4435)
(NASA-CR-197193; NAS 1.26:197193) Avail: CASI HC A05/MF A01

On the Moon or Mars, it is necessary to have an anchor, or a stable, fixed point able to support the forces necessary to rescue a stuck vehicle, act as a stake for a tent in a Martian gale, act as a fulcrum in the erection of general construction poles, or support tent-like regolith shields. The anchor emplacement system must be highly autonomous. It must supply the energy and stability for anchor deployment. The goal of the anchor emplacement system project is to design and build a prototype anchor and to design a conceptual anchor emplacement system. Various anchors were tested in a 1.3 cubic meter test bed containing decomposed granite. A simulated lunar soil was created by adjusting the moisture and

compaction characteristics of the soil. We conducted tests on emplacement torque, amount of force the anchor could withstand before failure, anchor pull out force at various angles, and soil disturbances caused by placing the anchor. A single helix auger anchor performed best in this test bed based on energy to emplace, and the ultimate holding capacity. The anchor was optimized for ultimate holding capacity, minimum emplacement torque, and minimum soil disturbance in sandy soils yielding the following dimensions: helix diameter (4.45 cm), pitch (1.27 cm), blade thickness (0.15 cm), total length (35.56 cm), shaft diameter (0.78 cm), and a weight of 212.62 g. The experimental results showed that smaller diameter, single-helix augers held more force than larger diameter augers for a given depth. The emplacement system consists of a flywheel and a motor for power, sealed in a protective box supported by four legs. The flywheel system was chosen over a gear system based on its increased reliability in the lunar environment. Author (revised)

N95-12694*# University of Central Florida, Orlando, FL. Mechanical and Aerospace Engineering.

DESIGN AND TESTING OF A MODEL CELSS CHAMBER ROBOT Final Report

Mark Davis, Shawn DeZego, Kinzy Jones, Christopher Kewley, Mike Langlais, John McCarthy, Damon Penny, Tom Bonner, C. Ashley Funderburke, and Ruth Hailey et al 1994 315 p Prepared for Universities Space Research Association, Columbia, MD

(Contract NASw-4435)

(NASA-CR-197196; NAS 1.26:197196) Avail: CASI HC A14/MF A03

A robot system for use in an enclosed environment was designed and tested. The conceptual design will be used to assist in research performed by the Controlled Ecological Life Support System (CELSS) project. Design specifications include maximum load capacity, operation at specified environmental conditions, low maintenance, and safety. The robot system must not be hazardous to the sealed environment, and be capable of stowing and deploying within a minimum area of the CELSS chamber facility. This design consists of a telescoping robot arm that slides vertically on a shaft positioned in the center of the CELSS chamber. The telescoping robot arm consists of a series of links which can be fully extended to a length equal to the radius of the working envelope of the CELSS chamber. The vertical motion of the robot arm is achieved through the use of a combination ball screw/ball spline actuator system. The robot arm rotates cylindrically about the vertical axis through use of a turntable bearing attached to a central mounting structure fitted to the actuator shaft. The shaft is installed in an overhead rail system allowing the entire structure to be stowed and deployed within the CELSS chamber. The overhead rail system is located above the chamber's upper lamps and extends to the center of the CELSS chamber. The mounting interface of the actuator shaft and rail system allows the entire actuator shaft to be detached and removed from the CELSS chamber. When the actuator shaft is deployed, it is held fixed at the bottom of the chamber by placing a square knob on the bottom of the shaft into a recessed square fitting in the bottom of the chamber floor. A support boot ensures the rigidity of the shaft. Three student teams combined into one group designed a model of the CELSS chamber robot that they could build. They investigated materials, availability, and strength in their design. After the model arm and stand were built, the class performed pre-tests on the entire system. A stability pre-test was used to determine whether the model robot arm would tip over on the stand when it was fully extended. Results showed the stand tipped when 50 Newtons were applied horizontally to the top of the vertical shaft while the arm was fully extended. This proved that it was stable. Another pre-test was the actuator slip test used to determine if there is an adequate coefficient of friction between the actuator drive wheels and drive cable to enable the actuator to fully extend and retract the arm. This pre-test revealed that the coefficient of friction was not large enough to prevent slippage. Sandpaper was glued to the drive wheel and this eliminated the slippage problem. The class preformed a fit test in the CELSS chamber to ensure that the completed robot arm is capable of reaching the entire working envelope. The robot was centered in the chamber and the arm was fully extended to the sides of the chamber. The arm was also able to retract to clear the drain pipes separating the upper and lower plant trays. Author (revised)

N95-12843*# National Aeronautics and Space Administration. Lewis Research Center, Cleveland, OH.

ANALYTICAL AND EXPERIMENTAL VIBRATION ANALYSIS OF A FAULTY GEAR SYSTEM

F. K. Choy (Akron Univ., OH.), M. J. Braun (Akron Univ., OH.), V. Polyshchuk (Akron Univ., OH.), J. J. Zakrajsek, D. P. Townsend, and R. F. Handschuh Oct. 1994 19 p Presented at the 1994 Fall Technical Workshop, St. Louis, MO, 24-26 Oct. 1994; sponsored by the American Gear Manufacturers' Association

(DA Proj. 1L1-62211-A-47-A; RTOP 505-62-36)

(NASA-TM-106689; E-9045; NAS 1.15:106689; ARL-TR-574) Avail: CASI HC A03/MF A01

A comprehensive analytical procedure was developed for predicting faults in gear transmission systems under normal operating conditions. A gear tooth fault model is developed to simulate the effects of pitting and wear on the vibration signal under normal operating conditions. The model uses changes in the gear mesh stiffness to simulate the effects of gear tooth faults. The overall dynamics of the gear transmission system is evaluated by coupling the dynamics of each individual gear-rotor system through gear mesh forces generated between each gear-rotor system and the bearing forces generated between the rotor and the gearbox structures. The predicted results were compared with experimental results obtained from a spiral bevel gear fatigue test rig at NASA Lewis Research Center. The Wigner-Ville Distribution (WVD) was used to give a comprehensive comparison of the predicted and experimental results. The WVD method applied to the experimental results were also compared to other fault detection techniques to verify the WVD's ability to detect the pitting damage, and to determine its relative performance. Overall results show good correlation between the experimental vibration data of the damaged test gear and the predicted vibration from the model with simulated gear tooth pitting damage. Results also verified that the WVD method can successfully detect and locate gear tooth wear and pitting damage. Author

N95-12854# National Inst. of Standards and Technology, Gaithersburg, MD. Robot Systems Div.

OVERVIEW OF NASREM: THE NASA/NBS STANDARD REFERENCE MODEL FOR TELEROBOT CONTROL SYSTEM ARCHITECTURE RE

J. S. Albus, R. Quintero, and R. Lumia Apr. 1994 14 p See also PB88-123773 and PB89-193940

(PB94-194560; NISTIR-5412) Avail: CASI HC A03/MF A01

The NASA/NBS Standard Reference Model for Telerobot Control System Architecture (NASREM) was developed by the National Institute of Standards and Technology (NIST) for the National Aeronautics and Space Administration (NASA) to provide a software control system architecture guideline for use by development contractors charged with building the Flight Telerobot Servicer (FTS) control system as part of the Freedom Space Station project. The original NASREM document describes a conceptual or domain-independent architecture, and suggests the outline of a functional or domain-specific architecture for FTS. This paper presents an overview of the NASREM conceptual architecture and reviews subsequent work at NIST in defining a functional architecture for the servo and primitive levels. This work suggests outlines for software and hardware architecture specifications, and software development environments to complement the NASREM conceptual and functional architectures. NTIS

N95-13083*# National Aeronautics and Space Administration. Lewis Research Center, Cleveland, OH.

COMPUTERIZED DESIGN AND GENERATION OF LOW-NOISE HELICAL GEARS WITH MODIFIED SURFACE TOPOLOGY

F. L. Litvin (Chicago Univ., Chicago, IL.), N. X. Chen (Chicago Univ., Chicago, IL.), J. Lu (Chicago Univ., Chicago, IL.), and R. F. Handschuh (Army Research Lab., Cleveland, OH.) Aug. 1994 33 p Presented at the 23rd Mechanisms Conference, Minneapolis, MN, 11-14 Sep. 1994, sponsored by the American Society of Mechanical Engineers Prepared in cooperation with ARL, Cleveland, OH

(RTOP 505-62-36; DA Proj. 1L1-62211-A-47-A)

(NASA-TM-106696; E-9056; NAS 1.15:106696; ARL-TR-573) Avail: CASI HC A03/MF A01

An approach for design and generation of low-noise helical gears with localized bearing contact is proposed. The approach is applied to double circular arc helical gears and modified involute helical gears. The reduction of noise and vibration is achieved by application of a predesigned parabolic

function of transmission errors that is able to absorb a discontinuous linear function of transmission errors caused by misalignment. The localization of the bearing contact is achieved by the mismatch of pinion-gear tooth surfaces. Computerized simulation of meshing and contact of the designed gears demonstrated that the proposed approach will produce a pair of gears that has a parabolic transmission error function even when misalignment is present. Numerical examples for illustration of the developed approach are given. Author

N95-13128# Babcock and Wilcox Co., Lynchburg, VA. Contract Research Div.

GUIDEWAY STRUCTURAL DESIGN AND POWER/PROPULSION/BRAKING IN RELATION TO GUIDEWAYS. VOLUME 3: APPENDIX B: MAGLEV GUIDEWAY STRUCTURAL DESIGN (Diskette Supplement) Final Report, Aug. 1991 - Jan. 1993

K. M. Falkowski, F. S. Key, and S. B. Kuznetsov Jan. 1993 65 p See also PB93-169902 Diskette supplement: 3.5-inch diskette
(Contract DTFR53-91-C-00065)
(PB93-169910; CRD-1277-Vol-3-App-B; DOT/FRA/NMI-92/25-Vol-3-App-B; NONP-NTIS-Suppl-DK-94-28026) Avail: CASI SET A06 (HC,DK)

This final report summarizes work completed in the investigation of the power, propulsion, and braking systems for five different electrodynamic (EDS) Maglev configurations. System requirements and recommendations, including a cost analysis, are determined for each configuration. The analysis considers variations in vehicle length, acceleration'/deceleration criteria, airgap clearance, and maximum propulsion thrust. Five different guideway configurations have been considered, each of which is based on air-core magnets made from low-temperature superconductors (LTSC) - (NbTi, Nb3Sn) or the newer high-T(sub c) ceramic superconductors (HTSCs). The material requirements and cost of the guideway electrical components were studied as a function of the energy conversion efficiency, the stator block length, armature current density, stator temperature rise, and other parameters. The propulsion design focused on a dual-parallel, linear synchronous motor (LSM) with thrust modulation achieved by applying a variable frequency and voltage along the guideway. Critical design parameters were estimated using a three-dimensional computer model for the inductances, magnetic fields, and electromagnetic forces. The study also addressed the conceptual design of the magnet, cryostat, and refrigeration subsystems. Magnetic fields, forces, AC losses, superconductor stability, heat loading, and refrigeration demands were analyzed; a specific design shows limits of passive shielding. NTIS

N95-13155 Department of the Navy, Washington, DC.

MODULAR HYDRAULIC CONTROL SYSTEM Patent

David C. Winyard, inventor (to Navy) and Waldemar C. Lindstrom, inventor (to Navy) 21 Jun. 1994 14 p Filed 30 Sep. 1992
(AD-D016401; US-Patent-5,322,003; US-Patent-Appl-SN-953342; US-Patent-Class-91-363) Avail: US Patent and Trademark Office

A system of modular electrohydraulic servovalves is centrally controlled and may be used to control the operation of critical hydraulic actuators. A programmable controller operates a group of modular servovalves which each deliver a portion of the total actuator fluid requirements. The flow rate, valve position, and valve pressure of each servovalve is monitored by the controller and compared to expected values in memory to determine whether a servovalve malfunction exists. If so, the controller maintains the required flow rate to the actuator by closing the malfunctioning valve and either activating a spare or proportionally increasing the flow rates of the remaining servovalves to compensate for the loss. DTIC

N95-13162# Pacific Northwest Lab., Richland, WA.

THE EFFECT OF PASSIVE DAMPING ON FEEDBACK CONTROL PERFORMANCE OF FLEXIBLE MANIPULATORS

J. Y. Lew and M. S. Evans Jun. 1994 8 p Presented at the 1994 American Control Conference, Baltimore, MD, 29 Jun. - 1 Jul. 1994
(Contract DE-AC06-76RL-01830)
(DE94-015000; PNL-SA-23330; CONF-9406133-2) Avail: CASI HC A02/MF A01

This paper discusses the effect of passive damping on long-reach manipulators. Specifically, this paper explains how the addition of structural damping affects the closed-loop system response of the manipulators. A single-link flexible manipulator is used to illustrate the effects of passive damping on the location of the system's pole s and zeros. The corresponding performance of the system with modified pole/zero locations is discussed. The analysis is performed including colocated and noncolocated flexible-link manipulators. DOE

N95-13183# Argonne National Lab., IL.

A SIMPLIFIED THERMOHYDRODYNAMIC MODEL FOR FLUID FILM BEARINGS

A. Z. Szeri (Pittsburgh Univ., Pittsburgh, PA.) Mar. 1994 78 p
(Contract W-31-109-eng-38)
(DE94-015011; ANL/OTM/CR-7) Avail: CASI HC A05/MF A01

We aim to develop a simplified yet realistic model of fluid film lubrication under thermohydrodynamic conditions, with significant thermal and elastic deformation of the bearing pads. The principal thrust is transfer of technology from the researcher to the industrial designer: the end product will include two user-friendly computer programs, one for journal bearings and the other for thrust bearings, to be used for bearing design in interactive mode on a personal computer. DOE

N95-13189 Department of the Navy, Washington, DC.

DUPLEX ROLLING ELEMENT BEARING MOUNTING FOR ENSURING PRELOAD CONTROL Patent

Thomas L. Daugherty, inventor (to Navy) 31 May 1994 4 p Filed 30 Sep. 1992
(AD-D016402; US-Patent-5,316,393; US-Patent-Appl-SN-953339; US-Patent-Class-384-517) Avail: US Patent and Trademark Office

An apparatus for mounting face-to-face angular contact bearings to ensure preload control is discussed. Face-to-face angular contact paired bearings have inner races and outer races. The inner races or the bearings are fitted on an element to be supported such as a shaft. The outer races of the bearings are fitted in a bearing housing with a first gap Al there between. Preloading of the bearings is achieved by inserting preload springs between external surfaces of the outer races and respective bearing housing surf aces. A second gap A2 may also be provided between the bearing housing and the external surface of one of the outer races to prevent a change in preload due to thermal gradients. DTIC

N95-13410 Technische Univ., Delft (Netherlands). Dept. of Mechanical Engineering and Marine Technology.

STUDY OF IN-PLANE DYNAMICS OF TIRES Ph.D. Thesis

S. Gong 20 Dec. 1993 183 p See also PB93-137594
(PB94-206893; ISBN-90-370-0092-4) Copyright Avail: Issuing Activity (National Technical Information Service (NTIS))

The in-plane dynamics of tires deals with the forces and motion in the plane of rotation of the wheel. Three aspects of tire in-plane dynamics can be identified: the rolling contact between the tire and the road surface; the transmission of forces and motion from the contact patch to the wheel axle; and the vibration of the tire treadband. The main objective of the investigation reported in this thesis is to develop a tire model which is suitable to study all three aspects of the in-plane dynamics of tires in both low and high frequency ranges. The tire model is finally validated by experimental modal analysis of a test tire. Laboratory tests are conducted to establish the modal shapes and natural frequencies of the test tire. The tests are carried out for two different configurations of the tire: one with the wheel rim fixed in space and one with the tire-wheel system suspended freely in the air. Good agreement is found between the experimental and theoretical results. NTIS

N95-13583*# National Aeronautics and Space Administration. Lewis Research Center, Cleveland, OH.

SEALS FLOW CODE DEVELOPMENT 1993

Anita D. Liang, comp. and Robert C. Hendricks, comp. Jul. 1994 380 p Workshop held in Cleveland, OH, 3-4 Nov. 1993
(RTOP 590-21-11)
(NASA-CP-10136; E-8643; NAS 1.55:10136) Avail: CASI HC A17/MF A03

Seals Workshop of 1993 code releases include SPIRALI for spiral grooved cylindrical and face seal configurations; IFACE for face seals with pockets, steps, tapers, turbulence, and cavitation; GFACE for gas face seals with 'lift pad' configurations; and SCISEAL, a CFD code for research and design of seals of cylindrical configuration. GUI (graphical user interface) and code usage was discussed with hands on usage of the codes, discussions, comparisons, and industry feedback. Other highlights for the Seals

Workshop-93 include environmental and customer driven seal requirements; 'what's coming'; and brush seal developments including flow visualization, numerical analysis, bench testing, T-700 engine testing, tribological pairing and ceramic configurations, and cryogenic and hot gas facility brush seal results. Also discussed are seals for hypersonic engines and dynamic results for spiral groove and smooth annular seals. For individual titles, see N95-13584 through N95-13609.

N95-13584*# Walowit (Jed A.), Inc., Clifton Park, NY.
PRESENTATION OF COMPUTER CODE SPIRALI FOR INCOMPRESSIBLE, TURBULENT, PLANE AND SPIRAL GROOVED CYLINDRICAL AND FACE SEALS
Jed A. Walowit *In* NASA. Lewis Research Center, Seals Flow Code Development 1993 Jul. 1994 p 7-20 (For primary document see N95-13583 02-37)
Avail: CASI HC A03/MF A03

A viewgraph presentation is made showing the capabilities of the computer code SPIRALI. Overall capabilities of SPIRALI include: computes rotor dynamic coefficients, flow, and power loss for cylindrical and face seals; treats turbulent, laminar, Couette, and Poiseuille dominated flows; fluid inertia effects are included; rotor dynamic coefficients in three (face) or four (cylindrical) degrees of freedom; includes effects of spiral grooves; user definable transverse film geometry including circular steps and grooves; independent user definable friction factor models for rotor and stator; and user definable loss coefficients for sudden expansions and contractions.
CASI

N95-13585*# Mechanical Technology, Inc., Latham, NY.
CODE GFACE: GAS LUBRICATED FACE SEALS IN LAMINAR REGIME
Wilbur Shapiro *In* NASA. Lewis Research Center, Seals Flow Code Development 1993 Jul. 1994 p 21-34 (For primary document see N95-13583 02-37)
Avail: CASI HC A03/MF A03

A viewgraph presentation is given of the capabilities of the computer code GFACE. Capabilities include: varying geometries, including Rayleigh step, tapered land, and hydrostatic; variable grid; z, x-x, and y-y degrees of freedom; can determine position as a function of load; and English or SI units.
CASI

N95-13586*# CFD Research Corp., Huntsville, AL.
SCISEAL: A CFD CODE FOR ANALYSIS OF FLUID DYNAMIC FORCES IN SEALS
Mahesh Athavale and Andrzej Przekwas *In* NASA. Lewis Research Center, Seals Flow Code Development 1993 Jul. 1994 p 35-58 (For primary document see N95-13583 02-37)
Avail: CASI HC A03/MF A03

A viewgraph presentation is made of the objectives, capabilities, and test results of the computer code SCISEAL. Currently, the seal code has: a finite volume, pressure-based integration scheme; colocated variables with strong conservation approach; high-order spatial differencing, up to third-order; up to second-order temporal differencing; a comprehensive set of boundary conditions; a variety of turbulence models and surface roughness treatment; moving grid formulation for arbitrary rotor whirl; rotor dynamic coefficients calculated by the circular whirl and numerical shaker methods; and small perturbation capabilities to handle centered and eccentric seals.
CASI

N95-13587*# Mechanical Technology, Inc., Latham, NY.
USER INTERFACE DEVELOPMENT
Bharat Aggrawal *In* NASA. Lewis Research Center, Seals Flow Code Development 1993 Jul. 1994 p 59-66 (For primary document see N95-13583 02-37)
Avail: CASI HC A02/MF A03

This viewgraph presentation describes the development of user interfaces for OS/2 versions of computer codes for the analysis of seals. Current status, new features, work in progress, and future plans are discussed.
CASI

N95-13588*# National Aeronautics and Space Administration. Lewis Research Center, Cleveland, OH.
ENVIRONMENTAL AND CUSTOMER-DRIVEN SEAL REQUIREMENTS
Robert C. Hendricks *In its* Seals Flow Code Development 1993 Jul. 1994 p 67-78 (For primary document see N95-13583 02-37)
Avail: CASI HC A03/MF A03

Public awareness of environmental hazards, well-publicized effects of hazardous leakages (Three Mile Island, Challenger), and a general concern for planet earth have precipitated emission limits that drive the design requirements for seals applications. Types of seals, barrier fluids, and the necessity of thin lubricating films and stable turbomachine operation to minimize leakage and material losses generated by rubbing contact are discussed.
Author

N95-13589*# Rotordynamics-Seal Research, Inc., North Highlands, CA.
BETA TESTING OF MTI SEAL CODES
Joseph Scharrer *In* NASA. Lewis Research Center, Seals Flow Code Development 1993 Jul. 1994 p 79-86 (For primary document see N95-13583 02-37)
Avail: CASI HC A02/MF A03

An evaluation of MTI seal codes is made by comparing cylindrical air and water seals. Results are presented in viewgraph format and show that: ICYL and GCYL geometry variations are desirable; load and direct stiffness calculations are good; damping and cross-coupled stiffness predictions are poor; added mass coefficients should be calculated; and variation in inlet tangential velocity is critical to design.
CASI

N95-13590*# EG and G Sealol, Cranston, RI.
EG AND G AND NASA FACE SEAL CODES COMPARISON
Prit Basu *In* NASA. Lewis Research Center, Seals Flow Code Development 1993 Jul. 1994 p 87-98 (For primary document see N95-13583 02-37)
Avail: CASI HC A03/MF A03

This viewgraph presentation presents the following results for the example comparison: EG&G code with face deformations suppressed and SPIRALG agree well with each other as well as with the experimental data; 0 rpm stiffness data calculated by EG&G code are about 70-100 percent lower than that by SPIRALG; there is no appreciable difference between 0 rpm and 16,000 rpm stiffness and damping coefficients calculated by SPIRALG; and the film damping above 500 psig calculated by SPIRALG is much higher than the O-Ring secondary seal damping (e.g. 50 lbf.s/in).
Derived from text

N95-13591*# National Aeronautics and Space Administration. Lewis Research Center, Cleveland, OH.
DEVELOPMENT OF A BRUSH SEALS PROGRAM LEADING TO CERAMIC BRUSH SEALS
Robert C. Hendricks, Ralph Flower, and Harold Howe *In its* Seals Flow Code Development 1993 Jul. 1994 p 99-118 Sponsored in part by Army (For primary document see N95-13583 02-37)
Avail: CASI HC A03/MF A03

Some events of a U.S. Army/NASA Lewis Research Center brush seals program are reviewed, and the development of ceramic brush seals is described. Some preliminary room-temperature flow data are given, and the results of testing metallic brushes in cryogenic nitrogen are discussed.
Author

N95-13592*# National Aeronautics and Space Administration. Lewis Research Center, Cleveland, OH.
BRUSH SEALS FOR CRYOGENIC APPLICATIONS
Margaret P. Proctor *In its* Seals Flow Code Development 1993 Jul. 1994 p 119-130 (For primary document see N95-13583 02-37)
Avail: CASI HC A03/MF A03

This viewgraph presentation presents test results of brush seals for cryogenic applications. Leakage for a single brush seal was two to three times less than for a 12-tooth labyrinth seal. The maximum temperature rise for a single brush seal was less than 50 R and occurred at 25 psid across the seal and 35,000 rpm. A static blowout test demonstrated sealing capability up to 550 psid. The seal limit was not obtained. The power loss for a single brush at 35,000 rpm and 175 psid was 2.45 hp. Two brushes far apart leak less than two brushes tight packed. Rotor wear was approximately 0.00075 mils and bristle wear was 1-3 mils after 4-1/2 hours.
Derived from text

N95-13593*# National Aeronautics and Space Administration. Lewis Research Center, Cleveland, OH.
HIGH TEMPERATURE SEAL TEST RIG **c09**
Harold E. Addy, Jr. *In its* Seals Flow Code Development 1993 Jul. 1994 p 131-132 (For primary document see N95-13583 02-37)
Avail: CASI HC A01/MF A03

The High Temperature Seals Test Rig Program at NASA's Lewis Research Center is a joint effort involving three separate federal government agencies. Testing has been underway at Lewis in this test rig since April, 1993. The rig was designed to run tests at temperatures to 800 F at pressures to 200 psia or at temperatures to 1300 to 1500 F at pressures to 65 psia. It was designed to run at speeds of up to 50,000 rpm which, for a 5.1 inch diameter disk, is a surface speed of about 1100 ft./sec. The rig was designed to allow easy replacement of the disks as well as the seals such that different disk materials and coatings may be tested.
Derived from text

N95-13594*# Technetics, Inc., DeLand, FL.
CERAMIC BRUSH SEALS DEVELOPMENT
Harold Howe *In* NASA. Lewis Research Center, Seals Flow Code Development 1993 Jul. 1994 p 133-150 (For primary document see N95-13583 02-37)
Avail: CASI HC A03/MF A03

The following topics are discussed in this viewgraph presentation: ceramic brush seals, research and development, manufacturing, brazed assembly development, controlling braze flow, fiber selection, and braze results.
CASI

N95-13595*# General Electric Co., Lynn, MA. Aircraft Engines.
BRUSH SEALS FOR TURBINE ENGINE FUEL CONSERVATION
Mike Sousa *In* NASA. Lewis Research Center, Seals Flow Code Development 1993 Jul. 1994 p 151-158 (For primary document see N95-13583 02-37)
Avail: CASI HC A02/MF A03

The program objective is to demonstrate brush seals for replacing labyrinth seals in turboprop engines. The approach taken was to design and procure brush seals with assistance from Sealol, modify and instrument an existing T407 low pressure turbine test rig, replace inner balance piston and outer balance piston labyrinth seals with brush seals, conduct cyclic tests to evaluate seal leakage at operating pressures and temperatures, and evaluate effect of seal pack width and rotor eccentricity. Results are presented in viewgraph format and show that brush seals offer performance advantages over labyrinth seals.
Derived from text

N95-13596*# Akron Univ., OH. Dept. of Mechanical Engineering.
BRUSH SEAL NUMERICAL SIMULATION: CONCEPTS AND ADVANCES
M. J. Braun and V. V. Kudriavtsev *In* NASA. Lewis Research Center, Seals Flow Code Development 1993 Jul. 1994 p 159-198 (For primary document see N95-13583 02-37)
Avail: CASI HC A03/MF A03

The development of the brush seal is considered to be most promising among the advanced type seals that are presently in use in the high speed turbomachinery. The brush is usually mounted on the stationary portions of the engine and has direct contact with the rotating element, in the process of limiting the 'unwanted' leakage flows between stages, or various engine cavities. This type of sealing technology is providing high (in comparison with conventional seals) pressure drops due mainly to the high packing density (around 100 bristles/sq mm), and brush compliance with the rotor motions. In the design of modern aerospace turbomachinery leakage flows between the stages must be minimal, thus contributing to the higher efficiency of the engine. Use of the brush seal instead of the labyrinth seal reduces the leakage flow by one order of magnitude. Brush seals also have been found to enhance dynamic performance, cost less, and are lighter than labyrinth seals. Even though industrial brush seals have been successfully developed through extensive experimentation, there is no comprehensive numerical methodology for the design or prediction of their performance. The existing analytical/numerical approaches are based on bulk flow models and do not allow the investigation of the effects of brush morphology (bristle arrangement), or brushes arrangement (number of brushes, spacing between them), on the pressure drops and flow leakage. An increase in the brush seal efficiency is clearly a complex problem that is closely related to the brush geometry and arrangement, and can be solved most likely only by means of a numerically distributed model.
Author

N95-13597*# EG and G Sealol, Cranston, RI. Fluid Components Technology Group.
CURRENT DEVELOPMENTS IN BRUSH SEALS
Bob Loewenthal *In* NASA. Lewis Research Center, Seals Flow Code Development 1993 Jul. 1994 p 199-208 (For primary document see N95-13583 02-37)
Avail: CASI HC A02/MF A03

The objective of the brush seal development program is to develop a comprehensive design methodology for brush seals using application requirements from engine manufacturers and experimental characterization of seal design and tribological pairs. The goals are to substantially lower leakage compared to labyrinth seals, seal life consistent with man-rated mission requirements, to investigate single and multiple staged brush seals, temperature up to 1200 F and surface speed up to 900 fps, and pressure drop across the seal of 50 psid. Test results are presented in viewgraph format.
Derived from text

N95-13598*# Crane (John), Inc., Morton Grove, IL.
COMPUTER TOOLS FOR FACE SEAL ANALYSES DEVELOPED AT JOHN CRANE
Shifeng Wu *In* NASA. Lewis Research Center, Seals Flow Code Development 1993 Jul. 1994 p 209-218 (For primary document see N95-13583 02-37)
Avail: CASI HC A02/MF A03

The purposes of the computer tools for face seal analysis are new product optimization, existing seals on new applications, existing seals on off-duty conditions, and trouble-shooting. Discussed in this viewgraph presentation are interface forces, friction/heat generation, heat transfer/temperature distribution, axisymmetric pressure/thermal distortion, leakage, and an example case.
CASI

N95-13599*# Detroit Diesel Allison, Indianapolis, IN.
COMPRESSOR DISCHARGE FILM RIDING FACE SEALS
John Munson *In* NASA. Lewis Research Center, Seals Flow Code Development 1993 Jul. 1994 p 219-226 (For primary document see N95-13583 02-37)
Avail: CASI HC A02/MF A03

Seals examined were the eight-pad Rayleigh step, the tapered spiral groove, and two hydrostatic seals. The spiral groove configuration is the preferred choice because of superior stiffness. Second choice is Rayleigh step because of combined higher operating film thickness and good stiffness at low clearance. Recess hydrostatic has reasonable performance, but stiffness falls off at low clearance. Also, pneumatic hammer characteristics must be investigated. Experience at high pressure ratios is limited. An advantage is that it would have good low speed performance.
Derived from text

N95-13600*# Wright Lab., Wright-Patterson AFB, OH. Aero Propulsion and Power Directorate.
AIR FORCE SEAL ACTIVITIES
Ellen R. Mayhew *In* NASA. Lewis Research Center, Seals Flow Code Development 1993 Jul. 1994 p 227-234 (For primary document see N95-13583 02-37)
Avail: CASI HC A02/MF A03

Seal technology development is an important part of the Air Force's participation in the Integrated High Performance Turbine Engine Technology (IHPTET) initiative, the joint DOD, NASA, ARPA, and industry endeavor to double turbine engine capabilities by the turn of the century. Significant performance and efficiency improvements can be obtained through reducing internal flow system leakage, but seal environment requirements continue to become more extreme as the engine thermodynamic cycles advance towards these IHPTET goals. Brush seal technology continues to be pursued by the Air Force to reduce leakage at the required conditions. Likewise, challenges in engine mainshaft air/oil seals are also being addressed. Counter-rotating intershaft applications within the IHPTET initiative involve very high rubbing velocities. This viewgraph presentation briefly describes past and current seal research and development programs and gives a

summary of seal applications in demonstrator and developmental engine testing. Author (revised)

N95-13601*# General Motors Corp., Lagrange, IL.
HIGH-SPEED SEAL AND BEARING TEST FACILITY **c09**
Jean B. Panos *In* NASA. Lewis Research Center, Seals Flow Code Development 1993 235-238 (SEE N95-13583 02-37) Jul. 1994 (For primary document see N95-13583 02-37)
Avail: CASI HC A01/MF A03

The following topics are discussed in this viewgraph presentation: high speed seal/bearing rig background, project status, facility features, test rig capabilities, EMD testing advantages, and future opportunities. CASI

N95-13602*# National Aeronautics and Space Administration. Lewis Research Center, Cleveland, OH.
HYPERSONIC ENGINE SEAL DEVELOPMENT AT NASA LEWIS RESEARCH CENTER
Bruce M. Steinetz *In its* Seals Flow Code Development 1993 Jul. 1994 p 239-248 (For primary document see N95-13583 02-37)
Avail: CASI HC A02/MF A03

NASA Lewis Research Center is developing advanced seal concepts and sealing technology for advanced combined cycle ramjet/scramjet engines being designed for the National Aerospace Plane (NASP). Technologies are being developed for both the dynamic seals that seal the sliding interfaces between articulating engine panels and sidewalls, and for the static seals that seal the heat exchanger to back-up structure interfaces. This viewgraph presentation provides an overview of the candidate engine seal concepts, seal material assessments, and unique test facilities used to assess the leakage and thermal performance of the seal concepts. Author (revised)

N95-13603*# Texas A&M Univ., College Station, TX. Turbomachinery Lab.
THEORETICAL VERSUS EXPERIMENTAL RESULTS FOR THE ROTORDYNAMIC COEFFICIENTS OF ECCENTRIC, SMOOTH, GAS ANNULAR SEAL ANNULAR GAS SEALS
Dara W. Childs and Chis Alexander *In* NASA. Lewis Research Center, Seals Flow Code Development 1993 Jul. 1994 p 249-266 (For primary document see N95-13583 02-37)
Avail: CASI HC A03/MF A03

This viewgraph presentation presents the following results: (1) The analytical results overpredict the experimental results for the direct stiffness values and incorrectly predict increasing stiffness with decreasing pressure ratios. (2) Theory correctly predicts increasing cross-coupled stiffness, K(sub YX), with increasing eccentricity and inlet preswirl. (3) Direct damping, C(sub XX), underpredicts the experimental results, but the analytical results do correctly show that damping increases with increasing eccentricity. (4) The whirl frequency values predicted by theory are insensitive to changes in the static eccentricity ratio. Although these values match perfectly with the experimental results at 16,000 rpm, the results at the lower speed do not correspond. (5) Theoretical and experimental mass flow rates match at 5000 rpm, but at 16,000 rpm the theoretical results overpredict the experimental mass flow rates. (6) Theory correctly shows the linear pressure profiles and the associated entrance losses with the specified rotor positions. Derived from text

N95-13604*# Texas A&M Univ., College Station, TX. Turbomachinery Lab.
TURBOMACHINERY LABORATORY TEXAS A AND M UNIVERSITY RESEARCH PROGRESS ON ANNULAR GAS SEALS
Dara W. Childs *In* NASA. Lewis Research Center, Seals Flow Code Development 1993 Jul. 1994 p 267-284 (For primary document see N95-13583 02-37)
Avail: CASI HC A03/MF A03

Three helically-grooved seals were tested and the results were compared to the MTI code SPIRALG. A smooth annular seal was tested at six eccentricity ratios from 0 to 0.5. The following are concluded in this viewgraph presentation: (1) Helical-grooved seals provide a substantial reduction in cross-coupled stiffness coefficients. Negative k(sub xy) values are obtained for no-swirl or low-swirl cases. (2) SPIRALG is completely unsuitable for the type of seal tested, namely, turbulent flow, wide grooves and lands, etc. (3) A good analysis code is needed to guide the design of helically-grooved annular seals including groove and smooth sections. Derived from text

N95-13605*# National Aeronautics and Space Administration. Lewis Research Center, Cleveland, OH.
PRESSURE MEASUREMENTS OF A THREE WAVE JOURNAL AIR BEARING
Florin Dimofte and Harold E. Addy, Jr. *In its* Seals Flow Code Development 1993 Jul. 1994 p 285-294 (For primary document see N95-13583 02-37)
Avail: CASI HC A02/MF A03

In order to validate theoretical predictions of a wave journal bearing concept, a bench test rig was assembled at NASA Lewis Research Center to measure the steady-state performance of a journal air bearing. The tester can run up to 30,000 RPM and the spindle has a run out of less than 1 micron. A three wave journal bearing (50 mm diameter and 58 mm length) has been machined at NASA Lewis. The pressures at 16 ports along the bearing circumference at the middle of the bearing length were measured and compared to the theoretical prediction. The bearing ran at speeds up to 15,000 RPM and certain loads. Good agreement was found between the measured and calculated pressures. Author

N95-13606*# Mechanical Technology, Inc., Latham, NY.
INCOMPRESSIBLE FACE SEALS: COMPUTER CODE IFACE
Antonio Artiles *In* NASA. Lewis Research Center, Seals Flow Code Development 1993 Jul. 1994 p 295-304 (For primary document see N95-13583 02-37)
Avail: CASI HC A02/MF A03

Capabilities of the computer code IFACE are given in viewgraph format. These include: two dimensional, incompressible, isoviscous flow; rotation of both rotor and housing; roughness in both rotor and housing; arbitrary film thickness distribution, including steps, pockets, and tapers; three degrees of freedom; dynamic coefficients; prescribed force and moments; pocket pressures or orifice size; turbulence, Couette and Poiseuille flow; cavitation; and inertia pressure drops at inlets to film. Derived from text

N95-13607*# National Aeronautics and Space Administration. Lewis Research Center, Cleveland, OH.
RELATIVE PERFORMANCE COMPARISON BETWEEN BASELINE LABYRINTH AND DUAL-BRUSH COMPRESSOR DISCHARGE SEALS IN A T-700 ENGINE TEST
Robert C. Hendricks, Thomas A. Griffin, Kristine R. Csavina, Arvind Pancholi, and Dvandra Sood *In its* Seals Flow Code Development 1993 Jul. 1994 p 305-324 (For primary document see N95-13583 02-37)
Avail: CASI HC A03/MF A03

In separate series of T-700 engine tests, direct comparisons were made between the forward-facing labyrinth and dual-brush compressor discharge seals. Compressor speeds to 43,000 rpm, surface speeds to 160 m/s (530 ft/s), pressures to 1 MPa (145 psi), and temperatures to 680 K (765 F) characterized these tests. The wear estimate for 40 hr of engine operations was less than 0.025 mm (0.001 in.) of the Haynes 25 alloy bristles running against a chromium-oxide-coated rub runner. The pressure drops were higher for the dual-brush than for the forward-facing labyrinth seal, implying better seal characteristics and engine performance for the brush seal. Modification of the secondary flow path requires that changes in cooling air and engine dynamics be accounted for. Author

N95-13608*# National Aeronautics and Space Administration. Lewis Research Center, Cleveland, OH.
SOME METALLOGRAPHIC RESULTS FOR BRUSH BRISTLES AND BRUSH SEGMENTS OF A SHROUD RING BRUSH SEAL TESTED IN A T-700 ENGINE
Robert C. Hendricks, Thomas A. Griffin, George A. Bobula, Robert C. Bill, David R. Hull, and Kristine R. Csavina *In its* Seals Flow Code Development 1993 Jul. 1994 p 325-366 (For primary document see N95-13583 02-37)
Avail: CASI HC A03/MF A03

Post-test investigation of a T-700 engine brush seal found regions void of bristles ('yanked out'), regions of bent-over bristles near the inlet, some 'snapped' bristles near the fence, and a more uniform smeared bristle interface between the first and last axial rows of bristles. Several bristles

and four brush segments were cut from the brush seal, wax mounted, polished, and analyzed. Metallographic analysis of the bristle near the rub tip showed tungsten-rich phases uniformly distributed throughout the bristle, no apparent change within 1 mu m of the interface, and possibly a small amount of titanium, which would represent a transfer from the rotor. Analysis of the bristle wear face showed nonuniform tungsten, which is indicative of material resolidification. The cut end contained oxides and internal fractures; the worn end was covered with oxide scale. Material losses due to wear and elastoplastic deformation within the shear zone and third-body lubrication effects in the contact zone are discussed. Author

N95-13609*# Technische Univ., Brunswick (Germany). Inst. fuer Maschinenelemente und Foerdertechnik.
NON-CONTACTING GAS LUBRICATED FACE SEALS FOR HIGH p x v-VALUES
J. Glienicke, A. Launert, H. Schums, and B. Kohring *In* NASA. Lewis Research Center, Seals Flow Code Development 1993 Jul. 1994 p 367-378 (For primary document see N95-13583 02-37)
(Contracts AIF-7089; AIF-8084)
Avail: CASI HC A03/MF A03

The authors discuss recently developed mathematical fundamentals concerning the calculation of noncontacting gas lubricated face seals. They carried out extensive experiments using three different designs at pressures up to 10 MPa and sliding velocities up to 110 m/s. A comparison between the experimental results and the calculations indicates that a stable operation without wear can be ensured in all cases, provided that the materials and geometrical parameters of the seal have been properly chosen.
Author (revised)

38 QUALITY ASSURANCE AND RELIABILITY

Includes product sampling procedures and techniques; and quality control.

N95-11813*# Pennsylvania State Univ., University Park, PA. Dept. of Engineering Science and Mechanics.
THE INFLUENCE OF FINITE-SIZE SOURCES IN ACOUSTO-ULTRASONICS Final Report
Brian N. Pavlakovic and Joseph L. Rose Aug. 1994 103 p
(Grant NAG3-1365; RTOP 505-90-51)
(NASA-CR-195374; E-9061; NAS 1.26:195374) Avail: CASI HC A06/MF A02

This work explores the effects that the finite normal axisymmetric traction loading of an infinite isotropic plate has on wave propagation in acousto-ultrasonics (AU), in which guided waves are created using two normal incidence transducers. Although the work also addresses the effects of the transducer pressure distribution and pulse shape, this thesis concentrates on two main questions: how does the transducer's diameter control the phase velocity and frequency spectrum of the response, and how does the plate thickness relate to the plate's excitability? The mathematics of the time-harmonic solution and the physical principles and the practical considerations for AU wave generation are explained. Transient sources are modeled by the linear superposition of the time-harmonic solutions found using the Hankel transform and they are then compared to experimental data to provide insight into the relation between the size of the transducer and the preferred phase velocity. Author (revised)

N95-11822# Technische Univ., Delft (Netherlands).
REVEALING HIDDEN DEFECTS: A HYBRID EVALUATION STRATEGY FOR STEEL STRUCTURES Ph.D. Thesis
D. J. Chinn 11 Oct. 1993 169 p
(PB94-191236; ISBN-90-6275-892-4) Copyright Avail: CASI HC A08/MF A02

A void exists between the capabilities of inspection and monitoring. The goal of this research is to develop a hybrid method which ideally incorporates the advantages of both inspection and monitoring. Economically, a hybrid method should allow localized inspection without extensive operations. This can be accomplished by testing large global areas with one set of measurements as in monitoring methods. Operations are facilitated if the hybrid method requires only long-range accessibility. With respect to performance, a hybrid method should detect, locate and characterize a full range of defects including small cracks, through-wall cracking and extensive longitudinal and circumferential cracking. In this way, fatigue crack growth can be tracked and repaired as necessary. For reliability, data from a hybrid method should be recordable and reproducible. NTIS

N95-11994* Oklahoma Univ., Norman, OK. School of Industrial Engineering.
A DECISION SUPPORT SYSTEM FOR TOLERANCE ALLOCATION (Diskette)
Pakize Simin Pulat and Shivakumar Raman Aug. 1993 138 p Diskette: 3.5-inch DSHD
(Grant NAG8-137)
(NASA-CR-195817; NAS 1.26:195817; NONP-NASA-DK-94-5869) Avail: CASI SET A09 (HC,DK)

Tolerance design for discrete parts requires extensive data, handbooks and/or complex mathematical models. Decision support expert systems are needed that integrate such information to simplify tolerance design. In this research, user-friendly decision support tools for automated tolerance allocation and tolerance analysis are developed. The tolerance allocation prototype can provide component tolerances based on assembly specification. Handbook-based tolerances or optimal tolerances can be designed based on user interaction. Tolerance analysis determines the assembly tolerance for a given chain of component tolerances based on different analysis models and a decision-chart. Other research conducted include a methodology for indirect tolerance transfer to manufacturing and a new methodology for simultaneous process selection and tolerance allocation. Author

N95-12381*# California State Univ., Fullerton, CA.
RELIABILITY AND COST ANALYSIS METHODS Final Report
Ronald C. Suich 1991 15 p Revised
(Grant NAG3-1100)
(NASA-CR-196326; NAS 1.26:196326) Avail: CASI HC A03/MF A01

In the design phase of a system, how does a design engineer or manager choose between a subsystem with .990 reliability and a more costly subsystem with .995 reliability? When is the increased cost justified? High reliability is not necessarily an end in itself but may be desirable in order to reduce the expected cost due to subsystem failure. However, this may not be the wisest use of funds since the expected cost due to subsystem failure is not the only cost involved. The subsystem itself may be very costly. We should not consider either the cost of the subsystem or the expected cost due to subsystem failure separately but should minimize the total of the two costs, i.e., the total of the cost of the subsystem plus the expected cost due to subsystem failure. This final report discusses the Combined Analysis of Reliability, Redundancy, and Cost (CARRAC) methods which were developed under Grant Number NAG 3-1100 from the NASA Lewis Research Center. CARRAC methods and a CARRAC computer program employ five models which can be used to cover a wide range of problems. The models contain an option which can include repair of failed modules. Author

N95-12391*# Alabama Univ., Huntsville, AL.
PROBABILITY OF DETECTION OF DEFECTS IN COATINGS WITH ELECTRONIC SHEAROGRAPHY Final Technical Report, 3 Jun. 1993 - 2 Jun. 1994
Gary A. Maddux, Charles M. Horton, Matthew D. Lansing, William J. Gnacek, and Patrick L. Newton Jul. 1994 22 p
(Contract NAS8-38609)
(NASA-CR-196201; UAH-5-33267; NAS 1.26:196201) Avail: CASI HC A03/MF A01

The goal of this research was to utilize statistical methods to evaluate the probability of detection (POD) of defects in coatings using electronic shearography. The coating system utilized in the POD studies was to be the paint system currently utilized on the external casings of the NASA Space Transportation System (STS) Revised Solid Rocket Motor (RSRM) boosters. The population of samples was to be large enough to determine the minimum defect size for 90 percent probability of detection of 95 percent confidence POD on these coatings. Also, the best methods to excite coatings on aerospace components to induce deformations for measurement by electronic shearography were to be determined. Author

N95-13406 Newcastle-upon-Tyne Univ., Newcastle (England). Dept. of Computing Science.
RELIABILITY ALLOCATION FOR A SYSTEM USING MARKOV ANALYSIS
R. Burnett and T. Anderson Jun. 1994 23 p
(PB94-205051; TRS-477) Copyright Avail: Issuing Activity (National Technical Information Service (NTIS))

This report proposes a method for allocating an appropriate reliability requirement to each module of a modular software system, using Markov analysis. A formula to calculate an estimate of the overall system reliability is established. From that formula, a procedure to allocate the reliability requirement for each module is derived using an optimization process, taking into account the known overall required level of reliability. NTIS

39 STRUCTURAL MECHANICS

Includes structural element design and weight analysis; fatigue; and thermal stress.

For applications see *05 Aircraft Design, Testing and Performance* and *18 Spacecraft Design, Testing and Performance.*

N95-11698# Polish Academy of Sciences, Warsaw (Poland). Inst. Podstawowych Problemow Techniki.
A STOCHASTIC MODEL OF FATIGUE CRACK GROWTH [STOCHASTYCZNY MODEL WZROSTU SZCZELINY ZMECZENIOWEJ]
Krzysztof Dolinski 1992 177 p In POLISH
(ISSN 0208-5658)
Avail: CASI HC A09/MF A02

In the process of modeling any mechanical phenomenon, we must always ask whether a purely deterministic approach in which all values are assumed to be clearly defined is adequate. Is it capable of describing the phenomenon in question accurately enough for our purposes? Will the solutions we obtain guarantee a design which is safe enough in terms of subsequent use of the structure it represents? Do the experimental results allow us to interpret the phenomenon in a purely deterministic manner and ignore their variance or attribute it to measurement error? It is not often that we can answer these questions in the affirmative, even though the answers will determine the accuracy and most importantly the adequacy of the deterministic concept for modeling other phenomena besides mechanical ones. Despite this, researchers will continue to construct deterministic models for a long time to come and use them as an idealization which will often suffice for practical purposes and at the same time will allow them to avoid the difficulties associated with the use of stochastic methods. But technological advances and the more stringent requirements for the safety and strength of structures have compelled us to use statistics, probability theory, and the theory of stochastic processes in order to account for the random character of the material and the loads it is subjected to and thus abandon our deterministic interpretation of the variables which describe the phenomenon in question. Transl. by SCITRAN

N95-11711*# General Electric Co., Cincinnati, OH.
ENGINE STRUCTURES ANALYSIS SOFTWARE: COMPONENT SPECIFIC MODELING (COSMO) Final Report
R. L. McKnight, R. J. Maffeo, and S. Schwartz Cleveland, OH NASA Aug. 1994 74 p
(Contract NAS3-26617; RTOP 505-63-5B)
(NASA-CR-195378; E-9093; NAS 1.26:195378) Avail: CASI HC A04/MF A01

A component specific modeling software program has been developed for propulsion systems. This expert program is capable of formulating the component geometry as finite element meshes for structural analysis which, in the future, can be spun off as NURB geometry for manufacturing. COSMO currently has geometry recipes for combustors, turbine blades, vanes, and disks. Component geometry recipes for nozzles, inlets, frames, shafts, and ducts are being added. COSMO uses component recipes that work through neutral files with the Technology Benefit Estimator (T/BEST) program which provides the necessary base parameters and loadings. This report contains the users manual for combustors, turbine blades, vanes, and disks. Author (revised)

N95-11768 ESDU International Ltd., London (England).
PIPELINE VIBRATIONS. COMPUTER PROGRAM FOR THE PREDICTION OF FLUID TRANSIENTS IN FLEXIBLE, UNBRANCHED THREE-DIMENSIONAL PIPING SYSTEMS
May 1994 50 p
(ISSN 0141-4011)
(ESDU-93031; ISBN-0-85679-884-3) Avail: ESDU

ESDU 93031 directly accounts for the mutual coupling between internal pressure and flow conditions, and the stresses and structural motion of the pipework. The system must consist of straight pipes each of uniform cross section and material properties and each aligned with one of a set of orthogonal axes. It is assumed that all bends remain right angles and do not flex. Externally-acting rigid supports can be modelled at any location in any or all the three translational and three rotational degrees of freedom. The system can have a reservoir or a centrifugal pump (running at constant speed or running down after trip) at the upstream end, and a reservoir or a valve (opening, closing or fixed) at the downstream end. Data on the pump characteristics and rotor inertia are required (although default data are included) and allowance may be made for backflow. The valve may be closed instantaneously, with a linear area change with time, or an area/time closure curve may be input. Output includes steady-state values, together with maximum and minimum values and their location, of pressure, velocity, pipe displacement, axial and shear forces in the walls, and torsional and bending moments in the walls; the time variation of user-chosen variables at selected locations over the run time can also be provided. Criteria by which it can be established whether structural coupling is important are defined and their use discussed. The program is available on disc in the software volume as ESDUpac A9331 running only under MS DOS in the user-friendly ESDUview shell that prompts for all the input data and provides context-sensitive help facilities. Author

N95-11769 ESDU International Ltd., London (England).
STIFFNESSES OF LAMINATED FLAT PLATES
Apr. 1994 24 p Supersedes ESDU-75002
(ISSN 0141-4097; ISSN 0958-0360)
(ESDU-94003; ESDU-75002; ISBN-0-85679-890-8) Avail: ESDU

ESDU 94003 gives formulae for the in-plane and flexural stiffnesses of laminated flat plates built-up from thin orthotropic layers that may have different material properties, thicknesses, and orientations of their principal axes of orthotropy. The influence of the lay-up arrangement on the plate stiffnesses is explained. A complete list of possible forms of the stiffness matrices is provided with in each case examples of possible lay-up arrangements that will give them. Although it is normally convenient to use the central plane of the plate as the reference plane, subsequent calculations may be simplified by adopting another parallel reference plane; formulae are given for the values of the coupled in-plane and flexural stiffness matrix and the flexural stiffness matrix of the plate for such a shift of reference plane. The in-plane stiffness matrix is unaffected. A worked example illustrates the calculation of the stiffnesses. The relationship between the stiffnesses of a layer and the complete matrix of the elastic constants for an anisotropic solid is included. The relationship of the stiffnesses of both isotropic plates and sandwich panels with the laminated plate stiffnesses is also given. Equations are given relating the stress and strain in a layer in one axis system to those in another. The formulae apply to composite plates with systematic fibrous reinforcements in metallic or non-metallic matrices. Author

N95-11770 ESDU International Ltd., London (England).
STRESS ANALYSIS OF LAMINATED FLAT PLATES
Apr. 1994 16 p Supersedes ESDU-74039
(ISSN 0141-4097; ISSN 0958-0360)
(ESDU-94004; ESDU-74039; ISBN-0-85679-891-6) Avail: ESDU

ESDU 94004 gives equations for the strains and stresses, and curvatures where appropriate, in laminated flat plates as a result of either loading actions or the differential contractions and expansions that occur due to temperature changes in the usual working environment or temperature change from the curing temperature to the working temperature, or a combination of both effects. The plates may be built-up from orthotropic layers having different material elastic and thermal properties, thicknesses, and orientations of their principal axes of orthotropy. The equations apply to balanced laminates, when no curvature will be induced by the thermal effects. They also apply to unbalanced laminates in which case equations

give the stresses induced by thermal effects when the plate is held flat, either with or without an in-plane loading. Worked examples for the stresses in a balanced plate due to external loading and built-in stresses in the faceplate of a sandwich panel illustrate the use of the equations. Author

N95-11771 ESDU International Ltd., London (England).
BUCKLING OF FLAT RECTANGULAR ORTHOTROPIC PLATES
Apr. 1994 22 p Supersedes ESDU-73003
(ISSN 0141-4097; ISSN 0958-0360)
(ESDU-94005; ESDU-73003; ISBN-0-85679-892-4) Avail: ESDU

ESDU 94005 introduces a Fortran program, A9405, that calculates the buckling load for the plate for uniform, in-plane uniaxial or biaxial direct loading with or without shear. The program deals with all symmetrical combinations of clamped and simply-supported edge conditions and takes account of out-of-plane shear deformations. It applies to isotropic materials, sandwich panels and specially-orthtropic laminated plates. The input to the program includes the plate stiffnesses; ESDU 68029 gives guidance on estimating them for a sandwich panel and ESDU 81047 provides a program to calculated the stiffnesses for a laminated plate from the layer properties. Given one or two of the applied load components, the program will calculate a specified load to cause buckling (or warn that buckling has already occurred); alternatively, given the ratios of the three loads one to another it will provide that loads in the same ratio at buckling. The full input and output to the program is explained, and illustrated with worked examples, and warning messages that may be output are indicated. The program is provided on disc (uncompiled) in the software volume and compiled within ESDUview, a user-friendly shell running under MS DOS that prompts on screen for input data. Author

N95-11772 ESDU International Ltd., London (England).
ELASTIC BUCKLING OF UNBALANCED LAMINATED FIBRE REINFORCED COMPOSITE PLATES (RECTANGULAR PLATES OF AsBtDs TYPE, ALL EDGES SIMPLY-SUPPORTED UNDER BIAXIAL LOADING)
Apr. 1994 32 p Supersedes ESDU-86020
(ISSN 0141-4097; ISSN 0958-0360)
(ESDU-94006; ESDU-86020; ISBN-0-85679-893-2) Avail: ESDU

ESDU 94006 introduces a Fortran program, ESDUpac A9406, for calculating the buckling loading of composite plates for which in both the direct and flexural stiffness matrices the first two terms in the last column and last row are zero and in the coupling stiffness matrix the first two terms of the first two rows and the last term of the third row are zero. Such stiffness matrices arise when the fibers are all laid to make the same angle with a plate edge, but the angles are of opposite signs in each pair of laminae equidistant from the centre plane. The plate is assumed to be initial flat and rectangular, with loading applied uniformly along the edges. No account is taken of through-the-thickness shear deformation. Uniaxial or biaxial loading (in which one load can be tensile) is treated; under biaxial loading either one load may be fixed, and the other at buckling determined, or the ratio of the load may be fixed, and the loads in that ratio at buckling found. Example curves illustrate the variation of the buckling load with plate aspect ratio showing the influence of the coupling stiffness matrix. The full input and output to the program is explained and illustrated with worked examples. The program is provided on disc (uncompiled) in the software volume and compiled within ESDUview, a user-friendly shell running under MS DOS that prompts on screen for input data. Author

N95-11773 ESDU International Ltd., London (England).
ELASTIC BUCKLING OF CYLINDRICALLY CURVED LAMINATED FIBRE REINFORCED COMPOSITE PANELS WITH ALL EDGES SIMPLY-SUPPORTED UNDER BIAXIAL LOADING
Apr. 1994 20 p Supersedes ESDU-87025
(ISSN 0141-4097; ISSN 0958-0360)
(ESDU-94007; ESDU-87025; ISBN-0-85679-894-0) Avail: ESDU

ESDU 94007 introduces a Fortran program, ESDUpac A9407, that calculates the buckling value of a uniform in-plane axial loading on the panel, with or without an additional circumferential loading due to normal pressure. Also output are the longitudinal buckle half wavelengths and, when pressure is considered, the circumferential buckle half wavelengths. The program applies to specially-orthotropic lay-ups, and will treat other lay-ups as if they were specially-orthotropic. It is based on elastic, thin plate, small deflection theory assuming the material to be homogeneous and orthotropic with the principal axes of orthotropy aligned with the rectangular plate edges. Through thickness shear is neglected. The equations on which the program is based are given, the input to the program is described in detail, its validation discussed, and specimen input and output of several worked examples are included. The program is provided on disc (uncompiled) in the software volume and compiled within ESDUview, a user-friendly shell running under MS DOS that prompts on screen for input data. Author

N95-11814*# National Aeronautics and Space Administration. Langley Research Center, Hampton, VA.
LINEAR PROOF MASS ACTUATOR
Sidney E. Holloway, III Sep. 1994 20 p
(RTOP 233-01-01-06)
(NASA-TM-109143; NAS 1.15:109143) Avail: CASI HC A03/MF A01

This paper describes the mechanical design, analysis, fabrication, testing, and lessons learned by developing a uniquely designed spaceflight-like actuator. The linear proof mass actuator (LPMA) was designed to attach to both a large space structure and a ground test model without modification. Previous designs lacked the power to perform in a terrestrial environment while other designs failed to produce the desired accelerations or frequency range for spaceflight applications. Thus, the design for a unique actuator was conceived and developed at NASA Langley Research Center. The basic design consists of four large mechanical parts (mass, upper housing, lower housing, and center support) and numerous smaller supporting components including an accelerometer, encoder, and four drive motors. Fabrication personnel were included early in the design phase of the LPMA as part of an integrated manufacturing process to alleviate potential difficulties in machining an already challenging design. Operating testing of the LPMA demonstrated that the actuator is capable of various types of load functions. Author (revised)

N95-11815*# National Aeronautics and Space Administration. Langley Research Center, Hampton, VA.
ACCURATE INTERLAMINAR STRESS RECOVERY FROM FINITE ELEMENT ANALYSIS
Alexander Tessler and H. Ronald Riggs Sep. 1994 13 p
(RTOP 505-63-53-01)
(NASA-TM-109149; NAS 1.15:109149) Avail: CASI HC A03/MF A01

The accuracy and robustness of a two-dimensional smoothing methodology is examined for the problem of recovering accurate interlaminar shear stress distributions in laminated composite and sandwich plates. The smoothing methodology is based on a variational formulation which combines discrete least-squares and penalty-constraint functionals in a single variational form. The smoothing analysis utilizes optimal strains computed at discrete locations in a finite element analysis. These discrete strain data are smoothed with a smoothing element discretization, producing superior accuracy strains and their first gradients. The approach enables the resulting smooth strain field to be practically C1-continuous throughout the domain of smoothing, exhibiting superconvergent properties of the smoothed quantity. The continuous strain gradients are also obtained directly from the solution. The recovered strain gradients are subsequently employed in the integration o equilibrium equations to obtain accurate interlaminar shear stresses. The problem is a simply-supported rectangular plate under a doubly sinusoidal load. The problem has an exact analytic solution which serves as a measure of goodness of the recovered interlaminar shear stresses. The method has the versatility of being applicable to the analysis of rather general and complex structures built of distinct components and materials, such as found in aircraft design. For these types of structures, the smoothing is achieved with 'patches', each patch covering the domain in which the smoothed quantity is physically continuous. Author

N95-11865*# National Aeronautics and Space Administration. Lewis Research Center, Cleveland, OH.
THE ROLE OF CRACK FORMATION IN CHEVRON-NOTCHED FOUR-POINT BEND SPECIMENS
Anthony M. Calomino and Louis J. Ghosn Aug. 1994 21 p
(Contract NCC3-331; RTOP 505-63-52)
(NASA-TM-106631; E-8948; NAS 1.15:106631) Avail: CASI HC A03/MF A01

The failure sequence following crack formation in a chevron-notched

four-point bend 1 specimen is examined in a parametric study using the Bluhm slice synthesis model. Premature failure resulting from crack formation forces which exceed those required to propagate a crack beyond alpha (min) is examined together with the critical crack length and critical crack front length. An energy based approach is used to establish factors which forecast the tendency of such premature failure due to crack formation for any selected chevron-notched geometry. A comparative study reveals that, for constant values of alpha (1) and alpha (0), the dimensionless beam compliance and stress intensity factor are essentially independent of specimen width and thickness. The chevron tip position, alpha (0) has its primary effect on the force required to initiate a sharp crack. Small values for alpha (0) maximize the stable region length, however, the premature failure tendency is also high for smaller alpha (0) values. Improvements in premature failure resistance can be realized for larger values of alpha (0) with only a minor reduction in the stable region length. The stable region length is also maximized for larger chevron based positions, alpha (1) but the chance for premature failure is also raised. Smaller base positions improve the premature failure resistance with only minor decreases in the stable region length. Chevron geometries having a good balance of premature failure resistance, stable region length, and crack front length are 0.20 less than or equal to alpha (0) is less than or equal to 0.30 and 0.70 is less than or equal to alpha (1) is less than or equal to 0.80.

Author

N95-11879# National Aerospace Lab., Bangalore (India). Structural Integrity Div.

A STUDY OF FATIGUE CRACK GROWTH IN LUGS UNDER SPECTRUM LOADING

R. Sunder and Raghu V. Prakash May 1994 25 p Presented at the 3rd ASTM Symposium on Advances in Fatigue Lifetime Predictive Techniques, Montreal, Quebec, 16-17 May 1994 Sponsored by Aeronautical Development Agency

(NAL Proj. T0-177)

(NAL-PD-SN-9407) Avail: CASI HC A03/MF A01

Optical fractography and special load sequencing were used to characterize the growth of naturally initiating fatigue cracks under FALSTAFF spectrum loading in lugs with bushes fitted to varying degrees of interference. The same technique was used to obtain a stress intensity calibration under constant amplitude loading. This calibration, combined with crack growth analyses using the hysteretic closure concept and Rainflow cycle count, correlated well with experimental observations of growth rate down to crack depth of 100 microns. Available analytical stress intensity solutions do not appear to explain observed high crack growth rates, particularly as crack size diminishes to part through dimensions.

Author

N95-11924# National Aeronautical Lab., Bangalore (India). Structural Integrity Div.

A STUDY OF NATURALLY INITIATING NOTCH ROOT FATIGUE CRACKS UNDER SPECTRUM LOADING

Raghu V. Prakash, R. Sunder, and E. I. Mitchenko May 1994 28 p Presented at the 3rd ASTM Symposium on Advances in Fatigue Lifetime Predictive Techniques, Montreal, Quebec, 16-17 May 1994 Sponsored by Aeronautical Development Agency and Dept. of Science and Technology

(NAL Proj. T-0-107)

(NAL-PD-SN-9406) Avail: CASI HC A03/MF A01

The kinetics of short cracks at notches were studied in 2014-T6511 Al-Cu alloy extruded bar stock under modified versions of FALSTAFF and TWIST load spectra. Experiments were conducted on test coupons of different thickness and at different stress levels. The effects of these and other parameters on the density and growth rate patterns of multiple cracks was investigated. The quality of fractographic crack growth rate measurements was found to be superior to surface replica technique. It was also observed that artificially initiated fatigue cracks grow slower than naturally initiated ones. Interaction of naturally initiating multiple cracks was quantified.

Author

N95-11948*# Virginia Polytechnic Inst. and State Univ., Blacksburg, VA. Dept. of Engineering Science and Mechanics.

INTERLAMINAR STRESS ANALYSIS OF DROPPED-PLY LAMINATED PLATES AND SHELLS BY A MIXED METHOD Ph.D. Thesis

Peter N. Harrison, Eric R. Johnson, and James H. Starnes, Jr. May 1994 173 p

(Grant NAG1-343)

(NASA-CR-196851; NAS 1.26:196851; VPI-E-94-04; CCMS-94-04) Avail: CASI HC A08/MF A02

A mixed method of approximation based on Reissner's variational principle is developed for the linear analysis of interlaminar stresses in laminated composites, with special interest in laminates that contain terminated internal plies (dropped-ply laminates). Two models are derived, one for problems of generalized plane deformation and the other for the axisymmetric response of shells of revolution. A layerwise approach is taken in which the stress field is assumed with an explicit dependence on the thickness coordinate in each layer. The dependence of the stress field on the thickness coordinate is determined such that the three-dimensional equilibrium equations are satisfied by the approximation. The solution domain is reduced to one dimension by integration through the thickness. Continuity of tractions and displacements between layers is imposed. The governing two-point boundary value problem is composed of a system of both differential and algebraic equations (DAE's) and their associated boundary conditions. Careful evaluation of the system of DAE's was required to arrive at a form that allowed application of a one-step finite difference approximation. A two-stage Gauss implicit Runge-Kutta finite difference scheme was used for the solution because of its relatively high degree of accuracy. Patch tests of the two models revealed problems with solution accuracy for the axisymmetric model of a cylindrical shell loaded by internal pressure. Parametric studies of dropped-ply laminate characteristics and their influence on the interlaminar stresses were performed using the generalized plane deformation model. Eccentricity of the middle surface of the laminate through the ply drop-off was found to have a minimal effect on the interlaminar stresses under longitudinal compression, transverse tension, and in-plane shear. A second study found the stiffness change across the ply termination to have a much greater influence on the interlaminar stresses.

Author

N95-11954*# National Aeronautics and Space Administration. Lewis Research Center, Cleveland, OH.

PROBABILISTIC SIMULATION OF THE HUMAN FACTOR IN STRUCTURAL RELIABILITY

Christos C. Chamis and Surendra N. Singhal Sep. 1994 13 p

(Contract NAS3-25266; RTOP 584-03-11)

(NASA-TM-106498; E-8489; NAS 1.15:106498) Avail: CASI HC A03/MF A01

The formal approach described herein computationally simulates the probable ranges of uncertainties for the human factor in probabilistic assessments of structural reliability. Human factors such as marital status, professional status, home life, job satisfaction, work load, and health are studied by using a multifactor interaction equation (MFIE) model to demonstrate the approach. Parametric studies in conjunction with judgment are used to select reasonable values for the participating factors (primitive variables). Subsequently performed probabilistic sensitivity studies assess the suitability of the MFIE as well as the validity of the whole approach. Results show that uncertainties range from 5 to 30 percent for the most optimistic case, assuming 100 percent for no error (perfect performance).

Author

N95-12108# Polish Academy of Sciences, Warsaw (Poland). Inst. of Basic Problems of Technology.

THE USE OF AN ACOUSTIC EMISSION METHOD TO ESTIMATE THE EFFECT OF MANUFACTURING PROCESS AND SERVICE FACTORS ON THE FAILURE OF CONCRETE [WYKORZYSTANIE METODY EMISJI AKUSTYCZNEJ W OCENIE WPLYWU CZYNNIKOW TECHNOLOGICZNYCH I EKSPLOATACYJNYCH NO PROCES NISZCZENIA BETONU]

Jerzy Hola (Wroclaw Polytechnic Electronic Engineering Inst., Poland.) and Jerzy Ranachowski 1992 27 p In POLISH

(ISSN 0208-5658)

Avail: CASI HC A03/MF A01

This article presents the results of research on the effect of several important manufacturing process factors on the failure of concrete involving the use of acoustic emission as the research method. The authors focus special attention on such factors as the grain-size distribution of the aggregate, moisture, and heat treatment. The authors also discuss the importance of critical stresses in the concrete and how to determine them

by means of acoustic emission measurements. The authors provide a bibliography with detailed information on the subject. Author

N95-12511 Naval Postgraduate School, Monterey, CA.
A STUDY OF THE DEFORMATION OF HELICAL SPRINGS UNDER ECCENTRIC LOADING M.S. Thesis
Andrew R. Leech Jun. 1994 66 p Limited Reproducibility: More than 20% of this document may be affected by microfiche quality
(AD-A283448) Avail: CASI HC A04

Much analysis has been done to date on the deformation of helical springs due to normal loadings. The aim of this study is to design a helical spring that will deform under eccentric loading a desired amount due to a given force. Under the assumptions of linear stress strain relationships, the spring will be designed in terms of its material properties and its geometry. The deformation of the spring will be made possible utilizing a Shape Memory Alloy (SMA) active element that undergoes phase transformation upon heating above a certain temperature. Two models for spring deformation have been considered. In the first model we study the differential compression of a spring using SMA wire actuators, and in the second model we investigate the bending of an SMA rod placed inside the spring. Our efforts were a first step towards the development of a structural skeleton for a minimally invasive surgical manipulator. DTIC

N95-12620*# Auburn Univ., AL. Dept. of Electrical Engineering.
DESIGN OF A ZVS PWM INVERTER FOR A BRUSHLESS DC MOTOR IN AN EMA APPLICATION
J. Brett Bell, R. M. Nelms, and Michael T. Shepherd 1993 8 p
(Contract NAS8-39131)
(NASA-CR-195808; NAS 1.26:195808) Avail: CASI HC A02/MF A01

The Component Development Division of the Propulsion Laboratory at Marshall Space Flight Center (MSFC) is currently investigating the use of electromechanical actuators for use in space transportation applications such as Thrust Vector Control (TVC). These high power servomechanisms will require rugged, reliable, and compact power electronic modules capable of modulating several hundred amperes of current at up to 270 Vdc. This paper will discuss the design and implementation of a zero-voltage-switched PWM (Pulse Width Modulation) inverter which operates from a 270 Vdc source at currents up to 100 A. Author (revised)

N95-12631# Polish Academy of Sciences, Warsaw (Poland). Inst. of Basic Problems of Technology.
AN ANALYSIS OF THE LOAD-BEARING CAPACITY OF MEMBERS OF SQUARE CROSS SECTION WITH A SERIES OF PERPENDICULAR NOTCHES [ANALIZA NOSNOSCI GRANICZNEJ ELEMENTOW O PRZEKROJU KWADRATOWYM Z SZEREGIEM WYCIEC O PROFILU PROSTOKATNYM]
Jozef Miastkowski and Ryszard Szczebiot 1993 37 p In POLISH
(ISSN 0208-5658)
Avail: CASI HC A03/MF A01

The authors analyze the load-bearing capacity of structural members with square cross sections which have been weakened on their perimeters by a series of perpendicular notches. The analysis is based on complete solutions for axisymmetric bars with perpendicular notches and estimates of load-bearing capacity obtained from kinematically acceptable failure mechanisms. A procedure for determining the optimal distance (spacing) between the notches in the case of bars weakened by a series of perpendicular notches is described. The practical value of the analysis presented was confirmed by the results of experiments conducted on aluminum alloy test pieces of square cross section for plastic working weakened by two peripheral perpendicular notches. Author (revised)

N95-12775# Technische Univ., Delft (Netherlands).
EFFECT OF SHEAR LIPS, LOADING TRANSITIONS AND TEST FREQUENCY ON CONSTANT DELTA K AND CONSTANT LOAD AMPLITUDE FATIGUE TESTS Ph.D. Thesis
F. A. Veer 5 Oct. 1993 200 p
(PB94-192440) Avail: CASI HC A09/MF A03

The scope of this thesis is: to investigate the fatigue crack growth behavior of several materials during constant load amplitude and constant Delta K type fatigue tests; to look at the basic parameters that control the crack growth rate in these materials; and to study the presence or absence of shear lip development in these materials. Chapter 1 contains a review of the literature regarding fatigue crack growth. Chapters 2, 3, and 4 deal with experimental technique, crack tip plasticity and reproducibility of test results respectively. Chapters 5 and 6 deal with the results obtained on materials that did not form shear lips. Chapter 7 will deal with the basics of shear lip development and with the effect of shear lips. Chapters 8 and 9 will deal with the results obtained on materials that do form shear lips. Chapter 10 will deal with the problem of frequency effects on shear lip development. The final chapter compares and discusses the results obtained on different materials. NTIS

N95-12784# Los Alamos National Lab., NM.
MECHANICAL BEHAVIOR OF (238)UO2, (238)PuO2, AND (239)PuO2 AS A FUNCTION OF STRAIN RATE AND TEMPERATURE
M. G. Stout, R. W. Ellis, and R. A. Pereyra 25 Oct. 1994 35 p
(Contract W-7405-eng-36)
(DE94-015718; LA-12811-MS) Avail: CASI HC A03/MF A01

The mechanical response of (238)UO2 was measured as a function of strain rate and temperature. We evaluated material produced by two processing schedules: hot pressing followed by a grain stabilization; and cold pressing plus a sintering treatments. The response of these two materials was identical, within the scatter of our data. We complemented our data with that published in the literature, after having made the appropriate corrections for grain size, porosity, and stoichiometry. The entire collection of data was used to evaluate the Follansbee-Kocks mechanical threshold stress (MTS) model for the prediction of yield stress as a function of strain rate and temperature. We used this model to predict the yield stress of (238)UO2 for strain rates between (dot(var epsilon)) = 10(exp -5) and 10(exp 3) s(exp -1) and temperatures from 800 to 1600 C. These predictions provided the basis for constructing a deformation/fracture map for both urania and plutonia. Examination of the maps indicates that for compressive loading and impact strain rates, the (238)UO2 will be an excellent mock material for (238)PuO2. Under these conditions both the strength and deformation and the fracture modes are consistent between these two materials. DOE

N95-12818*# National Aeronautics and Space Administration. Lewis Research Center, Cleveland, OH.
LARGE-DISPLACEMENT STRUCTURAL DURABILITY ANALYSES OF SIMPLE BEND SPECIMEN EMULATING ROCKET NOZZLE LINERS
Vinod K. Arya (Toledo Univ., OH.) and Gary R. Halford Jun. 1994 17 p
Original contains color illustrations
(Contract NCC3-120; RTOP 505-63-5B)
(NASA-TM-106521; E-8644; NAS 1.15:106521) Avail: CASI HC A03/MF A01; 7 functional color pages

Large-displacement elastic and elastic-plastic, finite-element stress-strain analyses of an oxygen-tree high-conductivity (OFHC) copper plate specimen were performed using an updated Lagrangian formulation. The plate specimen is intended for low-cost experiments that emulate the most important thermomechanical loading and failure modes of a more complex rocket nozzle. The plate, which is loaded in bending at 593 C, contains a centrally located and internally pressurized channel. The cyclic crack initiation lives were estimated using the results from the analyses and isothermal strain-controlled low-cycle fatigue data for OFHC copper. A comparison of the predicted and experimental cyclic lives showed that an elastic analysis predicts a longer cyclic life than that observed in experiments by a factor greater than 4. The results from elastic-plastic analysis for the plate bend specimen, however, predicted a cyclic life in close agreement with experiment, thus justifying the need for the more rigorous stress-strain analysis. Author (revised)

N95-12861*# Alabama Univ., Huntsville, AL. Dept. of Mechanical and Aerospace Engineering.
STRESS RELAXATION FUNCTIONS: METHODS OF APPROXIMATION (Diskette Supplement) Final Report
Mark V. Bower and Frederick S. Gant Apr. 1994 54 p Diskette supplement: 5.25-inch DSDD
(Grant NAG8-850)
(NASA-CR-195830; NAS 1.26:195830; NONP-NASA-Suppl-DK-94-28025)
Avail: CASI SET A06 (HC,DK)

A new method of determining Prony series coefficients is presented. This method, the domain of influence method (DOI), capitalizes on characteristics of the exponential decay curve to adjust its parameters to

fit a set of data. This method was applied to viscoelastic stress relaxation data. The method is general and can be used to develop exponential decay curves to represent other types of data where appropriate. The DOI method does not include any error correction within itself. To improve the results of the DOI method some form of error correction is necessary. The nonlinearity of the Prony series does not lend itself to common methods of error minimization. Optimization methods can be applied to this problem. These methods use the functional behavior of the problem under study to minimize or maximize some characteristic of the problem. Here the function minimized was an error function between the DOI estimated Prony series and the viscoelastic data. Optimization was achieved by adjusting the Prony series coefficients to minimize that error. The DOI method was encoded in FORTRAN and integrated with commercially available optimization routines to produce a tool called Viscoelastic Coefficient Determination or VCD. A description of this code including a discussion of the salient features is presented. An example is used to demonstrate the DOI method, illustrate the operation of VCD, and demonstrate the capabilities of the method and the software. A code listing appears in the appendix. Author (revised)

N95-12947# Finnish Centre for Radiation and Nuclear Safety, Helsinki (Finland).

VALIDITY OF FRACTURE TOUGHNESS DETERMINED WITH SMALL BEND SPECIMENS [PIENILLAE TAIVUTUSSAUVOILLA MITATUN MURTUMISSITKEYDEN PAETEVYYS]

K. Wallin (Technical Research Centre of Finland, Espoo, Finland.), R. Rintamaa (Technical Research Centre of Finland, Espoo, Finland.), and M. Valo (Technical Research Centre of Finland, Espoo, Finland.) Feb. 1994 28 p In FINNISH

(DE94-624157; STUK-YTO-TR-63) Avail: CASI HC A03/MF A01 (US Sales Only)

This report considers the validity of fracture toughness estimates obtained with small bend specimens in relation to fracture toughness estimates obtained with large specimens. The study is based upon the analysis and comparison of actual test results. The results prove the validity of the fracture toughness determined based upon small bend specimens, especially when the results are only used to determine the fracture toughness transition temperature T(sub o). In this case the possible error is typically less than 5 deg C and at most 10 deg C. It can be concluded that small bend specimens are very suitable for the estimation of fracture toughness in the case of brittle fracture, provided the results are corrected for statistical size effects. DOE

N95-13096*# Texas A&M Univ., College Station, TX. Dept. of Mechanical Engineering.

COMPARISON OF SYMBOLIC AND NUMERICAL INTEGRATION METHODS FOR AN ASSUMED-STRESS HYBRID SHELL ELEMENT

Govind Rengarajan, Norman F. Knight, Jr., and Mohammad A. Aminpour 1993 15 p

(Contract NAS1-19317; NAG1-1374; NAG1-1505)

(NASA-CR-195945; NAS 1.26:195945) Avail: CASI HC A03/MF A01

Hybrid shell elements have long been regarded with reserve by the commercial finite element developers despite the high degree of reliability and accuracy associated with such formulations. The fundamental reason is the inherent higher computational cost of the hybrid approach as compared to the displacement-based formulations. However, a noteworthy factor in favor of hybrid elements is that numerical integration to generate element matrices can be entirely avoided by the use of symbolic integration. In this paper, the use of the symbolic computational approach is presented for an assumed-stress hybrid shell element with drilling degrees of freedom and the significant time savings achieved is demonstrated through an example. Author

N95-13162*# Clemson Univ., SC. Dept. of Mechanical Engineering.

NONLINEAR STRUCTURAL RESPONSE USING ADAPTIVE DYNAMIC RELAXATION ON A MASSIVELY-PARALLEL-PROCESSING SYSTEM

David R. Oakley and Norman F. Knight, Jr. 15 Jun. 1994 43 p

(Grant NAG1-1505)

(NASA-CR-196491; NAS 1.26:196491) Avail: CASI HC A03/MF A01

A parallel adaptive dynamic relaxation (ADR) algorithm has been developed for nonlinear structural analysis. This algorithm has minimal memory requirements, is easily parallelizable and scalable to many processors, and is generally very reliable and efficient for highly nonlinear problems. Performance evaluations on single-processor computers have shown that the ADR algorithm is reliable and highly vectorizable, and that it is competitive with direct solution methods for the highly nonlinear problems considered. The present algorithm is implemented on the 512-processor Intel Touchstone DELTA system at Caltech, and it is designed to minimize the extent and frequency of interprocessor communication. The algorithm has been used to solve for the nonlinear static response of two and three dimensional hyperelastic systems involving contact. Impressive relative speedups have been achieved and demonstrate the high scalability of the ADR algorithm. For the class of problems addressed, the ADR algorithm represents a very promising approach for parallel-vector processing. Author

N95-13163*# Clemson Univ., SC. Dept. of Mechanical Engineering.

IMPROVED ASSUMED-STRESS HYBRID SHELL ELEMENT WITH DRILLING DEGREES OF FREEDOM FOR LINEAR STRESS, BUCKLING, AND FREE VIBRATION ANALYSES

Govind Rengarajan, Mohammad A. Aminpour, and Norman F. Knight, Jr. 1992 51 p

(Contract NAS1-19317; NAG1-1374; NAG1-1505)

(NASA-CR-192816; NAS 1.26:192816) Avail: CASI HC A04/MF A01

An improved four-node quadrilateral assumed-stress hybrid shell element with drilling degrees of freedom is presented. The formulation is based on Hellinger-Reissner variational principle and the shape functions are formulated directly for the four-node element. The element has 12 membrane degrees of freedom and 12 bending degrees of freedom. It has nine independent stress parameters to describe the membrane stress resultant field and 13 independent stress parameters to describe the moment and transverse shear stress resultant field. The formulation encompasses linear stress, linear buckling, and linear free vibration problems. The element is validated with standard tests cases and is shown to be robust. Numerical results are presented for linear stress, buckling, and free vibration analyses. Author

N95-13235*# National Aeronautics and Space Administration. Lewis Research Center, Cleveland, OH.

ACTIVITIES OF THE STRUCTURES DIVISION, LEWIS RESEARCH CENTER Annual Report, 1990

1990 71 p

(NASA-TM-108081; NAS 1.15:108081; DAAP-LEW-137682) Copyright Avail: CASI HC A04/MF A01

The purpose of the NASA Lewis Research Center, Structures Division's 1990 Annual Report is to give a brief, but comprehensive, review of the technical accomplishments of the Division during the past calendar year. The report is organized topically to match the Center's Strategic Plan. Over the years, the Structures Division has developed the technology base necessary for improving the future of aeronautical and space propulsion systems. In the future, propulsion systems will need to be lighter, to operate at higher temperatures and to be more reliable in order to achieve higher performance. Achieving these goals is complex and challenging. Our approach has been to work cooperatively with both industry and universities to develop the technology necessary for state-of-the-art advancement in aeronautical and space propulsion systems. The Structures Division consists of four branches: Structural Mechanics, Fatigue and Fracture, Structural Dynamics, and Structural Integrity. This publication describes the work of the four branches by three topic areas of Research: (1) Basic Discipline; (2) Aeropropulsion; and (3) Space Propulsion. Each topic area is further divided into the following: (1) Materials; (2) Structural Mechanics; (3) Life Prediction; (4) Instruments, Controls, and Testing Techniques; and (5) Mechanisms. The publication covers 78 separate topics with a bibliography containing 159 citations. We hope you will find the publication interesting as well as useful. Author

N95-13576 DELAB, Trondheim (Norway).

ACTIVE VIBRATION CONTROL USING A DISTRIBUTED CONTROLLER Ph.D. Thesis

M. J. Newman 11 Mar. 1994 217 p Sponsored by Norges Forskningsraad

(PB94-207073; STF40-A94048) Avail: Issuing Activity (National Technical Information Service (NTIS))

This thesis deals with active vibration control, using distributed actuators and sensors applied to a beam. In the theory, a 'quality factor' is defined

to evaluate the use of shaped distributed actuators and sensors to beams with known normal mode shapes. Experiments are reported where the shaped actuators and sensors have been implemented using polyvinylidene fluoride (PVDF) piezoelectric plastic with shaped electrodes. The loss factors in normal modes have been increased by the active system up to 7 fold over and above the passive loss factors. NTIS

42 GEOSCIENCES (GENERAL)

N95-12231* Oregon State Univ., Corvallis, OR. Marine Science Center.
COMMUNICATIONS PLAN
30 Jun. 1994 66 p Revised Original contains color illustrations
(NASA-CR-196435; NAS 1.26:196435) Avail: Issuing Activity; 18 functional color pages

The mission of the HMSC public wing is to increase public appreciation and awareness of marine and coastal environments, promote wise stewardship, and communicate the results of marine research conducted by the OSU and cooperating agencies at the center. In the course of the communications planning phase, the power and potential for HMSC to affect public perception of and attitudes toward science and marine research have been recognized. This focusing has resulted in the definition of a 'priority audience': adult citizens in the general public whose decisions about research, resources, and policies will shape the future of local and global marine environments. The goals of this study are to: (1) develop an interpretive approach and thematic framework for exhibits; (2) develop a design approach to the interpretive elements; and (3) provide input to the architects to ensure the marriage of interpretation and architecture as the building design proceeds. Derived from text

43 EARTH RESOURCES AND REMOTE SENSING

Includes remote sensing of earth resources by aircraft and spacecraft; photogrammetry; and aerial photography.

For instrumentation see *35 Instrumentation and Photography.*

N95-11783# Lawrence Livermore National Lab., Livermore, CA.
HIGH AVERAGE POWER PARAMETRIC FREQUENCY CONVERSION-NEW CONCEPTS AND NEW PUMP SOURCES
S. P. Velsko and M. S. Webb Mar. 1994 9 p Presented at the OE/LASE 1994: Conference on Optics, Electro-Optics, and Laser Applications in Science and Engineering, Los Angeles, CA, 22-29 Jan. 1994
(Contract W-7405-eng-48)
(DE94-013652; UCRL-JC-116760; CONF-940142-40) Avail: CASI HC A02/MF A01

A number of applications, including long range remote sensing and antisensor technology, require high average power tunable radiation in several distinct spectral regions. Of the many issues which determine the deployability of optical parametric oscillators (OPOS) and related systems, efficiency and simplicity are among the most important. It is only recently that the advent of compact diode laser pumped solid state lasers has produced pump sources for parametric oscillators which can make compact, efficient, high average power tunable sources possible. In this paper we outline several different issues in parametric oscillator and pump laser development which are currently under study at Lawrence Livermore National Laboratory. DOE

N95-11820# National Defence Research Establishment, Linkoeping (Sweden). Huvudavdelning foer Informationsteknologi.
OBJECT-ORIENTED INCREMENTAL MAP-GENERATION FOR MOBILE ROBOT NAVIGATION
H. Alayan and E. Jungert Sep. 1993 78 p
(PB94-190717; FOA-C-30729-3.4) Avail: CASI HC A05/MF A01

An approach to map the external environment of an autonomous robot is described. The model is designed mainly for indoor usage but has limited outdoor capabilities as well. The resulting implementation should be used for incremental mapping of the surrounding environment in which the robot is navigating. The map generation is a process on a low level. On the low level, the free space is represented as a type of trapezoid. On the top level, a connectivity graph is generated and represented in symbolic form. A description of the analysis and design method is presented in this work. NTIS

N95-11831 Optical Society of America, Washington, DC.
OPTICAL REMOTE SENSING OF THE ATMOSPHERE. TECHNICAL DIGEST 1993. VOLUME 5: POSTCONFERENCE EDITION Final Report, 5 Mar. 1993 - 4 Mar. 1994
Jarus W. Quinn Jun. 1994 522 p Conference held in Salt Lake City, UT, 8-12 Mar. 1993 Limited Reproducibility: More than 20% of this document may be affected by microfiche quality
(Contract DAAH04-93-G-0041)
(AD-A281446; ARO-31110.1-GS-CF-Vol-5) Avail: CASI HC A22

The agenda of sessions includes water vapor, space & ground based remote sensing, clouds and ECLIP, winds, ozone, aerosols, spectroscopy and new developments. DTIC

N95-11880# Geodetic Inst., Helsinki (Finland).
THE PROGRAM FOR THE 1993 ADJUSTMENT OF THE FINNISH FIRST-ORDER TERRESTRIAL TRIANGULATION
Jorma Jokela, Markku Poutanen, and Raimo Konttinen 1994 26 p
(ISSN 0355-1962)
(Rept-94:3; ISBN-951-711-174-6) Avail: CASI HC A03/MF A01

This report presents an adjustment program for all sizes of classical geodetic horizontal networks up to several hundreds of unknowns. The data file can consist of direction, distance, and azimuth observations. The adjustment is made on a predefined ellipsoid (here International 1924), and the program performs the reductions of the angles to this ellipsoid. In this program version, the distances, however, must be reduced on the ellipsoid beforehand. The number of fixed points must be at least two if no azimuth observations exist. With azimuths included, one fixed point only is required. The output of the program is the adjusted coordinates of all the unknown points, their standard errors, error ellipses for the adjusted coordinates and the calculated directions and distances of the neighboring stations. Depending on the program options, more detailed outputs can also be produced. The program was used for the 1993 adjustment of the Finnish first-order triangulation network, which consists of more than 350 stations and over 700 unknowns. Author

N95-11881# Geodetic Inst., Helsinki (Finland).
FINAL RESULTS OF THE BALTIC SEA LEVEL 1990 GPS CAMPAIGN. RESEARCH WORKS OF THE SSG 5.147 OF THE INTERNATIONAL ASSOCIATION OF GEODESY
Juhani Kakkuri, ed. 1994 63 p
(ISSN 0355-1962)
(Rept-94:2; ISBN-951-711-172-X) Avail: CASI HC A04/MF A01

The Baltic Sea Level Project is an international cooperation program between the countries on the Baltic Sea. The goal of the cooperation is unification of the vertical datums. Two GPS observation campaigns were arranged to achieve the goal: a two week campaign in October 1990 (the first campaign) and a one week campaign in June 1993 (the second campaign). In this report the final results of the first campaign are shown. Derived from text

N95-11950# Geodetic Inst., Helsinki (Finland).
OBSERVATION RESULTS: ANGLE MEASUREMENTS IN 1964-1965, 1971, 1984 AND 1986-1987
Raimo Konttinen 1994 71 p
(ISSN 0085-6932)
(Rept-118; ISBN-951-711-171-1) Avail: CASI HC A04/MF A01

This publication presents results of the angle measurements made in the Rauma - Aland chain (1964-65) and in the Niinisalo base extension (1971), Inari (1984 and 1986), and Utsjoki (1986-87) nets. The results published here have been used, for instance, in the final adjustment of the Finnish first order terrestrial triangulation network. Derived from text

N95-11997*# National Aeronautics and Space Administration. Goddard Space Flight Center, Greenbelt, MD.
DIFFERENTIAL ABSORPTION LIDAR MEASUREMENTS OF ATMOSPHERIC WATER VAPOR USING A PSEUDONOISE CODE MODULATED AlGaAs LASER Thesis

Jonathan A. R. Rall Jul. 1994 155 p
(RTOP 924-00-00)
(NASA-TM-104610; Rept-94B00103; NAS 1.15:104610) Avail: CASI HC A08/MF A02

Lidar measurements using pseudonoise code modulated AlGaAs lasers are reported. Horizontal path lidar measurements were made at night to terrestrial targets at ranges of 5 and 13 km with 35 mW of average power and integration times of one second. Cloud and aerosol lidar measurements were made to thin cirrus clouds at 13 km altitude with Rayleigh (molecular) backscatter evident up to 9 km. Average transmitter power was 35 mW and measurement integration time was 20 minutes. An AlGaAs laser was used to characterize spectral properties of water vapor absorption lines at 811.617, 816.024, and 815.769 nm in a multipass absorption cell using derivative spectroscopy techniques. Frequency locking of an AlGaAs laser to a water vapor absorption line was achieved with a laser center frequency stability measured to better than one-fifth of the water vapor Doppler linewidth over several minutes. Differential absorption lidar measurements of atmospheric water vapor were made in both integrated path and range-resolved modes using an externally modulated AlGaAs laser. Mean water vapor number density was estimated from both integrated path and range-resolved DIAL measurements and agreed with measured humidity values to within 6.5 percent and 20 percent, respectively. Error sources were identified and their effects on estimates of water vapor number density calculated. Author

N95-12297# Instituto de Pesquisas Espaciais, Sao Jose dos Campos (Brazil).
PROPOSAL OF A METHODOLOGY TO EVALUATE URBAN QUALITY OF LIFE USING CONVENTIONAL AND REMOTE SENSING DATA, GEOGRAPHIC INFORMATION SYSTEM, AND A DATABASE M.S. Thesis [PROPOSTA METODOLOGICA PARA AVALIACAO DA QUALIDADE DE VIDA URBANA A PARTIR DE DADOS CONVENCIONAIS E DE SENSORIAMENTO REMOTO, SISTEMA DE INFORMACOES GEOGRAFICAS E BANCO DE DADOS GEORRELACIONAL]
Vania Aparecida Ceccato Feb. 1994 149 p In PORTUGESE
(INPE-5552-TDI/536) Avail: CASI HC A07/MF A02

A methodology of urban quality of life evaluation using conventional and remote sensing data (aerial photographs in the scale of 1:10,000, orbital images SPOT-panchromatic in paper-1:25,000 and digital TM-LANDSAT), a Geographic Information System (GIS) and a georelational database, was developed. The proposal was based on an urban quality of life model involving the following variables: infrastructure, income, health criminality, pattern of built space and green areas. To do so, the potentiality of texture patterns as well as classes of vegetation index, was evaluated on an exploratory basis as social and environmental indicators. The conventional data and those related to remote sensing composed the database file and were manipulated in order to be integrated to a GIS. Therefore, making it possible the production of cartographic representations of each model variable, as well as the integration of them all, representing different patterns of quality of life. The methodology proved useful to urban quality of life diagnoses of Rio Claro-SP, mainly when compared with the quality defined by the population's perception. It is suggested that the methodology be tested in other cities with minor changes, aiming at improving the model developed. Author

N95-12301# Instituto de Pesquisas Espaciais, Sao Jose dos Campos (Brazil).
DIGITAL IMAGE PROCESSING TECHNIQUES FOR IMAGE-MAPPING APPLICATIONS M.S. Thesis [TECNICAS DE PROCESSAMENTO DIGITAL DE IMAGENS PARA APLICACOES NO MAPEAMENTO POR CARTA-IMAGEM]
Marcos Antonio Timbo Elmiro Mar. 1994 131 p In PORTUGESE
(INPE-5546-TDI/532) Avail: CASI HC A07/MF A02

Many important activities, especially those related to survey of natural resources are supported by national systematic maps in order to provide a confident base to place the results. Unfortunately, because traditional mapping is a very expensive and slow task, the basic national cartographic coverage is poorly established. Image-Mapping techniques can provide a fast and cost-effective alternate solution to avoid dependency on traditional maps. This paper presents the basic guidelines for a methodology to produce Image-Maps using an entirely digital approach. Within this methodology three main steps are deeply discussed, followed by algorithm developments and computer program implementations. The first step is digital mosaicking using a gray level adjustment of image tiles and an irregular join line for connecting them. The second step is a removal of cloud coverage by multitemporal data replacement. And the final step is application of special image enhancement techniques for local feature improvement. The results pointed out that digital mosaicking can produce resulting image with no visible differences between source images; image coverage can be significantly improved by cloud removal based on multitemporal data; and special purpose enhancement techniques improve the image visual quality, aiding the interpretation task. From that results it was possible to draw some conclusions indicating that Image-Mapping activities can be significantly improved by using digital approaches as proposed by this work. Author

N95-12379*# National Aeronautics and Space Administration. Langley Research Center, Hampton, VA.
DESIGN STUDIES OF LARGE APERTURE, HIGH-RESOLUTION EARTH SCIENCE MICROWAVE RADIOMETERS COMPATIBLE WITH SMALL LAUNCH VEHICLES
Lyle C. Schroeder, M. C. Bailey, Richard F. Harrington, Bruce M. Kendall, and Thomas G. Campbell Sep. 1994 26 p
(RTOP 506-59-64-01)
(NASA-TP-3469; L-17359; NAS 1.60:3469) Avail: CASI HC A03/MF A01

High-spatial-resolution microwave radiometer sensing from space with reasonable swath widths and revisit times favors large aperture systems. However, with traditional precision antenna design, the size and weight requirements for such systems are in conflict with the need to emphasize small launch vehicles. This paper describes tradeoffs between the science requirements, basic operational parameters, and expected sensor performance for selected satellite radiometer concepts utilizing novel lightweight compactly packaged real apertures. Antenna, feed, and radiometer subsystem design and calibration are presented. Preliminary results show that novel lightweight real aperture coupled with state-of-the-art radiometer designs are compatible with small launch systems, and hold promise for high-resolution earth science measurements of sea ice, precipitation, soil moisture, sea surface temperature, and ocean wind speeds. Author (revised)

N95-12428# New Mexico State Univ., Las Cruces, NM. Dept. of Mathematical Sciences.
THE DIFFERENTIAL GEODESY OF THE SPHERICAL REPRESENTATION
J. D. Zund 13 May 1994 50 p
(Contract F19628-89-K-0044)
(AD-A282212; AD-E202070; PL-TR-94-2143; SR-6) Avail: CASI HC A03/MF A01

This report contains a detailed exposition of the theory of the spherical representation of surfaces in Gaussian differential geometry and its application in differential geodesy. The theory is developed in a new unified approach which is then applicable to the Marussi-Hotline theory of differential geodesy. Our presentation is logically a completion and continuation of the sketch of the theory given in Chapter 11 of Martin Hotine's Mathematical Geodesy (U.S. Department of Commerce, Washington, D.C., 1969). DTIC

N95-12527# Maryland Univ., College Park, MD. Computer Vision Lab.
SITE MODEL BASED IMAGE REGISTRATION AND CHANGE DETECTION, RADIUS Annual Report No. 1, Sep. 1992 - Sep. 1993
R. Chellappa, C. Rodriguez, Q. Zheng, A. Rosenfeld, and L. S. Davis Jun. 1994 81 p
(Contract DACA76-92-C-0024)
(AD-A282796; TEC-0055) Avail: CASI HC A05/MF A01

The University of Maryland (with TASC as a subcontractor) is one of a group of institutions doing research on aerial image understanding in support of the RADIUS program. The emphasis of our research is on knowledge-based change detection (CD) using site models and the domain expertise of image analysts IAs). We are designing a system that allows the IA to specify what are to be considered as significant changes through quick look (QL) profiles, and to select appropriate image understanding algorithms for detecting these changes. Before CD can be attempted, the acquired images have to be registered to the site model. Two algorithms for image registration have been developed. When no information about

the camera is available, we use an efficient constrained search mechanism for image-to-image registration. When an approximate camera model is available, as in RADIUS applications, we use a fast image-to-site model registration algorithm which first projects the site model into the new image domain using the given approximate camera model, and then use five control points to do camera resection and to obtain an accurate camera mode. To enable efficient transfer of technology to the IAs, we have developed our algorithms under the RADIUS Common Development Environment (RCDE). DTIC

N95-12634 Massachusetts Univ., Amherst, MA. Dept. of Physics and Astronomy.

NEAR-INFRARED IMAGING OF SELECTED AREAS Final Report, 8 Aug. 1991 - 7 May 1994

S. G. Kleinmann 7 May 1994 20 p Limited Reproducibility: More than 20% of this document may be affected by microfiche quality

(Contract F19628-91-K-0021)

(AD-A283519) Avail: CASI HC A03

The observational program described here consists of multi-color near-infrared imaging of selected areas on the sky. The scientific goals are to provide a database for development of algorithms for efficient extraction of sources both in sparse and in crowded areas, and to check current models of the sky. The practical goals are to test a variety of observing techniques in preparation of a new-infrared all-sky survey DTIC

N95-13142# Edgewood Arsenal, Aberdeen Proving Ground, MD. Research Development and Engineering Center.

VAPOR DETECTION SENSITIVITY AS A FUNCTION OF OPTICAL RESOLUTION FOR A SINGLE LORENTZIAN BAND Final Report, Dec. 1993 - Apr. 1994

Dennis F. Flanigan Jul. 1994 27 p

(DA Proj. 101-62622-A-553)

(AD-A283444; ERDEC-TR-173) Avail: CASI HC A03/MF A01

The objective of this effort is twofold: to begin the development of a computer model for passive infrared (IR) remote sensing vapor detection systems and to provide guidance for the determination of optimum spectral resolution for the remote detection of organic vapors. The target bands are modeled as Lorentzian bands; this allows a fairly simple analytical approach. Several sensor models are compared including: a detector limited sensor model according to Wolfe, and two background limited incident photon (BLIP) models based on work by Wolfe and Kingston. The measures of sensitivity are signal to noise ratio (SNR), noise equivalent concentration pathlength (NECL), and noise equivalent delta(T) (NEDT), all as a function of optical bandwidth. Signal to noise ratio, NECL, and NEDT values are computed for a typical broad and narrow band associated with organophosphorus compounds. Additionally, the simulant sulfur hexafluoride (SF6) is evaluated. The results show that gains in sensitivity may be possible in existing remote sensors if the current optical resolution 4/cm is reduced to 8/cm or 16/cm, although this must be done carefully to ensure no loss in discrimination. It is clear that present systems are limited by detector technology. With true background limited performance and careful optimization to a particular problem, sensitivity improvements of 50 may be possible. DTIC

N95-13159# Instituto de Pesquisas Espaciais, Sao Jose dos Campos (Brazil).

ESTIMATION OF ABOVE-GROUND PHYTOMASS IN A TROPICAL FOREST USING TM-LANDSAT 5 E HRV-SPOT 1 DATA M.S. Thesis [ESTIMATIVA DE FITOMASSA AEREA EM REGIAO DE FLORESTA TROPICAL COM USO DE DADOS TM-LANDSAT 5 E HRV-SPOT 1]

Newton Jordao Zerbini Nov. 1992 134 p In PORTUGESE

(INPE-5500-TDI/515) Avail: CASI HC A07/MF A02

The Amazon forest has been the subject of much debate due to the extent of human intervention occurring there. The Brazilian Amazon, with 3.5 million sq km, requires efficient systems of data collection for rational management of its forest resources. The present dissertation develops a quantitative method for determining the biomass of tropical forest using satellite imagery from TM-LANDSAT 5 and HRV-SPOT in an area to be inundated for hydroelectricity. The study determined the correlation of biomass above-ground and tree measurements with spectral response and elevation in four samples: dense forest on dry land - undulated relief (samples 1 and 4), dense forest on dry land - flat relief (sample 2), and floodplain forest (sample 3). The forest samples were divided into three vertical levels for analysis. In comparison with the other forest levels, the spectral variables combined with the biomass variables did not permit the quantification of the biomass in the highest level of the forest. Regression analysis identified the equations for quantifying biomass. The proposed method is practical and gave significant results using either image index or image fraction for both TM-LANDSAT or HRV-SPOT data. Of the twelve models tested, a linear model gave a significant relationship for the biomass in the intermediate and low levels with spectral and elevation variables. It is recommended that future studies determine the most efficient model to quantify the biomass in the three levels of the forest. Author (revised)

N95-13290 RAND Corp., Santa Monica, CA.

MapView USER'S GUIDE

Larry McDonough, Scott Bailey, and Allison Koehler 1993 75 p Limited Reproducibility: More than 20% of this document may be affected by microfiche quality

(AD-A282469) Avail: Issuing Activity (Defense Technical Information Center (DTIC))

MapView is a general-purpose, object-oriented graphics program that was developed as part of the Theater Level Campaign/NonLinear Combat (TLC/NLC) project at RAND. Every attempt has been made to generalize the functionality of the program for use by other projects. MapView is written in the C programming language and runs under the X11 Release 5 windowing environment with Sun Microsystems' OPEN LOOK Toolkit. The program enables scenario generation through a flexible, user-friendly interface that defines graphic objects, places them on an underlying image, and modifies or queries them as desired. In addition, MapView can process a file of commands that define and modify graphic objects and create animated simulation output. DTIC

N95-13350# Instituto de Pesquisas Espaciais, Sao Jose dos Campos (Brazil).

AVHRR/NOAA IMAGES TO DETECT AND QUANTIFY DEFORESTATION IN AMAZON FOREST: RELATIONS WITH TM/LANDSAT DATA M.S. Thesis [IMAGENS DO SISTEMA SENSOR AVHRR/NOAA NA DETECCAO E AVALIACAO DE DESMATAMENTOS NA FLORESTA AMAZONICA: RELACOES COM DADOS DO SISTEMA TM/LANDSAT]

Silvana Amaral 1992 190 p In PORTUGESE

(INPE-5501-TDI/516) Avail: CASI HC A09/MF A02

This work analyzes the use of AVHRR (Advanced Very High Resolution Radiometer)/NOAA images to detect and evaluate deforestation in the Amazon Forest using TM/Landsat images for validation and calibration of the results. A pilot methodology was developed for the region of 'Serra do Roncador', MT, where deforestation is caused by large agriculture and cattle projects. An AVHRR image with spatial resolution of 2 km and geometrically corrected was used to classify areas of deforestation and forest. The identification of these classes and the comparison and validation of the area estimates with the visual interpretation of the TM (Thematic Mappers)/ Landsat images were based and on the use of Geographical Information System. The correlation results of forested and deforestation areas from AVHRR were compared to TM data using statistical analyses. Strong linear correlation and regression was found between the data sets (R(exp 2) = 0.93). An application of the model for the region of Sao Jose do Xingu, MT, with a deforestation pattern similar to that found in the first region, presented adequate results with average errors of 3 percent for the total forest area. The results corroborated the use of AVHRR band 3 to detect and monitor alterations in forest areas. TM/Landsat data are necessary to calibrate estimates of areas. Author (revised)

N95-13352# Instituto de Pesquisas Espaciais, Sao Jose dos Campos (Brazil).

USE OF REMOTE SENSING AND GEOGRAPHIC INFORMATION SYSTEM TECHNIQUES IN INTEGRATED STUDIES OF WATERSHEDS M.S. Thesis [TECNICAS DE SENSORIAMENTO REMOTO E SISTEMAS GEOGRAFICOS DE INFORMACOES NO ESTUDO INTEGRADO DE BACIAS HIDROGRAFICAS]

Alexandre Grimaldi deCastro May 1992 154 p In PORTUGESE

(INPE-5494-TDI/511) Avail: CASI HC A08/MF A02

This study was designed to assess the multitemporal patterns of soil loss at Ribeirao Bonito watershed State of Sao Paulo, Brazil. The potential of integrated use of remote sensing and GIS in environmental studies was

evaluated. The applicability of the Universal Soil Loss Equation model seems satisfactory. Meanwhile, there was observed some analytical and operational restrictions related to both systems. Technical improvements are necessary to solve difficulties related to digital image processing and integration of remote sensing and GIS. The main impediment was represented by the absence of specific quality control procedures during acquisition processing, analysis conversion and final products presentation. Author

44 ENERGY PRODUCTION AND CONVERSION

Includes specific energy conversion systems, e.g., fuel cells; global sources of energy; geophysical conversion; and windpower.

For related information see also *07 Aircraft Propulsion and Power, 20 Spacecraft Propulsion and Power,* and *28 Propellants and Fuels.*

N95-11798# Helsinki Univ. of Technology, Espoo (Finland). Dept. of Technical Physics.

TKKMOD: A COMPUTER SIMULATION PROGRAM FOR AN INTEGRATED WIND DIESEL SYSTEM. VERSION 1.0: DOCUMENT AND USER GUIDE

L. M. Manninen 10 Dec. 1993 45 p

(ISSN 0358-0741)

(PB94-179090; TKK-F-C155; ISBN-951-22-1910-7) Avail: CASI HC A03/MF A01

The document describes TKKMOD, a simulation model developed at Helsinki University of Technology for a specific wind-diesel system layout, with special emphasis on the battery submodel and its use in simulation. The model has been included into the European wind-diesel modeling software package WDLTOOLS under the CEC JOULE project 'Engineering Design Tools for Wind-Diesel Systems' (JOUR-0078). WDLTOOLS serves as the user interface and processes the input and output data of different logistic simulation models developed by the project participants. TKKMOD cannot be run without this shell. The report only describes the simulation principles and model specific parameters of TKKMOD and gives model specific user instructions. The input and output data processing performed outside this model is described in the documentation of the shell. The simulation model is utilized for calculation of long-term performance of the reference system configuration for given wind and load conditions. The main results are energy flows, losses in the system components, diesel fuel consumption, and the number of diesel engine starts. NTIS

N95-11799# Helsinki Univ. of Technology, Espoo (Finland). Dept. of Technical Physics.

DATA ACQUISITION SYSTEM OF THE NANOSAW-2 STAND ALONE WIND DIESEL PLANT. DOCUMENT AND USER'S GUIDE

L. M. Manninen 10 Dec. 1993 34 p

(ISSN 0358-0741)

(PB94-179108; TKK-F-C157; ISBN-951-22-1912-3) Avail: CASI HC A03/MF A01

This document is the report of a wind-diesel measurement and modeling project. A measurement system comprising signal transducers, wiring, data logger, and data acquisition software has been constructed. The system produces comprehensive data of high quality. Remote control of measurement system and monitoring of plant status is also possible. The selected data logging unit has proved to be reliable. The logger and software can also be applied to other data acquisition applications with minor changes. Chapters 2 and 3 describe the physical measurement system excluding the data logger. The data acquisition including the hardware (data logger) and the software are discussed in chapter 4. Chapter 5 contains the user instructions. NTIS

N95-11846# Helsinki Univ. of Technology, Espoo (Finland). Dept. of Technical Physics.

VALIDATION RESULTS OF WIND DIESEL SIMULATION MODEL TKKMOD

L. M. Manninen 1993 11 p

(ISSN 0358-0741)

(PB94-179157; TKK-F-C156; ISBN-951-22-1911-5) Avail: CASI HC A03/MF A01

The document summarizes the results of TKKMOD validation procedure. TKKMOD is a simulation model developed at Helsinki University of Technology for a specific wind-diesel system layout. The model has been included into the European wind-diesel modeling software package WDLTOOLS under the CEC JOULE project Engineering Design Tools for Wind-Diesel Systems (JOUR-0078). The simulation model is utilized for calculation of long-term performance of the reference system configuration for given wind and load conditions. The main results are energy flows, energy losses in the system components, diesel fuel consumption, and the number of diesel engine starts. The work has been funded through the Finnish Advanced Energy System R&D Programme (NEMO). The validation has been performed using the data from EFI (Norwegian Electric Power Institute), since data from the Finnish reference system is not yet available. The EFI system has a slightly different configuration with similar overall operating principles and approximately same battery capacity. The validation data set, 394 hours of measured data, is from the first prototype wind-diesel system on the island FROYA off the Norwegian coast. NTIS

N95-11903*# National Aeronautics and Space Administration. Lewis Research Center, Cleveland, OH.

EMITTANCE THEORY FOR THIN FILM SELECTIVE EMITTER

Donald L. Chubb, Roland A. Lowe, and Brian S. Good Aug. 1994 18 p Presented at the First Conference on Thermophotovoltaic Generation of Electricity, Copper Mountain, CO, 24-26 Jul. 1994; sponsored by Midwest Research Inst.

(RTOP 233-01-0A)

(NASA-TM-106727; E-9097; NAS 1.15:106727) Avail: CASI HC A03/MF A01

Thin films of high temperature garnet materials such as yttrium aluminum garnet (YAG) doped with rare earths are currently being investigated as selective emitters. This paper presents a radiative transfer analysis of the thin film emitter. From this analysis the emitter efficiency and power density are calculated. Results based on measured extinction coefficients for erbium-YAG and holmium-YAG are presented. These results indicated that emitter efficiencies of 50 percent and power densities of several watts/sq cm are attainable at moderate temperatures (less than 1750 K). Author

N95-12647# National Renewable Energy Lab., Golden, CO.

SOLAR RADIATION DATA MANUAL FOR FLAT-PLATE AND CONCENTRATING COLLECTORS

M. A. Dunlap, ed. 1994 257 p

(Contract DE-AC36-83CH-10093)

(DE93-018229; NREL/TP-463-5607) Copyright Avail: CASI HC A12/MF A03

For designers and engineers of solar energy-related systems, the Solar Radiation Data Manual for Flat-Plate and Concentrating Collectors gives the solar resource available for various types of collectors for the US and its territories. The data in the manual were modeled using hourly values of direct beam and diffuse horizontal solar radiation from the National Solar Radiation Data Base (NSRDB). The NSRDB contains modeled (93%) and measured (7%) global horizontal, diffuse horizontal, and direct beam solar radiation for 1961-1990. DOE

N95-12650# Los Alamos National Lab., NM.

EFFECT OF OPERATING PARAMETERS AND ANODE GAS IMPURITIES UPON POLYMER ELECTROLYTE FUEL CELLS

K. R. Weisbrod and N. E. Vanderborgh 1994 7 p Presented at the 29th Intersociety Energy Conversion Engineering Conference, Monterey, CA, 7-12 Aug. 1994

(Contract W-7405-eng-36)

(DE94-014464; LA-UR-94-1876; CONF-940812-12) Avail: CASI HC A02/MF A01

PEM fuel cells are actively under development for transportation and other applications. Integration of a PEM fuel cell stack with a methanol reformer requires an understanding of single cell performance under a range of operating conditions using anode gas contaminated with impurities. The effect of temperature, pressure, and anode gas impurities on single cell PEM performance was investigated with platinum black electrodes. Single cell performance remained unchanged as temperature was varied between 80 and 100 at 3 atm pressure. High water partial pressures at 120C produced a mass transfer limiting current. While operation at 120C did not reverse CO2 poisoning, anode air addition proved effective. Air

injection also decreased CO poisoning at injected concentrations up to 200 ppm CO. Higher single cell tolerance was observed for CH3OH than CO. Up to 1 mole % CH3OH in the gas phase reduced the current density by less than 10%. DOE

N95-13126# California Univ., Berkeley. Lawrence Berkeley Lab, CA.
PROCEEDINGS OF THE EIGHTEENTH DOE SOLAR PHOTOCHEMISTRY RESEARCH CONFERENCE
1994 180 p Conference held in Tahoe City, CA, 5-9 Jun. 1994
(Contract DE-AC03-76SF-00098)
(DE94-014926; LBL-35647; CONF-9406158) Avail: CASI HC A09/MF A02

This annual conference brings together grantees and contractors of the DOE Division of Chemical Sciences engaged in fundamental research on solar photochemical energy conversion. It provides a focus for a wide spectrum of activities which contribute to providing the knowledge base and concepts needed for the capture and chemical conversion of solar energy. The research will provide the foundations for solar technologies of the future, in which light-induced charge separation processes will be applied to conversion of light energy to chemical energy, e.g., production of alcohols from CO2, H2 from water, NH3 from atm. N2, etc. The plenary lecture addresses photoconversion by nanocrystalline films of oxide semiconductors. The topical sessions feature presentations on charge transfer at semiconductor-liquid electrolyte junctions, long-range vectorial electron transfer in macromolecular arrays, transition metal photophysics, electronic structure and solvent effects on electron transfer processes, artificial assemblies for photosynthesis, and the photosynthetic bacterial reaction center. This volume contains the agenda for the meeting and abstracts of the 30 formal presentations and 56 posters. DOE

45 ENVIRONMENT POLLUTION

Includes atmospheric, noise, thermal, and water pollution.

N95-11742# Allied-Signal Aerospace Co., Kansas City, MO.
TRICHLOROETHYLENE EMISSIONS REDUCTIONS ACHIEVED BY ENCLOSING SOLVENT SPRAY DEGREASING OPERATIONS
B. M. Stone Jun. 1994 10 p Presented at the Pollution Prevention Conference, Denver, CO, 3-5 May 1994
(Contract DE-AC04-76DP-00613)
(DE94-013741; KCP-613-5378; CONF-940578-8) Avail: CASI HC A02/MF A01

Allied Signal Inc., Kansas City Division (KCD), produces precision electrical and mechanical parts at the US Department of Energy's Kansas City Plant (KCP). The KCD, in cooperation with the DOE and Sandia National Labs (SNL), has completed a goal to eliminate chlorinated hydrocarbons from production processes to the maximum extent practical. This has resulted in many cleaning operations converting from chlorinated hydrocarbon solvents, such as trichloroethylene (TCE), to other processes. Solvent spray cleaning operations which use TCE today do not have a practical alternative. KCP has implemented the use of enclosed ventilation booths. This reduces the amount of TCE emitted into the air by 71 percent. This report documents the use of the enclosed booth, cost of installation, and benefits of the booth. DOE

N95-11743# Joint Publications Research Service, Arlington, VA.
JPRS REPORT: SCIENCE AND TECHNOLOGY. CENTRAL EURASIA: LIFE SCIENCES
8 Dec. 1993 73 p Transl. into ENGLISH from various Russian articles
(JPRS-ULS-93-014) Avail: CASI HC A04/MF A01

Translations are presented covering the following subject areas: aerospace medicine, agricultural science, biochemistry, biotechnology, environment, genetics, immunology, medicine, microbiology, nonionizing radiation effects, physiology, public health, psychology, and radiation biology. CASI

N95-11745# Pacific Northwest Lab., Richland, WA.
GLOBAL ICE SHEET MODELING
T. J. Hughes and J. L. Fastook May 1994 165 p
(Contract DE-AC06-76RL-01830)
(DE94-013744; PNL-9414) Avail: CASI HC A08/MF A02

The University of Maine conducted this study for Pacific Northwest Laboratory (PNL) as part of a global climate modeling task for site characterization of the potential nuclear waste respository site at Yucca Mountain, NV. The purpose of the study was to develop a global ice sheet dynamics model that will forecast the three-dimensional configuration of global ice sheets for specific climate change scenarios. The objective of the third (final) year of the work was to produce ice sheet data for glaciation scenarios covering the next 100,000 years. This was accomplished using both the map-plane and flowband solutions of our time-dependent, finite-element gridpoint model. The theory and equations used to develop the ice sheet models are presented. Three future scenarios were simulated by the model and results are discussed. DOE

N95-11784# Allied-Signal Aerospace Co., Kansas City, MO.
IMPROVING THE EFFICIENCY OF HIGH PURITY WATER SYSTEMS
Michael Bukay (Bukay, Michael and Associates, San Rafael, CA.) and D. Youngberg May 1994 23 p Presented at the Ultrapure Water Expo, Philadelphia, PA, 9-11 May 1994
(Contract DE-AC04-76DP-00613)
(DE94-013742; KCP-613-5290; CONF-9405174-1) Avail: CASI HC A03/MF A01

High purity water (HPW) production involves the consumption of substantial amounts of energy, precious potable water, harsh/hazardous chemicals, and other environmental/impact materials. The discharge of some of the waste products from HPW systems is also a concern. The purpose of this paper is to discuss techniques to improve the efficiency of HPW production and thereby reduce any negative effects on the environment. It provides specific examples of how end-users and equipment suppliers are increasing the efficiency of their pretreatment, reverse osmosis, ion-exchange, and sanitization technology while frequently citing capital and operating cost reductions. DOE

N95-11826 Technische Univ., Delft (Netherlands). Interfaculty Reactor Inst.
ENVIRONMENTAL LICHENOLOGY: BIOMONITORING TRACE-ELEMENT AIR POLLUTION Ph.D. Thesis
J. E. Sloof 27 Sep. 1993 196 p Limited Reproducibility: More than 20% of this document may be affected by microfiche quality
(PB94-191335; ISBN-90-73861-12-8) Copyright Avail: CASI HC A09

In this thesis several experiments have been described on the applicability of lichens as biomonitors for trace-element air pollution. The aim of the thesis was to gain knowledge about the relationships between trace-element concentrations in lichens and concentrations in air particulate matter and/or depositions of trace elements on a regional and national scale, and about the processes involved in the element uptake and release by lichens. NTIS

N95-11845* National Aeronautics and Space Administration. Goddard Space Flight Center, Greenbelt, MD.
GREENHOUSE EFFECT DETECTION EXPERIMENT (GEDEX). SELECTED DATA SETS (Optical Disc)
Lola M. Olsen and Archibald Warnock, III 1992 The GEDEX Atmospheric Temperature Workshop was held in Columbia, MD, Jul. 1991 Sponsored by NASA, Washington Optical disc: 2 CD-ROM disks formatted to CDF version 2.1
(NASA-TM-109952; NAS 1.15:109952; NONP-NASA-CD-94-24404) Avail: Issuing Activity (NASA Goddard Space Flight Center, Distributed Active Archive Center, Greenbelt, MD 20771)

This CD-ROM contains selected data sets compiled by the participants of the Greenhouse Effect Detection Experiment (GEDEX) workshop on atmospheric temperature. The data sets include surface, upper air, and/or satellite-derived measurements of temperature, solar irradiance, clouds, greenhouse gases, fluxes, albedo, aerosols, ozone, and water vapor, along with Southern Oscillation Indices and Quasi-Biennial Oscillation statistics. CASI

N95-11848 Environmental Protection Agency, Research Triangle Park, NC. Office of Air Quality Planning and Standards.
DIRECTORY OF OAQPS INFORMATION SERVICES, MAY 1994
May 1994 33 p See also PB93-196624 Limited Reproducibility: More than 20% of this document may be affected by microfiche quality

(PB94-181310; EPA/452/B-94/010) Avail: Issuing Activity (National Technical Information Service (NTIS))

The Office of Air Quality Planning and Standards (OAQPS) provides many types of information services to EPA Headquarters and Regional Offices, State and local air pollution control agencies, consultants, industry, and the general public. The goal of the directory is to provide a brief listing of these services so that users can more easily determine what is available and how to obtain it. Information is grouped into four major areas: pollutant/program services technical support services, administrative support services, and compliance services. Each major area is further divided into sub-categories. Within each subcategory, line items describing information services are categorized by the type of delivery mechanism used. These include electronic bulletin boards, clearinghouses, reports and other documents, newsletters, support centers, workshops, and direct training such as classroom and self instructional courses. NTIS

N95-11849 Environmental Protection Agency, Washington, DC. Office of Air and Radiation.

IMPLEMENTATION STRATEGY FOR THE CLEAN AIR ACT AMMENDMENTS OF 1990. UPDATE, MAY 1994

May 1994 23 p See also PB94-129715 Limited Reproducibility: More than 20% of this document may be affected by microfiche quality

(PB94-180700; EPA/410/K-94/001) Avail: CASI HC A03

This is the fourth in a series of Implementation Strategy documents issued to inform Congress and the public on the status of activities implementing the Clean Air Act Amendments of 1990. The paragraphs immediately following present highlights of the past year's activities, as well as a summary of achievements to date. The remainder of the document consists of a cumulate list of significant actions already taken to carry out the 1990 Amendments, as well as a two year projection of future activities. NTIS

N95-11893 Environmental Protection Agency, Research Triangle Park, NC. Office of Air Quality Planning and Standards.

SO2 GUIDELINE DOCUMENT Final Report

A. M. Smith Feb. 1994 241 p Limited Reproducibility: More than 20% of this document may be affected by microfiche quality

(PB94-181393; EPA/452/R-94/008) Avail: CASI HC A11

The SO2 guideline document is a compilation of currently available policy and guidance for SO2 programs. It is intended only to provide a guide to SO2 policy and guidance in effect at the time of the document's preparation and does not present any new policy or guidance. Each chapter summarizes relevant policy and guidance and provides detailed references to guide the user to more complete sources found in the appendix and elsewhere. References include statutory and regulatory sources, Federal Register notices, and US EPA guidance documents and memoranda, and questions and answers. The guideline covers topics such as air quality status, air quality monitoring and modeling, and control strategies. NTIS

N95-11931*# Scripps Institution of Oceanography, La Jolla, CA.

TRACE GAS EMISSIONS TO THE ATMOSPHERE BY BIOMASS BURNING IN THE WEST AFRICAN SAVANNAS Final Report, 1 Oct. 1991 - 31 Mar. 1994

Robert J. Frouin, Samuel F. Iacobellis, Herisoa Razafimpanilo, and Richard C. J. Somerville 28 Aug. 1994 111 p

(Grant NAGw-2727)

(NASA-CR-196758; NAS 1.26:196758) Avail: CASI HC A06/MF A02

Savanna fires and atmospheric carbon dioxide (CO2) detection and estimating burned area using Advanced Very High Resolution Radiometer—(AVHRR) reflectance data are investigated in this two part research project. The first part involves carbon dioxide flux estimates and a three-dimensional transport model to quantify the effect of north African savanna fires on atmospheric CO2 concentration, including CO2 spatial and temporal variability patterns and their significance to global emissions. The second article describes two methods used to determine burned area from AVHRR data. The article discusses the relationship between the percentage of burned area and AVHRR channel 2 reflectance (the linear method) and Normalized Difference Vegetation Index (NDVI) (the nonlinear method). A comparative performance analysis of each method is described. CASI

N95-12110*# Western Commercial Space Center, Inc., Lompoc, CA.

ENVIRONMENTAL PROCESS IMPROVEMENT FEASIBILITY STUDY AND DEMONSTRATION PROGRAM Final Report, 1 Jun. 1993 - 27 May 1994

Rodger L. Martin 2 Jun. 1994 177 p Prepared for Tennessee Univ., Tullahoma, TN and Calspan Corp., Tullahoma, TN

(Grant NAGw-1195; AF Proj. 9310)

(NASA-CR-196789; NAS 1.26:196789) Avail: CASI HC A09/MF A02

This report is the final product of an environmental study conducted by Western Commercial Space Center, Inc. under contract to Tennessee-Calspan Center for Space Transportation and Applied Research. The purpose of this investigation is to accurately document the current environmental and permitting processes associated with commercial space launch activity at Vandenberg AFB, and make recommendations to streamline those processes. The particular areas of interest focus on: identifying applicable Federal, state, and local laws, Department of Defense directives, and Air force regulations; defining the environmental process on Vandenberg AFB and how it relates with other agencies, including Federal and state regulatory agencies; and defining the air quality permit process. Study investigation results are applied to an example Pilot Space Launch Vehicle (PSLV) planning to launch from Vandenberg AFB. The PSLV space hardware is analyzed with respect to environmental and permitting issues associated with vehicle processing, facilities required (existing or new), and launch. The PSLV verified the earlier findings of the study and gave insight into streamlining recommendations. Author (revised)

N95-12356# Environmental Protection Agency, Washington, DC. Information Access Branch.

ACCESS EPA

1993 636 p

(PB93-170041; EPA-220/B-93-008; ISBN-0-16-041867-4) Avail: CASI HC A99/MF A06; SOD HC

Access EPA is a directory of U.S. Environmental Protection Agency (EPA) and other public sector environmental information resources. First published in 1991, this is the third, revised edition of the directory. There is information for everyone interested in the environment: citizens, consumers, householders; scientists; federal, state, local, and tribal governments; business people; and students and researchers. Contact information and a description of services is given for each information resource. Each chapter begins with a brief introduction and table of contents. In some instances, supplementary material is provided at the end of the chapter. With the exception of chapter 7, State Environmental Libraries, each of the chapters describes EPA information. Included after the eight chapters of information contacts are the following reference tools: acronyms that appear throughout ACCESS EPA; an index of library and information services by state; and a name/title/subject index. Derived from text

N95-12384*# National Academy of Sciences - National Research Council, Washington, DC. Commission on Geosciences, Environment, and Resources.

SOLAR INFLUENCES ON GLOBAL CHANGE

1994 173 p Sponsored by NASA, Washington, NSF, NOAA, Geological Survey, Dept. of Agriculture, and Office of Naval Research

(Grant NSF OCE-93-13563)

(NASA-CR-196966; NAS 1.26:196966; LC-94-67788; ISBN-0-309-05148-7) Copyright Avail: CASI HC A08/MF A02

Monitoring of the Sun and the Earth has yielded new knowledge essential to this debate. There is now no doubt that the total radiative energy from the Sun that heats the Earth's surface changes over decadal time scales as a consequence of solar activity. Observations indicate as well that changes in ultraviolet radiation and energetic particles from the Sun, also connected with the solar activity, modulate the layer of ozone that protects the biosphere from the solar ultraviolet radiation. This report reassesses solar influences on global change in the light of this new knowledge of solar and atmospheric variability. Moreover, the report considers climate change to be encompassed within the broader concept of global change; thus the biosphere is recognized to be part of a larger, coupled Earth system. Implementing a program to continuously monitor solar irradiance over the next several decades will provide the opportunity to estimate solar influences on global change, assuming continued maintenance of observations of climate and other potential forcing mechanisms. In the lower atmosphere, an increase in solar radiation is expected to cause global warming. In the stratosphere, however, the two

effects produce temperature changes of opposite sign. A monitoring program that would augment long term observations of tropospheric parameters with similar observations of stratospheric parameters could separate these diverse climate perturbations and perhaps isolate a greenhouse footprint of climate change. Monitoring global change in the troposphere is a key element of all facets of the United States Global Change Research Program (USGCRP), not just of the study of solar influences on global change. The need for monitoring the stratosphere is also important for global change research in its own right because of the stratospheric ozone layer.

Derived from text

N95-12462# University Corp. for Atmospheric Research, Boulder, CO.
REPORTS TO THE NATION ON OUR CHANGING PLANET. EL NINO AND CLIMATE PREDICTION, NO. 3, SPRING 1994
John M. Wallace (Washington Univ., Seattle, WA.) and Shawna Vogel Jun. 1994 26 p LIMITED REPRODUCIBILITY: More than 20% of this document may be affected by color photographs Original contains color illustrations
(Grant NOAA-27GP0232-1)
Avail: CASI HC A03/MF A01

Climate prediction helps societies plan their lives, agricultural needs, and economic needs around the fluctuating seasonal changes that occur. El Nino, a sporadically occurring warm ocean current affecting climate in the Pacific, typically appears around December and lasts for several months. Detrimental effects include: (1) a scarcity of marine life which decreases available food supplies and depresses the fishing industries; (2) heavy rains that bring their own losses and disasters; (3) exposure and destruction of coral reefs in the western Pacific due to sea-level rises in the east; and (4) sometimes an increase in mosquito-borne diseases. Positive effects include: (1) generation of or increase in fresh water supplies; (2) production of temporary habitats for migrating fish trapped during flooding; and (3) proliferation of some marine food supplies from animals that thrive in warmer water temperatures. Typically, losses from El Ninos are dramatically larger than gains. Worldwide, scientists now understand how El Ninos develop, affect the ocean, and possibly can be predicted with the help of satellite imagery and the global tracking of sea surface temperatures. Ocean winds cause upwelling, which reduces phytoplankton available to the higher marine food chain. Ocean winds and sea currents have a symbiotic relationship and when the responses between them become intense, small perturbations can occur that eventually cause an El Nino to develop. From satellite observations, scientists have developed numerical prediction models that depict occurring climatic processes. These models allow understanding of how specific systems operate, how El Nino occurrence conditions are generated, how to predict El Nino climatic patterns and their effects, and how to better manage agricultural, marine, and water resources. CASI

N95-12771 Helsinki Univ. of Technology, Espoo (Finland). Metrology Research Inst.
DEVELOPMENT OF UV IRRADIANCE STANDARDS
E. Ikonen, M. L. Junttila, and K. Jokela Jan. 1993 16 p Limited Reproducibility: More than 20% of this document may be affected by microfiche quality
(PB94-181005; ISBN-951-22-2069-5) Avail: CASI HC A03

Precision measurements of solar ultraviolet (UV) radiation are needed for the assessment of health and environmental effects associated with the depletion of stratospheric ozone. The possibility of large ozone depletions over the Northern Europe combined with the relatively high UV sensitivity of the population are reasons justifying increased efforts for solar UV measurements in the Nordic Countries. Moreover, reflection from snow considerably increases ocular and facial doses in spring. Presently, the most accurate UV measurements are carried out at 15% uncertainty level with absolutely calibrated spectroradiometers. To provide meaningful estimates of the solar UV trends at the few percent uncertainty level, calibration of spectroradiometers must, at least, be stable at 1% level over time scales of ten years or more. The best way to do this is to establish a detector based primary standard which can be used for direct calibration of spectroradiometers. We have available at the Finnish Center for Radiation and Nuclear Safety and at the Helsinki University of Technology the necessary basic equipment needed for the new calibration system.

NTIS

N95-12776# Rijksinstituut voor Volksgezondheid en Milieuhygieene, Bilthoven (Netherlands).
ALLOCATING CO2-EMISSIONS BY USING EQUITY RULES AND OPTIMIZATION
M. A. Janssen, M. G. J. DenElzen, and J. Rotmans Dec. 1992 53 p
(PB94-192861; RIVM-222901012) Avail: CASI HC A04/MF A01

In order to reduce the risks of a climate change, a major problem in developing an effective international policy, is the allocation of the responsibility for reducing greenhouse gas emissions among regions. This report presents two approaches to provide for the allocation problem of emission reductions of the most important greenhouse gas: CO2. The first deals with a description of the emission debt concept. The authors use an equity rule by which all past and future dwellers on earth are permitted to emit an equal CO2 quotum per year. Furthermore, the level of the equal emission quotum is dependent on the policy related CO2-equivalent concentration targets. In the second approach the allocation problem is formulated as an optimization problem. This contains an 'optimal' trade off between rough estimates for social and economic consequences of reducing fossil CO2-emissions in order to meet policy targets, as expressed in a CO2-equivalent concentration level. NTIS

N95-12777# Rijksinstituut voor de Volksgezondheid, Bilthoven (Netherlands).
THE ADDITIONAL PROGRAMME ON AMMONIA Final Report
G. M. F. Boermans and J. W. Erisman Mar. 1993 44 p
(PB94-193075; RIVM-222105002) Avail: CASI HC A03/MF A01

In this report results of the additional monitoring program on NH3 are reported. The aim of this project was to evaluate long-range transport model (TREND) results on NH3 concentrations in high density emission areas. For this evaluation, continuous ammonia concentrations were measured during one year at two locations in the Netherlands (Vredepeel and Lunteren). The Vredepeel as well as the Lunteren fixed point is located in rural areas with a large amount of intensive farming systems. Furthermore, the representativeness of these fixed point measurements was investigated using mobile measurements and a short term/short range transport model for NH3 Short-term Local scale Ammonia transport Model (SLAM). The measuring strategy developed for this research provides a good tool for estimating the representativeness of a single point measurement for a larger area surrounding the fixed point. NTIS

N95-12786*# Alabama Univ., Huntsville, AL. Scientific Information Systems Lab.
[A DATA AND INFORMATION SYSTEM FOR PROCESSING, ARCHIVAL, AND DISTRIBUTION OF DATA FOR GLOBAL CHANGE RESEARCH] Final Report, 26 May 1993 - 25 May 1994
Sara J. Graves 15 Aug. 1994 7 p
(Contract NCC8-21; NAG8-904)
(NASA-CR-196770; NAS 1.26:196770) Avail: CASI HC A02/MF A01

Work on this project was focused on information management techniques for Marshall Space Flight Center's EOSDIS Version 0 Distributed Active Archive Center (DAAC). The centerpiece of this effort has been participation in EOSDIS catalog interoperability research, the result of which is a distributed Information Management System (IMS) allowing the user to query the inventories of all the DAAC's from a single user interface. UAH has provided the MSFC DAAC database server for the distributed IMS, and has contributed to definition and development of the browse image display capabilities in the system's user interface. Another important area of research has been in generating value-based metadata through data mining. In addition, information management applications for local inventory and archive management, and for tracking data orders were provided.

Derived from text

N95-12798*# Georgia Inst. of Tech., Atlanta, GA. College of Computing.
PARALLELIZATION AND VISUAL ANALYSIS OF MULTIDIMENSIONAL FIELDS: APPLICATION TO OZONE PRODUCTION, DESTRUCTION, AND TRANSPORT IN THREE DIMENSIONS Annual Progress Report
Karsten Schwan Oct. 1994 31 p
(Grant NAGw-3886)
(NASA-CR-195971; NAS 1.26:195971) Avail: CASI HC A03/MF A01

Atmospheric modeling is a grand challenge problem for several reasons, including its inordinate computational requirements and its generation of

large amounts of data concurrent with its use of very large data sets derived from measurement instruments like satellites. In addition, atmospheric models are typically run several times, on new data sets or to reprocess existing data sets, to investigate or reinvestigate specific chemical or physical processes occurring in the earth's atmosphere, to understand model fidelity with respect to observational data, or simply to experiment with specific model parameters or components. Derived from text

N95-12832*# Harvard Univ., Cambridge, MA. Dept. of Chemistry
DEVELOPMENT OF TECHNIQUES FOR THE IN SITU OBSERVATION OF OH AND HO2 FOR STUDIES OF THE IMPACT OF HIGH-ALTITUDE SUPERSONIC AIRCRAFT ON THE STRATOSPHERE Final Technical Report, 1 Aug. 1990 - 31 Jul. 1993
James G. Anderson 8 Sep. 1994 23 p
(Contract NCC2-693)
(NASA-CR-196759; NAS 1.26:196759) Avail: CASI HC A03/MF A01

This three-year project supported the construction, calibration, and deployment of a new instrument to measure the OH and HO2 radicals on the NASA ER-2 aircraft. The instrument has met and exceeded all of its design goals. The instrumentation represents a true quantum leap in performance over that achieved in previous HO(x) instruments built in our group. Sensitivity for OH was enhanced by over two orders of magnitude as the weight fell from approximately 1500 to less than 200 Kg. Reliability has been very high: HO(x) data are available for all flights during the first operational mission, the Stratospheric Photochemistry, Aerosols, and Dynamics Expedition (SPADE). The results of that experiment have been reported in the scientific literature and at conferences. Additionally, measurements of H2O and O3 were made and have been reported in the scientific literature. The measurements demonstrated the important role that OH and HO2 play in determining the concentration of ozone in the lower stratosphere. During the SPADE, campaign the measurements demonstrated that the catalytic removal is dominated by processes involving the odd-hydrogen and halogen radicals-and extremely important constraint for photochemical models that are being used to assess the potential deleterious effects of super-sonic aircraft effluent on the burden of stratospheric ozone. Derived from text

N95-12855# Environmental Protection Agency, Ann Arbor, MI. Certification Div.
REGULATORY IMPACT ANALYSIS AND REGULATORY SUPPORT DOCUMENT: CONTROL OF AIR POLLUTION; DETERMINATION OF SIGNIFICANCE FOR NONROAD SOURCES AND EMISSION STANDARDS FOR NEW NONROAD COMPRESSION-IGNITION ENGINES AT OR ABOVE 37 KILOWATTS (50 HORSEPOWER) Final Report
T. Trimble, D. R. North, K. A. H. Green, M. A. Sabourin, and D. A. Guerrieri 27 May 1994 180 p
(PB94-194594) Avail: CASI HC A09/MF A02

The regulatory impact analysis and support document provides additional information in support of the Final Rulemaking (FRM). This FRM will regulate all new nonroad compression-ignition engines greater than or equal to 37 kilowatts (50 hp), except engines which propel or are used on marine vessels, aircraft engines, engines which propel locomotives, and engines regulated by the Mining, Safety, and Health Administration. The regulated engines are hereafter referred to as nonroad large CI engines. The goal of this regulation is to substantially reduce NOx emission and smoke from nonroad large CI engines beginning in the 1996 model year. NTIS

N95-12926# Lawrence Livermore National Lab., Livermore, CA.
INTERPOLATION OF SCATTERED TEMPERATURE DATA MEASUREMENTS ONTO A WORLDWIDE REGULAR GRID USING RADIAL BASIS FUNCTIONS WITH APPLICATIONS TO GLOBAL WARMING
E. J. Kansa, M. C. Axelrod, and J. R. Kercher May 1994 5 p Presented at the World Congress on Computational and Applied Mathematics, Atlanta, GA, 11-15 Jul. 1994
(Contract W-7405-eng-48)
(DE94-014745; UCRL-JC-117247; CONF-940719-5) Avail: CASI HC A01/MF A01

Our current research into the response of natural ecosystems to a hypothesized climatic change requires that we have estimates of various meteorological variables on a regularly spaced grid of points on the surface of the earth. Unfortunately, the bulk of the world's meteorological measurement stations is located at airports that tend to be concentrated on the coastlines of the world or near populated areas. We can also see that the spatial density of the station locations is extremely non-uniform with the greatest density in the USA, followed by Western Europe. Furthermore, the density of airports is rather sparse in desert regions such as the Sahara, the Arabian, Gobi, and Australian deserts; likewise the density is quite sparse in cold regions such as Antarctica Northern Canada, and interior northern Russia. The Amazon Basin in Brazil has few airports. The frequency of airports is obviously related to the population centers and the degree of industrial development of the country. We address the following problem here. Given values of meteorological variables, such as maximum monthly temperature, measured at the more than 5,500 airport stations, interpolate these values onto a regular grid of terrestrial points spaced by one degree in both latitude and longitude. This is known as the scattered data problem. DOE

N95-13192# Instituto de Pesquisas Espaciais, Sao Jose dos Campos (Brazil).
CESIUM-137 AND NATURAL RADIONUCLIDES IN SOILS FROM SOUTHERN BRAZIL AND IN SOILS AND OTHERS ENVIRONMENTAL SAMPLES FROM ANTARCTIC [CESIO-137 E RADIONUCLIDEOS NATURAIS EM SOLOS DO SUL DO BRASIL E EM SOLOS E OUTRAS AMOSTRAS AMBIENTAIS DA ANTARTICA]
Luiz Alexandre Schuch Apr. 1993 168 p In PORTUGESE
(INPE-5505-TDI-517) Avail: CASI HC A08/MF A02

This work presents a study of environmental artificial and natural radioactivity levels in soil samples from Southern Brazil and in soils and other environmental samples from Antarctica. Artificial radioactivity was determined by measuring Cs-137 which is a 30.1 year half-life man-made radionuclide produced in the past by atmospheric tests of nuclear weapons. Natural radioactivity was determined by measuring some radionuclides belonging to Th-232 and U-238 natural radioactive families, and of K-40 concentrations. Several types of soil from Southern Brazil and soil samples, marine sediments, lichens, mosses, and algae collected at King George and other nearby islands (South Shetland Archipelago, Antarctica) were analyzed. A gamma-ray spectrometer was used to measure radioactivity levels of the collected samples and its overall characteristics are analyzed. Measurements on the collected samples have shown: low radioactivity levels when compared with similar samples from the Northern Hemisphere; the characteristic latitudinal variation of the fallout product Cs-137; higher Cs-137 lixiviation when compared with that of natural radionuclides in soils collected at different dates; the impossibility to measure in collected soil samples fallout products from Chernobyl nuclear accident that occured in April, 1986; and low correlation of Cs-137 concentrations with some pedological parameters. A high linear correlation was observed between the integrated Cs-137 concentrations, in Bqm(exp -2), and organic carbon, in individual vertical soil profiles. However this is not observed when the integrated Cs-137 concentrations are compared in all the profiles, with the mean value of organic carbon for each profile. It was also observed that among environmental samples from Antarctic, lichens and mosses have shown the highest Cs-137 concentrations. These results are being used to select the species that will be used for yearly fallout follow-up among the most abundant ones. Author (revised)

46 GEOPHYSICS

Includes aeronomy; upper and lower atmosphere studies; ionospheric and magnetospheric physics; and geomagnetism.

For space radiation see *93 Space Radiation.*

N95-11730# Geological Survey, Denver, CO.
PRELIMINARY SEISMICITY AND FOCAL MECHANISMS FOR THE SOUTHERN GREAT BASIN OF NEVADA AND CALIFORNIA, JANUARY 1992 - SEPTEMBER 1992
S. C. Harmsen 1994 213 p
(Contract DE-AI08-92NV-10874)
(DE94-013589; USGS-OFR-93-369) Avail: CASI HC A10/MF A03

The telemetered southern Great Basin seismic network (SGBSN) is operated for the Department of Energy's Yucca Mountain Project (YMP). The US Geological Survey, Branch of Earthquake and Landslide Hazards, maintained this network until September 30, 1992, at which time all

operational and analysis responsibilities were transferred to the University of Nevada at Reno Seismological Laboratory (UNRSL). This report contains preliminary earthquake and chemical explosion hypocenter listings and preliminary earthquake focal mechanism solutions for USGS/SGBSN data for the period January 1, 1992 through September 30, 1992, 15:00 UTC. DOE

N95-11732# Los Alamos National Lab., NM.
MICROMORPHOLOGY, MINERALOGY, AND GENESIS OF SOILS AND FRACTURE FILLS AND THE PAJARITO PLATEAU, NEW MEXICO Ph.D. Thesis
D. W. Davenport (Texas Technological Univ., Lubbock, TX.) Dec. 1993 109 p
(Contract W-7405-eng-36)
(DE94-013612; LA-SUB-94-84) Avail: CASI HC A06/MF A02

The town of Los Alamos, and the Los Alamos National Laboratory (LANL), are located on the Pajarito Plateau in north-central New Mexico. Environmental concerns have recently focused attention on the numerous fractures in the Bandelier Tuff, the series of volcanic rock units that make up most of the plateau. These fractures have come into question as possible conduits for transport of contaminants downward through the tuff. This study arose out of a need to evaluate the potential for contaminant transport in the fractures. Because the fractures are typically filled, or partially filled, with soil-like material, and appear to be physically continuous with the soils on the surface of the Pajarito Plateau, it was decided to approach the question of the fractures from a soil genesis and morphology standpoint. Specifically, it was believed that soil characterization techniques, including soil micromorphological and mineralogical analyses, could provide information about the dominant processes (past and present) acting in the soils and fractures. The specific objectives of this research were to investigate: (1) the physical, mineralogical and chemical nature of fracture-filling materials in the Bandelier Tuff, as well as associated surface soils; (2) the relationships among fracture-fills, tuff bedrock, and surface soils of the Pajarito Plateau; (3) the processes responsible for the development of the fracture-fills; and (4) the likely sequence of events leading to the present morphology of the soils and fracture-fills. DOE

N95-11741# Lawrence Livermore National Lab., Livermore, CA.
HIGH PERFORMANCE CLIMATE SYSTEM MODELING USING A DOMAIN AND TASK DECOMPOSITION MESSAGE-PASSING APPROACH
J. J. Ambrosiano, J. Bolstad, A. J. Bourgeois, J. C. Brown, B. Chan, W. P. Dannevik, P. G. Eltgroth, B. Grant, C. Matarazzo, and A. A. Mirin et al Mar. 1994 9 p Presented at the Scalable High Performance Computing Conference, Knoxville, TN, 23 May 1994
(Contract W-7405-eng-48)
(DE94-013739; UCRL-JC-115610; CONF-9405100-9) Avail: CASI HC A02/MF A01

We have developed a Climate System Modeling Framework (CSMF) for high-performance systems, designed to schedule and couple multiple physics simulations packages in a flexible and transportable manner. Some of the major packages in the CSMF include models of atmospheric and oceanic circulation and chemistry, land surface and sea ice processes, and trace gas biogeochemistry. Parallelism is achieved through both domain decomposition and process-level concurrency, with data transfer and synchronization accomplished through message-passing. Both machine transportability and architecture-dependent optimization are handled through libraries and conditional compile directives. Preliminary experiments with the CSMF have been executed on a number of high-performance platforms, including the Intel Paragon, the TMC CM-5 and the Meiko CS-2, and we are in the very early stages of optimization. Progress to date is presented. DOE

N95-11801*# SRI International Corp., Menlo Park, CA. Geoscience and Engineering Center.
MAGNETOSPHERIC-IONOSPHERIC POYNTING FLUX Final Report
Jeffrey P. Thayer Aug. 1994 76 p Original contains color illustrations
(Contract NAS5-31214; SRI Proj. 2432)
(NASA-CR-196856; NAS 1.26:196856) Avail: CASI HC A05/MF A01; 8 functional color pages

Over the past three years of funding SRI, in collaboration with the University of Texas at Dallas, has been involved in determining the total electromagnetic energy flux into the upper atmosphere from DE-B electric and magnetic field measurements and modeling the electromagnetic energy flux at high latitudes, taking into account the coupled magnetosphere-ionosphere system. This effort has been very successful in establishing the DC Poynting flux as a fundamental quantity in describing the coupling of electromagnetic energy between the magnetosphere and ionosphere. The DE-B satellite electric and magnetic field measurements were carefully scrutinized to provide, for the first time, a large data set of DC, field-aligned, Poynting flux measurement. Investigations describing the field-aligned Poynting flux observations from DE-B orbits under specific geomagnetic conditions and from many orbits were conducted to provide a statistical average of the Poynting flux distribution over the polar cap. The theoretical modeling effort has provided insight into the observations by formulating the connection between Poynting's theorem and the electromagnetic energy conversion processes that occur in the ionosphere. Modeling and evaluation of these processes has helped interpret the satellite observations of the DC Poynting flux and improved our understanding of the coupling between the ionosphere and magnetosphere. Author

N95-11836# National Oceanic and Atmospheric Administration, Washington, DC. Sounding Implementation Branch.
TOVS OPERATIONAL SOUNDING UPGRADES: 1990-1992
Anthony L. Reale, Michael W. Chalfant, Robert V. Wagoner, Timothy J. Gardner, and Leah W. Casey Mar. 1994 76 p Original contains color illustrations
(NOAA-TR-NESDIS-76) Avail: CASI HC A05/MF A01

The TIROS Operational Vertical Sounder (TOVS) on board NOAA polar orbiting satellites provides a global set of radiometric observations which are used to compute NESDIS operational sounding products. The TOVS consists of the High-resolution Infrared Radiation Sounder (HIRS), Microwave Sounding Unit (MSU), and Stratospheric Sounding Unit (SSU) instruments (Smith, 1979). Sounding products of atmospheric temperature and moisture are produced with the primary objective of providing global data for use in operational numerical weather prediction forecast models. Two operational NOAA satellites in sun synchronous orbits, six hours apart, provide an average of four sounding observations daily for most locations on the earth. The soundings are particularly useful in remote ocean regions where conventional meteorological observations are sparse. The horizontal resolution and spatial density of the derived soundings ranges from about 50 km to 300 km depending on the satellite scan angle and cloud conditions. The vertical resolution ranges from about 3 to 5 km, but for user convenience is defined at 40 pressure levels ranging from 1000 to .1 hPa for temperature, and at the 15 lowest levels from 1000 to 300 hPa for moisture. These are then converted to 18 values of layer mean virtual temperature and geopotential heights, and 3 layers of precipitable water, which are the standard operational sounding products distributed to users and archived. The TOVS radiance temperatures and ancillary data for each sounding are also provided . The 40 TOVS pressure levels and 21 layers comprising the products are listed in Appendix A. Author

N95-12103*# National Aeronautics and Space Administration, Washington, DC.
PRESENT STATE OF KNOWLEDGE OF THE UPPER ATMOSPHERE1993: AN ASSESSMENT REPORT, PART 2
Michael J. Kurylo, Jack A. Kaye, Robert F. Hampson, and Anne-Marie Schmoltner Jan. 1994 149 p
(NASA-RP-1337; NAS 1.61:1337) Avail: CASI HC A07/MF A02

This document is issued in response to the Clean Air Act Amendment of 1990, Public Law 101-549, which mandates that the National Aeronautics and Space Administration (NASA) and other key agencies submit triennial reports to Congress and the Environmental Protection Agency. NASA is charged with the responsibility to report on the state of our knowledge of the earth's upper atmosphere, particularly the stratosphere. Part 2 (this document) presents summaries of several scientific assessments of our current understanding of the chemical composition and physical structure of the stratosphere, in particular how the abundance and distribution of ozone is predicted to change in the future. These reviews include: (Section B) 'Scientific Assessment of Ozone Depletion: 1991'; (Section C) 'Methyl bromide and the Ozone Layer: A Summary of Current Understanding', published in 1992; (Section D) 'Concentrations, Lifetimes, and Trends of Chlorofluorocarbons (CFC's), Halons, and Related Molecules in the Atmosphere'; (Section E) 'The Atmospheric Effects of Stratospheric Aircraft:

Interim Assessment Report of the NASA High-Speed Research Program'; (Section F) 'Chemical Kinetics and Photochemical Data for Use in Stratospheric Modeling'; and (Section G) a list of the contributors to this report. Author (revised)

N95-12112# Polish Academy of Sciences, Warsaw (Poland). Inst. of Physical Acoustics.

AN ESTIMATE OF THE EVOLUTION OF THE ACOUSTIC EMISSION SPECTRUM OF ROCKS ON THE BASIS OF CHANGES IN ITS AVERAGE FREQUENCY IN THE PROCESS OF DEFORMATION [OCENA EWOLUCJI WIDMA EMISJI AKUSTYCZNEJ SKAL NA PODSTAWIE ZMIAN JEGO SREDNIEJ CZESTOTLIWOSCI W PROCESIE DEFORMACJI]

Anna Jaroszewska and Zygmunt Palka 1992 21 p
(ISSN 0208-5658)
Avail: CASI HC A03/MF A01

In this article the authors propose and apply a new procedure for estimating the evolution of the frequency spectrum of the acoustic emission of rocks based on determining its average frequency as a function of uniaxial compression. The authors analyzed dolomite, dolomite limestone, and sandstone samples and observed that the average frequency increases as a function of loading time and then decreases dramatically immediately prior to the failure of the samples. These results are consistent with earlier results obtained by the authors with another method and the dominant trends in the acoustic emission frequency spectrum of the rocks under uniaxial compression. But the results of this study indicate that the proposed method is more accurate and effective in predicting the actual time of failure of the rocks. Author

N95-12130*# National Aeronautics and Space Administration. Goddard Space Flight Center, Greenbelt, MD.

FORTRAN PROGRAMS TO PROCESS MAGSAT DATA FOR LITHOSPHERIC, EXTERNAL FIELD, AND RESIDUAL CORE COMPONENTS

Douglas E. Alsdorf (Ohio State Univ., Columbus.) and Ralph R. B. vonFrese (Ohio State Univ., Columbus.) Sep. 1994 188 p Sponsored by Amoco Oil Co.; Arco Chemical Co.; Exxon Corp.; Texaco, Inc.; Unocal Corp.; Ohio Supercomputer Center
(Grant NAGw-973; RTOP 921-00-00)
(NASA-TM-104612; Rept-94B00142; NAS 1.15:104612) Avail: CASI HC A09/MF A02

The FORTRAN programs supplied in this document provide a complete processing package for statistically extracting residual core, external field and lithospheric components in Magsat observations. To process the individual passes: (1) orbits are separated into dawn and dusk local times and by altitude, (2) passes are selected based on the variance of the magnetic field observations after a least-squares fit of the core field is removed from each pass over the study area, and (3) spatially adjacent passes are processed with a Fourier correlation coefficient filter to separate coherent and non-coherent features between neighboring tracks. In the second state of map processing: (1) data from the passes are normalized to a common altitude and gridded into dawn and dusk maps with least squares collocation, (2) dawn and dusk maps are correlated with a Fourier correlation efficient filter to separate coherent and non-coherent features; the coherent features are averaged to produce a total field grid, (3) total field grids from all altitudes are continued to a common altitude, correlation filtered for coherent anomaly features, and subsequently averaged to produce the final total field grid for the study region, and (4) the total field map is differentially reduced to the pole. Author

N95-12226*# National Aeronautics and Space Administration. Goddard Space Flight Center, Greenbelt, MD.

TECHNICAL REPORT SERIES ON GLOBAL MODELING AND DATA ASSIMILATION. VOLUME 2: DIRECT SOLUTION OF THE IMPLICIT FORMULATION OF FOURTH ORDER HORIZONTAL DIFFUSION FOR GRIDPOINT MODELS ON THE SPHERE

Yong Li (General Sciences Corp., Laurel, MD.), S. Moorthi (National Meteorological Center, Camp Springs, MD.), J. Ray Bates, and Max J. Suarez Oct. 1994 48 p
(Contract NAS5-32332; RTOP 910-00-00)
(NASA-TM-10406; Rept-94B00143; NAS 1.15: 10406) Avail: CASI HC A03/MF A01

High order horizontal diffusion of the form K Delta(exp 2m) is widely used in spectral models as a means of preventing energy accumulation at the shortest resolved scales. In the spectral context, an implicit formation of such diffusion is trivial to implement. The present note describes an efficient method of implementing implicit high order diffusion in global finite difference models. The method expresses the high order diffusion equation as a sequence of equations involving Delta(exp 2). The solution is obtained by combining fast Fourier transforms in longitude with a finite difference solver for the second order ordinary differential equation in latitude. The implicit diffusion routine is suitable for use in any finite difference global model that uses a regular latitude/longitude grid. The absence of a restriction on the timestep makes it particularly suitable for use in semi-Lagrangian models. The scale selectivity of the high order diffusion gives it an advantage over the uncentering method that has been used to control computational noise in two-time-level semi-Lagrangian models. Author

N95-12244*# Arizona State Univ., Tempe, AZ.

UV EXTINCTION AND IR EMISSION IN DIFFUSE H2 REGIONS Final Technical Report, 15 Aug. 1991 - 14 Aug. 1994

Per A. Aannestad 1994 33 p
(Grant NAG5-1743)
(NASA-CR-196939; NAS 1.26:196939) Avail: CASI HC A03/MF A01

HII regions occupy a unique position in our understanding of the physical relationships between stars, the interstellar medium, and galactic structure. Observations show a complex interaction between a newly formed hot star and its surroundings. In particular, the ultraviolet radiation from the stars modifies the pre-existing dust, which again affects both the amount of ionizing radiation absorbed by the gas, and the infrared spectrum emitted by the heated dust. The aim of this project was to use UV and far-UV observations to gain information on the nebular dust, and to use this dust to model the far-IR emission, for a consistent picture of a few selected diffuse HII regions. Using archival data from the IUE and Voyager data banks and computed model atmospheres, we have deduced extinction curves for early-types stars. The requisite spectral resolution turned out to be a major task. We have successfully modelled these curves in terms of a multi-component, multi-size distribution of dust grains, and interpret the differences in the curves as primarily due to the presence or non-presence of intermediate size grains (0.01 to 0.04 micron). Much smaller (0.005 micron) grains must also be present. Finally, we have made calculations of the temperature fluctuations and the corresponding infra-red emission in such small grains. Author (revised)

N95-12468*# Illinois Univ., Champaign, IL.

THE TERRESTRIAL GRAVITATIONAL WAVE ENVIRONMENT FROM KNOWN SOURCES Final Technical Report, 1 Jan. 1992 - 31 Dec. 1993

Ronald F. Webbink 1993 4 p
(Grant NAGw-2996)
(NASA-CR-196167; NAS 1.26:196167) Avail: CASI HC A01/MF A01

The objective of this project was to produce a gravitational wave spectral line list of all known binary stars producing expected strain amplitudes at Earth in excess of h = 10 (exp -21), or gravitational wave fluxes in excess of F = 10 (exp -12) erg cm(exp -2) s(exp -1). These strain and flux limits lie above the anticipated detection thresholds for space-borne laser interferometers capable of detecting gravitational radiation in the 10 micron Hz to 1 Hz frequency range. The source list was intended to provide frequency (including each harmonic), amplitude and phase (for each polarization and harmonic), and celestial coordinates for each system, lacking only the orientation of the principal polarization axis with respect to the pole of the coordinate system, and the sign of the source phase and frequency (or, equivalently, of the sense of rotation of the strain tensor with time) from providing a complete source description. Such a spectral line list would lay essential groundwork for high-sensitivity, low-frequency searches for gravitational radiation. Author

N95-12506# California Univ., Davis, CA. Dept. of Civil Engineering.

TRIAXIAL AND TORSIONAL SHEAR TEST RESULTS FOR SAND Final Report

Bruce L. Kutter, Yie-Ruey Chen, and C. K. Shen Jun. 1994 195 p
(Contract N47408-89-C-1058)
(AD-A282725; NFESC-CR-94.003-SHR) Avail: CASI HC A09/MF A03

This report presents the results of the laboratory tests conducted in triaxial and torsional apparatus. The purposes of this report are not only to

support the calibration and verification of the bounding surface hypoplasticity model for granular soil but to provide a valuable data base for future research in numerical model simulation and design. Under this contract, two experiments were carried out: (1) Laboratory samples in the triaxial apparatus and hollow cylinder torsional apparatus; and (2) Centrifuge model tests including two and three-dimensional structures subjected to static and dynamic loadings. This report presents the results of triaxial tests including drained and undrained, monotonic and cyclic, and stress and strain controlled tests. The maximum stress ratio achieved in drained triaxial tests was significantly larger than that in undrained triaxial tests. Results of six hollow cylinder torsional and rotational shear tests are also presented. The results from different types are compared. Finally, the conclusions of these laboratory tests are also discussed. The test results indicate that the shape of phase transformation and failure surfaces were different when viewed in the pi-plane. It was also found that samples subject to rotational shear may be less likely to develop larger strain during undrained cycling than samples in triaxial compression/extension cyclic tests at similar stress ratios. DTIC

N95-12508# Phillips Lab., Hanscom AFB, MA.
DETERMINATION OF THE AURORAL OVAL Q INDEX FROM THE AIR WEATHER SERVICE K INDEX Interim Report
B. S. Dandekar 18 Oct. 1993 32 p
(AD-A282764; AD-E202000; PL-TR-93-2267; ERP-1136) Avail: CASI HC A03/MF A01

The AWS determines the auroral oval diameter in real time as a function of the Kp index from the particle precipitation measured aboard Defense Meteorological Satellites (DMSP). For the Q index needed to drive the auroral algorithm in the AWS polar ionospheric model, Hardy determined a relation between the Kp and the Q index. The analysis indicates that the auroral oval index Q computed from the AWS-K is overestimated. A least-squared deviation circle is fitted to the data base used in the Hardy algorithm. Using a four-year data set of Kp and Q observations, a new relation between the planetary magnetic activity index Kp and Q is determined to rectify this overestimation of the Q index. The new relation is :Q=0.964 Kp-0.3 for Kp less than 2 + and 0=2.04 Kp-2.7 for Kp greater than 2 +. The improved, more precise Q values obtained from this relation will improve prediction of the auroral oval phenomena that affect the performance of the real time operational systems. DTIC

N95-12534 Colorado Univ., Boulder, CO.
REACTIONS OF ATMOSPHERIC CLUSTER IONS Annual Technical Report, 1 Jun. 1993 - 31 May 1994
Stephen R. Leone and Veronica M. Bierbaum 28 Jun. 1994 2 p Limited Reproducibility: More than 20% of this document may be affected by microfiche quality
(Contract F49620-93-1-0372)
(AD-A282598; AFOSR-94-0459TR) Avail: CASI HC A01

In our first year of AASERT support, we have developed the necessary instrumentation and computer programs for measuring the mobilities of cluster ions using ion modulation/arrival time techniques. As a test of the methodology, we have carried out a systematic study of the mobility of CO+ in helium buffer gas as a function of drift field and have found excellent agreement with previous results. Studies of the mobilities and reactions of atmospheric cluster ions using our SIFT instrument are being initiated. DTIC

N95-12544 Naval Oceanographic Office, Bay Saint Louis, MS.
A UNIFIED APPROACH TO GEOPOTENTIAL FIELD MODELING
John M. Quinn and Donald L. Shiel Jul. 1993 118 p Limited Reproducibility: More than 20% of this document may be affected by microfiche quality
(AD-A283453; NOO-TR-308) Avail: CASI HC A06

It is shown that when both vector and gradient tensor components of a potential field are simultaneously available, inverse problems, such as determining the depth to the oceanic magnetic basement, can be split into a purely geometric problem, which seeks to determine the dimension and position parameters of one or more prisms and a purely geophysical problem, which seeks to determine the physical properties (i.e., the magnetization, polarization, density, etc.) of the prism. The geometrical problem is nonlinear and must be solved iteratively using standard stochastic or least-squares inversion techniques, while the geophysical problem is linear and may be solved by direct inversion once the geometric parameters have been established. DTIC

N95-12649# Los Alamos National Lab., NM.
AN OBSERVATIONAL TEST OF MAGNETOSPHERIC MAGNETIC FIELD MAPPING
L. A. Weiss, M. F. Thomsen, G. D. Reeves, E. W. Hones, and D. J. McComas 1994 4 p Presented at the 8th International Symposium on Solar Terrestrial Physics, Sendai, Japan, 6-10 Jun. 1994
(Contract W-7405-eng-36)
(DE94-014461; LA-UR-94-2129; CONF-9406192-3) Avail: CASI HC A01/MF A01

The distortion of the geomagnetic field is a key signature of the response of the magnetosphere to the solar wind input. A number of empirical models have been devised to estimate the magnetic field direction and magnitude at any point within the magnetosphere under a variety of conditions. We describe a technique whereby the field-line mapping predicted by such models is tested by matching measurements of magnetospheric plasma energy spectra obtained by Los Alamos instruments at geosynchronous orbit with spectra obtained by instruments on the polar-orbiting DMSP satellites (at an altitude of about 800 km) at times when the two satellites are in approximate magnetic conjugacy. With up to three geosynchronous satellites and as many as four DMSP satellites in operation at any given time, there are a very large number of such two-satellite conjunctions, allowing the model mappings to be tested under a wide range of local times and geomagnetic activity. Preliminary results from the application of this technique are presented for one week of data from March, 1991. DOE

N95-12686 Australian Geological Survey Organisation, Canberra, Australian Capital Territory (Australia).
AGSO 1993: YEARBOOK OF THE AUSTRALIAN GEOLOGICAL SURVEY ORGANISATION. GEOSCIENTIFIC RESEARCH AND DATABASE DEVELOPMENT FOR THE YEAR 1 JULY 1992 TO 30 JUNE 1993
1994 178 p
(ISSN 1039-5679)
Copyright Avail: Issuing Activity

The Australian Geological Survey Organization (AGSO) has a mission to build a vigorous, client driven national geoscientific mapping effort to encourage economically and environmentally sustainable management of Australian's mineral, energy, soil, and water resources. The 1992-93 yearbook focuses on: (1) report by the Mineral and Environmental Group which is focused on the Richard Review that emphasized on national mapping through the national Geoscience Mapping Accord; (2) report by the Petroleum and Marine Geoscience Group which consists of a comprehensive evaluation of the Continental Margins Program (provides regional geoscience data) and the Richard Review that indicates AGSO's general program direction over the preceding years; (3) database coordination and research (operate, develop, and implement AGSO information technology strategy); and (4) program delivery which provides cartographic products and related services in support to the AGSO's program objectives. CASI

N95-12949*# California Univ., Los Angeles, CA. Dept. of Earth and Space Sciences.
NEOTECTONICS OF ASIA: THIN-SHELL FINITE-ELEMENT MODELS WITH FAULTS
Xianghong Kong and Peter Bird Jul. 1994 46 p Submitted for publication
(Grant NAGw-3042)
(NASA-CR-196436; NAS 1.26:196436) Avail: CASI HC A03/MF A01

As India pushed into and beneath the south margin of Asia in Cenozoic time, it added a great volume of crust, which may have been (1) emplaced locally beneath Tibet, (2) distributed as regional crustal thickening of Asia, (3) converted to mantle eclogite by high-pressure metamorphism, or (4) extruded eastward to increase the area of Asia. The amount of eastward extrusion is especially controversial: plane-stress computer models of finite strain in a continuum lithosphere show minimal escape, while laboratory and theoretical plane-strain models of finite strain in a faulted lithosphere show escape as the dominant mode. We suggest computing the present (or neo)tectonics by use of the known fault network and available data on fault activity, geodesy, and stress to select the best model. We apply a

new thin-shell method which can represent a faulted lithosphere of realistic rheology on a sphere, and provided predictions of present velocities, fault slip rates, and stresses for various trial rheologies and boundary conditions. To minimize artificial boundaries, the models include all of Asia east of 40 deg E and span 100 deg on the globe. The primary unknowns are the friction coefficient of faults within Asia and the amounts of shear traction applied to Asia in the Himalayan and oceanic subduction zones at its margins. Data on Quaternary fault activity prove to be most useful in rating the models. Best results are obtained with a very low fault friction of 0.085. This major heterogeneity shows that unfaulted continum models cannot be expected to give accurate simulations of the orogeny. But, even with such weak faults, only a fraction of the internal deformation is expressed as fault slip; this means that rigid microplate models cannot represent the kinematics either. A universal feature of the better models is that eastern China and southeast Asia flow rapidly eastward with respect to Siberia. The rate of escape is very sensitive to the level of shear traction in the Pacific subduction zones, which is below 6 MPa. Because this flow occurs across a wide range of latitudes, the net eastward escape is greater than the rate of crustal addition in the Himalaya. The crustal budget is balanced by extension and thinning, primarily within the Tibetan plateau and the Baikal rift. The low level of deviation stresses in the best models suggests that topographic stress plays a major role in the orogeny; thus, we have to expect that different topography in the past may have been linked with fundamentally different modes of continental collision. Author (revised)

N95-13025*# New Mexico Univ., Albuquerque, NM. Dept. of Earth and Planetary Science.

[FACTORS INFLUENCING THE RATES, PROCESSES AND MAGNITUDE OF ACCUMULATION OF CARBON IN DESERT SOILS]

Leslie D. McFadden 1994 30 p Sponsored in part by NSF

(Grant NAG5-1828)

(NASA-CR-196820; NAS 1.26:196820) Avail: CASI HC A03/MF A01

This report summarizes research funded through NASA's Soil Landscape Climate Program which includes studies of the systematics of carbon storage and flux in the terrestrial environment, specifically terrestrial soils. Efforts focussed on the nature of carbon behavior in arid environments, where the majority of the carbon is present as inorganic carbon stored as pedogenic carbonate in desert calcic soils. Studies were supported of soils in two areas of western North America's major deserts: the Mojave Desert and the Chihuahuan Desert. Part 1 of this report summarizes the results of research conducted in the area of the Providence Mountains, California in the eastern Mojave Desert. Part 2 of this report summarizes the results of research in the Sevilleta Wildlife Refuge in central New Mexico, one of the sites of the UMN Biology Department's Long Term Ecological Research. Author (revised)

N95-13136# Scripps Institution of Oceanography, La Jolla, CA. Inst. of Geophysics and Planetary Physics.

NONLINEAR HYSTERESIS IN AN ENDOCHRONIC SOLID Final Technical Report, 1 Nov. 1988 - 3 Nov. 1993

Jean-Bernard Minster 4 Jan. 1994 34 p

(Contract F19628-88-K-0039)

(AD-A283142; PL-TR-94-2005; AD-E202062) Avail: CASI HC A03/MF A01

Propagation of seismic waves in the nearfield where rock rheology is demonstrably nonlinear raises unique difficulties. Nonlinearity arises primarily in two forms at intermediate to large strains: (1) nonlinear elasticity and (2) amplitude-dependent attenuation. The proper representation of nonlinear constitutive equations for rocks in this regime is a potentially important ingredient of quantitative source models. We have shown previously that nonlinear one-dimensional wave propagation can result in spectral distortions at all wavelengths. This effect is strongly pulse-shape dependent, and therefore calls for three-dimensional capability. More recently, we found that our approximate description of the phenomenology in the nonlinear regime was inadequate and unable to simulate new laboratory observations. We describe an intrinsically nonlinear rheological model, based on the endochronic framework of K. Valanis, which replicates the main features of observed hysteresis loops in the strain regime of interest and is easily reduced to differential form. The resulting differential equations can be readily solved numerically. Thus, this model is suitable for finite difference and finite element stress wave codes. Ultimately, a complete description of the rheology in terms of a thermodynamically valid constitutive equation is really what should be used in numerical simulations, if it can be developed and validated experimentally. DTIC

N95-13190*# Texas Univ., Dallas, TX.

IONOSPHERIC DYNAMICS INSTRUMENT INVESTIGATION FOR THE TIMED MISSION Final Report

R. A. Heelis Sep. 1994 80 p

(Contract NAS5-32571)

(NASA-CR-196198; NAS 1.26:196198; TIMED-IDI) Avail: CASI HC A05/MF A01

The primary science objectives for the Ionospheric Dynamics Instrument (IDI) investigation are related to the global response of the ITM to energy inputs from the magnetosphere and an understanding of the ways in which electric fields are internally generated by neutral atmosphere motions in the lower thermosphere and mesosphere. At low and mid latitudes the electric fields are generated by neutral atmosphere motions and temporal resolution on time scales of a second will adequately describe the global field and allow its relationship to neutral wind motion to be established. However, the redistribution of current systems and the electrodynamics associated with plasma structures requires temporal sampling rates at the highest possible frequencies. The results of these studies are presented graphically. Derived from text

N95-13293 Colorado Univ., Boulder, CO. Boulder Lab. for Atmospheric and Space Physics.

GRAVITY WAVE FORCING AND INFLUENCES NEAR THE MESOPAUSE Final Technical Report

David C. Fritts 1994 4 p Limited Reproducibility: More than 20% of this document may be affected by microfiche quality

(Contract N00014-92-J-2005)

(AD-A282482) Avail: CASI HC A01

Our goals in this research were to address gravity wave effects near the mesopause using largely analytic and modeling techniques. A first approach employed an analytic description of the gravity wave field to develop a parameterization scheme for the most important wave effects at greater altitudes that was based on the observed characteristics of the wave spectrum. A second approach was intended to apply pseudo-spectral collocation techniques for studies of wave excitation, instability, dissipation, and interaction processes thought to play important roles in the circulation, structure, and variability throughout the atmosphere. DTIC

N95-13434 Technische Univ., Delft (Netherlands).

FINITE ELEMENT METHODS IN RESISTIVITY LOGGING Ph.D. Thesis

J. R. Lovell 14 Sep. 1993 208 p

(PB94-206919; ISBN-90-5326-008-0) Copyright Avail: Issuing Activity (National Technical Information Service (NTIS))

Resistivity measurements are used in geophysical logging to help determine hydrocarbon reserves. The derivation of formation parameters from resistivity measurements is a complicated nonlinear procedure often requiring additional geological information. This requires an excellent understanding of tool physics, both to design new tools and interpret the measurements of existing tools. The Laterolog measurements in particular are difficult to interpret because the response is very nonlinear as a function of electrical conductivity, unlike Induction measurements. Forward modeling of the Laterolog is almost invariably done with finite element codes which require the inversion of large sparse matrices. Modern techniques can be used to accelerate this inversion. Moreover, an understanding of the tool physics can help refine these numerical techniques. NTIS

47 METEOROLOGY AND CLIMATOLOGY

Includes weather forecasting and modification.

N95-11758*# Wisconsin Univ., Madison, WI. Cooperative Inst. of Meteorological Satellite Studies.

IMPLEMENTATION OF A STATE OF THE ART AUTOMATED SYSTEM FOR THE PRODUCTION OF CLOUD/WATER VAPOR MOTION WINDS FROM GEOSTATIONARY SATELLITES Progress Report, 1 Jan. - 30 June 1994

Christopher Velden Aug. 1994 18 p
(Grant NAG8-974)
(NASA-CR-196817; NAS 1.26:196817) Avail: CASI HC A03/MF A01

Significant progress was attained in this reporting period towards the overall goal of improving the CIMSS satellite wind algorithms through incorporation of new processing options, and testing/evaluating these options on data sets and through case studies. Several new strategies were implemented, and these are outlined. In addition, data from GOES-8 have recently become available during system check-out and evaluation. Initial testing and software adjustments necessary to handle this new and improved data are briefly touched upon in this summary, and will be a main focus of the remaining funds and efforts under this contract. Derived from text

N95-12392# Colorado State Univ., Fort Collins, CO. Dept. of Atmospheric Science.
DYNAMICAL STUDIES IN HURRICANE INTENSITY CHANGE
Michael T. Montgomery Jun. 1994 87 p
(Contract N00014-93-1-0456)
(AD-A282406) Avail: CASI HC A05/MF A01

My research objective is to elucidate and quantify a variety of dynamical processes believed important in hurricane intensity change. As a continuation of my collaboration with scientists at the Hurricane Research Division in Miami, the asymmetric stability problem for rapidly rotating vortices has recently been examined within the framework of asymmetric balance (AB) theory. In this paper the theorem of Charney and Stern is generalized to cover rapidly rotating (i.e. large Rossby number) baroclinic vortices. The theory is applied to observational data from hurricane Gloria of 1985, and Gloria is shown to satisfy the necessary condition for exponential instability. In order to determine whether such instabilities are realized and what role they may play in intensification cycles of hurricanes, a complete eigenvalue analysis is planned for the upcoming year. DTIC

N95-12423 Naval Postgraduate School, Monterey, CA.
TROPICAL CYCLONE DEVELOPMENT AND INTENSIFICATION UNDER MODERATE TO STRONG VERTICAL WIND SHEAR M.S. Thesis
Debra K. Smith Mar. 1994 119 p Limited Reproducibility: More than 20% of this document may be affected by microfiche quality
(AD-A282185) Avail: Issuing Activity (Defense Technical Information Center (DTIC))

A study was conducted to understand the physical mechanisms by which a tropical cyclone is able to develop and be maintained under moderate to strong vertical wind shear. The general approach was to describe case studies of three tropical cyclones in the western North Pacific that developed and/or intensified in the lee of another tropical cyclone. The data resources include high temporal and spatial resolution visible and infrared satellite imagery, operational subjective and objective analyses, plus special Tropical Cyclone Motion (TCM-90) high resolution (50 km) analyses and multi-quadric analyses. The three tropical cyclones developed and/or intensified under moderate to strong vertical wind shear that exceeded threshold values. The vertical wind shear was time dependent due to complex interactions with the leading tropical cyclone outflow, adjacent tropical upper tropospheric trough, and large-scale environment. Diurnal variability in strength of convection and outflow against the impinging flow led to fully exposed, partially exposed, or covered middle to lower tropospheric cyclonic circulation. Special characteristics of the monsoon trough circulation must create and sustain the tropical cyclone circulation against the tendency for the vertical wind shear to ventilate the vertical thermal and convective structure. DTIC

N95-12624 Battelle Columbus Labs., Research Triangle Park, NC.
METHODS OF MODELING RADIANT ENERGY EXCHANGE IN RADIATION FOG AND CLOUDS Final Report, Jun. 1992 - Mar. 1993
John M. Davis Jun. 1994 103 p Limited Reproducibility: More than 20% of this document may be affected by microfiche quality
(Contract DAAL03-91-C-0034)
(AD-A283509; ARL-CR-103) Avail: Issuing Activity (Defense Technical Information Center (DTIC))

This report describes several types of parameterizations commonly used in cloud and fog models to calculate the effects of radiant energy exchange in both the infrared and solar portions of the spectrum. The types of parameterizations used in several models of radiation fog have been summarized in the main text and detailed in the appendix, along with a few summaries of supporting studies. In general, the treatment of radiant exchange includes spectral resolution at the level of band models, whether band models are used explicitly or whether the radiation stream has been divided using a sum of exponentials approach. All of the studies use a plane parallel approximation in one form or another and all assume spherical particles for droplets and aerosols. The more sophisticated studies use a delta-two stream approach to account for the effects of multiple scattering. A few of the models include a prognostic equation that links the change in the microphysical distribution with the radiation field. The more advanced models also include a carefully designed surface flux exchange model. The strengths and deficiencies of the approaches are discussed and recommendations of a proper radiative parameterization are listed. DTIC

N95-12905 Mitre Corp., Bedford, MA.
THUNDERSTORM HYPOTHESIS REASONER Final Report
Alice M. Mulvehill Feb. 1994 31 p Limited Reproducibility: More than 20% of this document may be affected by microfiche quality
(Contract F19628-94-C-0001)
(AD-A282664; MTR-94B0000071) Avail: Issuing Activity (Defense Technical Information Center (DTIC))

THOR is a knowledge-based system which incorporates techniques from signal processing, pattern processing, and artificial intelligence (AI) in order to determine the boundary of small thunderstorms which develop and dissipate over the area encompassed by the Kennedy Space Center and the Cape Canaveral Air Force Station. THOR interprets electric field mill data (derived from a network of electric field mills) by using heuristics and algorithms about thunderstorms that have been obtained from several domain specialists. THOR generates two forms of output: contour plots which visually describe the electric field activity over the network and a verbal interpretation of the activity. THOR uses signal processing and pattern recognition to detect signatures associated with noise or thunderstorm behavior in a near real time fashion from over 31 electrical field mills. THOR's AI component generates hypotheses identifying areas which are under a threat from storm activity, such as lightning. THOR runs on a VAX/VMS at the Kennedy Space Center. Its software is a coupling of C and Fortran programs, several signal processing packages, and an expert system development shell. DTIC

N95-12839*# National Aeronautics and Space Administration. Langley Research Center, Hampton, VA.
SATELLITE ESTIMATES OF SHORTWAVE SURFACE RADIATION AND ATMOSPHERIC METEOROLOGY FOR THE BOREAS EXPERIMENT REGION
C. D. Moats (Lockheed Engineering and Sciences Co., Hampton, VA.), C. H. Whitlock, S. R. LeCroy, and R. C. DiPasquale Sep. 1994 57 p
(RTOP 578-12-23-70)
(NASA-TM-109132; NAS 1.15:109132) Avail: CASI HC A04/MF A01

This report provides background data for the Boreal Ecosystem Atmosphere Study (BOREAS) sites, including daily, seasonal, interannual, and spatial variability of shortwave (SW) radiation at the Earth's surface. This background data, from the Version 1.1 SW data set, was provided by the Surface Radiation Budget (SRB) Climatology Project established by the World Climate Research Program (WCRP). Author

N95-12927# Lawrence Livermore National Lab., Livermore, CA.
THE IMPACT OF ELEVATION DATA REPRESENTATION ON NOCTURNAL DRAINAGE WIND SIMULATIONS
H. Walker and J. M. Leone, Jr. Apr. 1994 6 p Presented at the 6th Conference on Mesoscale Processes, Portland, OR, 18-22 Jul. 1994
(Contract W-7405-eng-48)
(DE94-014752; UCRL-JC-115986; CONF-940769-5) Avail: CASI HC A02/MF A01

This document contains information about SABLE, an atmospheric model developed by Lawrence Livermore National Laboratory. The model is a hydrostatic mesoscale model that represents surface-atmosphere interactions affected by complex terrain. SABLE is used to evaluate the impacts of elevation on drainage systems. The simulation also encompasses wind effects on nocturnal drainage. DOE

N95-12996# Federal Aviation Administration, Atlantic City, NJ.
TERMINAL DOPPLER WEATHER RADAR BUILD 5A OPERATIONAL TEST AND EVALUATION (OT/E) INTEGRATION AND OT/E OPERATIONAL TEST PLAN
Radame Martinez, Peter Guthlein, Steven Viveiros, and Donne Wedge Jul. 1994 46 p
(AD-A283052; DOT/FAA/CT-TN94-19) Avail: CASI HC A03/MF A01

The Terminal Doppler Weather Radar (TDWR) Build 5A Enhancement Operational Test and Evaluation (OT&E) Integration and OT&E Operational Test Plan provides the overall philosophy and approach to Build 5A OT&E testing, and identifies OT&E objectives, responsibilities, and resources. The TDWR Build 5A enhancement provides connectivity to the Low Level Wind Shear Alert System (LLWAS) 2 to display LLWAS 2 wind data along with TDWR hazardous weather data on TDWR geographical situation displays (GSD) and ribbon display terminals (RDT). The TDWR Build 5A OT&E is scheduled to occur at the TDWR site in Memphis, TN, March through May 1994. DTIC

N95-12997# Army Research Lab., White Sands Missle Range, NM.
SUPERMARIAH: A SIMILARITY-BASED METHOD FOR DETERMINING WIND, TEMPERATURE, AND HUMIDITY PROFILE STRUCTURE IN THE SURFACE BOUNDARY LAYER Final Report
Henry Rachele, Frank V. Hansen, Arnold Tunick, and Lisa Manguso Jun. 1994 41 p
(AD-A283058; ARL-TR-264) Avail: CASI HC A03/MF A01

Supermariah is a new methodology for estimating the surface layer similarity scaling constants for wind, temperature, and specific humidity, using data from tower-borne sensors. It is conceptually based on the Dynamic Similarity of Flows Theory. We discuss the origin and logic of the Mariah approach (the predecessor of SuperMariah) and then present the extension of Mariah resulting in SuperMariah. This report reviews the complete set of model equations and presents several examples to illustrate comparisons of the Mariah, SuperMariah, and the more traditional O'KEYPS formulations. DTIC

N95-13095# National Oceanic and Atmospheric Administration, Washington, DC. Synoptic Analysis Branch.
CATALOGUE OF HEAVY RAINFALL CASES OF SIX INCHES OR MORE OVER THE CONTINENTAL US DURING 1993
Richard Borneman and Charles Kadin Aug. 1994 160 p
(NOAA-TR-NESDIS-80) Avail: CASI HC A08/MF A02

The year of 1992 was a very active one for heavy rainfall events over the continental United States. Flash flooding occurred in many parts of the country, with excessive rainfall taking place during each month of the year. A catalog with meteorological charts and satellite imagery was developed and published (NOAA Technical Report NESDIS 66) to acquaint meteorologists with many of these events and familiarize them with some of the factors that played a significant role in their occurrence. As much as 1992 turned out to be a major problem for the many areas affected by floods, 1993 turned out to be a true nightmare. 'The Great Flood of 1993,' centered over the middle and upper Mississippi Valley, was the most noteworthy event of the year. Over a 2 to 3 month period, a persistent jet stream interacted with tropical moisture that resulted in repetitive showers and thunderstorms over the region. Widespread and prolonged flooding caused billions of dollars in crop losses and property damage. In addition, a series of strong winter storms plagued California at the beginning of the year. As was the case with the first edition of the catalog, this year's edition highlights 24 hour heavy rainfall amounts of 6 inches or more. Additionally, it has been expanded to include more data and statistics, and some comparisons are made between 1992 and 1993. Author

N95-13134# Massachusetts Univ., Lowell, MA.
SHORT TERM WEATHER FORECASTING IN REAL TIME IN A BASE WEATHER STATION SETTING
Frank P. Colby, Jr. and Keith L. Seitter Oct. 1993 56 p
(Contract F19628-91-K-0040)
(AD-A283141; PL-TR-94-2048; AD-E202122; SR-2) Avail: CASI HC A04/MF A01

Several changes have been made to the mesoscale model during the past year, and they are highlighted in this report. Those changes include improvements to the initialization routines, adjustments to the boundary conditions, and the addition of simple clouds and precipitation. One model run which includes precipitation is discussed in some detail. DTIC

N95-13137# Hughes STX, Inc., Lexington, MA.
STOCHASTIC INDEXING
Albert R. Boehm 21 Jan. 1994 12 p
(Contract F19628-93-C-0051)
(AD-A283143; PL-TR-94-2012; AD-E202111; SR-1) Avail: CASI HC A03/MF A01

A documentation of the computer program for Stochastic Indexing (SED) is presented. A new method of 'storing' and retrieving randomly generated features is described. DTIC

N95-13268# Los Alamos National Lab., NM.
TESTS OF A NEW CLOUD TREATMENT IN AN ATMOSPHERIC GENERAL CIRCULATION MODEL
J. E. Kristjansson Dec. 1993 17 p Presented at the Center for Nonlinear Studies International Conference on Modeling the Forces of Nature, Los Alamos, NM, 17-21 May 1993
(Contract W-7405-eng-36)
(DE94-013138; LA-UR-94-1848; CONF-9305289-3) Avail: CASI HC A03/MF A01

We present a new cloud treatment in an atmospheric climate model. The water (or ice) content of clouds is introduced as a prognostic variable, subject to both advective and diffusive transport. In the first phase of the study, the cloud water does not affect the radiative properties of clouds. We then find differences in precipitation and cloud fields, but little effect on the overall climate. In the second phase the cloud water determines the reflectivity of the clouds. This causes large changes in the global circulation, largely due to enhanced reflection from high tropical cirrus clouds. As a third step, the cloud emissivity is also based on the cloud water content. This greatly enhances the outgoing terrestrial radiation and brings the model's radiative budget quite close to the observed. DOE

48 OCEANOGRAPHY

Includes biological, dynamic, and physical oceanography; and marine resources.

For related information see also *43 Earth Resources and Remote Sensing.*

N95-11706*# Colorado Univ., Boulder, CO. Div. of Cryospheric and Polar Processes.
PARAMETERIZATION AND SCALING OF ARCTIC ICE CONDITIONS IN THE CONTEXT OF ICE-ATMOSPHERE PROCESSES Annual Progress Report No. 3
R. G. Barry, J. Heinrichs, K. Steffen, J. A. Maslanik, J. Key, M. C. Serreze, and R. W. Weaver Sep. 1994 26 p
(Grant NAGw-2598)
(NASA-CR-196831; NAS 1.26:196831) Avail: CASI HC A03/MF A01

This report summarizes achievements during year three of our project to investigate the use of ERS-1 SAR data to study Arctic ice and ice/atmosphere processes. The project was granted a one year extension, and goals for the final year are outlined. The specific objects of the project are to determine how the development and evolution of open water/thin ice areas within the interior ice pack vary under different atmospheric synoptic regimes; compare how open water/thin ice fractions estimated from large-area divergence measurements differ from fractions determined by summing localized openings in the pack; relate these questions of scale and process to methods of observation, modeling, and averaging over time and space; determine whether SAR data might be used to calibrate ice concentration estimates from medium and low-rate bit sensors (AVHRR and DMSP-OLS) and the special sensor microwave imager (SSM/I); and investigate methods to integrate SAR data for turbulent heat flux parametrization at the atmosphere interface with other satellite data. Derived from text

N95-11787 CoasTec, Baton Rouge, LA.
NEW YORK BIGHT STUDY. REPORT 4: GEOGRAPHIC INFORMATION SYSTEMS AND RELATIONAL DATABASE MANAGEMENT SYSTEM DEVELOPMENT

Matteson W. Hiland and Mark R. Byrnes May 1994 88 p Limited Reproducibility: More than 20% of this document may be affected by microfiche quality
(Contract DACW39-93-C-0066)
(AD-A281716; CERC-TR-94-4) Avail: Issuing Activity (Defense Technical Information Center (DTIC))

The general objective of the information management component of the New York Bight Study was to develop a District-based system (a geographic information system or GIS) to store, manipulate, and analyze the data sets associated with and developed by the New York Bight study. To accomplish this objective, the following efforts were required: database development, hardware/software acquisition, system installation, input of database attributes and graphic elements, and training of New York District personnel. Intergraph hardware and software were chosen as the system platform. Oracle database software was selected because it is one of the more common relational database management systems that provides comprehensive relational database (RDB) functions and data storage capabilities. The selection of a base map projection and coordinate system was one of the first decisions made in the process of loading graphic data. Several files were loaded into the system including: digitized shoreline files, graphic representations of gauge locations, tide data, satellite images, model output for water surface elevation, temperature, salinity, and dissolved oxygen, wave hindcast data, and ship observation data. Appendix A presents a basic user training guide. Project training was focused to create geographic map displays from measured data and model output, and to perform analyses on these data. Training was performed in the manner that reflected the types of projects undertaken by the New York District and addressed problems or questions of interest to the New York District. DTIC

N95-11900 National Oceanic and Atmospheric Administration, Miami, FL. Atlantic Oceanographic and Meteorological Labs.
HYDROGRAPHIC, CARBON DIOXIDE, NUTRIENT AND PRODUCTIVITY MEASUREMENTS FROM THE SOUTH ATLANTIC DURING JULY AND AUGUST OF 1991
E. B. Forde, J. C. Hendee, and R. Wanninkhof Apr. 1994 96 p Limited Reproducibility: More than 20% of this document may be affected by microfiche quality
(PB94-180668; NOAA-DR-ERL-AOML-24) Avail: CASI HC A05

From July 11 to September 2, 1991, the National Oceanic and Atmospheric Administration's (NOAA) Carbon Dioxide (CO_2) and Radiatively Important Trace Species (RITS) programs participated in an oceanographic research cruise conducted aboard the NOAA ship MALCOLM BALDRIGE. This report presents the research from that cruise that was conducted for the CO_2 program, which has recently been renamed the Ocean-Atmospheric Carbon Exchange Study (OACES). The report contains tables of the following data: hydrography from each CTD cast at the bottle trip depths, (including salinity, oxygen and nutrients), discrete carbon parameters, underway carbon parameter values, and data from productivity casts. Descriptions of sampling techniques and analytical methods used in the collection and processing of these data are also presented. NTIS

N95-11920*# National Aeronautics and Space Administration. Goddard Space Flight Center, Albuquerque, NM.
SeaWiFS TECHNICAL REPORT SERIES. VOLUME 19: CASE STUDIES FOR SeaWiFS CALIBRATION AND VALIDATION, PART 2
Stanford B. Hooker, ed., James G. Acker, ed., Elaine R. Firestone, ed., Charles R. McClain, Robert S. Fraser, James T. McLean, Michael Darzi, James K. Firestone, Frederick S. Patt, and Brian D. Schieber et al Aug. 1994 74 p
(NASA-TM-104566-Vol-19-Pt-2; Rept-94B00115; NAS 1.15:104566-Vol-19-Pt-2) Avail: CASI HC A04/MF A01

This document provides brief reports, or case studies, on a number of investigations and data set development activities sponsored by the Calibration and Validation Team (CVT) within the Sea-viewing Wide Field-of-view Sensor (SeaWiFS) Project. Chapter 1 is a comparison with the atmospheric correction of Coastal Zone Color Scanner (CZCS) data using two independent radiative transfer formulations. Chapter 2 is a study on lunar reflectance at the SeaWiFS wavelengths which was useful in establishing the SeaWiFS lunar gain. Chapter 3 reports the results of the first ground-based solar calibration of the SeaWiFS instrument. The experiment was repeated in the fall of 1993 after the instrument was modified to reduce stray light; the results from the second experiment will be provided in the next case studies volume. Chapter 4 is a laboratory experiment using trap detectors which may be useful tools in the calibration round-robin program. Chapter 5 is the original data format evaluation study conducted in 1992 which outlines the technical criteria used in considering three candidate formats, the hierarchical data format (HDF), the common data format (CDF), and the network CDF (netCDF). Chapter 6 summarizes the meteorological data sets accumulated during the first three years of CZCS operation which are being used for initial testing of the operational SeaWiFS algorithms and systems and would be used during a second global processing of the CZCS data set. Chapter 7 describes how near-real time surface meteorological and total ozone data required for the atmospheric correction algorithm will be retrieved and processed. Finally, Chapter 8 is a comparison of surface wind products from various operational meteorological centers and field observations. Surface winds are used in the atmospheric correction scheme to estimate glint and foam radiances.
Author

N95-12151*# National Aeronautics and Space Administration. Goddard Space Flight Center, Albuquerque, NM.
SeaWiFS TECHNICAL REPORT SERIES. VOLUME 22: PRELAUNCH ACCEPTANCE REPORT FOR THE SeaWiFS RADIOMETER
Stanford B. Hooker, ed., Elaine R. Firestone, ed., James G. Acker, ed., Robert A. Barnes, William L. Barnes, Wayne E. Esaias, and Charles R. McClain Sep. 1994 35 p
(NASA-TM-104556-Vol-22; Rept-94B00126-Vol-22; NAS 1.15:104556-Vol-22) Avail: CASI HC A03/MF A01

The final acceptance, or rejection, of the Sea-viewing Wide Field-of-view Sensor (SeaWiFS) will be determined by the instrument's on-orbit operation. There is, however, an extensive set of laboratory measurements describing the operating characteristics of the radiometer. Many of the requirements in the Ocean Color Data Mission (OCDM) specifications can be checked only by laboratory measurements. Here, the calibration review panel examines the laboratory characterization and calibration of SeaWiFS in the light of the OCDM performance specification. Overall, the performance of the SeaWiFS instrument meets or exceeds the requirements of the OCDM contract in all but a few unimportant details. The detailed results of this examination are presented here by following the outline of the specifications, as found in the Contract. The results are presented in the form of requirements and compliance pairs. These results give conclusions on many, but not all, of the performance specifications. The acceptance by this panel of the performance of SeaWiFS must only be considered as an intermediate conclusion. The ultimate acceptance (or rejection) of the SeaWiFS data set will rely on the measurements made by the instrument on orbit.
Author

N95-12359*# National Aeronautics and Space Administration. Goddard Space Flight Center, Greenbelt, MD.
SeaWiFS TECHNICAL REPORT SERIES. VOLUME 23: SeaWiFS PRELAUNCH RADIOMETRIC CALIBRATION AND SPECTRAL CHARACTERIZATION
Robert A. Barnes (ManTech, Inc., Wallops Island, VA.), Alan W. Holmes (Santa Barbara Research Center, CA.), William L. Barnes, Wayne E. Esaias, Charles R. McClain, Tomas Svitek, Stanford B. Hooker, Elaine R. Firestone, and James G. Acker Oct. 1994 58 p
(NASA-TM-104566-Vol-23; Rept-94B00144-Vol-23; NAS 1.15:104566-Vol-23) Avail: CASI HC A04/MF A01

Based on the operating characteristics of the Sea-viewing Wide Field-of-view Sensor (SeaWiFS), calibration equations have been developed that allow conversion of the counts from the radiometer into Earth-existing radiances. These radiances are the geophysical properties the instrument has been designed to measure. SeaWiFS uses bilinear gains to allow high sensitivity measurements of ocean-leaving radiances and low sensitivity measurements of radiances from clouds, which are much brighter than the ocean. The calculation of these bilinear gains is central to the calibration equations. Several other factors within these equations are also included. Among these are the spectral responses of the eight SeaWiFS bands. A band's spectral response includes the ability of the band to isolate a portion of the electromagnetic spectrum and the amount of light that lies outside of that region. The latter is termed out-of-band response. In the calibration procedure, some of the counts from the instrument are produced by radiance in the out-of-band region. The number of those counts for

each band is a function of the spectral shape of the source. For the SeaWiFS calibration equations, the out-of-band responses are converted from those for the laboratory source into those for a source with the spectral shape of solar flux. The solar flux, unlike the laboratory calibration, approximates the spectral shape of the Earth-existing radiance from the oceans. This conversion modifies the results from the laboratory radiometric calibration by 1-4 percent, depending on the band. These and other factors in the SeaWiFS calibration equations are presented here, both for users of the SeaWiFS data set and for researchers making ground-based radiance measurements in support of Sea WiFS. Author

N95-12540 Brown Univ., Providence, RI. Div. of Applied Mathematics.
DYNAMICAL SYSTEMS AND OCEANOGRAPHY Final Report, 1 Apr. - 31 Dec. 1993
Christopher Jones, Steven Wiggins, and George Haller 25 Apr. 1994 10 p Limited Reproducibility: More than 20% of this document may be affected by microfiche quality
(Contract N00014-93-1-0675)
(AD-A282635) Avail: CASI HC A02

The workshop on 'Dynamical Systems and Oceanography' was held in Little Compton, RI on May 20-21, 1993. The participants were from both the dynamical systems and oceanography communities and were brought together with the goal of brainstorming on the future directions that the application of dynamical systems techniques to oceanography might take. The result of the conference was a white paper that is appended to this report. The workshop was organized into two separate days. On the first day, discussions revolved around the use of geometric techniques from dynamical systems in studying the mixing properties of the ocean. Main lectures were given by Wiggins (dynamical systems) and Samelson (oceanography). Fruitful discussions were held involving all participants on this topic. Short lectures were also given by Kirwan, Brown, and Richardson. On the second day, focus was put on the use of dynamical systems in understanding instabilities. A lecture was given by Pratt(oceanography) on the current problems of interest and also one by Jones (dynamical systems) on the available modern techniques. DTIC

N95-12590# Colorado Univ., Boulder, CO. Dept. of Mathematics.
NONLINEAR PROBLEMS IN FLUID DYNAMICS AND INVERSE SCATTERING: LANGMUIR CIRCULATIONS IN OCEAN SURFACE LAYERS Annual Report, 1 Oct. 1993 - 30 Sep. 1994
Duane P. Sather 31 Jul. 1994 3 p
(Contract N00014-94-1-0194)
(AD-A282934) Avail: CASI HC A01/MF A01

Research investigations on the interaction of surface waves, wind and currents in stratified ocean layers have been carried out. The research program involves the development of appropriate models for general physical situations (e.g., systems of coupled nonlinear partial differential equations) as well as the analysis of these models for certain specific problems such as Langmuir circulations and double-diffusive convection. During the period of the report, two papers were published and four papers were accepted for publication. Some of the results obtained and the methods used in these papers are outlined in this report. DTIC

N95-12998# Washington Univ., Seattle, WA. Applied Physics Lab.
OCEAN ACOUSTIC TOMOGRAPHY: SINGLE SLICE AND MOVING SHIP EXPERIMENTS
Bruce M. Howe and Peter F. Worcester Jul. 1994 50 p
(Contracts N00014-91-J-4055; N00014-91-J-4117; N00039-91-C-0072)
(AD-A283059; APL-UW-TR-9308) Avail: CASI HC A03/MF A01

The results of the ocean acoustic tomography work that supported the development of matched field processing (MFP) are summarized. This report focuses on two experiments. In Slice89 a single source transmitted to a vertical hydrophone array. This experiment improved our understanding of the single slice transfer function from scales of internal waves to 1000 km. It demonstrated the importance of unresolved high wavenumber ocean mesoscale variability to acoustic propagation. Any coherent signal processing technique must be robust against both internal wave variability and unresolved high wavenumber mesoscale variability, as both contribute roughly comparable amounts of travel time variance. The Acoustic Mid-Ocean Dynamics Experiment - Moving Ship Tomography Experiment (AMODE-MST) was a large mapping effort to address the primary goal of this tomography effort: to determine the precision with which the ocean mesoscale sound speed field can be measured for input into matched field (or other) processing of long-range acoustic transmissions. The experiment demonstrated that tomographic techniques can be used to measure the sound speed structure over a large area with high resolution. DTIC

51 LIFE SCIENCES (GENERAL)

N95-11728# Marci (J. M.) Spectroscopic Society, Prague, Stredocesky (Czechoslovakia).
ABSTRACTS FROM THE INTERNATIONAL CONFERENCE ON NUCLEAR ANALYTICAL METHODS IN THE LIFE SCIENCES Abstracts Only
31 Jan. 1994 210 p Conference held in Prague, Czechoslovakia, 13-17 Sep. 1993
(DE94-621923; INIS-MF-13811; CONF-930954) Avail: CASI HC A10/MF A03 (US Sales Only)

The proceedings contain short communications of 133 papers presented at the conference. All these contributions have been inputted to international nuclear information system (INIS). The majority of papers deal with the determination of trace elements in biological and environmental samples using neutron activation analysis, X-ray fluorescence analysis, proton-induced X-ray emission (PIXE) analysis and tracer techniques. DOE

N95-11737# Rensselaer Polytechnic Inst., Troy, NY.
MICROBIAL COMMUNITIES IN SUBSURFACE ENVIRONMENTS: DIVERSITY, ORIGIN, AND EVOLUTION
S. A. Nierzwicki-Bauer 2 May 1994 10 p
(Contract DE-FG02-90ER-60989)
(DE94-013699; DOE/ER-60989/4) Avail: CASI HC A02/MF A01

This report summarizes the progress made from 9-1-93 to 5-1-94 on this DOE grant. As participants in the subsurface science program, the authors are assessing the influence of environmental conditions on the distribution and evolution of subsurface microorganisms employing molecular techniques. The approach utilizes 16S rRNA targeted oligonucleotide probes, polymerase chain reaction (PCR) amplification of gene sequences, and sequencing techniques. Continued progress towards identifying target sequences for selected microbial types and groups is being made by analysis of rRNA sequence data for subsurface microorganisms and other microorganisms in the rRNA databases. Hybridization probes for these target sequences are being produced and used to classify isolated strains of subsurface microbes into focus clades useful for testing origins hypotheses. DOE

N95-11810*# National Aeronautics and Space Administration. Ames Research Center, Moffett Field, CA.
EFFECTS OF ORAL GLUCOSE ON EXERCISE THERMOREGULATION IN MEN AFTER WATER IMMERSION
Alan S. Dearborn (San Francisco Univ., CA.), Andrew C. Ertl (California Univ., Davis, CA.), John E. Greenleaf, Paul R. Barnes, Catherine G. R. Jackson, and Jennifer L. Breckler Aug. 1994 34 p
(RTOP 199-18-12-07)
(NASA-TM-108825; A-94085; NAS 1.15:108825) Avail: CASI HC A03/MF A01

To test the hypothesis elevated blood glucose would attenuate the rise in exercise rectal temperature, six men age 35 plus or minus S.D. 7 years participated in each of three trials by 4-hr water immersion to the neck: (1) 2.0 g/kg body wt of oral glucose (33.8 percent wt./vol.) was consumed followed by 80 min controlled rest (Glu/Rest), and 70 min horizontal supine cycle exercise at 62.8 percent plus or minus S.E. 0.5 percent (1.97 plus or minus 0.02 L/min) of peak O2 uptake followed by 10 min recovery (2) with (Glu/Ex) and (3) without prior flucose (No Glu/Ex). Blood samples were taken at -25, 0, 15, 45, and 68 min of exercise and after plus 10 min of recovery for measurement of hemoglobin, hematocrit, and blood glucose. Both mean skin (T sub sk) (from six sites) and rectal temperatures (T sub re) were monitored continuously. Sweat rate was measured by resistanc hygrometry. The mean of delta PV for the exercise trials was -12.2 plus or minus 2.1 percent. Mean blood glucose for the Glu/Ex trial was higher than that of the No Glu/Ex trial was (108.4 equal or minus 3.9 and 85.6 plus or minus 1.6 mg/dl, respectively, P less than

0.05. At the end of exercise T(sub sk) for the Glu/Ex trial was lower than for No Glu/Ex(32.0 plus or minus 0.3 and 32.4 equals or minus 0.2 C, respectively, P less than 0.05); T(sub re) for the Glu/Ex trial was lower than for No Glu/Es (38.22 plus or minus 0.17 and 38.60 plus or minus 0.11 C, respectively, P less than 0.05); and forearm sweat rate for the Glu/Ex trial (0.34 plus or minus 0.04 and 0.43 plus or minus g/sq cm, respectively, P less than 0.05). These data suggest that elevation of blood glucose prior to horizontal exercise following hypohydration attenuates the increase in body temperature without altering heat production or exercise hypovolemia. Author

N95-11902# Technische Univ., Delft (Netherlands). Interfaculty Reactor Inst.

COPPER METABOLISM IN RATS FED ASCORBIC ACID OR RESTRICTED AMOUNTS OF COPPER Ph.D. Thesis [KOPERHUISHOUDING BIJ RATTEN NA VERSTREKKING VAN ASCORBINEZUUR-RIJKE OF KOPER-ARME VOEDERS]

G. J. vandenBerg 25 Nov. 1993 156 p

(PB94-191343; ISBN-90-73861-18-7) Avail: CASI HC A08/MF A02

The effects of feeding supplements of ascorbic acid on dietary copper availability and copper status were studied in rats. Male outbred Wistar (Hsd/Cpb:Wu) rats used were fed on purified diets adequate in copper (5 mg/kg) without or with 1 or 10 g ascorbic acid/kg diet. In Chapters 1 and 2 the mechanisms are described by which dietary ascorbic acid influences copper metabolisms; the effects of a very high concentration (10 g ascorbic acid/kg diet) are compared with those of a pharmacological one (1 g/kg diet). The third Chapter describes a whole-body counting technique and the use of radiotracers which allow determination of true copper absorption in vivo. Chapter 4 describes the influence of ascorbic acid on true copper absorption and biliary excretion. Chapter 6 deals with the effects of ascorbic acid on intestinal copper solubility. A model for copper uptake is proposed in which reducing agents, ascorbic acid or a membrane bound NADH reductase, are involved (Chapter 9). Finally, in the general discussion the results presented are summarized and integrated. NTIS

N95-12006*# National Aeronautics and Space Administration. Ames Research Center, Moffett Field, CA.

VESTIBULAR AFFERENT RESPONSES TO LINEAR ACCELERATIONS IN THE ALERT SQUIRREL MONKEY

Christopher J. Somps, Robert H. Schor, and David L. Tomko Aug. 1994 18 p

(RTOP 199-16-12)

(NASA-TM-4581; A-94058; NAS 1.15:4581) Avail: CASI HC A03/MF A01

The spontaneous activity of 40 otolith afferents and 44 canal afferents was recorded in 4 alert, intact squirrel monkeys. Polarization vectors and response properties of otolith afferents were determined during static re-orientations relative to gravity and during Earth-horizontal, sinusoidal, linear oscillations. Canal afferents were tested for sensitivity to linear accelerations. For regular otolith afferents, a significant correlation between upright discharge rate and sensitivity to dynamic acceleration in the horizontal plane was observed. This correlation was not present in irregular units. The sensitivity of otolith afferents to both static tilts and dynamic linear acceleration was much greater in irregularly discharging units than in regularly discharging units. The spontaneous activity and static and dynamic response properties of regularly discharging otolith afferents were similar to those reported in barbiturate-anesthetized squirrel monkeys. Irregular afferents also had similar dynamic response properties when compared to anesthetized monkeys. However, this sample of irregular afferents in alert animals had higher resting discharge rates and greater sensitivity to static tilts. The majority of otolith polarization vectors were oriented near the horizontal in the plane of the utricular maculae; however, directions of maximum sensitivity were different during dynamic and static testing. Canal afferents were not sensitive to static tilts or linear oscillations of the head. Author

N95-12310 National Academy of Sciences - National Research Council, Washington, DC. Committee on National Needs for Biomedical and Behavioral Research Personnel.

MEETING THE NATION'S NEEDS FOR BIOMEDICAL AND BEHAVIORAL SCIENTISTS

1994 166 p

(LC-94-66477; ISBN-0-309-05086-3) Copyright Avail: Issuing Activity

The subject of this report is the nation's future need for biomedical and behavioral research scientists and the role the National Research Service Awards (NRSA) program can play in meeting those needs. This is the tenth in the continuing series of reports to the National Institutes of Health (NIH) and the U.S. Congress on this subject. The committee's deliberations and recommendations centered on three major activities. First, a Panel on Estimation Procedures was established to provide numerical analysis of educational and employment prospects and national needs for biomedical and behavioral research personnel. The panel concluded that existing mathematical models are inadequate to predict need and their recommendations for alternative strategies are presented in Chapter 2. Second, the committee convened a public hearing to gather views from a broad constituency associated with NRSA programs. Both written and oral testimony were considered by the committee and their conclusions are reflected in the recommendations stated within the report. Third, the committee met as a group on four separate occasions and, as a panel of experts, discussed and debated information and recommendations. The consensus of these meetings forms the basis for the recommendations included in this report. Author (revised)

N95-12393# Puerto Rico Univ., San Juan. Inst. of Neurobiology.

NEURAL NETWORKS: STRUCTURE AND REPAIR. PART 1: GROUND SQUIRREL VISUAL SYSTEM. PART 2: FORMATION, MAINTENANCE AND PLASTICITY OF SYNAPTIC CONNECTIONS Progress Report, 1993 - 1994

Nidza Lugo-Garcia, Damien P. Kuffler, and Rosa E. Blanco 27 Jul. 1994 4 p

(Contract N00014-89-J-3070)

(AD-A282420) Avail: CASI HC A01/MF A01

This project uses the visual system of squirrels, with special emphasis on the retina, to study the normal organization of neural networks. Over the past year we have added to our knowledge of the organization of the retinal ganglion cell layer: (1) We have determined that only 50% of the cells in the ganglion cell layer are retinal ganglion cells. (2) Retinal ganglion cells projecting to the superior colliculus have been identified using Cholera Toxin subunit B (CTB) as a retrograde tracer. The ZIDAS and Neurolucida image analysis systems have been used to characterize the dendritic tree of the medium-sized cells from this group. Differences in the organization of the dendritic tree suggest that these cells comprise more than one subpopulation. (3) Experiments to determine whether retinal ganglion cells project to more than one retinal projection target have revealed that ganglion cells in this species do not project bilaterally to any significant degree. DTIC

N95-12614 Edgewood Research Development and Engineering Center, Aberdeen Proving Ground, MD.

ACUTE INHALATION OF EXPLOSIVELY DISSEMINATED CARBON FIBERS IN RATS Final Report, Nov. 1991 - Apr. 1992

Roger J. Hilaski, Jeffrey D. Bergmann, David C. Burnett, William T. Muse, Jr., and Sandra A. Thomson May 1994 111 p Limited Reproducibility: More than 20% of this document may be affected by microfiche quality

(DA Proj. 1C4-63627-DE-79)

(AD-A280556; ERDEC-TR-084) Avail: CASI HC A06

Carbon fibers are lightweight, high tensile strength synthetic strands used commercially and in military applications for aircraft and electromagnetic obscuration. Fibers with respirable diameters less than 3.5 micrometers and lengths greater than 10 micrometers will deposit by interception in the bronchi. Recent XM81 grenade field studies indicated that explosive dissemination produced fibers with diameters less than 3.0 micrometers and lengths less than 100 micrometers, making some of the fibrous smoke respirable. Carbon fibers were explosively generated to determine if the resultant aerosol is respirable and if it adversely affects rodents. Groups of 344 male Fischer rats were exposed to one of the three concentrations of carbon fibers for 30 min. Air-exposed and fuse/fuelexposed rats served as the controls. Exposed rats and respective control groups were submitted for bronchoalveolar lavage; biochemical, physiological, and pathological evaluation at 24 hr and 14 and 90 days post exposure. Also, SEM analysis was used to characterize the size range of the fibers and to determine fiber deposition in trachea and lung tissues. Aerosol samples were collected for mutagenicity testing. Initial results indicated the presence of fiber fragments and combustion products in the respirable range. However, there

were no adverse changes in the biological responses of the rats from short-term exposure to XM81 grenade aerosols. DTIC

N95-12677# Pacific Northwest Lab., Richland, WA.
RATIONAL ENZYME REDESIGN
R. L. Ornstein May 1994 5 p Presented at the LIGNIN Workshop on Research Needs in LIGNIN Biosynthesis and Biodegradation, Pacific Grove, CA, 25-26 May 1994
(Contract DE-AC06-76RL-01830)
(DE94-014565; PNL-SA-24337; CONF-9405190-1) Avail: CASI HC A01/MF A01

Protein engineering is first a means of elucidating structure-function relations in an enzyme, and second, a means of changing a protein to make it serve a different, but generally related, purpose. In principle, one may change the functional characteristics of an enzyme by altering its substrate specificity, kinetics, optimum range of activity, and chemical mechanism. Obviously one cannot make all possible combinations of amino acid changes for even the smallest enzyme, so the essential question is which changes to make. The intent of rational protein/enzyme redesign is to alter a protein/enzyme in a timely and premeditated fashion. This article provides an outline of the process of rational enzyme redesign. DOE

N95-12827*# Emory Univ., Atlanta, GA. Dept. of Physiology.
EFFECT OF DECREASED GRAVITY ON CIRCULATION IN THE RAT
Final Technical Report, 1 May 1985 - 31 Jan. 1987
Vojin P. Popovic 1 Jul. 1987 92 p
(Grant NAG2-87)
(NASA-CR-196946; NAS 1.26:196946) Avail: CASI HC A05/MF A01

It has been reported that hypokinesia and bed rest induce cardiovascular changes similar to those observed in space flights. Using an animal model that was developed in our laboratory and that was extensively studied and characterized in our laboratory and other laboratories in this country and abroad, we have studied circulatory mechanisms that occur during exposure to hypokinesia (with or without negative tilt) as well as during readaptation to control conditions (free activity). We believe that this study contributes to better understanding of mammalian circulatory mechanisms that operate under 1-g force and will serve to provide control data to be compared with cardiovascular data obtained in conditions of a Space lab. Because survey and anesthesia drastically decrease cardiac output and other circulatory parameters in rats, only unanesthetized rats were used in experiments. Aorta and right atrium of the animals were permanently cannulated fifteen to twenty days before experiments. Arterial and right ventricular blood pressures, cardiac output, cerebral and other regional blood flow, ECG, other cardiovascular parameters, and oxygen consumption were measured with techniques routinely used in our laboratory. Specifically, we undertook the following investigations during the period of three years: (1) A study of circulatory changes (right ventricular pressure, arterial blood pressure, heart rate, cardiac output) during exposure of rats to hypokinetic conditions. Used the head down tilted Holton-Musacchia system in order to compare the results with the results already obtained on unrestrained rats, (2) Humoral changes were investigated in animals exposed to hypokinesia; also, lymphocyte and neutrophil levels in hypokinetic animals (with or without tilt) were determined to ascertain the level of induced stress and possible changes observed in weightless animals, and (3) circulating blood volume was determined during and after hypokinesia.
Author

N95-12941*# Louisville Univ., KY. Dept. of Microbiology and Immunology.
SPACEFLIGHT AND IMMUNE RESPONSES OF RHESUS MONKEYS
Final Report
Gerald Sonnenfeld Sep. 1994 14 p
(Grant NAG2-624)
(NASA-CR-196846; NAS 1.26:196846) Avail: CASI HC A03/MF A01

Evidence from both human and rodent studies indicates that alterations in immunological parameters occur after space flight. The objective of this project is to determine the effects of space flight on immune responses of Rhesus monkeys. The expected significance of the work is a determination of the range of immunological functions of the Rhesus monkey, a primate similar in many ways to man, affected by space flight. Changes in immune responses that could yield alterations in resistance to infection may be determined as well as the duration of alterations in immune responses. Additional information on the nature of cellular interactions for the generation of immune responses may also be obtained. Derived from text

N95-13176# California Univ., Davis, CA. Primate Research Center.
CONSEQUENCES OF PROLONGED INHALATION OF OZONE ON FISCHER-344/N RATS: COLLABORATIVE STUDIES. PART 1: CONTENT AND CROSS-LINKING OF LUNG COLLAGEN
J. A. Last, T. R. Gelzleichter, J. Harkema, and S. Hawk Apr. 1994 50 p Prepared in cooperation with Lovelace Biomedical and Environmental Research Inst., Albuquerque, NM and Inhalation Toxicology Research Inst., Albuquerque, NM
(Contract RFA-90-1)
(PB94-182748; HEI/RR-65-1/94-Pt-1) Copyright Avail: CASI HC A03/MF A01

Male and female rats were exposed either to filtered air (controls) or to 0.12, 0.5, or 1.0 parts per million ozone for six hours per day, five days per week, for 20 months. Biochemical analysis indicated excess collagen in the female rats exposed to 0.5 to 1.0 ppm ozone. Collagen in the lungs of the females also contained relatively more hyroxylysine-derived cross links than did the lung collagen from age-matched control animals that had breathed only filtered air. Exposure of Fischer-344 rats for 20 months to 0.5 or 1.0 ppm ozone was associated with excess fibrotic lung collagen deposition as defined histologically. The authors conclude that chronic exposure of rats to 20 months to ozone at concentrations of 0.5 ppm or above for six hours per day, five days per week, causes mild to moderate lung fibrosis, as defined histologically and, in female rats, biochemically. The significance of these observations with regard to health risks to humans chronically inhaling ozone at ambient levels in polluted air remains to be determined. DTIC

N95-13271# Ohio State Univ., Columbus.
REGULATION OF ALTERNATIVE CO2 FIXATION PATHWAYS IN PROKARYOTIC AND EUKARYOTIC PHOTOSYNTHETIC ORGANISMS
R. Tabita 1993 12 p
(Contract DE-FG02-91ER-20033)
(DE94-013180; DOE/ER-20033/2) Avail: CASI HC A03/MF A01

The goal of this project is to determine how photosynthetic microorganisms regulate the assimilation of CO2 via pathways alternative to the usual Calvin-Benson-Bassham reductive pentose phosphate scheme, particularly in the molecular basis for switches in CO2 metabolic paths. We have identified proteins on one-dimensional and two-dimensional SDS gels that appear differentially expressed in R. sphaeroides strain 16PHC which may be due to a mutation or change in some locus that controls the expression of several genes and their products. Similar observations were made relative to R. rubrum I-19 and the wild-type, namely that additional protein bands were observed in extracts of I-19 compared to the wild-type when both were grown photoheterotrophically with malate as electron donor and CO2 as the obligatory electron acceptor. The results of Tn5 mutagenesis of R. sphaeroides 16PHC resulted in the isolation of several strains that effectively changed back to the 16 phenotype; i.e., no malate-dependent phototrophic growth with CO2 as electron acceptor. We have found that both wild-type R. sphaeroides and R. rubrum, and the respective RubisCO negative mutant strains, are all capable of photolithoautotrophic growth using reduced sulfur compounds as electron donors and CO2 as the sole carbon source and electron acceptor. The fact that the RubisCO negative are capable of photoautotrophic growth is an exciting development for us because it proves that alternative or nonCalvin CO2 fixation pathways are extremely important to the overall carbon metabolism of these organisms. Moreover, wild-type strains turn off the synthesis of RubisCO under these cultural conditions. Thus, there appears to be separate autotrophic CO2 fixation pathways in these organisms, and a major emphasis has been placed to identify how these bacteria can grow autotrophically and fix CO2 in the absence of RubisCO. DOE

N95-13373# Brandeis Univ., Waltham, MA.
CONFORMATION OF MEMBRANE PROTEINS: BACTERIORHODOPSIN
Final Report, 1 Nov. 1992 - 15 Apr. 1994
Gerald D. Fasman 13 May 1994 6 p
(Contract DAAH04-93-G-0007)
(AD-A281282; ARO-29714.1-LS) Avail: CASI HC A02/MF A01

Bacteriorhodopsin, from the purple membrane (PM) of Halobacterium

halobium, was chemically modified with methoxypolyethylene glycol (MW = 5000) succinimidyl carbonate. The polyethylene glycolbacteriorhodopsin (m-PEG-SC-BR33) conjugate, containing one PEG chain, was water soluble. The secondary structure of the conjugate in water appeared partially denatured but was shown to contain a-helical segments by circular dichroism (CD) spectroscopy. The isolated bacteriorhodopsin conjugate, with added retinal, was refolded in a mixed detergent-lipid micelle and had an absorption maximum at 555 nm. The refolded conjugate was transferred into vesicles which pumped protons, upon illumination, as efficiently as did native BR. Modification of the PM with methoxypolyethylene glycol did not alter the native structure or inhibit proton pumping, and therefore it is suggested that the glycol polymer is present as a covalently linked moiety to residues unnecessary for proton pumping and proper folding. The site of attachment of mPEG was determined to be either at Lys 129 or Lys 159, with position Lys 129 the most probable site of attachment. The m-PEG-SC-BR33 could be stepwise refolded to the native conformation by the addition of trifluoroethanol to lower the dielectric constant, simulating the insertion of the BR into the phospholipid bilayer. DTIC

N95-13408# Technische Univ., Delft (Netherlands).
MODELLING OF BIOPOTENTIAL RECORDINGS AND ITS IMPLICATIONS FOR INSTRUMENTATION DESIGN Ph.D. Thesis
A. C. M. vanRijn 8 Nov. 1993 153 p Sponsored by Stichting voor de Technische Wetenschappen
(PB94-206844) Avail: CASI HC A08/MF A02

The thesis describes the results of a five year research project where the measurement situation during the recording of bioelectric events was analyzed. This analysis was used as a basis for the design of instrumentation. The analysis starts with the transducers in bioelectric recordings: the electrodes. Part 1 is completed with a chapter on the main specifications of the systems to be developed. In Part 2, several hardware implementations based on the developed theory are described. They include the following: (1) the design of amplifiers for bioelectric events; (2) the transmission of the biomedical signals from the isolated front-end to the signal processing hardware; (3) the use of optical fibers, and (4) wireless telemetry systems. NTIS

N95-13423*# Benson (Robert H.), Springfield, VA.
LIFE SCIENCES CENTRIFUGE FACILITY ASSESSMENT Final Report, 15 Aug. - 15 Sep. 1994
Robert H. Benson 15 Sep. 1994 8 p
(NASA Order H-22787-D)
(NASA-CR-196848; NAS 1.26:196848; MSFC-1) Avail: CASI HC A02/MF A01

This report provides an assessment of the status of the Centrifuge Facility being developed by ARC for flight on the International Space Station Alpha. The assessment includes technical status, schedules, budgets, project management, performance of facility relative to science requirements, and identifies risks and issues that need to be considered in future development activities. Author

N95-11966*# National Aeronautics and Space Administration. Ames Research Center, Moffett Field, CA.
ON THE ISOLATION OF HALOPHILIC MICROORGANISMS FROM SALT DEPOSITS OF GREAT GEOLOGICAL AGE
Helga Stan-Lotter and Ewald Denner *In its* Technical Paper Contest for Women 1992. Space Challenges: Earth and Beyond 1993 p 137-144
(For primary document see N95-11955 02-99)
Avail: CASI HC A02/MF A03

52 AEROSPACE MEDICINE

Includes physiological factors; biological effects of radiation; and effects of weightlessness on man and animals.

N95-11702# Civil Aeromedical Inst., Oklahoma City, OK.
ELIMINATION OF QUININE IN TWO SUBJECTS AFTER INGESTION OF TONIC WATER: AN EXPLORATORY STUDY Final Report
Vicky L. White, Dennis V. Canfield, and Jerry R. Hordinsky Aug. 1994 9 p
(DOT/FAA/AM-94/16) Avail: CASI HC A02/MF A01

Biological specimens from eight fatal aviation accidents out of 775 fatal aviation accidents analyzed in 1991 and 1992 were found to contain quinine. In one case, the investigators sought to identify the source of quinine found in the pilot. It was suggested that the quinine might have come from the consumption of tonic water. Since no recent use of quinine or tonic water could be found, the investigators asked how long quinine could be detected in a urine specimen. A limited research project was undertaken to provide a preliminary range of the approximate length of time quinine could be detected in urine and blood. Each of two male subjects was given a 20 oz. bottle of tonic water, which contained 35 mg of quinine. Quinine was detected using standard laboratory thin layer chromatography (TLC) and high performance liquid chromatography (HPLC) methods. Quinine has such diverse applications as a treatment for muscle cramps and malaria, in addition to being an additive in tonic water. Since adverse effects have been identified at plasma concentrations between 10-15 micro-g/mL, no performance effects would be expected from the maximum concentrations of quinine found (0.291 micro-g/mL) in this study after the ingestion of one 20 oz. bottle of tonic water. However, based on this study, the possibility of prolonged detection (over eight days) of quinine should (1) serve as a warning against using this as a sign of recent use of quinine directly or in association with alcohol, and (2) alert the investigators to inquire about disorders or conditions that might impair performance, but for which quinine treatment was terminated days before the accident. Author

N95-11708*# Texas Univ., Austin, TX. Dept. of Biomedical Engineering.
PRECONDITIONING ELECTROMYOGRAPHIC DATA FOR AN UPPER EXTREMITY MODEL USING NEURAL NETWORKS
D. J. Roberson, M. Fernjallah, R. E. Barr, and R. V. Gonzalez 1994 3 p
(Contract NAS9-18773)
(NASA-CR-196877; NAS 1.26:196877) Avail: CASI HC A01/MF A01

A back propagation neural network has been employed to precondition the electromyographic signal (EMG) that drives a computational model of the human upper extremity. This model is used to determine the complex relationship between EMG and muscle activation, and generates an optimal muscle activation scheme that simulates the actual activation. While the experimental and model predicted results of the ballistic muscle movement are very similar, the activation function between the start and the finish is not. This neural network preconditions the signal in an attempt to more closely model the actual activation function over the entire course of the muscle movement. Author

N95-11744# Joint Publications Research Service, Arlington, VA.
JPRS REPORT: SCIENCE AND TECHNOLOGY. CENTRAL EURASIA: LIFE SCIENCES
20 Oct. 1993 64 p Transl. into ENGLISH from various Russian articles
(JPRS-ULS-93-012) Avail: CASI HC A04/MF A01

Translations are presented covering the following areas of the life sciences: biochemistry, biophysics, biotechnology, environment, epidemiology, immunology, medicine, microbiology, nonionizing radiation effects, pharmacology, toxicology, physiology, public health, and radiation biology. CASI

N95-11806# Polish Academy of Sciences, Warsaw (Poland). Inst. Podstawowych Problemow Techniki.
A NUMERICAL ANALYSIS OF THE DISTRIBUTION OF STRESSES IN LUNG PARENCHYMA WHICH ACCOUNTS FOR THE INTERACTIONS BETWEEN THE TISSUE SKELETON AND FLOWING AIR Ph.D. Thesis [NUMERYCZNA ANALIZA ROZKLADU NAPREZEN W MIAZSZU PLUCNYM Z UWZGLEDNIENIEM ODDZIALYWAN MIEDZY SZKIELETEM TKANKOWYM A PRZEPLYWAJACYM POWIETRZEM]
Piotr Kowalczyk 1993 93 p In POLISH
(ISSN 0208-5658)
Avail: CASI HC A05/MF A01

This article presents a numerical model which enables the approximate determination of the distribution of strains and stresses in lung tissue during respiration. It includes the formulation of a basic system of differential equations for the problem, time and space sampling of the system and the development of an algorithm for solving the system, and implementation of the system in a computer program. The computer model accounts for the non-linear mechanical properties of the tissue, their extensive

deformation, and the effect of variations in the distribution of gas pressure and flow in the air spaces of the lungs. Part 1 explains the basic approach to the subject and briefly discusses extant research on the mechanics of the respiration process. Part 2 presents a physical model of the problem. It also contains a brief discussion of the anatomy and physiology of the lungs. Then follows a discussion of extant knowledge of the mechanical properties of lung tissue and a critical overview of previously used constitutional models of lung tissue. The following subsection contains an analysis of air flow in respiratory tracts and presents a model of the mechanical relationships between this flow and the deformation of the tissue skeleton. It consists of a system of discretely modelled air ducts embedded in a two-phase porous medium which fills the spaces of the lungs. Next the author writes a system of differential equations for the problem which includes an equation for flow in the respiratory tree, an equation for equilibrium in the lung tissue, and an equation for gas filtration in the tissue, along with their respective boundary and initial conditions. The author introduces the concept of a contact layer along with an additional equilibrium equation for the purpose of simplifying the numerical realization of a mixed boundary condition for displacements and stresses. In Part 3 the author presents a numerical algorithm which provides an approximate solution of the equations of the problem by means of an increment version of the finite element method. The author gives a matrix formulation of a conjugate problem in which the unknown variables at each step are the increments of flows in the components of the respiratory tree and the increments of displacements and pressures at the nodes of the finite element grid. The author describes an iterative procedure for solving the problem with an implicit numerical time integration scheme. Examples of numerical computations performed by means of the aforementioned algorithm implemented in a computer program are discussed in Part 4. Among other subjects, the author studied the static characteristics of a model of the human lungs under the action of the tissue's own weight and the effect of the inhalation rate on local ventilation and stresses in different regions of the lungs. Part 5 contains a critical analysis of the model and its results and recommendations for further research in the field. It also summarizes the original work embodied in the thesis. Author (revised)

N95-11808*# New England Deaconess Hospital, Boston, MA. Lab. of Cancer Biology.

MORPHOLOGICAL DIFFERENTIATION OF COLON CARCINOMA CELL LINES IN ROTATING WALL VESSELS Final Report, 1 Jun. 1991 - 31 May 1994

J. M. Jessup 1994 76 p

(Grant NAG9-520)

(NASA-CR-196780; Rept-115-38-8515; NAS 1.26:196780) Avail: CASI HC A05/MF A01

The objectives of this project were to determine whether (1) microgravity permits unique, three-dimensional cultures of neoplastic human colon tissues and (2) this culture interaction produces novel intestinal growth and differentiation factors. The initial phase of this project tested the efficacy of simulated microgravity for the cultivation and differentiation of human colon carcinoma in rotating wall vessels (RWV's) on microcarrier beads. The RWV's simulate microgravity by randomizing the gravity vector in an aqueous medium under a low shear stress environment in unit gravity. This simulation achieves approximately a one-fifth g environment that allows cells to 'float' and form three-dimensional relationships with less shear stress than in other stirred aqueous medium bioreactors. In the second phase of this project we assessed the ability of human colon carcinoma lines to adhere to various substrates because adhesion is the first event that must occur to create three-dimensional masses. Finally, we tested growth factor production in the last phase of this project. Author

N95-11887*# National Aeronautics and Space Administration. Lyndon B. Johnson Space Center, Houston, TX.

EVALUATION OF COSTAR MASS HANDLING CHARACTERISTICS IN AN ENVIRONMENT. A SIMULATION OF THE HUBBLE SPACE TELESCOPE SERVICE MISSION

Sudhakar L. Rajulu (Lockheed Engineering and Sciences Co., Houston, TX.), Glenn K. Klute, and Lauren Fletcher Aug. 1994 59 p

(NASA-TP-3489; S-775; NAS 1.60:3489) Avail: CASI HC A04/MF A01

The STS-61 Shuttle mission, which took place in December 1993, was solely aimed at servicing the Hubble Space Telescope (HST). Successful completion of this mission was critical to NASA since it was necessary to rectify a flaw in the HST mirror. In addition, NASA had never scheduled a mission with such a high quantity of complex extravehicular activity. To meet the challenge of this mission, the STS-61 crew trained extensively in the Weightless Environment Test Facility at the Johnson Space Center and in the Neutral Buoyancy Simulator at the Marshall Space Flight Center. However, it was suspected that neutral buoyancy training might induce negative training by virtue of the viscous damping effect present in water. The mockups built for this training also did not have the mass properties of the actual orbital replacement units (ORUs). It was felt that the crew should be further trained on mockups with similar mass characteristics. A comprehensive study was designed to address these issues. The study was quantitative, and instrumentation was set up to measure and quantify the forces and moments experienced during ORU mass handling and remote manipulator system run conditions. Author

N95-12376*# Mount Sinai School of Medicine, New York, NY. Dept. of Neurology.

REDUCTION OF OCULAR COUNTER-ROLLING BY ADAPTATION TO SPACE Final Report

Mingjia Dai, Leigh McGarvie, Inessa Kozlovskaya, Mischa Sirota, Theodore Raphan, and Bernard Cohen 15 Nov. 1993 23 p

(Grants NAG2-573; NAG2-703)

(NASA-CR-196279; NAS 1.26:196279) Avail: CASI HC A03/MF A01

We studied the three-dimensional vestibulo-ocular reflex (VOR) of rhesus monkeys before and after the COSMOS Biosatellite 2229 Mission of 1992-1993. This included tests of ocular counter-rolling (OCR), the gain of the vestibulo-ocular reflex (VOR), and spatial orientation of velocity storage. A four-axis vestibular and oculomotor stimulator was transported to the Institute of Biomedical Problems in Moscow for the pre- and postflight ground-based testing. Twelve normal juvenile male rhesus monkey were implanted surgically with eye coils and tested 60-90 days before spaceflight. Two monkey (7906 and 6151), selected from the twelve as flight animals, flew from 12/29/92 to 1/10/93. Upon recovery, they were tested for 11 days postflight along with three control animals. Compensatory ocular torsion was produced in two ways: (1) Lateral head tilts evoked OCR through otolith-ocular reflexes. OCR was also measured dynamically during off-vertical axis rotation (OVAR). (2) Rotation about a naso-occipital axis that was either vertical of horizontal elicited torsional nystagmus through semicircular canal-ocular reflexes (roll VOR). OCR from the otoliths was substantially reduced (70 percent) for 11 days after reentry on both modes of testing. The gain of the roll VOR was also decreased, but less than OCR. These data demonstrate that there was a long-lasting depression of torsional or roll eye movements after adaptation to microgravity in these monkeys, especially those movements produced by the otolith organs.

Author (revised)

N95-12405# Army Aeromedical Research Lab., Fort Rucker, AL.

BIOMEDICAL IMAGING

James E. Bruckart Apr. 1994 30 p

(AD-A282221) Avail: CASI HC A03/MF A01

This paper has been prepared for submission to the Advisory Group for Aerospace Research and Development (AGARD) Working Group 20 as a chapter on three-dimensional image collection for a report on 3D anthropometry. The principal 3D anthropometry data acquisition task, imaging the human body, presents technical barriers. The ultimate choice of an imaging technique depends on the specific details of an object that require reproduction and the precision required from the task. This report details the technologies in surface and subsurface imaging systems for research and commercial applications. DTIC

N95-12406# Army Aeromedical Research Lab., Fort Rucker, AL.

DYNAMIC SINE WAVE RESPONSE MEASUREMENTS OF CRT DISPLAYS USING SINUSOIDAL COUNTERPHASE MODULATION

Robert W. Verona, Howard H. Beasley, John S. Martin, and Victor Klymenko Apr. 1994 20 p

(AD-A282222; USAARL-94-22) Avail: CASI HC A03/MF A01

The current practice of basing the performance of cathode ray tube (CRT) displays on static image quality figures-of-merit fails to provide a valid assessment of a display's ability to reproduce real-world scenes where there is relative motion within the scene or between the sensor and scene. Techniques which provide assessment of a display's capability to reproduce

spatial information in a dynamic environment are needed. One technique based on response to sinusoidal counterphase modulation is presented.
DTIC

N95-12535 Massachusetts General Hospital, Boston, MA.
ULTRASHORT LASER PULSE EFFECTS IN OCULAR AND RELATED MEDIA: LASER-INDUCED SHOCK WAVE PROPAGATION AND RETINAL DAMAGE Annual Technical Report, 15 Apr. 1993 - 14 Apr. 1994
T. F. Deutsch, A. G. Doukas, T. Flotte, K. Dorey, and S. Lee Jun. 1994 8 p Limited Reproducibility: More than 20% of this document may be affected by microfiche quality
(Contract F49620-93-1-0290)
(AD-A282599; AFOSR-94-0464TR) Avail: Issuing Activity (Defense Technical Information Center (DTIC))

The goals of this project are: (1) to develop assays for functional damage to retinal cells by pressure waves (stress transients); (2) to determine the acoustic properties of the aqueous and vitreous humors of the eye; and (3) to examine the effect of pressure waves to the retinal pigment epithelium in vitro. During this first year our efforts have been directed primarily at the first goal, with some initial efforts on the second. During this period we developed the capability of growing human retinal pigment epithelium (RPE) cells in culture, incorporating them in test capillaries, recovering them after exposure to stress transients and assessing cell damage.
DTIC

N95-12542 Shock Society, Augusta, GA.
SUMMARY OF THE SIXTEENTH ANNUAL CONFERENCE ON SHOCK Summary Report
10 Jul. 1994 9 p Conference held in Santa Fe, NM, 13-16 Jun. 1993 Limited Reproducibility: More than 20% of this document may be affected by microfiche quality
(Contract N00014-93-1-0951)
(AD-A282643) Avail: CASI HC A02

Thirty-two abstracts were selected for presentation in four mini-symposia which cover topics including adhesion molecules, mediators, endotoxin/sepsis, and hemorrhage/ischemia - reperfusion. In addition, 194 abstracts were scheduled as poster presentationsin three sessions: 'Hemorrhage/Isechemia - Reperfusion', 'Mediators', and 'Endotoxin/Sepsis.' A workshop, 'Basic Molecular Biology Concepts and Techniques', was scheduled. Symposia dealing with 'Biological Roles of Nitric Oxide in Sepsis and Tissue Injury', 'Molecular Mechanisms in Shock', and 'New Insights into Mediator Interactions in Sepsis and Ards', were complimented with a debate on 'Controversies in Shock Research.'
CASI

N95-12593 Edgewood Arsenal, Aberdeen Proving Ground, MD. Research, Development and Engineering Center.
COMPARISON OF SUBMAXIMAL CYCLING AND TREADMILL EXERCISE AT SIMILAR WORK RATES Final Report, Nov. 1991 - Jun. 1992
David M. Caretti Jul. 1994 15 p Limited Reproducibility: More than 20% of this document may be affected by microfiche quality
(DA Proj. 101-62622-A-553)
(AD-A283430; ERDEC-TR-175) Avail: Issuing Activity (Defense Technical Information Center (DTIC))

The increased use of both the treadmill and cycle ergometer for exercise testing during respirator wear has escalated the need to compare the physiological response relationships between modes. This study compared circulatory, respiratory, and metabolic responses of submaximal cycling and treadmill exercise of similar work rates in 8 males and 6 females to determine whether the two exercise modes elicited different responses. Gender differences for each exercise mode were also assessed. Subjects cycled or walked for 5 min at each of five incremental external work rates of 60, 90, 120, 150, and 180 W. Measurements of HR, V(T), F(b)' V(E)' V(O2), and V(CO2) were obtained for each minute of exercise. Varying differences were observed in the respiratory and metabolic responses within gender groups to exercise between cycling and treadmill exercise of equal work rates with cycling eliciting greater responses at intensities of greater than 120 W. For cycling and treadmill exercise, females had significantly higher HR and F(b) than males at intensities greater than 90 W, but metabolic responses were similar between gender groups. These results suggest that both exercise modes are useful for protocols evaluating the physiological effects of mask wear during low levels of physical exertion. However, treadmill exercise seems better suited for testing at higher submaximal work rates.
DTIC

N95-12792*# National Aeronautics and Space Administration. Ames Research Center, Moffett Field, CA.
CREW FACTORS IN FLIGHT OPERATIONS 9: EFFECTS OF PLANNED COCKPIT REST ON CREW PERFORMANCE AND ALERTNESS IN LONG-HAUL OPERATIONS
Mark R. Rosekind, R. Curtis Graeber, David F. Dinges, Linda J. Connell, Michael S. Rountree, Cheryl L. Spinweber, and Kelly A. Gillen Sep. 1994 80 p
(RTOP 505-64-53)
(NASA-TM-108839; A-94134; NAS 1.15:108839; DOT/FAA/92/24) Avail: CASI HC A05/MF A01

This study examined the effectiveness of a planned cockpit rest period to improve alertness and performance in long-haul flight operations. The Rest Group (12 crew members) was allowed a planned 40 minute rest period during the low workload, cruise portion of the flight, while the No-Rest Group (9 crew members) had a 40 minute planned control period when they maintained usual flight activities. Measures used in the study included continuous ambulatory recordings of brain wave and eye movement activity, a reaction time/vigilance task, a wrist activity monitor, in-flight fatigue and alertness ratings, a daily log for noting sleep periods, meals, exercise, flight and duty periods, and the NASA Background Questionnaire. The Rest Group pilots slept on 93 percent of the opportunities, falling asleep in 5.6 minutes and sleeping for 25.8 minutes. This nap was associated with improved physiological alertness and performance compared to the No-Rest Group. The benefits of the nap were observed through the critical descent and landing phases of flight. The nap did not affect layover sleep or the cumulative sleep debt. The nap procedures were implemented with minimal disruption to usual flight operations and there were no reported or identified concerns regarding safety.
Author

N95-12919 Rome Lab., Griffiss AFB, NY.
RADIOFREQUENCY/MICROWAVE RADIATION BIOLOGICAL EFFECTS AND SAFETY STANDARDS: A REVIEW Report, Jun. 1988 - May 1993
Scott M. Bolen Jun. 1994 31 p Limited Reproducibility: More than 20% of this document may be affected by microfiche quality
(AF Proj. 4506)
(AD-A282886; RL-TR-94-53) Avail: Issuing Activity (Defense Technical Information Center (DTIC))

The study of human exposure to radiofrequency/microwave (RF/MW) radiation has been the subject of widespread investigation and analysis. It is known that electromagnetic radiation has a biological effect on human tissue. An attempt has been made by researchers to quantify the effects of radiation exposure on the human body and to set guidelines for safe exposure levels. A review of the pertinent findings is presented along with the American National Standards Institute (ANSI) recommended safety standard and the United States Air Force permissible exposure limit for RF/MW radiation. An overview of research conducted in the Soviet Union and Eastern Europe is also included in this report.
DTIC

N95-13054 Army Aeromedical Research Lab., Fort Rucker, AL.
AVIATION EPIDEMIOLOGY DATA REGISTER: CARDIOVASCULAR DISEASE SCREENING OUTCOMES IN THE NORTH DAKOTA ARMY NATIONAL GUARD AVIATOR COHORT Final Report
Kevin T. Mason and S. G. Shannon Jun. 1994 30 p Limited Reproducibility: More than 20% of this document may be affected by microfiche quality
(DA Proj. 301-62787-A-878)
(AD-A283064; USAARL-94-31) Avail: CASI HC A03

This study compared the aeromedical cardiovascular disease screening outcomes between the North Dakota Army National Guard (NDARNG) aviator cohort and a peer cohort composed of all other Army National Guard (ARNG) aviators. Each cohort included aviators age 40 or older which is the age aviators enter the cardiovascular disease screening program for the detection of disease. The study was based on analysis of factors found in the U.S. Army Aviation Epidemiology Data Register. Analyses were conducted using nonparametric, relative risk, odds ratio, and matched pair case control methods.
DTIC

N95-13177 European Office of Aerospace Research and Development, FPO New York, NY.
EFFECTS OF NOISE ON HEARING 5TH INTERNATIONAL SYMPOSIUM
14 May 1994 59 p Symposium held in Gothenburg, Sweden, 12-14 May 1994 Limited Reproducibility: More than 20% of this document may be affected by microfiche quality
(AD-A281439) Avail: CASI HC A04

Abstracts for oral presentations include the following: The Effects of Acoustic Trauma, Other Cochlear Injury and Death on Basilar-membrane Responses to Sound; Noise Induced Expression of Heat Shock Proteins in the Cochlea; Genetic Susceptibility to Noise-Induced Hearing Loss in Mice; Sensory Cell Regeneration and Functional Recovery Following Acoustic Trauma and Aminoglycoside Ototoxicity; The Effects of Noise on Cochlear Blood Flow; Efferent and Priming Modulation of Noise-Induced Hearing Loss; Threshold Shift Dynamics Following Interrupted Impact or Continuous Noise Exposure; Interactions Between Age-related and Noise-induced Hearing Loss; Effects of Intense Noise on Fegal Sheep Auditory Brainstem Response; Underwater Hearing and Occupational Noise Exposure; International Review of Field Studies of Hearing Protector Attenuation; Current Standards for Occupational Exposure to Noise; and more. Abstracts for posters are also included. CASI

N95-13230* National Aeronautics and Space Administration, Washington, DC.
AEROSPACE MEDICINE AND BIOLOGY: A CONTINUING BIBLIOGRAPHY WITH INDEXES (SUPPLEMENT 394)
Dec. 1992 41 p
(NASA-SP-7011(394); NAS 1.21:7011(394)) Avail: CASI HC A03

This bibliography lists 71 reports, articles and other documents introduced into the NASA Scientific and Technical Information System during Nov. 1994. Subject coverage includes: aerospace medicine and physiology, life support systems and man/system technology, protective clothing, exobiology and extraterrestrial life, planetary biology, and flight crew behavior and performance. Author

N95-13270*# Texas Univ., Austin, TX. Dept. of Mechanical Engineering.
A MUSCULOSKELETAL MODEL OF THE ELBOW JOINT COMPLEX
Roger V. Gonzalez, Ronald E. Barr, and Lawrence D. Abraham 1993 2 p
(Grant NAG9-588)
(NASA-CR-195812; NAS 1.26:195812) Avail: CASI HC A01/MF A01

This paper describes a musculoskeletal model that represents human elbow flexion-extension and forearm pronation-supination. Musculotendon parameters and the skeletal geometry were determined for the musculoskeletal model in the analysis of ballistic elbow joint complex movements. The key objective was to develop a computational model, guided by optimal control, to investigate the relationship among patterns of muscle excitation, individual muscle forces, and movement kinematics. The model was verified using experimental kinematic, torque, and electromyographic data from volunteer subjects performing both isometric and ballistic elbow joint complex movements. In general, the model predicted kinematic and muscle excitation patterns similar to what was experimentally measured. Author

53 BEHAVIORAL SCIENCES

Includes psychological factors; individual and group behavior; crew training and evaluation; and psychiatric research.

N95-11872 National Defence Research Establishment, Stockholm (Sweden). Huvudavdeling foer Maensklig Prestation och Funktion.
TANK CREW PERFORMANCE RELATED TO COGNITIVE ABILITY AND MOTIVATION OF THE TANK CREW MEMBERS [PRESTATION HOS STRIDSVAGNSBESAETTNINGAR RELATERAD TILL KOGNITIV FOERMAGA OCH MOTIVATION HOS BESAETTNINGSMEDLEMMARNA]
C. Wallenius Dec. 1993 33 p In SWEDISH
(PB94-190642; FOA-C-50103-5.3) Avail: Issuing Activity (National Technical Information Service (NTIS))

Tank crews from three Swedish armored regiments were divided into three criterion groups with regard to performance: below average, average, and above average. Cognitive ability, ability to structure, emotional commitment, experience of control and appraisal of person-related and task-related group cohesion respectively, were studied at the individual level in the three criterion groups (n=130). The results showed that individuals who belonged to tank crew whose performance was below average had a lower emotional commitment and perceived less task-related group cohesion. On the other hand, these individuals showed on average a better ability to structure and, to some extent, greater experience of control, compared with individuals in groups that were assessed as average in performance. There were no differences between the three criterion groups with reference to cognitive ability or person-related group cohesion. Implications of the results for selection and training are discussed. NTIS

N95-11942 Massachusetts Inst. of Tech., Cambridge. Artificial Intelligence Lab.
HOW ARE THREE-DIMENSIONAL OBJECTS REPRESENTED IN THE BRAIN?
Heinrich H. Buelthoff, Shimon Y. Edelman, and Michael J. Tarr 18 Apr. 1994 20 p Limited Reproducibility: More than 20% of this document may be affected by microfiche quality
(Contracts N00014-92-J-1879; N00014-93-1-0385)
(AD-A282367; AI-M-1479) Avail: Issuing Activity (Defense Technical Information Center (DTIC))

We discuss a variety of psychophysical experiments that explore different aspects of the problem of object recognition and representation in human vision. In all experiments, subjects were presented with realistically rendered images of computer-generated three-dimensional objects, with tight control over stimulus shape, surface properties, illumination, and viewpoint, as well as subjects' prior exposure to the stimulus objects. Contrary to the predictions of the paradigmatic theory of recognition, which holds that object representations are viewpoint invariant, performance in all experiments was consistently viewpoint dependent, was only partially aided by binocular stereo and other depth information, was specific to viewpoints that were familiar, and was systematically disrupted by rotation in depth more than by deforming the two-dimensional images of the stimuli. The emerging concept of multiple-views representation supported by these results is consistent with recently advanced computational theories of recognition based on view interpolation. Moreover, in several simulated experiments employing the same stimuli used in experiments with human subjects, models based on multiple-views representations replicated many of the psychophysical results concerning the observed pattern of human performance. DTIC

N95-12133# Advisory Group for Aerospace Research and Development, Neuilly-Sur-Seine (France). Aerospace Medical Panel.
PSYCHOPHYSIOLOGICAL ASSESSMENT METHODS (INCLUDING A REGISTER OF PSYCHOPHYSIOLOGISTS ON MICROFICHES) [METHODES D'EVALUATION PSYCHOPHYSIOLOGIQUE (LISTE DE PSYCHOPHYSIOLOGUES INCLUSE SUR MICROFICHES)]
John A. Caldwell (Army Aeromedical Research Lab., Fort Rucker, AL.), Glenn F. Wilson, Muzaffer Cetinguc, Anthony W. K. Gaillard, Alexander Gunder, Didier Lagarde, Scott Makeig, Grete Myhre, and Nicola A. Wright May 1994 157 p Original contains color illustrations
(AGARD-AR-324; ISBN-92-835-0747-9) Copyright Avail: CASI HC A08/MF A02

The study of human-centered operationally-relevant problems in aerospace and aviation research and development can be enhanced by the inclusion of psychophysiological techniques. By measuring physiological variables in conjunction with performance and subjective measures, a more thorough understanding about the processes underlying performance can be obtained. This report presents a summary of the general utility of psychophysiological assessments, the types of applied problems which can be addressed with these assessments, and the qualities of several psychophysiological techniques. In addition, safety and ethical considerations, guidelines for making determinations about the most appropriate research strategy, and three research examples are discussed. The report concludes with a series of appendixes which offer the reader information on how to collect and analyze each of the psychophysiological measures. This Advisory Report was sponsored by the Aerospace Medical Panel of the Advsiory Group for Aerospace Research and Development (AGARD). Author

N95-12495# Johns Hopkins Univ., Baltimore, MD. School of Medicine.
VISUAL PSYCHOPHYSICS OF EGOMOTION Final Report

Kathleen Turano 30 Jun. 1994 10 p
(Grant AF-AFOSR-0154-91)
(AD-A282547; AFOSR-94-0450TR) Avail: CASI HC A02/MF A01

Human observers' ability to perceive self motion using information contained within optic-flow patterns was investigated. Subjects discriminated changes in heading direction as stimulus parameters were manipulated. Some of the results were surprising and difficult to explain in the context of current theories. In order to better understand the results, the role of eye movements in self-motion detection and in speed discrimination was investigated. The end product is a model that can account for the findings. The optimal stimulus for motion detection was also explored to define the shape (x,y,t) of the human motion sensors, which are believed to be involved in the early processing stages of self-motion perception. A computational model for the extraction of 3D motion information from 2D motion information was also developed. The neural network model was able to qualitatively account for the human observer's ability to detect changes in heading direction. DTIC

N95-13019# Civil Aeromedical Inst., Oklahoma City, OK.
AGE 60 RULE RESEARCH. PART 1: BIBLIOGRAPHIC DATABASE Final Report
Washington Oct. 1994 181 p Prepared in cooperation with Hilton Systems, Inc., Cherry Hill, NJ
(Contract DTFA02-90-C-90125; FAA Task AM-A-94-HRR-138)
(DOT/FAA/AM-94/20-Pt-1) Avail: CASI HC A09/MF A02

As part of their research contract with the FAA to study issues related to the 'Age 60 Rule' for pilot mandatory retirement, Hilton Systems, Inc. in collaboration with Lehigh University faculty and research facilities compiled this extensive bibliography. Topics included pilot aging, performance, health and physiological factors, as well as other aviation and pilot related topics. Citations were included from a variety of sources including international and military studies. The bibliography was organized in three sections. The first section presents a bibliographic listing on the above topics. The second section provides a listing of publications by authors active in related fields. Finally, the third section provides citations from the driving literature. Author

N95-13020# Civil Aeromedical Inst., Oklahoma City, OK.
AGE 60 RULE. PART 2: AIRLINE PILOT AGE AND PERFORMANCE. A REVIEW OF THE SCIENTIFIC LITERATURE Final Report
D. T. Hyland (Lehigh Univ., Bethlehem, PA.), E. J. Kay (Lehigh Univ., Bethlehem, PA.), J. D. Deimler (Hilton Systems, Inc., Cherry Hill, NJ.), and E. B. Gurman (University of Southern Mississippi, Hattiesburg, MS.)
Washington Oct. 1994 138 p
(Contract DTFA02-90-C-90125; FAA Task AM-A-91-HRR-138)
(DOT/FAA/AM-94/21-Pt-2; Rept-8025-1A-Pt-2) Avail: CASI HC A07/MF A02

This review of the literature establishes the scientific foundation for subsequent studies on the 'Age 60 Rule' research conducted under a contract with Hilton Systems, Inc. The scientific literature relevant to the two separate scientific approaches required by the contract is reviewed. The document first provides a review of the Age 60 Rule, as well as the theoretical and methodological considerations critical to the study of aging and the assessment of individual pilot performance. A proposed model is presented to form a framework for the research. Pilot behaviors affected by aging and/or experience are reviewed. Specific performance assessment batteries are reviewed in detail in Appendix A. Issues related to measuring complex pilot performance are discussed. Recommendations and criteria for developing a performance methodology are presented. The second part of the literature review provides a discussion of the issued related to the analyses of existing data to assess the relationship between pilot age, experience, and accident rates. This section provides a critical review of existing analyses and presents recommendations for an improved analytical methodology. Author

N95-13199# Hilton Systems, Inc., Cherry Hill, NJ.
AGE 60 STUDY. PART 4: EXPERIMENTAL EVALUATION OF PILOT PERFORMANCE Final Report
D. T. Hyland (Lehigh Univ., Bethlehem, PA.), E. J. Kay (Lehigh Univ., Bethlehem, PA.), and J. D. Deimler Oct. 1994 66 p
(Contract DTFA02-90-C-90125)
(Rept-8025-4B; DOT/FAA/AM-94/23) Avail: CASI HC A04/MF A01

The purpose of this study was to examine the feasibility of developing an individually-based pilot performance assessment, as well as design an experimental methodology to empirically examine the relationship between pilot aging and performance. Pilot performance was measured with both domain-dependent, as well as domain independent assessments to test a decrement with compensation model of expertise and aging. Computerized cognitive test batteries, COGSREEN and WOMBAT, were selected as domain-independent measures. Flitescript and whole task performance in the B727 simulator were domain-dependent measures. Forty B727-rated pilots were recruited from air carriers and the FAA. Pilots were males between the ages of 41 and 71 years (M=53.9, sd=8.1). All pilots had a minimum of 5000 hours of total flight time with a wide range of total and recent hours in type. Three simulator scenarios were designed to assess pilot performance on routine and emergency/abnormal maneuvers. Simulator performance measures were based on a deviation score and an evaluator rating. The relationships between the following measures were assessed by examination of the correlations between: (1) flying experience and simulator performance, (2) predictor test scores and simulator performance, (3) interrelationship between the predictor tests, and (4) age, flying experience, predictor test scores and simulator performance. Finally, pilot perceptions of each measure were assessed. COGSCREEN total composite scores were significantly correlated with evaluator ratings on emergency/abnormal maneuvers. Neither WOMBAT nor Flitescript were found to correlate with simulator performance. Pilot age was significantly correlated with performance on the predictor tests. A pattern of inter-correlations among pilot age, COGSCREEN and simulator performance is discussed. Author (revised)

N95-13375# Maryland Univ., College Park, MD. Office of Research Administration and Advancement.
COORDINATED ACTION IN 3-D SPACE Final Report, 15 Dec. 1990 - 31 Mar. 1994
Robert M. Steinman 31 May 1994 6 p
(Grant AF-AFOSR-0124-91)
(AD-A281284; AFOSR-94-0401TR) Avail: CASI HC A02/MF A01

Unique hardware and novel software were developed to study natural patterns of head and eye movements during inspection and manipulation of objects in nearby 3-D space. Emphasis was placed on natural tasks in which subjects looked at and handled real objects in a natural visual environment with the head and torso free to move naturally. Two quite different mechanistic models of gaze control were tested: (a) an 'on-line' feedback model and (b) a 'single packet' model that bases accurate gaze control on preplanned patterns of coordinated movements of the head and eyes. We found that the VOR was not turned-off during gaze-shifts, as currently believed, but that it was not effective in compensating for abrupt displacements of the head as had been believed previously. The speed and accuracy of button presses produced by tapping and the correlation of these performance measures with binocular gaze-errors were also studied. These studies were performed to determine how accurate binocular fixation must be in order to insure rapid and accurate tapping in nearby 3-D space. We found that effective performance was possible with binocular gaze-errors about the size of the human fovea (2 deg - 3 deg). DTIC

N95-13433 Newcastle-upon-Tyne Univ., Newcastle (England). Dept. of Computing Science.
SCENE ANALYSIS: A BRIEF SURVEY
C. Robertson and G. M. Megson Mar. 1994 33 p See also AD-A162662
(PB94-205085; TRS-480) Copyright Avail: Issuing Activity (National Technical Information Service (NTIS))

A brief survey of scene analysis is presented. In particular we consider the complex and highly parallel process of image gathering in the eye and contrast this with current computer-based image analysis. A number of classical scene analysis techniques based on statistical methods are also outlined. NTIS

54 MAN/SYSTEM TECHNOLOGY AND LIFE SUPPORT

Includes human engineering; biotechnology; and space suits and protective clothing.

For related information see also *16 Space Transportation.*

N95-11778# Technische Univ., Delft (Netherlands). Faculteit der Werktuigbouwkunde en Maritime Techniek.

DESIGN ISSUES OF HUMAN OPERATOR SUPPORT SYSTEMS Ph.D. Thesis

A. M. Sassen 24 Aug. 1993 235 p

(PB94-191376; ISBN-90-370-0090-8) Copyright Avail: CASI HC A11/MF A03

The thesis begins with an overview of the tasks of a human operator in a supervisory control system. This analysis results in an overview of possible human operator support systems. In Chapter 3, a number of problems have been identified which may account for a lack of acceptance of knowledge based support systems. Chapter 4 consists of a description of technology that is available to construct human operator support systems. It describes three different approaches to build diagnostic systems: the rule-based approach, systems that reason from first principles, and the multilevel flow modeling approach. All three are illustrated with examples taken from the domain of a nuclear power plant simulation. Chapter 5 contains an overview of the programming environment for expert systems constrained in reasoning time (PERFECT). PERFECT is aimed at providing the necessary engineering support in real-time knowledge based system development. Chapter 6 contains a description and the results of an evaluation of the diagnostic system of the generic nuclear plant as developed with PERFECT. The last chapter contains a summary of the conclusions of earlier chapters. Moreover, recommendations are made for further research. NTIS

N95-11811*# National Aeronautics and Space Administration. Lyndon B. Johnson Space Center, Houston, TX.

CARBON DIOXIDE AND WATER VAPOR PRODUCTION AT REST AND DURING EXERCISE. A REPORT ON DATA COLLECTION FOR THE CREW AND THERMAL SYSTEMS DIVISION

Stuart M. C. Lee (Krug Life Sciences, Inc., Houston, TX.) and Steven F. Siconolfi Aug. 1994 13 p

(NASA-TP-3500; S-781; NAS 1.60:3500) Avail: CASI HC A03/MF A01

The current environmental control device in the shuttle uses lithium hydroxide (LiOH) filter canisters to remove carbon dioxide (CO2) from the cabin air, requiring several bulky filter canisters that can only be used once and must be changed frequently. To alleviate a stowage problem and decrease launch weight, the Crew and Thermal Systems Division (CTSD) at the NASA Johnson Space Center has been researching a system to be used on future shuttle missions. This system uses two beds of solid amine material to absorb CO2 and water, later desorbing them to space vacuum. In this way the air scrubbing medium is regenerable and reusable. To identify the efficacy of this regenerable CO2 removal system (RCRS), CTSD began investigations in the shuttle mockup. The purpose of this investigation was to support the CTSD program by determining mean levels of carbon dioxide and water vapor production in normal, healthy males and females age-matched with the astronaut corps. Subjects' responses were measured at rest and during exercise at intensity levels equivalent to normal shuttle operation activities. The results were used to assess the adjustments made to RCRS and are reported as a reference for future investigations in shuttle environmental control. Author

N95-11873 National Defence Research Establishment, Stockholm (Sweden). Huvudavdelning foer Maensklig Prestation och Funktion.

VISIT TO UDRI AND USAF, ARMSTRONG LAB., WILLIAMS AFB, PHOENIX, USA, FEBRUARY 8-11, 1993 [BESOEK VID UDRI OCH USAF-ARMSTRONG LAB., WILLIAMS AFB, PHOENIX, USA. FLYGTEKNISK OCH HUMANVETENSKAPLIG FORSKNING I DISTRIBUERADE FLYGTRAENINGSSIMULATORER, 1993-02-08-11]

G. Derefeldt and U. Engdahl Nov. 1993 58 p In SWEDISH

(PB94-190659; FOA-A-50020-5.2) Avail: Issuing Activity (National Technical Information Service (NTIS))

The document reports on a visit on 11-18 Feb. 1993 to the University of Dayton Research Institute (UDRI) and to AL/HRA (Aircrew Training Research Division, Human Resources Directorate, USAF-Armstrong Laboratory, Williams Air Force Base) in Arizona, USA. The main purpose of the journey was to stengthen the contacts in the field of color presentations, visual displays in flight simulation, situational awareness and night vision devices (NVD). AL/HRA is the Air Force's premier organization for research and development in aircrew training techniques and technologies. Its basic mission is to increase aircrew effectiveness and to provide enhanced training systems for combat preparation. For better aircrew training at lower cost, new aircrew training system technology is advanced and the training effectiveness of that technology is evaluated. At Armstrong Lab, work is concentrated in three primary areas: (1) Basic research (concentrated in visual attention and cognitive processing); (2) Training effectiveness (to make optimal use of existing and future training resources); and (3) Technology development (including exploratory and advanced work on aircrew training devices). Personnel from UDRI are involved in both the basic research and the training effectiveness areas, which includes visual requirements and the adaptation of these requirements to visual simulation. NTIS

N95-11878*# National Aeronautics and Space Administration. Lyndon B. Johnson Space Center, Houston, TX.

HUMAN FACTORS ASSESSMENTS OF THE STS-57 SPACEHAB-1 MISSION

Frances E. Mount, Sue Adam, Tim McKay, Mihriban Whitmore, Darlene Merced-Moore, Tina Holden, Charles Wheelwright, Anton Koros, Sr., Michael ONeal, and Jennifer Toole et al Aug. 1994 42 p

(Contracts NAS9-17900; NAS9-18800)

(NASA-TM-104802; S-779; NAS 1.15:104802) Avail: CASI HC A03/MF A01

SpaceHab-1 (STS-57) was the first of six scheduled Commercial Middeck Augmentation Module (CMAM) missions seeking to offer entrepreneurial companies an opportunity to use the resource of microgravity. The SpaceHab module, which occupies about one-fourth of the payload bay, is approximately 2-3/4 meters (9 feet) long and 4 meters (13.5 feet) in diameter. It provides a shirt-sleeve working environment and contains the storage space equivalent of 50 middeck lockers, considerably over and above the number of experiments that can be carried in the orbiter middeck alone. A modified Spacelab tunnel links the SpaceHab module to the middeck. While in orbit, the orbiter payload bay doors remain open, exposing the padded exterior of the lab and tunnel to space until preparation for reentry at the end of the flight. The crew for SpaceHab-1 was comprised of four males and two females, each of whom participated in some part of the human factors assessment (HFA) evaluation. The HFA was one of over twenty experiments manifested on this maiden flight of the SpaceHab module. HFA consisted of HFA-EPROC, HFA-LIGHT, HFA-SOUND, HFA-QUEST, and HFA-TRANS. The goal of HFA-EPROC was to assess the advantages and disadvantages of paper versus computer presentation for procedural tasks. The next two evaluations investigated the module's lighting and acoustic environment. HFA-TRANS sought to evaluate the design of the SpaceHab tunnel and to characterize translation through it. HFA-QUEST represented a consolidation of the in-flight questions generated by the HFA principal investigators involved in the acoustic, lighting, and translation studies. Author (revised)

N95-11905*# National Aeronautics and Space Administration. Ames Research Center, Moffett Field, CA.

INTERVIEWS WITH THE APOLLO LUNAR SURFACE ASTRONAUTS IN SUPPORT OF PLANNING FOR EVA SYSTEMS DESIGN

Mary M. Connors, Dean B. Eppler, and Daniel G. Morrow Sep. 1994 21 p

(RTOP 199-06-12)

(NASA-TM-108846; A-94131; NAS 1.15:108846) Avail: CASI HC A03/MF A01

Focused interviews were conducted with the Apollo astronauts who landed on the moon. The purpose of these interviews was to help define extravehicular activity (EVA) system requirements for future lunar and planetary missions. Information from the interviews was examined with particular attention to identifying areas of consensus, since some commonality of experience is necessary to aid in the design of advanced systems. Results are presented under the following categories: mission approach; mission structure; suits; portable life support systems; dust control;

gloves; automation; information, displays, and controls; rovers and remotes; tools; operations; training; and general comments. Research recommendations are offered, along with supporting information. Author

N95-11908# National Inst. of Standards and Technology, Gaithersburg, MD. Factory Automation Systems Div.
BODY DIMENSIONS FOR APPAREL
Y. T. T. Lee Apr. 1994 30 p See also PB93-158665 Sponsored by Defense Logistics Agency
(PB94-187739; NISTIR-5411) Avail: CASI HC A03/MF A01

This report represents a compilation of body dimensions that are used in the manufacturing and fitting of apparel. It is the result of a comparison of five body measurements reports, including documentations of national and international apparel sizing standards. The information in this report will provide the basis for the development of the information model of made-to-measure pattern making. It will also contribute to the conducting of future body measurements survey and the development of new or improved sizing standards for apparel. NTIS

N95-11949*# Wisconsin Univ., Madison, WI. Dept. of Horticulture.
GROWTH OF POTATOES FOR CELSS
T. W. Tibbitts, W. Cao, and R. M. Wheeler Cleveland, OH NASA Aug. 1994 200 p
(Contract NCC2-301)
(NASA-CR-177646; A-94129; NAS 1.26:177646) Avail: CASI HC A09/MF A03

This report summarizes research on the utilization of white potatoes (Solanum tuberosum L.) for space life support systems at the University of Wisconsin-Madison over the period of 1984 to 1993. At full maturity the tuber productivity was 37.5 gm(exp -2) d(exp -1), equating to a growing area requirement for one human (2800 kcal d(exp -1)) of 10.1 m(exp -2). A recirculating nutrient system using slanted trays produced best potato growth and tuber yields when a 2-3 cm layer of gravel or arcillite media was utilized. Potato production was close to maximum under lighting levels of 400 micromol m(exp -2) s(exp -1) of photosynthetic photo flux (PPF) for 24 hours or 800 micromol m(exp -2) s(exp -1) for 12 hours, alternating diurnal temperatures of 22 C and 14 C, relative humidity of 85 percent, and a carbon dioxide level of 1000 micromol m(exp -1). The range of effective concentrations of each separate nutrient is reported. The extensive studies with potatoes in this project have demonstrated that this crop has high productivity of nutritous tubers with a high harvest index in controlled environments, and can fulfill a significant portion of the energy and protein requirements for humans in space. Author

N95-12132*# Food and Agrosystems, Inc., Sunnyvale, CA.
METHODOLOGIES FOR PROCESSING PLANT MATERIAL INTO ACCEPTABLE FOOD ON A SMALL SCALE
Thomas R. Parks, John N. Bindon, Anthony J. G. Bowles, Peter Golbitz, Rauno A. Lampi, and Robert F. Marquardt Sep. 1994 258 p
(Contract NAS2-13404; SBIR-12.04-8450B)
(NASA-CR-177647; A-94130; NAS 1.26:177647) Avail: CASI HC A12/MF A03

Based on the Controlled Environment Life Support System (CELSS) production of only four crops, wheat, white potatoes, soybeans, and sweet potatoes; a crew size of twelve; a daily planting/harvesting regimen; and zero-gravity conditions, estimates were made on the quantity of food that would need to be grown to provide adequate nutrition; and the corresponding amount of biomass that would result. Projections were made of the various types of products that could be made from these crops, the unit operations that would be involved, and what menu capability these products could provide. Equipment requirements to perform these unit operations were screened to identify commercially available units capable of operating (or being modified to operate) under CELSS/zero-gravity conditions. Concept designs were developed for those equipment needs for which no suitable units were commercially available. Prototypes of selected concept designs were constructed and tested on a laboratory scale, as were selected commercially available units. This report discusses the practical considerations taken into account in the various design alternatives, some of the many product/process factors that relate to equipment development, and automation alternatives. Recommendations are made on both general and specific areas in which it was felt additional investigation would benefit CELSS missions. Author

N95-12354# Federal Aviation Administration, Oklahoma City, OK. Civil Aeromedical Inst.
SIMULTANEOUS GAS-CHROMATOGRAPHIC DETERMINATION OF FOUR TOXIC GASES GENERALLY PRESENT IN COMBUSTION ATMOSPHERES Final Report
Boyd R. Endecott, Donald C. Sanders, and Arvind K. Chaturvedi Sep. 1994 12 p
(DOT/FAA/AM-94/18) Avail: CASI HC A03/MF A01

Measurement of combustion gases produced by burning aircraft cabin materials poses a continuing limitation for smoke toxicity research. Since toxic effects of gases depend on both their concentrations and durations of exposures, frequent atmosphere sampling is necessary to define the concentration-time curve. A gas chromatographic method was developed for the simultaneous analyses of carbon monoxide (CO), hydrogen sulfide (H2S), sulfur dioxide (SO2), and hydrogen cyanide (HCN). The method utilized an MTI M200 dual-column gas chromatograph (GC) equipped with 4-m molecular sieve-5A and 8-m PoraPlot-U capillary columns and two low-volume, high sensitivity thermal conductivity detectors. Detectability (ppm)/retention times (seconds) for the gases were: CO (100/28); H2S (50/26); SO2 (125/76); HCN (60/108). The method was effective for determining the gases in mixtures and in the combustion atmospheres generated by burning wool (CO, HCN, and H2S) and modacrylic (CO and HCN) fabrics. Common atmospheric gaseous or combustion products (oxygen, carbon dioxide, nitrogen, water vapor, and other volatiles) did not interfere with the analyses. However, filtration of the combustion atmospheres was necessary to prevent restriction of the GC sampling inlet by smoke particulates. The speed, sensitivity, and selectivity of this method make it suitable for smoke toxicity research and for evaluating performance of passenger protective breathing equipment. Author

N95-12361*# Universities Space Research Association, Columbia, MD.
M.E.366-J EMBODIMENT DESIGN PROJECT: PORTABLE FOOT RESTRAINT
Randall Heaton, Eikar Meyer, Davey Schmidt, and Kevin Enders 25 Apr. 1994 49 p
(Contract NASw-4435)
(NASA-CR-197163; NAS 1.26:197163) Avail: CASI HC A03/MF A01

During space shuttle operations, astronauts require support to carry out tasks in the weightless environment. In the past, portable foot restraints (PFR) with orientations adjustable in pitch, roll, and yaw provided this support for payload bay operations. These foot restraints, however, were designed for specific tasks with a load limit of 111.2 Newtons. Since the original design, new applications for foot restraints have been identified. New designs for the foot restraints have been created to boost the operational work load to 444.8 Newtons and decrease setup times. What remains to be designed is an interface between the restraint system and the extravehicular mobility unit (EMU) boots. NASA provided a proposed locking device involving a spring-loaded mechanism. This locking mechanism must withstand loads of 1334.4 Newtons in any direction and weigh less than 222.4 Newtons. This paper develops an embodiment design for the interface between the PFR and the EMU boots. This involves design of the locking mechanism and a removable cleat that allows the boot to interface with this mechanism. The design team used the Paul Beitz engineering methodology to present the systematic development, structural analysis, and production considerations of the embodiment design. This methodology provides a basis for understanding the justification behind the decisions made in the design. Author

N95-12555*# Universities Space Research Association, Columbia, MD.
THE EMBODIMENT DESIGN OF THE HEAT REJECTION SYSTEM FOR THE PORTABLE LIFE SUPPORT SYSTEM
Sue Stuckwisch, Jason Francois, Julia Laughlin, Lee Phillips, and Carlos A. Carrion 25 Apr. 1994 51 p
(Contract NASw-4435)
(NASA-CR-197178; NAS 1.26:197178) Avail: CASI HC A04/MF A01

The Portable Life Support System (PLSS) provides a suitable environment for the astronaut in the Extravehicular Mobility Unit (EMU), and the heat rejection system controls the thermal conditions in the space suit. The current PLSS sublimates water to the space environment; therefore, the system loses mass. Since additional supplies of fluid must be available on the Space Shuttle, NASA desires a closed heat rejecting system. This document presents the embodiment design for a radiative plate heat rejection

system without mass transfer to the space environment. This project will transform the concept variant into a design complete with material selection, dimensions of the system, layouts of the heat rejection system, suggestions for manufacturing, and financial viability. Author

N95-12629*# Universities Space Research Association, Columbia, MD.
INTEGRAL HABITAT TRANSPORT SYSTEM
Bill Elliott, Scott Frazer, Joey Higgs, Jason Huff, and Tigree Milam 8 Mar. 1994 12 p
(Contract NASw-4435)
(NASA-CR-197156; NAS 1.26:197156) Avail: CASI HC A03/MF A01

In the 1993 Fall quarter, the ME 4182 design class was sponsored to study various scenarios that needed to be studied for Martian travel. The class was sponsored by NASA and there were several different design projects. The design that group three chose was an integral transport system for a Martian habitat. An integral transport system means the design had to be one that was attached to the habitat. There were several criteria that the design had to meet. Group three performed an in depth study of the Martian environment and looked at several different design ideas. The concept group three developed involved the use of kinematic linkages and the use of Martian gravity to move the habitat. The various design concepts, the criteria matrices and all other aspects that helped group three develop their design can be found in their 1993 ME 4182 design report. Now it is Winter quarter 1994 and group three is faced with another problem. The problem is building a working prototype of their Fall design. The limitations this quarter were the parts. The group had to make the prototype work with existing manufactured parts or make the parts themselves in a machine shop. The prototype was scaled down roughly about twelve times smaller than the original design. The following report describes the actions taken by group three to build a working model. Derived from text

N95-13055 Army Aeromedical Research Lab., Fort Rucker, AL.
STANDARDS RELEVANT TO A NATO ANTHROPOMETRY SURVEY USING 3D IMAGING TOOLS
James E. Bruckart Jun. 1994 20 p Limited Reproducibility: More than 20% of this document may be affected by microfiche quality
(DA Proj. 301-62787-A-878)
(AD-A283065; USAARL-94-30) Avail: CASI HC A03

Designers of aircraft cockpits and aircrew equipment have long recognized the importance of accurate measurements of the flying population. The success of three dimensional anthropometry and its usability for design and fitting are dependent largely on the adoption of standards for digital image display, transformation, storage, and communication. Standards are required for image data obtained from surface or volumetric scanner systems, as well as reduced and analyzed data. There are hundreds of data formats already in use by various disciplines for all sorts of data. In this paper, we will discuss what is desired in a format for three dimensional biomedical image data and several formats already available. DTIC

N95-11962*# National Aeronautics and Space Administration. Ames Research Center, Moffett Field, CA.
TECHNIQUES FOR OPTIMAL CROP SELECTION IN A CONTROLLED ECOLOGICAL LIFE SUPPORT SYSTEM
Ann McCormack, Cory Finn, and Betsy Dunsky *In its* Technical Paper Contest for Women 1992. Space Challenges: Earth and Beyond 1993 p 81-96 See also N93-12018 (For primary document see N95-11955 02-99)
Avail: CASI HC A03/MF A03

N95-11964*# National Aeronautics and Space Administration. Ames Research Center, Moffett Field, CA.
TRAINING FOR LIFE SCIENCE EXPERIMENTS IN SPACE AT THE NASA AMES RESEARCH CENTER
Annette T. Rodrigues and A. Christopher Maese *In its* Technical Paper Contest for Women 1992. Space Challenges: Earth and Beyond 1993 p 111-128 (For primary document see N95-11955 02-99)
Avail: CASI HC A03/MF A03

N95-11970*# National Aeronautics and Space Administration. Ames Research Center, Moffett Field, CA.
MEETING THE CHALLENGE OF MANNED LUNAR AND MARTIAN EXPLORATION
Rebecca C. Williamson *In its* Technical Paper Contest for Women 1992. Space Challenges: Earth and Beyond 1993 p 195-205 (For primary document see N95-11955 02-99)
Avail: CASI HC A03/MF A03

N95-13214*# Georgia Tech Research Inst., Atlanta, GA.
EVALUATION OF CANDIDATE MILLIMETER WAVE SENSORS FOR SYNTHETIC VISION
Neal T. Alexander, Brian H. Hudson, and Jim D. Echard *In* NASA. Langley Research Center, Airborne Windshear Detection and Warning Systems. Fifth and Final Combined Manufacturers' and Technologists' Conference, Part 2 Jul. 1994 p 747-764 (For primary document see N95-13203 02-03)
Avail: CASI HC A03/MF A04

55 SPACE BIOLOGY

Includes exobiology; planetary biology; and extraterrestrial life.

N95-13026*# Georgia Inst. of Tech., Atlanta, GA. School of Electrical and Computer Engineering.
SEARCH FOR EXTRATERRESTRIAL INTELLIGENCE/HIGH RESOLUTION MICROWAVE SURVEY TEAM MEMBER Final Report, 1 Mar. 1991 - 31 Aug. 1994
Paul G. Steffes 1994 21 p
(Grant NAG2-700)
(NASA-CR-196478; NAS 1.26:196478) Avail: CASI HC A03/MF A01

This final report summarizes activities conducted during the three years of the NASA High Resolution Microwave Survey (HRMS). With primary interest in the Sky Survey activity, the principal investigator attended nine Working Group meetings and traveled independently to conduct experiments or present results at other meetings. The major activity involved evaluating the effects of spaceborne radio frequency interference (RFI) on both the SETI sky survey and targeted search. The development of a database of all unclassified earth or biting and deep space transmitters, along with accompanying search software, was a key accomplishment. The software provides information about potential sources of interference and gives complete information regarding the frequencies, positions and levels of interference generated by the spacecraft. A complete description of this search system (called HRS, or HRMS RFI Search) is provided. Other accomplishments include development of a 32,000 channel Fast-Fourier-Transform Spectrum analyzer for use in studies of interference from satellites and in a 1.4 mm SETI observational study. The latest revision of HRS has now been distributed to the extended radio astronomy and SETI community. Author (revised)

59 MATHEMATICAL AND COMPUTER SCIENCES (GENERAL)

N95-11914*# National Aeronautics and Space Administration. Lyndon B. Johnson Space Center, Houston, TX.
SOFTWARE ANALYSIS HANDBOOK: SOFTWARE COMPLEXITY ANALYSIS AND SOFTWARE RELIABILITY ESTIMATION AND PREDICTION
Alice T. Lee, Todd Gunn, Tuan Pham, and Ron Ricaldi Aug. 1994 96 p
(NASA-TM-104799; S-774; NAS 1.15:104799) Avail: CASI HC A05/MF A01

This handbook documents the three software analysis processes the Space Station Software Analysis team uses to assess space station software, including their backgrounds, theories, tools, and analysis procedures. Potential applications of these analysis results are also presented. The first section describes how software complexity analysis provides quantitative

information on code, such as code structure and risk areas, throughout the software life cycle. Software complexity analysis allows an analyst to understand the software structure, identify critical software components, assess risk areas within a software system, identify testing deficiencies, and recommend program improvements. Performing this type of analysis during the early design phases of software development can positively affect the process, and may prevent later, much larger, difficulties. The second section describes how software reliability estimation and prediction analysis, or software reliability, provides a quantitative means to measure the probability of failure-free operation of a computer program, and describes the two tools used by JSC to determine failure rates and design tradeoffs between reliability, costs, performance, and schedule. Author (revised)

N95-11932*# Institute for Computer Applications in Science and Engineering, Hampton, VA.
[RESEARCH IN PROGRESS IN APPLIED MATHEMATICS, NUMERICAL ANALYSIS, FLUID MECHANICS, AND COMPUTER SCIENCE] Final Semiannual Report, 1 Oct. 1993 - 31 Mar. 1994
Jun. 1994 77 p
(Contracts NAS1-19480; NAS1-18605; NAS1-18107; NAS1-17070; NAS1-17130; NAS1-15810; NAS1-16394; NAS1-14101; NAS1-14472; RTOP 505-90-52-01)
(NASA-CR-194942; NAS 1.26:194942) Avail: CASI HC A05/MF A01

This report summarizes research conducted at the Institute for Computer Applications in Science and Engineering in applied mathematics, fluid mechanics, and computer science during the period October 1, 1993 through March 31, 1994. The major categories of the current ICASE research program are: (1) applied and numerical mathematics, including numerical analysis and algorithm development; (2) theoretical and computational research in fluid mechanics in selected areas of interest to LaRC, including acoustics and combustion; (3) experimental research in transition and turbulence and aerodynamics involving LaRC facilities and scientists; and (4) computer science. Author (revised)

60 COMPUTER OPERATIONS AND HARDWARE

Includes hardware for computer graphics, firmware, and data processing.

For components see *33 Electronics and Electrical Engineering.*

N95-12413# Mitre Corp., Bedford, MA. C-3 Div.
EXPLOITATION OF VIRTUAL REALITY ARCHITECTURES Final Report
H. Veron, D. A. Southard, R. B. Mitchell, P. J. Hezel, and J. L. Segal
Jun. 1994 123 p
(Contract F19628-94-C-0001)
(AD-A282263; MTR93-B-0000191; RL-TR-94-79) Avail: CASI HC A06/MF A02

A computer interface technology known as virtual reality (VR) has received a great deal of attention because it provides a new paradigm for interfacing humans to computer-generated synthetic environments. VR is a natural outgrowth of several enabling technologies: workstations, computer graphics, visualization, displays, interactive devices, and software. The user can then directly manipulate simulated objects and leave behind the limitations of the physical world. The goal of this project was to examine VR for potential application in command, control, battle management, and situation awareness. Work focused on establishing and developing an optimized hardware and software architecture for a variety of applications. The purpose of this report is to provide a technical summary of MITRE's findings. The report begins with a user-interface device description and evaluation and a description of the software requirements for integrating these devices in a VR platform and the implications on the software architecture. The report then describes the Virtual Environment Architecture (VEA), the software architecture used to develop a real-time stand-alone interactive VR platform, including rationale, tradeoffs, performance issues, and use of a knowledge-base. Finally, the report describes a scenario developed for demonstrating the utility of the VR platform in a battle management prototype application. DTIC

N95-12516# Carnegie-Mellon Univ., Pittsburgh, PA. School of Computer Science.
ON-LINE DATA RECONSTRUCTION IN REDUNDANT DISK ARRAYS Ph.D. Thesis
Mark Holland May 1994 255 p
(Contract MDA972-90-C-0035)
(AD-A282709; CMU-CS-94-164) Avail: CASI HC A12/MF A03

There exists a wide variety of applications in which data availability must be continuous, that is, where the system is never taken off-line and any interruption in the accessibility of stored data causes significant disruption in the service provided by the application. Examples include on-line transaction processing systems such as airline reservation systems and automated teller networks in banking systems. In addition, there exist many applications for which a high degree of data availability is important, but continuous operation is not required. An example is a research and development environment, where access to a centrally-stored CAD system is often necessary to make progress on a design project. These applications and many others mandate both high performance and high availability from their storage subsystems. Redundant disk arrays are systems in which a high level of I/O performance is obtained by grouping together a large number of small disks, rather than building one large, expensive drive. The high component count of such systems leads to unacceptably high rates of data loss due to component failure, and so they typically incorporate redundancy to achieve fault tolerance. DTIC

N95-12524# Carnegie-Mellon Univ., Pittsburgh, PA. Dept. of Computer Science.
USING SECURE COPROCESSORS Ph.D. Thesis
Bennet Yee May 1994 97 p
(Contracts F19628-93-C-0193; F33615-90-C-1465)
(AD-A281255; CMU-CS-94-149) Avail: CASI HC A05/MF A02

How do we build distributed systems that are secure? Cryptographic techniques can be used to secure the communications between physically separated systems, but this is not enough: we must be able to guarantee the privacy of the cryptographic keys and the integrity of the cryptographic functions, in addition to the integrity of the security kernel and access control databases we have on the machines. Physical security is a central assumption upon which secure distributed systems are built; without this foundation even the best cryptosystem or the most secure kernel will crumble. In this thesis, the author addresses the distributed security problem by proposing the addition of a small, physically secure hardware module, a secure coprocessor, to standard workstations and PC's. The central axiom is that secure coprocessors are able to maintain the privacy of the data they process. This thesis attacks the distributed security problem from multiple sides. First, the author analyzes the security properties of existing system components, both at the hardware and software level. Second, the author demonstrates how physical security requirements may be isolated to the secure coprocessor, and shows how security properties may be bootstrapped using cryptographic techniques from this central nucleus of security within a combined hardware/software architecture. DTIC

N95-12826*# Institute for Computer Applications in Science and Engineering, Hampton, VA.
DESIGN CONSIDERATION FOR PARALLEL GRAPHICS LIBRARIES Final Report
Thomas W. Crockett Jun. 1994 24 p Presented at the 1994 Intel Supercomputer Users Group Conference Submitted for publication
(Contracts NAS1-18605; NAS1-19480; RTOP 505-90-52-01)
(NASA-CR-194935; NAS 1.26:194935; ICASE-94-49) Avail: CASI HC A03/MF A01

Applications which run on parallel supercomputers are often characterized by massive datasets. Converting these vast collections of numbers to visual form has proven to be a powerful aid to comprehensions. For a variety of reasons, it may be described to provide this visual feedback at runtime. One way to accomplish this is to exploit the available parallelism to perform graphics operations in place. In order to do this we need appropriate parallel rendering algorithms and library interfaces. This paper provides a tutorial introduction to some of the issues which arise in designing parallel graphics libraries and their underlying rendering algorithms. The focus is on polygon rendering for distributed memory message-passing systems. We illustrate our discussion with examples from PGL, a parallel

graphics library which has been developed on the Intel family of parallel systems. Author (revised)

N95-13436 Newcastle-upon-Tyne Univ., Newcastle (England). Dept. of Computing Science.
DELTA-4: AN OPEN ARCHITECTURE FOR DEPENDABLE SYSTEMS
P. A. Barrett and N. A. Speirs Jan. 1994 10 p
(PB94-195641; TRS-457) Copyright Avail: Issuing Activity (National Technical Information Service (NTIS))

The Delta-4 project, carried out within the framework of the European Strategic Program for Research in Information Technology (ESPRIT), has defined an open, fault-tolerant, distributed computing architecture for use in application areas such as computer-integrated manufacturing, process control and office automation. The Delta-4 approach to fault-tolerance is based upon the replication of software components on distinct host computers using a range of different replication strategies. The paper presents an overview of the Delta-4 architecture and of the facilities which it provides for supporting the requirements of real-time systems with respects to throughput and response. The problems of replica divergence are discussed, and a solution based on message selection and pre-emption synchronization messages is proposed. NTIS

N95-13557 DELAB, Trondheim (Norway).
NORWEGIAN CONTRIBUTION TO THE SWG ON APSE PROGRAMME Final Report
K. J. Wedde 31 Jan. 1994 57 p See also PB92-151356
(PB94-202397; STF40-A94027) Avail: Issuing Activity (National Technical Information Service (NTIS))

The Norwegian contribution to the Special Working Group (SWG) on Ada Programming Support Environments (APSE) was to develop the Symbolic Debugger (SDB). The report summarizes the major accomplishments and lessons learned throughout the project. The major accomplishments are: (1) A SDB has been developed and implemented on VAX/VMS and Sun3/SunOS host machines, able to debug programs on the host and on a MC68020 remote target; and (2) The demonstration of portability and transportability of Ada programs. The lessons learned are: (1) More emphasis should have been put on planning the project and establishing standards and routines; (2) Clear communication is required of the level of information and cooperation needed; and (3) The 'parallel development' approach is essential in successful development of large systems. NTIS

61 COMPUTER PROGRAMMING AND SOFTWARE

Includes computer programs, routines, alogorithms, and specific applications, e.g., CAD/CAM.

N95-11761*# Notre Dame Univ., IN. Image and Signal Analysis Lab.
IMPROVED IMAGE DECOMPRESSION FOR REDUCED TRANSFORM CODING ARTIFACTS
Thomas P. ORourke and Robert L. Stevenson 1994 10 p Presented at the 1994 SPIE and IS/T's Symposium on Electronic Imaging Science and Technology, San Jose, CA, Feb. 1994 Submitted for publication
(Grant NAG3-1549)
(NASA-CR-196805; NAS 1.26:196805) Avail: CASI HC A02/MF A01

The perceived quality of images reconstructed from low bit rate compression is severely degraded by the appearance of transform coding artifacts. This paper proposes a method for producing higher quality reconstructed images based on a stochastic model for the image data. Quantization (scalar or vector) partitions the transform coefficient space and maps all points in a partition cell to a representative reconstruction point, usually taken as the centroid of the cell. The proposed image estimation technique selects the reconstruction point within the quantization partition cell which results in a reconstructed image which best fits a non-Gaussian Markov random field (MRF) image model. This approach results in a convex constrained optimization problem which can be solved iteratively. At each iteration, the gradient projection method is used to update the estimate based on the image model. In the transform domain, the resulting coefficient reconstruction points are projected to the particular quantization partition cells defined by the compressed image. Experimental results will be shown for images compressed using scalar quantization of block DCT and using vector quantization of subband wavelet transform. The proposed image decompression provides a reconstructed image with reduced visibility of transform coding artifacts and superior perceived quality. Author

N95-11762*# Notre Dame Univ., IN. Image and Signal Analysis Lab.
VECTOR QUANTIZATION FOR EFFICIENT CODING OF UPPER SUBBANDS
W. J. Zeng (Princeton Univ., NJ.) and Y. F. Huang [1994] 27 p
(Grant NAG3-1549)
(NASA-CR-196804; NAS 1.26:196804) Avail: CASI HC A03/MF A01

This paper examines the application of vector quantization (VQ) to exploit both intra-band and inter-band redundancy in subband coding. The focus here is on the exploitation of inter-band dependency. It is shown that VQ is particularly suitable and effective for coding the upper subbands. Three subband decomposition-based VQ coding schemes are proposed here to exploit the inter-band dependency by making full use of the extra flexibility of VQ approach over scalar quantization. A quadtree-based variable rate VQ (VRVQ) scheme which takes full advantage of the intra-band and inter-band redundancy is first proposed. Then, a more easily implementable alternative based on an efficient block-based edge estimation technique is employed to overcome the implementational barriers of the first scheme. Finally, a predictive VQ scheme formulated in the context of finite state VQ is proposed to further exploit the dependency among different subbands. A VRVQ scheme proposed elsewhere is extended to provide an efficient bit allocation procedure. Simulation results show that these three hybrid techniques have advantages, in terms of peak signal-to-noise ratio (PSNR) and complexity, over other existing subband-VQ approaches.
Author (revised)

N95-11763*# Notre Dame Univ., IN. Dept. of Electrical Engineering.
ACHIEVING UNEQUAL ERROR PROTECTION WITH CONVOLUTIONAL CODES
D. G. Mills, D. J. Costello, Jr., and R. Palazzo, Jr. Aug. 1994 21 p Presented at the IEEE Transactions on Information Theory Conference
(Grants NAG5-557; NAG3-1549; NSF EID-90-17558; FAPESP-94/4845-7)
(NASA-CR-196803; NAS 1.26:196803) Avail: CASI HC A03/MF A01

This paper examines the unequal error protection capabilities of convolutional codes. Both time-invariant and periodically time-varying convolutional encoders are examined. The effective free distance vector is defined and is shown to be useful in determining the unequal error protection (UEP) capabilities of convolutional codes. A modified transfer function is used to determine an upper bound on the bit error probabilities for individual input bit positions in a convolutional encoder. The bound is heavily dependent on the individual effective free distance of the input bit position. A bound relating two individual effective free distances is presented. The bound is a useful tool in determining the maximum possible disparity in individual effective free distances of encoders of specified rate and memory distribution. The unequal error protection capabilities of convolutional encoders of several rates and memory distributions are determined and discussed. Author

N95-11764*# Notre Dame Univ., IN. Dept. of Electrical Engineering.
[AN EFFICIENT SYSTEM FOR RELIABLY TRANSMITTING IMAGE AND VIDEO DATA OVER LOW BIT RATE NOISY CHANNELS] Interim Report
Daniel J. Costello, Jr., Y. F. Huang, and Robert L. Stevenson 1 Sep. 1994 12 p
(Grant NAG3-1549)
(NASA-CR-196802; NAS 1.26:196802) Avail: CASI HC A03/MF A01

This research project is intended to develop an efficient system for reliably transmitting image and video data over low bit rate noisy channels. The basic ideas behind the proposed approach are the following: employ statistical-based image modeling to facilitate pre- and post-processing and error detection, use spare redundancy that the source compression did not remove to add robustness, and implement coded modulation to improve bandwidth efficiency and noise rejection. Over the last six months, progress has been made on various aspects of the project. Through our studies of the integrated system, a list-based iterative Trellis decoder has been developed. The decoder accepts feedback from a post-processor which

can detect channel errors in the reconstructed image. The error detection is based on the Huber Markov random field image model for the compressed image. The compression scheme used here is that of JPEG (Joint Photographic Experts Group). Experiments were performed and the results are quite encouraging. The principal ideas here are extendable to other compression techniques. In addition, research was also performed on unequal error protection channel coding, subband vector quantization as a means of source coding, and post processing for reducing coding artifacts. Our studies on unequal error protection (UEP) coding for image transmission focused on examining the properties of the UEP capabilities of convolutional codes. The investigation of subband vector quantization employed a wavelet transform with special emphasis on exploiting interband redundancy. The outcome of this investigation included the development of three algorithms for subband vector quantization. The reduction of transform coding artifacts was studied with the aid of a non-Gaussian Markov random field model. This results in improved image decompression. These studies are summarized and the technical papers included in the appendices.

Derived from text

N95-11843 Institute of Electrical and Electronics Engineers, New York, NY.

PROCEEDINGS: THE ELEVENTH IEEE WORKSHOP ON REAL-TIME OPERATING SYSTEMS AND SOFTWARE

19 May 1994 125 p Workshop held in Seattle, WA, 18-19 May 1994 Limited Reproducibility: More than 20% of this document may be affected by microfiche quality

(AD-A281738) Avail: CASI HC A06

The Institute of Electrical and Electronic Engineers (IEEE) Workshop on Real-Time Operating Systems and Software is a forum that covers recent advances in real-time computing, a field that is becoming an essential part of computer science and engineering. It brings together practitioners and researchers from academia, industry, and government, to explore the best current ideas on real-time software and operating systems, and to evaluate the maturity and directions of real-time system technology. As the demand for the functionalities and reliabilities of real-time systems continue to grow, our intellectual and engineering abilities are being challenged to come up with practical solutions to the problems faced in design and development of complex real-time systems.

DTIC

N95-11918*# NYMA, Inc., Brook Park, OH.

A MODEL-BASED EXPERT SYSTEM FOR SPACE POWER DISTRIBUTION DIAGNOSTICS Final Report

Todd M. Quinn and Richard F. Schlegelmilch Sep. 1994 23 p

(Contract NAS3-27186; RTOP 233-03-04)

(NASA-CR-195336; E-8879; NAS 1.26:195336) Avail: CASI HC A03/MF A01

When engineers diagnose system failures, they often use models to confirm system operation. This concept has produced a class of advanced expert systems that perform model-based diagnosis. A model-based diagnostic expert system for the Space Station Freedom electrical power distribution test bed is currently being developed at the NASA Lewis Research Center. The objective of this expert system is to autonomously detect and isolate electrical fault conditions. Marple, a software package developed at TRW, provides a model-based environment utilizing constraint suspension. Originally, constraint suspension techniques were developed for digital systems. However, Marple provides the mechanisms for applying this approach to analog systems such as the test bed, as well. The expert system was developed using Marple and Lucid Common Lisp running on a Sun Sparc-2 workstation. The Marple modeling environment has proved to be a useful tool for investigating the various aspects of model-based diagnostics. This report describes work completed to date and lessons learned while employing model-based diagnostics using constraint suspension within an analog system.

Author

N95-11923*# National Aeronautics and Space Administration. Marshall Space Flight Center, Huntsville, AL.

DEVELOPMENT OF HOMOTOPY ALGORITHMS FOR FIXED-ORDER MIXED H2/H(INFINITY) CONTROLLER SYNTHESIS

M. Whorton, H. Buschek, and A. J. Calise Washington Sep. 1994 29 p

(NASA-TP-3507; M-759; NAS 1.60:3507) Avail: CASI HC A03/MF A01

A major difficulty associated with H-infinity and mu-synthesis methods is the order of the resulting compensator. Whereas model and/or controller reduction techniques are sometimes applied, performance and robustness properties are not preserved. By directly constraining compensator order during the optimization process, these properties are better preserved, albeit at the expense of computational complexity. This paper presents a novel homotopy algorithm to synthesize fixed-order mixed H2/H-infinity compensators. Numerical results are presented for a four-disk flexible structure to evaluate the efficiency of the algorithm.

Author

N95-11941 East Tennessee State Univ., Johnson City, TN. Dept. of Computer and Information Sciences.

REAL WORLD SOFTWARE ENGINEERING Final Report, 28 Sep. 1992 - 31 May 1994

Donald Gotterbarn, Robert Riser, and Suzanne Smith 15 Jul. 1994 1002 p Limited Reproducibility: More than 20% of this document may be affected by microfiche quality

(Contract DAAL03-92-G-0411)

(AD-A282365; ARO-30996.4-MA) Avail: Issuing Activity (Defense Technical Information Center (DTIC))

Based on our experience teaching software engineering, we at East Tennessee State University are convinced that a one-semester software engineering course cannot adequately cover all aspects of the software development process and still provide students with meaningful project experience. Current software engineering course models emphasize either the product or the process. These models rarely finish a realistic product or do so by marginal treatment of significant aspects of the life cycle. For example, while concentrating on implementation details, topics such as detailed design reviews, configuration management, and maintenance are minimized. To address this problem, East Tennessee State University is expanding and changing its undergraduate curriculum in software engineering. Integral to this effort, we are incorporating into the undergraduate curriculum lessons learned while developing and teaching software engineering courses at the graduate level. This proposal was to develop a two-semester undergraduate course which presents real-world software engineering. The course provides a thorough coverage of the software development process with realistic project experience. The course is designed to present software engineering in a layered approach where interrelated topics are presented repeatedly in increasing depth. Furthermore, the relationship of software engineering principles to software development is emphasized by the careful coordination of project and lecture stages.

DTIC

N95-12005*# Institute for Computer Applications in Science and Engineering, Hampton, VA.

ON BOTTLENECK PARTITIONING k-ARY n-CUBES Final Report

David M. Nicol (College of William and Mary, Williamsburg, VA.) and Weizhen Mao (College of William and Mary, Williamsburg, VA.) Hampton, VA NASA Aug. 1994 12 p Submitted for publication

(Contract NAS1-19480; RTOP 505-90-52-01)

(NASA-CR-194966; NAS 1.26:194966; ICASE-94-72) Avail: CASI HC A03/MF A01

Graph partitioning is a topic of extensive interest, with applications to parallel processing. In this context graph nodes typically represent computation, and edges represent communication. One seeks to distribute the workload by partitioning the graph so that every processor has approximately the same workload, and the communication cost (measured as a function of edges exposed by the partition) is minimized. Measures of partition quality vary; in this paper we consider a processor's cost to be the sum of its computation and communication costs, and consider the cost of a partition to be the bottleneck, or maximal processor cost induced by the partition. For a general graph the problem of finding an optimal partitioning is intractable. In this paper we restrict our attention to the class of k-art n-cube graphs with uniformly weighted nodes. Given mild restrictions on the node weight and number of processors, we identify partitions yielding the smallest bottleneck. We also demonstrate by example that some restrictions are necessary for the partitions we identify to be optimal. In particular, there exist cases where partitions that evenly partition nodes need not be optimal.

Author

N95-12014*# Alabama Univ., Huntsville, AL. Dept. of Electrical and Computer Engineering.

ADVANCED COMPUTER ARCHITECTURE SPECIFICATION FOR AUTOMATED WELD SYSTEMS Final Report, 14 Jul. 1993 - 26 May 1994

Constantine Katsinis Jun. 1994 18 p

(Contract NAS8-38609)

(NASA-CR-194006; NAS 1.26:194006) Avail: CASI HC A03/MF A01

This report describes the requirements for an advanced automated weld system and the associated computer architecture, and defines the overall system specification from a broad perspective. According to the requirements of welding procedures as they relate to an integrated multiaxis motion control and sensor architecture, the computer system requirements are developed based on a proven multiple-processor architecture with an expandable, distributed-memory, single global bus architecture, containing individual processors which are assigned to specific tasks that support sensor or control processes. The specified architecture is sufficiently flexible to integrate previously developed equipment, be upgradable and allow on-site modifications. Author

N95-12300# Instituto de Pesquisas Espaciais, Sao Jose dos Campos (Brazil).

AN EXPERIMENTAL ENVIRONMENT FOR SOFTWARE ENGINEERING M.S. Thesis [UM AMBIENTE EXPERIMENTAL PARA A ENGENHARIA DE SOFTWARE]

Nilson Santanna Aug. 1993 181 p In PORTUGESE

(INPE-5540-TDI/528) Avail: CASI HC A09/MF A02

Software systems are becoming increasingly useful in a great variety of knowledge areas. Software Engineering, following this trend, has become an area with a large quantity of emerging methodologies, models and tools (known by the general name of Software Engineering Techniques) covering the entire software life cycle. These techniques will keep being proposed and so it is necessary to know them all well. This paper presents an experimental environment (Experimental Environment for Software Engineering - AEES) that has been developed in order to obtain data from controlled experiments which use Software Engineering Techniques. The results obtained through the analysis of these data will increase the knowledge about these techniques and their use. Integrating AEES with a software development environment allows for the application of experimental results to projects, achieving higher levels of quality and productivity. Author

N95-12366# Helsinki Univ. of Technology, Espoo (Finland). Digital Systems Lab.

EFFICIENT DETECTION OF DEADLOCKS IN PETRI NETS

K. Varpaaniemi Oct. 1993 63 p

(PB94-179405; ISBN-951-22-1775-9) Avail: CASI HC A04/MF A01

Reachability analysis is a powerful formal method for analysis of concurrent and distributed finite state systems. It suffers from the state space explosion problem, however: the state space of a system can be far too large to be completely generated. The report considers two promising methods, Valmari's stubborn set method and Godefroid's sleep set method, to avoid generating all of the state space when searching for undesirable reachable terminal states, also called deadlocks. Petri nets are a widely used model for concurrent and distributed systems. This report shows that the stubborn set method and the sleep set method can be combined without any of the assumptions previously placed on the stubborn sets as far as the detection of reachable terminal states in place/transition nets, a class of Petri nets, is concerned. This report emphasizes the value of dynamically stubborn sets as a useful generalization of stubborn sets and shows some results that improve the understanding of the stubborn set method. NTIS

N95-12497# Carnegie-Mellon Univ., Pittsburgh, PA. School of Computer Science.

B* PROBABILITY BASED SEARCH

Hans J. Berliner and Chris McConnell 27 Jun. 1994 74 p

(Grant NSF IRI-91-05202)

(AD-A282551; CMU-CS-94-168) Avail: CASI HC A04/MF A01

We describe a search algorithm for two-player games that relies on selectivity rather than brute-force to achieve success. The key ideas behind the algorithm are: (1) stopping when one alternative is clearly better than all the others; and (2) focusing the search on the place where the most progress can likely be made toward being able to stop. Critical to this process is identifying uncertainty about the ultimate value of any move. The lower bound on uncertainty is the best estimate of the real value of a move, while the upper bound is its optimistic value, based on some measure of unexplored potential. Uncertainty is represented as probability densities. The search develops those parts of the tree where moving existing bounds would be most likely to succeed and make the most progress toward terminating the search. Termination is achieved when the established real value of the best move is so good that the likelihood of this being achieved by any other alternative is minimal. DTIC

N95-12500 Aerospace Medical Research Labs., Brooks AFB, TX. Human Resources Directorate.

GUIDED APPROACH TO INSTRUCTIONAL DESIGN ADVISING (GAIDA): HOW TO CREATE GAIDA COMPATIBLE LESSONS, VOLUME 2 Interim Report, Aug. 1993 - Apr. 1994

Larry K. Whitehead May 1994 29 p Limited Reproducibility: More than 20% of this document may be affected by microfiche quality

(AF Proj. 1121)

(AD-A282645; AL/HR-TP-1994-0013-Vol-2) Avail: CASI HC A03

The Guided Approach to Instructional Design Advising (GAIDA) software is based on the idea that a novice can produce effective computer-based instruction by following appropriate guidance given through a computer-base.. system. This paper (volume 2 of 2) describes how to generate computer-based lessons that will be compatible with the GAIDA software. DTIC

N95-12504 Carnegie-Mellon Univ., Pittsburgh, PA. Dept. of Computer Science.

PERFORMANCE MEASUREMENTS OF THE MULTIMEDIA TESTBED ON REAL-TIME MACH

Roger B. Dannenberg, David B. Anderson, Tom Neuendorffer, and Dean Rubine Apr. 1994 20 p Limited Reproducibility: More than 20% of this document may be affected by microfiche quality

(AD-A282658; CMU-CS-94-141) Avail: Issuing Activity (Defense Technical Information Center (DTIC))

Multimedia has generated widespread interest in real-time support within general purpose operating systems. Multimedia also places new demands on operating systems for interprocess communication. The Multimedia Testbed is a set of applications that stress consistent low-latency response and efficient interprocess communication for large blocks of data. The Multimedia Testbed was ported to Real-Time Mach in the hopes of providing predictable low-latency response and, consequently, good synchronization and low jitter as required for multimedia applications. Our work compares the performance of Real-Time Mach with that of Mach 3.0. Although the fixed-priority scheduling, of Real-Time Mach is a substantial improvement, user threads are still preempted by device drivers, and the overall real-time performance is not suitable for multimedia applications. We discuss areas where Real-Time Mach needs improvement. DTIC

N95-12541# Carnegie-Mellon Univ., Pittsburgh, PA. School of Computer Science.

A PRACTICAL APPROACH TO DRAWING UNDIRECTED GRAPHS

Daniel Tunkelang Jun. 1994 29 p

(AD-A282641; CMU-CS-94-161) Avail: CASI HC A03/MF A01

Although there is extensive research on drawing graphs, none of the published methods are satisfactory for drawing general undirected graphs. Generating drawings which are optimal with respect to several aesthetic criteria is known to be NP-hard, so all published approaches to the problem have used heuristics. These heuristics are too slow to be practical for graphs of moderate size, and they do not produce consistently good drawings for general graphs. Moreover, they rely on general optimization methods, because problem-specific methods require a deeper theoretical understanding of the graph drawing problem. This paper presents an algorithm to generate two-dimensional drawings of undirected graphs. The algorithm uses a combination of heuristics to obtain drawings which are near-optimal with respect to an aesthetic cost function. The algorithm is incremental in nature, but preprocesses the graph to determine an order for node placement. The algorithm uses a local optimization strategy that effectively manages the trade-off between speed and output quality. Finally, the algorithm uses a variety of techniques to speed up computation of the

aesthetic cost function. The paper discusses this algorithm in the context of previous work and open problems. The algorithm is compared with the force-directed algorithm of Fruchterman and Reingold and the simulated annealing algorithm of Davidson and Harel in terms of output quality. Finally, the paper considers what work is necessary to create a truly effective algorithm for drawing undirected graphs. DTIC

N95-12588# Rhode Island Univ., Kingston, RI.
ACTIVE NODAL TASK SEEKING FOR HIGH-PERFORMANCE, ULTRA-DEPENDABLE COMPUTING Semiannual Report, 15 Jan. - 15 Jul. 1994
Jien-Chung Lo, Donald W. Tufts, and James W. Cooley Jul. 1994 29 p
(Contract N00014-94-1-0479; NSF MIP-93-08085)
(AD-A282924) Avail: CASI HC A03/MF A01

The Active Nodal Task Seeking (ANTS) approach to the design of multicomputer systems is named for its basic component: an Active Nodal Task-Seeker (ANT). In this system, there is no load balancing or load sharing, instead, each ANT computing node is actively finding out how it can contribute to the execution of the needed tasks. A run-time partition is established such that some of the ANT computing nodes are under exhaustive diagnosis at any given time. An ANTS multicomputer system can achieve a mean time to failure of more than 20 years with just 8 computing nodes and 3 buses, while the minimum requirements are 3 computing nodes and 1 bus, and with a worst case computing node failure rate of 5 x 0.0001 per hour. This work has been motivated by the need to develop high-performance multicomputer systems for radar, active and passive sonar, and electronic warfare that can provide ultra-dependable performance for more than 20 years without field repairs. We argue that high performance is also an attribute of an ANTS computing system, because the overhead of dynamic task scheduling is reduced and because efficient use is made of the available processing resources. DTIC

N95-12774# Technische Univ., Delft (Netherlands).
EXPERIMENTS WITH FORMAL METHODS IN SOFTWARE ENGINEERING Ph.D. Thesis
N. Plat 21 Sep. 1993 232 p See also PB90-211632 and PB92-104926
(PB94-192416; ISBN-90-9006392-7) Copyright Avail: CASI HC A11/MF A03

The industrial take-up of formal methods for software development has, so far, been rather slow. The thesis addresses the reasons for this phenomenon through a number of experiments, each involving the formal method Vienna Development Method (VDM), and its specification language: VDM-SL. The issue of standardization and tool support is discussed. The application of VDM in the framework of a widely used standard for software development is analyzed: DoD-STD-2167A. The relationship between formal methods and the commonly used 'structured' methods for software development is analyzed through examining mappings from data flow diagrams to VDM specifications, and through the construction of a prototype combined structured/formal method, called SVDM, based on one such mapping. SVDM is further illustrated through a case study in which a simple lift system is developed. The research in this thesis shows that the industrial take-up of formal methods can best be pursued through a gradual introduction of formal methods in software processes. NTIS

N95-12796*# Aerojet-General Corp., Azusa, CA. Electronic Systems Plant.
EARTH OBSERVING SYSTEM (EOS)/ADVANCED MICROWAVE SOUNDING UNIT-A (AMSU-A) Monthly Report No. 20, 1-31 Aug. 1994
Sep. 1994 119 p
(Contract NAS5-32314; RTOP 422-00-00)
(NASA-CR-189379; Rept-10300-12; NAS 1.26:189379; CDRL-529) Avail: CASI HC A06/MF A02

This is the twentieth monthly report for the Earth Observing System/Advanced Microwave Sounding Unit-A (EOS/AMSU-A), Contract NAS5-32314, and covers the period from 1 August 1994 through 31 August 1994. This period is the eighth month of the Implementation Phase which provides for the design, fabrication, assembly, and test of the first EOS/AMSU-A, the Protoflight Model. During this period the number one priority for the program continued to be the issuance of Requests for Quotations (RFQ) to suppliers and the procurement of the long-lead receiver components. Significant effort was also dedicated to preparation and conduct of internal design reviews and preparation for the PDR scheduled in September. An overview of the program status, including key events, action items, and documentation submittals, is provided in Section 2 of this report. The Program Manager's 'Priority Issues' are defined in Section 3. Section 4 through 7 provide detailed progress reports for the system engineering effort, each subsystem, performance assurance, and configuration/data management. Contractual matters are discussed in Section 8.
Derived from text

N95-12893# Oak Ridge National Lab., TN.
PARALLEL ALGORITHMS FOR THE SPECTRAL TRANSFORM METHOD
I. T. Foster (Argonne National Lab., IL.) and P. H. Worley Apr. 1994 46 p
(Contract DE-AC05-84OR-21400)
(DE94-015458; ORNL/TM-12507) Avail: CASI HC A03/MF A01

The spectral transform method is a standard numerical technique for solving partial differential equations on a sphere and is widely used in atmospheric circulation models. Recent research has identified several promising algorithms for implementing this method on massively parallel computers; however, no detailed comparison of the different algorithms has previously been attempted. In this paper, we describe these different parallel algorithms and report on computational experiments that we have conducted to evaluate their efficiency on parallel computers. The experiments used a testbed code that solves the nonlinear shallow water equations or a sphere; considerable care was taken to ensure that the experiments provide a fair comparison of the different algorithms and that the results are relevant to global models. We focus on hypercube- and mesh-connected multicomputers with cut-through routing, such as the Intel iPSC/860, DELTA, and Paragon, and the nCUBE/2, but also indicate how the results extend to other parallel computer architectures. The results of this study are relevant not only to the spectral transform method but also to multidimensional FFTs and other parallel transforms. DOE

N95-12922 Carnegie-Mellon Univ., Pittsburgh, PA. Software Engineering Inst.
SECOND DEPENDABLE SOFTWARE TECHNOLOGY EXCHANGE
Jun. 1994 39 p Limited Reproducibility: More than 20% of this document may be affected by microfiche quality
(Contract F19628-90-C-0003)
(AD-A283367; CMU/SEI-94-SR-06) Avail: Issuing Activity (Defense Technical Information Center (DTIC))

On March 24 and 25, 1994, the Open Attribute Engineering Project hosted the Second Dependable Software Technology Exchange. The exchange, sponsored by the Air Force Phillips Laboratories, the Office of Naval Research, and the Air Force Space and Missile Systems Center, brought together researchers and system developers, providing an opportunity for the researchers to learn the needs of the developers and for the developers to learn about techniques being investigated by the researchers. This report summarizes what transpired at the meeting.
DTIC

N95-13051 Institute for Defense Analyses, Alexandria, VA.
AN EXAMINATION OF SELECTED SOFTWARE TESTING TOOLS: 1993 SUPPLEMENT Final Report
Christine Youngblut and Bill Brykczynski Oct. 1993 196 p See also AD-A261941 Limited Reproducibility: More than 20% of this document may be affected by microfiche quality
(Contract MDA903-89-C-0003)
(AD-A283060; IDA-P-2925; IDA/HQ-93-044715; AD-E501812) Avail: CASI HC A09

This paper reports on the examination of eight additional tools for testing Ada code. It is a supplement to IDA Paper P-2769, An Examination of Selected Software Testing Tools: 1992, which reported on 27 tools that provide for test management, problem reporting, and static and dynamic analysis of Ada code. The tool discussions provide software development managers with information that will help them gain an understanding of the current capabilities of tools that are commercially available, the functionality of these tools, and how they can aid the development and support of Ada software. The newly examined tools provide static and dynamic analysis capabilities. They were applied to sample Ada programs in order to assess their functionality. Each tool was then described in terms of its functionality, ease of use, and documentation and support.

Problems encountered during the examination and other pertinent observations were also recorded. Available testing tools offer important opportunities for increasing software quality and reducing development and support costs. The wide variety of functionality provided by tools in the same category, however, and, in some cases, lack of tool maturity, require careful tool selection on behalf of a potential user. DTIC

N95-13077# Oak Ridge National Lab., TN.
COMPUTER-AIDED DESIGN-VERIFICATION VECTOR GENERATION
C. E. Stroud (Kentucky Univ., Lexington, KY.) and M. N. Ericson 1994 5 p Presented at the 7th Annual IEEE International Application Specific Integrated Circuit Conference and Exhibit, Rochester, NY, 19-23 Sep. 1994
(Contract DE-AC05-84OR-21400)
(DE94-014022; CONF-9409161-1) Avail: CASI HC A01/MF A01

This paper describes the features and usage of a CAD tool that assists ASIC designers in the generation of design-verification vectors. The designer describes the ASIC interfaces as well as the desired operations to be performed in an assembly language type format from which the CAD tool generates the actual input stimulus and timing relationships for the design verification simulation. DOE

N95-13157# California Univ., Berkeley. Lawrence Berkeley Lab, CA.
ADVANCES IN SPARK
F. Buhl, E. Erdem, J. M. Nataf, F. Winkelmann, M. A. Moshier, and E. F. Sowell Mar. 1994 43 p Presented at the 3rd International Conference on System Simulation in Buildings, Liege, Belgium, 3-5 Dec. 1990 Revised
(Contract DE-AC03-76SF-00098)
(DE94-014935; LBL-29419-Rev-1; CONF-901295-2-Rev-1) Avail: CASI HC A03/MF A01

The Simulation Problem Analysis and Research Kernel (SPARK), formerly SPANK, was originally described in a paper presented at the Second International Conference on System Simulation in Buildings in 1986. Since that time, it has undergone several enhancements and has been integrated into a larger software system for building energy analysis. Among the enhancements is the capability to simulate dynamic problems. Also, symbolic manipulation techniques are now used to generate objects and macro objects from equations expressed as text. Currently underway is the development of a graphical user interface. Newer developments include a reevaluation of the semantics of dynamic problem definition, which will ultimately result in much greater generality in user specification of numerical methods. This paper reports on these developments and indicates directions for future SPARK development. DOE

N95-13198*# National Aeronautics and Space Administration. Langley Research Center, Hampton, VA.
WORLD WIDE WEB IMPLEMENTATION OF THE LANGLEY TECHNICAL REPORT SERVER
Michael L. Nelson, Gretchen L. Gottlich, and David J. Bianco Sep. 1994 32 p
(RTOP 505-90-53-02)
(NASA-TM-109162; NAS 1.15:109162) Avail: CASI HC A03/MF A01

On January 14, 1993, NASA Langley Research Center (LaRC) made approximately 130 formal, 'unclassified, unlimited' technical reports available via the anonymous FTP Langley Technical Report Server (LTRS). LaRC was the first organization to provide a significant number of aerospace technical reports for open electronic dissemination. LTRS has been successful in its first 18 months of operation, with over 11,000 reports distributed and has helped lay the foundation for electronic document distribution for NASA. The availability of World Wide Web (WWW) technology has revolutionized the Internet-based information community. This paper describes the transition of LTRS from a centralized FTP site to a distributed data model using the WWW, and suggests how the general model for LTRS can be applied to other similar systems. Author

N95-13339# Columbia Univ., New York, NY.
ALGORITHMS FOR MATHEMATICAL PROGRAMMING
D. Goldfarb 1994 15 p
(Contract DE-FG02-92ER-25126)
(DE94-013544; DOE/ER-25126/1) Avail: CASI HC A03/MF A01

The objective is development, analysis, and implementation of algorithms for solving mathematical programming problems. Focus is on simplex algorithms, interior point algorithms, and algorithms that combine interior point and multiplier penalty approaches. DOE

N95-13370# Pennsylvania State Univ., University Park, PA. Applied Research Lab.
WEIGHTED PARZEN WINDOWS FOR PATTERN CLASSIFICATION
G. A. Babich and L. H. Sibul May 1994 73 p
(Contract N00014-90-J-1365)
(AD-A281222; PSU/ARL-TR-94-10) Avail: CASI HC A04/MF A01

This thesis presents a novel pattern recognition approach, named Weighted Parzen Windows (WPW). This technique uses a nonparametric supervised learning algorithm to estimate the underlying density function for each set of training data. Classification is accomplished by using the estimated density functions in a minimum risk strategy. The proposed approach reduces the effective size of the training data without introducing significant classification error. Furthermore, it is shown that Bayes-Gaussian, minimum Euclidean-distance, Parzen-window, and nearest-neighbor classifiers can be viewed as special cases of the WPW technique. Experimental results are presented to demonstrate the performance of the WPW algorithm as compared to traditional classifiers. DTIC

N95-13420*# Institute for Computer Applications in Science and Engineering, Hampton, VA.
ADAPTIVE RELAXATION FOR THE STEADY-STATE ANALYSIS OF MARKOV CHAINS Final Report
Graham Horton (Erlangen-Nuremberg Univ., Germany.) Jun. 1994 15 p Presented at the Numerical Solutions of Markov Chains Conference Submitted for publication
(Contract NAS1-19480; RTOP 505-90-52-01)
(NASA-CR-194944; NAS 1.26:194944; ICASE-94-55) Avail: CASI HC A03/MF A01

We consider a variant of the well-known Gauss-Seidel method for the solution of Markov chains in steady state. Whereas the standard algorithm visits each state exactly once per iteration in a predetermined order, the alternative approach uses a dynamic strategy. A set of states to be visited is maintained which can grow and shrink as the computation progresses. In this manner, we hope to concentrate the computational work in those areas of the chain in which maximum improvement in the solution can be achieved. We consider the adaptive approach both as a solver in its own right and as a relaxation method within the multi-level algorithm. Experimental results show significant computational savings in both cases. Author

N95-13432 Newcastle-upon-Tyne Univ., Newcastle (England). Dept. of Computing Science.
RECOVERY BLOCKS
B. Randell and J. Xu Apr. 1994 26 p See also PB94-148806 and PB94-148830
(PB94-205077; TRS-479) Copyright Avail: Issuing Activity (National Technical Information Service (NTIS))

This chapter reviews the development of the recovery block approach to software fault tolerance and subsequent work based on this approach. It starts with an account of the development and implementations of the basic recovery block scheme in the early 1970s at Newcastle, and then goes on to describe work at Newcastle and elsewhere on extensions to the basic scheme, recovery in concurrent systems, and linguistic support for recovery blocks based on the use of object-oriented programming concepts. NTIS

N95-13438 Newcastle-upon-Tyne Univ., Newcastle (England). Dept. of Computing Science.
SOME VERY COMPOSITIONAL TEMPORAL PROPERTIES
B. Moszkowski Dec. 1993 26 p
(PB94-195666; TRS-466) Copyright Avail: Issuing Activity (National Technical Information Service (NTIS))

A logic for reasoning about sequential and parallel behavior must support some form of compositionality. That is, much of the proof of a system should be decomposible into proofs of its parts. The authors discuss some important and easily described classes of properties which are readily imported and exported between temporal scopes. The authors call such properties very compositional since they support a methodology of specification and proof which is especially modular and reusable. Their

presentation uses Interval Temporal Logic (ITL) as the notation in which all behavior is described and proved. They give a powerful and elegant ITL proof system. It has been used by them to rigorously prove hundreds of theorems and derived inference rules, including a number for parallel systems involving message-passing, timing constraints and shared write-access. They believe that very compositional properties will be of interest to anyone involved with the specification and verification of computer systems. NTIS

N95-13571 DELAB, Trondheim (Norway).
SURRENDER USER'S MANUAL, SECOND EDITION
M. Granhaug 13 Dec. 1993 162 p See also LA-4796 and PB92-203298
(PB94-206950; STF40-A93169) Avail: Issuing Activity (National Technical Information Service (NTIS))

This report describes a Fortran and C subroutine package for rendering bivariate surfaces (z = f(x,y)) as 3D perspective plots with hidden lines removed or as contour maps. Line drawing and/or polygon filling may be used to present both kinds of plots. The package in addition contains routines for viewing selection and for adding 3D axes and other annotation. GPGS-F is used for all basic graphic functions, thus the package is machine and device independent. The report is aimed at application programmers with some programming experience. NTIS

62 COMPUTER SYSTEMS

Includes computer networks and special application computer systems.

N95-11734# Oak Ridge National Lab., TN.
IMPACT ANALYSIS ON A MASSIVELY PARALLEL COMPUTER
T. Zacharia and G. A. Aramayo 1994 5 p Presented at the DOE Defense Programs Packaging Workshop, Knoxville, TN, 16-19 May 1994
(Contract DE-AC05-84OR-21400)
(DE94-013624; CONF-9405109-9) Avail: CASI HC A01/MF A01

Advanced mathematical techniques and computer simulation play a major role in evaluating and enhancing the design of beverage cans, industrial, and transportation containers for improved performance. Numerical models are used to evaluate the impact requirements of containers used by the Department of Energy (DOE) for transporting radioactive materials. Many of these models are highly compute-intensive. An analysis may require several hours of computational time on current supercomputers despite the simplicity of the models being studied. As computer simulations and materials databases grow in complexity, massively parallel computers have become important tools. Massively parallel computational research at the Oak Ridge National Laboratory (ORNL) and its application to the impact analysis of shipping containers is briefly described in this paper. DOE

N95-11838# Helsinki Univ. of Technology, Espoo (Finland). Lab. of Signal Processing and Computer Technology.
DESIGN OF SYSTOLIC ALGORITHMS AND ARCHITECTURES FOR DIGITAL SIGNAL PROCESSING Ph.D. Thesis
W. Ling 17 Dec. 1993 86 p
(PB94-179256; ISBN-951-22-1855-0) Avail: CASI HC A05/MF A01

In this thesis, the design methods of systolic algorithms and architectures are studied. Several systolic algorithms and systolic architectures have been developed for implementations of different transformations, the least squares problem, and the circular convolution. A new systolic algorithm based on the even-odd decomposition method is first proposed. The algorithm provides an efficient way to reduce the array size of the discrete Fourier transform and the discrete Hartley transform. Using this algorithm, several important systolic architectures are derived, where the sizes of the arrays are only one fourth or one sixteenth of the original size. Next, two systolic architectures for the least squares problem are introduced. The algorithms and their mapping to the implementation are studied and each is shown to have some advantages over existing architectures. One of them is derived using the orthogonal-inverse updating algorithm. By this means, the resulting architecture is decreased from two triangular systolic arrays to only one. Finally, an algorithm for performing the circular convolution is proposed based on the Chinese remainder theorem. NTIS

N95-11857# Rochester Univ., NY. Dept. of Computer Science.
EAGER COMBINING: A COHERENCY PROTOCOL FOR INCREASING EFFECTIVE NETWORK AND MEMORY BANDWIDTH IN SHARED-MEMORY MULTIPROCESSORS
Ricardo Bianchini and Thomas J. LeBlanc Jan. 1994 26 p
(Contract N00014-92-J-1801; ARPA Order 8930)
(AD-A281501; TR-485) Avail: CASI HC A03/MF A01

One common cause of poor performance in large-scale shared-memory multiprocessors is limited memory or interconnection network bandwidth. Producer/consumer data, where one processor (the producer) writes data that many other processors (the consumers) must read, is a common sharing pattern in parallel programs that generates a nonuniform distribution of references. In this paper we quantify the performance impact of producer/consumer sharing as a function of memory and network bandwidth, and argue that the contention caused by this form of sharing can severely impact performance on large-scale machines. We then propose a new coherency protocol, called eager combining, which is designed to alleviate this contention. The protocol replicates the producer's data among multiple memory modules, thereby effectively increasing both the memory and network bandwidth of the producer, and dramatically decreasing the remote access latency of consumers. We then compare eager combining to other techniques for reducing or eliminating contention, and use execution-driven simulation of parallel programs on a large-scale multiprocessor to show that eager combining can improve performance by a factor of four or more for programs with producer/consumer data on machines with hundreds of processors. Author (DTIC)

N95-11858# Rochester Univ., NY. Dept. of Computer Science.
A PRELIMINARY EVALUATION OF CACHE-MISS-INITIATED PREFETCHING TECHNIQUES IN SCALABLE MULTIPROCESSORS
Ricardo Bianchini and Thomas J. LeBlanc May 1994 27 p
(Contract N00014-92-J-1801; ARPA Order 8930)
(AD-A281502; TR-515) Avail: CASI HC A03/MF A01

Prefetching is an important technique for reducing the average latency of memory accesses in scalable cache-coherent multiprocessors. Aggressive prefetching can significantly reduce the number of cache misses, but may introduce bursty network and memory traffic, and increase data sharin and cache pollution. Given that we anticipate enormous increases in both network bandwidth and latency, we examine whether aggressive prefetching triggered by a miss (cache-miss-initiated prefetching) can substantially improve the running time of parallel programs. Using execution-driven simulation of parallel programs on scalable cache-coherent machine, we study the performance of three cache-miss-initiated prefetching techniques: large cache blocks, sequential prefetching, and hybrid prefetching. Large cache blocks (which fetch multiple words within a single block) and sequential prefetching (which fetches multiple consecutive blocks) are well-known prefetching strategies. Hybrid prefetching is a novel technique combining hardware and software support for stride-directed prefetching. Our simulation results show that large cache blocks rarely provide significant performance improvements; the improvement in the miss rate is often too small (or nonexistent) to offset a corresponding increase in the miss penalty. Our results also show that sequential and hybrid prefetching perform better than prefetching via large cache blocks, and that hybrid prefetching performs at least as well as sequential prefetching. DTIC

N95-11863*# Hampton Univ., VA. Dept. of Mathematics
PERFORMANCE ANALYSIS OF THREE DIMENSIONAL INTEGRAL EQUATION COMPUTATIONS ON A MASSIVELY PARALLEL COMPUTER M.S. Thesis
Terry G. Logan Aug. 1994 60 p
(Grant NAG1-1170)
(NASA-CR-196747; NAS 1.26:196747) Avail: CASI HC A04/MF A01

The purpose of this study is to investigate the performance of the integral equation computations using numerical source field-panel method in a massively parallel processing (MPP) environment. A comparative study of computational performance of the MPP CM-5 computer and conventional Cray-YMP supercomputer for a three-dimensional flow problem is made. A serial FORTRAN code is converted into a parallel CM-FORTRAN code. Some performance results are obtained on CM-5 with 32, 62, 128 nodes along with those on Cray-YMP with a single processor. The comparison of the performance indicates that the parallel CM-FORTRAN code near or

out-performs the equivalent serial FORTRAN code for some cases.
Author

N95-12414# Massachusetts Inst. of Tech., Cambridge. Artificial Intelligence Lab.
EXPLORING THE PARALLELISM EXPOSED BY PARTIAL EVALUATION
Andrew Berlin and Rajeev J. Surati May 1994 9 p
(Contract N00014-92-J-4097; NSF MIP-90-01651)
(AD-A282284; AI-M-1414A) Avail: CASI HC A02/MF A01

We describe the key role played by partial evaluation in the Supercomputer Toolkit, a parallel computing system for scientific applications that effectively exploits the vast amount of parallelism exposed by partial evaluation. The Supercomputer Toolkit parallel processor and its associated partial evaluation-based compiler have been used extensively by scientists at M.I.T., and have made possible recent results in astrophysics showing that the motion of the planets in our solar system is chaotically unstable.
DTIC

N95-12418# Naval Air Warfare Center, Warminster, PA. Systems and Software Technology Dept.
POSIX DELTA DOCUMENT FOR THE NEXT-GENERATION COMPUTER RESOURCES (NGCR) OPERATING SYSTEMS INTERFACE STANDARD BASELINE, VERSION 4 Interim Report
F. Prindle 1 Jun. 1994 115 p
(AD-A282324; NAWCADWAR-94109-70) Avail: CASI HC A06/MF A02

The objective of the Next-Generation Computer Resources (NGCR) Program is to standardize computer and computer component interfaces for the Navy's next generation of mission-critical computing systems. The NGCR Operating Systems Standards Working Group (OSSWG) will either select a set of interface standards from commercial sources or jointly develop such standards with industry. Previously, the OSSWG established operating systems interface requirements for these standards. In this document, the OSSWG evaluates how effectively its established requirements are met by the Portable Operating System Interface (POSIX) standards, which have been selected as the baseline for the NGCR Program.
DTIC

N95-12523# Illinois Univ., Urbana, IL. Center for Reliable and High-Performance Computing.
A FRAMEWORK FOR EXPLOITING DATA AND FUNCTIONAL PARALLELISM ON DISTRIBUTED MEMORY MULTICOMPUTERS
Shankar Ramaswamy, Sachin Sapatnekar, and Prithviraj Banerjee 21 Jun. 1994 40 p Sponsored by ONR
(AD-A281194; UILU-ENG-94-2224; CRHC-94-10) Avail: CASI HC A03/MF A01

Recent research efforts have shown the benefits of integrating functional and data parallelism over using either pure data parallelism or pure functional parallelism. The work in this paper presents a theoretical framework for deciding on a good execution strategy for a given program based on the available functional and data parallelism in the program. The framework is based on assumptions about the form of computation and communication cost functions for multicomputer systems. We present mathematical functions for these costs and show that these functions are realistic. The framework also requires specification of the available functional and data parallelism for a given problem. For this purpose, we have developed a graphical programming tool. Currently, we have tested our approach using three benchmark programs on the Thinking Machines CM-5 and Intel Paragon. Results presented show that the approach is very effective and can provide a two- to three-fold increase in speedups over approaches using only data parallelism.
DTIC

N95-13269# Fermi National Accelerator Lab., Batavia, IL.
ANALYZING TERABYTES OF DATA AT FERMILAB
S. Wolbers May 1994 8 p Presented at the Meeting on Computing in High-Energy Physics, San Francisco, CA, 21-27 Apr. 1994
(Contract DE-AC02-76CH-03000)
(DE94-013149; FNAL/C-94/112; CONF-940492-4) Avail: CASI HC A02/MF A01

Computing demands of high energy physics are increasing steadily due to the demands of larger datasets and increasingly sophisticated detector systems and analysis techniques. Fermilab has been meeting these demands by the use of many different computing techniques. Most of these techniques attempt to utilize the most cost-effective computing resources while providing effective solutions to the problems that are created by multi-Terabyte data samples and large collaborations. New strategies are being developed to allow improved access to the data.
DOE

N95-13353 Toronto Univ. (Ontario). Inst. for Aerospace Studies.
AN ITERATIVE APPROACH TO MULTIBODY SIMULATION DYNAMICS SUITABLE FOR PARALLEL IMPLEMENTATION
I. Sharf and G. M. T. DEleuterio Sep. 1994 33 p Sponsored by Natural Sciences and Engineering Research Council of Canada, Institute for Space and Terrestrial Science and Institute for Robotics and Intelligent Systems
(ISSN 0082-5263)
(UTIAS-TN-276) Copyright Avail: Issuing Activity

This report presents a new solution procedure for simulation dynamics of multibody systems. The method is applicable to open chains with general (rotational and/or translational) interbody constraints. It is based on obtaining an explicit solution for the joint constraint forces by means of iterative techniques. We show that the algorithm possesses a parallel structure which matches the topology of the system. The computer simulation of the algorithm is described and numerical results for a 3-link (5 degree-of-freedom) anthropomorphic manipulator are presented. Comparison of several different iterative schemes indicates that the conjugate-gradient Jacobi method is computationally most efficient. An estimate for the parallel efficiency of this scheme is obtained by combining the theoretical bound for parallel complexity with an approximate overhead cost associated with parallel implementation.
Author

N95-13404 Newcastle-upon-Tyne Univ., Newcastle (England). Dept. of Computing Science.
PARALLEL PRECONDITIONERS FOR THE CONJUGATE GRADIENT METHOD
R. Cook, M. Pakzad, and C. Phillips Jan. 1994 15 p See also PB91-192187
(PB94-201605; TRS-467) Copyright Avail: Issuing Activity (National Technical Information Service (NTIS))

We consider parallel implementations of the conjugate gradient method applicable to both shared memory multiprocessors and local memory multicomputers. The basic method consists of a sequence of linear algebra steps, each of which can be readily parallelized at the cost of a certain amount of synchronization of communication. In practice the method is usually modified by the incorporation of an appropriate preconditioning step which improves the convergence characteristics. One of the more popular preconditioners is based on the use of incomplete factorization and in a parallel environment the forward and backward substitutions associated with the preconditioning step can be a limiting factor. We consider two related ways of improving the potential for parallelism at the cost of an increase in the number of iterations and quantify the effect by means of numerical examples.
NTIS

N95-13407 Newcastle-upon-Tyne Univ., Newcastle (England). Dept. of Computing Science.
UNIFORMISATION TECHNIQUES FOR INTEGRAL RECURRENCE EQUATIONS
L. Rapanotti and G. M. Megson 17 Mar. 1994 27 p See also PB93-152304 and PB93-200277
(PB94-205069; TRS-478) Copyright Avail: Issuing Activity (National Technical Information Service (NTIS))

Uniformization plays a central role for the derivation of systolic array designs. The authors present a new uniformization technique for a class of integral recurrence equations, i.e., equations whose data dependencies are defined through integral functions. This uniformization technique extends the more traditional technique for affine recurrences in a sound and consistent way, allowing us to overcome some of the limitations of the existing methods, while preserving their syntactic and semantic frameworks. Our technique is based on the reduction/decomposition of integral recurrences into their atomic components and their subsequent uniformization. The authors illustrate the method by considering modulo index functions occurring in signal processing systems, this demonstrates that synthesis methods can be applied to more general classes of iterative algorithms.
NTIS

N95-13556# Argonne National Lab., IL.
AN INFORMAL INTRODUCTION TO PARALLEL PROCESSORS
K. W. Hopkins (Southwest Baptist Univ., Bolivar, MO.) 1994 9 p
(Contract W-31-109-eng-38)
(DE94-016347; ANL/MCS/PP-77112) Avail: CASI HC A02/MF A01

In the summer of 1992, I had the opportunity to participate in a Faculty Research Program at Argonne National Laboratory. During that time I came in contact with some developments in computer science that were unfamiliar to me as a mathematician. Since most mathematicians have some exposure to computers, but certainly are not computer scientists, I felt it was appropriate to write a paper summarizing my introduction to parallel processing. This paper is not meant to be a full explanation of the topic, but an informal introduction for the 'mathematical layman'. DOE

63 CYBERNETICS

Includes feedback and control theory, artificial intelligence, robotics and expert systems.

For related information see also *54 Man/System Technology and Life Support.*

N95-11825# Technische Univ., Delft (Netherlands).
AUTONOMOUS MOTION ON WHEELS Ph.D. Thesis
P. vanTurennout 18 Jan. 1994 260 p
(PB94-191327; ISBN-90-9006530-X) Copyright Avail: CASI HC A12/MF A03

The main focus of the thesis is the autonomous motion of mobile robots, in particular those on wheels. Chapter 2 starts with a short introduction to planning activities. Planning is the main function of the navigator, which delivers the input to the guidance system. Chapter 3 discusses the modelling of wheeled mobile robots. Both the kinematics and dynamics are treated and are illustrated with examples of the two most used configurations: a differential-drive type robot (with two driven wheels) and a tricycle-type robot (with a steered and driven front wheel). Chapter 4 deals with the guidance system. The chapter starts with the subject of trajectory generation. The chapter ends with showing the controller's performance as obtained from experiments with the PAVLOV robot, including a wall-following example. Chapter 5 describes the localization problem. Three localization methods are described and investigated for their accuracies. Chapter 6 summarizes the contents of the thesis and presents the conclusions. NTIS

N95-11853# Minnesota Univ., Minneapolis, MN. Dept. of Electrical Engineering.
AN INTERPOLATION THEORETIC APPROACH TO CONTROL Final Report, 1 Jan. 1991 - 31 Mar. 1994
Allen Tannenbaum 11 Apr. 1994 19 p
(Contract DAAL03-91-G-0019)
(AD-A281465; ARO-27365.15-MA) Avail: CASI HC A03/MF A01

Our work has been concerned with the utilization of new interpolation and operator theoretic methods for the study of problems in robust control. We have worked on possible nonlinear generalizations of H infinity optimization theory and investigated corresponding intriguing questions in causality which arise in this context. In regard to our work on mu-synthesis and analysis, as well as the multivariable gain margin problem, we have developed a new type of interpolation method which is not norm-based. This is in contrast to the classical Nevanlinna-Pick theory which is used in H infinity design. This line of research leads to spectral radius and structured interpolation extensions of the Nevanlinna-Pick framework. We have also discovered a new lifting technique for the robust stability analysis of systems with several kinds of structured perturbations. We worked in distributed (infinite dimensional) H infinity control based on our skew Toeplitz methods. These have been applied to certain benchmark examples, e.g., delay systems that appear in aircraft control, and certain flexible beam problems. We have also been applying new curve evolution methods for problems in visual tracking. DTIC

N95-11909# National Inst. of Standards and Technology, Gaithersburg, MD.
PREDICTION OF GEOMETRIC-THERMAL MACHINE TOOL ERRORS BY ARTIFICIAL NEURAL NETWORKS
D. E. Gilsinn and M. A. Donmez Apr. 1994 149 p Sponsored by NRL
(PB94-186673; NISTIR-5367) Avail: CASI HC A07/MF A02

In machining operations, the precision of the workpiece dimensions depends on the accuracy of the relative position of the cutting tool and the workplace. Among the key factors that affect the accuracy of this relative position are the geometric errors of the machine tool and the thermal effects on these geometric errors. Recent work on developing models to predict volumetric errors on NC lathes has led to a syntheses technique that combines the modeling of individual axis related geometric-thermal components by way of a rigid body kinematic model to produce predicted errors in the work volume of the machine. An alternative method of modeling these component errors is described in this report. Neural network computing is shown to be a viable technique for developing mappings between machine tool component error measurements and the vector consisting of both a component slide position and the temperature state of the machine as reported by the thermal sensors. The conjugate gradient algorithm, used to compute the optimum neural network weights for the machine tool error components, is described. A case study of the mapping results for one component error of an actual NC lathe is given. Finally, the source codes for the neural network algorithm and the conjugate gradient algorithm are given in FORTRAN. NTIS

N95-11998*# Texas A&M Univ., College Station, TX. Dept. of Mechanical Engineering.
SELF CALIBRATING AUTOTRAC Final Report
Louis J. Everett 21 Sep. 1994 24 p
(Grant NAG9-629)
(NASA-CR-196930; NAS 1.26:196930) Avail: CASI HC A03/MF A01

The work reported here demonstrates how to automatically compute the position and attitude of a targeting reflective alignment concept (TRAC) camera relative to the robot end effector. In the robotics literature this is known as the sensor registration problem. The registration problem is important to solve if TRAC images need to be related to robot position. Previously, when TRAC operated on the end of a robot arm, the camera had to be precisely located at the correct orientation and position. If this location is in error, then the robot may not be able to grapple an object even though the TRAC sensor indicates it should. In addition, if the camera is significantly far from the alignment it is expected to be at, TRAC may give incorrect feedback for the control of the robot. A simple example is if the robot operator thinks the camera is right side up but the camera is actually upside down, the camera feedback will tell the operator to move in an incorrect direction. The automatic calibration algorithm requires the operator to translate and rotate the robot arbitrary amounts along (about) two coordinate directions. After the motion, the algorithm determines the transformation matrix from the robot end effector to the camera image plane. This report discusses the TRAC sensor registration problem.
Author (revised)

N95-12109# Polish Academy of Sciences, Warsaw (Poland). Independent Lab. for the Mechanics of Discrete Systems.
THE USE OF NEURON NETS TO STABILIZE DYNAMIC SYSTEMS [ZASTOSOWANIE SIECI NEURONOWYCH DO STABILIZACJI UKLADOW DYNAMICZNYCH]
Andrzej Ossowski 1992 65 p In POLISH
(ISSN 0208-5658)
Avail: CASI HC A04/MF A01

This article is a brief introduction to the subject of neuron (neuron-like) nets and their application to problems of dynamic system control and stabilization. The author discusses the following subjects: basic trends and motivating factors for the development of this branch of knowledge and models and functions of the neuron and the basic structures and definitions characteristic of neuron nets. The author goes on to discuss the principles of a method of optimal Lyapunov functions for studying dynamic systems, which he uses as the basis for examining problems of optimal stabilization of a multidimensional, multi-input linear system with control constraints. The author demonstrates that the stabilization problem can be solved by a certain neuron net acting as a stabilizer in a feedback system. The author describes the structure of this net in a general case and analyzes its operation. Author

N95-12367# Helsinki Univ. of Technology, Espoo (Finland). Lab. of Telecommunications Technology.

SCHEDULING IN AN INPUT AND OUTPUT QUEUING THREE-STAGE PACKET SWITCH BY USING NEURAL NETWORKS

J. Ma and K. Rahko 11 May 1993 8 p Presented at the Conference on Signal Processing (ICSP 1993), Peking, China, 26-30 Oct. 1993

(PB94-179413; ISBN-951-22-1849-6) Avail: CASI HC A02/MF A01

This paper presents a neural network application in packet switching systems where a neural network central controller is used to assign an optimal path resource arrangement for a three-stage Clos' packet switch with input and output buffers. The Clos' switch has a low cost of switching points, but it requires scheduling. In this paper, we propose a neural network algorithm to perform the scheduling. Since the input packet traffic can be written as a traffic matrix in every time slot, the optimal path arrangement is to assign the traffic matrix into a set of permutation matrices. We map the path arrangement to the neural networks and give the related neural network equations. The neural networks are a modified Hopfield model, which are constructed in three-dimension space, each neural network plane is associated with a middle stage switch, and they perform the path arrangement operations by computing the minimal energy of neurons. The simulation results show that the neural networks can rapidly complete the optimal scheduling after a very short convergence time. NTIS

N95-12395 North Carolina State Univ., Raleigh, NC.

OUTDOOR LANDMARK RECOGNITION USING HYBRID FRACTAL VISION SYSTEM AND NEURAL NETWORKS

1 Jul. 1994 10 p Limited Reproducibility: More than 20% of this document may be affected by microfiche quality

(Contract N00014-93-1200)

(AD-A282506) Avail: Issuing Activity (Defense Technical Information Center (DTIC))

Landmarks are useful cues for autonomous mobile robot navigation. Due to the changing imaging conditions, the appearance of the landmarks is varying in outdoor environments. We will develop a novel system to detect and recognize the landmarks. The developed system will be able to overcome changes in scale, lighting, etc. The proposed approach is based on a two-step method, using both fractal based object classifier and neural network based object identifier. Since fractals are inherently scale invariant over a finite range of scales, they make good models for outdoor scene objects. Since neural networks have fast recognition capabilities, they are a good choice in real time mobile robot applications. DTIC

N95-12411 Massachusetts Inst. of Tech., Cambridge. Artificial Intelligence Lab.

AN ANALYSIS OF THE EFFECT OF GAUSSIAN ERROR IN OBJECT RECOGNITION

Karen B. Sarachik Feb. 1994 123 p Limited Reproducibility: More than 20% of this document may be affected by microfiche quality

(Contract N00014-91-J-4038; NSF IRI-89-00267)

(AD-A282260; TR-1469) Avail: CASI HC A06

Object recognition is complicated by clutter, occlusion, and sensor error. Since pose hypotheses are based on image feature locations, these effects can lead to false negatives and positives. In a typical recognition algorithm, pose hypotheses are tested against the image, and a score is assigned to each hypothesis. We use a statistical model to determine the score distribution associated with correct and incorrect pose hypotheses, and use binary hypothesis testing techniques to distinguish between them. Using this approach we can compare algorithms and noise models, and automatically choose values for internal system thresholds to minimize the probability of making a mistake. DTIC

N95-12470*# Vanderbilt Univ., Nashville, TN. School of Engineering.

DEVELOPMENT OF ROBOSIM FOR ACADEMIC/INDUSTRIAL USE (Diskette Supplement)

George E. Cook, Csaba Biegl, and James F. Springfield, Jr. 21 Jul. 1994 180 p Diskette supplement: IBM compatible 3.5-inch diskette in DOS version Original contains color illustrations

(Grant NAG8-116)

(NASA-CR-196148; NAS 1.26:196148; NONP-NASA-Suppl-DK-94-16044)

Avail: CASI SET A11 (HC,DK); 5 functional color pages

The objectives of this research were to provide enhancements to a graphical simulation system, ROBOSIM, consisting of additional features considered essential for many applications, to port the package into a form compatible with lower cost and more useful engineering workstations, and to develop learning aids and documentation for users of the software package. In order to remain fully compatible with its original FORTRAN-coded, mainframe computer implementation, the facilities of ROBOSIM were expanded without changing its structure. This was accomplished by porting the FORTRAN code to C, keeping ROBOSIM as the kernel, and adding features to the front and back ends. Features added to the simulator include a modeling environment and an interactive simulation environment plus a number of advanced capabilities. The advanced features of the simulator include: composite objects supporting the linking of separate objects into a composite object which can be operated on as a unit while preserving the separate accessibility of its components; configuration management with the provision of an automatic configuration selection mechanism based on a set of heuristic rules; collision detection which provides a way to check for collisions during a simulation run; collision avoidance where the simulator provides a heuristic path planning algorithm which is capable of recovering from collision situations to provide collision-free path plans; and interface to control physical robots with the capability of generating command sequences for real robot controllers. Included in this report is a Manual, Tutorial, and Installation Instructions for installing and using ROBOSIM and disks containing the program and all examples. Author

N95-12782*# Massachusetts Inst. of Tech., Cambridge. Space Engineering Research Center.

ROBUST CONTROL DESIGN WITH REAL PARAMETER UNCERTAINTY USING ABSOLUTE STABILITY THEORY Ph.D. Thesis

Jonathan P. How and Steven R. Hall Jan. 1993 194 p

(Grants NAGw-2014; NAGw-1335)

(NASA-CR-196971; NAS 1.26:196971; SERC-1-93) Avail: CASI HC A09/MF A03

The purpose of this thesis is to investigate an extension of mu theory for robust control design by considering systems with linear and nonlinear real parameter uncertainties. In the process, explicit connections are made between mixed mu and absolute stability theory. In particular, it is shown that the upper bounds for mixed mu are a generalization of results from absolute stability theory. Both state space and frequency domain criteria are developed for several nonlinearities and stability multipliers using the wealth of literature on absolute stability theory and the concepts of supply rates and storage functions. The state space conditions are expressed in terms of Riccati equations and parameter-dependent Lyapunov functions. For controller synthesis, these stability conditions are used to form an overbound of the H2 performance objective. A geometric interpretation of the equivalent frequency domain criteria in terms of off-axis circles clarifies the important role of the multiplier and shows that both the magnitude and phase of the uncertainty are considered. A numerical algorithm is developed to design robust controllers that minimize the bound on an H2 cost functional and satisfy an analysis test based on the Popov stability multiplier. The controller and multiplier coefficients are optimized simultaneously, which avoids the iteration and curve-fitting procedures required by the D-K procedure of mu synthesis. Several benchmark problems and experiments on the Middeck Active Control Experiment at M.I.T. demonstrate that these controllers achieve good robust performance and guaranteed stability bounds. Author

N95-12811*# Case Western Reserve Univ., Cleveland, OH. Dept. of Systems Engineering.

INTELLIGENT CONTROL SYSTEMS RESEARCH Final Report

Kenneth A. Loparo Sep. 1994 14 p Sponsored by NASA. Lewis Research Center

(Grant NAG3-768; DA Proj. 1L1-61102-AH-45; RTOP 505-62-0E)

(NASA-CR-195380; E-9113; NAS 1.26:195380; ARL-CR-187) Avail: CASI HC A03/MF A01

Results of a three phase research program into intelligent control systems are presented. The first phase looked at implementing the lowest or direct level of a hierarchical control scheme using a reinforcement learning approach assuming no a priori information about the system under control. The second phase involved the design of an adaptive/optimizing level of the hierarchy and its interaction with the direct control level. The third and final phase of the research was aimed at combining the results of the

previous phases with some a priori information about the controlled system. Author

N95-12835# Carnegie-Mellon Univ., Pittsburgh, PA. Dept. of Computer Science.
POPULATION-BASED INCREMENTAL LEARNING. A METHOD FOR INTEGRATING GENETIC SEARCH BASED FUNCTION OPTIMIZATION AND COMPETITIVE LEARNING
Shumeet Baluja 2 Jun. 1994 40 p
(AD-A282654; CMU-CS-94-163) Avail: CASI HC A03/MF A01

Genetic algorithms (GA's) are biologically motivated adaptive systems which have been used, with varying degrees of success, for function optimization. In this study, an abstraction of the basic genetic algorithm, the Equilibrium Genetic Algorithm (EGA), and the GA in turn, are reconsidered within the framework of competitive learning. This new perspective reveals a number of different possibilities for performance improvements. This paper explores population-based incremental learning (PBIL), a method of combining the mechanisms of a operational genetic algorithm with simple competitive learning. The combination of these two methods reveals a tool which is far simpler than a GA, and which out-performs a GA on large set of optimization problems in terms of both speed and accuracy. This paper presents an empirical analysis of where the proposed technique will outperform genetic algorithms, and describes a class of problems in which a genetic algorithm may be able to perform better. Extensions to this algorithm are discussed and analyzed. PBIL and extensions are compared with a standard GA on twelve problems, including standard numerical optimization functions, traditional GA test suite problems, and NP-Complete problems DTIC

N95-12864# Sandia National Labs., Albuquerque, NM.
LEARNING ONE-DIMENSIONAL GEOMETRIC PATTERNS UNDER ONE-SIDED RANDOM MISCLASSIFICATION NOISE
P. W. Goldberg and S. A. Goldman 1994 11 p Presented at the Conference on Computational Learning Theory, New Brunswick, NJ, 10-15 Jul. 1994
(Contract DE-AC04-94AL-85000)
(DE94-014659; SAND-94-1383C; CONF-940794-1) Avail: CASI HC A03/MF A01

Developing the ability to recognize a landmark from a visual image of a robot's current location is a fundamental problem in robotics. The authors consider the problem of PAC-learning the concept class of geometric patterns where the target geometric pattern is a configuration of k points in the real line. Each instance is a configuration of n points on the real line, where it is labeled according to whether or not it visually resembles the target pattern. They relate the concept class of geometric patterns to the landmark recognition problem and then present a polynomial-time algorithm that PAC-learns the class of one-dimensional geometric patterns when the negative examples are corrupted by a large amount of random misclassification noise. DOE

N95-12866# Sandia National Labs., Albuquerque, NM.
LEARNING UNIONS OF BOXES WITH MEMBERSHIP AND EQUIVALENCE QUERIES
P. W. Goldberg, S. A. Goldman, and H. D. Mathias 1994 10 p Presented at the Conference on Computational Learning Theory, New Brunswick, NJ, 10-15 Jul. 1994
(Contract DE-AC04-94AL-85000)
(DE94-014662; SAND-94-1384C; CONF-940794-2) Avail: CASI HC A02/MF A01

The authors present two algorithms that use membership and equivalence queries to exactly identify the concepts given by the union of s discretized axis-parallel boxes in d-dimensional discretized Euclidean space where there are n discrete values that each coordinate can have. The first algorithm receives at most sd counterexamples and uses time and membership queries polynomial in s and log n for d any constant. Further, all equivalence queries made can be formulated as the union of O(sd log(s)) axis-parallel boxes. Next, they introduce a new complexity measure that better captures the complexity of a union of boxes than simply the number of boxes and dimensions. Their new measure, sigma, is the number of segments in the target polyhedron where a segment is a maximum portion of one of the sides of the polyhedron that lies entirely inside or entirely outside each of the other halfspaces defining the polyhedron. They then present an improvement of their first algorithm that uses time and queries polynomial in sigma and log n. The hypothesis class used here is decision trees of height at most 2sd. Further they can show that the time and queries used by this algorithm are polynomial in d and log n for s any constant thus generalizing the exact learnability of DNF formulas with a constant number of terms. In fact, this single algorithm is efficient for either s or d constant. DOE

N95-12884 SRI International Corp., Menlo Park, CA.
REPRESENTATION, MODELING AND RECOGNITION OF OUTDOOR SCENES Annual Report No. 2
Martin A. Fischler and Robert C. Bolles Apr. 1994 57 p Limited Reproducibility: More than 20% of this document may be affected by microfiche quality
(Contract DACA76-92-C-0008)
(AD-A283361; TEC-0057) Avail: CASI HC A04

The primary goal of this project was to advance the state-of-the-art in scene interpretation for autonomous systems that operate in natural terrain. In particular, techniques are being developed for representing knowledge about complex cultural and natural environments so that a computer vision system can successfully plan, navigate, recognize, and manipulate objects and answer questions or make decisions relevant to this knowledge. The results include the development of representations and associated methods for rapidly modeling natural terrain, from multiple images, at a level or organization higher than that of the conventional dense array of depths. In particular, we have developed an approach for integration of information acquired from multiple views of a scene that uses a new class of geometric primitives; it allows easy expression of known constraints and observed data, and also allows the use of practical optimization based solution techniques. This work will provide an effective way of allowing a robotic system to incrementally build a progressively more accurate and complete model of the environment in which it is operating. Work is also progressing on the problem of recognizing import classes of natural and manmade objects, especially roads, trees, rocks, and terrain features. DTIC

N95-13124# Brookhaven National Lab., Upton, NY.
NEURAL NETWORKS AND ORBIT CONTROL IN ACCELERATORS
E. Bozoki and A. Friedman 1994 4 p Presented at the 4th European Particle Accelerator Conference, London, England, 27 Jun. - 1 Jul. 1994
(Contract DE-AC02-76CH-00016)
(DE94-014877; BNL-60586; CONF-940618-9) Avail: CASI HC A01/MF A01

An overview of the architecture, workings and training of Neural Networks is given. We stress the aspects which are important for the use of Neural Networks for orbit control in accelerators and storage rings, especially its ability to cope with the nonlinear behavior of the orbit response to 'kicks' and the slow drift in the orbit response during long-term operation. Results obtained for the two NSLS storage rings with several network architectures and various training methods for each architecture are given. DOE

N95-13369# Brown Univ., Providence, RI. Div. of Applied Mathematics.
STOCHASTIC CONTROL AND NONLINEAR ESTIMATION Final Technical Report, 1 Apr. 1992 - 31 Mar. 1994
Wendell H. Fleming and Harold J. Kushner 19 May 1994 5 p
(Contract F49620-92-J-0081)
(AD-A281219; AFOSR-94-0393TR) Avail: CASI HC A01/MF A01

Work during this period concerned risk sensitive stochastic control, and related questions about differential games. This theory provides a link between stochastic and deterministic (robust control) approaches to disturbance attenuation problems. Other work developed efficient, general stochastic approximation methods for improving the operation of continuous or discrete event dynamical systems over a long time period. Applications to communication problems include large controlled multiplexing systems, which are approximated by diffusion type processes. The method yields a very efficient way of approximation as well as good numerical methods. DTIC

64 NUMERICAL ANALYSIS

Includes iteration, difference equations, and numerical approximation.

N95-11839# Helsinki Univ. of Technology, Espoo (Finland). Digital Systems Lab.

CONSTRUCTING COMBINATORIAL DESIGNS BY LOCAL SEARCH

K. J. Nurmela Nov. 1993 84 p

(PB94-179272; ISBN-951-22-1857-7) Avail: CASI HC A05/MF A01

Probabilistic search heuristics are used in search for covering designs, packing designs, and t-designs. Each covering design gives an upper bound for C(sub lambda)(v,m,k,t), the minimum size of a t - (v,m,k,lambda) covering design, while each packing design gives a lower bound for D(sub lambda)(v,m,k,t), the maximum size of a t - (v,m,k,lambda) packing design, and each t-design establishes the existence of such a design. The designs are constructed using probabilistic combinatorial optimization methods including simulated annealing, tabu search, threshold accepting, great deluge algorithm, and record-to-record travel. Implementation issues of these algorithms, such as cost functions and neighborhood structures, are discussed. Comparisons of the performance of these algorithms on some designs is carried out. Some elementary search methods including steepest descent algorithm and random walk are included in the comparisons. Finally, the results of the searches are tabulated. The object class heirarchy of the program (written in C++) and brief class descriptions are presented in the appendix. NTIS

N95-11850 Rensselaer Polytechnic Inst., Troy, NY.

WORKSHOP ON ADAPTIVE METHODS FOR PARTIAL DIFFERENTIAL EQUATIONS Final Report, 1 Jan. 1992 - 31 May 1993

Joseph E. Flaherty and Mark S. Shephard Jun. 1994 8 p Limited Reproducibility: More than 20% of this document may be affected by microfiche quality

(Contract DAAL03-92-G-0009)

(AD-A281416; ARO-29079.1-MA-CF) Avail: CASI HC A02

During this workshop, approximately 100 participants (whose names are appended) from industry, academia, Department of Defense, and other national laboratories heard talks on the theory and practice of adaptive approaches in several mathematical areas and physical disciplines. Also, for the first time in this series of workshops, a full day tutorial was held on May 17, covering some of the more germane issues in adaptivity. This tutorial discussed topics ranging from the underlying principles of a priori error estimation, to adaptive methods for transient problems, to computational geometric approaches for automatic three-dimensional finite element mesh generation. DTIC

N95-11861 California Univ., Santa Barbara, CA.

VISCOSITY SOLUTIONS OF FULLY NONLINEAR EQUATIONS

Michael G. Crandall 4 Apr. 1994 7 p Limited Reproducibility: More than 20% of this document may be affected by microfiche quality

(Contract DAAL03-90-G-0102)

(AD-A281725; ARO-27869.4-MA) Avail: CASI HC A02

The eight publications produced by the project established a number of basic results in the theory of viscosity solutions of fully nonlinear differential equations of first and second order in finite and infinite dimensions. These equations arise in the dynamic programming theory of control and differential games (the finite dimensional theory for ode and the infinite dimensional theory for pde dynamics). Being fully nonlinear, the equations do not typically admit regular or classical solutions, and the appropriate notion is that of viscosity solutions. Two major advances in the first order infinite dimensional case consisted of determining the precise notion appropriate to a class of infinite dimensional problems with unbounded terms arising from the pde dynamics, and the examination of a limit case in which the value function is not a solution, but the maximal subsolution. Significant contributions to the second order theory include a new exposition of the finite dimensional theory based on results from previous funding, an infinite dimensional generalization of the foundational result used in this exposition, and the extension of the theory to second order equations in infinite dimensions with unbounded first order terms. DTIC

N95-11883*# Research Inst. for Advanced Computer Science, Moffett Field, CA.

STABILITY AND ERROR ESTIMATION FOR COMPONENT ADAPTIVE GRID METHODS

Joseph Oliger and Xiaolei Zhu Aug. 1994 28 p

(Contracts NAS2-13721; N00014-89-J-0185; N00014-90-J-1344; NSF DMS-93-18166)

(NASA-CR-196492; NAS 1.26:196492; RIACS-TR-94-14) Avail: CASI HC A03/MF A01

Component adaptive grid (CAG) methods for solving hyperbolic partial differential equations (PDE's) are discussed in this paper. Applying recent stability results for a class of numerical methods on uniform grids. The convergence of these methods for linear problems on component adaptive grids is established here. Furthermore, the computational error can be estimated on CAG's using the stability results. Using these estimates, the error can be controlled on CAG's. Thus, the solution can be computed efficiently on CAG's within a given error tolerance. Computational results for time dependent linear problems in one and two space dimensions are presented. Author

N95-11922*# Institute for Computer Applications in Science and Engineering, Hampton, VA.

MICROWAVE HEATING AND JOINING OF CERAMIC CYLINDERS: A MATHEMATICAL MODEL Final Report

Michael R. Booty (New Jersey Inst. of Tech., Newark, NJ.) and Gregory A. Kriegsmann (New Jersey Inst. of Tech., Newark, NJ.) Jul. 1994 17 p Submitted for publication

(Contracts NAS1-19480; RTOP 505-90-52-01; AF-AFOSR-0252-91; DE-FG02-94ER-25196; NSF DMS-93-05828)

(NASA-CR-194962; NAS 1.26:194962; ICASE-94-69) Avail: CASI HC A03/MF A01

A thin cylindrical ceramic sample is placed in a single mode microwave applicator in such a way that the electric field strength is allowed to vary along its axis. The sample can either be a single rod or two rods butted together. We present a simple mathematical model which describes the microwave heating process. It is built on the assumption that the Biot number of the material is small, and that the electric field is known and uniform throughout the cylinder's cross-section. The model takes the form of a nonlinear parabolic equation of reaction-diffusion type, with a spatially varying reaction term that corresponds to the spatial variation of the electromagnetic field strength in the waveguide. The equation is analyzed and a solution is found which develops a hot spot near the center of the cylindrical sample and which then propagates outwards until it stabilizes. The propagation and stabilization phenomenon concentrates the microwave energy in a localized region about the center where elevated temperatures may be desirable. Author

N95-12007 Massachusetts Inst. of Tech., Cambridge. Artificial Intelligence Lab.

THE QUADRIC REFERENCE SURFACE: THEORY AND APPLICATIONS

Amnon Shashua and Sebastian Toelg Jun. 1994 11 p Limited Reproducibility: More than 20% of this document may be affected by microfiche quality

(Contracts N00014-92-J-1879; N00014-93-1-0385)

(AD-A282379; AI-M-1448; CBCL-85) Avail: CASI HC A03

The conceptual component of this work is about reference surfaces which are the dual of reference frames often used for shape representation purposes. The theoretical component of this work involves the question of whether one can find a unique (and simple) mapping that aligns two arbitrary perspective views of an opaque textured quadric surface in 3D, given (1) few corresponding points in the two views, or (2) the outline conic of the surface in one view (only) and few corresponding points in the two views. The practical component of this work is concerned with applying the theoretical results as tools for the task of achieving full correspondence between views of arbitrary objects. DTIC

N95-12501 Naval Postgraduate School, Monterey, CA. Dept. of Mathematics.

MEASURES OF CHANGE AND THE DETERMINATION OF EQUIVALENT CHANGE Technical Report, Apr. - Jun. 1994

C. L. Frenzen 6 Jun. 1994 33 p Limited Reproducibility: More than

20% of this document may be affected by microfiche quality
(AD-A282647; NPS-MA-94-002) Avail: CASI HC A03

Equivalent change in percentages, probabilities, or other variables belonging to a finite interval cannot be properly determined using methods appropriate for the real or positive real numbers, since these may require a variable to fall outside its interval of definition. A general theory for determining equivalent change on any open interval G of real numbers is developed. Properties for measures of change are proposed which give G a group structure order isomorphic to the naturally ordered additive group of real numbers. Different group operations on G determine numerically different measures of change, and numerically different results for equivalent change. Requiring the group product on G to be a rational function of its factors yields familiar results for equivalent change on the real and positive real numbers, and a function recently proposed by Ng when G is the open unit interval. Ng's function is not uniquely characterized by his twelve 'reasonable' properties, but is uniquely determined when the group product on G depends rationally on its factors. Geometrical interpretations of these results for the real numbers, positive real numbers, and the open unit interval are also given. DTIC

N95-12552# Maryland Univ., College Park, MD. Inst. for Physical Science and Technology.

IS THE POLLUTION EFFECT OF THE FEM AVOIDABLE FOR THE HELMHOLTZ EQUATION CONSIDERING HIGH WAVE NUMBERS? Final Report

Ivo M. Babuska and Stefan A. Sauter May 1994 46 p
(Contract N00014-93-I-1031)
(AD-A282585; BN-1172) Avail: CASI HC A03/MF A01

Using the Galerkin FEM to solve the Helmholtz equation, the error of the corresponding solution differs from the error of the best approximation substantially, and this effect increases with higher wave numbers k. In the one dimensional case, we will define a stabilized variant of the FEM which fits in the setting of the generalized FEM (GFEM). This variant will produce a FE-solution being very close to the best approximation, and we can prove quasioptimal error estimates without any pollution effect. This situation changes essentially in the higher dimensional case. We will show that for every GFEM there exists a domain and a solution of the Helmholtz equation which cannot be approximated without any pollution. Numerical examples will illustrate the improvement of the stabilized FEM compared with the Galerkin FEM. DTIC

N95-12577# Institut des Hautes Etudes Scientifiques, Bures-sur-Yvette (France).

EXTENSION OF A THEOREM OF GEHRING AND POMMERENKE

M. Chuaqui and B. Osgood Aug. 1993 12 p
(PB94-180858; IHES/M/93/45) Avail: CASI HC A03/MF A01

This paper demonstrates that the Gehring-Pommerenke theorem can be extended to a wider class of univalence criteria introduced by Nehari. NTIS

N95-12603# Institut des Hautes Etudes Scientifiques, Bures-sur-Yvette (France).

EXTENSIONS AND CONTRACTIONS OF THE LIE ALGEBRA OF Q-PSEUDODIFFERENTIAL SYMBOLS

B. Khesin, V. Lyubashenko, and C. Roger Feb. 1994 40 p Prepared for National Science Foundation, Arlington, VA
(Grant NSF DMS-93-07086)
(PB94-192374; IHES/M/94/13) Avail: CASI HC A03/MF A01

The authors construct cocycles on the Lie algebras of pseudo- and q-pseudodifferential symbols of one variable and on their close relatives: the sine-algebra and the Poisson algebra on two-torus. A 'quantum' Godbillon-Vey cocycle on (pseudo)-differential operators appears in this construction as a natural generalization of the Gelfand-Fuchs 3-cocycle on periodic vector fields. They describe a nontrivial embedding of the Virasoro algebra into (a completion of) q-pseudodifferential symbols, and propose q-analogs of the KP and KdV-hierarchies admitting an infinite number of conserved charges. NTIS

N95-12808# Institut des Hautes Etudes Scientifiques, Bures-sur-Yvette (France).

ASPECTS OF LONG TIME BEHAVIOUR OF SOLUTIONS OF NONLINEAR HAMILTONIAN EVOLUTION EQUATIONS

J. Bourgain Mar. 1994 42 p
(PB94-192382; IHES/M/94/18) Avail: CASI HC A03/MF A01

In the paper the authors will be mainly concerned with the behavior of solutions of (space periodic) nonlinear wave equations and nonlinear Schrodinger equations. Most of the techniques used have a wider range of applicability however. They are interested in nonlinear Hamiltonian PDE in a general (nonintegrable or close to integrable) context where one does not expect KAM results. Assuming local existence of solutions established, there are many issues to be addressed about their behavior for t approaches infinity and the following properties of the flow in phase space: (1) global existence behavior; (2) asymptotic stability; (3) behavior of higher Sobolev norms of smooth solutions when t approaches infinity, spreading of energy to higher modes; and (4) recurrence properties in time. NTIS

N95-12820# Helsinki Univ. of Technology, Espoo (Finland). Systems Analysis Lab.

GAUSSIAN PAIRED COMPARISON MODELS

U. Pulkkinen Dec. 1993 26 p Prepared in cooperation with Technical Research Centre of Finland, Espoo, Finland
(PB94-179025; ISBN-951-22-1889-5) Avail: CASI HC A03/MF A01

Bayesian paired comparison models based on the Gaussian additive error models for the use of expert judgements are formulated. Some limiting properties of the models are investigated. It is observed that the posterior variance cannot be made arbitrarily small by increasing the number of experts. The posterior distributions are determined by using the Gibbs sampler and numerical examples are discussed. The value of information lost in the paired comparison process is analyzed from the Bayesian point of view. NTIS

N95-13340# China Nuclear Information Centre, Beijing (China).

INVERSE OPERATOR THEORY METHOD MATHEMATICS-MECHANIZATION FOR THE SOLUTIONS OF NONLINEAR EQUATIONS AND SOME TYPICAL APPLICATIONS IN NONLINEAR PHYSICS

Jinqing Fang (Academia Sinica, Beijing, China.) and Weiguang Yao (Academia Sinica, Beijing, China.) Dec. 1992 28 p
(DE94-624804; CNIC-00700; IAE-0115) Avail: CASI HC A03/MF A01 (US Sales Only)

Inverse operator theory method (IOTM) has developed rapidly in the last few years. It is an effective and useful procedure for quantitative solution of nonlinear or stochastic continuous dynamical systems. Solutions are obtained in series form for deterministic equations, and in the case of stochastic equations it gives statistic measures of the solution process. A very important advantage of the IOTM is to eliminate a number of restrictions and assumptions on the nature of stochastic processes. Therefore, it provides more realistic solutions. The IOTM and its mathematics-mechanization (MM) are briefly introduced. They are used successfully to study the chaotic behaviors of the nonlinear dynamical systems for the first time in the world. As typical examples, the Lorentz equation, generalized Duffing equation and two coupled generalized Duffing equations are investigated by the use of the IOTM and the MM. The results are in good agreement with ones obtained by the Runge-Kutta method (RKM). It has higher accuracy and faster convergence. So the IOTM realized by the MM is potentially valuable in nonlinear science. DOE

N95-13437 Newcastle-upon-Tyne Univ., Newcastle (England). Dept. of Computing Science.

VISUALIZING PARALLEL NUMERICAL SOFTWARE PERFORMANCE ON A SHARED MEMORY MULTIPROCESSOR

P. A. Lee and C. Phillips Dec. 1993 14 p
(PB94-195658; TRS-458) Copyright Avail: Issuing Activity (National Technical Information Service (NTIS))

The authors consider here the use of a software package which can be used to monitor and visualize the behavior, with respect to data accesses, of parallel software in a multiprocessor environment supporting shared memory. The purpose of such monitoring is two-fold: (1) to aid in the understanding of the behavior of a given algorithm; and (2) to support the debugging of that software. To illustrate the use of this package the authors analyze its facilities in connection with a parallel implementation of block Gaussian elimination to solve a system of equations which arises when a certain spectral method is employed to solve an elliptic partial

differential equation in two dimensions. The authors outline the method, indicate the synchronization mechanisms which are necessary to ensure that the correct sequence of operations take place, and briefly describe the facilities provided by Encore Parallel Fortran which support these mechanisms. They then examine the facilities of the visualization software and indicate how these were adapted to monitor accesses to a packed storage representation of a block sparse array. Finally they illustrate the use of the software in the context of the solution of a particular partial differential equation. NTIS

N95-13439 Rutherford Appleton Lab., Chilton (England). Computational Modeling Div.
IMPLEMENTING A LINEAR EQUATION SOLVER IN THE CFD CODE PHOENICS
M. K. Boparai Dec. 1993 72 p
(PB94-195757; RAL-93-102) Avail: Issuing Activity (National Technical Information Service (NTIS))

The CFD code PHOENICS, one of the most widely used commercial codes, is intended to be 'expandable', allowing experienced users to interface their own modelling features to the processing module. The report describes the feasibility of implementing a user-defined linear equation solver using a simple conjugate gradient algorithm, in the flow-solving module of PHOENICS, without access to the main source code. It shows how the data can be efficiently accessed and stored with reference to the large central storage array of PHOENICS and this can be used as a starting point for incorporating more complex solvers and other features. The problem of heat conduction in a cube which leads to the solution of a system of linear equations is used to test the method. The new user-written routines including a matrix-vector multiplier are given in the appendices, and the way they are interfaced, built and linked with the PHOENICS modules is also shown. Note that the report does not assess the code in any way. NTIS

N95-13560 Newcastle-upon-Tyne Univ., Newcastle (England). Dept. of Computing Science.
CATEGORY THEORY: THE MATHEMATICS FOR THE HUMANITIES
M. A. Heather and B. N. Rossiter Feb. 1994 18 p See also PB93-195444 and PB93-220770 Prepared in cooperation with Northumbria Univ., Newcastle-upon-Tyne, England
(PB94-205044; TRS-476) Copyright Avail: Issuing Activity (National Technical Information Service (NTIS))

The humanities have long sought a formal basis in logic and set theory especially in the understanding of language and linguistics. Constructive mathematics now offers category theory developed in the second half of this century as an all-embracing formal language which may prove to be the ultimate breakthrough the humanities have long been seeking. The paper provides two examples--one at the very abstract level of adjointness between discourse in speech writing and the electronic format. At a much lower level the same mathematical formalism can represent methods of optimization in organizing dictionary data on disk. NTIS

N95-13573 Selskapet for Industriell og Teknisk Forskning, Oslo (Norway). Div. for Informatics.
APPROXIMATION OF SCATTERED DATA USING SMOOTH GRID FUNCTIONS
E. Arge, M. Daehlen, and A. Tveito 10 Jan. 1994 25 p Sponsored by Royal Norwegian Council for Scientific and Industrial Research
(PB94-207016; STF33-A94003) Avail: Issuing Activity (National Technical Information Service (NTIS))

We present a three-stage scheme for constructing smooth grid functions approximating data defined over scattered point sets. The scheme is useful for approximating large scattered data sets and is particularly successful when the data points are unevenly distributed. The paper includes several examples of grid surface construction over the plane. NTIS

65 STATISTICS AND PROBABILITY

Includes data sampling and smoothing; Monte Carlo method; and stochastic processes.

N95-13061# Los Alamos National Lab., NM.
MEAN IMPORTANCE MEASURES FOR GROUPS OF EVENTS IN FAULT TREES
F. E. Haskin (New Mexico Univ., Albuquerque, NM.), Min Huang (New Mexico Univ., Albuquerque, NM.), M. K. Sasser, and D. W. Stack 12 Oct. 1993 84 p
(Contract W-7405-eng-36)
(DE94-015416; LA-Sub-94-82) Avail: CASI HC A05/MF A01

The method of moments is applied to precisely determine the mean values of three importance measures: risk reduction, partial derivative, and variance reduction. Variance reduction calculations, in particular, are significantly improved by eliminating the imprecision associated with Monte Carlo estimates. The three importance measures are extended to permit analyses of the relative importance of groups of basic and initiating events. The partial derivative importance measure is extended by assessing the contribution of a group of events to the gradient of the top event frequency. The group importance measures are quantified for the overall fuel damage equation and for 14 dominant accident sequences from an independent probabilistic safety assessment of the K Production Reactor. This application demonstrates both the utility and the versatility of the group importance measures. DOE

66 SYSTEMS ANALYSIS

Includes mathematical modeling; network analysis; and operations research.

No abstracts in this category.

67 THEORETICAL MATHEMATICS

Includes topology and number theory.

N95-12364 Rutherford Appleton Lab., Chilton (England).
HALL CONDUCTANCE AS A TOPOLOGICAL INVARIANT
G. I. Watson Mar. 1994 32 p
(PB94-179330; RAL-94-030) Avail: Issuing Activity (National Technical Information Service (NTIS))

These lecture notes form an informal review of work published around 1982-88 on the topological approach to the theory of the integer quantum Hall effect (IQHE). The scope is the 'TKNN' paper (Thouless et al. 1982) and subsequent work inspired by it. The author will give several versions of the reasoning and try to explain some of the mathematical jargon which sometimes appears. NTIS

70 PHYSICS (GENERAL)

For precision time and time interval (PTTI) see *35 Instrumentation and Photography;* for geophysics, astrophysics or solar physics see *46 Geophysics, 90 Astrophysics,* or *92 Solar Physics.*

N95-11731# Oak Ridge National Lab., TN.
DESIGN AND CONSTRUCTION OF THE ASTRONAUTICS REFRIGERATOR MAGNET
L. Dresner May 1994 31 p
(Contract DE-AC05-84OR-21400)
(DE94-013599; ORNL/TM-12730) Avail: CASI HC A03/MF A01

This document reports on the design, construction, and testing of a 7-Tesla, 4-in. bore superconducting magnet for use in the Astronautics Refrigerator Experiment. The magnet is a single-strand, layer-wound, potted solenoid wound with Formvar-insulated SSC strands. The magnet was

constructed by American Magnetics, Inc. of Oak Ridge and has been installed in the Astronautics Refrigerator Experiment at the Astronautics Technology Center in Madison, Wisconsin. DOE

N95-12229 Alenia Spazio S.p.A., Turin (Italy).
STEP: AN INTERNATIONAL COLLABORATION IN FUNDAMENTAL PHYSICS
Monica Jarnot, ed., Jean-Pierre Blaser, Francis Everitt, Yusuf Jafry, Robin Laurance, Anna Nobili, Ho Jung Paik, Ruedeger Reinhard, Reiner Rummel, and Jon Salmon et al Mar. 1993 24 p Prepared in cooperation with Centre National d'Etudes Spatiales, Paris (France), Deutsche Aerospace A.G., Munich (Germany), International Centre for Relativistic Astrophysics, Rome (Italy), JPL, Pasadena, CA, Lockheed Missiles and Space Co., Palo Alto, CA, Matra Marconi Space, Toulouse (France), Rutherford Appleton Lab., Chilton (England), and Stanford Univ., CA Original contains color illustrations
Avail: Issuing Activity

STEP, the Satellite Test of the Equivalence Principle, is a joint European-U.S. space program to investigate one the strangest phenomena in physics: the fact that gravity makes all bodies fall with the same acceleration. Interpreted by Isaac Newton as the outcome of an equivalence between two distinct properties of a body, weight and quantity of matter, this 'universality of free fall' was reinterpreted by Albert Einstein in terms of an even wider equivalence between the laws of physics in different accelerated reference frames, a principle which Einstein made the basis for his general theory of relativity. STEP will advance the testing of equivalence into regions where the principle may break down. It will also provide a near-ideal space laboratory for other new experiments in gravitation, elementary particle physics, and geodesy. Derived from text

N95-12426# Naval Surface Warfare Center, Bethesda, MD.
LAWS OF INFRARED SIMILITUDE Final Report
Peter O. Cervenka and Lou Massa Jan. 1994 29 p
(AD-A282209; CARDIVNSWC-TR-94/002) Avail: CASI HC A03/MF A01

Accurate physical scale models of complex systems are found to be of great use in fields as diverse as aerodynamics, fluid mechanics, radar, or nuclear physics. It now appears that the concept of scale modeling may offer distinct advantages to those interested in the study of thermodynamic processes that occur in large physical structures. In this investigation, it is shown from a study of the heat equation and its boundary conditions that physical scale modeling can be used to simulate realistic systems operating in realistic outdoor environments. The thermal properties of the construction materials used in the system under study are allowed to vary with position, thus allowing the structure to be divided into a number of compartments. Physical effects which involve heat exchange between the structure and the ocean, or with the atmosphere, are investigated. Both time-dependent and time-independent cases are examined. DTIC

N95-12728# California Inst. of Tech., Pasadena, CA. Graduate Aeronautical Labs.
ON THE STRAIN AND STRAIN-RATE DEPENDENCE OF THE FRACTION OF PLASTIC WORK CONVERTED TO HEAT: AN EXPERIMENTAL STUDY USING HIGH SPEED INFRARED DETECTORS AND THE KOLSKY BAR
J. J. Mason, A. J. Rosakis, and G. Ravichandran Nov. 1992 32 p Submitted for publication Sponsored in part by NSF
(Contract N00014-90-J-1340)
(SM-92-33) Avail: CASI HC A03/MF A01

The conversion of plastic work to heat at high strain-rates gives rise to significant temperature increase which contributes to thermal softening in the constitutive response of many materials. This investigation systematically examines the rate of conversion of plastic work to heat in metals using a Kolsky (split Hopkinson) pressure bar and a high speed infrared detector array. Several experiments are performed, and the work rate to heat rate conversion fraction, the relative rate at which plastic work is converted to heat, is reported for 4340 steel, 2024 aluminum, and Ti-6Al-4V titanium alloys undergoing high strain and high strain-rate deformation. The functional dependence of this quantity upon strain and strain-rate is also reported for these metals. This quality represents the strength of the coupling term between temperature and mechanical fields in thermomechanical problems involving plastic flow. The experimental measurement of this constitutive function is important since it is an integral part of the formulation of coupled thermomechanical field equations, and it plays an important role in failure mode selection -- such as the formation of adiabatic shear bands -- in metals deforming at high strain-rates.
Author

N95-12994# California Univ., Riverside, CA. Dept. of Mathematics.
SPECTRAL ANALYSIS, ESTIMATION, AND PREDICTION OF MULTIPLE HARMONIZABLE RANDOM FIELDS AND TIME SERIES Final Report, May 1990 - Jan. 1994
M. M. Rao Jan. 1994 11 p
(Contract N00014-90-J-1705)
(AD-A283042) Avail: CASI HC A03/MF A01

A summary is presented of the work accomplished on the recently concluded ONR Grant No. N00014-90-J-1705 by the P.I. and his students. Presented are research papers and reports, books, participation in conferences, graduate student training and support, and research scholars visiting the principal investigator. CASI

N95-13143# Naval Postgraduate School, Monterey, CA.
ENHANCEMENT OF EMAG: A 2-D ELECTROSTATIC AND MAGNETOSTATIC SOLVER FOR MATLAB M.S. Thesis
David P. Wells Sep. 1994 135 p
(AD-A283446) Avail: CASI HC A07/MF A02

This thesis presents the theory and development involved in the enhancement of EMAG, a two dimensional electrostatic and magnetostatic solver, to allow it to solve problems involving rotational symmetry. EMAG 2.0 solves rotationally symmetric problems using discrete forms of the Poisson equations for electrostatics and magnetostatics in cylindrical coordinates. EMAG 2.0 is written entirely in MATLAB script format. It allows users to define electrostatic or magnetostatic problems on a 2-D grid and solve the problem for the potentials at uniformly spaced nodes on the grid. Graphical displays allow the users to visualize contour or mesh plots of potential, vector plots of electric or magnetic fields, and to calculate the charge or current enclosed in a user defined region of the grid. The EMAG 2.0 computational grid has a simulated open boundary which is generated by the transparent grid termination (TGT) technique. This boundary is unique to the type of system being solved. This thesis presents and compares two different methods for generating this boundary, one involving a probabilistic model of the system and the other using a direct matrix solution approach. Optimization of the transparent grid termination technique is also explored. DTIC

N95-13144# Naval Postgraduate School, Monterey, CA.
A CALIBRATION OF THE NAVAL POSTGRADUATE SCHOOL MIDDLE ULTRAVIOLET SPECTROGRAPH AND AN ANALYSIS OF THE OII 2470 A EMISSION OBTAINED BY THE MIDDLE ULTRAVIOLET SPECTROGRAPH M.S. Thesis
Hewitt M. Hymas Jun. 1994 72 p
(AD-A283449) Avail: CASI HC A04/MF A01

The NPS middle ultraviolet spectrograph, MUSTANG, instrument was tested using standard techniques to determine the wavelength calibration and overall sensitivity. The instrument was launched on March 10, 1994 on a NASA sounding rocket from Poker Flats, Alaska. Post-flight calibration indicates the wavelength calibration did not change as a result of the launch and no significant change in the sensitivity calibration. Ultraviolet dayglow spectra of the earth's ionosphere from 1800 A to 3400 A were obtained during a similar launch on March 19, 1992 from White Sands Missile Range, New Mexico. Data were obtained on the downleg of this earlier experiment and range in altitude from 115 km to 320 km. Analysis of the data from 2420 A to 2490 A was conducted to obtain the intensity profile of the OII 2470.4 A multiplet. The analysis used synthetic spectra generated for the N2 Vegard-Kaplan and the nitric-oxide gamma band emissions. DTIC

71 ACOUSTICS

Includes sound generation, transmission and attenuation. For noise pollution see *45 Environmental Pollution.*

N95-11856# Washington Univ., Seattle, WA. Applied Physics Lab.
SYNCHRONOUS PICOSECOND SONOLUMINESCENCE Annual Summary Report, 31 May 1993 - 1 Jun. 1994
Lawrence A. Crum 7 Jul. 1994 36 p
(Contract N00014-93-1-0322)
(AD-A281498) Avail: CASI HC A03/MF A01

If acoustic cavitation is produced in a liquid, the implosion of cavities can heat the internal contents of the bubble to incandescent temperatures. The electromagnetic emissions associated with this energy concentration can often be seen with the naked eye. This phenomenon, in which light is generated by sound, is called sonoluminescence. A particular form of this phenomenon is called single-bubble sonoluminescence. This form is much easier to study because the fundamental bubble dynamics that lead to bubble collapse and the associated electromagnetic emissions can be ascertained. Also, in single bubble sonoluminescence it is likely that the bubble collapse is spherically symmetric, resulting in an amplification of this already violent phenomenon. The intent of this project is to investigate the phenomenon of single bubble sonoluminescence, and from knowledge gained here, to be able to provide useful information concerning the more general phenomenon of multiple-bubble sonoluminescence. DTIC

N95-11906# National Inst. of Standards and Technology, Gaithersburg, MD. Ultrasonics Group.
NIST CALIBRATION OF ASTM E127-TYPE ULTRASONIC REFERENCE BLOCKS
J. A. Slotwinski and G. V. Blessing May 1994 49 p See also PB-258105
(PB94-191640; NISTIR-5430) Avail: CASI HC A03/MF A01

This document describes the procedures and instrumentation used by the National Institute of Standards and Technology (NIST) in calibrating aluminum ultrasonic reference blocks. The Ultrasonics Group performs this calibration service for technological and industrial customers The calibration is based on the American Society of Testing and Materials (ASTM) recognized practice for calibrating aluminum reference blocks, designated E127-92a. Instructions for requesting calibrations of ultrasonic rsference blocks are contained in Appendix 1 of this document. The NIST ultrasonic reference block calibration service was originated in the late 1970's, and is described in the NBS Technical Note 924 (PB258105). At that time, the application of one master block for use as a reference standard was considered to be a temporary or interim measure. Today NIST uses this master block to set the ultrasonic system sensitivity in all calibrations of ultrasonic reference block sets. In addition, there are several newly implemented practices employed for checking the calibration system characteristics, both over a period of years and in preparation for a particular calibration. This current document updates the NBS Technical Note 924 in describing these practices for our calibration procedure. NTIS

N95-12013# Polish Academy of Sciences, Warsaw (Poland). Inst. Podstawowych Problemow Techniki.
SOUND EMISSION IN MATERIALS AND CONSTRUCTION ELEMENT TESTING [SCHALLEMISSION IN STOFF-UND BAUELEMENTENPRUFUNG]
Jerzy Ranachowski and Feliks Rejmund 1993 30 p In GERMAN
(ISSN 0208-5658)
Avail: CASI HC A03/MF A01

This research paper is the first Polish article on application of sound emissions for studying materials and construction elements. Using measurement apparatus developed and manufactured at IPPT.PAN results are presented and information is presented about measurement methods. Research is divided into six classifications: investigation of construction ceramics, superconducting ceramics, metals, concrete, and concrete construction elements. Lesser known areas include measurement of bones using sound emission and electrical properties in ceramics and composites under mechanical loading. Author (revised)

N95-12341*# National Aeronautics and Space Administration. Langley Research Center, Hampton, VA.
EN ROUTE NOISE LEVELS FROM PROPFAN TEST ASSESSMENT AIRPLANE
Donald P. Garber (Lockheed Engineering and Sciences Co., Hampton, VA.) and William L. Willshire, Jr. Sep. 1994 32 p
(RTOP 535-03-11-02)
(NASA-TP-3451; L-17339; NAS 1.60-3451) Avail: CASI HC A03/MF A01

The en route noise test was designed to characterize propagation of propfan noise from cruise altitudes to the ground. In-flight measurements of propfan source levels and directional patterns were made by a chase plane flying in formation with the propfan test assessment (PTA) airplane. Ground noise measurements were taken during repeated flights over a distributed microphone array. The microphone array on the ground was used to provide ensemble-averaged estimates of mean flyover noise levels, establish confidence limits for those means, and measure propagation-induced noise variability. Even for identical nominal cruise conditions, peak sound levels for individual overflights varied substantially about the average, particularly when overflights were performed on different days. Large day-to-day variations in peak level measurements appeared to be caused by large day-to-day differences in propagation conditions and tended to obscure small variations arising from operating conditions. A parametric evaluation of the sensitivity of this prediction method to weather measurement and source level uncertainties was also performed. In general, predictions showed good agreement with measurements. However, the method was unable to predict short-term variability of ensemble-averaged data within individual overflights. Although variations in absorption appear to be the dominant factor in variations of peak sound levels recorded on the ground, accurate predictions of those levels require that a complete description of operational conditions be taken into account. The comprehensive and integrated methods presented in this paper have adequately predicted ground-measured sound levels. On average, peak sound levels were predicted within 3 dB for each of the three different cruise conditions. Author

N95-12396 Naval Research Lab., Washington, DC.
UNIFORM SPECTRAL AMPLITUDE WINDOWING FOR HYPERBOLIC FREQUENCY MODULATED WAVEFORMS Report, 1 Dec. 1993 - 20 Jan. 1994
David M. Drumheller 11 Jul. 1994 12 p Limited Reproducibility: More than 20% of this document may be affected by microfiche quality
(DA Proj. RJ1-4-B-87)
(AD-A282508; NRL/FR/7140-94-9713) Avail: CASI HC A03

The hyperbolic frequency-modulated (HFM) waveform has been used in experimental and scientific low-frequency sonar systems because it possesses the pulse compression property and is Doppler-tolerant. This report presents a class of HFM waveforms that possess a flat spectrum, and as such is useful for the direct measurement of a target frequency response and the development of classification algorithms. DTIC

N95-12597# National Defence Research Establishment, Stockholm (Sweden). Dept. of Weapon Systems, Effects and Protection.
STUDY OF ADAPTIVE HIGH RESOLUTION FREQUENCY ESTIMATION TECHNIQUES WITH HYDROACOUSTICAL APPLICATIONS
P. Sundstroem Mar. 1994 92 p
(PB94-179512; FOA-C-20970-2.2) Avail: CASI HC A05/MF A01

The problem under consideration in this master's thesis is the estimation of sinusoids in noise, especially in the context of hydroacoustical applications. The emphasis is on adaptive high resolution frequency estimation methods based on the signal subspace approach. For comparative reasons the authors have, however, included a section treating a traditional way of frequency estimation whose main feature is the fitting of an auto regressive process to the data. A new method for extracting frequencies from a subspace is derived. This method is closely related to the well-known Esprit (Estimating of Signal Parameters via Rotational Invariance Techniques) method for frequency estimation, but has the advantage that it uses only real numbers in the computations. Thereafter, thorough analysis of a few ways of estimating subspaces are performed and extensive simulation results are presented, both for the case of computer generated data and for the case of live data. A class of algorithms, that in this work has shown to be superior in performance compared to the traditional autoregressive fitting

method, is presented as a new way of estimating frequencies in noise. An algorithm from this class is named a TRE (Total Least Squares Real Esprit) algorithm and consists of a subspace approximation technique of choice and the real Esprit method for the extraction of the desired frequencies. NTIS

N95-13154 Department of the Navy, Washington, DC.
WELD ACOUSTIC MONITOR Patent
Richard A. Morris, inventor (to Navy), Ronald C. Tate, inventor (to Navy), and Milton A. Matteson, inventor (to Navy) 26 Apr. 1994 7 p Filed 31 Jul. 1992
(AD-D016400; US-Patent-5,306,893; US-Patent-Appl-SN-922425; US-Patent-Class-219-130) Avail: US Patent and Trademark Office

A system for real-time analysis of weld quality in an arc welding process is discussed. The system includes a transducer which receives acoustic signals generated during the welding process. The acoustic signals are then sampled and digitized. A signal processor calculates the root mean square and peak amplitudes of the digitized signals and transforms the digitized signal into a frequency domain signal. A data processor divides the frequency domain signal into a plurality of frequency bands and calculates the average power for each band. The average power values, in addition to the peak and root mean square amplitude values, are input to an artificial neural network for analysis of weld quality. Arc current and/or arc voltage signals may be input to the A/D converter alone or in combination with the acoustic signal data for subsequent signal processing and neural network analysis. DTIC

N95-13575 DELAB, Trondheim (Norway).
RESPONSE TO NOISE AROUND VAERNES AND BODOE AIRPORTS
T. Gjestland, I. L. N. Granoeien, and K. H. Liasjoe 31 Dec. 1993 63 p
(PB94-207065; STF40-A93136) Avail: Issuing Activity (National Technical Information Service (NTIS))

The report presents the results from social surveys around two airports in Norway. The traffic at these airports consists of a mix of civil and military aircraft. The survey includes three military aircraft exercises with a significant increase in the daily noise levels. These exercises do not seem to alter the respondents' general assessment of noise annoyance. NTIS

72 ATOMIC AND MOLECULAR PHYSICS

Includes atomic structure, electron properties, and molecular spectra.

N95-11747# Kiev Univ. (USSR). Inst. Yadernykh Issledovanij.
SMALL ANGLE NEUTRON SCATTERING IN SURFACE-ACTIVE AGENTS MIXTURES
L. A. Bulavin, V. M. Garamus, and Yu. M. Ostanevich 1993 8 p
(DE94-624057; KIYal-93-3) Avail: CASI HC A02/MF A01 (US Sales Only)

The method of study of micelle structure by small angle neutron scattering is studied. The determination of maximum size, radius of gyration, average scattering density of micelles is presented. The way of study of distribution of scattering density in micelle is described. The problem of micelles interaction is discussed. DOE

N95-11791# Lawrence Livermore National Lab., Livermore, CA. Chemistry and Materials Science Dept.
STRUCTURE AND PERFORMANCE OF CARBON AEROGEL ELECTRODES
R. W. Pekala, S. T. Mayer, J. F. Poco, and J. L. Kaschmitter Mar. 1994 10 p Presented at the Spring Meeting of the Materials Research Society, San Francisco, CA, 4-8 Apr. 1994
(Contract W-7405-eng-48)
(DE94-014746; UCRL-JC-116422; CONF-940411-39) Avail: CASI HC A02/MF A01

The chemistry and physics of small clusters of atoms (1-100 nm) has received considerable attention in recent years because these assemblies often have properties between the molecular and bulk solid-state limits. The different properties can be explained in terms of the large fraction of atoms that are at the surface of a cluster as compared to the interior. Although the synthesis and properties of metal and semiconductor clusters, metallocarbohedrenes, fullerenes, and nanotubes are the subject of extensive investigations, little attention has been paid to cluster-assembled porous materials. This oversight is of particular interest to us since we believe that aerogels are one of the few monolithic materials presently available where the benefits of cluster assembly can be demonstrated. In particular, the unique optical, thermal, acoustic, mechanical, and electrical properties of aerogels are directly related to their nanostructure, which is composed of interconnected particles (3-30 nm) with small interstitial pores (less than 50 nm). This structure leads to extremely high surface areas (400-1100 m(exp 2)/g) with a large fraction of the atoms covering the surface of the interconnected particles. As a result of these structural features, carbon aerogels are finding applications as electrodes in supercapacitors with high energy and power densities. DOE

N95-11817# Kyoto Univ., Kumatori (Japan). Research Reactor Inst.
RADIATION-INDUCED STRUCTURAL CHANGES, 4
Yoshimasa Hama, ed. (Waseda Univ., Tokyo, Japan.), Tomochika Matsuyama, ed., and Masaaki Ogasawara, ed. Oct. 1993 53 p
(DE94-753223; KURRI-TR-383) Avail: CASI HC A04/MF A01

This seminar was held for discussion on recent progress in experimental investigation of positron and its application to material science. Fundamental characteristics of positronium, measuring method, molecular structure of positronium, and its annihilation and reaction, in liquid phase positronium chemistry are reported. The nonthermal positrons (0.25-2.5 keV) are occurred in KURRI-LINAC, slow positrons are found out by moderating with solid xenon film. Positronium formation in insulating materials are reported. Positron lifetime and insulating rupture strength are measured with epoxy resin and fluororesin changing bridging density, experimental materials temperature, gamma ray dose Free-volume studies on polymer in multiphase systems are evaluated using the method of spin labeling, the molecular dynamics of polymer chains are discussed. The anisotropy diffusion process on structural relaxation of linear polymers are described, introducing the molecular dynamics simulation of polarization and stress relaxation of ferroelectric polymers. DOE

N95-11818# Kyoto Univ., Uji (Japan). Inst. for Theoretical Physics.
CONTRIBUTION OF HADRONIC INTERMEDIATE STATES IN NONLEPTONIC WEAK DECAYS OF K, CHARM AND B MESONS
K. Terasaki Jun. 1993 32 p
(DE94-753399; YITP/U-93-16) Avail: CASI HC A03/MF A01

We demonstrate that contributions of hadronic intermediate states are important in nonleptonic weak decays of K and charm mesons. Among various hadrons, exotic mesons can play an essential role in charm meson decays and also in the small violation of the so-called (Delta)I = 1/2 rule in K (yields) (pi)(pi) decays. The same technique is applied to B meson decays. DOE

N95-11828 Case Western Reserve Univ., Cleveland, OH. Dept. of Macromolecular Science.
CHIRAL RECOGNITION IN MOLECULAR AND MACROMOLECULAR PAIRS OF (S)- AND (R)-1-CYANO-2-METHYLPROPYL 4'(4-(8-VINYLOXYOCTYLOXY)BENZOYL) BIPHENYL-4-CARBOXYLATE ENANTIOMERS Report No. 10
V. Percec and Q. Zheng 30 Jun. 1994 57 p Limited Reproducibility: More than 20% of this document may be affected by microfiche quality
(Contract N00014-89-J-1828)
(AD-A281438) Avail: CASI HC A04

In the field of liquid crystals chiral molecular recognition was observed in various layered phases of enantiomeric pairs of low molar mass liquid crystals, although very little understanding of the influence of structural parameters on its manifestation is available. Molecular recognition in enantiomeric and diasteromeric pairs of macromolecular liquid crystals has not been studied, mainly because of the lack of the techniques available to synthesize enantiomeric and diastereomeric pairs of liquid crystalline polymers with well controlled molecular weight and narrow molecular weight distribution. Recently we initiated a systematic series of investigations on the chiral molecular recognition by studying the relationship between molecular, macromolecular and supramolecular structures and the extent of manifestation of heterochiral recognition. The methodology used in our research involves the synthesis of enantiomeric and diastereomeric mesogenic vinyl ethers and of the corresponding homopolymers and copolymers by living cationic polymerization and copolymerization reactions.

Living cationic polymerization provides homogeneous polymers and copolymers with well controlled molecular weight, composition and narrow molecular weight distribution. DTIC

N95-11851# Kansas State Univ., Manhattan, KS. Dept. of Chemistry.
SCANNING TUNNELING MICROSCOPY/ATOMIC FORCE MICROSCOPY FOR STUDY OF NANOSCALE METAL OXIDE PARTICLES (DESTRUCTIVE ADSORBENTS) Final Report, 1 Sep. 1993 - 31 Aug. 1994
Kenneth J. Klabunde and Dong Park 15 Jun. 1994 9 p
(Contract DAAH04-93-G-0457)
(AD-A281417; ARO-32398.1-CH-DPS) Avail: CASI HC A02/MF A01

A modern scanning tunneling microscopy/atomic force microscopy instrument was purchased. This instrument is allowing physical characterization of nanoscale particles of metal oxides. These particles are known to be effective reagents for the destruction of military toxins as well as chlorocarbons by a process we call destructive adsorption. DTIC

N95-11894 Los Alamos National Lab., NM.
THE CASCADE-DEUTERON SYSTEM
S. B. Carr, I. R. Afnan, and B. F. Gibson 1994 3 p Presented at the International Conference on Hypernuclear and Strange Particle Physics, Vancouver, Ontario, 4-8 Jul. 1994 Limited Reproducibility: More than 20% of this document may be affected by microfiche quality
(Contract W-7405-eng-36)
(DE94-011650; LA-UR-94-1175; CONF-940725-1) Avail: CASI HC A01

Recently there has been considerable speculation about the possible existence of the 'H' dibaryon, as a deeply bound six quark state. This in turn has generated considerable interest in doubly strange Lambda(Lambda) hypernuclei such as sub Lambda(Lambda)-He-6 would argue strongly against the existence of a deeply bound 'H'. To examine this problem, we have considered the interaction of a Xi hyperon with a deuteron in a full three-body analysis. We have included coupling between the Xi - N and the Lambda - Lambda channels within the framework of separable two-body interactions. Ultimately, we will perform the full break-up calculations with the hope of shedding some light on the interpretation of the neutron spectrum observed in Xi(-) capture on the deuteron. We present an outline of how we derived the AGS equations for the Xi(N)N system. DOE

N95-12012# Brookhaven National Lab., Upton, NY.
STRANGE HADRONIC MATTER
C. B. Dover, D. J. Millener, A. Gal, C. Greiner, J. Schaffner, and H. Stoecker Sep. 1993 5 p Presented at the 13th International Conference on Particles and Nuclei, Perugia, Italy, 27 Jun. - 3 Jul. 1993
(Contract DE-AC02-76CH-00016)
(DE94-001493; BNL-49500; CONF-930637-8) Avail: CASI HC A01/MF A01

The authors have investigated the domain of stability of multi-strange hadronic systems, made up of nucleons and hyperons (p, n, (Lambda), (Xi)(sup 0), (Xi)(sup (minus))) in a relativistic mean field approach. They find a large class of such objects which are stable against strong decay, including the bulk limit A (yields) (infinity). Using interactions tailored to reproduce the observed binding energies of (Lambda), (Xi) and (Lambda)(Lambda) hypernuclei, they estimate binding energies per baryon as large as E(sub B)/A (approx) (minus)22 MeV, with large strangeness per baryon f(sub s) (approx) 1-1.2 and small charge per baryon f(sub q) (approx) (minus)0.1 to 0. These multi-strange systems have typical baryon densities of 2-3 times that of ordinary nuclear matter. DOE

N95-12101# Polish Academy of Sciences, Warsaw (Poland). Inst. of Basic Problems of Technology.
THE FIELD EMISSION OF ELECTRONS IN VACUUM INSULATION SYSTEMS [EMISJA POLOWA ELEKTRONOW W PROZNIOWYCH UKLADACH IZOLACYJNYCH]
Wladyslaw Opydo (Poznan Technical Univ., Poland.) and Jerzy Ranachowski 1992 15 p
(ISSN 0208-5658)
Avail: CASI HC A03/MF A01

This article presents an overview of the field electron emission mechanisms which may occur in practical vacuum insulation systems. In addition to the mechanism of field electron emission from microscopic bulges on the cathode surface, the authors discuss the relatively new subject of field electron emission from nonmetallic microcraters in the surface of the cathode. Considering the need for a certain amount of standardization, the authors present the basic equations which they used to determine the electron emission characteristics of the surface of the cathode on the basis of the ampere-voltage characteristic of the insulation system, i.e. the gain factor for electrical field strength amplified by electron-emitting microscopic cathode surface irregularities and the field of the electron-emitting surface. Author

N95-12365 Rutherford Appleton Lab., Chilton (England).
MUON SITES AND ELECTRONIC STRUCTURE
S. F. J. Cox Mar. 1994 22 p
(PB94-179348; RAL-94-034) Avail: Issuing Activity (National Technical Information Service (NTIS))

The lecture concerns the sites adopted by positive muons implanted in different materials. It examines how the nature of the material determines the muons' environment, as relevant to micro-SR studies. The terms muon state or muonium state are often used (these are not to be confused with the spin states). The guiding principle is that muons, likes protons, cannot remain as the free particles once thermalized in matter, whether in gases, liquids, or solids. They seek to lower their energy by association with electrons, in inert materials by the formation of muonium - the bound state with a single electron - and in more reactive hosts by becoming intimately incorporated into the structure of the lattices or molecules. Physicists refer to this as localization and local electronic structure; chemists refer to it simply as bonding. Analogies with the chemical behavior of protons or atomic hydrogen are invaluable, provided proper account is taken of the larger zero-point energy of the muon when confined or bound. The relevant properties of atomic muonium are given, followed by a description of how these are modified in various hosts: dielectric, semiconducting, molecular, and metallic. The various possibilities are well illustrated by the muonium states observed in the different allotropes of carbon. NTIS

N95-12369# Fermi National Accelerator Lab., Batavia, IL.
SEARCH FOR SUPERSYMMETRY AT CDF
May 1994 11 p Presented at the 27th International Conference on High Energy Physics, Glasgow, Scotland, 21-27 Jul. 1994
(Contract DE-AC02-76CH-03000)
(DE94-014264; FNAL/C-94/149-E; CONF-940722-6) Avail: CASI HC A03/MF A01

We have conducted a search for trilepton events from supersymmetry (SUSY) in p(bar p) collisions at radical s = 1.8 TeV. In the minimal supersymmetric standard model (MSSM), trilepton events are expected from chargino-neutralino ((tilde chi)(sub 1)(sup +/-)(tilde chi)(sub 2)(sup 0)) pair production, with subsequent decay into leptons. In all possible combinations of electron and muon channels in 19 pb(sup -1) data, we observe no events which pass our trilepton selection criteria. Employing the GUT hypothesis within the framework of the MSSM, our preliminary analysis excludes M((tilde chi)(sub 1)(sup +/-)) less than 46 GeV/c(exp 2) for -500 less than mu less than -400 GeV, 2.0 less than tan(beta) less than 15.0, and M(tilde q) = 1.2 x M(tilde g). DOE

N95-12370# Fermi National Accelerator Lab., Batavia, IL.
MEASUREMENT OF THE POLARIZATION IN THE DECAY B(EXP 0) YIELDS J/PSI K(EXP *0) IN (BAR p)p COLLISIONS AT THE SQUARE ROOT OF s = 1.8 TeV
26 May 1994 10 p Presented at the 27th International Conference on High Energy Physics, Glasgow, Scotland, 21-27 Jul. 1994
(Contract DE-AC02-76CH-03000)
(DE94-014265; FNAL/C-94/127-E; CONF-940722-3) Avail: CASI HC A02/MF A01

This paper reports on the measurement of the polarization in the decay B(exp 0) yields J/psi K(exp *0) using data collected at the collider detector at Fermilab in (bar p)p collisions at square root of s = 1.8 TeV. B(exp 0) mesons were reconstructed through the decay chain B(exp 0) yields J/psi K(exp *0), J/psi yields mu(+)mu(-), K(exp *0) yields K(+)pi(-). A sample of 50 +/- 11 events was used in the measurement, yielding the result Gamma(sub L)/Gamma = 0.66 +/- 0.10 (stat) (sub -0.10) (sup +0.08) (sys). DOE

N95-12522# Case Western Reserve Univ., Cleveland, OH. Dept. of Macromolecular Science.

POLYMER EFFECT ON HETEROCHIRAL MOLECULAR RECOGNITION IN MOLECULAR AND MACROMOLECULAR PAIRS OF LIQUID CRYSTALS OF (R)- AND (S)-2-CHLORO-4-METHYLPENTYL 4'-((8-(VINYLOXY)OCTYL)OXY)BIPHENYL-4-CAROXYLATE ENANTIOMERS

Virgil Percec and Hiroji Oda 30 Jun. 1994 53 p

(Contract N00014-89-J-1828)

(AD-A281193) Avail: CASI HC A04/MF A01

(R)-2-Chloro-4-methylpentyl 4'-(8-vinyl oxy octyl oxy) biphenyl-4-carboxylate ((R)-8) (R greater than 95%) and (S)-2 Chloro-4-methylpentyl 4'-(8-vinyl oxy octyl oxy) biphenyl-4- carboxylate ((S)-8) (S greater than 95%) enantiomers and their corresponding homopolymers and copolymers with well defined molecular weight and narrow molecular weight distribution were synthesized and characterized. The phase behaviors of (R)-8 and poly ((R)-8) are identical to those of (S)-8 and poly ((S)-8) respectively. Both monomers display monotropic SA and SC* phases and a crystalline phase, while the corresponding polymers exhibit enantiotropic SA, SC*, and SX (unidentified smectic) mesophases. The SA-I transition of the binary mixture of (R)-8 with (S)-8 is 0.4 C higher in the 50/50 mixture than the theoretical value expected for an ideal solution, demonstrating the presence of heterochiral molecular recognition between the two enantiomers in their SA phase. Heterochiral recognition was not detected in the SC* phase of any of the enantiomeric pairs investigated. In the polymer mixtures, the chiral recognition observed in the SA phase of the monomer mixtures is enhanced with increasing the degree of polymerization (DP) up to about 10 to reach a positive deviation of 1.3 C from the theoretical ideal value.

DTIC

N95-12617 Pennsylvania State Univ., University Park, PA. Dept. of Chemistry.

ATOMIC SCALE DYNAMICS OF A TWO-DIMENSIONAL GAS-SOLID INTERFACE Technical Report No. 16, 1 Jun. 1994 - 31 May 1995

S. J. Stranick, M. M. Kamna, and P. S. Weiss 3 Jun. 1994 14 p Limited Reproducibility: More than 20% of this document may be affected by microfiche quality

(Contract N00014-91-J-1630)

(AD-A282646) Avail: CASI HC A03

We have imaged the interface between a two-dimensional molecular gas and a two-dimensional molecular solid using a low temperature ultrahigh vacuum scanning tunneling microscope. The solid consists of benzene molecules strongly bound to step edges on a Cu(111) surface. These benzene molecules on the Cu(111) terraces move freely as a two-dimensional gas at 77K. We observed exchange between the two phases at the interface and the transient occupation of well defined sites at this interface. On mesas of the Cu surface, the two-dimensional gas is held in a cage of the solid as in a two-dimensional nanometer scale gas bulb.

DTIC

N95-12829# Brookhaven National Lab., Upton, NY.

RESONANT X-RAY SCATTERING IN 5f MAGNETISM

G. H. Lander (Joint Research Centre of the European Communities, Karlsruhe, Karlsruhe, Germany.), W. G. Stirling (Keele Univ., England.), S. Langridge (Keele Univ., England.), and D. Gibbs 1994 15 p Presented at the International Conference on Magnetism, Warsaw, Poland, 22-26 Aug. 1994

(Contract DE-AC02-76CH-00016)

(DE94-013753; BNL-60451; CONF-940819-1) Avail: CASI HC A03/MF A01

Large enhancements of the magnetic cross section of photons occurs when the energy is tuned near to an absorption edge. Examples of this effect in the actinides at the M(sub IV) edge are presented. The excellent resolution available with x-ray synchrotron beams has allowed new features in both the magnetic structure and the critical regime to be determined. The technique is also sensitive to the near-surface region. Some of the possibilities with the new 3rd-generation synchrotrons will be discussed.

DOE

N95-12882 Florida Univ., Gainesville, FL. Quantum Theory Project.

PROCEEDINGS OF US-LATIN AMERICAN WORKSHOP ON MOLECULAR AND MATERIALS SCIENCES: THEORETICAL AND COMPUTATIONAL ASPECTS

David A. Micha 9 Aug. 1994 50 p Workshop held in Gainesville, FL, 10-12 Mar. 1993 Limited Reproducibility: More than 20% of this document may be affected by microfiche quality

(Contract N00014-91-1-0199)

(AD-A283359; TR-1) Avail: CASI HC A03

This workshop has been made possible by the financial support of the US National Science Foundation, International Programs Division, and by the Office of Naval Research, Physics Division. The early support by the ONR was essential in the beginning stages of the workshop organization; the NSF was very helpful speeding up their reviewing procedure to provide support on a tight schedule. The University of Florida, through its Departments of Chemistry and of Physics, and its Quantum Theory Project, provided help with its staff and with funds at critical times. The workshop attendants from Latin American countries helped this gathering in a very important way, by requesting and obtaining matching funds at their home institutions to travel to the USA. The program of the workshop evolved in response to suggestions from its participants. To begin with, it was decided to organize a short course on molecular and materials sciences based mostly on lectures by the Faculty of the Quantum Theory Project and other US institutions, and to request suggestions on its content from Latin American scientists associated to the University of Florida in past years' activities. These suggestions indicated a wish for additional contributions by participants in an informal conference format. The present programs combine the two aims, with a series of half hour overviews followed by long discussions with the participation of the attendants, and with half hour presentations by the attendants on subjects of their disciplines.

DTIC

N95-12905# Fermi National Accelerator Lab., Batavia, IL.

SCINTILLATING FIBER DETECTOR PERFORMANCE, DETECTOR GEOMETRIES, TRIGGER, AND ELECTRONICS ISSUES FOR SCINTILLATING FIBER TRACKING

A. E. Baumbaugh Jun. 1994 9 p Presented at the 6th Pisa Meeting on Advanced Detectors, Elba, Italy, 22-28 May 1994

(Contract DE-AC02-76CH-03000)

(DE94-015525; FNAL/C-94/183; CONF-9405168-4) Avail: CASI HC A02/MF A01

Scintillating fiber tracking technology has made great advances and has demonstrated great potential for high speed charged particle tracking and triggering. The small detector sizes and fast scintillation fluors available make them very promising for use at high luminosity experiments at today's and tomorrow's colliding and fixed target experiments where high rate capability is essential. This talk will discuss the current state of Scintillating fiber performance and current Visual Light Photon Counter (VLPC) characteristics. The primary topic will be some of the system design and integration issues which should be considered by anyone attempting to design a scintillating fiber tracking system which includes a high speed tracking trigger. Design constraints placed upon the detector system by the electronics and mechanical sub-systems will be discussed. Seemingly simple and unrelated decisions can have far reaching effects on overall system performance. SDC and DO example system designs will be discussed.

DOE

N95-12943# Fermi National Accelerator Lab., Batavia, IL.

INCLUSIVE JET AND TWO-JET DIFFERENTIAL CROSS SECTIONS AT CDF

Jun. 1994 13 p Presented at the 27th International Conference on High Energy Physics, Glasgow, Scotland, 21-27 Jul. 1994

(Contract DE-AC02-76CH-03000)

(DE94-015543; FNAL/C-94/159-E; CONF-940722-16) Avail: CASI HC A03/MF A01

The CDF collaboration collected 19.5 pb(sup -1) of data during the 1992-93 collider run at Fermilab. Using these data the inclusive jet cross section is measured in the pseudorapidity (eta) range 0.1-0.7. The transverse energy (E(sub T)) range of the jets extends from 15 to 440 GeV. The measured cross section is compared with next-to-leading order (Omicron(alpha(sub s)(sup 3))) QCD predictions for various parton distributions and different choices of renormalization scale. A new limit on

Lambda(sub c), a term representing quark substructure, is derived. The two-jet differential cross section is measured by determining the E(sub T) spectrum of central jets (0.1 less than the absolute value of eta less than 0.7) for different eta intervals of the second jet which span the range 0.1 less than the absolute value of eta less than 3.0. The results are compared with leading order QCD calculations. DOE

N95-13104# Los Alamos National Lab., NM.
PARTICLE-PRODUCTION MECHANISM IN RELATIVISTIC HEAVY-ION COLLISIONS
B. W. Bush and J. R. Nix 1994 10 p Presented at the 7th International Conference on Nuclear Reaction Mechanisms, Vaienna, Italy, 6-11 Jun. 1994
(Contract W-7405-eng-36)
(DE94-014427; LA-UR-94-2179; CONF-9406200-1) Avail: CASI HC A02/MF A01

We discuss the production of particles in relativistic heavy-ion collisions through the mechanism of massive bremsstrahlung, in which massive mesons are emitted during rapid nucleon acceleration. This mechanism is described within the framework of classical hadrodynamics for extended nucleons, corresponding to nucleons of finite size interacting with massive meson fields. This new theory provides a natural covariant microscopic approach to relativistic heavy-ion collisions that includes automatically spacetime nonlocality and retardation, nonequilibrium phenomena, interactions among all nucleons, and particle production. Inclusion of the finite nucleon size cures the difficulties with preacceleration and runaway solutions that have plagued the classical theory of self-interacting point particles. For the soft reactions that dominate nucleon-nucleon collisions, a significant fraction of the incident center-of-mass energy is radiated through massive bremsstrahlung. In the present version of the theory, this radiated energy is in the form of neutral scalar (sigma) and neutral vector (omega) mesons, which subsequently decay primarily into pions with some photons also. Additional meson fields that are known to be important from nucleon-nucleon scattering experiments should be incorporated in the future, in which case the radiated energy would also contain isovector pseudoscalar (pi)(+), (pi)(-), (pi)(0), isovector scalar (delta)(+), (delta)(-), (delta)(0), isovector vector (rho)(+), (rho)(-), (rho)(0), and neutral pseudoscalar (eta) mesons. DOE

N95-13141# Florida Univ., Gainesville, FL. Quantum Theory Project.
US-LATIN AMERICAN WORKSHOP ON MOLECULAR AND MATERIALS SCIENCES: THEORETICAL AND COMPUTATIONAL ASPECTS
David A. Micha 9 Aug. 1994 40 p Workshop held in Gainesville, FL, 8-10 Feb. 1994
(Contract N00014-93-1-0199)
(AD-A283428; TR-2) Avail: CASI HC A03/MF A01

Partial contents include: time-dependent theory of photoabsorption processes; molecular simulation of a chemical reaction in supercritical water; many-body methods for electron correlation; conformational studies of PAF and PAF-antagonists; electric properties of atomic anions; theoretical interpretation of the Li4(-) spectrum using path integrals and ab initio methods; energy levels and structure of tetra-atomic van der Vaals clusters; technology for modern computational science: the John Slater Computing Facility; carbohydrates on the stabilization of biological structures: molecular dynamics simulation; the role of quantum chemistry in heterogeneous catalysis; and corrections to the Born-Oppenheimer approximation by means of perturbation theory. CASI

N95-13160# Fermi National Accelerator Lab., Batavia, IL.
PHOTON PRODUCTION AT CDF AND D0
R. M. Harris Apr. 1994 10 p Presented at the 29th Moriond Meeting on Quantum Chromodynamics and High Energy Hadronic Interactions, Les Arcs, France, 12-26 Mar. 1994
(Contract DE-AC02-76CH-03000)
(DE94-014985; FNAL/C-94/101-E; CONF-940327-6) Avail: CASI HC A02/MF A01

We present measurements of isolated prompt photon production in (bar p)p collisions at (radical)s = 1.8 TeV from the Fermilab experiments CDF and D0. Precision measurements of prompt photon production from CDF constrain the gluon distribution of the proton, and recent results from D0 agree with CDF and QCD. The pseudorapidity distribution of the jet in photon events at CDF is used to constrain parton distributions. Gauge boson (g,(gamma),W) + jet angular distributions at CDF show good agreement with QCD and illustrate the spin of quarks and gluons. Diphoton candidate mass distributions from CDF are used to search for new physics and measure the background to Higgs(yields)(gamma)(gamma). Finally, CDF searches for resonances in the W+jet and -(gamma)+jet mass distributions, and thereby excludes excited states of composite quarks for mass M* less than 540 GeV/c(exp 2) at 95 percent confidence level. DOE

N95-13161# Fermi National Accelerator Lab., Batavia, IL.
A SEARCH FOR A HEAVY NEUTRAL GAUGE BOSON DECAYING INTO DIELECTRONS IN (-p)p COLLISIONS AT THE SQUARE ROOT OF s = 1.8 TeV
Jun. 1994 9 p Presented at the 27th International Conference on High Energy Physics, Glasgow, Scotland, 21-27 Jul. 1994
(Contract DE-AC02-76CH-03000)
(DE94-014987; FNAL/C-94/156-E; CONF-940722-9) Avail: CASI HC A02/MF A01

We have searched for the production of a heavy neutral gauge boson (Zeta)(prime) decaying into dielectrons in (bar p)p collisions at (radical)s = 1.8 TeV. The data are obtained using the CDF detector during 1992-1993 run, and correspond to an integrated luminosity of 19.6 +/- 0.7 pb(exp -1). We present a 95 percent confidence level upper limit on the production cross section times branching ratio of (Zeta)(prime) decaying into dielectrons as a function of (Zeta)(prime) mass. We also present lower mass limits for (Zeta)(prime) bosons using standard model coupling strengths, the predictions of several E(sub 6) models, and the Alternative Left-Right model. DOE

N95-13169# Fermi National Accelerator Lab., Batavia, IL.
MULTI-JET ANALYSIS FOR THE TOP SEARCH AT THE FERMILAB COLLIDER
Jun. 1994 10 p Presented at the 27th International Conference on High Energy Physics, Glasgow, Scotland, 21-27 Jul. 1994
(Contract DE-AC02-76CH-03000)
(DE94-014988; FNAL/C-94/152-E; CONF-940722-8) Avail: CASI HC A02/MF A01

The search for a top signal in the multi-jet sample is presented. The t(anti t) decays considered here are the Standard Model ones in which both W's decay into a quark pair, thus generating a nominal 6-jets topology. Despite the enormous initial background rate, a reasonable signal-to-background ratio has been achieved once the SVX detector is used for b-tagging the events. Application of the method to the existing data set is presented, along with expectations for future runs. DOE

N95-13170# Fermi National Accelerator Lab., Batavia, IL.
A PRECISION MEASUREMENT OF THE PROMPT PHOTON CROSS SECTION IN p(-p) COLLISIONS AT THE SQUARE ROOT OF s = 1.8 TeV
S. E. Kuhlmann (Argonne National Lab., IL.) Jun. 1994 13 p Presented at the 27th International Conference on High Energy Physics, Glasgow, Scotland, 21-27 Jul. 1994
(Contract DE-AC02-76CH-03000)
(DE94-014989; FNAL/C-94/148-E; CONF-940722-10) Avail: CASI HC A03/MF A01

A prompt photon cross section measurement from the CDF experiment at the Fermilab p(bar p) Collider is presented Detector and trigger upgrades, as well as six times the integrated luminosity compared with our previous publication, have contributed to a much more precise measurement and extended P(sub T) range. As before, the cross section agrees qualitatively with QCD calculations but has a steeper slope at low P(sub T). DOE

N95-13173# Argonne National Lab., IL.
ENERGY DISSIPATION BY A LONGITUDINAL RAMAN PROCESS
U. Fano (Chicago Univ., Chicago, IL.) and Mitio Inokuti 1994 8 p
(Contract W-31-109-eng-38)
(DE94-015027; ANL/ER/PP-78774) Avail: CASI HC A02/MF A01

The concept of a longitudinal Raman process is introduced to encompass the indirect transmission of energy from slow electrons to nuclei through the reversible polarization of surrounding electrons. Experimental approaches are sought to assess this process quantitatively. DOE

N95-13178 Oregon State Univ., Corvallis, OR.
MATTER-WAVE INTERFEROMETRY WITH LASER COOLED ATOMS Summary Report
David McIntyre 27 May 1994 3 p Limited Reproducibility: More than 20% of this document may be affected by microfiche quality
(AD-A282484) Avail: Issuing Activity (Defense Technical Information Center (DTIC))

This program is investigating matter-wave interferometry with laser cooled atoms. A slow beam of laser cooled rubidium atoms will be used as the matter-wave source. The atom optical elements are microfabricated amplitude transmission gratings which will be used in a three-grating interferometer to split and recombine the rubidium beam. The interferometer will be a useful new tool for precision atomic physics and a sensitive inertial sensor DTIC

N95-13242 Direction des Recherches, Etudes et Techniques, Paris (France). Centre de Documentation de l'Armement.
POLYATOMIC ION IMPACT ON SOLID SURFACES AND RELATED PHENOMENA [COLLISION D'IONS POLYATOMIQUES AVEC DES SURFACES SOLIDES ET PHENOMENES ASSOCIES]
1994 6 p In FRENCH
(PB94-201258) Avail: Issuing Activity (National Technical Information Service (NTIS))

This report sums up an international, interdisciplinary colloquium entitled Polyatomic Ion Impact on Solids and Related Phenomena, which was held in Saint Malo, France in June of 1993. The common focus of the symposium was the impact of a beam of fast aggregates on a solid surface. The goal was to come up with a few guidelines in choosing projectiles and targets, and to identify the cases in which the use of polyatomic beams is clearly more advantageous than the use of atomic, electron, or photon beams. Participants described the various types of aggregate sources now being used in a wide variety of aggregate beams, and compared models used to simulate the primary and secondary effects of aggregate/target interaction using various incident speeds and target types. Presentations on the secondary emissions and induced flaws of fast aggregates showed there is still much theoretical and experimental work to be done to slow down the electrons of aggregate fragments in matter. The conference highlighted the value of several 'star' aggregates such as buckyballs, metals, hydrogen, and bimolecules. NTIS

N95-13273# Academy of Sciences of the Ukraine, Kiev. Ibnst. Teoreticheskoj Fiziki.
ON THE CHARGED VECTOR PARTICLE SCATTERING ON A VECTOR PARTICLE
V. K. Tartakovskij and V. A. Cherednichenko 1993 21 p
(DE94-622787; ITF-93-26) Avail: CASI HC A03/MF A01 (US Sales Only)

According to the quantum electrodynamics the elastic scattering differential cross-section of the relativistic charged vector particle by the identical and nonidentical ones is obtained in the general explicit form both in an arbitrary coordinate system and in a concrete one. The nonrelativistic and ultrarelativistic limit cases are examined. DOE

N95-13274# Academy of Sciences of the Ukraine, Kiev. Inst. Teoreticheskoj Fiziki.
THE ODDERON IN THE DEEP-INELASTIC LEPTON-HADRON SCATTERING
B. V. Struminskij 1993 5 p
(DE94-622791; ITF-93-29) Avail: CASI HC A01/MF A01 (US Sales Only)

The study of the structure function F(sub 3) for the deep-inelastic neutrino-nucleon scattering in the region of small x can be used in order to determine the odderon parameters. DOE

N95-13275# Academy of Sciences of the Ukraine, Kiev. Inst. Teoreticheskoj Fiziki.
STUDY OF THE NUCLEAR-COULOMB LOW-ENERGY SCATTERING PARAMETERS ON THE BASIS OF THE p-MATRIX APPROACH
V. A. Babenko and N. M. Petrov 1993 11 p
(DE94-622811; ITP-93-60) Avail: CASI HC A03/MF A01 (US Sales Only)

The P-matrix approach application to the description of two charged strongly interacting particles nuclear-Coulomb scattering parameters is considered. The nuclear-Coulomb scattering length and effective range explicit expressions in terms of the P-matrix parameters are found. The nuclear-Coulomb low-energy parameters expansions in powers of small parameter beta identical to R/a(sub b), involving terms with big logarithms, are obtained. The nuclear-Coulomb scattering length and effective range for the square-well and the delta-shell short range potentials are found in an explicit form. DOE

N95-13338# Argonne National Lab., IL.
A BRIGHTNESS COMPARISON OF THERMIONIC ELECTRON SOURCES IN A TEM
R. E. Cook Mar. 1994 3 p Presented at the Microscopy Society of America and Microbeam Analysis Society Joint Meeting, New Orleans, LA, 31 Jul. - 5 Aug. 1994
(Contract W-31-109-eng-38)
(DE94-013300; ANL/MSD/CP-82370; CONF-940753-14) Avail: CASI HC A01/MF A01

In the quest for thermionic electron sources brighter than the standard tungsten filament, manufacturers have given us first LaB(sub 6) and then CeB(sub 6) single crystals. This paper compares these 3 electron sources under typical operating conditions in a Philips EM420T transmission microscope. DOE

N95-13376# South Carolina Univ., Columbia, SC. Dept. of Chemistry.
POTENTIAL MOLECULAR WIRES BY AN ITERATIVE DIVERGENT/CONVERGENT APPROACH. DOUBLING OF MOLECULAR LENGTH AT EACH ITERATION
Darren L. Pearson, Jeffry S. Schumm, LeRoy Jones, II, and James M. Tour 28 Jun. 1994 9 p
(Contract N00014-89-J-3062)
(AD-A281292; TR-37-ONR) Avail: CASI HC A02/MF A01

We have devised an iterative convergent/divergent approach to conjugated oligomers that might serve as molecular wires. The molecular length doubles with each iteration. The systems prepared are completely monodispersed and based upon oligo(thiophene-ethynylene)s (1) and oligo(phenylene-ethynylene)s at 100 A and 128 A long, respectively. The optical and size exclusion chromatography (SEC) properties are discussed. Methods are outlined to attach end groups that might serve as molecular alligator clips. DTIC

N95-13536# China Nuclear Information Centre, Beijing (China).
RESPONSE OF HIGH T(SUB c) SUPERCONDUCTING JOSEPHSON JUNCTION TO NUCLEAR RADIATION
Honglin Ding (Academia Sinica, Beijing, China.), Wanchang Zhang (Academia Sinica, Beijing, China.), and Xiufeng Zhang (Academia Sinica, Beijing, China.) Oct. 1992 11 p
(DE94-624705; CNIC-00682; IAE-0114) Avail: CASI HC A03/MF A01 (US Sales Only)

The development of nuclear radiation detectors and research on high T(sub c) superconducting nuclear radiation detectors are introduced. The emphases are: (1) the principle of using thin-film and thick-film Josephson junctions (bridge junction) based on high T(sub c) YBCO superconductors to detect nuclear radiation; (2) the fabrication of thin film and thick-film Josephson junction; and (3) response of junction to low energy gamma-rays of 59.5 keV emitted from (exp 241)Am and beta-rays of 546 keV. The results show that a detector for measuring nuclear radiation spectrum made of high T(sub c) superconducting thin-film or thick-film, especially, thick-film Josephson junction, certainly can be developed. DOE

73 NUCLEAR AND HIGH-ENERGY PHYSICS

Includes elementary and nuclear particles; and reactor theory. For space radiation see *93 Space Radiation.*

N95-11750# Kyoto Univ., Kumatori (Japan). Research Reactor Inst.
SUMMARY REPORTS OF ACTIVITIES UNDER VISITING RESEARCH PROGRAM, 1993
Oct. 1993 64 p
(DE94-753222; KURRI-TR-381) Avail: CASI HC A04/MF A01

The summary reports of activities under visiting research program in

the Research Reactor Institute, Kyoto University, in fiscal year 1992 are included. In this report, 104 summaries of researches using the Kyoto University Reactor (KUR) and 9 summaries of the researches using the Kyoto University Critical Assembly (KUCA) are collected. DOE

N95-11779# Los Alamos National Lab., NM.
AUTONOMOUS POWER SYSTEM FOR REMOTE LOCATIONS
S. S. Voss, N. W. Brown, V. I. Serbin, I. M. Vishnepolsky, V. I. Korindyasov, and N. Khlopkin 1994 7 p Presented at the 29th Intersociety Energy Conversion Engineering Conference, Monterey, CA, 7-12 Aug. 1994
(Contract W-7405-eng-36)
(DE94-013244; LA-UR-94-1555; CONF-940812-5) Avail: CASI HC A02/MF A01

The Russian technical specialists of Krasnaya Zvezda (Red Star) and Kurchatov Institute of Atomic Energy (KIAE) of Moscow were tasked in the early 1970's to develop a compact, transportable power system that would work reliably and autonomously at remote locations. The original system specifications required that it be able to operate for several years without maintenance in sea water at a depth of 6 km. To meet these requirements the Russia specialists designed a compact nuclear system with water coolant coupled to a thermoelectric power conversion subsystem. The goal was to design a system that was scalable from 300 kWth to 300 MWth. A proof-of-principle system, the GAMMA reactor system, was designed, constructed and tested at KIAE. The system construction was completed in 1981 and testing began the same year. The GAMMA reactor system is still operational today. The follow-on system for remote sites is the ELENA reactor system. It has not been built, but the final assembly drawings have been completed and are ready to be used. The ELENA was designed to provide both direct electric power and local space heating. It can also be used for desalination. The design of the ELENA meets post-Chernobyl safety requirements and includes features to assure its safety under autonomous operation. This paper provides an overview of the GAMMA and ELENA power systems including their design criteria, testing, and transportation to remote sites. It also includes discussion on an evaluation and technology transfer program that could make this system available for use throughout the world. DOE

N95-11792# Maryland Univ., College Park, MD.
BEAMS 92: PROCEEDINGS
D. Mosher, ed. and G. Cooperstein, ed. 1993 704 p Presented at the 9th International Conference on High Power Particle Beams, Washington, DC, 25-29 May 1992
(Contract DE-FG05-92ER-54160)
(DE94-014783; DOE/ER-54160/1-Vol-1; CONF-920515-Vol-1) Avail: CASI HC A99/MF A06

This report contains papers on the following topics: ion beam; electron beam, bremsstrahlung, and diagnostics; radiating Z-pinch; microwaves; electron lasers; advanced accelerators; beam and pulsed power applications; and pulsed power. DOE

N95-11910# Air Force Inst. of Tech., Wright-Patterson AFB, OH.
MIXED CLUSTERS FROM THE COEXPANSION OF C2F6 AND N2 IN A PULSED, SUPERSONIC EXPANSION CLUSTER ION SOURCE AND BEAM DEFLECTION TIME-OF-FLIGHT MASS SPECTROMETER: A FIRST APPLICATION Ph.D. Thesis
Steven D. Thompson 1994 165 p
(AD-A282044; AFIT/CI/CIA-94-012D) Avail: CASI HC A08/MF A02

The following topics are discussed: (1) cluster ion genesis; (2) cluster ion detection; (3) Ion source; (4) pulse valve; (5) e-gun; (6) Ion optics; (7) a first order model; and (8) a modified Bakker's model. DTIC

N95-12102*# Johns Hopkins Univ., Laurel, MD. Applied Physics Lab.
STUDIES OF ELECTROMAGNETIC ION CYCLOTRON WAVES USING AMPTE/CCE AND DYNAMICS EXPLORER Final Report, 1 Jun. 1991 - 31 Aug. 1994
Robert E. Erlandson 31 Aug. 1994 12 p
(Grant NAG5-160-1)
(NASA-CR-196437; NAS 1.26:196437) Avail: CASI HC A03/MF A01

The overall objective of this research is to investigate the generation and propagation of electromagnetic ion cyclotron (EMIC) waves in the frequency range from 0.2 to 5 Hz (Pc 1 frequency band). Data used in this research were acquired by the AMPTE/CCE, DE-1, and DE-2 satellites. One of the primary questions addressed in this research is the role which EMIC waves have on the transfer of energy from the equatorial magnetosphere to the ionosphere. The primary result from this research is that some fraction of EMIC waves, generated in the equatorial magnetosphere, are Landau damped in the ionosphere and are therefore a heat source for ionospheric electrons. This result as well as other results are summarized below. Author

N95-12147*# Alabama Univ., Huntsville, AL. Center for Space Plasma and Aeronomic Research.
RESEARCH ON ORBITAL PLASMA-ELECTRODYNAMICS (ROPE) Progress Report, 27 Mar. - 29 Jun. 1994
S. T. Wu and K. Wright Aug. 1994 44 p Submitted for publication
(Contract NAS8-37107)
(NASA-CR-196929; NAS 1.26:196929) Avail: CASI HC A03/MF A01

Since the development of probe theory by Langmuir and Blodgett, the problem of current collection by a charged spherically or cylindrically symmetric body has been investigated by a number of authors. This paper overviews the development of a fully three-dimensional particle simulation code which can be used to understand the physics of current collection in three dimensions and can be used to analyze data resulting from the future tethered satellite system (TSS). According to the TSS configurations, two types of particle simulation models were constructed: a simple particle simulation (SIPS) and a super particle simulation (SUPS). The models study the electron transient response and its asymptotic behavior around a three dimensional, highly biased satellite. The potential distribution surrounding the satellite is determined by solving Laplace's equation in the SIPS model and by solving Poisson's equation in the SUPS model. Thus, the potential distribution in space is independent of the density distribution of the particles in the SUPS model but it does depend on the density distribution of the particles in the SUPS model. The evolution of the potential distribution in the SUPS model is described. When the spherical satellite is charged to a highly positive potential and immersed in a plasma with a uniform magnetic field, the formation of an electron torus in the equatorial plane (the plane in perpendicular to the magnetic field) and elongation of the torus along the magnetic field are found in both the SIPS and the SUPS models but the shape of the torus is different. The areas of high potential that exist in the polar regions in the SUPS model exaggerate the elongation of the electron torus along the magnetic field. The current collected by the satellite for different magentic field strengths is investigated in both models. Due to the nonlinear effects present in SUPS, the oscillating phenomenon of the current collection curve during the first 10 plasma periods can be seen (this does not appear in SIPS). From the parametric studies, it appears that the oscillating phenomenon of the current collection curve occurs only when the magnetic field strength is less than 0.2 gauss for the present model. Author (revised)

N95-12665*# California Univ., Los Angeles, CA. School of Engineering and Applied Science.
ION ENGINE PROPELLED EARTH-MARS CYCLER WITH NUCLEAR THERMAL PROPELLED TRANSFER VEHICLE, VOLUME 2 Final Report
Rudolf X. Meyer, Myles Baker, and Joseph Melko 1994 64 p Prepared for Universities Space Research Association, Columbia, MD
(Contract NASw-4435)
(NASA-CR-197208; NAS 1.26:197208) Avail: CASI HC A04/MF A01

The goal of this project was to perform a preliminary design of a long term, reusable transportation system between earth and Mars which would be capable of providing both artificial gravity and shelter from solar flare radiation. The heart of this system was assumed to be a Cycler spacecraft propelled by an ion propulsion system. The crew transfer vehicle was designed to be propelled by a nuclear-thermal propulsion system. Several Mars transportation system architectures and their associated space vehicles were designed. Author

74 OPTICS

Includes light phenomena; and optical devices.
For lasers see *36 Lasers and Masers.*

N95-11841# National Inst. of Standards and Technology, Gaithersburg, MD. Radiometric Physics Div.
OPTICAL METROLOGY AND MORE. PROGRAMS AND SERVICES OF THE RADIOMETRIC PHYSICS DIVISION, PHYSICS LABORATORY
S. Bruce May 1994 24 p
(PB94-191707; NISTIR-5429) Avail: CASI HC A03/MF A01

The Radiometric Physics Division is the primary unit within NIST for carrying out the basic mission of promoting accurate and useful optical radiation measurements in the ultraviolet, visible, and infrared regions. This brochure describes the programs and projects that comprise the work represented by this division. NTIS

N95-12390*# Alabama Univ., Huntsville, AL. Center for Applied Optics.
LIDAR PERFORMANCE ANALYSIS Final Report, 23 Oct. 1992 - 22 Nov. 1993
Gary D. Spiers 15 Aug. 1994 75 p
(Contract NAS8-38609)
(NASA-CR-196510; NAS 1.26:196510) Avail: CASI HC A04/MF A01

Section 1 details the theory used to build the lidar model, provides results of using the model to evaluate AEOLUS design instrument designs, and provides snapshots of the visual appearance of the coded model. Appendix A contains a Fortran program to calculate various forms of the refractive index structure function. This program was used to determine the refractive index structure function used in the main lidar simulation code. Appendix B contains a memo on the optimization of the lidar telescope geometry for a line-scan geometry. Appendix C contains the code for the main lidar simulation and brief instruction on running the code. Appendix D contains a Fortran code to calculate the maximum permissible exposure for the eye from the ANSI Z136.1-1992 eye safety standards. Appendix E contains a paper on the eye safety analysis of a space-based coherent lidar presented at the 7th Coherent Laser Radar Applications and Technology Conference, Paris, France, 19-23 July 1993. Derived from text

N95-12415# Air Force Inst. of Tech., Wright-Patterson AFB, OH.
FIBRE OPTIC SENSORS USING ADIABATICALLY TAPERED SINGLE MODE FIBRES Ph.D. Thesis
Zoe M. Hale Feb. 1994 210 p
(AD-A282306; AFIT/CI/CIA-94-011D) Avail: CASI HC A10/MF A03

The ultimate goal of the research presented in this dissertation was to determine if an adiabatically tapered single mode fiber could be used as an effective basis for a chemical or biological sensor. This required a phased investigation examining: (1) The evanescent absorption behavior of the tapered fiber; (2) The fluorescent capture efficiency of the tapered fiber; (3) The effect of immobilizing an indicator to the surface of the tapered fiber; (4) A suitable configuration for the tapered fiber to allow simple application of selective elements as well as interaction with the sample solution; (5) The new configuration in conjunction with a simple immobilization method and model analytes; and (6) The new configuration in conjunction in a realistic chemical or biological assay. DTIC

N95-12427# Army Aeromedical Research Lab., Fort Rucker, AL.
SEMIAUTOMATED METHODOLOGY FOR MEASUREMENT OF FIELD-OF-VIEW, MAGNIFICATION, AND DISTORTION OF NIGHT VISION DEVICES AS DEFINED IN MIL-A-49425(CR) Final Report
John S. Martin, Howard H. Beasley, Robert W. Vernona, and Clarence E. Rash May 1994 59 p
(AD-A282210; USAARL-94-25) Avail: CASI HC A04/MF A01

As new and improved designs for night vision imaging systems based on the principle of image intensification are produced, it is advantageous to have a system which can accurately and quickly assess the performance of various configurations of intensifiers and associated optics. Parameters which define system performance include field-of-view (FOV), magnification, and distortion. The availability of precision positioners and personal computers enable the measurement of performance as specified in Military Specification MIL-A-49425 (CR), Aviator's Night Vision Imaging System AN/AVS-6(V)1. AN/AVS-6(V)2, with a high degree of accuracy and repeatability. A measurement system which provides high flexibility in the evaluation of image intensification devices is described. DTIC

N95-12538 California Univ., Santa Barbara, CA. Dept. of Electrical and Computer Engineering.
STUDIES OF OPTICAL PHASE CONJUGATORS AND APPLICATIONS Final Report, 1 Jul. 1991 - 30 Sep. 1993
Pochi Yeh 30 Sep. 1993 88 p Limited Reproducibility: More than 20% of this document may be affected by microfiche quality
(Grant AF-AFOSR-0299-91)
(AD-A282626; AFOSR-94-0419TR) Avail: CASI HC A05

The main objective of this research is to theoretically investigate the physics of various optical phase conjugation processes (e.g., four-wave mixing, stimulated Brillouin scattering, photorefractive self- or mutually pumped phase conjugators) in nonlinear optical media (photorefractive crystals, optical fibers, etc.), and to explore theoretically and/or experimentally various kinks of applications of optical phase conjugation and nonlinear optical processes. DTIC

N95-12598 Swedish Inst. for Materials Testing, Boras (Sweden).
CALIBRATION OF OPTICAL WAVELENGTH AT 1300 nm AND 1550 nm USING MOLECULAR ABSORPTION LINES [KALIBRERING AV LJUSVAGLAENGD VID 1300 NM OCH 1550 NM MED HJAELP AV MOLEKYLAERA ABSORPTIONSLINJER]
S. Mogren 1994 40 p In SWEDISH
(PB94-180080; SP-RAPP-1994:07) Avail: Issuing Activity (National Technical Information Service (NTIS))

A simple system for the calibration of the wavelength scale of a diffraction grating monochromator, which is used for spectral measurements of laser diode sources in the near infrared region has been developed. The calibration system is based on an absorption cell containing gas molecules as a wavelength standard. The measurement system consists of an edge emitting LED source, connected to a single mode fiber, which radiates the monochromator via the absorption cell. A special coupler, a fiber-cell-fiber with gradient index lenses has been developed for this purpose. A cooled germanium detector is connected to the output slit of the monochromator. The absorption is detected by the connected optical power meter, which transfers the data to a computer for calculation and presentation. Measurements of the absorption of isotopically clean acetylene gas (12)C2H2, in the wavelength region of 1,550 nm and methane gas at a wavelength of 1,300 nm have been done. NTIS

N95-12659*# Hampton Univ., VA. Dept. of Physics
SPACEBORNE PHOTONICS INSTITUTE Final Technical Report
D. D. Venable, U. O. Farrukh, K. S. Han, I. H. Hwang, N. W. Jalufka, C. W. Lowe, B. M. Tabibi, C. J. Lee, D. Lyons, and A. Maclin Jul. 1994 27 p
(Grant NAG1-1091)
(NASA-CR-196784; NAS 1.26:196784) Avail: CASI HC A03/MF A01

This report describes in chronological detail the development of the Spaceborne Photonics Institute as a sustained research effort at Hampton University in the area of optical physics. This provided the research expertise to initiate a PhD program in Physics. Research was carried out in the areas of: (1) modelling of spaceborne solid state laser systems; (2) amplified spontaneous emission in solar pumped iodine lasers; (3) closely simulated AM0 CW solar pumped iodine laser and repeatedly short pulsed iodine laser oscillator; (4) a materials spectroscopy and growth program; and (5) laser induced fluorescence and atomic and molecular spectroscopy. CASI

N95-12736*# Physitron, Inc., Huntsville, AL.
LARGE AREA SOFT X-RAY COLLIMATOR TO FACILITATE X-RAY OPTICS TESTING Semiannual Progress Report, 1 Mar. - 1 Sep. 1994
Samuel L. Espy 27 Sep. 1994 6 p
(NASA Order H-19648-D)
(NASA-CR-196923; NAS 1.26:196923; PHY-94R028) Avail: CASI HC A02/MF A01

The first objective of this program is to design a nested conical foil x-ray optic which will collimate x-rays diverging from a point source. The collimator could then be employed in a small, inexpensive x-ray test stand which would be used to test various x-ray optics and detector systems. The second objective is to demonstrate the fabrication of the x-ray reflectors

for this optic using lacquer-smoothing and zero-stress electroforming techniques. Author (revised)

N95-13106# Los Alamos National Lab., NM.
VISIBLE/INFRARED RADIOMETRIC CALIBRATION STATION
D. A. Byrd, W. B. Maier, II, S. C. Bender, R. F. Holland, F. D. Michaud, A. L. Luettgen, R. W. Christensen, and T. R. OBrian 1994 16 p Presented at the Annual Meeting of the Society of Photo-Optical Instrumentation Engineers, San Diego, CA, 24-29 Jul. 1994
(Contract W-7405-eng-36)
(DE94-014459; LA-UR-94-2127; CONF-940723-3) Avail: CASI HC A03/MF A01

We have begun construction of a visible/infrared radiometric calibration station that will allow for absolute calibration of optical and IR remote sensing instruments with clear apertures less than 16 inches in diameter in a vacuum environment. The calibration station broadband sources will be calibrated at the National Institute of Standards and Technology (NIST) and allow for traceable absolute radiometric calibration to within (+/-) 3 percent in the visible and near IR (0.4-2.5 micrometers), and less than (+/-) 1 percent in the infrared, up to 12 micrometers. Capabilities for placing diffraction limited images or for sensor full-field flooding will exist. The facility will also include the calibration of polarization and spectral effects, spatial resolution, field of view performance, and wavefront characterization. The configuration of the vacuum calibration station consists of an off-axis 21 inch, f/3.2, parabolic collimator with a scanning fold flat in collimated space. The sources are placed, via mechanisms to be described, at the focal plane of the off-axis parabola. Vacuum system pressure will be in the 10(exp -6) Torr range. The broadband white-light source is a custom de sign by LANL with guidance from Labsphere Inc. The continuous operating radiance of the integrating sphere will be from 0.0-0.006 W/sq cm/Sr/micrometer (upper level quoted for (approximately) 500 nm wavelength). The blackbody source is also custom designed at LANL with guidance from NIST. The blackbody temperature will be controllable between 250-350 K. Both of the above sources have 4.1 inch apertures with estimated radiometric instability at less than 1 percent. The designs of each of these units will be described. The monochromator and interferometer light sources are outside the vacuum, but all optical relay and beam shaping optics are enclosed within the vacuum calibration station. These sources are described, as well as the methodology for alignment and characterization. DOE

N95-13248 Technische Univ., Delft (Netherlands).
OBJECT RECOGNITION FOR FLEXIBLE ASSEMBLY USING STEREO VISION Ph.D. Thesis
J. Buurman 6 Dec. 1993 165 p
(PB94-204427; ISBN-90-6275-938-6) Copyright Avail: Issuing Activity (National Technical Information Service (NTIS))

A computer vision system is described for object recognition in a flexible assembly cell. The thesis supplies some background theory on the subjects of stereo vision and recognition. It then introduces the Delft Intelligent Assembly Cell (DIAC) project and states the problem to be solved. Its stereo vision and recognition systems are described individually, and then their combination is evaluated. The acquisition of models is described, either from computer aided design (CAD) models or from a learning procedure using the same stereo vision system and algorithms similar to those in recognition. Finally, the thesis concludes with a discussion of results. NTIS

N95-13374 Northwestern Univ., Evanston, IL.
RATIONAL DESIGN, CONSTRUCTION, AND PROCESSING OF HIGH-PERFORMANCE NONLINEAR, OPTICAL MATERIALS Final Report, 1 Dec. 1992 - 28 Feb. 1994
T. J. Marks, G. K. Wong, and M. A. Ratner 1 Jun. 1994 14 p
Limited Reproducibility: More than 20% of this document may be affected by microfiche quality
(Contract F49620-93-1-0114)
(AD-A281283; AFOSR-94-0416TR) Avail: CASI HC A03

This project consists of a collaborative synthetic, processing, physical characterization, and theoretical program aimed at the rational design, construction, evaluation, and fundamental understanding of new types of maximum-performance molecule/polymer-based materials exhibiting high second-order (X(sup 2)) optical nonlinearities. Areas of emphasis include poled chromophore-functionalized glassy polymers, poled chromophore-embedded crosslinkable matrices, chromophoric self-assembled superlattices, the theoretical design and analysis of novel chromophores and chromophore environments, theoretical studies of poling dynamics, studies of optical damage phenomena, and fabrication of new types of NLO waveguides. Each research component of this highly interactive effort builds upon work already in progress as well as upon strong on-going collaborations in laser optics and quantum theory. DTIC

N95-13421# Oak Ridge National Lab., TN.
EYE-GAZE DETERMINATION OF USER INTENT AT THE COMPUTER INTERFACE
J. H. Goldberg (Pennsylvania State Univ., University Park, PA.) and J. C. Schryver 1993 13 p Presented at the 7th European Eye Movement Conference, Durham, England, 31 Aug. - 3 Sep. 1993
(Contract DE-AC05-84OR-21400)
(DE94-012337; CONF-9308228-1) Avail: CASI HC A03/MF A01

Determination of user intent at the computer interface through eye-gaze monitoring can significantly aid applications for the disabled, as well as telerobotics and process control interfaces. Whereas current eye-gaze control applications are limited to object selection and x/y gazepoint tracking, a methodology was developed here to discriminate a more abstract interface operation: zooming-in or out. This methodology first collects samples of eye-gaze location looking at controlled stimuli, at 30 Hz, just prior to a user's decision to zoom. The sample is broken into data frames, or temporal snapshots. Within a data frame, all spatial samples are connected into a minimum spanning tree, then clustered, according to user defined parameters. Each cluster is mapped to one in the prior data frame, and statistics are computed from each cluster. These characteristics include cluster size, position, and pupil size. A multiple discriminant analysis uses these statistics both within and between data frames to formulate optimal rules for assigning the observations into zooming, zoom-out, or no zoom conditions. The statistical procedure effectively generates heuristics for future assignments, based upon these variables. Future work will enhance the accuracy and precision of the modeling technique, and will empirically test users in controlled experiments. DOE

N95-13532# Lawrence Livermore National Lab., Livermore, CA.
AN ADAPTIVE OPTICS PACKAGE DESIGNED FOR ASTRONOMICAL USE WITH A LASER GUIDE STAR TUNED TO AN ABSORPTION LINE OF ATOMIC SODIUM
J. T. Salmon, K. Avicola, and J. M. Brase et al 11 Apr. 1994 11 p Presented at the Society of Photo-Optical Instrumentation Engineers (SPIE) Conference, Kona Beach, HI, 13-18 Mar. 1994
(Contract W-7405-eng-48)
(DE94-012391; UCRL-JC-114939; CONF-940391-7) Avail: CASI HC A03/MF A01

We present the design and implementation of a very compact adaptive optic system that senses the return light from a sodium guide-star and controls a deformable mirror and a pointing mirror to compensate atmospheric perturbations in the wavefront. The deformable mirror has 19 electrostrictive actuators and triangular subapertures. The wavefront sensor is a Hartmann sensor with lenslets on triangular centers. The high-bandwidth steering mirror assembly incorporates an analog controller that samples the tilt with an avalanche photodiode quad cell. An (line integral)/25 imaging leg focuses the light into a science camera that can either obtain long-exposure images or speckle data. In laboratory tests overall Strehl ratios were improved by a factor of 3 when a mylar sheet was used as an aberrator. The crossover frequency at unity gain is 30 Hz. DOE

N95-13574 DELAB, Trondheim (Norway).
FIBER-OPTIC SENSORS AND THE APPLICATION TO CONDITIONAL MONITORING FOR MECHANICAL STRUCTURES
L. Bjerkan, K. Johannessen, and N. Ryen 16 Feb. 1994 100 p Sponsored by Royal Norwegian Council for Scientific and Industrial Research
(PB94-207057; STF40-A94035) Avail: Issuing Activity (National Technical Information Service (NTIS))

The report summarizes the fiber-optic sensor activities in 1993 at DELAB. The aim of the project has been to collect information on existing fiber-optic sensor technology and perform a few demonstrations of the industrial capabilities. The results have been presented to Norwegian industry

and will hopefully form a basis for industrial development projects. The results of the project have been reported in short memos that have been distributed to the interested industry on a running basis. The memos that have not been written exclusively for a partner are included in the appendix. Fiber-optic sensors have been studied in general and compared to alternative sensors techniques. The possibility of having completely optical sensors with no electrical signals except in a central processing unit is advantageous. The sensors can thereby be made resistant to electromagnetic interference, attenuation due to long transmission lengths and aging due to environmental stress. Strain sensors have been the focus of the project. However, other mechanical parameters are converted either deliberately or through unavoidable noise factors to measurable strain. The sensors are also sensitive to temperature change. The theoretical basis has been described and applied particularly to polarimetric and Bragg grating sensors. NTIS

75 PLASMA PHYSICS

Includes magnetohydrodynamics and plasma fusion.

For ionospheric plasmas see *46 Geophysics*. For space plasmas see *90 Astrophysics*.

N95-11746# Brookhaven National Lab., Upton, NY.
REVIEW OF ELECTRON BEAM MICROINSTABILITIES AND THEIR RELEVANCE TO EBIS DEVICES
A. Hershcovitch 31 May 1994 18 p Presented at the 6th International Symposium on Electron Beam Ion Sources and Their Applications, Stockholm, Sweden, 20-23 Jun. 1994
(Contract DE-AC02-76CH-00016)
(DE94-013755; BNL-60497; CONF-9406180-2) Avail: CASI HC A03/MF A01

Plasma kinetic theory and some examples of microinstabilities are briefly reviewed. Although the velocity space configuration of any EBIS is inherently susceptible to a number of classical beam microinstabilities, the small radial dimension of an electron beam ion source (EBIS) plasma may prevent modes from occurring in EBIS traps due to physical limitation. In EBIS devices with high electron beam compression, where the potential for beam microinstabilities is great, the radial dimension is smaller than the Debye length, which renders plasma kinetic theory invalid. Potential for parametric instabilities exists due to coupling of structure excited modes into plasma modes by various mode-mode coupling 'decay' processes. DOE

N95-11754# Sandia National Labs., Albuquerque, NM.
TARGET AREA CHAMBER SYSTEM DESIGN FOR THE NATIONAL IGNITION FACILITY
R. Wavrik, J. Boyes, C. Olson, F. Dempsey, R. Garcia, V. Karpenko, A. Anderson, M. Tobin, and J. Latkowski 1994 6 p Presented at the 11th Topical Meeting on the Technology of Fusion Energy, New Orleans, LA, 19-24 Jun. 1994
(Contract DE-AC04-94AL-85000)
(DE94-013347; SAND-94-1603C; CONF-940630-10) Avail: CASI HC A02/MF A01

The National Ignition Facility (NIF) is a proposed Department of Energy facility which will contribute to the resolution of important Defense Program and inertial fusion energy issues for energy production in the future. The NIF will consist of a laser system with 192 independent beamlets transported to a target chamber. The target chamber is a multipurpose structure that provides the interface between the target and the laser optics. The chamber must be capable of achieving moderate vacuum levels in reasonable times; it must remain dimensionally stable within micron tolerances, provide support for the optics, diagnostics, and target positioner; it must minimize the debris from the x ray and laser light environments; and it must be capable of supporting external neutron shielding. The chamber must also be fabricated from a low activation material. The fusion reaction in the target gives off neutrons, x rays, and gamma rays. The x rays and gamma rays interact with the interior of the target chamber wall while neutrons penetrate the wall. In order to minimize the neutron activation of components outside the target chamber and to absorb gammas emitted from the activated chamber, shielding will be placed immediately outside the chamber. The target chamber contains the target positioner. The target positioner moves the target from outside the chamber to the center of the chamber and positions the target at the focal spot of the laser beams. The target positioner must be survivable in a harsh radioactive environment. The materials used must be low activation and have a high stiffness to weight ratio to maintain target stability. This paper describes the conceptual design of the target chamber, target positioner, and shielding for the NIF. DOE

N95-11786# Lawrence Livermore National Lab., Livermore, CA.
A 250 GHz MICROWAVE INTERFEROMETER FOR DIVERTOR EXPERIMENTS ON D3-D
R. A. James, D. G. Nilson, R. D. Stever, D. N. Hill, and T. A. Casper 31 Jan. 1994 15 p Presented at the 10th Topical Conference on High-Temperature Plasma Diagnostics, Rochester, NY, 8-12 May 1994
(Contract W-7405-eng-48)
(DE94-014056; UCRL-JC-116276; CONF-940552-11) Avail: CASI HC A03/MF A01

A new 250 GHz, two-frequency microwave interferometer system has been developed to diagnose divertor plasmas on D3-D. This diagnostic will measure the line-averaged density across both the inner and outer, lower divertor legs. With a cut-off density of over 7 x 10(exp 14) cm(exp -3), temporal measurements of ELM's, MARF's, and plasma detachment are expected. The outer leg system will use a double pass method while the inner leg system will be single pass. Two special three dimensional carbon composite tiles are used, one to protect the microwave antennas mounted directly under the strike point and the other as the outer leg reflecting surface. Performance, design constraints, and the thermal-mechanical design of the three dimensional carbon composite tiles are discussed. DOE

N95-11837 Naval Postgraduate School, Monterey, CA.
ANODE SHEATH CONTRIBUTIONS IN PLASMA THRUSTERS M.S. Thesis
John F. Riggs Mar. 1994 114 p Limited Reproducibility: More than 20% of this document may be affected by microfiche quality
(AD-A280395) Avail: Issuing Activity (Defense Technical Information Center (DTIC))

Contributions of the anode to Magnetoplasmadynamic (MPD) thruster performance are considered. High energy losses at this electrode, surface erosion, and sheath/ionization effects must be controlled in designs of practical interest. Current constriction or spotting at the anode, evolving into localized surface damage and considerable throat erosion, is shown to be related to the electron temperature's T(sub e) rise above the gas temperature T(sub o). An elementary one-dimensional description of a collisional sheath which highlights the role of T(sub e) is presented. Computations to model the one-dimensional sheath are attempted using a set of five coupled first-order, nonlinear differential equations describing the electric field, as well as the species current and number densities. For a large temperature nonequilibrium (i.e., T(sub e) greater than T(sub o)), the one-dimensional approach fails to give reasonable answers and a multidimensional description is deemed necessary. Thus, anode spotting may be precipitated by the elevation of T sub e among other factors. A review of transpiration cooling as a means of recouping some anode power is included. Active anode cooling via transpiration cooling would result in (1) quenching T(sub e), (2) adding 'hot' propellant to exhaust, and (3) reducing the local electron Hall parameter. DTIC

N95-11886# Institute of Plasma Physics, Prague (Czechoslovakia).
VELOCITY SPREAD OF REB GENERATED BY HIGH CURRENT DIODE
P. Vrba May 1994 17 p
(IPPCZ-339) Avail: CASI HC A03/MF A01

Theoretical analysis and numerical simulations of Relativistic Electron Beam (REB) generation in high current diode immersed in external magnetic field has been done. The calculations confirmed that the generated beam is homogeneous and monoenergetic in a broad central region. In the case of cylindrical diode, the mixing of electron trajectories has been only observed in a narrow periphery beam region. The angle between particle trajectories and external longitudinal magnetic field varies chaotically from 0 to 25 deg. This phenomenon suppresses the excitation of two stream instability excited by REB in the plasma column. Author

N95-11916# Institute of Plasma Physics, Prague (Czechoslovakia).
THE REFLECTION OF RELATIVISTIC ELECTRON BEAM BY VIRTUAL CATHODE

P. Vrba May 1994 18 p
(IPPCZ-338) Avail: CASI HC A03/MF A01

We studied the formation of Virtual Cathode (VC) by the Relativistic Electron Beam (REB) propagating through the terminating foil into a vacuum region in experimental devices REBEX. The beam properties (homogeneity and angular spread of particles velocities) and arising electromagnetic fields (e.g. equipotentials of VC, internal azimuthal magnetic field) were determined numerically by the help of 2d relativistic electromagnetic current-line code 'POISSON 2'. We were interested in obtaining the dependence of reflection coefficient of scattered REB by formatting VC on total beam current, beam energy, external magnetic field, and on the length of vacuum drift tube. The results obtained are useful for additional plasma heating mechanism via two stream instability generated by oscillating REB. Author

N95-12371# Los Alamos National Lab., NM.
PLASMA AND ION BEAM PROCESSING AT LOS ALAMOS
D. J. Rej, H. A. Davis, and I. Henins et al 1994 4 p Presented at the 10th International Conference on High Power Particle Beams, San Diego, CA, 20-24 Jun. 1994
(Contract W-7405-eng-36)
(DE94-014293; LA-UR-94-2032; CONF-940634-7) Avail: CASI HC A01/MF A01

Efforts are underway at Los Alamos National Laboratory to utilize plasma and intense ion beam science and technology for the processing of advanced materials. A major theme involves surface modification of materials, e.g., etching, deposition, alloying, and implantation. In this paper, we concentrate on two programs, plasma source ion implantation and high-intensity pulsed ion beam deposition. DOE

N95-12429# National Inst. for Fusion Science, Nagoya (Japan).
PHYSICS OF HIGH ENERGY DENSITY PLASMAS PRODUCED BY PULSED POWER
Hidenori Akiyama, ed. (Kumamoto Univ., Japan.) Jun. 1994 114 p Meeting held in Nagoya, Japan, 17-18 Dec. 1993 Original contains color illustrations
(ISSN 0915-6348)
(NIFS-Proc-18) Avail: CASI HC A06/MF A02

Papers presented at the December 1993 meeting to address the physics of high energy density plasmas are compiled. The papers cover several research and applications areas including ion beam generation, z-pinch, plasma focusing, railguns, high energy plasma flows, and pulsed ion and electron beams. For individual titles, see N95-12430 through N95-12451.

N95-12430# Tokushima Univ. (Japan). Faculty of Engineering.
RESISTIVITY VARIATION OF FUSE AS AN OPENING SWITCH
Naoyuki Shimomura, Masayoshi Nagata, and Hidenori Akiyama *In* National Inst. for Fusion Science, Physics of High Energy Density Plasmas Produced by Pulsed Power Jun. 1994 p 1-8 (For primary document see N95-12429 02-75)
Avail: CASI HC A02/MF A02

Resistance variation of thin copper wires in water as an opening switch was studied to obtain the basic data for design of an inductive energy storage pulsed power generator. The dimensions of a wire influence not only wire resistance but the relation between the resistivity and the energy deposited in the wire of unit mass. The dependence of the changing rate of wire resistivity on the resistivity was obtained using the energy balance equation for exploding wires. The phases of wire explosion were clearly confirmed and the influence of the dimension was removed from the relation between the resistivity and the deposited energy in the early phase of the wire vaporization. Author (revised)

N95-12431# Osaka Univ., Osaka (Japan). Inst. of Laser Engineering.
BEAM DIVERGENCE CHARACTERISTIC OF TWO-STAGE ION DIODE
Nobutake Shirai, Kazuhito Yasuike, Genji Takahashi, Norihisa Shomoto, Kazuhiro Yamamoto, Kazuo Imasaki, Chiyoe Yamanaka, Shuji Miyamoto, and Sadao Nakai *In* National Inst. for Fusion Science, Physics of High Energy Density Plasmas Produced by Pulsed Power Jun. 1994 p 9-15 (For primary document see N95-12429 02-75)
Avail: CASI HC A02/MF A02

The improvement of beam divergence by a two-stage diode is being studied at ILE Osaka University. We measured 750 keV carbon beam divergence by using a Shadow-Box with CR-39. We used the track analyzer (LUZEX III) that could measure and digitize the position of tracks, track diameter and shape of tracks to count a number of tracks on CR-39 and obtained results of beam divergence at first stage and second stage with track diameter resolution. Author

N95-12432# Osaka Univ., Osaka (Japan). Inst. of Laser Engineering.
NEW MULTI-DIMENSIONAL DIAGNOSTICS METHOD FOR INTENSE ION BEAMS
Kazuhito Yasuike, Nobutake Shirai, Genji Takahashi, Norihisa Shoumoto, Kazuhiro Yamamoto, Kazuo Imasaki, Chiyoe Yamanaka, Shuji Miyamoto, and Sadao Nakai *In* National Inst. for Fusion Science, Physics of High Energy Density Plasmas Produced by Pulsed Power Jun. 1994 p 16-25 (For primary document see N95-12429 02-75)
Avail: CASI HC A02/MF A02

We have developed a new diagnostic method for intense ion beams, called an arrayed pinhole camera (APC). An arrayed pinhole camera can measure spatial distributions of beam divergence and flux with time resolution. We measured proton and carbon beams of energy about 0.2 MeV, generated by a beam-extraction type applied-B diode. Achieved performances of this APC are a spatial resolution on anode of 1 mm, an effective divergence resolution of better than 10 mrad and a time resolution of 10 ns. Author (revised)

N95-12433# Nagoya Inst. of Tech. (Japan). Lab. of Beam Technology.
EVALUATION OF DYNAMIC PRESSURE OF ABLATION PLASMA PRODUCED BY INTENSE, PULSED, ION BEAM
Xiangdong Kang, Katsumi Masugata, and Kiyoshi Yatsui *In* National Inst. for Fusion Science, Physics of High Energy Density Plasmas Produced by Pulsed Power Jun. 1994 p 26-35 (For primary document see N95-12429 02-75)
Avail: CASI HC A02/MF A02

Basic characteristics of an ablation plasma produced by an intense, pulsed, ion beam have been evaluated from the measurement of ion-flux density by using a biased-ion collector. The target mass loss is detected by the measurement of the weights of the target before and after the shot. A one-dimensional hydrodynamic model is introduced by assuming a high-power, light-ion beam-driven expansion and the following adiabatic expansion into vacuum. Using this model, it is possible to deduce the pressure from the data of the ion flux and the mass loss of the target. This method is also applicable to other intense pulsed energy sources such as lasers or electron beams. Author

N95-12434# Himeji Inst. of Tech. (Japan). Dept. of Electrical Engineering.
A STUDY ON SUCCESSIVE GENERATION OF INTENSE PULSED ION BEAMS BY THE INVERSE PINCH ION DIODE
Yoshiyuki Hashimoto, Mitsuyasu Yatsuzuka, and Sadao Nobuhara *In* National Inst. for Fusion Science, Physics of High Energy Density Plasmas Produced by Pulsed Power Jun. 1994 p 36-45 (For primary document see N95-12429 02-75)
Avail: CASI HC A02/MF A02

Successive generation of intense pulsed ion beams was studied experimentally by the inverse pinch ion diode. When the anode of metals or plastics is used as an ion source, the diode impedance and the ion beam current were changed with every shot of operation. In the case of a copper anode, the ion current at the tenth shot was reduced to one half or one third than that at the first shot. Using soda-lime glass (Na2O CaO 5SiO2) surface of which vacuum oil or Aquadag was coated as the ion source, the diode impedance and the ion current remained constant during 25-30 shots. Using the vacuum oil ion source, the most dominant species in the ion beam was C(3+) which has energy in the range of 150-200 keV. The current density of the ion beam at 120 mm behind the anode was about 100 A/sq cm. Author (revised)

N95-12435# Niigata Univ. (Japan). Dept. of Electrical Engineering.
MEASUREMENTS OF 20 GHz HIGH-POWER MICROWAVES OUTPUT FROM A LARGE DIAMETER PLASMA FILLED BACKWARD WAVE OSCILLATOR
Ken-Ichi Kurashina, Wonsop Kim, Kazuo Ogura, Kazuo Minami, Tsuguhiro Watanabe, and Syouji Sugito *In* National Inst. for Fusion Science, Physics of High Energy Density Plasmas Produced by Pulsed Power Jun.

1994 p 46-54 (For primary document see N95-12429 02-75)
Avail: CASI HC A02/MF A02

A large diameter plasma filled backward wave oscillator (BWO) is investigated experimentally. The parameters of slow wave structure are chosen so that the oscillation frequency is about 20 GHz at 60 keV beam energy. Plasma is produced by the beam and it has favorable effects on beam propagation and Cerenkov oscillation. The output power of the BWO with plasma is observed to be 3-6 times that of vacuum BWO. The power level is several kW and efficiency is about 0.01 percent. The output power is strongly enhanced when the guiding magnetic field approaches the fundamental electron cyclotron resonance. A maximum power of 490 kW with an efficiency of 4 percent is achieved even for a relatively low beam energy of 60 keV. Author (revised)

N95-12436# Himeji Inst. of Tech. (Japan). Dept. of Electrical Engineering.
PLASMA EFFECTS ON ELECTRON BEAM DYNAMICS IN A VIRTUAL CATHODE OSCILLATOR
Mitsuyasu Yatsuzuka, Kenji Nagakawa, Yoshiyuki Hashimoto, and Sadao Nobuhara *In* National Inst. for Fusion Science, Physics of High Energy Density Plasmas Produced by Pulsed Power Jun. 1994 p 55-65 Sponsored by Ministry of Education, Science and Culture and Himeji City Fund for Development of Science and Industry (For primary document see N95-12429 02-75)
Avail: CASI HC A03/MF A02

High-power microwave generation in an axially-extracted virtual cathode oscillator has been studied experimentally. The microwave emission of 1.2 GW at frequencies in the range of 15 GHz is observed in the presence of an annular electron beam operated at a 330 kV and 20 kA. The electron beam current in the diode region is well characterized by the electron space-charge-limited current in bipolar flow, which is well below the critical current defined for diode pinching. The observed microwave emission is accompanied by the strongly pinched electron beam which results from the formation anode plasma. The essential feature of such a pinching effect for the microwave generation is confirmed by the absence of emission when the pinch of the electron beam is suppressed by the application of the axial magnetic field. Author (revised)

N95-12437# Nissin Electric Mfg. Co. Ltd., Tokyo, Tokyo (Japan).
STUDY ON SURFACE TREATMENT BY PULSED ELECTRON BEAMS
Shigeru Kato, Kenta Naito, Satoru Senbayashi, Yuu Kawakita, and Musuhi Hakoda *In* National Inst. for Fusion Science, Physics of High Energy Density Plasmas Produced by Pulsed Power Jun. 1994 p 66-75 Original contains color illustrations (For primary document see N95-12429 02-75)
Avail: CASI HC A02/MF A02

We developed a pulsed electron beam system for surface treatment use. It features high peak power density and broad area beams, which result in the possibility of advanced surface treatment. We experimentally demonstrated surface hardening, amorphizing and alloying with this system. A description of the performance of the system and results of surface treatment experiments are presented. Author (revised)

N95-12438# Japan Steel Works Ltd., Takanodai, Chiba (Japan).
PRESENT STATUS OF OHMIC IGNITION CHEMICAL LAUNCHER EXPERIMENT
K. Ikuta, Y. Aso, K. Fujioka, Y. Uehara, S. Nakamura, and K. Yamamoto *In* National Inst. for Fusion Science, Physics of High Energy Density Plasmas Produced by Pulsed Power Jun. 1994 p 76-80 (For primary document see N95-12429 02-75)
Avail: CASI HC A01/MF A02

This paper describes the first successful demonstration of a centrifugal mass separator packaged in a cartridge of the ohmic ignition chemical (OIC) gun in order to extract hot hydrogen from the reaction products of OIC interaction between water and aluminum. Author (revised)

N95-12439# Kumamoto Univ. (Japan). Dept. of Electrical Engineering and Computer Science.
GAS-PUFF Z-PINCH DRIVEN BY INDUCTIVE ENERGY STORAGE PULSED POWER GENERATOR ASO-2
K. Imasaka, K. Hasegawa, H. Akiyama, and S. Maeda *In* National Inst. for Fusion Science, Physics of High Energy Density Plasmas Produced by Pulsed Power Jun. 1994 p 81-89 (For primary document see N95-12429 02-75)
Avail: CASI HC A02/MF A02

An inductive energy storage pulsed power generator ASO-2 with two-staged opening switches was used as a power source of a gas-puff z-pinch and was compared with a fast bank with the same energy. A uniform discharge and a z-pinch implosion occurred at higher driving current than that of a fast bank. The intensity of soft x-rays driven by ASO-2 with only one-staged opening switch (copper wire fuses) was much increased in comparison with that driven by the fast bank. From the observation of hot spots by a pin-hole camera, the spatial positions of the hot spots did not move much shot to shot. These results are very important for applications of the gas-puff z-pinch in industry. Author

N95-12440# Nihon Univ., Tokyo (Japan). Atomic Energy Research Inst.
CONTRACTION PHASE OF A GAS-PUFF Z-PINCH
Kinya Moriyama, Keiichi Takasugi, Tetsu Miyamoto, and Koichi Sato *In* National Inst. for Fusion Science, Physics of High Energy Density Plasmas Produced by Pulsed Power Jun. 1994 p 90-98 (For primary document see N95-12429 02-75)
Avail: CASI HC A02/MF A02

The dynamics of a gas-puff z-pinch plasma was investigated using a Kerr-cell camera. A large amplitude Rayleigh-Taylor instability was observed to develop during the contraction of the plasma. Two types of gas nozzles were examined to reduce axial nonuniformity, and it was confirmed that the uniform z-pinch was produced by the choice of the nozzle. Author

N95-12441# Tokyo Inst. of Tech. (Japan).
CONTROL OF INITIAL MASS ON METAL VAPOR PUFF Z-PINCH
Seizo Furuya, Kenji Arai, Eiji Goto, and Shozo Ishii *In* National Inst. for Fusion Science, Physics of High Energy Density Plasmas Produced by Pulsed Power Jun. 1994 p 99-106 (For primary document see N95-12429 02-75)
Avail: CASI HC A02/MF A02

The high energy density z-pinch plasma created by injecting metal vapor between the electrodes has been examined experimentally. In the metal vapor puff z-pinch, an initial mass of metal vapor greatly affects the pinch characteristics. To control the metal vapor spatial distribution and the puffed vapor velocity, a discharge current with a square wave is employed to produce the metal vapor. We have constructed the LC ladder discharge circuit which can generate the current pulse with 10 microsecs in pulse width. Ag metal vapor is ejected by the discharge through a small hole drilled at the center of the electrode. Author

N95-12442# Tokyo Inst. of Tech. (Japan).
Z-PINCH PLASMA BY SOLID FINE PARTICLE INJECTION
Takahiro Hoshide, Qing-Pin Ai, Daiju Itagaki, and Shozo Ishii *In* National Inst. for Fusion Science, Physics of High Energy Density Plasmas Produced by Pulsed Power Jun. 1994 p 107-113 (For primary document see N95-12429 02-75)
Avail: CASI HC A02/MF A02

We have proposed z-pinch plasma by solid fine particle injection to create high energy density plasma. This scheme is superior in high repetition rate operation. It is possible to control the plasma point that radiates intense soft X-rays when the mass and the fine particle injection method are chosen properly. The solid fine particles are injected through a small hole drilled at the center of the main electrode. The particles are accelerated by a pulsed electrostatic field which is applied between the electrodes placed under the main electrode. Injection characteristics are experimentally examined for Cu particles of 1 micron in diameter. Author

N95-12443# Gunma Univ., Kiryu (Japan). Dept. of Electronic Engineering.
MONOCHROMATIC X RAY IMAGING IN PLASMA FOCUS EXPERIMENT
N. Hisatome, J. Du, T. Yamamoto, K. Shimoda, and K. Hirano *In* National Inst. for Fusion Science, Physics of High Energy Density Plasmas Produced by Pulsed Power Jun. 1994 p 114-126 (For primary document see N95-12429 02-75)
Avail: CASI HC A03/MF A02

A monochromatic, soft x-ray imaging spectrometer is designed and examined using a plasma produced by a plasma focus device. In this spectrometer a pinhole image is recorded simultaneously with a

monochromatic image. This provides identification of the wavelength if the soft x-ray source fluctuates from shot to shot such as in Z pinch or plasma focus. The monochromatic image of the Argon K-lines are successfully obtained and displayed in 3D. The resolution power and dispersion is obtained in-situ and compared with calculations. Author

N95-12444# Gunma Univ., Kiryu (Japan). Dept. of Electronic Engineering.

HOT SPOTS OBSERVATION IN A DENSE PLASMA FOCUS

Yoshio Takahama, Min Han, Takeshi Yanagidaira, and Katsumi Hirano *In* National Inst. for Fusion Science, Physics of High Energy Density Plasmas Produced by Pulsed Power Jun. 1994 p 127-134 (For primary document see N95-12429 02-75)

Avail: CASI HC A02/MF A02

Hot spots in a dense plasma focus are investigated with a time-resolved and filtered pinhole camera system through Ar K-lines. In conjuction with these observations, a Moire Schlieren technique is used to observe the macroscopic plasma behavior. The hot spots are generated at the disruption of the plasma column by growing of macroscopic instabilities. On both sides of the disrupted region, the hot spots appear and emit intense K-lines of argon for nearly 15 ns. A spatial distribution of Ar K-line emission with calibration is obtained using the pinhole camera system. The maximum intensity, approx. 2 x 10(exp 13) (photons/(s x sq mm x sq mrad 0.02 percent BW)), is observed when 6 percent of argon is added to the 4 Torr hydrogen. Author

N95-12445# Gunma Univ., Kiryu (Japan). Dept. of Electronic Engineering.

OBSERVATION OF A SOFT X RAY EMITTING CORE IN A DENSE PLASMA FOCUS

A. Yoshida, K. Shimoda, H. Kitaoka, and K. Hirano *In* National Inst. for Fusion Science, Physics of High Energy Density Plasmas Produced by Pulsed Power Jun. 1994 p 135-145 (For primary document see N95-12429 02-75)

Avail: CASI HC A03/MF A02

A filamentary core and hot spots with strong X-ray emission are observed in a medium size plasma focus facility of working gas of hydrogen with Ar admixture. Macroscopic plasma behavior and the brightness of the soft X-ray source, hot spots in the plasma are observed with a Moire Schlieren technique and a filtered pinhole camera. It is recognized that the radius of the filamentary core is in the sub-mm range in spite of the radius of the plasma column being several times greater than that of the core. The maximum brightness of the soft X-ray is approx. 10(exp 16)(photons/(s x sq mm x sq mrad x 0.01 percent BW)). Author

N95-12446# Moscow Physical-Engineering Inst. (Russia). Scientific Research Inst. of Technical Glass.

THE RESULTS OF THE STUDY OF COMPACT GAS-PUFF AND VACUUM SPARK PLASMA SOURCES OF SXR WITH GLASS-CAPILLARY CONVERTERS (GCC)

Alla Shlyaptseva, Victor Kantsyrev, Andrei Inozemtsev, and Oleg Petrukhin *In* National Inst. for Fusion Science, Physics of High Energy Density Plasmas Produced by Pulsed Power Jun. 1994 p 146-162 (For primary document see N95-12429 02-75)

Avail: CASI HC A03/MF A02

The results are presented dealing with the working out and study of the SXR compact plasma source. The experimental set up included a compact new 'gas-puff' source with parameters being better than the traditional ones and a new type of SXR source - low-inductance vacuum spark (LIVS) with glass-capillary converters (GCC) of SXR. The compact plasma 'gas-puff' source had the high value of the z approx. (1-2) 10(exp -2) (conversion coefficient of initial energy supply into SXR); a small effective size of emission region and greater resource. The characteristics of LIVS with GCC were studied. GCC consisting of about several hundreds of glass capillaries allowed us to focus SXR, to change the cross section of SXR beams to plasma sources, and to change SXR spectrum. The possibility was shown of using of GCC in plasma diagnostics of powerful plasma devices: for X-ray microscopy and to study the influence of SXR on the solid state surface. Author

N95-12447# Nihon Univ., Tokyo (Japan). Atomic Energy Research Inst.

COMMON UNDERSTANDINGS OF PHENOMENA IN Z-PINCHES

Keiichi Takasugi, Hideaki Suzuki, Kinya Moriyama, and Tetsu Miyamoto *In* National Inst. for Fusion Science, Physics of High Energy Density Plasmas Produced by Pulsed Power Jun. 1994 p 163-172 (For primary document see N95-12429 02-75)

Avail: CASI HC A02/MF A02

Common problems which are observed in gas-puff z-pinch experiments are discussed. The crowbar of plasma current is observed in z-pinches which automatically occurs due to short circuiting near the power feed. The emissivity of x-ray increases with z of the operating gas. The higher the z of the gas, the larger the input energy during the contraction. Author

N95-12448# Tokyo Inst. of Tech., Yokahama (Japan). Dept. of Energy Sciences.

HIGH RESOLUTION DIAGNOSTICS OF INTENSE ION DIODES AND KEY ISSUES FOR BRIGHT LIGHT ION BEAM GENERATION

Kazuhiko Horioka *In* National Inst. for Fusion Science, Physics of High Energy Density Plasmas Produced by Pulsed Power Jun. 1994 p 173-180 (For primary document see N95-12429 02-75)

Avail: CASI HC A02/MF A02

Progress in the diagnostic techniques of high power vacuum gaps has stimulated the development of analytical and numerical calculation of the diode physics. These developments have made clear the diode physics and key issues for bright light ion beam generation. In this report, recent diagnostic techniques of the acceleration gaps are reviewed and those issues are briefly discussed. Author

N95-12449# Kumamoto Univ. (Japan). Dept. of Electrical Engineering and Computer Science.

BEHAVIORS OF PLASMA ARMATURE IN THE AUGMENTED RAILGUN USING A PERMANENT MAGNET

S. Katsuki, H. Akiyama, and S. Maeda *In* National Inst. for Fusion Science, Physics of High Energy Density Plasmas Produced by Pulsed Power Jun. 1994 p 181-190 (For primary document see N95-12429 02-75)

Avail: CASI HC A02/MF A02

Augmentation of the magnetic field for electromagnetic railguns is a quite effective method to suppress the ablation of bore materials since it allows a decrease of the plasma armature current without a decrease of the Lorentz force for the acceleration. Another constructive effect of the augmentation on a plasma armature was observed in our experiment, that is to say, an external magnetic field for the augmentation compresses the plasma armature in the axial direction and suppresses the broadening of the plasma armature. In this paper, the behavior of a plasma armature in the augmented railgun using a permanent magnet is investigated in comparison with that in the railgun without the augmentation. Author

N95-12450# Kanazawa Univ. (Japan). Dept. of Physics.

STRONG BEAM-PLASMA TURBULENCE

M. Masuzaki, R. Ando, M. Yoshikawa, K. Kobayashi, H. Koguchi, D. Yamada, and K. Kamada *In* National Inst. for Fusion Science, Physics of High Energy Density Plasmas Produced by Pulsed Power Jun. 1994 p 191-200 Sponsored by Ministry of Education, Science and Culture (For primary document see N95-12429 02-75)

Avail: CASI HC A02/MF A02

High-power broadband microwave radiation was observed when an intense relativistic electron beam was injected into an unmagnetized gun-produced plasma. From spectroscopic measurements of hf strong electric fields in the plasma, it was found that our beam-plasma system is in the strong Langmuir turbulent state. A preliminary result indicating the relation between the radiation and the turbulence is shown. Author

N95-12451# Saga Univ. (Japan). Dept. of Electrical Engineering.

PLASMA OPENING SWITCH BY LASER-PRODUCED PLASMA WITH DIFFERENT KINDS OF ION SPECIES

Satoshi Ihara, Hidenori Akiyama, Susumu Kohno, Sunao Katsuki, Sadao Maeda, and Chobei Yamabe *In* National Inst. for Fusion Science, Physics of High Energy Density Plasmas Produced by Pulsed Power Jun. 1994 p 201-209 (For primary document see N95-12429 02-75)

Avail: CASI HC A02/MF A02

We have already proposed using laser-produced plasma as the plasma source of the plasma opening switch (POS). A POS using laser-produced

plasma has a possibility to be operated repeatedly by focusing the laser light on the target surface repeatedly. Other advantages are that the parameters of plasmas are kept constant for many shots, and the kinds of ion species can be changed easily by changing the targets for plasma production. In this paper, the operation of POS using the laser-produced plasma is experimentally investigated by changing the target materials (Al, Cu, W) as plasma sources. Author

N95-12641*# Universities Space Research Association, Columbia, MD.
FUSION POWERED HUMAN TRANSPORT TO MARS (UWFR94)
John Cappellari, Susan Grota, David Hagedorn, Yoshi Hirai, Mark Remmel, Deanna Schmidt, Matt Sveum, and Helena Wandow 1994 108 p
(Contract NASw-4435)
(NASA-CR-197184; NAS 1.26:197184) Avail: CASI HC A06/MF A02

In the future, two important technological dreams will have become reality: fusion will be a viable power source, and human settlement on Mars will be feasible, desirable, and even necessary. Merging these two concepts is especially attractive for the aerospace engineer because of the high specific power that will be possible with fusion (on the order 10 kW/kg). The UWFR94, a large, fusion-powered, human-transport ship, is designed to transport 100 passengers between earth and Mars in approximately thirty days. This relatively short transit time, which mitigates the need for artificial gravity, is made possible by a Polywell inertial electrostatic fusion reactor capable of 20 kW/kg. The mass of each reactor is 37 metric tons and the fuel used is (3)He-(3)He. The electricity generated drives the propulsion system, composed of nine ion thrusters and 780 tons of xenon propellant. The payload consists of three independent, identical cylinders housing the crew, and has a mass of approximately 400 tons. The aluminum cylinders' radius and length are 3 and 12 meters, respectively, with a thickness of 6 cm (15 cm in the solar flare safe rooms). Atmospheric reentry is avoided by constructing and repairing the UWFR94 in space, and by transferring crew and cargo to shuttle-like vehicles for transportation to the planet upon arrival. Author

N95-12757# Los Alamos National Lab., NM.
GENERATION OF ULTRA-HIGH MAGNETIC FIELDS FOR AGEX
M. G. Sheppard, C. M. Fowler, and B. L. Freeman Aug. 1994 11 p
(Contract W-7405-eng-36)
(DE94-015171; LA-12773) Avail: CASI HC A03/MF A01

Generation of ultra-high magnetic fields of 10-25 MG (0.4-2.5 MJ/cm(sup 3)) using high-explosive-driven magnetic flux-compression is one approach which could enhance the US Above Ground EXperimental (AGEX) capability. The beginnings of a US-Russian collaboration to generate 20 MG by extending flux-compression technology are described. The first joint experiments, planned for November 1993 at Los Alamos, will test the Russian MC-1 10 MG generator and will be followed by several high-temperature superconductor experiments. Equation-of-state experiments involving isentropic compression at pressures of several megabars are being considered as follow-on joint experiments. Magnetohydrodynamic (MHD) calculations of the MC-1 experiments using the ID MHD code RAVEN are presented, including comparisons and benchmarks against previous Russian experiments and calculations. The first joint experiments will use Russian hardware and US high-explosive. Gaining practical experience with the MC-1 and benchmarking the RAVEN predictions for the performance of the modified generator are important first steps towards reaching the 20 MG goal. DOE

N95-12758 Oak Ridge National Lab., TN.
FEEDBACK CONTROL AND STABILIZATION EXPERIMENTS ON THE TEXAS EXPERIMENTAL TOKAMAK (TEXT)
T. Uckan, B. A. Carreras, B. Richards, A. J. Wootton, R. D. Bengtson, R. Bravenec, G. X. Li, P. D. Hurwitz, P. E. Phillips, and W. L. Rowan Jun. 1994 17 p Limited Reproducibility: More than 20% of this document may be affected by microfiche quality
(Contract DE-AC05-84OR-21400)
(DE94-015214; ORNL/TM-12757) Avail: CASI HC A03

Plasma edge feedback experiments on the Texas Experimental Tokamak (TEXT) have been successful in controlling the edge plasma potential fluctuation level. The feedback wave-launcher, consisting of electrostatic probes located in the shadow of the limiter, is driven by the local edge potential fluctuations. In general, the edge potential fluctuations are modified in a broad frequency band. Moreover, it is observed that the potential fluctuations can be reduced (less than or equal to 100 kHz) without enhancing other modes, or excited (10 to 12 kHz), depending on the phase difference between the driver and the launcher signal, and gain of the system. This turbulence modification is achieved not only locally but also halfway around the torus and has about 2 cm of poloidal extent. Experiments on the characterization of the global plasma parameters with the edge feedback are discussed. Effects of the edge feedback on the estimated fluctuation-induced radial particle flux as well as on the local plasma parameters are presented. DOE

N95-12759# Edgerton, Germeshausen and Grier, Inc., Idaho Falls, ID.
VACUUM SYSTEM OPERATING EXPERIENCE REVIEW FOR FUSION APPLICATIONS
L. C. Cadwallader Mar. 1994 63 p
(Contract DE-AC07-76ID-01570)
(DE94-015267; EGG-FSP-11037; ITER/US-93/TE/SA-18) Avail: CASI HC A04/MF A01

This report presents a review of vacuum system operating experiences from particle accelerator, fusion experiment, space simulation chamber, and other applications. Safety relevant operating experiences and accident information are discussed. Quantitative order-of-magnitude estimates of vacuum system component failure rates and accident initiating event frequencies are presented for use in risk assessment, reliability, and availability studies. Safety concerns with vacuum systems are discussed, including personnel safety, foreign material intrusion, and factors relevant to vacuum systems being the primary confinement boundary for tritium and activated dusts. This information should be useful to fusion system designers and safety analysts, such as the team working on the Engineering Design Activities for the International Thermonuclear Experimental Reactor. DOE

N95-12853*# SRI International Corp., Menlo Park, CA. Geoscience and Engineering Center.
GUEST INVESTIGATOR PROGRAM STUDY: PHYSICS OF EQUATORIAL PLASMA BUBBLES Final Report
Roland T. Tsunoda Oct. 1994 23 p
(Contract NAS5-31215; SRI Proj. 2431)
(NASA-CR-196150; NAS 1.26:196150) Avail: CASI HC A03/MF A01

Plasma bubbles are large-scale (10 to 100 km) depletions in plasma density found in the night-time equatorial ionosphere. Their formation has been found to entail the upward transport of plasma over hundreds of kilometers in altitude, suggesting that bubbles play significant roles in the physics of many of the diverse and unique features found in the low-latitude ionosphere. In the simplest scenario, plasma bubbles appear first as perturbations in the bottomside F layer, which is linearly unstable to the gravitationally driven Rayleigh-Taylor instability. Once initiated, bubbles develop upward through the peak of the F layer into its topside (sometimes to altitudes in excess of 1000 km), a behavior predicted by the nonlinear form of the same instability. While good general agreement has been found between theory and observations, little is known about the detailed physics associated with plasma bubbles. Our research activity centered around two topics: the shape of plasma bubbles and associated electric fields, and the day-to-day variability in the occurrence of plasma bubbles. The first topic was pursued because of a divergence in view regarding the nonlinear physics associated with plasma bubble development. While the development of perturbations in isodensity contours in the bottomside F layer into plasma bubbles is well accepted, some believed bubbles to be cylinder-like closed regions of depleted plasma density that floated upward leaving a turbulent wake behind them (e.g., Woodman and LaHoz, 1976; Ott, 1978; Kelley and Ott, 1978). Our results, summarized in a paper submitted to the Journal of Geophysical Research, consisted of incoherent scatter radar measurements that showed unambiguously that the depleted region is wedgelike and not cylinderlike, and a case study and modeling of SM-D electric field instrument (EFI) measurements that showed that the absence of electric-field perturbations outside the plasma-depleted region is a distinct signature of wedge-shaped plasma bubbles. The second topic was pursued because the inability to predict the day-to-day occurrence of plasma bubbles indicated inadequate knowledge of the physics of plasma bubbles. An understanding of bubble formation requires an understanding of the roles of the various terms in the linearized growth rate of the collisional Rayleigh-Taylor instability. In our study, we examined electric-field perturbations found in SM-D EFI data and found that the seeding is more likely to be produced in the E region rather than the F region. The results

of this investigation are presented in the Appendix of this report and will be submitted for publication in the Journal of Geophysical Research.
Author

N95-12867 Texas Univ., Austin, TX. Inst. for Fusion Studies.
HELICAL TEMPERATURE PERTURBATIONS ASSOCIATED WITH TEARING MODES IN TOKAMAK PLASMAS
R. Fitzpatrick Jun. 1994 45 p Limited Reproducibility: More than 20% of this document may be affected by microfiche quality
(Contract DE-FG05-80ET-53088)
(DE94-014708; DOE/ET-53088/663) Avail: CASI HC A03

An investigation is made into the electron temperature perturbations associated with tearing modes in tokamak plasmas, with a view to determining the mode structure using Electron Cyclotron Emission (ECE) data. It is found that there is a critical magnetic island width below which the conventional picture where the temperature is flattened inside the separatrix is invalid. This effect comes about because of the stagnation of magnetic field lines in the vicinity of the rational surface and the finite parallel thermal conductivity of the plasma. For islands whose widths lie below the critical value there is no flattening of the electron temperature inside the separatrix. Such islands have quite different ECE signatures to conventional magnetic islands. In fact the two island types could, in principle, be differentiated experimentally. It should also be possible to map out the outer ideal magnetohydrodynamical eigenfunctions using ECE data. Islands whose widths are much less than the critical value are not destabilized by the perturbed bootstrap current, unlike conventional magnetic islands. This effect is found to have a number of very interesting consequences and may, indeed, provide an explanation for some puzzling experimental results regarding error field induced magnetic reconnection. All islands whose widths are much greater than the critical width possess a boundary layer on the separatrix which enables heat to be transported from one side of the island to the other via the X-point region. The structure of this boundary layer is described in some detail. Finally, the critical island width is found to be fairly substantial in conventional tokamak plasmas, provided that the long mean free path nature of parallel heat transport and the anomalous nature of perpendicular heat transport are taken into account in the calculation. DOE

N95-12897# Rice Univ., Houston, TX. Dept. of Space Physics and Astronomy.
RADIATIVE PROPERTIES OF STRONGLY MAGNETIZED PLASMAS
J. C. Weisheit Nov. 1993 5 p
(Contract DE-FG05-91ER-14213)
(DE94-015487; DOE/ER-14213/4) Avail: CASI HC A01/MF A01

The influence of strong magnetic fields on quantum phenomena continues to be a topic of much interest to physicists and astronomers investigating a wide array of problems: the formation of high energy-density plasmas in pulsed power experiments, the crustal structure and radiative properties of neutron stars, transport coefficients of matter irradiated by subpicosecond lasers, the spectroscopy of magnetic white dwarf stars, the quantum Hall effect, etc. The passage of time finds more questions being asked than being answered in this subject, where even the hydrogen atom 'paradigm' remains a major challenge. This theoretical program consists of two distinct parts: (1) investigation into the structure and transport properties of many-electron atoms in fields B is greater than than 10(exp 8) Gauss; and (2) extension of spectral lineshape methods for diagnosing fields in strongly magnetized plasmas. Research during the past year continued to be focused on the first topic, primarily because of the interest and skills of Dr. E.P. Lief, the postdoctoral research associate who was hired to work on the proposal. DOE

N95-12944# General Atomic Co., San Diego, CA.
FUSION PROGRAMS IN APPLIED PLASMA PHYSICS
Jul. 1993 45 p
(Contract DE-FG03-92ER-54150)
(DE94-015853; GA-A-21347) Avail: CASI HC A03/MF A01

This report summarizes the progress made in theoretical and experimental research funded by US Department of Energy Grant No. DE-FG03-92ER54150, during the period July 11, 1992 through May 31, 1993. Four main tasks are reported: applied plasma physics theory, alpha particle diagnostic, edge and current density diagnostic, and plasma rotation drive. The report also discusses the research plans for the theory and experimental programs for the next grant year. Reports and publications supported by the grant during this period are listed in the final section.
DOE

N95-13024*# Iowa Univ., Iowa City, IA. Dept. of Physics and Astronomy.
WAVES IN SPACE PLASMAS (WISP) Final Report
Wynne Calvert 2 Aug. 1994 42 p
(Grant NAG5-1926)
(NASA-CR-196432; NAS 1.26:196432) Avail: CASI HC A03/MF A01

Activities under this project have included participation in the Waves in Space Plasmas (WISP) program, a study of the data processing requirements for WISP, and theoretical studies of radio sounding, ducting, and magnetoionic theory. An analysis of radio sounding in the magnetosphere was prepared. Author

N95-13107# China Nuclear Information Centre, Beijing (China).
A NUMERICAL CALCULATION METHOD FOR THE KINETIC BALLOONING MODE EIGEN-EQUATION WITH THREE COMPONENTS
Guofang Sui (Southwest Inst. of Physics, Sichuan, China.) and Hailin Zhou (Southwest Inst. of Physics, Sichuan, China.) Oct. 1992 10 p In CHINESE
(DE94-625048; CNIC-00691; SIP-0056) Avail: CASI HC A02/MF A01 (US Sales Only)

A numerical method is described to solve the kinetic ballooning mode eigen-equation with three components. The effect of high velocity particles on the ballooning mode instability is studied. Results obtained from the theoretical calculation can successfully explain the phenomena observed in the experiments. DOE

N95-13280# Argonne National Lab., IL.
MHD PRESSURE DROPS AND THERMAL HYDRAULIC ANALYSIS FOR THE ITER BREEDING BLANKET DESIGN
Thanh Q. Hua and Y. Gohar Jun. 1994 23 p Presented at the ISFNT-3: 3rd International Symposium on Fusion Nuclear Technology, Los Angeles, CA, 27 Jun. - 1 Jul. 1994
(Contract W-31-109-eng-38)
(DE94-015085; ANL/TD/CP-81660; CONF-940664-19) Avail: CASI HC A03/MF A01

The breeding blanket design of the International Thermonuclear Experimental Reactor (ITER) is a self-cooled liquid lithium system with a vanadium structure. Electrical insulation of the coolant channel surfaces from the liquid metal is required to reduce the magnetohydrodynamic (MHD) pressure to less than 1 MPa. Insulation is provided by AlN coating at the channel surfaces in contact with lithium. MHD pressure drop and thermal hydraulic analysis of the blanket design is carried out subject to pressure, temperature, and stress considerations. Design windows relating the lithium flow velocity, MHD pressure, and structural temperature are formulated. The requirements of the insulator coating and characterization of the coating effectiveness are presented. Effects on the MHD pressure drop due to uniform cracks through the coating layer is also analyzed. DOE

N95-13285# Lawrence Livermore National Lab., Livermore, CA.
ABSORPTION OF INTENSE MICROWAVES AND ION ACOUSTIC TURBULENCE DUE TO HEAT TRANSPORT
J. S. DeGroot (California Univ., Davis, CA.), J. M. Liu (California Univ., Davis, CA.), and J. P. Matte (Quebec Univ., Montreal, Quebec.) Feb. 1994 11 p Presented at the 11th International Workshop on Laser Interaction and Related Plasma Phenomena, Monterey, CA, 25-29 Oct. 1993
(Contract W-7405-eng-48)
(DE94-015140; UCRL-JC-116212; CONF-931048-15) Avail: CASI HC A03/MF A01

Measurements and calculations of the inverse bremsstrahlung absorption of intense microwaves are presented. The isotropic component of the electron distribution becomes flat-topped in agreement with detailed Fokker-Planck calculations. The plasma heating is reduced due to the flat-topped distributions in agreement with calculations. The calculations show that the heat flux at high microwave powers is very large, q(sub max) (approx) 0.3 n(sub e)v(sub e)T(sub e). A new particle model to calculate the heat transport inhibition due to ion acoustic turbulence in ICF plasmas is also presented. One-dimensional PIC calculations of ion acoustic

turbulence excited due to heat transport are presented. The 2-D PIC code is presently being used to perform calculations of heat flux inhibition due to ion acoustic turbulence. DOE

N95-13341# China Nuclear Information Centre, Beijing (China).
IMPROVEMENTS OF HCN LASER HETERODYNE INTERFEROMETER FOR MEASURING PLASMA DENSITY
Dingguo Bi (Southwest Inst. of Physics, Sichuan, China.) Oct. 1992 12 p In CHINESE
(DE94-625037; CNIC-00679; SIP-0054) Avail: CASI HC A03/MF A01 (US Sales Only)

The improvements of a measuring method and laser performance in the HCN laser heterodyne interferometer system for plasma density measuring are introduced. A Fabry-Perot type output coupler which has optimal reflectance and transmittance is used to obtain maximum output power. The laser output power and frequency are stabilized by a microcomputer aided feedback control system. The fluctuation of output power is less than +/- 1% and the fluctuation of frequency is less than +/- 77 kHz. There is no longer any frequency drift or power drift during long term operation. A new method for measuring phase shift in heterodyne interferometer is suggested. The phase shift is directly obtained from the probe beam, which reflects the variation of plasma density, without comparing with reference beat. The low limit of measurable phase shift is depending on the frequency of clock and the upper limit is infinite. DOE

N95-13422# Oak Ridge National Lab., TN.
L-H TRANSITION IN TOKAMAKS AND STELLARATORS
K. C. Shaing, C. T. Hsu, and P. J. Christenson 1993 6 p Presented at the IAEA Meeting on H-Mode Physics, Naka, Japan, 15-17 Nov. 1993
(Contract DE-AC05-84OR-21400)
(DE94-013257; CONF-9311147-8) Avail: CASI HC A02/MF A01

It is shown that the bifurcation dynamics in the H-mode theory based on the ion orbit loss and nonlinear viscosity is not sensitive to the radial pressure and temperature gradients after bifurcation. This allows the poloidal flow velocity to be opposite to that of the poloidal E x B velocity in the H-mode phase if the pressure gradient is steep. Here, E(B) is the electric (magnetic) field. The theory is also extended to stellarator configurations to demonstrate that the tokamak H-mode theory can be tested in a controlled manner in those devices. A set of poloidal and toroidal momentum evolution equations is derived in which the radial current density outside the last closed flux surface is expressed in terms of the radial integral of the poloidal current density into the diverter plates. This facilitates the calculation of the radial electric field profile across the separatrix. DOE

N95-13529# Texas Univ., Austin, TX. Fusion Research Center.
LOCKED MODES IN TEXT-U TOKAMAK
A. Vannucci (Sao Paulo Univ., Brazil.) and S. C. McCool Apr. 1994 19 p
(Contract DE-FG03-94ER-54241)
(DE94-011595; FRCR-4454241/130; DOE/ER-54241/130) Avail: CASI HC A03/MF A01

Locked mode coils for detecting radial magnetic field perturbations B(sub r) were recently constructed and installed on the TEXT-U tokamak. The measured experimental signals showed that both minor and major disruptive instabilities were almost always preceded by a growth in B(sub r). For some plasma discharges with long duration precursors, a mode lock occurs before the disruption takes place. However, detailed investigation showed that the modes were still rotating in the toroidal direction but with a very low frequency of about 50 Hz. The results of the analysis done confirmed that the m=1/m=2 mode coupling is the main triggering mechanism for the disruptions. Only after the coupling has taken place, when the frequency of the MHD (Magnetohydrodynamic) activity measured with Mirnov coils has dropped from about 10 kHz to near 5 kHz and the characteristic deformation of the sawteeth has occurred, are fluctuating radial magnetic fields picked up by the locked mode coils. DOE

N95-13538# China Nuclear Information Centre, Beijing (China).
EFFECT OF STOCHASTIC DAMPING RESONANCE WAVE PACKET ON ENERGETIC ALPHA PARTICLE TRANSPORT
Wenxiao Qu (Southwest Inst. of Physics, Sichuan, China.) Dec. 1992 9 p In CHINESE
(DE94-625041; CNIC-00655; SIP-0049) Avail: CASI HC A02/MF A01 (US Sales Only)

Generally, the velocity of alpha particles produced by fusion is much greater than ion thermal velocity, but much smaller than electron thermal velocity. By using this property, a technique to enhance the radial transport of resonant energetic alpha particles with stochastic injection of damping resonance wave packet is suggested. The effect of the enhanced radial transport of resonant energetic alpha particles on the alpha particle distribution function and its possible use in the tokamak reactors is discussed. DOE

N95-13539# China Nuclear Information Centre, Beijing (China).
DENSITY GRADIENT EFFECTS IN THE TOKAMAK EDGE TURBULENCE WITH TEMPERATURE GRADIENT DRIVING
Shuanghui Hu (Southwest Inst. of Physics, Sichuan, China.), Lin Huang (Southwest Inst. of Physics, Sichuan, China.), and Xiaoming Qiu (Southwest Inst. of Physics, Sichuan, China.) Oct. 1992 9 p
(DE94-625042; CNIC-00659; SIP-0051) Avail: CASI HC A02/MF A01 (US Sales Only)

Based on magnetohydrodynamics, a new theoretical model is established. In this model the density gradient effects are added into the tokamak edge turbulence with temperature gradient driving. The physical mechanism and the density gradient effects in evolution of this turbulence are discussed. The fluctuation levels and the associated diffusion coefficients at the turbulent saturation are calculated. The theoretical results are in agreement with the experimental ones on TEXT. DOE

N95-13540# Academy of Sciences of the Ukraine, Kharkov. Fiziko-Tekhnicheskij Inst.
EXCITATION OF FAST MAGNETO-ACOUSTIC WAVES IN UNHOMOGENEOUS PLASMA OF A LARGE SIZE TOKAMAK [VOZBUZHDENIE BMZV V NEODNORODNOJ PLAZME TOKAMAKA BOL'SHIKH RAZEROV]
I. A. Girka, A. V. Longinov, and K. N. Stepanov 1993 32 p In RUSSIAN
(DE94-625050; KFTI-93-9) Avail: CASI HC A03/MF A01 (US Sales Only)

The excitation of fast magneto-acoustic waves by a small size current turn in plasma of large dimensions with linear density profile at the boundary is considered. Simple analytical solutions for plasma and antenna impedance in various absorption regimes are obtained. The dependence of impedance antenna performances on plasma and antenna parameters (gradient of Alfven refraction index, frequency, longitudinal and azimuthal wave numbers, distance from antenna to camera wall and to plasma) are analyzed. DOE

N95-13541# China Nuclear Information Centre, Beijing (China).
THE EXPERIMENT AND ANALYSIS OF TAILORING V(SUB L) AND I(SUB P) WITH ZnO VOLTAGE-SENSITIVE RESISTOR ON HT-6M
Shuping Fan (Academia Sinica, Hefei, China.), Baohua Liu (Academia Sinica, Hefei, China.), Minyou Ye (Academia Sinica, Hefei, China.), and Jiarong Luo (Academia Sinica, Hefei, China.) Dec. 1992 11 p
(DE94-625074; CNIC-00641; ASIPP-0034) Avail: CASI HC A03/MF A01 (US Sales Only)

The idea of improving plateau with ZnO 'varistor' (voltage sensitive resistor) is presented. The result of tailoring V(sub L) and I(sub P) experiment on HT-6M tokamak is introduced. An improved tens millisecond plateau was achieved ((Delta) V(sub L)/V(sub L) less than 5%, (Delta)I(sub p)/I(sub p) less than 5%, (Delta)N(sub e)/N(sub e) less than 10%). Obviously, it is of great importance for many diagnostic measurements and further physics experiments to have the constant distribution of temperature and density. A simplified analysis of the actual poloidal circuit of HT-6M is given. The numerical simulation and the result of experiment are compared. The operating principle of the varistor and its application on iron core transformer tokamak in plateau and rising phase are mentioned. DOE

N95-13555# Lawrence Livermore National Lab., Livermore, CA.
TIME-RESOLVED ELECTRON THERMAL CONDUCTION BY PROBING OF PLASMA FORMATION IN TRANSPARENT SOLIDS WITH HIGH POWER SUBPICOSECOND LASER PULSES Ph.D. Thesis
B. T. V. Vu Feb. 1994 170 p
(Contract W-7405-eng-48)
(DE94-015170; UCRL-LR-117409) Avail: CASI HC A08/MF A02

This dissertation work includes a series of experimental measurements in a search for better understanding of high temperature (10(exp 4)- 10(exp 6) K) and high density plasmas (10(exp 22)-10(exp 24)cm/cc) produced by irradiating a transparent solid target with high intensity (10(exp 13) - 10(exp 15)W/cm(exp 2)) and subpicosecond (10(exp minus 12)-10(exp minus 13)s) laser pulses. Experimentally, pump and probe schemes with both frontside (vacuum-plasma side) and backside (plasma-bulk material side) probes are used to excite and interrogate or probe the plasma evolution, thereby providing useful insights into the plasma formation mechanisms. A series of different experiments has been carried out so as to characterize plasma parameters and the importance of various nonlinear processes. Experimental evidence shows that electron thermal conduction is supersonic in a time scale of the first picosecond after laser irradiation, so fast that it was often left unresolved in the past. The experimental results from frontside probing demonstrate that upon irradiation with a strong (pump) laser pulse, a thin high temperature (approximately 40eV) super-critical density (approximately 10(exp 23)/cu cm) plasma layer is quickly formed at the target surface which in turn becomes strongly reflective and prevents further transmission of the remainder of the laser pulse. In the bulk region behind the surface, it is also found that a large sub-critical (approximately 10(exp 18)/cu cm) plasma is produced by inverse Bremsstrahlung absorption and collisional ionization. The bulk underdense plasma is evidenced by large absorption of the backside probe light. A simple and analytical model, modified from the avalanche model, for plasma evolution in transparent materials is proposed to explain the experimental results. Elimination of the bulk plasma is then experimentally illustrated by using targets overcoated with highly absorptive films. DOE

76 SOLID-STATE PHYSICS

Includes superconductivity.

For related information, see also *33 Electronics and Electrical Engineering* and *36 Lasers and Masers.*

N95-11739# Brookhaven National Lab., Upton, NY.
THE MAGNETIC STRUCTURE OF HOLMIUM-ERBIUM SUPERLATTICES
D. F. McMorrow (Risoe National Lab., Roskilde, Denmark.), J. A. Simpson (Oxford Univ., Oxford, England.), R. A. Cowley (Oxford Univ., Oxford, England.), D. A. Jehan (Oxford Univ., Oxford, England.), R. C. C. Ward (Oxford Univ., Oxford, England.), M. R. Wells (Oxford Univ., Oxford, England.), T. R. Thurston, and D. Gibbs 1994 8 p Presented at the International Conference on Magnetism, Warsaw, Poland, 22-26 Aug. 1994
(Contract DE-AC02-76CH-00016)
(DE94-013728; BNL-60489; CONF-940819-3) Avail: CASI HC A02/MF A01

The effect of completing crystal-field anisotropies on magnetic order has been investigated in a series of Ho/Er superlattices using neutron and resonant x-ray magnetic diffraction techniques. The neutron diffraction reveals that for temperatures in the interval T(sub N)(Er) less than or equal to T less than or equal to T(sub N)(Ho) the Ho basal-plane order propagates coherently through the paramagnetic Er, and that below T(sub N)(Er) the longitudinal component of the Er moments fails to order across the Ho block. The magnetic superlattice peaks observed in the x-ray scattering display an anomalous energy dependence: a sharp resonance is found at L(sub III)(Ho), with no resonance visible at L(sub III)(Er). These results are discussed with reference to models of exchange in metallic superlattices. DOE

N95-11740# Brookhaven National Lab., Upton, NY.
ATOMIC STRUCTURE MODIFICATIONS OF DIAMOND-LIKE NANOCOMPOSITE FILMS: OBSERVATION BY RAMAN SPECTROSCOPY, FTIR AND STM
B. Dorfman (Polytechnic Univ., Farmingdale, NY.), M. Abraizov (Polytechnic Univ., Farmingdale, NY.), F. H. Pollak (Polytechnic Univ., Farmingdale, NY.), D. Yan (City Univ. of New York, Brooklyn, NY.), M. Strongin, X.-Q. Yang, and Z.-Y. Rong 1994 6 p Presented at the Spring Meeting of the Materials Research Society, San Francisco, CA, 4-8 Apr. 1994
(Contract DE-AC02-76CH-00016)
(DE94-013732; BNL-60467; CONF-940411-34) Avail: CASI HC A02/MF A01

Raman spectroscopy, FTIR and scanning tunneling microscopy (STM) were used to study diamond-like nanocomposite (DLN) and metal containing DLN (Me-DLN) films. The FTIR spectra showed no appreciable absorption from the C-H stretch vibration band in DLN when 1 kV rf bias voltage was applied. Thermal annealing (450 deg C for 2 hrs) of (1) DLN and Cr-DLN films caused no change in the Raman spectra while (2) for Pt-DLN films there was a blue shift of both the crystalline (G) and microcrystalline (D) graphite-like features, an increase in the I(sub D)/I(sub G) intensity ratio and a decrease in the linewidths. The changes observed were more pronounced in the film with the highest Pt concentration. The STM image of this Pt-DLN film revealed a structure of aromatic graphite rings. DOE

N95-11748# Kiev Univ. (USSR). Inst. Yadernykh Issledovanij.
AN INVESTIGATION OF Mn Si BY THE SR-TECHNIQUE
N. D. Marchuk and O. I. Guzhva 1993 14 p
(DE94-624058; KIYaI-93-9) Avail: CASI HC A03/MF A01 (US Sales Only)

The nature of a spin fluctuation and spin relaxation in manganese monosilicide have been considered. The systematized experimental data of SR-measurements made in manganese monosilicide have been presented. In comparison with the well-known data taken by NMR-technique an analysis was made of the new results of SR-measurements in manganese monosilicide. DOE

N95-11819# Kyoto Univ., Kumatori (Japan). Research Reactor Inst.
RADIATION-INDUCED STRUCTURAL CHANGES, 3
Yasuhiro Kondo, ed. (Tohoku Univ., Sendai, Japan.), Tomochika Matsuyama, ed., and Masaaki Ogasawara, ed. May 1993 56 p
(DE94-753401; KURRI-TR-376) Avail: CASI HC A04/MF A01

This meeting is the fourth of series meetings on the structural change in materials induced by ionizing radiation. The present meeting was organized to discuss specifically on the x-ray storage phosphors such as BaFBr:Eu(2+) or RbI(x)Br(1-x):Tl and to get a clear understanding of the present status of the research on the storage mechanisms, nature of the rare earth impurities, and the optical properties of BaFBr. It was also expected that all the participants became aware of unsolved problems in these storage materials and that some of them would start research work on the storage phosphors. Therefore this report was edited mainly to provide basic knowledge correlated with the storage phosphors and related phenomena rather than to report simply on the experimental results. DOE

N95-11842 Harvard Univ., Cambridge, MA. Dept. of Chemistry.
OPTICAL AND MAGNETIC RESONANCE INVESTIGATIONS OF 3D IONS IN SINGLE CRYSTAL HOSTS: CANDIDATES FOR TUNABLE SOLID-STATE LASERS Final Report, 1 May 1990 - 31 Dec. 1993
David J. Single 25 Apr. 1994 181 p Limited Reproducibility: More than 20% of this document may be affected by microfiche quality
(Contract DAAL03-90-G-0113)
(AD-A281726; ARO-27425.5-PH) Avail: CASI HC A09

A comprehensive report is presented on electron paramagnetic resonance (EPR) and correlated optical spectroscopic studies conducted in our laboratory on a new class of solid-state materials with potential utility as near infrared radiation (IR) lasers. All of the studied materials involve oxide host lattices (silicates, vanadates, and germanates) doped with 3D transition metal-ions (chromium and manganese). The novelty of the materials is connected to the tetrahedral coordination and unusual oxidation state of the dopant ions. EPR spectroscopy is to determine the elemental identity of the dopant ions, the 'spin' of the ions and hence their oxidation numbers, and the crystallographic position of the ion hence its coordination number. These properties are then attached to relevant optical centers through magnetic resonance correlated optical spectroscopies, such as optical Zeeman spectroscopy. In the Cr:forsterite laser system, our results prove that the near IR lasing center is tetrahedral Cr3(+). In Mn:Ba3(VO4)2 EPR spectroscopy shows that tetrahedral Mn5(+) and Mn4(+) centers are both present in the material; a novel spin-echo pulsed laser double resonance method is introduced to prove that the tetrahedral Mn5(+) is the active center. DTIC

N95-11855# Displaytech, Inc., Boulder, CO.
DESIGN AND SYNTHESIS OF TIGHT PITCH FLCs FOR ANALOG VOLTAGE-LIMITED ELECTRO-OPTIC MODULATORS Final Report, 30 Sep. 1991 - 29 Mar. 1994
William N. Thurmes 27 May 1994 47 p

(Contract DAAL03-91-C-0051)
(AD-A281472; DTI-144F; ARO-29367.2-EL-SB2) Avail: CASI HC A03/MF A01

The goal of this project was to make liquid crystal materials suitable for use in a deformable-helix ferroelectric liquid crystal (DHFLC) device for analog light transmission. Towards this goal, 141 new compounds were synthesized with potential in DHF mixtures, including compounds with novel chiral tails and cores. One class of achiral dopants was found to amplify the C* pitch induction abilities of chiral dopants. A subset of this family also helped decrease the crystallization point of mixtures. Other compounds showed tight C* pitch and high polarization. Still other compounds had C* pitch and N* pitch of opposite signs, making them useful for N* pitch compensation. Several compounds, which increase the birefringence of mixtures while increasing solubility, are also reported. The newly synthesized compounds were extensively evaluated for relevant properties. Formulation efforts with these new materials resulted in new DHFLC mixtures with tight C* pitch (0.13 microns), long N* pitch, and very wide (less than -30 C to 73 C) C* phases. These could potentially be used in fast-switching analog display devices. The mixtures were evaluated in FLC cells. Further research is required to optimize the LC cells and driving electronics to take full advantage of the newly formulated DHF mixtures. DTIC

N95-11862# Sandia National Labs., Albuquerque, NM.
PRESSURE STUDIES OF ALKALI, ALKALINE EARTH AND RARE EARTH DOPED C60 SUPERCONDUCTORS
J. E. Schirber, W. R. Bayless, A. R. Kortan, E. Ozdas, O. Zhou, D. Murphy, and J. E. Fischer 1994 5 p Presented at the 185th Electrochemical Society Meeting, San Francisco, CA, 22-27 May 1994
(Contract DE-AC04-94AL-85000)
(DE94-013345; SAND-94-0063C; CONF-940529-14) Avail: CASI HC A01/MF A01

Pressure studies of the superconducting transition temperature T(sub c) of the alkali metal doped C60 compounds helped to establish a universal curve of T(sub c) versus lattice constant upon which nearly all of these materials lie. Various theoretical schemes incorporate this finding and suggest that only the lattice parameter and not the details of the dopant determine T(sub c). Ca5C60, the highest T(sub c) member of the alkaline earth doped C60 superconductor has a T(sub c) which lies on this universal curve so this material, from these considerations, should have the same large negative pressure derivative as the alkali doped superconductors. We have measured dT(sub c)/dP for Ca5C60 and for Yb(sub x)C60 (x near 3) and find small and positive values indicating that the theoretical models must be expanded to include band structure effects. DOE

N95-11876*# National Aeronautics and Space Administration. Lewis Research Center, Cleveland, OH.
RADIATIVE PERFORMANCE OF RARE EARTH GARNET THIN FILM SELECTIVE EMITTERS
Roland A. Lowe (Kent State Univ., OH.), Donald L. Chubb, and Brian S. Good Aug. 1994 9 p Presented at the First Conference on Thermophotovoltaic Generation of Electricity, Copper Mountain, CO, 24-26 Jul. 1994; sponsored by Midwest Research Inst.
(RTOP 233-01-0A)
(NASA-TM-106722; E-9068; NAS 1.15:106722) Avail: CASI HC A02/MF A01

In this paper we present the first emitter efficiency results for the thin film 40 percent Er-1.5 percent Ho YAG (Yttrium Aluminum Garnet, Y3Al5O12) and 25 percent Ho YAG selective emitter at 1500 K with a platinum substrate. Spectral emittance and emissive power measurements were made (1.2 less than lambda less than 3.2 microns). Emitter efficiency and power density are significantly improved with the addition of multiple rare earth dopants. Predicted efficiency results are presented for an optimized (equal power density in the Er, (4)I(sub 15/2)-(4)I(sub 13/2) at 1.5 microns, and Ho, (5)I(sub 7)-(5)I(sub 8) at 2.0 micron emission bands) Er-Ho YAG thin film selective emitter. Author

N95-11882*# National Aeronautics and Space Administration. Lewis Research Center, Cleveland, OH.
DETERMINATION OF A TRANSIENT HEAT TRANSFER PROPERTY OF ACRYLIC USING THERMOCHROMIC LIQUID CRYSTALS
James D. Heidmann May 1994 9 p Presented at the 32nd Aerospace Sciences Meeting, Reno, NV, 10-13 Jan. 1994; sponsored by AIAA
(RTOP 505-62-10)
(NASA-TM-106541; E-8684; NAS 1.15:106541) Avail: CASI HC A02/MF A01

An experiment was performed to determine a transient heat transfer property of acrylic. The experiment took advantage of the known analytical solution for heat conduction in a homogeneous semi-infinite solid with a constant surface heat flux. Thermochromic liquid crystals were used to measure the temperature nonintrusively. The relevant property in this experiment was the transient thermal conduction coefficient h(sub t), which is the square root of the product of density p, specific heat c(sub p), and thermal conductivity k (i.e., square root of pc(sub p)k). A value of 595.6 W square root of s/sq m K was obtained for h(sub t), with a standard deviation of 5.1 W square root of s/sq m K. Although there is no generally accepted value for h(sub t), a commonly used one is 580 W square root of s/sq m K, which is almost 3 percent less than the h(sub t) value obtained in this experiment. Since these results were highly repeatable and since there is no definitive value for h(sub t), the new value is recommended for future use. Author

N95-11899# Joint Inst. for Nuclear Research, Dubna (USSR).
MEASUREMENT OF SYNCHROTRON RADIATION TRANSMISSION OF INFRARED RANGE BY YBa2Cu3O(7-DELTA) FILM IN SUPERCONDUCTING STATE [IZMERENIE PROPUSKANIYA SINKHROTRONOGO IZLUCHENIYA INFRAKRASNOGO DIAPAZONA PLENKOJ YBA2CU3O(7-DELTA) V SVERKHPROVODYASHCHEM SOSTOYANII]
N. R. Skintej, S. I. Tyutyunnikov, V. N. Shalyapin, and N. I. Balalykin 1993 3 p In RUSSIAN Submitted for publication
(DE94-623270; JINR-R-14-93-411) Avail: CASI HC A01/MF A01 (US Sales Only)

The results of the energy gap measurement of superconducting film YBa2Cu3O(7-delta) the base of MgO with the temperature T=20 K are presented. The measurements were made on the synchrotron radiation beam of the impulse electron storage facility. The determination of the energy gap was made by reconstruction of the transmission spectrum from the integral equation decision, involving signal time response from the detector of the infrared radiation, transmitted through the film. The measured value 2(Delta) MeV near T=20 K agrees with the Bardeen-Cooper-Schiffer theory in the limits of the measurement accuracy. DOE

N95-11921*# Alabama Univ., Huntsville, AL. Center for Microgravity and Materials Research.
CONVECTIVE FLOW EFFECTS ON PROTEIN CRYSTAL GROWTH Semiannual Progress Report No. 3, 31 Jan. - 1 Aug. 1994
Franz Rosenberger and Lisa A. Monaco 1994 33 p
(Grant NAG8-950)
(NASA-CR-196790; NAS 1.26:196790) Avail: CASI HC A03/MF A01

A high-resolution microscopic interferometric setup for the monitoring of protein morphologies has been developed. Growth or dissolution of a crystal can be resolved with a long-term depth resolution of 200 A and a lateral resolution of 2 microns. This capability of simultaneously monitoring the interfacial displacement with high local depth resolution has yielded several novel results. We have found with lysozyme that (1) the normal growth rate is oscillatory, and (2) depending on the impurity content of the solution, the growth step density is either greater or lower at the periphery of a facet than in its center. The repartitioning of Na plus and Cl minus ions between lysozyme solutions and crystals was studied for a wide range of crystallization conditions. A nucleation-growth-repartitioning model was developed, to interpret the large body of data in unified way. The results strongly suggest that (1) the ion to lysozyne ratio in the crystal depends mostly on kinetic rather than crystallographic parameters, and (2) lysozyme crystals possess a salt-rich core with a diameter electron microscopy results appear to confirm this finding, which could have far-reaching consequences for x-ray diffraction studies. A computational model for diffusive-convective transport in protein crystallization has been applied to a realistic growth cell geometry, taking into account the findings of the above repartitioning studies and our kinetics data for the growth of lysozyme. The results show that even in the small cell employed, protein concentration nonuniformities and gravity-driven solutal convection can be significant. The calculated convection velocities are of the same order to magnitude as those found in earlier experiments. As expected, convective transport, i.e., at Og, lysozyme crystal growth remains kinetically limited.

The salt distribution in the crystal is predicted to be non-uniform at both 1g and 0g, as a consequence of protein depletion in the solution. Static and dynamic light scattering studies in undersaturated and supersaturated solutions have been performed. Diffusivities in undersaturated solutions, were found to vary with lysozyme concentrations. Depending on the salt concentration, the diffusivities either increase or decrease. Interestingly, the corresponding static scattering intensities behave oppositely, Our current analysis indicates that these changes are inconsistent with aggregation in undersaturated solutions. However, the data are compatible with concentration-dependent changes of the interactions between protein and salt. Author (revised)

N95-11993 Georgia Univ., Athens. Dept. of Chemistry.
ELECTROCHEMICAL EPITAXY
Huang M. Baoming, Tedd E. Lister, and John L. Stickney 25 Jun. 1994 42 p Limited Reproducibility: More than 20% of this document may be affected by microfiche quality
(Contract N00014-19-J-1919)
(AD-A282403; TR-14) Avail: CASI HC A03

This chapter discusses epitaxy in electrodeposition. The paper mostly discusses compound epitaxy in electrodeposition. This can include the surface compounds formed by the underpotential deposition (UPD) on one element on a second element. It also includes the formation of thin films and bulk compounds on various substrates. A discussion of electrochemical atomic layer epitaxy is included as well. DTIC

N95-12004 Texas Univ., Austin, TX. Dept. of Chemistry and Biochemistry.
APPLICATION OF SCANNING TUNNELING MICROSCOPY TO STUDIES OF ELECTRODE SURFACES Final Report, May 1991 - Jun. 1994
Allen J. Bard Jul. 1994 7 p Limited Reproducibility: More than 20% of this document may be affected by microfiche quality
(Contract N00014-91-J-1752)
(AD-A282383) Avail: Issuing Activity (Defense Technical Information Center (DTIC))

This project involved the study of a variety of different surfaces and structures in gaseous and liquid environments using the scanning tunneling microscope (STM) and other scanning probe microscopes with the aim of obtaining a better understanding of electrode surfaces and the processes occuring on these surfaces. With the STM we investigated chemical changes on the surface of electrodes, e.g., corrosion, passivation, and biochemical activities, and studied the energetics for electron transfer at the surfaces of semiconductors. We also investigated nanostructures (for example, very small semiconductor particles, porous Si, and self-assembled monolayers) using this technique. DTIC

N95-12386*# Alabama Univ., Huntsville, AL. Materials Processing Lab.
OPTICAL ANALYSIS OF CRYSTAL GROWTH Final Report
Gary L. Workman, Andrea Passeur, and Sabrina Harper 24 Aug. 1994 60 p
(Contract NAS8-38609)
(NASA-CR-196514; NAS 1.26:196514) Avail: CASI HC A04/MF A01

Processing and data reduction of holographic images from Spacelab presents some interesting challenges in determining the effects of microgravity on crystal growth processes. Evaluation of several processing techniques, including the Computerized Holographic Image Processing System and the image processing software ITEX150, will provide fundamental information for holographic analysis of the space flight data. Author

N95-12425# Colorado School of Mines, Golden, CO.
IN-SITU X-RAY ANALYSIS OF THE ELECTROLYTE-SOLID INTERFACE Final Report
T. E. Furtak 31 May 1994 31 p
(Contract N00014-90-J-1326)
(AD-A282203) Avail: CASI HC A03/MF A01

This project was undertaken to advance the experimental technology of x-ray absorption spectroscopy in the study of electrochemical interfaces. The objective was to establish the standard by which subsequent measurements would be evaluated. To this end we paid a great deal of attention to the details of the control of a large sample, the potential pitfalls related to artifacts in the data, and to high quality analyses of the results. These goals were met. Extended x-ray absorption fine structure (EXAFS) is capable of revealing the near neighbor environment of a specific element in a complicated system. By placing a monolayer of a foreign metal on an electrode, and studying this material, we hoped to reveal the geometry of the electrolyte in the first layer next to the sample. We chose Cu on Pt as the prototype, partly for its suitability regarding x-ray absorption edges, and also for its exemplary role as a strongly bound electrochemically controlled adsorption system. Our experimental design was based upon use of an unusually large sample (47 cm2) to obtain large signals. The sample was excited with grazing incidence x-rays, and the absorption structure associated with the Cu was monitored through the Cu Ka emission. We used a specially designed sample and electrolyte control system that enabled experiments to be performed with both p-and s-polarized incident radiation. DTIC

N95-12602# Materials Research Society, Pittsburg, PA.
DIAGNOSTIC TECHNIQUES FOR SEMICONDUCTOR MATERIALS PROCESSING
O. J. Glembocki, S. W. Pang, F. H. Pollak, G. M. Crean, and G. Larrabee May 1994 519 p Proceedings of the Volume 324 Materials Research Society Symposium held in Boston, MA, 29 Nov. - 2 Dec. 1993
(AD-A282810) Avail: CASI HC A22/MF A04

The symposium focused on various aspects of process diagnostics and device processing. Diagnostic techniques which were considered fell into two classes: invasive and non invasive. Optical characterization techniques were the most widely applied characterization tools used in both materials and process monitoring. Techniques such as reflectance difference, ellipsometry, reflectance, absorption, light scattering, photoreflectance, Raman scattering and thermal wave modulated reflectance were shown to be powerful probes of various materials properties. The materials properties that were probed included surface stoichiometry and morphology, etch damage, Fermi level pinning position and thin film properties such as thickness, alloy content, and interfacial roughness. Real time diagnostics such as ellipsometry and reflectance difference were shown to be sensitive tools of materials properties during processing. DTIC

N95-12635 Department of the Navy, Washington, DC.
APPARATUS AND METHOD FOR FORMING TEXTURED BULK HIGH TEMPERATURE SUPERCONDUCTING MATERIALS Patent
John P. Wehrle, inventor (to Navy), Barbara F. Howell, inventor (to Navy), and James G. Morris, III, inventor (to Navy) 3 May 1994 6 p Filed 23 Mar. 1992
(AD-D016394; US-Patent-5,308,800; US-Patent-Appl-SN-858363; US-Patent-Class-505-400) Avail: US Patent and Trademark Office

Discussed is an apparatus and method for fabricating textured pseudosingle crystal bulk superconducting materials, featuring introduction of a pressure gradient and/or of a magnetic field for enhancement of melt-texturing directional solidification techniques using a steep temperature gradient furnace for increasing temperatures at which superconductive properties can be maintained in superconducting materials. The strengths of the temperature gradient, pressure gradient and/or magnetic field can be optimally varied, resulting information of superconducting material exhibiting superconductive properties at higher temperatures than previously achievable. DTIC

N95-12923 State Univ. of New York, Buffalo, NY. Dept. of Chemistry.
LOW OXIDATION STATE GALLIUM COMPOUNDS. SYNTHESIS AND CHARACTERIZATION OF Ga(CH2CMe3)n Technical Report No. 40
O. T. Beachley, Jr., John C. Pazik, and Matthew J. Noble 15 Aug. 1994 22 p Limited Reproducibility: More than 20% of this document may be affected by microfiche quality
(Contract N00014-90-J-1530)
(AD-A283369) Avail: Issuing Activity (Defense Technical Information Center (DTIC))

The new organogallium(I) compound (Ga(CH2CMe3))n has been prepared by the reduction of Ga(CH2CMe3)2Cl by using either sodium or lithium with naphthalene in THF. When the reagents were combined at -78 C, a yellow intermediate, a neopentylgallium(III) derivative of dihydronaphthalene C10H8(Ga(CH2CMe3)2)2 dot 2 MCl (M = Li, Na) was formed. Warming of the solution to 0-25 C resulted in decomposition of the yellow intermediate and formation of a reddish brown solution of Ga(CH2CMe3))n, Ga(H2CMe3)3, C10H8, and either NaCl or LiCl. The gallium(I) product was a vitreous solid and was characterized by complete

elemental analyses, hydrolyses with HCl/H2O and with DCl/D2O, oxidation with HgCl2 and with I2, cryoscopic molecular weight studies in benzene solution, and IR and NMR spectroscopic studies. All data support the conclusion that (Ga(CH2CMe3))n exists as a mixture of species which are gallium cages. The numbers of gallium atoms in these cages might range from 6 to 12 atoms. DTIC

N95-12948# Academy of Sciences of the Ukraine, Kharkov. Fiziko-Tekhnicheskij Inst.
RADIATION AMORPHIZATION OF MATERIALS [RADIATSIONNAYA AMORFIZATSIYA MATERIALOV]
I. M. Neklyudov and T. P. Chernyaeva 1993 76 p In RUSSIAN Revised
(DE94-624184; KFTI-93-02-Rev) Avail: CASI HC A05/MF A01 (US Sales Only)

The results of experimental and theoretical research on radiation amorphization are presented in this analytical review. Mechanism and driving forces of radiation amorphization are described; kinetic and thermodynamic conditions of amorphization are formulated. Compositional criteria of radiation amorphization are presented which allow us to predict irradiation behavior of materials and their tendency to radiation amorphization. Mechanisms of transition from crystalline state to amorphous state are considered depending on dose, temperature, structure of primary radiation damage, and flux level. DOE

N95-13059# General Electric Co., Schenectady, NY. Atomic Power Lab.
EVALUATION OF THE IMPROVEMENT IN THE FIGURE OF MERIT OF Bi2Te3 - BASED ALLOYS WITH ADDITION OF ULTRAFINE SCATTERING CENTERS
J. P. Fleurial (California Inst. of Tech., Pasadena, CA.) Sep. 1993 15 p
(Contract DE-AC12-76SN-00052)
(DE94-015363; KAPL-4767) Avail: CASI HC A03/MF A01

The addition of ultrafine scattering centers into Bi2Te3-based materials and their impact on the thermal and electrical transport properties in a 200-500 K temperature range are discussed. Based on previous theoretical efforts, the resulting improvements in the figure of merit of these heavily doped thermoelectric semiconductors were calculated as a function of composition, temperature, doping level, particulate size and concentration. Determination of the lattice thermal conductivity of the various alloys was conducted by considering phonon-phonon, carrier-phonon, point defect and inert scattering center scattering mechanisms. Degradation of the electrical properties due to the increase scattering rate was also taken into account. Practical application of these results is considered. DOE

N95-13078# Los Alamos National Lab., NM.
POLYCRYSTAL MODELS TO FIT EXPERIMENTS
U. F. Kocks and C. T. Necker 1994 14 p Presented at the Riso International Symposium on Materials Science: Numerical Predictions of Deformation Processes and the Behavior of Real Materials, Riso, Denmark, 5-9 Sep. 1994
(Contract W-7405-eng-36)
(DE94-014419; LA-UR-94-2141; CONF-9409173-1) Avail: CASI HC A03/MF A01

Two problems in the modeling of polycrystal plasticity are addressed in which some parameter can best be determined by matching with experiment, although the principles of the underlying mechanisms are presumed known. One of these problems is the transition from 'full constraints' (FC) to 'relaxed constraints' (RC) with increasing flatness of t he grains. Observed qualitative transitions in texture with strain, such as a transient orthotropic symmetry in torsion textures, can help identify the rate at which the FC-to-RC transition takes place. The second problem is that of the material dependence of deformation textures among the FCC metals which, it is argued, can only be due to a change in deformation modes, i.e., in the shape of the single-crystal yield surface. A heuristic assumption of an increasing importance of (111)(211)-slip as the stacking-fault energy decreases explains the qualitative trend. The quantitative parameter needed has been determined for copper from a match of prediction and experiment over a range of strains. DOE

N95-13081# Los Alamos National Lab., NM.
Be-9 AND B-11 NMR STUDY OF SUPERCONDUCTIVITY IN BORON DOPED UBe13
E. T. Ahrens, R. H. Heffner, P. C. Hammel, A. P. Reyes, J. L. Smith, and W. G. Clark Jun. 1994 10 p Presented at the SCES 1994, Amsterdam, Netherlands, Aug. 1994
(Contract W-7405-eng-36)
(DE94-014432; LA-UR-94-1984; CONF-9408113-1) Avail: CASI HC A02/MF A01

We present Be-9 and B-11 NMR spin-lattice relaxation rate (1/T(sub 1)) measurements in UBe(13-x)B(x) for x = 0.03 and 0.07 over the temperature range 0.096 K to 2 K. The temperature dependence of 1/T(sub 1) shows a strong B concentration dependence, especially at low temperatures. We interpret this behavior as consistent with gapless superconductivity induced by the addition of B impurities. The ratio of the Be-9 to B-11 1/T(sub 1) increases with decreasing temperature below (Tc) indicating additional contributions to the Be-9 relaxation rate, possibly from nuclear spin diffusion to normal-state vortex cores or paramagnetic impurities. DOE

N95-13086# Los Alamos National Lab., NM.
MASS CONSERVATION IN GRAIN GROWTH
D. T. Wu 1994 5 p Presented at the Spring Meeting of the Materials Research Society, San Francisco, CA, 4-8 Apr. 1994
(Contract W-7405-eng-36)
(DE94-014456; LA-UR-94-1918; CONF-940411-40) Avail: CASI HC A01/MF A01

Several alternatives to Hillert's work on grain growth have been proposed. Unfortunately some of these theories have been shown to violate mass conservation. The authors have shown that applying local mass conservation to grain growth leads to a correction term in the current representing the interaction between a grain and its surrounding. They also showed that Hillert's model of grain growth is equivalent to a mean field theory in which all grains want to shrink. The mass conserving backflux give a physical justification for the critical radius in Hillert's theory. DOE

N95-13125# Brookhaven National Lab., Upton, NY.
ROLE OF IMPLANTATION-INDUCED DEFECTS IN SURFACE-ORIENTED DIFFUSION OF FLUORINE IN SILICON
C. Szeles (Eoetvoes Lorand Univ., Budapest, Hungary.), B. Nielsen, P. Asoka-Kumar, K. G. Lynn, and M. Anderle 1994 5 p Presented at the 10th International Conference on Positron Annihilation, Beijing, China, 23-29 May 1994
(Contract DE-AC02-76CH-00016)
(DE94-014905; BNL-60537; CONF-9405170-5) Avail: CASI HC A01/MF A01

The annealing behavior open-volume defects introduced in Si(100) crystals during fluorine implantation and their role in the surface-oriented diffusion of F impurities were investigated by variable-energy positron beam depth profiling. The defects become mobile and undergo recovery at temperatures well below the onset of fluorine diffusion at 550 C as seen by secondary ion mass spectroscopy (SIMS). The results suggests that after irradiation and annealing the F occupies substitutional sites to which positrons are insensitive. The anomalous F diffusion seen in SIMS has been explained through a two-step diffusion mechanism, in which the diffusion kinetics is determined by dissociation of the substitutional F into an interstitial F and a vacancy, followed by their rapid diffusion to the surface. DOE

N95-13150 Department of the Navy, Washington, DC.
SUBSTRATE TEMPERATURE CONTROL APPARATUS AND TECHNIQUE FOR CVD REACTORS Patent
Keith A. Snail, inventor (to Navy) and Thomas P. Thorpe, inventor (to Navy) 7 Jun. 1994 13 p Filed 18 May 1993
(AD-D016387; US-Patent-5,318,801; US-Patent-Appl-SN-062889; US-Patent-Class-427-248.1) Avail: US Patent and Trademark Office

One of the critical experimental parameters affecting the quality and growth rate of chemical vapor deposition species, such as, diamond is the substrate temperature. An apparatus and technique for the precise control of the substrate temperature in a chemical vapor deposition environment has been developed. In a preferred embodiment, the technique uses a variable gas mixture in conjunction with the disclosed apparatus of the present invention to precisely control the temperature of the substrate to within at least + or - 20 deg C, for extended periods of time and over large area substrates on the order of 1 in. in diameter or larger. DTIC

N95-13168# Lehigh Univ., Bethlehem, PA. Center for Solid State Studies.
[ACTIVITIES OF LEHIGH UNIVERSITY] Quarterly Progress Report
1994 3 p
(Contract N00014-92-J-1308)
(AD-A282098) Avail: CASI HC A01/MF A01

We have repeated the work discussed in a previous report on the effect of Germanium Implantation on hot carrier injection. This process does indeed result in a large reduction in the hot carrier injection. Measurements have demonstrated that this implantation increases the electron trapping in SiO2 due to the localization of the Germanium at the Si-SiO2 interface because there was a much larger increase in the interface trap density if the implant was done before the oxidation. We have also verified that the Germanium does not have a measurable effect on the MOSFET device characteristics. Derived from text

N95-13272# Argonne National Lab., IL.
MAGNETIC RESPONSE OF ULTRATHIN Fe ON MgO: A POLARISED NEUTRON REFLECTOMETRY STUDY
S. Adenwalla, Y. Park, G. P. Felcher, and M. Teitelman May 1994 10 p Presented at the 6th Joint Conference on Magnetism and Magnetic Materials, Albuquerque, NM, 20-23 Jun. 1994
(Contract W-31-109-eng-38)
(DE94-013192; ANL/IPNS/CP-83050; CONF-940629-6) Avail: CASI HC A02/MF A01

The magnetization of ultrathin bcc Fe films (two and three monolayers) on MgO was measured and compared with the behavior predicted for a two-dimensional ferromagnet. The experiment indicated that no hysteresis was present in the magnetization. Instead, the magnetization at low temperature was affected by a marked field cooling effect. These observations lead to the conclusion that films of Fe on MgO of such thickness exhibit superparamagnetic behavior as if they were not entirely continuous. In contrast, films thicker than five monolayers exhibit a magnetic response close to that of bulk iron. DOE

N95-13277# Academy of Sciences of the Ukraine, Kiev. Inst. Teoreticheskoj Fiziki.
ABOUT THE STRUCTURE OF THE SUPERCONDUCTING ORDER PARAMETER OF 2 D FERMI SYSTEM WITH AN ARBITRARY PARTICLE DENSITY
E. V. Gorbar, V. M. Loktev, and V. S. Nikolaev 1993 15 p
(DE94-623268; ITP-93-42) Avail: CASI HC A03/MF A01 (US Sales Only)

Starting from the model Hamiltonian for the Fermi-system on the simple square lattice the structure of the superconducting order parameter is investigated for the arbitrary number of carriers. It is shown that pairing of s+id type is more advantageous energetically. Meanwhile the dependence of the s-gap on the number of carriers has a nonmonotonic ('bell-like') form. DOE

N95-13299 University of Southern Mississippi, Hattiesburg, MS. Dept. of Polymer Science.
A CRAMPS AND 13C CP/MAS NMR EXAMINATION OF SOLID-SOLID TRANSITIONS IN N-HEXATRIACONTANE (C36H74) Technical Report, 1 Jun. 1993 - 31 May 1994
Michael J. Stewart and Lon J. Mathias 15 Jul. 1994 3 p Limited Reproducibility: More than 20% of this document may be affected by microfiche quality
(Contract N00014-89-J-1225)
(AD-A282497; TR-71) Avail: Issuing Activity (Defense Technical Information Center (DTIC))

The normal paraffins can undergo several transitions before melting and may thus serve as interesting model compounds for polyethylene, which also undergoes solid-solid transitions, the strongest and best-known being the so-called alpha transition. Our examination of n-Hexatriacontane (C36) has been greatly furthered by the use of the solid-state H-1 NMR technique known as CRAMPS (combined rotation and multiple pulse spectroscopy). This technique, combined with DSC and C-13 CP/MAS NMR, has allowed us to make tentative assignments for the molecular motions occurring at different temperatures below the melting point. DTIC

N95-13337# Argonne National Lab., IL.
QUENCHED QCD AT FINITE DENSITY
J. B. Kogut (Illinois Univ., Urbana, IL.), M. P. Lombardo (Illinois Univ., Urbana, IL.), and D. K. Sinclair 31 Jan. 1994 41 p
(Contract W-31-109-eng-38)
(DE94-011522; ANL-HEP-TR-93-115) Avail: CASI HC A03/MF A01

Simulations of quenched QCD at relatively small but nonzero chemical potential mu on 32 times 16(sup 3) lattices indicate that the nucleon screening mass decreases linearly as mu increases predicting a critical chemical potential of one-third the nucleon mass, M(sub N)/3, by extrapolation. The meson spectrum does not change as mu increases over the same range, from zero to m(sub pi)/2. Past studies of quenched lattice QCD have suggested that there is phase transition at mu=m(sub pi)/2. The authors provide alternative explanations for these results, and find a number of technical reasons why standard lattice simulation techniques suffer from greatly enhanced fluctuations and finite size effects for mu ranging from m(sub pi)/2 to m(sub N)/3. They find evidence for such problems in their simulations, and suggest that they can be surmounted by improved measurement techniques. DOE

N95-13409 Technische Univ., Delft (Netherlands). Dept. of Mechanical Engineering and Marine Technology.
FRACTIONAL SUSPENSION CRYSTALLIZATION OF ORGANIC COMPOUNDS Ph.D. Thesis
P. J. Jansens 5 Apr. 1994 233 p
(PB94-206851; ISBN-90-370-0097-5) Copyright Avail: Issuing Activity (National Technical Information Service (NTIS))

The thesis is focused on the development and optimization of the operation of equipment for fractional suspension crystallization (FSC) processes. General objectives of the whole research project were: (1) To review and evaluate the different fractional crystallization techniques and processes; (2) To optimize the operating conditions for a cocurrent cascade of crystallizers (the CDC) with respect to the filterability of the produced crystals, because this parameter determines the separation efficiency and the production capacity of the downstream solid/liquid separator(s); (3) To analyze transport forces, purification mechanism and fluid dynamics in a TNO-Thijssen wash column in order to provide a sound basis for technical feasibility studies and future scale-up of this apparatus; (4) To investigate the technical feasibility of caprolactam purification with a FSC process comprising a CDC and a TNO-Thijssen wash column. NTIS

77 THERMODYNAMICS AND STATISTICAL PHYSICS

Includes quantum mechanics; theoretical physics; and Bose and Fermi statistics.

For related information see also *25 Inorganic and Physical Chemistry* and *34 Fluid Mechanics and Heat Transfer.*

N95-12512 Air Force Inst. of Tech., Wright-Patterson AFB, OH.
IMPINGEMENT FLOW HEAT TRANSFER MEASUREMENTS OF TURBINE BLADES USING A JET ARRAY Ph.D. Thesis
Kenneth W. VanTreuren Aug. 1994 269 p Limited Reproducibility: More than 20% of this document may be affected by microfiche quality
(AD-A283450; AFIT/CI/CIA-94-030D) Avail: CASI HC A12

The requirement for increased gas turbine engine performance has led to the use of much higher turbine entry temperature (TET). The higher temperatures require active cooling of the turbine blade using compressor bleed air. Arrays of impinging jets are one method currently used to reduce the blade temperature on the midspan and leading edge. Air flows through small holes in a blade insert and is directed on the inside surface of a turbine blade to reduce local surface temperature. The engine situation was represented by a 10-20 times scale model tested in the internal cooling transient facility at the University of Oxford. The geometry chosen was for a widely spaced array with a jet spacing of 8d and a plate thickness to jet diameter of 1.2. Experiments were accomplished for a range of impingement plate to target surface spacings, z/d, (1, 2 and 4) and jet Reynolds numbers, Re(sub j), (10,000 - 40,000) with both staggered and inline array hole configurations. The transient liquid crystal technique, both peak intensity narrowband and hue temperature history wideband,

enabled the determination of heat transfer coefficient and adiabatic wall temperature. For the first time, local detail of heat transfer on the target surface as well as observation of the crossflow influence on the jet at the target surface are possible. A large variation in heat transfer exists between the stagnation point and channel passage between jets (2-4 times) which was unknown in previous experiments. DTIC

N95-12553 Emory Univ., Atlanta, GA.
MAGNETO-OPTICAL PROPERTIES OF QUANTUM STRUCTURES WITH REDUCED DIMENSIONALITY Final Technical Report, 1 Dec. 1990 - 31 Mar. 1994
Krishan K. Bajaj 31 Mar. 1994 80 p Limited Reproducibility: More than 20% of this document may be affected by microfiche quality
(Grant AF-AFOSR-0056-91)
(AD-A282597; AFOSR-94-0434TR) Avail: Issuing Activity (Defense Technical Information Center (DTIC))

We have reported the results of the calculations of the exciton binding energies and oscillator strengths in type II quantum well structures both in the absence and in the presence of a magnetic field using a variety of variational and perturbation approaches. We have reported the results of the calculations of the energy levels of excitons and hydrogenic impurities in coupled double quantum well structures in the presence of a magnetic field. We have also described the results of our calculations of the energy levels of excitons and hydrogenic donors in quantum well wires in the presence of a magnetic field. We have also described the results of our calculation of the binding energies of hydrogenic donors in quantum dots in the presence of magnetic field. We have reported the results of our calculations of the energy level of hydrogenic impurities and excitons in dielectric quantum wells in the presence of electric and magnetic fields. And finally, we have presented results of our calculations of the exciton binding energies in ionic quantum well structures. DTIC

N95-13074# Lawrence Livermore National Lab., Livermore, CA.
THERMODYNAMIC CONSTANTS FOR ACTINIDE OXIDES AND OXYHYDROXIDES RELEVANT TO ACTINIDE VOLATILITY CALCULATIONS FOR THERMAL OXIDATION PROCESSES
Bartley B. Ebbinghaus and Oscar H. Krikorian 27 Oct. 1993 11 p
(Contract W-7405-eng-48)
(DE94-007762; UCRL-ID-115386) Avail: CASI HC A03/MF A01

The purpose of this report is to provide input of thermodynamic data on actinide volatilities to EERC for use in their computer code for modeling of metal volatilities in incinerators. It is also anticipated that the data may be documented later in an EPA sponsored 'Metals Bible.' It should be noted that only upper limits for the volatility of PuO2(s) due to PuO3(g) and PuO2 (OH2)(g) and the volatility of AmO2 in PuO2(s) due to AmO3(g) and AmO2 (OH2)(g) could be set. The data on the americium vapor species are intended for calculations where AmO2 is present as a solid solution in PuO2(s). DOE

N95-13172# Sandia National Labs., Albuquerque, NM.
MAGNETIC FIELD INDUCED MINIGAP IN DOUBLE QUANTUM WELLS
J. A. Simmons, S. K. Lyo, J. F. Klem, and N. E. Harff 1994 5 p Presented at the Conference on the Application of High Magnetic Fields, Cambridge, MA, 8-12 Aug. 1994
(Contract DE-AC04-94AL-85000)
(DE94-015013; SAND-94-1748C; CONF-940847-1) Avail: CASI HC A01/MF A01

We report discovery of a partial energy gap, or minigap, in strongly coupled double quantum wells (QW's), due to an anticrossing of the two QW dispersion curves. The anticrossing and minigap are induced by an in-plane magnetic field B(sub (parallel)), and give rise to large distortions in the Fermi surface and density of states, including a Van Hove singularity. Sweeping B(sub (parallel)) moves the minigap through the Fermi level, with the upper and lower gap edges producing a sharp maximum and minimum in the low-temperature in-plane conductance, in agreement with theoretical calculations. The gap energy may be directly determined from the data. DOE

N95-13572 Selskapet for Industriell og Teknisk Forskning, Oslo (Norway). Dept. of Instrumentation.
CHAOTIC TIME SERIES. PART 1: ESTIMATION OF INVARIANT PROPERTIES IN STATE SPACE
D. Kugiumtzis, B. Lillekjendlie, and N. Christophersen 19 Jan. 1994 28 p See also PB94-207115 Prepared in cooperation with Oslo Univ., Norway
(PB94-206968; STF31-A93045-Pt-1) Avail: Issuing Activity (National Technical Information Service (NTIS))

Certain deterministic non-linear systems may show chaotic behavior. Time series derived from such systems seem stochastic when analyzed with linear techniques. However, uncovering the deterministic structure is important because it allows for construction of more realistic and better models and thus improved predictive capabilities. This paper describes key features of chaotic systems including strange attractors and Lyapunov exponents. The emphasis is on state space reconstruction techniques that are used to estimate these properties, given scalar observations. Data generated from equations known to display chaotic behavior are used for illustration. A compilation of applications to real data from widely different fields is given. If chaos is found to be present, one may proceed to build non-linear models, which is the topic of the second paper in this series. NTIS

80 SOCIAL SCIENCES (GENERAL)

Includes educational matters.

N95-11765*# Ohio Aerospace Inst., Brook Park.
NASA/OAI RESEARCH ASSOCIATES PROGRAM Final Technical Report, 19 Mar. 1990 - 31 Dec. 1992
Theo G. Keith, Jr. Aug. 1994 65 p
(Contract NCC3-169)
(NASA-CR-196824; NAS 1.26:196824) Avail: CASI HC A04/MF A01

The intent of this activity was the development of a cooperative program between the Ohio Aerospace Institute and the NASA Lewis Research Center with the objective of better preparing recent university graduates for careers in government aerospace research laboratories. The selected individuals were given the title of research associate. To accomplish the aims of this effort: (1) the research associates were introduced to the NASA Lewis Research Center and its mission/programs, (2) the research associates directly participated in NASA research and development programs, and (3) the research associates were given continuing educational opportunities in specialized areas. A number of individuals participated in this project during the discourse of this cooperative agreement. Attached are the research summaries of eight of the research associates. These reports give a very good picture of the research activities that were conducted by the associates. Author

N95-12385 National Academy of Sciences - National Research Council, Washington, DC. Commission on Engineering and Technical Systems.
TOWARD INFRASTRUCTURE IMPROVEMENT: AN AGENDA FOR RESEARCH
James P. Gould, ed. and Andrew C. Lemer, ed. 1994 142 p
(Grant NSF MSS-91-16411)
(LC-94-67335; ISBN-0-309-05144-4) Copyright Avail: Issuing Activity

Millions of Americans rely on the services of the nation's infrastructure, arguably the most extensive system in the history of mankind. Most of the time and in most places, the roads, water supplies, waste-disposal facilities, and other elements of infrastructure serve efficiently and reliably the wide range of economic and social activities comprising our daily lives, and few people really notice that the system is there. But sometimes a ruptured water main, street repairs, or the destruction from a major storm or earthquake provides unfortunate reminders of the infrastructure's significance. The product of centuries of technological development and decades of construction, maintenance, and management, the system has developed for the most part as separate and distinct power plants, roads, pipelines, and waste repositories, built and operated by a myriad of government agencies, independent authorities, and private corporations. Decisions made in earlier times - when populations were smaller, land was less intensively used, and we understood less about our environment - leave us with facilities that are aging and often incapable of serving today's demands, some of them urgent. At the same time, extraordinary advances in electronics, biotechnology, materials, and other scientific and technical fields offer unprecedented opportunities for enhancing the system's performance. Decisions made today foreclose opportunities when we lack

ability to project consequences. Our infrastructure can be improved, and research is a wellspring for improvement. The National Science Foundation (NSF), created to increase the nation's base of scientific and engineering knowledge and strengthen its ability to conduct research in all areas of science and engineering, has been working to define the scope and extent of a program in Civil Infrastructure Systems (CIS). The NSF asked the National Research Council's (NRC) Building Research Board (BRB), in cooperation with the Geotechnical Board (GEOB), to undertake a study to provide advice on an infrastructure research agenda. This report documents the work and recommendations of the committee appointed to undertake that study. Derived from text

N95-11956*# Micro Craft, Inc., Moffett Field, CA.
EDUCATION: A SECOND CAREER
Kong Cha Authement *In* NASA. Ames Research Center, Technical Paper Contest for Women 1992. Space Challenges: Earth and Beyond 1993 p 1-4 (For primary document see N95-11955 02-99)
Avail: CASI HC A01/MF A03

N95-11958*# National Aeronautics and Space Administration. Ames Research Center, Moffett Field, CA.
ENGINEERING THE FUTURE WITH AMERICA'S HIGH SCHOOL STUDENTS
M. A. Farrance (General Electric Co., Moffett Field, CA.) and J. W. Jenner *In its* Technical Paper Contest for Women 1992. Space Challenges: Earth and Beyond 1993 p 21-35 (For primary document see N95-11955 02-99)
Avail: CASI HC A03/MF A03

N95-11959*# National Aeronautics and Space Administration. Ames Research Center, Moffett Field, CA.
USING EMERGENT ORDER TO SHAPE A SPACE SOCIETY
Amara L. Graps *In its* Technical Paper Contest for Women 1992. Space Challenges: Earth and Beyond 1993 p 37-47 (For primary document see N95-11955 02-99)
Avail: CASI HC A03/MF A03

81 ADMINISTRATION AND MANAGEMENT

Includes management planning and research.

N95-11944 RAND Corp., Santa Monica, CA.
CASE STUDY OF RISK MANAGEMENT IN THE USAF B-1B BOMBER PROGRAM
Susan J. Bodilly 1993 64 p Limited Reproducibility: More than 20% of this document may be affected by microfiche quality
(Contract F49620-91-C-0003)
(AD-A282371; RAND/N-3616-AF) Avail: Issuing Activity (Defense Technical Information Center (DTIC))

This case study was undertaken in conjunction with six others to develop a better understanding of the risks involved in weapon system development and whether government policies effectively aid in the management of those risks to reduce the probability or severity of negative outcomes. The purpose of the larger study of seven Air Force procurement programs is to provide information that might improve the decision environment in which weapon systems are procured and thus to increase the probability of positive outcomes. This case focuses on the procurement of the B-1B bomber and covers the procurement of the entire aircraft platform and its component systems. The B-1B, with a direct program acquisition cost of $20.5 billion in 1981 dollars, represents a mixed array of technical advances depending on the component part examined. The case study identifies risk-related decisions made early in the program prior to or at the start of full-scale development. The assessments of risk and its subsequent management are then tracked to show how the early risk management decisions affected the program. The term risk, as used throughout this paper, is the probability that, given that an activity is undertaken, an event will occur that has negative outcomes for those involved. This case study (1) identifies acquisition practices that shape and manage risk and (2) suggests possible improvements. DTIC

N95-12618*# Mississippi State Univ., Mississippi State, MS. Dept. of Industrial Engineering.
AN INVESTIGATION OF THE USE OF TEMPORAL DECOMPOSITION IN SPACE MISSION SCHEDULING Final Report, 14 Sep. 1993 - 1 Aug. 1994
Stanley E. Bullington and Venkat Narayanan Jul. 1994 63 p
(Grant NAG8-1012)
(NASA-CR-196420; NAS 1.26:196420) Avail: CASI HC A04/MF A01

This research involves an examination of techniques for solving scheduling problems in long-duration space missions. The mission timeline is broken up into several time segments, which are then scheduled incrementally. Three methods are presented for identifying the activities that are to be attempted within these segments. The first method is a mathematical model, which is presented primarily to illustrate the structure of the temporal decomposition problem. Since the mathematical model is bound to be computationally prohibitive for realistic problems, two heuristic assignment procedures are also presented. The first heuristic method is based on dispatching rules for activity selection, and the second heuristic assigns performances of a model evenly over timeline segments. These heuristics are tested using a sample Space Station mission and a Spacelab mission. The results are compared with those obtained by scheduling the missions without any problem decomposition. The applicability of this approach to large-scale mission scheduling problems is also discussed. Author

N95-11963*# Sterling Software, Inc., Moffett Field, CA.
DEVELOPMENT OF A CHANGE MANAGEMENT SYSTEM
Cathy Bonifas Parks *In* NASA. Ames Research Center, Technical Paper Contest for Women 1992. Space Challenges: Earth and Beyond 1993 p 97-110 (For primary document see N95-11955 02-99)
Avail: CASI HC A03/MF A03

82 DOCUMENTATION AND INFORMATION SCIENCE

Includes information management; information storage and retrieval technology; technical writing; graphic arts; and micrography.

For computer documentation see *61 Computer Programming and Software.*

N95-11788# Technosoft, Inc., Cincinnati, OH.
INTELLIGENT KNOWLEDGE-BASED ENGINEERING Final Report, 1 Jul. 1993 - 1 Jan. 1994
Adel Chemaly May 1994 28 p
(Contract F33615-93-C-5360)
(AD-A281906; WL-TR-94-4065) Avail: CASI HC A03/MF A01

This report presents a successful approach and implementation for integrating product and process design. The generation of a process plan as an integrated part of a free-form feature-based parametric design system is discussed. The success of the approach, detailed in this report, for an automated process planner integrated with a design system, comes from its capability to reason about and automatically extract a manufacturing representation from the part design geometry. By analyzing the part geometry, and planning around the problems that could be encountered in machining, the automated planner can overcome the difficulties in automating the process plan. No user assistance is required and it does not rely on retrieving and/or modifying the process plans of similar parts stored in a database. DTIC

N95-11824# Technische Univ., Delft (Netherlands). Dept. of Mechanical Engineering and Marine Technology.
VALIDATING MEDICAL KNOWLEDGE BASED SYSTEMS Ph.D. Thesis
C. vanDaalen 24 Aug. 1993 297 p
(PB94-191301; ISBN-90-370-0089-4) Copyright Avail: CASI HC A13/MF A03

The research described in this thesis concerns the validation of medical knowledge based systems in general, and of the medical knowledge based system PLEXUS in particular. First, the background of the research is described. The review of literature on performance evaluation of medical knowledge based systems is described in Chapter 2. The architecture of

the knowledge based system PLEXUS is discussed in Chapter 3. The setup and results of the laboratory evaluation are discussed in Chapter 4, and the setup and results of the clinical evaluation are described in Chapter 5. The study of the attitudes of physicians and process-operators towards knowledge-based systems is described in Chapter 6. The conclusions which can be drawn from the evaluation studies that were performed are discussed in Chapter 7. An analysis of the results of the investigations has led to general recommendations regarding the design and validation of medical knowledge based systems. These recommendations are also mentioned in the last chapter. NTIS

N95-12358*# National Aeronautics and Space Administration, Washington, DC.

CENDI INDEXING WORKSHOP

Oct. 1994 300 p Workshop held at NASA, Washington, 21-22 Sep. 1994

(NASA-CP-10160; NAS 1.55:10160) Avail: CASI HC A13/MF A03

The CENDI Indexing Workshop held at NASA Headquarters, Two Independence Square, 300 E Street, Washington, DC, on September 21-22, 1994 focused on the following topics: machine aided indexing, indexing quality, an indexing pilot project, the MedIndEx Prototype, Department of Energy/Office of Scientific and Technical Information indexing activities, high-tech coding structures, category indexing schemes, and the Government Information Locator Service. This publication consists mostly of viewgraphs related to the above noted topics. In an appendix is a description of the Government Information Locator Service. Author (revised)

N95-12383*# National Aeronautics and Space Administration, Washington, DC.

NASA STI PROGRAM SEMINAR: ELECTRONIC DOCUMENTS

29 Sep. 1994 120 p

(NASA-TM-109928; NAS 1.15:109928) Avail: CASI HC A06/MF A02

The theme of this NASA Scientific and Technical Information Program Seminar was electronic documents. Topics covered included Electronic Documents Management at the CASI, the Impact of Electronic Publishing on User Expectations and Searching Image Record Management, Secondary Publisher Considerations for Electronic Journal Literature, and the Technical Manual Publishing On Demand System (TMPODS). Author

N95-12502 Carnegie-Mellon Univ., Pittsburgh, PA. Dept. of Computer Science.

AN EMPIRICAL STUDY OF A HIGHLY AVAILABLE FILE SYSTEM

Brian D. Noble Feb. 1994 14 p Limited Reproducibility: More than 20% of this document may be affected by microfiche quality

(Contract F33615-90-C-1465; ARPA Order 7597)

(AD-A282655; CMU-CS-94-120) Avail: Issuing Activity (Defense Technical Information Center (DTIC))

In this paper we present results from a six-month empirical study of the high availability aspects of the Coda File System. We report on the service failures experienced by Coda clients, and show that such failures are masked successfully. We also explore the effectiveness and resource costs of key aspects of server replication and disconnected operation, the two high availability mechanisms of Coda. Wherever possible, we compare our measurements to simulation-based predictions from earlier papers and to anecdotal evidence from users. Finally, we explore how users take advantage of the support provided by Coda for mobile computing. DTIC

N95-12916 Naval Research Lab., Washington, DC.

INFORMATION TECHNOLOGY DIVISION'S TECHNICAL PAPER ABSTRACTS

Cathy J. Wiley 5 Jul. 1994 105 p Limited Reproducibility: More than 20% of this document may be affected by microfiche quality

(AD-A282682; NRL/MR/5510-94-7497) Avail: CASI HC A06

Information Technology Division's Technical Paper Abstracts 1993 documents the accomplishments of projects at the seven branches of the Information Technology Division. The seven branches are: Navy Center for Applied Research in Artificial Intelligence (NCARAI) including: machine learning, intelligent decision aids, interactive systems, sensor-based systems, and neural networks; Communications Systems; Human-Computer Interaction; Center for Computer High Assurance Systems; Transmission Technology; Advanced Information Technology; and Center for Computational Sciences. Points of contact are indicated for acquiring additional technical information about the projects. DTIC

N95-12995# Mississippi State Univ., Bay Saint Louis, MS. Center for Air Sea Technology.

DESIGN OF AN INTELLIGENT SUPPORT SYSTEM FOR SCIENTIFIC DATABASES

Patrick Perrin and Frederick Petry 1 Aug. 1994 38 p

(Contract N00014-92-J-4109)

(AD-A283043; CAST-TR-94-2) Avail: CASI HC A03/MF A01

This report describes progress made in designing an Intelligent Support System (ISS) for automatic data analysis and efficient data exploitation in numerical scientific databases, with an application to environmental databases used for ocean modeling and prediction. Improvements made to the Automatic Data Analysis System (ADAS) by combining the features of two machine learning techniques (i.e., data clustering and inductive learning by decision tree) to generate sets of production rules that efficiently describe the observational raw data contained in the scientific databases are explained. Data clustering allows the system to classify the raw data into clusters, which the system learns by induction to build the decision trees, from which are deduced the production rules. Also described is the design of a robust computational model of conversation (ENTRETIEN) for interactive natural language man-machine interfacing, based on case grammar theory. Such a system allows the user to naturally communicate with the system for efficient and effective information retrieval. ENTRETIEN conducts the conversation to recognize the user's intentions. To include the automatically generated production rules into the knowledge base of an expert system and to add the facilities of the natural language interface represent our final goal in building an intelligent support system for efficient exploitation of large scientific databases. DTIC

N95-13123# Los Alamos National Lab., NM.

SHIFTING OUR FOCUS: COMMUNICATING SCIENCE TO A NEW, NONTECHNICAL CULTURE

A. Garnett, G. Hollen, A. Longshore, A. Mauzy, and A. Reeves 1994 8 p Presented at the IPCC Conference, Banff, Canada, Sep. 1994

(Contract W-7405-eng-36)

(DE94-014258; LA-UR-94-1791; CONF-9409164-1) Avail: CASI HC A02/MF A01

Congress' decision to close down the $11 billion Superconducting Supercollider is spreading anxiety throughout the scientific community. As funding for the nation's research laboratories becomes increasingly scarce, technical communicators in these organizations must focus much of their communications efforts on a new culture: Congress and the public. We discuss how to characterize this new audience and the importance of evaluating communication products, and we highlight some strategies for interpreting science to nonscientists more effectively. DOE

N95-13167# Army Cold Regions Research and Engineering Lab., Hanover, NH.

BIBLIOGRAPHY ON COLD REGIONS SCIENCE AND TECHNOLOGY, VOLUME 47, PART 1 Report, 1993

Stuart G. Hibben 1993 232 p

(AD-A281879) Avail: CASI HC A11/MF A03

This is a continuing publication of the Cold Regions Bibliography Project in the Science and Technology Division of the Library of Congress. The present volume contains material accessioned between October 1992 and September 1993. It contains full citations of 5273 items, in many cases with abstracts. indexing for the volume is issued as Volume 46, Part 2. Derived from text

N95-13245 Selskapet for Industriell og Teknisk Forskning, Trondheim (Norway). Div. for Information Technology.

TOOLKITS FOR CONSTRUCTION AND MANIPULATION OF GEOGRAPHICAL DATA

M. Daehlen 27 Dec. 1993 46 p

(PB94-202587; STF33-A93044) Avail: Issuing Activity (National Technical Information Service (NTIS))

The publication is a collection of tutorial notes on mathematical toolkits for construction and manipulation of spatio-temporal data within geographical information systems. NTIS

83 ECONOMICS AND COST ANALYSIS

Includes cost effectiveness studies.

No abstracts in this category.

84 LAW, POLITICAL SCIENCE AND SPACE POLICY

Includes NASA appropriation hearings; aviation law; space law and policy; international law; international cooperation; and patent policy.

N95-11866*# National Aeronautics and Space Administration. Lewis Research Center, Cleveland, OH.
INTELLECTUAL PROPERTY RIGHTS AT THE NATIONAL AERONAUTICS AND SPACE ADMINISTRATION, LEWIS RESEARCH CENTER
Vernon E. Williams Sep. 1994 67 p
(NASA-TM-106731; E-9107; NAS 1.15:106731) Avail: CASI HC A04/MF A01

At a fundamental level, intellectual property is the core work product of a technical organization. The National Aeronautics and Space Administration (NASA), produces a variety of intellectual property including: patents, trademarks, data rights, copyright and rights associated with National Security. For a scientific organization to properly manage its work product it has to manage its intellectual property. This paper endeavors to describe how the intellectual property rights are generated and allocated at NASA. The author then goes on to discuss how the intellectual property might be managed to meet the objectives of program implementation, technology transfer and security. Author

N95-11871 National Defence Research Establishment, Stockholm (Sweden). Huvudavdelning foer informationsteknologi.
CONTRIBUTIONS TO CD SPACE COMMITTEE, 1993. SUMMARY AND COMMENTS [CD RYMDKOMMITTEARBETE 1993. SAMMANFATTNING OCH KOMMENTARER]
U. Ekblad Nov. 1993 58 p In SWEDISH See also PB92-195312
(PB94-190618; FOA-A-30087-9.4) Avail: Issuing Activity (National Technical Information Service (NTIS))

The report gives a summary of the contributions in the space area to the UN Conference on Disarmament in Geneva and its Space Committee on the Prevention of an Arms Race in Outer Space (PAROS) during the 1992 sessions. Commentaries are also given. NTIS

85 URBAN TECHNOLOGY AND TRANSPORTATION

Includes applications of space technology to urban problems; technology transfer; technology assessment; and surface and mass transportation.

For related information see also *03 Air Transportation and Safety, 16 Space Transportation,* and *44 Energy Production and Conversion.*

No abstracts in this category.

88 SPACE SCIENCES (GENERAL)

No abstracts in this category.

89 ASTRONOMY

Includes radio, gamma-ray, and infrared astronomy, and astrometry.

N95-12234*# Illinois Univ., Urbana, IL. Dept. of Astronomy.
A CATALOGUE OF POTENTIALLY BRIGHT CLOSE BINARY GRAVITATIONAL WAVE SOURCES Final Technical Report
Ronald F. Webbink 1985 481 p
(Grant NAGw-2996)
(NASA-CR-196934; NAS 1.26:196934) Avail: CASI HC A21/MF A04

This is a current print-out of results of a survey, undertaken in the spring of 1985, to identify those known binary stars which might produce significant gravitational wave amplitudes at earth, either dimensionless strain amplitudes exceeding a threshold h = 10(exp -21), or energy fluxes exceeding F = 10(exp -12) erg cm(exp -2) s(exp -1). All real or putative binaries brighter than a certain limiting magnitude (calculated as a function of primary spectral type, orbital period, orbital eccentricity, and bandpass) are included. All double degenerate binaries and Wolf-Rayet binaries with known or suspected orbital periods have also been included. The catalog consists of two parts: a listing of objects in ascending order of Right Ascension (Equinox B1950), followed by an index, listing of objects by identification number according to all major stellar catalogs. The object listing is a print-out of the spreadsheets on which the catalog is currently maintained. It should be noted that the use of this spreadsheet program imposes some limitations on the display of entries. Text entries which exceed the cell size may appear in truncated form, or may run into adjacent columns. Greek characters are not available; they are represented here by the first two or three letters of their Roman names, the first letter appearing as a capital or lower-case letter according to whether the capital or lower-case Greek character is represented. Neither superscripts nor subscripts are available; they appear here in normal position and type-face. The index provides the Right Ascension and Declination of objects sorted by catalogue number. Author (revised)

N95-12304*# National Aeronautics and Space Administration, Washington, DC.
X-RAY AND GAMMA RAY ASTRONOMY DETECTORS
Rudolf Decher, Brian D. Ramsey, and Robert Austin 1994 80 p
(NASA-SP-517; NAS 1.21:517; LC-94-92211) Avail: CASI HC A05/MF A01

X-ray and gamma ray astronomy was made possible by the advent of space flight. Discovery and early observations of celestial x-rays and gamma rays, dating back almost 40 years, were first done with high altitude rockets, followed by Earth-orbiting satellites> once it became possible to carry detectors above the Earth's atmosphere, a new view of the universe in the high-energy part of the electromagnetic spectrum evolved. Many of the detector concepts used for x-ray and gamma ray astronomy were derived from radiation measuring instruments used in atomic physics, nuclear physics, and other fields. However, these instruments, when used in x-ray and gamma ray astronomy, have to meet unique and demanding requirements related to their operation in space and the need to detect and measure extremely weak radiation fluxes from celestial x-ray and gamma ray sources. Their design for x-ray and gamma ray astronomy has, therefore, become a rather specialized and rapidly advancing field in which improved sensitivity, higher energy and spatial resolution, wider spectral coverage, and enhanced imaging capabilities are all sought. This text is intended as an introduction to x-ray and gamma ray astronomy instruments. It provides an overview of detector design and technology and is aimed at scientists, engineers, and technical personnel and managers associated with this field. The discussion is limited to basic principles and design concepts and provides examples of applications in past, present, and future space flight missions.
Author (revised)

N95-12373*# Georgia Univ., Athens.
A DEEP X-RAY SURVEY OF THE PLEIADES CLUSTER AND THE B6-A3 MAIN SEQUENCE STARS IN ORION Final Report, 15 Jun. 1991 - 14 Jun. 1993
Jean-Pierre Caillault 14 Jun. 1993 4 p
(Grant NAG5-1608)
(NASA-CR-196190; NAS 1.26:196190) Avail: CASI HC A01/MF A01

We have obtained deep ROSAT images of three regions within the Pleiades open cluster. We have detected 317 X-ray sources in these ROSAT PSPC images, 171 of which we associate with certain probable members of the Pleiades cluster. We detect nearly all Pleiades members with spectral types later than G0 and within 25 arcminutes of our three field centers where our sensitivity is highest. This has allowed us to derive for the first time the luminosity function for the G, K, and M dwarfs of an open cluster without the need to use statistical techniques to account for the presence of upper limits in the data sample. Because of our high X-ray detection frequency down to the faint limit of the optical catalog, we suspect that some of our unidentified X-ray sources are previously unknown, very low-mass members of the Pleiades. A large fraction of the Pleiades members detected with ROSAT have published rotational velocities. Plots of L(sub x)/L(sub bol) versus spectroscopic rotational velocity show tightly correlated 'saturation' type relations for stars with (B - V)(sub O) greater than 0.60. For each of several color ranges, X-ray luminosities rise rapidly with increasing rotation rate until v sin i approximately equals 15 km/s, and then remain essentially flat for rotation rates up to at least v sin i approximately equal to 100 km/s. The dispersion in rotation among low-mass stars in the Pleiades is by far the dominant contributor to the dispersion in L(subx) at a given mass. Only about 35 percent of the B.A. and early F stars in the Pleiades are detected as X-ray sources in our survey. There is no correlation between X-ray flux and rotation for these stars. The X-ray luminosity function for the early-type Pleiades stars appears to be bimodal, with only a few exceptions. We either detect these stars at fluxes in the range found for low-mass stars or we derive X-ray limits below the level found for most Pleiades dwarfs. The X-ray spectra for the early-type Pleiades stars detected by ROSAT are indistinguishable from the spectra of the low-mass Pleiades members. We believe that the simple explanation for this behavior is that the early-type Pleiades stars are not themselves intrinsic X-ray sources and that the X-ray sources and that the X-ray emission actually arises from low-mass companions to these stars. Author

N95-12388*# Georgia Univ., Athens.
AN X-RAY SEARCH FOR PMS STARS IN TRANSLUCENT MOLECULAR CLOUDS Annual Report, 15 Oct. 1992 - 14 Oct. 1994
Jean-Pierre Caillault 14 Oct. 1994 5 p
(Grant NAG5-1610)
(NASA-CR-196151; NAS 1.26:196151) Avail: CASI HC A01/MF A01

The work outlined in this paper identifies 108 plausible T Tauri candidates in the regions of two high latitude translucent molecular clouds. Follow-up optical spectroscopy of these candidates is needed to resolve the question of whether or not star formation is present in these clouds. We have recently submitted a proposal to use the Kitt Peak National Observatory 2.1 meter telescope to take medium resolution spectra of the 14 PMS candidate X-ray sources in MBM 40 to determine spectral types and search for indicators of youth (strong Li absorption; H alpha emission) and we will submit a similar proposal to study the X-ray sources in MBM 55. Only spectra will provide an unambiguous determination of their pedigree. As part of an ongoing study of star formation at high galactic latitude we intend to analyze data in the ROSAT archives to investigate the possibility of star formation in all of the high latitude translucent molecular clouds observed. We believe that this project may yield a significant increase in our understanding of the star formation process for low-mass stars and of the nature of the translucent clouds. Derived from text

N95-12463*# Alabama Univ., Huntsville, AL.
BATSE OBSERVATIONS OF 3C273
W.S. Paciesas, R. S. Mallozzi, G. N. Pendleton, B. A. Harmon, C. A. Wilson, S. N. Zhang, and G. J. Fishman 1994 5 p
(Contract NAS8-38609)
(NASA-CR-196185; NAS 1.26:196185) Avail: CASI HC A01/MF A01

The quasar 3C273 has been detected by all instruments on CGRO. The emission from this source is monitored continuously by BATSE using Earth occultation. We present results of a preliminary analysis of BATSE data, including light curves of the 3C273 flux covering approximately 150 days in the interval April-August 1991 and approximately 350 days in the interval July 1992-April 1993. The source intensity in the energy range 50-300 keV is typically approx. 0.002 ph cm(exp -2)s(exp -1). We find weak evidence for variations of as much as a factor of 3 in the intensity. We derive spectral parameters of 3C273 during the intervals TJD 8422-8435 (15-28 June 1991) and TJD 8532-8546 (3-17 October 1991) for comparison with other CGRO instruments. Author (revised)

N95-12464*# Alabama Univ., Huntsville, AL.
BATSE OBSERVATIONS OF NOVA MUSCAE 1991
W. S. Paciesas, M. S. Briggs, G. N. Pendleton, B. A. Harmon, C. A. Wilson, S. N. Zhang, and G. J. Fishman [1993] 4 p
(Contract NAS8-38609)
(NASA-CR-196416; NAS 1.26:196416) Avail: CASI HC A01/MF A01

The Compton Burst and Transient Source Experiment (BATSE) detected hard x-ray flux from Nova Muscae 1991 (GS/GRS 1124-68) during an interval of approximately 100 days beginning approximately 130 days after the January 1991 main outburst. The light curve during this secondary outburst is roughly symmetric, reaching a maximum around mid-July 1991 at an intensity of approximately 15 percent of the peak intensity during the main outburst. The hard x-ray spectrum displays a soft-to-hard evolution during the rise to maximum; the post-maximum spectral evolution is less well determined. We compare our observations with those of the GRANAT/SIGMA experiment, which covered the initial outburst well but missed most of the secondary outburst. Author

N95-12465*# Space Telescope Science Inst., Baltimore, MD.
HOT ABSORBERS AND THE X-RAY SPECTRA OF BL LAC OBJECTS Final Report, Oct. 1991 - Feb. 1994
C. Megan Urry Feb. 1994 2 p
(Grant NAG5-1671)
(NASA-CR-196196; NAS 1.26:196196) Avail: CASI HC A01/MF A01

This is the final report to the National Aeronautics and Space Administration (NASA) concerning NASA grant NAG5-1671. This grant was awarded to Dr. C. Megan Urry of the Space Telescope Science Institute in response to a proposal, entitled 'Hot Absorbers and the X-Ray Spectra of BL Lac Objects.' The grant was originally awarded in October 1991 and expired in February 1994. The purpose of this project was to detect spectral features in high signal-to-noise Rosat PSPC spectra of X-ray-bright BL Lac objects. We were granted observations of three targets: PKS2155-304, Mrk421, and Mrk501. All three were bright and yielded 5,000-30,000 photons in the good PSPC data. Author

N95-12466*# Space Telescope Science Inst., Baltimore, MD.
X-RAY TEMPORAL AND SPECTRAL STUDIES OF BLAZARS WITH THE GINGA SATELLITE Final Report, Feb. 1988 - Mar. 1994
C. Megan Urry Mar. 1994 3 p
(Grant NAG8-697)
(NASA-CR-196330; NAS 1.26:196330) Avail: CASI HC A01/MF A01

This is the final report to the National Aeronautics and Space Administration (NASA) concerning NASA grant NAG8-697. This grant was awarded to Dr. C. Megan Urry of the Space Telescope Science Institute in response to a proposal, entitled 'X-Ray Temporal and Spectral Studies of Blazars with the Ginga Satellite', to collaborate with Japanese colleagues in using the Ginga X-ray satellite. The grant was originally awarded on 2/27/88 and expired on 3/31/94. The Ginga X-ray satellite had unprecedented sensitivity in the 2-20 keV energy band, allowing us to make detailed temporal and spectral studies of a large number of blazars, which are a kind of unusually luminous and variable active galactic nuclei. We were successful with several proposals and were able to observe a number of different active galactic nuclei. Our investigations under this grant fall broadly into two categories: (1) Ginga observations of blazars, usually in conjunction with simultaneous multiwavelength observations using other facilities; and (2) the application of calculated pair plasma spectra to the X-ray colors of active galactic nuclei. These are described in turn. Author (revised)

N95-12633 Massachusetts Univ., Amherst, MA.
THE TWO MICRON ALL SKY SURVEY: SURVEY RATIONALE AND INITIAL TESTING
S. G. Kleinmann, M. G. Lysaght, W. L. Pughe, S. E. Schneider, and M. F.

Skrutskie 1994 7 p Limited Reproducibility: More than 20% of this document may be affected by microfiche quality
(AD-A283514) Avail: CASI HC A02

This paper summarizes the essential parameters of the 2MASS project and the rationale behind those choices, and gives an overview of results obtained with a prototype camera that has been in operation since May 1992. We conclude with a list of expected data products and a statements of the daya release policy. Derived from text

N95-12788*# Citadel Coll., Charleston, SC. Dept. of Physics.
PHOTOGRAPHIC REGION ELEMENTAL ABUNDANCE ANALYSES OF DR. DAVID S. LECKRONE'S GTO HST STARS 2 Final Report
Saul J. Adelman 6 Sep. 1994 23 p
(Grant NAG5-1551)
(NASA-CR-196756; NAS 1.26:196756) Avail: CASI HC A03/MF A01

Activities are presented for the grant-funded work at the Dominion Astrophysical (DAO) and Casleo Observatories. A comparison is planned for the spectrograms taken at both observatories of similar stars. It is reported that of the Northern Hemisphere program stars, only 112 Her remains to be analyzed. A preliminary solution for the components of this binary system has been found. The new ATLAS9 models have been used to reevaluate the effective temperatures and surface gravities derived for all program stars. Model atmospheres are being calculated by extensive grids on workstations upgraded to the DEC 3000 model 300X running Open VMS. An attached paper describes a plan to obtain the needed gf values as well as some first applications of astrophysical gf values, the most important of which was Vega. CASI

N95-12821*# Space Telescope Science Inst., Baltimore, MD.
FOC SV SUPPORT AND SCIENCE DATA ANALYSIS Final Report, 15 Aug. 1992 - May 1994
J. Chris Blades May 1994 9 p
(Grant NAG5-1733)
(NASA-CR-196764; NAS 1.26:196764) Avail: CASI HC A02/MF A01

The main activity of NASA grant NAG5-1733 has been the study of Planetary Nebulae in the Magellanic Clouds through observations using the ESA Faint Object Camera conducted during Hubble Space Telescope (HST) Observing Cycles 1 and 2 in the pre-Costar era and in Cycle 4 with Costar and the FOC. A table of the observations obtained during these observing periods is attached along with figures showing the final images. Both the table and the figures are intended for publication later this year in the Astrophysical journal. Work that had been carried out under this grant included: astrometric measurement of ground-based images and preparation of detailed observing proposals; re-calibration of FOC images; deconvolution; and data analysis and measurement. The work has resulted in two papers, the first already published and the second in preparation by Blades, Osmer and Barlow. A reprint of the first paper is attached. The second paper will enlarge upon the results described in the first paper, bearing in mind the much larger sample of objects. Finally, the recently acquired images in Cycle 4 with the corrected optics will allow us to make direct and quantitative comparison between the pre- and post-correction for FOC. This work will be carried out under a separate grant. All the observations concerning Planetary Nebulae as described in an earlier status report have been collected and measured. In addition, a preliminary study of the photometric response of the FOC was begun under this grant but not completed because the analysis of the Cycle 2 Planetary Nebulae took much longer and was much more difficult than originally envisaged (due to the spherical aberration problem). However, because our data covers a long time period, we shall be able to deduce the photometric properties now using the actual PN themselves. This work will be carried out under a separate grant. Derived from text

N95-12992*# Alabama Univ., Huntsville, AL.
FNAS UAH UVSP AND COMPLIMENTARY DATA ANALYSIS AND MODELING Final Report
Juan M. Fontenla 25 May 1994 4 p
(Contract NAS8-38609)
(NASA-CR-194005; NAS 1.26:194005) Avail: CASI HC A01/MF A01

Several data sets obtained by the UVSP and HXIS instruments on board SMM were studied. From these data, several events of sequences of events were selected that are specially representative of the plethora of active region energetic phenomena that was simultaneously observed by UVSP and HXIS. The selection criteria was to have available both types of observations in active region flares that are not so bright that the UVSP instrument was switched off for protection, and at the same time flares that are not so dim in X-Rays that HXIS will have collected significant data. Another criteria of secondary importance was to select events where auxiliary optical data is available. Author (revised)

N95-13012*# Southwest Research Inst., San Antonio, TX. Instrumentation and Space Research Div.
THE DETECTABILITY OF EXTRASOLAR TERRESTRIAL AND GIANT PLANETS DURING THEIR LUMINOUS FINAL ACCRETION
S. Alan Stern 1994 18 p Submitted for publication
(Grant NAGw-3023)
(NASA-CR-196147; NAS 1.26:196147) Avail: CASI HC A03/MF A01

One of the outstanding scientific questions in astronomy is the frequency at which solar systems form. Answering this question is an observational challenge because extrasolar planets are intrinsically difficult to directly detect. The direct detectability of planets is examined during the short but unique epoch of giant impacts that is a hallmark of the standard theory of planetary formation. Sufficiently large impacts during this era are capable of creating a luminous, 1500-2500 K photosphere, which can persist for timescales exceeding 103 years in some cases. The detectability of such events and the number of young stars one would need to examine to expect to find a luminous terrestrial class planet after a giant impact are examined. With emerging IR interferometric technology, thermally-luminous earth-sized objects can be detected in nearby star forming regions in 1-2 nights observing time. Unfortunately, predictions indicate that approximately 250 young stars would have to be searched to expect to find one hot, terrestrial-sized planet. By comparison, the detection of Saturn and Uranus/Neptune-sized planets after a giant impact requires only 1-2 hours of observing time. A single Keck-class telescope should be able to determine whether such planets are common in the nearest star forming regions by examining about less than 100 young stars over a few tens of nights. The results obtained herein suggest a new strategy for the detection of solar systems with the potential for the observational confirmation of the standard theory of late-stage planetary accretion. Author (revised)

N95-13056*# Johns Hopkins Univ., Baltimore, MD. Dept. of Physics and Astronomy.
A STUDY OF A MULTI-PINNED PHASE CCD DETECTOR FOR USE AS A STAR TRACKER Final Report
Scott D. Friedman 21 Jul. 1994 10 p
(Grant NAG5-1119)
(NASA-CR-196287; NAS 1.26:196287) Avail: CASI HC A02/MF A01

This grant has supported studies of the use of charge coupled devices (CCD's) in star trackers in a number of different areas. Among the tasks we have pursued are the following: (1) radiation modeling and the increase in noise equivalent angle as a result of exposure to protons and bremsstrahlung gamma rays; (2) the development of pattern matching software to identify field locations from a CCD image and a pre-existing map of the local area; (3) observations of various stellar fields from the 24 inch telescope at the Offit Observatory at JHU, primarily to test the pattern matching software (these included crowded fields as well as moving objects, like comets); and (4) tracking of very faint objects to determine the faint limit of the CCD system. Author (revised)

90 ASTROPHYSICS

Includes cosmology; celestial mechanics; space plasmas; and interstellar and interplanetary gases and dust.

For related information see also *75 Plasma Physics*.

N95-11928*# Lockheed Missiles and Space Co., Palo Alto, CA.
INVESTIGATION OF PHYSICAL PARAMETERS IN STELLAR FLARES OBSERVED BY GINGA Final Report, 20 Jul. 1993 - 19 Sep. 1994
Robert A. Stern 19 Sep. 1994 37 p
(Contract NAS8-39936)
(NASA-CR-196823; NAS 1.26:196823) Avail: CASI HC A03/MF A01

This program involves analysis and interpretation of results from GINGA Large Area Counter (LAC) observations from a group of large stellar x-ray flares. All LAC data are re-extracted using the standard Hayashida method

of LAC background subtraction and analyzed using various models available with the XSPEC spectral fitting program. Temperature-emission measure histories are available for a total of 5 flares observed by GINGA. These will be used to compare physical parameters of these flares with solar and stellar flare models. Author

N95-12939*# Columbia Univ., New York, NY. Dept. of Physics.
RESEARCH IN ASTROPHYSICAL PROCESSES Final Research Status Report, Jul. 1986 - Jun. 1994
Malvin A. Ruderman Aug. 1994 12 p
(Contract NCC5-37)
(NASA-CR-196773; NAS 1.26:196773) Avail: CASI HC A03/MF A01

Work completed under this grant is summarized in the following areas:(1) radio pulsar turn on and evaporation of companions in very low mass x-ray binaries and in binary radio pulsar systems; (2) effects of magnetospheric pair production on the radiation from gamma-ray pulsars; (3) radiation transfer in the atmosphere of an illuminated companion star; (4) evaporation of millisecond pulsar companions;(5) formation of planets around pulsars; (6) gamma-ray bursts; (7) quasi-periodic oscillations in low mass x-ray binaries; (8) origin of high mass x-ray binaries, runaway OB stars, and the lower mass cutoff for core collapse supernovae; (9) dynamics of planetary atmospheres; (10) two point closure modeling of stationary, forced turbulence; (11) models for the general circulation of Saturn; and (12) compressible convection in stellar interiors. Derived from text

N95-12940*# Alabama Univ., Huntsville, AL. Center for Space Plasma and Aeronomic Research.
MAGNETOSPHERIC SPACE PLASMA INVESTIGATIONS Semiannual Progress Report, Feb. - Jul. 1994
Richard H. Comfort and James L. Horwitz Aug. 1994 8 p
(Grant NAG8-239)
(NASA-CR-196793; NAS 1.26:196793) Avail: CASI HC A02/MF A01

A time dependent semi-kinetic model that includes self collisions and ion-neutral collisions and chemistry was developed. Light ion outflow in the polar cap transition region was modeled and compared with data results. A model study of wave heating of O+ ions in the topside transition region was carried out using a code which does local calculations that include ion-neutral and Coulomb self collisions as well as production and loss of O+. Another project is a statistical study of hydrogen spin curve characteristics in the polar cap. A statistical study of the latitudinal distribution of core plasmas along the L=4.6 field line using DE-1/RIMS data was completed. A short paper on dual spacecraft estimates of ion temperature profiles and heat flows in the plasmasphere ionosphere system was prepared. An automated processing code was used to process RIMS data from 1981 to 1984. Derived from text

N95-12950*# Illinois Univ., Urbana, IL.
THE X-RAY STRUCTURE OF THE SUPERNOVA REMNANT W49B Final Report, 15 Jul. 1992 - 14 Jan. 1994
John R. Dickel, Rosa Murphy, You-Hua Chu, Guillermo Garcia, and Daniel Goscha 1994 4 p
(Grant NAG5-2018)
(NASA-CR-196482; NAS 1.26:196482) Avail: CASI HC A01/MF A01

Comparison of x-ray and radio images of W49B and other supernova remnants (SNR) provides detailed information on the mechanisms responsible for the emission and on the evolution of the remnants. There is faint x-ray emission from all parts of W49B but most of it is concentrated near the center of the remnant, unlike the radio emission which arises in a shell near the periphery. This structure indicates that this SNR is in the adolescent phase of its lifetime. Derived from text

91 LUNAR AND PLANETARY EXPLORATION

Includes planetology; and manned and unmanned flights.

For spacecraft design or space stations see *18 Spacecraft Design, Testing and Performance.*

N95-11704*# Vexcel Corp., Boulder, CO.
VENUS SURFACE ROUGHNESS AND MAGELLAN STEREO DATA Progress Report
Kelly E. Maurice, Franz W. Leberl, L. Norikane, and Scott Hensley 14 Sep. 1994 65 p Original contains color illustrations
(Contract NASw-4854)
(NASA-CR-196821; NAS 1.26:196821; VDAP-R1) Avail: CASI HC A04/MF A01; 13 functional color pages

Presented are results of some studies to develop tools useful for the analysis of Venus surface shape and its roughness. Actual work was focused on Maxwell Montes. The analyses employ data acquired by means of NASA's Magellan satellite. The work is primarily concerned with deriving measurements of the Venusian surface using Magellan stereo SAR. Roughness was considered by means of a theoretical analyses based on digital elevation models (DEM's), on single Magellan radar images combined with radiometer data, and on the use of multiple overlapping Magellan radar images from cycles 1, 2, and 3, again combined with collateral radiometer data. Author

N95-12011*# California Inst. of Tech., Pasadena, CA. Geological and Planetary Science Div.
QUANTITATIVE UNDERSTANDING OF THE CYCLES OF OXIDIZED AND REDUCED SULFUR ON VENUS Final Technical Report, 1 Mar. 1992 - 28 Feb. 1994
Yuk L. Yung 28 Feb. 1994 29 p
(Grant NAG2-764)
(NASA-CR-196924; NAS 1.26:196924) Avail: CASI HC A03/MF A01

The evolution of the Venus atmosphere is determined by the supply of gases from the interior of the planet and outer space, and by the loss of particles to space over time. In particular, questions pertaining to the initial inventory of water and the current and past rates of outgassing can be addressed by studying the loss rates of H, D, He3 and He4. The photochemistry of the H2SO4 clouds may also have played an important role in regulating the amount of water above the cloud tops, and hence limit the rate of escape of hydrogen from the planet. Thus the problems of evolution and chemistry are intimately related. In our proposal the principal tasks we undertook to advance our understanding of the origin and evolution of water on Venus included: (1) escape of light atoms from Venus and (2) develop a photochemical model of sulfate formation. In the last two years we have made progress on Task 1 regarding how light atoms can escape from the exosphere of Venus with the development of a Monte Carlo program and in Task 2 have developed a thorough update on the SO2 photochemistry that had been previously carried out. Author (revised)

N95-12190*# National Aeronautics and Space Administration. Ames Research Center, Moffett Field, CA.
SCIENCE OBJECTIVES AND PERFORMANCE OF A RADIOMETER AND WINDOW DESIGN FOR ATMOSPHERIC ENTRY EXPERIMENTS
Roger A. Craig (MCAT Inst., Moffett Field, CA.), William C. Davy (Eloret Corp., Santa Clara, CA.), and Ellis E. Whiting (Eloret Corp., Santa Clara, CA.) Aug. 1994 18 p
(RTOP 232-01-04)
(NASA-TM-4637; A-94069; NAS 1.15:4637) Avail: CASI HC A03/MF A01

This paper describes the techniques developed for measuring stagnation-point radiation in NASA's cancelled Aeroassist Flight Experiment (AFE). It specifies the need for such a measurement; the types and requirements for the needed instruments; the Radiative Heating Experiment (RHE) developed for the AFE; the requirements, design parameters, and performance of the window developed for the RHE; the procedures and summary of the technique; and results of the arc-jet wind tunnel experiment conducted to demonstrate the overall concept. Subjects emphasized are the commercial implications of the knowledge to be gained by this experiment in connection with the Aeroassisted Space Transfer Vehicle (ASTV), the nonequilibrium nature of the radiation, concerns over the contribution of vacuum-ultraviolet radiation to the overall radiation, and the limit on the flight environment of the vehicle imposed by the limitations on the window material. Results show that a technique exists with which the stagnation-point radiation can be measured in flight in an environment of interest to commercial ASTV applications. Author (revised)

N95-12307*# Texas Univ., Austin, TX. Dept. of Aerospace Engineering and Engineering Mechanics.
A ROBOTIC EXPLORATION MISSION TO MARS AND PHOBOS Final Report
Justin H. Kerr, Erin Defosse, Quang Ho, Ernisto Barriga, Grant Davis,

Steve McCourt, and Matt Smith 29 Nov. 1993 149 p
(Contract NASw-4435)
(NASA-CR-197168; NAS 1.26:197168; RFP-ASE274L-0893) Avail: CASI HC A07/MF A02

This report discusses the design of a robotic exploration to Mars and Phobos. It begins with the mission's background and objectives, followed by a detailed explanation of various elements of Project Aeneas, including science, spacecraft, probes, and orbital trajectories. In addition, a description of Argos Space Endeavours, management procedures, and overall project costs are presented. Finally, a list of recommendations for future design activity is included. Author (revised)

N95-12362*# Universities Space Research Association, Columbia, MD.
LUNAR LANDER PROJECT: A STUDY ON FUTURE MANNED MISSIONS TO THE MOON
1966 77 p
(Contract NASw-4435)
(NASA-CR-197177; NAS 1.26:197177) Avail: CASI HC A05/MF A01

This project is based on designing a small lunar probe which will conduct research relating to future manned missions to the moon. The basic design calls for two experiments to be run. The first of these experiments is an enclosed environment section which will be exposed to solar radiation while on the moon. The purpose of this experiment is to determine the effect of radiation on an enclosed environment and how different shielding materials can be used to moderate this effect. The eight compartments will have the following covering materials: glass, polarized glass, plexiglass, polyurethane, and boron impregnated versions of the polyurethane and plexiglass. The enclosed atmosphere will be sampled by a mass spectrometer to determine elemental breakdown of its primary constituents. This is needed so that an accurate atmospheric processing system can be designed for a manned mission. The second experiment is a seismic study of the moon. A small penetrating probe will be shot into the lunar surface and data will be collected onboard the lander by an electronic seismograph which will store the data in the data storage unit for retrieval and transmission once every twenty-three hours. The project is designed to last ten years with possible extended life for an additional nine years at which point power requirements prevent proper functioning of the various systems. Author

N95-12529*# Cincinnati Univ., OH. Space Engineering Research Center.
DESIGN OF AN UNMANNED MARTIAN POLAR EXPLORATION SYSTEM Final Report
Curt Baldwin, Denny Chitwood, Brian DeMann, Jordan DuCheny, Richard Hampton, Jesse Kuhns, Amy Mercer, Shawn Newman, Chris Patrick, and Tony Polakowski et al 30 Jul. 1994 520 p
(Contract NASw-4435)
(NASA-CR-197160; NAS 1.26:197160) Avail: CASI HC A22/MF A04

The design of an unmanned Martian polar exploration system is presented. The system elements include subsystems for transportation of material from earth to Mars, study of the Martian north pole, power generation, and communications. Early next century, three Atlas 2AS launch vehicles will be used to insert three Earth-Mars transfer vehicles, or buses, into a low-energy transfer orbit. Capture at Mars will be accomplished by aerobraking into a circular orbit. Each bus contains four landers and a communications satellite. Six of the twelve total landers will be deployed at 60 deg intervals along 80 deg N, and the remaining six landers at 5 deg intervals along 30 deg E from 65 deg N to 90 deg N by a combination of retrorockets and parachutes. The three communications satellites will be deployed at altitudes of 500 km in circular polar orbits that are 120 deg out of phase. These placements maximize the polar coverage of the science and communications subsystems. Each lander contains scientific equipment, two microrovers, power supplies, communications equipment, and a science computer. The lander scientific equipment includes a microweather station, seismometer, thermal probe, x-ray spectrometer, camera, and sounding rockets. One rover, designed for short-range (less than 2 km) excursions from the lander, includes a mass spectrometer for mineral analysis, an auger/borescope system for depth profiling, a deployable thermal probe, and charge coupled device cameras for terrain visualization/navigation. The second rover, designed for longer-range (2-5 km) excursions from the lander, includes radar sounding/mapping equipment, a seismometer, and laser ranging devices. Power for all subsystems is supplied by a combination of solar cells, Ni-H batteries, and radioisotope thermoelectric generators. Communications are sequenced from rovers, sounding rockets, and remote sensors to the lander, then to the satellites, through the Deep Space Network to and from earth. Author (revised)

N95-12533*# Wisconsin Univ., Madison, WI. Dept. of Mechanical Engineering.
VENUS CLOUD BOBBER MISSION: A LONG TERM SURVEY OF THE VENUSIAN SURFACE
James Wai, Cheryl Derengowski, Russ Lautzenhiser, Matt Emerson, and Yongho Choi 9 May 1994 121 p
(Contract NASw-4435)
(NASA-CR-197174; NAS 1.26:197174) Avail: CASI HC A06/MF A02

We have examined the Venus Balloon concept in order to further develop the ideas and concepts behind it, and to creatively apply them to the design of the major Venus Balloon components. This report presents our models of the vertical path taken by the Venus Balloon and the entry into Venusian atmosphere. It also details our designs of the balloon, gondola, heat exchanger, power generator, and entry module. A vehicle is designed for a ballistic entry into the Venusian atmosphere, and an atmospheric model is created. The model is then used to set conditions. The shape and material of the vehicle are optimized, and the dimensions of the vehicle are then determined. Equipment is chosen and detailed that will be needed to collect and transmit information and control the mission. A gondola is designed that will enable this sensitive electronic equipment to survive in an atmosphere of very high temperature and pressure. This shape and the material of the shell are optimized, and the size is minimized. Insulation and supporting structures are designed to protect the payload equipment and to minimize mass. A method of cooling the gondola at upper altitudes was established. Power needs of the gondola equipment are determined. Power generation options are discussed and two separate thermoelectric generation models are outlined. Author (revised)

N95-12826*# Washington Univ., Seattle, WA. Dept. of Aeronautics and Astronautics.
PROJECT HYREUS: MARS SAMPLE RETURN MISSION UTILIZING IN SITU PROPELLANT PRODUCTION Final Report
Anita Abrego, Chris Bair, Anthony Hink, Jae Kim, Amber Koch, Ross Kruse, Dung Ngo, Heather Nicholson, Laurie Nill, and Craig Perras et al 31 Jul. 1993 384 p Prepared for Universities Space Research Association, Columbia, MD
(Contract NASw-4435)
(NASA-CR-197189; NAS 1.26:197189) Avail: CASI HC A17/MF A03

Project Hyreus is an unmanned Mars sample return mission that utilizes propellants manufactured in situ from the Martian atmosphere for the return voyage. A key goal of the mission is to demonstrate the considerable benefits of using indigenous resources and to test the viability of this approach as a precursor to manned Mars missions. The techniques, materials, and equipment used in Project Hyreus represent those that are currently available or that could be developed and readied in time for the proposed launch date in 2003. Project Hyreus includes such features as a Mars-orbiting satellite equipped with ground-penetrating radar, a large rover capable of sample gathering and detailed surface investigations, and a planetary science array to perform on-site research before samples are returned to Earth. Project Hyreus calls for the Mars Landing Vehicle to land in the Mangala Valles region of Mars, where it will remain for approximately 1.5 years. Methane and oxygen propellant for the Earth return voyage will be produced using carbon dioxide from the Martian atmosphere and a small supply of hydrogen brought from Earth. This process is key to returning a large Martian sample to Earth with a single Earth launch. Author

N95-12952*# California State Polytechnic Univ., Pomona, CA. Dept. of Geological Sciences.
PERIGLACIAL AND GLACIAL ANALOGS FOR MARTIAN LANDFORMS Final Technical Report, 1 Oct. 1984 - 31 Dec. 1992
Lisa A. Rossbacher 31 Dec. 1992 9 p
(Grant NAGw-0715)
(NASA-CR-196772; NAS 1.26:196772) Avail: CASI HC A02/MF A01

The list of useful terrestrial analogs for Martian landforms has been expanded to include: features developed by desiccation processes; catastrophic flood features associated with boulder-sized materials; and

sorted ground developed at a density boundary. Quantitative analytical techniques developed for physical geography have been adapted and applied to planetary studies, including: quantification of the patterns of polygonally fractured ground to describe pattern randomness independent of pattern size, with possible correlation to the mechanism of origin and quantification of the relative area of a geomorphic feature or region in comparison to planetary scale. Information about Martian geomorphology studied in this project was presented at professional meetings world-wide, at seven colleges and universities, in two interactive televised courses, and as part of two books. Overall, this project has expanded the understanding of the range of terrestrial analogs for Martian landforms, including identifying several new analogs. The processes that created these terrestrial features are characterized by both cold temperatures and low humidity, and therefore both freeze-thaw and desiccation processes are important. All these results support the conclusion that water has played a significant role in the geomorphic history of Mars. Author (revised)

N95-13497*# Georgia Inst. of Tech., Atlanta, GA. School of Mechanical Engineering.

LUNAR VERTICAL-SHAFT MINING SYSTEM

Steven D. Introne, ed., Roy Krause, Erik Williams, Keith Baskette, Frederick Martich, Brad Weaver, Jeff Meve, Kyle Alexander, Ron Dailey, and Matt White et al Mar. 1994 179 p

(Contract NASw-4435)

(NASA-CR-197154; NAS 1.26:197154) Avail: CASI HC A09/MF A02

This report proposes a method that will allow lunar vertical-shaft mining. Lunar mining allows the exploitation of mineral resources imbedded within the surface. The proposed lunar vertical-shaft mining system is comprised of five subsystems: structure, materials handling, drilling, mining, and planning. The structure provides support for the exploration and mining equipment in the lunar environment. The materials handling subsystem moves mined material outside the structure and mining and drilling equipment inside the structure. The drilling process bores into the surface for the purpose of collecting soil samples, inserting transducer probes, or locating ore deposits. Once the ore deposits are discovered and pinpointed, mining operations bring the ore to the surface. The final subsystem is planning, which involves the construction of the mining structure. Author (revised)

92 SOLAR PHYSICS

Includes solar activity, solar flares, solar radiation and sunspots.

For related information see *93 Space Radiation.*

N95-12243# Polish Academy of Sciences, Warsaw (Poland). Inst. of Basic Problems of Technology.

A MODEL OF THE DENSITY OF SOLAR RADIATION ENERGY ON AN ARBITRARY PLANE IDENTIFICATION FOR WARSAW [MODEL GESTOSCI ENERGII PROMIENIOWANIA SLONECZNEGO NA DOWOLNA PLASZCZYZNE IDENTYFIKACJA DLA WARSZAWY]

Stefan Owczarek 1993 42 p In POLISH

(ISSN 0208-5658)

Avail: CASI HC A03/MF A01

The author presents a mathematical model of the density of solar radiation energy on an arbitrarily inclined surface of the earth. The model is described by means of vector calculus within the framework of spherical geometry and the theory of the extinction and propagation of solar radiation. The concept of the model was borrowed from publications in the field cited in the article and was supplemented with the author's own ideas. They include the condition of the shadow of the plate, the concept of the radiation effect as the sum of two states, one corresponding to total cloudlessness and the other corresponding to total cloudiness, and a numerical realization of a discrete description. The use of a discrete description made it possible to calculate the components of the intensity of the radiation at any point on the earth, at any time of day, and at any time of the year as well as a composite representation, namely energy density in any time period. The possibility of determining energy density in any time period makes the model an extremely useful practical tool in the construction and operation of solar energy conversion systems. The author used his model to write a numerical program in Pascal for calculating solar radiation energy density on a plane with any azimuth and any angle of inclination relative to the horizon. The author identified the model on the basis of statistics on the average daily amounts of radiation in specific months of the year on a horizontal plane in Warsaw. The article includes tables with the results of calculations of average daily solar radiation energy fluxes in specific months of the year as well as the components of solar radiation energy density in the warm season on plates with specific azimuths and angles of inclination in the vicinity of Warsaw. Transl. by (SCITRAN)

N95-12667*# National Aeronautics and Space Administration. Goddard Space Flight Center, Greenbelt, MD.

NIMBUS-7 EARTH RADIATION BUDJET COMPACT SOLAR DATA SET USER'S GUIDE

H. Lee Kyle (Research and Data Systems, Inc., Greenbelt, MD.), Lanning M. Penn (Research and Data Systems, Inc., Greenbelt, MD.), Douglas Hoyt (Research and Data Systems, Inc., Greenbelt, MD.), Douglas Love (Scientific Management and Applied Research Technologies, Inc., Silver Spring, MD.), Sastri Vemury (Scientific Management and Applied Research Technologies, Inc., Silver Spring, MD.), and Brenda J. Vallette (Research and Data Systems, Inc., Greenbelt, MD.) Washington Aug. 1994 55 p

(Contract NAS5-31331; RTOP 665-10-70)

(NASA-RP-1346; Rept-94B00108; NAS 1.61:1346) Avail: CASI HC A04/MF A01

Nimbus-7 Earth Radiation Budget (ERB) solar measurements extend from November 16, 1978, to December 13, 1993, but with data gaps in 1992 and 1993. The measurements include the total solar irradiance plus six broadband spectral components. The Channel 10c total irradiance data appears very stable, and the calibration, well done. A number of characterization problems remain in the spectral measurements. In the original program, the solar and Earth flux measurements were intermixed and spread over about 170 computer tapes. For easier access, the solar data have been collected into two compact data sets. All of the data are collected into 14 Summary Solar Tapes (SST's). In addition, two Channel 10c Solar Tapes (CST's) give a separate listing of the stable total solar irradiance measurements. Channel 10c calibration and orbital irradiance values are given on separate PC disks. This document gives data descriptions and formats, together with quality control and calibration procedures.

Author

N95-13582*# Science Applications, Inc., San Diego, CA.

STRUCTURE AND DYNAMICS OF THE SOLAR CORONA Final Report, 1993 - 1994

D. D. Schnack 19 Oct. 1994 24 p Original contains color illustrations

(Contract NASw-4579)

(NASA-CR-196978; NAS 1.26:196978; SAIC-94/1151) Avail: CASI HC A03/MF A01; 7 functional color pages

Advanced computational techniques were used to study solar coronal heating and coronal mass ejections. A three dimensional, time dependent resistive magnetohydrodynamic code was used to study the dynamic response of a model corona to continuous, slow, random magnetic footpoint displacements in the photosphere. Three dimensional numerical simulations of the response of the corona to simple smooth braiding flows in the photosphere were calculated to illustrate and understand the spontaneous formation of current filaments. Two dimensional steady state helmet streamer configurations were obtained by determining the time asymptotic state of the interaction of an initially one dimensinal transponic solar wind with a spherical potential dipole field. The disruption of the steady state helmet streamer configuration was studied as a response to shearing of the magnetic footpoints of the closed field lines under the helmet. CASI

93 SPACE RADIATION

Includes cosmic radiation; and inner and outer earth's radiation belts.

For biological effects of radiation see *52 Aerospace Medicine.* For theory see *73 Nuclear and High-Energy Physics.*

N95-11757# Sandia National Labs., Albuquerque, NM.

BASIC MECHANISMS OF RADIATION EFFECTS IN THE NATURAL SPACE RADIATION ENVIRONMENT

J. R. Schwank 1994 109 p Presented at the 31st Annual International Nuclear and Space Radiation Effects Conference, Tucson, AZ, 18-22 Jul. 1994

(Contract DE-AC04-94AL-85000)
(DE94-013445; SAND-94-1580C; CONF-940726-12) Avail: CASI HC A06/MF A02

Four general topics are covered in respect to the natural space radiation environment: (1) particles trapped by the earth's magnetic field; (2) cosmic rays; (3) radiation environment inside a spacecraft; and (4) laboratory radiation sources. The interaction of radiation with materials is described by ionization effects and displacement effects. Total-dose effects on MOS devices is discussed with respect to: measurement techniques, electron-hole yield, hole transport, oxide traps, interface traps, border traps, device properties, case studies, and special concerns for commercial devices. Other device types considered for total-dose effects are SOI devices and nitrided oxide devices. Lastly, single event phenomena are discussed with respect to charge collection mechanisms and hard errors. DOE

N95-12469*# Radiophysics, Inc., Boulder, CO.
NON-DIPOLAR MAGNETIC FIELD MODELS AND PATTERNS OF RADIO EMISSION: URANUS AND NEPTUNE COMPARED Final Report, 3 Aug. 1993 - 15 Sep. 1994
D. R. Evans 15 Sep. 1994 69 p
(Contract NASw-4801)
(NASA-CR-196412; NAS 1.26:196412) Avail: CASI HC A04/MF A01

The magnetic field geometries of Uranus and Neptune are superficially similar, and are similarly unlike those of other planets: the field strengths are similar, and they contain extraordinarily large non-dipolar components. As a corollary, the best dipolar field models of each of the two planets comprises a dipole that is considerably offset from the planetary center and tilted away from the rotational axis. However, in other respects the best field models of the two planets are quite different. Uranus has a quadrupole model in which all the terms are well determined and in which none of the higher order terms is determined. To represent the magnetometer data acquired during Voyager's Neptune encounter requires a model of order 8 (instead of Uranus' order 2), yet many of the coefficients are poorly determined. A second model, an octupole model comprising the terms up to order three of the order 8 model, has been suggested by the magnetometer team as being useful; its use, however, is limited only to the region outside of about 2R(exp N), whereas planetary radio emissions have their sources well inside this surface. Computer code has been written that permits an analysis of the detailed motion of low energy charged particles moving in general planetary magnetic fields. At Uranus, this code reveals the existence of an isolated region of the inner magnetosphere above the day side in which particles may be trapped, separate from the more general magnetospheric trapping. An examination of the so-call ordinary mode uranian radio emissions leads us to believe that these emissions are in fact extraordinary mode emissions coming from particles trapped in this isolated region. A similar attempt to discover trapping regions at Neptune has proved, unfortunately, to be impossible. This arises from three factors: (1) the computation needed to track particles in an eighth order field is more than an order of magnitude greater than that needed to perform a similar calculation in a quadrupole field, and is beyond the capacity of workstation-class computers; (2) the octupole field model is known to be in error by too large an ammount for it, or any similarly truncated version of the eighth order model, to produce trustworthy results; (3) the eighth order model can, in effect, be infinitely varied without affecting the field strength along the spacecraft trajectory. Author (revised)

N95-12886*# Joint Inst. for Lab.. Astrophysics, Boulder, CO.
GAMMA-RAY BURST CONSTRAINTS ON THE GALACTIC FREQUENCY OF EXTRA-SOLAR OORT CLOUDS
J. Michael Shull and S. Alan Stern Jun. 1994 21 p Revised
(Grants NAGw-3023; NAGw-766)
(NASA-CR-196197; NAS 1.26:196197) Avail: CASI HC A03/MF A01

With the strong CGRO/BATSE evidence that most gamma-ray bursts do not come from galactic neutron stars, models involving the accretion of a comet onto a neutron star (NS) no longer appear to be strong contenders for explaining the majority of bursts. If this is the case, then it is worth asking whether the lack of an observed galactic gamma-ray burst population provides a useful constraint on the number of comets and comet clouds in the galaxy. Owing to the previously unrecognized structural weakness of cometary nuclei, we find the capture cross sections for comet-NS events to be much higher than previously published estimates, with tidal breakup at distances R(sub b) approximately equals to 4 x 10(exp 10) cm from the NS. As a result, impacts of comets onto field NS's penetrating the Oort Clouds of other stars are found to dominate all other galactic NS-comet capture rates by a factor of 100. This in turn predicts that if comet clouds are common, there should be a significant population of repeater sources with (1) a galactic distribution, (2) space-correlated repetition, and (3) a wide range of peak luminosities and luminosity time histories. If all main sequences stars have Oort Clouds like our own, we predict approximately 4000 such repeater sources in the Milky Way at any time, each repeating on timescales of months to years. Based on estimates of the sensitivity of the CGRO/BATSE instrument and assuming isotropic gamma-ray beaming from such events, we estimate that a population of approximately 20-200 of these galactic NS-Oort Cloud gamma-ray repeater sources should be detectable by CGRO. In addition, if giant planet formation is common in the galaxy, we estimate that the accretion of isolated comets injected to the interstellar medium by giant planet formation should produce an additional source of galactic, nonrepeating events. Comparing these estimates to the three to four soft gamma-ray repeater sources detected by BATSE, one is forced to conclude that (1) comet impacts on NS's are inefficient at producing gamma-rays; or (2) the gamma-rays from such events are highly beamed; or (3) the fraction of stars in the galaxy with Oort Cloud like our own is not higher than a few percent. Author

N95-13023*# Pennsylvania State Univ., University Park, PA. Dept. of Astronomy and Astrophysics.
SEARCH FOR INVERSE COMPTON X-RAYS FROM THE LOBES OF FORNAX A X-RAYS FROM RADIO GALAXIES STRADDLING THE FANAROFF-RILEY TRANSITION Final Technical Report
Eric D. Feigelson 1 Aug. 1994 9 p Original contains color illustrations
(Grant NAG5-1959)
(NASA-CR-196433; NAS 1.26:196433) Avail: CASI HC A02/MF A01; 1 functional color page

Two related studies of radio galaxies are covered in this report. The first is a search for inverse Compton x-rays from the lobes of Fornax A. In this study, a ROSAT position sensitive proportional counter image of Fornax A (NGC 1316) is presented, and after image processing, it was observed that the x-ray emission closely mimicked the radio emission. A second study involved x-rays from radio galaxies straddling the Fanaroff-Riley transition which divides radio galaxies into two broad morphological groups based on whether the lobe radio power is greater or less than a critical value. ROSAT HRI observations were obtained from four bright radio galaxies around the transition to search for x-ray indications of either nuclear engine or ambient medium differences. CASI

99 GENERAL

N95-11797# Helsinki Univ. of Technology, Otaniemi (Finland). Applied Electronics Lab.
[ACTIVITIES OF THE HELSINSKI UNIVERSITY OF TECHNOLOGY, APPLIED ELECTRONICS LABORATORY] Annual Report, 1991 - 1992
V. Kontra and A. Vuori 1993 27 p
(ISSN 0784-8498)
(PB94-179074; ISBN-951-22-1724-4) Avail: CASI HC A03/MF A01

In this report, the teaching, research, and publication activities in the Applied Electronics Laboratory of the Helsinki University of Technology during the period 1991-1992 are described. Research is mainly directed towards instrumentation using electronics. Application areas cover a variety of subjects from industrial and administrative purposes to medical and research institutes. During this period the project of hardware and software design of the ultrasonic guidance radar for the visually impaired was brought to a conclusion. A great deal of time and effort has been spent on the construction of the Radioastron satellite receiver. In 1992 a project on variable road signs was started. The purpose of the research in this project is to construct a road side display using LED technology, with varying messages and graphics. Contents include introduction; personnel; ordinary courses; research; theses; conferences, study tours, and visits; and publications. NTIS

N95-11830 Massachusetts Inst. of Tech., Cambridge. Lab. of Electronics.

THE RESEARCH LABORATORY OF ELECTRONICS Progress Report No. 136, 1 Jan. - 31 Dec. 1993

Jonathan Allen Jun. 1994 448 p Limited Reproducibility: More than 20% of this document may be affected by microfiche quality

(Contract DAAL03-92-C-0001)

(AD-A281445; ARO-28925.90-EL-JSEP) Avail: CASI HC A19

This progress report presents the following research projects: (1) solid state physics, electronics and optics; (2) applied physics; (3) systems and signals; (4) bioelectronics; and (5) language, speech and hearing. DTIC

N95-11955*# National Aeronautics and Space Administration. Ames Research Center, Moffett Field, CA.

TECHNICAL PAPER CONTEST FOR WOMEN 1992. SPACE CHALLENGES: EARTH AND BEYOND

Robin Orans, ed. 1993 220 p

(NASA-TM-109953; NAS 1.15:109953) Avail: CASI HC A10/MF A03

Two of the major concerns of the NASA Ames Research Center (NASA ARC) Advisory Committee for Women (ACW) are that recruitment of women scientists, engineers, and technicians needs to increase and that barriers to advancement need to be removed for improved representation of women in middle and upper management and scientific positions. One strategy that addressed this concern was the ACW sponsorship of a Technical Paper Contest for Women at Ames Research Center. Other sponsors of the Contest were the Ames Equal Opportunity Council and the Ames Contractor Council. The Technical Paper Contest for Women greatly increased the visibility of both the civil service women and the women who work for contractors at Ames. The women had the opportunity to hone their written and oral presentation skills. Networking among Ames women increased. For individual titles, see N95-11956 through N95-11971.

N95-11956*# Micro Craft, Inc., Moffett Field, CA.

EDUCATION: A SECOND CAREER **c80**

Kong Cha Authement *In* NASA. Ames Research Center, Technical Paper Contest for Women 1992. Space Challenges: Earth and Beyond 1993 p 1-4 (For primary document see N95-11955 02-99)

Avail: CASI HC A01/MF A03

Education provides women with the freedom to choose their destiny and forge a life for themselves if desired or necessary. Many women are denied the opportunity of education while growing up and must attempt to achieve such schooling later in life. For most women the decision to pursue this education can represent a very traumatic moment in their lives. Having faced the dilemma and decided to proceed, results in a very satisfying feeling when success has been achieved. Author (revised)

N95-11957*# National Aeronautics and Space Administration. Ames Research Center, Moffett Field, CA.

THE DEVELOPMENT AND APPLICATION OF THE SELF-ADAPTIVE GRID CODE, SAGE **c34**

Carol B. Davies *In its* Technical Paper Contest for Women 1992. Space Challenges: Earth and Beyond 1993 p 5-20 (For primary document see N95-11955 02-99)

Avail: CASI HC A03/MF A03

The multidimensional self-adaptive grid code, SAGE, has proven to be a flexible and useful tool in the solution of complex flow problems. Both 2- and 3-D examples given in this report show the code to be reliable and to substantially improve flowfield solutions. Since the adaptive procedure is a marching scheme the code is extremely fast and uses insignificant CPU time compared to the corresponding flow solver. The SAGE program is also machine and flow solver independent. Significant effort was made to simplify user interaction, though some parameters still need to be chosen with care. It is also difficult to tell when the adaption process has provided its best possible solution. This is particularly true if no experimental data are available or if there is a lack of theoretical understanding of the flow. Another difficulty occurs if local features are important but missing in the original grid; the adaption to this solution will not result in any improvement, and only grid refinement can result in an improved solution. These are complex issues that need to be explored within the context of each specific problem. Derived from text

N95-11958*# National Aeronautics and Space Administration. Ames Research Center, Moffett Field, CA.

ENGINEERING THE FUTURE WITH AMERICA'S HIGH SCHOOL STUDENTS **c80**

M. A. Farrance (General Electric Co., Moffett Field, CA.) and J. W. Jenner *In its* Technical Paper Contest for Women 1992. Space Challenges: Earth and Beyond 1993 p 21-35 (For primary document see N95-11955 02-99)

Avail: CASI HC A03/MF A03

The number of students enrolled in engineering is declining while the need for engineers is increasing. One contributing factor is that most high school students have little or no knowledge about what engineering is, or what engineers do. To teach young students about engineering, engineers need good tools. This paper presents a course of study developed and used by the authors in a junior college course for high school students. Students learned about engineering through independent student projects, in-class problem solving, and use of career information resources. Selected activities from the course can be adapted to teach students about engineering in other settings. Among the most successful techniques were the student research paper assignments, working out a solution to an engineering problem as a class exercise, and the use of technical materials to illustrate engineering concepts and demonstrate 'tools of the trade'. Author

N95-11959*# National Aeronautics and Space Administration. Ames Research Center, Moffett Field, CA.

USING EMERGENT ORDER TO SHAPE A SPACE SOCIETY **c80**

Amara L. Graps *In its* Technical Paper Contest for Women 1992. Space Challenges: Earth and Beyond 1993 p 37-47 (For primary document see N95-11955 02-99)

Avail: CASI HC A03/MF A03

A fast-growing movement in the scientific community is reshaping the way that we view the world around us. The short-hand name for this movement is 'chaos'. Chaos is a science of the global, nonlinear nature of systems. The center of this set of ideas is that simple, deterministic systems can breed complexity. Systems as complex as the human body, ecology, the mind or a human society. While it is true that simple laws can breed complexity, the other side is that complex systems can breed order. It is the latter that I will focus on in this paper. In the past, nonlinear was nearly synonymous with unsolvable because no general analytic solutions exist. Mathematically, an essential difference exists between linear and nonlinear systems. For linear systems, you just break up the complicated system into many simple pieces and patch together the separated solutions for each piece to form a solution to the full problem. In contrast, solutions to a nonlinear system cannot be added to form a new solution. The system must be treated in its full complexity. While it is true that no general analytical approach exists for reducing a complex system such as a society, it can be modeled. The technical involves a mathematical construct called phase space. In this space stable structures can appear which I use as analogies for the stable structures that appear in a complex system such as an ecology, the mind or a society. The common denominator in all of these systems is that they rely on a process called feedback loops. Feedback loops link the microscopic (individual) parts to the macroscopic (global) parts. The key, then, in shaping a space society, is in effectively using feedback loops. This paper will illustrate how one can model a space society by using methods that chaoticists have developed over the last hundred years. And I will show that common threads exist in the modeling of biological, economical, philosophical, and sociological systems. Author

N95-11960*# Bentley Engineering, Moffett Field, CA.

ARCHITECTURAL DESIGN OF THE SCIENCE COMPLEX AT ELIZABETH CITY STATE UNIVERSITY **c09**

Soheila Jahromi *In* NASA. Ames Research Center, Technical Paper Contest for Women 1992. Space Challenges: Earth and Beyond 1993 p 49-67 (For primary document see N95-11955 02-99)

Avail: CASI HC A03/MF A03

This paper gives an overall view of the architectural design process and elements in taking an idea from conception to execution. The project presented is an example for this process. Once the need for a new structure is established, an architect studies the requirements, opinions and limits in creating a structure that people will exist in, move through,

and use. Elements in designing a building include factors such as volume and surface, light and form changes of scale and view, movement and stasis. Some of the other factors are functions and physical conditions of construction. Based on experience, intuition, and boundaries, an architect will utilize all elements in creating a new building. In general, the design process begins with studying the spatial needs which develop into an architectural program. A comprehensive and accurate architectural program is essential for having a successful building. The most attractive building which does not meet the functional needs of its users has failed at the primary reason for its existence. To have a good program an architect must have a full understanding of the daily functions that will take place in the building. The architectural program along with site characteristics are among a few of the important guidelines in studying the form, adjacencies, and circulation for the structure itself and also in relation to the adjacent structures. Conceptual studies are part of the schematic design, which is the first milestone in the design process. The other reference points are design development and construction documents. At each milestone, review and coordination with all the consultants is established, and the user is essential in refining the project. In design development phase, conceptual diagrams take shape, and architectural, structural, mechanical, and electrical systems are developed. The final phase construction documents convey all the information required to construct the building. The design process and elements described were applied in the following project. Author

N95-11961*# National Aeronautics and Space Administration. Ames Research Center, Moffett Field, CA.

THE BIOLOGICAL FLIGHT RESEARCH FACILITY **c09**

Catherine C. Johnson *In its* Technical Paper Contest for Women 1992. Space Challenges: Earth and Beyond 1993 p 69-80 (For primary document see N95-11955 02-99)

Avail: CASI HC A03/MF A03

NASA Ames Research Center (ARC) is building a research facility, the Biological Flight Research Facility (BFRF), to meet the needs of life scientists to study the long-term effects of variable gravity on living systems. The facility will be housed on Space Station Freedom and is anticipated to operate for the lifetime of the station, approximately thirty years. It will allow plant and animal biologists to study the role of gravity, or its absence, at varying gravity intensities for varying periods of time and with various organisms. The principal difference between current Spacelab missions and those on Space Station Freedom, other than length of mission, will be the capability to perform on-orbit science procedures and the capability to simulate earth gravity. Initially the facility will house plants and rodents in habitats which can be maintained at microgravity or can be placed on a 2.5 meter diameter centrifuge. However, the facility is also being designed to accommodate future habitats for small primates, avian, and aquatic specimens. The centrifuge will provide 1 g for controls and will also be able to provide gravity from 0.01 to 2.0 g for threshold gravity studies as well as hypergravity studies. Included in the facility are a service unit for providing clean chambers for the specimens and a glovebox for manipulating the plant and animal specimens and for performing experimental protocols. The BFRF will provide the means to conduct basic experiments to gain an understanding of the effects of microgravity on the structure and function of plants and animals, as well as investigate the role of gravity as a potential countermeasure for the physiological changes observed in microgravity. Author

N95-11962*# National Aeronautics and Space Administration. Ames Research Center, Moffett Field, CA.

TECHNIQUES FOR OPTIMAL CROP SELECTION IN A CONTROLLED ECOLOGICAL LIFE SUPPORT SYSTEM **c54**

Ann McCormack, Cory Finn, and Betsy Dunsky *In its* Technical Paper Contest for Women 1992. Space Challenges: Earth and Beyond 1993 p 81-96 See also N93-12018 (For primary document see N95-11955 02-99)

Avail: CASI HC A03/MF A03

A Controlled Ecological Life Support System (CELSS) utilizes a plant's natural ability to regenerate air and water while being grown as a food source in a closed life support system. Current plant research is directed toward obtaining quantitative empirical data on the regenerative ability of each species of plant and the system volume and power requirements. Two techniques were adapted to optimize crop species selection while at the same time minimizing the system volume and power requirements. Each allows the level of life support supplied by the plants to be selected, as well as other system parameters. The first technique uses decision analysis in the form of a spreadsheet. The second method, which is used as a comparison with and validation of the first, utilizes standard design optimization techniques. Simple models of plant processes are used in the development of these methods. Author

N95-11963*# Sterling Software, Inc., Moffett Field, CA.

DEVELOPMENT OF A CHANGE MANAGEMENT SYSTEM **c81**

Cathy Bonifas Parks *In* NASA. Ames Research Center, Technical Paper Contest for Women 1992. Space Challenges: Earth and Beyond 1993 p 97-110 (For primary document see N95-11955 02-99)

Avail: CASI HC A03/MF A03

The complexity and interdependence of software on a computer system can create a situation where a solution to one problem causes failures in dependent software. In the computer industry, software problems arise and are often solved with 'quick and dirty' solutions. But in implementing these solutions, documentation about the solution or user notification of changes is often overlooked, and new problems are frequently introduced because of insufficient review or testing. These problems increase when numerous heterogeneous systems are involved. Because of this situation, a change management system plays an integral part in the maintenance of any multisystem computing environment. At the NASA Ames Advanced Computational Facility (ACF), the Online Change Management System (OCMS) was designed and developed to manage the changes being applied to its multivendor computing environment. This paper documents the research, design, and modifications that went into the development of this change management system (CMS). Author

N95-11964*# National Aeronautics and Space Administration. Ames Research Center, Moffett Field, CA.

TRAINING FOR LIFE SCIENCE EXPERIMENTS IN SPACE AT THE NASA AMES RESEARCH CENTER **c54**

Annette T. Rodrigues and A. Christopher Maese *In its* Technical Paper Contest for Women 1992. Space Challenges: Earth and Beyond 1993 p 111-128 (For primary document see N95-11955 02-99)

Avail: CASI HC A03/MF A03

As this country prepares for exploration to other planets, the need to understand the affects of long duration exposure to microgravity is evident. The National Aeronautics and Space Administration (NASA) Ames Research Center's Space Life Sciences Payloads Office is responsible for a number of non-human life sciences payloads on NASA's Space Shuttle's Spacelab. Included in this responsibility is the training of those individuals who will be conducting the experiments during flight, the astronauts. Preparing a crew to conduct such experiments requires training protocols that build on simple tasks. Once a defined degree of performance proficiency is met for each task, these tasks are combined to increase the complexity of the activities. As tasks are combined into in-flight operations, they are subjected to time constraints and the crew enhances their skills through repetition. The science objectives must be completely understood by the crew and are critical to the overall training program. Completion of the in-flight activities is proof of success. Because the crew is exposed to the background of early research and plans for post-flight analyses, they have a vested interest in the flight activities. The salient features of this training approach is that it allows for flexibility in implementation, consideration of individual differences, and a greater ability to retain experiment information. This training approach offers another effective alternative training tool to existing methodologies. Author

N95-11965*# National Aeronautics and Space Administration. Ames Research Center, Moffett Field, CA.

THE RHESUS MEASUREMENT SYSTEM: A NEW INSTRUMENT FOR SPACE RESEARCH **c09**

Julie E. Schonfeld and John W. Hines *In its* Technical Paper Contest for Women 1992. Space Challenges: Earth and Beyond 1993 p 129-136 (For primary document see N95-11955 02-99)

Avail: CASI HC A02/MF A03

The Rhesus Research Facility (RRF) is a research environment designed to study the effects of microgravity using rhesus primates as human surrogates. This experimental model allows investigators to study numerous aspects of microgravity exposure without compromising crew member activities. Currently, the RRF is slated for two missions to collect its data,

the first mission is SLS-3, due to fly in late 1995. The RRF is a joint effort between the United States and France. The science and hardware portions of the project are being shared between the National Aeronautics and Space Administration (NASA) and France's Centre National D'Etudes Spatiales (CNES). The RRF is composed of many different subsystems in order to acquire data, provide life support, environmental enrichment, computer facilities and measurement capabilities for two rhesus primates aboard a nominal sixteen day mission. One of these subsystems is the Rhesus Measurement System (RMS). The RMS is designed to obtain in-flight physiological measurements from sensors interfaced with the subject. The RMS will acquire, preprocess, and transfer the physiologic data to the Flight Data System (FDS) for relay to the ground during flight. The measurements which will be taken by the RMS during the first flight will be respiration, measured at two different sites; electromyogram (EMG) at three different sites; electroencephalogram (EEG); electrocardiogram (ECG); and body temperature. These measurements taken by the RMS will assist the research team in meeting the science objectives of the RRF project.

Derived from text

N95-11966*# National Aeronautics and Space Administration. Ames Research Center, Moffett Field, CA.

ON THE ISOLATION OF HALOPHILIC MICROORGANISMS FROM SALT DEPOSITS OF GREAT GEOLOGICAL AGE **c51**

Helga Stan-Lotter and Ewald Denner *In its* Technical Paper Contest for Women 1992. Space Challenges: Earth and Beyond 1993 p 137-144 (For primary document see N95-11955 02-99)

Avail: CASI HC A02/MF A03

From salt sediments of Triassic or Permian age from various locations in the world halophilic microorganisms were isolated. Molecular characteristics of several of the isolates suggested they belong to the archaebacteria. One group appears to represent novel strains; several properties of one such isolate, strain Bip, are described here. The existence of viable microorganisms in ancient sediment would have great implications with respect to our notions on evolution, the research for life in extraterrestrial environments, and the longterm survival of functional biological structures. Of crucial importance is thus the question if these microorganisms existed in the salt since the time of deposition or invaded at some later date. Some suggestions to address these issues experimentally are discussed.

Author

N95-11967*# Eloret Corp., Palo Alto, CA.

COMPUTATIONAL FLOW PREDICTIONS FOR HYPERSONIC DRAG DEVICES **c02**

Susan A. Tokarcik and Ethiraj Venkatapathy *In* NASA. Ames Research Center, Technical Paper Contest for Women 1992. Space Challenges: Earth and Beyond 1993 p 145-170 (For primary document see N95-11955 02-99)

Avail: CASI HC A03/MF A03

The effectiveness of two types of hypersonic decelerators is examined: mechanically deployable flares and inflatable ballutes. Computational fluid dynamics (CFD) is used to predict the flowfield around a solid rocket motor (SRM) with a deployed decelerator. The computations are performed with an ideal gas solver using an effective specific heat ratio of 1.15. The results from the ideal gas solver are compared to computational results from a thermochemical nonequilibrium solver. The surface pressure coefficient, the drag, and the extend of the compression corner separation zone predicted by the ideal gas solver compare well with those predicted by the nonequilibrium solver. The ideal gas solver is computationally inexpensive and is shown to be well suited for preliminary design studies. The computed solutions are used to determine the size and shape of the decelerator that are required to achieve a drag coefficient of 5. Heat transfer rates to the SRM and the decelerators are predicted to estimate the amount of thermal protection required.

Author

N95-11968*# National Aeronautics and Space Administration. Ames Research Center, Moffett Field, CA.

TEST MODEL DESIGNS FOR ADVANCED REFRACTORY CERAMIC MATERIALS **c27**

Huy Kim Tran *In its* Technical Paper Contest for Women 1992. Space Challenges: Earth and Beyond 1993 p 171-182 (For primary document see N95-11955 02-99)

Avail: CASI HC A03/MF A03

The next generation of space vehicles will be subjected to severe aerothermal loads and will require an improved thermal protection system (TPS) and other advanced vehicle components. In order to ensure the satisfactory performance system (TPS) and other advanced vehicle materials and components, testing is to be performed in environments similar to space flight. The design and fabrication of the test models should be fairly simple but still accomplish test objectives. In the Advanced Refractory Ceramic Materials test series, the models and model holders will need to withstand the required heat fluxes of 340 to 817 W/sq cm or surface temperatures in the range of 2700 K to 3000 K. The model holders should provide one dimensional (1-D) heat transfer to the samples and the appropriate flow field without compromising the primary test objectives. The optical properties such as the effective emissivity, catalytic efficiency coefficients, thermal properties, and mass loss measurements are also taken into consideration in the design process. Therefore, it is the intent of this paper to demonstrate the design schemes for different models and model holders that would accommodate these test requirements and ensure the safe operation in a typical arc jet facility.

Author

N95-11969*# National Aeronautics and Space Administration. Ames Research Center, Moffett Field, CA.

THE CROP GROWTH RESEARCH CHAMBER **c14**

Kimberly Wagenbach *In its* Technical Paper Contest for Women 1992. Space Challenges: Earth and Beyond 1993 p 183-193 (For primary document see N95-11955 02-99)

Avail: CASI HC A03/MF A03

The Crop Growth Research Chamber (CGRC) has been defined by CELSS principle investigators and science advisory panels as a necessary ground-based tool in the development of a regenerative life support system. The focus of CGRC research will be on the biomass production component of the CELSS system. The ground-based Crop Growth Research Chamber is for the study of plant growth and development under stringently controlled environments isolated from the external environment. The chamber has importance in three areas of CELSS activities: (1) crop research; (2) system control and integration, and (3) flight hardware design and experimentation. The laboratory size of the CGRC will be small enough to allow duplication of the unit, the conducting of controlled experiments, and replication of experiments, but large enough to provide information representative of larger plant communities. Experiments will focus on plant growth in a wide variety of environments and the effects of those environments on plant production of food, water, oxygen, toxins, and microbes. To study these effects in a closed system, tight control of the environment is necessary.

Author

N95-11970*# National Aeronautics and Space Administration. Ames Research Center, Moffett Field, CA.

MEETING THE CHALLENGE OF MANNED LUNAR AND MARTIAN EXPLORATION **c54**

Rebecca C. Williamson *In its* Technical Paper Contest for Women 1992. Space Challenges: Earth and Beyond 1993 p 195-205 (For primary document see N95-11955 02-99)

Avail: CASI HC A03/MF A03

As the U.S. space program plans for a return to the Lunar surface and ultimately for a mission to Mars, space units and portable life support systems will have to keep pace to meet the exploration mission requirements. The systems currently in use with the Shuttle program will not be adequate for exploration on the Martian surface or for extensive exploration and work on the Lunar surface. Currently, there are too many unknowns regarding locomotion and work physiology in reduced gravity to accurately design advanced suits and life support systems for routine extravehicular activity (EVA). It would be unwise and costly to arbitrarily develop new designs without first studying how the human body moves and works in these environments. This paper discusses the current state of the art of EVA space suit and PLSS design to meet the need of advanced exploration missions. Current research underway in the Extravehicular Systems Branch at Ames Research Center aimed at advanced system design is highlighted.

Author

N95-11971*# Eloret Corp., Palo Alto, CA.

INTERFEROGRAMS, SCHLIEREN, AND SHADOWGRAPHS CONSTRUCTED FROM REAL- AND IDEAL-GAS, TWO- AND THREE-DIMENSIONAL COMPUTED FLOWFIELDS **c34**

Leslie A. Yates *In* NASA. Ames Research Center, Technical Paper Contest for Women 1992. Space Challenges: Earth and Beyond 1993 p 207-218 See also N93-21356 (For primary document see N95-11955 02-99)
(Contract NCC2-583)
Avail: CASI HC A03/MF A03

The construction of interferograms, schlieren, and shadowgraphs from computed flowfield solutions permits one-to-one comparisons of computed and experimental results. A method of constructing these images from both ideal- and real-gas, two and three-dimensional computed flowfields is described. The computational grids can be structured or unstructured, and multiple grids are an option. Constructed images are shown for several types of computed flows including nozzle, wake, and reacting flows; comparisons to experimental images are also shown. In addition, th sensitivity of these images to errors in the flowfield solution is demonstrated, and the constructed images can be used to identify problem areas in the computations. Author

N95-12002 Joint Publications Research Service, Arlington, VA.
JPRS REPORT: SCIENCE AND TECHNOLOGY. CENTRAL EURASIA
20 Sep. 1994 48 p Transl. into ENGLISH from various Russian articles (JPRS-UST-94-020) Copyright Avail: Issuing Activity

Translated articles cover the following topics: fracture strength of superhard composites; photodetector with silicon avalanche photodiode for highly precise laser range finders; sources of optical radiation in picosecond range in injection lasers for pulsed-light range finding; highly precise laser range finders and laser systems for industrial use; multifunctional sounding systems with CO2 lasers and coherent signal reception; stand for in situ tests of optical sounders and pulsed light range finders; collecting and processing information in pulsed laser range finders; receiving channel of pulsed laser range finder with correlation signal selection; coherent reception of optical signal in scanning laser sounding systems; use of hybrid integrating optical correlator for processing signal of heterodyne laser range finder; optical processors for processing large files of sounding signals; discrete signal accumulation in laser sounders; calculating S-parameters of interdigital acoustic surface wave transducers; influence of ground surface on structure of pulse signal in millimeter wave band; influence that attenuation of light waves has on two-beam amplification of three-dimensional diffraction grating; two-dimensional radar imaging of moving objects by combined aperture synthesis and tomography; metastable deep centers in Si(1-x)Ge(x) single crystals; luminescence of multiple quantum wells of GaAs/Al(x)Ga(1-x)As in structures for infrared photocells; influence of hydrogenation on photoluminescence of GaAs/AlGaAs structures with quantum wells; investigation of interrelation between conditions of growth and quality of heteroboundary in selectivity doped heterostructures InP/In(1-x)Ga(x)As grown by liquid-phase epitaxy; processes of lasing, recombination and ionization in silicon and germanium crystals: kinetics of nonequilibrium carriers; fatigue resistance of high-temperature alloys under cyclic changes of temperature: Report 1: methods and results of study; and characteristics of cyclic resistance to cracks of aluminum alloys under combined modes of biaxial loading. CASI

N95-12003 Joint Publications Research Service, Arlington, VA.
JPRS REPORT: SCIENCE AND TECHNOLOGY. CENTRAL EURASIA
19 Sep. 1994 48 p Transl. into ENGLISH from various Russian articles (JPRS-UST-94-019) Copyright Avail: Issuing Activity

Translated articles cover the following topics: detection capability of pulsed optical sounders under influence of backscattered noise; mean strength of optical sounding signal in turbulent atmosphere; methods of determining the zero signal of linear accelerometers in the earth's gravitational field; development of methods and means for the automated control of failure warnings in aircraft and spacecraft systems during operation; automated system for the measurement of telemetric parameters; measuring the attenuation of laser radiation in different types of clouds; estimates of electron concentration in an artificial plasma cloud released into ionosphere; identification of cumulus rain and storm clouds in meteosat photographs; and interpolation of data from field oceanological observations. CASI

N95-12223# National Technical Information Service, Springfield, VA.
DIRECTORY OF FEDERAL LABORATORY AND TECHNOLOGY RESOURCES
Oct. 1993 730 p Prepared in cooperation with Wheeling Coll., WV (PB93-100097; ISBN-0-934213-40-2) Avail: CASI HC A99/MF A06

The Directory of Federal Laboratory and Technology Resources cross-references more than 1900 Federal laboratories and engineering centers in five ways, including by subject, by state, and by laboratory. A special listing includes the Technology Transfer office and contact person for every Federal laboratory. Twenty nine categories of science areas are included. CASI

N95-12303# National Technical Information Service, Springfield, VA.
CATALOG OF GOVERNMENT INVENTIONS AVAILABLE FOR LICENSING, 1991
Jan. 1992 192 p
(PB92-100171; ISBN-0-934213-35-6) Avail: CASI HC A09/MF A02

This catalog is designed to make it easy for businesses to scan and identify promising Government inventions from all agencies. More than 1,200 inventions were issued in 1991. Their summaries are listed in this catalog under 48 subject areas so that readers can quickly browse in their specific area of interest. To further enhance the value of the catalog, detailed subject and inventor indexes are included. Author

N95-12342# National Technical Information Service, Springfield, VA.
CATALOG OF GOVERNMENT INVENTIONS AVAILABLE FOR LICENSING, 1992
Jan. 1993 302 p
(PB93-128205; ISBN-0-934213-38-0) Avail: CASI HC A14/MF A03

This catalog is designed to make it easy for businesses to scan and identify promising inventions from all government agencies. More than 1,100 inventions were issued in 1992. Their summaries are listed in this catalog under 48 subject areas so that readers can quickly browse in their specific area of interest. To further enhance the value of the catalog, detailed subject and inventor indexes are included. Author

N95-12610# Nagoya Univ., Aichi (Japan). Solar Terrestrial Lab.
SOLAR-TERRESTRIAL ENVIRONMENT LABORATORY, NAGOYA UNIVERSITY Annual Report, 1993-1994
1994 92 p Original contains color illustrations
Avail: CASI HC A05/MF A01

Research progress in the following areas is covered: atmospheric environment, ionospheric and magnetospheric environment, heliospheric environment, and integrated studies. A publication list covering books and articles in the referred journals in the field and in the proceedings of international conferences from April 1992 to March 1994 is presented. Other areas covered include the following: staff, management system, collaborative research activities, international relations, education, research-related activities, public service, observatory programs, and facilities. CASI

N95-12697# Electronics and Telecommunications Research Inst., Daejon (Republic of Korea).
[ETRI BROCHURE: HISTORY, MISSION, AND ACTIVITY HIGHLIGHTS] Annual Report
1994 83 p Original contains color illustrations
Avail: CASI HC A05/MF A01

This annual report describes the activities carried out by the ETRI affiliate of the Korean Ministry of Communications during 1994. In addition to a brief description of the Institute, highlights are presented for research activities in the following areas: (1) R&D on basic and advanced technology including physical science research, communications science research, information science research, and materials and engineering research; (2) Semiconductors including high speed digital process design, advanced semiconductor devices, and compound semiconductor devices; (3) Computers including development of a high performance computer, multimedia, and distributed systems software; (4) Telecommunications including intelligent networks, communications processing, transmission, B-ISDN technologies, human interfaces, TDX-ISDN and applications systems, ATM switching, digital mobile communication systems, radio wave resource utilization, and satellite communications; and (5) Information technology with standardization in information and telecommunications, development and support of applications technologies, computer applications, and the activities of a technical information center. CASI

N95-12699# Toronto Univ. (Ontario). Inst. for Aerospace Studies.
[ACTIVITIES OF THE INSTITUTE FOR AEROSPACE STUDIES OF TORONTO UNIVERSITY] Annual Progress Report, 1992 and 1993
1993 119 p Original contains color illustrations
Avail: CASI HC A06/MF A02

This annual report highlights activities in both the undergraduate and graduate programs in Aerospace Engineering and provides summary reports on the various experimental facilities and research activities in: Flight Mechanics (flight simulation and air cushion technology); Fluid Mechanics (low speed aerodynamics, aircraft design, nonstationary flows and shock waves, unsteady gas dynamics, aeroacoustics, combustion, propulsion, hypersonic aerodynamics, and computational fluid dynamics); Solid Mechanics (structural mechanics, advanced composites, and materials processing in space); Spacecraft Mechanics (robotics, space dynamics and control); Engineering Physics (applied mass spectroscopy, fusion energy,plasma materials, tokamaks, fiber optic sensors and smart materials and structures). CASI

N95-12946# Technical Univ. of Prague (Czechoslovakia).
PROCEEDINGS OF THE CTU SEMINAR 1994, PART C
30 Apr. 1994 212 p Seminar held in Prague, Czechoslovakia, 17-20 Jan. 1994
(DE94-624078; INIS-MF-13872-Pt-C; CONF-940184-Pt-C) Avail: CASI HC A10/MF A03

The proceedings consist of 3 parts (A, B, C). Part C is divided into the following sections: Environmental Engineering, Mechanics, Materials Engineering, Reliability, Electronics and Optics. Out of 96 short communications contained in the proceedings, 6 items were input to the INIS system. DOE

Typical Subject Index Listing

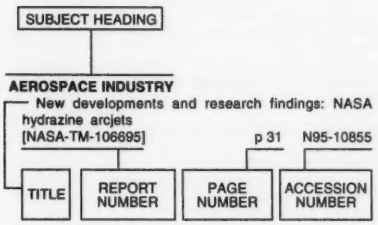

The subject heading is a key to the subject content of the document. Titles, report numbers, and accession numbers of pertinent documents are provided under each subject heading. When the title is insufficiently descriptive of the document content, a title extension is added, separated from the title by three hyphens. The report number helps to indicate the type of document cited (e.g., NASA report, NASA translation, NASA contractor report). The accession number is the number by which the document abstracts are arranged in this journal and by which the document is sold or requested. The page number helps you locate the citation in the abstract section. The titles, with title extensions if present, are arranged under each subject heading in ascending accession number order. The subject headings have been selected from the latest revision of the *NASA Thesaurus*.

A

ABLATION
Evaluation of dynamic pressure of ablation plasma produced by intense, pulsed, ion beam
p 365 N95-12433

ABSORPTION SPECTRA
Calibration of optical wavelength at 1300 nm and 1550 nm using molecular absorption lines
[PB94-180080] p 362 N95-12598

ABSORPTION SPECTROSCOPY
Differential absorption lidar measurements of atmospheric water vapor using a pseudonoise code modulated AlGaAs laser
[NASA-TM-104610] p 314 N95-11997
In-situ x-ray analysis of the electrolyte-solid interface
[AD-A282203] p 373 N95-12425

ABSTRACTS
Abstracts from the International Conference on Nuclear Analytical Methods in the Life Sciences
[DE94-621923] p 329 N95-11728

ACCELERATED LIFE TESTS
Accelerated testing of coatings for protection against atmospheric corrosion
[PB94-202579] p 276 N95-13244

ACCELERATION
Vestibular afferent responses to linear accelerations in the alert squirrel monkey
[NASA-TM-4581] p 330 N95-12006
Actuability of underactuated manipulators
[AD-A282788] p 300 N95-12526

ACCELERATORS
Neural networks and orbit control in accelerators
[DE94-014877] p 350 N95-13124

ACCELEROMETERS
Pressure measurements on an F/A-18 twin vertical tail in buffeting flow. Volume 3: Buffet power spectral densities
[AD-A281444] p 230 N95-11829

ACCEPTOR MATERIALS
Electronic energy transfer in new polymer nanocomposite assemblies
[AD-A282233] p 274 N95-12407

ACCIDENTS
Vacuum system operating experience review for fusion applications
[DE94-015267] p 368 N95-12759

ACCUMULATORS
Solar radiation data manual for flat-plate and concentrating collectors
[DE93-018229] p 317 N95-12647

ACETYLENE
Synthetic method for ethynylation of aromatic compounds
[AD-D016398] p 261 N95-13151

ACIDITY
Phenoxythiocarbonylation and deoxygenation of aryl trifluoromethyl carbinols
[AD-A280519] p 260 N95-12613

ACOUSTIC EMISSION
Sound emission in materials and construction element testing p 355 N95-12013
The use of an acoustic emission method to estimate the effect of manufacturing process and service factors on the failure of concrete p 311 N95-12108
An estimate of the evolution of the acoustic emission spectrum of rocks on the basis of changes in its average frequency in the process of deformation p 323 N95-12112
Comprehensive and critical literature review on insitu micro-sensors for application in tribology
[AD-A281646] p 296 N95-13165

ACOUSTIC EXCITATION
On the interaction of jet noise with a nearby flexible structure
[NASA-CR-194934] p 290 N95-11812
Synchronous picosecond sonoluminescence
[AD-A281498] p 355 N95-11856

ACOUSTIC IMAGING
Sound emission in materials and construction element testing p 355 N95-12013

ACOUSTIC MEASUREMENT
High frequency thermoacoustic refrigerator
[AD-A280925] p 279 N95-12772
Weld acoustic monitor
[AD-D016400] p 356 N95-13154

ACOUSTIC PROPAGATION
The influence of finite-size sources in acousto-ultrasonics
[NASA-CR-195374] p 308 N95-11813
Measurements of atmospheric turbulence effects on tail rotor acoustics
[NASA-TM-108843] p 232 N95-12360
Ocean acoustic tomography: Single slice and moving ship experiments
[AD-A283059] p 329 N95-12998

ACOUSTIC PROPERTIES
Structure and performance of carbon aerogel electrodes
[DE94-014746] p 356 N95-11791
Ultrashort laser pulse effects in ocular and related media: Laser-induced shock wave propagation and retinal damage
[AD-A282599] p 334 N95-12535

ACOUSTIC VELOCITY
Ocean acoustic tomography: Single slice and moving ship experiments
[AD-A283059] p 329 N95-12998

ACOUSTICS
The Research Laboratory of Electronics
[AD-A281445] p 386 N95-11830
A laboratory vacuum apparatus for magnetron sputtering of thin Z ZnO piezoelectric films, magnetron sputtering p 296 N95-12111

ACRYLATES
Multifunctional acrylic ether monomers, their polymers, and polymerizable epoxide derivatives from simple alpha-substitution of alkyl acrylates
[AD-A282513] p 273 N95-12400

ACRYLIC RESINS
Determination of a transient heat transfer property of acrylic using thermochromic liquid crystals
[NASA-TM-106541] p 372 N95-11882
Multifunctional acrylic ether monomers, their polymers, and polymerizable epoxide derivatives from simple alpha-substitution of alkyl acrylates
[AD-A282513] p 273 N95-12400

ACTINIDE SERIES
Resonant x-ray scattering in 5f magnetism
[DE94-013753] p 358 N95-12829

ACTIVATED CARBON
Novel activated carbon impregnants consisting of transition metal complexes. Part 1: Background, syntheses and characterizations
[AD-A282583] p 259 N95-12551

ACTIVATION
Modular hydraulic control system
[AD-D016401] p 304 N95-13155

ACTIVATION ANALYSIS
Summary reports of activities under visiting research program, 1993
[DE94-753222] p 360 N95-11750

ACTIVATION ENERGY
Tuning through the critical regime of the metal-insulator-transition in conducting polymers by pressure and magnetic field
[PB94-179165] p 272 N95-11847

ACTIVE CONTROL
Active vibration control using a distributed controller
[PB94-207073] p 313 N95-13576

ACTIVE GALACTIC NUCLEI
X-ray temporal and spectral studies of blazars with the Ginga satellite
[NASA-CR-196330] p 380 N95-12466

ACTIVITY (BIOLOGY)
Vestibular afferent responses to linear accelerations in the alert squirrel monkey
[NASA-TM-4581] p 330 N95-12006
Phenoxythiocarbonylation and deoxygenation of aryl trifluoromethyl carbinols
[AD-A280519] p 260 N95-12613

ACTUATORS
Design and application of electromechanical actuators for deep space missions
[NASA-CR-196791] p 299 N95-11701
Linear Proof Mass Actuator
[NASA-TM-109143] p 310 N95-11814
The development of a highly reliable power management and distribution system for civil transport aircraft
[NASA-TM-106697] p 243 N95-11867
Robust control of underactuated manipulators: Analysis and implementation
[AD-A282836] p 301 N95-12587
Design of a ZVS PWM inverter for a brushless DC motor in an EMA application
[NASA-CR-195808] p 312 N95-12620
Annular suspension and pointing system with controlled DC electromagnets
[NASA-CR-197206] p 302 N95-12666
A precision measurement of the prompt photon cross section in p(-p) collisions at the square root of s = 1.8 TeV
[DE94-014989] p 359 N95-13170
Active vibration control using a distributed controller
[PB94-207073] p 313 N95-13576

ADA (PROGRAMMING LANGUAGE)
An examination of selected software testing tools: 1993 supplement
[AD-A283060] p 344 N95-13051
Norwegian contribution to the SWG on APSE programme
[PB94-202397] p 341 N95-13557

ADAPTIVE CONTROL
Workshop on Adaptive Methods for Partial Differential Equations
[AD-A281416] p 351 N95-11850
Experimental evaluation of shape memory alloy actuation technique in adaptive antenna design concepts
[NASA-CR-194983] p 284 N95-12896

Mach number control in the High Speed Wind Tunnel of NLR
[PB94-201670] p 246 N95-13243

ADAPTIVE FILTERS

Locally connected adaptive Gabor filter for real-time motion compensation
[AD-A282544] p 286 N95-12494

ADAPTIVE OPTICS

An adaptive optics package designed for astronomical use with a laser guide star tuned to an absorption line of atomic sodium
[DE94-012391] p 363 N95-13532

ADDING CIRCUITS

Digital filter designs that are free of limit cycles
[AD-A282885] p 287 N95-12918

ADDITIVES

Heat transfer additives for adsorption cooling system fluids, phase 2
[PB94-187135] p 290 N95-11840

Tuning through the critical regime of the metal-insulator-transition in conducting polymers by pressure and magnetic field
[PB94-179165] p 272 N95-11847

Additives in bituminous materials and fuel-resistant sealers
[DOT/FAA/CT-94/78] p 273 N95-12131

Influence of additives on structure and thermal stability of ammonium nitrate
[PB94-206943] p 278 N95-13435

ADJOINTS

Category theory: The mathematics for the humanities
[PB94-205044] p 353 N95-13560

ADSORBENTS

Scanning tunneling microscopy/atomic force microscopy for study of nanoscale metal oxide particles (destructive adsorbents)
[AD-A281417] p 357 N95-11851

ADSORPTION

Heat transfer additives for adsorption cooling system fluids, phase 2
[PB94-187135] p 290 N95-11840

Self assembly of n-alkanethiolate monolayers on silver nano-structures: Determination of the apparent thickness of the monolayer by scanning tunneling microscopy
[AD-A282322] p 274 N95-12417

Hydrogen bonding and molecular orientation in water/fluorine adlayers on silver(110)
[AD-A282652] p 268 N95-13549

ADVANCED VERY HIGH RESOLUTION RADIOMETER

Trace gas emissions to the atmosphere by biomass burning in the west African savannas
[NASA-CR-196758] p 319 N95-11931

AVHRR/NOAA images to detect and quantify deforestation in Amazon Forest: Relations with TM/LANDSAT data
[INPE-5501-TDI/516] p 316 N95-13350

AERIAL PHOTOGRAPHY

Proposal of a methodology to evaluate urban quality of life using conventional and remote sensing data, geographic information system, and a database
[INPE-5552-TDI/536] p 315 N95-12297

Site model based image registration and change detection, RADIUS
[AD-A282796] p 315 N95-12527

AERIAL RECONNAISSANCE

Site model based image registration and change detection, RADIUS
[AD-A282796] p 315 N95-12527

AEROACOUSTICS

On the interaction of jet noise with a nearby flexible structure
[NASA-CR-194934] p 290 N95-11812

Effect of nonzero surface admittance on receptivity and stability of compressible boundary layer
[NASA-CR-4621] p 292 N95-12105

En route noise levels from propfan test assessment airplane
[NASA-TP-3451] p 355 N95-12341

Activities of the Institute for Aerospace Studies of Toronto University p 390 N95-12699

AERODYNAMIC BALANCE

Symmetric steady manoeuvre loads on rigid aircraft of classical configuration at subsonic speeds
[ESDU-94009] p 238 N95-11774

AERODYNAMIC CHARACTERISTICS

Gemini: A long-range cargo transport
[NASA-CR-197149] p 239 N95-12626

The Balsa bullet: A high speed, low-cost general aviation aircraft for Aeroworld
[NASA-CR-197165] p 240 N95-12638

Experimental aerodynamic characteristics of a generic hypersonic accelerator configuration at Mach numbers 1.5 and 2.0 -- conducted in the Langley Unitary Plan Wind Tunnel
[NASA-TM-4413] p 233 N95-12770

Hypersonic vehicle model and control law development using H(infinity) and micron synthesis
[NASA-TM-4562] p 255 N95-12838

Methodology for sensitivity analysis, approximate analysis, and design optimization in CFD for multidisciplinary applications
[NASA-CR-196981] p 294 N95-13201

Mach number control in the High Speed Wind Tunnel of NLR
[PB94-201670] p 246 N95-13243

AERODYNAMIC COEFFICIENTS

A simple analytical aerodynamic model of Langley Winged-Cone Aerospace Plane concept
[NASA-CR-194987] p 252 N95-12175

Dynamic ground effects flight test of an F-15 aircraft
[NASA-TM-4604] p 231 N95-12191

AERODYNAMIC CONFIGURATIONS

Optimum aerodynamic design via boundary control
[NASA-CR-195882] p 230 N95-11877

Experimental Aerodynamics Division
[NAL-SP-9404] p 229 N95-12166

The FC-1D: The profitable alternative Flying Circus Commercial Aviation Group
[NASA-CR-197152] p 240 N95-12628

AERODYNAMIC DRAG

Computational flow predictions for hypersonic drag devices p 233 N95-11967

A simple analytical aerodynamic model of Langley Winged-Cone Aerospace Plane concept
[NASA-CR-194987] p 252 N95-12175

AERODYNAMIC FORCES

Numerical analysis of tangential slot blowing on a generic chined forebody
[NASA-TM-108845] p 231 N95-11927

AERODYNAMIC HEAT TRANSFER

Investigation of advanced counterrotation blade configuration concepts for high speed turboprop systems. Task 8: Cooling flow/heat transfer analysis
[NASA-CR-195359] p 244 N95-11901

Investigation of advanced counterrotation blade configuration concepts for high speed turboprop systems. Task 8: Cooling flow/heat transfer analysis user's manual
[NASA-CR-195360] p 244 N95-11951

AERODYNAMIC HEATING

An axisymmetric analog two-layer convective heating procedure with application to the evaluation of Space Shuttle Orbiter wing leading edge and windward surface heating
[NASA-CR-188343] p 251 N95-11937

Science objectives and performance of a radiometer and window design for atmospheric entry experiments
[NASA-TM-4637] p 382 N95-12190

AERODYNAMIC INTERFERENCE

A wall interference assessment and correction system
[NASA-CR-196940] p 292 N95-12228

AERODYNAMIC LOADS

Test model designs for advanced refractory ceramic materials p 277 N95-11968

AERODYNAMIC NOISE

En route noise levels from propfan test assessment airplane
[NASA-TP-3451] p 355 N95-12341

Measurements of atmospheric turbulence effects on tail rotor acoustics
[NASA-TM-108843] p 232 N95-12360

AERODYNAMICS

Pressure measurements on an F/A-18 twin vertical tail in buffeting flow. Volume 3: Buffet power spectral densities
[AD-A281444] p 230 N95-11829

Optimum aerodynamic design via boundary control
[NASA-CR-195882] p 230 N95-11877

Research in progress in applied mathematics, numerical analysis, fluid mechanics, and computer science
[NASA-CR-194942] p 340 N95-11932

Flight dynamics of an unmanned aerial vehicle
[AD-A282259] p 239 N95-12410

Laws of infrared similitude
[AD-A282209] p 354 N95-12426

Activities of the Institute for Aerospace Studies of Toronto University p 390 N95-12699

Aeronautical engineering: A continuing bibliography with indexes (supplement 309)
[NASA-SP-7037(309)] p 229 N95-12894

Mach number control in the High Speed Wind Tunnel of NLR
[PB94-201670] p 246 N95-13243

AEROELASTICITY

Parallel aeroelastic computations for wing and wing-body configurations
[NASA-CR-196835] p 230 N95-11766

Aeroelastic simulation of higher harmonic control
[NASA-CR-4623] p 230 N95-11911

Studies on the flow induced by an oscillating airfoil in a uniform stream
[PB94-204450] p 233 N95-13250

AEROGELS

Structure and performance of carbon aerogel electrodes
[DE94-014746] p 356 N95-11791

AERONAUTICAL ENGINEERING

Aeronautics and space technology, past, present, and future p 229 N95-11892

Aeronautical engineering: A continuing bibliography with indexes (supplement 309)
[NASA-SP-7037(309)] p 229 N95-12894

AEROSOLS

Optical Remote Sensing of the Atmosphere. Technical digest 1993. Volume 5: Postconference edition
[AD-A281446] p 314 N95-11831

Acute inhalation of explosively disseminated carbon fibers in rats
[AD-A280556] p 330 N95-12614

AEROSPACE ENGINEERING

Aeronautics and space technology, past, present, and future p 229 N95-11892

JPRS report: Science and technology. Central Eurasia: Space
[JPRS-USP-94-006] p 247 N95-12000

Activities of the Institute for Aerospace Studies of Toronto University p 390 N95-12699

AEROSPACE ENVIRONMENTS

Basic mechanisms of radiation effects in the natural space radiation environment
[DE94-013445] p 384 N95-11757

Preliminary digital control system design for the petite amateur Navy satellite (PANSAT)
[AD-A282804] p 253 N95-12528

Proposal for the design of a zero gravity tool storage device
[NASA-CR-197150] p 302 N95-12627

Detailed component design for a Compact Environmental Anomaly Sensor (CEASE)
[AD-A283144] p 256 N95-13138

AEROSPACE MEDICINE

Elimination of quinine in two subjects after ingestion of tonic water: An exploratory study
[DOT/FAA/AM-94/16] p 332 N95-11702

Effects of oral glucose on exercise thermoregulation in men after water immersion
[NASA-TM-108825] p 329 N95-11810

Psychophysiological assessment methods (including a register of psychophysiologists on microfiches)
[AGARD-AR-324] p 335 N95-12133

The performance of child restraint devices in transport airplane passenger seats
[DOT/FAA/AM-94/19] p 234 N95-12146

Spaceflight and immune responses of Rhesus monkeys
[NASA-CR-196846] p 331 N95-12941

Age 60 Rule research. Part 1: Bibliographic database
[DOT/FAA/AM-94/20-PT-1] p 336 N95-13019

Age 60 Rule. Part 2: Airline pilot age and performance. A review of the scientific literature
[DOT/FAA/AM-94/21-PT-2] p 336 N95-13020

Aviation epidemiology data register: Cardiovascular disease screening outcomes in the North Dakota Army National Guard aviator cohort
[AD-A283064] p 334 N95-13054

Aerospace medicine and biology: A continuing bibliography with indexes (supplement 394)
[NASA-SP-7011(394)] p 335 N95-13230

AEROSPACE PLANES

A simple analytical aerodynamic model of Langley Winged-Cone Aerospace Plane concept
[NASA-CR-194987] p 252 N95-12175

AEROSPACE SAFETY

Evaluation of wiring constructions for space applications
[NASA-TM-106735] p 256 N95-13194

AEROSPACE SCIENCES

Technical paper contest for women 1992. Space challenges: Earth and beyond
[NASA-TM-109953] p 386 N95-11955

JPRS report: Science and technology. Central Eurasia: Space
[JPRS-USP-94-006] p 247 N95-12000

AEROSPACE SYSTEMS

Activities of the Structures Division, Lewis Research Center
[NASA-TM-108081] p 313 N95-13235

AEROTHERMODYNAMICS

Test model designs for advanced refractory ceramic materials p 277 N95-11968

AFFERENT NERVOUS SYSTEMS

Vestibular afferent responses to linear accelerations in the alert squirrel monkey
[NASA-TM-4581] p 330 N95-12006

AFRICA
Trace gas emissions to the atmosphere by biomass burning in the west African savannas
[NASA-CR-196758] p 319 N95-11931
AFTERBODIES
Supersonic base flow investigation over axisymmetric afterbodies
[PB94-180957] p 232 N95-12578
AGE FACTOR
Age 60 Rule research. Part 1: Bibliographic database
[DOT/FAA/AM-94/20-PT-1] p 336 N95-13019
Age 60 Rule. Part 2: Airline pilot age and performance. A review of the scientific literature
[DOT/FAA/AM-94/21-PT-2] p 336 N95-13020
AGGREGATES
The use of an acoustic emission method to estimate the effect of manufacturing process and service factors on the failure of concrete p 311 N95-12108
Marginal aggregates in flexible pavements: Background survey and experimental plan
[DOT/FAA/CT-94/58] p 246 N95-12216
AGING (BIOLOGY)
Age 60 Rule research. Part 1: Bibliographic database
[DOT/FAA/AM-94/20-PT-1] p 336 N95-13019
Age 60 Rule. Part 2: Airline pilot age and performance. A review of the scientific literature
[DOT/FAA/AM-94/21-PT-2] p 336 N95-13020
Age 60 study. Part 4: Experimental evaluation of pilot performance
[REPT-8025-4B] p 336 N95-13199
AGING (MATERIALS)
Additives in bituminous materials and fuel-resistant sealers
[DOT/FAA/CT-94/78] p 273 N95-12131
AIR BREATHING ENGINES
Shock-tunnel combustor testing for hypersonic vehicles
[NASA-CR-196836] p 246 N95-11938
AFOSR Contractors Meeting in Propulsion
[AD-A282729] p 257 N95-12507
AIR CARGO
Design of a high capacity long range cargo aircraft
[NASA-CR-197176] p 239 N95-12363
AIR DROP OPERATIONS
Athena: Advanced air launched space booster
[NASA-CR-197148] p 258 N95-12604
AIR DUCTS
Study of a vortical/axial type flameholders with variable angle blades
[INPE-5558-TDI/538] p 266 N95-12302
AIR FLOW
A numerical analysis of the distribution of stresses in lung parenchyma which accounts for the interactions between the tissue skeleton and flowing air
p 332 N95-11806
Structure of a swirl-stabilized, combusting spray
[NASA-TM-106724] p 243 N95-11890
Impingement flow heat transfer measurements of turbine blades using a jet array
[AD-A283450] p 375 N95-12512
An implementation of a chemical and thermal nonequilibrium flow solver on unstructured meshes and application to blunt bodies
[NASA-CR-194967] p 293 N95-12619
AIR JETS
Planar Rayleigh scattering and laser-induced fluorescence for visualization of a hot, Mach 2 annular air jet
[NASA-TM-4576] p 247 N95-13196
AIR LAND INTERACTIONS
The impact of elevation data representation on nocturnal drainage wind simulations
[DE94-014752] p 326 N95-12927
AIR LAUNCHING
Athena: Advanced air launched space booster
[NASA-CR-197148] p 258 N95-12604
AIR LAW
A study of aircraft post-crash fuel fire mitigation
[AD-A282208] p 234 N95-12499
AIR POLLUTION
Trichloroethylene emissions reductions achieved by enclosing solvent spray degreasing operations
[DE94-013741] p 318 N95-11742
Environmental lichenology: Biomonitoring trace-element air pollution
[PB94-191335] p 318 N95-11826
Directory of OAQPS information services, May 1994
[PB94-181310] p 318 N95-11848
Implementation strategy for the Clean Air Act Ammendments of 1990. Update, May 1994
[PB94-180700] p 319 N95-11849
Allocating CO2-emissions by using equity rules and optimization
[PB94-192861] p 320 N95-12776
The Additional Programme on Ammonia
[PB94-193075] p 320 N95-12777
Regulatory impact analysis and regulatory support document: Control of air pollution; determination of significance for nonroad sources and emission standards for new nonroad compression-ignition engines at or above 37 kilowatts (50 horsepower)
[PB94-194594] p 321 N95-12855
Proceedings of the CTU Seminar 1994, Part C
[DE94-624078] p 390 N95-12946
AIR QUALITY
Implementation strategy for the Clean Air Act Ammendments of 1990. Update, May 1994
[PB94-180700] p 319 N95-11849
SO2 guideline document
[PB94-181393] p 319 N95-11893
Present state of knowledge of the upper atmosphere1993: An assessment report, part 2
[NASA-RP-1337] p 322 N95-12103
AIR SAMPLING
Simultaneous gas-chromatographic determination of four toxic gases generally present in combustion atmospheres
[DOT/FAA/AM-94/18] p 338 N95-12354
Development of techniques for the in situ observation of OH and HO2 for studies of the impact of high-altitude supersonic aircraft on the stratosphere
[NASA-CR-196759] p 321 N95-12832
AIR SEA ICE INTERACTIONS
Parameterization and scaling of Arctic ice conditions in the context of ice-atmosphere processes
[NASA-CR-196831] p 327 N95-11706
AIR TRAFFIC CONTROLLERS (PERSONNEL)
Ground-based wake vortex monitoring, prediction, and ATC interface p 235 N95-13209
AIR WATER INTERACTIONS
Reports to the Nation on our changing planet. El Nino and climate prediction, no. 3, spring 1994
p 320 N95-12462
AIRBORNE EQUIPMENT
Remote sensing of turbulence in the clear atmosphere with 2-micron lidars p 236 N95-13213
AIRBORNE/SPACEBORNE COMPUTERS
An avionics scenario and command model description for Space Generic Open Avionics Architecture (SGOAA)
[NASA-CR-188330] p 242 N95-11913
The design and development of signal-processing algorithms for an airborne x-band Doppler weather radar
[NASA-CR-196888] p 281 N95-12374
AIRCRAFT ACCIDENTS
Elimination of quinine in two subjects after ingestion of tonic water: An exploratory study
[DOT/FAA/AM-94/16] p 332 N95-11702
Age 60 Rule. Part 2: Airline pilot age and performance. A review of the scientific literature
[DOT/FAA/AM-94/21-PT-2] p 336 N95-13020
AIRCRAFT ANTENNAS
Electromagnetic on-aircraft antenna radiation in the presence of composite plates
[NASA-CR-196126] p 284 N95-12856
AIRCRAFT COMPARTMENTS
Viper cabin-fuselage structural design concept with engine installation and wing structural design
[NASA-CR-197162] p 239 N95-12305
Simultaneous gas-chromatographic determination of four toxic gases generally present in combustion atmospheres
[DOT/FAA/AM-94/18] p 338 N95-12354
Cabin fuselage structural design with engine installation and control system
[NASA-CR-197173] p 240 N95-12639
Cabin-fuselage-wing structural design concept with engine installation
[NASA-CR-197172] p 242 N95-12993
AIRCRAFT CONFIGURATIONS
Impact of agility requirements on configuration synthesis
[NASA-CR-4627] p 238 N95-11952
Design of a high capacity long range cargo aircraft
[NASA-CR-197176] p 239 N95-12363
Design of a vehicle based system to prevent ozone loss
[NASA-CR-197199] p 242 N95-12702
AIRCRAFT CONTROL
Optimum aerodynamic design via boundary control
[NASA-CR-195882] p 230 N95-11877
Piloted evaluation of an integrated methodology for propulsion and airframe control design
[NASA-TM-106741] p 245 N95-12763
AIRCRAFT DESIGN
Symmetric steady manoeuvre loads on rigid aircraft of classical configuration at subsonic speeds
[ESDU-94009] p 238 N95-11774
Effects of mass on aircraft sidearm controller characteristics
[NASA-TM-104277] p 244 N95-11868
Optimum aerodynamic design via boundary control
[NASA-CR-195882] p 230 N95-11877
Impact of agility requirements on configuration synthesis
[NASA-CR-4627] p 238 N95-11952
Conceptual design of the AE481 Demon Remotely Piloted Vehicle (RPV)
[NASA-CR-197164] p 238 N95-12294
Viper cabin-fuselage structural design concept with engine installation and wing structural design
[NASA-CR-197162] p 239 N95-12305
Design of a high capacity long range cargo aircraft
[NASA-CR-197176] p 239 N95-12363
The Elite: A high speed, low-cost general aviation aircraft for Aeroworld
[NASA-CR-197161] p 239 N95-12530
Icarus Rewaxed: A high speed, low-cost general aviation aircraft for Aeroworld
[NASA-CR-197155] p 239 N95-12609
Gemini: A long-range cargo transport
[NASA-CR-197149] p 239 N95-12626
The FC-1D: The profitable alternative Flying Circus Commercial Aviation Group
[NASA-CR-197152] p 240 N95-12628
Triton 2 (1B)
[NASA-CR-197188] p 240 N95-12636
The OFP-6M transport jet
[NASA-CR-197159] p 240 N95-12637
The Balsa bullet: A high speed, low-cost general aviation aircraft for Aeroworld
[NASA-CR-197165] p 240 N95-12638
Central coast designs: The Eightball Express. Taking off with convention, cruising with improvements and landing with absolute success
[NASA-CR-197181] p 241 N95-12643
LCX: Proposal for a low-cost commercial transport
[NASA-CR-197186] p 241 N95-12645
A preliminary design proposal for a maritime patrol strike aircraft: MPS-2000 Condor
[NASA-CR-197182] p 241 N95-12689
Design and construction of a remote piloted flying wing
[NASA-CR-197195] p 241 N95-12695
Activities of the Institute for Aerospace Studies of Toronto University p 390 N95-12699
Integrated design and manufacturing for the high speed civil transport
[NASA-CR-197183] p 241 N95-12700
Design and testing of an oblique all-wing supersonic transport
[NASA-CR-196394] p 242 N95-12785
Cabin-fuselage-wing structural design concept with engine installation
[NASA-CR-197172] p 242 N95-12993
AIRCRAFT ENGINES
NASA's Hypersonic Research Engine Project: A review
[NASA-TM-107759] p 244 N95-12860
Activities of the Structures Division, Lewis Research Center
[NASA-TM-106081] p 313 N95-13235
Evaluation of alternative in-flight fire suppressants for full-scale testing in simulated aircraft engine nacelles and dry bays
[PB94-203403] p 236 N95-13247
The development of the F100-PW-220 and F110-GE-100 engines: A case study of risk assessment and risk management
[AD-A282467] p 244 N95-13289
AIRCRAFT FUEL SYSTEMS
High frequency flow/structural interaction in dense subsonic fluids handbook
[NASA-CR-194007] p 230 N95-11807
AIRCRAFT FUELS
A study of aircraft post-crash fuel fire mitigation
[AD-A282208] p 234 N95-12499
AIRCRAFT HAZARDS
Airborne Windshear Detection and Warning Systems. Fifth and Final Combined Manufacturers' and Technologists' Conference, part 2
[NASA-CP-10139-PT-2] p 234 N95-13203
Certification methodology applied to the NASA experimental radar system p 235 N95-13205
Characteristics of civil aviation atmospheric hazards
p 235 N95-13208
Doppler radar detection of vortex hazard indicators
p 236 N95-13212
Evaluation of candidate millimeter wave sensors for synthetic vision p 236 N95-13214
AIRCRAFT ICING
User's manual for the NASA Lewis ice accretion/heat transfer prediction code with electrothermal deicer input
[NASA-CR-4530] p 291 N95-11888
Role of wind tunnels and computer codes in the certification and qualification of rotorcraft for flight in forecast icing
[NASA-TM-106747] p 233 N95-13197

AIRCRAFT INDUSTRY
Design and construction of a remote piloted flying wing
[NASA-CR-197195] p 241 N95-12695
AIRCRAFT INSTRUMENTS
Flight test of takeoff performance monitoring system
[NASA-TP-3403] p 245 N95-12664
AIRCRAFT LANDING
Dynamic ground effects flight test of an F-15 aircraft
[NASA-TM-4604] p 231 N95-12191
Evaluation of candidate millimeter wave sensors for synthetic vision p 236 N95-13214
Passive MMW camera for low visibility landings p 236 N95-13215
AIRCRAFT MANEUVERS
Examples of flight path optimisation using a multivariate gradient-search method. Addendum A: Variation of optimum flight profile parameters with range
[ESDU-94016-ADD-A] p 238 N95-11794
AIRCRAFT MODELS
Pressure measurements on an F/A-18 twin vertical tail in buffeting flow. Volume 3: Buffet power spectral densities
[AD-A281444] p 230 N95-11829
Icarus Rewaxed: A high speed, low-cost general aviation aircraft for Aeroworld
[NASA-CR-197155] p 239 N95-12609
Electromagnetic on-aircraft antenna radiation in the presence of composite plates
[NASA-CR-196126] p 284 N95-12856
AIRCRAFT NOISE
En route noise levels from propfan test assessment airplane
[NASA-TP-3451] p 355 N95-12341
AIRCRAFT PERFORMANCE
Examples of flight path optimisation using a multivariate gradient-search method. Addendum A: Variation of optimum flight profile parameters with range
[ESDU-94016-ADD-A] p 238 N95-11794
Flight investigation of the use of a nose gear jump strut to reduce takeoff ground roll distance of STOL aircraft
[NASA-TM-108819] p 238 N95-12225
Design of a high capacity long range cargo aircraft
[NASA-CR-197176] p 239 N95-12363
The FC-1D: The profitable alternative Flying Circus Commercial Aviation Group
[NASA-CR-197152] p 240 N95-12628
Flight test of takeoff performance monitoring system
[NASA-TP-3403] p 245 N95-12664
AIRCRAFT PILOTS
Age 60 Rule research. Part 1: Bibliographic database
[DOT/FAA/AM-94/20-PT-1] p 336 N95-13019
Age 60 Rule. Part 2: Airline pilot age and performance. A review of the scientific literature
[DOT/FAA/AM-94/21-PT-2] p 336 N95-13020
Aviation epidemiology data register: Cardiovascular disease screening outcomes in the North Dakota Army National Guard aviator cohort
[AD-A283064] p 334 N95-13054
AIRCRAFT PRODUCTION
Integrated design and manufacturing for the high speed civil transport
[NASA-CR-197183] p 241 N95-12700
AIRCRAFT SAFETY
Simultaneous gas-chromatographic determination of four toxic gases generally present in combustion atmospheres
[DOT/FAA/AM-94/18] p 338 N95-12354
A study of aircraft post-crash fuel fire mitigation
[AD-A282208] p 234 N95-12499
Evaluation of alternative in-flight fire suppressants for full-scale testing in simulated aircraft engine nacelles and dry bays
[PB94-203403] p 236 N95-13247
AIRCRAFT STABILITY
Determining the accuracy of maximum likelihood parameter estimates with colored residuals
[NASA-CR-194893] p 244 N95-11869
AIRCRAFT STRUCTURES
On the interaction of jet noise with a nearby flexible structure
[NASA-CR-194934] p 290 N95-11812
Development of an Automated Nondestructive Inspection (ANDI) system for commercial aircraft, phase 1
[AD-A283500] p 234 N95-12623
Triton 2 (1B)
[NASA-CR-197188] p 240 N95-12636
AIRCRAFT WAKES
Airborne Windshear Detection and Warning Systems. Fifth and Final Combined Manufacturers' and Technologists' Conference, part 2
[NASA-CP-10139-PT-2] p 234 N95-13203
Aircraft wake RCS measurement p 235 N95-13210
Wake vortex detection at Denver Stapleton Airport with a pulsed 2-micron coherent lidar p 236 N95-13211
Doppler radar detection of vortex hazard indicators p 236 N95-13212
Remote sensing of turbulence in the clear atmosphere with 2-micron lidars p 236 N95-13213
AIRFOIL PROFILES
Application of two procedures for dual-point design of transonic airfoils
[NASA-TP-3466] p 231 N95-12176
AIRFOILS
Optimum aerodynamic design via boundary control
[NASA-CR-195882] p 230 N95-11877
Control theory based airfoil design using the Euler equations
[NASA-CR-196360] p 230 N95-11884
User's manual for the NASA Lewis ice accretion/heat transfer prediction code with electrothermal deicer input
[NASA-CR-4530] p 291 N95-11888
Application of two procedures for dual-point design of transonic airfoils
[NASA-TP-3466] p 231 N95-12176
Studies on the flow induced by an oscillating airfoil in a uniform stream
[PB94-204450] p 233 N95-13250
AIRLINE OPERATIONS
On-line data reconstruction in redundant disk arrays
[AD-A282709] p 340 N95-12516
The FC-1D: The profitable alternative Flying Circus Commercial Aviation Group
[NASA-CR-197152] p 240 N95-12628
The OFP-6M transport jet
[NASA-CR-197159] p 240 N95-12637
AIRPORTS
Moisture induced pressures in concrete airfield pavements
[AD-A281974] p 245 N95-11789
Gemini: A long-range cargo transport
[NASA-CR-197149] p 239 N95-12626
The Balsa bullet: A high speed, low-cost general aviation aircraft for Aeroworld
[NASA-CR-197165] p 240 N95-12638
Certification of windshear performance with RTCA class D radomes p 235 N95-13206
Airport surveillance using a solid state coherent lidar p 235 N95-13207
Ground-based wake vortex monitoring, prediction, and ATC interface p 235 N95-13209
Wake vortex detection at Denver Stapleton Airport with a pulsed 2-micron coherent lidar p 236 N95-13211
Evaluation of candidate millimeter wave sensors for synthetic vision p 236 N95-13214
Response to noise around Vaernes and Bodoe airports
[PB94-207065] p 356 N95-13575
AIRSPEED
Flight dynamics of an unmanned aerial vehicle
[AD-A282259] p 239 N95-12410
Remote sensing of turbulence in the clear atmosphere with 2-micron lidars p 236 N95-13213
ALBEDO
Satellite estimates of shortwave surface radiation and atmospheric meteorology for the BOREAS experiment region
[NASA-TM-109132] p 326 N95-12839
ALCOHOLS
Thermal conductivity of gaseous oxygenated aliphatic hydrocarbons. Alcohols, aldehydes, ketones and ethers
[ESDU-94018] p 265 N95-11795
Phenoxythiocarbonylation and deoxygenation of aryl trifluoromethyl carbinols
[AD-A280519] p 260 N95-12613
Hydrolysis and condensation of tin (4) alkoxide compounds: The control of structural evolution
[AD-A282789] p 267 N95-12807
ALDEHYDES
Thermal conductivity of gaseous oxygenated aliphatic hydrocarbons. Alcohols, aldehydes, ketones and ethers
[ESDU-94018] p 265 N95-11795
Synthetic method for ethynylation of aromatic compounds
[AD-D016398] p 261 N95-13151
ALERTNESS
Crew factors in flight operations 9: Effects of planned cockpit rest on crew performance and alertness in long-haul operations
[NASA-TM-108839] p 334 N95-12792
ALGEBRA
Extensions and contractions of the Lie algebra of q-pseudodifferential symbols
[PB94-192374] p 352 N95-12603
Parallel preconditioners for the conjugate gradient method
[PB94-201605] p 347 N95-13404
ALGORITHMS
Object-oriented incremental map-generation for mobile robot navigation
[PB94-190717] p 314 N95-11820
Design of systolic algorithms and architectures for digital signal processing
[PB94-179256] p 346 N95-11838
Constructing combinatorial designs by local search
[PB94-179272] p 351 N95-11839
An analysis of the effect of Gaussian error in object recognition
[AD-A282260] p 349 N95-12411
Minimal fixturing of frictionless assemblies: Complexity and algorithms
[AD-A282724] p 300 N95-12505
A practical approach to drawing undirected graphs
[AD-A282641] p 343 N95-12541
Near-infrared imaging of selected areas
[AD-A283519] p 316 N95-12634
Learning unions of boxes with membership and equivalence queries
[DE94-014662] p 350 N95-12866
Parallel algorithms for the spectral transform method
[DE94-015458] p 344 N95-12893
Simulating the energy performance of holographic glazings
[DE94-014969] p 296 N95-13158
Nonlinear structural response using adaptive dynamic relaxation on a massively-parallel-processing system
[NASA-CR-196491] p 313 N95-13162
Methodology for sensitivity analysis, approximate analysis, and design optimization in CFD for multidisciplinary applications
[NASA-CR-196981] p 294 N95-13201
Object recognition for flexible assembly using stereo vision
[PB94-204427] p 363 N95-13248
Numerical time dependent sheet cavitation simulations using a higher order panel method
[PB94-204435] p 294 N95-13249
Algorithms for mathematical programming
[DE94-013544] p 345 N95-13339
An iterative approach to multibody simulation dynamics suitable for parallel implementation
[UTIAS-TN-276] p 347 N95-13353
Weighted Parzen windows for pattern classification
[AD-A281222] p 345 N95-13370
Adaptive relaxation for the steady-state analysis of Markov chains
[NASA-CR-194944] p 345 N95-13420
Finite element methods in resistivity logging
[PB94-206919] p 325 N95-13434
Visualizing parallel numerical software performance on a shared memory multiprocessor
[PB94-195658] p 352 N95-13437
Implementing a linear equation solver in the CFD code PHOENICS
[PB94-195757] p 353 N95-13439
ALIGNMENT
Alignment and experiment of the HL-1 x ray bent-crystal spectrometer
[DE94-624719] p 297 N95-13537
ALIPHATIC HYDROCARBONS
Thermal conductivity of gaseous oxygenated aliphatic hydrocarbons. Alcohols, aldehydes, ketones and ethers
[ESDU-94018] p 265 N95-11795
ALKALIES
Pressure studies of alkali, alkaline earth and rare earth doped C60 superconductors
[DE94-013345] p 372 N95-11862
ALKALINE BATTERIES
Proceedings of the 36th Power Sources Conference
[AD-A281443] p 288 N95-13164
ALKALOIDS
Elimination of quinine in two subjects after ingestion of tonic water: An exploratory study
[DOT/FAA/AM-94/16] p 332 N95-11702
ALKANES
Triple sorbent thermal desorption/gas chromatography/mass spectrometry determination of vapor phase organic contaminants
[DE94-013634] p 264 N95-11735
Vapour pressures and critical points of liquids. Polycyclic phenyl and cyclohexyl compounds
[ESDU-94001] p 266 N95-12128
Orthobaric densities and molar volumes of liquids. Polycyclic phenyl and cyclohexyl compounds
[ESDU-94002] p 266 N95-12129
ALKYL COMPOUNDS
Amine catalyzed intramolecular imidization of alkyl and aryl phthalamates, kinetics and mechanism in deuterated chloroform
[AD-A281741] p 259 N95-11844
Multifunctional acrylic ether monomers, their polymers, and polymerizable epoxide derivatives from simple alpha-substitution of alkyl acrylates
[AD-A282513] p 273 N95-12400
Phosphazene-containing amine as curing agent for phthalonitrile-base polymer
[AD-D016375] p 276 N95-13179

ALLOYING
Growth of Au on Ni(110): A BFS modelling of surface alloy phases
[NASA-TM-106732] p 270 N95-12104
Study on surface treatment by pulsed electron beams
p 366 N95-12437
First principles investigation of the Ir-Zr-Nb ternary system
[AD-A282644] p 270 N95-12543
CGF cartridge development, volume 1
[NASA-CR-196508] p 270 N95-12830
ALPHA PARTICLES
Fusion programs in applied plasma physics
[DE94-015853] p 369 N95-12944
Effect of stochastic damping resonance wave packet on energetic alpha particle transport
[DE94-625041] p 370 N95-13538
ALTERNATIVES
Methodologies for processing plant material into acceptable food on a small scale
[NASA-CR-177647] p 338 N95-12132
ALUMINIDES
Symposium on Structural Intermetallics: Perspectives on Science and Technology, volume 1
[AD-A283378] p 271 N95-12925
ALUMINUM
NIST calibration of ASTM E127-type ultrasonic reference blocks
[PB94-191640] p 355 N95-11906
Adherend surface effects on epoxy cure by NMR
[AD-A282165] p 274 N95-12420
Analysis for Be-7 and Be-10 on LDEF materials and their sources
[NASA-CR-193989] p 268 N95-13084
ALUMINUM ALLOYS
Certain aspects of the melting, casting and welding of Ni3Al alloys
[DE94-013628] p 269 N95-11897
Effect of pre-welding heat-treatments on welding a two-phase Ni3Al alloy
[DE94-014409] p 270 N95-12372
An analysis of the load-bearing capacity of members of square cross section with a series of perpendicular notches p 312 N95-12631
On the strain and strain-rate dependence of the fraction of plastic work converted to heat: An experimental study using high speed infrared detectors and the Kolsky bar
[SM-92-33] p 354 N95-12728
Thin-film model studies of interfacial reactions in intermetallic matrix composites
[AD-A283360] p 263 N95-12883
Synchrotron studies of narrow band materials
[DE94-013698] p 271 N95-13554
ALUMINUM ARSENIDES
The Research Laboratory of Electronics
[AD-A281445] p 386 N95-11830
ALUMINUM COMPOUNDS
Investigation of the effects of solid rocket motor propellant composition on plume signature
[AD-A283365] p 258 N95-12885
ALUMINUM GALLIUM ARSENIDE LASERS
Differential absorption lidar measurements of atmospheric water vapor using a pseudonoise code modulated AlGaAs laser
[NASA-TM-104610] p 314 N95-11997
ALUMINUM NITRIDES
Pseudomorphic semiconducting heterostructures from combinations of AlN, GaN and selected SiC polytypes: Theoretical advancement and its coordination with experimental studies of nucleation, growth, characterization and device development
[AD-A281218] p 289 N95-13368
ALUMINUM OXIDES
Adherend surface effects on epoxy cure by NMR
[AD-A282165] p 274 N95-12420
ALUMINUM SILICATES
Surface roughness characterization of various ceramic fibers using AFM and low voltage SEM
[DE94-013635] p 272 N95-11736
ALVEOLI
A numerical analysis of the distribution of stresses in lung parenchyma which accounts for the interactions between the tissue skeleton and flowing air
p 332 N95-11806
AMAZON REGION (SOUTH AMERICA)
Estimation of above-ground phytomass in a tropical forest using TM-LANDSAT 5 E HRV-SPOT 1 data
[INPE-5500-TDI/515] p 316 N95-13159
AVHRR/NOAA images to detect and quantify deforestation in Amazon Forest: Relations with TM/LANDSAT data
[INPE-5501-TDI/516] p 316 N95-13350
AMBIENT TEMPERATURE
Stress analysis of laminated flat plates
[ESDU-94004] p 309 N95-11770
AMERICIUM
Thermodynamic constants for actinide oxides and oxyhydroxides relevant to actinide volatility calculations for thermal oxidation processes
[DE94-007762] p 376 N95-13074
AMERICIUM 241
Response of high T(sub c) superconducting Josephson junction to nuclear radiation
[DE94-624705] p 360 N95-13536
AMIDES
Amine catalyzed intramolecular imidization of alkyl and aryl phthalamates, kinetics and mechanism in deuterated chloroform
[AD-A281741] p 259 N95-11844
Synthesis and characterization of thianthrene-based polyamides
[AD-A282512] p 273 N95-12399
AMINES
Amine catalyzed intramolecular imidization of alkyl and aryl phthalamates, kinetics and mechanism in deuterated chloroform
[AD-A281741] p 259 N95-11844
Adherend surface effects on epoxy cure by NMR
[AD-A282165] p 274 N95-12420
Phosphazene-containing amine as curing agent for phthalonitrile-base polymer
[AD-D016375] p 276 N95-13179
AMINO ACIDS
Rational enzyme redesign
[DE94-014565] p 331 N95-12677
AMMONIA
The Additional Programme on Ammonia
[PB94-193075] p 320 N95-12777
AMMONIUM NITRATES
Influence of additives on structure and thermal stability of ammonium nitrate
[PB94-206943] p 278 N95-13435
AMORPHOUS MATERIALS
Radiation amorphization of materials
[DE94-624184] p 374 N95-12948
Structure-phase state of thick amorphous and microcrystalline chromium-carbon films deposited by ion-plasma sputtering
[DE94-624236] p 277 N95-13535
AMPLIFICATION
Microbial communities in subsurface environments: Diversity, origin, and evolution
[DE94-013699] p 329 N95-11737
Tropical cyclone development and intensification under moderate to strong vertical wind shear
[AD-A282185] p 326 N95-12423
AMPOULES
CGF cartridge development, volume 1
[NASA-CR-196508] p 270 N95-12830
ANALOG DATA
Part A: A data acquisition/controller system. Part B: Supplement to a data acquisition/controller system
[AD-A283373] p 285 N95-12924
ANALOG SIMULATION
An iterative approach to multibody simulation dynamics suitable for parallel implementation
[UTIAS-TN-276] p 347 N95-13353
Numerical simulations of creep in ductile-phase toughened intermetallic matrix composites
[DE94-014744] p 264 N95-13533
ANALYSIS (MATHEMATICS)
Using emergent order to shape a space society
p 377 N95-11959
ANALYTIC FUNCTIONS
Extension of a theorem of Gehring and Pommerenke
[PB94-180858] p 352 N95-12577
Numerical simulations of creep in ductile-phase toughened intermetallic matrix composites
[DE94-014744] p 264 N95-13533
ANALYTICAL CHEMISTRY
Vapour pressures and critical points of liquids. Polycyclic phenyl and cyclohexyl compounds
[ESDU-94001] p 266 N95-12128
Orthobaric densities and molar volumes of liquids. Polycyclic phenyl and cyclohexyl compounds
[ESDU-94002] p 266 N95-12129
ANCHORS (FASTENERS)
M.E.366-J embodiment design project: Portable foot restraint
[NASA-CR-197163] p 338 N95-12361
A lunar/Martian anchor emplacement system
[NASA-CR-197193] p 302 N95-12690
ANGLE OF ATTACK
Pressure measurements on an F/A-18 twin vertical tail in buffeting flow. Volume 3: Buffet power spectral densities
[AD-A281444] p 230 N95-11829
Water tunnel flow visualization study of a 4.4 percent scale X-31 forebody
[NASA-TM-104276] p 230 N95-11898
A simple analytical aerodynamic model of Langley Winged-Cone Aerospace Plane concept
[NASA-CR-194987] p 252 N95-12175
ANGULAR DISTRIBUTION
Photon production at CDF and D0
[DE94-014985] p 359 N95-13160
ANGULAR VELOCITY
The reflection of relativistic electron beam by virtual cathode
[IPPCZ-338] p 364 N95-11916
Hypersonic Gas-Surface Energy Accommodation Test Facility
[DE94-014468] p 232 N95-12652
ANISOTROPIC MEDIA
Plane-wave reflection from uniaxial chiral interface and its application to polarization transformation
[PB94-184496] p 283 N95-12580
Proceedings of Bianisotropics 1993: Seminar on Electrodynamics of Chiral and Bianisotropic Media
[PB94-179314] p 283 N95-12595
ANISOTROPY
The magnetic structure of holmium-erbium superlattices
[DE94-013728] p 371 N95-11739
Stiffnesses of laminated flat plates
[ESDU-94003] p 309 N95-11769
Scale disparity and spectral transfer in anisotropic numerical turbulence
[NASA-CR-194956] p 291 N95-11929
Origin of optical anisotropy in strained In(x)Ga(1-x)As/InP and In(y)Al(1-y)As/InP heterostructures
[AD-A283152] p 271 N95-13140
ANNEALING
Effect of pre-welding heat-treatments on welding a two-phase Ni3Al alloy
[DE94-014409] p 270 N95-12372
Study on surface treatment by pulsed electron beams
p 366 N95-12437
Role of implantation-induced defects in surface-oriented diffusion of fluorine in silicon
[DE94-014905] p 374 N95-13125
ANNIHILATION REACTIONS
Studies of positron induced luminescence from polymers
[DE94-013622] p 272 N95-11733
Radiation-induced structural changes, 4
[DE94-753223] p 356 N95-11817
Search for supersymmetry at CDF
[DE94-014264] p 357 N95-12369
Measurement of the polarization in the decay B(exp 0) yields J/psi K(exp *0) in (bar p)p collisions at the square root of s = 1.8 TeV
[DE94-014265] p 357 N95-12370
ANNULAR SUSPENSION AND POINTING SYSTEM
Introduction to magnetic bearings
[NASA-CR-197187] p 302 N95-12640
Annular suspension and pointing system with controlled DC electromagnets
[NASA-CR-197206] p 302 N95-12666
ANODES
Anode sheath contributions in plasma thrusters
[AD-A280395] p 364 N95-11837
Effect of operating parameters and anode gas impurities upon polymer electrolyte fuel cells
[DE94-014464] p 317 N95-12650
ANTARCTIC REGIONS
CESIUM-137 and natural radionuclides in soils from Southern Brazil and in soils and others environmental samples from Antarctic
[INPE-5505-TDI-517] p 321 N95-13192
ANTENNA ARRAYS
An investigation of the channel crosstalk in optical heterodyne controlled phased array radars
[AD-A281227] p 285 N95-13371
ANTENNA DESIGN
Design studies of large aperture, high-resolution Earth science microwave radiometers compatible with small launch vehicles
[NASA-TP-3469] p 315 N95-12379
Experimental evaluation of shape memory alloy actuation technique in adaptive antenna design concepts
[NASA-CR-194983] p 284 N95-12896
ANTENNA RADIATION PATTERNS
Analysis of cylindrical wrap-around and doubly conformal patch antennas by way of the finite element-artificial absorber method
[NASA-CR-195211] p 281 N95-12382
Electromagnetic on-aircraft antenna radiation in the presence of composite plates
[NASA-CR-196126] p 284 N95-12856
Experimental evaluation of shape memory alloy actuation technique in adaptive antenna design concepts
[NASA-CR-194983] p 284 N95-12896

ANTHRACENE
Studies of positron induced luminescence from polymers
[DE94-013622] p 272 N95-11733
ANTHROPOMETRY
Biomedical imaging
[AD-A282221] p 333 N95-12405
Standards relevant to a NATO anthropometry survey using 3D imaging tools
[AD-A283065] p 339 N95-13055
APOLLO PROJECT
Interviews with the Apollo lunar surface astronauts in support of planning for EVA systems design
[NASA-TM-108846] p 337 N95-11905
APPLICATION SPECIFIC INTEGRATED CIRCUITS
Computer-aided design-verification vector generation
[DE94-014022] p 345 N95-13077
APPLICATIONS PROGRAMS (COMPUTERS)
Sloshing analysis of tanks containing multiple fluid layers
[DE94-013333] p 290 N95-11753
Application of multivariate optimisation techniques to determination of optimum flight path trajectories
[ESDU-94012] p 238 N95-11793
Validation results of wind diesel simulation model TKKMOD
[PB94-179157] p 317 N95-11846
Performance analysis of three dimensional integral equation computations on a massively parallel computer
[NASA-CR-196747] p 346 N95-11863
The program for the 1993 adjustment of the Finnish first-order terrestrial triangulation
[REPT-94:3] p 314 N95-11880
A model-based expert system for space power distribution diagnostics
[NASA-CR-195336] p 342 N95-11918
Computer modeling the fatigue crack growth rate behavior of metals in corrosive environments
[NASA-CR-194982] p 269 N95-11933
FORTRAN programs to process Magsat data for lithospheric, external field, and residual core components
[NASA-TM-104612] p 323 N95-12130
Principles of GPS one-way data processing for high precision positioning applications: Algorithms and software issues p 237 N95-12177
Efficient and effective handling of cycle slips in global positioning system data p 237 N95-12230
Development of ROBOSIM for academic/industrial use
[NASA-CR-196148] p 349 N95-12470
ETRI brochure: History, mission, and activity highlights p 389 N95-12697
Experiments with formal methods in software engineering
[PB94-192416] p 344 N95-12774
HLLV avionics requirements study and electronic filing system database development
[NASA-CR-193993] p 243 N95-13027
A study of a multi-pinned phase CCD detector for use as a star tracker
[NASA-CR-196287] p 381 N95-13056
Role of wind tunnels and computer codes in the certification and qualification of rotorcraft for flight in forecast icing
[NASA-TM-106747] p 233 N95-13197
Visualizing parallel numerical software performance on a shared memory multiprocessor
[PB94-195658] p 352 N95-13437
Seals Flow Code Development 1993
[NASA-CP-10136] p 304 N95-13583
Presentation of computer code SPIRALI for incompressible, turbulent, plane and spiral grooved cylindrical and face seals p 305 N95-13584
Code GFACE: Gas lubricated face seals in laminar regime p 305 N95-13585
SCISEAL: A CFD code for analysis of fluid dynamic forces in seals p 305 N95-13586
User interface development p 305 N95-13587
Beta testing of MTI seal codes p 305 N95-13589
EG and G and NASA face seal codes comparison p 305 N95-13590
Incompressible face seals: Computer code IFACE p 307 N95-13606
APPROXIMATION
Stress relaxation functions: Methods of approximation
[NASA-CR-195830] p 312 N95-12861
Linear approximations of delays in buffers receiving correlated ATM cell streams
[PB94-207099] p 286 N95-13577
AQUEOUS SOLUTIONS
Self assembly of n-alkanethiolate monolayers on silver nano-structures: Determination of the apparent thickness of the monolayer by scanning tunneling microscopy
[AD-A282322] p 274 N95-12417
CeO2-ZrO2 powder synthesis by way of alcohol dehydration of aqueous salt solutions
[INPE-5484-PRE/1783] p 276 N95-13191
ARC DISCHARGES
PASP PLUS Transient Pulse Monitor (TPM): Preflight characterization report
[AD-A282582] p 283 N95-12550
ARC JET ENGINES
AFOSR Contractors Meeting in Propulsion
[AD-A282729] p 257 N95-12507
A low-erosion starting technique for high-performance arcjets
[NASA-TM-106627] p 259 N95-13347
ARC MELTING
Description of a high temperature quenching furnace for the study of the directional solidification of nickel-base superalloys
[DE94-013812] p 271 N95-13544
ARC WELDING
Weld acoustic monitor
[AD-D016400] p 356 N95-13154
ARCHAEBACTERIA
On the isolation of halophilic microorganisms from salt deposits of great geological age p 332 N95-11966
ARCHITECTURE
Architectural design of the science complex at Elizabeth City State University p 247 N95-11960
Communications plan --- Design of the public wing of the Oregon State University Hatfield Marine Science Center
[NASA-CR-196435] p 314 N95-12231
ARCHITECTURE (COMPUTERS)
Parallel methods for the flight simulation model
[DE94-013330] p 245 N95-11752
Design of systolic algorithms and architectures for digital signal processing
[PB94-179256] p 346 N95-11838
Performance analysis of three dimensional integral equation computations on a massively parallel computer
[NASA-CR-196747] p 346 N95-11863
An avionics scenario and command model description for Space Generic Open Avionics Architecture (SGOAA)
[NASA-CR-188330] p 242 N95-11913
Advanced computer architecture specification for automated weld systems
[NASA-CR-194006] p 343 N95-12014
Exploitation of virtual reality architectures
[AD-A282263] p 340 N95-12413
Space Station Module Power Management and Distribution System (SSM/PMAD)
[NASA-CR-193991] p 258 N95-12819
Overview of NASREM: The NASA/NBS standard reference model for telerobot control system architecture re
[PB94-194560] p 303 N95-12854
Quantum cellular automata
[AD-A283351] p 287 N95-12881
Methodology for sensitivity analysis, approximate analysis, and design optimization in CFD for multidisciplinary applications
[NASA-CR-196981] p 294 N95-13201
Uniformisation techniques for integral recurrence equations
[PB94-205069] p 347 N95-13407
An informal introduction to parallel processors
[DE94-016347] p 348 N95-13556
ARCTIC REGIONS
Parameterization and scaling of Arctic ice conditions in the context of ice-atmosphere processes
[NASA-CR-196831] p 327 N95-11706
ARGON
Alignment and experiment of the HL-1 x ray bent-crystal spectrometer
[DE94-624719] p 297 N95-13537
ARID LANDS
Factors influencing the rates, processes and magnitude of accumulation of carbon in desert soils
[NASA-CR-196820] p 325 N95-13025
ARMATURES
Behaviors of plasma armature in the augmented railgun using a permanent magnet p 367 N95-12449
AROMATIC COMPOUNDS
Synthesis and characterization of thianthrene-based polyamides
[AD-A282512] p 273 N95-12399
ARTIFICIAL INTELLIGENCE
Autonomous motion on wheels
[PB94-191327] p 348 N95-11825
An analysis of the effect of Gaussian error in object recognition
[AD-A282260] p 349 N95-12411
Thunderstorm hypothesis reasoner
[AD-A282664] p 326 N95-12805
Population-based incremental learning. A method for integrating genetic search based function optimization and competitive learning
[AD-A282654] p 350 N95-12835
Learning unions of boxes with membership and equivalence queries
[DE94-014662] p 350 N95-12866
Information Technology Division's technical paper abstracts
[AD-A282882] p 378 N95-12916
ASCORBIC ACID
Copper metabolism in rats fed ascorbic acid or restricted amounts of copper
[PB94-191343] p 330 N95-11902
ASIA
Neotectonics of Asia: Thin-shell finite-element models with faults
[NASA-CR-196436] p 324 N95-12949
ASPHALT
Additives in bituminous materials and fuel-resistant sealers
[DOT/FAA/CT-94/78] p 273 N95-12131
Marginal aggregates in flexible pavements: Background survey and experimental plan
[DOT/FAA/CT-94/58] p 246 N95-12216
ASSEMBLY LANGUAGE
Computer-aided design-verification vector generation
[DE94-014022] p 345 N95-13077
ASTRONAUT LOCOMOTION
Human factors assessments of the STS-57 SpaceHab-1 mission
[NASA-TM-104802] p 337 N95-11878
ASTRONAUT MANEUVERING EQUIPMENT
Interviews with the Apollo lunar surface astronauts in support of planning for EVA systems design
[NASA-TM-108846] p 337 N95-11905
ASTRONAUT PERFORMANCE
Human factors assessments of the STS-57 SpaceHab-1 mission
[NASA-TM-104802] p 337 N95-11878
ASTRONAUT TRAINING
Training for life science experiments in space at the NASA Ames Research Center p 339 N95-11964
ASTRONAUTS
Interviews with the Apollo lunar surface astronauts in support of planning for EVA systems design
[NASA-TM-108846] p 337 N95-11905
Proposal for the design of a zero gravity tool storage device
[NASA-CR-197150] p 302 N95-12627
MOOSE: Manned On-Orbit Servicing Equipment
[NASA-CR-197151] p 254 N95-12790
ASTRONOMICAL CATALOGS
The terrestrial gravitational wave environment from known sources
[NASA-CR-196167] p 323 N95-12468
ASTRONOMICAL INTERFEROMETRY
The detectability of extrasolar terrestrial and giant planets during their luminous final accretion
[NASA-CR-196147] p 381 N95-13012
ASTRONOMICAL PHOTOGRAPHY
Photographic region elemental abundance analyses of Dr. David S. Leckrone's GTO HST stars 2
[NASA-CR-196756] p 381 N95-12788
ASTRONOMICAL PHOTOMETRY
FOC SV support and science data analysis
[NASA-CR-196764] p 381 N95-12821
A study of a multi-pinned phase CCD detector for use as a star tracker
[NASA-CR-196287] p 381 N95-13056
ASTROPHYSICS
Exploring the parallelism exposed by partial evaluation
[AD-A282284] p 347 N95-12414
BATSE observations of 3C273
[NASA-CR-196185] p 380 N95-12463
BATSE observations of Nova Muscae 1991
[NASA-CR-196416] p 380 N95-12464
Hot absorbers and the x-ray spectra of BL Lac objects
[NASA-CR-196196] p 380 N95-12465
X-ray temporal and spectral studies of blazars with the Ginga satellite
[NASA-CR-196330] p 380 N95-12466
FOC SV support and science data analysis
[NASA-CR-196764] p 381 N95-12821
Gamma-ray burst constraints on the galactic frequency of extra-solar Oort clouds
[NASA-CR-196197] p 385 N95-12886
Research in astrophysical processes
[NASA-CR-196773] p 382 N95-12939
Summaries of papers presented at the High Resolution Spectroscopy Topical Meeting. Technical digest series. Volume 1: Post conference edition
[AD-A281261] p 268 N95-13372

ASYMMETRY
Water tunnel flow visualization study of a 4.4 percent scale X-31 forebody
[NASA-TM-104276] p 230 N95-11898
Design, synthesis and characterization of novel nonlinear optical polymers
[AD-A282201] p 274 N95-12424
ATLANTIC OCEAN
Hydrographic, carbon dioxide, nutrient and productivity measurements from the south Atlantic during July and August of 1991
[PB94-180668] p 328 N95-11900
ATMOSPHERIC BOUNDARY LAYER
Efficient parabolic equation solution of radiowave propagation in an inhomogeneous atmosphere and over irregular terrain: Formulation
[AD-A282648] p 284 N95-12834
SuperMariah: A similarity-based method for determining wind, temperature, and humidity profile structure in the surface boundary layer
[AD-A283058] p 327 N95-12997
ATMOSPHERIC CHEMISTRY
Quantitative understanding of the cycles of oxidized and reduced sulfur on Venus
[NASA-CR-196924] p 382 N95-12011
Present state of knowledge of the upper atmosphere1993: An assessment report, part 2
[NASA-RP-1337] p 322 N95-12103
Quantum chemical study of methane oxidation species
[NASA-CR-196158] p 265 N95-12107
Reactions of atmospheric cluster ions
[AD-A282598] p 324 N95-12534
Parallelization and visual analysis of multidimensional fields: Application to ozone production, destruction, and transport in three dimensions
[NASA-CR-195971] p 320 N95-12798
Development of techniques for the in situ observation of OH and HO2 for studies of the impact of high-altitude supersonic aircraft on the stratosphere
[NASA-CR-196759] p 321 N95-12832
ATMOSPHERIC CIRCULATION
High performance climate system modeling using a domain and task decomposition message-passing approach
[DE94-013739] p 322 N95-11741
Dynamical studies in hurricane intensity change
[AD-A282406] p 326 N95-12392
Parallelization and visual analysis of multidimensional fields: Application to ozone production, destruction, and transport in three dimensions
[NASA-CR-195971] p 320 N95-12798
Parallel algorithms for the spectral transform method
[DE94-015458] p 344 N95-12893
ATMOSPHERIC COMPOSITION
High performance climate system modeling using a domain and task decomposition message-passing approach
[DE94-013739] p 322 N95-11741
Greenhouse Effect Detection Experiment (GEDEX). Selected data sets
[NASA-TM-109952] p 318 N95-11845
Hydrographic, carbon dioxide, nutrient and productivity measurements from the south Atlantic during July and August of 1991
[PB94-180668] p 328 N95-11900
Trace gas emissions to the atmosphere by biomass burning in the west African savannas
[NASA-CR-196758] p 319 N95-11931
Present state of knowledge of the upper atmosphere1993: An assessment report, part 2
[NASA-RP-1337] p 322 N95-12103
Reactions of atmospheric cluster ions
[AD-A282598] p 324 N95-12534
Development of UV irradiance standards
[PB94-181005] p 320 N95-12771
Spacecraft maximum allowable concentrations for selected airborne contaminants, volume 1
[NASA-CR-196446] p 255 N95-12879
ATMOSPHERIC CORRECTION
SeaWiFS technical report series. Volume 19: Case studies for SeaWiFS calibration and validation, part 2
[NASA-TM-104566-VOL-19-PT-2] p 328 N95-11920
ATMOSPHERIC DIFFUSION
Concentration fluctuation models: A comparative study
[CUED/A-AERO/TR-24] p 292 N95-11939
Technical report series on global modeling and data assimilation. Volume 2: Direct solution of the implicit formulation of fourth order horizontal diffusion for gridpoint models on the sphere
[NASA-TM-10406] p 323 N95-12226
ATMOSPHERIC EFFECTS
Accelerated testing of coatings for protection against atmospheric corrosion
[PB94-202579] p 276 N95-13244
ATMOSPHERIC ENTRY
Science objectives and performance of a radiometer and window design for atmospheric entry experiments
[NASA-TM-4637] p 382 N95-12190
Venus cloud bobber mission: A long term survey of the Venusian surface
[NASA-CR-197174] p 383 N95-12533
ATMOSPHERIC GENERAL CIRCULATION MODELS
Technical report series on global modeling and data assimilation. Volume 2: Direct solution of the implicit formulation of fourth order horizontal diffusion for gridpoint models on the sphere
[NASA-TM-10406] p 323 N95-12226
Tests of a new cloud treatment in an atmospheric general circulation model
[DE94-013138] p 327 N95-13268
ATMOSPHERIC MODELS
High performance climate system modeling using a domain and task decomposition message-passing approach
[DE94-013739] p 322 N95-11741
Global ice sheet modeling
[DE94-013744] p 318 N95-11745
Present state of knowledge of the upper atmosphere1993: An assessment report, part 2
[NASA-RP-1337] p 322 N95-12103
Determination of the auroral oval Q index from the air weather service K index
[AD-A282764] p 324 N95-12508
Parallelization and visual analysis of multidimensional fields: Application to ozone production, destruction, and transport in three dimensions
[NASA-CR-195971] p 320 N95-12798
The impact of elevation data representation on nocturnal drainage wind simulations
[DE94-014752] p 326 N95-12927
Short term weather forecasting in real time in a base weather station setting
[AD-A283141] p 327 N95-13134
Gravity wave forcing and influences near the mesopause
[AD-A282482] p 325 N95-13293
ATMOSPHERIC MOISTURE
TOVS operational sounding upgrades: 1990-1992
[NOAA-TR-NESDIS-76] p 322 N95-11836
Differential absorption lidar measurements of atmospheric water vapor using a pseudonoise code modulated AlGaAs laser
[NASA-TM-104610] p 314 N95-11997
Tests of a new cloud treatment in an atmospheric general circulation model
[DE94-013138] p 327 N95-13268
ATMOSPHERIC PHYSICS
Magnetospheric-ionospheric Poynting flux
[NASA-CR-196856] p 322 N95-11801
Guest investigator program study: Physics of equatorial plasma bubbles
[NASA-CR-196150] p 368 N95-12853
Gravity wave forcing and influences near the mesopause
[AD-A282482] p 325 N95-13293
ATMOSPHERIC PRESSURE
Influence of additives on structure and thermal stability of ammonium nitrate
[PB94-206943] p 278 N95-13435
ATMOSPHERIC RADIATION
Satellite estimates of shortwave surface radiation and atmospheric meteorology for the BOREAS experiment region
[NASA-TM-109132] p 326 N95-12839
ATMOSPHERIC SOUNDING
TOVS operational sounding upgrades: 1990-1992
[NOAA-TR-NESDIS-76] p 322 N95-11836
Differential absorption lidar measurements of atmospheric water vapor using a pseudonoise code modulated AlGaAs laser
[NASA-TM-104610] p 314 N95-11997
Waves in Space Plasmas (WISP)
[NASA-CR-196432] p 369 N95-13024
ATMOSPHERIC TEMPERATURE
TOVS operational sounding upgrades: 1990-1992
[NOAA-TR-NESDIS-76] p 322 N95-11836
Greenhouse Effect Detection Experiment (GEDEX). Selected data sets
[NASA-TM-109952] p 318 N95-11845
Interpolation of scattered temperature data measurements onto a worldwide regular grid using radial basis functions with applications to global warming
[DE94-014745] p 321 N95-12926
ATOMIC CLUSTERS
Structure and performance of carbon aerogel electrodes
[DE94-014746] p 356 N95-11791
ATOMIC COLLISIONS
Quantitative understanding of the cycles of oxidized and reduced sulfur on Venus
[NASA-CR-196924] p 382 N95-12011
ATOMIC FORCE MICROSCOPY
Scanning tunneling microscopy/atomic force microscopy for study of nanoscale metal oxide particles (destructive adsorbents)
[AD-A281417] p 357 N95-11851
ATOMIC INTERACTIONS
Atomic scale dynamics of a two-dimensional gas-solid interface
[AD-A282646] p 358 N95-12617
Advanced cryogenic propellants
[AD-A282451] p 277 N95-12729
ATOMIC STRUCTURE
Atomic structure modifications of diamond-like nanocomposite films: Observation by Raman spectroscopy, FTIR and STM
[DE94-013732] p 371 N95-11740
Muon sites and electronic structure
[PB94-179348] p 357 N95-12365
Radiative properties of strongly magnetized plasmas
[DE94-015487] p 369 N95-12897
Atomic structures and compositions of internal interfaces
[DE94-013594] p 271 N95-13543
ATOMIZERS
Structure of a swirl-stabilized, combusting spray
[NASA-TM-106724] p 243 N95-11890
ATOMS
Protein crystal growth in low gravity
[NASA-CR-196980] p 279 N95-13202
ATTACK AIRCRAFT
A preliminary design proposal for a maritime patrol strike aircraft: MPS-2000 Condor
[NASA-CR-197182] p 241 N95-12689
ATTITUDE CONTROL
Modelling and simulation of Space Station Freedom berthing dynamics and control
[NASA-TM-109151] p 252 N95-11947
Analytical investigation of the dynamics of tethered constellations in Earth orbit, phase 2
[NASA-CR-196509] p 252 N95-12106
Cryogenic On-Orbit Liquid Depot Storage, Acquisition, and Transfer Satellite (COLD-SAT)
[NASA-CR-185249] p 259 N95-13237
AUDITORY PERCEPTION
Effects of Noise on Hearing 5th International Symposium
[AD-A281439] p 335 N95-13177
AUGER EFFECT
Laser physics of Nd(exp 3+)-doped phosphate glasses
[DE94-015141] p 299 N95-13534
AURORAS
Determination of the auroral oval Q index from the air weather service K index
[AD-A282764] p 324 N95-12508
AUSTENITE
Novel concepts in weld science: Role of gradients and composite structure
[DE94-015482] p 271 N95-12895
AUSTRALIA
AGSO 1993: Yearbook of the Australian Geological Survey Organisation. Geoscientific research and database development for the year 1 July 1992 to 30 June 1993
p 324 N95-12686
AUTOMATA THEORY
Quantum cellular automata
[AD-A283351] p 287 N95-12881
AUTOMATED GUIDEWAY TRANSIT VEHICLES
Guideway structural design and power/propulsion/braking in relation to guideways. Volume 3: Appendix B: Maglev guideway structural design
[PB93-169910] p 304 N95-13128
AUTOMATIC CONTROL
Autonomous power system for remote locations
[DE94-013244] p 361 N95-11779
Population-based incremental learning. A method for integrating genetic search based function optimization and competitive learning
[AD-A282654] p 350 N95-12835
AUTONOMOUS NAVIGATION
Object-oriented incremental map-generation for mobile robot navigation
[PB94-190717] p 314 N95-11820
Autonomous motion on wheels
[PB94-191327] p 348 N95-11825
Essential kinematics for autonomous vehicles
[AD-A282456] p 300 N95-12394
Outdoor landmark recognition using hybrid fractal vision system and neural networks
[AD-A282506] p 349 N95-12395

Human-like robots for space and hazardous environments
[NASA-CR-197171] p 301 N95-12532

AUXILIARY POWER SOURCES
Moisture induced pressures in concrete airfield pavements
[AD-A281974] p 245 N95-11789

AVALANCHE DIODES
An acoustic charge transport imager for high definition television applications
[NASA-CR-196806] p 280 N95-11760

AVIATION METEOROLOGY
Terminal Doppler Weather Radar Build 5A Operational Test and Evaluation (OT/E) integration and OT/E operational test plan
[AD-A283052] p 327 N95-12996

AVIATION PSYCHOLOGY
The selective use of functional optical variables in the control of forward speed
[NASA-TM-108849] p 229 N95-12227
Crew factors in flight operations 9: Effects of planned cockpit rest on crew performance and alertness in long-haul operations
[NASA-TM-108839] p 334 N95-12792

AVIONICS
The development of a highly reliable power management and distribution system for civil transport aircraft
[NASA-TM-106697] p 243 N95-11867
An avionics scenario and command model description for Space Generic Open Avionics Architecture (SGOAA)
[NASA-CR-188330] p 242 N95-11913
Cabin fuselage structural design with engine installation and control system
[NASA-CR-197173] p 240 N95-12639
HLLV avionics requirements study and electronic filing system database development
[NASA-CR-193993] p 243 N95-13027

AWARDS
Technical paper contest for women 1992. Space challenges: Earth and beyond
[NASA-TM-109953] p 386 N95-11955

AXISYMMETRIC BODIES
Interlaminar stress analysis of dropped-ply laminated plates and shells by a mixed method
[NASA-CR-196851] p 311 N95-11946

AZIMUTH
Magnetic field generation in shock waves
[AD-A282234] p 281 N95-12408
Monopulse tracker operating characteristics measurement error performance for azimuth tracking
[AD-A281188] p 282 N95-12521

AZOLES
Novel thermooxidatively stable poly(ether-imide-benzoxazole) and poly(ester-imide-benzoxazole)
[AD-A282381] p 273 N95-12008

B

B STARS
Research in astrophysical processes
[NASA-CR-196773] p 382 N95-12939

B-1 AIRCRAFT
Moisture induced pressures in concrete airfield pavements
[AD-A281974] p 245 N95-11789
Case study of risk management in the USAF B-1B bomber program
[AD-A282371] p 377 N95-11944

BACKWARD WAVE TUBES
Measurements of 20 GHz high-power microwaves output from a large diameter plasma filled backward wave oscillator p 365 N95-12435

BACTERIA
Conformation of membrane proteins: Bacteriorhodopsin
[AD-A281282] p 331 N95-13373

BACTERIOLOGY
On the isolation of halophilic microorganisms from salt deposits of great geological age p 332 N95-11966

BALLOON SOUNDING
Venus cloud bobber mission: A long term survey of the Venusian surface
[NASA-CR-197174] p 383 N95-12533

BALLOONING MODES
A numerical calculation method for the kinetic ballooning mode eigen-equation with three components
[DE94-625048] p 369 N95-13107

BALLOONS
Venus cloud bobber mission: A long term survey of the Venusian surface
[NASA-CR-197174] p 383 N95-12533

BALLUTES
Computational flow predictions for hypersonic drag devices p 233 N95-11967

BALSA
The Balsa bullet: A high speed, low-cost general aviation aircraft for Aeroworld
[NASA-CR-197165] p 240 N95-12638

BALTIC SEA
Final results of the Baltic Sea Level 1990 GPS Campaign. Research works of the SSG 5.147 of the International Association of Geodesy
[REPT-94:2] p 314 N95-11881

BANDWIDTH
Frequency doubler (from 4.7 to 9.4 GHz) using a diode
[AD-A282784] p 287 N95-12525

BARIUM COMPOUNDS
Radiation-induced structural changes, 3
[DE94-753401] p 371 N95-11819

BARIUM OXIDES
Measurement of synchrotron radiation transmission of infrared range by YBa2Cu3O(7-delta) film in superconducting state
[DE94-623270] p 372 N95-11899

BARS
On the strain and strain-rate dependence of the fraction of plastic work converted to heat: An experimental study using high speed infrared detectors and the Kolsky bar
[SM-92-33] p 354 N95-12728

BARYONS
The cascade-deuteron system
[DE94-011650] p 357 N95-11894

BASE FLOW
Supersonic base flow investigation over axisymmetric afterbodies
[PB94-180957] p 232 N95-12578

BAUXITE
Analysis for Be-7 and Be-10 on LDEF materials and their sources
[NASA-CR-193989] p 268 N95-13084

BAYES THEOREM
Gaussian paired comparison models
[PB94-179025] p 352 N95-12820

BAYS (TOPOGRAPHIC FEATURES)
New York bight study. Report 4: Geographic information systems and relational database management system development
[AD-A281716] p 327 N95-11787
Evaluation of alternative in-flight fire suppressants for full-scale testing in simulated aircraft engine nacelles and dry bays
[PB94-203403] p 236 N95-13247

BEACONS
Advanced S-Band studies using the TDRSS communications satellite
[NASA-CR-196931] p 281 N95-12010

BEAM CURRENTS
The reflection of relativistic electron beam by virtual cathode
[IPPCZ-338] p 364 N95-11916
A study on successive generation of intense pulsed ion beams by the inverse pinch ion diode p 365 N95-12434
Plasma effects on electron beam dynamics in a virtual cathode oscillator p 366 N95-12436

BEAMFORMING
New multi-dimensional diagnostics method for intense ion beams p 365 N95-12432

BEARINGS
Duplex rolling element bearing mounting for ensuring preload control
[AD-D016402] p 304 N95-13189
High-speed seal and bearing test facility p 247 N95-13601

BELL AIRCRAFT
Ten-year ground exposure of composite materials used on the Bell Model 206L helicopter flight service program
[NASA-TP-3468] p 262 N95-12357

BENDING
A study of the deformation of helical springs under eccentric loading
[AD-A283448] p 312 N95-12511

BENDING MOMENTS
Gemini: A long-range cargo transport
[NASA-CR-197149] p 239 N95-12626

BENZENE
Towards tailored interphase formation utilizing surface-active benzylsulfonium salts as cationic initiators
[AD-A282511] p 262 N95-12398
Atomic scale dynamics of a two-dimensional gas-solid interface
[AD-A282646] p 358 N95-12617

BERYLLIUM ISOTOPES
Be-9 and B-11 NMR study of superconductivity in boron doped UBe13
[DE94-014432] p 374 N95-13081
Analysis for Be-7 and Be-10 on LDEF materials and their sources
[NASA-CR-193989] p 268 N95-13084

BETA PARTICLES
Response of high T(sub c) superconducting Josephson junction to nuclear radiation
[DE94-624705] p 360 N95-13536

BIBLIOGRAPHIES
Research activities of the Center for the Space Processing of Engineering Materials
[NASA-CR-196484] p 259 N95-11891
NASA's Hypersonic Research Engine Project: A review
[NASA-TM-107759] p 244 N95-12860
Aeronautical engineering: A continuing bibliography with indexes (supplement 309)
[NASA-SP-7037(309)] p 229 N95-12894
Age 60 Rule research. Part 1: Bibliographic database
[DOT/FAA/AM-94/20-PT-1] p 336 N95-13019
Bibliography on cold regions science and technology, volume 47, part 1
[AD-A281879] p 378 N95-13167

BINARY ALLOYS
Growth of Au on Ni(110): A BFS modelling of surface alloy phases
[NASA-TM-106732] p 270 N95-12104

BINARY CODES
Method of phased magnitude correlation using binary sequences
[AD-D016397] p 284 N95-12646

BINARY DATA
An analysis of the effect of Gaussian error in object recognition
[AD-A282260] p 349 N95-12411
Method of phased magnitude correlation using binary sequences
[AD-D016397] p 284 N95-12646

BINARY STARS
A catalogue of potentially bright close binary gravitational wave sources
[NASA-CR-196934] p 379 N95-12234
The terrestrial gravitational wave environment from known sources
[NASA-CR-196167] p 323 N95-12468

BINARY SYSTEMS (MATERIALS)
Atomic structures and compositions of internal interfaces
[DE94-013594] p 271 N95-13543

BINOCULAR VISION
Coordinated action in 3-D space
[AD-A281284] p 336 N95-13375

BIOASSAY
Fibre optic sensors using adiabatically tapered single mode fibres
[AD-A282306] p 362 N95-12415

BIOASTRONAUTICS
The Biological Flight Research Facility p 247 N95-11961
The rhesus measurement system: A new instrument for space research p 247 N95-11965
Meeting the nation's needs for biomedical and behavioral scientists
[LC-94-66477] p 330 N95-12310
Reduction of ocular counter-rolling by adaptation to space
[NASA-CR-196279] p 333 N95-12376

BIOCHEMICAL OXYGEN DEMAND
Consequences of prolonged inhalation of ozone on Fischer-344/N rats: Collaborative studies. Part 1: Content and cross-linking of lung collagen
[PB94-182748] p 331 N95-13176

BIOCHEMISTRY
Copper metabolism in rats fed ascorbic acid or restricted amounts of copper
[PB94-191343] p 330 N95-11902

BIODYNAMICS
Preconditioning electromyographic data for an upper extremity model using neural networks
[NASA-CR-196877] p 332 N95-11708

BIOELECTRICITY
Modelling of biopotential recordings and its implications for instrumentation design
[PB94-206844] p 332 N95-13408

BIOINSTRUMENTATION
The rhesus measurement system: A new instrument for space research p 247 N95-11965

BIOLOGICAL EFFECTS
Radiofrequency/microwave radiation biological effects and safety standards: A review
[AD-A282886] p 334 N95-12919

BIOLOGICAL MODELS (MATHEMATICS)
A numerical analysis of the distribution of stresses in lung parenchyma which accounts for the interactions between the tissue skeleton and flowing air p 332 N95-11806

BIOMASS
Trace gas emissions to the atmosphere by biomass burning in the west African savannas
[NASA-CR-196758] p 319 N95-11931

Estimation of above-ground phytomass in a tropical forest using TM-LANDSAT 5 E HRV-SPOT 1 data
[INPE-5500-TDI/515] p 316 N95-13159

BIOMEDICAL DATA
Standards relevant to a NATO anthropometry survey using 3D imaging tools
[AD-A283065] p 339 N95-13055
Modelling of biopotential recordings and its implications for instrumentation design
[PB94-206844] p 332 N95-13408

BIONICS
The Research Laboratory of Electronics
[AD-A281445] p 386 N95-11830

BIOSPHERE
Satellite estimates of shortwave surface radiation and atmospheric meteorology for the BOREAS experiment region
[NASA-TM-109132] p 326 N95-12839

BIOSYNTHESIS
Rational enzyme redesign
[DE94-014565] p 331 N95-12677

BIOTECHNOLOGY
The laser and its applications on environment and biotechnology research
[DE94-013831] p 299 N95-13076

BIPLANES
Gemini: A long-range cargo transport
[NASA-CR-197149] p 239 N95-12626

BIPOLAR TRANSISTORS
Silicon carbide and sicaln heterojunction bipolar transistor structures
[AD-D016403] p 288 N95-13181

BISMALEIMIDE
Damage tolerance of candidate thermoset composites for use on single stage to orbit vehicles
[NASA-TP-3506] p 261 N95-11816
Glass reinforced-diallylbisphenol/maleimide composites with modified interphases
[AD-A282496] p 264 N95-13298

BISMUTH TELLURIDES
Evaluation of the improvement in the figure of merit of Bi2Te3 - based alloys with addition of ultrafine scattering centers
[DE94-015363] p 374 N95-13059

BISPHENOLS
Adherend surface effects on epoxy cure by NMR
[AD-A282165] p 274 N95-12420
Glass reinforced-diallylbisphenol/maleimide composites with modified interphases
[AD-A282496] p 264 N95-13298

BIT ERROR RATE
Achieving unequal error protection with convolutional codes
[NASA-CR-196803] p 341 N95-11763

BITUMENS
Additives in bituminous materials and fuel-resistant sealers
[DOT/FAA/CT-94/78] p 273 N95-12131

BL LACERTAE OBJECTS
Hot absorbers and the x-ray spectra of BL Lac objects
[NASA-CR-196196] p 380 N95-12465

BLAZARS
X-ray temporal and spectral studies of blazars with the Ginga satellite
[NASA-CR-196330] p 380 N95-12466

BLOCK COPOLYMERS
Additives in bituminous materials and fuel-resistant sealers
[DOT/FAA/CT-94/78] p 273 N95-12131

BLOCKS
NIST calibration of ASTM E127-type ultrasonic reference blocks
[PB94-191640] p 355 N95-11906

BLOOD CIRCULATION
Effect of decreased gravity on circulation in the rat
[NASA-CR-196946] p 331 N95-12827

BLOOD FLOW
Effect of decreased gravity on circulation in the rat
[NASA-CR-196946] p 331 N95-12827

BLOOD PRESSURE
Effect of decreased gravity on circulation in the rat
[NASA-CR-196946] p 331 N95-12827

BLOOD VOLUME
Effect of decreased gravity on circulation in the rat
[NASA-CR-196946] p 331 N95-12827

BLOWING
Numerical analysis of tangential slot blowing on a generic chined forebody
[NASA-TM-108845] p 231 N95-11927

BLUNT BODIES
An implementation of a chemical and thermal nonequilibrium flow solver on unstructured meshes and application to blunt bodies
[NASA-CR-194967] p 293 N95-12619

BODY CENTERED CUBIC LATTICES
Magnetic response of ultrathin Fe on MgO: A polarised neutron reflectometry study
[DE94-013192] p 375 N95-13272

BODY-WING CONFIGURATIONS
Parallel aeroelastic computations for wing and wing-body configurations
[NASA-CR-196835] p 230 N95-11766
Symmetric steady manoeuvre loads on rigid aircraft of classical configuration at subsonic speeds
[ESDU-94009] p 238 N95-11774
Integrated design and manufacturing for the high speed civil transport
[NASA-CR-197183] p 241 N95-12700
Cabin-fuselage-wing structural design concept with engine installation
[NASA-CR-197172] p 242 N95-12993

BOILERS
Composites (CFCCs) for low cost energy and cleaner environment
[DE94-013601] p 272 N95-11781

BOLTZMANN-VLASOV EQUATION
Review of electron beam microinstabilities and their relevance to EBIS devices
[DE94-013755] p 364 N95-11746

BONDED JOINTS
Towards tailored interphase formation utilizing surface-active benzylsulfonium salts as cationic initiators
[AD-A282511] p 262 N95-12398

BONDING
Towards tailored interphase formation utilizing surface-active benzylsulfonium salts as cationic initiators
[AD-A282511] p 262 N95-12398
Ferric chloride graphite intercalation compounds prepared from graphite fluoride
[NASA-TM-106447] p 261 N95-12783

BONE MARROW
Spaceflight and immune responses of Rhesus monkeys
[NASA-CR-196846] p 331 N95-12941

BONES
Sound emission in materials and construction element testing p 355 N95-12013

BOOSTER RECOVERY
Liquid flyback booster pre-phase: A study assessment
[NASA-TM-104801] p 248 N95-11934

BORIDES
A brightness comparison of thermionic electron sources in a TEM
[DE94-013300] p 360 N95-13338

BORON
Be-9 and B-11 NMR study of superconductivity in boron doped UBe13
[DE94-014432] p 374 N95-13081

BORON ALLOYS
Synchrotron studies of narrow band materials
[DE94-013698] p 271 N95-13554

BORON ISOTOPES
Be-9 and B-11 NMR study of superconductivity in boron doped UBe13
[DE94-014432] p 374 N95-13081

BORON NITRIDES
Ceramic composites with ceramic fibers
[AD-D016315] p 275 N95-13175

BOSONS
A search for a heavy neutral gauge boson decaying into dielectrons in (-p)p collisions at the square root of s = 1.8 TeV
[DE94-014987] p 359 N95-13161

BOUNDARIES
Triaxial and torsional shear test results for sand
[AD-A282725] p 323 N95-12506

BOUNDARY CONDITIONS
A wall interference assessment and correction system
[NASA-CR-196940] p 292 N95-12228
Boundary conditions for unsteady compressible flows
[NASA-TM-106737] p 293 N95-12380
Analysis of cylindrical wrap-around and doubly conformal patch antennas by way of the finite element-artificial absorber method
[NASA-CR-195211] p 281 N95-12382
Laws of infrared similitude
[AD-A282209] p 354 N95-12426
Studies on the flow induced by an oscillating airfoil in a uniform stream
[PB94-204450] p 233 N95-13250
Fundamental and experimental studies on the catalytic combustion of methane
[PB94-205895] p 268 N95-13251
Finite element methods in resistivity logging
[PB94-206919] p 325 N95-13434

BOUNDARY LAYER CONTROL
Effect of nonzero surface admittance on receptivity and stability of compressible boundary layer
[NASA-CR-4621] p 292 N95-12105

BOUNDARY LAYER FLOW
Effect of nonzero surface admittance on receptivity and stability of compressible boundary layer
[NASA-CR-4621] p 292 N95-12105
Computation of turbulent boundary layers employing the defect wall-function method
[NASA-CR-4629] p 293 N95-12859
Fundamental and experimental studies on the catalytic combustion of methane
[PB94-205895] p 268 N95-13251

BOUNDARY LAYER STABILITY
Effect of nonzero surface admittance on receptivity and stability of compressible boundary layer
[NASA-CR-4621] p 292 N95-12105

BOUNDARY LAYER TRANSITION
Numerical simulation of particle-wave interaction on boundary layers
[AD-A282184] p 293 N95-12422

BOUNDARY LAYERS
Numerical simulation of particle-wave interaction on boundary layers
[AD-A282184] p 293 N95-12422
Fundamental and experimental studies on the catalytic combustion of methane
[PB94-205895] p 268 N95-13251

BOUNDARY VALUE PROBLEMS
Interlaminar stress analysis of dropped-ply laminated plates and shells by a mixed method
[NASA-CR-196851] p 311 N95-11946

BRAGG ANGLE
Alignment and experiment of the HL-1 x ray bent-crystal spectrometer
[DE94-624719] p 297 N95-13537

BRAIDED COMPOSITES
Failure analysis of woven and braided fabric reinforced composites
[NASA-CR-194981] p 262 N95-11926
Test methods for textile composites
[NASA-CR-4609] p 262 N95-12793

BRAIN
How are three-dimensional objects represented in the brain?
[AD-A282367] p 335 N95-11942

BRAKES (FOR ARRESTING MOTION)
Computational flow predictions for hypersonic drag devices p 233 N95-11967

BRAKING
Guideway structural design and power/propulsion/braking in relation to guideways. Volume 3: Appendix B: Maglev guideway structural design
[PB93-169910] p 304 N95-13128

BRAZIL
Estimation of above-ground phytomass in a tropical forest using TM-LANDSAT 5 E HRV-SPOT 1 data
[INPE-5500-TDI/515] p 316 N95-13159
CESIUM-137 and natural radionuclides in soils from Southern Brazil and in soils and others environmental samples from Antarctic
[INPE-5505-TDI-517] p 321 N95-13192
Use of remote sensing and geographic information system techniques in integrated studies of watersheds
[INPE-5494-TDI/511] p 316 N95-13352

BREADBOARD MODELS
Space Station Module Power Management and Distribution System (SSM/PMAD)
[NASA-CR-193991] p 258 N95-12619

BREATHING APPARATUS
Simultaneous gas-chromatographic determination of four toxic gases generally present in combustion atmospheres
[DOT/FAA/AM-94/18] p 338 N95-12354

BREMSSTRAHLUNG
Beams 92: Proceedings
[DE94-014783] p 361 N95-11792
A study of a multi-pinned phase CCD detector for use as a star tracker
[NASA-CR-196287] p 381 N95-13056
Particle-production mechanism in relativistic heavy-ion collisions
[DE94-014427] p 359 N95-13104
Absorption of intense microwaves and ion acoustic turbulence due to heat transport
[DE94-015140] p 369 N95-13285

BRIGHTNESS
Matter-wave interferometry with laser cooled atoms
[AD-A282484] p 360 N95-13178
A brightness comparison of thermionic electron sources in a TEM
[DE94-013300] p 360 N95-13338

BRIGHTNESS DISTRIBUTION
Hot absorbers and the x-ray spectra of BL Lac objects
[NASA-CR-196196] p 380 N95-12465

BRITTLENESS
Computer modeling the fatigue crack growth rate behavior of metals in corrosive environments
[NASA-CR-194982] p 269 N95-11933
BROADBAND
Target recognition in ultra-wideband SAR imagery
[AD-A283462] p 282 N95-12547
200 MHz channel sounder, open description
[PB94-202538] p 285 N95-13559
BRONCHI
Acute inhalation of explosively disseminated carbon fibers in rats
[AD-A280556] p 330 N95-12614
BRUSH SEALS
Development of a brush seals program leading to ceramic brush seals p 305 N95-13591
Brush seals for cryogenic applications p 305 N95-13592
Ceramic brush seals development p 306 N95-13594
Brush seals for turbine engine fuel conservation p 306 N95-13595
Brush seal numerical simulation: Concepts and advances p 306 N95-13596
Current developments in brush seals p 306 N95-13597
Air Force seal activities p 306 N95-13600
Relative performance comparison between baseline labyrinth and dual-brush compressor discharge seals in a T-700 engine test p 307 N95-13607
Some metallographic results for brush bristles and brush segments of a shroud ring brush seal tested in a T-700 engine p 307 N95-13608
BUBBLES
Synchronous picosecond sonoluminescence
[AD-A281498] p 355 N95-11856
BUCKLING
Buckling of flat rectangular orthotropic plates
[ESDU-94005] p 310 N95-11771
Elastic buckling of unbalanced laminated fibre reinforced composite plates (rectangular plates of AsBtDs type, all edges simply-supported under biaxial loading)
[ESDU-94006] p 310 N95-11772
Cabin-fuselage-wing structural design concept with engine installation
[NASA-CR-197172] p 242 N95-12993
Improved assumed-stress hybrid shell element with drilling degrees of freedom for linear stress, buckling, and free vibration analyses
[NASA-CR-192816] p 313 N95-13163
BUFFER STORAGE
Buffer size and switching capacity study in packet switches of broadband ISDN
[PB94-179421] p 281 N95-12368
BUFFETING
Pressure measurements on an F/A-18 twin vertical tail in buffeting flow. Volume 3: Buffet power spectral densities
[AD-A281444] p 230 N95-11829
BUILDINGS
Architectural design of the science complex at Elizabeth City State University p 247 N95-11960
Communications plan --- Design of the public wing of the Oregon State University Hatfield Marine Science Center
[NASA-CR-196435] p 314 N95-12231
Advances in SPARK
[DE94-014935] p 345 N95-13157
BURNING RATE
Study of vortical/axial type flameholders with variable angle blades
[INPE-5558-TDI/538] p 266 N95-12302
BURSTS
BATSE observations of Nova Muscae 1991
[NASA-CR-196416] p 380 N95-12464

C

C-5 AIRCRAFT
Aircraft wake RCS measurement p 235 N95-13210
CADMIUM
Atomic structures and compositions of internal interfaces
[DE94-013594] p 271 N95-13543
CADMIUM ALLOYS
Atomic structures and compositions of internal interfaces
[DE94-013594] p 271 N95-13543
CALIBRATING
NIST calibration of ASTM E127-type ultrasonic reference blocks
[PB94-191640] p 355 N95-11906
SeaWiFS technical report series. Volume 19: Case studies for SeaWiFS calibration and validation, part 2
[NASA-TM-104566-VOL-19-PT-2] p 328 N95-11920
Self calibrating autoTRAC
[NASA-CR-196930] p 348 N95-11998
SeaWiFS technical report series. Volume 23: SeaWiFS prelaunch radiometric calibration and spectral characterization
[NASA-TM-104566-VOL-23] p 328 N95-12359
A new algorithm for five-hole probe calibration, data reduction, and uncertainty analysis
[NASA-TM-106458] p 232 N95-12378
Calibration of optical wavelength at 1300 nm and 1550 nm using molecular absorption lines
[PB94-180080] p 362 N95-12598
Nimbus-7 Earth Radiation Budjet compact solar data set user's guide
[NASA-RP-1346] p 384 N95-12667
Development of UV irradiance standards
[PB94-181005] p 320 N95-12771
Strain gage selection in loads equations using a genetic algorithm
[NASA-CR-4597] p 242 N95-12831
Visible/infrared radiometric calibration station
[DE94-014459] p 363 N95-13106
A calibration of the Naval Postgraduate School middle ultraviolet spectrograph and an analysis of the OII 2470 A emission obtained by the middle ultraviolet spectrograph
[AD-A283449] p 354 N95-13144
CAMERAS
Site model based image registration and change detection, RADIUS
[AD-A282796] p 315 N95-12527
Passive MMW camera for low visibility landings p 236 N95-13215
CANARD CONFIGURATIONS
Experimental aerodynamic characteristics of a generic hypersonic accelerator configuration at Mach numbers 1.5 and 2.0 --- conducted in the Langley Unitary Plan Wind Tunnel
[NASA-TM-4413] p 233 N95-12770
CANCER
Morphological differentiation of colon carcinoma cell lines in rotating wall vessels
[NASA-CR-196780] p 333 N95-11808
CANS
GASCAN 2 payload integration
[NASA-CR-197200] p 278 N95-12701
CAPACITORS
Proceedings of the 36th Power Sources Conference
[AD-A281443] p 288 N95-13164
CARBAMATES (TRADENAME)
One-step synthesis of dithiocarbamates from metal powders
[NASA-TM-106558] p 260 N95-12692
CARBON
Structure and performance of carbon aerogel electrodes
[DE94-014746] p 356 N95-11791
Synthesis and solid-state NMR characterization of 13C- and 15N-labelled n-methylphthalimide: A model compound for studying polyimides
[AD-A282510] p 273 N95-12397
Phenoxythiocarbonylation and deoxygenation of aryl trifluoromethyl carbinols
[AD-A280519] p 260 N95-12613
Structure-phase state of thick amorphous and microcrystalline chromium-carbon films deposited by ion-plasma sputtering
[DE94-624236] p 277 N95-13535
CARBON COMPOUNDS
Ferric chloride graphite intercalation compounds prepared from graphite fluoride
[NASA-TM-106447] p 261 N95-12783
CARBON CYCLE
Hydrographic, carbon dioxide, nutrient and productivity measurements from the south Atlantic during July and August of 1991
[PB94-180668] p 328 N95-11900
Factors influencing the rates, processes and magnitude of accumulation of carbon in desert soils
[NASA-CR-196820] p 325 N95-13025
CARBON DIOXIDE
Carbon dioxide and water vapor production at rest and during exercise. A report on data collection for the Crew and Thermal Systems Division
[NASA-TP-3500] p 337 N95-11811
Hydrographic, carbon dioxide, nutrient and productivity measurements from the south Atlantic during July and August of 1991
[PB94-180668] p 328 N95-11900
Allocating CO2-emissions by using equity rules and optimization
[PB94-192861] p 320 N95-12776
Project Genesis: Mars in situ propellant technology demonstrator mission
[NASA-CR-197166] p 277 N95-12822
Project Hyreus: Mars sample return mission utilizing in situ propellant production
[NASA-CR-197189] p 383 N95-12826
Regulation of alternative CO2 fixation pathways in prokaryotic and eukaryotic photosynthetic organisms
[DE94-013180] p 331 N95-13271
CARBON DIOXIDE CONCENTRATION
Hydrographic, carbon dioxide, nutrient and productivity measurements from the south Atlantic during July and August of 1991
[PB94-180668] p 328 N95-11900
Trace gas emissions to the atmosphere by biomass burning in the west African savannas
[NASA-CR-196758] p 319 N95-11931
Allocating CO2-emissions by using equity rules and optimization
[PB94-192861] p 320 N95-12776
CARBON FIBER REINFORCED PLASTICS
Damage tolerance of candidate thermoset composites for use on single stage to orbit vehicles
[NASA-TP-3506] p 261 N95-11816
CARBON FIBERS
Acute inhalation of explosively disseminated carbon fibers in rats
[AD-A280556] p 330 N95-12614
CARBON MONOXIDE
Reactions of atmospheric cluster ions
[AD-A282598] p 324 N95-12534
CARBONATES
Acquisition of a gas source mass spectrometer for paleoclimatology and paleoceanography research
[AD-A282634] p 266 N95-12539
Factors influencing the rates, processes and magnitude of accumulation of carbon in desert soils
[NASA-CR-196820] p 325 N95-13025
Evaluation of alternative in-flight fire suppressants for full-scale testing in simulated aircraft engine nacelles and dry bays
[PB94-203403] p 236 N95-13247
CARBOXYLATES
Polymer effect on heterochiral molecular recognition in molecular and macromolecular pairs of liquid crystals of (R)- and (S)-2-chloro-4-methylpentyl 4'-((8-(vinyloxy)octyl)oxy)biphenyl-4-caroxylate rs
[AD-A281193] p 358 N95-12522
Synthesis and decomposition of a novel carboxylate precursor to indium oxide
[NASA-TM-106555] p 260 N95-12693
CARBOXYLIC ACIDS
Synthesis and characterization of thianthrene-based polyamides
[AD-A282512] p 273 N95-12399
CARDIOVASCULAR SYSTEM
Aviation epidemiology data register: Cardiovascular disease screening outcomes in the North Dakota Army National Guard aviator cohort
[AD-A283064] p 334 N95-13054
CARGO AIRCRAFT
Design of a high capacity long range cargo aircraft
[NASA-CR-197176] p 239 N95-12363
Gemini: A long-range cargo transport
[NASA-CR-197149] p 239 N95-12626
The OFP-6M transport jet
[NASA-CR-197159] p 240 N95-12637
CARRIER DENSITY (SOLID STATE)
About the structure of the superconducting order parameter of 2 D Fermi system with an arbitrary particle density
[DE94-623268] p 375 N95-13277
CARRIER INJECTION
Activities of Lehigh University
[AD-A282098] p 375 N95-13168
CARTRIDGES
CGF cartridge development, volume 1
[NASA-CR-196508] p 270 N95-12830
CASCADE FLOW
Measurements of pressure and thermal wakes in a transonic turbine cascade
[AD-A283464] p 232 N95-12548
CASSEGRAIN ANTENNAS
Experimental evaluation of shape memory alloy actuation technique in adaptive antenna design concepts
[NASA-CR-194983] p 284 N95-12896
CASTINGS
Certain aspects of the melting, casting and welding of Ni3Al alloys
[DE94-013628] p 269 N95-11897
CATALOGS (PUBLICATIONS)
A catalogue of potentially bright close binary gravitational wave sources
[NASA-CR-196934] p 379 N95-12234
Catalog of government inventions available for licensing, 1991
[PB92-100171] p 389 N95-12303

Catalog of government inventions available for licensing, 1992
[PB93-128205] p 389 N95-12342
A data and information system for processing, archival, and distribution of data for global change research
[NASA-CR-196770] p 320 N95-12786
Catalogue of heavy rainfall cases of six inches or more over the continental US during 1993
[NOAA-TR-NESDIS-80] p 327 N95-13095

CATALYSIS
Amine catalyzed intramolecular imidization of alkyl and aryl phthalamates, kinetics and mechanism in deuterated chloroform
[AD-A281741] p 259 N95-11844
Microemulsions as reaction media: Literature review
[PB94-184553] p 267 N95-12585
Fundamental and experimental studies on the catalytic combustion of methane
[PB94-205895] p 268 N95-13251

CATALYSTS
Microemulsions as reaction media: Literature review
[PB94-184553] p 267 N95-12585

CATHODE RAY TUBES
Dynamic sine wave response measurements of CRT displays using sinusoidal counterphase modulation
[AD-A282222] p 333 N95-12406

CATHODES
The reflection of relativistic electron beam by virtual cathode
[IPPCZ-338] p 364 N95-11916
Plasma effects on electron beam dynamics in a virtual cathode oscillator p 366 N95-12436

CATIONS
Towards tailored interphase formation utilizing surface-active benzylsulfonium salts as cationic initiators
[AD-A282511] p 262 N95-12398

CAVITATION FLOW
Synchronous picosecond sonoluminescence
[AD-A281498] p 355 N95-11856
Numerical time dependent sheet cavitation simulations using a higher order panel method
[PB94-204435] p 294 N95-13249

CAVITIES
Design and construction of the astronautics refrigerator magnet
[DE94-013599] p 353 N95-11731
Tetravalent chromium (Cr(4+)) as laser-active ion for tunable solid-state lasers
[NASA-CR-196481] p 298 N95-12951

CELL DIVISION
Morphological differentiation of colon carcinoma cell lines in rotating wall vessels
[NASA-CR-196780] p 333 N95-11808

CENTER OF MASS
Precision tethered satellite attitude control
[NASA-CR-196950] p 254 N95-12766

CENTRAL PROCESSING UNITS
Fiber-optic sensors and the application to conditional monitoring for mechanical structures
[PB94-207057] p 363 N95-13574

CENTRIFUGES
The Biological Flight Research Facility
p 247 N95-11961
Life Sciences Centrifuge Facility assessment
[NASA-CR-196848] p 332 N95-13423

CERAMIC BONDING
Microwave heating and joining of ceramic cylinders: A mathematical model
[NASA-CR-194962] p 351 N95-11922

CERAMIC COATINGS
Effects of piston surface treatments on performance and emissions of a methanol-fueled, direct injection, stratified charge engine
[DE94-011851] p 302 N95-12648

CERAMIC FIBERS
Surface roughness characterization of various ceramic fibers using AFM and low voltage SEM
[DE94-013635] p 272 N95-11736
Composites (CFCCs) for low cost energy and cleaner environment
[DE94-013601] p 272 N95-11781
Test Plans. Lightweight Durable TPS: Tasks 1,2,4,5, and 6
[NASA-CR-196867] p 262 N95-11835
Microwave heating and joining of ceramic cylinders: A mathematical model
[NASA-CR-194962] p 351 N95-11922
Tensile creep and stress-rupture behavior of polymer derived SiC fibers
[NASA-TM-106692] p 263 N95-12813
Ceramic composites with ceramic fibers
[AD-D016315] p 275 N95-13175
Ceramic brush seals development
p 306 N95-13594

CERAMIC MATRIX COMPOSITES
Surface roughness characterization of various ceramic fibers using AFM and low voltage SEM
[DE94-013635] p 272 N95-11736
Composites (CFCCs) for low cost energy and cleaner environment
[DE94-013601] p 272 N95-11781
The effect of irradiation on the stability and properties of monolithic silicon carbide and SiC(f)/SiC composites up to 25 dpa
[DE94-014568] p 263 N95-12862
Ceramic composites with ceramic fibers
[AD-D016315] p 275 N95-13175

CERAMICS
Composites (CFCCs) for low cost energy and cleaner environment
[DE94-013601] p 272 N95-11781
Test model designs for advanced refractory ceramic materials p 277 N95-11968
Intelligent processing of ferroelectric thin films
[AD-A282833] p 275 N95-12586
VAMAS round robin on fractography of ceramics. Swedish results
[PB94-180155] p 275 N95-12600
Apparatus and method for forming textured bulk high temperature superconducting materials
[AD-D016394] p 373 N95-12635
Hydrolysis and condensation of tin (4) alkoxide compounds: The control of structural evolution
[AD-A282789] p 267 N95-12807
Ceramic manufacturing: Optimizing a multivariable system
[DE94-015016] p 276 N95-13184
CeO2-ZrO2 powder synthesis by way of alcohol dehydration of aqueous salt solutions
[INPE-5484-PRE/1783] p 276 N95-13191
CVD techniques for the synthesis or modification of porous ceramics
[PB94-206836] p 276 N95-13284
Equipment for investigation of cryogenic compaction of nanosize silicon nitride powders
[DE94-013593] p 277 N95-13530
Development of a brush seals program leading to ceramic brush seals p 305 N95-13591
Ceramic brush seals development
p 306 N95-13594

CERIUM
Synchrotron studies of narrow band materials
[DE94-013698] p 271 N95-13554

CERIUM COMPOUNDS
A brightness comparison of thermionic electron sources in a TEM
[DE94-013300] p 360 N95-13338

CERIUM OXIDES
CeO2-ZrO2 powder synthesis by way of alcohol dehydration of aqueous salt solutions
[INPE-5484-PRE/1783] p 276 N95-13191

CERTIFICATION
Role of wind tunnels and computer codes in the certification and qualification of rotorcraft for flight in forecast icing
[NASA-TM-106747] p 233 N95-13197
Windshear certification data base for forward-look detection systems p 234 N95-13204
Certification methodology applied to the NASA experimental radar system p 235 N95-13205

CESIUM 137
CESIUM-137 and natural radionuclides in soils from Southern Brazil and in soils and others environmental samples from Antarctic
[INPE-5505-TDI-517] p 321 N95-13192

CHALLENGER (ORBITER)
Memorial service for the mission 51-L crew (edited)
[NASA-TM-109900] p 250 N95-13133

CHAMBERS
Target area chamber system design for the National Ignition Facility
[DE94-013347] p 364 N95-11754

CHANGE DETECTION
Site model based image registration and change detection, RADIUS
[AD-A282796] p 315 N95-12527

CHAOS
Using emergent order to shape a space society
p 377 N95-11959
Inverse operator theory method mathematics-mechanization for the solutions of nonlinear equations and some typical applications in nonlinear physics
[DE94-624804] p 352 N95-13340

CHARACTERIZATION
Surface roughness characterization of various ceramic fibers using AFM and low voltage SEM
[DE94-013635] p 272 N95-11736
Space Station Freedom propulsion activities
[NASA-TM-108604] p 256 N95-13236

CHARGE CARRIERS
Photogeneration of charge carriers in bilayer assemblies of conjugated rigid-rod polymers
[AD-A282625] p 275 N95-12537

CHARGE COUPLED DEVICES
A study of a multi-pinned phase CCD detector for use as a star tracker
[NASA-CR-196287] p 381 N95-13056
Laser based combustion laboratory at NTH/SINTEF applied thermodynamics
[PB94-202603] p 299 N95-13246

CHARGE TRANSFER DEVICES
An acoustic charge transport imager for high definition television applications
[NASA-CR-196806] p 280 N95-11760

CHARGED PARTICLES
On the charged vector particle scattering on a vector particle
[DE94-622787] p 360 N95-13273
Study of the nuclear-coulomb low-energy scattering parameters on the basis of the p-matrix approach
[DE94-622811] p 360 N95-13275

CHECKOUT
An examination of selected software testing tools: 1993 supplement
[AD-A283060] p 344 N95-13051
Norwegian contribution to the SWG on APSE programme
[PB94-202397] p 341 N95-13557

CHEMICAL ANALYSIS
Micromorphology, mineralogy, and genesis of soils and fracture fills and the Pajarito Plateau, New Mexico
[DE94-013612] p 322 N95-11732
Triple sorbent thermal desorption/gas chromatography/mass spectrometry determination of vapor phase organic contaminants
[DE94-013634] p 264 N95-11735
UV and fluorescence studies for vinyl polymerization
[AD-A281187] p 274 N95-12520

CHEMICAL BONDS
Muon sites and electronic structure
[PB94-179348] p 357 N95-12365
Phenoxythiocarbonylation and deoxygenation of aryl trifluoromethyl carbinols
[AD-A280519] p 260 N95-12613
Ferric chloride graphite intercalation compounds prepared from graphite fluoride
[NASA-TM-106447] p 261 N95-12783

CHEMICAL ENERGY
Proceedings of the Eighteenth DOE Solar Photochemistry Research Conference
[DE94-014926] p 318 N95-13126

CHEMICAL ENGINEERING
Chemical Engineering Seminar 1993
[PB94-184538] p 266 N95-12584

CHEMICAL EXPLOSIONS
Preliminary seismicity and focal mechanisms for the Southern Great Basin of Nevada and California, January 1992 - September 1992
[DE94-013589] p 321 N95-11730

CHEMICAL PROPERTIES
Novel activated carbon impregnants consisting of transition metal complexes. Part 1: Background, syntheses and characterizations
[AD-A282583] p 259 N95-12551

CHEMICAL REACTION CONTROL
Thermal polymerization of styrene in the presence of stable radicals and inhibitors
[AD-A280926] p 275 N95-12773

CHEMICAL REACTIONS
Microemulsions as reaction media: Literature review
[PB94-184553] p 267 N95-12585
Kinetics and characterization of tungsten CVD processes
[PB94-206901] p 271 N95-13411

CHEMICAL TESTS
Screen test for cadmium and nickel plates as developed and used within the Aerospace Corporation
[NASA-CR-196961] p 270 N95-12148

CHEMICAL VAPOR INFILTRATION
CVD techniques for the synthesis or modification of porous ceramics
[PB94-206836] p 276 N95-13284

CHILDREN
The performance of child restraint devices in transport airplane passenger seats
[DOT/FAA/AM-94/19] p 234 N95-12146

CHIPS (ELECTRONICS)
An acoustic charge transport imager for high definition television applications
[NASA-CR-196806] p 280 N95-11760

CHIRALITY
Proceedings of Bianisotropics 1993: Seminar on Electrodynamics of Chiral and Bianisotropic Media
[PB94-179314] p 283 N95-12595

CHLORIDES
Thianthrene-based poly(benzoxazole)s
[AD-A282326] p 274 N95-12419
Ferric chloride graphite intercalation compounds prepared from graphite fluoride
[NASA-TM-106447] p 261 N95-12783
CHLOROCARBONS
Trichloroethylene emissions reductions achieved by enclosing solvent spray degreasing operations
[DE94-013741] p 318 N95-11742
Progress on resonance ionization detection of combustion radicals
[DE94-015339] p 267 N95-12762
Method for laser-assisted etching of III-V and II-VI semiconductor compounds using chlorofluorocarbon ambients
[AD-D016385] p 298 N95-12779
CHLOROFLUOROCARBONS
Present state of knowledge of the upper atmosphere1993: An assessment report, part 2
[NASA-RP-1337] p 322 N95-12103
CHLOROFORM
Amine catalyzed intramolecular imidization of alkyl and aryl phthalamates, kinetics and mechanism in deuterated chloroform
[AD-A281741] p 259 N95-11844
CHLOROPHYLLS
Hydrographic, carbon dioxide, nutrient and productivity measurements from the south Atlantic during July and August of 1991
[PB94-180668] p 328 N95-11900
CHOLESKY FACTORIZATION
Study of adaptive high resolution frequency estimation techniques with hydroacoustical applications
[PB94-179512] p 355 N95-12597
CHROMIUM
Tetravalent chromium (Cr(4+)) as laser-active ion for tunable solid-state lasers
[NASA-CR-196481] p 298 N95-12951
CHROMIUM CARBIDES
Structure-phase state of thick amorphous and microcrystalline chromium-carbon films deposited by ion-plasma sputtering
[DE94-624236] p 277 N95-13535
CHROMIUM COMPOUNDS
Structure-phase state of thick amorphous and microcrystalline chromium-carbon films deposited by ion-plasma sputtering
[DE94-624236] p 277 N95-13535
CHROMOPHORES
Electronic energy transfer in new polymer nanocomposite assemblies
[AD-A282233] p 274 N95-12407
Rational design, construction, and processing of high-performance nonlinear, optical materials
[AD-A281283] p 363 N95-13374
CHRONIC CONDITIONS
Consequences of prolonged inhalation of ozone on Fischer-344/N rats: Collaborative studies. Part 1: Content and cross-linking of lung collagen
[PB94-182748] p 331 N95-13176
CIRCUIT BOARDS
A high-performance constant-temperature hot-wire anemometer
[NASA-CR-177645] p 295 N95-11896
CIRCUITS
Modeling of transformers using circuit simulators
[DE94-014656] p 287 N95-12863
CIRCULAR ORBITS
Selection process for trade study: Reusable Hydrogen Composite Tank System (RHCTS)
[NASA-CR-196874] p 251 N95-11809
CITIES
Proposal of a methodology to evaluate urban quality of life using conventional and remote sensing data, geographic information system, and a database
[INPE-5552-TDI/536] p 315 N95-12297
CIVIL AVIATION
High speed civil transport aerodynamic optimization
[NASA-CR-196960] p 232 N95-12389
Integrated design and manufacturing for the high speed civil transport
[NASA-CR-197183] p 241 N95-12700
Evaluation of alternative in-flight fire suppressants for full-scale testing in simulated aircraft engine nacelles and dry bays
[PB94-203403] p 236 N95-13247
CLASSIFIERS
Outdoor landmark recognition using hybrid fractal vision system and neural networks
[AD-A282506] p 349 N95-12395
CLEAR AIR TURBULENCE
Airborne Windshear Detection and Warning Systems. Fifth and Final Combined Manufacturers' and Technologists' Conference, part 2
[NASA-CP-10139-PT-2] p 234 N95-13203
Characteristics of civil aviation atmospheric hazards
p 235 N95-13208
Aircraft wake RCS measurement p 235 N95-13210
Doppler radar detection of vortex hazard indicators
p 236 N95-13212
Remote sensing of turbulence in the clear atmosphere with 2-micron lidars p 236 N95-13213
CLIMATE
Solar influences on global change
[NASA-CR-196966] p 319 N95-12384
CLIMATE CHANGE
Global ice sheet modeling
[DE94-013744] p 318 N95-11745
Solar influences on global change
[NASA-CR-196966] p 319 N95-12384
Development of UV irradiance standards
[PB94-181005] p 320 N95-12771
Allocating CO2-emissions by using equity rules and optimization
[PB94-192861] p 320 N95-12776
Periglacial and glacial analogs for Martian landforms
[NASA-CR-196772] p 383 N95-12952
CLIMATOLOGY
Global ice sheet modeling
[DE94-013744] p 318 N95-11745
Factors influencing the rates, processes and magnitude of accumulation of carbon in desert soils
[NASA-CR-196820] p 325 N95-13025
Tests of a new cloud treatment in an atmospheric general circulation model
[DE94-013138] p 327 N95-13268
CLOSED ECOLOGICAL SYSTEMS
Growth of potatoes for CELSS
[NASA-CR-177646] p 338 N95-11949
Techniques for optimal crop selection in a controlled ecological life support system p 339 N95-11962
The crop growth research chamber
p 248 N95-11969
Methodologies for processing plant material into acceptable food on a small scale
[NASA-CR-177647] p 338 N95-12132
Design and testing of a model CELSS chamber robot
[NASA-CR-197196] p 303 N95-12694
CLOTHING
Body dimensions for apparel
[PB94-187739] p 338 N95-11908
CLOUD COVER
TOVS operational sounding upgrades: 1990-1992
[NOAA-TR-NESDIS-76] p 322 N95-11836
A model of the density of solar radiation energy on an arbitrary plane identification for Warsaw
p 384 N95-12243
Tests of a new cloud treatment in an atmospheric general circulation model
[DE94-013138] p 327 N95-13268
CLOUD PHYSICS
Methods of modeling radiant energy exchange in radiation fog and clouds
[AD-A283509] p 326 N95-12624
CLOUDS (METEOROLOGY)
SeaWiFS technical report series. Volume 23: SeaWiFS prelaunch radiometric calibration and spectral characterization
[NASA-TM-104566-VOL-23] p 328 N95-12359
Stochastic indexing
[AD-A283143] p 327 N95-13137
Tests of a new cloud treatment in an atmospheric general circulation model
[DE94-013138] p 327 N95-13268
CLUSTER ANALYSIS
Eye-gaze determination of user intent at the computer interface
[DE94-012337] p 363 N95-13421
CLUSTERS
Mixed clusters from the coexpansion of C2F6 and n2 in a pulsed, supersonic expansion cluster ion source and beam deflection time-of-flight mass spectrometer: A first application
[AD-A282044] p 361 N95-11910
CLUTTER
An analysis of the effect of Gaussian error in object recognition
[AD-A282260] p 349 N95-12411
CMOS
Self-checking state machine realizations in CMOS
[AD-A282177] p 286 N95-12421
COBALT
Raman structural studies of the nickel electrode
[NASA-CR-196331] p 289 N95-13344
COBALT ALLOYS
Synchrotron studies of narrow band materials
[DE94-013698] p 271 N95-13554
COCKPITS
Draft standard for color active matrix liquid crystal displays (AMLCDs) in US Military aircraft. Recommended best practices
[AD-A282950] p 243 N95-12591
CODE DIVISION MULTIPLE ACCESS
200 MHz channel sounder, open description
[PB94-202538] p 285 N95-13559
CODERS
Achieving unequal error protection with convolutional codes
[NASA-CR-196803] p 341 N95-11763
CODING
Vector quantization for efficient coding of upper subbands
[NASA-CR-196804] p 341 N95-11762
Trellis-based source and channel coding
[PB94-204443] p 285 N95-13405
COHERENT RADAR
Lidar performance analysis
[NASA-CR-196510] p 362 N95-12390
Wake vortex detection at Denver Stapleton Airport with a pulsed 2-micron coherent lidar p 236 N95-13211
COHERENT RADIATION
Free electron lasers and other advanced sources of light: Scientific research opportunities p 297 N95-12375
COLD PRESSING
Mechanical behavior of (238)UO2, (238)PuO2, and (239)PuO2 as a function of strain rate and temperature
[DE94-015718] p 312 N95-12784
COLD WEATHER
Bibliography on cold regions science and technology, volume 47, part 1
[AD-A281879] p 378 N95-13167
COLLAGENS
Consequences of prolonged inhalation of ozone on Fischer-344/N rats: Collaborative studies. Part 1: Content and cross-linking of lung collagen
[PB94-182748] p 331 N95-13176
COLLIMATION
Large area soft x-ray collimator to facilitate x-ray optics testing
[NASA-CR-196923] p 362 N95-12736
COLLIMATORS
Large area soft x-ray collimator to facilitate x-ray optics testing
[NASA-CR-196923] p 362 N95-12736
COLLISION AVOIDANCE
Development of ROBOSIM for academic/industrial use
[NASA-CR-196148] p 349 N95-12470
COLLISION PARAMETERS
Development of ROBOSIM for academic/industrial use
[NASA-CR-196148] p 349 N95-12470
COLLISIONS
Photon production at CDF and D0
[DE94-014985] p 359 N95-13160
A search for a heavy neutral gauge boson decaying into dielectrons in (-p)p collisions at the square root of s = 1.8 TeV
[DE94-014987] p 359 N95-13161
A precision measurement of the prompt photon cross section in p(-p) collisions at the square root of s = 1.8 TeV
[DE94-014989] p 359 N95-13170
Numerical simulations of drop collisions
[NASA-TM-106751] p 295 N95-13550
COLLOIDS
Small angle neutron scattering in surface-active agents mixtures
[DE94-624057] p 356 N95-11747
Microemulsions as reaction media: Literature review
[PB94-184553] p 267 N95-12585
COLOR VISION
Visit to UDRI and USAF, Armstrong Lab., Williams AFB, Phoenix, USA, February 8-11, 1993
[PB94-190659] p 337 N95-11873
COMBINATORIAL ANALYSIS
Constructing combinatorial designs by local search
[PB94-179272] p 351 N95-11839
Population-based incremental learning. A method for integrating genetic search based function optimization and competitive learning
[AD-A282654] p 350 N95-12835
Passive MMW camera for low visibility landings
p 236 N95-13215
COMBUSTIBLE FLOW
Shock tube investigations of combustion phenomena in supersonic flows
[PB94-175262] p 265 N95-11796
COMBUSTION
Analysis of cost: Combustion flame CVD diamond deposition
[AD-A282527] p 273 N95-12403

Laser based combustion laboratory at NTH/SINTEF applied thermodynamics
[PB94-202603] p 299 N95-13246
Fundamental and experimental studies on the catalytic combustion of methane
[PB94-205895] p 268 N95-13251

COMBUSTION CHAMBERS
Engine structures analysis software: Component Specific Modeling (COSMO)
[NASA-CR-195378] p 309 N95-11711
Shock-tunnel combustor testing for hypersonic vehicles
[NASA-CR-196836] p 246 N95-11938
Study of a vortical/axial type flameholders with variable angle blades
[INPE-5558-TDI/538] p 266 N95-12302
Open-chamber combustion study
[PB94-184090] p 301 N95-12579
Fundamental and experimental studies on the catalytic combustion of methane
[PB94-205895] p 268 N95-13251

COMBUSTION PHYSICS
Shock tube investigations of combustion phenomena in supersonic flows
[PB94-175262] p 265 N95-11796
Backdraft phenomena
[PB94-193927] p 267 N95-12852

COMBUSTION PRODUCTS
Trace gas emissions to the atmosphere by biomass burning in the west African savannas
[NASA-CR-196758] p 319 N95-11931
Simultaneous gas-chromatographic determination of four toxic gases generally present in combustion atmospheres
[DOT/FAA/AM-94/18] p 338 N95-12354
Progress on resonance ionization detection of combustion radicals
[DE94-015339] p 267 N95-12762

COMETARY COLLISIONS
Gamma-ray burst constraints on the galactic frequency of extra-solar Oort clouds
[NASA-CR-196197] p 385 N95-12886

COMETS
Gamma-ray burst constraints on the galactic frequency of extra-solar Oort clouds
[NASA-CR-196197] p 385 N95-12886

COMMAND AND CONTROL
Exploitation of virtual reality architectures
[AD-A282263] p 340 N95-12413
Lessons learned from experiments conducted on radar data management systems
[AD-A282896] p 284 N95-12920

COMMERCIAL AIRCRAFT
The performance of child restraint devices in transport airplane passenger seats
[DOT/FAA/AM-94/19] p 234 N95-12146
The FC-1D: The profitable alternative Flying Circus Commercial Aviation Group
[NASA-CR-197152] p 240 N95-12628
Central coast designs: The Eightball Express. Taking off with convention, cruising with improvements and landing with absolute success
[NASA-CR-197181] p 241 N95-12643
LCX: Proposal for a low-cost commercial transport
[NASA-CR-197186] p 241 N95-12645

COMMUNICATING
Shifting our focus: Communicating science to a new, nontechnical culture
[DE94-014258] p 378 N95-13123

COMMUNICATION CABLES
Part A: A data acquisition/controller system. Part B: Supplement to a data acquisition/controller system
[AD-A283373] p 285 N95-12924

COMMUNICATION EQUIPMENT
Project ECHO: Electronic Communications from Halo Orbit
[NASA-CR-197190] p 283 N95-12644

COMMUNICATION NETWORKS
Systems engineering technology for networks
[NASA-CR-196853] p 280 N95-11804
Buffer size and switching capacity study in packet switches of broadband ISDN
[PB94-179421] p 281 N95-12368
Modeling and implementation of a packet routing switch for satellite communications
[AD-A282262] p 282 N95-12412
Information Technology Division's technical paper abstracts
[AD-A282882] p 378 N95-12916

COMMUNICATION SATELLITES
Advanced S-Band studies using the TDRSS communications satellite
[NASA-CR-196931] p 281 N95-12010
Preliminary digital control system design for the petite amateur Navy satellite (PANSAT)
[AD-A282804] p 253 N95-12528
Lifetime and reentry prediction for the Petite Amateur Navy Satellite (PANSAT)
[AD-A283366] p 255 N95-12921

COMMUNICATION THEORY
Stochastic control and nonlinear estimation
[AD-A281219] p 350 N95-13369

COMPACTING
Equipment for investigation of cryogenic compaction of nanosize silicon nitride powders
[DE94-013593] p 277 N95-13530

COMPANION STARS
Research in astrophysical processes
[NASA-CR-196773] p 382 N95-12939

COMPARATORS
5-volt low level serial transceiver
[AD-D016399] p 288 N95-13153

COMPARISON
EG and G and NASA face seal codes comparison
p 305 N95-13590

COMPARTMENTS
Laws of infrared similitude
[AD-A282209] p 354 N95-12426

COMPATIBILITY
Integrated sensor bus
[PB94-206810] p 288 N95-13252

COMPENSATORS
Development of homotopy algorithms for fixed-order mixed H2/H(infinity) controller synthesis
[NASA-TP-3507] p 342 N95-11923
Annular suspension and pointing system with controlled DC electromagnets
[NASA-CR-197206] p 302 N95-12666

COMPILERS
Exploring the parallelism exposed by partial evaluation
[AD-A282284] p 347 N95-12414
A framework for exploiting data and functional parallelism on distributed memory multicomputers
[AD-A281194] p 347 N95-12523

COMPLEX COMPOUNDS
Novel activated carbon impregnants consisting of transition metal complexes. Part 1: Background, syntheses and characterizations
[AD-A282583] p 259 N95-12551
One-step synthesis of dithiocarbamates from metal powders
[NASA-TM-106558] p 260 N95-12692

COMPLEX SYSTEMS
Proceedings: The Eleventh IEEE Workshop on Real-Time Operating Systems and Software
[AD-A281738] p 342 N95-11843
Using emergent order to shape a space society
p 377 N95-11959
Laws of infrared similitude
[AD-A282209] p 354 N95-12426

COMPONENT RELIABILITY
Reliability and cost analysis methods
[NASA-CR-196326] p 308 N95-12381
On-line data reconstruction in redundant disk arrays
[AD-A282709] p 340 N95-12516

COMPOSITE MATERIALS
Optimal experimental designs for the estimation of thermal properties of composite materials
[NASA-CR-196792] p 261 N95-11700
Composites (CFCCs) for low cost energy and cleaner environment
[DE94-013601] p 272 N95-11781
The synthesis and structure of polyphosphazenes
[AD-A281723] p 272 N95-11832
Test Plans. Lightweight Durable TPS: Tasks 1,2,4,5, and 6
[NASA-CR-196867] p 262 N95-11835
Ten-year ground exposure of composite materials used on the Bell Model 206L helicopter flight service program
[NASA-TP-3468] p 262 N95-12357
Enhancement of luminescence in polymer nanocomposites
[AD-A282539] p 262 N95-12404
Nanometer scale phase separation in mixed composition self-assembled monolayers
[AD-A282671] p 266 N95-12514
Diagnostic techniques for semiconductor materials processing
[AD-A282810] p 373 N95-12602
Ferric chloride graphite intercalation compounds prepared from graphite fluoride
[NASA-TM-106447] p 261 N95-12783
Computer modelling of cyclic deformation of high-temperature materials
[AD-A282457] p 263 N95-12833
Micromechanics Analysis Code (MAC). User guide: Version 1.0
[NASA-TM-106706] p 264 N95-13193

COMPOSITE PROPELLANTS
Stress relaxation functions: Methods of approximation
[NASA-CR-195830] p 312 N95-12861

COMPOSITE STRUCTURES
Elastic buckling of cylindrically curved laminated fibre reinforced composite panels with all edges simply-supported under biaxial loading
[ESDU-94007] p 310 N95-11773
Selection process for trade study: Graphite Composite Primary Structure (GCPS)
[NASA-CR-196866] p 261 N95-11803
Test Plan. GCPS Task 4, subtask 4.2 thrust structure development
[NASA-CR-196869] p 251 N95-11833
Trade study plan for Graphite Composite Primary Structure (GCPS)
[NASA-CR-196868] p 261 N95-11834
Army Research Office Workshop on Dynamic Response of Composite Structures
[AD-A281471] p 262 N95-11854
Trade study plan for Reusable Hydrogen Composite Tank System (RHCTS)
[NASA-CR-196871] p 252 N95-11945
Electromagnetic on-aircraft antenna radiation in the presence of composite plates
[NASA-CR-196126] p 284 N95-12856
Novel concepts in weld science: Role of gradients and composite structure
[DE94-015482] p 271 N95-12895

COMPOSITION (PROPERTY)
Nanometer scale phase separation in mixed composition self-assembled monolayers
[AD-A282671] p 266 N95-12514

COMPRESSIBLE BOUNDARY LAYER
Effect of nonzero surface admittance on receptivity and stability of compressible boundary layer
[NASA-CR-4621] p 292 N95-12105

COMPRESSIBLE FLOW
Performance analysis of three dimensional integral equation computations on a massively parallel computer
[NASA-CR-196747] p 346 N95-11863
Computer code for determination of thermally perfect gas properties
[NASA-TP-3447] p 231 N95-11995
Boundary conditions for unsteady compressible flows
[NASA-TM-106737] p 293 N95-12380

COMPRESSIVE STRENGTH
Triaxial and torsional shear test results for sand
[AD-A282725] p 323 N95-12506
Test methods for textile composites
[NASA-CR-4609] p 262 N95-12793

COMPRESSORS
Object-oriented technology for compressor simulation
[NASA-TM-106723] p 243 N95-11864
Compressor discharge film riding face seals
p 306 N95-13599

COMPTON EFFECT
Search for inverse Compton x-rays from the lobes of Fornax A x-rays from radio galaxies straddling the Fanaroff-Riley transition
[NASA-CR-196433] p 385 N95-13023

COMPUTATIONAL FLUID DYNAMICS
LES, DNS and RANS for the analysis of high-speed turbulent reacting flows
[NASA-CR-196822] p 289 N95-11705
Parallel aeroelastic computations for wing and wing-body configurations
[NASA-CR-196835] p 230 N95-11766
A numerical analysis of the distribution of stresses in lung parenchyma which accounts for the interactions between the tissue skeleton and flowing air
p 332 N95-11806
High frequency flow/structural interaction in dense subsonic fluids handbook
[NASA-CR-194007] p 230 N95-11807
Performance analysis of three dimensional integral equation computations on a massively parallel computer
[NASA-CR-196747] p 346 N95-11863
Object-oriented technology for compressor simulation
[NASA-TM-106723] p 243 N95-11864
Analysis and design of numerical schemes for gas dynamics 1: Artificial diffusion, upwind biasing, limiters and their effect on accuracy and multigrid convergence
[NASA-CR-196477] p 290 N95-11875
Investigation of advanced counterrotation blade configuration concepts for high speed turboprop systems. Task 8: Cooling flow/heat transfer analysis
[NASA-CR-195359] p 244 N95-11901
Research in progress in applied mathematics, numerical analysis, fluid mechanics, and computer science
[NASA-CR-194942] p 340 N95-11932
Methods of ensuring realizability for non-realizable second order closures
[NASA-TM-106681] p 291 N95-11935
An axisymmetric analog two-layer convective heating procedure with application to the evaluation of Space Shuttle Orbiter wing leading edge and windward surface heating
[NASA-CR-188343] p 251 N95-11937

Investigation of advanced counterrotation blade configuration concepts for high speed turboprop systems. Task 8: Cooling flow/heat transfer analysis user's manual
[NASA-CR-195360] p 244 N95-11951
Computational flow predictions for hypersonic drag devices p 233 N95-11967
FDNS code to predict wall heat fluxes or wall temperatures in rocket nozzles
[NASA-CR-196925] p 292 N95-11999
High speed civil transport aerodynamic optimization
[NASA-CR-196960] p 232 N95-12389
Numerical computations with ABAQUS/Explicit, DYNA3D, and DYSMAS/L
[AD-A282249] p 293 N95-12409
Supersonic base flow investigation over axisymmetric afterbodies
[PB94-180957] p 232 N95-12578
Nonlinear problems in fluid dynamics and inverse scattering: Langmuir circulations in ocean surface layers
[AD-A282934] p 329 N95-12590
Computation of turbulent boundary layers employing the defect wall-function method
[NASA-CR-4629] p 293 N95-12859
Validation of the RPLUS3D code for supersonic inlet applications involving three-dimensional shock wave-boundary layer interactions
[NASA-TM-106579] p 233 N95-13058
Numerical time dependent sheet cavitation simulations using a higher order panel method
[PB94-204435] p 294 N95-13249
Implementing a linear equation solver in the CFD code PHOENICS
[PB94-195757] p 353 N95-13439
Numerical simulations of drop collisions
[NASA-TM-106751] p 295 N95-13550
Seals Flow Code Development 1993
[NASA-CP-10136] p 304 N95-13583
Code GFACE: Gas lubricated face seals in laminar regime p 305 N95-13585
SCISEAL: A CFD code for analysis of fluid dynamic forces in seals p 305 N95-13586
Brush seal numerical simulation: Concepts and advances p 306 N95-13596
Incompressible face seals: Computer code IFACE p 307 N95-13606

COMPUTATIONAL GEOMETRY
Toolkits for construction and manipulation of geographical data
[PB94-202587] p 378 N95-13245

COMPUTATIONAL GRIDS
Workshop on Adaptive Methods for Partial Differential Equations
[AD-A281416] p 351 N95-11850
Stability and error estimation for Component Adaptive Grid methods
[NASA-CR-196492] p 351 N95-11883
The development and application of the self-adaptive grid code, SAGE p 295 N95-11957
An investigation of the vortex method
[DE94-014931] p 294 N95-13156

COMPUTER AIDED DESIGN
The potential of genetic algorithms for conceptual design of rotor systems
[NASA-CR-196813] p 237 N95-11699
Intelligent knowledge-based engineering
[AD-A281906] p 377 N95-11788
High frequency flow/structural interaction in dense subsonic fluids handbook
[NASA-CR-194007] p 230 N95-11807
The Research Laboratory of Electronics
[AD-A281445] p 386 N95-11830
Application of two procedures for dual-point design of transonic airfoils
[NASA-TP-3466] p 231 N95-12176
High speed civil transport aerodynamic optimization
[NASA-CR-196960] p 232 N95-12389
On-line data reconstruction in redundant disk arrays
[AD-A282709] p 340 N95-12516
Large area soft x-ray collimator to facilitate x-ray optics testing
[NASA-CR-196923] p 362 N95-12736
Techniques for designing rotorcraft control systems
[NASA-CR-196192] p 245 N95-12791
Computer-aided design-verification vector generation
[DE94-014022] p 345 N95-13077
Computerized design and generation of low-noise helical gears with modified surface topology
[NASA-TM-106696] p 303 N95-13083
Advances in SPARK
[DE94-014935] p 345 N95-13157
A simplified thermohydrodynamic model for fluid film bearings
[DE94-015011] p 304 N95-13183
Object recognition for flexible assembly using stereo vision
[PB94-204427] p 363 N95-13248
Seals Flow Code Development 1993
[NASA-CP-10136] p 304 N95-13583
Beta testing of MTI seal codes p 305 N95-13589
Computer tools for face seal analyses developed at John Crane p 306 N95-13598

COMPUTER AIDED MANUFACTURING
Intelligent knowledge-based engineering
[AD-A281906] p 377 N95-11788

COMPUTER AIDED MAPPING
MapView user's guide
[AD-A282469] p 316 N95-13290

COMPUTER ANIMATION
MapView user's guide
[AD-A282469] p 316 N95-13290

COMPUTER ASSISTED INSTRUCTION
High frequency flow/structural interaction in dense subsonic fluids handbook
[NASA-CR-194007] p 230 N95-11807
Guided Approach to Instructional Design Advising (GAIDA): How to create GAIDA compatible lessons, volume 2
[AD-A282645] p 343 N95-12500

COMPUTER COMPONENTS
POSIX delta document for the Next-Generation Computer Resources (NGCR) operating systems interface standard baseline, version 4
[AD-A282324] p 347 N95-12418

COMPUTER DESIGN
Design of systolic algorithms and architectures for digital signal processing
[PB94-179256] p 346 N95-11838
Active Nodal Task Seeking for high-performance, ultra-dependable computing
[AD-A282924] p 344 N95-12588
Quantum cellular automata
[AD-A283351] p 287 N95-12881

COMPUTER GRAPHICS
Exploitation of virtual reality architectures
[AD-A282263] p 340 N95-12413
A practical approach to drawing undirected graphs
[AD-A282641] p 343 N95-12541
Flight test of takeoff performance monitoring system
[NASA-TP-3403] p 245 N95-12664
Design consideration for parallel graphics libraries
[NASA-CR-194935] p 340 N95-12828
Advances in SPARK
[DE94-014935] p 345 N95-13157
Toolkits for construction and manipulation of geographical data
[PB94-202587] p 378 N95-13245

COMPUTER INFORMATION SECURITY
Using secure coprocessors
[AD-A281255] p 340 N95-12524
Information Technology Division's technical paper abstracts
[AD-A282882] p 378 N95-12916

COMPUTER NETWORKS
An empirical study of a highly available file system
[AD-A282655] p 378 N95-12502

COMPUTER PROGRAM INTEGRITY
An experimental environment for software engineering
[INPE-5540-TDI/528] p 343 N95-12300

COMPUTER PROGRAMMING
An experimental environment for software engineering
[INPE-5540-TDI/528] p 343 N95-12300
Exploitation of virtual reality architectures
[AD-A282263] p 340 N95-12413
Experiments with formal methods in software engineering
[PB94-192416] p 344 N95-12774
Population-based incremental learning. A method for integrating genetic search based function optimization and competitive learning
[AD-A282654] p 350 N95-12835
The Second Workshop on Principles and Practice of Constraint Programming
[AD-A281731] p 229 N95-13166
Norwegian contribution to the SWG on APSE programme
[PB94-202397] p 341 N95-13557

COMPUTER PROGRAMS
High performance climate system modeling using a domain and task decomposition message-passing approach
[DE94-013739] p 322 N95-11741
Pipeline vibrations. Computer program for the prediction of fluid transients in flexible, unbranched three-dimensional piping systems
[ESDU-93031] p 309 N95-11768
A numerical analysis of the distribution of stresses in lung parenchyma which accounts for the interactions between the tissue skeleton and flowing air p 332 N95-11806
Burst transmission in the HF band: A system analysis and proposal for improvement
[PB94-190733] p 280 N95-11821
Object-oriented technology for compressor simulation
[NASA-TM-106723] p 243 N95-11864
TLIFE: A program for spur, helical and spiral bevel transmission life and reliability modeling
[NASA-CR-4622] p 300 N95-11889
The development and application of the self-adaptive grid code, SAGE p 295 N95-11957
Computer code for determination of thermally perfect gas properties
[NASA-TP-3447] p 231 N95-11995
Digital image processing techniques for image-mapping applications
[INPE-5546-TDI/532] p 315 N95-12301
Numerical computations with ABAQUS/Explicit, DYNA3D, and DYSMAS/L
[AD-A282249] p 293 N95-12409
Exploitation of virtual reality architectures
[AD-A282263] p 340 N95-12413
Non-dipolar magnetic field models and patterns of radio emission: Uranus and Neptune compared
[NASA-CR-196412] p 385 N95-12469
Wideband electromagnetic scattering program. Fourier-based radar imaging techniques
[AD-A282540] p 282 N95-12493
Locally connected adaptive Gabor filter for real-time motion compensation
[AD-A282544] p 286 N95-12494
NPS state vector analysis and relative motion plotting software for STS-51
[AD-A282909] p 249 N95-12510
Site model based image registration and change detection, RADIUS
[AD-A282796] p 315 N95-12527
An implementation of a chemical and thermal nonequilibrium flow solver on unstructured meshes and application to blunt bodies
[NASA-CR-194967] p 293 N95-12619
Method of phased magnitude correlation using binary sequences
[AD-D016397] p 284 N95-12646
Flight test of takeoff performance monitoring system
[NASA-TP-3403] p 245 N95-12664
Microfabricated hydrogen sensor technology for aerospace and commercial applications
[NASA-TM-106703] p 284 N95-12674
Overview of NASREM: The NASA/NBS standard reference model for telerobot control system architecture re
[PB94-194560] p 303 N95-12854
A hitchhiker's guide to microscopy and microanalysis using telecommunications, Email and The Internet
[DE94-013299] p 285 N95-13057
Validation of the RPLUS3D code for supersonic inlet applications involving three-dimensional shock wave-boundary layer interactions
[NASA-TM-106579] p 233 N95-13058
Thermodynamic constants for actinide oxides and oxyhydroxides relevant to actinide volatility calculations for thermal oxidation processes
[DE94-007762] p 376 N95-13074
A simplified thermohydrodynamic model for fluid film bearings
[DE94-015011] p 304 N95-13183
Numerical time dependent sheet cavitation simulations using a higher order panel method
[PB94-204435] p 294 N95-13249
Delta-4: An open architecture for dependable systems
[PB94-195641] p 341 N95-13436
Implementing a linear equation solver in the CFD code PHOENICS
[PB94-195757] p 353 N95-13439
CRYOCOL: A computer program to calculate the cryogenic distillation of hydrogen isotopes
[DE94-622012] p 268 N95-13531
An informal introduction to parallel processors
[DE94-016347] p 348 N95-13556

COMPUTER SYSTEMS DESIGN
An avionics scenario and command model description for Space Generic Open Avionics Architecture (SGOAA)
[NASA-CR-188330] p 242 N95-11913
The design and development of signal-processing algorithms for an airborne x-band Doppler weather radar
[NASA-CR-196888] p 281 N95-12374
Exploitation of virtual reality architectures
[AD-A282263] p 340 N95-12413
Design consideration for parallel graphics libraries
[NASA-CR-194935] p 340 N95-12828
Overview of NASREM: The NASA/NBS standard reference model for telerobot control system architecture re
[PB94-194560] p 303 N95-12854
Analyzing terabytes of data at Fermilab
[DE94-013149] p 347 N95-13269

COMPUTER SYSTEMS PERFORMANCE
Eager combining: A coherency protocol for increasing effective network and memory bandwidth in shared-memory multiprocessors
[AD-A281501] p 346 N95-11857
A preliminary evaluation of cache-miss-initiated prefetching techniques in scalable multiprocessors
[AD-A281502] p 346 N95-11858
Performance analysis of three dimensional integral equation computations on a massively parallel computer
[NASA-CR-196747] p 346 N95-11863
Active Nodal Task Seeking for high-performance, ultra-dependable computing
[AD-A282924] p 344 N95-12588
Some very compositional temporal properties
[PB94-195666] p 345 N95-13438
COMPUTER SYSTEMS PROGRAMS
Proceedings: The Eleventh IEEE Workshop on Real-Time Operating Systems and Software
[AD-A281738] p 342 N95-11843
Development of a change management system
p 377 N95-11963
Reliability allocation for a system using Markov analysis
[PB94-205051] p 309 N95-13406
COMPUTER TECHNIQUES
Parallel methods for the flight simulation model
[DE94-013330] p 245 N95-11752
Research in progress in applied mathematics, numerical analysis, fluid mechanics, and computer science
[NASA-CR-194942] p 340 N95-11932
Space Station Module Power Management and Distribution System (SSM/PMAD)
[NASA-CR-193991] p 258 N95-12819
Computer-aided design-verification vector generation
[DE94-014022] p 345 N95-13077
Enhancement of EMAG: A 2-D electrostatic and magnetostatic solver for MATLAB
[AD-A283446] p 354 N95-13143
Scene analysis: A brief survey
[PB94-205085] p 336 N95-13433
COMPUTER VISION
Self calibrating autoTRAC
[NASA-CR-196930] p 348 N95-11998
An analysis of the effect of Gaussian error in object recognition
[AD-A282260] p 349 N95-12411
Learning one-dimensional geometric patterns under one-sided random misclassification noise
[DE94-014659] p 350 N95-12864
Representation, modeling and recognition of outdoor scenes
[AD-A283361] p 350 N95-12884
Object recognition for flexible assembly using stereo vision
[PB94-204427] p 363 N95-13248
Scene analysis: A brief survey
[PB94-205085] p 336 N95-13433
COMPUTERIZED SIMULATION
Impact analysis on a massively parallel computer
[DE94-013624] p 346 N95-11734
Parallel methods for the flight simulation model
[DE94-013330] p 245 N95-11752
TKKMOD: A computer simulation program for an integrated wind diesel system. Version 1.0: Document and user guide
[PB94-179090] p 317 N95-11798
Burst transmission in the HF band: A system analysis and proposal for improvement
[PB94-190733] p 280 N95-11821
Validation results of wind diesel simulation model TKKMOD
[PB94-179157] p 317 N95-11846
Research on Orbital Plasma-Electrodynamics (ROPE)
[NASA-CR-196929] p 361 N95-12147
Numerical computations with ABAQUS/Explicit, DYNA3D, and DYSMAS/L
[AD-A282249] p 293 N95-12409
Development of ROBOSIM for academic/industrial use
[NASA-CR-196148] p 349 N95-12470
First principles investigation of the Ir-Zr-Nb ternary system
[AD-A282644] p 270 N95-12543
Intelligent control systems research
[NASA-CR-195380] p 349 N95-12811
Computer modelling of cyclic deformation of high-temperature materials
[AD-A282457] p 263 N95-12833
Modeling of transformers using circuit simulators
[DE94-014656] p 287 N95-12863
Neotectonics of Asia: Thin-shell finite-element models with faults
[NASA-CR-196436] p 324 N95-12949
An investigation of the vortex method
[DE94-014931] p 294 N95-13156
Advances in SPARK
[DE94-014935] p 345 N95-13157
Simulating the energy performance of holographic glazings
[DE94-014969] p 296 N95-13158
Windshear certification data base for forward-look detection systems p 234 N95-13204
Certification methodology applied to the NASA experimental radar system p 235 N95-13205
Certification of windshear performance with RTCA class D radomes p 235 N95-13206
Mach number control in the High Speed Wind Tunnel of NLR
[PB94-201670] p 246 N95-13243
A musculoskeletal model of the elbow joint complex
[NASA-CR-195812] p 335 N95-13270
CRYOCOL: A computer program to calculate the cryogenic distillation of hydrogen isotopes
[DE94-622012] p 268 N95-13531
Atomic structures and compositions of internal interfaces
[DE94-013594] p 271 N95-13543
COMPUTERS
JPRS report: Science and technology. Central Eurasia
[JPRS-UST-94-017] p 247 N95-12001
Exploring the parallelism exposed by partial evaluation
[AD-A282284] p 347 N95-12414
POSIX delta document for the Next-Generation Computer Resources (NGCR) operating systems interface standard baseline, version 4
[AD-A282324] p 347 N95-12418
CONCENTRATION (COMPOSITION)
Spacecraft maximum allowable concentrations for selected airborne contaminants, volume 1
[NASA-CR-196446] p 255 N95-12879
CONCENTRATORS
Environmental lichenology: Biomonitoring trace-element air pollution
[PB94-191335] p 318 N95-11826
CONCRETES
Moisture induced pressures in concrete airfield pavements
[AD-A281974] p 245 N95-11789
The use of an acoustic emission method to estimate the effect of manufacturing process and service factors on the failure of concrete p 311 N95-12108
Marginal aggregates in flexible pavements: Background survey and experimental plan
[DOT/FAA/CT-94/58] p 246 N95-12216
CONCURRENT ENGINEERING
Intelligent knowledge-based engineering
[AD-A281906] p 377 N95-11788
Integrated design and manufacturing for the high speed civil transport
[NASA-CR-197183] p 241 N95-12700
The Second Workshop on Principles and Practice of Constraint Programming
[AD-A281731] p 229 N95-13166
CONCURRENT PROCESSING
Efficient detection of deadlocks in Petri nets
[PB94-179405] p 343 N95-12366
Recovery blocks
[PB94-205077] p 345 N95-13432
Some very compositional temporal properties
[PB94-195666] p 345 N95-13438
CONDENSATION
Hydrolysis and condensation of tin (4) alkoxide compounds: The control of structural evolution
[AD-A282789] p 267 N95-12807
CONDUCTING POLYMERS
Tuning through the critical regime of the metal-insulator-transition in conducting polymers by pressure and magnetic field
[PB94-179165] p 272 N95-11847
CONDUCTIVE HEAT TRANSFER
Determination of a transient heat transfer property of acrylic using thermochromic liquid crystals
[NASA-TM-106541] p 372 N95-11882
User's manual for the NASA Lewis ice accretion/heat transfer prediction code with electrothermal deicer input
[NASA-CR-4530] p 291 N95-11888
Implementing a linear equation solver in the CFD code PHOENICS
[PB94-195757] p 353 N95-13439
Time-resolved electron thermal conduction by probing of plasma formation in transparent solids with high power subpicosecond laser pulses
[DE94-015170] p 370 N95-13555
CONFERENCES
Abstracts from the International Conference on Nuclear Analytical Methods in the Life Sciences
[DE94-621923] p 329 N95-11728
Beams 92: Proceedings
[DE94-014783] p 361 N95-11792
Proceedings: The Eleventh IEEE Workshop on Real-Time Operating Systems and Software
[AD-A281738] p 342 N95-11843
NASA STI Program Seminar: Electronic documents
[NASA-TM-109928] p 378 N95-12383
Physics of High Energy Density Plasmas Produced by Pulsed Power
[NIFS-PROC-18] p 365 N95-12429
Modeling of split-core transformers for power transmission
[AD-A282782] p 287 N95-12509
Dynamical systems and oceanography
[AD-A282635] p 329 N95-12540
Summary of the Sixteenth Annual Conference on Shock
[AD-A282643] p 334 N95-12542
Proceedings of Bianisotropics 1993: Seminar on Electrodynamics of Chiral and Bianisotropic Media
[PB94-179314] p 283 N95-12595
Diagnostic techniques for semiconductor materials processing
[AD-A282610] p 373 N95-12602
Proceedings of US-Latin American Workshop on Molecular and Materials Sciences: Theoretical and Computational Aspects
[AD-A283359] p 358 N95-12882
Symposium on Structural Intermetallics: Perspectives on Science and Technology, volume 1
[AD-A283378] p 271 N95-12925
Proceedings of the CTU Seminar 1994, Part C
[DE94-624078] p 390 N95-12946
WOCSDICE 1994: European Workshop on Compound Semiconductor Devices and Integrated Circuits
[AD-A283062] p 288 N95-13052
Proceedings of the Eighteenth DOE Solar Photochemistry Research Conference
[DE94-014926] p 318 N95-13126
US-Latin American Workshop on Molecular and Materials Sciences: Theoretical and Computational Aspects
[AD-A283428] p 359 N95-13141
Proceedings of the 36th Power Sources Conference
[AD-A281443] p 288 N95-13164
Effects of Noise on Hearing 5th International Symposium
[AD-A281439] p 335 N95-13177
Summaries of papers presented at the High Resolution Spectroscopy Topical Meeting. Technical digest series. Volume 1: Post conference edition
[AD-A281261] p 268 N95-13372
CONFIDENCE LIMITS
En route noise levels from propfan test assessment airplane
[NASA-TP-3451] p 355 N95-12341
A search for a heavy neutral gauge boson decaying into dielectrons in (-p)p collisions at the square root of s = 1.8 TeV
[DE94-014987] p 359 N95-13161
CONFIGURATION MANAGEMENT
Development of a change management system
p 377 N95-11963
Development of ROBOSIM for academic/industrial use
[NASA-CR-196148] p 349 N95-12470
CONGRESSIONAL REPORTS
Implementation strategy for the Clean Air Act Ammendments of 1990. Update, May 1994
[PB94-180700] p 319 N95-11849
Present state of knowledge of the upper atmosphere1993: An assessment report, part 2
[NASA-RP-1337] p 322 N95-12103
Space Shuttle: NASA's plans for repairing or replacing a damaged or destroyed orbiter. Report to the Chairman, Subcommittee on Investigations and Oversight, Committee on Science, Space, and Technology, House of Representatives
[GAO/NSIAD-94-197] p 249 N95-12851
CONJUGATE GRADIENT METHOD
Prediction of geometric-thermal machine tool errors by artificial neural networks
[PB94-186873] p 348 N95-11909
Parallel preconditioners for the conjugate gradient method
[PB94-201605] p 347 N95-13404
Implementing a linear equation solver in the CFD code PHOENICS
[PB94-195757] p 353 N95-13439
CONJUGATION
Electronic energy transfer in new polymer nanocomposite assemblies
[AD-A282233] p 274 N95-12407
Design, synthesis and characterization of novel nonlinear optical polymers
[AD-A282201] p 274 N95-12424

CONNECTION MACHINE
Performance analysis of three dimensional integral equation computations on a massively parallel computer
[NASA-CR-196420] p 346 N95-11863
CONSECUTIVE EVENTS
An investigation of the use of temporal decomposition in space mission scheduling
[NASA-CR-196420] p 377 N95-12618
CONSERVATION LAWS
Relativistic theory of superfluidity with two condensates
[DE94-624073] p 290 N95-11749
Mass conservation in grain growth
[DE94-014456] p 374 N95-13086
CONSTRAINTS
The performance of child restraint devices in transport airplane passenger seats
[DOT/FAA/AM-94/19] p 234 N95-12146
M.E.366-J embodiment design project: Portable foot restraint
[NASA-CR-197163] p 338 N95-12361
The Second Workshop on Principles and Practice of Constraint Programming
[AD-A281731] p 229 N95-13166
CONSTRICTIONS
Anode sheath contributions in plasma thrusters
[AD-A280395] p 364 N95-11837
CONSTRUCTION
Design and construction of the astronautics refrigerator magnet
[DE94-013599] p 353 N95-11731
Development of nanostructure fabrication technology and new electron-quantum wave devices
[AD-A281724] p 286 N95-11860
Toward infrastructure improvement: An agenda for research
[LC-94-67335] p 376 N95-12385
A lunar/Martian anchor emplacement system
[NASA-CR-197193] p 302 N95-12690
Approximation of scattered data using smooth grid functions
[PB94-207016] p 353 N95-13573
CONTACTORS
Status of hollow cathode heater development for the Space Station plasma contactor
[NASA-CR-195364] p 258 N95-12622
CONTAINERLESS MELTS
Ground based research in microgravity materials processing
[NASA-CR-196815] p 278 N95-11759
CONTAMINANTS
Triple sorbent thermal desorption/gas chromatography/mass spectrometry determination of vapor phase organic contaminants
[DE94-013634] p 264 N95-11735
Supercritical fluid (SCF) technologies: Assessment of applicability to installation restoration processes
[AD-A281504] p 290 N95-11859
Spacecraft maximum allowable concentrations for selected airborne contaminants, volume 1
[NASA-CR-196446] p 255 N95-12879
CONTAMINATION
Effect of operating parameters and anode gas impurities upon polymer electrolyte fuel cells
[DE94-014464] p 317 N95-12650
Analysis for Be-7 and Be-10 on LDEF materials and their sources
[NASA-CR-193989] p 268 N95-13084
CONTINGENCY
Tactical satellite orbital simulation and requirements study
[AD-A282314] p 282 N95-12416
CONTINUOUS RADIATION
Two-tone test method for determining frequency-domain transfer functions
[AD-A283452] p 282 N95-12513
CONTINUOUS WAVE LASERS
Spaceborne Photonics Institute
[NASA-CR-196784] p 362 N95-12659
Method of laser processing ferroelectric materials
[AD-D016386] p 298 N95-12780
CONTRACTION
Contraction phase of a gas-puff z-pinch
p 366 N95-12440
CONTRACTORS
Proceedings of the Eighteenth DOE Solar Photochemistry Research Conference
[DE94-014926] p 318 N95-13126
CONTROL BOARDS
Introduction to magnetic bearings
[NASA-CR-197187] p 302 N95-12640
CONTROL SIMULATION
Piloted evaluation of an integrated methodology for propulsion and airframe control design
[NASA-TM-106741] p 245 N95-12763
CONTROL STABILITY
Robust control design with real parameter uncertainty using absolute stability theory
[NASA-CR-196971] p 349 N95-12782
CONTROL SYSTEMS DESIGN
Effects of mass on aircraft sidearm controller characteristics
[NASA-TM-104277] p 244 N95-11868
Development of homotopy algorithms for fixed-order mixed H2/H(infinity) controller synthesis
[NASA-TP-3507] p 342 N95-11923
Actuability of underactuated manipulators
[AD-A282788] p 300 N95-12526
Preliminary digital control system design for the petite amateur Navy satellite (PANSAT)
[AD-A282804] p 253 N95-12528
Design of a ZVS PWM inverter for a brushless DC motor in an EMA application
[NASA-CR-195808] p 312 N95-12620
Cabin fuselage structural design with engine installation and control system
[NASA-CR-197173] p 240 N95-12639
Piloted evaluation of an integrated methodology for propulsion and airframe control design
[NASA-TM-106741] p 245 N95-12763
Precision tethered satellite attitude control
[NASA-CR-196650] p 254 N95-12766
Robust control design with real parameter uncertainty using absolute stability theory
[NASA-CR-196971] p 349 N95-12782
Techniques for designing rotorcraft control systems
[NASA-CR-196192] p 245 N95-12791
Intelligent control systems research
[NASA-CR-195380] p 349 N95-12811
Hypersonic vehicle model and control law development using H(infinity) and micron synthesis
[NASA-TM-4562] p 255 N95-12838
Overview of NASREM: The NASA/NBS standard reference model for telerobot control system architecture re
[PB94-184560] p 303 N95-12854
Modular hydraulic control system
[AD-D016401] p 304 N95-13155
CONTROL THEORY
An interpolation theoretic approach to control
[AD-A281465] p 348 N95-11853
Optimum aerodynamic design via boundary control
[NASA-CR-195882] p 230 N95-11877
Control theory based airfoil design using the Euler equations
[NASA-CR-196360] p 230 N95-11884
Development of homotopy algorithms for fixed-order mixed H2/H(infinity) controller synthesis
[NASA-TP-3507] p 342 N95-11923
Robust control design with real parameter uncertainty using absolute stability theory
[NASA-CR-196971] p 349 N95-12782
Stochastic control and nonlinear estimation
[AD-A281219] p 350 N95-13369
CONTROLLABILITY
Techniques for designing rotorcraft control systems
[NASA-CR-196192] p 245 N95-12791
Duplex rolling element bearing mounting for ensuring preload control
[AD-D016402] p 304 N95-13189
CONTROLLED ATMOSPHERES
Methodologies for processing plant material into acceptable food on a small scale
[NASA-CR-177647] p 338 N95-12132
CONTROLLERS
Effects of mass on aircraft sidearm controller characteristics
[NASA-TM-104277] p 244 N95-11868
Scheduling in an input and output queuing three-stage packet switch by using neural networks
[PB94-179413] p 349 N95-12367
Robust control of underactuated manipulators: Analysis and implementation
[AD-A282836] p 301 N95-12587
Active vibration control using a distributed controller
[PB94-207073] p 313 N95-13576
CONVECTION-DIFFUSION EQUATION
Convective flow effects on protein crystal growth
[NASA-CR-196790] p 372 N95-11921
CONVECTIVE FLOW
Analysis and design of numerical schemes for gas dynamics. 2: Artificial diffusion and discrete shock structure
[NASA-CR-196476] p 290 N95-11874
Analysis and design of numerical schemes for gas dynamics 1: Artificial diffusion, upwind biasing, limiters and their effect on accuracy and multigrid convergence
[NASA-CR-196477] p 290 N95-11875
Convective flow effects on protein crystal growth
[NASA-CR-196790] p 372 N95-11921
CONVECTIVE HEAT TRANSFER
An axisymmetric analog two-layer convective heating procedure with application to the evaluation of Space Shuttle Orbiter wing leading edge and windward surface heating
[NASA-CR-188343] p 251 N95-11937
CONVERGENCE
Loads for pulsed power cylindrical implosion experiments
[DE94-014429] p 299 N95-13080
Parallel preconditioners for the conjugate gradient method
[PB94-201605] p 347 N95-13404
CONVERSION
Federal metric progress in 1993
[PB94-196029] p 279 N95-11907
COOLING SYSTEMS
Heat transfer additives for adsorption cooling system fluids, phase 2
[PB94-187135] p 290 N95-11840
The embodiment design of the heat rejection system for the portable life support system
[NASA-CR-197178] p 338 N95-12555
Visible/infrared radiometric calibration station
[DE94-014459] p 383 N95-13106
Description of a high temperature quenching furnace for the study of the directional solidification of nickel-base superalloys
[DE94-013812] p 271 N95-13544
COORDINATES
Essential kinematics for autonomous vehicles
[AD-A282456] p 300 N95-12394
COPOLYMERIZATION
Chiral recognition in molecular and macromolecular pairs of (S)- and (R)-1-cyano-2-methylpropyl 4'(4-(8-vinyloxyoctyloxy)benzoyl) biphenyl-4-carboxylate enantiomers
[AD-A281438] p 356 N95-11828
COPOLYMERS
Chiral recognition in molecular and macromolecular pairs of (S)- and (R)-1-cyano-2-methylpropyl 4'(4-(8-vinyloxyoctyloxy)benzoyl) biphenyl-4-carboxylate enantiomers
[AD-A281438] p 356 N95-11828
Enhancement of luminescence in polymer nanocomposites
[AD-A282539] p 262 N95-12404
COPPER
Copper metabolism in rats fed ascorbic acid or restricted amounts of copper
[PB94-191343] p 330 N95-11902
Atomic scale dynamics of a two-dimensional gas-solid interface
[AD-A282646] p 358 N95-12617
Large-displacement structural durability analyses of simple bend specimen emulating rocket nozzle liners
[NASA-TM-106521] p 312 N95-12818
Polycrystal models to fit experiments
[DE94-014419] p 374 N95-13078
Electrochemical deposition of metal nano-disk structures using the scanning tunneling microscope
[AD-A282464] p 268 N95-13288
COPPER ALLOYS
Atomic structures and compositions of internal interfaces
[DE94-013594] p 271 N95-13543
COPPER OXIDES
Measurement of synchrotron radiation transmission of infrared range by YBa2Cu3O(7-delta) film in superconducting state
[DE94-623270] p 372 N95-11899
COPPER SELENIDES
Room-temperature synthesis of CuInQ2 (Q = S or Se) in non-aqueous solution using an organoindium reagent
[NASA-TM-106557] p 260 N95-12662
COPYRIGHTS
Intellectual property rights at the National Aeronautics and Space Administration, Lewis Research Center
[NASA-TM-106731] p 379 N95-11866
Parallel preconditioners for the conjugate gradient method
[PB94-201605] p 347 N95-13404
CORONAL LOOPS
FNAS UAH UVSP and complimentary data analysis and modeling
[NASA-CR-194005] p 381 N95-12992
CORROSION
Composites (CFCCs) for low cost energy and cleaner environment
[DE94-013601] p 272 N95-11781
CORROSION PREVENTION
Accelerated testing of coatings for protection against atmospheric corrosion
[PB94-202579] p 276 N95-13244

CORROSION TESTS
Accelerated testing of coatings for protection against atmospheric corrosion
[PB94-202579] p 276 N95-13244
COSMIC DUST
UV extinction and IR emission in diffuse H2 regions
[NASA-CR-196939] p 323 N95-12244
COSMIC RAYS
Basic mechanisms of radiation effects in the natural space radiation environment
[DE94-013445] p 384 N95-11757
COST ANALYSIS
Reliability and cost analysis methods
[NASA-CR-196326] p 308 N95-12381
Analysis of cost: Combustion flame CVD diamond deposition
[AD-A282527] p 273 N95-12403
Athena: Advanced air launched space booster
[NASA-CR-197148] p 258 N95-12604
COST REDUCTION
Design of a high capacity long range cargo aircraft
[NASA-CR-197176] p 239 N95-12363
Space facilities: Meeting future needs for research, development, and operations
[NASA-CR-194821] p 248 N95-12474
Central coast designs: The Eightball Express. Taking off with convention, cruising with improvements and landing with absolute success
[NASA-CR-197181] p 241 N95-12643
COSTS
Conceptual design of an Orbital Debris Defense System
[NASA-CR-197211] p 254 N95-12696
Ceramic manufacturing: Optimizing a multivariable system
[DE94-015016] p 276 N95-13184
Parallel preconditioners for the conjugate gradient method
[PB94-201605] p 347 N95-13404
COUETTE FLOW
Nonlinear problems in fluid dynamics and inverse scattering: Langmuir circulations in ocean surface layers
[AD-A282934] p 329 N95-12590
COULOMB COLLISIONS
Magnetospheric space plasma investigations
[NASA-CR-196793] p 382 N95-12940
Study of the nuclear-coulomb low-energy scattering parameters on the basis of the p-matrix approach
[DE94-622811] p 360 N95-13275
COUPLED MODES
Locked modes in TEXT-U tokamak
[DE94-011595] p 370 N95-13529
COVARIANCE
Study of adaptive high resolution frequency estimation techniques with hydroacoustical applications
[PB94-179512] p 355 N95-12597
CRACK INITIATION
The role of crack formation in chevron-notched four-point bend specimens
[NASA-TM-106631] p 310 N95-11865
A study of naturally initiating notch root fatigue cracks under spectrum loading
[NAL-PD-SN-9405] p 311 N95-11924
Computer modeling the fatigue crack growth rate behavior of metals in corrosive environments
[NASA-CR-194982] p 269 N95-11933
CRACK PROPAGATION
A stochastic model of fatigue crack growth
p 309 N95-11698
Micromorphology, mineralogy, and genesis of soils and fracture fills and the Pajarito Plateau, New Mexico
[DE94-013612] p 322 N95-11732
Revealing hidden defects: A hybrid evaluation strategy for steel structures
[PB94-191236] p 308 N95-11822
The role of crack formation in chevron-notched four-point bend specimens
[NASA-TM-106631] p 310 N95-11865
A study of fatigue crack growth in lugs under spectrum loading
[NAL-PD-SN-9407] p 311 N95-11879
A study of naturally initiating notch root fatigue cracks under spectrum loading
[NAL-PD-SN-9406] p 311 N95-11924
Computer modeling the fatigue crack growth rate behavior of metals in corrosive environments
[NASA-CR-194982] p 269 N95-11933
Effect of shear lips, loading transitions and test frequency on constant delta K and constant load amplitude fatigue tests
[PB94-192440] p 312 N95-12775
Novel concepts in weld science: Role of gradients and composite structure
[DE94-015482] p 271 N95-12895
CRACK TIPS
Effect of shear lips, loading transitions and test frequency on constant delta K and constant load amplitude fatigue tests
[PB94-192440] p 312 N95-12775
CRACKING (FRACTURING)
A study of fatigue crack growth in lugs under spectrum loading
[NAL-PD-SN-9407] p 311 N95-11879
A study of naturally initiating notch root fatigue cracks under spectrum loading
[NAL-PD-SN-9406] p 311 N95-11924
Fatigue in single crystal nickel superalloys
[AD-A283459] p 270 N95-12546
Effect of shear lips, loading transitions and test frequency on constant delta K and constant load amplitude fatigue tests
[PB94-192440] p 312 N95-12775
CRACKS
Revealing hidden defects: A hybrid evaluation strategy for steel structures
[PB94-191236] p 308 N95-11822
CRASHWORTHINESS
Triton 2 (1B)
[NASA-CR-197188] p 240 N95-12636
CRAY COMPUTERS
Performance analysis of three dimensional integral equation computations on a massively parallel computer
[NASA-CR-196747] p 346 N95-11863
CREEP ANALYSIS
Novel concepts in weld science: Role of gradients and composite structure
[DE94-015482] p 271 N95-12895
CREEP PROPERTIES
Micromechanics Analysis Code (MAC). User guide: Version 1.0
[NASA-TM-106706] p 264 N95-13193
Numerical simulations of creep in ductile-phase toughened intermetallic matrix composites
[DE94-014744] p 264 N95-13533
CREEP RUPTURE STRENGTH
Tensile creep and stress-rupture behavior of polymer derived SiC fibers
[NASA-TM-106692] p 263 N95-12813
CREEP STRENGTH
Tensile creep and stress-rupture behavior of polymer derived SiC fibers
[NASA-TM-106692] p 263 N95-12813
CREEP TESTS
Tensile creep and stress-rupture behavior of polymer derived SiC fibers
[NASA-TM-106692] p 263 N95-12813
Numerical simulations of creep in ductile-phase toughened intermetallic matrix composites
[DE94-014744] p 264 N95-13533
CREW PROCEDURES (INFLIGHT)
Age 60 study. Part 4: Experimental evaluation of pilot performance
[REPT-8025-4B] p 336 N95-13199
CREWS
Tank crew performance related to cognitive ability and motivation of the tank crew members
[PB94-190642] p 335 N95-11872
CRITICAL FLOW
High frequency flow/structural interaction in dense subsonic fluids handbook
[NASA-CR-194007] p 230 N95-11807
CRITICAL POINT
Vapour pressures and critical points of liquids. Polycyclic phenyl and cyclohexyl compounds
[ESDU-94001] p 266 N95-12128
Orthobaric densities and molar volumes of liquids. Polycyclic phenyl and cyclohexyl compounds
[ESDU-94002] p 266 N95-12129
CRITICAL TEMPERATURE
Vapour pressures and critical points of liquids. Polycyclic phenyl and cyclohexyl compounds
[ESDU-94001] p 266 N95-12128
CROP GROWTH
Growth of potatoes for CELSS
[NASA-CR-177646] p 338 N95-11949
The crop growth research chamber
p 248 N95-11969
CROSS CORRELATION
Investigation of spectral-based techniques for classification of wideband transient signals in additive white Gaussian noise
[AD-A282954] p 283 N95-12592
CROSS FLOW
Modeling jets in cross flow
[NASA-CR-194965] p 291 N95-11930
CROSSLINKING
Rational design, construction, and processing of high-performance nonlinear, optical materials
[AD-A281283] p 363 N95-13374
CROSSTALK
An investigation of the channel crosstalk in optical heterodyne controlled phased array radars
[AD-A281227] p 285 N95-13371
CRUSTS
Neotectonics of Asia: Thin-shell finite-element models with faults
[NASA-CR-196436] p 324 N95-12949
CRYOGENIC FLUID STORAGE
STS propellant densification feasibility study data book
[NASA-TM-108467] p 278 N95-12857
Cryogenic On-Orbit Liquid Depot Storage, Acquisition, and Transfer satellite (COLD-SAT) feasibility study
[NASA-CR-185247] p 256 N95-13232
Feasibility study for a Cryogenic On-Orbit Liquid Depot-Storage, Acquisition and Transfer (COLD-SAT) satellite
[NASA-CR-185248] p 294 N95-13233
Feasibility study for the Cryogenic Orbital Nitrogen Experiment (CONE)
[NASA-CR-187231] p 294 N95-13234
CRYOGENIC ROCKET PROPELLANTS
Test plan. Task 5, subtask 5.2: Early on-orbit TPSdebris impact tests
[NASA-CR-196873] p 251 N95-11802
Advanced cryogenic propellants
[AD-A282451] p 277 N95-12729
CRYOGENICS
Feasibility study for the Cryogenic Orbital Nitrogen Experiment (CONE)
[NASA-CR-187231] p 294 N95-13234
Equipment for investigation of cryogenic compaction of nanosize silicon nitride powders
[DE94-013593] p 277 N95-13530
CRYOCOL: A computer program to calculate the cryogenic distillation of hydrogen isotopes
[DE94-622012] p 268 N95-13531
Brush seals for cryogenic applications
p 305 N95-13592
CRYPTOGRAPHY
Using secure coprocessors
[AD-A281255] p 340 N95-12524
CRYSTAL DEFECTS
Protein crystal growth in low gravity
[NASA-CR-196980] p 279 N95-13202
CRYSTAL GROWTH
Optical analysis of crystal growth
[NASA-CR-196514] p 373 N95-12386
CGF cartridge development, volume 1
[NASA-CR-196508] p 270 N95-12630
Substrate temperature control apparatus and technique for CVD reactors
[AD-D016387] p 374 N95-13150
CRYSTAL STRUCTURE
The magnetic structure of holmium-erbium superlattices
[DE94-013728] p 371 N95-11739
Atomic structure modifications of diamond-like nanocomposite films: Observation by Raman spectroscopy, FTIR and STM
[DE94-013732] p 371 N95-11740
Naval research reviews, volume 46, February 1994
[AD-A281435] p 265 N95-11827
Convective flow effects on protein crystal growth
[NASA-CR-196790] p 372 N95-11921
Fatigue in single crystal nickel superalloys
[AD-A283459] p 270 N95-12546
Synthesis and decomposition of a novel carboxylate precursor to indium oxide
[NASA-TM-106555] p 260 N95-12693
Substrate temperature control apparatus and technique for CVD reactors
[AD-D016387] p 374 N95-13150
Silicon carbide and sicaln heterojunction bipolar transistor structures
[AD-D016403] p 288 N95-13181
Raman structural studies of the nickel electrode
[NASA-CR-196331] p 289 N95-13344
CRYSTALLINITY
Chiral recognition in molecular and macromolecular pairs of (S)- and (R)-1-cyano-2-methylpropyl 4'(4-(8-vinyloxyoctyloxy)benzoyl) biphenyl-4-carboxylate enantiomers
[AD-A281438] p 356 N95-11828
Method of laser processing ferroelectric materials
[AD-D016386] p 298 N95-12780
CRYSTALLIZATION
Convective flow effects on protein crystal growth
[NASA-CR-196790] p 372 N95-11921
Radiation amorphization of materials
[DE94-624184] p 374 N95-12948
Fractional suspension crystallization of organic compounds
[PB94-206851] p 375 N95-13409

CRYSTALLOGRAPHY
Optical and magnetic resonance investigations of 3D ions in single crystal hosts: Candidates for tunable solid-state lasers
[AD-A281726] p 371 N95-11842
CRYSTALS
Radiation amorphization of materials
[DE94-624184] p 374 N95-12948
Fractional suspension crystallization of organic compounds
[PB94-206851] p 375 N95-13409
CUES
Outdoor landmark recognition using hybrid fractal vision system and neural networks
[AD-A282506] p 349 N95-12395
CULTURE TECHNIQUES
Morphological differentiation of colon carcinoma cell lines in rotating wall vessels
[NASA-CR-196780] p 333 N95-11808
CUMULATIVE DAMAGE
Analytical and experimental vibration analysis of a faulty gear system
[NASA-TM-106689] p 300 N95-12377
CURING
Phosphazene-containing amine as curing agent for phthalonitrile-base polymer
[AD-D016375] p 276 N95-13179
CURRENT DENSITY
Fusion programs in applied plasma physics
[DE94-015853] p 369 N95-12944
CURRENT SHEETS
Research on Orbital Plasma-Electrodynamics (ROPE)
[NASA-CR-196929] p 361 N95-12147
Structure and dynamics of the solar corona
[NASA-CR-196978] p 384 N95-13582
CURVATURE
Elastic buckling of cylindrically curved laminated fibre reinforced composite panels with all edges simply-supported under biaxial loading
[ESDU-94007] p 310 N95-11773
CURVE FITTING
Strain gage selection in loads equations using a genetic algorithm
[NASA-CR-4597] p 242 N95-12831
CURVED PANELS
Numerical computations with ABAQUS/Explicit, DYNA3D, and DYSMAS/L
[AD-A282249] p 293 N95-12409
CURVES (GEOMETRY)
The differential geodesy of the spherical representation
[AD-A282212] p 315 N95-12428
CUTTERS
Prediction of geometric-thermal machine tool errors by artificial neural networks
[PB94-186673] p 348 N95-11909
CYANOGEN
Progress on resonance ionization detection of combustion radicals
[DE94-015339] p 267 N95-12762
CYCLES
Provoking and measuring cell losses in ATM systems by importance sampling, control variables and load cycles
[PB94-202520] p 285 N95-13558
CYCLIC HYDROCARBONS
Orthobaric densities and molar volumes of liquids. Polycyclic phenyl and cyclohexyl compounds
[ESDU-94002] p 266 N95-12129
CYCLIC LOADS
A study of fatigue crack growth in lugs under spectrum loading
[NAL-PD-SN-9407] p 311 N95-11879
A study of naturally initiating notch root fatigue cracks under spectrum loading
[NAL-PD-SN-9406] p 311 N95-11924
Computer modelling of cyclic deformation of high-temperature materials
[AD-A282457] p 263 N95-12833
CYCLOGENESIS
Dynamical studies in hurricane intensity change
[AD-A282406] p 326 N95-12392
CYCLOHEXANE
Vapour pressures and critical points of liquids. Polycyclic phenyl and cyclohexyl compounds
[ESDU-94001] p 266 N95-12128
CYCLONES
Tropical cyclone development and intensification under moderate to strong vertical wind shear
[AD-A282185] p 326 N95-12423
CYCLOTRON RADIATION
Studies of electromagnetic ion cyclotron waves using AMPTE/CCE and dynamics explorer
[NASA-CR-196437] p 361 N95-12102
Helical temperature perturbations associated with tearing modes in tokamak plasmas
[DE94-014706] p 369 N95-12867
CYLINDRICAL ANTENNAS
Analysis of cylindrical wrap-around and doubly conformal patch antennas by way of the finite element-artificial absorber method
[NASA-CR-195211] p 281 N95-12382
CYLINDRICAL BODIES
Fabrication of large area Si cylindrical drift detectors
[DE94-013534] p 295 N95-11780
Numerical computations with ABAQUS/Explicit, DYNA3D, and DYSMAS/L
[AD-A282249] p 293 N95-12409
An implementation of a chemical and thermal nonequilibrium flow solver on unstructured meshes and application to blunt bodies
[NASA-CR-194967] p 293 N95-12619
Loads for pulsed power cylindrical implosion experiments
[DE94-014429] p 299 N95-13080
CYLINDRICAL COORDINATES
Enhancement of EMAG: A 2-D electrostatic and magnetostatic solver for MATLAB
[AD-A283446] p 354 N95-13143
CYLINDRICAL SHELLS
Interlaminar stress analysis of dropped-ply laminated plates and shells by a mixed method
[NASA-CR-196851] p 311 N95-11946
CYTOLOGY
Morphological differentiation of colon carcinoma cell lines in rotating wall vessels
[NASA-CR-196780] p 333 N95-11808

D

DAMAGE
Test plan. Task 5, subtask 5.2: Early on-orbit TPSdebris impact tests
[NASA-CR-196873] p 251 N95-11802
VAMAS round robin on fractography of ceramics. Swedish results
[PB94-180155] p 275 N95-12600
DAMAGE ASSESSMENT
Moisture induced pressures in concrete airfield pavements
[AD-A281974] p 245 N95-11789
Debris/ice/TPS assessment and integrated photographic analysis of Shuttle Mission STS-65
[NASA-TM-109205] p 249 N95-12224
Ultrashort laser pulse effects in ocular and related media: Laser-induced shock wave propagation and retinal damage
[AD-A282599] p 334 N95-12535
Mean importance measures for groups of events in fault trees
[DE94-015416] p 353 N95-13061
DAMPING
Design of passive piezoelectric damping for space structures
[NASA-CR-4625] p 252 N95-12165
The effect of passive damping on feedback control performance of flexible manipulators
[DE94-015000] p 304 N95-13182
Effect of stochastic damping resonance wave packet on energetic alpha particle transport
[DE94-625041] p 370 N95-13538
DATA ACQUISITION
Data acquisition system of the NANOSAW-2 stand alone wind diesel plant. Document and user's guide
[PB94-179108] p 317 N95-11799
Proposal of a methodology to evaluate urban quality of life using conventional and remote sensing data, geographic information system, and a database
[INPE-5552-TDI/536] p 315 N95-12297
Biomedical imaging
[AD-A282221] p 333 N95-12405
Part A: A data acquisition/controller system. Part B: Supplement to a data acquisition/controller system
[AD-A283373] p 285 N95-12924
DATA BASE MANAGEMENT SYSTEMS
New York bight study. Report 4: Geographic information systems and relational database management system development
[AD-A281716] p 327 N95-11787
Design of an intelligent support system for scientific databases
[AD-A283043] p 378 N95-12995
DATA BASES
Impact analysis on a massively parallel computer
[DE94-013624] p 346 N95-11734
New York bight study. Report 4: Geographic information systems and relational database management system development
[AD-A281716] p 327 N95-11787
Intelligent knowledge-based engineering
[AD-A281906] p 377 N95-11788
High frequency flow/structural interaction in dense subsonic fluids handbook
[NASA-CR-194007] p 230 N95-11807
Hypersonic turbulent boundary-layer and free shear database
[NASA-CR-177610] p 292 N95-11992
An empirical study of a highly available file system
[AD-A282655] p 378 N95-12502
Triaxial and torsional shear test results for sand
[AD-A282725] p 323 N95-12506
Nimbus-7 Earth Radiation Budjet compact solar data set user's guide
[NASA-RP-1346] p 384 N95-12667
AGSO 1993: Yearbook of the Australian Geological Survey Organisation. Geoscientific research and database development for the year 1 July 1992 to 30 June 1993
p 324 N95-12686
The Second Workshop on Principles and Practice of Constraint Programming
[AD-A281731] p 229 N95-13166
Windshear certification data base for forward-look detection systems p 234 N95-13204
Object recognition for flexible assembly using stereo vision
[PB94-204427] p 363 N95-13248
DATA COMPRESSION
AIRSAR software: Computer programs for preprocessing of JPL compressed polarimetric SAR data
[PB94-179116] p 280 N95-11800
DATA CORRELATION
FORTRAN programs to process Magsat data for lithospheric, external field, and residual core components
[NASA-TM-104612] p 323 N95-12130
DATA FLOW ANALYSIS
Experiments with formal methods in software engineering
[PB94-192416] p 344 N95-12774
DATA MANAGEMENT
On bottleneck partitioning k-ary n-cubes
[NASA-CR-194966] p 342 N95-12005
A data and information system for processing, archival, and distribution of data for global change research
[NASA-CR-196770] p 320 N95-12786
Lessons learned from experiments conducted on radar data management systems
[AD-A282896] p 284 N95-12920
Analyzing terabytes of data at Fermilab
[DE94-013149] p 347 N95-13269
DATA PROCESSING
Implementation of a state of the art automated system for the production of cloud/water vapor motion winds from geostationary satellites
[NASA-CR-196817] p 325 N95-11758
New York bight study. Report 4: Geographic information systems and relational database management system development
[AD-A281716] p 327 N95-11787
FORTRAN programs to process Magsat data for lithospheric, external field, and residual core components
[NASA-TM-104612] p 323 N95-12130
Principles of GPS one-way data processing for high precision positioning applications: Algorithms and software issues p 237 N95-12177
Efficient and effective handling of cycle slips in global positioning system data p 237 N95-12230
CENDI Indexing Workshop
[NASA-CP-10160] p 378 N95-12358
Standards relevant to a NATO anthropometry survey using 3D imaging tools
[AD-A283065] p 339 N95-13055
Multi-jet analysis for the top search at the Fermilab Collider
[DE94-014988] p 359 N95-13169
Toolkits for construction and manipulation of geographical data
[PB94-202587] p 378 N95-13245
Analyzing terabytes of data at Fermilab
[DE94-013149] p 347 N95-13269
DATA PROCESSING EQUIPMENT
Certification of windshear performance with RTCA class D radomes p 235 N95-13206
DATA REDUCTION
SeaWiFS technical report series. Volume 19: Case studies for SeaWiFS calibration and validation, part 2
[NASA-TM-104566-VOL-19-PT-2] p 328 N95-11920
Efficient and effective handling of cycle slips in global positioning system data p 237 N95-12230
A new algorithm for five-hole probe calibration, data reduction, and uncertainty analysis
[NASA-TM-106458] p 232 N95-12378

DATA RETRIEVAL
HLLV avionics requirements study and electronic filing system database development
[NASA-CR-193993] p 243 N95-13027
DATA SMOOTHING
Approximation of scattered data using smooth grid functions
[PB94-207016] p 353 N95-13573
DATA STORAGE
Stochastic indexing
[AD-A283143] p 327 N95-13137
DATA STRUCTURES
Object-oriented incremental map-generation for mobile robot navigation
[PB94-190717] p 314 N95-11820
DATA SYSTEMS
Development of an Automated Nondestructive Inspection (ANDI) system for commercial aircraft, phase 1
[AD-A283500] p 234 N95-12623
Part A: A data acquisition/controller system. Part B: Supplement to a data acquisition/controller system
[AD-A283373] p 285 N95-12924
DATA TRANSMISSION
An efficient system for reliably transmitting image and video data over low bit rate noisy channels
[NASA-CR-196802] p 341 N95-11764
Burst transmission in the HF band: A system analysis and proposal for improvement
[PB94-190733] p 280 N95-11821
Information Technology Division's technical paper abstracts
[AD-A282882] p 378 N95-12916
5-volt low level serial transceiver
[AD-D016399] p 288 N95-13153
Integrated sensor bus
[PB94-206810] p 288 N95-13252
Trellis-based source and channel coding
[PB94-204443] p 285 N95-13405
Modelling of biopotential recordings and its implications for instrumentation design
[PB94-206844] p 332 N95-13408
DAYGLOW
A calibration of the Naval Postgraduate School middle ultraviolet spectrograph and an analysis of the OII 2470 A emission obtained by the middle ultraviolet spectrograph
[AD-A283449] p 354 N95-13144
DEATH
Memorial service for the mission 51-L crew (edited)
[NASA-TM-109900] p 250 N95-13133
DEBONDING (MATERIALS)
Probability of detection of defects in coatings with electronic shearography
[NASA-CR-196201] p 308 N95-12391
DEBRIS
Debris/ice/TPS assessment and integrated photographic analysis of Shuttle Mission STS-65
[NASA-TM-109205] p 249 N95-12224
DEBYE LENGTH
Review of electron beam microinstabilities and their relevance to EBIS devices
[DE94-013755] p 364 N95-11746
DECISION MAKING
A decision support system for tolerance allocation
[NASA-CR-195817] p 308 N95-11994
DECODERS
An efficient system for reliably transmitting image and video data over low bit rate noisy channels
[NASA-CR-196802] p 341 N95-11764
DECOMPOSITION
High performance climate system modeling using a domain and task decomposition message-passing approach
[DE94-013739] p 322 N95-11741
Thianthrene-based poly(benzoxazole)s
[AD-A282326] p 274 N95-12419
Synthesis and decomposition of a novel carboxylate precursor to indium oxide
[NASA-TM-106555] p 260 N95-12693
DECONTAMINATION
Supercritical fluid (SCF) technologies: Assessment of applicability to installation restoration processes
[AD-A281504] p 290 N95-11859
DEEP SPACE NETWORK
Project ECHO: Electronic Communications from Halo Orbit
[NASA-CR-197190] p 283 N95-12644
DEFECTS
Revealing hidden defects: A hybrid evaluation strategy for steel structures
[PB94-191236] p 308 N95-11822
Theory of complex defects on DNA polymer chain
[AD-A282619] p 275 N95-12536
VAMAS round robin on fractography of ceramics. Swedish results
[PB94-180155] p 275 N95-12600
DEFENSE PROGRAM
Burst transmission in the HF band: A system analysis and proposal for improvement
[PB94-190733] p 280 N95-11821
Air Force seal activities p 306 N95-13600
DEFLECTION
Numerical computations with ABAQUS/Explicit, DYNA3D, and DYSMAS/L
[AD-A282249] p 293 N95-12409
Flight dynamics of an unmanned aerial vehicle
[AD-A282259] p 239 N95-12410
DEFOCUSING
Defocus measurement using a liquid crystal point diffraction interferometer
[NASA-TM-106687] p 296 N95-12748
DEFORESTATION
AVHRR/NOAA images to detect and quantify deforestation in Amazon Forest: Relations with TM/LANDSAT data
[INPE-5501-TDI/516] p 316 N95-13350
DEFORMATION
An estimate of the evolution of the acoustic emission spectrum of rocks on the basis of changes in its average frequency in the process of deformation
p 323 N95-12112
A study of the deformation of helical springs under eccentric loading
[AD-A283448] p 312 N95-12511
Polycrystal models to fit experiments
[DE94-014419] p 374 N95-13078
DEGREES OF FREEDOM
Pipeline vibrations. Computer program for the prediction of fluid transients in flexible, unbranched three-dimensional piping systems
[ESDU-93031] p 309 N95-11768
Design of passive piezoelectric damping for space structures
[NASA-CR-4625] p 252 N95-12165
Improved assumed-stress hybrid shell element with drilling degrees of freedom for linear stress, buckling, and free vibration analyses
[NASA-CR-192816] p 313 N95-13163
DEHYDRATION
CeO2-ZrO2 powder synthesis by way of alcohol dehydration of aqueous salt solutions
[INPE-5484-PRE/1783] p 276 N95-13191
DEICERS
User's manual for the NASA Lewis ice accretion/heat transfer prediction code with electrothermal deicer input
[NASA-CR-4530] p 291 N95-11888
DEICING
User's manual for the NASA Lewis ice accretion/heat transfer prediction code with electrothermal deicer input
[NASA-CR-4530] p 291 N95-11888
DELTA LAUNCH VEHICLE
Project ECHO: Electronic Communications from Halo Orbit
[NASA-CR-197190] p 283 N95-12644
Project Genesis: Mars in situ propellant technology demonstrator mission
[NASA-CR-197166] p 277 N95-12822
DELTA WINGS
Design and construction of a remote piloted flying wing
[NASA-CR-197195] p 241 N95-12695
Experimental aerodynamic characteristics of a generic hypersonic accelerator configuration at Mach numbers 1.5 and 2.0 — conducted in the Langley Unitary Plan Wind Tunnel
[NASA-TM-4413] p 233 N95-12770
DENDRITIC CRYSTALS
Influence of additives on structure and thermal stability of ammonium nitrate
[PB94-206943] p 278 N95-13435
DENSE PLASMAS
Physics of High Energy Density Plasmas Produced by Pulsed Power
[NIFS-PROC-18] p 365 N95-12429
Hot spots observation in a dense plasma focus
p 367 N95-12444
Observation of a soft x ray emitting core in a dense plasma focus p 367 N95-12445
DENSIFICATION
STS propellant densification feasibility study data book
[NASA-TM-108467] p 278 N95-12857
CVD techniques for the synthesis or modification of porous ceramics
[PB94-206836] p 276 N95-13284
Equipment for investigation of cryogenic compaction of nanosize silicon nitride powders
[DE94-013593] p 277 N95-13530
DENSITY (MASS/VOLUME)
Orthobaric densities and molar volumes of liquids. Polycyclic phenyl and cyclohexyl compounds
[ESDU-94002] p 266 N95-12129
DENSITY DISTRIBUTION
Development of nonintrusive, scatter-independent techniques for measurement of liquid density inside dense sprays
[NASA-CR-196413] p 293 N95-12387
Density gradient effects in the tokamak edge turbulence with temperature gradient driving
[DE94-625042] p 370 N95-13539
DENSITY MEASUREMENT
Development of nonintrusive, scatter-independent techniques for measurement of liquid density inside dense sprays
[NASA-CR-196413] p 293 N95-12387
Improvements of HCN laser heterodyne interferometer for measuring plasma density
[DE94-625037] p 370 N95-13341
DEOXYGENATION
Phenoxythiocarbonylation and deoxygenation of aryl trifluoromethyl carbinols
[AD-A280519] p 260 N95-12613
DEOXYRIBONUCLEIC ACID
Microbial communities in subsurface environments: Diversity, origin, and evolution
[DE94-013699] p 329 N95-11737
Theory of complex defects on DNA polymer chain
[AD-A282619] p 275 N95-12536
DEPOSITION
Plasma and ion beam processing at Los Alamos
[DE94-014293] p 365 N95-12371
Nanometer scale phase separation in mixed composition self-assembled monolayers
[AD-A282671] p 266 N95-12514
DESALINIZATION
Autonomous power system for remote locations
[DE94-013244] p 361 N95-11779
DESERTIFICATION
Factors influencing the rates, processes and magnitude of accumulation of carbon in desert soils
[NASA-CR-196820] p 325 N95-13025
DESERTS
Tactical satellite orbital simulation and requirements study
[AD-A282314] p 282 N95-12416
DESIGN
Design and construction of the astronautics refrigerator magnet
[DE94-013599] p 353 N95-11731
DESIGN ANALYSIS
Requirements report for SSTO vertical take-off/horizontal landing vehicle
[NASA-CR-196875] p 251 N95-11777
Selection process for trade study: Reusable Hydrogen Composite Tank System (RHCTS)
[NASA-CR-196874] p 251 N95-11809
Object-oriented technology for compressor simulation
[NASA-TM-106723] p 243 N95-11864
Software analysis handbook: Software complexity analysis and software reliability estimation and prediction
[NASA-TM-104799] p 339 N95-11914
Architectural design of the science complex at Elizabeth City State University p 247 N95-11960
Frequency doubler (from 4.7 to 9.4 GHz) using a diode
[AD-A282784] p 287 N95-12525
Status of hollow cathode heater development for the Space Station plasma contactor
[NASA-CR-195364] p 258 N95-12622
External Device to Incrementally Skid the Habitat (E-DISH)
[NASA-CR-197147] p 301 N95-12625
Proposal for the design of a zero gravity tool storage device
[NASA-CR-197150] p 302 N95-12627
Triton 2 (1B)
[NASA-CR-197188] p 240 N95-12636
PowerSat: A technology demonstration of a solar power satellite
[NASA-CR-197210] p 253 N95-12661
Design and testing of a model CELSS chamber robot
[NASA-CR-197196] p 303 N95-12694
Optimization of aerospace structures
[NASA-CR-196763] p 242 N95-12787
Digital filter designs that are free of limit cycles
[AD-A282885] p 287 N95-12918
Guideway structural design and power/propulsion/braking in relation to guideways. Volume 3: Appendix B: Maglev guideway structural design
[PB93-169910] p 304 N95-13128

Methodology for sensitivity analysis, approximate analysis, and design optimization in CFD for multidisciplinary applications
[NASA-CR-196981] p 294 N95-13201
Space Station Freedom propulsion activities
[NASA-TM-108604] p 256 N95-13236

DESIGN TO COST
Test Plan. GCPS Task 4, subtask 4.2 thrust structure development
[NASA-CR-196869] p 251 N95-11833
The FC-1D: The profitable alternative Flying Circus Commercial Aviation Group
[NASA-CR-197152] p 240 N95-12628
The OFP-6M transport jet
[NASA-CR-197159] p 240 N95-12637

DESORPTION
Hydrogen bonding and molecular orientation in water/fluorine adlayers on silver(110)
[AD-A282652] p 268 N95-13549

DESULFURIZING
Hydrogen desulfurization of nickel: Thermodynamics and kinetics
[AD-A282581] p 266 N95-12549

DETECTION
Self-checking state machine realizations in CMOS
[AD-A282177] p 286 N95-12421

DETERIORATION
Ten-year ground exposure of composite materials used on the Bell Model 206L helicopter flight service program
[NASA-TP-3468] p 262 N95-12357
Influence of additives on structure and thermal stability of ammonium nitrate
[PB94-206943] p 278 N95-13435

DEUTERIUM
Advanced cryogenic propellants
[AD-A282451] p 277 N95-12729

DEUTERIUM COMPOUNDS
Amine catalyzed intramolecular imidization of alkyl and aryl phthalamates, kinetics and mechanism in deuterated chloroform
[AD-A281741] p 259 N95-11844

DEUTERONS
The cascade-deuteron system
[DE94-011650] p 357 N95-11894

DIAMETERS
Acute inhalation of explosively disseminated carbon fibers in rats
[AD-A280556] p 330 N95-12614

DIAMOND FILMS
Analysis of cost: Combustion flame CVD diamond deposition
[AD-A282527] p 273 N95-12403

DIAMONDS
Atomic structure modifications of diamond-like nanocomposite films: Observation by Raman spectroscopy, FTIR and STM
[DE94-013732] p 371 N95-11740
Substrate temperature control apparatus and technique for CVD reactors
[AD-D016387] p 374 N95-13150

DICARBOXYLIC ACIDS
Synthesis and characterization of thianthrene-based polyamides
[AD-A282512] p 273 N95-12399

DICHROISM
Synchrotron studies of narrow band materials
[DE94-013696] p 271 N95-13554

DICTIONARIES
Category theory: The mathematics for the humanities
[PB94-205044] p 353 N95-13560

DIELECTRIC PROPERTIES
Radiation-induced structural changes, 4
[DE94-753223] p 356 N95-11817

DIELECTRICS
Radiation-induced structural changes, 4
[DE94-753223] p 356 N95-11817
Light beam and pulse propagation in nonlinear dielectrics
[AD-A282548] p 282 N95-12496

DIENES
All-hydrocarbon composite resins based on cyclopentadiene
[AD-A282495] p 276 N95-13296

DIESEL ENGINES
TKKMOD: A computer simulation program for an integrated wind diesel system. Version 1.0: Document and user guide
[PB94-179090] p 317 N95-11798
Data acquisition system of the NANOSAW-2 stand alone wind diesel plant. Document and user's guide
[PB94-179108] p 317 N95-11799
Validation results of wind diesel simulation model TKKMOD
[PB94-179157] p 317 N95-11846
Open-chamber combustion study
[PB94-184090] p 301 N95-12579
Diesel-fired self-pumping water heater
[AD-A283063] p 279 N95-13053

DIETS
Copper metabolism in rats fed ascorbic acid or restricted amounts of copper
[PB94-191343] p 330 N95-11902

DIFFERENTIAL ABSORPTION LIDAR
Differential absorption lidar measurements of atmospheric water vapor using a pseudonoise code modulated AlGaAs laser
[NASA-TM-104610] p 314 N95-11997

DIFFERENTIAL EQUATIONS
Anode sheath contributions in plasma thrusters
[AD-A280395] p 364 N95-11837
Viscosity solutions of fully nonlinear equations
[AD-A281725] p 351 N95-11861
Extensions and contractions of the Lie algebra of q-pseudodifferential symbols
[PB94-192374] p 352 N95-12603

DIFFERENTIAL GEOMETRY
The differential geodesy of the spherical representation
[AD-A282212] p 315 N95-12428

DIFFERENTIATION (BIOLOGY)
Morphological differentiation of colon carcinoma cell lines in rotating wall vessels
[NASA-CR-196780] p 333 N95-11808

DIFFRACTION
Simulating the energy performance of holographic glazings
[DE94-014969] p 296 N95-13158

DIFFUSE RADIATION
Solar radiation data manual for flat-plate and concentrating collectors
[DE93-018229] p 317 N95-12647

DIFFUSION
Analysis and design of numerical schemes for gas dynamics. 2: Artificial diffusion and discrete shock structure
[NASA-CR-196476] p 290 N95-11874
Convective flow effects on protein crystal growth
[NASA-CR-196790] p 372 N95-11921
Role of implantation-induced defects in surface-oriented diffusion of fluorine in silicon
[DE94-014905] p 374 N95-13125
Density gradient effects in the tokamak edge turbulence with temperature gradient driving
[DE94-625042] p 370 N95-13539

DIFFUSION COEFFICIENT
Density gradient effects in the tokamak edge turbulence with temperature gradient driving
[DE94-625042] p 370 N95-13539

DIFFUSION THEORY
Convective flow effects on protein crystal growth
[NASA-CR-196790] p 372 N95-11921
Concentration fluctuation models: A comparative study
[CUED/A-AERO/TR-24] p 292 N95-11939
Technical report series on global modeling and data assimilation. Volume 2: Direct solution of the implicit formulation of fourth order horizontal diffusion for gridpoint models on the sphere
[NASA-TM-10406] p 323 N95-12226

DIFFUSIVITY
Analysis and design of numerical schemes for gas dynamics. 2: Artificial diffusion and discrete shock structure
[NASA-CR-196476] p 290 N95-11874
Analysis and design of numerical schemes for gas dynamics 1: Artificial diffusion, upwind biasing, limiters and their effect on accuracy and multigrid convergence
[NASA-CR-196477] p 290 N95-11875

DIGITAL DATA
Digital image processing techniques for image-mapping applications
[INPE-5546-TDI/532] p 315 N95-12301
Certification of windshear performance with RTCA class D radomes p 235 N95-13206
Trellis-based source and channel coding
[PB94-204443] p 285 N95-13405

DIGITAL ELECTRONICS
Integrated sensor bus
[PB94-206810] p 288 N95-13252

DIGITAL FILTERS
Digital filter designs that are free of limit cycles
[AD-A282885] p 287 N95-12918

DIGITAL SYSTEMS
A model-based expert system for space power distribution diagnostics
[NASA-CR-195336] p 342 N95-11918
Preliminary digital control system design for the petite amateur Navy satellite (PANSAT)
[AD-A282804] p 253 N95-12526
ETRI brochure: History, mission, and activity highlights p 389 N95-12697

DIGITAL TECHNIQUES
Part A: A data acquisition/controller system. Part B: Supplement to a data acquisition/controller system
[AD-A283373] p 285 N95-12924

DIMENSIONAL MEASUREMENT
Body dimensions for apparel
[PB94-187739] p 338 N95-11908

DIMENSIONAL STABILITY
The effect of irradiation on the stability and properties of monolithic silicon carbide and SiC(f)/SiC composites up to 25 dpa
[DE94-014568] p 263 N95-12862

DIMENSIONLESS NUMBERS
The role of crack formation in chevron-notched four-point bend specimens
[NASA-TM-106631] p 310 N95-11865

DIODES
Velocity spread of REB generated by high current diode
[IPPCZ-339] p 364 N95-11886
Beam divergence characteristic of two-stage ion diode p 365 N95-12431
High resolution diagnostics of intense ion diodes and key issues for bright light ion beam generation p 367 N95-12448
Frequency doubler (from 4.7 to 9.4 GHz) using a diode
[AD-A282784] p 287 N95-12525
The future of diode pumped solid state lasers and their applicability to the automotive industry
[DE94-014736] p 298 N95-12868

DIRECTIONAL CONTROL
Numerical analysis of tangential slot blowing on a generic chined forebody
[NASA-TM-108845] p 231 N95-11927

DIRECTIONAL SOLIDIFICATION (CRYSTALS)
Apparatus and method for forming textured bulk high temperature superconducting materials
[AD-D016394] p 373 N95-12635
Description of a high temperature quenching furnace for the study of the directional solidification of nickel-base superalloys
[DE94-013812] p 271 N95-13544

DIRECTORIES
Directory of OAQPS information services, May 1994
[PB94-181310] p 318 N95-11848
Directory of Federal laboratory and technology resources
[PB93-100097] p 389 N95-12223
Access EPA
[PB93-170041] p 319 N95-12356

DISARMAMENT
Contributions to CD Space Committee, 1993. Summary and comments
[PB94-190618] p 379 N95-11871

DISCOVERY (ORBITER)
NPS state vector analysis and relative motion plotting software for STS-51
[AD-A282909] p 249 N95-12510
Infrared spectral measurement of Space Shuttle glow
[AD-A282883] p 250 N95-12917

DISCRIMINANT ANALYSIS (STATISTICS)
Eye-gaze determination of user intent at the computer interface
[DE94-012337] p 363 N95-13421

DISPLACEMENT
Large-displacement structural durability analyses of simple bend specimen emulating rocket nozzle liners
[NASA-TM-106521] p 312 N95-12818

DISPLAY DEVICES
Activities of the Helsinski University of Technology, Applied Electronics Laboratory
[PB94-179074] p 385 N95-11797
Design and synthesis of tight pitch FLCs for analog voltage-limited electro-optic modulators
[AD-A281472] p 371 N95-11855
Visit to UDRI and USAF, Armstrong Lab., Williams AFB, Phoenix, USA, February 8-11, 1993
[PB94-190659] p 337 N95-11873
Dynamic sine wave response measurements of CRT displays using sinusoidal counterphase modulation
[AD-A282222] p 333 N95-12406
Exploitation of virtual reality architectures
[AD-A282263] p 340 N95-12413
NPS state vector analysis and relative motion plotting software for STS-51
[AD-A282909] p 249 N95-12510
Flight test of takeoff performance monitoring system
[NASA-TP-3403] p 245 N95-12684

DISRUPTING
Locked modes in TEXT-U tokamak
[DE94-011595] p 370 N95-13529

DISTANCE
Examples of flight path optimisation using a multivariate gradient-search method. Addendum A: Variation of optimum flight profile parameters with range
[ESDU-94016-ADD-A] p 238 N95-11794
DISTILLATION
CRYOCOL: A computer program to calculate the cryogenic distillation of hydrogen isotopes
[DE94-622012] p 268 N95-13531
DISTRIBUTED PARAMETER SYSTEMS
An interpolation theoretic approach to control
[AD-A281465] p 348 N95-11853
DISTRIBUTED PROCESSING
Efficient detection of deadlocks in Petri nets
[PB94-179405] p 343 N95-12366
An empirical study of a highly available file system
[AD-A282655] p 378 N95-12502
Using secure coprocessors
[AD-A281255] p 340 N95-12524
Active Nodal Task Seeking for high-performance, ultra-dependable computing
[AD-A282924] p 344 N95-12588
A data and information system for processing, archival, and distribution of data for global change research
[NASA-CR-196770] p 320 N95-12786
Delta-4: An open architecture for dependable systems
[PB94-195641] p 341 N95-13436
An informal introduction to parallel processors
[DE94-016347] p 348 N95-13556
DISTRIBUTION FUNCTIONS
Stationary plasma thruster ion velocity distribution
[NASA-CR-195379] p 257 N95-11919
DISULFIDES
One-step synthesis of dithiocarbamates from metal powders
[NASA-TM-106558] p 260 N95-12692
DIURNAL VARIATIONS
Tropical cyclone development and intensification under moderate to strong vertical wind shear
[AD-A282185] p 326 N95-12423
DMSP SATELLITES
Determination of the auroral oval Q index from the air weather service K index
[AD-A282764] p 324 N95-12508
Initial analysis and modeling results from the Polar Orbiting Geomagnetic Survey (POGS) satellite
[AD-A283454] p 253 N95-12545
DOCUMENT STORAGE
CENDI Indexing Workshop
[NASA-CP-10160] p 378 N95-12358
World wide web implementation of the Langley technical report server
[NASA-TM-109162] p 345 N95-13198
DOLOMITE (MINERAL)
An estimate of the evolution of the acoustic emission spectrum of rocks on the basis of changes in its average frequency in the process of deformation
p 323 N95-12112
DOPED CRYSTALS
Optical and magnetic resonance investigations of 3D ions in single crystal hosts: Candidates for tunable solid-state lasers
[AD-A281726] p 371 N95-11842
Pressure studies of alkali, alkaline earth and rare earth doped C60 superconductors
[DE94-013345] p 372 N95-11862
Radiative performance of rare earth garnet thin film selective emitters
[NASA-TM-106722] p 372 N95-11876
Photogeneration of charge carriers in bilayer assemblies of conjugated rigid-rod polymers
[AD-A282625] p 275 N95-12537
Advanced cryogenic propellants
[AD-A282451] p 277 N95-12729
Evaluation of the improvement in the figure of merit of Bi2Te3 - based alloys with addition of ultrafine scattering centers
[DE94-015363] p 374 N95-13059
Be-9 and B-11 NMR study of superconductivity in boron doped UBe13
[DE94-014432] p 374 N95-13081
Silicon carbide and sicaln heterojunction bipolar transistor structures
[AD-D016403] p 288 N95-13181
Laser physics of Nd(exp 3+)-doped phosphate glasses
[DE94-015141] p 299 N95-13534
DOPPLER EFFECT
Experimental and theoretical study of neon-like selenium x-ray laser spectral line profiles
[DE94-015327] p 298 N95-12761
Stimulated scattering of a slow electromagnetic wave excited by the relativistic electron beam
[DE94-625049] p 285 N95-13343
Summaries of papers presented at the High Resolution Spectroscopy Topical Meeting. Technical digest series. Volume 1: Post conference edition
[AD-A281261] p 268 N95-13372
Alignment and experiment of the HL-1 x ray bent-crystal spectrometer
[DE94-624719] p 297 N95-13537
DOPPLER RADAR
The design and development of signal-processing algorithms for an airborne x-band Doppler weather radar
[NASA-CR-196888] p 281 N95-12374
Lidar performance analysis
[NASA-CR-196510] p 362 N95-12390
Terminal Doppler Weather Radar Build 5A Operational Test and Evaluation (OT/E) integration and OT/E operational test plan
[AD-A283052] p 327 N95-12996
Airborne Windshear Detection and Warning Systems. Fifth and Final Combined Manufacturers' and Technologists' Conference, part 2
[NASA-CP-10139-PT-2] p 234 N95-13203
Doppler radar detection of vortex hazard indicators
p 236 N95-13212
DOSIMETERS
Detailed component design for a Compact Environmental Anomaly Sensor (CEASE)
[AD-A283144] p 256 N95-13138
DRAG
Control theory based airfoil design using the Euler equations
[NASA-CR-196360] p 230 N95-11884
DRAG DEVICES
Computational flow predictions for hypersonic drag devices p 233 N95-11967
DRAG REDUCTION
Application of two procedures for dual-point design of transonic airfoils
[NASA-TP-3466] p 231 N95-12176
The FC-1D: The profitable alternative Flying Circus Commercial Aviation Group
[NASA-CR-197152] p 240 N95-12628
DRAINAGE
The impact of elevation data representation on nocturnal drainage wind simulations
[DE94-014752] p 326 N95-12927
5-volt low level serial transceiver
[AD-D016399] p 288 N95-13153
DRILLING
Lunar vertical-shaft mining system
[NASA-CR-197154] p 384 N95-13497
DROP SIZE
Structure of a swirl-stabilized, combusting spray
[NASA-TM-106724] p 243 N95-11890
DROP TOWERS
Ground based research in microgravity materials processing
[NASA-CR-196815] p 278 N95-11759
DUCTILITY
Numerical simulations of creep in ductile-phase toughened intermetallic matrix composites
[DE94-014744] p 264 N95-13533
DUPLEXERS
Duplex rolling element bearing mounting for ensuring preload control
[AD-D016402] p 304 N95-13189
DURABILITY
Ten-year ground exposure of composite materials used on the Bell Model 206L helicopter flight service program
[NASA-TP-3468] p 262 N95-12357
DYADICS
Singularity of the Green dyadics for bi-isotropic
[PB94-184504] p 283 N95-12581
DYE LASERS
Laser based combustion laboratory at NTH/SINTEF applied thermodynamics
[PB94-202603] p 299 N95-13246
DYES
Simultaneous three-dimensional velocity and mixing measurements by use of laser Doppler velocimetry and fluorescence probes in a water tunnel
[NASA-TP-3454] p 246 N95-13553
DYNAMIC CHARACTERISTICS
Determining the accuracy of maximum likelihood parameter estimates with colored residuals
[NASA-CR-194893] p 244 N95-11869
Atomic scale dynamics of a two-dimensional gas-solid interface
[AD-A282646] p 358 N95-12617
DYNAMIC CONTROL
The use of neuron nets to stabilize dynamic systems
p 348 N95-12109
Flight dynamics of an unmanned aerial vehicle
[AD-A282259] p 239 N95-12410
DYNAMIC MODELS
Using emergent order to shape a space society
p 377 N95-11959
Hypersonic vehicle model and control law development using H(infinity) and micron synthesis
[NASA-TM-4562] p 255 N95-12838
Analytical and experimental vibration analysis of a faulty gear system
[NASA-TM-106689] p 303 N95-12843
DYNAMIC PRESSURE
Pressure measurements on an F/A-18 twin vertical tail in buffeting flow. Volume 3: Buffet power spectral densities
[AD-A281444] p 230 N95-11829
Evaluation of dynamic pressure of ablation plasma produced by intense, pulsed, ion beam
p 365 N95-12433
DYNAMIC PROGRAMMING
Viscosity solutions of fully nonlinear equations
[AD-A281725] p 351 N95-11861
DYNAMIC RESPONSE
Army Research Office Workshop on Dynamic Response of Composite Structures
[AD-A281471] p 262 N95-11854
Dynamic sine wave response measurements of CRT displays using sinusoidal counterphase modulation
[AD-A282222] p 333 N95-12406
Flight dynamics of an unmanned aerial vehicle
[AD-A282259] p 239 N95-12410
Development of the CSI phase-3 evolutionary model testbed
[NASA-CR-4630] p 256 N95-13195
Structure and dynamics of the solar corona
[NASA-CR-196978] p 384 N95-13582
DYNAMIC STABILITY
Flight dynamics of an unmanned aerial vehicle
[AD-A282259] p 239 N95-12410
DYNAMIC STRUCTURAL ANALYSIS
Engine structures analysis software: Component Specific Modeling (COSMO)
[NASA-CR-195378] p 309 N95-11711
High frequency flow/structural interaction in dense subsonic fluids handbook
[NASA-CR-194007] p 230 N95-11807
Modelling and simulation of Space Station Freedom berthing dynamics and control
[NASA-TM-109151] p 252 N95-11947
Design of passive piezoelectric damping for space structures
[NASA-CR-4625] p 252 N95-12165
Analytical and experimental vibration analysis of a faulty gear system
[NASA-TM-106689] p 300 N95-12377
Large-displacement structural durability analyses of simple bend specimen emulating rocket nozzle liners
[NASA-TM-106521] p 312 N95-12818
Analytical and experimental vibration analysis of a faulty gear system
[NASA-TM-106689] p 303 N95-12843
Improved assumed-stress hybrid shell element with drilling degrees of freedom for linear stress, buckling, and free vibration analyses
[NASA-CR-192816] p 313 N95-13163
The effect of passive damping on feedback control performance of flexible manipulators
[DE94-015000] p 304 N95-13182
Activities of the Structures Division, Lewis Research Center
[NASA-TM-106081] p 313 N95-13235
DYNAMIC TESTS
Vestibular afferent responses to linear accelerations in the alert squirrel monkey
[NASA-TM-4581] p 330 N95-12006
DYNAMICAL SYSTEMS
Using emergent order to shape a space society
p 377 N95-11959
Dynamical systems and oceanography
[AD-A282635] p 329 N95-12540
Inverse operator theory method mathematics-mechanization for the solutions of nonlinear equations and some typical applications in nonlinear physics
[DE94-624804] p 352 N95-13340
Stochastic control and nonlinear estimation
[AD-A281219] p 350 N95-13369

E

EARTH ATMOSPHERE
Optical Remote Sensing of the Atmosphere. Technical digest 1993. Volume 5: Postconference edition
[AD-A281446] p 314 N95-11831
Quantum chemical study of methane oxidation species
[NASA-CR-196158] p 265 N95-12107

Parallelization and visual analysis of multidimensional fields: Application to ozone production, destruction, and transport in three dimensions
[NASA-CR-195971] p 320 N95-12798
Tests of a new cloud treatment in an atmospheric general circulation model
[DE94-013138] p 327 N95-13268
EARTH GRAVITATION
Satellite laser ranging and gravity field modeling accuracy
[NASA-CR-196057] p 248 N95-12837
EARTH IONOSPHERE
Determination of the auroral oval Q index from the air weather service K index
[AD-A282764] p 324 N95-12508
EARTH MAGNETOSPHERE
Inner Magnetosphere Imager (IMI) solar terrestrial probe class mission preliminary design study report
[NASA-TM-108464] p 252 N95-11948
FORTRAN programs to process Magsat data for lithospheric, external field, and residual core components
[NASA-TM-104612] p 323 N95-12130
A magnetic shield/dual purpose mission
[NASA-CR-197192] p 255 N95-13006
EARTH OBSERVATIONS (FROM SPACE)
Proposal of a methodology to evaluate urban quality of life using conventional and remote sensing data, geographic information system, and a database
[INPE-5552-TDI/536] p 315 N95-12297
Digital image processing techniques for image-mapping applications
[INPE-5546-TDI/532] p 315 N95-12301
EARTH OBSERVING SYSTEM (EOS)
Earth Observing System (EOS)/Advanced Microwave Sounding Unit-A (AMSU-A)
[NASA-CR-189379] p 344 N95-12796
Development of the CSI phase-3 evolutionary model testbed
[NASA-CR-4630] p 256 N95-13195
EARTH ORBITAL ENVIRONMENTS
Infrared spectral measurement of Space Shuttle glow
[AD-A282883] p 250 N95-12917
EARTH ORBITS
Analytical investigation of the dynamics of tethered constellations in Earth orbit, phase 2
[NASA-CR-196509] p 252 N95-12106
MOOSE: Manned On-Orbit Servicing Equipment
[NASA-CR-197151] p 254 N95-12790
EARTH RADIATION BUDGET
Nimbus-7 Earth Radiation Budjet compact solar data set user's guide
[NASA-RP-1346] p 384 N95-12667
EARTH RESOURCES
Digital image processing techniques for image-mapping applications
[INPE-5546-TDI/532] p 315 N95-12301
Factors influencing the rates, processes and magnitude of accumulation of carbon in desert soils
[NASA-CR-196820] p 325 N95-13025
EARTH SCIENCES
JPRS report: Science and technology. Central Eurasia
[JPRS-UST-94-017] p 247 N95-12001
JPRS report: Science and technology. Central Eurasia
[JPRS-UST-94-020] p 389 N95-12002
JPRS report: Science and technology. Central Eurasia
[JPRS-UST-94-019] p 389 N95-12003
EARTH-MARS TRAJECTORIES
A robotic exploration mission to Mars and Phobos
[NASA-CR-197168] p 382 N95-12307
EARTH-MOON TRAJECTORIES
Project ECHO: Electronic Communications from Halo Orbit
[NASA-CR-197190] p 283 N95-12644
EARTHQUAKES
Preliminary seismicity and focal mechanisms for the Southern Great Basin of Nevada and California, January 1992 - September 1992
[DE94-013589] p 321 N95-11730
ECCENTRICITY
A catalogue of potentially bright close binary gravitational wave sources
[NASA-CR-196934] p 379 N95-12234
Theoretical versus experimental results for the rotordynamic coefficients of eccentric, smooth, gas annular seal annular gas seals p 307 N95-13603
Turbomachinery Laboratory Texas A and M University research progress on annular gas seals p 307 N95-13604
ECONOMIC ANALYSIS
Composites (CFCCs) for low cost energy and cleaner environment
[DE94-013601] p 272 N95-11781
ECOSYSTEMS
Design and testing of a model CELSS chamber robot
[NASA-CR-197196] p 303 N95-12694
EDDY CURRENTS
Development of an Automated Nondestructive Inspection (ANDI) system for commercial aircraft, phase 1
[AD-A283500] p 234 N95-12623
EDGE LOADING
An analysis of the load-bearing capacity of members of square cross section with a series of perpendicular notches p 312 N95-12631
EDITING
Efficient and effective handling of cycle slips in global positioning system data p 237 N95-12230
EDITING ROUTINES (COMPUTERS)
Efficient and effective handling of cycle slips in global positioning system data p 237 N95-12230
EDUCATION
Real world software engineering
[AD-A282365] p 342 N95-11941
Education: A second career p 377 N95-11956
Engineering the future with America's high school students p 377 N95-11958
Spaceborne Photonics Institute
[NASA-CR-196784] p 362 N95-12659
Activities of the Institute for Aerospace Studies of Toronto University p 390 N95-12699
EFFLUENTS
Development of techniques for the in situ observation of OH and HO2 for studies of the impact of high-altitude supersonic aircraft on the stratosphere
[NASA-CR-196759] p 321 N95-12832
EIGENVALUES
A numerical calculation method for the kinetic ballooning mode eigen-equation with three components
[DE94-625048] p 369 N95-13107
EIGENVECTORS
A numerical calculation method for the kinetic ballooning mode eigen-equation with three components
[DE94-625048] p 369 N95-13107
EL NINO
Reports to the Nation on our changing planet. El Nino and climate prediction, no. 3, spring 1994 p 320 N95-12462
ELASTIC BENDING
Large-displacement structural durability analyses of simple bend specimen emulating rocket nozzle liners
[NASA-TM-106521] p 312 N95-12818
ELASTIC BUCKLING
Elastic buckling of unbalanced laminated fibre reinforced composite plates (rectangular plates of AsBtDs type, all edges simply-supported under biaxial loading)
[ESDU-94006] p 310 N95-11772
Elastic buckling of cylindrically curved laminated fibre reinforced composite panels with all edges simply-supported under biaxial loading
[ESDU-94007] p 310 N95-11773
ELASTIC DEFORMATION
A numerical analysis of the distribution of stresses in lung parenchyma which accounts for the interactions between the tissue skeleton and flowing air p 332 N95-11806
Computer modelling of cyclic deformation of high-temperature materials
[AD-A282457] p 263 N95-12833
A simplified thermohydrodynamic model for fluid film bearings
[DE94-015011] p 304 N95-13183
ELASTIC PLATES
Elastic buckling of cylindrically curved laminated fibre reinforced composite panels with all edges simply-supported under biaxial loading
[ESDU-94007] p 310 N95-11773
ELASTIC SCATTERING
The cascade-deuteron system
[DE94-011650] p 357 N95-11894
On the charged vector particle scattering on a vector particle
[DE94-622787] p 360 N95-13273
ELASTOMERS
The synthesis and structure of polyphosphazenes
[AD-A281723] p 272 N95-11832
ELBOW (ANATOMY)
A musculoskeletal model of the elbow joint complex
[NASA-CR-195812] p 335 N95-13270
ELECTRIC ARCS
Recycle requirements for Nasa's 30 cm xenon ion thruster
[NASA-TM-106668] p 258 N95-12750
ELECTRIC CURRENT
The experiment and analysis of tailoring V(sub L) and I(sub P) with ZnO voltage-sensitive resistor on HT-6M
[DE94-625074] p 370 N95-13541
ELECTRIC EQUIPMENT TESTS
Screen test for cadmium and nickel plates as developed and used within the Aerospace Corporation
[NASA-CR-196961] p 270 N95-12148
Stepper motor
[NASA-CR-189373] p 287 N95-12795
ELECTRIC FIELDS
Influence of electrode geometry on the high-field characteristics of photoconductive silicon wafers
[DE94-014660] p 287 N95-12865
Ionospheric dynamics instrument investigation for the Timed Mission
[NASA-CR-196198] p 325 N95-13190
ELECTRIC IGNITION
A low-erosion starting technique for high-performance arcjets
[NASA-TM-106627] p 259 N95-13347
ELECTRIC MOTORS
Design of a ZVS PWM inverter for a brushless DC motor in an EMA application
[NASA-CR-195808] p 312 N95-12620
ELECTRIC NETWORKS
Design of passive piezoelectric damping for space structures
[NASA-CR-4625] p 252 N95-12165
ELECTRIC POTENTIAL
Power system applications for PASC converter systems
[DE94-013329] p 286 N95-11751
The experiment and analysis of tailoring V(sub L) and I(sub P) with ZnO voltage-sensitive resistor on HT-6M
[DE94-625074] p 370 N95-13541
ELECTRIC POWER PLANTS
Data acquisition system of the NANOSAW-2 stand alone wind diesel plant. Document and user's guide
[PB94-179108] p 317 N95-11799
ELECTRIC POWER TRANSMISSION
Modeling of split-core transformers for power transmission
[AD-A282782] p 287 N95-12509
ELECTRIC PROPULSION
A low-erosion starting technique for high-performance arcjets
[NASA-TM-106627] p 259 N95-13347
ELECTRIC ROCKET ENGINES
Anode sheath contributions in plasma thrusters
[AD-A280395] p 364 N95-11837
ELECTRIC SWITCHES
Resistivity variation of fuse as an opening switch p 365 N95-12430
ELECTRIC WIRE
Potential molecular wires by an iterative divergent/convergent approach. Doubling of molecular length at each iteration
[AD-A281292] p 360 N95-13376
ELECTRICAL FAULTS
A model-based expert system for space power distribution diagnostics
[NASA-CR-195336] p 342 N95-11918
Recycle requirements for Nasa's 30 cm xenon ion thruster
[NASA-TM-106668] p 258 N95-12750
ELECTRICAL IMPEDANCE
Power system applications for PASC converter systems
[DE94-013329] p 286 N95-11751
Electromagnetic on-aircraft antenna radiation in the presence of composite plates
[NASA-CR-196126] p 284 N95-12856
ELECTRICAL INSULATION
Evaluation of wiring constructions for space applications
[NASA-TM-106735] p 256 N95-13194
MHD pressure drops and thermal hydraulic analysis for the ITER breeding blanket design
[DE94-015085] p 369 N95-13280
ELECTRICAL PROPERTIES
Structure and performance of carbon aerogel electrodes
[DE94-014746] p 356 N95-11791
Sound emission in materials and construction element testing p 355 N95-12013
Evaluation of the improvement in the figure of merit of Bi2Te3 - based alloys with addition of ultrafine scattering centers
[DE94-015363] p 374 N95-13059
Evaluation of wiring constructions for space applications
[NASA-TM-106735] p 256 N95-13194
ELECTRICAL RESISTIVITY
Tuning through the critical regime of the metal-insulator-transition in conducting polymers by pressure and magnetic field
[PB94-179165] p 272 N95-11847
Resistivity variation of fuse as an opening switch p 365 N95-12430
Finite element methods in resistivity logging
[PB94-206919] p 325 N95-13434

ELECTRO-OPTICS
Design and synthesis of tight pitch FLCs for analog voltage-limited electro-optic modulators
[AD-A281472] p 371 N95-11855
Ultrawideband shipboard electrooptic electromagnetic environment monitoring
[AD-A282369] p 280 N95-11943
ELECTROACOUSTICS
An acoustic charge transport imager for high definition television applications
[NASA-CR-196806] p 280 N95-11760
ELECTROCARDIOGRAPHY
Modelling of biopotential recordings and its implications for instrumentation design
[PB94-206844] p 332 N95-13408
ELECTROCHEMISTRY
Electrochemical epitaxy
[AD-A282403] p 373 N95-11993
Application of scanning tunneling microscopy to studies of electrode surfaces
[AD-A282383] p 373 N95-12004
Hydrogen bonding and molecular orientation in water/fluorine adlayers on silver(110)
[AD-A282652] p 268 N95-13549
ELECTRODE MATERIALS
Raman structural studies of the nickel electrode
[NASA-CR-196331] p 289 N95-13344
ELECTRODEPOSITION
Electrochemical epitaxy
[AD-A282403] p 373 N95-11993
Electrochemical deposition of metal nano-disk structures using the scanning tunneling microscope
[AD-A282464] p 268 N95-13288
ELECTRODES
Structure and performance of carbon aerogel electrodes
[DE94-014746] p 356 N95-11791
Application of scanning tunneling microscopy to studies of electrode surfaces
[AD-A282383] p 373 N95-12004
Screen test for cadmium and nickel plates as developed and used within the Aerospace Corporation
[NASA-CR-196961] p 270 N95-12148
Effect of operating parameters and anode gas impurities upon polymer electrolyte fuel cells
[DE94-014464] p 317 N95-12650
Influence of electrode geometry on the high-field characteristics of photoconductive silicon wafers
[DE94-014660] p 287 N95-12865
Raman structural studies of the nickel electrode
[NASA-CR-196331] p 289 N95-13344
Modelling of biopotential recordings and its implications for instrumentation design
[PB94-206844] p 332 N95-13408
ELECTRODYNAMICS
Magnetospheric-ionospheric Poynting flux
[NASA-CR-196856] p 322 N95-11801
Proceedings of Bianisotropics 1993: Seminar on Electrodynamics of Chiral and Bianisotropic Media
[PB94-179314] p 283 N95-12595
ELECTROENCEPHALOGRAPHY
Modelling of biopotential recordings and its implications for instrumentation design
[PB94-206844] p 332 N95-13408
ELECTROKINETICS
A numerical calculation method for the kinetic ballooning mode eigen-equation with three components
[DE94-625048] p 369 N95-13107
ELECTROLUMINESCENCE
Silicon-based blue light emitting diode
[AD-A282382] p 286 N95-12009
ELECTROLYSIS
Electrochemical deposition of metal nano-disk structures using the scanning tunneling microscope
[AD-A282464] p 268 N95-13288
ELECTROLYTIC CELLS
Effect of operating parameters and anode gas impurities upon polymer electrolyte fuel cells
[DE94-014464] p 317 N95-12650
Proceedings of the 36th Power Sources Conference
[AD-A281443] p 288 N95-13164
ELECTROMAGNETIC ABSORPTION
Diagnostic techniques for semiconductor materials processing
[AD-A282810] p 373 N95-12602
Semiconductor photodetector device
[AD-D016314] p 288 N95-13174
Absorption of intense microwaves and ion acoustic turbulence due to heat transport
[DE94-015140] p 369 N95-13285
ELECTROMAGNETIC COMPATIBILITY
Integrated sensor bus
[PB94-206810] p 288 N95-13252
ELECTROMAGNETIC COUPLING
Magnetospheric-ionospheric Poynting flux
[NASA-CR-196856] p 322 N95-11801
ELECTROMAGNETIC FIELDS
Investigation of finite element: ABC methods for electromagnetic field simulation
[NASA-CR-196837] p 279 N95-11707
The reflection of relativistic electron beam by virtual cathode
[IPPCZ-338] p 364 N95-11916
Ultrawideband shipboard electrooptic electromagnetic environment monitoring
[AD-A282369] p 280 N95-11943
Finite element methods in resistivity logging
[PB94-206919] p 325 N95-13434
ELECTROMAGNETIC INTERACTIONS
PASP PLUS Transient Pulse Monitor (TPM): Preflight characterization report
[AD-A282582] p 283 N95-12550
ELECTROMAGNETIC INTERFERENCE
The development of a highly reliable power management and distribution system for civil transport aircraft
[NASA-TM-106697] p 243 N95-11867
Fiber-optic sensors and the application to conditional monitoring for mechanical structures
[PB94-207057] p 363 N95-13574
ELECTROMAGNETIC MEASUREMENT
PASP PLUS Transient Pulse Monitor (TPM): Preflight characterization report
[AD-A282582] p 283 N95-12550
ELECTROMAGNETIC PULSES
PASP PLUS Transient Pulse Monitor (TPM): Preflight characterization report
[AD-A282582] p 283 N95-12550
ELECTROMAGNETIC RADIATION
Studies of electromagnetic ion cyclotron waves using AMPTE/CCE and dynamics explorer
[NASA-CR-196437] p 361 N95-12102
Electromagnetic on-aircraft antenna radiation in the presence of composite plates
[NASA-CR-196126] p 284 N95-12856
Stimulated scattering of a slow electromagnetic wave excited by the relativistic electron beam
[DE94-625049] p 285 N95-13343
ELECTROMAGNETIC SCATTERING
Investigation of finite element: ABC methods for electromagnetic field simulation
[NASA-CR-196837] p 279 N95-11707
Analysis of cylindrical wrap-around and doubly conformal patch antennas by way of the finite element-artificial absorber method
[NASA-CR-195211] p 281 N95-12382
Wideband electromagnetic scattering program. Fourier-based radar imaging techniques
[AD-A282540] p 282 N95-12493
Electromagnetic on-aircraft antenna radiation in the presence of composite plates
[NASA-CR-196126] p 284 N95-12856
Stimulated scattering of a slow electromagnetic wave excited by the relativistic electron beam
[DE94-625049] p 285 N95-13343
ELECTROMAGNETIC SPECTRA
X-ray and gamma ray astronomy detectors
[NASA-SP-517] p 379 N95-12304
SeaWiFS technical report series. Volume 23: SeaWiFS prelaunch radiometric calibration and spectral characterization
[NASA-TM-104566-VOL-23] p 328 N95-12359
ELECTROMAGNETIC WAVE TRANSMISSION
Light beam and pulse propagation in nonlinear dielectrics
[AD-A282548] p 282 N95-12496
ELECTROMAGNETISM
Singularity of the Green dyadics for bi-isotropic
[PB94-184504] p 283 N95-12581
Proceedings of Bianisotropics 1993: Seminar on Electrodynamics of Chiral and Bianisotropic Media
[PB94-179314] p 283 N95-12595
ELECTROMAGNETS
Annular suspension and pointing system with controlled DC electromagnets
[NASA-CR-197206] p 302 N95-12666
ELECTROMECHANICAL DEVICES
Design and application of electromechanical actuators for deep space missions
[NASA-CR-196791] p 299 N95-11701
Design of a ZVS PWM inverter for a brushless DC motor in an EMA application
[NASA-CR-195808] p 312 N95-12620
Military applications of microelectromechanical systems
[AD-A282470] p 289 N95-13291
ELECTROMECHANICS
Recycle requirements for Nasa's 30 cm xenon ion thruster
[NASA-TM-106668] p 258 N95-12750
ELECTROMYOGRAPHY
Preconditioning electromyographic data for an upper extremity model using neural networks
[NASA-CR-196877] p 332 N95-11708
ELECTRON BEAMS
Review of electron beam microinstabilities and their relevance to EBIS devices
[DE94-013755] p 364 N95-11746
Beams 92: Proceedings
[DE94-014783] p 361 N95-11792
Development of nanostructure fabrication technology and new electron-quantum wave devices
[AD-A281724] p 286 N95-11860
Free electron lasers and other advanced sources of light: Scientific research opportunities p 297 N95-12375
Plasma effects on electron beam dynamics in a virtual cathode oscillator p 366 N95-12436
Study on surface treatment by pulsed electron beams p 366 N95-12437
ELECTRON BOMBARDMENT
Studies of positron induced luminescence from polymers
[DE94-013622] p 272 N95-11733
ELECTRON DENSITY (CONCENTRATION)
Magnetic field generation in shock waves
[AD-A282234] p 281 N95-12408
Experimental and theoretical study of neon-like selenium x-ray laser spectral line profiles
[DE94-015327] p 298 N95-12761
ELECTRON DIFFRACTION
Naval research reviews, volume 46, February 1994
[AD-A281435] p 265 N95-11827
Structure-phase state of thick amorphous and microcrystalline chromium-carbon films deposited by ion-plasma sputtering
[DE94-624236] p 277 N95-13535
ELECTRON DISTRIBUTION
Absorption of intense microwaves and ion acoustic turbulence due to heat transport
[DE94-015140] p 369 N95-13285
ELECTRON EMISSION
The field emission of electrons in vacuum insulation systems p 357 N95-12101
A brightness comparison of thermionic electron sources in a TEM
[DE94-013300] p 360 N95-13338
ELECTRON ENERGY
Pioneer Venus orbiter electron temperature probe
[NASA-CR-196844] p 257 N95-11805
Anode sheath contributions in plasma thrusters
[AD-A280395] p 364 N95-11837
Magnetic field generation in shock waves
[AD-A282234] p 281 N95-12408
Helical temperature perturbations associated with tearing modes in tokamak plasmas
[DE94-014708] p 369 N95-12867
ELECTRON GUNS
Mixed clusters from the coexpansion of C2F6 and n2 in a pulsed, supersonic expansion cluster ion source and beam deflection time-of-flight mass spectrometer: A first application
[AD-A282044] p 361 N95-11910
ELECTRON IRRADIATION
Study on surface treatment by pulsed electron beams p 366 N95-12437
Time-resolved electron thermal conduction by probing of plasma formation in transparent solids with high power subpicosecond laser pulses
[DE94-015170] p 370 N95-13555
ELECTRON PARAMAGNETIC RESONANCE
Optical and magnetic resonance investigations of 3D ions in single crystal hosts: Candidates for tunable solid-state lasers
[AD-A281726] p 371 N95-11842
ELECTRON SCATTERING
Evaluation of the improvement in the figure of merit of Bi2Te3 - based alloys with addition of ultrafine scattering centers
[DE94-015363] p 374 N95-13059
Energy dissipation by a longitudinal Raman process
[DE94-015027] p 359 N95-13173
ELECTRON SOURCES
A brightness comparison of thermionic electron sources in a TEM
[DE94-013300] p 360 N95-13338
ELECTRON TRAJECTORIES
Velocity spread of REB generated by high current diode
[IPPCZ-339] p 364 N95-11886
ELECTRON TRANSFER
Magnetic field generation in shock waves
[AD-A282234] p 281 N95-12408
Proceedings of the Eighteenth DOE Solar Photochemistry Research Conference
[DE94-014926] p 318 N95-13126

Activities of Lehigh University
[AD-A282098] p 375 N95-13168
ELECTRONIC AIRCRAFT
Conceptual design of the AE481 Demon Remotely Piloted Vehicle (RPV)
[NASA-CR-197164] p 238 N95-12294
ELECTRONIC BULLETIN BOARDS
A hitchhiker's guide to microscopy and microanalysis using telecommunications, Email and The Internet
[DE94-013299] p 285 N95-13057
ELECTRONIC EQUIPMENT
Vulnerability assessment of a space based weapon platform electronics system exposed to a thermonuclear weapon detonation
[DE94-013415] p 250 N95-11755
Scintillating fiber detector performance, detector geometries, trigger, and electronics issues for scintillating fiber tracking
[DE94-015525] p 358 N95-12905
ELECTRONIC EQUIPMENT TESTS
Self-checking state machine realizations in CMOS
[AD-A282177] p 286 N95-12421
ELECTRONIC MAIL
A hitchhiker's guide to microscopy and microanalysis using telecommunications, Email and The Internet
[DE94-013299] p 285 N95-13057
ELECTRONIC MODULES
Using secure coprocessors
[AD-A281255] p 340 N95-12524
Design of a ZVS PWM inverter for a brushless DC motor in an EMA application
[NASA-CR-195808] p 312 N95-12620
Space Station Module Power Management and Distribution System (SSM/PMAD)
[NASA-CR-193991] p 258 N95-12819
ELECTRONIC WARFARE
Ultrawideband shipboard electrooptic electromagnetic environment monitoring
[AD-A282369] p 280 N95-11943
ELECTRONS
Studies of positron induced luminescence from polymers
[DE94-013622] p 272 N95-11733
The field emission of electrons in vacuum insulation systems p 357 N95-12101
Studies of electromagnetic ion cyclotron waves using AMPTE/CCE and dynamics explorer
[NASA-CR-196437] p 361 N95-12102
Free electron lasers and other advanced sources of light: Scientific research opportunities p 297 N95-12375
ELECTROPHYSIOLOGY
Modelling of biopotential recordings and its implications for instrumentation design
[PB94-206844] p 332 N95-13408
ELECTROSTATIC CHARGE
PASP PLUS Transient Pulse Monitor (TPM): Preflight characterization report
[AD-A282582] p 283 N95-12550
ELECTROSTATIC PROBES
Feedback control and stabilization experiments on the Texas Experimental Tokamak (TEXT)
[DE94-015214] p 368 N95-12758
ELECTROSTATIC PROPULSION
Fusion powered human transport to Mars (UWFR94)
[NASA-CR-197184] p 368 N95-12641
ELECTROSTATICS
Enhancement of EMAG: A 2-D electrostatic and magnetostatic solver for MATLAB
[AD-A283446] p 354 N95-13143
ELEMENTARY PARTICLE INTERACTIONS
The odderon in the deep-inelastic lepton-hadron scattering
[DE94-622791] p 360 N95-13274
ELEVATION
The impact of elevation data representation on nocturnal drainage wind simulations
[DE94-014752] p 326 N95-12927
ELLIPSOMETRY
Diagnostic techniques for semiconductor materials processing
[AD-A282810] p 373 N95-12602
ELLIPTIC DIFFERENTIAL EQUATIONS
Visualizing parallel numerical software performance on a shared memory multiprocessor
[PB94-195658] p 352 N95-13437
ELLIPTICAL POLARIZATION
Plane-wave reflection from uniaxial chiral interface and its application to polarization transformation
[PB94-184496] p 283 N95-12580
EMBEDDING
Extensions and contractions of the Lie algebra of q-pseudodifferential symbols
[PB94-192374] p 352 N95-12603
EMBRITTLEMENT
Studies of low temperature, low flux radiation embrittlement of nuclear reactor structural materials
[DE94-013710] p 269 N95-11738
EMISSION
Trichloroethylene emissions reductions achieved by enclosing solvent spray degreasing operations
[DE94-013741] p 318 N95-11742
Observation of a soft x ray emitting core in a dense plasma focus p 367 N95-12445
EMISSION SPECTRA
Investigation of physical parameters in stellar flares observed by GINGA
[NASA-CR-196823] p 381 N95-11928
An estimate of the evolution of the acoustic emission spectrum of rocks on the basis of changes in its average frequency in the process of deformation p 323 N95-12112
BATSE observations of 3C273
[NASA-CR-196185] p 380 N95-12463
Hot absorbers and the x-ray spectra of BL Lac objects
[NASA-CR-196196] p 380 N95-12465
The terrestrial gravitational wave environment from known sources
[NASA-CR-196167] p 323 N95-12468
Effects of sample formulation on the analysis of heavy metals by x-ray fluorescence
[AD-A282733] p 267 N95-12836
A calibration of the Naval Postgraduate School middle ultraviolet spectrograph and an analysis of the OII 2470 A emission obtained by the middle ultraviolet spectrograph
[AD-A283449] p 354 N95-13144
EMISSIVITY
Common understandings of phenomena in z-pinches p 367 N95-12447
EMITTERS
Radiative performance of rare earth garnet thin film selective emitters
[NASA-TM-106722] p 372 N95-11876
Emittance theory for thin film selective emitter
[NASA-TM-106727] p 317 N95-11903
Silicon carbide and sicaln heterojunction bipolar transistor structures
[AD-D016403] p 288 N95-13181
EMOTIONAL FACTORS
Tank crew performance related to cognitive ability and motivation of the tank crew members
[PB94-190642] p 335 N95-11872
Characteristics of civil aviation atmospheric hazards p 235 N95-13208
EMULSIONS
Microemulsions as reaction media: Literature review
[PB94-184553] p 267 N95-12585
END EFFECTORS
Self calibrating autoTRAC
[NASA-CR-196930] p 348 N95-11998
ENERGETIC PARTICLES
Effect of stochastic damping resonance wave packet on energetic alpha particle transport
[DE94-625041] p 370 N95-13538
ENERGY ABSORPTION
Absorption of intense microwaves and ion acoustic turbulence due to heat transport
[DE94-015140] p 369 N95-13285
ENERGY ABSORPTION FILMS
Radiative performance of rare earth garnet thin film selective emitters
[NASA-TM-106722] p 372 N95-11876
Emittance theory for thin film selective emitter
[NASA-TM-106727] p 317 N95-11903
ENERGY BUDGETS
User's manual for the NASA Lewis ice accretion/heat transfer prediction code with electrothermal deicer input
[NASA-CR-4530] p 291 N95-11888
Satellite estimates of shortwave surface radiation and atmospheric meteorology for the BOREAS experiment region
[NASA-TM-109132] p 326 N95-12639
ENERGY CONSERVATION
Composites (CFCCs) for low cost energy and cleaner environment
[DE94-013601] p 272 N95-11781
Advanced Industrial Materials Program
[DE94-015528] p 279 N95-12942
Simulating the energy performance of holographic glazings
[DE94-014969] p 296 N95-13158
ENERGY CONVERSION EFFICIENCY
Radiative performance of rare earth garnet thin film selective emitters
[NASA-TM-106722] p 372 N95-11876
Emittance theory for thin film selective emitter
[NASA-TM-106727] p 317 N95-11903
ENERGY DISSIPATION
Anode sheath contributions in plasma thrusters
[AD-A280395] p 364 N95-11837
Energy dissipation by a longitudinal Raman process
[DE94-015027] p 359 N95-13173
ENERGY REQUIREMENTS
PowerSat: A technology demonstration of a solar power satellite
[NASA-CR-197210] p 253 N95-12661
ENERGY STORAGE
TKKMOD: A computer simulation program for an integrated wind diesel system. Version 1.0: Document and user guide
[PB94-179090] p 317 N95-11798
Gas-puff Z-pinch driven by inductive energy storage pulsed power generator ASO-2 p 366 N95-12439
ENERGY TECHNOLOGY
PowerSat: A technology demonstration of a solar power satellite
[NASA-CR-197210] p 253 N95-12661
Proceedings of the 36th Power Sources Conference
[AD-A281443] p 288 N95-13164
ENERGY TRANSFER
Magnetospheric-ionospheric Poynting flux
[NASA-CR-196856] p 322 N95-11801
Scale disparity and spectral transfer in anisotropic numerical turbulence
[NASA-CR-194956] p 291 N95-11929
Towards tailored interphase formation utilizing surface-active benzylsulfonium salts as cationic initiators
[AD-A282511] p 262 N95-12398
Electronic energy transfer in new polymer nanocomposite assemblies
[AD-A282233] p 274 N95-12407
Methods of modeling radiant energy exchange in radiation fog and clouds
[AD-A283509] p 326 N95-12624
Proceedings of the Eighteenth DOE Solar Photochemistry Research Conference
[DE94-014926] p 318 N95-13126
ENGINE AIRFRAME INTEGRATION
Cabin-fuselage-wing structural design concept with engine installation
[NASA-CR-197172] p 242 N95-12993
ENGINE DESIGN
Viper cabin-fuselage structural design concept with engine installation and wing structural design
[NASA-CR-197162] p 239 N95-12305
Open-chamber combustion study
[PB94-184090] p 301 N95-12579
Mars methane engine
[NASA-CR-197205] p 302 N95-12668
Regulatory impact analysis and regulatory support document: Control of air pollution; determination of significance for nonroad sources and emission standards for new nonroad compression-ignition engines at or above 37 kilowatts (50 horsepower)
[PB94-194594] p 321 N95-12855
NASA's Hypersonic Research Engine Project: A review
[NASA-TM-107759] p 244 N95-12860
ENGINE MONITORING INSTRUMENTS
High temperature strain gage technology for gas turbine engines
[NASA-CR-191177] p 295 N95-11996
ENGINE PARTS
Brush seals for turbine engine fuel conservation p 306 N95-13595
Air Force seal activities p 306 N95-13600
Hypersonic engine seal development at NASA Lewis Research Center p 307 N95-13602
Relative performance comparison between baseline labyrinth and dual-brush compressor discharge seals in a T-700 engine test p 307 N95-13607
Some metallographic results for brush bristles and brush segments of a shroud ring brush seal tested in a T-700 engine p 307 N95-13608
ENGINE TESTS
Shock-tunnel combustor testing for hypersonic vehicles
[NASA-CR-196836] p 246 N95-11938
Mars methane engine
[NASA-CR-197205] p 302 N95-12668
NASA's Hypersonic Research Engine Project: A review
[NASA-TM-107759] p 244 N95-12860
Relative performance comparison between baseline labyrinth and dual-brush compressor discharge seals in a T-700 engine test p 307 N95-13607
Some metallographic results for brush bristles and brush segments of a shroud ring brush seal tested in a T-700 engine p 307 N95-13608
ENGINEERING
JPRS report: Science and technology. Central Eurasia: Life sciences
[JPRS-ULS-93-014] p 318 N95-11743

JPRS report: Science and technology. Central Eurasia: Life sciences
[JPRS-ULS-93-012] p 332 N95-11744
Engineering the future with America's high school students p 377 N95-11958
JPRS report: Science and technology. Central Eurasia
[JPRS-UST-94-017] p 247 N95-12001
JPRS report: Science and technology. Central Eurasia
[JPRS-UST-94-020] p 389 N95-12002
JPRS report: Science and technology. Central Eurasia
[JPRS-UST-94-019] p 389 N95-12003

ENGINEERS
Technical paper contest for women 1992. Space challenges: Earth and beyond
[NASA-TM-109953] p 386 N95-11955
Engineering the future with America's high school students p 377 N95-11958

ENTHALPY
Thermophysical properties of MtBE (methyl tertbutyl ether)
[ESDU-94010] p 265 N95-11775

ENVIRONMENT EFFECTS
Global ice sheet modeling
[DE94-013744] p 318 N95-11745
Improving the efficiency of high purity water systems
[DE94-013742] p 318 N95-11784

ENVIRONMENT MODELS
SO2 guideline document
[PB94-181393] p 319 N95-11893

ENVIRONMENT PROTECTION
Directory of OAQPS information services, May 1994
[PB94-181310] p 318 N95-11848
Implementation strategy for the Clean Air Act Ammendments of 1990. Update, May 1994
[PB94-180700] p 319 N95-11849
SO2 guideline document
[PB94-181393] p 319 N95-11893
Access EPA
[PB93-170041] p 319 N95-12356
A study of aircraft post-crash fuel fire mitigation
[AD-A282208] p 234 N95-12499
Design of a vehicle based system to prevent ozone loss
[NASA-CR-197199] p 242 N95-12702
Environmental and customer-driven seal requirements p 305 N95-13588

ENVIRONMENTAL CONTROL
Carbon dioxide and water vapor production at rest and during exercise. A report on data collection for the Crew and Thermal Systems Division
[NASA-TP-3500] p 337 N95-11811

ENVIRONMENTAL ENGINEERING
Communications plan — Design of the public wing of the Oregon State University Hatfield Marine Science Center
[NASA-CR-196435] p 314 N95-12231
Proceedings of the CTU Seminar 1994, Part C
[DE94-624078] p 390 N95-12946

ENVIRONMENTAL MONITORING
Activities of the Helsinski University of Technology, Applied Electronics Laboratory
[PB94-179074] p 385 N95-11797
AIRSAR software: Computer programs for preprocessing of JPL compressed polarimetric SAR data
[PB94-179116] p 280 N95-11800
SeaWiFS technical report series. Volume 19: Case studies for SeaWiFS calibration and validation, part 2
[NASA-TM-104566-VOL-19-PT-2] p 328 N95-11920
Millimeter-wave radiometric utility study
[AD-A282524] p 281 N95-12402

ENVIRONMENTAL SURVEYS
Environmental process improvement feasibility study and demonstration program
[NASA-CR-196789] p 319 N95-12110

ENZYMES
Rational enzyme redesign
[DE94-014565] p 331 N95-12677

EPIDEMIOLOGY
Aviation epidemiology data register: Cardiovascular disease screening outcomes in the North Dakota Army National Guard aviator cohort
[AD-A283064] p 334 N95-13054

EPITAXY
Electrochemical epitaxy
[AD-A282403] p 373 N95-11993

EPITHELIUM
Morphological differentiation of colon carcinoma cell lines in rotating wall vessels
[NASA-CR-196780] p 333 N95-11808

EPOXY COMPOUNDS
Multifunctional acrylic ether monomers, their polymers, and polymerizable epoxide derivatives from simple alpha-substitution of alkyl acrylates
[AD-A282513] p 273 N95-12400

EPOXY RESINS
Damage tolerance of candidate thermoset composites for use on single stage to orbit vehicles
[NASA-TP-3506] p 261 N95-11816
Radiation-induced structural changes, 4
[DE94-753223] p 356 N95-11817
Adherend surface effects on epoxy cure by NMR
[AD-A282165] p 274 N95-12420
Elimination of internal contamination on semiconductor devices (protective coatings)
[DE94-015868] p 275 N95-12945
The structural basis for fatigue failure initiation in glassy polymers
[DE94-015415] p 275 N95-13060

EQUATIONS
Stress analysis of laminated flat plates
[ESDU-94004] p 309 N95-11770

EQUATIONS OF MOTION
The effect of passive damping on feedback control performance of flexible manipulators
[DE94-015000] p 304 N95-13182

EQUATIONS OF STATE
Generation of ultra-high magnetic fields for AGEX
[DE94-015171] p 368 N95-12757

EQUINOXES
A catalogue of potentially bright close binary gravitational wave sources
[NASA-CR-196934] p 379 N95-12234

EQUIPMENT SPECIFICATIONS
Methodologies for processing plant material into acceptable food on a small scale
[NASA-CR-177647] p 338 N95-12132
Stepper motor
[NASA-CR-189373] p 287 N95-12795

EQUIPOTENTIALS
The reflection of relativistic electron beam by virtual cathode
[IPPCZ-338] p 364 N95-11916

EQUIVALENCE
STEP: An international collaboration in fundamental physics p 354 N95-12229
Learning unions of boxes with membership and equivalence queries
[DE94-014662] p 350 N95-12866

ERBIUM
The magnetic structure of holmium-erbium superlattices
[DE94-013728] p 371 N95-11739

ERGOMETERS
Comparison of submaximal cycling and treadmill exercise at similar work rates
[AD-A283430] p 334 N95-12593

EROSION
Moisture induced pressures in concrete airfield pavements
[AD-A281974] p 245 N95-11789

ERROR ANALYSIS
Stability and error estimation for Component Adaptive Grid methods
[NASA-CR-196492] p 351 N95-11883
Prediction of geometric-thermal machine tool errors by artificial neural networks
[PB94-186673] p 348 N95-11909
A new algorithm for five-hole probe calibration, data reduction, and uncertainty analysis
[NASA-TM-106458] p 232 N95-12378
Initial analysis and modeling results from the Polar Orbiting Geomagnetic Survey (POGS) satellite
[AD-A283454] p 253 N95-12545
Is the pollution effect of the FEM avoidable for the Helmholtz equation considering high wave numbers?
[AD-A282585] p 352 N95-12552
Gaussian paired comparison models
[PB94-179025] p 352 N95-12820
Satellite laser ranging and gravity field modeling accuracy
[NASA-CR-196057] p 248 N95-12837

ERROR CORRECTING CODES
Achieving unequal error protection with convolutional codes
[NASA-CR-196803] p 341 N95-11763
An efficient system for reliably transmitting image and video data over low bit rate noisy channels
[NASA-CR-196802] p 341 N95-11764
Burst transmission in the HF band: A system analysis and proposal for improvement
[PB94-190733] p 280 N95-11821

ERROR DETECTION CODES
Achieving unequal error protection with convolutional codes
[NASA-CR-196803] p 341 N95-11763

ERROR FUNCTIONS
Computerized design and generation of low-noise helical gears with modified surface topology
[NASA-TM-106696] p 303 N95-13083

ESTIMATES
Meeting the nation's needs for biomedical and behavioral scientists
[LC-94-66477] p 330 N95-12310

ESTIMATING
An estimate of the evolution of the acoustic emission spectrum of rocks on the basis of changes in its average frequency in the process of deformation p 323 N95-12112
Study of adaptive high resolution frequency estimation techniques with hydroacoustical applications
[PB94-179512] p 355 N95-12597

ETCHING
Method for laser-assisted etching of III-V and II-VI semiconductor compounds using chlorofluorocarbon ambients
[AD-D016385] p 298 N95-12779

ETHERS
Thermophysical properties of MtBE (methyl tertbutyl ether)
[ESDU-94010] p 265 N95-11775
Thermal conductivity of gaseous oxygenated aliphatic hydrocarbons. Alcohols, aldehydes, ketones and ethers
[ESDU-94018] p 265 N95-11795
Chiral recognition in molecular and macromolecular pairs of (S)- and (R)-1-cyano-2-methylpropyl 4'(4-(8-vinyloxyoctyloxy)benzoyl) biphenyl-4-carboxylate enantiomers
[AD-A281438] p 356 N95-11828
Multifunctional acrylic ether monomers, their polymers, and polymerizable epoxide derivatives from simple alpha-substitution of alkyl acrylates
[AD-A282513] p 273 N95-12400
Adherend surface effects on epoxy cure by NMR
[AD-A282165] p 274 N95-12420

ETHYL ALCOHOL
CeO2-ZrO2 powder synthesis by way of alcohol dehydration of aqueous salt solutions
[INPE-5484-PRE/1783] p 276 N95-13191

ETHYLENE COMPOUNDS
Additives in bituminous materials and fuel-resistant sealers
[DOT/FAA/CT-94/78] p 273 N95-12131

EUKARYOTES
Regulation of alternative CO2 fixation pathways in prokaryotic and eukaryotic photosynthetic organisms
[DE94-013180] p 331 N95-13271

EULER EQUATIONS OF MOTION
Control theory based airfoil design using the Euler equations
[NASA-CR-196360] p 230 N95-11884
Boundary conditions for unsteady compressible flows
[NASA-TM-106737] p 293 N95-12380

EVALUATION
Validating medical knowledge based systems
[PB94-191301] p 377 N95-11824

EVANESCENCE
Fibre optic sensors using adiabatically tapered single mode fibres
[AD-A282306] p 362 N95-12415

EVOLUTION (LIBERATION)
Quantitative understanding of the cycles of oxidized and reduced sulfur on Venus
[NASA-CR-196924] p 382 N95-12011

EXCIMER LASERS
Method for laser-assisted etching of III-V and II-VI semiconductor compounds using chlorofluorocarbon ambients
[AD-D016385] p 298 N95-12779

EXCITONS
Radiation-induced structural changes, 3
[DE94-753401] p 371 N95-11819
Photogeneration of charge carriers in bilayer assemblies of conjugated rigid-rod polymers
[AD-A282625] p 275 N95-12537
Magneto-optical properties of quantum structures with reduced dimensionality
[AD-A282597] p 376 N95-12553

EXERCISE PHYSIOLOGY
Carbon dioxide and water vapor production at rest and during exercise. A report on data collection for the Crew and Thermal Systems Division
[NASA-TP-3500] p 337 N95-11811

EXHAUST EMISSION
Regulatory impact analysis and regulatory support document: Control of air pollution; determination of significance for nonroad sources and emission standards for new nonroad compression-ignition engines at or above 37 kilowatts (50 horsepower)
[PB94-194594] p 321 N95-12855
Aircraft wake RCS measurement p 235 N95-13210

EXHAUST GASES
Allocating CO2-emissions by using equity rules and optimization
[PB94-192861] p 320 N95-12776

Regulatory impact analysis and regulatory support document: Control of air pollution; determination of significance for nonroad sources and emission standards for new nonroad compression-ignition engines at or above 37 kilowatts (50 horsepower)
[PB94-194594] p 321 N95-12855

EXOBIOLOGY
Aerospace medicine and biology: A continuing bibliography with indexes (supplement 394)
[NASA-SP-7011(394)] p 335 N95-13230

EXPERIENCE
Age 60 study. Part 4: Experimental evaluation of pilot performance
[REPT-8025-4B] p 336 N95-13199

EXPERIMENT DESIGN
Optimal experimental designs for the estimation of thermal properties of composite materials
[NASA-CR-196792] p 261 N95-11700
Design and application of electromechanical actuators for deep space missions
[NASA-CR-196791] p 299 N95-11701
GASCAN 2 payload integration
[NASA-CR-197200] p 278 N95-12701

EXPERT SYSTEMS
Design issues of human operator support systems
[PB94-191376] p 337 N95-11778
Validating medical knowledge based systems
[PB94-191301] p 377 N95-11824
A model-based expert system for space power distribution diagnostics
[NASA-CR-195336] p 342 N95-11918
A decision support system for tolerance allocation
[NASA-CR-195817] p 308 N95-11994
Thunderstorm hypothesis reasoner
[AD-A282664] p 326 N95-12805
Intelligent control systems research
[NASA-CR-195380] p 349 N95-12811

EXPLODING WIRES
Resistivity variation of fuse as an opening switch
p 365 N95-12430

EXPLOITATION
Exploitation of virtual reality architectures
[AD-A282263] p 340 N95-12413
Lunar vertical-shaft mining system
[NASA-CR-197154] p 384 N95-13497

EXPLOSIVES
Generation of ultra-high magnetic fields for AGEX
[DE94-015171] p 368 N95-12757

EXPONENTS
Chaotic time series. Part 1: Estimation of invariant properties in state space
[PB94-206968] p 376 N95-13572

EXPOSURE
Simultaneous gas-chromatographic determination of four toxic gases generally present in combustion atmospheres
[DOT/FAA/AM-94/18] p 338 N95-12354
Ten-year ground exposure of composite materials used on the Bell Model 206L helicopter flight service program
[NASA-TP-3468] p 262 N95-12357
Radiofrequency/microwave radiation biological effects and safety standards: A review
[AD-A282886] p 334 N95-12919

EXTINCTION
UV extinction and IR emission in diffuse H2 regions
[NASA-CR-196939] p 323 N95-12244

EXTRASOLAR PLANETS
The detectability of extrasolar terrestrial and giant planets during their luminous final accretion
[NASA-CR-196147] p 381 N95-13012

EXTRATERRESTRIAL INTELLIGENCE
Search for extraterrestrial intelligence/High Resolution Microwave Survey team member
[NASA-CR-196478] p 339 N95-13026

EXTRATERRESTRIAL RADIATION
Basic mechanisms of radiation effects in the natural space radiation environment
[DE94-013445] p 384 N95-11757

EXTRATERRESTRIAL RESOURCES
Project Genesis: Mars in situ propellant technology demonstrator mission
[NASA-CR-197166] p 277 N95-12822
Project Hyreus: Mars sample return mission utilizing in situ propellant production
[NASA-CR-197189] p 383 N95-12826

EXTRAVEHICULAR ACTIVITY
Evaluation of COSTAR mass handling characteristics in an environment. A simulation of the Hubble Space Telescope service mission
[NASA-TP-3489] p 333 N95-11887
Interviews with the Apollo lunar surface astronauts in support of planning for EVA systems design
[NASA-TM-108846] p 337 N95-11905
Meeting the challenge of manned lunar and Martian exploration p 339 N95-11970

EXTRAVEHICULAR MOBILITY UNITS
M.E.366-J embodiment design project: Portable foot restraint
[NASA-CR-197163] p 338 N95-12361
The embodiment design of the heat rejection system for the portable life support system
[NASA-CR-197178] p 338 N95-12555

EYE (ANATOMY)
Scene analysis: A brief survey
[PB94-205085] p 336 N95-13433

EYE MOVEMENTS
Visual psychophysics of egomotion
[AD-A282547] p 335 N95-12495
Coordinated action in 3-D space
[AD-A281284] p 336 N95-13375
Eye-gaze determination of user intent at the computer interface
[DE94-012337] p 363 N95-13421

F

F REGION
Guest investigator program study: Physics of equatorial plasma bubbles
[NASA-CR-196150] p 368 N95-12853

F-15 AIRCRAFT
Dynamic ground effects flight test of an F-15 aircraft
[NASA-TM-4604] p 231 N95-12191
The development of the F100-PW-220 and F110-GE-100 engines: A case study of risk assessment and risk management
[AD-A282467] p 244 N95-13289

F-16 AIRCRAFT
The development of the F100-PW-220 and F110-GE-100 engines: A case study of risk assessment and risk management
[AD-A282467] p 244 N95-13289

FABRICATION
Fabrication of large area Si cylindrical drift detectors
[DE94-013534] p 295 N95-11780
Selection process for trade study: Graphite Composite Primary Structure (GCPS)
[NASA-CR-196866] p 261 N95-11803
Test Plans. Lightweight Durable TPS: Tasks 1,2,4,5, and 6
[NASA-CR-196867] p 262 N95-11835
Development of nanostructure fabrication technology and new electron-quantum wave devices
[AD-A281724] p 286 N95-11860
Silicon-based blue light emitting diode
[AD-A282382] p 286 N95-12009
Frequency doubler (from 4.7 to 9.4 GHz) using a diode
[AD-A282784] p 287 N95-12525

FABRY-PEROT INTERFEROMETERS
Studies of optical phase conjugators and applications
[AD-A282626] p 362 N95-12538
Improvements of HCN laser heterodyne interferometer for measuring plasma density
[DE94-625037] p 370 N95-13341

FACE CENTERED CUBIC LATTICES
Polycrystal models to fit experiments
[DE94-014419] p 374 N95-13078

FACILITIES
Target area chamber system design for the National Ignition Facility
[DE94-013347] p 364 N95-11754

FACTORIZATION
Parallel preconditioners for the conjugate gradient method
[PB94-201605] p 347 N95-13404

FAILURE
The use of an acoustic emission method to estimate the effect of manufacturing process and service factors on the failure of concrete p 311 N95-12108

FAILURE ANALYSIS
Moisture induced pressures in concrete airfield pavements
[AD-A281974] p 245 N95-11789
Failure analysis of woven and braided fabric reinforced composites
[NASA-CR-194981] p 262 N95-11926
Yield-before-break fracture mechanics analysis of high strength steel pressure vehicles
[AD-A282518] p 270 N95-12401

FAILURE MODES
An analysis of the load-bearing capacity of members of square cross section with a series of perpendicular notches p 312 N95-12631
Analytical and experimental vibration analysis of a faulty gear system
[NASA-TM-106689] p 303 N95-12843
The structural basis for fatigue failure initiation in glassy polymers
[DE94-015415] p 275 N95-13060

FALLOUT
CESIUM-137 and natural radionuclides in soils from Southern Brazil and in soils and others environmental samples from Antarctic
[INPE-5505-TDI-517] p 321 N95-13192

FAR INFRARED RADIATION
UV extinction and IR emission in diffuse H2 regions
[NASA-CR-196939] p 323 N95-12244

FAR ULTRAVIOLET RADIATION
The laser and its applications on environment and biotechnology research
[DE94-013831] p 299 N95-13076

FARM CROPS
Techniques for optimal crop selection in a controlled ecological life support system p 339 N95-11962
Methodologies for processing plant material into acceptable food on a small scale
[NASA-CR-177647] p 338 N95-12132

FATIGUE (MATERIALS)
A stochastic model of fatigue crack growth
p 309 N95-11698
High frequency flow/structural interaction in dense subsonic fluids handbook
[NASA-CR-194007] p 230 N95-11807
Revealing hidden defects: A hybrid evaluation strategy for steel structures
[PB94-191236] p 308 N95-11822
Fatigue in single crystal nickel superalloys
[AD-A283459] p 270 N95-12546
Effect of shear lips, loading transitions and test frequency on constant delta K and constant load amplitude fatigue tests
[PB94-192440] p 312 N95-12775
CGF cartridge development, volume 1
[NASA-CR-196508] p 270 N95-12830
Thermomechanical fatigue damage/failure mechanisms in SCS-6/Timetal 21S (0/90)s composite
[NASA-CR-191115] p 263 N95-13082

FATIGUE LIFE
Modeling and life prediction methodology for Titanium Matrix Composites subjected to mission profiles
[NASA-TM-109148] p 269 N95-11915
Large-displacement structural durability analyses of simple bend specimen emulating rocket nozzle liners
[NASA-TM-106521] p 312 N95-12818
Computer modelling of cyclic deformation of high-temperature materials
[AD-A282457] p 263 N95-12833
Cabin-fuselage-wing structural design concept with engine installation
[NASA-CR-197172] p 242 N95-12993
Thermomechanical fatigue damage/failure mechanisms in SCS-6/Timetal 21S (0/90)s composite
[NASA-CR-191115] p 263 N95-13082

FATIGUE TESTS
A study of fatigue crack growth in lugs under spectrum loading
[NAL-PD-SN-9407] p 311 N95-11879
A study of naturally initiating notch root fatigue cracks under spectrum loading
[NAL-PD-SN-9406] p 311 N95-11924
High temperature strain gage technology for gas turbine engines
[NASA-CR-191177] p 295 N95-11996
Effect of shear lips, loading transitions and test frequency on constant delta K and constant load amplitude fatigue tests
[PB94-192440] p 312 N95-12775
Analytical and experimental vibration analysis of a faulty gear system
[NASA-TM-106689] p 303 N95-12843

FAULT DETECTION
A model-based expert system for space power distribution diagnostics
[NASA-CR-195336] p 342 N95-11918
Efficient detection of deadlocks in Petri nets
[PB94-179405] p 343 N95-12366
Probability of detection of defects in coatings with electronic shearography
[NASA-CR-196201] p 308 N95-12391
Analytical and experimental vibration analysis of a faulty gear system
[NASA-TM-106689] p 303 N95-12843

FAULT TOLERANCE
Test plan. GCPS task 7, subtask 7.1: IHM development
[NASA-CR-106876] p 250 N95-11767
Stability and error estimation for Component Adaptive Grid methods
[NASA-CR-196492] p 351 N95-11883
On-line data reconstruction in redundant disk arrays
[AD-A282709] p 340 N95-12516
Recycle requirements for Nasa's 30 cm xenon ion thruster
[NASA-TM-106668] p 258 N95-12750

Delta-4: An open architecture for dependable systems
[PB94-195641] p 341 N95-13436
FAULT TREES
Mean importance measures for groups of events in fault trees
[DE94-015416] p 353 N95-13061
FEED SYSTEMS
High frequency flow/structural interaction in dense subsonic fluids handbook
[NASA-CR-194007] p 230 N95-11807
Various advanced design projects promoting engineering education
[NASA-CR-197170] p 258 N95-12630
FEEDBACK
The use of neuron nets to stabilize dynamic systems
p 348 N95-12109
Provoking and measuring cell losses in ATM systems by importance sampling, control variables and load cycles
[PB94-202520] p 285 N95-13558
FEEDBACK CONTROL
Annular suspension and pointing system with controlled DC electromagnets
[NASA-CR-197206] p 302 N95-12666
Feedback control and stabilization experiments on the Texas Experimental Tokamak (TEXT)
[DE94-015214] p 368 N95-12758
The effect of passive damping on feedback control performance of flexible manipulators
[DE94-015000] p 304 N95-13182
FEMALES
Technical paper contest for women 1992. Space challenges: Earth and beyond
[NASA-TM-109953] p 386 N95-11955
Education: A second career p 377 N95-11956
FERMI LIQUIDS
Synchrotron studies of narrow band materials
[DE94-013698] p 271 N95-13554
FERMI SURFACES
Magnetic field induced minigap in double quantum wells
[DE94-015013] p 376 N95-13172
FERMI-DIRAC STATISTICS
About the structure of the superconducting order parameter of 2 D Fermi system with an arbitrary particle density
[DE94-623268] p 375 N95-13277
FERRITES
Novel concepts in weld science: Role of gradients and composite structure
[DE94-015482] p 271 N95-12895
FERROELECTRICITY
Design and synthesis of tight pitch FLCs for analog voltage-limited electro-optic modulators
[AD-A281472] p 371 N95-11855
Intelligent processing of ferroelectric thin films
[AD-A282833] p 275 N95-12586
Method of laser processing ferroelectric materials
[AD-D016386] p 298 N95-12780
FERROMAGNETISM
Magnetic response of ultrathin Fe on MgO: A polarised neutron reflectometry study
[DE94-013192] p 375 N95-13272
FIBER COMPOSITES
Surface roughness characterization of various ceramic fibers using AFM and low voltage SEM
[DE94-013635] p 272 N95-11736
Elastic buckling of unbalanced laminated fibre reinforced composite plates (rectangular plates of AsBtDs type, all edges simply-supported under biaxial loading)
[ESDU-94006] p 310 N95-11772
Ceramic composites with ceramic fibers
[AD-D016315] p 275 N95-13175
Numerical simulations of creep in ductile-phase toughened intermetallic matrix composites
[DE94-014744] p 264 N95-13533
FIBER OPTICS
Ultrawideband shipboard electrooptic electromagnetic environment monitoring
[AD-A282369] p 280 N95-11943
Fibre optic sensors using adiabatically tapered single mode fibres
[AD-A282306] p 362 N95-12415
Studies of optical phase conjugators and applications
[AD-A282626] p 362 N95-12538
Activities of the Institute for Aerospace Studies of Toronto University p 390 N95-12699
Comprehensive and critical literature review on insitu micro-sensors for application in tribology
[AD-A281646] p 296 N95-13165
Fiber-optic sensors and the application to conditional monitoring for mechanical structures
[PB94-207057] p 363 N95-13574
FIBER ORIENTATION
Thermomechanical fatigue damage/failure mechanisms in SCS-6/Timetal 21S (0/90)s composite
[NASA-CR-191115] p 263 N95-13082
FIBER-MATRIX INTERFACES
Glass reinforced-diallylbisphenol/maleimide composites with modified interphases
[AD-A282496] p 264 N95-13298
FIBERS
Surface roughness characterization of various ceramic fibers using AFM and low voltage SEM
[DE94-013635] p 272 N95-11736
FIBERS (MATHEMATICS)
Hall conductance as a topological invariant
[PB94-179330] p 353 N95-12364
FIBROSIS
Consequences of prolonged inhalation of ozone on Fischer-344/N rats: Collaborative studies. Part 1: Content and cross-linking of lung collagen
[PB94-182748] p 331 N95-13176
FIELD COILS
A magnetic shield/dual purpose mission
[NASA-CR-197192] p 255 N95-13006
FIELD EFFECT TRANSISTORS
Ku-band high efficiency GaAs MMIC power amplifiers
[NASA-CR-182156] p 288 N95-13231
FIELD EMISSION
The field emission of electrons in vacuum insulation systems p 357 N95-12101
FIELD OF VIEW
SeaWiFS technical report series. Volume 22: Prelaunch acceptance report for the SeaWiFS radiometer
[NASA-TM-104566-VOL-22] p 328 N95-12151
SeaWiFS technical report series. Volume 23: SeaWiFS prelaunch radiometric calibration and spectral characterization
[NASA-TM-104566-VOL-23] p 328 N95-12359
Semiautomated methodology for measurement of field-of-view, magnification, and distortion of night vision devices as defined in MIL-A-49425(CR)
[AD-A282210] p 362 N95-12427
FIELD STRENGTH
The field emission of electrons in vacuum insulation systems p 357 N95-12101
Non-dipolar magnetic field models and patterns of radio emission: Uranus and Neptune compared
[NASA-CR-196412] p 385 N95-12469
FIELD THEORY (PHYSICS)
Quenched QCD at finite density
[DE94-011522] p 375 N95-13337
FIGHTER AIRCRAFT
Impact of agility requirements on configuration synthesis
[NASA-CR-4627] p 238 N95-11952
FIGURE OF MERIT
Evaluation of the improvement in the figure of merit of Bi2Te3 - based alloys with addition of ultrafine scattering centers
[DE94-015363] p 374 N95-13059
FILE MAINTENANCE (COMPUTERS)
Development of a change management system
p 377 N95-11963
FILM COOLING
Investigation of advanced counterrotation blade configuration concepts for high speed turboprop systems. Task 8: Cooling flow/heat transfer analysis
[NASA-CR-195359] p 244 N95-11901
FDNS code to predict wall heat fluxes or wall temperatures in rocket nozzles
[NASA-CR-196925] p 292 N95-11999
FILM THICKNESS
Electronic energy transfer in new polymer nanocomposite assemblies
[AD-A282233] p 274 N95-12407
FINE STRUCTURE
Raman structural studies of the nickel electrode
[NASA-CR-196331] p 289 N95-13344
FINES
Scanning tunneling microscopy/atomic force microscopy for study of nanoscale metal oxide particles (destructive adsorbents)
[AD-A281417] p 357 N95-11851
FINGERS
Minimal fixturing of frictionless assemblies: Complexity and algorithms
[AD-A282724] p 300 N95-12505
FINITE DIFFERENCE THEORY
Parallel aeroelastic computations for wing and wing-body configurations
[NASA-CR-196835] p 230 N95-11766
Interlaminar stress analysis of dropped-ply laminated plates and shells by a mixed method
[NASA-CR-196851] p 311 N95-11946
Numerical simulations of drop collisions
[NASA-TM-106751] p 295 N95-13550
FINITE ELEMENT METHOD
Investigation of finite element: ABC methods for electromagnetic field simulation
[NASA-CR-196837] p 279 N95-11707
Impact analysis on a massively parallel computer
[DE94-013624] p 346 N95-11734
Global ice sheet modeling
[DE94-013744] p 318 N95-11745
Sloshing analysis of tanks containing multiple fluid layers
[DE94-013333] p 290 N95-11753
Parallel aeroelastic computations for wing and wing-body configurations
[NASA-CR-196835] p 230 N95-11766
Accurate interlaminar stress recovery from finite element analysis
[NASA-TM-109149] p 310 N95-11815
Analysis of cylindrical wrap-around and doubly conformal patch antennas by way of the finite element-artificial absorber method
[NASA-CR-195211] p 281 N95-12382
Minimal fixturing of frictionless assemblies: Complexity and algorithms
[AD-A282724] p 300 N95-12505
Triaxial and torsional shear test results for sand
[AD-A282725] p 323 N95-12506
Modeling of split-core transformers for power transmission
[AD-A282782] p 287 N95-12509
Is the pollution effect of the FEM avoidable for the Helmholtz equation considering high wave numbers?
[AD-A282585] p 352 N95-12552
Neotectonics of Asia: Thin-shell finite-element models with faults
[NASA-CR-196436] p 324 N95-12949
Comparison of symbolic and numerical integration methods for an assumed-stress hybrid shell element
[NASA-CR-195945] p 313 N95-13096
Improved assumed-stress hybrid shell element with drilling degrees of freedom for linear stress, buckling, and free vibration analyses
[NASA-CR-192816] p 313 N95-13163
Numerical simulations of creep in ductile-phase toughened intermetallic matrix composites
[DE94-014744] p 264 N95-13533
FINITE VOLUME METHOD
Control theory based airfoil design using the Euler equations
[NASA-CR-196360] p 230 N95-11884
Validation of the RPLUS3D code for supersonic inlet applications involving three-dimensional shock wave-boundary layer interactions
[NASA-TM-106579] p 233 N95-13058
FINLAND
Observation results: Angle measurements in 1964-1965, 1971, 1984 and 1986-1987
[REPT-118] p 314 N95-11950
FIRE CONTROL
Evaluation of alternative in-flight fire suppressants for full-scale testing in simulated aircraft engine nacelles and dry bays
[PB94-203403] p 236 N95-13247
FIRES
Comparison of the KAMELEON fire model to large-scale open pool fire data
[DE94-013441] p 264 N95-11756
Trace gas emissions to the atmosphere by biomass burning in the west African savannas
[NASA-CR-196758] p 319 N95-11931
Fire propagation in concurrent flows
[PB94-193844] p 267 N95-12778
FISSION WEAPONS
Vulnerability assessment of a space based weapon platform electronics system exposed to a thermonuclear weapon detonation
[DE94-013415] p 250 N95-11755
FITTING
Body dimensions for apparel
[PB94-187739] p 338 N95-11908
FIXED WINGS
Flight dynamics of an unmanned aerial vehicle
[AD-A282259] p 239 N95-12410
FLAME HOLDERS
Study of a vortical/axial type flameholders with variable angle blades
[INPE-5558-TDI/538] p 266 N95-12302
FLAME PROPAGATION
Comparison of the KAMELEON fire model to large-scale open pool fire data
[DE94-013441] p 264 N95-11756
A study of aircraft post-crash fuel fire mitigation
[AD-A282206] p 234 N95-12499
AFOSR Contractors Meeting in Propulsion
[AD-A282729] p 257 N95-12507
Fire propagation in concurrent flows
[PB94-193844] p 267 N95-12778

Backdraft phenomena
[PB94-193927] p 267 N95-12852

FLAME RETARDANTS
Phosphazene-containing amine as curing agent for phthalonitrile-base polymer
[AD-D016375] p 276 N95-13179

FLAME TEMPERATURE
Comparison of the KAMELEON fire model to large-scale open pool fire data
[DE94-013441] p 264 N95-11756
Analysis of cost: Combustion flame CVD diamond deposition
[AD-A282527] p 273 N95-12403

FLAMES
Analysis of cost: Combustion flame CVD diamond deposition
[AD-A282527] p 273 N95-12403
Fire propagation in concurrent flows
[PB94-193844] p 267 N95-12778
Backdraft phenomena
[PB94-193927] p 267 N95-12852

FLAT PANEL DISPLAYS
Draft standard for color active matrix liquid crystal displays (AMLCDs) in US Military aircraft. Recommended best practices
[AD-A282950] p 243 N95-12591

FLAT PLATES
Stiffnesses of laminated flat plates
[ESDU-94003] p 309 N95-11769
Stress analysis of laminated flat plates
[ESDU-94004] p 309 N95-11770
Buckling of flat rectangular orthotropic plates
[ESDU-94005] p 310 N95-11771
Validation of the RPLUS3D code for supersonic inlet applications involving three-dimensional shock wave-boundary layer interactions
[NASA-TM-106579] p 233 N95-13058

FLATNESS
Polycrystal models to fit experiments
[DE94-014419] p 374 N95-13078

FLEXIBILITY
Integrated sensor bus
[PB94-206810] p 268 N95-13252

FLEXIBLE BODIES
Development of homotopy algorithms for fixed-order mixed H2/H(infinity) controller synthesis
[NASA-TP-3507] p 342 N95-11923

FLIGHT CHARACTERISTICS
Parallel methods for the flight simulation model
[DE94-013330] p 245 N95-11752

FLIGHT CONDITIONS
Role of wind tunnels and computer codes in the certification and qualification of rotorcraft for flight in forecast icing
[NASA-TM-106747] p 233 N95-13197

FLIGHT CONTROL
The development of a highly reliable power management and distribution system for civil transport aircraft
[NASA-TM-106697] p 243 N95-11867
Optimum aerodynamic design via boundary control
[NASA-CR-195882] p 230 N95-11877
Dynamic ground effects flight test of an F-15 aircraft
[NASA-TM-4604] p 231 N95-12191
Flight dynamics of an unmanned aerial vehicle
[AD-A282259] p 239 N95-12410
Triton 2 (1B)
[NASA-CR-197188] p 240 N95-12636
Piloted evaluation of an integrated methodology for propulsion and airframe control design
[NASA-TM-106741] p 245 N95-12763
Techniques for designing rotorcraft control systems
[NASA-CR-196192] p 245 N95-12791
Overview of NASREM: The NASA/NBS standard reference model for telerobot control system architecture re
[PB94-194560] p 303 N95-12854

FLIGHT CREWS
Visit to UDRI and USAF, Armstrong Lab., Williams AFB, Phoenix, USA, February 8-11, 1993
[PB94-190659] p 337 N95-11873
Crew factors in flight operations 9: Effects of planned cockpit rest on crew performance and alertness in long-haul operations
[NASA-TM-108839] p 334 N95-12792
Aviation epidemiology data register: Cardiovascular disease screening outcomes in the North Dakota Army National Guard aviator cohort
[AD-A283064] p 334 N95-13054
Standards relevant to a NATO anthropometry survey using 3D imaging tools
[AD-A283065] p 339 N95-13055

FLIGHT FATIGUE
Crew factors in flight operations 9: Effects of planned cockpit rest on crew performance and alertness in long-haul operations
[NASA-TM-108839] p 334 N95-12792

FLIGHT HAZARDS
Windshear certification data base for forward-look detection systems p 234 N95-13204
Characteristics of civil aviation atmospheric hazards p 235 N95-13208

FLIGHT MANAGEMENT SYSTEMS
Airborne Windshear Detection and Warning Systems. Fifth and Final Combined Manufacturers' and Technologists' Conference, part 2
[NASA-CP-10139-PT-2] p 234 N95-13203

FLIGHT MECHANICS
Activities of the Institute for Aerospace Studies of Toronto University p 390 N95-12699

FLIGHT OPERATIONS
Crew factors in flight operations 9: Effects of planned cockpit rest on crew performance and alertness in long-haul operations
[NASA-TM-108839] p 334 N95-12792

FLIGHT OPTIMIZATION
Application of multivariate optimisation techniques to determination of optimum flight path trajectories
[ESDU-94012] p 238 N95-11793
Examples of flight path optimisation using a multivariate gradient-search method. Addendum A: Variation of optimum flight profile parameters with range
[ESDU-94016-ADD-A] p 238 N95-11794

FLIGHT PATHS
Application of multivariate optimisation techniques to determination of optimum flight path trajectories
[ESDU-94012] p 238 N95-11793
Examples of flight path optimisation using a multivariate gradient-search method. Addendum A: Variation of optimum flight profile parameters with range
[ESDU-94016-ADD-A] p 238 N95-11794
Airborne Windshear Detection and Warning Systems. Fifth and Final Combined Manufacturers' and Technologists' Conference, part 2
[NASA-CP-10139-PT-2] p 234 N95-13203
Ground-based wake vortex monitoring, prediction, and ATC interface p 235 N95-13209
Doppler radar detection of vortex hazard indicators p 236 N95-13212

FLIGHT SAFETY
Age 60 Rule research. Part 1: Bibliographic database
[DOT/FAA/AM-94/20-PT-1] p 336 N95-13019
Age 60 Rule. Part 2: Airline pilot age and performance. A review of the scientific literature
[DOT/FAA/AM-94/21-PT-2] p 336 N95-13020
White Sands Test Facility
[NASA-TM-109901] p 249 N95-13129
Role of wind tunnels and computer codes in the certification and qualification of rotorcraft for flight in forecast icing
[NASA-TM-106747] p 233 N95-13197

FLIGHT SIMULATION
Parallel methods for the flight simulation model
[DE94-013330] p 245 N95-11752
Visit to UDRI and USAF, Armstrong Lab., Williams AFB, Phoenix, USA, February 8-11, 1993
[PB94-190659] p 337 N95-11873
Activities of the Institute for Aerospace Studies of Toronto University p 390 N95-12699
Piloted evaluation of an integrated methodology for propulsion and airframe control design
[NASA-TM-106741] p 245 N95-12763

FLIGHT SIMULATORS
Effects of mass on aircraft sidearm controller characteristics
[NASA-TM-104277] p 244 N95-11868
Age 60 study. Part 4: Experimental evaluation of pilot performance
[REPT-8025-4B] p 336 N95-13199

FLIGHT TESTS
Dynamic ground effects flight test of an F-15 aircraft
[NASA-TM-4604] p 231 N95-12191
Flight investigation of the use of a nose gear jump strut to reduce takeoff ground roll distance of STOL aircraft
[NASA-TM-108819] p 238 N95-12225
Flight dynamics of an unmanned aerial vehicle
[AD-A282259] p 239 N95-12410
Flight test of takeoff performance monitoring system
[NASA-TP-3403] p 245 N95-12664

FLORIDA
A comparison of two sites for the purpose of satellite laser ranging
[AD-A283149] p 299 N95-13139

FLOW CHARACTERISTICS
Fire propagation in concurrent flows
[PB94-193844] p 267 N95-12778

FLOW DISTRIBUTION
A shadowgraph study of the National Launch System's 1 1/2 stage vehicle configuration and Heavy Lift Launch Vehicle configuration --- Using the Marshall Space Flight Center's 14-Inch Trisonic Wind Tunnel
[NASA-RP-1347] p 229 N95-11710
High frequency flow/structural interaction in dense subsonic fluids handbook
[NASA-CR-194007] p 230 N95-11807
Structure of a swirl-stabilized, combusting spray
[NASA-TM-106724] p 243 N95-11880
Numerical analysis of tangential slot blowing on a generic chined forebody
[NASA-TM-108845] p 231 N95-11927
The development and application of the self-adaptive grid code, SAGE p 295 N95-11957
Computational flow predictions for hypersonic drag devices p 233 N95-11967
Test model designs for advanced refractory ceramic materials p 277 N95-11968
Interferograms, schlieren, and shadowgraphs constructed from real- and ideal-gas, two- and three-dimensional computed flowfields p 295 N95-11971
Experimental Aerodynamics Division
[NAL-SP-9404] p 229 N95-12166
Supersonic base flow investigation over axisymmetric afterbodies
[PB94-180957] p 232 N95-12578
Numerical time dependent sheet cavitation simulations using a higher order panel method
[PB94-204435] p 294 N95-13249

FLOW EQUATIONS
Control theory based airfoil design using the Euler equations
[NASA-CR-196360] p 230 N95-11884
A new Reynolds stress algebraic equation model
[NASA-TM-106644] p 292 N95-11953
Parallel algorithms for the spectral transform method
[DE94-015458] p 344 N95-12893

FLOW MEASUREMENT
A new algorithm for five-hole probe calibration, data reduction, and uncertainty analysis
[NASA-TM-106458] p 232 N95-12378
Impingement flow heat transfer measurements of turbine blades using a jet array
[AD-A283450] p 375 N95-12512
Planar Rayleigh scattering and laser-induced fluorescence for visualization of a hot, Mach 2 annular air jet
[NASA-TM-4576] p 247 N95-13196
Simultaneous three-dimensional velocity and mixing measurements by use of laser Doppler velocimetry and fluorescence probes in a water tunnel
[NASA-TP-3454] p 246 N95-13553

FLOW VELOCITY
Laser Doppler velocimeter measurements of boundary layer velocity and turbulent intensities in Mach 2.5 flow
[NASA-CR-196861] p 289 N95-11709
Fire propagation in concurrent flows
[PB94-193844] p 267 N95-12778
Simultaneous three-dimensional velocity and mixing measurements by use of laser Doppler velocimetry and fluorescence probes in a water tunnel
[NASA-TP-3454] p 246 N95-13553

FLOW VISUALIZATION
A shadowgraph study of the National Launch System's 1 1/2 stage vehicle configuration and Heavy Lift Launch Vehicle configuration --- Using the Marshall Space Flight Center's 14-Inch Trisonic Wind Tunnel
[NASA-RP-1347] p 229 N95-11710
Water tunnel flow visualization study of a 4.4 percent scale X-31 forebody
[NASA-TM-104276] p 230 N95-11898
Interferograms, schlieren, and shadowgraphs constructed from real- and ideal-gas, two- and three-dimensional computed flowfields p 295 N95-11971
Planar Rayleigh scattering and laser-induced fluorescence for visualization of a hot, Mach 2 annular air jet
[NASA-TM-4576] p 247 N95-13196
Simultaneous three-dimensional velocity and mixing measurements by use of laser Doppler velocimetry and fluorescence probes in a water tunnel
[NASA-TP-3454] p 246 N95-13553

FLUID DYNAMICS
Modeling jets in cross flow
[NASA-CR-194965] p 291 N95-11930
Evaluation of alternative in-flight fire suppressants for full-scale testing in simulated aircraft engine nacelles and dry bays
[PB94-203403] p 236 N95-13247
Fractional suspension crystallization of organic compounds
[PB94-206851] p 375 N95-13409

FLUID FILMS
A simplified thermohydrodynamic model for fluid film bearings
[DE94-015011] p 304 N95-13183

FLUID FLOW
Pipeline vibrations. Computer program for the prediction of fluid transients in flexible, unbranched three-dimensional piping systems
[ESDU-93031] p 309 N95-11768
Brush seal numerical simulation: Concepts and advances p 306 N95-13596
FLUID MANAGEMENT
Cryogenic On-Orbit Liquid Depot Storage, Acquisition, and Transfer satellite (COLD-SAT) feasibility study
[NASA-CR-185247] p 256 N95-13232
Feasibility study for a Cryogenic On-Orbit Liquid Depot-Storage, Acquisition and Transfer (COLD-SAT) satellite
[NASA-CR-185248] p 294 N95-13233
Feasibility study for the Cryogenic Orbital Nitrogen Experiment (CONE)
[NASA-CR-187231] p 294 N95-13234
Cryogenic On-Orbit Liquid Depot Storage, Acquisition, and Transfer Satellite (COLD-SAT)
[NASA-CR-185249] p 259 N95-13237
FLUID MECHANICS
Sloshing analysis of tanks containing multiple fluid layers
[DE94-013333] p 290 N95-11753
Laws of infrared similitude
[AD-A282209] p 354 N95-12426
Activities of the Institute for Aerospace Studies of Toronto University p 390 N95-12699
FLUID PRESSURE
Scaling fluid content-pressure relations of different fluid systems in porous media
[DE94-013349] p 294 N95-13075
FLUID-SOLID INTERACTIONS
Application of scanning tunneling microscopy to studies of electrode surfaces
[AD-A282383] p 373 N95-12004
FLUORESCENCE
Fibre optic sensors using adiabatically tapered single mode fibres
[AD-A282306] p 362 N95-12415
UV and fluorescence studies for vinyl polymerization
[AD-A281187] p 274 N95-12520
Laser spectroscopy of GdO: Ligand field assignments of 4f7(8S)6p reversing 4f7(8)6s transitions
[AD-A282827] p 268 N95-13180
Simultaneous three-dimensional velocity and mixing measurements by use of laser Doppler velocimetry and fluorescence probes in a water tunnel
[NASA-TP-3454] p 246 N95-13553
FLUORIDES
Phase A design study of microgravity fluoride fiber puller
[NASA-CR-196513] p 279 N95-12752
Ferric chloride graphite intercalation compounds prepared from graphite fluoride
[NASA-TM-106447] p 261 N95-12783
FLUORINATION
Ferric chloride graphite intercalation compounds prepared from graphite fluoride
[NASA-TM-106447] p 261 N95-12783
FLUORINE
Role of implantation-induced defects in surface-oriented diffusion of fluorine in silicon
[DE94-014905] p 374 N95-13125
Hydrogen bonding and molecular orientation in water/fluorine adlayers on silver(110)
[AD-A282652] p 268 N95-13549
FLUORINE COMPOUNDS
Method for laser-assisted etching of III-V and II-VI semiconductor compounds using chlorofluorocarbon ambients
[AD-D016385] p 298 N95-12779
FLUOROCARBONS
Method for laser-assisted etching of III-V and II-VI semiconductor compounds using chlorofluorocarbon ambients
[AD-D016385] p 298 N95-12779
Evaluation of alternative in-flight fire suppressants for full-scale testing in simulated aircraft engine nacelles and dry bays
[PB94-203403] p 236 N95-13247
FLUX DENSITY
Magnetospheric-ionospheric Poynting flux
[NASA-CR-196856] p 322 N95-11801
FLUX TRANSFER EVENTS
Ionospheric dynamics instrument investigation for the Timed Mission
[NASA-CR-196196] p 325 N95-13190
FLY BY WIRE CONTROL
The development of a highly reliable power management and distribution system for civil transport aircraft
[NASA-TM-106697] p 243 N95-11867
FLYWHEELS
A lunar/Martian anchor emplacement system
[NASA-CR-197193] p 302 N95-12690
FOCUSING
New multi-dimensional diagnostics method for intense ion beams p 365 N95-12432
FOG
Methods of modeling radiant energy exchange in radiation fog and clouds
[AD-A283509] p 326 N95-12624
FOILS (MATERIALS)
Experimental and theoretical study of neon-like selenium x-ray laser spectral line profiles
[DE94-015327] p 298 N95-12761
FOKKER-PLANCK EQUATION
Absorption of intense microwaves and ion acoustic turbulence due to heat transport
[DE94-015140] p 369 N95-13265
FOLDING STRUCTURES
Design studies of large aperture, high-resolution Earth science microwave radiometers compatible with small launch vehicles
[NASA-TP-3469] p 315 N95-12379
FOOD PRODUCTION (IN SPACE)
Growth of potatoes for CELSS
[NASA-CR-177646] p 338 N95-11949
Techniques for optimal crop selection in a controlled ecological life support system p 339 N95-11962
FOREARM
A musculoskeletal model of the elbow joint complex
[NASA-CR-195812] p 335 N95-13270
FOREBODIES
Water tunnel flow visualization study of a 4.4 percent scale X-31 forebody
[NASA-TM-104276] p 230 N95-11898
Numerical analysis of tangential slot blowing on a generic chined forebody
[NASA-TM-108845] p 231 N95-11927
FORECASTING
The role of crack formation in chevron-notched four-point bend specimens
[NASA-TM-106631] p 310 N95-11865
FOREST FIRE DETECTION
Trace gas emissions to the atmosphere by biomass burning in the west African savannas
[NASA-CR-196758] p 319 N95-11931
FORESTS
AIRSAR software: Computer programs for preprocessing of JPL compressed polarimetric SAR data
[PB94-179116] p 280 N95-11800
Satellite estimates of shortwave surface radiation and atmospheric meteorology for the BOREAS experiment region
[NASA-TM-109132] p 326 N95-12839
FORMALISM
Experiments with formal methods in software engineering
[PB94-192416] p 344 N95-12774
Category theory: The mathematics for the humanities
[PB94-205044] p 353 N95-13560
FORSTERITE
Tetravalent chromium (Cr(4+)) as laser-active ion for tunable solid-state lasers
[NASA-CR-196481] p 298 N95-12951
FORTRAN
FORTRAN programs to process Magsat data for lithospheric, external field, and residual core components
[NASA-TM-104612] p 323 N95-12130
Visualizing parallel numerical software performance on a shared memory multiprocessor
[PB94-195658] p 352 N95-13437
SURRENDER user's manual, second edition
[PB94-206950] p 346 N95-13571
FOUR-WAVE MIXING
Wavelength-encoded processing in semiconductor lasers
[AD-A282649] p 297 N95-12751
FRACTALS
Outdoor landmark recognition using hybrid fractal vision system and neural networks
[AD-A282506] p 349 N95-12395
FRACTIONS
Fractional suspension crystallization of organic compounds
[PB94-206851] p 375 N95-13409
FRACTOGRAPHY
A study of fatigue crack growth in lugs under spectrum loading
[NAL-PD-SN-9407] p 311 N95-11879
VAMAS round robin on fractography of ceramics. Swedish results
[PB94-180155] p 275 N95-12600
Thermomechanical fatigue damage/failure mechanisms in SCS-6/Timetal 21S (0/90)s composite
[NASA-CR-191115] p 263 N95-13082
FRACTURE MECHANICS
Modeling and life prediction methodology for Titanium Matrix Composites subjected to mission profiles
[NASA-TM-109148] p 269 N95-11915
Computer modeling the fatigue crack growth rate behavior of metals in corrosive environments
[NASA-CR-194982] p 269 N95-11933
Yield-before-break fracture mechanics analysis of high strength steel pressure vehicles
[AD-A282518] p 270 N95-12401
Fatigue in single crystal nickel superalloys
[AD-A283459] p 270 N95-12546
Validity of fracture toughness determined with small bend specimens
[DE94-624157] p 313 N95-12947
FRACTURE STRENGTH
Towards tailored interphase formation utilizing surface-active benzylsulfonium salts as cationic initiators
[AD-A282511] p 262 N95-12398
Test methods for textile composites
[NASA-CR-4609] p 262 N95-12793
Validity of fracture toughness determined with small bend specimens
[DE94-624157] p 313 N95-12947
FRACTURES (MATERIALS)
Micromorphology, mineralogy, and genesis of soils and fracture fills and the Pajarito Plateau, New Mexico
[DE94-013612] p 322 N95-11732
VAMAS round robin on fractography of ceramics. Swedish results
[PB94-180155] p 275 N95-12600
FRACTURING
Micromorphology, mineralogy, and genesis of soils and fracture fills and the Pajarito Plateau, New Mexico
[DE94-013612] p 322 N95-11732
Analysis of the effects of surface pitting and wear on the vibrations of a gear transmission system
[NASA-TM-106678] p 301 N95-12621
FREE ELECTRON LASERS
Beams 92: Proceedings
[DE94-014783] p 361 N95-11792
Free electron lasers and other advanced sources of light: Scientific research opportunities p 297 N95-12375
FREE FLOW
Measurements of pressure and thermal wakes in a transonic turbine cascade
[AD-A283464] p 232 N95-12548
FREE VIBRATION
Improved assumed-stress hybrid shell element with drilling degrees of freedom for linear stress, buckling, and free vibration analyses
[NASA-CR-192816] p 313 N95-13163
FREIGHT COSTS
Design of a high capacity long range cargo aircraft
[NASA-CR-197176] p 239 N95-12363
FREQUENCIES
Studies of electromagnetic ion cyclotron waves using AMPTE/CCE and dynamics explorer
[NASA-CR-196437] p 361 N95-12102
An estimate of the evolution of the acoustic emission spectrum of rocks on the basis of changes in its average frequency in the process of deformation
p 323 N95-12112
Frequency doubler (from 4.7 to 9.4 GHz) using a diode
[AD-A282784] p 287 N95-12525
Feedback control and stabilization experiments on the Texas Experimental Tokamak (TEXT)
[DE94-015214] p 368 N95-12758
200 MHz channel sounder, open description
[PB94-202538] p 285 N95-13559
FREQUENCY DISTRIBUTION
An estimate of the evolution of the acoustic emission spectrum of rocks on the basis of changes in its average frequency in the process of deformation
p 323 N95-12112
FREQUENCY MEASUREMENT
Uniform spectral amplitude windowing for hyperbolic frequency modulated waveforms
[AD-A282508] p 355 N95-12396
FREQUENCY MODULATION
Uniform spectral amplitude windowing for hyperbolic frequency modulated waveforms
[AD-A282508] p 355 N95-12396
Wavelength-encoded processing in semiconductor lasers
[AD-A282649] p 297 N95-12751
FREQUENCY RANGES
The terrestrial gravitational wave environment from known sources
[NASA-CR-196167] p 323 N95-12468
Study of in-plane dynamics of tires
[PB94-206893] p 304 N95-13410

FREQUENCY RESPONSE
A high-performance constant-temperature hot-wire anemometer
[NASA-CR-177645] p 295 N95-11896
Uniform spectral amplitude windowing for hyperbolic frequency modulated waveforms
[AD-A282508] p 355 N95-12396
Two-tone test method for determining frequency-domain transfer functions
[AD-A283452] p 282 N95-12513
FREQUENCY SHIFT KEYING
Burst transmission in the HF band: A system analysis and proposal for improvement
[PB94-190733] p 280 N95-11821
The effect of Rician fading and partial-band interference on noise-normalized fast frequency-hopped MFSK receivers
[AD-A282805] p 283 N95-12601
FRICTION FACTOR
Presentation of computer code SPIRALI for incompressible, turbulent, plane and spiral grooved cylindrical and face seals p 305 N95-13584
FUEL CELLS
Effect of operating parameters and anode gas impurities upon polymer electrolyte fuel cells
[DE94-014464] p 317 N95-12650
Proceedings of the 36th Power Sources Conference
[AD-A281443] p 288 N95-13164
FUEL COMBUSTION
Comparison of the KAMELEON fire model to large-scale open pool fire data
[DE94-013441] p 264 N95-11756
Structure of a swirl-stabilized, combusting spray
[NASA-TM-106724] p 243 N95-11890
Open-chamber combustion study
[PB94-184090] p 301 N95-12579
Mars methane engine
[NASA-CR-197205] p 302 N95-12668
FUEL CONSUMPTION
Examples of flight path optimisation using a multivariate gradient-search method. Addendum A: Variation of optimum flight profile parameters with range
[ESDU-94016-ADD-A] p 238 N95-11794
FUEL CONTROL
Viper cabin-fuselage structural design concept with engine installation and wing structural design
[NASA-CR-197162] p 239 N95-12305
FUEL PRODUCTION
Project Genesis: Mars in situ propellant technology demonstrator mission
[NASA-CR-197166] p 277 N95-12622
Project Hyreus: Mars sample return mission utilizing in situ propellant production
[NASA-CR-197189] p 383 N95-12626
FUEL SPRAYS
Structure of a swirl-stabilized, combusting spray
[NASA-TM-106724] p 243 N95-11890
FUEL TANK PRESSURIZATION
Cryogenic On-Orbit Liquid Depot Storage, Acquisition, and Transfer Satellite (COLD-SAT)
[NASA-CR-185249] p 259 N95-13237
FUEL TANKS
Test plan. Task 5, subtask 5.2: Early on-orbit TPSdebris impact tests
[NASA-CR-196873] p 251 N95-11802
Trade study plan for Graphite Composite Primary Structure (GCPS)
[NASA-CR-196868] p 261 N95-11834
Various advanced design projects promoting engineering education
[NASA-CR-197170] p 258 N95-12630
FULL SCALE TESTS
Selection process for trade study: Graphite Composite Primary Structure (GCPS)
[NASA-CR-196866] p 261 N95-11803
Test Plan. GCPS Task 4, subtask 4.2 thrust structure development
[NASA-CR-196869] p 251 N95-11833
FULLERENES
Structure and performance of carbon aerogel electrodes
[DE94-014746] p 356 N95-11791
Pressure studies of alkali, alkaline earth and rare earth doped C60 superconductors
[DE94-013345] p 372 N95-11862
FURLABLE ANTENNAS
Design studies of large aperture, high-resolution Earth science microwave radiometers compatible with small launch vehicles
[NASA-TP-3469] p 315 N95-12379
FURNACES
CGF cartridge development, volume 1
[NASA-CR-196506] p 270 N95-12830
FUSELAGES
Symmetric steady manoeuvre loads on rigid aircraft of classical configuration at subsonic speeds
[ESDU-94009] p 238 N95-11774
Cabin fuselage structural design with engine installation and control system
[NASA-CR-197173] p 240 N95-12639
Cabin-fuselage-wing structural design concept with engine installation
[NASA-CR-197172] p 242 N95-12993
FUSES
Resistivity variation of fuse as an opening switch p 365 N95-12430
FUSION REACTORS
Fusion powered human transport to Mars (UWFR94)
[NASA-CR-197184] p 368 N95-12641
Vacuum system operating experience review for fusion applications
[DE94-015267] p 368 N95-12759
FUSION WEAPONS
Vulnerability assessment of a space based weapon platform electronics system exposed to a thermonuclear weapon detonation
[DE94-013415] p 250 N95-11755

G

GALACTIC NUCLEI
Research in astrophysical processes
[NASA-CR-196773] p 382 N95-12939
Search for inverse Compton x-rays from the lobes of Fornax A x-rays from radio galaxies straddling the Fanaroff-Riley transition
[NASA-CR-196433] p 385 N95-13023
GALACTIC STRUCTURE
UV extinction and IR emission in diffuse H2 regions
[NASA-CR-196939] p 323 N95-12244
GALERKIN METHOD
Is the pollution effect of the FEM avoidable for the Helmholtz equation considering high wave numbers?
[AD-A282585] p 352 N95-12552
GALLIUM ARSENIDES
The Research Laboratory of Electronics
[AD-A281445] p 386 N95-11830
Development of nanostructure fabrication technology and new electron-quantum wave devices
[AD-A281724] p 286 N95-11860
CGF cartridge development, volume 1
[NASA-CR-196506] p 270 N95-12830
Gaseous detectors of ultraviolet and visible photons
[DE94-014990] p 296 N95-13171
Ku-band high efficiency GaAs MMIC power amplifiers
[NASA-CR-182156] p 288 N95-13231
GALLIUM COMPOUNDS
Low oxidation state gallium compounds. Synthesis and characterization of Ga(CH2CMe3)n
[AD-A283369] p 373 N95-12923
GALLIUM NITRIDES
Pseudomorphic semiconducting heterostructures from combinations of AlN, GaN and selected SiC polytypes: Theoretical advancement and its coordination with experimental studies of nucleation, growth, characterization and device development
[AD-A281218] p 289 N95-13368
GAME THEORY
Viscosity solutions of fully nonlinear equations
[AD-A281725] p 351 N95-11861
B* probability based search
[AD-A282551] p 343 N95-12497
GAMMA RAY ASTRONOMY
X-ray and gamma ray astronomy detectors
[NASA-SP-517] p 379 N95-12304
BATSE observations of 3C273
[NASA-CR-196185] p 380 N95-12463
Gamma-ray burst constraints on the galactic frequency of extra-solar Oort clouds
[NASA-CR-196197] p 385 N95-12886
GAMMA RAY BURSTS
BATSE observations of 3C273
[NASA-CR-196185] p 380 N95-12463
Gamma-ray burst constraints on the galactic frequency of extra-solar Oort clouds
[NASA-CR-196197] p 385 N95-12886
GAMMA RAY OBSERVATORY
BATSE observations of 3C273
[NASA-CR-196185] p 380 N95-12463
GAMMA RAY SPECTRA
BATSE observations of 3C273
[NASA-CR-196185] p 380 N95-12463
GAMMA RAYS
Radiation-induced structural changes, 4
[DE94-753223] p 356 N95-11817
A study of a multi-pinned phase CCD detector for use as a star tracker
[NASA-CR-196267] p 381 N95-13056
GANGLIA
Neural networks: Structure and repair. Part 1: Ground squirrel visual system. Part 2: Formation, maintenance and plasticity of synaptic connections
[AD-A282420] p 330 N95-12393
GAPS
Effects of piston surface treatments on performance and emissions of a methanol-fueled, direct injection, stratified charge engine
[DE94-011851] p 302 N95-12648
GAS ANALYSIS
Simultaneous gas-chromatographic determination of four toxic gases generally present in combustion atmospheres
[DOT/FAA/AM-94/18] p 338 N95-12354
GAS BEARINGS
Pressure measurements of a three wave journal air bearing p 307 N95-13605
GAS CHROMATOGRAPHY
Triple sorbent thermal desorption/gas chromatography/mass spectrometry determination of vapor phase organic contaminants
[DE94-013634] p 264 N95-11735
Simultaneous gas-chromatographic determination of four toxic gases generally present in combustion atmospheres
[DOT/FAA/AM-94/18] p 338 N95-12354
GAS DETECTORS
Microfabricated hydrogen sensor technology for aerospace and commercial applications
[NASA-TM-106703] p 284 N95-12674
Vapor detection sensitivity as a function of optical resolution for a single Lorentzian band
[AD-A283444] p 316 N95-13142
GAS DYNAMICS
Analysis and design of numerical schemes for gas dynamics. 2: Artificial diffusion and discrete shock structure
[NASA-CR-196476] p 290 N95-11874
Analysis and design of numerical schemes for gas dynamics 1: Artificial diffusion, upwind biasing, limiters and their effect on accuracy and multigrid convergence
[NASA-CR-196477] p 290 N95-11875
Boundary conditions for unsteady compressible flows
[NASA-TM-106737] p 293 N95-12380
Activities of the Institute for Aerospace Studies of Toronto University p 390 N95-12699
GAS FLOW
Interferograms, schlieren, and shadowgraphs constructed from real- and ideal-gas, two- and three-dimensional computed flowfields p 295 N95-11971
Analysis of cost: Combustion flame CVD diamond deposition
[AD-A282527] p 273 N95-12403
Fire propagation in concurrent flows
[PB94-193844] p 267 N95-12778
GAS GIANT PLANETS
The detectability of extrasolar terrestrial and giant planets during their luminous final accretion
[NASA-CR-196147] p 381 N95-13012
GAS LUBRICANTS
Code GFACE: Gas lubricated face seals in laminar regime p 305 N95-13585
Non-contacting gas lubricated face seals for high p x v-values p 308 N95-13609
GAS SPECTROSCOPY
Acquisition of a gas source mass spectrometer for paleoclimatology and paleoceanography research
[AD-A282634] p 266 N95-12539
GAS TEMPERATURE
Anode sheath contributions in plasma thrusters
[AD-A280395] p 364 N95-11837
GAS TUNGSTEN ARC WELDING
Effect of pre-welding heat-treatments on welding a two-phase Ni3Al alloy
[DE94-014409] p 270 N95-12372
GAS TURBINE ENGINES
High temperature strain gage technology for gas turbine engines
[NASA-CR-191177] p 295 N95-11996
Impingement flow heat transfer measurements of turbine blades using a jet array
[AD-A283450] p 375 N95-12512
GAS-SOLID INTERFACES
Atomic scale dynamics of a two-dimensional gas-solid interface
[AD-A282646] p 358 N95-12617
Atomic structures and compositions of internal interfaces
[DE94-013594] p 271 N95-13543
GASEOUS DIFFUSION
Analysis and design of numerical schemes for gas dynamics 1: Artificial diffusion, upwind biasing, limiters and their effect on accuracy and multigrid convergence
[NASA-CR-196477] p 290 N95-11875

GASIFICATION
MSW to hydrogen --- municipie solid waste (MSW)
[DE94-014741] p 265 N95-11790
GATES (CIRCUITS)
Quantum cellular automata
[AD-A283351] p 287 N95-12881
GAUSSIAN ELIMINATION
Visualizing parallel numerical software performance on a shared memory multiprocessor
[PB94-195658] p 352 N95-13437
GEAR TEETH
Analytical and experimental vibration analysis of a faulty gear system
[NASA-TM-106689] p 300 N95-12377
Analysis of the effects of surface pitting and wear on the vibrations of a gear transmission system
[NASA-TM-106678] p 301 N95-12621
Analytical and experimental vibration analysis of a faulty gear system
[NASA-TM-106689] p 303 N95-12843
Computerized design and generation of low-noise helical gears with modified surface topology
[NASA-TM-106696] p 303 N95-13083
GEARS
TLIFE: A program for spur, helical and spiral bevel transmission life and reliability modeling
[NASA-CR-4622] p 300 N95-11889
Analytical and experimental vibration analysis of a faulty gear system
[NASA-TM-106689] p 300 N95-12377
Analysis of the effects of surface pitting and wear on the vibrations of a gear transmission system
[NASA-TM-106678] p 301 N95-12621
Analytical and experimental vibration analysis of a faulty gear system
[NASA-TM-106689] p 303 N95-12843
Computerized design and generation of low-noise helical gears with modified surface topology
[NASA-TM-106696] p 303 N95-13083
GELS
Elimination of internal contamination on semiconductor devices (protective coatings)
[DE94-015868] p 275 N95-12945
GENERAL AVIATION AIRCRAFT
The Elite: A high speed, low-cost general aviation aircraft for Aeroworld
[NASA-CR-197161] p 239 N95-12530
Icarus Rewaxed: A high speed, low-cost general aviation aircraft for Aeroworld
[NASA-CR-197155] p 239 N95-12609
The Balsa bullet: A high speed, low-cost general aviation aircraft for Aeroworld
[NASA-CR-197165] p 240 N95-12638
GENERAL OVERVIEWS
Hall conductance as a topological invariant
[PB94-179330] p 353 N95-12364
Radiofrequency/microwave radiation biological effects and safety standards: A review
[AD-A282886] p 334 N95-12919
GENETIC ALGORITHMS
The potential of genetic algorithms for conceptual design of rotor systems
[NASA-CR-196813] p 237 N95-11699
Strain gage selection in loads equations using a genetic algorithm
[NASA-CR-4597] p 242 N95-12831
Population-based incremental learning. A method for integrating genetic search based function optimization and competitive learning
[AD-A282654] p 350 N95-12835
GENETICS
Population-based incremental learning. A method for integrating genetic search based function optimization and competitive learning
[AD-A282654] p 350 N95-12835
GEODESY
The program for the 1993 adjustment of the Finnish first-order terrestrial triangulation
[REPT-94:3] p 314 N95-11880
STEP: An international collaboration in fundamental physics p 354 N95-12229
Efficient and effective handling of cycle slips in global positioning system data p 237 N95-12230
The differential geodesy of the spherical representation
[AD-A282212] p 315 N95-12428
GEODETIC COORDINATES
The program for the 1993 adjustment of the Finnish first-order terrestrial triangulation
[REPT-94:3] p 314 N95-11880
GEODETIC SURVEYS
Final results of the Baltic Sea Level 1990 GPS Campaign. Research works of the SSG 5.147 of the International Association of Geodesy
[REPT-94:2] p 314 N95-11881
Observation results: Angle measurements in 1964-1965, 1971, 1984 and 1986-1987
[REPT-118] p 314 N95-11950
GEOGRAPHIC INFORMATION SYSTEMS
New York bight study. Report 4: Geographic information systems and relational database management system development
[AD-A281716] p 327 N95-11787
Proposal of a methodology to evaluate urban quality of life using conventional and remote sensing data, geographic information system, and a database
[INPE-5552-TDI/536] p 315 N95-12297
AGSO 1993: Yearbook of the Australian Geological Survey Organisation. Geoscientific research and database development for the year 1 July 1992 to 30 June 1993 p 324 N95-12686
Toolkits for construction and manipulation of geographical data
[PB94-202587] p 378 N95-13245
Use of remote sensing and geographic information system techniques in integrated studies of watersheds
[INPE-5494-TDI/511] p 316 N95-13352
GEOLOGICAL FAULTS
Neotectonics of Asia: Thin-shell finite-element models with faults
[NASA-CR-196436] p 324 N95-12949
GEOLOGICAL SURVEYS
Preliminary seismicity and focal mechanisms for the Southern Great Basin of Nevada and California, January 1992 - September 1992
[DE94-013589] p 321 N95-11730
Finite element methods in resistivity logging
[PB94-206919] p 325 N95-13434
GEOLOGY
AGSO 1993: Yearbook of the Australian Geological Survey Organisation. Geoscientific research and database development for the year 1 July 1992 to 30 June 1993 p 324 N95-12686
GEOMAGNETIC TAIL
An observational test of magnetospheric magnetic field mapping
[DE94-014461] p 324 N95-12649
Structure and dynamics of the solar corona
[NASA-CR-196978] p 384 N95-13582
GEOMAGNETISM
Initial analysis and modeling results from the Polar Orbiting Geomagnetic Survey (POGS) satellite
[AD-A283454] p 253 N95-12545
GEOMETRIC RECTIFICATION (IMAGERY)
AVHRR/NOAA images to detect and quantify deforestation in Amazon Forest: Relations with TM/LANDSAT data
[INPE-5501-TDI/516] p 316 N95-13350
GEOMORPHOLOGY
Micromorphology, mineralogy, and genesis of soils and fracture fills and the Pajarito Plateau, New Mexico
[DE94-013612] p 322 N95-11732
Periglacial and glacial analogs for Martian landforms
[NASA-CR-196772] p 383 N95-12952
GEOPHYSICS
AGSO 1993: Yearbook of the Australian Geological Survey Organisation. Geoscientific research and database development for the year 1 July 1992 to 30 June 1993 p 324 N95-12686
Guest investigator program study: Physics of equatorial plasma bubbles
[NASA-CR-196150] p 368 N95-12853
Finite element methods in resistivity logging
[PB94-206919] p 325 N95-13434
GEOPOTENTIAL
A unified approach to geopotential field modeling
[AD-A283453] p 324 N95-12544
GEOSYNCHRONOUS ORBITS
An observational test of magnetospheric magnetic field mapping
[DE94-014461] p 324 N95-12649
MOOSE: Manned On-Orbit Servicing Equipment
[NASA-CR-197151] p 254 N95-12790
GEOTECHNICAL ENGINEERING
Toward infrastructure improvement: An agenda for research
[LC-94-67335] p 376 N95-12385
GERMANATES
Optical and magnetic resonance investigations of 3D ions in single crystal hosts: Candidates for tunable solid-state lasers
[AD-A281726] p 371 N95-11842
GERMANIUM
Activities of Lehigh University
[AD-A282098] p 375 N95-13168
GET AWAY SPECIALS (STS)
GASCAN 2 payload integration
[NASA-CR-197200] p 278 N95-12701
STS-68 post flight presentation
[NASA-TM-109959] p 250 N95-13131
GETTERS
Gaseous detectors of ultraviolet and visible photons
[DE94-014990] p 296 N95-13171
GLACIERS
Periglacial and glacial analogs for Martian landforms
[NASA-CR-196772] p 383 N95-12952
GLASS
Glass microsphere lubrication
[NASA-CR-197157] p 277 N95-13508
GLASS FIBER REINFORCED PLASTICS
Glass reinforced-diallylbisphenol/maleimide composites with modified interphases
[AD-A282496] p 264 N95-13298
GLASS FIBERS
Phase A design study of microgravity fluoride fiber puller
[NASA-CR-196513] p 279 N95-12752
GLASS LASERS
Laser physics of Nd(exp 3+)-doped phosphate glasses
[DE94-015141] p 299 N95-13534
GLASS TRANSITION TEMPERATURE
Thianthrene-based poly(benzoxazole)s
[AD-A282326] p 274 N95-12419
GLOBAL AIR POLLUTION
Trace gas emissions to the atmosphere by biomass burning in the west African savannas
[NASA-CR-196758] p 319 N95-11931
Present state of knowledge of the upper atmosphere1993: An assessment report, part 2
[NASA-RP-1337] p 322 N95-12103
GLOBAL POSITIONING SYSTEM
Principles of GPS one-way data processing for high precision positioning applications: Algorithms and software issues p 237 N95-12177
Efficient and effective handling of cycle slips in global positioning system data p 237 N95-12230
NPS state vector analysis and relative motion plotting software for STS-51
[AD-A282909] p 249 N95-12510
GLOBAL WARMING
A data and information system for processing, archival, and distribution of data for global change research
[NASA-CR-196770] p 320 N95-12786
Interpolation of scattered temperature data measurements onto a worldwide regular grid using radial basis functions with applications to global warming
[DE94-014745] p 321 N95-12926
GLUCOSE
Effects of oral glucose on exercise thermoregulation in men after water immersion
[NASA-TM-108825] p 329 N95-11810
GLUONS
Photon production at CDF and D0
[DE94-014985] p 359 N95-13160
GOLD
Growth of Au on Ni(110): A BFS modelling of surface alloy phases
[NASA-TM-106732] p 270 N95-12104
GONDOLAS
Venus cloud bobber mission: A long term survey of the Venusian surface
[NASA-CR-197174] p 383 N95-12533
GOVERNMENT PROCUREMENT
Case study of risk management in the USAF B-1B bomber program
[AD-A282371] p 377 N95-11944
GOVERNMENT/INDUSTRY RELATIONS
Test Plans. Lightweight Durable TPS: Tasks 1,2,4,5, and 6
[NASA-CR-196867] p 262 N95-11835
Catalog of government inventions available for licensing, 1992
[PB93-128205] p 389 N95-12342
Airborne Windshear Detection and Warning Systems. Fifth and Final Combined Manufacturers' and Technologists' Conference, part 2
[NASA-CP-10139-PT-2] p 234 N95-13203
Windshear certification data base for forward-look detection systems p 234 N95-13204
Certification methodology applied to the NASA experimental radar system p 235 N95-13205
GOVERNMENTS
Directory of Federal laboratory and technology resources
[PB93-100097] p 389 N95-12223
GRAIN BOUNDARIES
CGF cartridge development, volume 1
[NASA-CR-196508] p 270 N95-12830
Atomic structures and compositions of internal interfaces
[DE94-013594] p 271 N95-13543
GRAIN SIZE
Mass conservation in grain growth
[DE94-014456] p 374 N95-13086

GRAND UNIFIED THEORY
Search for supersymmetry at CDF
[DE94-014264] p 357 N95-12369
GRANULAR MATERIALS
Influence of additives on structure and thermal stability of ammonium nitrate
[PB94-206943] p 278 N95-13435
GRAPH THEORY
A practical approach to drawing undirected graphs
[AD-A282641] p 343 N95-12541
GRAPHICAL USER INTERFACE
HLLV avionics requirements study and electronic filing system database development
[NASA-CR-193993] p 243 N95-13027
User interface development p 305 N95-13587
GRAPHITE
Selection process for trade study: Graphite Composite Primary Structure (GCPS)
[NASA-CR-196866] p 261 N95-11803
Trade study plan for Graphite Composite Primary Structure (GCPS)
[NASA-CR-196868] p 261 N95-11834
Self assembly of n-alkanethiolate monolayers on silver nano-structures: Determination of the apparent thickness of the monolayer by scanning tunneling microscopy
[AD-A282322] p 274 N95-12417
Ferric chloride graphite intercalation compounds prepared from graphite fluoride
[NASA-TM-106447] p 261 N95-12783
GRAPHITIZATION
Ferric chloride graphite intercalation compounds prepared from graphite fluoride
[NASA-TM-106447] p 261 N95-12783
GRAPHS (CHARTS)
A practical approach to drawing undirected graphs
[AD-A282641] p 343 N95-12541
SURRENDER user's manual, second edition
[PB94-206950] p 346 N95-13571
GRASSLANDS
Trace gas emissions to the atmosphere by biomass burning in the west African savannas
[NASA-CR-196758] p 319 N95-11931
GRATINGS (SPECTRA)
Calibration of optical wavelength at 1300 nm and 1550 nm using molecular absorption lines
[PB94-180080] p 362 N95-12598
GRAVELS
Marginal aggregates in flexible pavements: Background survey and experimental plan
[DOT/FAA/CT-94/58] p 246 N95-12216
GRAVITATION
STEP: An international collaboration in fundamental physics p 354 N95-12229
GRAVITATION THEORY
STEP: An international collaboration in fundamental physics p 354 N95-12229
GRAVITATIONAL CONSTANT
STEP: An international collaboration in fundamental physics p 354 N95-12229
GRAVITATIONAL EFFECTS
The Biological Flight Research Facility p 247 N95-11961
From undersea to outer space: The STS-40 jellyfish experiment
[NASA-TM-109958] p 250 N95-13122
GRAVITATIONAL FIELDS
The terrestrial gravitational wave environment from known sources
[NASA-CR-196167] p 323 N95-12468
Satellite laser ranging and gravity field modeling accuracy
[NASA-CR-196057] p 248 N95-12837
GRAVITATIONAL PHYSIOLOGY
Effect of decreased gravity on circulation in the rat
[NASA-CR-196946] p 331 N95-12827
GRAVITATIONAL WAVES
A catalogue of potentially bright close binary gravitational wave sources
[NASA-CR-196934] p 379 N95-12234
The terrestrial gravitational wave environment from known sources
[NASA-CR-196167] p 323 N95-12468
GRAVITY WAVES
Gravity wave forcing and influences near the mesopause
[AD-A282482] p 325 N95-13293
GREEN'S FUNCTIONS
Singularity of the Green dyadics for bi-isotropic
[PB94-184504] p 283 N95-12581
Numerical time dependent sheet cavitation simulations using a higher order panel method
[PB94-204435] p 294 N95-13249
Studies on the flow induced by an oscillating airfoil in a uniform stream
[PB94-204450] p 233 N95-13250
GREENHOUSE EFFECT
Greenhouse Effect Detection Experiment (GEDEX). Selected data sets
[NASA-TM-109952] p 318 N95-11845
Allocating CO2-emissions by using equity rules and optimization
[PB94-192861] p 320 N95-12776
GRID GENERATION (MATHEMATICS)
The development and application of the self-adaptive grid code, SAGE p 295 N95-11957
An implementation of a chemical and thermal nonequilibrium flow solver on unstructured meshes and application to blunt bodies
[NASA-CR-194967] p 293 N95-12619
Enhancement of EMAG: A 2-D electrostatic and magnetostatic solver for MATLAB
[AD-A283446] p 354 N95-13143
GRIDS
Approximation of scattered data using smooth grid functions
[PB94-207016] p 353 N95-13573
GROOVES
Turbomachinery Laboratory Texas A and M University research progress on annular gas seals p 307 N95-13604
GROUND BASED CONTROL
Development of a spindle thermal error characterization and compensation sensor system for machining center accuracy enhancement
[AD-A280891] p 300 N95-11729
GROUND EFFECT (AERODYNAMICS)
Dynamic ground effects flight test of an F-15 aircraft
[NASA-TM-4604] p 231 N95-12191
GROUND EFFECT (COMMUNICATIONS)
Windshear certification data base for forward-look detection systems p 234 N95-13204
GROUND HANDLING
Mars Equipment Transport System
[NASA-CR-197158] p 301 N95-12554
GROUND SPEED
The selective use of functional optical variables in the control of forward speed
[NASA-TM-108849] p 229 N95-12227
GROUND STATE
Experimental and theoretical study of neon-like selenium x-ray laser spectral line profiles
[DE94-015327] p 298 N95-12761
GROUND STATIONS
Observation results: Angle measurements in 1964-1965, 1971, 1984 and 1986-1987
[REPT-118] p 314 N95-11950
Preliminary digital control system design for the petite amateur Navy satellite (PANSAT)
[AD-A282804] p 253 N95-12528
GROUND TESTS
Linear Proof Mass Actuator
[NASA-TM-109143] p 310 N95-11814
NASA's Hypersonic Research Engine Project: A review
[NASA-TM-107759] p 244 N95-12860
Development of the CSI phase-3 evolutionary model testbed
[NASA-CR-4630] p 256 N95-13195
GUN LAUNCHERS
Present status of ohmic ignition chemical launcher experiment p 366 N95-12438
GYROTROPISM
Proceedings of Bianisotropics 1993: Seminar on Electrodynamics of Chiral and Bianisotropic Media
[PB94-179314] p 283 N95-12595

H

H II REGIONS
UV extinction and IR emission in diffuse H2 regions
[NASA-CR-196939] p 323 N95-12244
H-INFINITY CONTROL
An interpolation theoretic approach to control
[AD-A281465] p 348 N95-11853
Development of homotopy algorithms for fixed-order mixed H2/H(infinity) controller synthesis
[NASA-TP-3507] p 342 N95-11923
HADRONS
Contribution of hadronic intermediate states in nonleptonic weak decays of K, charm and B mesons
[DE94-753399] p 356 N95-11818
Strange hadronic matter
[DE94-001493] p 357 N95-12012
Multi-jet analysis for the top search at the Fermilab Collider
[DE94-014988] p 359 N95-13169
HALL EFFECT
Hall conductance as a topological invariant
[PB94-179330] p 353 N95-12364
HALOGEN COMPOUNDS
Synthetic method for ethynylation of aromatic compounds
[AD-D016398] p 261 N95-13151
HALOPHILES
Conformation of membrane proteins: Bacteriorhodopsin
[AD-A281282] p 331 N95-13373
HALOS
Project ECHO: Electronic Communications from Halo Orbit
[NASA-CR-197190] p 283 N95-12644
HAMILTONIAN FUNCTIONS
Aspects of long time behaviour of solutions of nonlinear Hamiltonian evolution equations
[PB94-192382] p 352 N95-12808
HANDLING EQUIPMENT
Mars Equipment Transport System
[NASA-CR-197158] p 301 N95-12554
HARDENING (MATERIALS)
Study on surface treatment by pulsed electron beams p 366 N95-12437
Computer modelling of cyclic deformation of high-temperature materials
[AD-A282457] p 263 N95-12833
HARMONIC ANALYSIS
Spectral analysis, estimation, and prediction of multiple harmonizable random fields and time series
[AD-A283042] p 354 N95-12994
HARMONIC CONTROL
Aeroelastic simulation of higher harmonic control
[NASA-CR-4623] p 230 N95-11911
HARMONIC GENERATORS
Frequency doubler (from 4.7 to 9.4 GHz) using a diode
[AD-A282784] p 287 N95-12525
HARMONIC OSCILLATORS
Design, synthesis and characterization of novel nonlinear optical polymers
[AD-A282201] p 274 N95-12424
HARMONICS
Frequency doubler (from 4.7 to 9.4 GHz) using a diode
[AD-A282784] p 287 N95-12525
HARNESSES
The performance of child restraint devices in transport airplane passenger seats
[DOT/FAA/AM-94/19] p 234 N95-12146
HARRIER AIRCRAFT
Moisture induced pressures in concrete airfield pavements
[AD-A281974] p 245 N95-11789
HCN LASERS
Improvements of HCN laser heterodyne interferometer for measuring plasma density
[DE94-625037] p 370 N95-13341
HEAD DOWN TILT
Effect of decreased gravity on circulation in the rat
[NASA-CR-196946] p 331 N95-12827
HEAD MOVEMENT
Reduction of ocular counter-rolling by adaptation to space
[NASA-CR-196279] p 333 N95-12376
Coordinated action in 3-D space
[AD-A281284] p 336 N95-13375
HEARING
The Research Laboratory of Electronics
[AD-A281445] p 386 N95-11830
Effects of Noise on Hearing 5th International Symposium
[AD-A281439] p 335 N95-13177
HEART DISEASES
Aviation epidemiology data register: Cardiovascular disease screening outcomes in the North Dakota Army National Guard aviator cohort
[AD-A283064] p 334 N95-13054
HEART RATE
Effect of decreased gravity on circulation in the rat
[NASA-CR-196946] p 331 N95-12827
HEAT AFFECTED ZONE
Effect of pre-welding heat-treatments on welding a two-phase Ni3Al alloy
[DE94-014409] p 270 N95-12372
HEAT ENGINES
High temperature solid lubricant materials for heavy duty and advanced heat engines
[NASA-TM-106570] p 260 N95-12764
HEAT EXCHANGERS
Composites (CFCCs) for low cost energy and cleaner environment
[DE94-013601] p 272 N95-11781
High frequency thermoacoustic refrigerator
[AD-A280925] p 279 N95-12772
Diesel-fired self-pumping water heater
[AD-A283063] p 279 N95-13053

Oscillating-flow regenerator test rig
[NASA-CR-196982] p 246 N95-13200
HEAT FLUX
Determination of a transient heat transfer property of acrylic using thermochromic liquid crystals
[NASA-TM-106541] p 372 N95-11882
FDNS code to predict wall heat fluxes or wall temperatures in rocket nozzles
[NASA-CR-196925] p 292 N95-11999
Absorption of intense microwaves and ion acoustic turbulence due to heat transport
[DE94-015140] p 369 N95-13285
HEAT MEASUREMENT
Science objectives and performance of a radiometer and window design for atmospheric entry experiments
[NASA-TM-4637] p 382 N95-12190
HEAT RESISTANT ALLOYS
Fatigue in single crystal nickel superalloys
[AD-A283459] p 270 N95-12546
Hydrogen desulfurization of nickel: Thermodynamics and kinetics
[AD-A282581] p 266 N95-12549
Symposium on Structural Intermetallics: Perspectives on Science and Technology, volume 1
[AD-A283376] p 271 N95-12925
Description of a high temperature quenching furnace for the study of the directional solidification of nickel-base superalloys
[DE94-013812] p 271 N95-13544
HEAT SHIELDING
Test model designs for advanced refractory ceramic materials p 277 N95-11968
HEAT TRANSFER
Heat transfer additives for adsorption cooling system fluids, phase 2
[PB94-187135] p 290 N95-11840
Magnetic field generation in shock waves
[AD-A282234] p 281 N95-12408
Laws of infrared similitude
[AD-A282209] p 354 N95-12426
Impingement flow heat transfer measurements of turbine blades using a jet array
[AD-A283450] p 375 N95-12512
Advances in SPARK
[DE94-014935] p 345 N95-13157
MHD pressure drops and thermal hydraulic analysis for the ITER breeding blanket design
[DE94-015085] p 369 N95-13280
Absorption of intense microwaves and ion acoustic turbulence due to heat transport
[DE94-015140] p 369 N95-13285
HEAT TRANSFER COEFFICIENTS
Determination of a transient heat transfer property of acrylic using thermochromic liquid crystals
[NASA-TM-106541] p 372 N95-11882
HEATERS
Status of hollow cathode heater development for the Space Station plasma contactor
[NASA-CR-195364] p 258 N95-12622
HEATING
Cabin fuselage structural design with engine installation and control system
[NASA-CR-197173] p 240 N95-12639
HEATING EQUIPMENT
Diesel-fired self-pumping water heater
[AD-A283063] p 279 N95-13053
HEAVY LIFT LAUNCH VEHICLES
A shadowgraph study of the National Launch System's 1 1/2 stage vehicle configuration and Heavy Lift Launch Vehicle configuration --- Using the Marshall Space Flight Center's 14-Inch Trisonic Wind Tunnel
[NASA-RP-1347] p 229 N95-11710
HLLV avionics requirements study and electronic filing system database development
[NASA-CR-193993] p 243 N95-13027
HELICAL WINDINGS
Turbomachinery Laboratory Texas A and M University research progress on annular gas seals p 307 N95-13604
HELICOPTER CONTROL
Aeroelastic simulation of higher harmonic control
[NASA-CR-4623] p 230 N95-11911
Techniques for designing rotorcraft control systems
[NASA-CR-196192] p 245 N95-12791
HELICOPTER DESIGN
The potential of genetic algorithms for conceptual design of rotor systems
[NASA-CR-196813] p 237 N95-11699
HELICOPTER TAIL ROTORS
Measurements of atmospheric turbulence effects on tail rotor acoustics
[NASA-TM-108843] p 232 N95-12360
HELICOPTERS
Ten-year ground exposure of composite materials used on the Bell Model 206L helicopter flight service program
[NASA-TP-3468] p 262 N95-12357
Role of wind tunnels and computer codes in the certification and qualification of rotorcraft for flight in forecast icing
[NASA-TM-106747] p 233 N95-13197
HEMATITE
Ferric chloride graphite intercalation compounds prepared from graphite fluoride
[NASA-TM-106447] p 261 N95-12783
HEMODYNAMIC RESPONSES
Effect of decreased gravity on circulation in the rat
[NASA-CR-196946] p 331 N95-12827
HEPTANES
Structure of a swirl-stabilized, combusting spray
[NASA-TM-106724] p 243 N95-11890
HETEROJUNCTION DEVICES
Silicon carbide and sicaln heterojunction bipolar transistor structures
[AD-D016403] p 288 N95-13181
HEURISTIC METHODS
Constructing combinatorial designs by local search
[PB94-179272] p 351 N95-11839
Intelligent control systems research
[NASA-CR-195380] p 349 N95-12811
HEXYL COMPOUNDS
Orthobaric densities and molar volumes of liquids. Polycyclic phenyl and cyclohexyl compounds
[ESDU-94002] p 266 N95-12129
HIGGS BOSONS
Photon production at CDF and D0
[DE94-014985] p 359 N95-13160
HIGH ALTITUDE
Development of techniques for the in situ observation of OH and HO2 for studies of the impact of high-altitude supersonic aircraft on the stratosphere
[NASA-CR-196759] p 321 N95-12832
HIGH CURRENT
Velocity spread of REB generated by high current diode
[IPPCZ-339] p 364 N95-11886
HIGH DEFINITION TELEVISION
An acoustic charge transport imager for high definition television applications
[NASA-CR-196806] p 280 N95-11760
HIGH ENERGY ELECTRONS
Free electron lasers and other advanced sources of light: Scientific research opportunities p 297 N95-12375
A numerical calculation method for the kinetic ballooning mode eigen-equation with three components
[DE94-625048] p 369 N95-13107
HIGH ENERGY INTERACTIONS
Analyzing terabytes of data at Fermilab
[DE94-013149] p 347 N95-13269
HIGH FREQUENCIES
High frequency thermoacoustic refrigerator
[AD-A280925] p 279 N95-12772
HIGH IMPULSE
SolSTUS: Solar Source Thermal Upper Stage
[NASA-CR-197179] p 257 N95-13581
HIGH POWER LASERS
The future of diode pumped solid state lasers and their applicability to the automotive industry
[DE94-014736] p 298 N95-12868
Time-resolved electron thermal conduction by probing of plasma formation in transparent solids with high power subpicosecond laser pulses
[DE94-015170] p 370 N95-13555
HIGH PRESSURE
Non-contacting gas lubricated face seals for high p x v-values p 308 N95-13609
HIGH RESOLUTION
Development of nanostructure fabrication technology and new electron-quantum wave devices
[AD-A281724] p 286 N95-11860
Tropical cyclone development and intensification under moderate to strong vertical wind shear
[AD-A282185] p 326 N95-12423
Summaries of papers presented at the High Resolution Spectroscopy Topical Meeting. Technical digest series. Volume 1: Post conference edition
[AD-A281261] p 268 N95-13372
HIGH SPEED
Modeling and implementation of a packet routing switch for satellite communications
[AD-A282262] p 282 N95-12412
The Elite: A high speed, low-cost general aviation aircraft for Aeroworld
[NASA-CR-197161] p 239 N95-12530
The Balsa bullet: A high speed, low-cost general aviation aircraft for Aeroworld
[NASA-CR-197165] p 240 N95-12638
On the strain and strain-rate dependence of the fraction of plastic work converted to heat: An experimental study using high speed infrared detectors and the Kolsky bar
[SM-92-33] p 354 N95-12728
Non-contacting gas lubricated face seals for high p x v-values p 308 N95-13609
HIGH SPEED CAMERAS
An acoustic charge transport imager for high definition television applications
[NASA-CR-196806] p 280 N95-11760
HIGH SPEED PHOTOGRAPHY
Debris/ice/TPS assessment and integrated photographic analysis of Shuttle Mission STS-65
[NASA-TM-109205] p 249 N95-12224
HIGH STRENGTH
Acute inhalation of explosively disseminated carbon fibers in rats
[AD-A280556] p 330 N95-12614
HIGH STRENGTH STEELS
Yield-before-break fracture mechanics analysis of high strength steel pressure vehicles
[AD-A282518] p 270 N95-12401
HIGH TEMPERATURE
High temperature strain gage technology for gas turbine engines
[NASA-CR-191177] p 295 N95-11996
Thianthrene-based poly(benzoxazole)s
[AD-A282326] p 274 N95-12419
Computer modelling of cyclic deformation of high-temperature materials
[AD-A282457] p 263 N95-12833
Description of a high temperature quenching furnace for the study of the directional solidification of nickel-base superalloys
[DE94-013812] p 271 N95-13544
HIGH TEMPERATURE ENVIRONMENTS
Measurements of pressure and thermal wakes in a transonic turbine cascade
[AD-A283464] p 232 N95-12548
HIGH TEMPERATURE GAS COOLED REACTORS
Studies of low temperature, low flux radiation embrittlement of nuclear reactor structural materials
[DE94-013710] p 269 N95-11738
HIGH TEMPERATURE LUBRICANTS
High temperature solid lubricant materials for heavy duty and advanced heat engines
[NASA-TM-106570] p 260 N95-12764
HIGH TEMPERATURE PLASMAS
Physics of High Energy Density Plasmas Produced by Pulsed Power
[NIFS-PROC-18] p 365 N95-12429
Evaluation of dynamic pressure of ablation plasma produced by intense, pulsed, ion beam p 365 N95-12433
Z-pinch plasma by solid fine particle injection p 366 N95-12442
Time-resolved electron thermal conduction by probing of plasma formation in transparent solids with high power subpicosecond laser pulses
[DE94-015170] p 370 N95-13555
HIGH TEMPERATURE RESEARCH
Response of high T(sub c) superconducting Josephson junction to nuclear radiation
[DE94-624705] p 360 N95-13536
HIGH TEMPERATURE SUPERCONDUCTORS
Apparatus and method for forming textured bulk high temperature superconducting materials
[AD-D016394] p 373 N95-12635
Generation of ultra-high magnetic fields for AGEX
[DE94-015171] p 368 N95-12757
The dissipative mechanism of pinning of a superconducting current
[DE94-623252] p 289 N95-13276
About the structure of the superconducting order parameter of 2 D Fermi system with an arbitrary particle density
[DE94-623268] p 375 N95-13277
Processing, fabrication, and demonstration of HTS integrated microwave circuits
[AD-A282505] p 289 N95-13300
HIGH TEMPERATURE TESTS
High temperature seal test rig p 247 N95-13593
HIGHLY MANEUVERABLE AIRCRAFT
Impact of agility requirements on configuration synthesis
[NASA-CR-4627] p 236 N95-11952
HIGHWAYS
Development of ground-penetrating radar equipment for detecting pavement condition for preventive maintenance
[PB94-189537] p 280 N95-11904
HISTOCHEMICAL ANALYSIS
Morphological differentiation of colon carcinoma cell lines in rotating wall vessels
[NASA-CR-196780] p 333 N95-11808
HISTORIES
Aeronautics and space technology, past, present, and future p 229 N95-11892
NASA's Hypersonic Research Engine Project: A review
[NASA-TM-107759] p 244 N95-12660

HOLDERS
Test model designs for advanced refractory ceramic materials p 277 N95-11968
HOLES (MECHANICS)
Impingement flow heat transfer measurements of turbine blades using a jet array
[AD-A283450] p 375 N95-12512
HOLLOW CATHODES
Status of hollow cathode heater development for the Space Station plasma contactor
[NASA-CR-195364] p 258 N95-12622
HOLMIUM
The magnetic structure of holmium-erbium superlattices
[DE94-013728] p 371 N95-11739
HOLOGRAPHY
Optical analysis of crystal growth
[NASA-CR-196514] p 373 N95-12386
Simulating the energy performance of holographic glazings
[DE94-014969] p 296 N95-13158
HOMOTOPY THEORY
Development of homotopy algorithms for fixed-order mixed H2/H(infinity) controller synthesis
[NASA-TP-3507] p 342 N95-11923
Hall conductance as a topological invariant
[PB94-179330] p 353 N95-12364
HOPPERS
Project Genesis: Mars in situ propellant technology demonstrator mission
[NASA-CR-197166] p 277 N95-12822
HORIZONTAL SPACECRAFT LANDING
Requirements report for SSTO vertical take-off/horizontal landing vehicle
[NASA-CR-196875] p 251 N95-11777
Selection process for trade study: Reusable Hydrogen Composite Tank System (RHCTS)
[NASA-CR-196874] p 251 N95-11809
HORIZONTAL TAIL SURFACES
Symmetric steady manoeuvre loads on rigid aircraft of classical configuration at subsonic speeds
[ESDU-94009] p 238 N95-11774
HOT PRESSING
Mechanical behavior of (238)UO2, (238)PuO2, and (239)PuO2 as a function of strain rate and temperature
[DE94-015718] p 312 N95-12784
HOT-WIRE ANEMOMETERS
A high-performance constant-temperature hot-wire anemometer
[NASA-CR-177645] p 295 N95-11896
HOUSINGS
Duplex rolling element bearing mounting for ensuring preload control
[AD-D016402] p 304 N95-13189
HUBBLE SPACE TELESCOPE
Evaluation of COSTAR mass handling characteristics in an environment. A simulation of the Hubble Space Telescope service mission
[NASA-TP-3489] p 333 N95-11887
HUMAN BEINGS
Body dimensions for apparel
[PB94-187739] p 336 N95-11908
HUMAN BODY
Biomedical imaging
[AD-A282221] p 333 N95-12405
HUMAN FACTORS ENGINEERING
Design issues of human operator support systems
[PB94-191376] p 337 N95-11778
Human factors assessments of the STS-57 SpaceHab-1 mission
[NASA-TM-104802] p 337 N95-11878
Interviews with the Apollo lunar surface astronauts in support of planning for EVA systems design
[NASA-TM-108846] p 337 N95-11905
Probabilistic simulation of the human factor in structural reliability
[NASA-TM-106498] p 311 N95-11954
Communications plan --- Design of the public wing of the Oregon State University Hatfield Marine Science Center
[NASA-CR-196435] p 314 N95-12231
M.E.366-J embodiment design project: Portable foot restraint
[NASA-CR-197163] p 338 N95-12361
Visual psychophysics of egomotion
[AD-A282547] p 335 N95-12495
Proposal for the design of a zero gravity tool storage device
[NASA-CR-197150] p 302 N95-12627
Coordinated action in 3-D space
[AD-A281284] p 336 N95-13375
HUMAN PERFORMANCE
Tank crew performance related to cognitive ability and motivation of the tank crew members
[PB94-190642] p 335 N95-11872
Probabilistic simulation of the human factor in structural reliability
[NASA-TM-106498] p 311 N95-11954
HUMAN RESOURCES
Visit to UDRI and USAF, Armstrong Lab., Williams AFB, Phoenix, USA, February 8-11, 1993
[PB94-190659] p 337 N95-11873
HUMAN TOLERANCES
Effects of Noise on Hearing 5th International Symposium
[AD-A281439] p 335 N95-13177
HUMAN-COMPUTER INTERFACE
Population-based incremental learning. A method for integrating genetic search based function optimization and competitive learning
[AD-A282654] p 350 N95-12835
Information Technology Division's technical paper abstracts
[AD-A282882] p 378 N95-12916
Eye-gaze determination of user intent at the computer interface
[DE94-012337] p 363 N95-13421
User interface development p 305 N95-13587
HUMIDITY MEASUREMENT
Differential absorption lidar measurements of atmospheric water vapor using a pseudonoise code modulated AlGaAs laser
[NASA-TM-104610] p 314 N95-11997
SuperMariah: A similarity-based method for determining wind, temperature, and humidity profile structure in the surface boundary layer
[AD-A283058] p 327 N95-12997
HURRICANES
Dynamical studies in hurricane intensity change
[AD-A282406] p 326 N95-12392
HYBRID ROCKET ENGINES
Various advanced design projects promoting engineering education
[NASA-CR-197170] p 258 N95-12630
HYDRAULIC CONTROL
Modular hydraulic control system
[AD-D016401] p 304 N95-13155
HYDRAULIC EQUIPMENT
The development of a highly reliable power management and distribution system for civil transport aircraft
[NASA-TM-106697] p 243 N95-11867
Modular hydraulic control system
[AD-D016401] p 304 N95-13155
HYDRAULICS
MHD pressure drops and thermal hydraulic analysis for the ITER breeding blanket design
[DE94-015085] p 369 N95-13280
HYDROCARBON COMBUSTION
Mars methane engine
[NASA-CR-197205] p 302 N95-12668
HYDROCARBON FUELS
A study of aircraft post-crash fuel fire mitigation
[AD-A282208] p 234 N95-12499
HYDROCARBONS
Trichloroethylene emissions reductions achieved by enclosing solvent spray degreasing operations
[DE94-013741] p 318 N95-11742
Amine catalyzed intramolecular imidization of alkyl and aryl phthalamates, kinetics and mechanism in deuterated chloroform
[AD-A281741] p 259 N95-11844
A study of aircraft post-crash fuel fire mitigation
[AD-A282208] p 234 N95-12499
Phenoxythiocarbonylation and deoxygenation of aryl trifluoromethyl carbinols
[AD-A280519] p 260 N95-12613
Finite element methods in resistivity logging
[PB94-206919] p 325 N95-13434
HYDRODYNAMICS
Loads for pulsed power cylindrical implosion experiments
[DE94-014429] p 299 N95-13080
HYDROGEN
MSW to hydrogen --- municiple solid waste (MSW)
[DE94-014741] p 265 N95-11790
Hydrogen desulfurization of nickel: Thermodynamics and kinetics
[AD-A282581] p 266 N95-12549
Microfabricated hydrogen sensor technology for aerospace and commercial applications
[NASA-TM-106703] p 284 N95-12674
Advanced cryogenic propellants
[AD-A282451] p 277 N95-12729
HYDROGEN ATOMS
Quantitative understanding of the cycles of oxidized and reduced sulfur on Venus
[NASA-CR-196924] p 382 N95-12011
HYDROGEN BONDS
Amine catalyzed intramolecular imidization of alkyl and aryl phthalamates, kinetics and mechanism in deuterated chloroform
[AD-A281741] p 259 N95-11844
Hydrogen bonding and molecular orientation in water/fluorine adlayers on silver(110)
[AD-A282652] p 268 N95-13549
HYDROGEN FUELS
Test plan. Task 5, subtask 5.2: Early on-orbit TPSdebris impact tests
[NASA-CR-196873] p 251 N95-11802
Selection process for trade study: Reusable Hydrogen Composite Tank System (RHCTS)
[NASA-CR-196874] p 251 N95-11809
HYDROGEN ISOTOPES
CRYOCOL: A computer program to calculate the cryogenic distillation of hydrogen isotopes
[DE94-622012] p 268 N95-13531
HYDROGEN PRODUCTION
MSW to hydrogen --- municiple solid waste (MSW)
[DE94-014741] p 265 N95-11790
Project Hyreus: Mars sample return mission utilizing in situ propellant production
[NASA-CR-197189] p 383 N95-12826
HYDROGRAPHY
Hydrographic, carbon dioxide, nutrient and productivity measurements from the south Atlantic during July and August of 1991
[PB94-180668] p 328 N95-11900
HYDROLYSIS
Hydrolysis and condensation of tin (4) alkoxide compounds: The control of structural evolution
[AD-A282789] p 267 N95-12807
HYDROSTATIC PRESSURE
Oscillating-flow regenerator test rig
[NASA-CR-196982] p 246 N95-13200
HYDROSTATICS
Code GFACE: Gas lubricated face seals in laminar regime p 305 N95-13585
HYDROXYL EMISSION
Development of techniques for the in situ observation of OH and HO2 for studies of the impact of high-altitude supersonic aircraft on the stratosphere
[NASA-CR-196759] p 321 N95-12832
Laser based combustion laboratory at NTH/SINTEF applied thermodynamics
[PB94-202603] p 299 N95-13246
HYDROXYL RADICALS
Phenoxythiocarbonylation and deoxygenation of aryl trifluoromethyl carbinols
[AD-A280519] p 260 N95-12613
HYPERBOLIC DIFFERENTIAL EQUATIONS
Stability and error estimation for Component Adaptive Grid methods
[NASA-CR-196492] p 351 N95-11883
HYPERCUBE MULTIPROCESSORS
On bottleneck partitioning k-ary n-cubes
[NASA-CR-194966] p 342 N95-12005
HYPERNUCLEI
The cascade-deuteron system
[DE94-011650] p 357 N95-11894
Strange hadronic matter
[DE94-001493] p 357 N95-12012
HYPERSONIC AIRCRAFT
Shock-tunnel combustor testing for hypersonic vehicles
[NASA-CR-196836] p 246 N95-11938
A simple analytical aerodynamic model of Langley Winged-Cone Aerospace Plane concept
[NASA-CR-194987] p 252 N95-12175
HYPERSONIC BOUNDARY LAYER
Hypersonic turbulent boundary-layer and free shear database
[NASA-CR-177610] p 292 N95-11992
HYPERSONIC FLOW
Shock-tunnel combustor testing for hypersonic vehicles
[NASA-CR-196836] p 246 N95-11938
An implementation of a chemical and thermal nonequilibrium flow solver on unstructured meshes and application to blunt bodies
[NASA-CR-194967] p 293 N95-12619
Hypersonic Gas-Surface Energy Accommodation Test Facility
[DE94-014468] p 232 N95-12652
HYPERSONIC HEAT TRANSFER
An axisymmetric analog two-layer convective heating procedure with application to the evaluation of Space Shuttle Orbiter wing leading edge and windward surface heating
[NASA-CR-188343] p 251 N95-11937
HYPERSONIC INLETS
Shock-tunnel combustor testing for hypersonic vehicles
[NASA-CR-196836] p 246 N95-11938

HYPERSONIC SPEED
Shock-tunnel combustor testing for hypersonic vehicles
[NASA-CR-196836] p 246 N95-11938
HYPERSONIC VEHICLES
Experimental aerodynamic characteristics of a generic hypersonic accelerator configuration at Mach numbers 1.5 and 2.0 --- conducted in the Langley Unitary Plan Wind Tunnel
[NASA-TM-4413] p 233 N95-12770
Hypersonic vehicle model and control law development using H(infinity) and micron synthesis
[NASA-TM-4562] p 255 N95-12838
HYPERSONIC WIND TUNNELS
Mach number control in the High Speed Wind Tunnel of NLR
[PB94-201670] p 246 N95-13243
HYPERSONICS
Computational flow predictions for hypersonic drag devices p 233 N95-11967
Hypersonic turbulent boundary-layer and free shear database
[NASA-CR-177610] p 292 N95-11992
Experimental aerodynamic characteristics of a generic hypersonic accelerator configuration at Mach numbers 1.5 and 2.0 --- conducted in the Langley Unitary Plan Wind Tunnel
[NASA-TM-4413] p 233 N95-12770
HYPERVELOCITY LAUNCHERS
Present status of ohmic ignition chemical launcher experiment p 366 N95-12438
HYPOKINESIA
Effect of decreased gravity on circulation in the rat
[NASA-CR-196946] p 331 N95-12827
HYPOTHESES
An analysis of the effect of Gaussian error in object recognition
[AD-A282260] p 349 N95-12411
HYSTERESIS
Nonlinear hysteresis in an endochronic solid
[AD-A283142] p 325 N95-13136

I

ICE
Global ice sheet modeling
[DE94-013744] p 318 N95-11745
User's manual for the NASA Lewis ice accretion/heat transfer prediction code with electrothermal deicer input
[NASA-CR-4530] p 291 N95-11888
Bibliography on cold regions science and technology, volume 47, part 1
[AD-A281879] p 378 N95-13167
ICE FORMATION
User's manual for the NASA Lewis ice accretion/heat transfer prediction code with electrothermal deicer input
[NASA-CR-4530] p 291 N95-11888
Debris/ice/TPS assessment and integrated photographic analysis of Shuttle Mission STS-65
[NASA-TM-109205] p 249 N95-12224
ICE PREVENTION
User's manual for the NASA Lewis ice accretion/heat transfer prediction code with electrothermal deicer input
[NASA-CR-4530] p 291 N95-11888
ICE REPORTING
Parameterization and scaling of Arctic ice conditions in the context of ice-atmosphere processes
[NASA-CR-196831] p 327 N95-11706
IDEAL GAS
Thermophysical properties of MtBE (methyl tertbutyl ether)
[ESDU-94010] p 265 N95-11775
Interferograms, schlieren, and shadowgraphs constructed from real- and ideal-gas, two- and three-dimensional computed flowfields p 295 N95-11971
Computer code for determination of thermally perfect gas properties
[NASA-TP-3447] p 231 N95-11995
IGNITION
Target area chamber system design for the National Ignition Facility
[DE94-013347] p 364 N95-11754
Review of pulse ignition
[INPE-5569-PUD/063] p 265 N95-11885
Status of hollow cathode heater development for the Space Station plasma contactor
[NASA-CR-195364] p 258 N95-12622
IGNITION SYSTEMS
Review of pulse ignition
[INPE-5569-PUD/063] p 265 N95-11885
ILLUMINANCE
Simulating the energy performance of holographic glazings
[DE94-014969] p 296 N95-13158
ILLUMINATING
Cabin fuselage structural design with engine installation and control system
[NASA-CR-197173] p 240 N95-12639
IMAGE ANALYSIS
Optical analysis of crystal growth
[NASA-CR-196514] p 373 N95-12386
Millimeter-wave radiometric utility study
[AD-A282524] p 281 N95-12402
Target recognition in ultra-wideband SAR imagery
[AD-A283462] p 282 N95-12547
Learning one-dimensional geometric patterns under one-sided random misclassification noise
[DE94-014659] p 350 N95-12864
Representation, modeling and recognition of outdoor scenes
[AD-A283361] p 350 N95-12884
Scene analysis: A brief survey
[PB94-205085] p 336 N95-13433
IMAGE CLASSIFICATION
Weighted Parzen windows for pattern classification
[AD-A281222] p 345 N95-13370
IMAGE ENHANCEMENT
Digital image processing techniques for image-mapping applications
[INPE-5546-TDI/532] p 315 N95-12301
IMAGE INTENSIFIERS
Semiautomated methodology for measurement of field-of-view, magnification, and distortion of night vision devices as defined in MIL-A-49425(CR)
[AD-A282210] p 362 N95-12427
Laser based combustion laboratory at NTH/SINTEF applied thermodynamics
[PB94-202603] p 299 N95-13246
IMAGE MOTION COMPENSATION
Locally connected adaptive Gabor filter for real-time motion compensation
[AD-A282544] p 286 N95-12494
Visual psychophysics of egomotion
[AD-A282547] p 335 N95-12495
IMAGE PROCESSING
Improved image decompression for reduced transform coding artifacts
[NASA-CR-196805] p 341 N95-11761
Vector quantization for efficient coding of upper subbands
[NASA-CR-196804] p 341 N95-11762
An efficient system for reliably transmitting image and video data over low bit rate noisy channels
[NASA-CR-196802] p 341 N95-11764
AIRSAR software: Computer programs for preprocessing of JPL compressed polarimetric SAR data
[PB94-179116] p 280 N95-11800
UV extinction and IR emission in diffuse H2 regions
[NASA-CR-196939] p 323 N95-12244
Digital image processing techniques for image-mapping applications
[INPE-5546-TDI/532] p 315 N95-12301
An analysis of the effect of Gaussian error in object recognition
[AD-A282260] p 349 N95-12411
Visual psychophysics of egomotion
[AD-A282547] p 335 N95-12495
Site model based image registration and change detection, RADIUS
[AD-A282796] p 315 N95-12527
Standards relevant to a NATO anthropometry survey using 3D imaging tools
[AD-A283065] p 339 N95-13055
Object recognition for flexible assembly using stereo vision
[PB94-204427] p 363 N95-13248
Use of remote sensing and geographic information system techniques in integrated studies of watersheds
[INPE-5494-TDI/511] p 316 N95-13352
IMAGE RECONSTRUCTION
Improved image decompression for reduced transform coding artifacts
[NASA-CR-196805] p 341 N95-11761
BATSE observations of 3C273
[NASA-CR-196185] p 380 N95-12463
IMAGE RESOLUTION
Digital image processing techniques for image-mapping applications
[INPE-5546-TDI/532] p 315 N95-12301
Dynamic sine wave response measurements of CRT displays using sinusoidal counterphase modulation
[AD-A282222] p 333 N95-12406
Target recognition in ultra-wideband SAR imagery
[AD-A283462] p 282 N95-12547
IMAGING SPECTROMETERS
Monochromatic x ray imaging in plasma focus experiment p 366 N95-12443
IMAGING TECHNIQUES
Outdoor landmark recognition using hybrid fractal vision system and neural networks
[AD-A282506] p 349 N95-12395
Biomedical imaging
[AD-A282221] p 333 N95-12405
Self assembly of n-alkanethiolate monolayers on silver nano-structures: Determination of the apparent thickness of the monolayer by scanning tunneling microscopy
[AD-A282322] p 274 N95-12417
Semiautomated methodology for measurement of field-of-view, magnification, and distortion of night vision devices as defined in MIL-A-49425(CR)
[AD-A282210] p 362 N95-12427
Wideband electromagnetic scattering program. Fourier-based radar imaging techniques
[AD-A282540] p 282 N95-12493
Near-infrared imaging of selected areas
[AD-A283519] p 316 N95-12634
Laser based combustion laboratory at NTH/SINTEF applied thermodynamics
[PB94-202603] p 299 N95-13246
Use of remote sensing and geographic information system techniques in integrated studies of watersheds
[INPE-5494-TDI/511] p 316 N95-13352
IMIDES
Synthesis and solid-state NMR characterization of 13C- and 15N-labelled n-methylphthalimide: A model compound for studying polyimides
[AD-A282510] p 273 N95-12397
IMINES
Synthetic method for ethynylation of aromatic compounds
[AD-D016398] p 261 N95-13151
IMMOBILIZATION
Fibre optic sensors using adiabatically tapered single mode fibres
[AD-A282306] p 362 N95-12415
IMMUNOLOGY
Spaceflight and immune responses of Rhesus monkeys
[NASA-CR-196846] p 331 N95-12941
IMPACT DAMAGE
Damage tolerance of candidate thermoset composites for use on single stage to orbit vehicles
[NASA-TP-3506] p 261 N95-11816
Army Research Office Workshop on Dynamic Response of Composite Structures
[AD-A281471] p 262 N95-11854
IMPACT RESISTANCE
Damage tolerance of candidate thermoset composites for use on single stage to orbit vehicles
[NASA-TP-3506] p 261 N95-11816
IMPACT TESTS
Impact analysis on a massively parallel computer
[DE94-013624] p 346 N95-11734
Test plan. Task 5, subtask 5.2: Early on-orbit TPSdebris impact tests
[NASA-CR-196873] p 251 N95-11802
The performance of child restraint devices in transport airplane passenger seats
[DOT/FAA/AM-94/19] p 234 N95-12146
IMPINGEMENT
Impingement flow heat transfer measurements of turbine blades using a jet array
[AD-A283450] p 375 N95-12512
IMPLANTATION
Muon sites and electronic structure
[PB94-179348] p 357 N95-12365
IMPLOSIONS
Generation of ultra-high magnetic fields for AGEX
[DE94-015171] p 368 N95-12757
Loads for pulsed power cylindrical implosion experiments
[DE94-014429] p 299 N95-13080
IMPREGNATING
Novel activated carbon impregnants consisting of transition metal complexes. Part 1: Background, syntheses and characterizations
[AD-A282583] p 259 N95-12551
IMPULSES
200 MHz channel sounder, open description
[PB94-202538] p 285 N95-13559
IMPURITIES
Effect of operating parameters and anode gas impurities upon polymer electrolyte fuel cells
[DE94-014464] p 317 N95-12650
IN SITU MEASUREMENT
UV and fluorescence studies for vinyl polymerization
[AD-A281187] p 274 N95-12520
INCINERATORS
Composites (CFCCs) for low cost energy and cleaner environment
[DE94-013601] p 272 N95-11781

INCOMPRESSIBLE FLOW
Performance analysis of three dimensional integral equation computations on a massively parallel computer
[NASA-CR-196747] p 346 N95-11863
Presentation of computer code SPIRALI for incompressible, turbulent, plane and spiral grooved cylindrical and face seals p 305 N95-13584
Incompressible face seals: Computer code IFACE p 307 N95-13606

INDEXES (DOCUMENTATION)
Catalog of government inventions available for licensing, 1991
[PB92-100171] p 389 N95-12303
Catalog of government inventions available for licensing, 1992
[PB93-126205] p 389 N95-12342
CENDI Indexing Workshop
[NASA-CP-10160] p 378 N95-12358
HLLV avionics requirements study and electronic filing system database development
[NASA-CR-193993] p 243 N95-13027

INDIA
Experimental Aerodynamics Division
[NAL-SP-9404] p 229 N95-12166

INDIUM
The Research Laboratory of Electronics
[AD-A281445] p 386 N95-11830

INDIUM ALLOYS
A novel lead-free solder replacement
[DE94-013782] p 269 N95-11785

INDIUM ALUMINUM ARSENIDES
Origin of optical anisotropy in strained In(x)Ga(1-x)As/InP and In(y)Al(1-y)As/InP heterostructures
[AD-A283152] p 271 N95-13140

INDIUM ARSENIDES
The Research Laboratory of Electronics
[AD-A281445] p 386 N95-11830

INDIUM COMPOUNDS
Room-temperature synthesis of CuInQ2 (Q = S or Se) in non-aqueous solution using an organoindium reagent
[NASA-TM-106557] p 260 N95-12662
Synthesis and decomposition of a novel carboxylate precursor to indium oxide
[NASA-TM-106555] p 260 N95-12693

INDIUM GALLIUM ARSENIDES
Origin of optical anisotropy in strained In(x)Ga(1-x)As/InP and In(y)Al(1-y)As/InP heterostructures
[AD-A283152] p 271 N95-13140

INDIUM PHOSPHIDES
Origin of optical anisotropy in strained In(x)Ga(1-x)As/InP and In(y)Al(1-y)As/InP heterostructures
[AD-A283152] p 271 N95-13140

INDUSTRIAL WASTES
Supercritical fluid (SCF) technologies: Assessment of applicability to installation restoration processes
[AD-A281504] p 290 N95-11859

INDUSTRIES
POSIX delta document for the Next-Generation Computer Resources (NGCR) operating systems interface standard baseline, version 4
[AD-A282324] p 347 N95-12418
Fiber-optic sensors and the application to conditional monitoring for mechanical structures
[PB94-207057] p 363 N95-13574

INELASTIC SCATTERING
The odderon in the deep-inelastic lepton-hadron scattering
[DE94-622791] p 360 N95-13274

INERTIAL CONFINEMENT FUSION
Absorption of intense microwaves and ion acoustic turbulence due to heat transport
[DE94-015140] p 369 N95-13285

INERTIAL NAVIGATION
NPS state vector analysis and relative motion plotting software for STS-51
[AD-A282909] p 249 N95-12510

INFECTIOUS DISEASES
Spaceflight and immune responses of Rhesus monkeys
[NASA-CR-196846] p 331 N95-12941

INFLATABLE STRUCTURES
Design studies of large aperture, high-resolution Earth science microwave radiometers compatible with small launch vehicles
[NASA-TP-3469] p 315 N95-12379

INFORMATION DISSEMINATION
Directory of OAQPS information services, May 1994
[PB94-181310] p 318 N95-11848
Access EPA
[PB93-170041] p 319 N95-12356
CENDI Indexing Workshop
[NASA-CP-10160] p 378 N95-12358
NASA STI Program Seminar: Electronic documents
[NASA-TM-109928] p 378 N95-12383
A hitchhiker's guide to microscopy and microanalysis using telecommunications, Email and The Internet
[DE94-013299] p 285 N95-13057
World wide web implementation of the Langley technical report server
[NASA-TM-109162] p 345 N95-13198

INFORMATION MANAGEMENT
New York bight study. Report 4: Geographic information systems and relational database management system development
[AD-A281716] p 327 N95-11787
NASA STI Program Seminar: Electronic documents
[NASA-TM-109928] p 378 N95-12383
Toward infrastructure improvement: An agenda for research
[LC-94-67335] p 376 N95-12385
A data and information system for processing, archival, and distribution of data for global change research
[NASA-CR-196770] p 320 N95-12786
HLLV avionics requirements study and electronic filing system database development
[NASA-CR-193993] p 243 N95-13027

INFORMATION PROCESSING (BIOLOGY)
How are three-dimensional objects represented in the brain?
[AD-A282367] p 335 N95-11942

INFORMATION RETRIEVAL
Directory of OAQPS information services, May 1994
[PB94-181310] p 318 N95-11848
CENDI Indexing Workshop
[NASA-CP-10160] p 378 N95-12358
A data and information system for processing, archival, and distribution of data for global change research
[NASA-CR-196770] p 320 N95-12786
Design of an intelligent support system for scientific databases
[AD-A283043] p 378 N95-12995
HLLV avionics requirements study and electronic filing system database development
[NASA-CR-193993] p 243 N95-13027
A hitchhiker's guide to microscopy and microanalysis using telecommunications, Email and The Internet
[DE94-013299] p 285 N95-13057
World wide web implementation of the Langley technical report server
[NASA-TM-109162] p 345 N95-13198

INFORMATION SYSTEMS
Abstracts from the International Conference on Nuclear Analytical Methods in the Life Sciences
[DE94-621923] p 329 N95-11728
Directory of OAQPS information services, May 1994
[PB94-181310] p 318 N95-11848
Access EPA
[PB93-170041] p 319 N95-12356
NASA STI Program Seminar: Electronic documents
[NASA-TM-109928] p 378 N95-12383
ETRI brochure: History, mission, and activity highlights p 389 N95-12697
A data and information system for processing, archival, and distribution of data for global change research
[NASA-CR-196770] p 320 N95-12786
Aeronautical engineering: A continuing bibliography with indexes (supplement 309)
[NASA-SP-7037(309)] p 229 N95-12894
Information Technology Division's technical paper abstracts
[AD-A282882] p 378 N95-12916
A hitchhiker's guide to microscopy and microanalysis using telecommunications, Email and The Internet
[DE94-013299] p 285 N95-13057
Delta-4: An open architecture for dependable systems
[PB94-195641] p 341 N95-13436

INFORMATION THEORY
CENDI Indexing Workshop
[NASA-CP-10160] p 378 N95-12358

INFORMATION TRANSFER
Catalog of government inventions available for licensing, 1992
[PB93-126205] p 389 N95-12342

INFRARED ASTRONOMY
The Two Micron All Sky Survey: Survey rationale and initial testing
[AD-A283514] p 380 N95-12633
Near-infrared imaging of selected areas
[AD-A283519] p 316 N95-12634
The detectability of extrasolar terrestrial and giant planets during their luminous final accretion
[NASA-CR-196147] p 381 N95-13012

INFRARED DETECTORS
Optical Remote Sensing of the Atmosphere. Technical digest 1993. Volume 5: Postconference edition
[AD-A281446] p 314 N95-11831
The Two Micron All Sky Survey: Survey rationale and initial testing
[AD-A283514] p 380 N95-12633
On the strain and strain-rate dependence of the fraction of plastic work converted to heat: An experimental study using high speed infrared detectors and the Kolsky bar
[SM-92-33] p 354 N95-12728
High frequency thermoacoustic refrigerator
[AD-A280925] p 279 N95-12772
Visible/infrared radiometric calibration station
[DE94-014459] p 363 N95-13106
Vapor detection sensitivity as a function of optical resolution for a single Lorentzian band
[AD-A283444] p 316 N95-13142

INFRARED IMAGERY
Tropical cyclone development and intensification under moderate to strong vertical wind shear
[AD-A282185] p 326 N95-12423

INFRARED RADIATION
Measurement of synchrotron radiation transmission of infrared range by YBa2Cu3O(7-delta) film in superconducting state
[DE94-623270] p 372 N95-11899
Laws of infrared similitude
[AD-A282209] p 354 N95-12426
Methods of modeling radiant energy exchange in radiation fog and clouds
[AD-A283509] p 326 N95-12624
Visible/infrared radiometric calibration station
[DE94-014459] p 363 N95-13106

INFRARED SIGNATURES
Investigation of the effects of solid rocket motor propellant composition on plume signature
[AD-A283365] p 258 N95-12885

INFRARED SPECTRA
Atomic structure modifications of diamond-like nanocomposite films: Observation by Raman spectroscopy, FTIR and STM
[DE94-013732] p 371 N95-11740
UV extinction and IR emission in diffuse H2 regions
[NASA-CR-196939] p 323 N95-12244
Calibration of optical wavelength at 1300 nm and 1550 nm using molecular absorption lines
[PB94-180080] p 362 N95-12598
Infrared spectral measurement of Space Shuttle glow
[AD-A282883] p 250 N95-12917

INFRARED TELESCOPES
The Two Micron All Sky Survey: Survey rationale and initial testing
[AD-A283514] p 380 N95-12633

INHIBITORS
Thermal polymerization of styrene in the presence of stable radicals and inhibitors
[AD-A280926] p 275 N95-12773

INJECTION
Z-pinch plasma by solid fine particle injection p 366 N95-12442
Effects of piston surface treatments on performance and emissions of a methanol-fueled, direct injection, stratified charge engine
[DE94-011851] p 302 N95-12648

INJECTION LOCKING
An investigation of the channel crosstalk in optical heterodyne controlled phased array radars
[AD-A281227] p 285 N95-13371

INJECTORS
Triple sorbent thermal desorption/gas chromatography/mass spectrometry determination of vapor phase organic contaminants
[DE94-013634] p 264 N95-11735
Development of nonintrusive, scatter-independent techniques for measurement of liquid density inside dense sprays
[NASA-CR-196413] p 293 N95-12387

INLET NOZZLES
Shock-tunnel combustor testing for hypersonic vehicles
[NASA-CR-196836] p 246 N95-11938

INNER RADIATION BELT
Inner Magnetosphere Imager (IMI) solar terrestrial probe class mission preliminary design study report
[NASA-TM-108464] p 252 N95-11948
Non-dipolar magnetic field models and patterns of radio emission: Uranus and Neptune compared
[NASA-CR-196412] p 385 N95-12469

INORGANIC COMPOUNDS
The synthesis and structure of polyphosphazenes
[AD-A281723] p 272 N95-11832

INSOLATION
A model of the density of solar radiation energy on an arbitrary plane identification for Warsaw p 384 N95-12243

INSPECTION
Development of an Automated Nondestructive Inspection (ANDI) system for commercial aircraft, phase 1
[AD-A283500] p 234 N95-12623
INSTRUMENT ERRORS
AVHRR/NOAA images to detect and quantify deforestation in Amazon Forest: Relations with TM/LANDSAT data
[INPE-5501-TDI/516] p 316 N95-13350
INSTRUMENT ORIENTATION
SeaWiFS technical report series. Volume 22: Prelaunch acceptance report for the SeaWiFS radiometer
[NASA-TM-104566-VOL-22] p 328 N95-12151
INSULATION
The field emission of electrons in vacuum insulation systems p 357 N95-12101
INSULATORS
Synchrotron studies of narrow band materials
[DE94-013698] p 271 N95-13554
INTEGRAL EQUATIONS
Performance analysis of three dimensional integral equation computations on a massively parallel computer
[NASA-CR-196747] p 346 N95-11863
INTEGRATED CIRCUITS
WOCSDICE 1994: European Workshop on Compound Semiconductor Devices and Integrated Circuits
[AD-A283062] p 288 N95-13052
Ku-band high efficiency GaAs MMIC power amplifiers
[NASA-CR-182156] p 288 N95-13231
Integrated sensor bus
[PB94-206810] p 288 N95-13252
Processing, fabrication, and demonstration of HTS integrated microwave circuits
[AD-A282505] p 289 N95-13300
INTEGRATED LIBRARY SYSTEMS
Design consideration for parallel graphics libraries
[NASA-CR-194935] p 340 N95-12828
INTEGRATED MISSION CONTROL CENTER
Development of a spindle thermal error characterization and compensation sensor system for machining center accuracy enhancement
[AD-A280891] p 300 N95-11729
INTELLIGENCE
Intelligent control systems research
[NASA-CR-195380] p 349 N95-12811
INTERCALATION
Ferric chloride graphite intercalation compounds prepared from graphite fluoride
[NASA-TM-106447] p 261 N95-12783
INTERFERENCE
A wall interference assessment and correction system
[NASA-CR-196940] p 292 N95-12228
INTERFEROMETERS
Matter-wave interferometry with laser cooled atoms
[AD-A282484] p 360 N95-13178
INTERFEROMETRY
Interferograms, schlieren, and shadowgraphs constructed from real- and ideal-gas, two- and three-dimensional computed flowfields
p 295 N95-11971
Defocus measurement using a liquid crystal point diffraction interferometer
[NASA-TM-106687] p 296 N95-12748
INTERLAMINAR STRESS
Accurate interlaminar stress recovery from finite element analysis
[NASA-TM-109149] p 310 N95-11815
Interlaminar stress analysis of dropped-ply laminated plates and shells by a mixed method
[NASA-CR-196851] p 311 N95-11946
Test methods for textile composites
[NASA-CR-4609] p 262 N95-12793
INTERMETALLICS
Certain aspects of the melting, casting and welding of Ni3Al alloys
[DE94-013628] p 269 N95-11897
First principles investigation of the Ir-Zr-Nb ternary system
[AD-A282644] p 270 N95-12543
Thin-film model studies of interfacial reactions in intermetallic matrix composites
[AD-A283360] p 263 N95-12883
Symposium on Structural Intermetallics: Perspectives on Science and Technology, volume 1
[AD-A283378] p 271 N95-12925
Numerical simulations of creep in ductile-phase toughened intermetallic matrix composites
[DE94-014744] p 264 N95-13533
INTERMOLECULAR FORCES
Atomic scale dynamics of a two-dimensional gas-solid interface
[AD-A282646] p 358 N95-12617
INTERNAL COMBUSTION ENGINES
Open-chamber combustion study
[PB94-184090] p 301 N95-12579
Mars methane engine
[NASA-CR-197205] p 302 N95-12668
INTERNAL PRESSURE
Pipeline vibrations. Computer program for the prediction of fluid transients in flexible, unbranched three-dimensional piping systems
[ESDU-93031] p 309 N95-11768
INTERNETS
A hitchhiker's guide to microscopy and microanalysis using telecommunications, Email and The Internet
[DE94-013299] p 285 N95-13057
INTERPLANETARY COMMUNICATION
Design of an unmanned Martian polar exploration system
[NASA-CR-197160] p 383 N95-12529
INTERPOLATION
An interpolation theoretic approach to control
[AD-A281465] p 348 N95-11853
Interpolation of scattered temperature data measurements onto a worldwide regular grid using radial basis functions with applications to global warming
[DE94-014745] p 321 N95-12926
INTERPROCESSOR COMMUNICATION
Eager combining: A coherency protocol for increasing effective network and memory bandwidth in shared-memory multiprocessors
[AD-A281501] p 346 N95-11857
A preliminary evaluation of cache-miss-initiated prefetching techniques in scalable multiprocessors
[AD-A281502] p 346 N95-11858
On bottleneck partitioning k-ary n-cubes
[NASA-CR-194966] p 342 N95-12005
A framework for exploiting data and functional parallelism on distributed memory multicomputers
[AD-A281194] p 347 N95-12523
INTERSTELLAR MATTER
UV extinction and IR emission in diffuse H2 regions
[NASA-CR-196939] p 323 N95-12244
INTESTINES
Morphological differentiation of colon carcinoma cell lines in rotating wall vessels
[NASA-CR-196780] p 333 N95-11808
INTRAVEHICULAR ACTIVITY
Human factors assessments of the STS-57 SpaceHab-1 mission
[NASA-TM-104802] p 337 N95-11878
MOOSE: Manned On-Orbit Servicing Equipment
[NASA-CR-197151] p 254 N95-12790
INVENTIONS
Catalog of government inventions available for licensing, 1991
[PB92-100171] p 389 N95-12303
Catalog of government inventions available for licensing, 1992
[PB93-128205] p 389 N95-12342
INVENTORIES
Space facilities: Meeting future needs for research, development, and operations
[NASA-CR-194821] p 248 N95-12474
INVERSE KINEMATICS
Essential kinematics for autonomous vehicles
[AD-A282456] p 300 N95-12394
An iterative approach to multibody simulation dynamics suitable for parallel implementation
[UTIAS-TN-276] p 347 N95-13353
INVERSE SCATTERING
Nonlinear problems in fluid dynamics and inverse scattering: Langmuir circulations in ocean surface layers
[AD-A282934] p 329 N95-12590
INVERSIONS
A unified approach to geopotential field modeling
[AD-A283453] p 324 N95-12544
INVERTEBRATES
From undersea to outer space: The STS-40 jellyfish experiment
[NASA-TM-109958] p 250 N95-13122
INVERTERS
Design of a ZVS PWM inverter for a brushless DC motor in an EMA application
[NASA-CR-195808] p 312 N95-12620
INVISCID FLOW
An axisymmetric analog two-layer convective heating procedure with application to the evaluation of Space Shuttle Orbiter wing leading edge and windward surface heating
[NASA-CR-188343] p 251 N95-11937
An investigation of the vortex method
[DE94-014931] p 294 N95-13156
IODINE LASERS
Mode-locking a longitudinally pumped low pressure atomic iodine laser
[AD-A282363] p 297 N95-11940
Spaceborne Photonics Institute
[NASA-CR-196784] p 362 N95-12659
ION ACOUSTIC WAVES
Absorption of intense microwaves and ion acoustic turbulence due to heat transport
[DE94-015140] p 369 N95-13285
ION BEAMS
Review of electron beam microinstabilities and their relevance to EBIS devices
[DE94-013755] p 364 N95-11746
Beams 92: Proceedings
[DE94-014783] p 361 N95-11792
Mixed clusters from the coexpansion of C2F6 and n2 in a pulsed, supersonic expansion cluster ion source and beam deflection time-of-flight mass spectrometer: A first application
[AD-A282044] p 361 N95-11910
Plasma and ion beam processing at Los Alamos
[DE94-014293] p 365 N95-12371
Physics of High Energy Density Plasmas Produced by Pulsed Power
[NIFS-PROC-18] p 365 N95-12429
Beam divergence characteristic of two-stage ion diode
p 365 N95-12431
New multi-dimensional diagnostics method for intense ion beams p 365 N95-12432
Evaluation of dynamic pressure of ablation plasma produced by intense, pulsed, ion beam
p 365 N95-12433
A study on successive generation of intense pulsed ion beams by the inverse pinch ion diode
p 365 N95-12434
High resolution diagnostics of intense ion diodes and key issues for bright light ion beam generation
p 367 N95-12448
ION CURRENTS
A study on successive generation of intense pulsed ion beams by the inverse pinch ion diode
p 365 N95-12434
ION CYCLOTRON RADIATION
Studies of electromagnetic ion cyclotron waves using AMPTE/CCE and dynamics explorer
[NASA-CR-196437] p 361 N95-12102
ION DENSITY (CONCENTRATION)
Ionospheric dynamics instrument investigation for the Timed Mission
[NASA-CR-196198] p 325 N95-13190
ION DISTRIBUTION
Stationary plasma thruster ion velocity distribution
[NASA-CR-195379] p 257 N95-11919
Hydrogen bonding and molecular orientation in water/fluorine adlayers on silver(110)
[AD-A282652] p 268 N95-13549
ION ENGINES
Ion engine propelled Earth-Mars cycler with nuclear thermal propelled transfer vehicle, volume 2
[NASA-CR-197208] p 361 N95-12665
Recycle requirements for Nasa's 30 cm xenon ion thruster
[NASA-TM-106668] p 258 N95-12750
ION EXCHANGING
Improving the efficiency of high purity water systems
[DE94-013742] p 318 N95-11784
ION IMPACT
Polyatomic ion impact on solid surfaces and related phenomena
[PB94-201258] p 360 N95-13242
ION IMPLANTATION
Plasma and ion beam processing at Los Alamos
[DE94-014293] p 365 N95-12371
Role of implantation-induced defects in surface-oriented diffusion of fluorine in silicon
[DE94-014905] p 374 N95-13125
Activities of Lehigh University
[AD-A282098] p 375 N95-13168
ION PROPULSION
Ion engine propelled Earth-Mars cycler with nuclear thermal propelled transfer vehicle, volume 2
[NASA-CR-197208] p 361 N95-12665
Recycle requirements for Nasa's 30 cm xenon ion thruster
[NASA-TM-106668] p 258 N95-12750
ION SOURCES
Review of electron beam microinstabilities and their relevance to EBIS devices
[DE94-013755] p 364 N95-11746
Mixed clusters from the coexpansion of C2F6 and n2 in a pulsed, supersonic expansion cluster ion source and beam deflection time-of-flight mass spectrometer: A first application
[AD-A282044] p 361 N95-11910
Beam divergence characteristic of two-stage ion diode
p 365 N95-12431
A study on successive generation of intense pulsed ion beams by the inverse pinch ion diode
p 365 N95-12434

ION TEMPERATURE
Magnetospheric space plasma investigations
[NASA-CR-196793] p 382 N95-12940
IONIC COLLISIONS
Magnetospheric space plasma investigations
[NASA-CR-196793] p 382 N95-12940
Particle-production mechanism in relativistic heavy-ion collisions
[DE94-014427] p 359 N95-13104
IONIC CRYSTALS
Alignment and experiment of the HL-1 x ray bent-crystal spectrometer
[DE94-624719] p 297 N95-13537
IONIC MOBILITY
Reactions of atmospheric cluster ions
[AD-A282598] p 324 N95-12534
IONIC REACTIONS
Reactions of atmospheric cluster ions
[AD-A282598] p 324 N95-12534
IONIZATION
Experimental and theoretical study of neon-like selenium x-ray laser spectral line profiles
[DE94-015327] p 298 N95-12761
The laser and its applications on environment and biotechnology research
[DE94-013831] p 299 N95-13076
IONIZING RADIATION
Radiation-induced structural changes, 3
[DE94-753401] p 371 N95-11819
IONOSPHERIC COMPOSITION
Quantitative understanding of the cycles of oxidized and reduced sulfur on Venus
[NASA-CR-196924] p 382 N95-12011
IONOSPHERIC F-SCATTER PROPAGATION
Guest investigator program study: Physics of equatorial plasma bubbles
[NASA-CR-196150] p 368 N95-12853
IONOSPHERIC PROPAGATION
Principles of GPS one-way data processing for high precision positioning applications: Algorithms and software issues p 237 N95-12177
IONOSPHERICS
Principles of GPS one-way data processing for high precision positioning applications: Algorithms and software issues p 237 N95-12177
IRIDIUM ALLOYS
First principles investigation of the Ir-Zr-Nb ternary system
[AD-A282644] p 270 N95-12543
IRON
Magnetic response of ultrathin Fe on MgO: A polarised neutron reflectometry study
[DE94-013192] p 375 N95-13272
IRON COMPOUNDS
Ferric chloride graphite intercalation compounds prepared from graphite fluoride
[NASA-TM-106447] p 261 N95-12783
IRON OXIDES
Ferric chloride graphite intercalation compounds prepared from graphite fluoride
[NASA-TM-106447] p 261 N95-12783
IRRADIANCE
Development of UV irradiance standards
[PB94-181005] p 320 N95-12771
IRRADIATION
Radiation-induced structural changes, 4
[DE94-753223] p 356 N95-11817
Role of implantation-induced defects in surface-oriented diffusion of fluorine in silicon
[DE94-014905] p 374 N95-13125
Development of radiation hard scintillators
[DE94-013204] p 296 N95-13287
ISOPROPYL ALCOHOL
CeO2-ZrO2 powder synthesis by way of alcohol dehydration of aqueous salt solutions
[INPE-5484-PRE/1783] p 276 N95-13191
ISOTOPE SEPARATION
CRYOCOL: A computer program to calculate the cryogenic distillation of hydrogen isotopes
[DE94-622012] p 268 N95-13531
ISOTROPIC MEDIA
Singularity of the Green dyadics for bi-isotropic
[PB94-184504] p 283 N95-12581
ISOTROPY
Buckling of flat rectangular orthotropic plates
[ESDU-94005] p 310 N95-11771
ITERATION
Parallel preconditioners for the conjugate gradient method
[PB94-201605] p 347 N95-13404
ITERATIVE SOLUTION
A unified approach to geopotential field modeling
[AD-A283453] p 324 N95-12544
An iterative approach to multibody simulation dynamics suitable for parallel implementation
[UTIAS-TN-276] p 347 N95-13353
Adaptive relaxation for the steady-state analysis of Markov chains
[NASA-CR-194944] p 345 N95-13420
IUE
UV extinction and IR emission in diffuse H2 regions
[NASA-CR-196939] p 323 N95-12244

J

JET AIRCRAFT NOISE
On the interaction of jet noise with a nearby flexible structure
[NASA-CR-194934] p 290 N95-11812
JET ENGINES
Engine structures analysis software: Component Specific Modeling (COSMO)
[NASA-CR-195378] p 309 N95-11711
The development of the F100-PW-220 and F110-GE-100 engines: A case study of risk assessment and risk management
[AD-A282467] p 244 N95-13289
JET EXHAUST
Moisture induced pressures in concrete airfield pavements
[AD-A281974] p 245 N95-11789
JET FLOW
On the interaction of jet noise with a nearby flexible structure
[NASA-CR-194934] p 290 N95-11812
Modeling jets in cross flow
[NASA-CR-194965] p 291 N95-11930
Simultaneous three-dimensional velocity and mixing measurements by use of laser Doppler velocimetry and fluorescence probes in a water tunnel
[NASA-TP-3454] p 246 N95-13553
JOSEPHSON JUNCTIONS
Response of high T(sub c) superconducting Josephson junction to nuclear radiation
[DE94-624705] p 360 N95-13536
JOURNAL BEARINGS
A simplified thermohydrodynamic model for fluid film bearings
[DE94-015011] p 304 N95-13183
Pressure measurements of a three wave journal air bearing p 307 N95-13605

K

K-EPSILON TURBULENCE MODEL
Modification of the two-equation turbulence model in NPARC to a Chien low Reynolds number k-epsilon formulation
[NASA-TM-106710] p 231 N95-11917
KAONS
Contribution of hadronic intermediate states in nonleptonic weak decays of K, charm and B mesons
[DE94-753399] p 356 N95-11818
KERR MAGNETOOPTICAL EFFECT
Studies of optical phase conjugators and applications
[AD-A282626] p 362 N95-12538
KETONES
Thermal conductivity of gaseous oxygenated aliphatic hydrocarbons. Alcohols, aldehydes, ketones and ethers
[ESDU-94018] p 265 N95-11795
KEVLAR (TRADEMARK)
Ten-year ground exposure of composite materials used on the Bell Model 206L helicopter flight service program
[NASA-TP-3468] p 262 N95-12357
KINEMATICS
Essential kinematics for autonomous vehicles
[AD-A282456] p 300 N95-12394
KINETIC THEORY
Review of electron beam microinstabilities and their relevance to EBIS devices
[DE94-013755] p 364 N95-11746
KINETICS
Amine catalyzed intramolecular imidization of alkyl and aryl phthalamates, kinetics and mechanism in deuterated chloroform
[AD-A281741] p 259 N95-11844
Adherend surface effects on epoxy cure by NMR
[AD-A282165] p 274 N95-12420
Hydrogen desulfurization of nickel: Thermodynamics and kinetics
[AD-A282581] p 266 N95-12549
Kinetics and characterization of tungsten CVD processes
[PB94-206901] p 271 N95-13411
KNOWLEDGE BASED SYSTEMS
Intelligent knowledge-based engineering
[AD-A281906] p 377 N95-11788
Validating medical knowledge based systems
[PB94-191301] p 377 N95-11824
Space Station Module Power Management and Distribution System (SSM/PMAD)
[NASA-CR-193991] p 258 N95-12819
Design of an intelligent support system for scientific databases
[AD-A283043] p 378 N95-12995
KNOWLEDGE BASES (ARTIFICIAL INTELLIGENCE)
Thunderstorm hypothesis reasoner
[AD-A282664] p 326 N95-12805
Population-based incremental learning. A method for integrating genetic search based function optimization and competitive learning
[AD-A282654] p 350 N95-12835
KP INDEX
Determination of the auroral oval Q index from the air weather service K index
[AD-A282764] p 324 N95-12508
KUTTA-JOUKOWSKI CONDITION
Numerical time dependent sheet cavitation simulations using a higher order panel method
[PB94-204435] p 294 N95-13249

L

LABORATORIES
Directory of Federal laboratory and technology resources
[PB93-100097] p 389 N95-12223
Solar-Terrestrial Environment Laboratory, Nagoya University p 389 N95-12610
LABORATORY EQUIPMENT
A laboratory vacuum apparatus for magnetron sputtering of thin Z ZnO piezoelectric films, magnetron sputtering p 296 N95-12111
LABYRINTH SEALS
Relative performance comparison between baseline labyrinth and dual-brush compressor discharge seals in a T-700 engine test p 307 N95-13607
LAGRANGIAN EQUILIBRIUM POINTS
Project ECHO: Electronic Communications from Halo Orbit
[NASA-CR-197190] p 283 N95-12644
LAMINAR BOUNDARY LAYER
Validation of the RPLUS3D code for supersonic inlet applications involving three-dimensional shock wave-boundary layer interactions
[NASA-TM-106579] p 233 N95-13058
LAMINAR FLOW
Code GFACE: Gas lubricated face seals in laminar regime p 305 N95-13585
LAMINATES
Stiffnesses of laminated flat plates
[ESDU-94003] p 309 N95-11769
Stress analysis of laminated flat plates
[ESDU-94004] p 309 N95-11770
Buckling of flat rectangular orthotropic plates
[ESDU-94005] p 310 N95-11771
Elastic buckling of unbalanced laminated fibre reinforced composite plates (rectangular plates of AsBtDs type, all edges simply-supported under biaxial loading)
[ESDU-94006] p 310 N95-11772
Elastic buckling of cylindrically curved laminated fibre reinforced composite panels with all edges simply-supported under biaxial loading
[ESDU-94007] p 310 N95-11773
Accurate interlaminar stress recovery from finite element analysis
[NASA-TM-109149] p 310 N95-11815
Interlaminar stress analysis of dropped-ply laminated plates and shells by a mixed method
[NASA-CR-196851] p 311 N95-11946
Test methods for textile composites
[NASA-CR-4609] p 262 N95-12793
Glass reinforced-diallylbisphenol/maleimide composites with modified interphases
[AD-A282496] p 264 N95-13298
LANDFORMS
Periglacial and glacial analogs for Martian landforms
[NASA-CR-196772] p 383 N95-12952
LANDING GEAR
Flight investigation of the use of a nose gear jump strut to reduce takeoff ground roll distance of STOL aircraft
[NASA-TM-108819] p 238 N95-12225
Gemini: A long-range cargo transport
[NASA-CR-197149] p 239 N95-12626
LANDING LOADS
Viper cabin-fuselage structural design concept with engine installation and wing structural design
[NASA-CR-197162] p 239 N95-12305
Gemini: A long-range cargo transport
[NASA-CR-197149] p 239 N95-12626
LANDING MODULES
Design of an unmanned Martian polar exploration system
[NASA-CR-197160] p 383 N95-12529

LANDING SITES
External Device to Incrementally Skid the Habitat (E-DISH)
[NASA-CR-197147] p 301 N95-12625
LANDMARKS
Using landmarks for the vehicle location measurement
[PB94-184512] p 237 N95-12582
Learning one-dimensional geometric patterns under one-sided random misclassification noise
[DE94-014659] p 350 N95-12864
LANDSAT SATELLITES
AVHRR/NOAA images to detect and quantify deforestation in Amazon Forest: Relations with TM/LANDSAT data
[INPE-5501-TDI/516] p 316 N95-13350
LANTHANUM COMPOUNDS
A brightness comparison of thermionic electron sources in a TEM
[DE94-013300] p 360 N95-13338
LARGE SPACE STRUCTURES
Design of passive piezoelectric damping for space structures
[NASA-CR-4625] p 252 N95-12165
LASER ANNEALING
Method of laser processing ferroelectric materials
[AD-D016386] p 298 N95-12780
LASER APPLICATIONS
Ultrashort laser pulse effects in ocular and related media: Laser-induced shock wave propagation and retinal damage
[AD-A282599] p 334 N95-12535
Progress on resonance ionization detection of combustion radicals
[DE94-015339] p 267 N95-12762
Method for laser-assisted etching of III-V and II-VI semiconductor compounds using chlorofluorocarbon ambients
[AD-D016385] p 298 N95-12779
The future of diode pumped solid state lasers and their applicability to the automotive industry
[DE94-014736] p 298 N95-12868
LASER ARRAYS
Diode-pumped micro-laser arrays
[AD-A282494] p 299 N95-13294
LASER BEAMS
Matter-wave interferometry with laser cooled atoms
[AD-A282484] p 360 N95-13178
Laser based combustion laboratory at NTH/SINTEF applied thermodynamics
[PB94-202603] p 299 N95-13246
LASER CAVITIES
Wavelength-encoded processing in semiconductor lasers
[AD-A282649] p 297 N95-12751
LASER DOPPLER VELOCIMETERS
Laser Doppler velocimeter measurements of boundary layer velocity and turbulent intensities in Mach 2.5 flow
[NASA-CR-196861] p 289 N95-11709
Lidar performance analysis
[NASA-CR-196510] p 362 N95-12390
Simultaneous three-dimensional velocity and mixing measurements by use of laser Doppler velocimetry and fluorescence probes in a water tunnel
[NASA-TP-3454] p 246 N95-13553
LASER FUSION
Target area chamber system design for the National Ignition Facility
[DE94-013347] p 364 N95-11754
LASER GUIDANCE
An adaptive optics package designed for astronomical use with a laser guide star tuned to an absorption line of atomic sodium
[DE94-012391] p 363 N95-13532
LASER HEATING
Experimental and theoretical study of neon-like selenium x-ray laser spectral line profiles
[DE94-015327] p 298 N95-12761
LASER INDUCED FLUORESCENCE
Stationary plasma thruster ion velocity distribution
[NASA-CR-195379] p 257 N95-11919
Spaceborne Photonics Institute
[NASA-CR-196784] p 362 N95-12659
Development of techniques for the in situ observation of OH and HO2 for studies of the impact of high-altitude supersonic aircraft on the stratosphere
[NASA-CR-196759] p 321 N95-12832
Planar Rayleigh scattering and laser-induced fluorescence for visualization of a hot, Mach 2 annular air jet
[NASA-TM-4576] p 247 N95-13196
Laser based combustion laboratory at NTH/SINTEF applied thermodynamics
[PB94-202603] p 299 N95-13246
LASER INTERFEROMETRY
Matter-wave interferometry with laser cooled atoms
[AD-A282484] p 360 N95-13178
Improvements of HCN laser heterodyne interferometer for measuring plasma density
[DE94-625037] p 370 N95-13341
LASER MATERIALS
Tetravalent chromium (Cr(4+)) as laser-active ion for tunable solid-state lasers
[NASA-CR-196481] p 298 N95-12951
Laser physics of Nd(exp 3+)-doped phosphate glasses
[DE94-015141] p 299 N95-13534
LASER MODE LOCKING
Mode-locking a longitudinally pumped low pressure atomic iodine laser
[AD-A282363] p 297 N95-11940
LASER PLASMAS
Plasma opening switch by laser-produced plasma with different kinds of ion species p 367 N95-12451
LASER PUMPING
High average power parametric frequency conversion-new concepts and new pump sources
[DE94-013652] p 314 N95-11783
Mode-locking a longitudinally pumped low pressure atomic iodine laser
[AD-A282363] p 297 N95-11940
Tetravalent chromium (Cr(4+)) as laser-active ion for tunable solid-state lasers
[NASA-CR-196481] p 298 N95-12951
Diode-pumped micro-laser arrays
[AD-A282494] p 299 N95-13294
Stimulated scattering of a slow electromagnetic wave excited by the relativistic electron beam
[DE94-625049] p 285 N95-13343
LASER RANGE FINDERS
Satellite laser ranging and gravity field modeling accuracy
[NASA-CR-196057] p 248 N95-12837
A comparison of two sites for the purpose of satellite laser ranging
[AD-A283149] p 299 N95-13139
LASER SPECTROSCOPY
Differential absorption lidar measurements of atmospheric water vapor using a pseudonoise code modulated AlGaAs laser
[NASA-TM-104610] p 314 N95-11997
Laser spectroscopy of GdO: Ligand field assignments of 4f7(8S)6p reversing 4f7(8)6s transitions
[AD-A282827] p 268 N95-13180
LASER TARGETS
Target area chamber system design for the National Ignition Facility
[DE94-013347] p 364 N95-11754
Plasma opening switch by laser-produced plasma with different kinds of ion species p 367 N95-12451
Time-resolved electron thermal conduction by probing of plasma formation in transparent solids with high power subpicosecond laser pulses
[DE94-015170] p 370 N95-13555
LASERS
The laser and its applications on environment and biotechnology research
[DE94-013831] p 299 N95-13076
LATEX
Additives in bituminous materials and fuel-resistant sealers
[DOT/FAA/CT-94/78] p 273 N95-12131
LATHES
Prediction of geometric-thermal machine tool errors by artificial neural networks
[PB94-186673] p 348 N95-11909
LATTICE PARAMETERS
Pressure studies of alkali, alkaline earth and rare earth doped C60 superconductors
[DE94-013345] p 372 N95-11862
One-step synthesis of dithiocarbamates from metal powders
[NASA-TM-106558] p 260 N95-12692
LAUNCH VEHICLE CONFIGURATIONS
A revolutionary lunar space transportation system architecture using extraterrestrial LOX-augmented NTR propulsion
[NASA-TM-106726] p 249 N95-11703
Trade study plan for Reusable Hydrogen Composite Tank System (RHCTS)
[NASA-CR-196871] p 252 N95-11945
Orion: Design of a system for assured low-cost human access to space
[NASA-CR-197185] p 253 N95-12564
LAUNCH VEHICLES
Converting the Minuteman missile into a small satellite launch system
[NASA-CR-197169] p 249 N95-12531
Orion: Design of a system for assured low-cost human access to space
[NASA-CR-197185] p 253 N95-12564
Athena: Advanced air launched space booster
[NASA-CR-197148] p 258 N95-12604
Various advanced design projects promoting engineering education
[NASA-CR-197170] p 258 N95-12630
LAUNCHING SITES
Environmental process improvement feasibility study and demonstration program
[NASA-CR-196789] p 319 N95-12110
LAW (JURISPRUDENCE)
Environmental process improvement feasibility study and demonstration program
[NASA-CR-196789] p 319 N95-12110
LAWS
Laws of infrared similitude
[AD-A282209] p 354 N95-12426
LEAD ACID BATTERIES
TKKMOD: A computer simulation program for an integrated wind diesel system. Version 1.0: Document and user guide
[PB94-179090] p 317 N95-11798
LEAD ZIRCONATE TITANATES
Method of laser processing ferroelectric materials
[AD-D016386] p 298 N95-12780
LEADING EDGES
Impingement flow heat transfer measurements of turbine blades using a jet array
[AD-A283450] p 375 N95-12512
LEAKAGE
Microfabricated hydrogen sensor technology for aerospace and commercial applications
[NASA-TM-106703] p 284 N95-12674
Environmental and customer-driven seal requirements p 305 N95-13588
Brush seals for cryogenic applications p 305 N95-13592
Air Force seal activities p 306 N95-13600
LEAR JET AIRCRAFT
Effects of mass on aircraft sidearm controller characteristics
[NASA-TM-104277] p 244 N95-11868
Aircraft wake RCS measurement p 235 N95-13210
LEARNING
Intelligent control systems research
[NASA-CR-195380] p 349 N95-12811
LEAST SQUARES METHOD
A unified approach to geopotential field modeling
[AD-A283453] p 324 N95-12544
LECTURES
Real world software engineering
[AD-A282365] p 342 N95-11941
LEPTONS
Search for supersymmetry at CDF
[DE94-014264] p 357 N95-12369
A search for a heavy neutral gauge boson decaying into dielectrons in (-p)p collisions at the square root of s = 1.8 TeV
[DE94-014987] p 359 N95-13161
LIBRARIES
Access EPA
[PB93-170041] p 319 N95-12356
CENDI Indexing Workshop
[NASA-CP-10160] p 378 N95-12358
LICENSING
Catalog of government inventions available for licensing, 1991
[PB92-100171] p 389 N95-12303
LICHENS
Environmental lichenology: Biomonitoring trace-element air pollution
[PB94-191335] p 318 N95-11826
LIE GROUPS
Extensions and contractions of the Lie algebra of q-pseudodifferential symbols
[PB94-192374] p 352 N95-12603
LIFE (DURABILITY)
Activities of the Structures Division, Lewis Research Center
[NASA-TM-108081] p 313 N95-13235
LIFE SCIENCES
Abstracts from the International Conference on Nuclear Analytical Methods in the Life Sciences
[DE94-621923] p 329 N95-11728
JPRS report: Science and technology. Central Eurasia: Life sciences
[JPRS-ULS-93-014] p 318 N95-11743
JPRS report: Science and technology. Central Eurasia: Life sciences
[JPRS-ULS-93-012] p 332 N95-11744
JPRS report: Science and technology. Central Eurasia
[JPRS-UST-94-017] p 247 N95-12001
JPRS report: Science and technology. Central Eurasia
[JPRS-UST-94-020] p 389 N95-12002
JPRS report: Science and technology. Central Eurasia
[JPRS-UST-94-019] p 389 N95-12003
Aerospace medicine and biology: A continuing bibliography with indexes (supplement 394)
[NASA-SP-7011(394)] p 335 N95-13230

Life Sciences Centrifuge Facility assessment
[NASA-CR-196848] p 332 N95-13423

LIFE SUPPORT SYSTEMS
Methodologies for processing plant material into acceptable food on a small scale
[NASA-CR-177647] p 338 N95-12132
Aerospace medicine and biology: A continuing bibliography with indexes (supplement 394)
[NASA-SP-7011(394)] p 335 N95-13230

LIFT
A simple analytical aerodynamic model of Langley Winged-Cone Aerospace Plane concept
[NASA-CR-194987] p 252 N95-12175
Cabin-fuselage-wing structural design concept with engine installation
[NASA-CR-197172] p 242 N95-12993

LIFT DRAG RATIO
The OFP-6M transport jet
[NASA-CR-197159] p 240 N95-12637
The Balsa bullet: A high speed, low-cost general aviation aircraft for Aeroworld
[NASA-CR-197165] p 240 N95-12638

LIGANDS
Novel activated carbon impregnants consisting of transition metal complexes. Part 1: Background, syntheses and characterizations
[AD-A282583] p 259 N95-12551
Laser spectroscopy of GdO: Ligand field assignments of 4f7(8S)6p reversing 4f7(8)6s transitions
[AD-A282827] p 268 N95-13180

LIGHT (VISIBLE RADIATION)
Visible/infrared radiometric calibration station
[DE94-014459] p 363 N95-13106

LIGHT AMPLIFIERS
Wavelength-encoded processing in semiconductor lasers
[AD-A282649] p 297 N95-12751

LIGHT BEAMS
Light beam and pulse propagation in nonlinear dielectrics
[AD-A282548] p 282 N95-12496

LIGHT CURVE
BATSE observations of Nova Muscae 1991
[NASA-CR-196416] p 380 N95-12464

LIGHT EMISSION
Studies of positron induced luminescence from polymers
[DE94-013622] p 272 N95-11733
Free electron lasers and other advanced sources of light: Scientific research opportunities p 297 N95-12375

LIGHT EMITTING DIODES
Activities of the Helsinski University of Technology, Applied Electronics Laboratory
[PB94-179074] p 385 N95-11797
Silicon-based blue light emitting diode
[AD-A282382] p 286 N95-12009
Wavelength-encoded processing in semiconductor lasers
[AD-A282649] p 297 N95-12751
Pseudomorphic semiconducting heterostructures from combinations of AlN, GaN and selected SiC polytypes: Theoretical advancement and its coordination with experimental studies of nucleation, growth, characterization and device development
[AD-A281218] p 289 N95-13368

LIGHT GAS GUNS
Present status of ohmic ignition chemical launcher experiment p 366 N95-12438

LIGHT IONS
Magnetospheric space plasma investigations
[NASA-CR-196793] p 382 N95-12940

LIGHT SCATTERING
Diagnostic techniques for semiconductor materials processing
[AD-A282810] p 373 N95-12602

LIGHTNING
Thunderstorm hypothesis reasoner
[AD-A282664] p 326 N95-12805

LIGNIN
Rational enzyme redesign
[DE94-014565] p 331 N95-12677

LINE SPECTRA
BATSE observations of Nova Muscae 1991
[NASA-CR-196416] p 380 N95-12464
Calibration of optical wavelength at 1300 nm and 1550 nm using molecular absorption lines
[PB94-180080] p 362 N95-12598
Photographic region elemental abundance analyses of Dr. David S. Leckrone's GTO HST stars 2
[NASA-CR-196756] p 381 N95-12788

LINEAR EQUATIONS
Implementing a linear equation solver in the CFD code PHOENICS
[PB94-195757] p 353 N95-13439

LINEAR POLARIZATION
Plane-wave reflection from uniaxial chiral interface and its application to polarization transformation
[PB94-184496] p 283 N95-12580

LINGUISTICS
Recovery blocks
[PB94-205077] p 345 N95-13432
Category theory: The mathematics for the humanities
[PB94-205044] p 353 N95-13560

LIQUID ALLOYS
Certain aspects of the melting, casting and welding of Ni3Al alloys
[DE94-013628] p 269 N95-11897

LIQUID CRYSTALS
Chiral recognition in molecular and macromolecular pairs of (S)- and (R)-1-cyano-2-methylpropyl 4'(4-(8-vinyloxyoctyloxy)benzoyl) biphenyl-4-carboxylate enantiomers
[AD-A281438] p 356 N95-11828
Synthesis, structure and properties of segmented polymers containing mesogens
[AD-A281419] p 272 N95-11852
Design and synthesis of tight pitch FLCs for analog voltage-limited electro-optic modulators
[AD-A281472] p 371 N95-11855
Determination of a transient heat transfer property of acrylic using thermochromic liquid crystals
[NASA-TM-106541] p 372 N95-11882
Polymer effect on heterochiral molecular recognition in molecular and macromolecular pairs of liquid crystals of (R)- and (S)-2-chloro-4-methylpentyl 4'-((8-(vinyloxy)octyl)oxy)biphenyl-4-caroxylate
rs
[AD-A281193] p 358 N95-12522
Draft standard for color active matrix liquid crystal displays (AMLCDs) in US Military aircraft. Recommended best practices
[AD-A282950] p 243 N95-12591
Defocus measurement using a liquid crystal point diffraction interferometer
[NASA-TM-106687] p 296 N95-12748

LIQUID HYDROGEN
Trade study plan for Reusable Hydrogen Composite Tank System (RHCTS)
[NASA-CR-196871] p 252 N95-11945
STS propellant densification feasibility study data book
[NASA-TM-108467] p 278 N95-12857
Cryogenic On-Orbit Liquid Depot Storage, Acquisition, and Transfer Satellite (COLD-SAT)
[NASA-CR-185249] p 259 N95-13237

LIQUID LITHIUM
MHD pressure drops and thermal hydraulic analysis for the ITER breeding blanket design
[DE94-015085] p 369 N95-13280

LIQUID NITROGEN
Feasibility study for the Cryogenic Orbital Nitrogen Experiment (CONE)
[NASA-CR-187231] p 294 N95-13234

LIQUID OXYGEN
A revolutionary lunar space transportation system architecture using extraterrestrial LOX-augmented NTR propulsion
[NASA-TM-106726] p 249 N95-11703
Development of nonintrusive, scatter-independent techniques for measurement of liquid density inside dense sprays
[NASA-CR-196413] p 293 N95-12387
STS propellant densification feasibility study data book
[NASA-TM-108467] p 278 N95-12857

LIQUID PHASES
Radiation-induced structural changes, 4
[DE94-753223] p 356 N95-11817

LIQUID PROPELLANT ROCKET ENGINES
AFOSR Contractors Meeting in Propulsion
[AD-A282729] p 257 N95-12507

LIQUID ROCKET PROPELLANTS
Project Hyreus: Mars sample return mission utilizing in situ propellant production
[NASA-CR-197189] p 383 N95-12826
STS propellant densification feasibility study data book
[NASA-TM-108467] p 278 N95-12857

LIQUID SLOSHING
Sloshing analysis of tanks containing multiple fluid layers
[DE94-013333] p 290 N95-11753

LIQUID WASTES
Sloshing analysis of tanks containing multiple fluid layers
[DE94-013333] p 290 N95-11753

LIQUID-LIQUID INTERFACES
Numerical simulations of drop collisions
[NASA-TM-106751] p 295 N95-13550

LIQUIDS
Vapour pressures and critical points of liquids. Polycyclic phenyl and cyclohexyl compounds
[ESDU-94001] p 266 N95-12128
Orthobaric densities and molar volumes of liquids. Polycyclic phenyl and cyclohexyl compounds
[ESDU-94002] p 266 N95-12129

LITERATURE
Comprehensive and critical literature review on insitu micro-sensors for application in tribology
[AD-A281646] p 296 N95-13165

LITHOGRAPHY
Development of nanostructure fabrication technology and new electron-quantum wave devices
[AD-A281724] p 286 N95-11860

LITHOSPHERE
FORTRAN programs to process Magsat data for lithospheric, external field, and residual core components
[NASA-TM-104612] p 323 N95-12130
Neotectonics of Asia: Thin-shell finite-element models with faults
[NASA-CR-196436] p 324 N95-12949

LOAD CARRYING CAPACITY
High frequency flow/structural interaction in dense subsonic fluids handbook
[NASA-CR-194007] p 230 N95-11807

LOAD TESTS
Effect of shear lips, loading transitions and test frequency on constant delta K and constant load amplitude fatigue tests
[PB94-192440] p 312 N95-12775
Test methods for textile composites
[NASA-CR-4609] p 262 N95-12793
Tensile creep and stress-rupture behavior of polymer derived SiC fibers
[NASA-TM-106692] p 263 N95-12813
Strain gage selection in loads equations using a genetic algorithm
[NASA-CR-4597] p 242 N95-12831

LOADING MOMENTS
Optimization of aerospace structures
[NASA-CR-196763] p 242 N95-12787
Strain gage selection in loads equations using a genetic algorithm
[NASA-CR-4597] p 242 N95-12831

LOADS (FORCES)
Symmetric steady manoeuvre loads on rigid aircraft of classical configuration at subsonic speeds
[ESDU-94009] p 238 N95-11774
Interlaminar stress analysis of dropped-ply laminated plates and shells by a mixed method
[NASA-CR-196851] p 311 N95-11946
An analysis of the load-bearing capacity of members of square cross section with a series of perpendicular notches p 312 N95-12631
Cabin fuselage structural design with engine installation and control system
[NASA-CR-197173] p 240 N95-12639
Effects of piston surface treatments on performance and emissions of a methanol-fueled, direct injection, stratified charge engine
[DE94-011851] p 302 N95-12648
Design and testing of a model CELSS chamber robot
[NASA-CR-197196] p 303 N95-12694
Loads for pulsed power cylindrical implosion experiments
[DE94-014429] p 299 N95-13080
Provoking and measuring cell losses in ATM systems by importance sampling, control variables and load cycles
[PB94-202520] p 285 N95-13558

LOGIC CIRCUITS
Quantum cellular automata
[AD-A283351] p 287 N95-12881
Integrated sensor bus
[PB94-206810] p 288 N95-13252

LOGIC DESIGN
The Second Workshop on Principles and Practice of Constraint Programming
[AD-A281731] p 229 N95-13166

LOGISTICS
Toward infrastructure improvement: An agenda for research
[LC-94-67335] p 376 N95-12385

LONG DURATION EXPOSURE FACILITY
Analysis for Be-7 and Be-10 on LDEF materials and their sources
[NASA-CR-193989] p 268 N95-13084

LONG DURATION SPACE FLIGHT
An investigation of the use of temporal decomposition in space mission scheduling
[NASA-CR-198420] p 377 N95-12618

LONG TERM EFFECTS
Ten-year ground exposure of composite materials used on the Bell Model 206L helicopter flight service program
[NASA-TP-3468] p 262 N95-12357
Periglacial and glacial analogs for Martian landforms
[NASA-CR-196772] p 383 N95-12952

LONGITUDINAL WAVES
Excitation of fast magneto-acoustic waves in unhomogeneous plasma of a large size tokamak
[DE94-625050] p 370 N95-13540
LOW COST
Composites (CFCCs) for low cost energy and cleaner environment
[DE94-013601] p 272 N95-11781
Orion: Design of a system for assured low-cost human access to space
[NASA-CR-197185] p 253 N95-12564
The Balsa bullet: A high speed, low-cost general aviation aircraft for Aeroworld
[NASA-CR-197165] p 240 N95-12638
LCX: Proposal for a low-cost commercial transport
[NASA-CR-197186] p 241 N95-12645
LOW NOISE
Computerized design and generation of low-noise helical gears with modified surface topology
[NASA-TM-106696] p 303 N95-13083
LOW PRESSURE
Mode-locking a longitudinally pumped low pressure atomic iodine laser
[AD-A282363] p 297 N95-11940
LOW REYNOLDS NUMBER
Modification of the two-equation turbulence model in NPARC to a Chien low Reynolds number k-epsilon formulation
[NASA-TM-106710] p 231 N95-11917
Scale disparity and spectral transfer in anisotropic numerical turbulence
[NASA-CR-194956] p 291 N95-11929
LOW TEMPERATURE
Studies of low temperature, low flux radiation embrittlement of nuclear reactor structural materials
[DE94-013710] p 269 N95-11738
LOW TEMPERATURE ENVIRONMENTS
Bibliography on cold regions science and technology, volume 47, part 1
[AD-A281879] p 378 N95-13167
LOW THRUST
SolSTUS: Solar Source Thermal Upper Stage
[NASA-CR-197179] p 257 N95-13581
LOW VISIBILITY
Evaluation of candidate millimeter wave sensors for synthetic vision p 236 N95-13214
Passive MMW camera for low visibility landings p 236 N95-13215
LOW VOLTAGE
Surface roughness characterization of various ceramic fibers using AFM and low voltage SEM
[DE94-013635] p 272 N95-11736
LUBRICATING OILS
Space hardware designs, volume 1
[NASA-CR-197209] p 253 N95-12663
LUBRICATION
High temperature solid lubricant materials for heavy duty and advanced heat engines
[NASA-TM-106570] p 260 N95-12764
Environmental and customer-driven seal requirements p 305 N95-13588
LUGS
A study of fatigue crack growth in lugs under spectrum loading
[NAL-PD-SN-9407] p 311 N95-11879
LUMINESCENCE
Studies of positron induced luminescence from polymers
[DE94-013622] p 272 N95-11733
Enhancement of luminescence in polymer nanocomposites
[AD-A282539] p 262 N95-12404
LUMINOSITY
X-ray temporal and spectral studies of blazars with the Ginga satellite
[NASA-CR-196330] p 380 N95-12466
LUNAR EXCAVATION EQUIPMENT
Lunar vertical-shaft mining system
[NASA-CR-197154] p 384 N95-13497
LUNAR EXPLORATION
Interviews with the Apollo lunar surface astronauts in support of planning for EVA systems design
[NASA-TM-108846] p 337 N95-11905
Meeting the challenge of manned lunar and Martian exploration p 339 N95-11970
Lunar Lander project: A study on future manned missions to the Moon
[NASA-CR-197177] p 383 N95-12362
LUNAR LANDING MODULES
Lunar Lander project: A study on future manned missions to the Moon
[NASA-CR-197177] p 383 N95-12362
LUNAR MINING
Lunar vertical-shaft mining system
[NASA-CR-197154] p 384 N95-13497
LUNAR PROBES
Lunar Lander project: A study on future manned missions to the Moon
[NASA-CR-197177] p 383 N95-12362
LUNAR RESOURCES
Glass microsphere lubrication
[NASA-CR-197157] p 277 N95-13508
LUNAR SOIL
A lunar/Martian anchor emplacement system
[NASA-CR-197193] p 302 N95-12690
Glass microsphere lubrication
[NASA-CR-197157] p 277 N95-13508
LUNAR SPACECRAFT
A revolutionary lunar space transportation system architecture using extraterrestrial LOX-augmented NTR propulsion
[NASA-TM-106726] p 249 N95-11703
LUNG MORPHOLOGY
A numerical analysis of the distribution of stresses in lung parenchyma which accounts for the interactions between the tissue skeleton and flowing air p 332 N95-11806
LUNGS
Consequences of prolonged inhalation of ozone on Fischer-344/N rats: Collaborative studies. Part 1: Content and cross-linking of lung collagen
[PB94-182748] p 331 N95-13176
LYSOZYME
Convective flow effects on protein crystal growth
[NASA-CR-196790] p 372 N95-11921
Protein crystal growth in low gravity
[NASA-CR-196980] p 279 N95-13202

M

MACH NUMBER
A shadowgraph study of the National Launch System's 1 1/2 stage vehicle configuration and Heavy Lift Launch Vehicle configuration --- Using the Marshall Space Flight Center's 14-Inch Trisonic Wind Tunnel
[NASA-RP-1347] p 229 N95-11710
Shock-tunnel combustor testing for hypersonic vehicles
[NASA-CR-196836] p 246 N95-11938
A simple analytical aerodynamic model of Langley Winged-Cone Aerospace Plane concept
[NASA-CR-194987] p 252 N95-12175
Performance measurements of the multimedia testbed on real-time Mach
[AD-A282658] p 343 N95-12504
An implementation of a chemical and thermal nonequilibrium flow solver on unstructured meshes and application to blunt bodies
[NASA-CR-194967] p 293 N95-12619
Experimental aerodynamic characteristics of a generic hypersonic accelerator configuration at Mach numbers 1.5 and 2.0 --- conducted in the Langley Unitary Plan Wind Tunnel
[NASA-TM-4413] p 233 N95-12770
Mach number control in the High Speed Wind Tunnel of NLR
[PB94-201670] p 246 N95-13243
MACHINE LEARNING
B* probability based search
[AD-A282551] p 343 N95-12497
Population-based incremental learning. A method for integrating genetic search based function optimization and competitive learning
[AD-A282654] p 350 N95-12835
Learning unions of boxes with membership and equivalence queries
[DE94-014662] p 350 N95-12866
Design of an intelligent support system for scientific databases
[AD-A283043] p 378 N95-12995
Weighted Parzen windows for pattern classification
[AD-A281222] p 345 N95-13370
MACHINE TOOLS
Development of a spindle thermal error characterization and compensation sensor system for machining center accuracy enhancement
[AD-A280891] p 300 N95-11729
Prediction of geometric-thermal machine tool errors by artificial neural networks
[PB94-186673] p 348 N95-11909
MACHINING
Development of a spindle thermal error characterization and compensation sensor system for machining center accuracy enhancement
[AD-A280891] p 300 N95-11729
Intelligent knowledge-based engineering
[AD-A281906] p 377 N95-11788
Prediction of geometric-thermal machine tool errors by artificial neural networks
[PB94-186673] p 348 N95-11909
MACROMOLECULES
Chiral recognition in molecular and macromolecular pairs of (S)- and (R)-1-cyano-2-methylpropyl 4'(4-(8-vinyloxyoctyloxy)benzoyl) biphenyl-4-carboxylate enantiomers
[AD-A281438] p 356 N95-11828
Design, synthesis and characterization of novel nonlinear optical polymers
[AD-A282201] p 274 N95-12424
Polymer effect on heterochiral molecular recognition in molecular and macromolecular pairs of liquid crystals of (R)- and (S)-2-chloro-4-methylpentyl 4'-((8-(vinyloxy)octyl)oxy)biphenyl-4-caroxylate rs
[AD-A281193] p 358 N95-12522
MAGELLANIC CLOUDS
FOC SV support and science data analysis
[NASA-CR-196764] p 381 N95-12821
MAGNESIUM OXIDES
Scanning tunneling microscopy/atomic force microscopy for study of nanoscale metal oxide particles (destructive adsorbents)
[AD-A281417] p 357 N95-11851
Measurement of synchrotron radiation transmission of infrared range by YBa2Cu3O(7-delta) film in superconducting state
[DE94-623270] p 372 N95-11899
Atomic structures and compositions of internal interfaces
[DE94-013594] p 271 N95-13543
MAGNETIC BEARINGS
Introduction to magnetic bearings
[NASA-CR-197187] p 302 N95-12640
MAGNETIC CIRCUITS
The experiment and analysis of tailoring V(sub L) and I(sub P) with ZnO voltage-sensitive resistor on HT-6M
[DE94-625074] p 370 N95-13541
MAGNETIC COILS
Locked modes in TEXT-U tokamak
[DE94-011595] p 370 N95-13529
MAGNETIC COMPRESSION
Generation of ultra-high magnetic fields for AGEX
[DE94-015171] p 368 N95-12757
MAGNETIC CORES
FORTRAN programs to process Magsat data for lithospheric, external field, and residual core components
[NASA-TM-104612] p 323 N95-12130
MAGNETIC DISKS
Study of magnetic recording media on glass substrates
[DE94-014740] p 296 N95-12869
MAGNETIC DISTURBANCES
Structure and dynamics of the solar corona
[NASA-CR-196978] p 384 N95-13582
MAGNETIC EFFECTS
FORTRAN programs to process Magsat data for lithospheric, external field, and residual core components
[NASA-TM-104612] p 323 N95-12130
Magneto-optical properties of quantum structures with reduced dimensionality
[AD-A282597] p 376 N95-12553
Apparatus and method for forming textured bulk high temperature superconducting materials
[AD-D016394] p 373 N95-12635
Radiative properties of strongly magnetized plasmas
[DE94-015487] p 369 N95-12897
MAGNETIC FIELD CONFIGURATIONS
The magnetic structure of holmium-erbium superlattices
[DE94-013728] p 371 N95-11739
Non-dipolar magnetic field models and patterns of radio emission: Uranus and Neptune compared
[NASA-CR-196412] p 385 N95-12469
An observational test of magnetospheric magnetic field mapping
[DE94-014461] p 324 N95-12649
Resonant x-ray scattering in 5f magnetism
[DE94-013753] p 358 N95-12829
FNAS UAH UVSP and complimentary data analysis and modeling
[NASA-CR-194005] p 381 N95-12992
Waves in Space Plasmas (WISP)
[NASA-CR-196432] p 369 N95-13024
MAGNETIC FIELDS
An investigation of Mn Si by the SR-technique
[DE94-624058] p 371 N95-11748
The Research Laboratory of Electronics
[AD-A281445] p 386 N95-11830
Tuning through the critical regime of the metal-insulator-transition in conducting polymers by pressure and magnetic field
[PB94-179165] p 272 N95-11847

Velocity spread of REB generated by high current diode
[IPPCZ-339] p 364 N95-11886
The reflection of relativistic electron beam by virtual cathode
[IPPCZ-338] p 364 N95-11916
FORTRAN programs to process Magsat data for lithospheric, external field, and residual core components
[NASA-TM-104612] p 323 N95-12130
Research on Orbital Plasma-Electrodynamics (ROPE)
[NASA-CR-196929] p 361 N95-12147
Magnetic field generation in shock waves
[AD-A282234] p 281 N95-12408
Initial analysis and modeling results from the Polar Orbiting Geomagnetic Survey (POGS) satellite
[AD-A283454] p 253 N95-12545
Generation of ultra-high magnetic fields for AGEX
[DE94-015171] p 368 N95-12757
Magnetospheric space plasma investigations
[NASA-CR-196793] p 382 N95-12940
A magnetic shield/dual purpose mission
[NASA-CR-197192] p 255 N95-13006
Magnetic field induced minigap in double quantum wells
[DE94-015013] p 376 N95-13172
Locked modes in TEXT-U tokamak
[DE94-011595] p 370 N95-13529

MAGNETIC FLUX
Magnetic field generation in shock waves
[AD-A282234] p 281 N95-12408

MAGNETIC ISLANDS
Helical temperature perturbations associated with tearing modes in tokamak plasmas
[DE94-014708] p 369 N95-12867
Locked modes in TEXT-U tokamak
[DE94-011595] p 370 N95-13529

MAGNETIC LEVITATION VEHICLES
Guideway structural design and power/propulsion/braking in relation to guideways. Volume 3: Appendix B: Maglev guideway structural design
[PB93-169910] p 304 N95-13128

MAGNETIC MATERIALS
Design and construction of the astronautics refrigerator magnet
[DE94-013599] p 353 N95-11731
Modeling of split-core transformers for power transmission
[AD-A282782] p 287 N95-12509

MAGNETIC PROPERTIES
Resonant x-ray scattering in 5f magnetism
[DE94-013753] p 358 N95-12829
Study of magnetic recording media on glass substrates
[DE94-014740] p 296 N95-12869

MAGNETIC RECORDING
Study of magnetic recording media on glass substrates
[DE94-014740] p 296 N95-12869

MAGNETIC RESONANCE
Optical and magnetic resonance investigations of 3D ions in single crystal hosts: Candidates for tunable solid-state lasers
[AD-A281726] p 371 N95-11842

MAGNETIC SHIELDING
A magnetic shield/dual purpose mission
[NASA-CR-197192] p 255 N95-13006

MAGNETIC SUSPENSION
Introduction to magnetic bearings
[NASA-CR-197187] p 302 N95-12640
Annular suspension and pointing system with controlled DC electromagnets
[NASA-CR-197206] p 302 N95-12666

MAGNETIZATION
Magnetic response of ultrathin Fe on MgO: A polarised neutron reflectometry study
[DE94-013192] p 375 N95-13272

MAGNETO-OPTICS
Magneto-optical properties of quantum structures with reduced dimensionality
[AD-A282597] p 376 N95-12553

MAGNETOACOUSTIC WAVES
Excitation of fast magneto-acoustic waves in unhomogeneous plasma of a large size tokamak
[DE94-625050] p 370 N95-13540

MAGNETOHYDRODYNAMIC STABILITY
Contraction phase of a gas-puff z-pinch
p 366 N95-12440

MAGNETOHYDRODYNAMICS
Locked modes in TEXT-U tokamak
[DE94-011595] p 370 N95-13529
Density gradient effects in the tokamak edge turbulence with temperature gradient driving
[DE94-625042] p 370 N95-13539

MAGNETOIONICS
Waves in Space Plasmas (WISP)
[NASA-CR-196432] p 369 N95-13024

MAGNETOPLASMADYNAMICS
Anode sheath contributions in plasma thrusters
[AD-A280395] p 364 N95-11837

MAGNETOSPHERE-IONOSPHERE COUPLING
Magnetospheric-ionospheric Poynting flux
[NASA-CR-196856] p 322 N95-11801

MAGNETOSPHERES
An observational test of magnetospheric magnetic field mapping
[DE94-014461] p 324 N95-12649
Magnetospheric space plasma investigations
[NASA-CR-196793] p 382 N95-12940
Waves in Space Plasmas (WISP)
[NASA-CR-196432] p 369 N95-13024

MAGNETOSTATICS
Enhancement of EMAG: A 2-D electrostatic and magnetostatic solver for MATLAB
[AD-A283446] p 354 N95-13143

MAGNETRON SPUTTERING
A laboratory vacuum apparatus for magnetron sputtering of thin Z ZnO piezoelectric films, magnetron sputtering
p 296 N95-12111

MAGSAT B SATELLITE
FORTRAN programs to process Magsat data for lithospheric, external field, and residual core components
[NASA-TM-104612] p 323 N95-12130

MAIN SEQUENCE STARS
A deep x-ray survey of the Pleiades cluster and the B6-A3 main sequence stars in Orion
[NASA-CR-196190] p 380 N95-12373

MAINTENANCE
Development of ground-penetrating radar equipment for detecting pavement condition for preventive maintenance
[PB94-189537] p 280 N95-11904
Cabin fuselage structural design with engine installation and control system
[NASA-CR-197173] p 240 N95-12639

MALES
Effects of oral glucose on exercise thermoregulation in men after water immersion
[NASA-TM-108825] p 329 N95-11810
Age 60 study. Part 4: Experimental evaluation of pilot performance
[REPT-8025-4B] p 336 N95-13199

MAN ENVIRONMENT INTERACTIONS
Present state of knowledge of the upper atmosphere1993: An assessment report, part 2
[NASA-RP-1337] p 322 N95-12103

MAN MACHINE SYSTEMS
Design issues of human operator support systems
[PB94-191376] p 337 N95-11778
MOOSE: Manned On-Orbit Servicing Equipment
[NASA-CR-197151] p 254 N95-12790
Population-based incremental learning. A method for integrating genetic search based function optimization and competitive learning
[AD-A282654] p 350 N95-12835
Aerospace medicine and biology: A continuing bibliography with indexes (supplement 394)
[NASA-SP-7011(394)] p 335 N95-13230

MANAGEMENT METHODS
A data and information system for processing, archival, and distribution of data for global change research
[NASA-CR-196770] p 320 N95-12786

MANAGEMENT PLANNING
Space facilities: Meeting future needs for research, development, and operations
[NASA-CR-194821] p 248 N95-12474
Space Shuttle: NASA's plans for repairing or replacing a damaged or destroyed orbiter. Report to the Chairman, Subcommittee on Investigations and Oversight, Committee on Science, Space, and Technology, House of Representatives
[GAO/NSIAD-94-197] p 249 N95-12851

MANAGEMENT SYSTEMS
The development of a highly reliable power management and distribution system for civil transport aircraft
[NASA-TM-106697] p 243 N95-11867
Development of a change management system
p 377 N95-11963
Toward infrastructure improvement: An agenda for research
[LC-94-67335] p 376 N95-12385
Space Station Module Power Management and Distribution System (SSM/PMAD)
[NASA-CR-193991] p 258 N95-12819
Lessons learned from experiments conducted on radar data management systems
[AD-A282896] p 284 N95-12920

MANEUVERABILITY
Impact of agility requirements on configuration synthesis
[NASA-CR-4627] p 238 N95-11952

MANEUVERS
Symmetric steady manoeuvre loads on rigid aircraft of classical configuration at subsonic speeds
[ESDU-94009] p 238 N95-11774

MANGANESE
An investigation of Mn Si by the SR-technique
[DE94-624058] p 371 N95-11748

MANIPULATORS
Essential kinematics for autonomous vehicles
[AD-A282456] p 300 N95-12394
Actuability of underactuated manipulators
[AD-A282788] p 300 N95-12526
Robust control of underactuated manipulators: Analysis and implementation
[AD-A282836] p 301 N95-12587
The effect of passive damping on feedback control performance of flexible manipulators
[DE94-015000] p 304 N95-13182
An iterative approach to multibody simulation dynamics suitable for parallel implementation
[UTIAS-TN-276] p 347 N95-13353

MANNED MARS MISSIONS
Nuclear rockets: High-performance propulsion for Mars
[DE94-013642] p 257 N95-11782
Meeting the challenge of manned lunar and Martian exploration p 339 N95-11970
Mars Equipment Transport System
[NASA-CR-197158] p 301 N95-12554
Integral habitat transport system
[NASA-CR-197156] p 339 N95-12629
Fusion powered human transport to Mars (UWFR94)
[NASA-CR-197184] p 368 N95-12641
Ion engine propelled Earth-Mars cycler with nuclear thermal propelled transfer vehicle, volume 2
[NASA-CR-197208] p 361 N95-12665

MANNED SPACE FLIGHT
Activities of the Space Studies Board of the National Research Council
[NASA-CR-195738] p 247 N95-12880

MANNED SPACECRAFT
Fusion powered human transport to Mars (UWFR94)
[NASA-CR-197184] p 368 N95-12641
Ion engine propelled Earth-Mars cycler with nuclear thermal propelled transfer vehicle, volume 2
[NASA-CR-197208] p 361 N95-12665
Project Freebird: An orbital transfer vehicle
[NASA-CR-197201] p 254 N95-12737

MANUALS
SO2 guideline document
[PB94-181393] p 319 N95-11893
Solar radiation data manual for flat-plate and concentrating collectors
[DE93-018229] p 317 N95-12647

MANUFACTURING
Intelligent knowledge-based engineering
[AD-A281906] p 377 N95-11788
Body dimensions for apparel
[PB94-187739] p 338 N95-11908
A decision support system for tolerance allocation
[NASA-CR-195817] p 308 N95-11994
The use of an acoustic emission method to estimate the effect of manufacturing process and service factors on the failure of concrete p 311 N95-12108
The future of diode pumped solid state lasers and their applicability to the automotive industry
[DE94-014736] p 298 N95-12868
Delta-4: An open architecture for dependable systems
[PB94-195641] p 341 N95-13436
Ceramic brush seals development
p 306 N95-13594

MAPPING
Proposal of a methodology to evaluate urban quality of life using conventional and remote sensing data, geographic information system, and a database
[INPE-5552-TDI/536] p 315 N95-12297
Digital image processing techniques for image-mapping applications
[INPE-5546-TDI/532] p 315 N95-12301
An observational test of magnetospheric magnetic field mapping
[DE94-014461] p 324 N95-12649
AGSO 1993: Yearbook of the Australian Geological Survey Organisation. Geoscientific research and database development for the year 1 July 1992 to 30 June 1993
p 324 N95-12686

MARINE CHEMISTRY
High performance climate system modeling using a domain and task decomposition message-passing approach
[DE94-013739] p 322 N95-11741

MARINE ENVIRONMENTS
Communications plan --- Design of the public wing of the Oregon State University Hatfield Marine Science Center
[NASA-CR-196435] p 314 N95-12231
MARKOV CHAINS
Adaptive relaxation for the steady-state analysis of Markov chains
[NASA-CR-194944] p 345 N95-13420
MARKOV PROCESSES
Improved image decompression for reduced transform coding artifacts
[NASA-CR-196805] p 341 N95-11761
Reliability allocation for a system using Markov analysis
[PB94-205051] p 309 N95-13406
MARS (PLANET)
Periglacial and glacial analogs for Martian landforms
[NASA-CR-196772] p 383 N95-12952
MARS BASES
External Device to Incrementally Skid the Habitat (E-DISH)
[NASA-CR-197147] p 301 N95-12625
Integral habitat transport system
[NASA-CR-197156] p 339 N95-12629
MARS EXPLORATION
A robotic exploration mission to Mars and Phobos
[NASA-CR-197168] p 382 N95-12307
Design of an unmanned Martian polar exploration system
[NASA-CR-197160] p 383 N95-12529
External Device to Incrementally Skid the Habitat (E-DISH)
[NASA-CR-197147] p 301 N95-12625
Mars methane engine
[NASA-CR-197205] p 302 N95-12668
MARS LANDING
A robotic exploration mission to Mars and Phobos
[NASA-CR-197168] p 382 N95-12307
Project Genesis: Mars in situ propellant technology demonstrator mission
[NASA-CR-197166] p 277 N95-12822
MARS PROBES
Design of an unmanned Martian polar exploration system
[NASA-CR-197160] p 383 N95-12529
SolSTUS: Solar Source Thermal Upper Stage
[NASA-CR-197179] p 257 N95-13581
MARS SAMPLE RETURN MISSIONS
Project Genesis: Mars in situ propellant technology demonstrator mission
[NASA-CR-197166] p 277 N95-12822
Project Hyreus: Mars sample return mission utilizing in situ propellant production
[NASA-CR-197189] p 383 N95-12826
MARS SURFACE
A lunar/Martian anchor emplacement system
[NASA-CR-197193] p 302 N95-12690
Project Hyreus: Mars sample return mission utilizing in situ propellant production
[NASA-CR-197189] p 383 N95-12826
Periglacial and glacial analogs for Martian landforms
[NASA-CR-196772] p 383 N95-12952
MASS
Effects of mass on aircraft sidearm controller characteristics
[NASA-TM-104277] p 244 N95-11868
MASS FLOW RATE
A low-erosion starting technique for high-performance arcjets
[NASA-TM-106627] p 259 N95-13347
MASS SPECTRA
Photon production at CDF and D0
[DE94-014985] p 359 N95-13160
A precision measurement of the prompt photon cross section in p(-p) collisions at the square root of s = 1.8 TeV
[DE94-014989] p 359 N95-13170
MASS SPECTROMETERS
Mixed clusters from the coexpansion of C2F6 and n2 in a pulsed, supersonic expansion cluster ion source and beam deflection time-of-flight mass spectrometer: A first application
[AD-A282044] p 361 N95-11910
Acquisition of a gas source mass spectrometer for paleoclimatology and paleoceanography research
[AD-A282634] p 266 N95-12539
The laser and its applications on environment and biotechnology research
[DE94-013831] p 299 N95-13076
Analysis for Be-7 and Be-10 on LDEF materials and their sources
[NASA-CR-193989] p 268 N95-13084
MASS SPECTROSCOPY
Triple sorbent thermal desorption/gas chromatography/mass spectrometry determination of vapor phase organic contaminants
[DE94-013634] p 264 N95-11735
Nanometer scale phase separation in mixed composition self-assembled monolayers
[AD-A282671] p 266 N95-12514
Diagnostic techniques for semiconductor materials processing
[AD-A282810] p 373 N95-12602
Role of implantation-induced defects in surface-oriented diffusion of fluorine in silicon
[DE94-014905] p 374 N95-13125
MASS TRANSFER
A study of aircraft post-crash fuel fire mitigation
[AD-A282208] p 234 N95-12499
Cryogenic On-Orbit Liquid Depot Storage, Acquisition, and Transfer Satellite (COLD-SAT)
[NASA-CR-185249] p 259 N95-13237
MASSIVELY PARALLEL PROCESSORS
Impact analysis on a massively parallel computer
[DE94-013624] p 346 N95-11734
Design consideration for parallel graphics libraries
[NASA-CR-194935] p 340 N95-12828
Nonlinear structural response using adaptive dynamic relaxation on a massively-parallel-processing system
[NASA-CR-196491] p 313 N95-13162
MATERIALS HANDLING
Lunar vertical-shaft mining system
[NASA-CR-197154] p 384 N95-13497
MATERIALS SCIENCE
Research activities of the Center for the Space Processing of Engineering Materials
[NASA-CR-196484] p 259 N95-11891
JPRS report: Science and technology. Central Eurasia
[JPRS-UST-94-017] p 247 N95-12001
JPRS report: Science and technology. Central Eurasia
[JPRS-UST-94-020] p 389 N95-12002
MATERIALS TESTS
Test model designs for advanced refractory ceramic materials p 277 N95-11968
MATHEMATICAL MODELS
A stochastic model of fatigue crack growth p 309 N95-11698
Impact analysis on a massively parallel computer
[DE94-013624] p 346 N95-11734
Parallel methods for the flight simulation model
[DE94-013330] p 245 N95-11752
Comparison of the KAMELEON fire model to large-scale open pool fire data
[DE94-013441] p 264 N95-11756
Autonomous motion on wheels
[PB94-191327] p 348 N95-11825
Pressure studies of alkali, alkaline earth and rare earth doped C60 superconductors
[DE94-013345] p 372 N95-11862
Determining the accuracy of maximum likelihood parameter estimates with colored residuals
[NASA-CR-194893] p 244 N95-11869
TLIFE: A program for spur, helical and spiral bevel transmission life and reliability modeling
[NASA-CR-4622] p 300 N95-11889
Microwave heating and joining of ceramic cylinders: A mathematical model
[NASA-CR-194962] p 351 N95-11922
Modeling jets in cross flow
[NASA-CR-194965] p 291 N95-11930
Probabilistic simulation of the human factor in structural reliability
[NASA-TM-106498] p 311 N95-11954
Using emergent order to shape a space society p 377 N95-11959
Analytical investigation of the dynamics of tethered constellations in Earth orbit, phase 2
[NASA-CR-196509] p 252 N95-12106
Research on Orbital Plasma-Electrodynamics (ROPE)
[NASA-CR-196929] p 361 N95-12147
A simple analytical aerodynamic model of Langley Winged-Cone Aerospace Plane concept
[NASA-CR-194987] p 252 N95-12175
A model of the density of solar radiation energy on an arbitrary plane identification for Warsaw p 384 N95-12243
Study of a vortical/axial type flameholders with variable angle blades
[INPE-5558-TDI/538] p 266 N95-12302
Outdoor landmark recognition using hybrid fractal vision system and neural networks
[AD-A282506] p 349 N95-12395
Triaxial and torsional shear test results for sand
[AD-A282725] p 323 N95-12506
Modeling of split-core transformers for power transmission
[AD-A282782] p 287 N95-12509
A unified approach to geopotential field modeling
[AD-A283453] p 324 N95-12544
An investigation of the use of temporal decomposition in space mission scheduling
[NASA-CR-196420] p 377 N95-12618
Gaussian paired comparison models
[PB94-179025] p 352 N95-12820
Hypersonic vehicle model and control law development using H(infinity) and micron synthesis
[NASA-TM-4562] p 255 N95-12838
Backdraft phenomena
[PB94-193927] p 267 N95-12852
A study of a multi-pinned phase CCD detector for use as a star tracker
[NASA-CR-196287] p 381 N95-13056
Mass conservation in grain growth
[DE94-014456] p 374 N95-13086
Nonlinear hysteresis in an endochronic solid
[AD-A283142] p 325 N95-13136
The effect of passive damping on feedback control performance of flexible manipulators
[DE94-015000] p 304 N95-13182
A simplified thermohydrodynamic model for fluid film bearings
[DE94-015011] p 304 N95-13183
Micromechanics Analysis Code (MAC). User guide: Version 1.0
[NASA-TM-106706] p 264 N95-13193
Object recognition for flexible assembly using stereo vision
[PB94-204427] p 363 N95-13248
Numerical time dependent sheet cavitation simulations using a higher order panel method
[PB94-204435] p 294 N95-13249
Studies on the flow induced by an oscillating airfoil in a uniform stream
[PB94-204450] p 233 N95-13250
Approximation of scattered data using smooth grid functions
[PB94-207016] p 353 N95-13573
Structure and dynamics of the solar corona
[NASA-CR-196978] p 384 N95-13582
Theoretical versus experimental results for the rotordynamic coefficients of eccentric, smooth, gas annular seal annular gas seals p 307 N95-13603
MATHEMATICAL PROGRAMMING
Algorithms for mathematical programming
[DE94-013544] p 345 N95-13339
CRYOCOL: A computer program to calculate the cryogenic distillation of hydrogen isotopes
[DE94-622012] p 268 N95-13531
MATRICES (CIRCUITS)
Power system applications for PASC converter systems
[DE94-013329] p 286 N95-11751
MATRICES (MATHEMATICS)
Implementing a linear equation solver in the CFD code PHOENICS
[PB94-195757] p 353 N95-13439
MATRIX MATERIALS
Damage tolerance of candidate thermoset composites for use on single stage to orbit vehicles
[NASA-TP-3506] p 261 N95-11816
Towards tailored interphase formation utilizing surface-active benzylsulfonium salts as cationic initiators
[AD-A282511] p 262 N95-12398
Energy dissipation by a longitudinal Raman process
[DE94-015027] p 359 N95-13173
CVD techniques for the synthesis or modification of porous ceramics
[PB94-206836] p 276 N95-13284
All-hydrocarbon composite resins based on cyclopentadiene
[AD-A282495] p 276 N95-13296
MAXIMUM LIKELIHOOD ESTIMATES
Determining the accuracy of maximum likelihood parameter estimates with colored residuals
[NASA-CR-194893] p 244 N95-11869
MAXIMUM PRINCIPLE
Analysis and design of numerical schemes for gas dynamics 1: Artificial diffusion, upwind biasing, limiters and their effect on accuracy and multigrid convergence
[NASA-CR-196477] p 290 N95-11875
MEASURE AND INTEGRATION
Comparison of symbolic and numerical integration methods for an assumed-stress hybrid shell element
[NASA-CR-195945] p 313 N95-13096
MEASURING INSTRUMENTS
The rhesus measurement system: A new instrument for space research p 247 N95-11965
Photon production at CDF and D0
[DE94-014985] p 359 N95-13160
A search for a heavy neutral gauge boson decaying into dielectrons in (-p)p collisions at the square root of s = 1.8 TeV
[DE94-014987] p 359 N95-13161

MECHANICAL ENGINEERING
Linear Proof Mass Actuator
[NASA-TM-109143] p 310 N95-11814
Various advanced design projects promoting engineering education
[NASA-CR-197170] p 258 N95-12630
Proceedings of the CTU Seminar 1994, Part C
[DE94-624078] p 390 N95-12946
MECHANICAL IMPEDANCE
Excitation of fast magneto-acoustic waves in unhomogeneous plasma of a large size tokamak
[DE94-625050] p 370 N95-13540
MECHANICAL PROPERTIES
Surface roughness characterization of various ceramic fibers using AFM and low voltage SEM
[DE94-013635] p 272 N95-11736
A novel lead-free solder replacement
[DE94-013782] p 269 N95-11785
Structure and performance of carbon aerogel electrodes
[DE94-014746] p 356 N95-11791
Thianthrene-based poly(benzoxazole)s
[AD-A282326] p 274 N95-12419
On the strain and strain-rate dependence of the fraction of plastic work converted to heat: An experimental study using high speed infrared detectors and the Kolsky bar
[SM-92-33] p 354 N95-12728
The effect of irradiation on the stability and properties of monolithic silicon carbide and SiC(f)/SiC composites up to 25 dpa
[DE94-014568] p 263 N95-12862
Novel concepts in weld science: Role of gradients and composite structure
[DE94-015482] p 271 N95-12895
MECHANICS (PHYSICS)
Laws of infrared similitude
[AD-A282209] p 354 N95-12426
MEDICAL PERSONNEL
Meeting the nation's needs for biomedical and behavioral scientists
[LC-94-66477] p 330 N95-12310
MEDICAL SERVICES
Meeting the nation's needs for biomedical and behavioral scientists
[LC-94-66477] p 330 N95-12310
MELTING
A CRAMPS and 13C CP/MAS NMR examination of solid-solid transitions in n-Hexatriacontane (C36H74)
[AD-A282497] p 375 N95-13299
MELTING POINTS
Vapour pressures and critical points of liquids. Polycyclic phenyl and cyclohexyl compounds
[ESDU-94001] p 266 N95-12128
Orthobaric densities and molar volumes of liquids. Polycyclic phenyl and cyclohexyl compounds
[ESDU-94002] p 266 N95-12129
MEMBRANES
The synthesis and structure of polyphosphazenes
[AD-A281723] p 272 N95-11832
Conformation of membrane proteins: Bacteriorhodopsin
[AD-A281282] p 331 N95-13373
MEMORY (COMPUTERS)
Parallel methods for the flight simulation model
[DE94-013330] p 245 N95-11752
A preliminary evaluation of cache-miss-initiated prefetching techniques in scalable multiprocessors
[AD-A281502] p 346 N95-11858
Design consideration for parallel graphics libraries
[NASA-CR-194935] p 340 N95-12828
Methodology for sensitivity analysis, approximate analysis, and design optimization in CFD for multidisciplinary applications
[NASA-CR-196981] p 294 N95-13201
MENTAL PERFORMANCE
Tank crew performance related to cognitive ability and motivation of the tank crew members
[PB94-190642] p 335 N95-11872
Probabilistic simulation of the human factor in structural reliability
[NASA-TM-106498] p 311 N95-11954
MEROMORPHIC FUNCTIONS
Extension of a theorem of Gehring and Pommerenke
[PB94-180658] p 352 N95-12577
MESOMETEOROLOGY
Short term weather forecasting in real time in a base weather station setting
[AD-A283141] p 327 N95-13134
MESON RESONANCE
Contribution of hadronic intermediate states in nonleptonic weak decays of K, charm and B mesons
[DE94-753399] p 356 N95-11818
MESONS
Contribution of hadronic intermediate states in nonleptonic weak decays of K, charm and B mesons
[DE94-753399] p 356 N95-11818
Measurement of the polarization in the decay B(exp 0) yields J/psi K(exp *0) in (bar p)p collisions at the square root of s = 1.8 TeV
[DE94-014265] p 357 N95-12370
MESOPAUSE
Gravity wave forcing and influences near the mesopause
[AD-A282482] p 325 N95-13293
MESOSCALE PHENOMENA
Short term weather forecasting in real time in a base weather station setting
[AD-A283141] p 327 N95-13134
MESOSPHERE
Ionospheric dynamics instrument investigation for the Timed Mission
[NASA-CR-196198] p 325 N95-13190
MESSAGE PROCESSING
Some very compositional temporal properties
[PB94-195666] p 345 N95-13438
MESSAGES
Integrated sensor bus
[PB94-206810] p 288 N95-13252
METABOLISM
Copper metabolism in rats fed ascorbic acid or restricted amounts of copper
[PB94-191343] p 330 N95-11902
Comparison of submaximal cycling and treadmill exercise at similar work rates
[AD-A283430] p 334 N95-12593
Regulation of alternative CO2 fixation pathways in prokaryotic and eukaryotic photosynthetic organisms
[DE94-013180] p 331 N95-13271
METAL CLUSTERS
Low oxidation state gallium compounds. Synthesis and characterization of Ga(CH2CMe3)n
[AD-A283369] p 373 N95-12923
METAL COATINGS
Structure-phase state of thick amorphous and microcrystalline chromium-carbon films deposited by ion-plasma sputtering
[DE94-624236] p 277 N95-13535
METAL FATIGUE
A study of fatigue crack growth in lugs under spectrum loading
[NAL-PD-SN-9407] p 311 N95-11879
A study of naturally initiating notch root fatigue cracks under spectrum loading
[NAL-PD-SN-9406] p 311 N95-11924
Computer modeling the fatigue crack growth rate behavior of metals in corrosive environments
[NASA-CR-194982] p 269 N95-11933
Computer modelling of cyclic deformation of high-temperature materials
[AD-A282457] p 263 N95-12833
METAL FILMS
Magnetic response of ultrathin Fe on MgO: A polarised neutron reflectometry study
[DE94-013192] p 375 N95-13272
Structure-phase state of thick amorphous and microcrystalline chromium-carbon films deposited by ion-plasma sputtering
[DE94-624236] p 277 N95-13535
METAL MATRIX COMPOSITES
Modeling and life prediction methodology for Titanium Matrix Composites subjected to mission profiles
[NASA-TM-109148] p 269 N95-11915
Thin-film model studies of interfacial reactions in intermetallic matrix composites
[AD-A283360] p 263 N95-12883
Thermomechanical fatigue damage/failure mechanisms in SCS-6/Timetal 21S (0/90)s composite
[NASA-CR-191115] p 263 N95-13082
METAL OXIDE SEMICONDUCTORS
Basic mechanisms of radiation effects in the natural space radiation environment
[DE94-013445] p 384 N95-11757
METAL OXIDES
Synthesis and decomposition of a novel carboxylate precursor to indium oxide
[NASA-TM-106555] p 260 N95-12693
Hydrolysis and condensation of tin (4) alkoxide compounds: The control of structural evolution
[AD-A282789] p 267 N95-12807
Synchrotron studies of narrow band materials
[DE94-013698] p 271 N95-13554
METAL PARTICLES
Z-pinch plasma by solid fine particle injection
p 366 N95-12442
METAL PLATES
Screen test for cadmium and nickel plates as developed and used within the Aerospace Corporation
[NASA-CR-196961] p 270 N95-12148
Large-displacement structural durability analyses of simple bend specimen emulating rocket nozzle liners
[NASA-TM-106521] p 312 N95-12818
METAL POWDER
One-step synthesis of dithiocarbamates from metal powders
[NASA-TM-106558] p 260 N95-12692
Effects of sample formulation on the analysis of heavy metals by x-ray fluorescence
[AD-A282733] p 267 N95-12836
METAL PROPELLANTS
Investigation of the effects of solid rocket motor propellant composition on plume signature
[AD-A283365] p 258 N95-12885
METAL SURFACES
Growth of Au on Ni(110): A BFS modelling of surface alloy phases
[NASA-TM-106732] p 270 N95-12104
Adherend surface effects on epoxy cure by NMR
[AD-A282165] p 274 N95-12420
Hydrogen bonding and molecular orientation in water/fluorine adlayers on silver(110)
[AD-A282652] p 268 N95-13549
METAL VAPORS
Control of initial mass on metal vapor puff z-pinch
p 366 N95-12441
Kinetics and characterization of tungsten CVD processes
[PB94-206901] p 271 N95-13411
METAL-METAL BONDING
Effect of pre-welding heat-treatments on welding a two-phase Ni3Al alloy
[DE94-014409] p 270 N95-12372
METAL-WATER REACTIONS
Hydrogen bonding and molecular orientation in water/fluorine adlayers on silver(110)
[AD-A282652] p 268 N95-13549
METALLIC PLASMAS
Control of initial mass on metal vapor puff z-pinch
p 366 N95-12441
METALLIZING
Electrochemical deposition of metal nano-disk structures using the scanning tunneling microscope
[AD-A282464] p 268 N95-13288
METALLOGRAPHY
Thermomechanical fatigue damage/failure mechanisms in SCS-6/Timetal 21S (0/90)s composite
[NASA-CR-191115] p 263 N95-13082
METAMORPHISM (GEOLOGY)
Neotectonics of Asia: Thin-shell finite-element models with faults
[NASA-CR-196436] p 324 N95-12949
METEOROLOGICAL CHARTS
Catalogue of heavy rainfall cases of six inches or more over the continental US during 1993
[NOAA-TR-NESDIS-80] p 327 N95-13095
METEOROLOGICAL INSTRUMENTS
The design and development of signal-processing algorithms for an airborne x-band Doppler weather radar
[NASA-CR-196888] p 281 N95-12374
METEOROLOGICAL PARAMETERS
Thunderstorm hypothesis reasoner
[AD-A282664] p 326 N95-12805
Interpolation of scattered temperature data measurements onto a worldwide regular grid using radial basis functions with applications to global warming
[DE94-014745] p 321 N95-12926
Windshear certification data base for forward-look detection systems p 234 N95-13204
Certification methodology applied to the NASA experimental radar system p 235 N95-13205
Airport surveillance using a solid state coherent lidar p 235 N95-13207
Characteristics of civil aviation atmospheric hazards p 235 N95-13208
Wake vortex detection at Denver Stapleton Airport with a pulsed 2-micron coherent lidar p 236 N95-13211
Evaluation of candidate millimeter wave sensors for synthetic vision p 236 N95-13214
METEOROLOGICAL RADAR
The design and development of signal-processing algorithms for an airborne x-band Doppler weather radar
[NASA-CR-196888] p 281 N95-12374
Terminal Doppler Weather Radar Build 5A Operational Test and Evaluation (OT/E) integration and OT/E operational test plan
[AD-A283052] p 327 N95-12996
Characteristics of civil aviation atmospheric hazards p 235 N95-13208
METEOROLOGICAL SATELLITES
Implementation of a state of the art automated system for the production of cloud/water vapor motion winds from geostationary satellites
[NASA-CR-196817] p 325 N95-11758
Determination of the auroral oval Q index from the air weather service K index
[AD-A282764] p 324 N95-12508

METEOROLOGY
Catalogue of heavy rainfall cases of six inches or more over the continental US during 1993
[NOAA-TR-NESDIS-80] p 327 N95-13095
METHANE
Quantum chemical study of methane oxidation species
[NASA-CR-196158] p 265 N95-12107
Mars methane engine
[NASA-CR-197205] p 302 N95-12668
Project Genesis: Mars in situ propellant technology demonstrator mission
[NASA-CR-197166] p 277 N95-12822
Project Hyreus: Mars sample return mission utilizing in situ propellant production
[NASA-CR-197189] p 383 N95-12826
Fundamental and experimental studies on the catalytic combustion of methane
[PB94-205895] p 268 N95-13251
METHOD OF CHARACTERISTICS
Analysis and design of numerical schemes for gas dynamics. 2: Artificial diffusion and discrete shock structure
[NASA-CR-196476] p 290 N95-11874
METHOD OF MOMENTS
Mean importance measures for groups of events in fault trees
[DE94-015416] p 353 N95-13061
METHYL COMPOUNDS
Thermophysical properties of MtBE (methyl tertbutyl ether)
[ESDU-94010] p 265 N95-11775
Synthesis and solid-state NMR characterization of 13C- and 15N-labelled n-methylphthalimide: A model compound for studying polyimides
[AD-A282510] p 273 N95-12397
METRICATION
Federal metric progress in 1993
[PB94-196029] p 279 N95-11907
METROLOGY
Optical metrology and more. Programs and services of the Radiometric Physics Division, Physics Laboratory
[PB94-191707] p 362 N95-11841
MICROBIOLOGY
Morphological differentiation of colon carcinoma cell lines in rotating wall vessels
[NASA-CR-196780] p 333 N95-11808
MICROBURSTS (METEOROLOGY)
Airborne Windshear Detection and Warning Systems. Fifth and Final Combined Manufacturers' and Technologists' Conference, part 2
[NASA-CP-10139-PT-2] p 234 N95-13203
Certification methodology applied to the NASA experimental radar system p 235 N95-13205
Certification of windshear performance with RTCA class D radomes p 235 N95-13206
MICROCRACKS
Effect of pre-welding heat-treatments on welding a two-phase Ni3Al alloy
[DE94-014409] p 270 N95-12372
Fatigue in single crystal nickel superalloys
[AD-A283459] p 270 N95-12546
MICROCRYSTALS
Atomic structure modifications of diamond-like nanocomposite films: Observation by Raman spectroscopy, FTIR and STM
[DE94-013732] p 371 N95-11740
Structure-phase state of thick amorphous and microcrystalline chromium-carbon films deposited by ion-plasma sputtering
[DE94-624236] p 277 N95-13535
MICROELECTRONICS
CVD techniques for the synthesis or modification of porous ceramics
[PB94-206836] p 276 N95-13284
MICROGRAVITY
Morphological differentiation of colon carcinoma cell lines in rotating wall vessels
[NASA-CR-196780] p 333 N95-11808
Proposal for the design of a zero gravity tool storage device
[NASA-CR-197150] p 302 N95-12627
Effect of decreased gravity on circulation in the rat
[NASA-CR-196946] p 331 N95-12827
From undersea to outer space: The STS-40 jellyfish experiment
[NASA-TM-109958] p 250 N95-13122
Protein crystal growth in low gravity
[NASA-CR-196980] p 279 N95-13202
Cryogenic On-Orbit Liquid Depot Storage, Acquisition, and Transfer satellite (COLD-SAT) feasibility study
[NASA-CR-185247] p 256 N95-13232
Feasibility study for a Cryogenic On-Orbit Liquid Depot-Storage, Acquisition and Transfer (COLD-SAT) satellite
[NASA-CR-185248] p 294 N95-13233
Feasibility study for the Cryogenic Orbital Nitrogen Experiment (CONE)
[NASA-CR-187231] p 294 N95-13234
Cryogenic On-Orbit Liquid Depot Storage, Acquisition, and Transfer Satellite (COLD-SAT)
[NASA-CR-185249] p 259 N95-13237
MICROGRAVITY APPLICATIONS
An examination of anticipated g-jitter on Space Station and its effects on materials processes
[NASA-TM-103775] p 278 N95-12703
MICROMACHINING
Military applications of microelectromechanical systems
[AD-A282470] p 289 N95-13291
MICROMECHANICS
Modeling and life prediction methodology for Titanium Matrix Composites subjected to mission profiles
[NASA-TM-109148] p 269 N95-11915
Failure analysis of woven and braided fabric reinforced composites
[NASA-CR-194981] p 262 N95-11926
Computer modelling of cyclic deformation of high-temperature materials
[AD-A282457] p 263 N95-12833
Micromechanics Analysis Code (MAC). User guide: Version 1.0
[NASA-TM-106706] p 264 N95-13193
Military applications of microelectromechanical systems
[AD-A282470] p 289 N95-13291
MICROMETEOROLOGY
SuperMariah: A similarity-based method for determining wind, temperature, and humidity profile structure in the surface boundary layer
[AD-A283058] p 327 N95-12997
MICROMINIATURIZATION
Diode-pumped micro-laser arrays
[AD-A282494] p 299 N95-13294
Kinetics and characterization of tungsten CVD processes
[PB94-206901] p 271 N95-13411
MICROORGANISMS
Microbial communities in subsurface environments: Diversity, origin, and evolution
[DE94-013699] p 329 N95-11737
Regulation of alternative CO2 fixation pathways in prokaryotic and eukaryotic photosynthetic organisms
[DE94-013180] p 331 N95-13271
MICROPARTICLES
Glass microsphere lubrication
[NASA-CR-197157] p 277 N95-13508
MICROPROCESSORS
Using secure coprocessors
[AD-A281255] p 340 N95-12524
MICROSTRIP ANTENNAS
Analysis of cylindrical wrap-around and doubly conformal patch antennas by way of the finite element-artificial absorber method
[NASA-CR-195211] p 281 N95-12382
MICROSTRUCTURE
Effect of pre-welding heat-treatments on welding a two-phase Ni3Al alloy
[DE94-014409] p 270 N95-12372
Study of magnetic recording media on glass substrates
[DE94-014740] p 296 N95-12869
The structural basis for fatigue failure initiation in glassy polymers
[DE94-015415] p 275 N95-13060
Some metallographic results for brush bristles and brush segments of a shroud ring brush seal tested in a T-700 engine p 307 N95-13608
MICROWAVE ANTENNAS
Design studies of large aperture, high-resolution Earth science microwave radiometers compatible with small launch vehicles
[NASA-TP-3469] p 315 N95-12379
MICROWAVE ATTENUATION
Absorption of intense microwaves and ion acoustic turbulence due to heat transport
[DE94-015140] p 369 N95-13285
MICROWAVE CIRCUITS
Processing, fabrication, and demonstration of HTS integrated microwave circuits
[AD-A282505] p 289 N95-13300
MICROWAVE IMAGERY
Parameterization and scaling of Arctic ice conditions in the context of ice-atmosphere processes
[NASA-CR-196831] p 327 N95-11706
Millimeter-wave radiometric utility study
[AD-A282524] p 281 N95-12402
Passive MMW camera for low visibility landings p 236 N95-13215
MICROWAVE INTERFEROMETERS
A 250 GHz microwave interferometer for divertor experiments on D3-D
[DE94-014056] p 364 N95-11786
MICROWAVE OSCILLATORS
Plasma effects on electron beam dynamics in a virtual cathode oscillator p 366 N95-12436
MICROWAVE POWER BEAMING
PowerSat: A technology demonstration of a solar power satellite
[NASA-CR-197210] p 253 N95-12661
MICROWAVE RADIOMETERS
Design studies of large aperture, high-resolution Earth science microwave radiometers compatible with small launch vehicles
[NASA-TP-3469] p 315 N95-12379
Earth Observing System (EOS)/Advanced Microwave Sounding Unit-A (AMSU-A)
[NASA-CR-189379] p 344 N95-12796
MICROWAVE SOUNDING
TOVS operational sounding upgrades: 1990-1992
[NOAA-TR-NESDIS-76] p 322 N95-11836
Earth Observing System (EOS)/Advanced Microwave Sounding Unit-A (AMSU-A)
[NASA-CR-189379] p 344 N95-12796
MICROWAVE TRANSMISSION
Principles of GPS one-way data processing for high precision positioning applications: Algorithms and software issues p 237 N95-12177
Search for extraterrestrial intelligence/High Resolution Microwave Survey team member
[NASA-CR-196478] p 339 N95-13026
MICROWAVES
Microwave heating and joining of ceramic cylinders: A mathematical model
[NASA-CR-194962] p 351 N95-11922
Measurements of 20 GHz high-power microwaves output from a large diameter plasma filled backward wave oscillator p 365 N95-12435
Strong beam-plasma turbulence p 367 N95-12450
Radiofrequency/microwave radiation biological effects and safety standards: A review
[AD-A282886] p 334 N95-12919
MILITARY OPERATIONS
Tactical satellite orbital simulation and requirements study
[AD-A282314] p 282 N95-12416
MILITARY TECHNOLOGY
Acute inhalation of explosively disseminated carbon fibers in rats
[AD-A280556] p 330 N95-12614
MapView user's guide
[AD-A282469] p 316 N95-13290
Military applications of microelectromechanical systems
[AD-A282470] p 289 N95-13291
MILKY WAY GALAXY
Gamma-ray burst constraints on the galactic frequency of extra-solar Oort clouds
[NASA-CR-196197] p 385 N95-12886
MILLIMETER WAVES
Millimeter-wave radiometric utility study
[AD-A282524] p 281 N95-12402
Evaluation of candidate millimeter wave sensors for synthetic vision p 236 N95-13214
Passive MMW camera for low visibility landings p 236 N95-13215
MINERAL DEPOSITS
On the isolation of halophilic microorganisms from salt deposits of great geological age p 332 N95-11966
Lunar vertical-shaft mining system
[NASA-CR-197154] p 384 N95-13497
MINERALOGY
Micromorphology, mineralogy, and genesis of soils and fracture fills and the Pajarito Plateau, New Mexico
[DE94-013612] p 322 N95-11732
MINUTEMAN ICBM
Converting the Minuteman missile into a small satellite launch system
[NASA-CR-197169] p 249 N95-12531
Minuteman 2 launched small satellite
[NASA-CR-197203] p 254 N95-12765
MIRRORS
Tetravalent chromium (Cr(4+)) as laser-active ion for tunable solid-state lasers
[NASA-CR-196481] p 298 N95-12951
An adaptive optics package designed for astronomical use with a laser guide star tuned to an absorption line of atomic sodium
[DE94-012391] p 363 N95-13532
MISSILE CONFIGURATIONS
Experimental Aerodynamics Division
[NAL-SP-9404] p 229 N95-12166

MISSILE SIGNATURES
Investigation of the effects of solid rocket motor propellant composition on plume signature
[AD-A283365] p 258 N95-12885
MISSILE TRAJECTORIES
Parallel methods for the flight simulation model
[DE94-013330] p 245 N95-11752
MISSILES
Parallel methods for the flight simulation model
[DE94-013330] p 245 N95-11752
MISSION PLANNING
Inner Magnetosphere Imager (IMI) solar terrestrial probe class mission preliminary design study report
[NASA-TM-108464] p 252 N95-11948
Meeting the challenge of manned lunar and Martian exploration p 339 N95-11970
Design of an unmanned Martian polar exploration system
[NASA-CR-197160] p 383 N95-12529
An investigation of the use of temporal decomposition in space mission scheduling
[NASA-CR-196420] p 377 N95-12618
Project Freebird: An orbital transfer vehicle
[NASA-CR-197201] p 254 N95-12737
MapView user's guide
[AD-A282469] p 316 N95-13290
SolSTUS: Solar Source Thermal Upper Stage
[NASA-CR-197179] p 257 N95-13581
MIXING LAYERS (FLUIDS)
Backdraft phenomena
[PB94-193927] p 267 N95-12852
MOBILE COMMUNICATION SYSTEMS
ETRI brochure: History, mission, and activity highlights p 389 N95-12697
MODAL RESPONSE
Development of the CSI phase-3 evolutionary model testbed
[NASA-CR-4630] p 256 N95-13195
MODELS
Object recognition for flexible assembly using stereo vision
[PB94-204427] p 383 N95-13248
Modelling of biopotential recordings and its implications for instrumentation design
[PB94-206844] p 332 N95-13408
MODULARITY
Reliability allocation for a system using Markov analysis
[PB94-205051] p 309 N95-13406
MODULATION TRANSFER FUNCTION
An investigation of the channel crosstalk in optical heterodyne controlled phased array radars
[AD-A281227] p 285 N95-13371
MODULATORS
Design and synthesis of tight pitch FLCs for analog voltage-limited electro-optic modulators
[AD-A281472] p 371 N95-11855
MOISTURE
Moisture induced pressures in concrete airfield pavements
[AD-A281974] p 245 N95-11789
The use of an acoustic emission method to estimate the effect of manufacturing process and service factors on the failure of concrete p 311 N95-12108
MOISTURE RESISTANCE
All-hydrocarbon composite resins based on cyclopentadiene
[AD-A282495] p 276 N95-13296
MOLECULAR BEAM EPITAXY
The magnetic structure of holmium-erbium superlattices
[DE94-013728] p 371 N95-11739
Pseudomorphic semiconducting heterostructures from combinations of AlN, GaN and selected SiC polytypes: Theoretical advancement and its coordination with experimental studies of nucleation, growth, characterization and device development
[AD-A281218] p 289 N95-13368
MOLECULAR BEAMS
Hypersonic Gas-Surface Energy Accommodation Test Facility
[DE94-014466] p 232 N95-12652
MOLECULAR BIOLOGY
Microbial communities in subsurface environments: Diversity, origin, and evolution
[DE94-013699] p 329 N95-11737
Convective flow effects on protein crystal growth
[NASA-CR-196790] p 372 N95-11921
Summary of the Sixteenth Annual Conference on Shock
[AD-A282643] p 334 N95-12542
Regulation of alternative CO2 fixation pathways in prokaryotic and eukaryotic photosynthetic organisms
[DE94-013180] p 331 N95-13271
MOLECULAR CHAINS
Radiation-induced structural changes, 4
[DE94-753223] p 356 N95-11817
Theory of complex defects on DNA polymer chain
[AD-A282619] p 275 N95-12536
MOLECULAR CLOUDS
An x-ray search for PMS stars in translucent molecular clouds
[NASA-CR-196151] p 380 N95-12388
MOLECULAR DYNAMICS
Radiation-induced structural changes, 4
[DE94-753223] p 356 N95-11817
Proceedings of US-Latin American Workshop on Molecular and Materials Sciences: Theoretical and Computational Aspects
[AD-A283359] p 358 N95-12882
US-Latin American Workshop on Molecular and Materials Sciences: Theoretical and Computational Aspects
[AD-A283428] p 359 N95-13141
MOLECULAR ELECTRONICS
Proceedings of US-Latin American Workshop on Molecular and Materials Sciences: Theoretical and Computational Aspects
[AD-A283359] p 358 N95-12882
Potential molecular wires by an iterative divergent/convergent approach. Doubling of molecular length at each iteration
[AD-A281292] p 360 N95-13376
MOLECULAR ENERGY LEVELS
Advanced cryogenic propellants
[AD-A282451] p 277 N95-12729
MOLECULAR EXCITATION
Theory of complex defects on DNA polymer chain
[AD-A282619] p 275 N95-12536
MOLECULAR GASES
Atomic scale dynamics of a two-dimensional gas-solid interface
[AD-A282646] p 358 N95-12617
MOLECULAR INTERACTIONS
Reactions of atmospheric cluster ions
[AD-A282598] p 324 N95-12534
Atomic scale dynamics of a two-dimensional gas-solid interface
[AD-A282646] p 358 N95-12617
Advanced cryogenic propellants
[AD-A282451] p 277 N95-12729
Summaries of papers presented at the High Resolution Spectroscopy Topical Meeting. Technical digest series. Volume 1: Post conference edition
[AD-A281261] p 268 N95-13372
Hydrogen bonding and molecular orientation in water/fluorine adlayers on silver(110)
[AD-A282652] p 268 N95-13549
MOLECULAR OSCILLATORS
Design, synthesis and characterization of novel nonlinear optical polymers
[AD-A282201] p 274 N95-12424
MOLECULAR SPECTRA
Calibration of optical wavelength at 1300 nm and 1550 nm using molecular absorption lines
[PB94-180080] p 362 N95-12598
MOLECULAR SPECTROSCOPY
Spaceborne Photonics Institute
[NASA-CR-196784] p 362 N95-12659
MOLECULAR STRUCTURE
Radiation-induced structural changes, 4
[DE94-753223] p 356 N95-11817
Naval research reviews, volume 46, February 1994
[AD-A281435] p 265 N95-11827
Chiral recognition in molecular and macromolecular pairs of (S)- and (R)-1-cyano-2-methylpropyl 4'(4-(8-vinyloxyoctyloxy)benzoyl) biphenyl-4-carboxylate enantiomers
[AD-A281438] p 356 N95-11828
The synthesis and structure of polyphosphazenes
[AD-A281723] p 272 N95-11832
Synthesis, structure and properties of segmented polymers containing mesogens
[AD-A281419] p 272 N95-11852
Enhancement of luminescence in polymer nanocomposites
[AD-A282539] p 262 N95-12404
Adherend surface effects on epoxy cure by NMR
[AD-A282165] p 274 N95-12420
MOLECULAR WEIGHT
Chiral recognition in molecular and macromolecular pairs of (S)- and (R)-1-cyano-2-methylpropyl 4'(4-(8-vinyloxyoctyloxy)benzoyl) biphenyl-4-carboxylate enantiomers
[AD-A281438] p 356 N95-11828
Polymer effect on heterochiral molecular recognition in molecular and macromolecular pairs of liquid crystals of (R)- and (S)-2-chloro-4-methylpentyl 4'-((8-(vinyloxy)octyl)oxy)biphenyl-4-caroxylate rs
[AD-A281193] p 358 N95-12522
MOMENTS OF INERTIA
Flight dynamics of an unmanned aerial vehicle
[AD-A282259] p 239 N95-12410
MOMENTUM THEORY
Analysis and design of numerical schemes for gas dynamics 1: Artificial diffusion, upwind biasing, limiters and their effect on accuracy and multigrid convergence
[NASA-CR-196477] p 290 N95-11875
MONKEYS
The rhesus measurement system: A new instrument for space research p 247 N95-11965
Vestibular afferent responses to linear accelerations in the alert squirrel monkey
[NASA-TM-4581] p 330 N95-12006
Reduction of ocular counter-rolling by adaptation to space
[NASA-CR-196279] p 333 N95-12376
Spaceflight and immune responses of Rhesus monkeys
[NASA-CR-196846] p 331 N95-12941
MONOCHROMATORS
Calibration of optical wavelength at 1300 nm and 1550 nm using molecular absorption lines
[PB94-180080] p 362 N95-12598
MONOMERS
Multifunctional acrylic ether monomers, their polymers, and polymerizable epoxide derivatives from simple alpha-substitution of alkyl acrylates
[AD-A282513] p 273 N95-12400
MONOPLANES
The Elite: A high speed, low-cost general aviation aircraft for Aeroworld
[NASA-CR-197161] p 239 N95-12530
Icarus Rewaxed: A high speed, low-cost general aviation aircraft for Aeroworld
[NASA-CR-197155] p 239 N95-12609
Triton 2 (1B)
[NASA-CR-197188] p 240 N95-12636
MONOPULSE RADAR
Monopulse tracker operating characteristics measurement error performance for azimuth tracking
[AD-A281188] p 282 N95-12521
MONTE CARLO METHOD
Vulnerability assessment of a space based weapon platform electronics system exposed to a thermonuclear weapon detonation
[DE94-013415] p 250 N95-11755
A study of a multi-pinned phase CCD detector for use as a star tracker
[NASA-CR-196287] p 381 N95-13056
Mean importance measures for groups of events in fault trees
[DE94-015416] p 353 N95-13061
MOON
Project ECHO: Electronic Communications from Halo Orbit
[NASA-CR-197190] p 283 N95-12644
A lunar/Martian anchor emplacement system
[NASA-CR-197193] p 302 N95-12690
MORPHOLOGY
Morphological differentiation of colon carcinoma cell lines in rotating wall vessels
[NASA-CR-196780] p 333 N95-11808
Enhancement of luminescence in polymer nanocomposites
[AD-A282539] p 262 N95-12404
Diagnostic techniques for semiconductor materials processing
[AD-A282810] p 373 N95-12602
MOSAICS
Digital image processing techniques for image-mapping applications
[INPE-5546-TDI/532] p 315 N95-12301
MOTION PERCEPTION
The selective use of functional optical variables in the control of forward speed
[NASA-TM-108849] p 229 N95-12227
Visual psychophysics of egomotion
[AD-A282547] p 335 N95-12495
MOTION SIMULATION
Numerical simulations of drop collisions
[NASA-TM-106751] p 295 N95-13550
MOTIVATION
Tank crew performance related to cognitive ability and motivation of the tank crew members
[PB94-190642] p 335 N95-11872
The use of neuron nets to stabilize dynamic systems p 348 N95-12109

MOUNTAINS
Factors influencing the rates, processes and magnitude of accumulation of carbon in desert soils
[NASA-CR-196820] p 325 N95-13025
MOUNTING
Duplex rolling element bearing mounting for ensuring preload control
[AD-D016402] p 304 N95-13189
MSM (SEMICONDUCTORS)
Development of nanostructure fabrication technology and new electron-quantum wave devices
[AD-A281724] p 286 N95-11860
MULTIGRID METHODS
Analysis and design of numerical schemes for gas dynamics 1: Artificial diffusion, upwind biasing, limiters and their effect on accuracy and multigrid convergence
[NASA-CR-196477] p 290 N95-11875
MULTIMEDIA
Performance measurements of the multimedia testbed on real-time Mach
[AD-A282658] p 343 N95-12504
ETRI brochure: History, mission, and activity highlights
p 389 N95-12697
MULTIPATH TRANSMISSION
Advanced S-Band studies using the TDRSS communications satellite
[NASA-CR-196931] p 281 N95-12010
MULTIPHASE FLOW
Scaling fluid content-pressure relations of different fluid systems in porous media
[DE94-013349] p 294 N95-13075
MULTIPROCESSING (COMPUTERS)
Parallel methods for the flight simulation model
[DE94-013330] p 245 N95-11752
Eager combining: A coherency protocol for increasing effective network and memory bandwidth in shared-memory multiprocessors
[AD-A281501] p 346 N95-11857
A preliminary evaluation of cache-miss-initiated prefetching techniques in scalable multiprocessors
[AD-A281502] p 346 N95-11858
Advanced computer architecture specification for automated weld systems
[NASA-CR-194006] p 343 N95-12014
A framework for exploiting data and functional parallelism on distributed memory multicomputers
[AD-A281194] p 347 N95-12523
Active Nodal Task Seeking for high-performance, ultra-dependable computing
[AD-A282924] p 344 N95-12588
Parallel preconditioners for the conjugate gradient method
[PB94-201605] p 347 N95-13404
Visualizing parallel numerical software performance on a shared memory multiprocessor
[PB94-195658] p 352 N95-13437
MULTISENSOR FUSION
Evaluation of candidate millimeter wave sensors for synthetic vision p 236 N95-13214
Passive MMW camera for low visibility landings
p 236 N95-13215
MULTISTAGE ROCKET VEHICLES
Converting the Minuteman missile into a small satellite launch system
[NASA-CR-197169] p 249 N95-12531
Orion: Design of a system for assured low-cost human access to space
[NASA-CR-197185] p 253 N95-12564
Athena: Advanced air launched space booster
[NASA-CR-197148] p 258 N95-12604
MUONIUM
Muon sites and electronic structure
[PB94-179348] p 357 N95-12365
MUONS
An investigation of Mn Si by the SR-technique
[DE94-624058] p 371 N95-11748
Muon sites and electronic structure
[PB94-179348] p 357 N95-12365
MUSCLES
A musculoskeletal model of the elbow joint complex
[NASA-CR-195812] p 335 N95-13270
MUSCULAR FUNCTION
Preconditioning electromyographic data for an upper extremity model using neural networks
[NASA-CR-196877] p 332 N95-11708
MUSCULOSKELETAL SYSTEM
A study of the deformation of helical springs under eccentric loading
[AD-A283448] p 312 N95-12511
A musculoskeletal model of the elbow joint complex
[NASA-CR-195812] p 335 N95-13270
MUSEUMS
Communications plan --- Design of the public wing of the Oregon State University Hatfield Marine Science Center
[NASA-CR-196435] p 314 N95-12231

N

NACELLES
Evaluation of alternative in-flight fire suppressants for full-scale testing in simulated aircraft engine nacelles and dry bays
[PB94-203403] p 236 N95-13247
NARROWBAND
Synchrotron studies of narrow band materials
[DE94-013698] p 271 N95-13554
NASA PROGRAMS
NASA/OAI Research Associates program
[NASA-CR-196824] p 376 N95-11765
Intellectual property rights at the National Aeronautics and Space Administration, Lewis Research Center
[NASA-TM-106731] p 379 N95-11866
Aeronautics and space technology, past, present, and future p 229 N95-11892
Technical paper contest for women 1992. Space challenges: Earth and beyond
[NASA-TM-109953] p 386 N95-11955
NASA's Hypersonic Research Engine Project: A review
[NASA-TM-107759] p 244 N95-12860
NASA SPACE PROGRAMS
Activities of the Space Studies Board of the National Research Council
[NASA-CR-195738] p 247 N95-12880
NATIONAL AEROSPACE PLANE PROGRAM
Hypersonic engine seal development at NASA Lewis Research Center p 307 N95-13602
NATIONAL LAUNCH VEHICLE PROGRAM
A shadowgraph study of the National Launch System's 1 1/2 stage vehicle configuration and Heavy Lift Launch Vehicle configuration --- Using the Marshall Space Flight Center's 14-Inch Trisonic Wind Tunnel
[NASA-RP-1347] p 229 N95-11710
NATURAL GAS
Open-chamber combustion study
[PB94-184090] p 301 N95-12579
Fundamental and experimental studies on the catalytic combustion of methane
[PB94-205895] p 268 N95-13251
NATURAL LANGUAGE PROCESSING
Design of an intelligent support system for scientific databases
[AD-A283043] p 378 N95-12995
NAVIER-STOKES EQUATION
Investigation of advanced counterrotation blade configuration concepts for high speed turboprop systems. Task 8: Cooling flow/heat transfer analysis
[NASA-CR-195359] p 244 N95-11901
Numerical simulation of particle-wave interaction on boundary layers
[AD-A282184] p 293 N95-12422
Supersonic base flow investigation over axisymmetric afterbodies
[PB94-180957] p 232 N95-12578
Validation of the RPLUS3D code for supersonic inlet applications involving three-dimensional shock wave-boundary layer interactions
[NASA-TM-106579] p 233 N95-13058
An investigation of the vortex method
[DE94-014931] p 294 N95-13156
Numerical simulations of drop collisions
[NASA-TM-106751] p 295 N95-13550
NAVIGATION INSTRUMENTS
Principles of GPS one-way data processing for high precision positioning applications: Algorithms and software issues p 237 N95-12177
NEAR FIELDS
Nonlinear hysteresis in an endochronic solid
[AD-A283142] p 325 N95-13136
NEAR INFRARED RADIATION
Optical and magnetic resonance investigations of 3D ions in single crystal hosts: Candidates for tunable solid-state lasers
[AD-A281726] p 371 N95-11842
Near-infrared imaging of selected areas
[AD-A283519] p 316 N95-12634
Visible/infrared radiometric calibration station
[DE94-014459] p 383 N95-13106
NEODYMIUM LASERS
Laser based combustion laboratory at NTH/SINTEF applied thermodynamics
[PB94-202603] p 299 N95-13246
Laser physics of Nd(exp 3+)-doped phosphate glasses
[DE94-015141] p 299 N95-13534
NEPTUNE (PLANET)
Non-dipolar magnetic field models and patterns of radio emission: Uranus and Neptune compared
[NASA-CR-196412] p 385 N95-12469
NETHERLANDS
The Additional Programme on Ammonia
[PB94-193075] p 320 N95-12777
NETS
The use of neuron nets to stabilize dynamic systems
p 348 N95-12109
NETWORK ANALYSIS
Algorithms for mathematical programming
[DE94-013544] p 345 N95-13339
NETWORK CONTROL
Systems engineering technology for networks
[NASA-CR-196853] p 280 N95-11804
NEURAL NETS
Preconditioning electromyographic data for an upper extremity model using neural networks
[NASA-CR-196877] p 332 N95-11708
Prediction of geometric-thermal machine tool errors by artificial neural networks
[PB94-186673] p 348 N95-11909
Scheduling in an input and output queuing three-stage packet switch by using neural networks
[PB94-179413] p 349 N95-12367
Neural networks: Structure and repair. Part 1: Ground squirrel visual system. Part 2: Formation, maintenance and plasticity of synaptic connections
[AD-A282420] p 330 N95-12393
Outdoor landmark recognition using hybrid fractal vision system and neural networks
[AD-A282506] p 349 N95-12395
Investigation of spectral-based techniques for classification of wideband transient signals in additive white Gaussian noise
[AD-A282954] p 283 N95-12592
Optimization of aerospace structures
[NASA-CR-196763] p 242 N95-12787
Population-based incremental learning. A method for integrating genetic search based function optimization and competitive learning
[AD-A282654] p 350 N95-12835
Neural networks and orbit control in accelerators
[DE94-014877] p 350 N95-13124
Weld acoustic monitor
[AD-D016400] p 356 N95-13154
NEUROGLIA
Neural networks: Structure and repair. Part 1: Ground squirrel visual system. Part 2: Formation, maintenance and plasticity of synaptic connections
[AD-A282420] p 330 N95-12393
NEURONS
The use of neuron nets to stabilize dynamic systems
p 348 N95-12109
Neural networks: Structure and repair. Part 1: Ground squirrel visual system. Part 2: Formation, maintenance and plasticity of synaptic connections
[AD-A282420] p 330 N95-12393
NEUROPHYSIOLOGY
Preconditioning electromyographic data for an upper extremity model using neural networks
[NASA-CR-196877] p 332 N95-11708
NEUTRAL ATMOSPHERES
Ionospheric dynamics instrument investigation for the Timed Mission
[NASA-CR-196198] p 325 N95-13190
NEUTRAL BUOYANCY SIMULATION
Evaluation of COSTAR mass handling characteristics in an environment. A simulation of the Hubble Space Telescope service mission
[NASA-TP-3489] p 333 N95-11887
NEUTRINOS
The odderon in the deep-inelastic lepton-hadron scattering
[DE94-622791] p 360 N95-13274
NEUTRON BEAMS
Summary reports of activities under visiting research program, 1993
[DE94-753222] p 360 N95-11750
NEUTRON DIFFRACTION
The magnetic structure of holmium-erbium superlattices
[DE94-013728] p 371 N95-11739
Small angle neutron scattering in surface-active agents mixtures
[DE94-624057] p 356 N95-11747
Summary reports of activities under visiting research program, 1993
[DE94-753222] p 360 N95-11750
NEUTRON IRRADIATION
The effect of irradiation on the stability and properties of monolithic silicon carbide and SiC(f)/SiC composites up to 25 dpa
[DE94-014568] p 263 N95-12862
NEUTRON SCATTERING
Small angle neutron scattering in surface-active agents mixtures
[DE94-624057] p 356 N95-11747

NEUTRON SPECTRA
The cascade-deuteron system
[DE94-011650] p 357 N95-11894
NEUTRON STARS
Gamma-ray burst constraints on the galactic frequency of extra-solar Oort clouds
[NASA-CR-196197] p 385 N95-12886
NEUTRONS
The magnetic structure of holmium-erbium superlattices
[DE94-013728] p 371 N95-11739
NEW MEXICO
A comparison of two sites for the purpose of satellite laser ranging
[AD-A283149] p 299 N95-13139
NICKEL
Growth of Au on Ni(110): A BFS modelling of surface alloy phases
[NASA-TM-106732] p 270 N95-12104
Raman structural studies of the nickel electrode
[NASA-CR-196331] p 289 N95-13344
NICKEL ALLOYS
Certain aspects of the melting, casting and welding of Ni3Al alloys
[DE94-013628] p 269 N95-11897
Effect of pre-welding heat-treatments on welding a two-phase Ni3Al alloy
[DE94-014409] p 270 N95-12372
Fatigue in single crystal nickel superalloys
[AD-A283459] p 270 N95-12546
Hydrogen desulfurization of nickel: Thermodynamics and kinetics
[AD-A282581] p 266 N95-12549
Thin-film model studies of interfacial reactions in intermetallic matrix composites
[AD-A283360] p 263 N95-12883
Description of a high temperature quenching furnace for the study of the directional solidification of nickel-base superalloys
[DE94-013812] p 271 N95-13544
NICKEL CADMIUM BATTERIES
Validation results of wind diesel simulation model TKKMOD
[PB94-179157] p 317 N95-11846
Screen test for cadmium and nickel plates as developed and used within the Aerospace Corporation
[NASA-CR-196961] p 270 N95-12148
NIGHT VISION
Visit to UDRI and USAF, Armstrong Lab., Williams AFB, Phoenix, USA, February 8-11, 1993
[PB94-190659] p 337 N95-11873
Semiautomated methodology for measurement of field-of-view, magnification, and distortion of night vision devices as defined in MIL-A-49425(CR)
[AD-A282210] p 362 N95-12427
NIMBUS 7 SATELLITE
Nimbus-7 Earth Radiation Budjet compact solar data set user's guide
[NASA-RP-1346] p 384 N95-12667
NIOBIUM ALLOYS
First principles investigation of the Ir-Zr-Nb ternary system
[AD-A282644] p 270 N95-12543
NITRIDING
Basic mechanisms of radiation effects in the natural space radiation environment
[DE94-013445] p 384 N95-11757
NITRILES
Phosphazene-containing amine as curing agent for phthalonitrile-base polymer
[AD-D016375] p 276 N95-13179
NITROGEN
Mixed clusters from the coexpansion of C2F6 and n2 in a pulsed, supersonic expansion cluster ion source and beam deflection time-of-flight mass spectrometer: A first application
[AD-A282044] p 361 N95-11910
Synthesis and solid-state NMR characterization of 13C- and 15N-labelled n-methylphthalimide: A model compound for studying polyimides
[AD-A282510] p 273 N95-12397
Feasibility study for the Cryogenic Orbital Nitrogen Experiment (CONE)
[NASA-CR-187231] p 294 N95-13234
NITROGEN DIOXIDE
Laser based combustion laboratory at NTH/SINTEF applied thermodynamics
[PB94-202603] p 299 N95-13246
NOAA SATELLITES
TOVS operational sounding upgrades: 1990-1992
[NOAA-TR-NESDIS-76] p 322 N95-11836
NOBLE METALS
Improving the efficiency of high purity water systems
[DE94-013742] p 318 N95-11784
NOISE INTENSITY
En route noise levels from propfan test assessment airplane
[NASA-TP-3451] p 355 N95-12341
Response to noise around Vaernes and Bodoe airports
[PB94-207065] p 356 N95-13575
NOISE POLLUTION
Effects of Noise on Hearing 5th International Symposium
[AD-A281439] p 335 N95-13177
NOISE PROPAGATION
En route noise levels from propfan test assessment airplane
[NASA-TP-3451] p 355 N95-12341
NOISE REDUCTION
Computerized design and generation of low-noise helical gears with modified surface topology
[NASA-TM-106696] p 303 N95-13083
NONDESTRUCTIVE TESTS
Test plan. GCPS task 7, subtask 7.1: IHM development
[NASA-CR-106876] p 250 N95-11767
Revealing hidden defects: A hybrid evaluation strategy for steel structures
[PB94-191236] p 308 N95-11822
Sound emission in materials and construction element testing p 355 N95-12013
Probability of detection of defects in coatings with electronic shearography
[NASA-CR-196201] p 308 N95-12391
Development of an Automated Nondestructive Inspection (ANDI) system for commercial aircraft, phase 1
[AD-A283500] p 234 N95-12623
NONEQUILIBRIUM FLOW
Predicting radiative heat transfer in thermochemical nonequilibrium flow fields. Theory and user's manual for the LORAN code
[NASA-TM-4564] p 291 N95-11936
An implementation of a chemical and thermal nonequilibrium flow solver on unstructured meshes and application to blunt bodies
[NASA-CR-194967] p 293 N95-12619
NONEQUILIBRIUM RADIATION
Predicting radiative heat transfer in thermochemical nonequilibrium flow fields. Theory and user's manual for the LORAN code
[NASA-TM-4564] p 291 N95-11936
NONINTRUSIVE MEASUREMENT
Stationary plasma thruster ion velocity distribution
[NASA-CR-195379] p 257 N95-11919
Development of nonintrusive, scatter-independent techniques for measurement of liquid density inside dense sprays
[NASA-CR-196413] p 293 N95-12387
Planar Rayleigh scattering and laser-induced fluorescence for visualization of a hot, Mach 2 annular air jet
[NASA-TM-4576] p 247 N95-13196
Simultaneous three-dimensional velocity and mixing measurements by use of laser Doppler velocimetry and fluorescence probes in a water tunnel
[NASA-TP-3454] p 246 N95-13553
NONLINEAR EQUATIONS
Anode sheath contributions in plasma thrusters
[AD-A280395] p 364 N95-11837
Viscosity solutions of fully nonlinear equations
[AD-A281725] p 351 N95-11861
Nonlinear problems in fluid dynamics and inverse scattering: Langmuir circulations in ocean surface layers
[AD-A282934] p 329 N95-12590
Aspects of long time behaviour of solutions of nonlinear Hamiltonian evolution equations
[PB94-192382] p 352 N95-12808
Inverse operator theory method mathematics-mechanization for the solutions of nonlinear equations and some typical applications in nonlinear physics
[DE94-624804] p 352 N95-13340
NONLINEAR EVOLUTION EQUATIONS
Aspects of long time behaviour of solutions of nonlinear Hamiltonian evolution equations
[PB94-192382] p 352 N95-12808
Time-resolved electron thermal conduction by probing of plasma formation in transparent solids with high power subpicosecond laser pulses
[DE94-015170] p 370 N95-13555
NONLINEAR OPTICS
Light beam and pulse propagation in nonlinear dielectrics
[AD-A282548] p 282 N95-12496
Studies of optical phase conjugators and applications
[AD-A282626] p 362 N95-12538
Rational design, construction, and processing of high-performance nonlinear, optical materials
[AD-A281283] p 363 N95-13374
NONLINEAR SYSTEMS
An interpolation theoretic approach to control
[AD-A281465] p 348 N95-11853
Using emergent order to shape a space society p 377 N95-11959
Robust control design with real parameter uncertainty using absolute stability theory
[NASA-CR-196971] p 349 N95-12782
Inverse operator theory method mathematics-mechanization for the solutions of nonlinear equations and some typical applications in nonlinear physics
[DE94-624804] p 352 N95-13340
NONLINEARITY
Design, synthesis and characterization of novel nonlinear optical polymers
[AD-A282201] p 274 N95-12424
Frequency doubler (from 4.7 to 9.4 GHz) using a diode
[AD-A282784] p 287 N95-12525
Aspects of long time behaviour of solutions of nonlinear Hamiltonian evolution equations
[PB94-192382] p 352 N95-12808
Digital filter designs that are free of limit cycles
[AD-A282885] p 287 N95-12918
Chaotic time series. Part 1: Estimation of invariant properties in state space
[PB94-206968] p 376 N95-13572
NONPARAMETRIC STATISTICS
Weighted Parzen windows for pattern classification
[AD-A281222] p 345 N95-13370
NORTH AMERICA
Ten-year ground exposure of composite materials used on the Bell Model 206L helicopter flight service program
[NASA-TP-3468] p 262 N95-12357
NOSE WHEELS
Flight investigation of the use of a nose gear jump strut to reduce takeoff ground roll distance of STOL aircraft
[NASA-TM-108819] p 238 N95-12225
NOTCH TESTS
A study of naturally initiating notch root fatigue cracks under spectrum loading
[NAL-PD-SN-9406] p 311 N95-11924
NOTCHES
An analysis of the load-bearing capacity of members of square cross section with a series of perpendicular notches p 312 N95-12631
NOVAE
BATSE observations of Nova Muscae 1991
[NASA-CR-196416] p 380 N95-12464
NOWCASTING
Short term weather forecasting in real time in a base weather station setting
[AD-A283141] p 327 N95-13134
NOZZLE FLOW
Interferograms, schlieren, and shadowgraphs constructed from real- and ideal-gas, two- and three-dimensional computed flowfields p 295 N95-11971
FDNS code to predict wall heat fluxes or wall temperatures in rocket nozzles
[NASA-CR-196925] p 292 N95-11999
NOZZLE WALLS
FDNS code to predict wall heat fluxes or wall temperatures in rocket nozzles
[NASA-CR-196925] p 292 N95-11999
NUCLEAR BINDING ENERGY
Strange hadronic matter
[DE94-001493] p 357 N95-12012
Magneto-optical properties of quantum structures with reduced dimensionality
[AD-A282597] p 376 N95-12553
NUCLEAR ELECTRIC POWER GENERATION
Autonomous power system for remote locations
[DE94-013244] p 361 N95-11779
Contributions to CD Space Committee, 1993. Summary and comments
[PB94-190618] p 379 N95-11871
NUCLEAR ELECTRIC PROPULSION
Fusion powered human transport to Mars (UWFR94)
[NASA-CR-197184] p 368 N95-12641
NUCLEAR MAGNETIC RESONANCE
Amine catalyzed intramolecular imidization of alkyl and aryl phthalamates, kinetics and mechanism in deuterated chloroform
[AD-A281741] p 259 N95-11844
Synthesis and solid-state NMR characterization of 13C- and 15N-labelled n-methylphthalimide: A model compound for studying polyimides
[AD-A282510] p 273 N95-12397
Adherend surface effects on epoxy cure by NMR
[AD-A282165] p 274 N95-12420

Be-9 and B-11 NMR study of superconductivity in boron doped UBe13
[DE94-014432] p 374 N95-13081
A CRAMPS and 13C CP/MAS NMR examination of solid-solid transitions in n-Hexatriacontane (C36H74)
[AD-A282497] p 375 N95-13299

NUCLEAR PHYSICS
Laws of infrared similitude
[AD-A282209] p 354 N95-12426
Effect of stochastic damping resonance wave packet on energetic alpha particle transport
[DE94-625041] p 370 N95-13538

NUCLEAR PROPULSION
A revolutionary lunar space transportation system architecture using extraterrestrial LOX-augmented NTR propulsion
[NASA-TM-106726] p 249 N95-11703
Nuclear rockets: High-performance propulsion for Mars
[DE94-013642] p 257 N95-11782
Ion engine propelled Earth-Mars cycler with nuclear thermal propelled transfer vehicle, volume 2
[NASA-CR-197208] p 361 N95-12665

NUCLEAR RADIATION
Response of high T(sub c) superconducting Josephson junction to nuclear radiation
[DE94-624705] p 360 N95-13536

NUCLEAR REACTIONS
Summary reports of activities under visiting research program, 1993
[DE94-753222] p 360 N95-11750
Synthesis and characterization of thianthrene-based polyamides
[AD-A282512] p 273 N95-12399

NUCLEAR REACTOR CONTROL
Design issues of human operator support systems
[PB94-191376] p 337 N95-11778

NUCLEAR REACTORS
Studies of low temperature, low flux radiation embrittlement of nuclear reactor structural materials
[DE94-013710] p 269 N95-11738

NUCLEAR ROCKET ENGINES
A revolutionary lunar space transportation system architecture using extraterrestrial LOX-augmented NTR propulsion
[NASA-TM-106726] p 249 N95-11703
Nuclear rockets: High-performance propulsion for Mars
[DE94-013642] p 257 N95-11782
Ion engine propelled Earth-Mars cycler with nuclear thermal propelled transfer vehicle, volume 2
[NASA-CR-197208] p 361 N95-12665

NUCLEAR VULNERABILITY
Vulnerability assessment of a space based weapon platform electronics system exposed to a thermonuclear weapon detonation
[DE94-013415] p 250 N95-11755

NUCLEATION
Convective flow effects on protein crystal growth
[NASA-CR-196790] p 372 N95-11921
Pseudomorphic semiconducting heterostructures from combinations of AlN, GaN and selected SiC polytypes: Theoretical advancement and its coordination with experimental studies of nucleation, growth, characterization and device development
[AD-A281218] p 289 N95-13368

NUCLEON-NUCLEON INTERACTIONS
Particle-production mechanism in relativistic heavy-ion collisions
[DE94-014427] p 359 N95-13104

NUCLEONS
The odderon in the deep-inelastic lepton-hadron scattering
[DE94-622791] p 360 N95-13274
Quenched QCD at finite density
[DE94-011522] p 375 N95-13337

NUCLEOPHILES
Synthesis and characterization of thianthrene-based polyamides
[AD-A282512] p 273 N95-12399

NUMERICAL ANALYSIS
Stability and error estimation for Component Adaptive Grid methods
[NASA-CR-196492] p 351 N95-11883
Numerical computations with ABAQUS/Explicit, DYNA3D, and DYSMAS/L
[AD-A282249] p 293 N95-12409
Approximation of scattered data using smooth grid functions
[PB94-207016] p 353 N95-13573

NUMERICAL CONTROL
Development of a spindle thermal error characterization and compensation sensor system for machining center accuracy enhancement
[AD-A280891] p 300 N95-11729
Power system applications for PASC converter systems
[DE94-013329] p 286 N95-11751
Data acquisition system of the NANOSAW-2 stand alone wind diesel plant. Document and user's guide
[PB94-179108] p 317 N95-11799
Neural networks and orbit control in accelerators
[DE94-014877] p 350 N95-13124
Equipment for investigation of cryogenic compaction of nanosize silicon nitride powders
[DE94-013593] p 277 N95-13530

NUMERICAL STABILITY
Stability and error estimation for Component Adaptive Grid methods
[NASA-CR-196492] p 351 N95-11883

NUMERICAL WEATHER FORECASTING
TOVS operational sounding upgrades: 1990-1992
[NOAA-TR-NESDIS-76] p 322 N95-11836
Technical report series on global modeling and data assimilation. Volume 2: Direct solution of the implicit formulation of fourth order horizontal diffusion for gridpoint models on the sphere
[NASA-TM-10406] p 323 N95-12226
Reports to the Nation on our changing planet. El Nino and climate prediction, no. 3, spring 1994
p 320 N95-12462
Thunderstorm hypothesis reasoner
[AD-A282664] p 326 N95-12805

NUTRIENTS
Hydrographic, carbon dioxide, nutrient and productivity measurements from the south Atlantic during July and August of 1991
[PB94-180668] p 328 N95-11900

O

O STARS
Research in astrophysical processes
[NASA-CR-196773] p 382 N95-12939

OBJECT-ORIENTED PROGRAMMING
Recovery blocks
[PB94-205077] p 345 N95-13432

OBLIQUE WINGS
Design and testing of an oblique all-wing supersonic transport
[NASA-CR-196394] p 242 N95-12785

OCCLUSION
An analysis of the effect of Gaussian error in object recognition
[AD-A282260] p 349 N95-12411

OCCULTATION
BATSE observations of 3C273
[NASA-CR-196185] p 380 N95-12463
Acute inhalation of explosively disseminated carbon fibers in rats
[AD-A280556] p 330 N95-12614

OCEAN COLOR SCANNER
SeaWiFS technical report series. Volume 22: Prelaunch acceptance report for the SeaWiFS radiometer
[NASA-TM-104556-VOL-22] p 328 N95-12151
SeaWiFS technical report series. Volume 23: SeaWiFS prelaunch radiometric calibration and spectral characterization
[NASA-TM-104566-VOL-23] p 328 N95-12359

OCEAN CURRENTS
Reports to the Nation on our changing planet. El Nino and climate prediction, no. 3, spring 1994
p 320 N95-12462
Nonlinear problems in fluid dynamics and inverse scattering: Langmuir circulations in ocean surface layers
[AD-A282934] p 329 N95-12590

OCEAN DYNAMICS
Dynamical systems and oceanography
[AD-A282635] p 329 N95-12540

OCEAN MODELS
Nonlinear problems in fluid dynamics and inverse scattering: Langmuir circulations in ocean surface layers
[AD-A282934] p 329 N95-12590

OCEAN SURFACE
Nonlinear problems in fluid dynamics and inverse scattering: Langmuir circulations in ocean surface layers
[AD-A282934] p 329 N95-12590

OCEAN TEMPERATURE
Reports to the Nation on our changing planet. El Nino and climate prediction, no. 3, spring 1994
p 320 N95-12462

OCEANOGRAPHIC PARAMETERS
Hydrographic, carbon dioxide, nutrient and productivity measurements from the south Atlantic during July and August of 1991
[PB94-180668] p 328 N95-11900

OCEANOGRAPHY
Final results of the Baltic Sea Level 1990 GPS Campaign. Research works of the SSG 5.147 of the International Association of Geodesy
[REPT-94:2] p 314 N95-11881
Hydrographic, carbon dioxide, nutrient and productivity measurements from the south Atlantic during July and August of 1991
[PB94-180668] p 328 N95-11900
SeaWiFS technical report series. Volume 22: Prelaunch acceptance report for the SeaWiFS radiometer
[NASA-TM-104556-VOL-22] p 328 N95-12151
Dynamical systems and oceanography
[AD-A282635] p 329 N95-12540
Ocean acoustic tomography: Single slice and moving ship experiments
[AD-A283059] p 329 N95-12998

OFFICE AUTOMATION
Delta-4: An open architecture for dependable systems
[PB94-195641] p 341 N95-13436

OHMIC DISSIPATION
Loads for pulsed power cylindrical implosion experiments
[DE94-014429] p 299 N95-13080
The dissipative mechanism of pinning of a superconducting current
[DE94-623252] p 289 N95-13276

OLIGOMERS
Potential molecular wires by an iterative divergent/convergent approach. Doubling of molecular length at each iteration
[AD-A281292] p 360 N95-13376

ON-LINE SYSTEMS
Self-checking state machine realizations in CMOS
[AD-A282177] p 286 N95-12421
On-line data reconstruction in redundant disk arrays
[AD-A282709] p 340 N95-12516
A hitchhiker's guide to microscopy and microanalysis using telecommunications, Email and The Internet
[DE94-013299] p 285 N95-13057
World wide web implementation of the Langley technical report server
[NASA-TM-109162] p 345 N95-13198

ONE DIMENSIONAL FLOW
Computer code for determination of thermally perfect gas properties
[NASA-TP-3447] p 231 N95-11995

OORT CLOUD
Gamma-ray burst constraints on the galactic frequency of extra-solar Oort clouds
[NASA-CR-196197] p 385 N95-12886

OPENINGS
Backdraft phenomena
[PB94-193927] p 267 N95-12852

OPERATING COSTS
The FC-1D: The profitable alternative Flying Circus Commercial Aviation Group
[NASA-CR-197152] p 240 N95-12628
The OFP-6M transport jet
[NASA-CR-197159] p 240 N95-12637
Central coast designs: The Eightball Express. Taking off with convention, cruising with improvements and landing with absolute success
[NASA-CR-197181] p 241 N95-12643
LCX: Proposal for a low-cost commercial transport
[NASA-CR-197186] p 241 N95-12645

OPERATING SYSTEMS (COMPUTERS)
Proceedings: The Eleventh IEEE Workshop on Real-Time Operating Systems and Software
[AD-A281738] p 342 N95-11843
POSIX delta document for the Next-Generation Computer Resources (NGCR) operating systems interface standard baseline, version 4
[AD-A282324] p 347 N95-12418
Performance measurements of the multimedia testbed on real-time Mach
[AD-A282658] p 343 N95-12504

OPERATORS (MATHEMATICS)
Inverse operator theory method mathematics-mechanization for the solutions of nonlinear equations and some typical applications in nonlinear physics
[DE94-624804] p 352 N95-13340

OPERATORS (PERSONNEL)
Design issues of human operator support systems
[PB94-191376] p 337 N95-11778

OPTICAL CORRECTION PROCEDURE
Defocus measurement using a liquid crystal point diffraction interferometer
[NASA-TM-106687] p 296 N95-12748

OPTICAL EQUIPMENT
Evaluation of COSTAR mass handling characteristics in an environment. A simulation of the Hubble Space Telescope service mission
[NASA-TP-3489] p 333 N95-11887

OPTICAL FIBERS
Phase A design study of microgravity fluoride fiber puller
[NASA-CR-196513] p 279 N95-12752
Modelling of biopotential recordings and its implications for instrumentation design
[PB94-206844] p 332 N95-13408
OPTICAL HETERODYNING
An investigation of the channel crosstalk in optical heterodyne controlled phased array radars
[AD-A281227] p 285 N95-13371
OPTICAL MATERIALS
Design, synthesis and characterization of novel nonlinear optical polymers
[AD-A282201] p 274 N95-12424
Rational design, construction, and processing of high-performance nonlinear, optical materials
[AD-A281283] p 363 N95-13374
OPTICAL MEASUREMENT
Visual psychophysics of egomotion
[AD-A282547] p 335 N95-12495
Defocus measurement using a liquid crystal point diffraction interferometer
[NASA-TM-106687] p 296 N95-12748
OPTICAL MEASURING INSTRUMENTS
Fiber-optic sensors and the application to conditional monitoring for mechanical structures
[PB94-207057] p 363 N95-13574
OPTICAL PROPERTIES
Radiation-induced structural changes, 3
[DE94-753401] p 371 N95-11819
Optical metrology and more. Programs and services of the Radiometric Physics Division, Physics Laboratory
[PB94-191707] p 362 N95-11841
Design, synthesis and characterization of novel nonlinear optical polymers
[AD-A282201] p 274 N95-12424
Studies of optical phase conjugators and applications
[AD-A282626] p 362 N95-12538
Magneto-optical properties of quantum structures with reduced dimensionality
[AD-A282597] p 376 N95-12553
Origin of optical anisotropy in strained In(x)Ga(1-x)As/InP and In(y)Al(1-y)As/InP heterostructures
[AD-A283152] p 271 N95-13140
OPTICAL PUMPING
Light beam and pulse propagation in nonlinear dielectrics
[AD-A282548] p 282 N95-12496
OPTICAL RADAR
Lidar performance analysis
[NASA-CR-196510] p 362 N95-12390
Airborne Windshear Detection and Warning Systems. Fifth and Final Combined Manufacturers' and Technologists' Conference, part 2
[NASA-CP-10139-PT-2] p 234 N95-13203
Airport surveillance using a solid state coherent lidar p 235 N95-13207
Wake vortex detection at Denver Stapleton Airport with a pulsed 2-micron coherent lidar p 236 N95-13211
Remote sensing of turbulence in the clear atmosphere with 2-micron lidars p 236 N95-13213
OPTICAL REFLECTION
Plane-wave reflection from uniaxial chiral interface and its application to polarization transformation
[PB94-184496] p 283 N95-12580
OPTICAL RESONANCE
Optical and magnetic resonance investigations of 3D ions in single crystal hosts: Candidates for tunable solid-state lasers
[AD-A281726] p 371 N95-11842
OPTICAL RESONATORS
High average power parametric frequency conversion-new concepts and new pump sources
[DE94-013652] p 314 N95-11783
OPTICAL SWITCHING
Wavelength-encoded processing in semiconductor lasers
[AD-A282649] p 297 N95-12751
OPTICAL TRACKING
A comparison of two sites for the purpose of satellite laser ranging
[AD-A283149] p 299 N95-13139
OPTICAL WAVEGUIDES
Wavelength-encoded processing in semiconductor lasers
[AD-A282649] p 297 N95-12751
OPTICS
Proceedings of the CTU Seminar 1994, Part C
[DE94-624078] p 390 N95-12946
OPTIMAL CONTROL
Development of homotopy algorithms for fixed-order mixed H2/H(infinity) controller synthesis
[NASA-TP-3507] p 342 N95-11923
Scheduling in an input and output queuing three-stage packet switch by using neural networks
[PB94-179413] p 349 N95-12367
Robust control design with real parameter uncertainty using absolute stability theory
[NASA-CR-196971] p 349 N95-12782
Techniques for designing rotorcraft control systems
[NASA-CR-196192] p 245 N95-12791
OPTIMIZATION
Optimization of aerospace structures
[NASA-CR-196763] p 242 N95-12787
Ceramic manufacturing: Optimizing a multivariable system
[DE94-015016] p 276 N95-13184
Methodology for sensitivity analysis, approximate analysis, and design optimization in CFD for multidisciplinary applications
[NASA-CR-196981] p 294 N95-13201
Reliability allocation for a system using Markov analysis
[PB94-205051] p 309 N95-13406
OPTOELECTRONIC DEVICES
WOCSDICE 1994: European Workshop on Compound Semiconductor Devices and Integrated Circuits
[AD-A283062] p 288 N95-13052
ORBIT CALCULATION
Satellite laser ranging and gravity field modeling accuracy
[NASA-CR-196057] p 248 N95-12837
ORBIT DECAY
Lifetime and reentry prediction for the Petite Amateur Navy Satellite (PANSAT)
[AD-A283366] p 255 N95-12921
ORBIT INSERTION
Project ECHO: Electronic Communications from Halo Orbit
[NASA-CR-197190] p 283 N95-12644
ORBIT TRANSFER VEHICLES
A revolutionary lunar space transportation system architecture using extraterrestrial LOX-augmented NTR propulsion
[NASA-TM-106726] p 249 N95-11703
Project Freebird: An orbital transfer vehicle
[NASA-CR-197201] p 254 N95-12737
ORBITAL ELEMENTS
Satellite laser ranging and gravity field modeling accuracy
[NASA-CR-196057] p 248 N95-12837
ORBITAL LIFETIME
Lifetime and reentry prediction for the Petite Amateur Navy Satellite (PANSAT)
[AD-A283366] p 255 N95-12921
ORBITAL MANEUVERS
A robotic exploration mission to Mars and Phobos
[NASA-CR-197168] p 382 N95-12307
Conceptual design of an Orbital Debris Defense System
[NASA-CR-197211] p 254 N95-12696
ORBITAL MECHANICS
Satellite laser ranging and gravity field modeling accuracy
[NASA-CR-196057] p 248 N95-12837
ORBITAL POSITION ESTIMATION
A data and information system for processing, archival, and distribution of data for global change research
[NASA-CR-196770] p 320 N95-12786
Satellite laser ranging and gravity field modeling accuracy
[NASA-CR-196057] p 248 N95-12837
ORBITAL SERVICING
Evaluation of COSTAR mass handling characteristics in an environment. A simulation of the Hubble Space Telescope service mission
[NASA-TP-3489] p 333 N95-11887
Project Freebird: An orbital transfer vehicle
[NASA-CR-197201] p 254 N95-12737
ORBITAL WORKERS
MOOSE: Manned On-Orbit Servicing Equipment
[NASA-CR-197151] p 254 N95-12790
ORBITS
Neural networks and orbit control in accelerators
[DE94-014877] p 350 N95-13124
ORDER-DISORDER TRANSFORMATIONS
Tuning through the critical regime of the metal-insulator-transition in conducting polymers by pressure and magnetic field
[PB94-179165] p 272 N95-11847
ORGANIC COMPOUNDS
Triple sorbent thermal desorption/gas chromatography/mass spectrometry determination of vapor phase organic contaminants
[DE94-013834] p 264 N95-11735
Fractional suspension crystallization of organic compounds
[PB94-206851] p 375 N95-13409
ORGANOMETALLIC COMPOUNDS
Novel activated carbon impregnants consisting of transition metal complexes. Part 1: Background, syntheses and characterizations
[AD-A282583] p 259 N95-12551
Low oxidation state gallium compounds. Synthesis and characterization of Ga(CH2CMe3)n
[AD-A283369] p 373 N95-12923
ORION NEBULA
A deep x-ray survey of the Pleiades cluster and the B6-A3 main sequence stars in Orion
[NASA-CR-196190] p 380 N95-12373
ORTHOTROPIC PLATES
Buckling of flat rectangular orthotropic plates
[ESDU-94005] p 310 N95-11771
OSCILLATING FLOW
Oscillating-flow regenerator test rig
[NASA-CR-196982] p 246 N95-13200
OSCILLATIONS
Studies on the flow induced by an oscillating airfoil in a uniform stream
[PB94-204450] p 233 N95-13250
OSCILLATOR STRENGTHS
Magneto-optical properties of quantum structures with reduced dimensionality
[AD-A282597] p 376 N95-12553
OSMOSIS
Improving the efficiency of high purity water systems
[DE94-013742] p 318 N95-11784
OTOLITH ORGANS
Vestibular afferent responses to linear accelerations in the alert squirrel monkey
[NASA-TM-4581] p 330 N95-12006
Reduction of ocular counter-rolling by adaptation to space
[NASA-CR-196279] p 333 N95-12376
OUTGASSING
Quantitative understanding of the cycles of oxidized and reduced sulfur on Venus
[NASA-CR-196924] p 382 N95-12011
OXIDATION
Certain aspects of the melting, casting and welding of Ni3Al alloys
[DE94-013628] p 269 N95-11897
Quantum chemical study of methane oxidation species
[NASA-CR-196158] p 265 N95-12107
Low oxidation state gallium compounds. Synthesis and characterization of Ga(CH2CMe3)n
[AD-A283369] p 373 N95-12923
Thermodynamic constants for actinide oxides and oxyhydroxides relevant to actinide volatility calculations for thermal oxidation processes
[DE94-007762] p 376 N95-13074
Atomic structures and compositions of internal interfaces
[DE94-013594] p 271 N95-13543
OXIDATION RESISTANCE
Novel thermooxidatively stable poly(ether-imide-benzoxazole) and poly(ester-imide-benzoxazole)
[AD-A282381] p 273 N95-12008
CGF cartridge development, volume 1
[NASA-CR-196508] p 270 N95-12830
OXIDATION-REDUCTION REACTIONS
Design, synthesis and characterization of novel nonlinear optical polymers
[AD-A282201] p 274 N95-12424
OXIDE FILMS
Emittance theory for thin film selective emitter
[NASA-TM-106727] p 317 N95-11903
OXIDES
Optical and magnetic resonance investigations of 3D ions in single crystal hosts: Candidates for tunable solid-state lasers
[AD-A281726] p 371 N95-11842
OXYGEN
Effects of oral glucose on exercise thermoregulation in men after water immersion
[NASA-TM-108825] p 329 N95-11810
Advanced cryogenic propellants
[AD-A282451] p 277 N95-12729
Project Genesis: Mars in situ propellant technology demonstrator mission
[NASA-CR-197166] p 277 N95-12822
OXYGEN PRODUCTION
Project Hyreus: Mars sample return mission utilizing in situ propellant production
[NASA-CR-197189] p 383 N95-12826
OXYGENATION
Thermal conductivity of gaseous oxygenated aliphatic hydrocarbons. Alcohols, aldehydes, ketones and ethers
[ESDU-94018] p 265 N95-11795

OZONE
Optical Remote Sensing of the Atmosphere. Technical digest 1993. Volume 5: Postconference edition
[AD-A281446] p 314 N95-11831
Consequences of prolonged inhalation of ozone on Fischer-344/N rats: Collaborative studies. Part 1: Content and cross-linking of lung collagen
[PB94-182748] p 331 N95-13176
OZONE DEPLETION
Present state of knowledge of the upper atmosphere1993: An assessment report, part 2
[NASA-RP-1337] p 322 N95-12103
Design of a vehicle based system to prevent ozone loss
[NASA-CR-197199] p 242 N95-12702
Development of UV irradiance standards
[PB94-181005] p 320 N95-12771
Parallelization and visual analysis of multidimensional fields: Application to ozone production, destruction, and transport in three dimensions
[NASA-CR-195971] p 320 N95-12798

P

PACIFIC OCEAN
Reports to the Nation on our changing planet. El Nino and climate prediction, no. 3, spring 1994
p 320 N95-12462
PACKET SWITCHING
Scheduling in an input and output queuing three-stage packet switch by using neural networks
[PB94-179413] p 349 N95-12367
Buffer size and switching capacity study in packet switches of broadband ISDN
[PB94-179421] p 281 N95-12368
Modeling and implementation of a packet routing switch for satellite communications
[AD-A282262] p 282 N95-12412
PACKET TRANSMISSION
Buffer size and switching capacity study in packet switches of broadband ISDN
[PB94-179421] p 281 N95-12368
PACKETS (COMMUNICATION)
Preliminary digital control system design for the petite amateur Navy satellite (PANSAT)
[AD-A282804] p 253 N95-12528
PAINTS
Probability of detection of defects in coatings with electronic shearography
[NASA-CR-196201] p 308 N95-12391
Accelerated testing of coatings for protection against atmospheric corrosion
[PB94-202579] p 276 N95-13244
PAIR PRODUCTION
Search for supersymmetry at CDF
[DE94-014264] p 357 N95-12369
PALEOBIOLOGY
On the isolation of halophilic microorganisms from salt deposits of great geological age p 332 N95-11966
PANEL METHOD (FLUID DYNAMICS)
Performance analysis of three dimensional integral equation computations on a massively parallel computer
[NASA-CR-196747] p 346 N95-11863
Numerical time dependent sheet cavitation simulations using a higher order panel method
[PB94-204435] p 294 N95-13249
Studies on the flow induced by an oscillating airfoil in a uniform stream
[PB94-204450] p 233 N95-13250
PANELS
Elastic buckling of cylindrically curved laminated fibre reinforced composite panels with all edges simply-supported under biaxial loading
[ESDU-94007] p 310 N95-11773
Introduction to magnetic bearings
[NASA-CR-197187] p 302 N95-12640
PAPERS
Technical paper contest for women 1992. Space challenges: Earth and beyond
[NASA-TM-109953] p 386 N95-11955
PARABOLIC ANTENNAS
Project ECHO: Electronic Communications from Halo Orbit
[NASA-CR-197190] p 283 N95-12644
PARABOLIC DIFFERENTIAL EQUATIONS
Efficient parabolic equation solution of radiowave propagation in an inhomogeneous atmosphere and over irregular terrain: Formulation
[AD-A282648] p 284 N95-12834
PARABOLIC REFLECTORS
External Device to Incrementally Skid the Habitat (E-DISH)
[NASA-CR-197147] p 301 N95-12625
PARAFFINS
A CRAMPS and 13C CP/MAS NMR examination of solid-solid transitions in n-Hexatriacontane (C36H74)
[AD-A282497] p 375 N95-13299
PARALLEL COMPUTERS
Impact analysis on a massively parallel computer
[DE94-013624] p 346 N95-11734
PARALLEL PROCESSING (COMPUTERS)
Impact analysis on a massively parallel computer
[DE94-013624] p 346 N95-11734
Parallel methods for the flight simulation model
[DE94-013330] p 245 N95-11752
Parallel aeroelastic computations for wing and wing-body configurations
[NASA-CR-196835] p 230 N95-11766
Performance analysis of three dimensional integral equation computations on a massively parallel computer
[NASA-CR-196747] p 346 N95-11863
On bottleneck partitioning k-ary n-cubes
[NASA-CR-194966] p 342 N95-12005
High speed civil transport aerodynamic optimization
[NASA-CR-196960] p 232 N95-12389
Exploring the parallelism exposed by partial evaluation
[AD-A282284] p 347 N95-12414
Parallelization and visual analysis of multidimensional fields: Application to ozone production, destruction, and transport in three dimensions
[NASA-CR-195971] p 320 N95-12798
Design consideration for parallel graphics libraries
[NASA-CR-194935] p 340 N95-12828
Population-based incremental learning. A method for integrating genetic search based function optimization and competitive learning
[AD-A282654] p 350 N95-12835
Parallel algorithms for the spectral transform method
[DE94-015458] p 344 N95-12893
Nonlinear structural response using adaptive dynamic relaxation on a massively-parallel-processing system
[NASA-CR-196491] p 313 N95-13162
Uniformisation techniques for integral recurrence equations
[PB94-205069] p 347 N95-13407
Some very compositional temporal properties
[PB94-195666] p 345 N95-13438
An informal introduction to parallel processors
[DE94-016347] p 348 N95-13556
PARALLEL PROGRAMMING
Eager combining: A coherency protocol for increasing effective network and memory bandwidth in shared-memory multiprocessors
[AD-A281501] p 346 N95-11857
A preliminary evaluation of cache-miss-initiated prefetching techniques in scalable multiprocessors
[AD-A281502] p 346 N95-11858
On bottleneck partitioning k-ary n-cubes
[NASA-CR-194966] p 342 N95-12005
A framework for exploiting data and functional parallelism on distributed memory multicomputers
[AD-A281194] p 347 N95-12523
Design consideration for parallel graphics libraries
[NASA-CR-194935] p 340 N95-12828
Norwegian contribution to the SWG on APSE programme
[PB94-202397] p 341 N95-13557
PARAMAGNETISM
Magnetic response of ultrathin Fe on MgO: A polarised neutron reflectometry study
[DE94-013192] p 375 N95-13272
PARAMETER IDENTIFICATION
Determining the accuracy of maximum likelihood parameter estimates with colored residuals
[NASA-CR-194893] p 244 N95-11869
PARAMETRIC AMPLIFIERS
High average power parametric frequency conversion-new concepts and new pump sources
[DE94-013652] p 314 N95-11783
PARTIAL DIFFERENTIAL EQUATIONS
Investigation of finite element: ABC methods for electromagnetic field simulation
[NASA-CR-196837] p 279 N95-11707
Workshop on Adaptive Methods for Partial Differential Equations
[AD-A281416] p 351 N95-11850
Viscosity solutions of fully nonlinear equations
[AD-A281725] p 351 N95-11861
Stability and error estimation for Component Adaptive Grid methods
[NASA-CR-196492] p 351 N95-11883
Aspects of long time behaviour of solutions of nonlinear Hamiltonian evolution equations
[PB94-192382] p 352 N95-12808
Visualizing parallel numerical software performance on a shared memory multiprocessor
[PB94-195658] p 352 N95-13437
PARTICLE ACCELERATORS
Vacuum system operating experience review for fusion applications
[DE94-015267] p 368 N95-12759
PARTICLE BEAMS
Beams 92: Proceedings
[DE94-014783] p 361 N95-11792
PARTICLE DECAY
Contribution of hadronic intermediate states in nonleptonic weak decays of K, charm and B mesons
[DE94-753399] p 356 N95-11818
Measurement of the polarization in the decay B(exp 0) yields J/psi K(exp *0) in (be- p)p collisions at the square root of s = 1.8 TeV
[DE94-014265] p 357 N95-12370
Multi-jet analysis for the top search at the Fermilab Collider
[DE94-014988] p 359 N95-13169
PARTICLE DIFFUSION
Feedback control and stabilization experiments on the Texas Experimental Tokamak (TEXT)
[DE94-015214] p 368 N95-12758
PARTICLE IMAGE VELOCIMETRY
Laser Doppler velocimeter measurements of boundary layer velocity and turbulent intensities in Mach 2.5 flow
[NASA-CR-196861] p 289 N95-11709
PARTICLE INTERACTIONS
Numerical simulation of particle-wave interaction on boundary layers
[AD-A282184] p 293 N95-12422
Inclusive jet and two-jet differential cross sections at CDF
[DE94-015543] p 358 N95-12943
PARTICLE PRECIPITATION
Determination of the auroral oval Q index from the air weather service K index
[AD-A282764] p 324 N95-12508
Ionospheric dynamics instrument investigation for the Timed Mission
[NASA-CR-196198] p 325 N95-13190
CVD techniques for the synthesis or modification of porous ceramics
[PB94-206836] p 276 N95-13284
PARTICLE PRODUCTION
Particle-production mechanism in relativistic heavy-ion collisions
[DE94-014427] p 359 N95-13104
PARTICLE SIZE DISTRIBUTION
Investigation of the effects of solid rocket motor propellant composition on plume signature
[AD-A283365] p 258 N95-12885
PARTICLE TRACKS
Scintillating fiber detector performance, detector geometries, trigger, and electronics issues for scintillating fiber tracking
[DE94-015525] p 358 N95-12905
PARTICLE TRAJECTORIES
Velocity spread of REB generated by high current diode
[IPPCZ-339] p 364 N95-11886
PARTICULATE SAMPLING
Effects of sample formulation on the analysis of heavy metals by x-ray fluorescence
[AD-A282733] p 267 N95-12836
CESIUM-137 and natural radionuclides in soils from Southern Brazil and in soils and others environmental samples from Antarctic
[INPE-5505-TDI-517] p 321 N95-13192
PARTICULATES
Environmental lichenology: Biomonitoring trace-element air pollution
[PB94-191335] p 318 N95-11826
PARTITIONS (MATHEMATICS)
On bottleneck partitioning k-ary n-cubes
[NASA-CR-194966] p 342 N95-12005
PARTONS
Photon production at CDF and D0
[DE94-014985] p 359 N95-13160
PASSENGER AIRCRAFT
The Elite: A high speed, low-cost general aviation aircraft for Aeroworld
[NASA-CR-197161] p 239 N95-12530
Icarus Rewaxed: A high speed, low-cost general aviation aircraft for Aeroworld
[NASA-CR-197155] p 239 N95-12609
The OFP-6M transport jet
[NASA-CR-197159] p 240 N95-12637
The Balsa bullet: A high speed, low-cost general aviation aircraft for Aeroworld
[NASA-CR-197165] p 240 N95-12638
Central coast designs: The Eightball Express. Taking off with convention, cruising with improvements and landing with absolute success
[NASA-CR-197181] p 241 N95-12643
LCX: Proposal for a low-cost commercial transport
[NASA-CR-197186] p 241 N95-12645

PASSENGERS
The performance of child restraint devices in transport airplane passenger seats
[DOT/FAA/AM-94/19] p 234 N95-12146
Characteristics of civil aviation atmospheric hazards
p 235 N95-13208

PATENTS
Intellectual property rights at the National Aeronautics and Space Administration, Lewis Research Center
[NASA-TM-106731] p 379 N95-11866
Catalog of government inventions available for licensing, 1991
[PB92-100171] p 389 N95-12303
Method for laser-assisted etching of III-V and II-VI semiconductor compounds using chlorofluorocarbon ambients
[AD-D016385] p 298 N95-12779
Method of laser processing ferroelectric materials
[AD-D016386] p 298 N95-12780

PATTERN RECOGNITION
How are three-dimensional objects represented in the brain?
[AD-A282367] p 335 N95-11942
Outdoor landmark recognition using hybrid fractal vision system and neural networks
[AD-A282506] p 349 N95-12395
An analysis of the effect of Gaussian error in object recognition
[AD-A282260] p 349 N95-12411
B* probability based search
[AD-A282551] p 343 N95-12497
Learning one-dimensional geometric patterns under one-sided random misclassification noise
[DE94-014659] p 350 N95-12864
Representation, modeling and recognition of outdoor scenes
[AD-A283361] p 350 N95-12884
A study of a multi-pinned phase CCD detector for use as a star tracker
[NASA-CR-196287] p 381 N95-13056
Object recognition for flexible assembly using stereo vision
[PB94-204427] p 363 N95-13248
Weighted Parzen windows for pattern classification
[AD-A281222] p 345 N95-13370

PATTERN REGISTRATION
Site model based image registration and change detection, RADIUS
[AD-A282796] p 315 N95-12527

PAVEMENTS
Moisture induced pressures in concrete airfield pavements
[AD-A281974] p 245 N95-11789
Development of ground-penetrating radar equipment for detecting pavement condition for preventive maintenance
[PB94-189537] p 280 N95-11904
Additives in bituminous materials and fuel-resistant sealers
[DOT/FAA/CT-94/78] p 273 N95-12131
Marginal aggregates in flexible pavements: Background survey and experimental plan
[DOT/FAA/CT-94/58] p 246 N95-12216

PAYLOAD INTEGRATION
GASCAN 2 payload integration
[NASA-CR-197200] p 278 N95-12701

PAYLOADS
Project ECHO: Electronic Communications from Halo Orbit
[NASA-CR-197190] p 283 N95-12644
Conceptual design of an Orbital Debris Defense System
[NASA-CR-197211] p 254 N95-12696
A magnetic shield/dual purpose mission
[NASA-CR-197192] p 255 N95-13006

PELLETS
Ground based research in microgravity materials processing
[NASA-CR-196815] p 278 N95-11759

PENETRATION
Passive MMW camera for low visibility landings
p 236 N95-13215

PEPTIDES
Naval research reviews, volume 46, February 1994
[AD-A281435] p 265 N95-11827

PERFORMANCE
Structure and performance of carbon aerogel electrodes
[DE94-014746] p 356 N95-11791

PERFORMANCE PREDICTION
Development of a spindle thermal error characterization and compensation sensor system for machining center accuracy enhancement
[AD-A280891] p 300 N95-11729
High performance climate system modeling using a domain and task decomposition message-passing approach
[DE94-013739] p 322 N95-11741
Object-oriented technology for compressor simulation
[NASA-TM-106723] p 243 N95-11864
Software analysis handbook: Software complexity analysis and software reliability estimation and prediction
[NASA-TM-104799] p 339 N95-11914
Modeling of split-core transformers for power transmission
[AD-A282782] p 287 N95-12509
Airport surveillance using a solid state coherent lidar
p 235 N95-13207

PERFORMANCE TESTS
Validating medical knowledge based systems
[PB94-191301] p 377 N95-11824
Status of hollow cathode heater development for the Space Station plasma contactor
[NASA-CR-195364] p 258 N95-12622
Terminal Doppler Weather Radar Build 5A Operational Test and Evaluation (OT/E) integration and OT/E operational test plan
[AD-A283052] p 327 N95-12996
Age 60 study. Part 4: Experimental evaluation of pilot performance
[REPT-8025-4B] p 336 N95-13199
Brush seals for cryogenic applications
p 305 N95-13592
Brush seals for turbine engine fuel conservation
p 306 N95-13595
Current developments in brush seals
p 306 N95-13597
Compressor discharge film riding face seals
p 306 N95-13599
Theoretical versus experimental results for the rotordynamic coefficients of eccentric, smooth, gas annular seal annular gas seals p 307 N95-13603
Turbomachinery Laboratory Texas A and M University research progress on annular gas seals
p 307 N95-13604
Pressure measurements of a three wave journal air bearing p 307 N95-13605
Relative performance comparison between baseline labyrinth and dual-brush compressor discharge seals in a T-700 engine test p 307 N95-13607

PERIODIC VARIATIONS
Free electron lasers and other advanced sources of light: Scientific research opportunities p 297 N95-12375
Reports to the Nation on our changing planet. El Nino and climate prediction, no. 3, spring 1994
p 320 N95-12462

PERMAFROST
Bibliography on cold regions science and technology, volume 47, part 1
[AD-A281879] p 378 N95-13167

PERMANENT MAGNETS
Behaviors of plasma armature in the augmented railgun using a permanent magnet p 367 N95-12449

PERSONAL COMPUTERS
TLIFE: A program for spur, helical and spiral bevel transmission life and reliability modeling
[NASA-CR-4622] p 300 N95-11889
Semiautomated methodology for measurement of field-of-view, magnification, and distortion of night vision devices as defined in MIL-A-49425(CR)
[AD-A282210] p 362 N95-12427

PERSONNEL
Visit to UDRI and USAF, Armstrong Lab., Williams AFB, Phoenix, USA, February 8-11, 1993
[PB94-190659] p 337 N95-11873
Meeting the nation's needs for biomedical and behavioral scientists
[LC-94-66477] p 330 N95-12310

PERSONNEL SELECTION
Tank crew performance related to cognitive ability and motivation of the tank crew members
[PB94-190642] p 335 N95-11872

PERTURBATION
Guest investigator program study: Physics of equatorial plasma bubbles
[NASA-CR-196150] p 368 N95-12853
Locked modes in TEXT-U tokamak
[DE94-011595] p 370 N95-13529

PETRI NETS
Efficient detection of deadlocks in Petri nets
[PB94-179405] p 343 N95-12366

PHARMACOLOGY
Copper metabolism in rats fed ascorbic acid or restricted amounts of copper
[PB94-191343] p 330 N95-11902

PHASE CONJUGATION
Studies of optical phase conjugators and applications
[AD-A282626] p 362 N95-12538

PHASE DETECTORS
A study of a multi-pinned phase CCD detector for use as a star tracker
[NASA-CR-196287] p 381 N95-13056

PHASE DIAGRAMS
Synthesis, structure and properties of segmented polymers containing mesogens
[AD-A281419] p 272 N95-11852

PHASE SHIFT
Improvements of HCN laser heterodyne interferometer for measuring plasma density
[DE94-625037] p 370 N95-13341

PHASE STABILITY (MATERIALS)
Structure-phase state of thick amorphous and microcrystalline chromium-carbon films deposited by ion-plasma sputtering
[DE94-624236] p 277 N95-13535

PHASE SWITCHING INTERFEROMETERS
Defocus measurement using a liquid crystal point diffraction interferometer
[NASA-TM-106687] p 296 N95-12748

PHASE TRANSFORMATIONS
A study of the deformation of helical springs under eccentric loading
[AD-A283448] p 312 N95-12511
Radiation amorphization of materials
[DE94-624184] p 374 N95-12948
A CRAMPS and 13C CP/MAS NMR examination of solid-solid transitions in n-Hexatriacontane (C36H74)
[AD-A282497] p 375 N95-13299
Influence of additives on structure and thermal stability of ammonium nitrate
[PB94-206943] p 278 N95-13435

PHASED ARRAYS
An investigation of the channel crosstalk in optical heterodyne controlled phased array radars
[AD-A281227] p 285 N95-13371

PHENOMENOLOGY
Relativistic theory of superfluidity with two condensates
[DE94-624073] p 290 N95-11749

PHENYLS
Amine catalyzed intramolecular imidization of alkyl and aryl phthalamates, kinetics and mechanism in deuterated chloroform
[AD-A281741] p 259 N95-11844
Orthobaric densities and molar volumes of liquids. Polycyclic phenyl and cyclohexyl compounds
[ESDU-94002] p 266 N95-12129

PHOBOS
A robotic exploration mission to Mars and Phobos
[NASA-CR-197168] p 382 N95-12307

PHOSPHATES
Laser physics of Nd(exp 3+)-doped phosphate glasses
[DE94-015141] p 299 N95-13534

PHOSPHAZENE
The synthesis and structure of polyphosphazenes
[AD-A281723] p 272 N95-11832

PHOSPHORS
Radiation-induced structural changes, 3
[DE94-753401] p 371 N95-11819

PHOTOCATHODES
Gaseous detectors of ultraviolet and visible photons
[DE94-014990] p 296 N95-13171

PHOTOCHEMICAL REACTIONS
Quantitative understanding of the cycles of oxidized and reduced sulfur on Venus
[NASA-CR-196924] p 382 N95-12011
Design, synthesis and characterization of novel nonlinear optical polymers
[AD-A282201] p 274 N95-12424
Development of techniques for the in situ observation of OH and HO2 for studies of the impact of high-altitude supersonic aircraft on the stratosphere
[NASA-CR-196759] p 321 N95-12832
Proceedings of the Eighteenth DOE Solar Photochemistry Research Conference
[DE94-014926] p 318 N95-13126

PHOTOCONDUCTORS
Influence of electrode geometry on the high-field characteristics of photoconductive silicon wafers
[DE94-014660] p 287 N95-12865

PHOTOELECTRIC EMISSION
Synchrotron studies of narrow band materials
[DE94-013698] p 271 N95-13554

PHOTOELECTROCHEMISTRY
Advanced cryogenic propellants
[AD-A282451] p 277 N95-12729

PHOTOEXCITATION
Photogeneration of charge carriers in bilayer assemblies of conjugated rigid-rod polymers
[AD-A282625] p 275 N95-12537

PHOTOIONIZATION
Progress on resonance ionization detection of combustion radicals
[DE94-015339] p 267 N95-12762
PHOTOLUMINESCENCE
Studies of positron induced luminescence from polymers
[DE94-013622] p 272 N95-11733
Photogeneration of charge carriers in bilayer assemblies of conjugated rigid-rod polymers
[AD-A282625] p 275 N95-12537
PHOTOMETERS
Development of nanostructure fabrication technology and new electron-quantum wave devices
[AD-A281724] p 286 N95-11860
Semiconductor photodetector device
[AD-D016314] p 288 N95-13174
PHOTONICS
Spaceborne Photonics Institute
[NASA-CR-196784] p 362 N95-12659
PHOTONS
Resonant x-ray scattering in 5f magnetism
[DE94-013753] p 358 N95-12829
Photon production at CDF and D0
[DE94-014985] p 359 N95-13160
Gaseous detectors of ultraviolet and visible photons
[DE94-014990] p 296 N95-13171
PHOTOSPHERE
Structure and dynamics of the solar corona
[NASA-CR-196978] p 384 N95-13582
PHOTOSYNTHESIS
Proceedings of the Eighteenth DOE Solar Photochemistry Research Conference
[DE94-014926] p 318 N95-13126
Regulation of alternative CO2 fixation pathways in prokaryotic and eukaryotic photosynthetic organisms
[DE94-013180] p 331 N95-13271
PHOTOVOLTAIC CELLS
Radiative performance of rare earth garnet thin film selective emitters
[NASA-TM-106722] p 372 N95-11876
Emittance theory for thin film selective emitter
[NASA-TM-106727] p 317 N95-11903
PHOTOVOLTAIC CONVERSION
Radiative performance of rare earth garnet thin film selective emitters
[NASA-TM-106722] p 372 N95-11876
Emittance theory for thin film selective emitter
[NASA-TM-106727] p 317 N95-11903
PHYSICAL EXERCISE
Effects of oral glucose on exercise thermoregulation in men after water immersion
[NASA-TM-108825] p 329 N95-11810
Carbon dioxide and water vapor production at rest and during exercise. A report on data collection for the Crew and Thermal Systems Division
[NASA-TP-3500] p 337 N95-11811
Comparison of submaximal cycling and treadmill exercise at similar work rates
[AD-A283430] p 334 N95-12593
PHYSIOLOGICAL EFFECTS
Summary of the Sixteenth Annual Conference on Shock
[AD-A282643] p 334 N95-12542
Effect of decreased gravity on circulation in the rat
[NASA-CR-196946] p 331 N95-12827
PHYSIOLOGICAL RESPONSES
Vestibular afferent responses to linear accelerations in the alert squirrel monkey
[NASA-TM-4581] p 330 N95-12006
Comparison of submaximal cycling and treadmill exercise at similar work rates
[AD-A283430] p 334 N95-12593
Spaceflight and immune responses of Rhesus monkeys
[NASA-CR-196846] p 331 N95-12941
PHYSIOLOGY
Psychophysiological assessment methods (including a register of psychophysiologists on microfiches)
[AGARD-AR-324] p 335 N95-12133
PHYTOTRONS
The crop growth research chamber
p 248 N95-11969
PIEZOELECTRIC CERAMICS
Design of passive piezoelectric damping for space structures
[NASA-CR-4625] p 252 N95-12165
PIEZOELECTRIC TRANSDUCERS
Computer modelling of cyclic deformation of high-temperature materials
[AD-A282457] p 263 N95-12833
PIEZOELECTRICITY
A laboratory vacuum apparatus for magnetron sputtering of thin Z ZnO piezoelectric films, magnetron sputtering
p 296 N95-12111
Active vibration control using a distributed controller
[PB94-207073] p 313 N95-13576
PILOT PERFORMANCE
Crew factors in flight operations 9: Effects of planned cockpit rest on crew performance and alertness in long-haul operations
[NASA-TM-108839] p 334 N95-12792
Age 60 Rule research. Part 1: Bibliographic database
[DOT/FAA/AM-94/20-PT-1] p 336 N95-13019
Age 60 Rule. Part 2: Airline pilot age and performance. A review of the scientific literature
[DOT/FAA/AM-94/21-PT-2] p 336 N95-13020
Age 60 study. Part 4: Experimental evaluation of pilot performance
[REPT-8025-4B] p 336 N95-13199
Evaluation of candidate millimeter wave sensors for synthetic vision p 236 N95-13214
PILOTLESS AIRCRAFT
Conceptual design of the AE481 Demon Remotely Piloted Vehicle (RPV)
[NASA-CR-197164] p 238 N95-12294
PINHOLE CAMERAS
New multi-dimensional diagnostics method for intense ion beams p 365 N95-12432
Hot spots observation in a dense plasma focus
p 367 N95-12444
PINNING
The dissipative mechanism of pinning of a superconducting current
[DE94-623252] p 289 N95-13276
PIONEER VENUS 1 SPACECRAFT
Pioneer Venus orbiter electron temperature probe
[NASA-CR-196844] p 257 N95-11805
PIPELINES
Pipeline vibrations. Computer program for the prediction of fluid transients in flexible, unbranched three-dimensional piping systems
[ESDU-93031] p 309 N95-11768
PIPELINING (COMPUTERS)
Design consideration for parallel graphics libraries
[NASA-CR-194935] p 340 N95-12828
PISTONS
Effects of piston surface treatments on performance and emissions of a methanol-fueled, direct injection, stratified charge engine
[DE94-011851] p 302 N95-12648
PITCHING MOMENTS
A simple analytical aerodynamic model of Langley Winged-Cone Aerospace Plane concept
[NASA-CR-194987] p 252 N95-12175
PITTING
Analytical and experimental vibration analysis of a faulty gear system
[NASA-TM-106689] p 300 N95-12377
Analysis of the effects of surface pitting and wear on the vibrations of a gear transmission system
[NASA-TM-106678] p 301 N95-12621
PLANE WAVES
Plane-wave reflection from uniaxial chiral interface and its application to polarization transformation
[PB94-184496] p 283 N95-12580
PLANETARY BASES
Mars Equipment Transport System
[NASA-CR-197158] p 301 N95-12554
PLANETARY EVOLUTION
The detectability of extrasolar terrestrial and giant planets during their luminous final accretion
[NASA-CR-196147] p 381 N95-13012
PLANETARY GEOLOGY
Periglacial and glacial analogs for Martian landforms
[NASA-CR-196772] p 383 N95-12952
PLANETARY IONOSPHERES
Pioneer Venus orbiter electron temperature probe
[NASA-CR-196844] p 257 N95-11805
PLANETARY MAGNETIC FIELDS
Non-dipolar magnetic field models and patterns of radio emission: Uranus and Neptune compared
[NASA-CR-196412] p 385 N95-12469
PLANETARY MAGNETOSPHERES
Non-dipolar magnetic field models and patterns of radio emission: Uranus and Neptune compared
[NASA-CR-196412] p 385 N95-12469
PLANETARY MAPPING
Venus surface roughness and Magellan stereo data
[NASA-CR-196821] p 382 N95-11704
PLANETARY NEBULAE
FOC SV support and science data analysis
[NASA-CR-196764] p 381 N95-12821
PLANETARY RADIATION
Non-dipolar magnetic field models and patterns of radio emission: Uranus and Neptune compared
[NASA-CR-196412] p 385 N95-12469
The detectability of extrasolar terrestrial and giant planets during their luminous final accretion
[NASA-CR-196147] p 381 N95-13012
PLANETARY SYSTEMS
The detectability of extrasolar terrestrial and giant planets during their luminous final accretion
[NASA-CR-196147] p 381 N95-13012
PLANETS
Research in astrophysical processes
[NASA-CR-196773] p 382 N95-12939
PLANTS (BOTANY)
Environmental lichenology: Biomonitoring trace-element air pollution
[PB94-191335] p 318 N95-11826
Techniques for optimal crop selection in a controlled ecological life support system p 339 N95-11962
PLASMA ANTENNAS
Excitation of fast magneto-acoustic waves in unhomogeneous plasma of a large size tokamak
[DE94-625050] p 370 N95-13540
PLASMA BUBBLES
Guest investigator program study: Physics of equatorial plasma bubbles
[NASA-CR-196150] p 368 N95-12853
PLASMA CONTROL
Control of initial mass on metal vapor puff z-pinch
p 366 N95-12441
L-H transition in tokamaks and stellarators
[DE94-013257] p 370 N95-13422
PLASMA CURRENTS
Guest investigator program study: Physics of equatorial plasma bubbles
[NASA-CR-196150] p 368 N95-12853
PLASMA DENSITY
A 250 GHz microwave interferometer for divertor experiments on D3-D
[DE94-014056] p 364 N95-11786
Stationary plasma thruster ion velocity distribution
[NASA-CR-195379] p 257 N95-11919
Improvements of HCN laser heterodyne interferometer for measuring plasma density
[DE94-625037] p 370 N95-13341
PLASMA DIAGNOSTICS
A 250 GHz microwave interferometer for divertor experiments on D3-D
[DE94-014056] p 364 N95-11786
Monochromatic x ray imaging in plasma focus experiment p 366 N95-12443
Hot spots observation in a dense plasma focus
p 367 N95-12444
High resolution diagnostics of intense ion diodes and key issues for bright light ion beam generation
p 367 N95-12448
Fusion programs in applied plasma physics
[DE94-015853] p 369 N95-12944
Improvements of HCN laser heterodyne interferometer for measuring plasma density
[DE94-625037] p 370 N95-13341
PLASMA DIODES
A study on successive generation of intense pulsed ion beams by the inverse pinch ion diode
p 365 N95-12434
PLASMA DYNAMICS
Guest investigator program study: Physics of equatorial plasma bubbles
[NASA-CR-196150] p 368 N95-12853
PLASMA ELECTRODES
Research on Orbital Plasma-Electrodynamics (ROPE)
[NASA-CR-196929] p 361 N95-12147
PLASMA ENGINES
Anode sheath contributions in plasma thrusters
[AD-A280395] p 364 N95-11837
Stationary plasma thruster ion velocity distribution
[NASA-CR-195379] p 257 N95-11919
PLASMA FOCUS
Monochromatic x ray imaging in plasma focus experiment p 366 N95-12443
Hot spots observation in a dense plasma focus
p 367 N95-12444
Observation of a soft x ray emitting core in a dense plasma focus p 367 N95-12445
PLASMA FREQUENCIES
Excitation of fast magneto-acoustic waves in unhomogeneous plasma of a large size tokamak
[DE94-625050] p 370 N95-13540
PLASMA GENERATORS
Physics of High Energy Density Plasmas Produced by Pulsed Power
[NIFS-PROC-18] p 365 N95-12429
Beam divergence characteristic of two-stage ion diode
p 365 N95-12431
Measurements of 20 GHz high-power microwaves output from a large diameter plasma filled backward wave oscillator p 365 N95-12435
Observation of a soft x ray emitting core in a dense plasma focus p 367 N95-12445
The results of the study of compact gas-puff and vacuum spark plasma sources of SXR with Glass-Capillary Converters (GCC) p 367 N95-12446

High resolution diagnostics of intense ion diodes and key issues for bright light ion beam generation
p 367 N95-12448
Plasma opening switch by laser-produced plasma with different kinds of ion species p 367 N95-12451

PLASMA GUNS
Physics of High Energy Density Plasmas Produced by Pulsed Power
[NIFS-PROC-18] p 365 N95-12429

PLASMA HEATING
Velocity spread of REB generated by high current diode
[IPPCZ-339] p 364 N95-11886
The reflection of relativistic electron beam by virtual cathode
[IPPCZ-338] p 364 N95-11916
An observational test of magnetospheric magnetic field mapping
[DE94-014461] p 324 N95-12649
Fusion programs in applied plasma physics
[DE94-015853] p 369 N95-12944
Absorption of intense microwaves and ion acoustic turbulence due to heat transport
[DE94-015140] p 369 N95-13285

PLASMA JETS
Magnetic field generation in shock waves
[AD-A282234] p 281 N95-12408
Locked modes in TEXT-U tokamak
[DE94-011595] p 370 N95-13529

PLASMA OSCILLATIONS
The reflection of relativistic electron beam by virtual cathode
[IPPCZ-338] p 364 N95-11916

PLASMA PHYSICS
Review of electron beam microinstabilities and their relevance to EBIS devices
[DE94-013755] p 364 N95-11746
Common understandings of phenomena in z-pinches
p 367 N95-12447
Fusion programs in applied plasma physics
[DE94-015853] p 369 N95-12944
A magnetic shield/dual purpose mission
[NASA-CR-197192] p 255 N95-13006

PLASMA PINCH
Observation of a soft x ray emitting core in a dense plasma focus p 367 N95-12445

PLASMA POTENTIALS
Feedback control and stabilization experiments on the Texas Experimental Tokamak (TEXT)
[DE94-015214] p 368 N95-12758

PLASMA PROBES
Research on Orbital Plasma-Electrodynamics (ROPE)
[NASA-CR-196929] p 361 N95-12147

PLASMA PROPULSION
Anode sheath contributions in plasma thrusters
[AD-A280395] p 364 N95-11837

PLASMA SPECTRA
X-ray temporal and spectral studies of blazars with the Ginga satellite
[NASA-CR-196330] p 380 N95-12466

PLASMA TURBULENCE
Strong beam-plasma turbulence p 367 N95-12450

PLASMA-ELECTROMAGNETIC INTERACTION
Radiative properties of strongly magnetized plasmas
[DE94-015487] p 369 N95-12897

PLASMA-PARTICLE INTERACTIONS
Evaluation of dynamic pressure of ablation plasma produced by intense, pulsed, ion beam
p 365 N95-12433
Plasma effects on electron beam dynamics in a virtual cathode oscillator p 366 N95-12436
Strong beam-plasma turbulence p 367 N95-12450

PLASMAS (PHYSICS)
Review of electron beam microinstabilities and their relevance to EBIS devices
[DE94-013755] p 364 N95-11746
Velocity spread of REB generated by high current diode
[IPPCZ-339] p 364 N95-11886
Magnetic field generation in shock waves
[AD-A282234] p 281 N95-12408
Contraction phase of a gas-puff z-pinch
p 366 N95-12440
Behaviors of plasma armature in the augmented railgun using a permanent magnet p 367 N95-12449
Status of hollow cathode heater development for the Space Station plasma contactor
[NASA-CR-195364] p 258 N95-12622
Radiative properties of strongly magnetized plasmas
[DE94-015487] p 369 N95-12897
Structure-phase state of thick amorphous and microcrystalline chromium-carbon films deposited by ion-plasma sputtering
[DE94-624236] p 277 N95-13535
Excitation of fast magneto-acoustic waves in unhomogeneous plasma of a large size tokamak
[DE94-625050] p 370 N95-13540
Time-resolved electron thermal conduction by probing of plasma formation in transparent solids with high power subpicosecond laser pulses
[DE94-015170] p 370 N95-13555

PLASMASPHERE
Magnetospheric space plasma investigations
[NASA-CR-196793] p 382 N95-12940
Waves in Space Plasmas (WISP)
[NASA-CR-196432] p 369 N95-13024
Ionospheric dynamics instrument investigation for the Timed Mission
[NASA-CR-196198] p 325 N95-13190

PLASTIC DEFORMATION
Yield-before-break fracture mechanics analysis of high strength steel pressure vehicles
[AD-A282518] p 270 N95-12401
On the strain and strain-rate dependence of the fraction of plastic work converted to heat: An experimental study using high speed infrared detectors and the Kolsky bar
[SM-92-33] p 354 N95-12728

PLASTIC FLOW
On the strain and strain-rate dependence of the fraction of plastic work converted to heat: An experimental study using high speed infrared detectors and the Kolsky bar
[SM-92-33] p 354 N95-12728

PLASTIC PROPERTIES
Triaxial and torsional shear test results for sand
[AD-A282725] p 323 N95-12506
Effect of shear lips, loading transitions and test frequency on constant delta K and constant load amplitude fatigue tests
[PB94-192440] p 312 N95-12775
Validity of fracture toughness determined with small bend specimens
[DE94-624157] p 313 N95-12947
Polycrystal models to fit experiments
[DE94-014419] p 374 N95-13078

PLATES (STRUCTURAL MEMBERS)
Interlaminar stress analysis of dropped-ply laminated plates and shells by a mixed method
[NASA-CR-196851] p 311 N95-11946
Electromagnetic on-aircraft antenna radiation in the presence of composite plates
[NASA-CR-196126] p 284 N95-12856

PLEIADES CLUSTER
A deep x-ray survey of the Pleiades cluster and the B6-A3 main sequence stars in Orion
[NASA-CR-196190] p 380 N95-12373

PLOTTING
NPS state vector analysis and relative motion plotting software for STS-51
[AD-A282909] p 249 N95-12510

PLUMES
Concentration fluctuation models: A comparative study
[CUED/A-AERO/TR-24] p 292 N95-11939

PLUTONIUM OXIDES
Mechanical behavior of (238)UO2, (238)PuO2, and (239)PuO2 as a function of strain rate and temperature
[DE94-015718] p 312 N95-12784
Thermodynamic constants for actinide oxides and oxyhydroxides relevant to actinide volatility calculations for thermal oxidation processes
[DE94-007762] p 376 N95-13074

PLY ORIENTATION
Interlaminar stress analysis of dropped-ply laminated plates and shells by a mixed method
[NASA-CR-196851] p 311 N95-11946

PNEUMATIC CONTROL
Flight investigation of the use of a nose gear jump strut to reduce takeoff ground roll distance of STOL aircraft
[NASA-TM-108819] p 238 N95-12225

PNEUMATIC PROBES
A new algorithm for five-hole probe calibration, data reduction, and uncertainty analysis
[NASA-TM-106458] p 232 N95-12378

PNEUMATICS
The development of a highly reliable power management and distribution system for civil transport aircraft
[NASA-TM-106697] p 243 N95-11867

POINT DEFECTS
Evaluation of the improvement in the figure of merit of Bi2Te3 - based alloys with addition of ultrafine scattering centers
[DE94-015363] p 374 N95-13059

POINT SOURCES
Large area soft x-ray collimator to facilitate x-ray optics testing
[NASA-CR-196923] p 362 N95-12736

POINTING CONTROL SYSTEMS
ASPOD modifications of 1993-1994
[NASA-CR-197204] p 254 N95-12698
Precision tethered satellite attitude control
[NASA-CR-196950] p 254 N95-12766

POISSON EQUATION
Research on Orbital Plasma-Electrodynamics (ROPE)
[NASA-CR-196929] p 361 N95-12147
Enhancement of EMAG: A 2-D electrostatic and magnetostatic solver for MATLAB
[AD-A283446] p 354 N95-13143

POLAR CAPS
Design of an unmanned Martian polar exploration system
[NASA-CR-197160] p 383 N95-12529
Magnetospheric space plasma investigations
[NASA-CR-196793] p 382 N95-12940

POLAR REGIONS
Magnetospheric-ionospheric Poynting flux
[NASA-CR-196856] p 322 N95-11801

POLAR SUBSTORMS
Waves in Space Plasmas (WISP)
[NASA-CR-196432] p 369 N95-13024

POLARIMETRY
AIRSAR software: Computer programs for preprocessing of JPL compressed polarimetric SAR data
[PB94-179116] p 280 N95-11800

POLARIZATION (CHARGE SEPARATION)
Proceedings of the Eighteenth DOE Solar Photochemistry Research Conference
[DE94-014926] p 318 N95-13126

POLARIZATION (SPIN ALIGNMENT)
Measurement of the polarization in the decay B(exp 0) yields J/psi K(exp *0) in (bar p)p collisions at the square root of s = 1.8 TeV
[DE94-014265] p 357 N95-12370

POLARIZED ELECTROMAGNETIC RADIATION
Plane-wave reflection from uniaxial chiral interface and its application to polarization transformation
[PB94-184496] p 283 N95-12580

POLICIES
SO2 guideline document
[PB94-181393] p 319 N95-11893

POLLUTION CONTROL
Directory of OAQPS information services, May 1994
[PB94-181310] p 318 N95-11848
Implementation strategy for the Clean Air Act Ammendments of 1990. Update, May 1994
[PB94-180700] p 319 N95-11849
Design of a vehicle based system to prevent ozone loss
[NASA-CR-197199] p 242 N95-12702
Regulatory impact analysis and regulatory support document: Control of air pollution; determination of significance for nonroad sources and emission standards for new nonroad compression-ignition engines at or above 37 kilowatts (50 horsepower)
[PB94-194594] p 321 N95-12855
Environmental and customer-driven seal requirements
p 305 N95-13588

POLLUTION MONITORING
SO2 guideline document
[PB94-181393] p 319 N95-11893
The Additional Programme on Ammonia
[PB94-193075] p 320 N95-12777
Proceedings of the CTU Seminar 1994, Part C
[DE94-624078] p 390 N95-12946

POLLUTION TRANSPORT
Concentration fluctuation models: A comparative study
[CUED/A-AERO/TR-24] p 292 N95-11939

POLYACETYLENE
Tuning through the critical regime of the metal-insulator-transition in conducting polymers by pressure and magnetic field
[PB94-179165] p 272 N95-11847

POLYAMIDE RESINS
Synthesis and characterization of thianthrene-based polyamides
[AD-A282512] p 273 N95-12399

POLYATOMIC MOLECULES
Polyatomic ion impact on solid surfaces and related phenomena
[PB94-201258] p 360 N95-13242

POLYCARBONATES
The structural basis for fatigue failure initiation in glassy polymers
[DE94-015415] p 275 N95-13060

POLYCRYSTALS
Polycrystal models to fit experiments
[DE94-014419] p 374 N95-13078

POLYGONS
SURRENDER user's manual, second edition
[PB94-206950] p 346 N95-13571

POLYIMIDE RESINS
Damage tolerance of candidate thermoset composites for use on single stage to orbit vehicles
[NASA-TP-3506] p 261 N95-11816

POLYIMIDES
Synthesis and solid-state NMR characterization of 13C- and 15N-labelled n-methylphthalimide: A model compound for studying polyimides
[AD-A282510] p 273 N95-12397
Characterization of the one step polyimide synthesis
[AD-A281216] p 276 N95-13367
POLYMER CHEMISTRY
Novel thermooxidatively stable poly(ether-imide-benzoxazole) and poly(ester-imide-benzoxazole)
[AD-A282381] p 273 N95-12008
Polymer effect on heterochiral molecular recognition in molecular and macromolecular pairs of liquid crystals of (R)- and (S)-2-chloro-4-methylpentyl 4'-((8-(vinyloxy)octyl)oxy)biphenyl-4-caroxylate rs
[AD-A281193] p 358 N95-12522
Characterization of the one step polyimide synthesis
[AD-A281216] p 276 N95-13367
POLYMERIZATION
Chiral recognition in molecular and macromolecular pairs of (S)- and (R)-1-cyano-2-methylpropyl 4'(4-(8-vinyloxyoctyloxy)benzoyl) biphenyl-4-carboxylate enantiomers
[AD-A281438] p 356 N95-11828
Multifunctional acrylic ether monomers, their polymers, and polymerizable epoxide derivatives from simple alpha-substitution of alkyl acrylates
[AD-A282513] p 273 N95-12400
UV and fluorescence studies for vinyl polymerization
[AD-A281187] p 274 N95-12520
Polymer effect on heterochiral molecular recognition in molecular and macromolecular pairs of liquid crystals of (R)- and (S)-2-chloro-4-methylpentyl 4'-((8-(vinyloxy)octyl)oxy)biphenyl-4-caroxylate rs
[AD-A281193] p 358 N95-12522
Thermal polymerization of styrene in the presence of stable radicals and inhibitors
[AD-A280926] p 275 N95-12773
Characterization of the one step polyimide synthesis
[AD-A281216] p 276 N95-13367
POLYMERS
Effect of operating parameters and anode gas impurities upon polymer electrolyte fuel cells
[DE94-014464] p 317 N95-12650
POLYNOMIALS
Minimal fixturing of frictionless assemblies: Complexity and algorithms
[AD-A282724] p 300 N95-12505
POLYPHENYLS
Vapour pressures and critical points of liquids. Polycyclic phenyl and cyclohexyl compounds
[ESDU-94001] p 266 N95-12128
POLYPYRROLES
Tuning through the critical regime of the metal-insulator-transition in conducting polymers by pressure and magnetic field
[PB94-179165] p 272 N95-11847
POLYSTYRENE
Studies of positron induced luminescence from polymers
[DE94-013622] p 272 N95-11733
Development of radiation hard scintillators
[DE94-013204] p 296 N95-13287
POLYTETRAFLUOROETHYLENE
Evaluation of wiring constructions for space applications
[NASA-TM-106735] p 256 N95-13194
POLYURETHANE RESINS
Synthesis, structure and properties of segmented polymers containing mesogens
[AD-A281419] p 272 N95-11852
Ten-year ground exposure of composite materials used on the Bell Model 206L helicopter flight service program
[NASA-TP-3468] p 262 N95-12357
POPULATIONS
Proposal of a methodology to evaluate urban quality of life using conventional and remote sensing data, geographic information system, and a database
[INPE-5552-TDI/536] p 315 N95-12297
Development of UV irradiance standards
[PB94-181005] p 320 N95-12771
POROSITY
Scaling fluid content-pressure relations of different fluid systems in porous media
[DE94-013349] p 294 N95-13075
CVD techniques for the synthesis or modification of porous ceramics
[PB94-206836] p 276 N95-13284
POROUS MATERIALS
Structure and performance of carbon aerogel electrodes
[DE94-014746] p 356 N95-11791
PORTABLE EQUIPMENT
Burst transmission in the HF band: A system analysis and proposal for improvement
[PB94-190733] p 280 N95-11821
Diesel-fired self-pumping water heater
[AD-A283063] p 279 N95-13053
PORTABLE LIFE SUPPORT SYSTEMS
Interviews with the Apollo lunar surface astronauts in support of planning for EVA systems design
[NASA-TM-108846] p 337 N95-11905
Meeting the challenge of manned lunar and Martian exploration p 339 N95-11970
The embodiment design of the heat rejection system for the portable life support system
[NASA-CR-197178] p 338 N95-12555
POSITION (LOCATION)
Using landmarks for the vehicle location measurement
[PB94-184512] p 237 N95-12582
RINGSAT
[NASA-CR-197167] p 253 N95-12632
POSITION SENSING
Self calibrating autoTRAC
[NASA-CR-196930] p 348 N95-11998
POSITIONING
Principles of GPS one-way data processing for high precision positioning applications: Algorithms and software issues p 237 N95-12177
POSITRONIUM
Radiation-induced structural changes, 4
[DE94-753223] p 356 N95-11817
POSITRONS
Studies of positron induced luminescence from polymers
[DE94-013622] p 272 N95-11733
Radiation-induced structural changes, 4
[DE94-753223] p 356 N95-11817
Role of implantation-induced defects in surface-oriented diffusion of fluorine in silicon
[DE94-014905] p 374 N95-13125
POSTFLIGHT ANALYSIS
STS-68 post flight presentation
[NASA-TM-109959] p 250 N95-13131
STS-61 mission highlights resource tape
[NASA-TM-109963] p 250 N95-13132
POSTLAUNCH REPORTS
Debris/ice/TPS assessment and integrated photographic analysis of Shuttle Mission STS-65
[NASA-TM-109205] p 249 N95-12224
POTABLE WATER
Elimination of quinine in two subjects after ingestion of tonic water: An exploratory study
[DOT/FAA/AM-94/16] p 332 N95-11702
Improving the efficiency of high purity water systems
[DE94-013742] p 318 N95-11784
POTATOES
Growth of potatoes for CELSS
[NASA-CR-177646] p 338 N95-11949
Methodologies for processing plant material into acceptable food on a small scale
[NASA-CR-177647] p 338 N95-12132
POTENTIAL FIELDS
A unified approach to geopotential field modeling
[AD-A283453] p 324 N95-12544
POTENTIAL FLOW
Control theory based airfoil design using the Euler equations
[NASA-CR-196360] p 230 N95-11884
POWDER (PARTICLES)
CeO2-ZrO2 powder synthesis by way of alcohol dehydration of aqueous salt solutions
[INPE-5484-PRE/1783] p 276 N95-13191
Equipment for investigation of cryogenic compaction of nanosize silicon nitride powders
[DE94-013593] p 277 N95-13530
POWDER METALLURGY
Ground based research in microgravity materials processing
[NASA-CR-196815] p 278 N95-11759
POWER AMPLIFIERS
Ku-band high efficiency GaAs MMIC power amplifiers
[NASA-CR-182156] p 288 N95-13231
POWER CONDITIONING
A model-based expert system for space power distribution diagnostics
[NASA-CR-195336] p 342 N95-11918
POWER FACTOR CONTROLLERS
Description of a high temperature quenching furnace for the study of the directional solidification of nickel-base superalloys
[DE94-013812] p 271 N95-13544
POWER SUPPLY CIRCUITS
Recycle requirements for Nasa's 30 cm xenon ion thruster
[NASA-TM-106668] p 258 N95-12750
POYNTING THEOREM
Magnetospheric-ionospheric Poynting flux
[NASA-CR-196856] p 322 N95-11801
PRE-MAIN SEQUENCE STARS
An x-ray search for PMS stars in translucent molecular clouds
[NASA-CR-196151] p 380 N95-12388
PRECIPITATES
Atomic structures and compositions of internal interfaces
[DE94-013594] p 271 N95-13543
PRECIPITATION (METEOROLOGY)
The design and development of signal-processing algorithms for an airborne x-band Doppler weather radar
[NASA-CR-196888] p 281 N95-12374
PRECISION
A precision measurement of the prompt photon cross section in p(-p) collisions at the square root of s = 1.8 TeV
[DE94-014989] p 359 N95-13170
PRECONDITIONING
Parallel preconditioners for the conjugate gradient method
[PB94-201605] p 347 N95-13404
PREDICTION ANALYSIS TECHNIQUES
Prediction of geometric-thermal machine tool errors by artificial neural networks
[PB94-186673] p 348 N95-11909
Modeling and life prediction methodology for Titanium Matrix Composites subjected to mission profiles
[NASA-TM-109148] p 269 N95-11915
First principles investigation of the Ir-Zr-Nb ternary system
[AD-A282644] p 270 N95-12543
Chaotic time series. Part 1: Estimation of invariant properties in state space
[PB94-206968] p 376 N95-13572
PREDICTIONS
Meeting the nation's needs for biomedical and behavioral scientists
[LC-94-66477] p 330 N95-12310
Lifetime and reentry prediction for the Petite Amateur Navy Satellite (PANSAT)
[AD-A283366] p 255 N95-12921
PREFLIGHT ANALYSIS
PASP PLUS Transient Pulse Monitor (TPM): Preflight characterization report
[AD-A282582] p 283 N95-12550
PRELAUNCH TESTS
White Sands Test Facility
[NASA-TM-109901] p 249 N95-13129
PREPROCESSING
AIRSAR software: Computer programs for preprocessing of JPL compressed polarimetric SAR data
[PB94-179116] p 280 N95-11800
PRESSES
Equipment for investigation of cryogenic compaction of nanosize silicon nitride powders
[DE94-013593] p 277 N95-13530
PRESSURE DISTRIBUTION
Application of two procedures for dual-point design of transonic airfoils
[NASA-TP-3466] p 231 N95-12176
PRESSURE EFFECTS
Ultrashort laser pulse effects in ocular and related media: Laser-induced shock wave propagation and retinal damage
[AD-A282599] p 334 N95-12535
PRESSURE GRADIENTS
Apparatus and method for forming textured bulk high temperature superconducting materials
[AD-D016394] p 373 N95-12635
L-H transition in tokamaks and stellarators
[DE94-013257] p 370 N95-13422
PRESSURE MEASUREMENT
Pressure measurements on an F/A-18 twin vertical tail in buffeting flow. Volume 3: Buffet power spectral densities
[AD-A281444] p 230 N95-11829
A new algorithm for five-hole probe calibration, data reduction, and uncertainty analysis
[NASA-TM-106458] p 232 N95-12376
Pressure measurements of a three wave journal air bearing p 307 N95-13605
PRESSURE PULSES
A low-erosion starting technique for high-performance arcjets
[NASA-TM-106627] p 259 N95-13347
PRESSURE RATIO
Pressure measurements on an F/A-18 twin vertical tail in buffeting flow. Volume 3: Buffet power spectral densities
[AD-A281444] p 230 N95-11829

PRESSURE REDUCTION
MHD pressure drops and thermal hydraulic analysis for the ITER breeding blanket design
[DE94-015085] p 369 N95-13280
PRESSURE SENSORS
Pressure measurements on an F/A-18 twin vertical tail in buffeting flow. Volume 3: Buffet power spectral densities
[AD-A281444] p 230 N95-11829
A new algorithm for five-hole probe calibration, data reduction, and uncertainty analysis
[NASA-TM-106458] p 232 N95-12378
PRESSURE VESSELS
Yield-before-break fracture mechanics analysis of high strength steel pressure vehicles
[AD-A282518] p 270 N95-12401
Oscillating-flow regenerator test rig
[NASA-CR-196982] p 246 N95-13200
PREVENTION
Contributions to CD Space Committee, 1993. Summary and comments
[PB94-190618] p 379 N95-11871
Design of a vehicle based system to prevent ozone loss
[NASA-CR-197199] p 242 N95-12702
PRINTED CIRCUITS
A high-performance constant-temperature hot-wire anemometer
[NASA-CR-177645] p 295 N95-11896
PROBABILITY DENSITY FUNCTIONS
LES, DNS and RANS for the analysis of high-speed turbulent reacting flows
[NASA-CR-196822] p 289 N95-11705
B* probability based search
[AD-A282551] p 343 N95-12497
The effect of Rician fading and partial-band interference on noise-normalized fast frequency-hopped MFSK receivers
[AD-A282805] p 283 N95-12601
PROBABILITY THEORY
Naval research reviews, volume 46, February 1994
[AD-A281435] p 265 N95-11827
Probability of detection of defects in coatings with electronic shearography
[NASA-CR-196201] p 308 N95-12391
An analysis of the effect of Gaussian error in object recognition
[AD-A282260] p 349 N95-12411
Measures of change and the determination of equivalent change
[AD-A282647] p 351 N95-12501
PROBLEM SOLVING
Engineering the future with America's high school students p 377 N95-11958
PROCESS CONTROL (INDUSTRY)
Design issues of human operator support systems
[PB94-191376] p 337 N95-11778
Chemical Engineering Seminar 1993
[PB94-184538] p 266 N95-12584
PROCUREMENT MANAGEMENT
Case study of risk management in the USAF B-1B bomber program
[AD-A282371] p 377 N95-11944
PRODUCT DEVELOPMENT
Status of hollow cathode heater development for the Space Station plasma contactor
[NASA-CR-195364] p 256 N95-12622
Design and testing of a model CELSS chamber robot
[NASA-CR-197196] p 303 N95-12694
Integrated design and manufacturing for the high speed civil transport
[NASA-CR-197163] p 241 N95-12700
PRODUCTION ENGINEERING
Intelligent knowledge-based engineering
[AD-A281906] p 377 N95-11788
Chemical Engineering Seminar 1993
[PB94-184538] p 266 N95-12584
CVD techniques for the synthesis or modification of porous ceramics
[PB94-206836] p 276 N95-13284
PRODUCTION MANAGEMENT
Development of a spindle thermal error characterization and compensation sensor system for machining center accuracy enhancement
[AD-A280891] p 300 N95-11729
PRODUCTIVITY
An experimental environment for software engineering
[INPE-5540-TDI/528] p 343 N95-12300
Advanced Industrial Materials Program
[DE94-015528] p 279 N95-12942
PROGRAM VERIFICATION (COMPUTERS)
Validation results of wind diesel simulation model TKKMOD
[PB94-179157] p 317 N95-11846
Software analysis handbook: Software complexity analysis and software reliability estimation and prediction
[NASA-TM-104799] p 339 N95-11914
Second Dependable Software Technology Exchange
[AD-A283367] p 344 N95-12922
An examination of selected software testing tools: 1993 supplement
[AD-A283060] p 344 N95-13051
The Second Workshop on Principles and Practice of Constraint Programming
[AD-A281731] p 229 N95-13166
Visualizing parallel numerical software performance on a shared memory multiprocessor
[PB94-195658] p 352 N95-13437
Beta testing of MTI seal codes p 305 N95-13589
PROGRAMMERS
SURRENDER user's manual, second edition
[PB94-206950] p 346 N95-13571
PROGRAMMING ENVIRONMENTS
Design issues of human operator support systems
[PB94-191376] p 337 N95-11778
An experimental environment for software engineering
[INPE-5540-TDI/528] p 343 N95-12300
A framework for exploiting data and functional parallelism on distributed memory multicomputers
[AD-A281194] p 347 N95-12523
Norwegian contribution to the SWG on APSE programme
[PB94-202397] p 341 N95-13557
PROJECT MANAGEMENT
Case study of risk management in the USAF B-1B bomber program
[AD-A282371] p 377 N95-11944
On bottleneck partitioning k-ary n-cubes
[NASA-CR-194966] p 342 N95-12005
Activities of the Space Studies Board of the National Research Council
[NASA-CR-195738] p 247 N95-12880
The development of the F100-PW-220 and F110-GE-100 engines: A case study of risk assessment and risk management
[AD-A282467] p 244 N95-13289
PROJECT PLANNING
Integrated propulsion technology demonstrator. Program plan
[NASA-CR-196870] p 257 N95-11823
PROJECT SETI
Search for extraterrestrial intelligence/High Resolution Microwave Survey team member
[NASA-CR-196478] p 339 N95-13026
PROJECTILES
Polyatomic ion impact on solid surfaces and related phenomena
[PB94-201258] p 360 N95-13242
PROJECTIVE GEOMETRY
The quadric reference surface: Theory and applications
[AD-A282379] p 351 N95-12007
PROKARYOTES
Regulation of alternative CO2 fixation pathways in prokaryotic and eukaryotic photosynthetic organisms
[DE94-013180] p 331 N95-13271
PRONY SERIES
Stress relaxation functions: Methods of approximation
[NASA-CR-195830] p 312 N95-12861
PROP-FAN TECHNOLOGY
En route noise levels from propfan test assessment airplane
[NASA-TP-3451] p 355 N95-12341
PROPANE
Design of a vehicle based system to prevent ozone loss
[NASA-CR-197199] p 242 N95-12702
PROPELLANT ACTUATED INSTRUMENTS
Design of a ZVS PWM inverter for a brushless DC motor in an EMA application
[NASA-CR-195808] p 312 N95-12620
PROPELLANT STORAGE
STS propellant densification feasibility study data book
[NASA-TM-108467] p 278 N95-12857
PROPELLANT TANKS
Trade study plan for Reusable Hydrogen Composite Tank System (RHCTS)
[NASA-CR-196871] p 252 N95-11945
PROPELLANT TRANSFER
Cryogenic On-Orbit Liquid Depot Storage, Acquisition, and Transfer satellite (COLD-SAT) feasibility study
[NASA-CR-185247] p 256 N95-13232
Feasibility study for a Cryogenic On-Orbit Liquid Depot-Storage, Acquisition and Transfer (COLD-SAT) satellite
[NASA-CR-185248] p 294 N95-13233
PROPELLANTS
Project Genesis: Mars in situ propellant technology demonstrator mission
[NASA-CR-197166] p 277 N95-12822
PROPELLER FANS
En route noise levels from propfan test assessment airplane
[NASA-TP-3451] p 355 N95-12341
PROPORTIONAL COUNTERS
The laser and its applications on environment and biotechnology research
[DE94-013831] p 299 N95-13076
PROPULSION
Guideway structural design and power/propulsion/braking in relation to guideways. Volume 3: Appendix B: Maglev guideway structural design
[PB93-169910] p 304 N95-13128
White Sands Test Facility
[NASA-TM-109901] p 249 N95-13129
Space Station Freedom propulsion activities
[NASA-TM-108604] p 256 N95-13236
PROPULSION SYSTEM CONFIGURATIONS
A revolutionary lunar space transportation system architecture using extraterrestrial LOX-augmented NTR propulsion
[NASA-TM-106726] p 249 N95-11703
Nuclear rockets: High-performance propulsion for Mars
[DE94-013642] p 257 N95-11782
Selection process for trade study: Graphite Composite Primary Structure (GCPS)
[NASA-CR-196866] p 261 N95-11803
Integrated propulsion technology demonstrator. Program plan
[NASA-CR-196870] p 257 N95-11823
Test Plan. GCPS Task 4, subtask 4.2 thrust structure development
[NASA-CR-196869] p 251 N95-11833
Shock-tunnel combustor testing for hypersonic vehicles
[NASA-CR-196836] p 246 N95-11938
Design and testing of an oblique all-wing supersonic transport
[NASA-CR-196394] p 242 N95-12785
Hypersonic vehicle model and control law development using H(infinity) and micron synthesis
[NASA-TM-4562] p 255 N95-12838
Guideway structural design and power/propulsion/braking in relation to guideways. Volume 3: Appendix B: Maglev guideway structural design
[PB93-169910] p 304 N95-13128
Activities of the Structures Division, Lewis Research Center
[NASA-TM-108081] p 313 N95-13235
PROPULSION SYSTEM PERFORMANCE
Nuclear rockets: High-performance propulsion for Mars
[DE94-013642] p 257 N95-11782
Shock-tunnel combustor testing for hypersonic vehicles
[NASA-CR-196836] p 246 N95-11938
Converting the Minuteman missile into a small satellite launch system
[NASA-CR-197169] p 249 N95-12531
Design and construction of a remote piloted flying wing
[NASA-CR-197195] p 241 N95-12695
STS propellant densification feasibility study data book
[NASA-TM-108467] p 278 N95-12857
Activities of the Structures Division, Lewis Research Center
[NASA-TM-108081] p 313 N95-13235
Space Station Freedom propulsion activities
[NASA-TM-108604] p 256 N95-13236
PROTECTIVE CLOTHING
Aerospace medicine and biology: A continuing bibliography with indexes (supplement 394)
[NASA-SP-7011(394)] p 335 N95-13230
PROTECTIVE COATINGS
Hydrogen desulfurization of nickel: Thermodynamics and kinetics
[AD-A282581] p 266 N95-12549
Elimination of internal contamination on semiconductor devices (protective coatings)
[DE94-015868] p 275 N95-12945
PROTEIN CRYSTAL GROWTH
Convective flow effects on protein crystal growth
[NASA-CR-196790] p 372 N95-11921
Protein crystal growth in low gravity
[NASA-CR-196980] p 279 N95-13202
PROTEIN SYNTHESIS
Convective flow effects on protein crystal growth
[NASA-CR-196790] p 372 N95-11921
PROTEINS
Rational enzyme redesign
[DE94-014565] p 331 N95-12677

Conformation of membrane proteins: Bacteriorhodopsin
[AD-A281282] p 331 N95-13373

PROTOCOL (COMPUTERS)
Eager combining: A coherency protocol for increasing effective network and memory bandwidth in shared-memory multiprocessors
[AD-A281501] p 346 N95-11857
Using secure coprocessors
[AD-A281255] p 340 N95-12524
Integrated sensor bus
[PB94-206810] p 288 N95-13252

PROTON IRRADIATION
A study of a multi-pinned phase CCD detector for use as a star tracker
[NASA-CR-196287] p 381 N95-13056

PROTON-PROTON REACTIONS
Measurement of the polarization in the decay B(exp 0) yields J/psi K(exp *0) in (bar p)p collisions at the square root of s = 1.8 TeV
[DE94-014265] p 357 N95-12370

PROTONS
Amine catalyzed intramolecular imidization of alkyl and aryl phthalamates, kinetics and mechanism in deuterated chloroform
[AD-A281741] p 259 N95-11844

PROTOTYPES
Selection process for trade study: Reusable Hydrogen Composite Tank System (RHCTS)
[NASA-CR-196874] p 251 N95-11809

PSYCHOLOGICAL EFFECTS
Ground-based wake vortex monitoring, prediction, and ATC interface p 235 N95-13209

PSYCHOLOGICAL TESTS
The selective use of functional optical variables in the control of forward speed
[NASA-TM-108849] p 229 N95-12227
Age 60 Rule. Part 2: Airline pilot age and performance. A review of the scientific literature
[DOT/FAA/AM-94/21-PT-2] p 336 N95-13020

PSYCHOPHYSICS
How are three-dimensional objects represented in the brain?
[AD-A282367] p 335 N95-11942
Visual psychophysics of egomotion
[AD-A282547] p 335 N95-12495

PSYCHOPHYSIOLOGY
Psychophysiological assessment methods (including a register of psychophysiologists on microfiches)
[AGARD-AR-324] p 335 N95-12133

PUBLIC HEALTH
Meeting the nation's needs for biomedical and behavioral scientists
[LC-94-66477] p 330 N95-12310

PUBLIC RELATIONS
Shifting our focus: Communicating science to a new, nontechnical culture
[DE94-014258] p 378 N95-13123

PULSARS
Research in astrophysical processes
[NASA-CR-196773] p 382 N95-12939

PULSE AMPLITUDE
Power system applications for PASC converter systems
[DE94-013329] p 286 N95-11751
Method of phased magnitude correlation using binary sequences
[AD-D016397] p 284 N95-12646

PULSE COMMUNICATION
Preliminary digital control system design for the petite amateur Navy satellite (PANSAT)
[AD-A282804] p 253 N95-12528
Trellis-based source and channel coding
[PB94-204443] p 285 N95-13405

PULSE COMPRESSION
Method of phased magnitude correlation using binary sequences
[AD-D016397] p 284 N95-12646

PULSE DOPPLER RADAR
Certification of windshear performance with RTCA class D radomes p 235 N95-13206

PULSE GENERATORS
Physics of High Energy Density Plasmas Produced by Pulsed Power
[NIFS-PROC-18] p 365 N95-12429
Resistivity variation of fuse as an opening switch p 365 N95-12430
A study on successive generation of intense pulsed ion beams by the inverse pinch ion diode p 365 N95-12434
Gas-puff Z-pinch driven by inductive energy storage pulsed power generator ASO-2 p 366 N95-12439
Plasma opening switch by laser-produced plasma with different kinds of ion species p 367 N95-12451

PULSE HEATING
Study on surface treatment by pulsed electron beams p 366 N95-12437

PULSE MODULATION
Light beam and pulse propagation in nonlinear dielectrics
[AD-A282548] p 282 N95-12496

PULSED LASERS
Ultrashort laser pulse effects in ocular and related media: Laser-induced shock wave propagation and retinal damage
[AD-A282599] p 334 N95-12535
Spaceborne Photonics Institute
[NASA-CR-196784] p 362 N95-12659
Time-resolved electron thermal conduction by probing of plasma formation in transparent solids with high power subpicosecond laser pulses
[DE94-015170] p 370 N95-13555

PULSES
Review of pulse ignition
[INPE-5569-PUD/063] p 265 N95-11885

PUMPS
Diesel-fired self-pumping water heater
[AD-A283063] p 279 N95-13053

PUPIL SIZE
Eye-gaze determination of user intent at the computer interface
[DE94-012337] p 363 N95-13421

PURIFICATION
Improving the efficiency of high purity water systems
[DE94-013742] p 318 N95-11784
Fractional suspension crystallization of organic compounds
[PB94-206851] p 375 N95-13409

PURITY
Improving the efficiency of high purity water systems
[DE94-013742] p 318 N95-11784

Q

Q FACTORS
Active vibration control using a distributed controller
[PB94-207073] p 313 N95-13576

QUALITATIVE ANALYSIS
Low oxidation state gallium compounds. Synthesis and characterization of Ga(CH2CMe3)n
[AD-A283369] p 373 N95-12923

QUALITY
Proposal of a methodology to evaluate urban quality of life using conventional and remote sensing data, geographic information system, and a database
[INPE-5552-TDI/536] p 315 N95-12297

QUALITY CONTROL
Nimbus-7 Earth Radiation Budjet compact solar data set user's guide
[NASA-RP-1346] p 384 N95-12667

QUANTUM CHEMISTRY
Quantum chemical study of methane oxidation species
[NASA-CR-196158] p 265 N95-12107
Proceedings of US-Latin American Workshop on Molecular and Materials Sciences: Theoretical and Computational Aspects
[AD-A283359] p 358 N95-12882
US-Latin American Workshop on Molecular and Materials Sciences: Theoretical and Computational Aspects
[AD-A283428] p 359 N95-13141

QUANTUM CHROMODYNAMICS
Inclusive jet and two-jet differential cross sections at CDF
[DE94-015543] p 358 N95-12943
Photon production at CDF and D0
[DE94-014985] p 359 N95-13160
Multi-jet analysis for the top search at the Fermilab Collider
[DE94-014988] p 359 N95-13169
A precision measurement of the prompt photon cross section in p(-p) collisions at the square root of s = 1.8 TeV
[DE94-014989] p 359 N95-13170
Quenched QCD at finite density
[DE94-011522] p 375 N95-13337

QUANTUM EFFICIENCY
Enhancement of luminescence in polymer nanocomposites
[AD-A282539] p 262 N95-12404
Photogeneration of charge carriers in bilayer assemblies of conjugated rigid-rod polymers
[AD-A282625] p 275 N95-12537

QUANTUM ELECTRODYNAMICS
On the charged vector particle scattering on a vector particle
[DE94-622787] p 360 N95-13273

QUANTUM ELECTRONICS
The Research Laboratory of Electronics
[AD-A281445] p 386 N95-11830
Development of nanostructure fabrication technology and new electron-quantum wave devices
[AD-A281724] p 286 N95-11860
Quantum cellular automata
[AD-A283351] p 287 N95-12881

QUANTUM MECHANICS
Magnetic field induced minigap in double quantum wells
[DE94-015013] p 376 N95-13172

QUANTUM THEORY
Hall conductance as a topological invariant
[PB94-179330] p 353 N95-12364
Proceedings of US-Latin American Workshop on Molecular and Materials Sciences: Theoretical and Computational Aspects
[AD-A283359] p 358 N95-12882

QUANTUM WELLS
Magneto-optical properties of quantum structures with reduced dimensionality
[AD-A282597] p 376 N95-12553
Magnetic field induced minigap in double quantum wells
[DE94-015013] p 376 N95-13172

QUARKS
The cascade-deuteron system
[DE94-011650] p 357 N95-11894
Quenched QCD at finite density
[DE94-011522] p 375 N95-13337

QUENCHING (ATOMIC PHYSICS)
Quenched QCD at finite density
[DE94-011522] p 375 N95-13337

QUENCHING (COOLING)
Description of a high temperature quenching furnace for the study of the directional solidification of nickel-base superalloys
[DE94-013812] p 271 N95-13544

R

RADAR
Activities of the Helsinski University of Technology, Applied Electronics Laboratory
[PB94-179074] p 385 N95-11797

RADAR ANTENNAS
An investigation of the channel crosstalk in optical heterodyne controlled phased array radars
[AD-A281227] p 285 N95-13371

RADAR CROSS SECTIONS
Analysis of cylindrical wrap-around and doubly conformal patch antennas by way of the finite element-artificial absorber method
[NASA-CR-195211] p 281 N95-12382
Wideband electromagnetic scattering program. Fourier-based radar imaging techniques
[AD-A282540] p 282 N95-12493

RADAR DATA
Lessons learned from experiments conducted on radar data management systems
[AD-A282896] p 284 N95-12920
Part A: A data acquisition/controller system. Part B: Supplement to a data acquisition/controller system
[AD-A283373] p 285 N95-12924

RADAR DETECTION
Development of ground-penetrating radar equipment for detecting pavement condition for preventive maintenance
[PB94-189537] p 280 N95-11904
Airborne Windshear Detection and Warning Systems. Fifth and Final Combined Manufacturers' and Technologists' Conference, part 2
[NASA-CP-10139-PT-2] p 234 N95-13203
Windshear certification data base for forward-look detection systems p 234 N95-13204
Certification methodology applied to the NASA experimental radar system p 235 N95-13205
Certification of windshear performance with RTCA class D radomes p 235 N95-13206
Airport surveillance using a solid state coherent lidar p 235 N95-13207
Ground-based wake vortex monitoring, prediction, and ATC interface p 235 N95-13209
Aircraft wake RCS measurement p 235 N95-13210
Wake vortex detection at Denver Stapleton Airport with a pulsed 2-micron coherent lidar p 236 N95-13211
Doppler radar detection of vortex hazard indicators p 236 N95-13212
Remote sensing of turbulence in the clear atmosphere with 2-micron lidars p 236 N95-13213

RADAR EQUIPMENT
Development of ground-penetrating radar equipment for detecting pavement condition for preventive maintenance
[PB94-189537] p 280 N95-11904
RADAR IMAGERY
Venus surface roughness and Magellan stereo data
[NASA-CR-196821] p 382 N95-11704
AIRSAR software: Computer programs for preprocessing of JPL compressed polarimetric SAR data
[PB94-179116] p 280 N95-11800
Wideband electromagnetic scattering program. Fourier-based radar imaging techniques
[AD-A282540] p 282 N95-12493
Target recognition in ultra-wideband SAR imagery
[AD-A283462] p 282 N95-12547
RADAR MAPS
Venus surface roughness and Magellan stereo data
[NASA-CR-196821] p 382 N95-11704
RADAR MEASUREMENT
Differential absorption lidar measurements of atmospheric water vapor using a pseudonoise code modulated AlGaAs laser
[NASA-TM-104610] p 314 N95-11997
The design and development of signal-processing algorithms for an airborne x-band Doppler weather radar
[NASA-CR-196888] p 281 N95-12374
Wideband electromagnetic scattering program. Fourier-based radar imaging techniques
[AD-A282540] p 282 N95-12493
Certification methodology applied to the NASA experimental radar system p 235 N95-13205
Aircraft wake RCS measurement p 235 N95-13210
RADAR SIGNATURES
Aircraft wake RCS measurement p 235 N95-13210
Wake vortex detection at Denver Stapleton Airport with a pulsed 2-micron coherent lidar p 236 N95-13211
RADAR TRACKING
Monopulse tracker operating characteristics measurement error performance for azimuth tracking
[AD-A281188] p 282 N95-12521
Lessons learned from experiments conducted on radar data management systems
[AD-A282896] p 284 N95-12920
RADIANCE
SeaWiFS technical report series. Volume 23: SeaWiFS prelaunch radiometric calibration and spectral characterization
[NASA-TM-104566-VOL-23] p 328 N95-12359
RADIANT FLUX DENSITY
Emittance theory for thin film selective emitter
[NASA-TM-106727] p 317 N95-11903
A model of the density of solar radiation energy on an arbitrary plane identification for Warsaw
p 384 N95-12243
BATSE observations of Nova Muscae 1991
[NASA-CR-196416] p 380 N95-12464
Methods of modeling radiant energy exchange in radiation fog and clouds
[AD-A283509] p 326 N95-12624
RADIANT HEATING
Methods of modeling radiant energy exchange in radiation fog and clouds
[AD-A283509] p 326 N95-12624
RADIATION DAMAGE
Radiation amorphization of materials
[DE94-624184] p 374 N95-12948
RADIATION DETECTORS
Response of high T(sub c) superconducting Josephson junction to nuclear radiation
[DE94-624705] p 360 N95-13536
RADIATION DISTRIBUTION
Methods of modeling radiant energy exchange in radiation fog and clouds
[AD-A283509] p 326 N95-12624
RADIATION DOSAGE
Basic mechanisms of radiation effects in the natural space radiation environment
[DE94-013445] p 384 N95-11757
Detailed component design for a Compact Environmental Anomaly Sensor (CEASE)
[AD-A283144] p 256 N95-13138
RADIATION EFFECTS
Summary reports of activities under visiting research program, 1993
[DE94-753222] p 360 N95-11750
Basic mechanisms of radiation effects in the natural space radiation environment
[DE94-013445] p 384 N95-11757
Radiation-induced structural changes, 4
[DE94-753223] p 356 N95-11817
A model of the density of solar radiation energy on an arbitrary plane identification for Warsaw
p 384 N95-12243
The effect of irradiation on the stability and properties of monolithic silicon carbide and SiC(f)/SiC composites up to 25 dpa
[DE94-014568] p 263 N95-12862
Radiofrequency/microwave radiation biological effects and safety standards: A review
[AD-A282886] p 334 N95-12919
Radiation amorphization of materials
[DE94-624184] p 374 N95-12948
RADIATION HARDENING
Development of radiation hard scintillators
[DE94-013204] p 296 N95-13287
RADIATION MEASUREMENT
Measurement of synchrotron radiation transmission of infrared range by YBa2Cu3O(7-delta) film in superconducting state
[DE94-623270] p 372 N95-11899
RADIATION MEASURING INSTRUMENTS
Ultrawideband shipboard electrooptic electromagnetic environment monitoring
[AD-A282369] p 280 N95-11943
X-ray and gamma ray astronomy detectors
[NASA-SP-517] p 379 N95-12304
RADIATION SOURCES
Basic mechanisms of radiation effects in the natural space radiation environment
[DE94-013445] p 384 N95-11757
Gas-puff Z-pinch driven by inductive energy storage pulsed power generator ASO-2 p 366 N95-12439
RADIATION TOLERANCE
Development of radiation hard scintillators
[DE94-013204] p 296 N95-13287
RADIATIVE HEAT TRANSFER
Emittance theory for thin film selective emitter
[NASA-TM-106727] p 317 N95-11903
Predicting radiative heat transfer in thermochemical nonequilibrium flow fields. Theory and user's manual for the LORAN code
[NASA-TM-4564] p 291 N95-11936
Science objectives and performance of a radiometer and window design for atmospheric entry experiments
[NASA-TM-4637] p 382 N95-12190
The embodiment design of the heat rejection system for the portable life support system
[NASA-CR-197178] p 338 N95-12555
RADIATIVE TRANSFER
Trace gas emissions to the atmosphere by biomass burning in the west African savannas
[NASA-CR-196758] p 319 N95-11931
Electronic energy transfer in new polymer nanocomposite assemblies
[AD-A282233] p 274 N95-12407
RADICALS
Towards tailored interphase formation utilizing surface-active benzylsulfonium salts as cationic initiators
[AD-A282511] p 262 N95-12398
Multifunctional acrylic ether monomers, their polymers, and polymerizable epoxide derivatives from simple alpha-substitution of alkyl acrylates
[AD-A282513] p 273 N95-12400
Progress on resonance ionization detection of combustion radicals
[DE94-015339] p 267 N95-12762
Thermal polymerization of styrene in the presence of stable radicals and inhibitors
[AD-A280926] p 275 N95-12773
RADIO ASTRONOMY
The x-ray structure of the supernova remnant W49B
[NASA-CR-196482] p 382 N95-12950
Search for extraterrestrial intelligence/High Resolution Microwave Survey team member
[NASA-CR-196478] p 339 N95-13026
RADIO BURSTS
Burst transmission in the HF band: A system analysis and proposal for improvement
[PB94-190733] p 280 N95-11821
RADIO EMISSION
Non-dipolar magnetic field models and patterns of radio emission: Uranus and Neptune compared
[NASA-CR-196412] p 385 N95-12469
Search for inverse Compton x-rays from the lobes of Fornax A x-rays from radio galaxies straddling the Fanaroff-Riley transition
[NASA-CR-196433] p 385 N95-13023
RADIO EQUIPMENT
Preliminary digital control system design for the petite amateur Navy satellite (PANSAT)
[AD-A282804] p 253 N95-12528
RADIO FREQUENCIES
Atomic structure modifications of diamond-like nanocomposite films: Observation by Raman spectroscopy, FTIR and STM
[DE94-013732] p 371 N95-11740
ETRI brochure: History, mission, and activity highlights
p 389 N95-12697
200 MHz channel sounder, open description
[PB94-202538] p 285 N95-13559
RADIO FREQUENCY HEATING
Microwave heating and joining of ceramic cylinders: A mathematical model
[NASA-CR-194962] p 351 N95-11922
RADIO FREQUENCY INTERFERENCE
RINGSAT
[NASA-CR-197167] p 253 N95-12632
Search for extraterrestrial intelligence/High Resolution Microwave Survey team member
[NASA-CR-196478] p 339 N95-13026
RADIO GALAXIES
Search for inverse Compton x-rays from the lobes of Fornax A x-rays from radio galaxies straddling the Fanaroff-Riley transition
[NASA-CR-196433] p 385 N95-13023
RADIO RECEIVERS
Activities of the Helsinski University of Technology, Applied Electronics Laboratory
[PB94-179074] p 385 N95-11797
Processing, fabrication, and demonstration of HTS integrated microwave circuits
[AD-A282505] p 289 N95-13300
RADIO TRANSMISSION
The effect of Rician fading and partial-band interference on noise-normalized fast frequency-hopped MFSK receivers
[AD-A282805] p 283 N95-12601
Efficient parabolic equation solution of radiowave propagation in an inhomogeneous atmosphere and over irregular terrain: Formulation
[AD-A282648] p 284 N95-12834
RADIO TRANSMITTERS
RINGSAT
[NASA-CR-197167] p 253 N95-12632
RADIO WAVES
Ultrawideband shipboard electrooptic electromagnetic environment monitoring
[AD-A282369] p 280 N95-11943
Efficient parabolic equation solution of radiowave propagation in an inhomogeneous atmosphere and over irregular terrain: Formulation
[AD-A282648] p 284 N95-12834
Radiofrequency/microwave radiation biological effects and safety standards: A review
[AD-A282886] p 334 N95-12919
RADIOACTIVE WASTES
Global ice sheet modeling
[DE94-013744] p 318 N95-11745
Sloshing analysis of tanks containing multiple fluid layers
[DE94-013333] p 290 N95-11753
RADIOACTIVITY
CESIUM-137 and natural radionuclides in soils from Southern Brazil and in soils and others environmental samples from Antarctic
[INPE-5505-TDI-517] p 321 N95-13192
RADIOIMMUNOASSAY
Spaceflight and immune responses of Rhesus monkeys
[NASA-CR-196846] p 331 N95-12941
RADIOMETERS
Optical metrology and more. Programs and services of the Radiometric Physics Division, Physics Laboratory
[PB94-191707] p 362 N95-11841
SeaWiFS technical report series. Volume 22: Prelaunch acceptance report for the SeaWiFS radiometer
[NASA-TM-104556-VOL-22] p 328 N95-12151
Science objectives and performance of a radiometer and window design for atmospheric entry experiments
[NASA-TM-4637] p 382 N95-12190
SeaWiFS technical report series. Volume 23: SeaWiFS prelaunch radiometric calibration and spectral characterization
[NASA-TM-104566-VOL-23] p 328 N95-12359
Visible/infrared radiometric calibration station
[DE94-014459] p 363 N95-13106
RADIOSONDES
Waves in Space Plasmas (WISP)
[NASA-CR-196432] p 369 N95-13024
RADOMES
Certification of windshear performance with RTCA class D radomes p 235 N95-13206
RAILGUN ACCELERATORS
Behaviors of plasma armature in the augmented railgun using a permanent magnet p 367 N95-12449
RAIN
Catalogue of heavy rainfall cases of six inches or more over the continental US during 1993
[NOAA-TR-NESDIS-80] p 327 N95-13095
RAIN FORESTS
Estimation of above-ground phytomass in a tropical forest using TM-LANDSAT 5 E HRV-SPOT 1 data
[INPE-5500-TDI/515] p 316 N95-13159

AVHRR/NOAA images to detect and quantify deforestation in Amazon Forest: Relations with TM/LANDSAT data
[INPE-5501-TDI/516] p 316 N95-13350

RAINSTORMS
Catalogue of heavy rainfall cases of six inches or more over the continental US during 1993
[NOAA-TR-NESDIS-80] p 327 N95-13095

RAMAN SPECTRA
Atomic structure modifications of diamond-like nanocomposite films: Observation by Raman spectroscopy, FTIR and STM
[DE94-013732] p 371 N95-11740
Optical Remote Sensing of the Atmosphere. Technical digest 1993. Volume 5: Postconference edition
[AD-A281446] p 314 N95-11831
Diagnostic techniques for semiconductor materials processing
[AD-A282810] p 373 N95-12602

RAMAN SPECTROSCOPY
Atomic structure modifications of diamond-like nanocomposite films: Observation by Raman spectroscopy, FTIR and STM
[DE94-013732] p 371 N95-11740
Raman structural studies of the nickel electrode
[NASA-CR-196331] p 289 N95-13344

RAMJET ENGINES
Hypersonic engine seal development at NASA Lewis Research Center p 307 N95-13602

RANDOM NOISE
Investigation of spectral-based techniques for classification of wideband transient signals in additive white Gaussian noise
[AD-A282954] p 283 N95-12592
Learning one-dimensional geometric patterns under one-sided random misclassification noise
[DE94-014659] p 350 N95-12864

RANDOM NUMBERS
Stochastic indexing
[AD-A283143] p 327 N95-13137

RANDOM PROCESSES
Improved image decompression for reduced transform coding artifacts
[NASA-CR-196805] p 341 N95-11761

RANDOM VARIABLES
Gaussian paired comparison models
[PB94-179025] p 352 N95-12820

RANDOM WALK
Constructing combinatorial designs by local search
[PB94-179272] p 351 N95-11839

RANGEFINDING
Satellite laser ranging and gravity field modeling accuracy
[NASA-CR-196057] p 248 N95-12837
A comparison of two sites for the purpose of satellite laser ranging
[AD-A283149] p 299 N95-13139

RARE EARTH ELEMENTS
Laser spectroscopy of GdO: Ligand field assignments of 4f7(8S)6p reversing 4f7(8)6s transitions
[AD-A282827] p 268 N95-13180

RARE GASES
Certain aspects of the melting, casting and welding of Ni3Al alloys
[DE94-013628] p 269 N95-11897
The laser and its applications on environment and biotechnology research
[DE94-013831] p 299 N95-13076

RATINGS
Age 60 study. Part 4: Experimental evaluation of pilot performance
[REPT-8025-4B] p 336 N95-13199

RATIONAL FUNCTIONS
Measures of change and the determination of equivalent change
[AD-A282647] p 351 N95-12501

RATIOS
Measures of change and the determination of equivalent change
[AD-A282647] p 351 N95-12501

RATS
Copper metabolism in rats fed ascorbic acid or restricted amounts of copper
[PB94-191343] p 330 N95-11902
Acute inhalation of explosively disseminated carbon fibers in rats
[AD-A280556] p 330 N95-12614
Effect of decreased gravity on circulation in the rat
[NASA-CR-196946] p 331 N95-12827
Consequences of prolonged inhalation of ozone on Fischer-344/N rats: Collaborative studies. Part 1: Content and cross-linking of lung collagen
[PB94-182748] p 331 N95-13176

RAYLEIGH SCATTERING
Planar Rayleigh scattering and laser-induced fluorescence for visualization of a hot, Mach 2 annular air jet
[NASA-TM-4576] p 247 N95-13196

REACTING FLOW
LES, DNS and RANS for the analysis of high-speed turbulent reacting flows
[NASA-CR-196822] p 289 N95-11705
Interferograms, schlieren, and shadowgraphs constructed from real- and ideal-gas, two- and three-dimensional computed flowfields
p 295 N95-11971
Fundamental and experimental studies on the catalytic combustion of methane
[PB94-205895] p 268 N95-13251

REACTION KINETICS
Rational enzyme redesign
[DE94-014565] p 331 N95-12677
Hydrolysis and condensation of tin (4) alkoxide compounds: The control of structural evolution
[AD-A282789] p 267 N95-12807
Characterization of the one step polyimide synthesis
[AD-A281216] p 276 N95-13367

REACTION-DIFFUSION EQUATIONS
Microwave heating and joining of ceramic cylinders: A mathematical model
[NASA-CR-194962] p 351 N95-11922

REACTIVITY
Thin-film model studies of interfacial reactions in intermetallic matrix composites
[AD-A283360] p 263 N95-12883

REACTOR DESIGN
Target area chamber system design for the National Ignition Facility
[DE94-013347] p 364 N95-11754

REACTOR MATERIALS
Studies of low temperature, low flux radiation embrittlement of nuclear reactor structural materials
[DE94-013710] p 269 N95-11738

REACTOR SAFETY
Vacuum system operating experience review for fusion applications
[DE94-015267] p 368 N95-12759
Mean importance measures for groups of events in fault trees
[DE94-015416] p 353 N95-13061

REACTOR TECHNOLOGY
Nuclear rockets: High-performance propulsion for Mars
[DE94-013642] p 257 N95-11782

REAGENTS
Room-temperature synthesis of CuInQ2 (Q = S or Se) in non-aqueous solution using an organoindium reagent
[NASA-TM-106557] p 260 N95-12662

REAL GASES
Interferograms, schlieren, and shadowgraphs constructed from real- and ideal-gas, two- and three-dimensional computed flowfields
p 295 N95-11971
Computer code for determination of thermally perfect gas properties
[NASA-TP-3447] p 231 N95-11995

REAL NUMBERS
Measures of change and the determination of equivalent change
[AD-A282647] p 351 N95-12501

REAL TIME OPERATION
Development of a spindle thermal error characterization and compensation sensor system for machining center accuracy enhancement
[AD-A280891] p 300 N95-11729
Proceedings: The Eleventh IEEE Workshop on Real-Time Operating Systems and Software
[AD-A281738] p 342 N95-11843
Locally connected adaptive Gabor filter for real-time motion compensation
[AD-A282544] p 286 N95-12494
Performance measurements of the multimedia testbed on real-time Mach
[AD-A282658] p 343 N95-12504
Determination of the auroral oval Q index from the air weather service K index
[AD-A282764] p 324 N95-12508
NPS state vector analysis and relative motion plotting software for STS-51
[AD-A282909] p 249 N95-12510
Short term weather forecasting in real time in a base weather station setting
[AD-A283141] p 327 N95-13134
An iterative approach to multibody simulation dynamics suitable for parallel implementation
[UTIAS-TN-276] p 347 N95-13353
Delta-4: An open architecture for dependable systems
[PB94-195641] p 341 N95-13436

RECEIVERS
The effect of Rician fading and partial-band interference on noise-normalized fast frequency-hopped MFSK receivers
[AD-A282805] p 283 N95-12601
200 MHz channel sounder, open description
[PB94-202538] p 285 N95-13559

RECOMMENDATIONS
Spacecraft maximum allowable concentrations for selected airborne contaminants, volume 1
[NASA-CR-196446] p 255 N95-12879

RECONNAISSANCE AIRCRAFT
Conceptual design of the AE481 Demon Remotely Piloted Vehicle (RPV)
[NASA-CR-197164] p 238 N95-12294
A preliminary design proposal for a maritime patrol strike aircraft: MPS-2000 Condor
[NASA-CR-197182] p 241 N95-12689

RECORDING INSTRUMENTS
Modelling of biopotential recordings and its implications for instrumentation design
[PB94-206844] p 332 N95-13408

RECTANGULAR PLATES
Buckling of flat rectangular orthotropic plates
[ESDU-94005] p 310 N95-11771
Elastic buckling of unbalanced laminated fibre reinforced composite plates (rectangular plates of AsBtDs type, all edges simply-supported under biaxial loading)
[ESDU-94006] p 310 N95-11772
Accurate interlaminar stress recovery from finite element analysis
[NASA-TM-109149] p 310 N95-11815

REDUNDANCY ENCODING
Vector quantization for efficient coding of upper subbands
[NASA-CR-196804] p 341 N95-11762

REDUNDANT COMPONENTS
Reliability and cost analysis methods
[NASA-CR-196326] p 308 N95-12381
On-line data reconstruction in redundant disk arrays
[AD-A282709] p 340 N95-12516

REENTRY VEHICLES
Conceptual design of an Orbital Debris Defense System
[NASA-CR-197211] p 254 N95-12696

REFERENCE SYSTEMS
NIST calibration of ASTM E127-type ultrasonic reference blocks
[PB94-191640] p 355 N95-11906

REFLECTANCE
Diagnostic techniques for semiconductor materials processing
[AD-A282810] p 373 N95-12602

REFLECTOR ANTENNAS
Experimental evaluation of shape memory alloy actuation technique in adaptive antenna design concepts
[NASA-CR-194983] p 284 N95-12896

REFRACTIVITY
Excitation of fast magneto-acoustic waves in unhomogeneous plasma of a large size tokamak
[DE94-625050] p 370 N95-13540

REFRACTORY MATERIALS
Test model designs for advanced refractory ceramic materials p 277 N95-11968
Apparatus and method for forming textured bulk high temperature superconducting materials
[AD-D016394] p 373 N95-12635

REFRIGERATORS
Design and construction of the astronautics refrigerator magnet
[DE94-013599] p 353 N95-11731
High frequency thermoacoustic refrigerator
[AD-A280925] p 279 N95-12772

REGENERATORS
Oscillating-flow regenerator test rig
[NASA-CR-196982] p 246 N95-13200

REGOLITH
A lunar/Martian anchor emplacement system
[NASA-CR-197193] p 302 N95-12690

REGULATIONS
SO2 guideline document
[PB94-181393] p 319 N95-11893
Environmental process improvement feasibility study and demonstration program
[NASA-CR-196789] p 319 N95-12110
Age 60 study. Part 4: Experimental evaluation of pilot performance
[REPT-8025-4B] p 336 N95-13199

REINFORCEMENT (PSYCHOLOGY)
Intelligent control systems research
[NASA-CR-195380] p 349 N95-12811

REINFORCING FIBERS
Modeling and life prediction methodology for Titanium Matrix Composites subjected to mission profiles
[NASA-TM-109148] p 269 N95-11915

REINFORCING MATERIALS
Towards tailored interphase formation utilizing surface-active benzylsulfonium salts as cationic initiators
[AD-A282511] p 262 N95-12398
REISSNER THEORY
Interlaminar stress analysis of dropped-ply laminated plates and shells by a mixed method
[NASA-CR-196851] p 311 N95-11946
RELATIVISTIC ELECTRON BEAMS
Velocity spread of REB generated by high current diode
[IPPCZ-339] p 364 N95-11886
The reflection of relativistic electron beam by virtual cathode
[IPPCZ-338] p 364 N95-11916
Strong beam-plasma turbulence p 367 N95-12450
Stimulated scattering of a slow electromagnetic wave excited by the relativistic electron beam
[DE94-625049] p 285 N95-13343
RELATIVISTIC PARTICLES
On the charged vector particle scattering on a vector particle
[DE94-622787] p 360 N95-13273
RELATIVISTIC THEORY
Relativistic theory of superfluidity with two condensates
[DE94-624073] p 290 N95-11749
RELAXATION (MECHANICS)
The structural basis for fatigue failure initiation in glassy polymers
[DE94-015415] p 275 N95-13060
RELAXATION METHOD (MATHEMATICS)
Adaptive relaxation for the steady-state analysis of Markov chains
[NASA-CR-194944] p 345 N95-13420
RELIABILITY
Revealing hidden defects: A hybrid evaluation strategy for steel structures
[PB94-191236] p 308 N95-11822
The development of a highly reliable power management and distribution system for civil transport aircraft
[NASA-TM-106697] p 243 N95-11867
Reliability allocation for a system using Markov analysis
[PB94-205051] p 309 N95-13406
RELIABILITY ANALYSIS
TLIFE: A program for spur, helical and spiral bevel transmission life and reliability modeling
[NASA-CR-4622] p 300 N95-11889
Software analysis handbook: Software complexity analysis and software reliability estimation and prediction
[NASA-TM-104799] p 339 N95-11914
Reliability and cost analysis methods
[NASA-CR-196326] p 308 N95-12381
Reliability allocation for a system using Markov analysis
[PB94-205051] p 309 N95-13406
RELIABILITY ENGINEERING
Illustrated structural application of universal first-order reliability method
[NASA-TP-3501] p 248 N95-11870
Reliability and cost analysis methods
[NASA-CR-196326] p 308 N95-12381
Second Dependable Software Technology Exchange
[AD-A283367] p 344 N95-12922
Proceedings of the CTU Seminar 1994, Part C
[DE94-624078] p 390 N95-12946
RELIEF MAPS
SURRENDER user's manual, second edition
[PB94-206950] p 346 N95-13571
REMOTE CONTROL
Data acquisition system of the NANOSAW-2 stand alone wind diesel plant. Document and user's guide
[PB94-179108] p 317 N95-11799
REMOTE MANIPULATOR SYSTEM
Evaluation of COSTAR mass handling characteristics in an environment. A simulation of the Hubble Space Telescope service mission
[NASA-TP-3489] p 333 N95-11887
Modelling and simulation of Space Station Freedom berthing dynamics and control
[NASA-TM-109151] p 252 N95-11947
REMOTE SENSING
Optical Remote Sensing of the Atmosphere. Technical digest 1993. Volume 5: Postconference edition
[AD-A281446] p 314 N95-11831
TOVS operational sounding upgrades: 1990-1992
[NOAA-TR-NESDIS-76] p 322 N95-11836
Trace gas emissions to the atmosphere by biomass burning in the west African savannas
[NASA-CR-196758] p 319 N95-11931
Proposal of a methodology to evaluate urban quality of life using conventional and remote sensing data, geographic information system, and a database
[INPE-5552-TDI/536] p 315 N95-12297
Millimeter-wave radiometric utility study
[AD-A282524] p 281 N95-12402
Satellite estimates of shortwave surface radiation and atmospheric meteorology for the BOREAS experiment region
[NASA-TM-109132] p 326 N95-12839
Visible/infrared radiometric calibration station
[DE94-014459] p 363 N95-13106
Remote sensing of turbulence in the clear atmosphere with 2-micron lidars p 236 N95-13213
Use of remote sensing and geographic information system techniques in integrated studies of watersheds
[INPE-5494-TDI/511] p 316 N95-13352
REMOTE SENSORS
Vapor detection sensitivity as a function of optical resolution for a single Lorentzian band
[AD-A283444] p 316 N95-13142
REMOTELY PILOTED VEHICLES
Conceptual design of the AE481 Demon Remotely Piloted Vehicle (RPV)
[NASA-CR-197164] p 238 N95-12294
Design and construction of a remote piloted flying wing
[NASA-CR-197195] p 241 N95-12695
REQUIREMENTS
Integrated propulsion technology demonstrator. Program plan
[NASA-CR-196870] p 257 N95-11823
RESEARCH
Activities of the Helsinki University of Technology, Applied Electronics Laboratory
[PB94-179074] p 385 N95-11797
AGSO 1993: Yearbook of the Australian Geological Survey Organisation. Geoscientific research and database development for the year 1 July 1992 to 30 June 1993
p 324 N95-12686
RESEARCH AND DEVELOPMENT
JPRS report: Science and technology. Central Eurasia: Life sciences
[JPRS-ULS-93-014] p 318 N95-11743
JPRS report: Science and technology. Central Eurasia: Life sciences
[JPRS-ULS-93-012] p 332 N95-11744
NASA/OAI Research Associates program
[NASA-CR-196824] p 376 N95-11765
JPRS report: Science and technology. Central Eurasia: Space
[JPRS-USP-94-006] p 247 N95-12000
JPRS report: Science and technology. Central Eurasia
[JPRS-UST-94-017] p 247 N95-12001
JPRS report: Science and technology. Central Eurasia
[JPRS-UST-94-020] p 389 N95-12002
JPRS report: Science and technology. Central Eurasia
[JPRS-UST-94-019] p 389 N95-12003
Experimental Aerodynamics Division
[NAL-SP-9404] p 229 N95-12166
Space facilities: Meeting future needs for research, development, and operations
[NASA-CR-194821] p 248 N95-12474
Activities of the Space Studies Board of the National Research Council
[NASA-CR-195738] p 247 N95-12880
Symposium on Structural Intermetallics: Perspectives on Science and Technology, volume 1
[AD-A283378] p 271 N95-12925
Advanced Industrial Materials Program
[DE94-015528] p 279 N95-12942
Bibliography on cold regions science and technology, volume 47, part 1
[AD-A281879] p 378 N95-13167
Air Force seal activities p 306 N95-13600
RESEARCH FACILITIES
The Biological Flight Research Facility
p 247 N95-11961
Directory of Federal laboratory and technology resources
[PB93-100097] p 389 N95-12223
Communications plan --- Design of the public wing of the Oregon State University Hatfield Marine Science Center
[NASA-CR-196435] p 314 N95-12231
Free electron lasers and other advanced sources of light: Scientific research opportunities p 297 N95-12375
Space facilities: Meeting future needs for research, development, and operations
[NASA-CR-194821] p 248 N95-12474
ETRI brochure: History, mission, and activity highlights
p 389 N95-12697
Activities of the Institute for Aerospace Studies of Toronto University p 390 N95-12699
RESEARCH MANAGEMENT
Activities of Lehigh University
[AD-A282098] p 375 N95-13168
RESEARCH PROJECTS
Project Hyreus: Mars sample return mission utilizing in situ propellant production
[NASA-CR-197189] p 383 N95-12826
RESEARCH VEHICLES
Experimental aerodynamic characteristics of a generic hypersonic accelerator configuration at Mach numbers 1.5 and 2.0 --- conducted in the Langley Unitary Plan Wind Tunnel
[NASA-TM-4413] p 233 N95-12770
RESIN MATRIX COMPOSITES
All-hydrocarbon composite resins based on cyclopentadiene
[AD-A282495] p 276 N95-13296
RESINS
Phosphazene-containing amine as curing agent for phthalonitrile-base polymer
[AD-D016375] p 276 N95-13179
RESONANCE
Progress on resonance ionization detection of combustion radicals
[DE94-015339] p 267 N95-12762
Photon production at CDF and D0
[DE94-014985] p 359 N95-13160
Effect of stochastic damping resonance wave packet on energetic alpha particle transport
[DE94-625041] p 370 N95-13538
RESONANCE SCATTERING
Resonant x-ray scattering in 5f magnetism
[DE94-013753] p 358 N95-12829
RESONANT FREQUENCIES
Effects of mass on aircraft sidearm controller characteristics
[NASA-TM-104277] p 244 N95-11868
Study of in-plane dynamics of tires
[PB94-206893] p 304 N95-13410
RESONATORS
High frequency thermoacoustic refrigerator
[AD-A280925] p 279 N95-12772
RESOURCE ALLOCATION
On bottleneck partitioning k-ary n-cubes
[NASA-CR-194966] p 342 N95-12005
RESPIRATION
A numerical analysis of the distribution of stresses in lung parenchyma which accounts for the interactions between the tissue skeleton and flowing air
p 332 N95-11806
Acute inhalation of explosively disseminated carbon fibers in rats
[AD-A280556] p 330 N95-12614
Consequences of prolonged inhalation of ozone on Fischer-344/N rats: Collaborative studies. Part 1: Content and cross-linking of lung collagen
[PB94-182748] p 331 N95-13176
RESPIRATORY PHYSIOLOGY
A numerical analysis of the distribution of stresses in lung parenchyma which accounts for the interactions between the tissue skeleton and flowing air
p 332 N95-11806
RESPONSE TIME (COMPUTERS)
Performance analysis of three dimensional integral equation computations on a massively parallel computer
[NASA-CR-196747] p 346 N95-11863
RETINA
Neural networks: Structure and repair. Part 1: Ground squirrel visual system. Part 2: Formation, maintenance and plasticity of synaptic connections
[AD-A282420] p 330 N95-12393
Ultrashort laser pulse effects in ocular and related media: Laser-induced shock wave propagation and retinal damage
[AD-A282599] p 334 N95-12535
RETIREMENT
Age 60 Rule research. Part 1: Bibliographic database
[DOT/FAA/AM-94/20-PT-1] p 336 N95-13019
Age 60 Rule. Part 2: Airline pilot age and performance. A review of the scientific literature
[DOT/FAA/AM-94/21-PT-2] p 336 N95-13020
REUSABLE LAUNCH VEHICLES
Requirements report for SSTO vertical take-off/horizontal landing vehicle
[NASA-CR-196875] p 251 N95-11777
Liquid flyback booster pre-phase: A study assessment
[NASA-TM-104801] p 248 N95-11934
REUSABLE SPACECRAFT
Ion engine propelled Earth-Mars cycler with nuclear thermal propelled transfer vehicle, volume 2
[NASA-CR-197208] p 361 N95-12665
MOOSE: Manned On-Orbit Servicing Equipment
[NASA-CR-197151] p 254 N95-12790
REVERSE OSMOSIS
Improving the efficiency of high purity water systems
[DE94-013742] p 318 N95-11784

REYNOLDS STRESS
Methods of ensuring realizability for non-realizable second order closures
[NASA-TM-106681] p 291 N95-11935
A new Reynolds stress algebraic equation model
[NASA-TM-106644] p 292 N95-11953
RHEOLOGY
Neotectonics of Asia: Thin-shell finite-element models with faults
[NASA-CR-196436] p 324 N95-12949
Nonlinear hysteresis in an endochronic solid
[AD-A283142] p 325 N95-13136
RIGGING
Mars Equipment Transport System
[NASA-CR-197158] p 301 N95-12554
RIGID ROTORS
Aeroelastic simulation of higher harmonic control
[NASA-CR-4623] p 230 N95-11911
RIGID STRUCTURES
Prediction of geometric-thermal machine tool errors by artificial neural networks
[PB94-186673] p 348 N95-11909
RISK
Test Plan. GCPS Task 4, subtask 4.2 thrust structure development
[NASA-CR-196869] p 251 N95-11833
Case study of risk management in the USAF B-1B bomber program
[AD-A282371] p 377 N95-11944
Conceptual design of an Orbital Debris Defense System
[NASA-CR-197211] p 254 N95-12696
Mean importance measures for groups of events in fault trees
[DE94-015416] p 353 N95-13061
Characteristics of civil aviation atmospheric hazards
p 235 N95-13208
The development of the F100-PW-220 and F110-GE-100 engines: A case study of risk assessment and risk management
[AD-A282467] p 244 N95-13289
ROADS
Study of in-plane dynamics of tires
[PB94-206893] p 304 N95-13410
ROBOT ARMS
Actuability of underactuated manipulators
[AD-A282788] p 300 N95-12526
Robust control of underactuated manipulators: Analysis and implementation
[AD-A282836] p 301 N95-12587
Design and testing of a model CELSS chamber robot
[NASA-CR-197196] p 303 N95-12694
ASPOD modifications of 1993-1994
[NASA-CR-197204] p 254 N95-12698
ROBOT CONTROL
Autonomous motion on wheels
[PB94-191327] p 348 N95-11825
Development of ROBOSIM for academic/industrial use
[NASA-CR-196148] p 349 N95-12470
Robust control of underactuated manipulators: Analysis and implementation
[AD-A282836] p 301 N95-12587
Overview of NASREM: The NASA/NBS standard reference model for telerobot control system architecture re
[PB94-194560] p 303 N95-12854
An iterative approach to multibody simulation dynamics suitable for parallel implementation
[UTIAS-TN-276] p 347 N95-13353
ROBOT DYNAMICS
Object-oriented incremental map-generation for mobile robot navigation
[PB94-190717] p 314 N95-11820
Robust control of underactuated manipulators: Analysis and implementation
[AD-A282836] p 301 N95-12587
Design and testing of a model CELSS chamber robot
[NASA-CR-197196] p 303 N95-12694
An iterative approach to multibody simulation dynamics suitable for parallel implementation
[UTIAS-TN-276] p 347 N95-13353
ROBOT SENSORS
Object-oriented incremental map-generation for mobile robot navigation
[PB94-190717] p 314 N95-11820
Self calibrating autoTRAC
[NASA-CR-196930] p 348 N95-11998
Development of an Automated Nondestructive Inspection (ANDI) system for commercial aircraft, phase 1
[AD-A283500] p 234 N95-12623
ROBOTICS
Self calibrating autoTRAC
[NASA-CR-196930] p 348 N95-11998
A robotic exploration mission to Mars and Phobos
[NASA-CR-197168] p 382 N95-12307
Development of ROBOSIM for academic/industrial use
[NASA-CR-196148] p 349 N95-12470
Minimal fixturing of frictionless assemblies: Complexity and algorithms
[AD-A282724] p 300 N95-12505
Human-like robots for space and hazardous environments
[NASA-CR-197171] p 301 N95-12532
ASPOD modifications of 1993-1994
[NASA-CR-197204] p 254 N95-12698
Project Freebird: An orbital transfer vehicle
[NASA-CR-197201] p 254 N95-12737
Representation, modeling and recognition of outdoor scenes
[AD-A283361] p 350 N95-12884
ROBOTS
Object-oriented incremental map-generation for mobile robot navigation
[PB94-190717] p 314 N95-11820
Autonomous motion on wheels
[PB94-191327] p 348 N95-11825
Essential kinematics for autonomous vehicles
[AD-A282456] p 300 N95-12394
Outdoor landmark recognition using hybrid fractal vision system and neural networks
[AD-A282506] p 349 N95-12395
Actuability of underactuated manipulators
[AD-A282788] p 300 N95-12526
Human-like robots for space and hazardous environments
[NASA-CR-197171] p 301 N95-12532
Overview of NASREM: The NASA/NBS standard reference model for telerobot control system architecture re
[PB94-194560] p 303 N95-12854
Learning one-dimensional geometric patterns under one-sided random misclassification noise
[DE94-014659] p 350 N95-12864
ROBUSTNESS (MATHEMATICS)
Accurate interlaminar stress recovery from finite element analysis
[NASA-TM-109149] p 310 N95-11815
An interpolation theoretic approach to control
[AD-A281465] p 348 N95-11853
Development of homotopy algorithms for fixed-order mixed H2/H(infinity) controller synthesis
[NASA-TP-3507] p 342 N95-11923
Robust control design with real parameter uncertainty using absolute stability theory
[NASA-CR-196971] p 349 N95-12782
Hypersonic vehicle model and control law development using H(infinity) and micron synthesis
[NASA-TM-4562] p 255 N95-12838
ROCK MECHANICS
Nonlinear hysteresis in an endochronic solid
[AD-A283142] p 325 N95-13136
ROCKET ENGINE DESIGN
Nuclear rockets: High-performance propulsion for Mars
[DE94-013642] p 257 N95-11782
Integrated propulsion technology demonstrator. Program plan
[NASA-CR-196870] p 257 N95-11823
Recycle requirements for Nasa's 30 cm xenon ion thruster
[NASA-TM-106668] p 258 N95-12750
SolSTUS: Solar Source Thermal Upper Stage
[NASA-CR-197179] p 257 N95-13581
ROCKET ENGINES
SolSTUS: Solar Source Thermal Upper Stage
[NASA-CR-197179] p 257 N95-13581
ROCKET EXHAUST
Investigation of the effects of solid rocket motor propellant composition on plume signature
[AD-A283365] p 258 N95-12885
ROCKET LININGS
Large-displacement structural durability analyses of simple bend specimen emulating rocket nozzle liners
[NASA-TM-106521] p 312 N95-12818
ROCKET NOZZLES
FDNS code to predict wall heat fluxes or wall temperatures in rocket nozzles
[NASA-CR-196925] p 292 N95-11999
Large-displacement structural durability analyses of simple bend specimen emulating rocket nozzle liners
[NASA-TM-106521] p 312 N95-12818
ROCKET-BORNE INSTRUMENTS
A calibration of the Naval Postgraduate School middle ultraviolet spectrograph and an analysis of the OII 2470 A emission obtained by the middle ultraviolet spectrograph
[AD-A283449] p 354 N95-13144
ROCKS
An estimate of the evolution of the acoustic emission spectrum of rocks on the basis of changes in its average frequency in the process of deformation
p 323 N95-12112
ROLLING CONTACT LOADS
Duplex rolling element bearing mounting for ensuring preload control
[AD-D016402] p 304 N95-13189
ROSAT MISSION
Search for inverse Compton x-rays from the lobes of Fornax A x-rays from radio galaxies straddling the Fanaroff-Riley transition
[NASA-CR-196433] p 385 N95-13023
ROTARY WINGS
The potential of genetic algorithms for conceptual design of rotor systems
[NASA-CR-196813] p 237 N95-11699
ROTATING DISKS
Engine structures analysis software: Component Specific Modeling (COSMO)
[NASA-CR-195378] p 309 N95-11711
ROTATING ENVIRONMENTS
Ion engine propelled Earth-Mars cycler with nuclear thermal propelled transfer vehicle, volume 2
[NASA-CR-197208] p 361 N95-12665
ROTATING PLASMAS
Fusion programs in applied plasma physics
[DE94-015853] p 369 N95-12944
Locked modes in TEXT-U tokamak
[DE94-011595] p 370 N95-13529
ROTOR AERODYNAMICS
Aeroelastic simulation of higher harmonic control
[NASA-CR-4623] p 230 N95-11911
Measurements of atmospheric turbulence effects on tail rotor acoustics
[NASA-TM-108843] p 232 N95-12360
ROTOR DYNAMICS
Aeroelastic simulation of higher harmonic control
[NASA-CR-4623] p 230 N95-11911
Analytical and experimental vibration analysis of a faulty gear system
[NASA-TM-106689] p 300 N95-12377
Presentation of computer code SPIRALI for incompressible, turbulent, plane and spiral grooved cylindrical and face seals p 305 N95-13584
SCISEAL: A CFD code for analysis of fluid dynamic forces in seals p 305 N95-13586
Theoretical versus experimental results for the rotordynamic coefficients of eccentric, smooth, gas annular seal annular gas seals p 307 N95-13603
ROTORS
Ceramic manufacturing: Optimizing a multivariable system
[DE94-015016] p 276 N95-13184
ROVING VEHICLES
Design of an unmanned Martian polar exploration system
[NASA-CR-197160] p 383 N95-12529
Human-like robots for space and hazardous environments
[NASA-CR-197171] p 301 N95-12532
Integral habitat transport system
[NASA-CR-197156] p 339 N95-12629
Space hardware designs, volume 1
[NASA-CR-197209] p 253 N95-12663
RUBIDIUM
Matter-wave interferometry with laser cooled atoms
[AD-A282484] p 360 N95-13178
RUDDERS
The development of a highly reliable power management and distribution system for civil transport aircraft
[NASA-TM-106697] p 243 N95-11867
RUNGE-KUTTA METHOD
Interlaminar stress analysis of dropped-ply laminated plates and shells by a mixed method
[NASA-CR-196851] p 311 N95-11946
RUNWAYS
Additives in bituminous materials and fuel-resistant sealers
[DOT/FAA/CT-94/78] p 273 N95-12131
Marginal aggregates in flexible pavements: Background survey and experimental plan
[DOT/FAA/CT-94/58] p 246 N95-12216
The Balsa bullet: A high speed, low-cost general aviation aircraft for Aeroworld
[NASA-CR-197165] p 240 N95-12638
RURAL AREAS
The Additional Programme on Ammonia
[PB94-193075] p 320 N95-12777
RUSSIAN FEDERATION
JPRS report: Science and technology. Central Eurasia: Life sciences
[JPRS-ULS-93-014] p 318 N95-11743

JPRS report: Science and technology. Central Eurasia: Life sciences
[JPRS-ULS-93-012] p 332 N95-11744
Autonomous power system for remote locations
[DE94-013244] p 361 N95-11779
JPRS report: Science and technology. Central Eurasia: Space
[JPRS-USP-94-006] p 247 N95-12000
JPRS report: Science and technology. Central Eurasia
[JPRS-UST-94-017] p 247 N95-12001
JPRS report: Science and technology. Central Eurasia
[JPRS-UST-94-020] p 389 N95-12002
JPRS report: Science and technology. Central Eurasia
[JPRS-UST-94-019] p 389 N95-12003
RUSSIAN SPACE PROGRAM
JPRS report: Science and technology. Central Eurasia: Space
[JPRS-USP-94-006] p 247 N95-12000

S

S MATRIX THEORY
Study of the nuclear-coulomb low-energy scattering parameters on the basis of the p-matrix approach
[DE94-622811] p 360 N95-13275
SABATIER REACTION
Project Genesis: Mars in situ propellant technology demonstrator mission
[NASA-CR-197166] p 277 N95-12822
Project Hyreus: Mars sample return mission utilizing in situ propellant production
[NASA-CR-197189] p 383 N95-12826
SAFETY
Lidar performance analysis
[NASA-CR-196510] p 362 N95-12390
Cabin fuselage structural design with engine installation and control system
[NASA-CR-197173] p 240 N95-12639
Design and testing of a model CELSS chamber robot
[NASA-CR-197196] p 303 N95-12694
Conceptual design of an Orbital Debris Defense System
[NASA-CR-197211] p 254 N95-12696
SAFETY FACTORS
Illustrated structural application of universal first-order reliability method
[NASA-TP-3501] p 248 N95-11870
Vacuum system operating experience review for fusion applications
[DE94-015267] p 368 N95-12759
Characteristics of civil aviation atmospheric hazards p 235 N95-13208
SAFETY MANAGEMENT
Radiofrequency/microwave radiation biological effects and safety standards: A review
[AD-A282886] p 334 N95-12919
SALINITY
Hydrographic, carbon dioxide, nutrient and productivity measurements from the south Atlantic during July and August of 1991
[PB94-180668] p 328 N95-11900
SALTS
On the isolation of halophilic microorganisms from salt deposits of great geological age p 332 N95-11966
SAMPLING
Provoking and measuring cell losses in ATM systems by importance sampling, control variables and load cycles
[PB94-202520] p 285 N95-13558
SANDS
Marginal aggregates in flexible pavements: Background survey and experimental plan
[DOT/FAA/CT-94/58] p 246 N95-12216
Triaxial and torsional shear test results for sand
[AD-A282725] p 323 N95-12506
SANDWICH STRUCTURES
Stiffnesses of laminated flat plates
[ESDU-94003] p 309 N95-11769
Buckling of flat rectangular orthotropic plates
[ESDU-94005] p 310 N95-11771
SATELLITE ANTENNAS
Experimental evaluation of shape memory alloy actuation technique in adaptive antenna design concepts
[NASA-CR-194983] p 284 N95-12896
SATELLITE ATTITUDE CONTROL
Precision tethered satellite attitude control
[NASA-CR-196850] p 254 N95-12766
Spacecraft attitude determination accuracy from mission experience
[NASA-TM-104613] p 255 N95-12858
SATELLITE COMMUNICATION
Modeling and implementation of a packet routing switch for satellite communications
[AD-A282262] p 282 N95-12412
Preliminary digital control system design for the petite amateur Navy satellite (PANSAT)
[AD-A282804] p 253 N95-12528
RINGSAT
[NASA-CR-197167] p 253 N95-12632
ETRI brochure: History, mission, and activity highlights p 389 N95-12697
SATELLITE CONSTELLATIONS
RINGSAT
[NASA-CR-197167] p 253 N95-12632
SATELLITE DESIGN
RINGSAT
[NASA-CR-197167] p 253 N95-12632
Minuteman 2 launched small satellite
[NASA-CR-197203] p 254 N95-12765
SATELLITE IMAGERY
Parameterization and scaling of Arctic ice conditions in the context of ice-atmosphere processes
[NASA-CR-196831] p 327 N95-11706
Tropical cyclone development and intensification under moderate to strong vertical wind shear
[AD-A282185] p 326 N95-12423
Catalogue of heavy rainfall cases of six inches or more over the continental US during 1993
[NOAA-TR-NESDIS-80] p 327 N95-13095
Estimation of above-ground phytomass in a tropical forest using TM-LANDSAT 5 E HRV-SPOT 1 data
[INPE-5500-TDI/515] p 316 N95-13159
AVHRR/NOAA images to detect and quantify deforestation in Amazon Forest: Relations with TM/LANDSAT data
[INPE-5501-TDI/516] p 316 N95-13350
SATELLITE INSTRUMENTS
Satellite laser ranging and gravity field modeling accuracy
[NASA-CR-196057] p 248 N95-12837
SATELLITE NAVIGATION SYSTEMS
Principles of GPS one-way data processing for high precision positioning applications: Algorithms and software issues p 237 N95-12177
SATELLITE NETWORKS
Systems engineering technology for networks
[NASA-CR-196853] p 280 N95-11804
SATELLITE OBSERVATION
Implementation of a state of the art automated system for the production of cloud/water vapor motion winds from geostationary satellites
[NASA-CR-196817] p 325 N95-11758
Minuteman 2 launched small satellite
[NASA-CR-197203] p 254 N95-12765
Satellite estimates of shortwave surface radiation and atmospheric meteorology for the BOREAS experiment region
[NASA-TM-109132] p 326 N95-12839
Waves in Space Plasmas (WISP)
[NASA-CR-196432] p 369 N95-13024
SATELLITE ORIENTATION
Spacecraft attitude determination accuracy from mission experience
[NASA-TM-104613] p 255 N95-12858
SATELLITE PERTURBATION
Satellite laser ranging and gravity field modeling accuracy
[NASA-CR-196057] p 248 N95-12837
SATELLITE POWER TRANSMISSION
PowerSat: A technology demonstration of a solar power satellite
[NASA-CR-197210] p 253 N95-12661
SATELLITE SOUNDING
Earth Observing System (EOS)/Advanced Microwave Sounding Unit-A (AMSU-A)
[NASA-CR-189379] p 344 N95-12796
SATELLITE TRACKING
A comparison of two sites for the purpose of satellite laser ranging
[AD-A283149] p 299 N95-13139
SATELLITE-BORNE INSTRUMENTS
Earth Observing System (EOS)/Advanced Microwave Sounding Unit-A (AMSU-A)
[NASA-CR-189379] p 344 N95-12796
SATELLITE-BORNE PHOTOGRAPHY
AVHRR/NOAA images to detect and quantify deforestation in Amazon Forest: Relations with TM/LANDSAT data
[INPE-5501-TDI/516] p 316 N95-13350
SATURN (PLANET)
Research in astrophysical processes
[NASA-CR-196773] p 382 N95-12939
SCALARS
Chaotic time series. Part 1: Estimation of invariant properties in state space
[PB94-206966] p 376 N95-13572
SCALE MODELS
Pressure measurements on an F/A-18 twin vertical tail in buffeting flow. Volume 3: Buffet power spectral densities
[AD-A281444] p 230 N95-11829
Laws of infrared similitude
[AD-A282209] p 354 N95-12426
Impingement flow heat transfer measurements of turbine blades using a jet array
[AD-A283450] p 375 N95-12512
Design and construction of a remote piloted flying wing
[NASA-CR-197195] p 241 N95-12695
Computer modelling of cyclic deformation of high-temperature materials
[AD-A282457] p 263 N95-12833
Development of the CSI phase-3 evolutionary model testbed
[NASA-CR-4630] p 256 N95-13195
Mach number control in the High Speed Wind Tunnel of NLR
[PB94-201670] p 246 N95-13243
SCALING LAWS
SuperMariah: A similarity-based method for determining wind, temperature, and humidity profile structure in the surface boundary layer
[AD-A283058] p 327 N95-12997
Scaling fluid content-pressure relations of different fluid systems in porous media
[DE94-013349] p 294 N95-13075
SCANNING ELECTRON MICROSCOPY
Surface roughness characterization of various ceramic fibers using AFM and low voltage SEM
[DE94-013635] p 272 N95-11736
SCANNING TUNNELING MICROSCOPY
Atomic structure modifications of diamond-like nanocomposite films: Observation by Raman spectroscopy, FTIR and STM
[DE94-013732] p 371 N95-11740
Scanning tunneling microscopy/atomic force microscopy for study of nanoscale metal oxide particles (destructive adsorbents)
[AD-A281417] p 357 N95-11851
Application of scanning tunneling microscopy to studies of electrode surfaces
[AD-A282383] p 373 N95-12004
Self assembly of n-alkanethiolate monolayers on silver nano-structures: Determination of the apparent thickness of the monolayer by scanning tunneling microscopy
[AD-A282322] p 274 N95-12417
Nanometer scale phase separation in mixed composition self-assembled monolayers
[AD-A282671] p 266 N95-12514
Electrochemical deposition of metal nano-disk structures using the scanning tunneling microscope
[AD-A282464] p 268 N95-13288
SCATTERING
Small angle neutron scattering in surface-active agents mixtures
[DE94-624057] p 356 N95-11747
Study of the nuclear-coulomb low-energy scattering parameters on the basis of the p-matrix approach
[DE94-622811] p 360 N95-13275
SCATTERING CROSS SECTIONS
Resonant x-ray scattering in 5f magnetism
[DE94-013753] p 358 N95-12829
Inclusive jet and two-jet differential cross sections at CDF
[DE94-015543] p 358 N95-12943
On the charged vector particle scattering on a vector particle
[DE94-622787] p 360 N95-13273
SCENE ANALYSIS
Representation, modeling and recognition of outdoor scenes
[AD-A283361] p 350 N95-12884
Scene analysis: A brief survey
[PB94-205085] p 336 N95-13433
SCHEDULES
Integrated propulsion technology demonstrator. Program plan
[NASA-CR-196870] p 257 N95-11823
SCHEDULING
Scheduling in an input and output queuing three-stage packet switch by using neural networks
[PB94-179413] p 349 N95-12367
An investigation of the use of temporal decomposition in space mission scheduling
[NASA-CR-196420] p 377 N95-12618
SCHLIEREN PHOTOGRAPHY
Interferograms, schlieren, and shadowgraphs constructed from real- and ideal-gas, two- and three-dimensional computed flowfields p 295 N95-11971
Optical analysis of crystal growth
[NASA-CR-196514] p 373 N95-12386

SCHOOLS
Engineering the future with America's high school students p 377 N95-11958
SCHROEDINGER EQUATION
Aspects of long time behaviour of solutions of nonlinear Hamiltonian evolution equations
[PB94-192382] p 352 N95-12808
SCIENTIFIC VISUALIZATION
Parallelization and visual analysis of multidimensional fields: Application to ozone production, destruction, and transport in three dimensions
[NASA-CR-195971] p 320 N95-12798
SCIENTISTS
Technical paper contest for women 1992. Space challenges: Earth and beyond
[NASA-TM-109953] p 386 N95-11955
SCINTILLATING FIBERS
Scintillating fiber detector performance, detector geometries, trigger, and electronics issues for scintillating fiber tracking
[DE94-015525] p 358 N95-12905
SCINTILLATION COUNTERS
Scintillating fiber detector performance, detector geometries, trigger, and electronics issues for scintillating fiber tracking
[DE94-015525] p 358 N95-12905
Development of radiation hard scintillators
[DE94-013204] p 296 N95-13287
SEA ICE
Parameterization and scaling of Arctic ice conditions in the context of ice-atmosphere processes
[NASA-CR-196831] p 327 N95-11706
SEA LEVEL
Final results of the Baltic Sea Level 1990 GPS Campaign. Research works of the SSG 5.147 of the International Association of Geodesy
[REPT-94:2] p 314 N95-11881
SEA SURFACE TEMPERATURE
Reports to the Nation on our changing planet. El Nino and climate prediction, no. 3, spring 1994
p 320 N95-12462
SEALERS
Additives in bituminous materials and fuel-resistant sealers
[DOT/FAA/CT-94/78] p 273 N95-12131
SEALING
Hypersonic engine seal development at NASA Lewis Research Center p 307 N95-13602
SEALS (STOPPERS)
Seals Flow Code Development 1993
[NASA-CP-10136] p 304 N95-13583
Presentation of computer code SPIRALI for incompressible, turbulent, plane and spiral grooved cylindrical and face seals p 305 N95-13584
Code GFACE: Gas lubricated face seals in laminar regime p 305 N95-13585
SCISEAL: A CFD code for analysis of fluid dynamic forces in seals p 305 N95-13586
Environmental and customer-driven seal requirements p 305 N95-13588
Beta testing of MTI seal codes p 305 N95-13589
EG and G and NASA face seal codes comparison p 305 N95-13590
High temperature seal test rig p 247 N95-13593
Computer tools for face seal analyses developed at John Crane p 306 N95-13598
Compressor discharge film riding face seals p 306 N95-13599
High-speed seal and bearing test facility p 247 N95-13601
Hypersonic engine seal development at NASA Lewis Research Center p 307 N95-13602
Theoretical versus experimental results for the rotordynamic coefficients of eccentric, smooth, gas annular seal annular gas seals p 307 N95-13603
Turbomachinery Laboratory Texas A and M University research progress on annular gas seals p 307 N95-13604
Incompressible face seals: Computer code IFACE p 307 N95-13606
Non-contacting gas lubricated face seals for high p x v-values p 308 N95-13609
SEARCH RADAR
Lessons learned from experiments conducted on radar data management systems
[AD-A282896] p 284 N95-12920
SEAT BELTS
The performance of child restraint devices in transport airplane passenger seats
[DOT/FAA/AM-94/19] p 234 N95-12146
SEISMIC WAVES
Nonlinear hysteresis in an endochronic solid
[AD-A283142] p 325 N95-13136
SEISMOLOGY
Preliminary seismicity and focal mechanisms for the Southern Great Basin of Nevada and California, January 1992 - September 1992
[DE94-013589] p 321 N95-11730
SELENIUM
Experimental and theoretical study of neon-like selenium x-ray laser spectral line profiles
[DE94-015327] p 298 N95-12761
SELF ADAPTIVE CONTROL SYSTEMS
The development and application of the self-adaptive grid code, SAGE p 295 N95-11957
Recycle requirements for Nasa's 30 cm xenon ion thruster
[NASA-TM-106668] p 258 N95-12750
Space Station Module Power Management and Distribution System (SSM/PMAD)
[NASA-CR-193991] p 258 N95-12819
SEMICONDUCTING FILMS
Kinetics and characterization of tungsten CVD processes
[PB94-206901] p 271 N95-13411
SEMICONDUCTOR DEVICES
Fabrication of large area Si cylindrical drift detectors
[DE94-013534] p 295 N95-11780
Radiative performance of rare earth garnet thin film selective emitters
[NASA-TM-106722] p 372 N95-11876
Elimination of internal contamination on semiconductor devices (protective coatings)
[DE94-015868] p 275 N95-12945
WOCSDICE 1994: European Workshop on Compound Semiconductor Devices and Integrated Circuits
[AD-A283062] p 288 N95-13052
Semiconductor photodetector device
[AD-D016314] p 288 N95-13174
SEMICONDUCTOR DIODES
Optical Remote Sensing of the Atmosphere. Technical digest 1993. Volume 5: Postconference edition
[AD-A281446] p 314 N95-11831
SEMICONDUCTOR LASERS
High average power parametric frequency conversion-new concepts and new pump sources
[DE94-013652] p 314 N95-11783
Optical Remote Sensing of the Atmosphere. Technical digest 1993. Volume 5: Postconference edition
[AD-A281446] p 314 N95-11831
Stationary plasma thruster ion velocity distribution
[NASA-CR-195379] p 257 N95-11919
Wavelength-encoded processing in semiconductor lasers
[AD-A282649] p 297 N95-12751
Diode-pumped micro-laser arrays
[AD-A282494] p 299 N95-13294
SEMICONDUCTORS (MATERIALS)
Structure and performance of carbon aerogel electrodes
[DE94-014746] p 356 N95-11791
Development of nanostructure fabrication technology and new electron-quantum wave devices
[AD-A281724] p 286 N95-11860
Radiative performance of rare earth garnet thin film selective emitters
[NASA-TM-106722] p 372 N95-11876
Emittance theory for thin film selective emitter
[NASA-TM-106727] p 317 N95-11903
Magneto-optical properties of quantum structures with reduced dimensionality
[AD-A282597] p 376 N95-12553
Diagnostic techniques for semiconductor materials processing
[AD-A282810] p 373 N95-12602
ETRI brochure: History, mission, and activity highlights p 389 N95-12697
Method for laser-assisted etching of III-V and II-VI semiconductor compounds using chlorofluorocarbon ambients
[AD-D016385] p 298 N95-12779
WOCSDICE 1994: European Workshop on Compound Semiconductor Devices and Integrated Circuits
[AD-A283062] p 288 N95-13052
Evaluation of the improvement in the figure of merit of Bi2Te3 - based alloys with addition of ultrafine scattering centers
[DE94-015363] p 374 N95-13059
Role of implantation-induced defects in surface-oriented diffusion of fluorine in silicon
[DE94-014905] p 374 N95-13125
Proceedings of the Eighteenth DOE Solar Photochemistry Research Conference
[DE94-014926] p 318 N95-13126
Origin of optical anisotropy in strained In(x)Ga(1-x)As/InP and In(y)Al(1-y)As/InP heterostructures
[AD-A283152] p 271 N95-13140
Semiconductor photodetector device
[AD-D016314] p 288 N95-13174
SENSITIVITY
SeaWiFS technical report series. Volume 23: SeaWiFS prelaunch radiometric calibration and spectral characterization
[NASA-TM-104566-VOL-23] p 328 N95-12359
Development of UV irradiance standards
[PB94-181005] p 320 N95-12771
Methodology for sensitivity analysis, approximate analysis, and design optimization in CFD for multidisciplinary applications
[NASA-CR-196981] p 294 N95-13201
SENSORIMOTOR PERFORMANCE
Coordinated action in 3-D space
[AD-A281284] p 336 N95-13375
SENSORS
An adaptive optics package designed for astronomical use with a laser guide star tuned to an absorption line of atomic sodium
[DE94-012391] p 363 N95-13532
SEQUENCING
Microbial communities in subsurface environments: Diversity, origin, and evolution
[DE94-013699] p 329 N95-11737
An investigation of the use of temporal decomposition in space mission scheduling
[NASA-CR-196420] p 377 N95-12618
SEQUENTIAL ANALYSIS
Mean importance measures for groups of events in fault trees
[DE94-015416] p 353 N95-13061
SERVICE LIFE
TLIFE: A program for spur, helical and spiral bevel transmission life and reliability modeling
[NASA-CR-4622] p 300 N95-11889
SERVOMECHANISMS
Design of a ZVS PWM inverter for a brushless DC motor in an EMA application
[NASA-CR-195808] p 312 N95-12620
Modular hydraulic control system
[AD-D016401] p 304 N95-13155
SET THEORY
Category theory: The mathematics for the humanities
[PB94-205044] p 353 N95-13560
SHADOWGRAPH PHOTOGRAPHY
A shadowgraph study of the National Launch System's 1 1/2 stage vehicle configuration and Heavy Lift Launch Vehicle configuration --- Using the Marshall Space Flight Center's 14-Inch Trisonic Wind Tunnel
[NASA-RP-1347] p 229 N95-11710
Interferograms, schlieren, and shadowgraphs constructed from real- and ideal-gas, two- and three-dimensional computed flowfields p 295 N95-11971
SHADOWS
Advanced S-Band studies using the TDRSS communications satellite
[NASA-CR-196931] p 281 N95-12010
SHAFTS (MACHINE ELEMENTS)
Analysis of the effects of surface pitting and wear on the vibrations of a gear transmission system
[NASA-TM-106678] p 301 N95-12621
Design and testing of a model CELSS chamber robot
[NASA-CR-197196] p 303 N95-12694
Study of in-plane dynamics of tires
[PB94-206893] p 304 N95-13410
SHAPE MEMORY ALLOYS
A study of the deformation of helical springs under eccentric loading
[AD-A283448] p 312 N95-12511
Experimental evaluation of shape memory alloy actuation technique in adaptive antenna design concepts
[NASA-CR-194983] p 284 N95-12896
SHAPES
Using emergent order to shape a space society p 377 N95-11959
The quadric reference surface: Theory and applications
[AD-A282379] p 351 N95-12007
SHEAR LAYERS
Hypersonic turbulent boundary-layer and free shear database
[NASA-CR-177610] p 292 N95-11992
SHEAR PROPERTIES
Effect of shear lips, loading transitions and test frequency on constant delta K and constant load amplitude fatigue tests
[PB94-192440] p 312 N95-12775
SHEAR STRENGTH
Test methods for textile composites
[NASA-CR-4609] p 262 N95-12793

SHEAR STRESS
Accurate interlaminar stress recovery from finite element analysis
[NASA-TM-109149] p 310 N95-11815
Computation of turbulent boundary layers employing the defect wall-function method
[NASA-CR-4629] p 293 N95-12859
SHEATHS
Anode sheath contributions in plasma thrusters
[AD-A260395] p 364 N95-11837
SHELLS (STRUCTURAL FORMS)
Comparison of symbolic and numerical integration methods for an assumed-stress hybrid shell element
[NASA-CR-195945] p 313 N95-13096
Improved assumed-stress hybrid shell element with drilling degrees of freedom for linear stress, buckling, and free vibration analyses
[NASA-CR-192816] p 313 N95-13163
SHOCK (PHYSIOLOGY)
Summary of the Sixteenth Annual Conference on Shock
[AD-A282643] p 334 N95-12542
SHOCK HEATING
Magnetic field generation in shock waves
[AD-A282234] p 281 N95-12408
SHOCK TUBES
Shock tube investigations of combustion phenomena in supersonic flows
[PB94-175262] p 265 N95-11796
SHOCK WAVE INTERACTION
Validation of the RPLUS3D code for supersonic inlet applications involving three-dimensional shock wave-boundary layer interactions
[NASA-TM-106579] p 233 N95-13058
SHOCK WAVES
Analysis and design of numerical schemes for gas dynamics. 2: Artificial diffusion and discrete shock structure
[NASA-CR-196476] p 290 N95-11874
Magnetic field generation in shock waves
[AD-A282234] p 281 N95-12408
Ultrashort laser pulse effects in ocular and related media: Laser-induced shock wave propagation and retinal damage
[AD-A282599] p 334 N95-12535
Activities of the Institute for Aerospace Studies of Toronto University p 390 N95-12699
SHORT CRACKS
A study of naturally initiating notch root fatigue cracks under spectrum loading
[NAL-PD-SN-9406] p 311 N95-11924
SHORT TAKEOFF AIRCRAFT
Flight investigation of the use of a nose gear jump strut to reduce takeoff ground roll distance of STOL aircraft
[NASA-TM-108819] p 238 N95-12225
A preliminary design proposal for a maritime patrol strike aircraft: MPS-2000 Condor
[NASA-CR-197182] p 241 N95-12689
SHORT WAVE RADIATION
Satellite estimates of shortwave surface radiation and atmospheric meteorology for the BOREAS experiment region
[NASA-TM-109132] p 326 N95-12639
SHUTTLE PALLET SATELLITES
NPS state vector analysis and relative motion plotting software for STS-51
[AD-A282909] p 249 N95-12510
SIDELOBES
Method of phased magnitude correlation using binary sequences
[AD-D016397] p 284 N95-12646
SIGNAL ANALYZERS
Weld acoustic monitor
[AD-D016400] p 356 N95-13154
SIGNAL DETECTION
Monopulse tracker operating characteristics measurement error performance for azimuth tracking
[AD-A281188] p 282 N95-12521
SIGNAL ENCODING
Achieving unequal error protection with convolutional codes
[NASA-CR-196803] p 341 N95-11763
SIGNAL FADING
Advanced S-Band studies using the TDRSS communications satellite
[NASA-CR-196931] p 281 N95-12010
The effect of Rician fading and partial-band interference on noise-normalized fast frequency-hopped MFSK receivers
[AD-A282805] p 283 N95-12601
SIGNAL PROCESSING
The Research Laboratory of Electronics
[AD-A281445] p 386 N95-11830
Optical Remote Sensing of the Atmosphere. Technical digest 1993. Volume 5: Postconference edition
[AD-A281446] p 314 N95-11831
Design of systolic algorithms and architectures for digital signal processing
[PB94-179256] p 346 N95-11838
The design and development of signal-processing algorithms for an airborne x-band Doppler weather radar
[NASA-CR-196888] p 281 N95-12374
Uniform spectral amplitude windowing for hyperbolic frequency modulated waveforms
[AD-A282508] p 355 N95-12396
Investigation of spectral-based techniques for classification of wideband transient signals in additive white Gaussian noise
[AD-A282954] p 283 N95-12592
Study of adaptive high resolution frequency estimation techniques with hydroacoustical applications
[PB94-179512] p 355 N95-12597
5-volt low level serial transceiver
[AD-D016399] p 288 N95-13153
Weld acoustic monitor
[AD-D016400] p 356 N95-13154
Certification of windshear performance with RTCA class D radomes p 235 N95-13206
Uniformisation techniques for integral recurrence equations
[PB94-205069] p 347 N95-13407
SIGNAL TRANSMISSION
Weld acoustic monitor
[AD-D016400] p 356 N95-13154
SIGNATURE ANALYSIS
Analysis of the effects of surface pitting and wear on the vibrations of a gear transmission system
[NASA-TM-106678] p 301 N95-12621
SILANES
Glass reinforced-diallylbisphenol/maleimide composites with modified interphases
[AD-A282496] p 264 N95-13298
SILICATES
Optical and magnetic resonance investigations of 3D ions in single crystal hosts: Candidates for tunable solid-state lasers
[AD-A281726] p 371 N95-11842
SILICON
Silicon-based blue light emitting diode
[AD-A282382] p 286 N95-12009
Influence of electrode geometry on the high-field characteristics of photoconductive silicon wafers
[DE94-014660] p 287 N95-12865
Role of implantation-induced defects in surface-oriented diffusion of fluorine in silicon
[DE94-014905] p 374 N95-13125
SILICON CARBIDES
Surface roughness characterization of various ceramic fibers using AFM and low voltage SEM
[DE94-013635] p 272 N95-11736
Modeling and life prediction methodology for Titanium Matrix Composites subjected to mission profiles
[NASA-TM-109148] p 269 N95-11915
Tensile creep and stress-rupture behavior of polymer derived SiC fibers
[NASA-TM-106692] p 263 N95-12813
The effect of irradiation on the stability and properties of monolithic silicon carbide and SiC(f)/SiC composites up to 25 dpa
[DE94-014568] p 263 N95-12862
Silicon carbide and sicaln heterojunction bipolar transistor structures
[AD-D016403] p 288 N95-13181
Pseudomorphic semiconducting heterostructures from combinations of AlN, GaN and selected SiC polytypes: Theoretical advancement and its coordination with experimental studies of nucleation, growth, characterization and device development
[AD-A281218] p 289 N95-13368
SILICON COMPOUNDS
Investigation of the effects of solid rocket motor propellant composition on plume signature
[AD-A283365] p 258 N95-12885
SILICON DIOXIDE
Certain aspects of the melting, casting and welding of Ni3Al alloys
[DE94-013628] p 269 N95-11897
Elimination of internal contamination on semiconductor devices (protective coatings)
[DE94-015868] p 275 N95-12945
Activities of Lehigh University
[AD-A282098] p 375 N95-13168
SILICON FILMS
Fabrication of large area Si cylindrical drift detectors
[DE94-013534] p 295 N95-11780
SILICON NITRIDES
Equipment for investigation of cryogenic compaction of nanosize silicon nitride powders
[DE94-013593] p 277 N95-13530
SILICON RADIATION DETECTORS
Fabrication of large area Si cylindrical drift detectors
[DE94-013534] p 295 N95-11780
SILVER
Self assembly of n-alkanethiolate monolayers on silver nano-structures: Determination of the apparent thickness of the monolayer by scanning tunneling microscopy
[AD-A282322] p 274 N95-12417
Electrochemical deposition of metal nano-disk structures using the scanning tunneling microscope
[AD-A282464] p 268 N95-13288
Hydrogen bonding and molecular orientation in water/fluorine adlayers on silver(110)
[AD-A282652] p 268 N95-13549
SILVER ALLOYS
A novel lead-free solder replacement
[DE94-013782] p 269 N95-11785
SIMILARITY NUMBERS
SuperMariah: A similarity-based method for determining wind, temperature, and humidity profile structure in the surface boundary layer
[AD-A283058] p 327 N95-12997
SIMPLEX METHOD
Algorithms for mathematical programming
[DE94-013544] p 345 N95-13339
SIMULATED ANNEALING
Constructing combinatorial designs by local search
[PB94-179272] p 351 N95-11839
SIMULATION
Object-oriented technology for compressor simulation
[NASA-TM-106723] p 243 N95-11864
Tactical satellite orbital simulation and requirements study
[AD-A282314] p 282 N95-12416
Numerical time dependent sheet cavitation simulations using a higher order panel method
[PB94-204435] p 294 N95-13249
Provoking and measuring cell losses in ATM systems by importance sampling, control variables and load cycles
[PB94-202520] p 285 N95-13558
SIMULATORS
Analytical investigation of the dynamics of tethered constellations in Earth orbit, phase 2
[NASA-CR-196509] p 252 N95-12106
Development of ROBOSIM for academic/industrial use
[NASA-CR-196148] p 349 N95-12470
Evaluation of alternative in-flight fire suppressants for full-scale testing in simulated aircraft engine nacelles and dry bays
[PB94-203403] p 236 N95-13247
SINE WAVES
Dynamic sine wave response measurements of CRT displays using sinusoidal counterphase modulation
[AD-A282222] p 333 N95-12406
SINGLE CRYSTALS
Optical and magnetic resonance investigations of 3D ions in single crystal hosts: Candidates for tunable solid-state lasers
[AD-A281726] p 371 N95-11842
Fatigue in single crystal nickel superalloys
[AD-A283459] p 270 N95-12546
A brightness comparison of thermionic electron sources in a TEM
[DE94-013300] p 360 N95-13338
SINGLE STAGE TO ORBIT VEHICLES
Test plan. GCPS task 7, subtask 7.1: IHM development
[NASA-CR-196876] p 250 N95-11767
Requirements report for SSTO vertical take-off/horizontal landing vehicle
[NASA-CR-196875] p 251 N95-11777
Test plan. Task 5, subtask 5.2: Early on-orbit TPSdebris impact tests
[NASA-CR-196873] p 251 N95-11802
Selection process for trade study: Graphite Composite Primary Structure (GCPS)
[NASA-CR-196866] p 261 N95-11803
Selection process for trade study: Reusable Hydrogen Composite Tank System (RHCTS)
[NASA-CR-196874] p 251 N95-11809
Damage tolerance of candidate thermoset composites for use on single stage to orbit vehicles
[NASA-TP-3506] p 261 N95-11816
Integrated propulsion technology demonstrator. Program plan
[NASA-CR-196870] p 257 N95-11823
Test Plan. GCPS Task 4, subtask 4.2 thrust structure development
[NASA-CR-196869] p 251 N95-11833
Trade study plan for Graphite Composite Primary Structure (GCPS)
[NASA-CR-196868] p 261 N95-11834
Test Plans. Lightweight Durable TPS: Tasks 1,2,4,5, and 6
[NASA-CR-196867] p 262 N95-11835

Trade study plan for Reusable Hydrogen Composite Tank System (RHCTS)
[NASA-CR-196871] p 252 N95-11945
Various advanced design projects promoting engineering education
[NASA-CR-197170] p 258 N95-12630
Hypersonic vehicle model and control law development using H(infinity) and micron synthesis
[NASA-TM-4562] p 255 N95-12838

SINGULARITY (MATHEMATICS)
A wall interference assessment and correction system
[NASA-CR-196940] p 292 N95-12228
Singularity of the Green dyadics for bi-isotropic
[PB94-184504] p 283 N95-12581

SINTERING
Microwave heating and joining of ceramic cylinders: A mathematical model
[NASA-CR-194962] p 351 N95-11922
Ceramic manufacturing: Optimizing a multivariable system
[DE94-015016] p 276 N95-13184

SITE SELECTION
A comparison of two sites for the purpose of satellite laser ranging
[AD-A283149] p 299 N95-13139

SIZE DETERMINATION
Body dimensions for apparel
[PB94-187739] p 338 N95-11908

SKIDDING
External Device to Incrementally Skid the Habitat (E-DISH)
[NASA-CR-197147] p 301 N95-12625

SKY SURVEYS (ASTRONOMY)
The Two Micron All Sky Survey: Survey rationale and initial testing
[AD-A283514] p 380 N95-12633
Near-infrared imaging of selected areas
[AD-A283519] p 316 N95-12634
Search for extraterrestrial intelligence/High Resolution Microwave Survey team member
[NASA-CR-196478] p 339 N95-13026

SLEEP
Crew factors in flight operations 9: Effects of planned cockpit rest on crew performance and alertness in long-haul operations
[NASA-TM-108839] p 334 N95-12792

SLOTS
Numerical analysis of tangential slot blowing on a generic chined forebody
[NASA-TM-108845] p 231 N95-11927

SMALL SCIENTIFIC SATELLITES
Inner Magnetosphere Imager (IMI) solar terrestrial probe class mission preliminary design study report
[NASA-TM-108464] p 252 N95-11948
Design studies of large aperture, high-resolution Earth science microwave radiometers compatible with small launch vehicles
[NASA-TP-3469] p 315 N95-12379
Converting the Minuteman missile into a small satellite launch system
[NASA-CR-197169] p 249 N95-12531
Minuteman 2 launched small satellite
[NASA-CR-197203] p 254 N95-12765
Lifetime and reentry prediction for the Petite Amateur Navy Satellite (PANSAT)
[AD-A283366] p 255 N95-12921

SMART STRUCTURES
Army Research Office Workshop on Dynamic Response of Composite Structures
[AD-A281471] p 262 N95-11854
Experimental evaluation of shape memory alloy actuation technique in adaptive antenna design concepts
[NASA-CR-194983] p 284 N95-12896

SMOKE
Simultaneous gas-chromatographic determination of four toxic gases generally present in combustion atmospheres
[DOT/FAA/AM-94/18] p 338 N95-12354

SNOW
Bibliography on cold regions science and technology, volume 47, part 1
[AD-A281879] p 378 N95-13167

SOCIOLOGY
Using emergent order to shape a space society
p 377 N95-11959

SODIUM
Evaluation of alternative in-flight fire suppressants for full-scale testing in simulated aircraft engine nacelles and dry bays
[PB94-203403] p 236 N95-13247

SOFTWARE ENGINEERING
Software analysis handbook: Software complexity analysis and software reliability estimation and prediction
[NASA-TM-104799] p 339 N95-11914
Real world software engineering
[AD-A282365] p 342 N95-11941
Development of a change management system
p 377 N95-11963
An experimental environment for software engineering
[INPE-5540-TDI/528] p 343 N95-12300
Guided Approach to Instructional Design Advising (GAIDA): How to create GAIDA compatible lessons, volume 2
[AD-A282645] p 343 N95-12500
Experiments with formal methods in software engineering
[PB94-192416] p 344 N95-12774
Second Dependable Software Technology Exchange
[AD-A283367] p 344 N95-12922
An examination of selected software testing tools: 1993 supplement
[AD-A283060] p 344 N95-13051
Reliability allocation for a system using Markov analysis
[PB94-205051] p 309 N95-13406
Recovery blocks
[PB94-205077] p 345 N95-13432

SOFTWARE RELIABILITY
Software analysis handbook: Software complexity analysis and software reliability estimation and prediction
[NASA-TM-104799] p 339 N95-11914
Space Station Module Power Management and Distribution System (SSM/PMAD)
[NASA-CR-193991] p 258 N95-12819
Second Dependable Software Technology Exchange
[AD-A283367] p 344 N95-12922

SOFTWARE TOOLS
Principles of GPS one-way data processing for high precision positioning applications: Algorithms and software issues p 237 N95-12177
HLLV avionics requirements study and electronic filing system database development
[NASA-CR-193993] p 243 N95-13027
An examination of selected software testing tools: 1993 supplement
[AD-A283060] p 344 N95-13051
Methodology for sensitivity analysis, approximate analysis, and design optimization in CFD for multidisciplinary applications
[NASA-CR-196981] p 294 N95-13201
Computer tools for face seal analyses developed at John Crane p 306 N95-13598

SOIL EROSION
Use of remote sensing and geographic information system techniques in integrated studies of watersheds
[INPE-5494-TDI/511] p 316 N95-13352

SOIL SCIENCE
Effects of sample formulation on the analysis of heavy metals by x-ray fluorescence
[AD-A282733] p 267 N95-12836
Factors influencing the rates, processes and magnitude of accumulation of carbon in desert soils
[NASA-CR-196820] p 325 N95-13025

SOILS
Triaxial and torsional shear test results for sand
[AD-A282725] p 323 N95-12506
Effects of sample formulation on the analysis of heavy metals by x-ray fluorescence
[AD-A282733] p 267 N95-12836
CESIUM-137 and natural radionuclides in soils from Southern Brazil and in soils and others environmental samples from Antarctic
[INPE-5505-TDI-517] p 321 N95-13192

SOL-GEL PROCESSES
Design, synthesis and characterization of novel nonlinear optical polymers
[AD-A282201] p 274 N95-12424

SOLAR ACTIVITY
Solar influences on global change
[NASA-CR-196966] p 319 N95-12384

SOLAR ACTIVITY EFFECTS
Solar influences on global change
[NASA-CR-196966] p 319 N95-12384

SOLAR ARRAYS
PASP PLUS Transient Pulse Monitor (TPM): Preflight characterization report
[AD-A282582] p 283 N95-12550
ASPOD modifications of 1993-1994
[NASA-CR-197204] p 254 N95-12698

SOLAR ATMOSPHERE
FNAS UAH UVSP and complimentary data analysis and modeling
[NASA-CR-194005] p 381 N95-12992

SOLAR CELLS
Introduction to magnetic bearings
[NASA-CR-197187] p 302 N95-12640
Solar radiation data manual for flat-plate and concentrating collectors
[DE93-018229] p 317 N95-12647
Hypersonic Gas-Surface Energy Accommodation Test Facility
[DE94-014468] p 232 N95-12652
PowerSat: A technology demonstration of a solar power satellite
[NASA-CR-197210] p 253 N95-12661
Proceedings of the 36th Power Sources Conference
[AD-A281443] p 288 N95-13164

SOLAR CORONA
Structure and dynamics of the solar corona
[NASA-CR-196978] p 384 N95-13582

SOLAR ENERGY
A model of the density of solar radiation energy on an arbitrary plane identification for Warsaw
p 384 N95-12243
Introduction to magnetic bearings
[NASA-CR-197187] p 302 N95-12640
Solar radiation data manual for flat-plate and concentrating collectors
[DE93-018229] p 317 N95-12647

SOLAR ENERGY CONVERSION
PowerSat: A technology demonstration of a solar power satellite
[NASA-CR-197210] p 253 N95-12661
Proceedings of the Eighteenth DOE Solar Photochemistry Research Conference
[DE94-014926] p 318 N95-13126
SolSTUS: Solar Source Thermal Upper Stage
[NASA-CR-197179] p 257 N95-13581

SOLAR FLARES
BATSE observations of 3C273
[NASA-CR-196185] p 380 N95-12463
FNAS UAH UVSP and complimentary data analysis and modeling
[NASA-CR-194005] p 381 N95-12992

SOLAR MAXIMUM MISSION
FNAS UAH UVSP and complimentary data analysis and modeling
[NASA-CR-194005] p 381 N95-12992

SOLAR OBSERVATORIES
Solar-Terrestrial Environment Laboratory, Nagoya University p 389 N95-12610

SOLAR PLANETARY INTERACTIONS
Pioneer Venus orbiter electron temperature probe
[NASA-CR-196844] p 257 N95-11805

SOLAR POWER SATELLITES
PowerSat: A technology demonstration of a solar power satellite
[NASA-CR-197210] p 253 N95-12661

SOLAR RADIATION
A model of the density of solar radiation energy on an arbitrary plane identification for Warsaw
p 384 N95-12243
Solar influences on global change
[NASA-CR-196966] p 319 N95-12384
Development of UV irradiance standards
[PB94-181005] p 320 N95-12771

SOLAR RADIATION SHIELDING
A magnetic shield/dual purpose mission
[NASA-CR-197192] p 255 N95-13006

SOLAR SAILS
Space hardware designs, volume 1
[NASA-CR-197209] p 253 N95-12663

SOLAR SYSTEM
Exploring the parallelism exposed by partial evaluation
[AD-A282284] p 347 N95-12414

SOLAR TERRESTRIAL INTERACTIONS
Solar-Terrestrial Environment Laboratory, Nagoya University p 389 N95-12610

SOLAR WIND
An observational test of magnetospheric magnetic field mapping
[DE94-014461] p 324 N95-12649
Structure and dynamics of the solar corona
[NASA-CR-196978] p 384 N95-13582

SOLAR-PUMPED LASERS
Spaceborne Photonics Institute
[NASA-CR-196784] p 362 N95-12659

SOLDERS
A novel lead-free solder replacement
[DE94-013782] p 269 N95-11785

SOLENOIDS
Velocity spread of REB generated by high current diode
[IPPCZ-339] p 364 N95-11886

SOLID CRYOGENS
Advanced cryogenic propellants
[AD-A282451] p 277 N95-12729

SOLID ELECTROLYTES
Effect of operating parameters and anode gas impurities upon polymer electrolyte fuel cells
[DE94-014464] p 317 N95-12650

SOLID LUBRICANTS
High temperature solid lubricant materials for heavy duty and advanced heat engines
[NASA-TM-106570] p 260 N95-12764

Glass microsphere lubrication
[NASA-CR-197157] p 277 N95-13508

SOLID MECHANICS
Activities of the Institute for Aerospace Studies of Toronto University p 390 N95-12699

SOLID PHASES
Atomic scale dynamics of a two-dimensional gas-solid interface
[AD-A282646] p 358 N95-12617
A CRAMPS and 13C CP/MAS NMR examination of solid-solid transitions in n-Hexatriacontane (C36H74)
[AD-A282497] p 375 N95-13299

SOLID PROPELLANT COMBUSTION
Investigation of the effects of solid rocket motor propellant composition on plume signature
[AD-A283365] p 258 N95-12885

SOLID PROPELLANT ROCKET ENGINES
Liquid flyback booster pre-phase: A study assessment
[NASA-TM-104801] p 248 N95-11934
Computational flow predictions for hypersonic drag devices p 233 N95-11967
AFOSR Contractors Meeting in Propulsion
[AD-A282729] p 257 N95-12507

SOLID STATE
Structure and performance of carbon aerogel electrodes
[DE94-014746] p 356 N95-11791

SOLID STATE DEVICES
Airport surveillance using a solid state coherent lidar p 235 N95-13207

SOLID STATE LASERS
Optical and magnetic resonance investigations of 3D ions in single crystal hosts: Candidates for tunable solid-state lasers
[AD-A281726] p 371 N95-11842
The future of diode pumped solid state lasers and their applicability to the automotive industry
[DE94-014736] p 298 N95-12868
Tetravalent chromium (Cr(4+)) as laser-active ion for tunable solid-state lasers
[NASA-CR-196481] p 298 N95-12951
Wake vortex detection at Denver Stapleton Airport with a pulsed 2-micron coherent lidar p 236 N95-13211
Diode-pumped micro-laser arrays
[AD-A282494] p 299 N95-13294

SOLID STATE PHYSICS
The Research Laboratory of Electronics
[AD-A281445] p 386 N95-11830
Synthesis and solid-state NMR characterization of 13C- and 15N-labelled n-methylphthalimide: A model compound for studying polyimides
[AD-A282510] p 273 N95-12397
Laser physics of Nd(exp 3+)-doped phosphate glasses
[DE94-015141] p 299 N95-13534

SOLID SURFACES
Polyatomic ion impact on solid surfaces and related phenomena
[PB94-201258] p 360 N95-13242

SOLID WASTES
MSW to hydrogen — municiple solid waste (MSW)
[DE94-014741] p 265 N95-11790

SOLIDS
Time-resolved electron thermal conduction by probing of plasma formation in transparent solids with high power subpicosecond laser pulses
[DE94-015170] p 370 N95-13555

SOLUBILITY
Thianthrene-based poly(benzoxazole)s
[AD-A282326] p 274 N95-12419

SOLVENT EXTRACTION
Supercritical fluid (SCF) technologies: Assessment of applicability to installation restoration processes
[AD-A281504] p 290 N95-11859
CeO2-ZrO2 powder synthesis by way of alcohol dehydration of aqueous salt solutions
[INPE-5484-PRE/1783] p 276 N95-13191

SOLVENTS
Trichloroethylene emissions reductions achieved by enclosing solvent spray degreasing operations
[DE94-013741] p 318 N95-11742

SONAR
Uniform spectral amplitude windowing for hyperbolic frequency modulated waveforms
[AD-A282508] p 355 N95-12396

SONOLUMINESCENCE
Synchronous picosecond sonoluminescence
[AD-A281496] p 355 N95-11856

SORBENTS
Triple sorbent thermal desorption/gas chromatography/mass spectrometry determination of vapor phase organic contaminants
[DE94-013634] p 264 N95-11735

SOUND PRESSURE
High frequency thermoacoustic refrigerator
[AD-A280925] p 279 N95-12772
Effects of Noise on Hearing 5th International Symposium
[AD-A281439] p 335 N95-13177

SOUND WAVES
En route noise levels from propfan test assessment airplane
[NASA-TP-3451] p 355 N95-12341
Weld acoustic monitor
[AD-D016400] p 356 N95-13154

SOUNDING
200 MHz channel sounder, open description
[PB94-202538] p 285 N95-13559

SOUTHERN HEMISPHERE
Tactical satellite orbital simulation and requirements study
[AD-A282314] p 282 N95-12416

SOUTHERN OSCILLATION
Reports to the Nation on our changing planet. El Nino and climate prediction, no. 3, spring 1994 p 320 N95-12462

SOYBEANS
Methodologies for processing plant material into acceptable food on a small scale
[NASA-CR-177647] p 338 N95-12132

SPACE COMMERCIALIZATION
Environmental process improvement feasibility study and demonstration program
[NASA-CR-196789] p 319 N95-12110
Cryogenic On-Orbit Liquid Depot Storage, Acquisition, and Transfer Satellite (COLD-SAT)
[NASA-CR-185249] p 259 N95-13237

SPACE COMMUNICATION
Tactical satellite orbital simulation and requirements study
[AD-A282314] p 282 N95-12416

SPACE DEBRIS
Contributions to CD Space Committee, 1993. Summary and comments
[PB94-190618] p 379 N95-11871
Conceptual design of an Orbital Debris Defense System
[NASA-CR-197211] p 254 N95-12696
ASPOD modifications of 1993-1994
[NASA-CR-197204] p 254 N95-12698

SPACE ENVIRONMENT SIMULATION
Development of the CSI phase-3 evolutionary model testbed
[NASA-CR-4630] p 256 N95-13195

SPACE ERECTABLE STRUCTURES
Various advanced design projects promoting engineering education
[NASA-CR-197170] p 258 N95-12630

SPACE EXPLORATION
Aeronautics and space technology, past, present, and future p 229 N95-11892
Interviews with the Apollo lunar surface astronauts in support of planning for EVA systems design
[NASA-TM-108846] p 337 N95-11905
Activities of the Space Studies Board of the National Research Council
[NASA-CR-195738] p 247 N95-12880

SPACE FLIGHT STRESS
Effect of decreased gravity on circulation in the rat
[NASA-CR-196946] p 331 N95-12827
Spaceflight and immune responses of Rhesus monkeys
[NASA-CR-196846] p 331 N95-12941

SPACE HABITATS
External Device to Incrementally Skid the Habitat (E-DISH)
[NASA-CR-197147] p 301 N95-12625
Integral habitat transport system
[NASA-CR-197156] p 339 N95-12629

SPACE HEATING (BUILDINGS)
Autonomous power system for remote locations
[DE94-013244] p 361 N95-11779

SPACE LABORATORIES
The Biological Flight Research Facility p 247 N95-11961

SPACE MANUFACTURING
Phase A design study of microgravity fluoride fiber puller
[NASA-CR-196513] p 279 N95-12752

SPACE MISSIONS
Evaluation of COSTAR mass handling characteristics in an environment. A simulation of the Hubble Space Telescope service mission
[NASA-TP-3489] p 333 N95-11887
An investigation of the use of temporal decomposition in space mission scheduling
[NASA-CR-196420] p 377 N95-12618
Proposal for the design of a zero gravity tool storage device
[NASA-CR-197150] p 302 N95-12627

SPACE PERCEPTION
How are three-dimensional objects represented in the brain?
[AD-A282367] p 335 N95-11942

SPACE PLASMAS
Magnetospheric space plasma investigations
[NASA-CR-196793] p 382 N95-12940
Waves in Space Plasmas (WISP)
[NASA-CR-196432] p 369 N95-13024

SPACE PROBES
A robotic exploration mission to Mars and Phobos
[NASA-CR-197168] p 382 N95-12307

SPACE PROCESSING
Ground based research in microgravity materials processing
[NASA-CR-196815] p 278 N95-11759
Research activities of the Center for the Space Processing of Engineering Materials
[NASA-CR-196484] p 259 N95-11891
Optical analysis of crystal growth
[NASA-CR-196514] p 373 N95-12386
Various advanced design projects promoting engineering education
[NASA-CR-197170] p 258 N95-12630
An examination of anticipated g-jitter on Space Station and its effects on materials processes
[NASA-TM-103775] p 278 N95-12703
Phase A design study of microgravity fluoride fiber puller
[NASA-CR-196513] p 279 N95-12752

SPACE RENDEZVOUS
NPS state vector analysis and relative motion plotting software for STS-51
[AD-A282909] p 249 N95-12510

SPACE SHUTTLE BOOSTERS
Liquid flyback booster pre-phase: A study assessment
[NASA-TM-104801] p 248 N95-11934

SPACE SHUTTLE MISSION 51-L
Memorial service for the mission 51-L crew (edited)
[NASA-TM-109900] p 250 N95-13133

SPACE SHUTTLE MISSIONS
Infrared spectral measurement of Space Shuttle glow
[AD-A282883] p 250 N95-12917
Lifetime and reentry prediction for the Petite Amateur Navy Satellite (PANSAT)
[AD-A283366] p 255 N95-12921
STS-65 mission highlights resource tape
[NASA-TM-108589] p 250 N95-13130
STS-68 post flight presentation
[NASA-TM-109959] p 250 N95-13131

SPACE SHUTTLE ORBITERS
An axisymmetric analog two-layer convective heating procedure with application to the evaluation of Space Shuttle Orbiter wing leading edge and windward surface heating
[NASA-CR-188343] p 251 N95-11937
Modelling and simulation of Space Station Freedom berthing dynamics and control
[NASA-TM-109151] p 252 N95-11947
Proposal for the design of a zero gravity tool storage device
[NASA-CR-197150] p 302 N95-12627
Space Shuttle: NASA's plans for repairing or replacing a damaged or destroyed orbiter. Report to the Chairman, Subcommittee on Investigations and Oversight, Committee on Science, Space, and Technology, House of Representatives
[GAO/NSIAD-94-197] p 249 N95-12851

SPACE SHUTTLE PAYLOADS
Human factors assessments of the STS-57 SpaceHab-1 mission
[NASA-TM-104802] p 337 N95-11878
STS propellant densification feasibility study data book
[NASA-TM-108467] p 278 N95-12857

SPACE SHUTTLES
NPS state vector analysis and relative motion plotting software for STS-51
[AD-A282909] p 249 N95-12510
Orion: Design of a system for assured low-cost human access to space
[NASA-CR-197185] p 253 N95-12564
Introduction to magnetic bearings
[NASA-CR-197187] p 302 N95-12640
Conceptual design of an Orbital Debris Defense System
[NASA-CR-197211] p 254 N95-12696
MOOSE: Manned On-Orbit Servicing Equipment
[NASA-CR-197151] p 254 N95-12790
Infrared spectral measurement of Space Shuttle glow
[AD-A282883] p 250 N95-12917
White Sands Test Facility
[NASA-TM-109901] p 249 N95-13129
STS-61 mission highlights resource tape
[NASA-TM-109963] p 250 N95-13132

SPACE STATION FREEDOM
A model-based expert system for space power distribution diagnostics
[NASA-CR-195336] p 342 N95-11918
Modelling and simulation of Space Station Freedom berthing dynamics and control
[NASA-TM-109151] p 252 N95-11947
An examination of anticipated g-jitter on Space Station and its effects on materials processes
[NASA-TM-103775] p 278 N95-12703
Space Station Freedom propulsion activities
[NASA-TM-106604] p 256 N95-13236
SPACE STATION PAYLOADS
The Biological Flight Research Facility
p 247 N95-11961
Life Sciences Centrifuge Facility assessment
[NASA-CR-196848] p 332 N95-13423
SPACE STATION POWER SUPPLIES
A model-based expert system for space power distribution diagnostics
[NASA-CR-195336] p 342 N95-11918
SPACE STATIONS
Analytical investigation of the dynamics of tethered constellations in Earth orbit, phase 2
[NASA-CR-196509] p 252 N95-12106
Status of hollow cathode heater development for the Space Station plasma contactor
[NASA-CR-195364] p 258 N95-12622
Introduction to magnetic bearings
[NASA-CR-197187] p 302 N95-12640
Optimization of aerospace structures
[NASA-CR-196763] p 242 N95-12787
Space Station Module Power Management and Distribution System (SSM/PMAD)
[NASA-CR-193991] p 258 N95-12819
Spacecraft maximum allowable concentrations for selected airborne contaminants, volume 1
[NASA-CR-196446] p 255 N95-12879
Activities of the Space Studies Board of the National Research Council
[NASA-CR-195738] p 247 N95-12880
Life Sciences Centrifuge Facility assessment
[NASA-CR-196848] p 332 N95-13423
SPACE STORAGE
Cryogenic On-Orbit Liquid Depot Storage, Acquisition, and Transfer satellite (COLD-SAT) feasibility study
[NASA-CR-185247] p 256 N95-13232
Feasibility study for a Cryogenic On-Orbit Liquid Depot-Storage, Acquisition and Transfer (COLD-SAT) satellite
[NASA-CR-185248] p 294 N95-13233
SPACE SUITS
Interviews with the Apollo lunar surface astronauts in support of planning for EVA systems design
[NASA-TM-108846] p 337 N95-11905
Meeting the challenge of manned lunar and Martian exploration p 339 N95-11970
SPACE TOOLS
Mars Equipment Transport System
[NASA-CR-197158] p 301 N95-12554
SPACE TRANSPORTATION
Design of an unmanned Martian polar exploration system
[NASA-CR-197160] p 383 N95-12529
Orion: Design of a system for assured low-cost human access to space
[NASA-CR-197185] p 253 N95-12564
Fusion powered human transport to Mars (UWFR94)
[NASA-CR-197184] p 368 N95-12641
Ion engine propelled Earth-Mars cycler with nuclear thermal propelled transfer vehicle, volume 2
[NASA-CR-197208] p 361 N95-12665
Cryogenic On-Orbit Liquid Depot Storage, Acquisition, and Transfer Satellite (COLD-SAT)
[NASA-CR-185249] p 259 N95-13237
SPACE TRANSPORTATION SYSTEM
A revolutionary lunar space transportation system architecture using extraterrestrial LOX-augmented NTR propulsion
[NASA-TM-106726] p 249 N95-11703
STS propellant densification feasibility study data book
[NASA-TM-108467] p 278 N95-12857
STS-65 mission highlights resource tape
[NASA-TM-108589] p 250 N95-13130
STS-61 mission highlights resource tape
[NASA-TM-109963] p 250 N95-13132
Cryogenic On-Orbit Liquid Depot Storage, Acquisition, and Transfer Satellite (COLD-SAT)
[NASA-CR-185249] p 259 N95-13237
SPACE TRANSPORTATION SYSTEM FLIGHTS
Evaluation of COSTAR mass handling characteristics in an environment. A simulation of the Hubble Space Telescope service mission
[NASA-TP-3489] p 333 N95-11887
Debris/ice/TPS assessment and integrated photographic analysis of Shuttle Mission STS-65
[NASA-TM-109205] p 249 N95-12224
STS-68 post flight presentation
[NASA-TM-109959] p 250 N95-13131
STS-61 mission highlights resource tape
[NASA-TM-109963] p 250 N95-13132
SPACE WEAPONS
Vulnerability assessment of a space based weapon platform electronics system exposed to a thermonuclear weapon detonation
[DE94-013415] p 250 N95-11755
SPACE-TIME FUNCTIONS
Particle-production mechanism in relativistic heavy-ion collisions
[DE94-014427] p 359 N95-13104
SPACEBORNE ASTRONOMY
X-ray and gamma ray astronomy detectors
[NASA-SP-517] p 379 N95-12304
BATSE observations of 3C273
[NASA-CR-196185] p 380 N95-12463
FOC SV support and science data analysis
[NASA-CR-196764] p 381 N95-12821
Search for extraterrestrial intelligence/High Resolution Microwave Survey team member
[NASA-CR-196478] p 339 N95-13026
SPACEBORNE EXPERIMENTS
Training for life science experiments in space at the NASA Ames Research Center p 339 N95-11964
The rhesus measurement system: A new instrument for space research p 247 N95-11965
STEP: An international collaboration in fundamental physics p 354 N95-12229
Lunar Lander project: A study on future manned missions to the Moon
[NASA-CR-197177] p 383 N95-12362
GASCAN 2 payload integration
[NASA-CR-197200] p 278 N95-12701
Cryogenic On-Orbit Liquid Depot Storage, Acquisition, and Transfer satellite (COLD-SAT) feasibility study
[NASA-CR-185247] p 256 N95-13232
Feasibility study for a Cryogenic On-Orbit Liquid Depot-Storage, Acquisition and Transfer (COLD-SAT) satellite
[NASA-CR-185248] p 294 N95-13233
SPACEBORNE LASERS
Lidar performance analysis
[NASA-CR-196510] p 362 N95-12390
Spaceborne Photonics Institute
[NASA-CR-196784] p 362 N95-12659
SPACECRAFT ANTENNAS
Design studies of large aperture, high-resolution Earth science microwave radiometers compatible with small launch vehicles
[NASA-TP-3469] p 315 N95-12379
SPACECRAFT BREAKUP
Lifetime and reentry prediction for the Petite Amateur Navy Satellite (PANSAT)
[AD-A283366] p 255 N95-12921
SPACECRAFT CABIN ATMOSPHERES
Carbon dioxide and water vapor production at rest and during exercise. A report on data collection for the Crew and Thermal Systems Division
[NASA-TP-3500] p 337 N95-11811
Spacecraft maximum allowable concentrations for selected airborne contaminants, volume 1
[NASA-CR-196446] p 255 N95-12879
SPACECRAFT CHARGING
Detailed component design for a Compact Environmental Anomaly Sensor (CEASE)
[AD-A283144] p 256 N95-13138
SPACECRAFT CONSTRUCTION MATERIALS
Damage tolerance of candidate thermoset composites for use on single stage to orbit vehicles
[NASA-TP-3506] p 261 N95-11816
Modeling and life prediction methodology for Titanium Matrix Composites subjected to mission profiles
[NASA-TM-109148] p 269 N95-11915
Test model designs for advanced refractory ceramic materials p 277 N95-11968
Evaluation of wiring constructions for space applications
[NASA-TM-106735] p 256 N95-13194
SPACECRAFT CONTAMINATION
Spacecraft maximum allowable concentrations for selected airborne contaminants, volume 1
[NASA-CR-196446] p 255 N95-12879
SPACECRAFT CONTROL
Modelling and simulation of Space Station Freedom berthing dynamics and control
[NASA-TM-109151] p 252 N95-11947
SPACECRAFT DESIGN
Trade study plan for Reusable Hydrogen Composite Tank System (RHCTS)
[NASA-CR-196871] p 252 N95-11945
Inner Magnetosphere Imager (IMI) solar terrestrial probe class mission preliminary design study report
[NASA-TM-108484] p 252 N95-11948
STEP: An international collaboration in fundamental physics p 354 N95-12229
Lunar Lander project: A study on future manned missions to the Moon
[NASA-CR-197177] p 383 N95-12362
Design of an unmanned Martian polar exploration system
[NASA-CR-197160] p 383 N95-12529
Venus cloud bobber mission: A long term survey of the Venusian surface
[NASA-CR-197174] p 383 N95-12533
Orion: Design of a system for assured low-cost human access to space
[NASA-CR-197185] p 253 N95-12564
Fusion powered human transport to Mars (UWFR94)
[NASA-CR-197184] p 368 N95-12641
Space hardware designs, volume 1
[NASA-CR-197209] p 253 N95-12663
Ion engine propelled Earth-Mars cycler with nuclear thermal propelled transfer vehicle, volume 2
[NASA-CR-197208] p 361 N95-12665
ASPOD modifications of 1993-1994
[NASA-CR-197204] p 254 N95-12698
Project Freebird: An orbital transfer vehicle
[NASA-CR-197201] p 254 N95-12737
Optimization of aerospace structures
[NASA-CR-196763] p 242 N95-12787
Feasibility study for a Cryogenic On-Orbit Liquid Depot-Storage, Acquisition and Transfer (COLD-SAT) satellite
[NASA-CR-185248] p 294 N95-13233
SPACECRAFT DOCKING
Modelling and simulation of Space Station Freedom berthing dynamics and control
[NASA-TM-109151] p 252 N95-11947
SPACECRAFT ELECTRONIC EQUIPMENT
Activities of the Helsinski University of Technology, Applied Electronics Laboratory
[PB94-179074] p 385 N95-11797
An avionics scenario and command model description for Space Generic Open Avionics Architecture (SGOAA)
[NASA-CR-188330] p 242 N95-11913
SPACECRAFT ENVIRONMENTS
Human factors assessments of the STS-57 SpaceHab-1 mission
[NASA-TM-104802] p 337 N95-11878
SPACECRAFT EQUIPMENT
Design and application of electromechanical actuators for deep space missions
[NASA-CR-196791] p 299 N95-11701
Linear Proof Mass Actuator
[NASA-TM-109143] p 310 N95-11814
Stepper motor
[NASA-CR-189373] p 287 N95-12795
SPACECRAFT GLOW
Infrared spectral measurement of Space Shuttle glow
[AD-A282883] p 250 N95-12917
SPACECRAFT INSTRUMENTS
SeaWiFS technical report series. Volume 19: Case studies for SeaWiFS calibration and validation, part 2
[NASA-TM-104566-VOL-19-PT-2] p 328 N95-11920
Design studies of large aperture, high-resolution Earth science microwave radiometers compatible with small launch vehicles
[NASA-TP-3469] p 315 N95-12379
Development of techniques for the in situ observation of OH and HO2 for studies of the impact of high-altitude supersonic aircraft on the stratosphere
[NASA-CR-196759] p 321 N95-12832
Spacecraft attitude determination accuracy from mission experience
[NASA-TM-104613] p 255 N95-12858
Detailed component design for a Compact Environmental Anomaly Sensor (CEASE)
[AD-A283144] p 256 N95-13138
SPACECRAFT LANDING
STS-65 mission highlights resource tape
[NASA-TM-108589] p 250 N95-13130
SPACECRAFT LAUNCHING
Liquid flyback booster pre-phase: A study assessment
[NASA-TM-104801] p 248 N95-11934
Environmental process improvement feasibility study and demonstration program
[NASA-CR-196789] p 319 N95-12110
Converting the Minuteman missile into a small satellite launch system
[NASA-CR-197169] p 249 N95-12531
Minuteman 2 launched small satellite
[NASA-CR-197203] p 254 N95-12765
STS-65 mission highlights resource tape
[NASA-TM-108589] p 250 N95-13130

SPACECRAFT LUBRICATION
Space hardware designs, volume 1
[NASA-CR-197209] p 253 N95-12663
Glass microsphere lubrication
[NASA-CR-197157] p 277 N95-13508
SPACECRAFT MAINTENANCE
Test plan. GCPS task 7, subtask 7.1: IHM development
[NASA-CR-106876] p 250 N95-11767
MOOSE: Manned On-Orbit Servicing Equipment
[NASA-CR-197151] p 254 N95-12790
Space Shuttle: NASA's plans for repairing or replacing a damaged or destroyed orbiter. Report to the Chairman, Subcommittee on Investigations and Oversight, Committee on Science, Space, and Technology, House of Representatives
[GAO/NSIAD-94-197] p 249 N95-12851
SPACECRAFT MODELS
Development of the CSI phase-3 evolutionary model testbed
[NASA-CR-4630] p 256 N95-13195
SPACECRAFT MODULES
Mars Equipment Transport System
[NASA-CR-197158] p 301 N95-12554
Project Freebird: An orbital transfer vehicle
[NASA-CR-197201] p 254 N95-12737
SPACECRAFT ORBITS
Project ECHO: Electronic Communications from Halo Orbit
[NASA-CR-197190] p 283 N95-12644
SPACECRAFT POWER SUPPLIES
Space Station Module Power Management and Distribution System (SSM/PMAD)
[NASA-CR-193991] p 258 N95-12819
SPACECRAFT PROPULSION
A revolutionary lunar space transportation system architecture using extraterrestrial LOX-augmented NTR propulsion
[NASA-TM-106726] p 249 N95-11703
Nuclear rockets: High-performance propulsion for Mars
[DE94-013642] p 257 N95-11782
Space Station Freedom propulsion activities
[NASA-TM-106604] p 256 N95-13236
SPACECRAFT RADIATORS
The embodiment design of the heat rejection system for the portable life support system
[NASA-CR-197178] p 338 N95-12555
SPACECRAFT RELIABILITY
Test plan. GCPS task 7, subtask 7.1: IHM development
[NASA-CR-106876] p 250 N95-11767
SPACECRAFT SHIELDING
Test model designs for advanced refractory ceramic materials p 277 N95-11968
Conceptual design of an Orbital Debris Defense System
[NASA-CR-197211] p 254 N95-12696
SPACECRAFT STRUCTURES
Design of passive piezoelectric damping for space structures
[NASA-CR-4625] p 252 N95-12165
SPACECREWS
Memorial service for the mission 51-L crew (edited)
[NASA-TM-109900] p 250 N95-13133
SPACELAB PAYLOADS
Training for life science experiments in space at the NASA Ames Research Center p 339 N95-11964
SPATIAL DISTRIBUTION
New multi-dimensional diagnostics method for intense ion beams p 365 N95-12432
Protein crystal growth in low gravity
[NASA-CR-196980] p 279 N95-13202
SPATIAL RESOLUTION
Tropical cyclone development and intensification under moderate to strong vertical wind shear
[AD-A282185] p 326 N95-12423
Visible/infrared radiometric calibration station
[DE94-014459] p 363 N95-13106
SPECIFIC HEAT
Optimal experimental designs for the estimation of thermal properties of composite materials
[NASA-CR-196792] p 261 N95-11700
Computer code for determination of thermally perfect gas properties
[NASA-TP-3447] p 231 N95-11995
SPECIFIC IMPULSE
A low-erosion starting technique for high-performance arcjets
[NASA-TM-106627] p 259 N95-13347
SolSTUS: Solar Source Thermal Upper Stage
[NASA-CR-197179] p 257 N95-13581
SPECIFICATIONS
Advanced computer architecture specification for automated weld systems
[NASA-CR-194006] p 343 N95-12014
SPECTRAL BANDS
Free electron lasers and other advanced sources of light: Scientific research opportunities p 297 N95-12375
SPECTRAL EMISSION
Radiative performance of rare earth garnet thin film selective emitters
[NASA-TM-106722] p 372 N95-11876
Emittance theory for thin film selective emitter
[NASA-TM-106727] p 317 N95-11903
BATSE observations of Nova Muscae 1991
[NASA-CR-196416] p 380 N95-12464
X-ray temporal and spectral studies of blazars with the Ginga satellite
[NASA-CR-196330] p 380 N95-12466
Progress on resonance ionization detection of combustion radicals
[DE94-015339] p 267 N95-12762
Alignment and experiment of the HL-1 x ray bent-crystal spectrometer
[DE94-624719] p 297 N95-13537
SPECTRAL LINE WIDTH
Experimental and theoretical study of neon-like selenium x-ray laser spectral line profiles
[DE94-015327] p 298 N95-12761
SPECTRAL METHODS
Technical report series on global modeling and data assimilation. Volume 2: Direct solution of the implicit formulation of fourth order horizontal diffusion for gridpoint models on the sphere
[NASA-TM-10406] p 323 N95-12226
SPECTRAL REFLECTANCE
Development of UV irradiance standards
[PB94-181005] p 320 N95-12771
Laser spectroscopy of GdO: Ligand field assignments of 4f7(8S)6p reversing 4f7(8)6s transitions
[AD-A282827] p 268 N95-13180
SPECTRAL RESOLUTION
Visible/infrared radiometric calibration station
[DE94-014459] p 363 N95-13106
Vapor detection sensitivity as a function of optical resolution for a single Lorentzian band
[AD-A283444] p 316 N95-13142
SPECTRAL THEORY
Emittance theory for thin film selective emitter
[NASA-TM-106727] p 317 N95-11903
SPECTROGRAMS
Photographic region elemental abundance analyses of Dr. David S. Leckrone's GTO HST stars 2
[NASA-CR-196756] p 381 N95-12788
SPECTROMETERS
Triple sorbent thermal desorption/gas chromatography/mass spectrometry determination of vapor phase organic contaminants
[DE94-013634] p 264 N95-11735
Alignment and experiment of the HL-1 x ray bent-crystal spectrometer
[DE94-624719] p 297 N95-13537
SPECTRORADIOMETERS
Development of UV irradiance standards
[PB94-181005] p 320 N95-12771
SPECTROSCOPIC ANALYSIS
Acquisition of a gas source mass spectrometer for paleoclimatology and paleoceanography research
[AD-A282634] p 266 N95-12539
SPECTROSCOPY
Optical Remote Sensing of the Atmosphere. Technical digest 1993. Volume 5: Postconference edition
[AD-A281446] p 314 N95-11831
Optical and magnetic resonance investigations of 3D ions in single crystal hosts: Candidates for tunable solid-state lasers
[AD-A281726] p 371 N95-11842
Summaries of papers presented at the High Resolution Spectroscopy Topical Meeting. Technical digest series. Volume 1: Post conference edition
[AD-A281261] p 268 N95-13372
Synchrotron studies of narrow band materials
[DE94-013698] p 271 N95-13554
SPECTRUM ANALYSIS
Investigation of physical parameters in stellar flares observed by GINGA
[NASA-CR-196823] p 381 N95-11928
BATSE observations of 3C273
[NASA-CR-196185] p 380 N95-12463
Investigation of spectral-based techniques for classification of wideband transient signals in additive white Gaussian noise
[AD-A282954] p 283 N95-12592
Photographic region elemental abundance analyses of Dr. David S. Leckrone's GTO HST stars 2
[NASA-CR-196756] p 381 N95-12788
Spectral analysis, estimation, and prediction of multiple harmonizable random fields and time series
[AD-A283042] p 354 N95-12994
SPEED CONTROL
The selective use of functional optical variables in the control of forward speed
[NASA-TM-108849] p 229 N95-12227
SPEED INDICATORS
Flight dynamics of an unmanned aerial vehicle
[AD-A282259] p 239 N95-12410
SPIN DYNAMICS
Radiation-induced structural changes, 4
[DE94-753223] p 356 N95-11817
SPIN STABILIZATION
Spacecraft attitude determination accuracy from mission experience
[NASA-TM-104613] p 255 N95-12858
SPIN-LATTICE RELAXATION
An investigation of Mn Si by the SR-technique
[DE94-624058] p 371 N95-11748
Be-9 and B-11 NMR study of superconductivity in boron doped UBe13
[DE94-014432] p 374 N95-13081
SPIN-ORBIT INTERACTIONS
Laser spectroscopy of GdO: Ligand field assignments of 4f7(8S)6p reversing 4f7(8)6s transitions
[AD-A282827] p 268 N95-13180
SPINDLES
Development of a spindle thermal error characterization and compensation sensor system for machining center accuracy enhancement
[AD-A280891] p 300 N95-11729
SPONTANEOUS EMISSION
Spaceborne Photonics Institute
[NASA-CR-196784] p 362 N95-12659
SPRAY CHARACTERISTICS
Development of nonintrusive, scatter-independent techniques for measurement of liquid density inside dense sprays
[NASA-CR-196413] p 293 N95-12387
SPRAYERS
Structure of a swirl-stabilized, combusting spray
[NASA-TM-106724] p 243 N95-11890
SPREAD SPECTRUM TRANSMISSION
Preliminary digital control system design for the petite amateur Navy satellite (PANSAT)
[AD-A282804] p 253 N95-12528
The effect of Rician fading and partial-band interference on noise-normalized fast frequency-hopped MFSK receivers
[AD-A282805] p 283 N95-12601
SPRINGS (ELASTIC)
A study of the deformation of helical springs under eccentric loading
[AD-A283448] p 312 N95-12511
SPUTTERING
Intelligent processing of ferroelectric thin films
[AD-A282833] p 275 N95-12586
Structure-phase state of thick amorphous and microcrystalline chromium-carbon films deposited by ion-plasma sputtering
[DE94-624236] p 277 N95-13535
STABILITY
The role of crack formation in chevron-notched four-point bend specimens
[NASA-TM-106631] p 310 N95-11865
Strange hadronic matter
[DE94-001493] p 357 N95-12012
Minimal fixturing of frictionless assemblies: Complexity and algorithms
[AD-A282724] p 300 N95-12505
A lunar/Martian anchor emplacement system
[NASA-CR-197193] p 302 N95-12690
Locked modes in TEXT-U tokamak
[DE94-011595] p 370 N95-13529
STABILIZATION
The use of neuron nets to stabilize dynamic systems p 348 N95-12109
Feedback control and stabilization experiments on the Texas Experimental Tokamak (TEXT)
[DE94-015214] p 368 N95-12758
STABILIZERS (FLUID DYNAMICS)
Pressure measurements on an F/A-18 twin vertical tail in buffeting flow. Volume 3: Buffet power spectral densities
[AD-A281444] p 230 N95-11829
Experimental aerodynamic characteristics of a generic hypersonic accelerator configuration at Mach numbers 1.5 and 2.0 --- conducted in the Langley Unitary Plan Wind Tunnel
[NASA-TM-4413] p 233 N95-12770
STAGNATION FLOW
Analysis and design of numerical schemes for gas dynamics. 2: Artificial diffusion and discrete shock structure
[NASA-CR-196476] p 290 N95-11874

STAGNATION POINT
Science objectives and performance of a radiometer and window design for atmospheric entry experiments
[NASA-TM-4637] p 382 N95-12190
STAGNATION PRESSURE
Numerical computations with ABAQUS/Explicit, DYNA3D, and DYSMAS/L
[AD-A282249] p 293 N95-12409
STANDARD MODEL (PARTICLE PHYSICS)
Search for supersymmetry at CDF
[DE94-014264] p 357 N95-12369
STANDARDIZATION
NIST calibration of ASTM E127-type ultrasonic reference blocks
[PB94-191640] p 355 N95-11906
Federal metric progress in 1993
[PB94-196029] p 279 N95-11907
ETRI brochure: History, mission, and activity highlights
p 389 N95-12697
Experiments with formal methods in software engineering
[PB94-192416] p 344 N95-12774
Standards relevant to a NATO anthropometry survey using 3D imaging tools
[AD-A283065] p 339 N95-13055
Equipment for investigation of cryogenic compaction of nanosize silicon nitride powders
[DE94-013593] p 277 N95-13530
STANDARDS
SO2 guideline document
[PB94-181393] p 319 N95-11893
NIST calibration of ASTM E127-type ultrasonic reference blocks
[PB94-191640] p 355 N95-11906
Draft standard for color active matrix liquid crystal displays (AMLCDs) in US Military aircraft. Recommended best practices
[AD-A282950] p 243 N95-12591
Regulatory impact analysis and regulatory support document: Control of air pollution; determination of significance for nonroad sources and emission standards for new nonroad compression-ignition engines at or above 37 kilowatts (50 horsepower)
[PB94-194594] p 321 N95-12855
STAR DISTRIBUTION
A study of a multi-pinned phase CCD detector for use as a star tracker
[NASA-CR-196287] p 381 N95-13056
STAR TRACKERS
A study of a multi-pinned phase CCD detector for use as a star tracker
[NASA-CR-196287] p 381 N95-13056
STARTING
A low-erosion starting technique for high-performance arcjets
[NASA-TM-106627] p 259 N95-13347
STATE VECTORS
NPS state vector analysis and relative motion plotting software for STS-51
[AD-A282909] p 249 N95-12510
STATIC STABILITY
Flight dynamics of an unmanned aerial vehicle
[AD-A282259] p 239 N95-12410
STATIONKEEPING
Analytical investigation of the dynamics of tethered constellations in Earth orbit, phase 2
[NASA-CR-196509] p 252 N95-12106
STATISTICAL ANALYSIS
AVHRR/NOAA images to detect and quantify deforestation in Amazon Forest: Relations with TM/LANDSAT data
[INPE-5501-TDI/516] p 316 N95-13350
Eye-gaze determination of user intent at the computer interface
[DE94-012337] p 363 N95-13421
STDN (NETWORK)
Systems engineering technology for networks
[NASA-CR-196853] p 280 N95-11804
STEADY FLOW
Analysis and design of numerical schemes for gas dynamics. 2: Artificial diffusion and discrete shock structure
[NASA-CR-196476] p 290 N95-11874
STEADY STATE CREEP
Numerical simulations of creep in ductile-phase toughened intermetallic matrix composites
[DE94-014744] p 264 N95-13533
STEEL STRUCTURES
Revealing hidden defects: A hybrid evaluation strategy for steel structures
[PB94-191236] p 308 N95-11822
STEELS
On the strain and strain-rate dependence of the fraction of plastic work converted to heat: An experimental study using high speed infrared detectors and the Kolsky bar
[SM-92-33] p 354 N95-12728
Validity of fracture toughness determined with small bend specimens
[DE94-624157] p 313 N95-12947
STEEPEST DESCENT METHOD
Constructing combinatorial designs by local search
[PB94-179272] p 351 N95-11839
STELLAR EVOLUTION
The x-ray structure of the supernova remnant W49B
[NASA-CR-196482] p 382 N95-12950
STELLAR FLARES
Investigation of physical parameters in stellar flares observed by GINGA
[NASA-CR-196823] p 381 N95-11928
STELLAR INTERIORS
Research in astrophysical processes
[NASA-CR-196773] p 382 N95-12939
STELLAR LUMINOSITY
A deep x-ray survey of the Pleiades cluster and the B6-A3 main sequence stars in Orion
[NASA-CR-196190] p 380 N95-12373
The terrestrial gravitational wave environment from known sources
[NASA-CR-196167] p 323 N95-12468
STELLAR MASS EJECTION
Structure and dynamics of the solar corona
[NASA-CR-196978] p 384 N95-13582
STELLAR MODELS
Investigation of physical parameters in stellar flares observed by GINGA
[NASA-CR-196823] p 381 N95-11928
STELLAR OSCILLATIONS
BATSE observations of Nova Muscae 1991
[NASA-CR-196416] p 380 N95-12464
STELLAR RADIATION
Investigation of physical parameters in stellar flares observed by GINGA
[NASA-CR-196823] p 381 N95-11928
STELLAR ROTATION
A deep x-ray survey of the Pleiades cluster and the B6-A3 main sequence stars in Orion
[NASA-CR-196190] p 380 N95-12373
STELLAR SPECTRA
A catalogue of potentially bright close binary gravitational wave sources
[NASA-CR-196934] p 379 N95-12234
An x-ray search for PMS stars in translucent molecular clouds
[NASA-CR-196151] p 380 N95-12388
The terrestrial gravitational wave environment from known sources
[NASA-CR-196167] p 323 N95-12468
Photographic region elemental abundance analyses of Dr. David S. Leckrone's GTO HST stars 2
[NASA-CR-196756] p 381 N95-12788
STELLAR SPECTROPHOTOMETRY
The terrestrial gravitational wave environment from known sources
[NASA-CR-196167] p 323 N95-12468
STELLAR STRUCTURE
FOC SV support and science data analysis
[NASA-CR-196764] p 381 N95-12821
STELLARATORS
L-H transition in tokamaks and stellarators
[DE94-013257] p 370 N95-13422
STEPPING MOTORS
Stepper motor
[NASA-CR-189373] p 287 N95-12795
STIFFNESS
Test methods for textile composites
[NASA-CR-4609] p 262 N95-12793
Cabin-fuselage-wing structural design concept with engine installation
[NASA-CR-197172] p 242 N95-12993
STIFFNESS MATRIX
Stiffnesses of laminated flat plates
[ESDU-94003] p 309 N95-11769
Elastic buckling of unbalanced laminated fibre reinforced composite plates (rectangular plates of AsBtDs type, all edges simply-supported under biaxial loading)
[ESDU-94006] p 310 N95-11772
STOCHASTIC PROCESSES
A stochastic model of fatigue crack growth
p 309 N95-11698
LES, DNS and RANS for the analysis of high-speed turbulent reacting flows
[NASA-CR-196822] p 289 N95-11705
A unified approach to geopotential field modeling
[AD-A283453] p 324 N95-12544
Spectral analysis, estimation, and prediction of multiple harmonizable random fields and time series
[AD-A283042] p 354 N95-12994
Stochastic indexing
[AD-A283143] p 327 N95-13137
Inverse operator theory method mathematics-mechanization for the solutions of nonlinear equations and some typical applications in nonlinear physics
[DE94-624804] p 352 N95-13340
Stochastic control and nonlinear estimation
[AD-A281219] p 350 N95-13369
Effect of stochastic damping resonance wave packet on energetic alpha particle transport
[DE94-625041] p 370 N95-13538
Chaotic time series. Part 1: Estimation of invariant properties in state space
[PB94-206968] p 376 N95-13572
Linear approximations of delays in buffers receiving correlated ATM cell streams
[PB94-207099] p 286 N95-13577
STOICHIOMETRY
Diagnostic techniques for semiconductor materials processing
[AD-A282810] p 373 N95-12602
STORAGE TANKS
Sloshing analysis of tanks containing multiple fluid layers
[DE94-013333] p 290 N95-11753
STORMS
Tactical satellite orbital simulation and requirements study
[AD-A282314] p 282 N95-12416
STOVL AIRCRAFT
Piloted evaluation of an integrated methodology for propulsion and airframe control design
[NASA-TM-106741] p 245 N95-12763
STRAIN GAGES
High temperature strain gage technology for gas turbine engines
[NASA-CR-191177] p 295 N95-11996
Strain gage selection in loads equations using a genetic algorithm
[NASA-CR-4597] p 242 N95-12831
STRAIN MEASUREMENT
High temperature strain gage technology for gas turbine engines
[NASA-CR-191177] p 295 N95-11996
STRAIN RATE
On the strain and strain-rate dependence of the fraction of plastic work converted to heat: An experimental study using high speed infrared detectors and the Kolsky bar
[SM-92-33] p 354 N95-12728
Mechanical behavior of (238)UO2, (238)PuO2, and (239)PuO2 as a function of strain rate and temperature
[DE94-015718] p 312 N95-12784
STRAKES
Water tunnel flow visualization study of a 4.4 percent scale X-31 forebody
[NASA-TM-104276] p 230 N95-11898
STRANGE ATTRACTORS
Chaotic time series. Part 1: Estimation of invariant properties in state space
[PB94-206968] p 376 N95-13572
STRANGENESS
Strange hadronic matter
[DE94-001493] p 357 N95-12012
STRATOSPHERE
Present state of knowledge of the upper atmosphere1993: An assessment report, part 2
[NASA-RP-1337] p 322 N95-12103
Development of techniques for the in situ observation of OH and HO2 for studies of the impact of high-altitude supersonic aircraft on the stratosphere
[NASA-CR-196759] p 321 N95-12832
STREAMS
Linear approximations of delays in buffers receiving correlated ATM cell streams
[PB94-207099] p 286 N95-13577
STRESS ANALYSIS
Stress analysis of laminated flat plates
[ESDU-94004] p 309 N95-11770
A numerical analysis of the distribution of stresses in lung parenchyma which accounts for the interactions between the tissue skeleton and flowing air
p 332 N95-11806
Computer modeling the fatigue crack growth rate behavior of metals in corrosive environments
[NASA-CR-194982] p 269 N95-11933
Interlaminar stress analysis of dropped-ply laminated plates and shells by a mixed method
[NASA-CR-196851] p 311 N95-11946
Mechanical behavior of (238)UO2, (238)PuO2, and (239)PuO2 as a function of strain rate and temperature
[DE94-015718] p 312 N95-12784
Optimization of aerospace structures
[NASA-CR-196763] p 242 N95-12787
Improved assumed-stress hybrid shell element with drilling degrees of freedom for linear stress, buckling, and free vibration analyses
[NASA-CR-192516] p 313 N95-13163

STRESS CORROSION CRACKING
Computer modeling the fatigue crack growth rate behavior of metals in corrosive environments
[NASA-CR-194982] p 269 N95-11933
STRESS DISTRIBUTION
Accurate interlaminar stress recovery from finite element analysis
[NASA-TM-109149] p 310 N95-11815
Interlaminar stress analysis of dropped-ply laminated plates and shells by a mixed method
[NASA-CR-196851] p 311 N95-11946
Computation of turbulent boundary layers employing the defect wall-function method
[NASA-CR-4629] p 293 N95-12859
STRESS INTENSITY FACTORS
The role of crack formation in chevron-notched four-point bend specimens
[NASA-TM-106631] p 310 N95-11865
A study of fatigue crack growth in lugs under spectrum loading
[NAL-PD-SN-9407] p 311 N95-11879
Computer modeling the fatigue crack growth rate behavior of metals in corrosive environments
[NASA-CR-194982] p 269 N95-11933
STRESS RELAXATION
Stress relaxation functions: Methods of approximation
[NASA-CR-195830] p 312 N95-12861
STRESS WAVES
The influence of finite-size sources in acousto-ultrasonics
[NASA-CR-195374] p 308 N95-11813
STRESS-STRAIN RELATIONSHIPS
Stiffnesses of laminated flat plates
[ESDU-94003] p 309 N95-11769
Stress analysis of laminated flat plates
[ESDU-94004] p 309 N95-11770
Modeling and life prediction methodology for Titanium Matrix Composites subjected to mission profiles
[NASA-TM-109148] p 269 N95-11915
Failure analysis of woven and braided fabric reinforced composites
[NASA-CR-194981] p 262 N95-11926
Numerical computations with ABAQUS/Explicit, DYNA3D, and DYSMAS/L
[AD-A262249] p 293 N95-12409
Triaxial and torsional shear test results for sand
[AD-A262725] p 323 N95-12506
A study of the deformation of helical springs under eccentric loading
[AD-A263448] p 312 N95-12511
Mechanical behavior of (238)UO2, (238)PuO2, and (239)PuO2 as a function of strain rate and temperature
[DE94-015718] p 312 N95-12784
Numerical simulations of creep in ductile-phase toughened intermetallic matrix composites
[DE94-014744] p 264 N95-13533
STRUCTURAL ANALYSIS
A stochastic model of fatigue crack growth
p 309 N95-11698
Parallel aeroelastic computations for wing and wing-body configurations
[NASA-CR-196835] p 230 N95-11766
Structure and performance of carbon aerogel electrodes
[DE94-014746] p 356 N95-11791
Army Research Office Workshop on Dynamic Response of Composite Structures
[AD-A281471] p 262 N95-11854
Computer modeling the fatigue crack growth rate behavior of metals in corrosive environments
[NASA-CR-194982] p 269 N95-11933
GASCAN 2 payload integration
[NASA-CR-197200] p 278 N95-12701
Optimization of aerospace structures
[NASA-CR-196763] p 242 N95-12787
Comparison of symbolic and numerical integration methods for an assumed-stress hybrid shell element
[NASA-CR-195945] p 313 N95-13096
Nonlinear structural response using adaptive dynamic relaxation on a massively-parallel-processing system
[NASA-CR-196491] p 313 N95-13162
STRUCTURAL DESIGN
Selection process for trade study: Graphite Composite Primary Structure (GCPS)
[NASA-CR-196866] p 261 N95-11803
Chiral recognition in molecular and macromolecular pairs of (S)- and (R)-1-cyano-2-methylpropyl 4'(4-(8-vinyloxyoctyloxy)benzoyl) biphenyl-4-carboxylate enantiomers
[AD-A281436] p 356 N95-11828
Architectural design of the science complex at Elizabeth City State University p 247 N95-11960
Viper cabin-fuselage structural design concept with engine installation and wing structural design
[NASA-CR-197162] p 239 N95-12305
M.E.366-J embodiment design project: Portable foot restraint
[NASA-CR-197163] p 338 N95-12361
Various advanced design projects promoting engineering education
[NASA-CR-197170] p 258 N95-12630
Cabin fuselage structural design with engine installation and control system
[NASA-CR-197173] p 240 N95-12639
Cabin-fuselage-wing structural design concept with engine installation
[NASA-CR-197172] p 242 N95-12993
Guideway structural design and power/propulsion/braking in relation to guideways. Volume 3: Appendix B: Maglev guideway structural design
[PB93-169910] p 304 N95-13128
STRUCTURAL DESIGN CRITERIA
High frequency flow/structural interaction in dense subsonic fluids handbook
[NASA-CR-194007] p 230 N95-11807
STRUCTURAL FAILURE
Army Research Office Workshop on Dynamic Response of Composite Structures
[AD-A281471] p 262 N95-11854
Illustrated structural application of universal first-order reliability method
[NASA-TP-3501] p 248 N95-11870
STRUCTURAL MEMBERS
An analysis of the load-bearing capacity of members of square cross section with a series of perpendicular notches p 312 N95-12631
STRUCTURAL RELIABILITY
Test plan. GCPS task 7, subtask 7.1: IHM development
[NASA-CR-106876] p 250 N95-11767
High frequency flow/structural interaction in dense subsonic fluids handbook
[NASA-CR-194007] p 230 N95-11807
Illustrated structural application of universal first-order reliability method
[NASA-TP-3501] p 248 N95-11870
Probabilistic simulation of the human factor in structural reliability
[NASA-TM-106498] p 311 N95-11954
STRUCTURAL VIBRATION
On the interaction of jet noise with a nearby flexible structure
[NASA-CR-194934] p 290 N95-11812
Army Research Office Workshop on Dynamic Response of Composite Structures
[AD-A281471] p 262 N95-11854
Analytical and experimental vibration analysis of a faulty gear system
[NASA-TM-106689] p 300 N95-12377
An examination of anticipated g-jitter on Space Station and its effects on materials processes
[NASA-TM-103775] p 278 N95-12703
The effect of passive damping on feedback control performance of flexible manipulators
[DE94-015000] p 304 N95-13182
STRUTS
Flight investigation of the use of a nose gear jump strut to reduce takeoff ground roll distance of STOL aircraft
[NASA-TM-108819] p 238 N95-12225
STUDENTS
Engineering the future with America's high school students p 377 N95-11958
STYRENES
Thermal polymerization of styrene in the presence of stable radicals and inhibitors
[AD-A280926] p 275 N95-12773
SUBROUTINES
SURRENDER user's manual, second edition
[PB94-206950] p 346 N95-13571
SUBSONIC FLOW
High frequency flow/structural interaction in dense subsonic fluids handbook
[NASA-CR-194007] p 230 N95-11807
SUBSONIC SPEED
Symmetric steady manoeuvre loads on rigid aircraft of classical configuration at subsonic speeds
[ESDU-94009] p 238 N95-11774
The development of a highly reliable power management and distribution system for civil transport aircraft
[NASA-TM-106697] p 243 N95-11867
SUBSTITUTES
Parallel preconditioners for the conjugate gradient method
[PB94-201605] p 347 N95-13404
SUBSTRATES
Rational enzyme redesign
[DE94-014565] p 331 N95-12677
Substrate temperature control apparatus and technique for CVD reactors
[AD-D016387] p 374 N95-13150
SUCTION
Effect of nonzero surface admittance on receptivity and stability of compressible boundary layer
[NASA-CR-4621] p 292 N95-12105
SULFATES
Quantitative understanding of the cycles of oxidized and reduced sulfur on Venus
[NASA-CR-196924] p 382 N95-12011
SULFONES
Adherend surface effects on epoxy cure by NMR
[AD-A282165] p 274 N95-12420
SULFUR
Hydrogen desulfurization of nickel: Thermodynamics and kinetics
[AD-A282581] p 266 N95-12549
SULFUR DIOXIDES
SO2 guideline document
[PB94-181393] p 319 N95-11893
SULFUR OXIDES
Quantitative understanding of the cycles of oxidized and reduced sulfur on Venus
[NASA-CR-196924] p 382 N95-12011
SUNSPOTS
FNAS UAH UVSP and complimentary data analysis and modeling
[NASA-CR-194005] p 381 N95-12992
SUPERCOMPUTERS
Impact analysis on a massively parallel computer
[DE94-013624] p 346 N95-11734
Exploring the parallelism exposed by partial evaluation
[AD-A282284] p 347 N95-12414
Design consideration for parallel graphics libraries
[NASA-CR-194935] p 340 N95-12828
SUPERCONDUCTING DEVICES
Guideway structural design and power/propulsion/braking in relation to guideways. Volume 3: Appendix B: Maglev guideway structural design
[PB93-169910] p 304 N95-13128
SUPERCONDUCTING FILMS
Measurement of synchrotron radiation transmission of infrared range by YBa2Cu3O(7-delta) film in superconducting state
[DE94-623270] p 372 N95-11899
Processing, fabrication, and demonstration of HTS integrated microwave circuits
[AD-A282505] p 289 N95-13300
Response of high T(sub c) superconducting Josephson junction to nuclear radiation
[DE94-624705] p 360 N95-13536
SUPERCONDUCTING MAGNETS
Design and construction of the astronautics refrigerator magnet
[DE94-013599] p 353 N95-11731
A magnetic shield/dual purpose mission
[NASA-CR-197192] p 255 N95-13006
SUPERCONDUCTING SUPER COLLIDER
Shifting our focus: Communicating science to a new, nontechnical culture
[DE94-014258] p 378 N95-13123
SUPERCONDUCTIVITY
Pressure studies of alkali, alkaline earth and rare earth doped C60 superconductors
[DE94-013345] p 372 N95-11862
Measurement of synchrotron radiation transmission of infrared range by YBa2Cu3O(7-delta) film in superconducting state
[DE94-623270] p 372 N95-11899
Be-9 and B-11 NMR study of superconductivity in boron doped UBe13
[DE94-014432] p 374 N95-13081
The dissipative mechanism of pinning of a superconducting current
[DE94-623252] p 289 N95-13276
About the structure of the superconducting order parameter of 2 D Fermi system with an arbitrary particle density
[DE94-623268] p 375 N95-13277
Response of high T(sub c) superconducting Josephson junction to nuclear radiation
[DE94-624705] p 360 N95-13536
SUPERCONDUCTORS (MATERIALS)
Pressure studies of alkali, alkaline earth and rare earth doped C60 superconductors
[DE94-013345] p 372 N95-11862
Measurement of synchrotron radiation transmission of infrared range by YBa2Cu3O(7-delta) film in superconducting state
[DE94-623270] p 372 N95-11899
SUPERCRITICAL FLUIDS
Supercritical fluid (SCF) technologies: Assessment of applicability to installation restoration processes
[AD-A281504] p 290 N95-11859

SUPERFLUIDITY
Relativistic theory of superfluidity with two condensates
[DE94-624073] p 290 N95-11749
SUPERHIGH FREQUENCIES
Advanced S-Band studies using the TDRSS communications satellite
[NASA-CR-196931] p 281 N95-12010
Ku-band high efficiency GaAs MMIC power amplifiers
[NASA-CR-182156] p 288 N95-13231
SUPERLATTICES
The magnetic structure of holmium-erbium superlattices
[DE94-013728] p 371 N95-11739
Rational design, construction, and processing of high-performance nonlinear, optical materials
[AD-A281283] p 363 N95-13374
SUPERNOVA REMNANTS
The x-ray structure of the supernova remnant W49B
[NASA-CR-196482] p 382 N95-12950
SUPERNOVAE
Research in astrophysical processes
[NASA-CR-196773] p 382 N95-12939
SUPERSATURATION
Convective flow effects on protein crystal growth
[NASA-CR-196790] p 372 N95-11921
SUPERSONIC AIRCRAFT
Development of techniques for the in situ observation of OH and HO2 for studies of the impact of high-altitude supersonic aircraft on the stratosphere
[NASA-CR-196759] p 321 N95-12832
SUPERSONIC BOUNDARY LAYERS
Laser Doppler velocimeter measurements of boundary layer velocity and turbulent intensities in Mach 2.5 flow
[NASA-CR-196861] p 289 N95-11709
SUPERSONIC COMBUSTION
Shock tube investigations of combustion phenomena in supersonic flows
[PB94-175262] p 265 N95-11796
AFOSR Contractors Meeting in Propulsion
[AD-A282729] p 257 N95-12507
Planar Rayleigh scattering and laser-induced fluorescence for visualization of a hot, Mach 2 annular air jet
[NASA-TM-4576] p 247 N95-13196
SUPERSONIC COMBUSTION RAMJET ENGINES
Shock-tunnel combustor testing for hypersonic vehicles
[NASA-CR-196836] p 246 N95-11938
NASA's Hypersonic Research Engine Project: A review
[NASA-TM-107759] p 244 N95-12860
SUPERSONIC FLOW
Shock tube investigations of combustion phenomena in supersonic flows
[PB94-175262] p 265 N95-11796
Analysis and design of numerical schemes for gas dynamics 1: Artificial diffusion, upwind biasing, limiters and their effect on accuracy and multigrid convergence
[NASA-CR-196477] p 290 N95-11875
Mixed clusters from the coexpansion of C2F6 and n2 in a pulsed, supersonic expansion cluster ion source and beam deflection time-of-flight mass spectrometer: A first application
[AD-A282044] p 361 N95-11910
Supersonic base flow investigation over axisymmetric afterbodies
[PB94-180957] p 232 N95-12578
SUPERSONIC INLETS
Validation of the RPLUS3D code for supersonic inlet applications involving three-dimensional shock wave-boundary layer interactions
[NASA-TM-106579] p 233 N95-13058
SUPERSONIC JET FLOW
Magnetic field generation in shock waves
[AD-A282234] p 281 N95-12408
SUPERSONIC TRANSPORTS
High speed civil transport aerodynamic optimization
[NASA-CR-196960] p 232 N95-12389
Integrated design and manufacturing for the high speed civil transport
[NASA-CR-197183] p 241 N95-12700
Design and testing of an oblique all-wing supersonic transport
[NASA-CR-196394] p 242 N95-12785
SUPERSONIC TURBINES
Measurements of pressure and thermal wakes in a transonic turbine cascade
[AD-A283464] p 232 N95-12548
SUPERSONIC WIND TUNNELS
Design and testing of an oblique all-wing supersonic transport
[NASA-CR-196394] p 242 N95-12785
Mach number control in the High Speed Wind Tunnel of NLR
[PB94-201670] p 246 N95-13243
SUPERSYMMETRY
Search for supersymmetry at CDF
[DE94-014264] p 357 N95-12369
SUPPLYING
Object recognition for flexible assembly using stereo vision
[PB94-204427] p 363 N95-13248
SUPPORT SYSTEMS
Design issues of human operator support systems
[PB94-191376] p 337 N95-11778
Meeting the challenge of manned lunar and Martian exploration p 339 N95-11970
A decision support system for tolerance allocation
[NASA-CR-195817] p 308 N95-11994
Design of an intelligent support system for scientific databases
[AD-A283043] p 378 N95-12995
SURFACE CRACKS
The structural basis for fatigue failure initiation in glassy polymers
[DE94-015415] p 275 N95-13060
SURFACE DEFECTS
Probability of detection of defects in coatings with electronic shearography
[NASA-CR-196201] p 308 N95-12391
SURFACE DIFFUSION
Hypersonic Gas-Surface Energy Accommodation Test Facility
[DE94-014468] p 232 N95-12652
SURFACE EMITTING LASERS
Wavelength-encoded processing in semiconductor lasers
[AD-A282649] p 297 N95-12751
Diode-pumped micro-laser arrays
[AD-A282494] p 299 N95-13294
SURFACE GEOMETRY
The quadric reference surface: Theory and applications
[AD-A282379] p 351 N95-12007
Effects of sample formulation on the analysis of heavy metals by x-ray fluorescence
[AD-A282733] p 267 N95-12836
SURFACE LAYERS
Growth of Au on Ni(110): A BFS modelling of surface alloy phases
[NASA-TM-106732] p 270 N95-12104
Nanometer scale phase separation in mixed composition self-assembled monolayers
[AD-A282671] p 266 N95-12514
SURFACE NAVIGATION
Using landmarks for the vehicle location measurement
[PB94-184512] p 237 N95-12582
SURFACE PROPERTIES
Application of scanning tunneling microscopy to studies of electrode surfaces
[AD-A282383] p 373 N95-12004
SURFACE REACTIONS
Application of scanning tunneling microscopy to studies of electrode surfaces
[AD-A282383] p 373 N95-12004
Atomic scale dynamics of a two-dimensional gas-solid interface
[AD-A282646] p 358 N95-12617
Thin-film model studies of interfacial reactions in intermetallic matrix composites
[AD-A283360] p 263 N95-12883
Polyatomic ion impact on solid surfaces and related phenomena
[PB94-201258] p 360 N95-13242
Hydrogen bonding and molecular orientation in water/fluorine adlayers on silver(110)
[AD-A282652] p 268 N95-13549
SURFACE ROUGHNESS
Venus surface roughness and Magellan stereo data
[NASA-CR-196821] p 382 N95-11704
Surface roughness characterization of various ceramic fibers using AFM and low voltage SEM
[DE94-013635] p 272 N95-11736
SURFACE ROUGHNESS EFFECTS
Effects of sample formulation on the analysis of heavy metals by x-ray fluorescence
[AD-A282733] p 267 N95-12836
Origin of optical anisotropy in strained In(x)Ga(1-x)As/InP and In(y)Al(1-y)As/InP heterostructures
[AD-A283152] p 271 N95-13140
SURFACE TEMPERATURE
Impingement flow heat transfer measurements of turbine blades using a jet array
[AD-A283450] p 375 N95-12512
SURFACE TREATMENT
Study on surface treatment by pulsed electron beams p 366 N95-12437
Effects of piston surface treatments on performance and emissions of a methanol-fueled, direct injection, stratified charge engine
[DE94-011851] p 302 N95-12648
SURFACE WAVES
Nonlinear problems in fluid dynamics and inverse scattering: Langmuir circulations in ocean surface layers
[AD-A282934] p 329 N95-12590
Efficient parabolic equation solution of radiowave propagation in an inhomogeneous atmosphere and over irregular terrain: Formulation
[AD-A282648] p 284 N95-12834
SURFACTANTS
Small angle neutron scattering in surface-active agents mixtures
[DE94-624057] p 356 N95-11747
Adherend surface effects on epoxy cure by NMR
[AD-A282165] p 274 N95-12420
Microemulsions as reaction media: Literature review
[PB94-184553] p 267 N95-12585
SURVEILLANCE
Millimeter-wave radiometric utility study
[AD-A282524] p 281 N95-12402
SURVEYS
Comprehensive and critical literature review on insitu micro-sensors for application in tribology
[AD-A281646] p 296 N95-13165
Response to noise around Vaernes and Bodoe airports
[PB94-207065] p 358 N95-13575
SURVIVAL
Test plan. Task 5, subtask 5.2: Early on-orbit TPSdebris impact tests
[NASA-CR-196873] p 251 N95-11802
SWEAT COOLING
Anode sheath contributions in plasma thrusters
[AD-A280395] p 364 N95-11837
SWEPT WINGS
Optimum aerodynamic design via boundary control
[NASA-CR-195882] p 230 N95-11877
SWIRLING
Structure of a swirl-stabilized, combusting spray
[NASA-TM-106724] p 243 N95-11890
SWITCHES
Modeling and implementation of a packet routing switch for satellite communications
[AD-A282262] p 282 N95-12412
Plasma opening switch by laser-produced plasma with different kinds of ion species p 367 N95-12451
SWITCHING CIRCUITS
Power system applications for PASC converter systems
[DE94-013329] p 286 N95-11751
Buffer size and switching capacity study in packet switches of broadband ISDN
[PB94-179421] p 281 N95-12368
SYMBOLS
Extensions and contractions of the Lie algebra of q-pseudodifferential symbols
[PB94-192374] p 352 N95-12603
SYMMETRY
Chiral recognition in molecular and macromolecular pairs of (S)- and (R)-1-cyano-2-methylpropyl 4'(4-(8-vinyloxyoctyloxy)benzoyl) biphenyl-4-carboxylate enantiomers
[AD-A281438] p 356 N95-11828
SYNAPSES
Neural networks: Structure and repair. Part 1: Ground squirrel visual system. Part 2: Formation, maintenance and plasticity of synaptic connections
[AD-A282420] p 330 N95-12393
SYNCHRONISM
Performance measurements of the multimedia testbed on real-time Mach
[AD-A282658] p 343 N95-12504
Parallel preconditioners for the conjugate gradient method
[PB94-201605] p 347 N95-13404
Provoking and measuring cell losses in ATM systems by importance sampling, control variables and load cycles
[PB94-202520] p 285 N95-13558
Linear approximations of delays in buffers receiving correlated ATM cell streams
[PB94-207099] p 286 N95-13577
SYNCHROTRON RADIATION
Measurement of synchrotron radiation transmission of infrared range by YBa2Cu3O(7-delta) film in superconducting state
[DE94-623270] p 372 N95-11899
Resonant x-ray scattering in 5f magnetism
[DE94-013753] p 358 N95-12829
SYNCHROTRONS
Synchrotron studies of narrow band materials
[DE94-013696] p 271 N95-13554

SYNTAX
Object-oriented technology for compressor simulation
[NASA-TM-106723] p 243 N95-11864
SYNTHESIS (CHEMISTRY)
Design and synthesis of tight pitch FLCs for analog voltage-limited electro-optic modulators
[AD-A281472] p 371 N95-11855
Synthesis and solid-state NMR characterization of 13C- and 15N-labelled n-methylphthalimide: A model compound for studying polyimides
[AD-A282510] p 273 N95-12397
Synthesis and characterization of thianthrene-based polyamides
[AD-A282512] p 273 N95-12399
Multifunctional acrylic ether monomers, their polymers, and polymerizable epoxide derivatives from simple alpha-substitution of alkyl acrylates
[AD-A282513] p 273 N95-12400
Novel activated carbon impregnants consisting of transition metal complexes. Part 1: Background, syntheses and characterizations
[AD-A282583] p 259 N95-12551
Room-temperature synthesis of CuInQ2 (Q = S or Se) in non-aqueous solution using an organoindium reagent
[NASA-TM-106557] p 260 N95-12662
One-step synthesis of dithiocarbamates from metal powders
[NASA-TM-106558] p 260 N95-12692
Synthesis and decomposition of a novel carboxylate precursor to indium oxide
[NASA-TM-106555] p 260 N95-12693
Low oxidation state gallium compounds. Synthesis and characterization of Ga(CH2CMe3)n
[AD-A283369] p 373 N95-12923
Synthetic method for ethynylation of aromatic compounds
[AD-D016398] p 261 N95-13151
Rational design, construction, and processing of high-performance nonlinear, optical materials
[AD-A281283] p 363 N95-13374
Potential molecular wires by an iterative divergent/convergent approach. Doubling of molecular length at each iteration
[AD-A281292] p 360 N95-13376
SYNTHETIC APERTURE RADAR
Parameterization and scaling of Arctic ice conditions in the context of ice-atmosphere processes
[NASA-CR-196831] p 327 N95-11706
AIRSAR software: Computer programs for preprocessing of JPL compressed polarimetric SAR data
[PB94-179116] p 280 N95-11800
Wideband electromagnetic scattering program. Fourier-based radar imaging techniques
[AD-A282540] p 282 N95-12493
Target recognition in ultra-wideband SAR imagery
[AD-A283462] p 282 N95-12547
SYNTHETIC RESINS
All-hydrocarbon composite resins based on cyclopentadiene
[AD-A282495] p 276 N95-13296
SYSTEM FAILURES
Vacuum system operating experience review for fusion applications
[DE94-015267] p 368 N95-12759
SYSTEMS ANALYSIS
Burst transmission in the HF band: A system analysis and proposal for improvement
[PB94-190733] p 280 N95-11821
Validating medical knowledge based systems
[PB94-191301] p 377 N95-11824
A high-performance constant-temperature hot-wire anemometer
[NASA-CR-177645] p 295 N95-11896
Efficient detection of deadlocks in Petri nets
[PB94-179405] p 343 N95-12366
An empirical study of a highly available file system
[AD-A282655] p 378 N95-12502
Space Station Module Power Management and Distribution System (SSM/PMAD)
[NASA-CR-193991] p 258 N95-12819
Object recognition for flexible assembly using stereo vision
[PB94-204427] p 363 N95-13248
Reliability allocation for a system using Markov analysis
[PB94-205051] p 309 N95-13406
SYSTEMS ENGINEERING
New York bight study. Report 4: Geographic information systems and relational database management system development
[AD-A281716] p 327 N95-11787
Systems engineering technology for networks
[NASA-CR-196853] p 280 N95-11804
Proceedings: The Eleventh IEEE Workshop on Real-Time Operating Systems and Software
[AD-A281738] p 342 N95-11843
Object-oriented technology for compressor simulation
[NASA-TM-106723] p 243 N95-11864
Meeting the challenge of manned lunar and Martian exploration p 339 N95-11970
Reliability and cost analysis methods
[NASA-CR-196326] p 308 N95-12381
Integrated design and manufacturing for the high speed civil transport
[NASA-CR-197183] p 241 N95-12700
Uniformisation techniques for integral recurrence equations
[PB94-205069] p 347 N95-13407
SYSTEMS INTEGRATION
Terminal Doppler Weather Radar Build 5A Operational Test and Evaluation (OT/E) integration and OT/E operational test plan
[AD-A283052] p 327 N95-12996
Use of remote sensing and geographic information system techniques in integrated studies of watersheds
[INPE-5494-TDI/511] p 316 N95-13352
SYSTEMS MANAGEMENT
New York bight study. Report 4: Geographic information systems and relational database management system development
[AD-A281716] p 327 N95-11787
SYSTEMS STABILITY
A high-performance constant-temperature hot-wire anemometer
[NASA-CR-177645] p 295 N95-11896
Robust control design with real parameter uncertainty using absolute stability theory
[NASA-CR-196971] p 349 N95-12782
SYSTOLIC ARRAYS
Design of systolic algorithms and architectures for digital signal processing
[PB94-179256] p 346 N95-11838

T

TAIL ASSEMBLIES
Pressure measurements on an F/A-18 twin vertical tail in buffeting flow. Volume 3: Buffet power spectral densities
[AD-A281444] p 230 N95-11829
Viper cabin-fuselage structural design concept with engine installation and wing structural design
[NASA-CR-197162] p 239 N95-12305
Experimental aerodynamic characteristics of a generic hypersonic accelerator configuration at Mach numbers 1.5 and 2.0 --- conducted in the Langley Unitary Plan Wind Tunnel
[NASA-TM-4413] p 233 N95-12770
TAIL SURFACES
Pressure measurements on an F/A-18 twin vertical tail in buffeting flow. Volume 3: Buffet power spectral densities
[AD-A281444] p 230 N95-11829
TAILLESS AIRCRAFT
Design and construction of a remote piloted flying wing
[NASA-CR-197195] p 241 N95-12695
TAKEOFF
Flight investigation of the use of a nose gear jump strut to reduce takeoff ground roll distance of STOL aircraft
[NASA-TM-108819] p 238 N95-12225
The Elite: A high speed, low-cost general aviation aircraft for Aeroworld
[NASA-CR-197161] p 239 N95-12530
The Balsa bullet: A high speed, low-cost general aviation aircraft for Aeroworld
[NASA-CR-197165] p 240 N95-12638
Flight test of takeoff performance monitoring system
[NASA-TP-3403] p 245 N95-12664
TAKEOFF RUNS
Flight investigation of the use of a nose gear jump strut to reduce takeoff ground roll distance of STOL aircraft
[NASA-TM-108819] p 238 N95-12225
TANKS (COMBAT VEHICLES)
Tank crew performance related to cognitive ability and motivation of the tank crew members
[PB94-190642] p 335 N95-11872
TARGET ACQUISITION
Monopulse tracker operating characteristics measurement error performance for azimuth tracking
[AD-A281188] p 282 N95-12521
TARGET RECOGNITION
Millimeter-wave radiometric utility study
[AD-A282524] p 281 N95-12402
Target recognition in ultra-wideband SAR imagery
[AD-A283462] p 282 N95-12547
TARGETS
Norwegian contribution to the SWG on APSE programme
[PB94-202397] p 341 N95-13557
Provoking and measuring cell losses in ATM systems by importance sampling, control variables and load cycles
[PB94-202520] p 285 N95-13558
TASK COMPLEXITY
Age 60 study. Part 4: Experimental evaluation of pilot performance
[REPT-8025-4B] p 336 N95-13199
TAYLOR INSTABILITY
Contraction phase of a gas-puff z-pinch p 366 N95-12440
TDR SATELLITES
Advanced S-Band studies using the TDRSS communications satellite
[NASA-CR-196931] p 281 N95-12010
TEARING MODES (PLASMAS)
Helical temperature perturbations associated with tearing modes in tokamak plasmas
[DE94-014708] p 369 N95-12867
TECHNOLOGIES
JPRS report: Science and technology. Central Eurasia: Life sciences
[JPRS-ULS-93-014] p 318 N95-11743
JPRS report: Science and technology. Central Eurasia: Life sciences
[JPRS-ULS-93-012] p 332 N95-11744
JPRS report: Science and technology. Central Eurasia: Space
[JPRS-USP-94-006] p 247 N95-12000
JPRS report: Science and technology. Central Eurasia
[JPRS-UST-94-017] p 247 N95-12001
JPRS report: Science and technology. Central Eurasia
[JPRS-UST-94-020] p 389 N95-12002
JPRS report: Science and technology. Central Eurasia
[JPRS-UST-94-019] p 389 N95-12003
Toward infrastructure improvement: An agenda for research
[LC-94-67335] p 376 N95-12385
TECHNOLOGY ASSESSMENT
Supercritical fluid (SCF) technologies: Assessment of applicability to installation restoration processes
[AD-A281504] p 290 N95-11859
Impact of agility requirements on configuration synthesis
[NASA-CR-4627] p 238 N95-11952
Symposium on Structural Intermetallics: Perspectives on Science and Technology, volume 1
[AD-A283378] p 271 N95-12925
Fractional suspension crystallization of organic compounds
[PB94-206851] p 375 N95-13409
TECHNOLOGY TRANSFER
Catalog of government inventions available for licensing, 1991
[PB92-100171] p 389 N95-12303
Catalog of government inventions available for licensing, 1992
[PB93-128205] p 389 N95-12342
Site model based image registration and change detection, RADIUS
[AD-A282796] p 315 N95-12527
Bibliography on cold regions science and technology, volume 47, part 1
[AD-A281879] p 378 N95-13167
TECHNOLOGY UTILIZATION
The future of diode pumped solid state lasers and their applicability to the automotive industry
[DE94-014736] p 298 N95-12868
Military applications of microelectromechanical systems
[AD-A282470] p 289 N95-13291
TECTONICS
Neotectonics of Asia: Thin-shell finite-element models with faults
[NASA-CR-196436] p 324 N95-12949
TELECOMMUNICATION
ETRI brochure: History, mission, and activity highlights p 389 N95-12697
TELEMETRY
Preliminary seismicity and focal mechanisms for the Southern Great Basin of Nevada and California, January 1992 - September 1992
[DE94-013589] p 321 N95-11730
TELEROBOTICS
Overview of NASREM: The NASA/NBS standard reference model for telerobot control system architecture re
[PB94-194560] p 303 N95-12854
TELESCOPES
An adaptive optics package designed for astronomical use with a laser guide star tuned to an absorption line of atomic sodium
[DE94-012391] p 363 N95-13532

TELEVISION CAMERAS
An acoustic charge transport imager for high definition television applications
[NASA-CR-196806] p 280 N95-11760
TEMPERATURE CONTROL
The embodiment design of the heat rejection system for the portable life support system
[NASA-CR-197178] p 338 N95-12555
Microfabricated hydrogen sensor technology for aerospace and commercial applications
[NASA-TM-106703] p 284 N95-12674
Substrate temperature control apparatus and technique for CVD reactors
[AD-D016387] p 374 N95-13150
TEMPERATURE DEPENDENCE
Thermal conductivity of gaseous oxygenated aliphatic hydrocarbons. Alcohols, aldehydes, ketones and ethers
[ESDU-94018] p 265 N95-11795
Computer code for determination of thermally perfect gas properties
[NASA-TP-3447] p 231 N95-11995
Validity of fracture toughness determined with small bend specimens
[DE94-624157] p 313 N95-12947
Be-9 and B-11 NMR study of superconductivity in boron doped UBe13
[DE94-014432] p 374 N95-13081
TEMPERATURE DISTRIBUTION
Interpolation of scattered temperature data measurements onto a worldwide regular grid using radial basis functions with applications to global warming
[DE94-014745] p 321 N95-12926
TEMPERATURE EFFECTS
Effect of operating parameters and anode gas impurities upon polymer electrolyte fuel cells
[DE94-014464] p 317 N95-12650
Mechanical behavior of (238)UO2, (238)PuO2, and (239)PuO2 as a function of strain rate and temperature
[DE94-015718] p 312 N95-12784
Novel concepts in weld science: Role of gradients and composite structure
[DE94-015482] p 271 N95-12895
Simulating the energy performance of holographic glazings
[DE94-014969] p 296 N95-13158
A simplified thermohydrodynamic model for fluid film bearings
[DE94-015011] p 304 N95-13183
Cryogenic On-Orbit Liquid Depot Storage, Acquisition, and Transfer Satellite (COLD-SAT)
[NASA-CR-185249] p 259 N95-13237
TEMPERATURE GRADIENTS
Apparatus and method for forming textured bulk high temperature superconducting materials
[AD-D016394] p 373 N95-12635
L-H transition in tokamaks and stellarators
[DE94-013257] p 370 N95-13422
TEMPERATURE MEASUREMENT
Optimal experimental designs for the estimation of thermal properties of composite materials
[NASA-CR-196792] p 261 N95-11700
Measurements of pressure and thermal wakes in a transonic turbine cascade
[AD-A283464] p 232 N95-12548
SuperMariah: A similarity-based method for determining wind, temperature, and humidity profile structure in the surface boundary layer
[AD-A283058] p 327 N95-12997
TEMPERATURE PROBES
Pioneer Venus orbiter electron temperature probe
[NASA-CR-196844] p 257 N95-11805
TEMPORAL DISTRIBUTION
Use of remote sensing and geographic information system techniques in integrated studies of watersheds
[INPE-5494-TDI/511] p 316 N95-13352
TEMPORAL RESOLUTION
Tropical cyclone development and intensification under moderate to strong vertical wind shear
[AD-A282185] p 326 N95-12423
An investigation of the use of temporal decomposition in space mission scheduling
[NASA-CR-196420] p 377 N95-12618
Ionospheric dynamics instrument investigation for the Timed Mission
[NASA-CR-196198] p 325 N95-13190
TENSILE CREEP
Tensile creep and stress-rupture behavior of polymer derived SiC fibers
[NASA-TM-106692] p 263 N95-12813
TENSILE STRENGTH
Failure analysis of woven and braided fabric reinforced composites
[NASA-CR-194981] p 262 N95-11926
Acute inhalation of explosively disseminated carbon fibers in rats
[AD-A280556] p 330 N95-12614
Test methods for textile composites
[NASA-CR-4609] p 262 N95-12793
TENSILE TESTS
Tensile creep and stress-rupture behavior of polymer derived SiC fibers
[NASA-TM-106692] p 263 N95-12813
TERMS
CENDI Indexing Workshop
[NASA-CP-10160] p 378 N95-12358
TERNARY SYSTEMS
First principles investigation of the Ir-Zr-Nb ternary system
[AD-A282644] p 270 N95-12543
TERRAIN
Efficient parabolic equation solution of radiowave propagation in an inhomogeneous atmosphere and over irregular terrain: Formulation
[AD-A282648] p 284 N95-12834
Representation, modeling and recognition of outdoor scenes
[AD-A283361] p 350 N95-12884
The impact of elevation data representation on nocturnal drainage wind simulations
[DE94-014752] p 326 N95-12927
Factors influencing the rates, processes and magnitude of accumulation of carbon in desert soils
[NASA-CR-196820] p 325 N95-13025
TERRESTRIAL PLANETS
The detectability of extrasolar terrestrial and giant planets during their luminous final accretion
[NASA-CR-196147] p 381 N95-13012
TEST FACILITIES
Evaluation of COSTAR mass handling characteristics in an environment. A simulation of the Hubble Space Telescope service mission
[NASA-TP-3489] p 333 N95-11887
Hypersonic Gas-Surface Energy Accommodation Test Facility
[DE94-014468] p 232 N95-12652
White Sands Test Facility
[NASA-TM-109901] p 249 N95-13129
High-speed seal and bearing test facility p 247 N95-13601
TEST PATTERN GENERATORS
Locally connected adaptive Gabor filter for real-time motion compensation
[AD-A282544] p 286 N95-12494
TEST STANDS
Design and application of electromechanical actuators for deep space missions
[NASA-CR-196791] p 299 N95-11701
Development of the CSI phase-3 evolutionary model testbed
[NASA-CR-4630] p 256 N95-13195
Oscillating-flow regenerator test rig
[NASA-CR-196982] p 246 N95-13200
High temperature seal test rig p 247 N95-13593
TETHERED SATELLITES
Analytical investigation of the dynamics of tethered constellations in Earth orbit, phase 2
[NASA-CR-196509] p 252 N95-12106
Research on Orbital Plasma-Electrodynamics (ROPE)
[NASA-CR-196929] p 361 N95-12147
Precision tethered satellite attitude control
[NASA-CR-196950] p 254 N95-12766
TETHERING
Analytical investigation of the dynamics of tethered constellations in Earth orbit, phase 2
[NASA-CR-196509] p 252 N95-12106
Precision tethered satellite attitude control
[NASA-CR-196950] p 254 N95-12766
TEXTURES
Polycrystal models to fit experiments
[DE94-014419] p 374 N95-13078
THEMATIC MAPPERS (LANDSAT)
AVHRR/NOAA images to detect and quantify deforestation in Amazon Forest: Relations with TM/LANDSAT data
[INPE-5501-TDI/516] p 316 N95-13350
THEOREM PROVING
Some very compositional temporal properties
[PB94-195666] p 345 N95-13438
THEOREMS
Relativistic theory of superfluidity with two condensates
[DE94-624073] p 290 N95-11749
Extension of a theorem of Gehring and Pommerenke
[PB94-180858] p 352 N95-12577
THERAPY
Summary of the Sixteenth Annual Conference on Shock
[AD-A282643] p 334 N95-12542
THERMAL ANALYSIS
Development of a spindle thermal error characterization and compensation sensor system for machining center accuracy enhancement
[AD-A280891] p 300 N95-11729
Investigation of advanced counterrotation blade configuration concepts for high speed turboprop systems. Task 8: Cooling flow/heat transfer analysis
[NASA-CR-195359] p 244 N95-11901
Microwave heating and joining of ceramic cylinders: A mathematical model
[NASA-CR-194962] p 351 N95-11922
Investigation of advanced counterrotation blade configuration concepts for high speed turboprop systems. Task 8: Cooling flow/heat transfer analysis user's manual
[NASA-CR-195360] p 244 N95-11951
Thianthrene-based poly(benzoxazole)s
[AD-A282326] p 274 N95-12419
AFOSR Contractors Meeting in Propulsion
[AD-A282729] p 257 N95-12507
THERMAL BATTERIES
Proceedings of the 36th Power Sources Conference
[AD-A281443] p 288 N95-13164
THERMAL CONDUCTIVITY
Optimal experimental designs for the estimation of thermal properties of composite materials
[NASA-CR-196792] p 261 N95-11700
Thermophysical properties of MtBE (methyl tertbutyl ether)
[ESDU-94010] p 265 N95-11775
Thermal conductivity of gaseous oxygenated aliphatic hydrocarbons. Alcohols, aldehydes, ketones and ethers
[ESDU-94018] p 265 N95-11795
Determination of a transient heat transfer property of acrylic using thermochromic liquid crystals
[NASA-TM-106541] p 372 N95-11882
Analysis of cost: Combustion flame CVD diamond deposition
[AD-A282527] p 273 N95-12403
The effect of irradiation on the stability and properties of monolithic silicon carbide and SiC(f)/SiC composites up to 25 dpa
[DE94-014568] p 263 N95-12862
Evaluation of the improvement in the figure of merit of Bi2Te3 - based alloys with addition of ultrafine scattering centers
[DE94-015363] p 374 N95-13059
THERMAL CONTROL COATINGS
Effects of piston surface treatments on performance and emissions of a methanol-fueled, direct injection, stratified charge engine
[DE94-011851] p 302 N95-12648
THERMAL CYCLING TESTS
A novel lead-free solder replacement
[DE94-013782] p 269 N95-11785
High temperature strain gage technology for gas turbine engines
[NASA-CR-191177] p 295 N95-11996
THERMAL EXPANSION
Thermomechanical fatigue damage/failure mechanisms in SCS-6/Timetal 21S (0/90)s composite
[NASA-CR-191115] p 263 N95-13082
THERMAL FATIGUE
Large-displacement structural durability analyses of simple bend specimen emulating rocket nozzle liners
[NASA-TM-106521] p 312 N95-12818
THERMAL INSULATION
Test Plans. Lightweight Durable TPS: Tasks 1,2,4,5, and 6
[NASA-CR-196867] p 262 N95-11835
THERMAL PROTECTION
A 250 GHz microwave interferometer for divertor experiments on D3-D
[DE94-014056] p 364 N95-11786
Test model designs for advanced refractory ceramic materials p 277 N95-11968
Debris/ice/TPS assessment and integrated photographic analysis of Shuttle Mission STS-65
[NASA-TM-109205] p 249 N95-12224
THERMAL STABILITY
Synthesis, structure and properties of segmented polymers containing mesogens
[AD-A281419] p 272 N95-11852
Novel thermooxidatively stable poly(ether-imide-benzoxazole) and poly(ester-imide-benzoxazole)
[AD-A282381] p 273 N95-12008
Thianthrene-based poly(benzoxazole)s
[AD-A282326] p 274 N95-12419
Influence of additives on structure and thermal stability of ammonium nitrate
[PB94-206943] p 278 N95-13435

THERMIONIC CATHODES
A brightness comparison of thermionic electron sources in a TEM
[DE94-013300] p 360 N95-13338
THERMIONIC EMITTERS
A brightness comparison of thermionic electron sources in a TEM
[DE94-013300] p 360 N95-13338
THERMOCHROMATIC MATERIALS
Determination of a transient heat transfer property of acrylic using thermochromic liquid crystals
[NASA-TM-106541] p 372 N95-11882
THERMOCLINES
Reports to the Nation on our changing planet. El Nino and climate prediction, no. 3, spring 1994
p 320 N95-12462
THERMODYNAMIC PROPERTIES
Modeling and life prediction methodology for Titanium Matrix Composites subjected to mission profiles
[NASA-TM-109148] p 269 N95-11915
Laws of infrared similitude
[AD-A282209] p 354 N95-12426
Hydrogen desulfurization of nickel: Thermodynamics and kinetics
[AD-A282581] p 266 N95-12549
On the strain and strain-rate dependence of the fraction of plastic work converted to heat: An experimental study using high speed infrared detectors and the Kolsky bar
[SM-92-33] p 354 N95-12728
Thermal polymerization of styrene in the presence of stable radicals and inhibitors
[AD-A280926] p 275 N95-12773
Thermodynamic constants for actinide oxides and oxyhydroxides relevant to actinide volatility calculations for thermal oxidation processes
[DE94-007762] p 376 N95-13074
Thermomechanical fatigue damage/failure mechanisms in SCS-6/Timetal 21S (0/90)s composite
[NASA-CR-191115] p 263 N95-13082
Evaluation of alternative in-flight fire suppressants for full-scale testing in simulated aircraft engine nacelles and dry bays
[PB94-203403] p 236 N95-13247
Influence of additives on structure and thermal stability of ammonium nitrate
[PB94-206943] p 278 N95-13435
THERMODYNAMICS
Relativistic theory of superfluidity with two condensates
[DE94-624073] p 290 N95-11749
Laws of infrared similitude
[AD-A282209] p 354 N95-12426
Laser based combustion laboratory at NTH/SINTEF applied thermodynamics
[PB94-202603] p 299 N95-13246
THERMOELECTRIC GENERATORS
Autonomous power system for remote locations
[DE94-013244] p 361 N95-11779
THERMOELECTRICITY
Autonomous power system for remote locations
[DE94-013244] p 361 N95-11779
Protein crystal growth in low gravity
[NASA-CR-196980] p 279 N95-13202
THERMOGRAPHY
Determination of a transient heat transfer property of acrylic using thermochromic liquid crystals
[NASA-TM-106541] p 372 N95-11882
THERMONUCLEAR EXPLOSIONS
Vulnerability assessment of a space based weapon platform electronics system exposed to a thermonuclear weapon detonation
[DE94-013415] p 250 N95-11755
THERMONUCLEAR REACTIONS
Generation of ultra-high magnetic fields for AGEX
[DE94-015171] p 368 N95-12757
THERMOPHYSICAL PROPERTIES
Thermophysical properties of MtBE (methyl tertbutyl ether)
[ESDU-94010] p 265 N95-11775
High temperature solid lubricant materials for heavy duty and advanced heat engines
[NASA-TM-106570] p 260 N95-12764
THERMOREGULATION
Effects of oral glucose on exercise thermoregulation in men after water immersion
[NASA-TM-108825] p 329 N95-11810
THERMOSETTING RESINS
Glass reinforced-diallylbisphenol/maleimide composites with modified interphases
[AD-A282496] p 264 N95-13298
THERMOSPHERE
Ionospheric dynamics instrument investigation for the Timed Mission
[NASA-CR-196198] p 325 N95-13190
THESES
Trellis-based source and channel coding
[PB94-204443] p 285 N95-13405
THICK FILMS
Pseudomorphic semiconducting heterostructures from combinations of AlN, GaN and selected SiC polytypes: Theoretical advancement and its coordination with experimental studies of nucleation, growth, characterization and device development
[AD-A281218] p 289 N95-13368
Structure-phase state of thick amorphous and microcrystalline chromium-carbon films deposited by ion-plasma sputtering
[DE94-624236] p 277 N95-13535
THICKNESS
The role of crack formation in chevron-notched four-point bend specimens
[NASA-TM-106631] p 310 N95-11865
Self assembly of n-alkanethiolate monolayers on silver nano-structures: Determination of the apparent thickness of the monolayer by scanning tunneling microscopy
[AD-A282322] p 274 N95-12417
THIN FILMS
Radiative performance of rare earth garnet thin film selective emitters
[NASA-TM-106722] p 372 N95-11876
Emittance theory for thin film selective emitter
[NASA-TM-106727] p 317 N95-11903
Electrochemical epitaxy
[AD-A282403] p 373 N95-11993
A laboratory vacuum apparatus for magnetron sputtering of thin Z ZnO piezoelectric films, magnetron sputtering
p 296 N95-12111
Plasma and ion beam processing at Los Alamos
[DE94-014293] p 365 N95-12371
Electronic energy transfer in new polymer nanocomposite assemblies
[AD-A282233] p 274 N95-12407
Intelligent processing of ferroelectric thin films
[AD-A282833] p 275 N95-12586
Diagnostic techniques for semiconductor materials processing
[AD-A282810] p 373 N95-12602
Space hardware designs, volume 1
[NASA-CR-197209] p 253 N95-12663
Method of laser processing ferroelectric materials
[AD-D016386] p 298 N95-12780
Thin-film model studies of interfacial reactions in intermetallic matrix composites
[AD-A283360] p 263 N95-12883
Magnetic response of ultrathin Fe on MgO: A polarised neutron reflectometry study
[DE94-013192] p 375 N95-13272
CVD techniques for the synthesis or modification of porous ceramics
[PB94-206836] p 276 N95-13284
Processing, fabrication, and demonstration of HTS integrated microwave circuits
[AD-A282505] p 289 N95-13300
Pseudomorphic semiconducting heterostructures from combinations of AlN, GaN and selected SiC polytypes: Theoretical advancement and its coordination with experimental studies of nucleation, growth, characterization and device development
[AD-A281218] p 289 N95-13368
Kinetics and characterization of tungsten CVD processes
[PB94-206901] p 271 N95-13411
THIN PLATES
Elastic buckling of cylindrically curved laminated fibre reinforced composite panels with all edges simply-supported under biaxial loading
[ESDU-94007] p 310 N95-11773
THIN WALLED SHELLS
Neotectonics of Asia: Thin-shell finite-element models with faults
[NASA-CR-196436] p 324 N95-12949
THIOLS
Self assembly of n-alkanethiolate monolayers on silver nano-structures: Determination of the apparent thickness of the monolayer by scanning tunneling microscopy
[AD-A282322] p 274 N95-12417
THREE AXIS STABILIZATION
Spacecraft attitude determination accuracy from mission experience
[NASA-TM-104613] p 255 N95-12858
THREE DIMENSIONAL BODIES
The quadric reference surface: Theory and applications
[AD-A282379] p 351 N95-12007
THREE DIMENSIONAL BOUNDARY LAYER
Validation of the RPLUS3D code for supersonic inlet applications involving three-dimensional shock wave-boundary layer interactions
[NASA-TM-106579] p 233 N95-13058
THREE DIMENSIONAL FLOW
Performance analysis of three dimensional integral equation computations on a massively parallel computer
[NASA-CR-196747] p 346 N95-11883
An investigation of the vortex method
[DE94-014931] p 294 N95-13156
Numerical time dependent sheet cavitation simulations using a higher order panel method
[PB94-204435] p 294 N95-13249
SCISEAL: A CFD code for analysis of fluid dynamic forces in seals p 305 N95-13586
THREE DIMENSIONAL MODELS
Validation of the RPLUS3D code for supersonic inlet applications involving three-dimensional shock wave-boundary layer interactions
[NASA-TM-106579] p 233 N95-13058
Numerical simulations of drop collisions
[NASA-TM-106751] p 295 N95-13550
THRESHOLDS (PERCEPTION)
Effects of Noise on Hearing 5th International Symposium
[AD-A281439] p 335 N95-13177
THRUST
Guideway structural design and power/propulsion/braking in relation to guideways. Volume 3: Appendix B: Maglev guideway structural design
[PB93-169910] p 304 N95-13128
THRUST AUGMENTATION
A revolutionary lunar space transportation system architecture using extraterrestrial LOX-augmented NTR propulsion
[NASA-TM-106726] p 249 N95-11703
THRUST BEARINGS
A simplified thermohydrodynamic model for fluid film bearings
[DE94-015011] p 304 N95-13183
THRUST CONTROL
Piloted evaluation of an integrated methodology for propulsion and airframe control design
[NASA-TM-106741] p 245 N95-12763
THRUST-WEIGHT RATIO
Selection process for trade study: Graphite Composite Primary Structure (GCPS)
[NASA-CR-196866] p 261 N95-11803
Test Plan. GCPS Task 4, subtask 4.2 thrust structure development
[NASA-CR-196869] p 251 N95-11833
Trade study plan for Graphite Composite Primary Structure (GCPS)
[NASA-CR-196868] p 261 N95-11834
The OFP-6M transport jet
[NASA-CR-197159] p 240 N95-12637
THRUSTORS
Stationary plasma thruster ion velocity distribution
[NASA-CR-195379] p 257 N95-11919
THUNDERSTORMS
Thunderstorm hypothesis reasoner
[AD-A282664] p 326 N95-12805
TIME DEPENDENCE
Stability and error estimation for Component Adaptive Grid methods
[NASA-CR-196492] p 351 N95-11883
Numerical time dependent sheet cavitation simulations using a higher order panel method
[PB94-204435] p 294 N95-13249
Equipment for investigation of cryogenic compaction of nanosize silicon nitride powders
[DE94-013593] p 277 N95-13530
TIME FUNCTIONS
Determination of the auroral oval Q index from the air weather service K index
[AD-A282764] p 324 N95-12508
TIME MEASUREMENT
X-ray and gamma ray astronomy detectors
[NASA-SP-517] p 379 N95-12304
TIME OF FLIGHT SPECTROMETERS
Mixed clusters from the coexpansion of C2F6 and n2 in a pulsed, supersonic expansion cluster ion source and beam deflection time-of-flight mass spectrometer: A first application
[AD-A282044] p 361 N95-11910
TIME SERIES ANALYSIS
Spectral analysis, estimation, and prediction of multiple harmonizable random fields and time series
[AD-A283042] p 354 N95-12994
Chaotic time series. Part 1: Estimation of invariant properties in state space
[PB94-206968] p 376 N95-13572
TIME SHARING
Eager combining: A coherency protocol for increasing effective network and memory bandwidth in shared-memory multiprocessors
[AD-A281501] p 346 N95-11857

TIN ALLOYS
A novel lead-free solder replacement
[DE94-013782] p 239 N95-11785
TIN COMPOUNDS
Hydrolysis and condensation of tin (4) alkoxide compounds: The control of structural evolution
[AD-A282789] p 267 N95-12807
TIRES
Study of in-plane dynamics of tires
[PB94-206893] p 304 N95-13410
TIROS SATELLITES
TOVS operational sounding upgrades: 1990-1992
[NOAA-TR-NESDIS-76] p 322 N95-11836
TITANIUM
Modeling and life prediction methodology for Titanium Matrix Composites subjected to mission profiles
[NASA-TM-109148] p 269 N95-11915
Thermomechanical fatigue damage/failure mechanisms in SCS-6/Timetal 21S (0/90)s composite
[NASA-CR-191115] p 263 N95-13082
TITANIUM ALLOYS
Computer modeling the fatigue crack growth rate behavior of metals in corrosive environments
[NASA-CR-194982] p 269 N95-11933
On the strain and strain-rate dependence of the fraction of plastic work converted to heat: An experimental study using high speed infrared detectors and the Kolsky bar
[SM-92-33] p 354 N95-12728
Thin-film model studies of interfacial reactions in intermetallic matrix composites
[AD-A283360] p 263 N95-12883
TOKAMAK DEVICES
Feedback control and stabilization experiments on the Texas Experimental Tokamak (TEXT)
[DE94-015214] p 368 N95-12758
Vacuum system operating experience review for fusion applications
[DE94-015267] p 368 N95-12759
Helical temperature perturbations associated with tearing modes in tokamak plasmas
[DE94-014708] p 369 N95-12867
L-H transition in tokamaks and stellarators
[DE94-013257] p 370 N95-13422
Alignment and experiment of the HL-1 x ray bent-crystal spectrometer
[DE94-624719] p 297 N95-13537
Density gradient effects in the tokamak edge turbulence with temperature gradient driving
[DE94-625042] p 370 N95-13539
The experiment and analysis of tailoring V(sub L) and I(sub P) with ZnO voltage-sensitive resistor on HT-6M
[DE94-625074] p 370 N95-13541
TOLERANCES (PHYSIOLOGY)
Effects of Noise on Hearing 5th International Symposium
[AD-A281439] p 335 N95-13177
TOMOGRAPHY
Ocean acoustic tomography: Single slice and moving ship experiments
[AD-A283059] p 329 N95-12998
TOOLS
Proposal for the design of a zero gravity tool storage device
[NASA-CR-197150] p 302 N95-12627
TOPOGRAPHY
Venus surface roughness and Magellan stereo data
[NASA-CR-196821] p 362 N95-11704
Observation results: Angle measurements in 1964-1965, 1971, 1984 and 1986-1987
[REPT-118] p 314 N95-11950
Self assembly of n-alkanethiolate monolayers on silver nano-structures: Determination of the apparent thickness of the monolayer by scanning tunneling microscopy
[AD-A282322] p 274 N95-12417
TOPOLOGY
Computerized design and generation of low-noise helical gears with modified surface topology
[NASA-TM-106696] p 303 N95-13083
Multi-jet analysis for the top search at the Fermilab Collider
[DE94-014988] p 359 N95-13169
TOROIDAL PLASMAS
Locked modes in TEXT-U tokamak
[DE94-011595] p 370 N95-13529
TORQUE
Stepper motor
[NASA-CR-189373] p 287 N95-12795
TORSION
Triaxial and torsional shear test results for sand
[AD-A282725] p 323 N95-12506
Polycrystal models to fit experiments
[DE94-014419] p 374 N95-13078
TORUSES
Research on Orbital Plasma-Electrodynamics (ROPE)
[NASA-CR-196929] p 361 N95-12147
TOUGHNESS
Towards tailored interphase formation utilizing surface-active benzylsulfonium salts as cationic initiators
[AD-A282511] p 262 N95-12398
TOWERS
Evaluation of candidate millimeter wave sensors for synthetic vision p 236 N95-13214
TOXICITY
Simultaneous gas-chromatographic determination of four toxic gases generally present in combustion atmospheres
[DOT/FAA/AM-94/18] p 338 N95-12354
TOXICOLOGY
Spacecraft maximum allowable concentrations for selected airborne contaminants, volume 1
[NASA-CR-196446] p 255 N95-12879
TOXINS AND ANTITOXINS
Neural networks: Structure and repair. Part 1: Ground squirrel visual system. Part 2: Formation, maintenance and plasticity of synaptic connections
[AD-A282420] p 330 N95-12393
TRACE CONTAMINANTS
Trace gas emissions to the atmosphere by biomass burning in the west African savannas
[NASA-CR-196758] p 319 N95-11931
Effects of sample formulation on the analysis of heavy metals by x-ray fluorescence
[AD-A282733] p 267 N95-12836
TRACE ELEMENTS
Environmental lichenology: Biomonitoring trace-element air pollution
[PB94-191335] p 318 N95-11826
Hydrographic, carbon dioxide, nutrient and productivity measurements from the south Atlantic during July and August of 1991
[PB94-180668] p 328 N95-11900
TRACKING (POSITION)
Conceptual design of an Orbital Debris Defense System
[NASA-CR-197211] p 254 N95-12696
Numerical simulations of drop collisions
[NASA-TM-106751] p 295 N95-13550
TRACKING RADAR
Monopulse tracker operating characteristics measurement error performance for azimuth tracking
[AD-A281188] p 282 N95-12521
Lessons learned from experiments conducted on radar data management systems
[AD-A282896] p 284 N95-12920
Doppler radar detection of vortex hazard indicators p 236 N95-13212
TRAFFIC
Response to noise around Vaernes and Bodoe airports
[PB94-207065] p 356 N95-13575
TRAFFIC CONTROL
Activities of the Helsinski University of Technology, Applied Electronics Laboratory
[PB94-179074] p 385 N95-11797
TRAINING AIRCRAFT
Triton 2 (1B)
[NASA-CR-197188] p 240 N95-12636
TRAINING SIMULATORS
Visit to UDRI and USAF, Armstrong Lab., Williams AFB, Phoenix, USA, February 8-11, 1993
[PB94-190659] p 337 N95-11873
TRAJECTORIES
Autonomous motion on wheels
[PB94-191327] p 348 N95-11825
TRAJECTORY OPTIMIZATION
Application of multivariate optimisation techniques to determination of optimum flight path trajectories
[ESDU-94012] p 238 N95-11793
TRAJECTORY PLANNING
Development of ROBOSIM for academic/industrial use
[NASA-CR-196148] p 349 N95-12470
TRANSDUCERS
Comprehensive and critical literature review on insitu micro-sensors for application in tribology
[AD-A281646] p 296 N95-13165
Modelling of biopotential recordings and its implications for instrumentation design
[PB94-206844] p 332 N95-13408
TRANSFER FUNCTIONS
Two-tone test method for determining frequency-domain transfer functions
[AD-A283452] p 282 N95-12513
TRANSFORMATIONS (MATHEMATICS)
Essential kinematics for autonomous vehicles
[AD-A282456] p 300 N95-12394
The differential geodesy of the spherical representation
[AD-A282212] p 315 N95-12428
TRANSFORMERS
Power system applications for PASC converter systems
[DE94-013329] p 286 N95-11751
Modeling of transformers using circuit simulators
[DE94-014656] p 287 N95-12863
TRANSISTORS
Basic mechanisms of radiation effects in the natural space radiation environment
[DE94-013445] p 384 N95-11757
Development of nanostructure fabrication technology and new electron-quantum wave devices
[AD-A281724] p 286 N95-11860
TRANSITION METALS
Novel activated carbon impregnants consisting of transition metal complexes. Part 1: Background, syntheses and characterizations
[AD-A282583] p 259 N95-12551
Synchrotron studies of narrow band materials
[DE94-013698] p 271 N95-13554
TRANSITION PRESSURE
Equipment for investigation of cryogenic compaction of nanosize silicon nitride powders
[DE94-013593] p 277 N95-13530
TRANSITION TEMPERATURE
Pressure studies of alkali, alkaline earth and rare earth doped C60 superconductors
[DE94-013345] p 372 N95-11862
TRANSMISSION EFFICIENCY
Efficient and effective handling of cycle slips in global positioning system data p 237 N95-12230
TRANSMISSION ELECTRON MICROSCOPY
Atomic structures and compositions of internal interfaces
[DE94-013594] p 271 N95-13543
TRANSMISSION LOSS
Buffer size and switching capacity study in packet switches of broadband ISDN
[PB94-179421] p 281 N95-12368
TRANSMISSIONS (MACHINE ELEMENTS)
TLIFE: A program for spur, helical and spiral bevel transmission life and reliability modeling
[NASA-CR-4622] p 300 N95-11889
Analytical and experimental vibration analysis of a faulty gear system
[NASA-TM-106689] p 300 N95-12377
TRANSMITTER RECEIVERS
5-volt low level serial transceiver
[AD-D016399] p 288 N95-13153
200 MHz channel sounder, open description
[PB94-202538] p 285 N95-13559
TRANSMITTERS
Flight dynamics of an unmanned aerial vehicle
[AD-A282259] p 239 N95-12410
Search for extraterrestrial intelligence/High Resolution Microwave Survey team member
[NASA-CR-196478] p 339 N95-13026
200 MHz channel sounder, open description
[PB94-202538] p 285 N95-13559
TRANSONIC FLOW
Analysis and design of numerical schemes for gas dynamics 1: Artificial diffusion, upwind biasing, limiters and their effect on accuracy and multigrid convergence
[NASA-CR-196477] p 290 N95-11875
TRANSONIC WIND TUNNELS
Mach number control in the High Speed Wind Tunnel of NLR
[PB94-201670] p 246 N95-13243
TRANSPARENCE
Time-resolved electron thermal conduction by probing of plasma formation in transparent solids with high power subpicosecond laser pulses
[DE94-015170] p 370 N95-13555
TRANSPORT AIRCRAFT
The development of a highly reliable power management and distribution system for civil transport aircraft
[NASA-TM-106697] p 243 N95-11867
The performance of child restraint devices in transport airplane passenger seats
[DOT/FAA/AM-94/19] p 234 N95-12146
The FC-1D: The profitable alternative Flying Circus Commercial Aviation Group
[NASA-CR-197152] p 240 N95-12628
LCX: Proposal for a low-cost commercial transport
[NASA-CR-197186] p 241 N95-12645
Design and testing of an oblique all-wing supersonic transport
[NASA-CR-196394] p 242 N95-12785
TRANSPORT PROPERTIES
Dynamical systems and oceanography
[AD-A282635] p 329 N95-12540
Radiative properties of strongly magnetized plasmas
[DE94-015487] p 369 N95-12897
Fusion programs in applied plasma physics
[DE94-015853] p 369 N95-12944

TRANSPUTERS
Modeling and implementation of a packet routing switch for satellite communications
[AD-A282262] p 282 N95-12412
TRAPEZOIDS
Object-oriented incremental map-generation for mobile robot navigation
[PB94-190717] p 314 N95-11820
TRAPPING
Non-dipolar magnetic field models and patterns of radio emission: Uranus and Neptune compared
[NASA-CR-196412] p 385 N95-12469
TREADMILLS
Comparison of submaximal cycling and treadmill exercise at similar work rates
[AD-A283430] p 334 N95-12593
TREADS
Study of in-plane dynamics of tires
[PB94-206893] p 304 N95-13410
TRELLIS CODING
Trellis-based source and channel coding
[PB94-204443] p 285 N95-13405
TRIANGULATION
The program for the 1993 adjustment of the Finnish first-order terrestrial triangulation
[REPT-94:3] p 314 N95-11880
Toolkits for construction and manipulation of geographical data
[PB94-202587] p 378 N95-13245
TRIBOLOGY
High temperature solid lubricant materials for heavy duty and advanced heat engines
[NASA-TM-106570] p 260 N95-12764
Comprehensive and critical literature review on insitu micro-sensors for application in tribology
[AD-A281646] p 296 N95-13165
A simplified thermohydrodynamic model for fluid film bearings
[DE94-015011] p 304 N95-13183
Computer tools for face seal analyses developed at John Crane p 306 N95-13598
TRISONIC WIND TUNNELS
Experimental Aerodynamics Division
[NAL-SP-9404] p 229 N95-12166
TROPICAL METEOROLOGY
Reports to the Nation on our changing planet. El Nino and climate prediction, no. 3, spring 1994
p 320 N95-12462
TROPICAL REGIONS
Guest investigator program study: Physics of equatorial plasma bubbles
[NASA-CR-196150] p 368 N95-12853
Ionospheric dynamics instrument investigation for the Timed Mission
[NASA-CR-196198] p 325 N95-13190
TROPICAL STORMS
Tropical cyclone development and intensification under moderate to strong vertical wind shear
[AD-A282185] p 326 N95-12423
TUBE CATHODES
Status of hollow cathode heater development for the Space Station plasma contactor
[NASA-CR-195364] p 258 N95-12622
TUNABLE LASERS
Optical and magnetic resonance investigations of 3D ions in single crystal hosts: Candidates for tunable solid-state lasers
[AD-A281726] p 371 N95-11842
Progress on resonance ionization detection of combustion radicals
[DE94-015339] p 267 N95-12762
Tetravalent chromium (Cr(4+)) as laser-active ion for tunable solid-state lasers
[NASA-CR-196481] p 298 N95-12951
TUNGSTEN
A brightness comparison of thermionic electron sources in a TEM
[DE94-013300] p 360 N95-13338
TUNGSTEN COMPOUNDS
Kinetics and characterization of tungsten CVD processes
[PB94-206901] p 271 N95-13411
TURBINE BLADES
Engine structures analysis software: Component Specific Modeling (COSMO)
[NASA-CR-195378] p 309 N95-11711
Investigation of advanced counterrotation blade configuration concepts for high speed turboprop systems. Task 8: Cooling flow/heat transfer analysis
[NASA-CR-195359] p 244 N95-11901
Impingement flow heat transfer measurements of turbine blades using a jet array
[AD-A283450] p 375 N95-12512
Measurements of pressure and thermal wakes in a transonic turbine cascade
[AD-A283464] p 232 N95-12548
TURBINE ENGINES
Air Force seal activities p 306 N95-13600
TURBINES
Impingement flow heat transfer measurements of turbine blades using a jet array
[AD-A283450] p 375 N95-12512
TURBOCOMPRESSORS
Ceramic manufacturing: Optimizing a multivariable system
[DE94-015016] p 276 N95-13184
TURBOFAN AIRCRAFT
A preliminary design proposal for a maritime patrol strike aircraft: MPS-2000 Condor
[NASA-CR-197182] p 241 N95-12689
TURBOFAN ENGINES
The OFP-6M transport jet
[NASA-CR-197159] p 240 N95-12637
TURBOGENERATORS
Composites (CFCCs) for low cost energy and cleaner environment
[DE94-013601] p 272 N95-11781
TURBOMACHINERY
Investigation of advanced counterrotation blade configuration concepts for high speed turboprop systems. Task 8: Cooling flow/heat transfer analysis user's manual
[NASA-CR-195360] p 244 N95-11951
TURBOPROP ENGINES
Investigation of advanced counterrotation blade configuration concepts for high speed turboprop systems. Task 8: Cooling flow/heat transfer analysis user's manual
[NASA-CR-195360] p 244 N95-11951
Brush seals for turbine engine fuel conservation
p 306 N95-13595
TURBULENCE
Modification of the two-equation turbulence model in NPARC to a Chien low Reynolds number k-epsilon formulation
[NASA-TM-106710] p 231 N95-11917
Scale disparity and spectral transfer in anisotropic numerical turbulence
[NASA-CR-194956] p 291 N95-11929
Hypersonic turbulent boundary-layer and free shear database
[NASA-CR-177610] p 292 N95-11992
Fire propagation in concurrent flows
[PB94-193844] p 267 N95-12778
Density gradient effects in the tokamak edge turbulence with temperature gradient driving
[DE94-625042] p 370 N95-13539
TURBULENCE EFFECTS
Measurements of atmospheric turbulence effects on tail rotor acoustics
[NASA-TM-108843] p 232 N95-12360
Measurements of pressure and thermal wakes in a transonic turbine cascade
[AD-A283464] p 232 N95-12548
Density gradient effects in the tokamak edge turbulence with temperature gradient driving
[DE94-625042] p 370 N95-13539
TURBULENCE MODELS
Methods of ensuring realizability for non-realizable second order closures
[NASA-TM-106681] p 291 N95-11935
A new Reynolds stress algebraic equation model
[NASA-TM-106644] p 292 N95-11953
Hypersonic turbulent boundary-layer and free shear database
[NASA-CR-177610] p 292 N95-11992
TURBULENT BOUNDARY LAYER
Laser Doppler velocimeter measurements of boundary layer velocity and turbulent intensities in Mach 2.5 flow
[NASA-CR-196861] p 289 N95-11709
Concentration fluctuation models: A comparative study
[CUED/A-AERO/TR-24] p 292 N95-11939
Hypersonic turbulent boundary-layer and free shear database
[NASA-CR-177610] p 292 N95-11992
Computation of turbulent boundary layers employing the defect wall-function method
[NASA-CR-4629] p 293 N95-12859
Validation of the RPLUS3D code for supersonic inlet applications involving three-dimensional shock wave-boundary layer interactions
[NASA-TM-106579] p 233 N95-13058
TURBULENT FLOW
LES, DNS and RANS for the analysis of high-speed turbulent reacting flows
[NASA-CR-196822] p 289 N95-11705
Pressure measurements on an F/A-18 twin vertical tail in buffeting flow. Volume 3: Buffet power spectral densities
[AD-A281444] p 230 N95-11829
Modification of the two-equation turbulence model in NPARC to a Chien low Reynolds number k-epsilon formulation
[NASA-TM-106710] p 231 N95-11917
Scale disparity and spectral transfer in anisotropic numerical turbulence
[NASA-CR-194956] p 291 N95-11929
Methods of ensuring realizability for non-realizable second order closures
[NASA-TM-106681] p 291 N95-11935
A new Reynolds stress algebraic equation model
[NASA-TM-106644] p 292 N95-11953
Measurements of pressure and thermal wakes in a transonic turbine cascade
[AD-A283464] p 232 N95-12548
Computation of turbulent boundary layers employing the defect wall-function method
[NASA-CR-4629] p 293 N95-12859
Methodology for sensitivity analysis, approximate analysis, and design optimization in CFD for multidisciplinary applications
[NASA-CR-196981] p 294 N95-13201
Fundamental and experimental studies on the catalytic combustion of methane
[PB94-205895] p 268 N95-13251
Presentation of computer code SPIRALI for incompressible, turbulent, plane and spiral grooved cylindrical and face seals p 305 N95-13584
TURBULENT JETS
Modeling jets in cross flow
[NASA-CR-194965] p 291 N95-11930
Planar Rayleigh scattering and laser-induced fluorescence for visualization of a hot, Mach 2 annular air jet
[NASA-TM-4576] p 247 N95-13196
TURBULENT MIXING
Hypersonic turbulent boundary-layer and free shear database
[NASA-CR-177610] p 292 N95-11992
TURBULENT WAKES
Measurements of pressure and thermal wakes in a transonic turbine cascade
[AD-A283464] p 232 N95-12548
TVD SCHEMES
Analysis and design of numerical schemes for gas dynamics 1: Artificial diffusion, upwind biasing, limiters and their effect on accuracy and multigrid convergence
[NASA-CR-196477] p 290 N95-11875
TWO BODY PROBLEM
Study of the nuclear-coulomb low-energy scattering parameters on the basis of the p-matrix approach
[DE94-622811] p 360 N95-13275
TWO DIMENSIONAL BOUNDARY LAYER
Effect of nonzero surface admittance on receptivity and stability of compressible boundary layer
[NASA-CR-4621] p 292 N95-12105
TWO DIMENSIONAL FLOW
Shock-tunnel combustor testing for hypersonic vehicles
[NASA-CR-196836] p 246 N95-11938
An investigation of the vortex method
[DE94-014931] p 294 N95-13156
Numerical time dependent sheet cavitation simulations using a higher order panel method
[PB94-204435] p 294 N95-13249
Studies on the flow induced by an oscillating airfoil in a uniform stream
[PB94-204450] p 233 N95-13250
TWO DIMENSIONAL MODELS
Fundamental and experimental studies on the catalytic combustion of methane
[PB94-205895] p 268 N95-13251
TWO PHASE FLOW
Scaling fluid content-pressure relations of different fluid systems in porous media
[DE94-013349] p 294 N95-13075

U

ULTRAHIGH FREQUENCIES
Advanced S-Band studies using the TDRSS communications satellite
[NASA-CR-196931] p 281 N95-12010
ULTRASONIC FLAW DETECTION
The influence of finite-size sources in acousto-ultrasonics
[NASA-CR-195374] p 308 N95-11813
ULTRASONIC RADIATION
The influence of finite-size sources in acousto-ultrasonics
[NASA-CR-195374] p 308 N95-11813
ULTRASONIC TESTS
Revealing hidden defects: A hybrid evaluation strategy for steel structures
[PB94-191236] p 308 N95-11822

ULTRASONIC WAVE TRANSDUCERS
The influence of finite-size sources in acousto-ultrasonics
[NASA-CR-195374] p 308 N95-11813
ULTRASONICS
NIST calibration of ASTM E127-type ultrasonic reference blocks
[PB94-191640] p 355 N95-11906
ULTRAVIOLET RADIATION
UV extinction and IR emission in diffuse H2 regions
[NASA-CR-196939] p 323 N95-12244
Solar influences on global change
[NASA-CR-196966] p 319 N95-12384
Development of UV irradiance standards
[PB94-181005] p 320 N95-12771
Gaseous detectors of ultraviolet and visible photons
[DE94-014990] p 296 N95-13171
ULTRAVIOLET SPECTRA
A calibration of the Naval Postgraduate School middle ultraviolet spectrograph and an analysis of the OII 2470 A emission obtained by the middle ultraviolet spectrograph
[AD-A283449] p 354 N95-13144
ULTRAVIOLET SPECTROMETERS
FNAS UAH UVSP and complimentary data analysis and modeling
[NASA-CR-194005] p 381 N95-12992
The laser and its applications on environment and biotechnology research
[DE94-013831] p 299 N95-13076
A calibration of the Naval Postgraduate School middle ultraviolet spectrograph and an analysis of the OII 2470 A emission obtained by the middle ultraviolet spectrograph
[AD-A283449] p 354 N95-13144
ULTRAVIOLET SPECTROSCOPY
UV and fluorescence studies for vinyl polymerization
[AD-A281187] p 274 N95-12520
UNCONTROLLED REENTRY (SPACECRAFT)
Lifetime and reentry prediction for the Petite Amateur Navy Satellite (PANSAT)
[AD-A283366] p 255 N95-12921
UNDERWATER ACOUSTICS
Study of adaptive high resolution frequency estimation techniques with hydroacoustical applications
[PB94-179512] p 355 N95-12597
Ocean acoustic tomography: Single slice and moving ship experiments
[AD-A283059] p 329 N95-12998
UNDERWATER VEHICLES
Numerical simulation of particle-wave interaction on boundary layers
[AD-A282184] p 293 N95-12422
UNIVERSAL TIME
Initial analysis and modeling results from the Polar Orbiting Geomagnetic Survey (POGS) satellite
[AD-A283454] p 253 N95-12545
UNIVERSITY PROGRAM
NASA/OAI Research Associates program
[NASA-CR-196824] p 376 N95-11765
Solar-Terrestrial Environment Laboratory, Nagoya University p 389 N95-12610
UNMANNED SPACECRAFT
Project Genesis: Mars in situ propellant technology demonstrator mission
[NASA-CR-197166] p 277 N95-12822
Project Hyreus: Mars sample return mission utilizing in situ propellant production
[NASA-CR-197189] p 383 N95-12826
UNSTEADY AERODYNAMICS
Aeroelastic simulation of higher harmonic control
[NASA-CR-4623] p 230 N95-11911
UNSTEADY FLOW
Boundary conditions for unsteady compressible flows
[NASA-TM-106737] p 293 N95-12380
Activities of the Institute for Aerospace Studies of Toronto University p 390 N95-12699
Studies on the flow induced by an oscillating airfoil in a uniform stream
[PB94-204450] p 233 N95-13250
UPPER ATMOSPHERE
Greenhouse Effect Detection Experiment (GEDEX). Selected data sets
[NASA-TM-109952] p 318 N95-11845
UPWELLING WATER
Reports to the Nation on our changing planet. El Nino and climate prediction, no. 3, spring 1994
p 320 N95-12462
URANIUM ALLOYS
Be-9 and B-11 NMR study of superconductivity in boron doped UBe13
[DE94-014432] p 374 N95-13081
URANIUM OXIDES
Mechanical behavior of (238)UO2, (238)PuO2, and (239)PuO2 as a function of strain rate and temperature
[DE94-015718] p 312 N95-12784
Thermodynamic constants for actinide oxides and oxyhydroxides relevant to actinide volatility calculations for thermal oxidation processes
[DE94-007762] p 376 N95-13074
URANUS (PLANET)
Non-dipolar magnetic field models and patterns of radio emission: Uranus and Neptune compared
[NASA-CR-196412] p 385 N95-12469
USER MANUALS (COMPUTER PROGRAMS)
Engine structures analysis software: Component Specific Modeling (COSMO)
[NASA-CR-195378] p 309 N95-11711
TKKMOD: A computer simulation program for an integrated wind diesel system. Version 1.0: Document and user guide
[PB94-179090] p 317 N95-11798
The program for the 1993 adjustment of the Finnish first-order terrestrial triangulation
[REPT-94:3] p 314 N95-11880
User's manual for the NASA Lewis ice accretion/heat transfer prediction code with electrothermal deicer input
[NASA-CR-4530] p 291 N95-11888
Predicting radiative heat transfer in thermochemical nonequilibrium flow fields. Theory and user's manual for the LORAN code
[NASA-TM-4564] p 291 N95-11936
Investigation of advanced counterrotation blade configuration concepts for high speed turboprop systems. Task 8: Cooling flow/heat transfer analysis user's manual
[NASA-CR-195360] p 244 N95-11951
Nimbus-7 Earth Radiation Budjet compact solar data set user's guide
[NASA-RP-1346] p 384 N95-12667
Stochastic indexing
[AD-A283143] p 327 N95-13137
Micromechanics Analysis Code (MAC). User guide: Version 1.0
[NASA-TM-106706] p 264 N95-13193
MapView user's guide
[AD-A282469] p 316 N95-13290
SURRENDER user's manual, second edition
[PB94-206950] p 346 N95-13571
USER REQUIREMENTS
A data and information system for processing, archival, and distribution of data for global change research
[NASA-CR-196770] p 320 N95-12786
Environmental and customer-driven seal requirements
p 305 N95-13588
UTILITIES
Toward infrastructure improvement: An agenda for research
[LC-94-67335] p 376 N95-12385

V

VACUUM APPARATUS
A laboratory vacuum apparatus for magnetron sputtering of thin Z ZnO piezoelectric films, magnetron sputtering
p 296 N95-12111
VACUUM MELTING
Description of a high temperature quenching furnace for the study of the directional solidification of nickel-base superalloys
[DE94-013812] p 271 N95-13544
VACUUM SYSTEMS
The field emission of electrons in vacuum insulation systems p 357 N95-12101
Vacuum system operating experience review for fusion applications
[DE94-015267] p 368 N95-12759
Description of a high temperature quenching furnace for the study of the directional solidification of nickel-base superalloys
[DE94-013812] p 271 N95-13544
VACUUM TUBES
The reflection of relativistic electron beam by virtual cathode
[IPPCZ-338] p 364 N95-11916
VALVES
Modular hydraulic control system
[AD-D016401] p 304 N95-13155
VANADATES
Optical and magnetic resonance investigations of 3D ions in single crystal hosts: Candidates for tunable solid-state lasers
[AD-A281726] p 371 N95-11842
VANADIUM
MHD pressure drops and thermal hydraulic analysis for the ITER breeding blanket design
[DE94-015085] p 369 N95-13280
VANADIUM ALLOYS
On the strain and strain-rate dependence of the fraction of plastic work converted to heat: An experimental study using high speed infrared detectors and the Kolsky bar
[SM-92-33] p 354 N95-12728
VANES
Engine structures analysis software: Component Specific Modeling (COSMO)
[NASA-CR-195378] p 309 N95-11711
VAPOR DEPOSITION
Analysis of cost: Combustion flame CVD diamond deposition
[AD-A282527] p 273 N95-12403
Intelligent processing of ferroelectric thin films
[AD-A282833] p 275 N95-12586
Loads for pulsed power cylindrical implosion experiments
[DE94-014429] p 299 N95-13080
Substrate temperature control apparatus and technique for CVD reactors
[AD-D016387] p 374 N95-13150
CVD techniques for the synthesis or modification of porous ceramics
[PB94-206836] p 276 N95-13284
Kinetics and characterization of tungsten CVD processes
[PB94-206901] p 271 N95-13411
VAPOR PHASES
Triple sorbent thermal desorption/gas chromatography/mass spectrometry determination of vapor phase organic contaminants
[DE94-013634] p 264 N95-11735
Atomic scale dynamics of a two-dimensional gas-solid interface
[AD-A282646] p 358 N95-12617
Scaling fluid content-pressure relations of different fluid systems in porous media
[DE94-013349] p 294 N95-13075
VAPOR PRESSURE
Vapour pressures and critical points of liquids. Polycyclic phenyl and cyclohexyl compounds
[ESDU-94001] p 266 N95-12128
VAPORS
Thermophysical properties of MtBE (methyl tertbutyl ether)
[ESDU-94010] p 265 N95-11775
Vapor detection sensitivity as a function of optical resolution for a single Lorentzian band
[AD-A283444] p 316 N95-13142
VARIABILITY
Ceramic manufacturing: Optimizing a multivariable system
[DE94-015016] p 276 N95-13184
VARIABLE STARS
The terrestrial gravitational wave environment from known sources
[NASA-CR-196167] p 323 N95-12468
VARIABLE SWEEP WINGS
A preliminary design proposal for a maritime patrol strike aircraft: MPS-2000 Condor
[NASA-CR-197182] p 241 N95-12689
VARIATIONS
Influence of additives on structure and thermal stability of ammonium nitrate
[PB94-206943] p 278 N95-13435
VARISTORS
The experiment and analysis of tailoring V(sub L) and I(sub P) with ZnO voltage-sensitive resistor on HT-6M
[DE94-625074] p 370 N95-13541
VAX COMPUTERS
Norwegian contribution to the SWG on APSE programme
[PB94-202397] p 341 N95-13557
VECTOR ANALYSIS
NPS state vector analysis and relative motion plotting software for STS-51
[AD-A282909] p 249 N95-12510
VECTOR MESONS
Particle-production mechanism in relativistic heavy-ion collisions
[DE94-014427] p 359 N95-13104
On the charged vector particle scattering on a vector particle
[DE94-622787] p 360 N95-13273
VECTOR PROCESSING (COMPUTERS)
Nonlinear structural response using adaptive dynamic relaxation on a massively-parallel-processing system
[NASA-CR-196491] p 313 N95-13162
VECTOR QUANTIZATION
Vector quantization for efficient coding of upper subbands
[NASA-CR-196804] p 341 N95-11762
An efficient system for reliably transmitting image and video data over low bit rate noisy channels
[NASA-CR-196802] p 341 N95-11764

VECTOR SPACES
A model of the density of solar radiation energy on an arbitrary plane identification for Warsaw
p 384 N95-12243
VECTORS (MATHEMATICS)
Implementing a linear equation solver in the CFD code PHOENICS
[PB94-195757] p 353 N95-13439
VEGETATION
Estimation of above-ground phytomass in a tropical forest using TM-LANDSAT 5 E HRV-SPOT 1 data
[INPE-5500-TDI/515] p 316 N95-13159
VEHICLE WHEELS
Study of in-plane dynamics of tires
[PB94-206893] p 304 N95-13410
VELOCITY DISTRIBUTION
Stationary plasma thruster ion velocity distribution
[NASA-CR-195379] p 257 N95-11919
Simultaneous three-dimensional velocity and mixing measurements by use of laser Doppler velocimetry and fluorescence probes in a water tunnel
[NASA-TP-3454] p 246 N95-13553
VELOCITY MEASUREMENT
A new algorithm for five-hole probe calibration, data reduction, and uncertainty analysis
[NASA-TM-106458] p 232 N95-12378
Hypersonic Gas-Surface Energy Accommodation Test Facility
[DE94-014468] p 232 N95-12652
Simultaneous three-dimensional velocity and mixing measurements by use of laser Doppler velocimetry and fluorescence probes in a water tunnel
[NASA-TP-3454] p 246 N95-13553
VENTILATION
Cabin fuselage structural design with engine installation and control system
[NASA-CR-197173] p 240 N95-12639
VENUS (PLANET)
Quantitative understanding of the cycles of oxidized and reduced sulfur on Venus
[NASA-CR-196924] p 382 N95-12011
VENUS ATMOSPHERE
Pioneer Venus orbiter electron temperature probe
[NASA-CR-196844] p 257 N95-11805
Venus cloud bobber mission: A long term survey of the Venusian surface
[NASA-CR-197174] p 383 N95-12533
VENUS CLOUDS
Quantitative understanding of the cycles of oxidized and reduced sulfur on Venus
[NASA-CR-196924] p 382 N95-12011
VENUS PROBES
Venus cloud bobber mission: A long term survey of the Venusian surface
[NASA-CR-197174] p 383 N95-12533
VENUS SURFACE
Venus surface roughness and Magellan stereo data
[NASA-CR-196821] p 382 N95-11704
VERTICAL AIR CURRENTS
Airborne Windshear Detection and Warning Systems. Fifth and Final Combined Manufacturers' and Technologists' Conference, part 2
[NASA-CP-10139-PT-2] p 234 N95-13203
VERTICAL LANDING
Moisture induced pressures in concrete airfield pavements
[AD-A281974] p 245 N95-11789
VERTICAL TAKEOFF
Moisture induced pressures in concrete airfield pavements
[AD-A281974] p 245 N95-11789
VERY LARGE SCALE INTEGRATION
Locally connected adaptive Gabor filter for real-time motion compensation
[AD-A282544] p 286 N95-12494
VERY LOW FREQUENCIES
BATSE observations of 3C273
[NASA-CR-196185] p 380 N95-12463
Locked modes in TEXT-U tokamak
[DE94-011595] p 370 N95-13529
VESTIBULAR NYSTAGMUS
Reduction of ocular counter-rolling by adaptation to space
[NASA-CR-196279] p 333 N95-12376
VESTIBULAR TESTS
Reduction of ocular counter-rolling by adaptation to space
[NASA-CR-196279] p 333 N95-12376
VIBRATION
Atomic structure modifications of diamond-like nanocomposite films: Observation by Raman spectroscopy, FTIR and STM
[DE94-013732] p 371 N95-11740
Pipeline vibrations. Computer program for the prediction of fluid transients in flexible, unbranched three-dimensional piping systems
[ESDU-93031] p 309 N95-11768
An implementation of a chemical and thermal nonequilibrium flow solver on unstructured meshes and application to blunt bodies
[NASA-CR-194967] p 293 N95-12619
Analysis of the effects of surface pitting and wear on the vibrations of a gear transmission system
[NASA-TM-106678] p 301 N95-12621
VIBRATION DAMPING
Aeroelastic simulation of higher harmonic control
[NASA-CR-4623] p 230 N95-11911
Active vibration control using a distributed controller
[PB94-207073] p 313 N95-13576
VIBRATION EFFECTS
An examination of anticipated g-jitter on Space Station and its effects on materials processes
[NASA-TM-103775] p 278 N95-12703
Analytical and experimental vibration analysis of a faulty gear system
[NASA-TM-106689] p 303 N95-12843
Computerized design and generation of low-noise helical gears with modified surface topology
[NASA-TM-106696] p 303 N95-13083
VIBRATION MODE
Theory of complex defects on DNA polymer chain
[AD-A282619] p 275 N95-12536
Active vibration control using a distributed controller
[PB94-207073] p 313 N95-13576
VIBRATIONAL STATES
Theory of complex defects on DNA polymer chain
[AD-A282619] p 275 N95-12536
VIDEO COMMUNICATION
An efficient system for reliably transmitting image and video data over low bit rate noisy channels
[NASA-CR-196802] p 341 N95-11764
VIDEO COMPRESSION
Improved image decompression for reduced transform coding artifacts
[NASA-CR-196805] p 341 N95-11761
Vector quantization for efficient coding of upper subbands
[NASA-CR-196804] p 341 N95-11762
An efficient system for reliably transmitting image and video data over low bit rate noisy channels
[NASA-CR-196802] p 341 N95-11764
VIDEO DATA
An efficient system for reliably transmitting image and video data over low bit rate noisy channels
[NASA-CR-196802] p 341 N95-11764
VIEWING
SURRENDER user's manual, second edition
[PB94-206950] p 346 N95-13571
VINYL POLYMERS
UV and fluorescence studies for vinyl polymerization
[AD-A281187] p 274 N95-12520
VINYLIDENE
Active vibration control using a distributed controller
[PB94-207073] p 313 N95-13576
VIRTUAL REALITY
Exploitation of virtual reality architectures
[AD-A282263] p 340 N95-12413
VISCOELASTICITY
Stress relaxation functions: Methods of approximation
[NASA-CR-195830] p 312 N95-12861
VISCOPLASTICITY
Micromechanics Analysis Code (MAC). User guide: Version 1.0
[NASA-TM-106706] p 264 N95-13193
VISCOSITY
Viscosity solutions of fully nonlinear equations
[AD-A281725] p 351 N95-11861
VISCOUS DAMPING
Evaluation of COSTAR mass handling characteristics in an environment. A simulation of the Hubble Space Telescope service mission
[NASA-TP-3489] p 333 N95-11887
VISCOUS FLOW
An investigation of the vortex method
[DE94-014931] p 294 N95-13156
Studies on the flow induced by an oscillating airfoil in a uniform stream
[PB94-204450] p 233 N95-13250
VISIBILITY
Airborne Windshear Detection and Warning Systems. Fifth and Final Combined Manufacturers' and Technologists' Conference, part 2
[NASA-CP-10139-PT-2] p 234 N95-13203
Characteristics of civil aviation atmospheric hazards
p 235 N95-13208
VISUAL ACUITY
Neural networks: Structure and repair. Part 1: Ground squirrel visual system. Part 2: Formation, maintenance and plasticity of synaptic connections
[AD-A282420] p 330 N95-12393
VISUAL PERCEPTION
Visit to UDRI and USAF, Armstrong Lab., Williams AFB, Phoenix, USA, February 8-11, 1993
[PB94-190659] p 337 N95-11873
The selective use of functional optical variables in the control of forward speed
[NASA-TM-108849] p 229 N95-12227
Visual psychophysics of egomotion
[AD-A282547] p 335 N95-12495
VISUAL PIGMENTS
Conformation of membrane proteins: Bacteriorhodopsin
[AD-A281282] p 331 N95-13373
VISUAL SIGNALS
Evaluation of candidate millimeter wave sensors for synthetic vision p 236 N95-13214
VITAMINS
Copper metabolism in rats fed ascorbic acid or restricted amounts of copper
[PB94-191343] p 330 N95-11902
VOIDS
Revealing hidden defects: A hybrid evaluation strategy for steel structures
[PB94-191236] p 308 N95-11822
The structural basis for fatigue failure initiation in glassy polymers
[DE94-015415] p 275 N95-13060
VOLTAGE CONVERTERS (DC TO DC)
Power system applications for PASC converter systems
[DE94-013329] p 286 N95-11751
VOLUMETRIC ANALYSIS
Orthobaric densities and molar volumes of liquids. Polycyclic phenyl and cyclohexyl compounds
[ESDU-94002] p 266 N95-12129
VORTICES
Relativistic theory of superfluidity with two condensates
[DE94-624073] p 290 N95-11749
Water tunnel flow visualization study of a 4.4 percent scale X-31 forebody
[NASA-TM-104276] p 230 N95-11898
Dynamical studies in hurricane intensity change
[AD-A282406] p 326 N95-12392
An investigation of the vortex method
[DE94-014931] p 294 N95-13156
Ground-based wake vortex monitoring, prediction, and ATC interface p 235 N95-13209
Wake vortex detection at Denver Stapleton Airport with a pulsed 2-micron coherent lidar p 236 N95-13211
Doppler radar detection of vortex hazard indicators
p 236 N95-13212
Simultaneous three-dimensional velocity and mixing measurements by use of laser Doppler velocimetry and fluorescence probes in a water tunnel
[NASA-TP-3454] p 246 N95-13553
VOYAGER 2 SPACECRAFT
Non-dipolar magnetic field models and patterns of radio emission: Uranus and Neptune compared
[NASA-CR-196412] p 385 N95-12469

W

WAKES
Measurements of atmospheric turbulence effects on tail rotor acoustics
[NASA-TM-108843] p 232 N95-12360
Ground-based wake vortex monitoring, prediction, and ATC interface p 235 N95-13209
WALKING MACHINES
Human-like robots for space and hazardous environments
[NASA-CR-197171] p 301 N95-12532
Integral habitat transport system
[NASA-CR-197156] p 339 N95-12629
WALL FLOW
A wall interference assessment and correction system
[NASA-CR-196940] p 292 N95-12228
Computation of turbulent boundary layers employing the defect wall-function method
[NASA-CR-4629] p 293 N95-12859
WALL TEMPERATURE
FDNS code to predict wall heat fluxes or wall temperatures in rocket nozzles
[NASA-CR-196925] p 292 N95-11999
WARNING SYSTEMS
Thunderstorm hypothesis reasoner
[AD-A282664] p 326 N95-12805

Terminal Doppler Weather Radar Build 5A Operational Test and Evaluation (OT/E) integration and OT/E operational test plan
[AD-A283052] p 327 N95-12996
Airborne Windshear Detection and Warning Systems. Fifth and Final Combined Manufacturers' and Technologists' Conference, part 2
[NASA-CP-10139-PT-2] p 234 N95-13203

WASTE TREATMENT
MSW to hydrogen --- municiple solid waste (MSW)
[DE94-014741] p 265 N95-11790
Supercritical fluid (SCF) technologies: Assessment of applicability to installation restoration processes
[AD-A281504] p 290 N95-11859

WASTE UTILIZATION
MSW to hydrogen --- municiple solid waste (MSW)
[DE94-014741] p 265 N95-11790

WATER
Evaluation of COSTAR, mass handling characteristics in an environment. A simulation of the Hubble Space Telescope service mission
[NASA-TP-3489] p 333 N95-11887
Quantitative understanding of the cycles of oxidized and reduced sulfur on Venus
[NASA-CR-196924] p 382 N95-12011
Development of techniques for the in situ observation of OH and HO2 for studies of the impact of high-altitude supersonic aircraft on the stratosphere
[NASA-CR-196759] p 321 N95-12832
Hydrogen bonding and molecular orientation in water/fluorine adlayers on silver(110)
[AD-A282652] p 268 N95-13549
Simultaneous three-dimensional velocity and mixing measurements by use of laser Doppler velocimetry and fluorescence probes in a water tunnel
[NASA-TP-3454] p 246 N95-13553

WATER COLOR
SeaWiFS technical report series. Volume 19: Case studies for SeaWiFS calibration and validation, part 2
[NASA-TM-104566-VOL-19-PT-2] p 328 N95-11920
SeaWiFS technical report series. Volume 22: Prelaunch acceptance report for the SeaWiFS radiometer
[NASA-TM-104556-VOL-22] p 328 N95-12151

WATER CONSUMPTION
Elimination of quinine in two subjects after ingestion of tonic water: An exploratory study
[DOT/FAA/AM-94/16] p 332 N95-11702

WATER FLOW
Periglacial and glacial analogs for Martian landforms
[NASA-CR-196772] p 383 N95-12952

WATER HEATING
Diesel-fired self-pumping water heater
[AD-A283063] p 279 N95-13053

WATER IMMERSION
Effects of oral glucose on exercise thermoregulation in men after water immersion
[NASA-TM-108825] p 329 N95-11810

WATER QUALITY
Improving the efficiency of high purity water systems
[DE94-013742] p 318 N95-11784

WATER TREATMENT
Improving the efficiency of high purity water systems
[DE94-013742] p 318 N95-11784

WATER TUNNEL TESTS
Water tunnel flow visualization study of a 4.4 percent scale X-31 forebody
[NASA-TM-104276] p 230 N95-11898
Simultaneous three-dimensional velocity and mixing measurements by use of laser Doppler velocimetry and fluorescence probes in a water tunnel
[NASA-TP-3454] p 246 N95-13553

WATER VAPOR
Implementation of a state of the art automated system for the production of cloud/water vapor motion winds from geostationary satellites
[NASA-CR-196817] p 325 N95-11758
Carbon dioxide and water vapor production at rest and during exercise. A report on data collection for the Crew and Thermal Systems Division
[NASA-TP-3500] p 337 N95-11811
Optical Remote Sensing of the Atmosphere. Technical digest 1993. Volume 5: Postconference edition
[AD-A281446] p 314 N95-11831
Differential absorption lidar measurements of atmospheric water vapor using a pseudonoise code modulated AlGaAs laser
[NASA-TM-104610] p 314 N95-11997

WATERSHEDS
Use of remote sensing and geographic information system techniques in integrated studies of watersheds
[INPE-5494-TDI/511] p 316 N95-13352

WAVE DIFFRACTION
Efficient parabolic equation solution of radiowave propagation in an inhomogeneous atmosphere and over irregular terrain: Formulation
[AD-A282648] p 284 N95-12834
Simulating the energy performance of holographic glazings
[DE94-014969] p 296 N95-13158

WAVE DISPERSION
Stimulated scattering of a slow electromagnetic wave excited by the relativistic electron beam
[DE94-625049] p 285 N95-13343
Excitation of fast magneto-acoustic waves in unhomogeneous plasma of a large size tokamak
[DE94-625050] p 370 N95-13540

WAVE DRAG
Application of two procedures for dual-point design of transonic airfoils
[NASA-TP-3466] p 231 N95-12176

WAVE EQUATIONS
Is the pollution effect of the FEM avoidable for the Helmholtz equation considering high wave numbers?
[AD-A282585] p 352 N95-12552
Aspects of long time behaviour of solutions of nonlinear Hamiltonian evolution equations
[PB94-192382] p 352 N95-12808

WAVE EXCITATION
Excitation of fast magneto-acoustic waves in unhomogeneous plasma of a large size tokamak
[DE94-625050] p 370 N95-13540

WAVE GENERATION
The influence of finite-size sources in acousto-ultrasonics
[NASA-CR-195374] p 308 N95-11813

WAVE PACKETS
Effect of stochastic damping resonance wave packet on energetic alpha particle transport
[DE94-625041] p 370 N95-13538

WAVE PROPAGATION
Investigation of finite element: ABC methods for electromagnetic field simulation
[NASA-CR-196837] p 279 N95-11707
Revealing hidden defects: A hybrid evaluation strategy for steel structures
[PB94-191236] p 308 N95-11822
Boundary conditions for unsteady compressible flows
[NASA-TM-106737] p 293 N95-12380
Efficient parabolic equation solution of radiowave propagation in an inhomogeneous atmosphere and over irregular terrain: Formulation
[AD-A282648] p 284 N95-12834
Nonlinear hysteresis in an endochronic solid
[AD-A283142] p 325 N95-13136

WAVE REFLECTION
Plane-wave reflection from uniaxial chiral interface and its application to polarization transformation
[PB94-184496] p 283 N95-12580

WAVEFORMS
Uniform spectral amplitude windowing for hyperbolic frequency modulated waveforms
[AD-A282508] p 355 N95-12396

WEAPON SYSTEM MANAGEMENT
Case study of risk management in the USAF B-1B bomber program
[AD-A282371] p 377 N95-11944
The development of the F100-PW-220 and F110-GE-100 engines: A case study of risk assessment and risk management
[AD-A282467] p 244 N95-13289

WEAPON SYSTEMS
Vulnerability assessment of a space based weapon platform electronics system exposed to a thermonuclear weapon detonation
[DE94-013415] p 250 N95-11755

WEAPONS DEVELOPMENT
Case study of risk management in the USAF B-1B bomber program
[AD-A282371] p 377 N95-11944
The development of the F100-PW-220 and F110-GE-100 engines: A case study of risk assessment and risk management
[AD-A282467] p 244 N95-13289

WEAR
Analytical and experimental vibration analysis of a faulty gear system
[NASA-TM-106689] p 300 N95-12377
Analysis of the effects of surface pitting and wear on the vibrations of a gear transmission system
[NASA-TM-106678] p 301 N95-12621
Non-contacting gas lubricated face seals for high p x v-values p 308 N95-13609

WEAR TESTS
Brush seals for cryogenic applications p 305 N95-13592
Relative performance comparison between baseline labyrinth and dual-brush compressor discharge seals in a T-700 engine test p 307 N95-13607
Some metallographic results for brush bristles and brush segments of a shroud ring brush seal tested in a T-700 engine p 307 N95-13608

WEATHER STATIONS
Short term weather forecasting in real time in a base weather station setting
[AD-A283141] p 327 N95-13134

WEATHERING
Ten-year ground exposure of composite materials used on the Bell Model 206L helicopter flight service program
[NASA-TP-3468] p 262 N95-12357
Accelerated testing of coatings for protection against atmospheric corrosion
[PB94-202579] p 276 N95-13244

WEDGES
Validation of the RPLUS3D code for supersonic inlet applications involving three-dimensional shock wave-boundary layer interactions
[NASA-TM-106579] p 233 N95-13058

WEIGHTLESSNESS
Spaceflight and immune responses of Rhesus monkeys
[NASA-CR-196846] p 331 N95-12941
Feasibility study for the Cryogenic Orbital Nitrogen Experiment (CONE)
[NASA-CR-187231] p 294 N95-13234

WEIGHTLESSNESS SIMULATION
Evaluation of COSTAR mass handling characteristics in an environment. A simulation of the Hubble Space Telescope service mission
[NASA-TP-3489] p 333 N95-11887

WELD STRENGTH
Weld acoustic monitor
[AD-D016400] p 356 N95-13154

WELDED JOINTS
Novel concepts in weld science: Role of gradients and composite structure
[DE94-015482] p 271 N95-12895

WELDING
Certain aspects of the melting, casting and welding of Ni3Al alloys
[DE94-013628] p 269 N95-11897
Advanced computer architecture specification for automated weld systems
[NASA-CR-194006] p 343 N95-12014

WETTABILITY
A novel lead-free solder replacement
[DE94-013782] p 269 N95-11785

WHEAT
Methodologies for processing plant material into acceptable food on a small scale
[NASA-CR-177647] p 338 N95-12132

WHITE NOISE
Investigation of spectral-based techniques for classification of wideband transient signals in additive white Gaussian noise
[AD-A282954] p 283 N95-12592

WIND (METEOROLOGY)
Reports to the Nation on our changing planet. El Nino and climate prediction, no. 3, spring 1994 p 320 N95-12462

WIND DIRECTION
Reports to the Nation on our changing planet. El Nino and climate prediction, no. 3, spring 1994 p 320 N95-12462

WIND MEASUREMENT
Implementation of a state of the art automated system for the production of cloud/water vapor motion winds from geostationary satellites
[NASA-CR-196817] p 325 N95-11758
Terminal Doppler Weather Radar Build 5A Operational Test and Evaluation (OT/E) integration and OT/E operational test plan
[AD-A283052] p 327 N95-12996

WIND SHEAR
Tropical cyclone development and intensification under moderate to strong vertical wind shear
[AD-A282185] p 326 N95-12423
Terminal Doppler Weather Radar Build 5A Operational Test and Evaluation (OT/E) integration and OT/E operational test plan
[AD-A283052] p 327 N95-12996
Airborne Windshear Detection and Warning Systems. Fifth and Final Combined Manufacturers' and Technologists' Conference, part 2
[NASA-CP-10139-PT-2] p 234 N95-13203
Windshear certification data base for forward-look detection systems p 234 N95-13204
Certification methodology applied to the NASA experimental radar system p 235 N95-13205
Certification of windshear performance with RTCA class D radomes p 235 N95-13206
Airport surveillance using a solid state coherent lidar p 235 N95-13207
Ground-based wake vortex monitoring, prediction, and ATC interface p 235 N95-13209

WIND TUNNEL APPARATUS
Test model designs for advanced refractory ceramic materials p 277 N95-11968

WIND TUNNEL MODELS
Test model designs for advanced refractory ceramic materials p 277 N95-11968
Experimental Aerodynamics Division
[NAL-SP-9404] p 229 N95-12166
A wall interference assessment and correction system
[NASA-CR-196940] p 292 N95-12228
Design and testing of an oblique all-wing supersonic transport
[NASA-CR-196394] p 242 N95-12785
Mach number control in the High Speed Wind Tunnel of NLR
[PB94-201670] p 246 N95-13243

WIND TUNNEL TESTS
A shadowgraph study of the National Launch System's 1 1/2 stage vehicle configuration and Heavy Lift Launch Vehicle configuration --- Using the Marshall Space Flight Center's 14-Inch Trisonic Wind Tunnel
[NASA-RP-1347] p 229 N95-11710
Shock-tunnel combustor testing for hypersonic vehicles
[NASA-CR-196836] p 246 N95-11938
Measurements of pressure and thermal wakes in a transonic turbine cascade
[AD-A283464] p 232 N95-12548
Supersonic base flow investigation over axisymmetric afterbodies
[PB94-180957] p 232 N95-12578
Experimental aerodynamic characteristics of a generic hypersonic accelerator configuration at Mach numbers 1.5 and 2.0 --- conducted in the Langley Unitary Plan Wind Tunnel
[NASA-TM-4413] p 233 N95-12770
Design and testing of an oblique all-wing supersonic transport
[NASA-CR-196394] p 242 N95-12785
NASA's Hypersonic Research Engine Project: A review
[NASA-TM-107759] p 244 N95-12860
Role of wind tunnels and computer codes in the certification and qualification of rotorcraft for flight in forecast icing
[NASA-TM-106747] p 233 N95-13197

WIND TUNNELS
Test model designs for advanced refractory ceramic materials p 277 N95-11968

WIND TURBINES
TKKMOD: A computer simulation program for an integrated wind diesel system. Version 1.0: Document and user guide
[PB94-179090] p 317 N95-11798
Data acquisition system of the NANOSAW-2 stand alone wind diesel plant. Document and user's guide
[PB94-179108] p 317 N95-11799
Validation results of wind diesel simulation model TKKMOD
[PB94-179157] p 317 N95-11846

WIND VELOCITY
Certification methodology applied to the NASA experimental radar system p 235 N95-13205

WIND VELOCITY MEASUREMENT
Lidar performance analysis
[NASA-CR-196510] p 362 N95-12390
SuperMariah: A similarity-based method for determining wind, temperature, and humidity profile structure in the surface boundary layer
[AD-A283058] p 327 N95-12997

WINDOWS (APERTURES)
Science objectives and performance of a radiometer and window design for atmospheric entry experiments
[NASA-TM-4637] p 382 N95-12190

WINDPOWER UTILIZATION
TKKMOD: A computer simulation program for an integrated wind diesel system. Version 1.0: Document and user guide
[PB94-179090] p 317 N95-11798
Data acquisition system of the NANOSAW-2 stand alone wind diesel plant. Document and user's guide
[PB94-179108] p 317 N95-11799
Validation results of wind diesel simulation model TKKMOD
[PB94-179157] p 317 N95-11846

WINDPOWERED GENERATORS
TKKMOD: A computer simulation program for an integrated wind diesel system. Version 1.0: Document and user guide
[PB94-179090] p 317 N95-11798

WING NACELLE CONFIGURATIONS
Cabin fuselage structural design with engine installation and control system
[NASA-CR-197173] p 240 N95-12639

WING ROOTS
Gemini: A long-range cargo transport
[NASA-CR-197149] p 239 N95-12626

WINGLETS
Design and construction of a remote piloted flying wing
[NASA-CR-197195] p 241 N95-12695

WINGS
Parallel aeroelastic computations for wing and wing-body configurations
[NASA-CR-196835] p 230 N95-11766
The development of a highly reliable power management and distribution system for civil transport aircraft
[NASA-TM-106697] p 243 N95-11867
Optimum aerodynamic design via boundary control
[NASA-CR-195882] p 230 N95-11877
Viper cabin-fuselage structural design concept with engine installation and wing structural design
[NASA-CR-197162] p 239 N95-12305
The FC-1D: The profitable alternative Flying Circus Commercial Aviation Group
[NASA-CR-197152] p 240 N95-12628
Cabin-fuselage-wing structural design concept with engine installation
[NASA-CR-197172] p 242 N95-12993
Numerical time dependent sheet cavitation simulations using a higher order panel method
[PB94-204435] p 294 N95-13249

WIRING
Evaluation of wiring constructions for space applications
[NASA-TM-106735] p 256 N95-13194

WOLF-RAYET STARS
A catalogue of potentially bright close binary gravitational wave sources
[NASA-CR-196934] p 379 N95-12234

WORKLOADS (PSYCHOPHYSIOLOGY)
Crew factors in flight operations 9: Effects of planned cockpit rest on crew performance and alertness in long-haul operations
[NASA-TM-108839] p 334 N95-12792

WORKSTATIONS
Exploitation of virtual reality architectures
[AD-A282263] p 340 N95-12413

WOVEN COMPOSITES
Failure analysis of woven and braided fabric reinforced composites
[NASA-CR-194981] p 262 N95-11926
Test methods for textile composites
[NASA-CR-4609] p 262 N95-12793

X

X RAY ABSORPTION
Development of nonintrusive, scatter-independent techniques for measurement of liquid density inside dense sprays
[NASA-CR-196413] p 293 N95-12387
In-situ x-ray analysis of the electrolyte-solid interface
[AD-A282203] p 373 N95-12425
Raman structural studies of the nickel electrode
[NASA-CR-196331] p 289 N95-13344

X RAY ANALYSIS
In-situ x-ray analysis of the electrolyte-solid interface
[AD-A282203] p 373 N95-12425

X RAY ASTRONOMY
Investigation of physical parameters in stellar flares observed by GINGA
[NASA-CR-196823] p 381 N95-11928
X-ray and gamma ray astronomy detectors
[NASA-SP-517] p 379 N95-12304
A deep x-ray survey of the Pleiades cluster and the B6-A3 main sequence stars in Orion
[NASA-CR-196190] p 380 N95-12373
An x-ray search for PMS stars in translucent molecular clouds
[NASA-CR-196151] p 380 N95-12388
BATSE observations of Nova Muscae 1991
[NASA-CR-196416] p 380 N95-12464
Hot absorbers and the x-ray spectra of BL Lac objects
[NASA-CR-196196] p 380 N95-12465
X-ray temporal and spectral studies of blazars with the Ginga satellite
[NASA-CR-196330] p 380 N95-12466
The x-ray structure of the supernova remnant W49B
[NASA-CR-196482] p 382 N95-12950

X RAY ASTROPHYSICS FACILITY
Activities of the Space Studies Board of the National Research Council
[NASA-CR-195738] p 247 N95-12880

X RAY BINARIES
Research in astrophysical processes
[NASA-CR-196773] p 382 N95-12939

X RAY DETECTORS
Large area soft x-ray collimator to facilitate x-ray optics testing
[NASA-CR-196923] p 362 N95-12736
Alignment and experiment of the HL-1 x ray bent-crystal spectrometer
[DE94-624719] p 297 N95-13537

X RAY DIFFRACTION
The magnetic structure of holmium-erbium superlattices
[DE94-013728] p 371 N95-11739
Resonant x-ray scattering in 5f magnetism
[DE94-013753] p 358 N95-12829
Raman structural studies of the nickel electrode
[NASA-CR-196331] p 289 N95-13344

X RAY FLUORESCENCE
Effects of sample formulation on the analysis of heavy metals by x-ray fluorescence
[AD-A282733] p 267 N95-12836
Proceedings of the CTU Seminar 1994, Part C
[DE94-624078] p 390 N95-12946

X RAY IMAGERY
Monochromatic x ray imaging in plasma focus experiment p 366 N95-12443

X RAY LASERS
Experimental and theoretical study of neon-like selenium x-ray laser spectral line profiles
[DE94-015327] p 298 N95-12761

X RAY OPTICS
Large area soft x-ray collimator to facilitate x-ray optics testing
[NASA-CR-196923] p 362 N95-12736

X RAY SCATTERING
Resonant x-ray scattering in 5f magnetism
[DE94-013753] p 358 N95-12829

X RAY SOURCES
A deep x-ray survey of the Pleiades cluster and the B6-A3 main sequence stars in Orion
[NASA-CR-196190] p 380 N95-12373
An x-ray search for PMS stars in translucent molecular clouds
[NASA-CR-196151] p 380 N95-12388
The results of the study of compact gas-puff and vacuum spark plasma sources of SXR with Glass-Capillary Converters (GCC) p 367 N95-12446
Hot absorbers and the x-ray spectra of BL Lac objects
[NASA-CR-196196] p 380 N95-12465
The x-ray structure of the supernova remnant W49B
[NASA-CR-196482] p 382 N95-12950
Search for inverse Compton x-rays from the lobes of Fornax A x-rays from radio galaxies straddling the Fanaroff-Riley transition
[NASA-CR-196433] p 385 N95-13023

X RAY SPECTRA
Investigation of physical parameters in stellar flares observed by GINGA
[NASA-CR-196823] p 381 N95-11928
BATSE observations of Nova Muscae 1991
[NASA-CR-196416] p 380 N95-12464
Hot absorbers and the x-ray spectra of BL Lac objects
[NASA-CR-196196] p 380 N95-12465
X-ray temporal and spectral studies of blazars with the Ginga satellite
[NASA-CR-196330] p 380 N95-12466
FNAS UAH UVSP and complimentary data analysis and modeling
[NASA-CR-194005] p 381 N95-12992

X RAY SPECTROSCOPY
In-situ x-ray analysis of the electrolyte-solid interface
[AD-A282203] p 373 N95-12425
Effects of sample formulation on the analysis of heavy metals by x-ray fluorescence
[AD-A282733] p 267 N95-12836
Alignment and experiment of the HL-1 x ray bent-crystal spectrometer
[DE94-624719] p 297 N95-13537

X RAY STARS
An x-ray search for PMS stars in translucent molecular clouds
[NASA-CR-196151] p 380 N95-12388

X RAYS
Target area chamber system design for the National Ignition Facility
[DE94-013347] p 364 N95-11754
Radiation-induced structural changes, 3
[DE94-753401] p 371 N95-11819
Gas-puff Z-pinch driven by inductive energy storage pulsed power generator ASO-2 p 366 N95-12439
Hot spots observation in a dense plasma focus p 367 N95-12444
Observation of a soft x ray emitting core in a dense plasma focus p 367 N95-12445
Common understandings of phenomena in z-pinches p 367 N95-12447
Large area soft x-ray collimator to facilitate x-ray optics testing
[NASA-CR-196923] p 362 N95-12736

X-31 AIRCRAFT
Water tunnel flow visualization study of a 4.4 percent scale X-31 forebody
[NASA-TM-104276] p 230 N95-11898
XENON
Radiation-induced structural changes, 4
[DE94-753223] p 356 N95-11817
Stationary plasma thruster ion velocity distribution
[NASA-CR-195379] p 257 N95-11919
Recycle requirements for Nasa's 30 cm xenon ion thruster
[NASA-TM-106668] p 258 N95-12750
XI HYPERONS
The cascade-deuteron system
[DE94-011650] p 357 N95-11894

Y

YAG LASERS
Laser based combustion laboratory at NTH/SINTEF applied thermodynamics
[PB94-202603] p 299 N95-13246
YAWING MOMENTS
Numerical analysis of tangential slot blowing on a generic chined forebody
[NASA-TM-108845] p 231 N95-11927
YBCO SUPERCONDUCTORS
Response of high T(sub c) superconducting Josephson junction to nuclear radiation
[DE94-624705] p 360 N95-13536
YIELD STRENGTH
Yield-before-break fracture mechanics analysis of high strength steel pressure vehicles
[AD-A282518] p 270 N95-12401
Mechanical behavior of (238)UO2, (238)PuO2, and (239)PuO2 as a function of strain rate and temperature
[DE94-015718] p 312 N95-12784
YTTRIUM OXIDES
Measurement of synchrotron radiation transmission of infrared range by YBa2Cu3O(7-delta) film in superconducting state
[DE94-623270] p 372 N95-11899
YTTRIUM-ALUMINUM GARNET
Radiative performance of rare earth garnet thin film selective emitters
[NASA-TM-106722] p 372 N95-11876
Emittance theory for thin film selective emitter
[NASA-TM-106727] p 317 N95-11903

Z

ZEEMAN EFFECT
Radiative properties of strongly magnetized plasmas
[DE94-015487] p 369 N95-12897
ZETA PINCH
Beams 92: Proceedings
[DE94-014783] p 361 N95-11792
Gas-puff Z-pinch driven by inductive energy storage pulsed power generator ASO-2 p 366 N95-12439
Contraction phase of a gas-puff z-pinch
p 366 N95-12440
Control of initial mass on metal vapor puff z-pinch
p 366 N95-12441
Z-pinch plasma by solid fine particle injection
p 366 N95-12442
Common understandings of phenomena in z-pinches
p 367 N95-12447
ZINC OXIDES
The experiment and analysis of tailoring V(sub L) and I(sub P) with ZnO voltage-sensitive resistor on HT-6M
[DE94-625074] p 370 N95-13541
ZIRCONIUM ALLOYS
First principles investigation of the Ir-Zr-Nb ternary system
[AD-A282644] p 270 N95-12543
ZIRCONIUM OXIDES
CeO2-ZrO2 powder synthesis by way of alcohol dehydration of aqueous salt solutions
[INPE-5484-PRE/1783] p 276 N95-13191

Typical Personal Author Index Listing

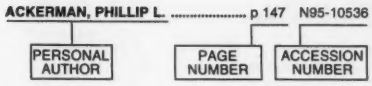

Listings in this index are arranged alphabetically by personal author. The page number helps you locate the citation in the abstract section. The accession number denotes the number by which the citation is identified.

A

AANNESTAD, PER A. ..... p 323 N95-12244
ABDALLA, VICTOR RACY ..... p 265 N95-11885
ABRAHAM, LAWRENCE D. ..... p 335 N95-13270
ABRAIZOV, M. ..... p 371 N95-11740
ABREGO, ANITA ..... p 383 N95-12826
ACEVES, ALEJANDRO ..... p 282 N95-12496
ACKER, JAMES G. ..... p 328 N95-11920
p 328 N95-12151
p 328 N95-12359
ACOSTA, FRANCISCO GARCIA ... p 277 N95-12822
ACUNA, MARIO H. ..... p 253 N95-12545
ADAM, SUE ..... p 337 N95-11878
ADAMO, RICHARD C. ..... p 283 N95-12550
ADDY, HAROLD E., JR. ..... p 247 N95-13593
p 307 N95-13605
ADELMAN, SAUL J. ..... p 381 N95-12788
ADENWALLA, S. ..... p 375 N95-13272
ADUMITROAIE, VIRGIL ..... p 289 N95-11705
AFNAN, I. R. ..... p 357 N95-11894
AGGRAWAL, BHARAT ..... p 305 N95-13587
AGOSTA, ROXANA M. ..... p 231 N95-11927
AHEARN, J. S. ..... p 263 N95-12883
AHLRICH, RANDY C. ..... p 246 N95-12216
AHMADJIAN, M. ..... p 250 N95-12917
AHRENS, E. T. ..... p 374 N95-13081
AI, QING-PIN ..... p 366 N95-12442
AKIYAMA, H. ..... p 366 N95-12439
p 367 N95-12449
AKIYAMA, HIDENORI ..... p 365 N95-12429
p 365 N95-12430
p 367 N95-12451
ALAYAN, H. ..... p 314 N95-11820
ALBERTELLI, JAMIL ..... p 255 N95-13006
ALBERTS, C. J. ..... p 234 N95-12623
ALBINSSON, M. ..... p 280 N95-11821
ALBUS, J. S. ..... p 303 N95-12854
ALDRICH, JACK B. ..... p 252 N95-12165
ALEXANDER, BILL ..... p 249 N95-12531
ALEXANDER, CHIS ..... p 307 N95-13603
ALEXANDER, KELLY ..... p 240 N95-12637
ALEXANDER, KYLE ..... p 384 N95-13497
ALEXANDER, NEAL T. ..... p 236 N95-13214
ALFANO, ROBERT R. ..... p 298 N95-12951
ALLARA, D. L. ..... p 266 N95-12514
ALLCOCK, HARRY R. ..... p 272 N95-11832
ALLEN, JONATHAN ..... p 386 N95-11830
ALLISON, DENNIS O. ..... p 231 N95-12176
ALLMAN, S. L. ..... p 299 N95-13076
ALSDORF, DOUGLAS E. ..... p 323 N95-12130
ALVAREZ, JAIME ..... p 240 N95-12628
AMARAL, SILVANA ..... p 316 N95-13350
AMBROSIANO, J. J. ..... p 322 N95-11741
AMINPOUR, MOHAMMAD A. ..... p 313 N95-13096
p 313 N95-13163
AMMERLAAN, J. A. M. ..... p 271 N95-13411
AN, MENG LIN ..... p 241 N95-12700
ANDERLE, M. ..... p 374 N95-13125
ANDERSON, A. ..... p 364 N95-11754
ANDERSON, BERNHARD H. ..... p 233 N95-13058
ANDERSON, DAVID B. ..... p 343 N95-12504
ANDERSON, HUGH ..... p 256 N95-13138
ANDERSON, JAMES G. ..... p 321 N95-12832
ANDERSON, SCOTT ..... p 277 N95-12822
ANDERSON, T. ..... p 309 N95-13406
ANDERSON, W. E. ..... p 299 N95-13080
ANDERTON, GARY L. ..... p 273 N95-12131
ANDO, R. ..... p 367 N95-12450
ANDRAS, MARIA T. ..... p 260 N95-12662
p 260 N95-12693
ANDREWS, EARL H. ..... p 244 N95-12860
ANDREWS, JASON ..... p 277 N95-12822
ANESES, CARLOS A. ..... p 254 N95-12737
ANGELONE, K. ..... p 254 N95-12790
ANKNEY, W. ..... p 248 N95-11934
ANNIS, CHARLES ..... p 270 N95-12546
APKARIAN, V. A. ..... p 277 N95-12729
ARAI, KENJI ..... p 366 N95-12441
ARAMAYO, G. A. ..... p 346 N95-11734
ARCHER, W. E. ..... p 287 N95-12863
ARGE, E. ..... p 353 N95-13573
ARIOTTI, SCOTT ..... p 242 N95-12993
ARMIJO, E. V. ..... p 299 N95-13080
ARNOLD, S. M. ..... p 264 N95-13193
ARTAKI, I. ..... p 269 N95-11785
ARTILES, ANTONIO ..... p 307 N95-13606
ARYA, VINOD K. ..... p 312 N95-12818
ASO, Y. ..... p 366 N95-12438
ASOKA-KUMAR, P. ..... p 374 N95-13125
ASPNES, D. E. ..... p 271 N95-13140
ATHAVALE, MAHESH ..... p 305 N95-13586
ATRE, S. V. ..... p 266 N95-12514
AUDINO, MICHAEL J. ..... p 270 N95-12401
AUSTIN, ROBERT ..... p 379 N95-12304
AUTHEMENT, KONG CHA ..... p 377 N95-11956
AVICOLA, K. ..... p 363 N95-13532
AVIS, DANIEL ..... p 239 N95-12530
AWE, CYNTHIA A. ..... p 229 N95-12227
AXELROD, M. C. ..... p 321 N95-12926

B

BABENKO, V. A. ..... p 360 N95-13275
BABICH, G. A. ..... p 345 N95-13370
BABUSKA, IVO M. ..... p 352 N95-12552
BAILEY, M. C. ..... p 315 N95-12379
BAILEY, SCOTT ..... p 316 N95-13290
BAILEY, WILLIAM J. ..... p 256 N95-13232
BAIR, CHRIS ..... p 383 N95-12826
BAJAJ, KRISHAN K. ..... p 376 N95-12553
BAKAJ, A. S. ..... p 277 N95-13535
BAKER, D. ..... p 255 N95-12858
BAKER, DONALD J. ..... p 262 N95-12357
BAKER, MYLES ..... p 361 N95-12665
BALAKRISHNAN, TANAPAAL ..... p 240 N95-12639
BALALYKIN, N. I. ..... p 372 N95-11899
BALDWIN, CURT ..... p 383 N95-12529
BALLA, R. JEFFREY ..... p 247 N95-13196
BALUJA, SHUMEET ..... p 350 N95-12835
BANERJEE, PRITHVIRAJ ..... p 347 N95-12523
BANFORD, MICHAEL ..... p 230 N95-11829
BAOMING, HUANG M. ..... p 373 N95-11993
BARAFF, DAVID ..... p 300 N95-12505
BARCLAY, THOMAS H. ..... p 273 N95-12400
BARD, ALLEN J. ..... p 373 N95-12004
BARENTS, MATT ..... p 239 N95-12609
BARKER, LEE A. ..... p 249 N95-12510
BARNES, PAUL R. ..... p 329 N95-11810
BARNES, ROBERT A. ..... p 328 N95-12151
p 328 N95-12359
BARNES, WILLIAM L. ..... p 328 N95-12151
p 328 N95-12359
BARNETT, LEE ..... p 235 N95-13206
BARR, R. E. ..... p 332 N95-11708
BARR, RONALD E. ..... p 335 N95-13270
BARRETT, P. A. ..... p 341 N95-13436
BARRIGA, ERNISTO ..... p 382 N95-12307
BARRON, ANDREW R. ..... p 260 N95-12662
BARRY, R. G. ..... p 327 N95-11706
BARTHELL, B. L. ..... p 299 N95-13080
BARTOS, J. J. ..... p 299 N95-13080
BASKETTE, KEITH ..... p 384 N95-13497
BASU, PRIT ..... p 305 N95-13590
BATES, J. RAY ..... p 323 N95-12226
BAUMBAUGH, A. E. ..... p 358 N95-12905
BAYLESS, W. R. ..... p 372 N95-11862
BAYLISS, A. ..... p 290 N95-11812
BEACH, R. ..... p 298 N95-12868
BEACHLEY, O. T., JR. ..... p 373 N95-12923
BEASLEY, HOWARD H. ..... p 333 N95-12406
p 362 N95-12427
BEDELL, LISA ..... p 301 N95-12625
BEDILLION, ERIK ..... p 254 N95-12696
BEDROSIAN, E. ..... p 282 N95-12416
BEEKMAN, DOUGLAS H. ..... p 256 N95-13232
BELL, J. ..... p 248 N95-11934
BELL, J. BRETT ..... p 312 N95-12620
BELL, R. S. ..... p 294 N95-13234
BELTRAN, L. ..... p 296 N95-13158
BENDER, S. C. ..... p 363 N95-13106
BENGTSON, R. D. ..... p 368 N95-12758
BENNETT, B. R. ..... p 271 N95-13140
BENSON, ROBERT H. ..... p 332 N95-13423
BERG, FREDERIC J. ..... p 260 N95-12613
BERGERMAN, MARCEL ..... p 301 N95-12587
BERGMANN, JEFFREY D. ..... p 330 N95-12614
BERLIN, ANDREW ..... p 347 N95-12414
BERLINER, HANS J. ..... p 343 N95-12497
BERNER, C. ..... p 232 N95-12578
BERNING, M. ..... p 248 N95-11934
BERNSTEIN, GARY H. ..... p 287 N95-12881
BERRY, M. ..... p 280 N95-11943
BI, DINGGUO ..... p 370 N95-13341
BIAGTAN, E. ..... p 296 N95-13287
BIANCHINI, RICARDO ..... p 346 N95-11857
p 346 N95-11858
BIANCO, DAVID J. ..... p 345 N95-13198
BIBEAU, C. ..... p 299 N95-13534
BICKFORD, R. L. ..... p 284 N95-12674
BIEGL, CSABA ..... p 349 N95-12470
BIERBAUM, VERONICA M. ..... p 324 N95-12534
BILL, ROBERT C. ..... p 307 N95-13608
BINDON, JOHN N. ..... p 338 N95-12132
BIRD, PETER ..... p 324 N95-12949
BIRINGEN, SEDAT ..... p 293 N95-12422
BIRKAN, M. A. ..... p 257 N95-12507
BISESE, ANNE ..... p 302 N95-12640
BISHOP, MIKE ..... p 240 N95-12639
BJERKAN, L. ..... p 363 N95-13574
BJOERGE, T. ..... p 299 N95-13246
BLADES, J. CHRIS ..... p 381 N95-12821
BLANCHETTE, RYAN L. ..... p 254 N95-12737
BLANCO, ROSA E. ..... p 330 N95-12393
BLASER, JEAN-PIERRE ..... p 354 N95-12229
BLESSING, G. V. ..... p 355 N95-11906
BLEVINS, GARY ..... p 254 N95-12696
BOBULA, GEORGE A. ..... p 307 N95-13608
BODILLY, SUSAN J. ..... p 377 N95-11944
BOEHM, ALBERT R. ..... p 327 N95-13137
BOERMANS, G. M. F. ..... p 320 N95-12777
BOHS, BRIAN ..... p 254 N95-12696
BOLEN, SCOTT ..... p 282 N95-12521
BOLEN, SCOTT M. ..... p 287 N95-12918
p 334 N95-12919
BOLLES, ROBERT C. ..... p 350 N95-12884
BOLSTAD, J. ..... p 322 N95-11741
BOLTON, D. ..... p 242 N95-12993
BOND, THOMAS H. ..... p 233 N95-13197
BONNER, TOM ..... p 303 N95-12694
BOOKER, COREY G. ..... p 258 N95-12604
BOOTY, MICHAEL R. ..... p 351 N95-11922
BOPARAI, M. K. ..... p 353 N95-13439
BORNEMAN, RICHARD ..... p 327 N95-13095
BOROVIK-ROMANOV, A. ..... p 296 N95-13171
BOROWSKI, STANLEY K. ..... p 249 N95-11703
BORRELLI, JASON ..... p 283 N95-12644
BOS, J. F. T. ..... p 246 N95-13243
BOSWELL, C. ..... p 254 N95-12790
BOURGAIN, J. ..... p 352 N95-12808
BOURGEOIS, A. J. ..... p 322 N95-11741
BOWEN, BARRY C. ..... p 249 N95-12224
BOWER, MARK V. ..... p 312 N95-12861

BOWLES, ANTHONY J. G. p 338 N95-12132
BOYES, J. p 364 N95-11754
BOZOKI, E. p 350 N95-13124
BOZZOLO, GUILLERMO p 270 N95-12104
BRACALENTE, EMEDIO M. p 235 N95-13205
BRACE, LARRY H. p 257 N95-11805
BRAGG, DAVID p 254 N95-12696
BRANN, DAVID M. p 254 N95-12737
BRASE, J. M. p 363 N95-13532
BRASOVEANU, D. p 255 N95-12858
BRASSEUR, JAMES G. p 291 N95-11929
BRAUN, M. J. p 300 N95-12377
p 303 N95-12843
p 306 N95-13596
BRAVENEC, R. p 368 N95-12758
BRAZELL, J. W. p 301 N95-12625
BRECKLER, JENNIFER L. p 329 N95-11810
BRENDLEY, KEITH W. p 289 N95-13291
BRENNAN, K. F. p 280 N95-11760
BRESLAUER, ALAN p 258 N95-12604
BREWER, JASON p 241 N95-12700
BRIGGS, M. S. p 380 N95-12464
BRIGHT, MICHELLE M. p 245 N95-12763
BRITT, CHARLES L. p 235 N95-13205
BRITT, DANIEL p 258 N95-12819
BRITTER, R. E. p 292 N95-11939
BRITTON, RANDALL K. p 233 N95-13197
BROGAN, NICK p 301 N95-12554
BROWN, CHRISTOPHER p 254 N95-12696
BROWN, DANSEN p 230 N95-11829
BROWN, DOUGLAS L. p 293 N95-12859
BROWN, GARRY p 253 N95-12661
BROWN, HENRY B., JR. p 278 N95-12701
BROWN, J. C. p 322 N95-11741
BROWN, N. W. p 361 N95-11779
BRUCE, S. p 362 N95-11841
BRUCKART, JAMES E. p 333 N95-12405
p 339 N95-13055
BRUNO, ANTHONY B. p 287 N95-12509
BRYANT, L. p 248 N95-11934
BRYKCZYNSKI, BILL p 344 N95-13051
BUDINOFF, J. p 254 N95-12790
BUELTHOFF, HEINRICH H. p 335 N95-11942
BUFKIN, A. p 248 N95-11934
BUHL, F. p 345 N95-13157
BUI, HUNG p 302 N95-12668
BUKAY, MICHAEL p 318 N95-11784
BULAVIN, L. A. p 356 N95-11747
BULLINGTON, STANLEY E. p 377 N95-12618
BULMAN, MELVIN J. p 249 N95-11703
BULZAN, DANIEL L. p 243 N95-11890
BURCHAM, FRANK W. p 231 N95-12191
BURKHARDT, LINDA A. p 256 N95-13194
BURNETT, DAVID C. p 330 N95-12614
BURNETT, R. p 309 N95-13406
BUSCHEK, H. p 342 N95-11923
BUSH, B. W. p 359 N95-13104
BUSH, H. p 299 N95-13080
BUURMAN, J. p 363 N95-13248
BUZBY, JARED G. p 278 N95-12701
BYRD, D. A. p 363 N95-13106
BYRNES, MARK R. p 327 N95-11787
BYUN, CHANSUP p 230 N95-11766

C

CADWALLADER, L. C. p 368 N95-12759
CADY, E. C. p 294 N95-13233
p 294 N95-13234
CAILLAULT, JEAN-PIERRE p 380 N95-12373
p 380 N95-12388
CAIN, L. p 248 N95-11934
CALDWELL, JOHN A. p 335 N95-12133
CALISE, A. J. p 342 N95-11923
CALOMINO, ANTHONY M. p 310 N95-11865
CALVERT, WYNNE p 369 N95-13024
CAMM, FRANK p 244 N95-13289
CAMPBELL, RICHARD L. p 231 N95-12176
CAMPBELL, STEVEN D. p 235 N95-13209
CAMPBELL, THOMAS G. p 315 N95-12379
CAMPOS, MARIO J. p 254 N95-12737
CANFIELD, DENNIS V. p 332 N95-11702
CANNON, M. R. p 243 N95-11864
CAO, W. p 338 N95-11949
CAO, Y. p 272 N95-11847
CAPOZZI, BRIAN p 239 N95-12609
CAPPELLARI, JOHN p 368 N95-12641
CARAM, J. p 248 N95-11934
CARETTI, DAVID M. p 334 N95-12593
CARLSSON, L. p 275 N95-12600
CARPENTER, BERNIE F. p 284 N95-12896
CARR, D. p 239 N95-12305
CARR, S. B. p 357 N95-11894
CARRERAS, B. A. p 368 N95-12758
CARRION, CARLOS A. p 338 N95-12555
p 302 N95-12627
CARRUTHERS, T. F. p 288 N95-13174
CARTER, JOHN P. p 281 N95-12408
CARVER, G. P. p 279 N95-11907
CASANOVA, JOSE p 254 N95-12696
CASEY, LEAH W. p 322 N95-11836
CASPER, T. A. p 364 N95-11786
CASTELLI, MICHAEL G. p 263 N95-13082
CASTILLO, T. p 275 N95-12945
CAVALCANTI, MARCELO p 285 N95-12924
CECCATO, VANIA APARECIDA p 315 N95-12297
CEPEDA, A. p 242 N95-12993
CERVENKA, PETER O. p 354 N95-12426
CESAR, E. p 282 N95-12416
CETINGUC, MUZAFFER p 335 N95-12133
CHALFANT, MICHAEL W. p 322 N95-11836
CHAMBERLAIN, I. p 254 N95-12790
CHAMBERS, LIN HARTUNG p 291 N95-11936
CHAMIS, CHRISTOS C. p 311 N95-11954
CHAN, B. p 322 N95-11741
CHAN, B. L. p 282 N95-12493
CHAN, SUNNY p 254 N95-12765
CHANDLER, T. p 290 N95-11840
CHATTERJEE, A. p 279 N95-11707
CHATURVEDI, ARVIND K. p 338 N95-12354
CHELLAPPA, R. p 315 N95-12527
CHEMALY, ADEL p 377 N95-11788
CHEN, C. H. p 299 N95-13076
CHEN, JIEFU p 297 N95-13537
CHEN, N. X. p 303 N95-13083
CHEN, W. p 277 N95-13530
CHEN, WEI p 295 N95-11780
CHEN, YIE-RUEY p 323 N95-12506
CHEREDNICHENKO, V. A. p 360 N95-13273
CHERNYAEVA, T. P. p 374 N95-12948
CHEW, LARRY p 289 N95-11709
CHILDS, DARA W. p 307 N95-13603
p 307 N95-13604
CHINN, D. J. p 308 N95-11822
CHITSOMBOON, TAWIT p 231 N95-11917
CHITWOOD, DENNY p 383 N95-12529
CHOI, YONGHO p 383 N95-12533
CHOU, STEPHEN Y. p 286 N95-11860
CHOUDHARI, MEELAN p 292 N95-12105
CHOWDHRY, RAJIV S. p 255 N95-12838
CHOY, F. K. p 300 N95-12377
p 301 N95-12621
p 303 N95-12843
CHRISTENSEN, R. W. p 363 N95-13106
CHRISTENSON, P. J. p 370 N95-13422
CHRISTOPHERSEN, N. p 376 N95-13572
CHU, CHING-MEI p 237 N95-12230
CHU, YOU-HUA p 382 N95-12950
CHUAQUI, M. p 352 N95-12577
CHUBB, DONALD L. p 372 N95-11876
p 317 N95-11903
CIECWIERZ, WOJCIECH p 296 N95-12111
CLARK, ERIC B. p 260 N95-12692
p 260 N95-12693
CLARK, J. p 282 N95-12416
CLARK, MICHELLE L. p 240 N95-12636
CLARK, W. G. p 374 N95-13081
CLEMENT, ANNE E. p 299 N95-13139
CLINTON, DUSTIN p 302 N95-12690
COBLEIGH, BRENT R. p 230 N95-11898
COCKRELL, B. p 248 N95-11934
COHEN, BERNARD p 333 N95-12376
COHEN, LISA E. p 254 N95-12737
COLBY, FRANK P., JR. p 327 N95-13134
COLEMAN, ANTHONY S. p 243 N95-11867
COLETTA, CHRIS p 302 N95-12668
COMFORT, RICHARD H. p 382 N95-12940
CONCHA, M. p 254 N95-12790
CONNELL, LINDA J. p 334 N95-12792
CONNORS, MARY M. p 337 N95-11905
COOK, GEORGE E. p 349 N95-12470
COOK, R. p 347 N95-13404
COOK, R. E. p 360 N95-13338
COOK, S. R. p 232 N95-12652
COOL, T. A. p 267 N95-12762
COOLEY, BRYAN p 283 N95-12644
COOLEY, JAMES W. p 344 N95-12588
COOPER, PAUL A. p 252 N95-11947
COOPERSTEIN, G. p 361 N95-11792
COOPERSTOCK, R. L. p 259 N95-12551
COPELAND, R. BRADEN p 255 N95-13006
COPIOLI, PAUL p 258 N95-12604
CORBAN, ROBERT R. p 249 N95-11703
CORCORAN, DANIEL J., III p 254 N95-12737
CORDA, STEPHEN p 231 N95-12191
CORNET, A. p 271 N95-13140
CORNILSEN, BAHNE C. p 289 N95-13344
CORRELL, ERIC p 255 N95-13006
CORRODO, M. p 254 N95-12790
COSMO, MARIO L. p 252 N95-12106
COSTA, ALFRED J. p 241 N95-12695
COSTELLO, D. J., JR. p 341 N95-11763
COSTELLO, DANIEL J., JR. p 341 N95-11764
COVELL, PETER F. p 233 N95-12770
COWAN, I. R. p 292 N95-11939
COWLEY, R. A. p 371 N95-11739
COX, JAMES F. p 254 N95-12737
COX, S. F. J. p 357 N95-12365
CRAIG, ROGER A. p 382 N95-12190
CRANDALL, MICHAEL G. p 351 N95-11861
CREAN, G. M. p 373 N95-12602
CREATH, KATHERINE p 296 N95-12748
CREDLE, BEN p 301 N95-12625
CRIBBS, DAVID p 254 N95-12696
CRIBBS, RICHARD p 253 N95-12663
CROCKETT, THOMAS W. p 340 N95-12828
CROSS, J. B. p 232 N95-12652
CROSSLEY, WILLIAM A. p 237 N95-11699
CROUCH, M. A. p 294 N95-13234
CRUM, LAWRENCE A. p 355 N95-11856
CSAVINA, KRISTINE R. p 307 N95-13607
p 307 N95-13608
CUFF, DANIEL J. p 255 N95-12921
CULVER, DONALD W. p 249 N95-11703
CURRAN, FRANCIS M. p 259 N95-13347
CURRY, D. p 248 N95-11934
CURRY, ROBERT E. p 231 N95-12191
CURRY, WILLIAM B. p 266 N95-12539
CURTIS, TREVOR J. p 254 N95-12737
CUSTODIO, O. p 254 N95-12790

D

DAEHLEN, M. p 378 N95-13245
p 353 N95-13573
DAGENAIS, M. p 297 N95-12751
DAI, MINGJIA p 333 N95-12376
DAILEY, RON p 384 N95-13497
DALES, CHRIS p 255 N95-13006
DAMKROGER, B. K. p 271 N95-13544
DANA, DAVID R. p 283 N95-12550
DANDEKAR, B. S. p 324 N95-12508
DANNENBERG, ROGER B. p 343 N95-12504
DANNEVIK, W. P. p 322 N95-11741
DAPKUNAS, S. J. p 277 N95-13530
DARZI, MICHAEL p 328 N95-11920
DAUGHERTY, THOMAS L. p 304 N95-13189
DAUSCH, DAVID p 275 N95-12586
DAVENPORT, D. W. p 322 N95-11732
DAVIDSON, J. L. p 259 N95-11891
DAVIDSON, M. p 296 N95-13287
DAVIES, CAROL B. p 295 N95-11957
DAVIS, D. A. p 256 N95-13195
DAVIS, DANA p 255 N95-13006
DAVIS, GRANT p 382 N95-12307
DAVIS, H. A. p 365 N95-12371
DAVIS, J. BRADLEY p 249 N95-12224
DAVIS, JOHN M. p 326 N95-12624
DAVIS, L. S. p 315 N95-12527
DAVIS, MARK p 303 N95-12694
DAVIS, NECHOLE p 255 N95-13006
DAVIS, R. F. p 289 N95-13368
DAVIS, RYAN EDWIN p 241 N95-12643
DAVY, WILLIAM C. p 382 N95-12190
DAWSON, ANNE MARIE p 241 N95-12643
DEANDRADENONO, MARIA DOCARMO p 276 N95-13191
DEARBORN, ALAN S. p 329 N95-11810
DEBOIS, ALAIN p 302 N95-12668
DEBOLE, MARCY p 283 N95-12644
DEC, JOHN p 241 N95-12700
DECARVALHO, JOAO ANDRADE, JR. p 265 N95-11885
DECASTRO, ALEXANDRE GRIMALDI p 316 N95-13352
DECHER, RUDOLF p 379 N95-12304
DEFOSSE, ERIN p 382 N95-12307
DEFREITASMUNIZ, WILSON p 266 N95-12302
DEGER, MATT p 277 N95-12822
DEGROOT, J. S. p 369 N95-13285
DEIMLER, J. D. p 336 N95-13020
p 336 N95-13199
DEKKER, J. P. p 276 N95-13284
DEKONINGGANS, H. J. p 294 N95-13249
DEKRAMER, CORNELIS p 287 N95-12795
DELALAMO, J. A. p 271 N95-13140
DELANEY, ROBERT A. p 244 N95-11901
p 244 N95-11951
DELEUTERIO, G. M. T. p 347 N95-13353
DELFRATE, JOHN p 230 N95-11898
DELLACORTE, C. p 260 N95-12764
DELNORE, VICTOR E. p 234 N95-13203
DELUCA, DANIEL P. p 270 N95-12546
DEMANN, BRIAN p 383 N95-12529
DEMEO, MARTHA E. p 252 N95-11947
DEMKO, RICHARD p 254 N95-12696
DEMPSEY, F. p 364 N95-11754

DEMUREN, A. O. p 291 N95-11930
DENELZEN, M. G. J. p 320 N95-12776
DENNER, EWALD p 332 N95-11966
DENNIS, MARK F. p 258 N95-13232
DEREFELDT, G. p 337 N95-11873
DERENGOWSKI, CHERYL p 383 N95-12533
DERIEUX, DAVID A. p 283 N95-12592
DETURK, ROBIN p 238 N95-11952
DEUTSCH, T. F. p 334 N95-12535
DEVENEY, M. F. p 287 N95-12863
DEWEESE, RICHARD p 234 N95-12146
DEZEGO, SHAWN p 303 N95-12694
DIBERARDINO, THOMAS p 261 N95-13151
DICARLO, J. A. p 263 N95-12813
DICKEL, JOHN R. p 382 N95-12950
DICKMAN, JOHN E. p 256 N95-13194
DIMOFTE, FLORIN p 307 N95-13605
DINDAL, A. B. p 264 N95-11735
DING, HONGLIN p 360 N95-13536
DINGES, DAVID F. p 334 N95-12792
DIPASQUALE, R. C. p 326 N95-12839
DISTEFANO, E. p 294 N95-13233
DIXON, CARL A. p 270 N95-12830
DODSON, LORI J. p 292 N95-11992
DOLEZAL, WILLIAM K. p 243 N95-12591
DOLINSKI, KRZYSZTOF p 309 N95-11698
DONMEZ, M. A. p 348 N95-11909
DONNELLY, M. K. p 286 N95-11751
DONOFRIO, KEVIN p 241 N95-12700
DOREY, K. p 334 N95-12535
DORFMAN, B. p 371 N95-11740
DOUGLAS, S. R. p 268 N95-13531
DOUGLASS, DEBORAH A. p 254 N95-12737
DOUKAS, A. G. p 334 N95-12535
DOVER, C. B. p 357 N95-12012
DOWDY p 253 N95-12632
DOWNARD, CATHERINE L. p 254 N95-12737
DOYLE, BARBARA J. p 278 N95-12701
DRESNER, L. p 353 N95-11731
DRUMHELLER, DAVID M. p 355 N95-12396
DRUMMOND, C. K. p 243 N95-11864
DU, J. p 366 N95-12443
DUAN, S. p 296 N95-12869
DUCHENY, JORDAN p 383 N95-12529
DUCK, ROB p 255 N95-13006
DUESBERY, M. S. p 263 N95-12833
DUNLAP, M. A. p 317 N95-12647
DUNSKY, BETSY p 339 N95-11962
DUONG, T. p 268 N95-13288
DUQUETTE, JAIME p 241 N95-12695
DURACINSKI, JON p 253 N95-12661
DURAJ, STAN A. p 260 N95-12692
p 260 N95-12693

E

EASTLAND, KEVIN p 240 N95-12638
EBBINGHAUS, BARTLEY B. p 376 N95-13074
EBY, STEVEN C. p 242 N95-12702
ECHARD, JIM D. p 236 N95-13214
ECKLES, WILLIAM E. p 260 N95-12692
EDELMAN, SHIMON Y. p 335 N95-11942
EDWARDS, JOE p 253 N95-12661
EKBLAD, U. p 379 N95-11871
ELGES, MICHAEL p 258 N95-12819
ELLIOTT, BILL p 339 N95-12629
ELLIS, R. W. p 312 N95-12784
ELLIS, VINCENT J. p 282 N95-12513
ELMIRO, MARCOS ANTONIO TIMBO
p 315 N95-12301
ELTGROTH, P. G. p 322 N95-11741
ELVANDER, JOSH p 253 N95-12564
EMERSON, MATT p 383 N95-12533
ENDECOTT, BOYD R. p 338 N95-12354
ENDERS, KEVIN p 338 N95-12361
ENGDAHL, U. p 337 N95-11873
EPPEL, JOSEPH C. p 238 N95-12225
EPPLER, DEAN B. p 337 N95-11905
ERDEM, E. p 345 N95-13157
ERICKSON, MATTHEW G. p 268 N95-13180
ERICSON, M. N. p 345 N95-13077
ERISMAN, J. W. p 320 N95-12777
ERLANDSON, ROBERT E. p 361 N95-12102
ERMAKOV, E. N. p 289 N95-13276
ERTL, ANDREW C. p 329 N95-11810
ESAIAS, WAYNE E. p 328 N95-12151
p 328 N95-12359
ESPENAK, F. p 250 N95-12917
ESPY, SAMUEL L. p 362 N95-12736
ESTES, ROBERT D. p 252 N95-12106
EVANS, D. R. p 385 N95-12469
EVANS, JAMES E. p 235 N95-13209
EVANS, M. S. p 304 N95-13182
EVERETT, LOUIS J. p 348 N95-11998
EVERITT, FRANCIS p 354 N95-12229

F

FAASSE, P. R. p 246 N95-13243
FALKOWSKI, K. M. p 304 N95-13128
FAN, SHUPING p 370 N95-13541
FAN, YIPING p 281 N95-12010
FANG, JINQING p 352 N95-13340
FANO, U. p 359 N95-13173
FANWICK, PHILLIP E. p 260 N95-12692
p 260 N95-12693
FARRANCE, M. A. p 377 N95-11958
FARRARA, RICHARD A. p 270 N95-12401
FARRENS, BRYAN p 239 N95-12609
FARRIS, RICHARD J. p 272 N95-11852
FARRUKH, U. O. p 362 N95-12659
FASMAN, GERALD D. p 331 N95-13373
FASTOOK, J. L. p 318 N95-11745
FAY, JONATHAN p 239 N95-12530
FAZAH, M. M. p 278 N95-12857
FEASTER, SANDI p 255 N95-13006
FECHT, PAUL HANS p 241 N95-12643
FEDRO, MARK J. p 262 N95-12793
FEIGELSON, ERIC D. p 385 N95-13023
FEIGELSON, ROBERT S. p 279 N95-13202
FELCHER, G. P. p 375 N95-13272
FERNANDEZ-PELLO, A. C. p 267 N95-12778
FERNJALLAH, M. p 332 N95-11708
FERRANTE, JOHN p 270 N95-12104
FICHTEL, EDWARD J. p 295 N95-11996
FINN, CORY p 339 N95-11962
FIRESTONE, ELAINE R. p 328 N95-11920
p 328 N95-12151
p 328 N95-12359
FIRESTONE, JAMES K. p 328 N95-11920
FISCHER, J. E. p 372 N95-11862
FISCHLER, MARTIN A. p 350 N95-12884
FISHMAN, G. J. p 380 N95-12463
p 380 N95-12464
FITZPATRICK, R. p 369 N95-12867
FLAHERTY, JOSEPH E. p 351 N95-11850
FLANIGAN, DENNIS F. p 316 N95-13142
FLEISCHMANN, C. M. p 267 N95-12852
FLEMING, WENDELL H. p 350 N95-13369
FLEMMING, ROBERT J. p 233 N95-13197
FLETCHER, LAUREN p 333 N95-11887
FLEURIAL, J. P. p 374 N95-13059
FLINT, JOHN H. p 236 N95-13213
FLOTTE, T. p 334 N95-12535
FLOWER, RALPH p 305 N95-13591
FOGARTY, PAUL W. p 254 N95-12698
FOLLEN, G. J. p 243 N95-11864
FOLLETT, W. H. p 294 N95-13233
FOMYIN, P. YI. p 290 N95-11749
FONTENLA, JUAN M. p 381 N95-12992
FORDE, E. B. p 328 N95-11900
FOREMAN, L. R. p 299 N95-13080
FORREST, DANA K. p 233 N95-12770
FOSTER, G. p 296 N95-13287
FOSTER, I. T. p 344 N95-12893
FOWLER, C. M. p 368 N95-12757
FRANCOIS, JASON p 338 N95-12555
p 302 N95-12627
FRANK, JEREMY p 258 N95-12604
FRASER, ROBERT S. p 328 N95-11920
FRAZER, SCOTT p 339 N95-12629
FRAZIER, WILLIAM E. p 266 N95-12549
FRECHET, JEAN M. p 259 N95-11844
FREEDMAN, JEROME E. p 236 N95-13212
FREEMAN, B. L. p 368 N95-12757
FRENZEN, C. L. p 351 N95-12501
FRIEDMAN, A. p 350 N95-13124
FRIEDMAN, SCOTT D. p 381 N95-13056
FRIEDMANN, PERETZ P. p 230 N95-11911
FRITTS, DAVID C. p 325 N95-13293
FROUIN, ROBERT J. p 319 N95-11931
FRY, ROMAN ZYABASH p 241 N95-12643
FUJIOKA, K. p 366 N95-12438
FULKERSON, DAN p 239 N95-12609
FUNDERBURKE, C. ASHLEY p 303 N95-12694
FURLER, R. p 296 N95-13158
FURTAK, T. E. p 373 N95-12425
FURUYA, SEIZO p 366 N95-12441

G

GAILLARD, ANTHONY W. K. p 335 N95-12133
GAL, A. p 357 N95-12012
GALLIANO, J. p 235 N95-13208
GANGLOFF, RICHARD P. p 269 N95-11933
GANN, R. G. p 236 N95-13247
GANT, FREDERICK S. p 312 N95-12861
GAO, CHUAN p 296 N95-12869
GARAMUS, V. M. p 356 N95-11747
GARBER, DONALD P. p 355 N95-12341
GARCIA, F. P. p 299 N95-13080
GARCIA, GUILLERMO p 382 N95-12950
GARCIA, R. p 364 N95-11754
GARDNER, TIMOTHY J. p 322 N95-11836
GARG, SANJAY p 245 N95-12763
GARNER, M. p 242 N95-12993
GARNETT, A. p 378 N95-13123
GARRETT, W. R. p 299 N95-13076
GARRISON, JAMES L., JR. p 252 N95-11947
GEDEON, D. R. p 246 N95-13200
GEIGER, MICHELLE p 301 N95-12554
p 277 N95-13508
GELZLEICHTER, T. R. p 331 N95-13176
GEORGIADIS, NICHOLAS J. p 231 N95-11917
GERBER, R. B. p 277 N95-12729
GERTSMANN, JOSEPH p 279 N95-13053
GHOSN, LOUIS J. p 310 N95-11865
GIBBS, D. p 371 N95-11739
p 358 N95-12829
GIBSON, B. F. p 357 N95-11894
GILLEN, KELLY A. p 334 N95-12792
GILSINN, D. E. p 348 N95-11909
GILSON, WILLIAM H. p 235 N95-13210
GIORI, KATHY L. p 283 N95-12550
GIRKA, I. A. p 370 N95-13540
GIVI, PEYMAN p 289 N95-11705
GJESTLAND, T. p 356 N95-13575
GLEMBOCKI, O. J. p 373 N95-12602
GLIENICKE, J. p 308 N95-13609
GNACEK, WILLIAM J. p 308 N95-12391
GOBBY, P. L. p 299 N95-13080
GOHAR, Y. p 369 N95-13280
GOLBITZ, PETER p 338 N95-12132
GOLDBERG, J. H. p 363 N95-13421
GOLDBERG, P. W. p 350 N95-12864
p 350 N95-12866
GOLDFARB, D. p 345 N95-13339
GOLDMAN, S. A. p 350 N95-12864
p 350 N95-12866
GOLDSBY, J. C. p 263 N95-12813
GOMEZ, V. M. p 299 N95-13080
GONG, S. p 304 N95-13410
GONZALEZ, R. V. p 332 N95-11708
GONZALEZ, RODOLFO p 249 N95-12531
GONZALEZ, ROGER V. p 335 N95-13270
GOOD, BRIAN S. p 372 N95-11876
p 317 N95-11903
GOODE, HENRY p 277 N95-13508
GORBAR, E. V. p 375 N95-13277
GOSCHA, DANIEL p 382 N95-12950
GOTO, EIJI p 368 N95-12441
GOTTERBARN, DONALD p 342 N95-11941
GOTTLICH, GRETCHEN L. p 345 N95-13198
GOULD, JAMES P. p 376 N95-12385
GOWDY, VAN p 234 N95-12146
GRADINARU, G. p 287 N95-12865
GRAEBER, R. CURTIS p 334 N95-12792
GRANHAUG, M. p 348 N95-13571
GRANOEIEN, I. L. N. p 356 N95-13575
GRANT, B. p 322 N95-11741
GRANT, PATRICK p 255 N95-13006
GRAPS, AMARA L. p 377 N95-11959
GRAVES, SARA J. p 320 N95-12786
GREEN, J. B. p 302 N95-12648
GREEN, K. A. H. p 321 N95-12855
GREENBERG, H. S. p 250 N95-11767
p 251 N95-11777
p 251 N95-11802
p 261 N95-11803
p 251 N95-11809
p 251 N95-11833
p 261 N95-11834
p 262 N95-11835
p 252 N95-11945
GREENLEAF, JOHN E. p 329 N95-11810
GREENWOOD, SEAN p 240 N95-12638
GREGORY, IRENE M. p 255 N95-12838
GREGORY, JOHN C. p 268 N95-13084
GREINER, C. p 357 N95-12012
GRETHLEIN, CHRISTIAN E. p 238 N95-11952
GRIFFIN, THOMAS A. p 307 N95-13607
p 307 N95-13608
GRITZO, L. A. p 264 N95-11756
GRONET, M. J. p 256 N95-13195
GROSSHANDLER, W. L. p 236 N95-13247
GROSSI, MARIO D. p 252 N95-12106
GROTA, SUSAN p 368 N95-12641
GUERRIERI, D. A. p 321 N95-12855
GULLAHORN, GORDON E. p 252 N95-12106
GUMUS, ILKER p 240 N95-12639
GUNDER, ALEXANDER p 335 N95-12133
GUNN, TODD p 339 N95-11914
GUNTHER, CHRISTIAN K. p 262 N95-12793
GUPTA, ANURAG p 241 N95-12700
GURLEY, KENNETH S. p 297 N95-11940
GURMAN, E. B. p 336 N95-13020

GURULE, V. A. ..... p 299 N95-13080
GUSSY, JOEL ..... p 240 N95-12639
GUSTFASON, H. ..... p 296 N95-13287
GUTHLEIN, PETER ..... p 327 N95-12996
GUTHRIE ..... p 253 N95-12632
GUZHVA, O. I. ..... p 371 N95-11748

H

HACKEL, L. ..... p 298 N95-12868
HAERTLING, GENE ..... p 275 N95-12586
HAGEDORN, DAVID ..... p 368 N95-12641
HAGEN, MARTIN J. ..... p 232 N95-12360
HAGOOD, NESBITT W., IV ..... p 252 N95-12165
HAILES, CHRIS ..... p 238 N95-12294
HAILEY, RUTH ..... p 303 N95-12694
HAKODA, MUSUHI ..... p 366 N95-12437
HALE, ZOE M. ..... p 362 N95-12415
HALFORD, GARY R. ..... p 312 N95-12818
HALL, EDWARD J. ..... p 244 N95-11901
p 244 N95-11951
HALL, STEVEN R. ..... p 349 N95-12782
HALLER, GEORGE ..... p 329 N95-12540
HAMA, YOSHIMASA ..... p 356 N95-11817
HAMMEL, P. C. ..... p 374 N95-13081
HAMMOUD, AHMAD N. ..... p 256 N95-13194
HAMPDEN-SMITH, M. J. ..... p 267 N95-12807
HAMPSON, ROBERT F. ..... p 322 N95-12103
HAMPTON, RICHARD ..... p 383 N95-12529
HAN, K. S. ..... p 362 N95-12659
HAN, MIN ..... p 367 N95-12444
HANDSCHUH, R. F. ..... p 300 N95-12377
p 301 N95-12621
p 303 N95-12843
p 303 N95-13083
HANNA, G. J. ..... p 294 N95-13233
p 294 N95-13234
HANNON, STEPHEN M. ..... p 235 N95-13207
p 236 N95-13211
HANSEN, FRANK V. ..... p 327 N95-12997
HANSEN, IRVING G. ..... p 243 N95-11867
HARDY, GORDON ..... p 238 N95-12225
HARFF, N. E. ..... p 376 N95-13172
HARIHARAN, S. I. ..... p 293 N95-12380
HARKEMA, J. ..... p 331 N95-13176
HARMON, B. A. ..... p 380 N95-12463
p 380 N95-12464
HARMON, J. ..... p 296 N95-13287
HARMSEN, S. C. ..... p 321 N95-11730
HARPER, SABRINA ..... p 373 N95-12386
HARRINGTON, BROOK ..... p 240 N95-12628
HARRINGTON, RICHARD F. ..... p 315 N95-12379
HARRIS, R. M. ..... p 359 N95-13160
HARRISON, PETER N. ..... p 311 N95-11946
HART, S. ..... p 280 N95-11943
HARTFIELD, ROY ..... p 293 N95-12387
HARTMAN, TROY ..... p 241 N95-12645
HASEGAWA, K. ..... p 366 N95-12439
HASHIMOTO, YOSHIYUKI ..... p 365 N95-12434
p 366 N95-12436
HASHMALL, J. ..... p 255 N95-12858
HASKEW, TIM A. ..... p 299 N95-11701
HASKIN, F. E. ..... p 353 N95-13061
HAWK, S. ..... p 331 N95-13176
HAYATDAVOUDI, MAZIAR ..... p 241 N95-12645
HAYDEN, J. S. ..... p 299 N95-13534
HEATHER, M. A. ..... p 353 N95-13560
HEATON, RANDALL ..... p 338 N95-12361
HEAVEN, MICHAEL C. ..... p 268 N95-13180
HEDMAN, MATT ..... p 277 N95-12822
HEEGAARD, P. E. ..... p 285 N95-13558
HEEGER, A. J. ..... p 272 N95-11847
HEELIS, R. A. ..... p 325 N95-13190
HEFFNER, R. H. ..... p 374 N95-13081
HEHEMANN, DAVID G. ..... p 260 N95-12692
p 260 N95-12693
HEIDEGGER, NATHAN J. ..... p 244 N95-11901
p 244 N95-11951
HEIDMANN, JAMES D. ..... p 372 N95-11882
HEIFETZ, ANDY ..... p 253 N95-12564
HEINRICHS, J. ..... p 327 N95-11706
HELVIK, B. E. ..... p 285 N95-13558
p 286 N95-13577
HENAGER, C. H., JR. ..... p 263 N95-12862
HENDEE, J. C. ..... p 328 N95-11900
HENDERSON, SCOTT ..... p 258 N95-12604
HENDERSON, ULESES C., JR. ..... p 246 N95-13553
HENDRICKS, ROBERT C. ..... p 304 N95-13583
p 305 N95-13588
p 305 N95-13591
p 307 N95-13607
p 307 N95-13608
HENEGHAN, BRIAN ..... p 240 N95-12637
HENINS, I. ..... p 365 N95-12371
HENRY, BRIAN ..... p 254 N95-12696
HENSHALL, G. A. ..... p 264 N95-13533
HENSLEY, SCOTT ..... p 382 N95-11704
HEPP, ALOYSIUS F. ..... p 260 N95-12662
p 260 N95-12692
p 260 N95-12693
HERMANN, M. ..... p 252 N95-11948
HERSHCOVITCH, A. ..... p 364 N95-11746
HESS, F. ..... p 295 N95-11780
HETTINGA, JOEL ..... p 241 N95-12645
HEZEL, P. J. ..... p 340 N95-12413
HIBBEN, STUART G. ..... p 378 N95-13167
HIGGINS, C. E. ..... p 264 N95-11735
HIGGS, JOEY ..... p 339 N95-12629
HIGHLEY, STEVEN R. ..... p 281 N95-12402
HILAND, MATTESON W. ..... p 327 N95-11787
HILASKI, ROGER J. ..... p 330 N95-12614
HILL, D. N. ..... p 364 N95-11786
HIMMEL, JEFFREY ..... p 287 N95-12525
HINDERS, KRISS ..... p 254 N95-12765
HINES, JOHN W. ..... p 247 N95-11965
HINK, ANTHONY ..... p 383 N95-12826
HINTON, DAVID A. ..... p 234 N95-13204
HIRAI, YOSHI ..... p 368 N95-12641
HIRANO, K. ..... p 366 N95-12443
p 367 N95-12445
HIRANO, KATSUMI ..... p 367 N95-12444
HISATOME, N. ..... p 366 N95-12443
HO, QUANG ..... p 382 N95-12307
HODGE, A. ..... p 261 N95-11816
HOFFBAUER, M. A. ..... p 232 N95-12652
HOKSTAD, P. R. ..... p 286 N95-13577
HOLA, JERZY ..... p 311 N95-12108
HOLDEN, TINA ..... p 337 N95-11878
HOLEN, J. ..... p 264 N95-11756
HOLLAND, MARK ..... p 340 N95-12516
HOLLAND, R. F. ..... p 363 N95-13106
HOLLEN, G. ..... p 378 N95-13123
HOLLENBERG, G. W. ..... p 263 N95-12862
HOLLINGER, JAMES P. ..... p 281 N95-12402
HOLLOWAY, SIDNEY E., III ..... p 310 N95-11814
HOLMES, ALAN W. ..... p 328 N95-12359
HOLMES, JOULES ..... p 240 N95-12637
HOLP, GRAHAM ..... p 301 N95-12625
HOLT, ANDREW ..... p 302 N95-12690
HONDA, MARK ..... p 253 N95-12663
HONES, E. W. ..... p 324 N95-12649
HONG, SEOUNG-SOO ..... p 260 N95-12613
HOOKER, STANFORD B. ..... p 328 N95-11920
p 328 N95-12151
p 328 N95-12359
HOOPER, MATT ..... p 241 N95-12645
HOPKINS, K. W. ..... p 348 N95-13556
HOPPER, DARREL G. ..... p 243 N95-12591
HORDINSKY, JERRY R. ..... p 332 N95-11702
HORIOKA, KAZUHIKO ..... p 367 N95-12448
HORTON, CHARLES M. ..... p 308 N95-12391
HORTON, GRAHAM ..... p 345 N95-13420
HORWITZ, JAMES L. ..... p 382 N95-12940
HOSHIDE, TAKAHIRO ..... p 366 N95-12442
HOU, GENE W. ..... p 294 N95-13201
HOW, JONATHAN P. ..... p 349 N95-12782
HOWE, BRUCE M. ..... p 329 N95-12998
HOWE, HAROLD ..... p 305 N95-13591
p 306 N95-13594
HOWELL, BARBARA F. ..... p 373 N95-12635
p 261 N95-13151
HOYT, DOUGLAS ..... p 384 N95-12667
HRIVNAK, LANCE ..... p 283 N95-12644
HSU, C. T. ..... p 370 N95-13422
HSU, FU-LIAN ..... p 260 N95-12613
HSU, SHAW L. ..... p 272 N95-11852
HU, SHUANGHUI ..... p 370 N95-13539
HUA, THANH Q. ..... p 369 N95-13280
HUANG, LIN ..... p 370 N95-13539
HUANG, MIN ..... p 353 N95-13061
HUANG, S. J. ..... p 276 N95-13367
HUANG, Y. F. ..... p 341 N95-11762
p 341 N95-11764
HUBER, ALAN C. ..... p 256 N95-13138
HUDSON, B. ..... p 236 N95-13212
HUDSON, BRIAN H. ..... p 236 N95-13214
HUECKEL, MACY ..... p 239 N95-12609
HUFF, JASON ..... p 339 N95-12629
HUFFAKER, R. MILTON ..... p 235 N95-13207
HUGHES, BRET ..... p 240 N95-12637
HUGHES, T. J. ..... p 318 N95-11745
HUI, DAVID ..... p 262 N95-11854
HULETT, L. D., JR. ..... p 272 N95-11733
HULL, DAVID R. ..... p 307 N95-13608
HUMBLE, GREG ..... p 249 N95-12531
HUNG, CHING-CHEH ..... p 261 N95-12783
HUNG, PEN-SHAN ..... p 237 N95-12177
HUNT, TERESA ..... p 253 N95-12564
HUNT, W. D. ..... p 280 N95-11760
HUNTER, GARY W. ..... p 284 N95-12674
HURME, M. ..... p 266 N95-12584
HURWITZ, P. D. ..... p 368 N95-12758
HUTH, G. ..... p 282 N95-12416
HWANG, I. H. ..... p 362 N95-12659
HYLAND, D. T. ..... p 336 N95-13020
p 336 N95-13199
HYMAS, HEWITT M. ..... p 354 N95-13144

I

IACOBELLIS, SAMUEL F. ..... p 319 N95-11931
IBANEZ-MEIER, RODRIGO ..... p 270 N95-12104
IDE, JAMES R. ..... p 256 N95-13194
IHARA, SATOSHI ..... p 367 N95-12451
IKONEN, E. ..... p 320 N95-12771
IKUTA, K. ..... p 366 N95-12438
IMASAKA, K. ..... p 366 N95-12439
IMASAKI, KAZUO ..... p 365 N95-12431
p 365 N95-12432
INGLEFIELD, PAUL T. ..... p 274 N95-12420
INOKUTI, MITIO ..... p 359 N95-13173
INOZEMTSEV, ANDREI ..... p 367 N95-12446
INTRONE, STEVE ..... p 301 N95-12625
INTRONE, STEVEN D. ..... p 384 N95-13497
IRELAND, GLEN J. ..... p 242 N95-12702
ISHII, SHOZO ..... p 366 N95-12441
p 366 N95-12442
ITAGAKI, DAIJU ..... p 366 N95-12442

J

JACKELS, CHARLES F. ..... p 265 N95-12107
JACKSON, CATHERINE G. R. ..... p 329 N95-11810
JACKSON, JENNIFER J. ..... p 254 N95-12698
JAFRY, YUSUF ..... p 354 N95-12229
JAHROMI, SOHEILA ..... p 247 N95-11960
JALUFKA, N. W. ..... p 362 N95-12659
JAMES, KELLY ..... p 254 N95-12696
JAMES, R. A. ..... p 364 N95-11786
JAMESON, ANTONY ..... p 290 N95-11874
p 290 N95-11875
p 230 N95-11877
p 230 N95-11884
JANASWAMY, RAMAKRISHNA ..... p 284 N95-12834
JANDA, K. C. ..... p 277 N95-12729
JANSA, E. D. ..... p 284 N95-12674
JANSENS, P. J. ..... p 375 N95-13409
JANSSEN, M. A. ..... p 320 N95-12776
JANTZ, ERIK ..... p 302 N95-12690
JARNOT, MONICA ..... p 354 N95-12229
JAROSZEWSKA, ANNA ..... p 323 N95-12112
JARRETT, WILLIAM L. ..... p 273 N95-12397
JEHAN, D. A. ..... p 371 N95-11739
JEN, G. ..... p 276 N95-13367
JENEKHE, S. A. ..... p 274 N95-12407
JENEKHE, SAMSON A. ..... p 262 N95-12404
p 275 N95-12537
JENKINS, JEFFREY D. ..... p 281 N95-12010
JENKINS, R. A. ..... p 264 N95-11735
JENNER, J. W. ..... p 377 N95-11958
JENNINGS, D. E. ..... p 250 N95-12917
JESSEN, TODD ..... p 275 N95-13175
JESSUP, J. M. ..... p 333 N95-11808
JOHANNESSEN, K. ..... p 363 N95-13574
JOHNSON, A. L. ..... p 268 N95-13549
JOHNSON, C. G. ..... p 273 N95-12397
JOHNSON, CATHERINE C. ..... p 247 N95-11961
JOHNSON, D. K. ..... p 293 N95-12380
JOHNSON, ERIC R. ..... p 311 N95-11946
JOHNSON, J. O. ..... p 250 N95-11755
JOHNSON, L. ..... p 252 N95-11948
JOHNSON, MATT ..... p 242 N95-12702
JOHNSON, R. A. ..... p 274 N95-12419
JOHNSON, R. M. ..... p 286 N95-11751
JOHNSON, RANDY A. ..... p 273 N95-12399
JOHNSON, ROBERT D. ..... p 273 N95-12400
JOHNSON, W. S. ..... p 269 N95-11915
JOHNSON, WALTER W. ..... p 229 N95-12227
JOKELA, JORMA ..... p 314 N95-11880
JOKELA, K. ..... p 320 N95-12771
JONES, CHRISTOPHER ..... p 329 N95-12540
JONES, KINZY ..... p 303 N95-12694
JONES, LEROY, II ..... p 360 N95-13376
JONES, R. H. ..... p 270 N95-12372
JUNGERT, E. ..... p 314 N95-11820
JUNTTILA, M. L. ..... p 320 N95-12771

K

KADIN, CHARLES ..... p 327 N95-13095
KAKKURI, JUHANI ..... p 314 N95-11881
KALEDIN, LEONID A. ..... p 268 N95-13180
KAMADA, K. ..... p 367 N95-12450
KAMNA, M. M. ..... p 358 N95-12617
KAN, S. H-T. ..... p 284 N95-12856

KANG, XIANGDONG ..... p 365 N95-12433
KANSA, E. J. ..... p 321 N95-12926
KANTSYREV, VICTOR ..... p 367 N95-12446
KAPOOR, KAMLESH ..... p 233 N95-13058
KARPENKO, V. ..... p 364 N95-11754
KARR, GERALD R. ..... p 292 N95-11999
KASCHMITTER, J. L. ..... p 356 N95-11791
KATNIK, GREGORY N. ..... p 249 N95-12224
KATO, SHIGERU ..... p 366 N95-12437
KATSINIS, CONSTANTINE ..... p 343 N95-12014
KATSUKI, S. ..... p 367 N95-12449
KATSUKI, SUNAO ..... p 367 N95-12451
KATZ, KENNETH ..... p 238 N95-12294
KAUFMAN, TERESA ..... p 302 N95-12690
KAUFMAN, W. M. ..... p 234 N95-12623
KAWAKITA, YUU ..... p 366 N95-12437
KAY, E. J. ..... p 336 N95-13020
p 336 N95-13199
KAYE, DANIEL S. ..... p 282 N95-12412
KAYE, JACK A. ..... p 322 N95-12103
KEFAUVER, W. NEILL ..... p 284 N95-12896
KEITH, THEO G., JR. ..... p 376 N95-11765
p 242 N95-12787
KELLER, J. ..... p 296 N95-13287
KELLER, TEDDY M. ..... p 276 N95-13179
KELLEY, J. B. ..... p 271 N95-13544
KELLY, ALONZO ..... p 300 N95-12394
KELLY, DAN ..... p 240 N95-12638
KEMPEL, L. C. ..... p 281 N95-12382
KENDALL, BRUCE M. ..... p 315 N95-12379
KERCHER, J. R. ..... p 321 N95-12926
KERN, S. ..... p 289 N95-13368
KERR, JUSTIN H. ..... p 382 N95-12307
KETTERING, MARK ..... p 240 N95-12637
KEWLEY, CHRISTOPHER ..... p 303 N95-12694
KEY, F. S. ..... p 304 N95-13128
KEY, J. ..... p 327 N95-11706
KHAN, AFSAR ..... p 253 N95-12661
KHAN, FITRATULLAH ..... p 285 N95-12924
KHESIN, B. ..... p 352 N95-12603
KHLOPKIN, N. ..... p 361 N95-11779
KHOSLA, PRADEEP ..... p 300 N95-12505
KIM, JAE ..... p 383 N95-12826
KIM, WONSOP ..... p 365 N95-12435
KIM, Y. S. ..... p 274 N95-12520
KIPP, JARED ..... p 277 N95-12822
KITAOKA, H. ..... p 367 N95-12445
KLABUNDE, KENNETH J. ..... p 357 N95-11851
KLEIN, VLADISLAV ..... p 244 N95-11869
KLEINMANN, S. G. ..... p 380 N95-12633
p 316 N95-12634
KLEM, J. F. ..... p 376 N95-13172
KLINE-SCHODER, ROBERT J. ..... p 254 N95-12766
KLUTE, GLENN K. ..... p 333 N95-11887
KLYMENKO, VICTOR ..... p 333 N95-12406
KNIGHT, NORMAN F., JR. ..... p 313 N95-13096
p 313 N95-13162
p 313 N95-13163
KOBAYASHI, K. ..... p 367 N95-12450
KOBAYASHI, TAKAHISA ..... p 277 N95-12822
KOCH, AMBER ..... p 383 N95-12826
KOCH, J. A. ..... p 298 N95-12761
KOCKS, U. F. ..... p 374 N95-13078
KODRES, C. A. ..... p 245 N95-11789
KOEHLER, ALLISON ..... p 316 N95-13290
KOGUCHI, H. ..... p 367 N95-12450
KOGUT, J. B. ..... p 375 N95-13337
KOHNO, SUSUMU ..... p 367 N95-12451
KOHRING, B. ..... p 308 N95-13609
KOLVER, JILL ..... p 238 N95-12294
KONDO, YASUHIRO ..... p 371 N95-11819
KONG, XIANGHONG ..... p 324 N95-12949
KONTRA, V. ..... p 385 N95-11797
KONTTINEN, RAIMO ..... p 314 N95-11880
p 314 N95-11950
KOOPMAN, FRITZ ..... p 241 N95-12695
KORINDYASOV, V. I. ..... p 361 N95-11779
KORONY, G. ..... p 287 N95-12865
KOROS, ANTON, SR. ..... p 337 N95-11878
KORTAN, A. R. ..... p 372 N95-11862
KOSTEN, SUSAN ..... p 279 N95-12752
KOWALCZYK, PIOTR ..... p 332 N95-11806
KOYAMA, L. ..... p 280 N95-11943
KOZLOVSKAYA, INESSA ..... p 333 N95-12376
KRAGH, MELODY ..... p 283 N95-12601
KRANER, H. W. ..... p 295 N95-11780
KRASNOPOLER, A. ..... p 268 N95-13549
KRAUSE, ROY ..... p 384 N95-13497
KRAUSE, SCOTT ..... p 241 N95-12695
KRIEGSMANN, GREGORY A. ..... p 351 N95-11922
KRIKORIAN, OSCAR H. ..... p 376 N95-13074
KRISTJANSSON, J. E. ..... p 327 N95-13268
KRUSE, ROSS ..... p 383 N95-12826
KUDRIAVTSEV, V. V. ..... p 306 N95-13596
KUFFLER, DAMIEN P. ..... p 330 N95-12393
KUGIUMTZIS, D. ..... p 376 N95-13572
KUHLMANN, S. E. ..... p 359 N95-13170
KUHNS, JESSE ..... p 383 N95-12529
KURASHINA, KEN-ICHI ..... p 365 N95-12435
KURYLO, MICHAEL J. ..... p 322 N95-12103
KUSHNER, HAROLD J. ..... p 350 N95-13369
KUTTER, BRUCE L. ..... p 323 N95-12506
KUYKENDALL ..... p 253 N95-12632
KUZNETSOV, S. B. ..... p 304 N95-13128
KYLE, H. LEE ..... p 384 N95-12667

L

LAANANEN, DAVID H. ..... p 237 N95-11699
LAGARDE, DIDIER ..... p 335 N95-12133
LALA, P. K. ..... p 286 N95-12421
LAMPI, RAUNO A. ..... p 338 N95-12132
LANCE, D. ..... p 261 N95-11816
LANDER, G. H. ..... p 358 N95-12829
LANDRY, CHRISTOPHER C. ..... p 260 N95-12662
LANE, J. ..... p 254 N95-12790
LANGLAIS, MIKE ..... p 303 N95-12694
LANGRIDGE, S. ..... p 358 N95-12829
LANSING, MATTHEW D. ..... p 308 N95-12391
LARA-CURZIO, E. ..... p 272 N95-11736
LARRABEE, G. ..... p 373 N95-12602
LAST, J. A. ..... p 331 N95-13176
LATKOWSKI, J. ..... p 364 N95-11754
LAU, K. C. ..... p 300 N95-11729
LAUGHLIN, JULIA ..... p 338 N95-12555
p 302 N95-12627
LAUNERT, A. ..... p 308 N95-13609
LAURANCE, ROBIN ..... p 354 N95-12229
LAUTZENHISER, RUSS ..... p 383 N95-12533
LE, TUAN ..... p 239 N95-12530
LEBERL, FRANZ W. ..... p 382 N95-11704
LEBLANC, THOMAS J. ..... p 346 N95-11857
p 346 N95-11858
LECROY, S. R. ..... p 326 N95-12839
LEE, ALICE T. ..... p 339 N95-11914
LEE, C. J. ..... p 362 N95-12659
LEE, CHRISTOPHER ..... p 300 N95-12526
LEE, CHRISTOPHER A. ..... p 242 N95-12785
LEE, E. S. ..... p 296 N95-13158
LEE, JAE MOON ..... p 241 N95-12700
LEE, NING-CHENG ..... p 269 N95-11785
LEE, P. A. ..... p 352 N95-13437
LEE, S. ..... p 334 N95-12535
LEE, STUART M. C. ..... p 337 N95-11811
LEE, Y. T. T. ..... p 338 N95-11908
LEECH, ANDREW R. ..... p 312 N95-12511
LEMER, ANDREW C. ..... p 376 N95-12385
LENHARD, R. J. ..... p 294 N95-13075
LENT, CRAIG S. ..... p 287 N95-12881
LEONARD, CHUCK ..... p 240 N95-12638
LEONE, J. M., JR. ..... p 326 N95-12927
LEONE, STEPHEN R. ..... p 324 N95-12534
LEONTSINIS, N. ..... p 254 N95-12790
LEU, DAVID L. ..... p 253 N95-12528
LEUNG, MAN-KIT ..... p 259 N95-11844
LEVINE, WILLIAM S. ..... p 245 N95-12791
LEW, J. Y. ..... p 304 N95-13182
LEWANDOWSKI, LAURAND H. ..... p 273 N95-12131
LEWIS, T. A. ..... p 272 N95-11733
LI, G. X. ..... p 368 N95-12758
LI, HAU ..... p 286 N95-12494
LI, HUA-XIN ..... p 270 N95-12372
LI, W. ..... p 268 N95-13288
LI, WEINJIE ..... p 274 N95-12417
LI, YONG ..... p 323 N95-12226
LI, ZHENG ..... p 295 N95-11780
LIANG, ANITA D. ..... p 304 N95-13583
LIANG, S. H. ..... p 259 N95-12551
LIASJOE, K. H. ..... p 356 N95-13575
LICCIONE, JOHN W. ..... p 243 N95-12591
LILLEKJENDLIE, B. ..... p 376 N95-13572
LINDBERG, R. ..... p 267 N95-12585
LINDELL, I. V. ..... p 283 N95-12580
p 283 N95-12581
LINDSTROM, WALDEMAR C. ..... p 304 N95-13155
LING, FREDERICK F. ..... p 296 N95-13165
LING, W. ..... p 346 N95-11838
LINTHICUM, K. ..... p 289 N95-13368
LISTER, TEDD E. ..... p 373 N95-11993
LITVIN, F. L. ..... p 303 N95-13083
LIU, BAOHUA ..... p 370 N95-13541
LIU, BAW-LIN ..... p 230 N95-11807
LIU, C. C. ..... p 284 N95-12674
LIU, J. M. ..... p 369 N95-13285
LO, C. F. ..... p 292 N95-12228
LO, JIEN-CHUNG ..... p 344 N95-12588
LOEWENTHAL, BOB ..... p 306 N95-13597
LOGAN, TERRY G. ..... p 346 N95-11863
LOKTEV, V. M. ..... p 375 N95-13277
LOMBARDO, M. P. ..... p 375 N95-13337
LONGINOV, A. V. ..... p 370 N95-13540
LONGSHORE, A. ..... p 378 N95-13123
LOOMIS, MARK P. ..... p 246 N95-11938
LOPARO, KENNETH A. ..... p 349 N95-12811
LORENZINI, ENRICO C. ..... p 252 N95-12106
LOUBRIEL, G. M. ..... p 287 N95-12865
LOVE, DOUGLAS ..... p 384 N95-12667
LOVELL, J. R. ..... p 325 N95-13434
LOWDEN, R. A. ..... p 272 N95-11736
LOWE, C. W. ..... p 362 N95-12659
LOWE, ROLAND A. ..... p 372 N95-11876
p 317 N95-11903
LU, J. ..... p 303 N95-13083
LU, JIE ..... p 297 N95-13537
LUCAS, G. E. ..... p 269 N95-11738
LUETTGEN, A. L. ..... p 363 N95-13106
LUGO-GARCIA, NIDZA ..... p 330 N95-12393
LUJAN, MICHAEL A. ..... p 240 N95-12628
LUMIA, R. ..... p 303 N95-12854
LUMLEY, JOHN L. ..... p 292 N95-11953
LUO, JIARONG ..... p 370 N95-13541
LUTZ, PATRICIA M. ..... p 261 N95-13151
LY, SIAO ..... p 301 N95-12625
LYNN, K. G. ..... p 374 N95-13125
LYO, S. K. ..... p 376 N95-13172
LYONS, D. ..... p 362 N95-12659
LYSAGHT, M. G. ..... p 380 N95-12633
LYUBASHENKO, V. ..... p 352 N95-12603

M

MA, C. Y. ..... p 264 N95-11735
MA, CHRISTINA ..... p 253 N95-12663
MA, J. ..... p 349 N95-12367
p 281 N95-12368
MACABANTAD, DOMINIQUE DUJALE
p 241 N95-12643
MACKAY, GORDON ..... p 249 N95-12531
MACKLEY, ERNEST A. ..... p 244 N95-12860
MACKNIGHT, WILLIAM J. ..... p 272 N95-11852
MACLIN, A. ..... p 362 N95-12659
MADANGARLI, V. P. ..... p 287 N95-12865
MADDUX, GARY A. ..... p 308 N95-12391
MAEDA, S. ..... p 366 N95-12439
p 367 N95-12449
MAEDA, SADAO ..... p 367 N95-12451
MAESE, A. CHRISTOPHER ..... p 339 N95-11964
MAESTRELLO, L. ..... p 290 N95-11812
MAFFEO, R. J. ..... p 309 N95-11711
MAGNUSSEN, B. F. ..... p 264 N95-11756
MAIER, W. B., II ..... p 363 N95-13106
MAKEIG, SCOTT ..... p 335 N95-12133
MAKEL, D. B. ..... p 284 N95-12674
MALGHAN, S. G. ..... p 277 N95-13530
MALLOZZI, R. S. ..... p 380 N95-12463
MANGUSO, LISA ..... p 327 N95-12997
MANNINEN, L. M. ..... p 317 N95-11798
p 317 N95-11799
p 317 N95-11846
MANZELLA, DAVID H. ..... p 257 N95-11919
MAO, WEIZHEN ..... p 342 N95-12005
MARCELO, MOHRLI ..... p 277 N95-12822
MARCHENKO, I. G. ..... p 277 N95-13535
MARCHESSEAULT, B. ..... p 239 N95-12305
MARCHUK, N. D. ..... p 371 N95-11748
MARDARE, DANIELA ..... p 275 N95-12773
MARK, KAREN ..... p 277 N95-12822
MARKLEY, F. ..... p 296 N95-13287
MARKS, T. J. ..... p 363 N95-13374
MARQUARDT, ROBERT F. ..... p 338 N95-12132
MARSHALL, ROBERT E. ..... p 235 N95-13208
MARTICH, FREDERICK ..... p 384 N95-13497
MARTIN, JAMES ..... p 302 N95-12690
MARTIN, JAMES L. ..... p 238 N95-12225
MARTIN, JOHN S. ..... p 333 N95-12406
p 362 N95-12427
MARTIN, RODGER L. ..... p 319 N95-12110
MARTIN, TIMOTHY A. ..... p 256 N95-13232
MARTIN, TRENT ..... p 254 N95-12765
MARTINEZ, RADAME ..... p 327 N95-12998
MARTINSON, ROBERT J. ..... p 236 N95-13213
MARTUCCI, THOMAS A., III ..... p 254 N95-12698
MARTYN ..... p 253 N95-12632
MASIULANIEC, KONSTANTY C. ..... p 291 N95-11888
MASLANIK, J. A. ..... p 327 N95-11706
MASON, J. J. ..... p 354 N95-12728
MASON, KEVIN T. ..... p 334 N95-13054
MASSA, LOU ..... p 354 N95-12426
MASUGATA, KATSUMI ..... p 365 N95-12433
MASUZAKI, M. ..... p 367 N95-12450
MATARAZZO, C. ..... p 322 N95-11741
MATHESON, MARK ..... p 277 N95-12822
MATHEWS, BRUCE D. ..... p 235 N95-13206
MATHIAS, H. D. ..... p 350 N95-12866
MATHIAS, L. J. ..... p 274 N95-12419
MATHIAS, LON J. ..... p 273 N95-12008
p 273 N95-12397

	p 262	N95-12398
	p 273	N95-12399
	p 273	N95-12400
	p 276	N95-13296
	p 264	N95-13298
	p 375	N95-13299
MATLOCK, D. K.	p 271	N95-12895
MATSUYAMA, TOMOCHIKA	p 356	N95-11817
	p 371	N95-11819
MATTE, J. P.	p 369	N95-13285
MATTERN, DUANE L.	p 245	N95-12763
MATTESON, MILTON A.	p 356	N95-13154
MATTIKALLI, RAJU	p 300	N95-12505
MATYJASZEWSKI, KRZYSZTOF	p 275	N95-12773
MAURICE, KELLY E.	p 382	N95-11704
MAUZY, A.	p 378	N95-13123
MAYER, S. T.	p 356	N95-11791
MAYHEW, ELLEN R.	p 306	N95-13600
MCCARTHY, JOHN	p 303	N95-12694
MCCLAIN, CHARLES R.	p 328	N95-11920
	p 328	N95-12151
	p 328	N95-12359
MCCOMAS, D. J.	p 324	N95-12649
MCCONNELL, CHRIS	p 343	N95-12497
MCCOOL, S. C.	p 370	N95-13529
MCCORKLE, T.	p 239	N95-12305
MCCORMACK, ANN	p 339	N95-11962
MCCOURT, STEVE	p 382	N95-12307
MCDANIEL, AMOS D.	p 295	N95-11996
MCDONOUGH, LARRY	p 316	N95-13290
MCFADDEN, LESLIE D.	p 325	N95-13025
MCGARITY, JOHN O.	p 256	N95-13138
MCGARVIE, LEIGH	p 333	N95-12376
MCGOWEN, JOHN A.	p 262	N95-12398
MCGREEVY, J. L.	p 290	N95-11812
MCHATY, ROD	p 249	N95-12531
MCILWAIN, MEL C.	p 249	N95-11703
MCINTYRE, DAVID	p 360	N95-13178
MCKAY, TIM	p 337	N95-11876
MCKNIGHT, R. L.	p 309	N95-11711
MCLEAN, JAMES T.	p 328	N95-11920
MCMILLIAN, SHANDY	p 254	N95-12765
MCMINN, JOHN D.	p 255	N95-12838
MCMORROW, D. F.	p 371	N95-11739
MCWITHEY, MICHAEL C.	p 242	N95-12702
MEGSON, G. M.	p 347	N95-13407
	p 336	N95-13433
MEISS, A. G.	p 240	N95-12636
MELKO, JOSEPH	p 361	N95-12665
MERCED-MOORE, DARLENE	p 337	N95-11878
MERCER, AMY	p 383	N95-12529
MERCER, CAROLYN R.	p 296	N95-12748
MERKLE, K. L.	p 271	N95-13543
MESEROLE, J. S.	p 294	N95-13233
	p 294	N95-13234
MEVE, JEFF	p 384	N95-13497
MEYER, EIKAR	p 338	N95-12361
MEYER, R. C.	p 301	N95-12579
MEYER, RUDOLF X.	p 253	N95-12663
	p 361	N95-12665
MEYERS, D. P.	p 301	N95-12579
MEZA, VICTOR J.	p 240	N95-12628
MEZYNSKI, ALEXIS	p 232	N95-12548
MIASTKOWSKI, JOZEF	p 312	N95-12631
MICHA, DAVID A.	p 358	N95-12882
	p 359	N95-13141
MICHAUD, F. D.	p 363	N95-13106
MICKEL, THU-HA T.	p 266	N95-12549
MICKELSON, ALAN R.	p 285	N95-13371
MIDDLETON, DAVID B.	p 245	N95-12664
MILAM, TIGREE	p 339	N95-12629
MILLENER, D. J.	p 357	N95-12012
MILLER, DUANE D.	p 260	N95-12613
MILLER, FRAN	p 235	N95-13206
MILLER, GREGORY A.	p 270	N95-12543
MILLER, ROBERT GLENN	p 241	N95-12643
MILLER, WILLIAM	p 258	N95-12819
MILLS, D. G.	p 341	N95-11763
MINAMI, KAZUO	p 365	N95-12435
MINECK, RAYMOND E.	p 231	N95-12176
MINGUET, PIERRE J.	p 262	N95-12793
MINSTER, JEAN-BERNARD	p 325	N95-13136
MIRDAMADI, M.	p 269	N95-11915
MIRI', A. A.	p 322	N95-11741
MITCHELL, R. B.	p 340	N95-12413
MITCHENKO, E. I.	p 311	N95-11924
MITLYNG, DAVID	p 240	N95-12628
MIYAMOTO, SHUJI	p 365	N95-12431
	p 365	N95-12432
MIYAMOTO, TETSU	p 366	N95-12440
	p 367	N95-12447
MOATS, C. D.	p 326	N95-12839
MOGREN, S.	p 362	N95-12598
MOMMA, LOURDES JUNKO	p 265	N95-11885
MONACO, LISA A.	p 372	N95-11921
MONCMAN, DEBORAH A.	p 261	N95-11700
MONTGOMERY, MICHAEL T.	p 326	N95-12392
MONTGOMERY, RAYMOND C.	p 252	N95-11947
MONTOYA, J.	p 235	N95-13208
MOORTHI, S.	p 323	N95-12226
MORE, K. L.	p 272	N95-11736
MORELLI, EUGENE A.	p 244	N95-11869
MORIYAMA, KINYA	p 366	N95-12440
	p 367	N95-12447
MORRIS, JAMES G., III	p 373	N95-12635
MORRIS, RICHARD A.	p 356	N95-13154
MORRISETTE, MONICA	p 241	N95-12700
MORROW, DANIEL G.	p 337	N95-11905
MOSES, D.	p 272	N95-11847
MOSHER, D.	p 361	N95-11792
MOSHER, MARIANNE	p 232	N95-12360
MOSHIER, M. A.	p 345	N95-13157
MOSZKOWSKI, B.	p 345	N95-13438
MOUNT, FRANCES E.	p 337	N95-11878
MOUSSOUROS, MINOS	p 293	N95-12409
MUEGGE, ED	p 256	N95-13194
MUELLER, CRAIG	p 241	N95-12700
MULLER, MATTHEW	p 254	N95-12698
MULVEHILL, ALICE M.	p 326	N95-12805
MUMMA, M. J.	p 250	N95-12917
MUNSON, JOHN	p 306	N95-13599
MURPHY, D.	p 372	N95-11862
MURPHY, ROSA	p 382	N95-12950
MURRAY, S. F.	p 296	N95-13165
MUSE, WILLIAM T., JR.	p 330	N95-12614
MUTHIAH, JENO	p 276	N95-13296
MYERS, CHRIS	p 258	N95-12819
MYHRE, GRETE	p 335	N95-12133

N

NAEGELI, D. W.	p 234	N95-12499
NAGAKAWA, KENJI	p 366	N95-12436
NAGATA, MASAYOSHI	p 365	N95-12430
NAGEL, R. L.	p 287	N95-12863
NAIK, RAJIV A.	p 262	N95-11926
NAITO, KENTA	p 366	N95-12437
NAKAI, SADAO	p 365	N95-12431
	p 365	N95-12432
NAKAMURA, S.	p 366	N95-12438
NARAYANAN, VENKAT	p 377	N95-12618
NATAF, J. M.	p 345	N95-13157
NATHAN, M.	p 263	N95-12883
NECKER, C. T.	p 374	N95-13078
NEHER, JASON R.	p 240	N95-12636
NEKLYUDOV, I. M.	p 374	N95-12948
NELMS, R. M.	p 312	N95-12620
NELSON, EMILY S.	p 278	N95-12703
NELSON, MICHAEL L.	p 345	N95-13198
NESPOR, JERALD D.	p 236	N95-13212
NESTOR, JULIE	p 238	N95-12294
NETTLES, A. T.	p 261	N95-11816
NEUENDORFFER, TOM	p 343	N95-12504
NEUHART, DAN H.	p 246	N95-13553
NEWMAN, M. J.	p 313	N95-13576
NEWMAN, SHAWN	p 383	N95-12529
NEWTON, PATRICK L.	p 308	N95-12391
NGO, DUNG	p 383	N95-12826
NGUYEN, J.	p 279	N95-11707
NGUYEN, PHONG	p 241	N95-12645
NICHOLSON, HEATHER	p 383	N95-12826
NICHOLSON, SHAUN R.	p 281	N95-12374
NICOL, DAVID M.	p 342	N95-12005
NICOLETTE, V. F.	p 264	N95-11756
NIEDERMEIER	p 253	N95-12632
NIELSEN, B.	p 374	N95-13125
NIELSEN, KENNETH	p 283	N95-12644
NIERZWICKI-BAUER, S. A.	p 329	N95-11737
NIKOLAEV, V. S.	p 375	N95-13277
NILL, LAURIE	p 383	N95-12826
NILSON, D. G.	p 364	N95-11786
NIX, J. R.	p 359	N95-13104
NOBARI, M. R. H.	p 295	N95-13550
NOBILI, ANNA	p 354	N95-12229
NOBLE, BRIAN D.	p 378	N95-12502
NOBLE, MATTHEW J.	p 373	N95-12923
NOBUHARA, SADAO	p 365	N95-12434
	p 366	N95-12436
NORIKANE, L.	p 382	N95-11704
NORTH, D. R.	p 321	N95-12855
NURMELA, K. J.	p 351	N95-11839
NYBERG, GREGORY	p 238	N95-11952

O

OAKLEY, DAVID R.	p 313	N95-13162
OBRIAN, T. R.	p 363	N95-13106
ODA, HIROJI	p 358	N95-12522
ODETTE, G. R.	p 269	N95-11738
ODONOGHUE, DENNIS P.	p 245	N95-12763
OFARRELL, J. M.	p 230	N95-11807
OGASAWARA, MASAAKI	p 356	N95-11817
	p 371	N95-11819
OGNIVENKO, V. V.	p 285	N95-13343
OGURA, KAZUO	p 365	N95-12435
OHANLON, SEAN	p 301	N95-12554
	p 277	N95-13508
OKANO	p 253	N95-12632
OLIGER, JOSEPH	p 351	N95-11883
OLSEN, LOLA M.	p 318	N95-11845
OLSON, C.	p 364	N95-11754
OLSON, D. L.	p 271	N95-12895
ONEAL, MICHAEL	p 337	N95-11878
ONEIL, PATRICK J.	p 238	N95-11952
OPYDO, WLADYSLAW	p 357	N95-12101
ORANS, ROBIN	p 386	N95-11955
ORAZI, R.	p 280	N95-11943
ORAZI, RICHARD J.	p 298	N95-12779
ORNSTEIN, R. L.	p 331	N95-12677
OROURKE, THOMAS P.	p 341	N95-11761
OSAHENI, JOHN A.	p 262	N95-12404
	p 275	N95-12537
OSBORNE, WILLIAM P.	p 281	N95-12010
OSGOOD, B.	p 352	N95-12577
OSSOWSKI, ANDRZEJ	p 348	N95-12109
OSTANEVICH, YU. M.	p 356	N95-11747
OWCZAREK, STEFAN	p 384	N95-12243
OZDAS, E.	p 372	N95-11862

P

PACIESAS, W. S.	p 380	N95-12464
PACIESAS, W.S.	p 380	N95-12463
PAIK, HO JUNG	p 354	N95-12229
PAKZAD, M.	p 347	N95-13404
PALAZZO, R., JR.	p 341	N95-11763
PALKA, ZYGMUNT	p 323	N95-12112
PAMADI, BANDU N.	p 252	N95-12175
PANCHOLI, ARVIND	p 307	N95-13607
PANG, S. W.	p 373	N95-12602
PANOS, JEAN B.	p 247	N95-13601
PANTAZIS, JOHN A.	p 256	N95-13138
PANWAR, T. S.	p 292	N95-11939
PAPAMICHAEL, K.	p 296	N95-13158
PAPPERT, S.	p 280	N95-11943
PARIKH, A. N.	p 266	N95-12514
PARK, DONG	p 357	N95-11851
PARK, Y.	p 375	N95-13272
PARKS, CATHY BONIFAS	p 377	N95-11963
PARKS, THOMAS R.	p 338	N95-12132
PASSEUR, ANDREA	p 373	N95-12386
PASTERNAK, A. D.	p 265	N95-11790
PATNAIK, SURYA N.	p 242	N95-12787
PATONIS, HRISTOS	p 258	N95-12604
PATRICK, B. O.	p 259	N95-12551
PATRICK, CHRIS	p 383	N95-12529
PATT, FREDERICK S.	p 328	N95-11920
PATTERSON, MIKE	p 238	N95-12294
PAVLAKOVIC, BRIAN N.	p 308	N95-11813
PAYNE, S. A.	p 299	N95-13534
PAZIK, JOHN C.	p 373	N95-12923
PEARSON, DARREN L.	p 360	N95-13376
PECHENIK, A.	p 277	N95-13530
PEIRO, F.	p 271	N95-13140
PEKALA, R. W.	p 356	N95-11791
PENDER, MICHAEL	p 284	N95-12646
PENDLETON, ED	p 230	N95-11829
PENDLETON, G. N.	p 380	N95-12463
	p 380	N95-12464
PENN, LANNING M.	p 384	N95-12667
PENNER, R. M.	p 268	N95-13288
PENNER, REGINALD M.	p 274	N95-12417
PENNY, DAMON	p 303	N95-12694
PERCEC, V.	p 356	N95-11828
PERCEC, VIRGIL	p 358	N95-12522
PEREYRA, R. A.	p 312	N95-12784
PEREZ, C. L.	p 250	N95-11755
PEREZ, GUSTAVO, JR.	p 241	N95-12643
PERLSTEIN, JERRY	p 275	N95-12537
PERRAS, CRAIG	p 383	N95-12826
PERRIN, PATRICK	p 378	N95-12995
PERSON, LEE H., JR.	p 245	N95-12664
PESKOV, V.	p 296	N95-13171
PETERSON, W.	p 248	N95-11934
PETRICEVIC, V.	p 298	N95-12951
PETROV, N. M.	p 360	N95-13275
PETRUKHIN, OLEG	p 367	N95-12446
PETRY, FREDERICK	p 378	N95-12995
PETTIT, CHRIS	p 230	N95-11829
PFEFFERLE, L. D.	p 268	N95-13251
PHAM, TUAN	p 339	N95-11914
PHAM, VU	p 249	N95-12531
PHAN, A. H.	p 270	N95-12148
PHILLIPS, C.	p 347	N95-13404
	p 352	N95-13437

PHILLIPS, LEE ..... p 338 N95-12555
p 302 N95-12627
PHILLIPS, P. E. ..... p 368 N95-12758
PHILLIPS, R. C. ..... p 299 N95-13076
PIELOCH, STUART ..... p 301 N95-12554
p 277 N95-13508
PIERCE, MARK W. ..... p 284 N95-12920
PIERMARINI, G. J. ..... p 277 N95-13530
PINERO, LUIS R. ..... p 258 N95-12750
PITTS, W. M. ..... p 236 N95-13247
PLA-DALMAU, A. ..... p 296 N95-13287
PLAT, N. ..... p 344 N95-12774
PLATZKE, MIKE ..... p 253 N95-12661
PLONKA, JOHN ..... p 258 N95-12604
POCO, J. F. ..... p 356 N95-11791
POEHLMANN, K. ..... p 282 N95-12416
POKORA, DARLENE C. ..... p 229 N95-11710
POLAKOWSKI, TONY ..... p 383 N95-12529
POLLAK, F. H. ..... p 371 N95-11740
p 373 N95-12602
POLYSHCHUK, V. ..... p 300 N95-12377
p 301 N95-12621
p 303 N95-12843
POPE, JONATHAN M. ..... p 269 N95-11933
POPOVIC, VOJIN P. ..... p 331 N95-12827
POROD, WOLFGANG ..... p 287 N95-12881
POUTANEN, MARKKU ..... p 314 N95-11880
POWERS, W. T. ..... p 284 N95-12674
PRABHU, RAMADAS K. ..... p 293 N95-12619
PRAKASH, RAGHU V. ..... p 311 N95-11879
p 311 N95-11924
PRASANNA, M. G. ..... p 300 N95-11889
PREGGER, BRUCE A. ..... p 266 N95-12549
PRESSESKY, J. L. ..... p 296 N95-12869
PRINDLE, F. ..... p 347 N95-12418
PROCTOR, FRED H. ..... p 234 N95-13204
PROCTOR, MARGARET P. ..... p 305 N95-13592
PRYOR, D. W., JR. ..... p 294 N95-13156
PRZEKWAS, ANDRZEJ ..... p 305 N95-13586
PUGHE, W. L. ..... p 380 N95-12633
PULAT, PAKIZE SIMIN ..... p 308 N95-11994
PULKKINEN, U. ..... p 352 N95-12820

Q

QIU, XIAOMING ..... p 370 N95-13539
QU, WENXIAO ..... p 370 N95-13538
QUINN, JARUS W. ..... p 314 N95-11831
p 268 N95-13372
QUINN, JOHN M. ..... p 324 N95-12544
p 253 N95-12545
QUINN, TODD M. ..... p 342 N95-11918
QUINTERO, R. ..... p 303 N95-12854

R

RACHELE, HENRY ..... p 327 N95-12997
RAHKO, K. ..... p 349 N95-12367
p 281 N95-12368
RAJULU, SUDHAKAR L. ..... p 333 N95-11887
RALL, JONATHAN A. R. ..... p 314 N95-11997
RAMAN, SHIVAKUMAR ..... p 308 N95-11994
RAMASWAMY, SHANKAR ..... p 347 N95-12523
RAMSEY, BRIAN D. ..... p 379 N95-12304
RAMSEY, KERI ..... p 239 N95-12609
RANACHOWSKI, JERZY ..... p 355 N95-12013
p 357 N95-12101
p 311 N95-12108
RANAUDO, RICHARD J. ..... p 245 N95-12763
RANDELL, B. ..... p 345 N95-13432
RAO, M. M. ..... p 354 N95-12994
RAPANOTTI, L. ..... p 347 N95-13407
RAPHAN, THEODORE ..... p 333 N95-12376
RASH, CLARENCE E. ..... p 362 N95-12427
RATHZ, TOM ..... p 278 N95-11759
RATNER, M. A. ..... p 363 N95-13374
RAUCH, G. C. ..... p 296 N95-12869
RAVICHANDRAN, G. ..... p 354 N95-12728
RAWLIN, VINCENT K. ..... p 258 N95-12750
RAZAFIMPANILO, HERISOA ..... p 319 N95-11931
READEY, M. J. ..... p 276 N95-13184
REALE, ANTHONY L. ..... p 322 N95-11836
REESE, CHARLES ..... p 258 N95-12604
REEVES, A. ..... p 378 N95-13123
REEVES, G. D. ..... p 324 N95-12649
REHAK, P. ..... p 295 N95-11780
REICHERT, BRUCE A. ..... p 232 N95-12378
REINHARD, RUEDEGER ..... p 354 N95-12229
REJ, D. J. ..... p 365 N95-12371
REJMUND, FELIKS ..... p 355 N95-12013
REMMEL, MARK ..... p 368 N95-12641
RENGARAJAN, GOVIND ..... p 313 N95-13096
p 313 N95-13163
REUTHER, JAMES ..... p 230 N95-11884
REYES, A. P. ..... p 374 N95-13081
RICALDI, RON ..... p 339 N95-11914
RICE, C. J. ..... p 250 N95-12917
RICHARDS, B. ..... p 368 N95-12758
RICHARDS, MARK A. ..... p 235 N95-13208
RICHARDSON, J. H. ..... p 265 N95-11790
RICHEY, EDWARD, III ..... p 269 N95-11933
RICHTER, G. N. ..... p 265 N95-11790
RIEDMAN, JOHN ..... p 253 N95-12661
RIGGS, H. RONALD ..... p 310 N95-11815
RIGGS, JOHN F. ..... p 364 N95-11837
RINTAMAA, R. ..... p 313 N95-12947
RISER, ROBERT ..... p 342 N95-11941
RITTENHOUSE, KIRK ..... p 235 N95-13206
ROBERSON, D. J. ..... p 332 N95-11708
ROBERSON, S. ..... p 289 N95-13368
ROBERTSON, C. ..... p 336 N95-13433
ROBINSON, LAWSON H. ..... p 230 N95-11911
ROBSON, CHRISTOPHER ..... p 253 N95-12663
RODRIGUES, ANNETTE T. ..... p 339 N95-11964
RODRIGUEZ, C. ..... p 315 N95-12527
ROGER, C. ..... p 352 N95-12603
ROGERS, PETE ..... p 253 N95-12661
ROGERS, R. S. ..... p 265 N95-11790
ROJAS, R. G. ..... p 284 N95-12856
ROLLINGS, RAYMOND S. ..... p 246 N95-12216
RONG, Z.-Y. ..... p 371 N95-11740
ROOFF, JOHN ..... p 240 N95-12638
ROSAKIS, A. J. ..... p 354 N95-12728
ROSBOROUGH, GEORGE W. ..... p 248 N95-12837
ROSE, JOSEPH L. ..... p 308 N95-11813
ROSEKIND, MARK R. ..... p 334 N95-12792
ROSENBERGER, FRANZ ..... p 372 N95-11921
ROSENFELD, A. ..... p 315 N95-12527
ROSSBACHER, LISA A. ..... p 383 N95-12952
ROSSITER, B. N. ..... p 353 N95-13560
ROTMANS, J. ..... p 320 N95-12776
ROUNTREE, MICHAEL S. ..... p 334 N95-12792
ROWAN, W. L. ..... p 368 N95-12758
ROWE, WILLIAM ..... p 235 N95-13206
ROWNEY, DAVID A. ..... p 254 N95-12698
RUBADEUX, K. L. ..... p 300 N95-11889
RUBIN, M. ..... p 296 N95-13158
RUBINE, DEAN ..... p 343 N95-12504
RUDDUCK, R. C. ..... p 282 N95-12493
RUDERMAN, MALVIN A. ..... p 382 N95-12939
RUDOLPH, RICHARD H. ..... p 240 N95-12636
RUETER, AMY ..... p 239 N95-12530
RUMMEL, REINER ..... p 354 N95-12229
RUSS, EDWIN J. ..... p 259 N95-13237
RUSSELL, STEPHEN D. ..... p 298 N95-12779
p 298 N95-12780
RUTKA, M. J. ..... p 288 N95-13252
RUTLEDGE, J. ..... p 277 N95-12729
RYAN, JAMES S. ..... p 232 N95-12389
RYBAK, S. C. ..... p 294 N95-13233
RYEN, N. ..... p 363 N95-13574

S

SABINI, GEORGE J. ..... p 289 N95-11705
SABIO, VINCENT ..... p 282 N95-12547
SABOURIN, M. A. ..... p 321 N95-12855
SAGDEO, PRADIP ..... p 238 N95-12294
SAIKI, E. M. ..... p 293 N95-12422
SALMON, J. T. ..... p 363 N95-13532
SALMON, JON ..... p 354 N95-12229
SANDERS, DONALD C. ..... p 338 N95-12354
SANDLIN, GLENN D. ..... p 281 N95-12402
SANGMEISTER, GARY ..... p 283 N95-12644
SANKOVIC, JOHN M. ..... p 259 N95-13347
SANTANNA, NILSON ..... p 343 N95-12300
SANTELLA, M. L. ..... p 269 N95-11897
SAPATNEKAR, SACHIN ..... p 347 N95-12523
SARACHIK, KAREN B. ..... p 349 N95-12411
SAROUGHIAN, ANDY ..... p 240 N95-12628
SASSEN, A. M. ..... p 337 N95-11778
SASSER, M. K. ..... p 353 N95-13061
SATHER, DUANE P. ..... p 329 N95-12590
SATO, KOICHI ..... p 366 N95-12440
SAUNIER, PAUL ..... p 288 N95-13231
SAUTER, STEFAN A. ..... p 352 N95-12552
SAVAGE, M. ..... p 300 N95-11889
SCHAFFNER, J. ..... p 357 N95-12012
SCHARRER, JOSEPH ..... p 305 N95-13589
SCHEIFLE, JOHN ..... p 253 N95-12545
SCHEIMAN, DANIEL A. ..... p 260 N95-12693
SCHEROCK, JEFF ..... p 240 N95-12638
SCHIEBER, BRIAN D. ..... p 328 N95-11920
SCHIRBER, J. E. ..... p 372 N95-11862
SCHLEGELMILCH, RICHARD F. ..... p 342 N95-11918
SCHMALE, D. T. ..... p 271 N95-13544
SCHMIDT, DAVEY ..... p 338 N95-12361
SCHMIDT, DEANNA ..... p 368 N95-12641
SCHMOLTNER, ANNE-MARIE ..... p 322 N95-12103
SCHNACK, D. D. ..... p 384 N95-13582
SCHNEIDER, MARK S. ..... p 242 N95-12702
SCHNEIDER, S. E. ..... p 380 N95-12633
SCHONFELD, JULIE E. ..... p 247 N95-11965
SCHOR, ROBERT H. ..... p 330 N95-12006
SCHROEDER, LYLE C. ..... p 315 N95-12379
SCHRYVER, J. C. ..... p 363 N95-13421
SCHUCH, LUIZ ALEXANDRE ..... p 321 N95-13192
SCHUENEMAN, G. ..... p 296 N95-13287
SCHUMM, JEFFRY S. ..... p 360 N95-13376
SCHUMS, H. ..... p 308 N95-13609
SCHUR, KEITH ..... p 243 N95-12591
SCHUSTER, JOHN R. ..... p 259 N95-13237
SCHWAN, KARSTEN ..... p 320 N95-12798
SCHWANK, J. R. ..... p 384 N95-11757
SCHWARTZ, A. ..... p 296 N95-12869
SCHWARTZ, S. ..... p 309 N95-11711
SCOTT, ELAINE P. ..... p 261 N95-11700
SCUILLION, T. ..... p 280 N95-11904
SEAL, DANIEL W. ..... p 238 N95-11952
SEAS, A. ..... p 298 N95-12951
SEGAL, J. L. ..... p 340 N95-12413
SEIDMAN, D. N. ..... p 271 N95-13543
SEITTER, KEITH L. ..... p 327 N95-13134
SELKOWITZ, S. ..... p 296 N95-13158
SELOW, JAN ..... p 238 N95-12294
SEMCHENKO, I. ..... p 283 N95-12595
SENBAYASHI, SATORU ..... p 366 N95-12437
SENCHISHIN, V. ..... p 296 N95-13287
SERBIN, V. I. ..... p 361 N95-11779
SERREZE, M. C. ..... p 327 N95-11706
SERVIDIO, DWAYNE M. ..... p 287 N95-12509
SETTLES, GARY S. ..... p 292 N95-11992
SEWELL, JESSE ..... p 289 N95-11709
SEXTON, DOUGLAS A. ..... p 298 N95-12779
p 298 N95-12780
SHABBIR, AAMIR ..... p 291 N95-11935
SHAING, K. C. ..... p 370 N95-13422
SHALYAPIN, V. N. ..... p 372 N95-11899
SHANNON, S. G. ..... p 334 N95-13054
SHAPIRO, WILBUR ..... p 305 N95-13585
SHARF, I. ..... p 347 N95-13353
SHARP, BRAD ..... p 254 N95-12765
SHASHUA, AMNON ..... p 351 N95-12007
SHAUGHNESSY, JOHN D. ..... p 255 N95-12838
SHAW, ROBERT J. ..... p 233 N95-13058
SHEN, C. K. ..... p 323 N95-12506
SHEPHARD, MARK S. ..... p 351 N95-11850
SHEPHERD, MICHAEL T. ..... p 312 N95-12620
SHEPPARD, M. G. ..... p 368 N95-12757
SHIEH, GEOFFREY S. ..... p 289 N95-11705
SHIEL, DONALD L. ..... p 324 N95-12544
p 253 N95-12545
SHIH, TSAN-HSING ..... p 291 N95-11935
p 292 N95-11953
SHIMODA, K. ..... p 366 N95-12443
p 367 N95-12445
SHIMOMURA, NAOYUKI ..... p 365 N95-12430
SHIRAI, NOBUTAKE ..... p 365 N95-12431
p 365 N95-12432
SHLYAPTSEVA, ALLA ..... p 367 N95-12446
SHOMOTO, NORIHISA ..... p 365 N95-12431
SHOUCRI, MERIT ..... p 236 N95-13215
SHOUMOTO, NORIHISA ..... p 365 N95-12432
SHULL, J. MICHAEL ..... p 385 N95-12886
SIBUL, L. H. ..... p 345 N95-13370
SICONOLFI, STEVEN F. ..... p 337 N95-11811
SIEGEL, M. W. ..... p 234 N95-12623
SIGLER, DOUGLAS L. ..... p 253 N95-12661
SIGNOR, DAVID B. ..... p 232 N95-12360
SIHVOLA, A. ..... p 283 N95-12595
SIHVOLA, A. H. ..... p 283 N95-12580
p 283 N95-12581
SIKKA, V. K. ..... p 269 N95-11897
SILVA, ALEX ..... p 240 N95-12628
SIMMONS, J. A. ..... p 376 N95-13172
SIMON, DONALD L. ..... p 245 N95-12763
SIMONSON, S. A. ..... p 263 N95-12862
SIMPSON, J. A. ..... p 371 N95-11739
SINCLAIR, D. K. ..... p 375 N95-13337
SINGH, R. ..... p 254 N95-12790
SINGH, RAJ ..... p 275 N95-12586
SINGHAL, SURENDRA N. ..... p 311 N95-11954
SINGLE, DAVID J. ..... p 371 N95-11842
SINN, M. T. ..... p 271 N95-13140
SIROTA, MISCHA ..... p 333 N95-12376
SKAAR, ERIC ..... p 275 N95-12586
SKEEN, J. T. ..... p 264 N95-11735
SKINTEJ, N. R. ..... p 372 N95-11899
SKOWRONSKI, LORI ..... p 302 N95-12640
SKRUTSKIE, M. F. ..... p 380 N95-12633
SLATTERY, J. A. ..... p 269 N95-11785
SLEPTSOV, A. N. ..... p 277 N95-13535
SLEPTSOV, S. N. ..... p 277 N95-13535
SLIVA, R. ..... p 281 N95-12382
SLOOF, J. E. ..... p 318 N95-11826

SLOTWINSKI, J. A. p 355 N95-11906
SMEETS, G. p 265 N95-11796
SMICK, DOUG p 241 N95-12700
SMITH, A. M. p 319 N95-11893
SMITH, DEBRA K. p 326 N95-12423
SMITH, GUY A. p 279 N95-12752
SMITH, J. L. p 374 N95-13081
SMITH, MATT p 382 N95-12307
SMITH, S. S. p 260 N95-11904
SMITH, SUZANNE p 342 N95-11941
SMOOKE, M. D. p 268 N95-13251
SNAIL, KEITH A. p 374 N95-13150
SNAZA, CLAY J. p 258 N95-12885
SOBOLESKI, CRAIG p 241 N95-12695
SOLARZ, R. p 298 N95-12868
SOMERVILLE, RICHARD C. J. p 319 N95-11931
SOMPS, CHRISTOPHER J. p 330 N95-12006
SONNENFELD, GERALD p 331 N95-12941
SOOD, DVANDRA p 307 N95-13607
SORRELLS, CINDY p 301 N95-12554
p 277 N95-13508
SOULAS, GEORGE C. p 258 N95-12622
SOUSA, MIKE p 306 N95-13595
SOUTHARD, D. A. p 340 N95-12413
SOVINSKY, J. R. p 269 N95-11785
SOWELL, E. F. p 345 N95-13157
SPEIRS, N. A. p 341 N95-13436
SPERA, DAVID A. p 256 N95-13236
SPERRY, DAVID J. p 256 N95-13138
SPIERS, GARY D. p 362 N95-12390
SPINWEBER, CHERYL L. p 334 N95-12792
SPRINGER, ANTHONY M. p 229 N95-11710
SPRINGFIELD, JAMES F., JR. p 349 N95-12470
SRIVATSAN, RAGHAVACHARI p 245 N95-12664
STACK, D. W. p 353 N95-13061
STAN-LOTTER, HELGA p 332 N95-11966
STARNES, JAMES H., JR. p 311 N95-11946
STAUDMEISTER, DOUGLAS p 239 N95-12530
STAVNES, MARK W. p 256 N95-13194
STEEB, RANDALL p 269 N95-13291
STEELE, SANDRA J. p 267 N95-12836
STEFFEN, K. p 327 N95-11706
STEFFES, PAUL G. p 339 N95-13026
STEGALL, R. L. p 236 N95-13212
STEINETZ, BRUCE M. p 307 N95-13602
STEINMAN, ROBERT M. p 336 N95-13375
STEINSMO, U. p 276 N95-13244
STEM, STEVEN p 239 N95-12530
STEPANOV, K. N. p 370 N95-13540
STEPHENSON, MARK T. p 231 N95-12191
STERN, ROBERT A. p 381 N95-11928
STERN, S. ALAN p 385 N95-12886
p 381 N95-13012
STEVENS, C. p 239 N95-12305
STEVENSON, ROBERT L. p 341 N95-11761
p 341 N95-11764
STEVER, R. D. p 364 N95-11786
STEWART, MICHAEL J. p 375 N95-13299
STICKNEY, JOHN L. p 373 N95-11993
STIRLING, W. G. p 358 N95-12829
STOCKWELL, ALAN E. p 252 N95-11947
STOECKER, H. p 357 N95-12012
STONE, B. M. p 318 N95-11742
STOOKSBURY, F. p 279 N95-12942
STOUT, M. G. p 312 N95-12784
STOVALL, JOHN R. p 242 N95-11913
STRANICK, S. J. p 266 N95-12514
p 358 N95-12617
STRONGIN, M. p 371 N95-11740
STROUD, C. E. p 345 N95-13077
STRUM, M. J. p 264 N95-13533
STRUMINSKIJ, B. V. p 360 N95-13274
STUCKWISCH, SUE p 338 N95-12555
p 302 N95-12627
STURISKY, HILTON p 241 N95-12700
STUVE, E. M. p 268 N95-13549
SUAREZ, MAX J. p 323 N95-12226
SUDARSHAN, T. S. p 287 N95-12865
SUGITO, SYOUJI p 365 N95-12435
SUGN, C. S. p 274 N95-12520
SUI, GUOFANG p 369 N95-13107
SUICH, RONALD C. p 308 N95-12381
SUMMERS, C. J. p 280 N95-11760
SUNDAR, RAJ A. p 273 N95-12008
p 264 N95-13296
SUNDER, R. p 311 N95-11879
p 311 N95-11924
SUNDSTROEM, P. p 355 N95-12597
SUNG, C. S. p 276 N95-13367
SURATI, RAJEEV J. p 347 N95-12414
SUSKO, DAVID p 241 N95-12695
SUZUKI, HIDEAKI p 367 N95-12447
SVEUM, MATT p 368 N95-12641
SVITEK, TOMAS p 328 N95-12359
SWIETLIK, C. p 245 N95-11752
SWITZER, GEORGE F. p 234 N95-13204
p 235 N95-13205
SYMKO, OREST G. p 279 N95-12772
SZCZEBIOT, RYSZARD p 312 N95-12631
SZELES, C. p 374 N95-13125
SZERI, A. Z. p 304 N95-13183

T

TABIBI, B. M. p 362 N95-12659
TABITA, R. p 331 N95-13271
TABOREK, P. p 277 N95-12729
TAIT, TERRY p 301 N95-12625
TAKAHAMA, YOSHIO p 367 N95-12444
TAKAHASHI, GENJI p 365 N95-12431
p 365 N95-12432
TAKASUGI, KEIICHI p 366 N95-12440
p 367 N95-12447
TALBOT, MATTHEW D. p 242 N95-12702
TAM, KWOK HUNG p 302 N95-12666
TAN, M. K. p 256 N95-13195
TANAKA, S. p 289 N95-13368
TANG, K. p 299 N95-13076
TANG, YU p 290 N95-11753
TANNENBAUM, ALLEN p 348 N95-11853
TARES, T. p 280 N95-11800
TARR, MICHAEL J. p 335 N95-11942
TARTAKOVSKIJ, V. K. p 360 N95-13273
TATE, RONALD C. p 356 N95-13154
TATUM, KENNETH E. p 231 N95-11995
TAULBEE, DALE B. p 289 N95-11705
TAYLOR, ARTHUR C., III p 294 N95-13201
TAYLOR, CHRIS p 242 N95-12702
TEALE, TIM p 240 N95-12628
TEITELMAN, M. p 375 N95-13272
TERASAKI, K. p 356 N95-11818
TESSLER, ALEXANDER p 310 N95-11815
THAYER, JEFFREY P. p 322 N95-11801
THOMPSON, STEVEN D. p 361 N95-11910
THOMSEN, M. F. p 324 N95-12649
THOMSON, J. ALEX p 236 N95-13211
THOMSON, SANDRA A. p 330 N95-12614
THORPE, THOMAS P. p 374 N95-13150
THORSNESS, C. B. p 265 N95-11790
THURMES, WILLIAM N. p 371 N95-11855
THURSTON, T. R. p 371 N95-11739
TIBBITTS, T. W. p 338 N95-11949
TICHY, F. p 299 N95-13246
TISHKOFF, J. M. p 257 N95-12507
TOBIN, M. p 364 N95-11754
TOELG, SEBASTIAN p 351 N95-12007
TOKARCIK, SUSAN A. p 233 N95-11967
TOLK, N. H. p 272 N95-11733
TOM, DONALD p 284 N95-12648
TOMKO, DAVID L. p 330 N95-12006
TOOLE, JENNIFER p 337 N95-11878
TOPP, DAVID A. p 244 N95-11901
p 244 N95-11951
TOUR, JAMES M. p 360 N95-13376
TOWNSEND, D. P. p 300 N95-12377
p 301 N95-12621
p 303 N95-12843
TRAN, HUY KIM p 277 N95-11968
TRAN, TRUNG H. p 288 N95-13153
TRANDEM, O. p 285 N95-13559
TREGRE, GREGORY J. p 276 N95-13296
TRETYAKOV, S. p 283 N95-12595
TRIEU, THAI-BA p 241 N95-12695
TRIEU, THUYBA p 241 N95-12695
TRIGGS, MIKE p 240 N95-12639
TRIMBLE, D. J. p 263 N95-12862
TRIMBLE, T. p 321 N95-12855
TRIPATHY, SUKANT p 274 N95-12424
TRYGGVASON, G. p 295 N95-13550
TSERNG, H. Q. p 288 N95-13231
TSUNODA, ROLAND T. p 368 N95-12853
TU, TINA p 262 N95-11835
TUFTS, DONALD W. p 344 N95-12588
TUNICK, ARNOLD p 327 N95-12997
TUNKELANG, DANIEL p 343 N95-12541
TURANO, KATHLEEN p 335 N95-12495
TURNER, D. p 239 N95-12305
TVEITO, A. p 353 N95-13573
TYUTYUNNIKOV, S. I. p 372 N95-11899

U

UCKAN, T. p 368 N95-12758
UEHARA, Y. p 366 N95-12438
ULLMAN, CHRISTOPHER p 258 N95-12604
UNDERWOOD, JOHN H. p 270 N95-12401
URAS, R. A. p 290 N95-11753
URRY, C. MEGAN p 380 N95-12465
p 380 N95-12466

V

VAEKIPARTA, R. M. K. p 272 N95-11847
VAJDOS, GREG p 254 N95-12765
VALLETTE, BRENDA J. p 384 N95-12667
VALO, M. p 313 N95-12947
VANDAALEN, C. p 377 N95-11824
VANDENBERG, G. J. p 330 N95-11902
VANDERBORGH, N. E. p 317 N95-12650
VANDERVLEUTEN, R. J. p 285 N95-13405
VANDRIEL, C. A. p 278 N95-13435
VANNUCCI, A. p 370 N95-13529
VANRIJN, A. C. M. p 332 N95-13408
VANTREUREN, KENNETH W. p 375 N95-12512
VANTRIET, ROBERT p 241 N95-12643
VANTURENNOUT, P. p 348 N95-11825
VANZANDT, L. L. p 275 N95-12536
VARPAANIEMI, K. p 343 N95-12366
VEER, F. A. p 312 N95-12775
VELDEN, CHRISTOPHER p 325 N95-11758
VELSKO, S. P. p 314 N95-11783
VEMURY, SASTRI p 384 N95-12667
VENABLE, D. D. p 362 N95-12659
VENKATAPATHY, ETHIRAJ p 233 N95-11967
VERDERAIME, V. p 248 N95-11870
VERNONA, ROBERT W. p 362 N95-12427
VERON, H. p 340 N95-12413
VERONA, ROBERT W. p 333 N95-12406
VIANCO, P. T. p 269 N95-11785
VIEIRA, J. p 242 N95-12993
VILCHINSKIJ, S. J. p 290 N95-11749
VIRTANEN, J. A. p 268 N95-13288
VIRTANEN, JORMA A. p 274 N95-12417
VISHNEPOLSKY, I. M. p 361 N95-11779
VIVEIROS, STEVEN p 327 N95-12996
VOGEL, SHAWNA p 320 N95-12462
VOLAKIS, J. L. p 281 N95-12382
VOLAKIS, JOHN L. p 279 N95-11707
VOLYNSHIKOVA, T. p 296 N95-13171
VONFLOTOW, ANDREAS H. p 252 N95-12165
VONFRESE, RALPH R. B. p 323 N95-12130
VOSS, S. S. p 361 N95-11779
VRBA, P. p 364 N95-11886
p 364 N95-11916
VU, B. T. V. p 370 N95-13555
VU, JOSEPHINE LYNN p 302 N95-12666
VUORI, A. p 385 N95-11797

W

WAARTS, R. p 299 N95-13294
WACHTER, JOSEPH P. p 259 N95-13237
WAGENBACH, KIMBERLY p 248 N95-11969
WAGNER, CHARLES A. p 244 N95-11868
WAGNER, G. R. p 289 N95-13300
WAGONER, ROBERT V. p 322 N95-11836
WAI, JAMES p 383 N95-12533
WALKER, H. p 326 N95-12927
WALKER, IRA J. p 233 N95-12770
WALLACE, JOHN M. p 320 N95-12462
WALLENIUS, C. p 335 N95-11872
WALLIN, K. p 313 N95-12947
WALLMAN, H. p 265 N95-11790
WALOWIT, JED A. p 305 N95-13584
WANDER, JOHN p 299 N95-11701
WANDOW, HELENA p 368 N95-12641
WANG, FEILING p 275 N95-12586
WANG, H. T. G. p 281 N95-12382
WANG, K. C. p 251 N95-11937
WANG, NING p 296 N95-13165
WANG, Z. p 233 N95-13250
WANNINKHOF, R. p 328 N95-11900
WARD, R. C. C. p 371 N95-11739
WARNOCK, ARCHIBALD, III p 318 N95-11845
WATANABE, TSUGUHIRO p 365 N95-12435
WATKINS, SETH p 255 N95-13006
WATKISS, ERIC J. p 239 N95-12410
WATMUFF, JONATHAN H. p 295 N95-11896
WATSON, C. W. p 257 N95-11782
WATSON, G. I. p 353 N95-12364
WAVRIK, R. p 364 N95-11754
WEAVER, BRAD p 384 N95-13497
WEAVER, R. W. p 327 N95-11706
WEBB, M. S. p 314 N95-11783
WEBB, RON p 253 N95-12661
WEBBINK, RONALD F. p 379 N95-12234
p 323 N95-12468
WEBER, REED p 302 N95-12690
WEDDE, K. J. p 341 N95-13557
WEDGE, DONNE p 327 N95-12996
WEHRLE, JOHN P. p 373 N95-12635
WEINER, STEPHEN P. p 256 N95-13232
WEISBROD, K. R. p 317 N95-12650
WEISE, TIMOTHY MICHAEL p 241 N95-12643

WEISHEIT, J. C. ..... p 369 N95-12897
WEISS, L. A. ..... p 324 N95-12649
WEISS, P. S. ..... p 358 N95-12617
WEISSHAAR, TERRENCE A. ..... p 239 N95-12363
WELLS, DAVID P. ..... p 354 N95-13143
WELLS, JENNIFER ..... p 240 N95-12637
WELLS, M. R. ..... p 371 N95-11739
WELLS, VALANA L. ..... p 237 N95-11699
WENDT, BRUCE J. ..... p 232 N95-12378
WEST, B. ..... p 302 N95-12648
WHALEN, J. M. ..... p 259 N95-12551
WHEELER, R. M. ..... p 338 N95-11949
WHEELWRIGHT, CHARLES ..... p 337 N95-11878
WHELAN, TODD ..... p 240 N95-12637
WHITE, MATT ..... p 384 N95-13497
WHITE, VICKY L. ..... p 332 N95-11702
WHITE, WILLIAM E. ..... p 267 N95-12836
WHITEHEAD, LARRY K. ..... p 343 N95-12500
WHITING, ELLIS E. ..... p 382 N95-12190
WHITLOCK, C. H. ..... p 326 N95-12839
WHITMORE, MIHRIBAN ..... p 337 N95-11878
WHORTON, M. ..... p 342 N95-11923
WIBISONO, BENEDICT C. ..... p 278 N95-12701
WIGGINS, STEVEN ..... p 329 N95-12540
WILEY, CATHY J. ..... p 378 N95-12916
WILLEN, G. S. ..... p 294 N95-13233
WILLETTE, CHRIS ..... p 277 N95-13508
WILLIAMS ..... p 253 N95-12632
WILLIAMS, DANIEL ..... p 254 N95-12698
WILLIAMS, ERIK ..... p 384 N95-13497
WILLIAMS, VERNON E. ..... p 379 N95-11866
WILLIAMSON, REBECCA C. ..... p 339 N95-11970
WILLSHIRE, WILLIAM L., JR. ..... p 355 N95-12341
WILSON, ALLEN W. ..... p 269 N95-11933
WILSON, C. A. ..... p 380 N95-12463
p 380 N95-12464
WILSON, GLENN F. ..... p 335 N95-12133
WILT, T. E. ..... p 264 N95-13193
WING, DAVID J. ..... p 246 N95-13553
WINKELMANN, F. ..... p 345 N95-13157
WINYARD, DAVID C. ..... p 304 N95-13155
WITKOWSKI, L. C. ..... p 288 N95-13231
WITTE, DAVID W. ..... p 231 N95-11995
WOLBERS, S. ..... p 347 N95-13269
WOLFE, MATTHEW ..... p 283 N95-12644
WOLFENBARGER, J. K. ..... p 265 N95-11790
WONG, G. K. ..... p 363 N95-13374
WOO, A. G. ..... p 281 N95-12382
WOOD, J. C. ..... p 260 N95-12764
WOOD, J. G. ..... p 246 N95-13200
WOOD, M. C. ..... p 266 N95-12514
WOODFORD, LYNN M. ..... p 256 N95-13194
WOOTTON, A. J. ..... p 368 N95-12758
WORCESTER, PETER F. ..... p 329 N95-12998
WORKMAN, GARY L. ..... p 278 N95-11759
p 373 N95-12386
p 279 N95-12752
WORLEY, P. H. ..... p 344 N95-12893
WRAY, RICHARD B. ..... p 242 N95-11913
WRIGHT, B. R. ..... p 234 N95-12499
WRIGHT, K. ..... p 361 N95-12147
WRIGHT, NICOLA A. ..... p 335 N95-12133
WRIGHT, WILLIAM B. ..... p 291 N95-11888
WU, D. T. ..... p 374 N95-13086
WU, Q. H. ..... p 284 N95-12674
WU, S. T. ..... p 361 N95-12147
WU, SHIFENG ..... p 306 N95-13598
WU, SHIH-CHIN ..... p 252 N95-11947
WURTELE, M. ..... p 288 N95-13231

X

XIONG, WEI-ZHONG ..... p 245 N95-11752
XU, J. ..... p 272 N95-11733
p 345 N95-13432
XU, YANGSHENG ..... p 300 N95-12526
p 301 N95-12587

Y

YAMABE, CHOBEI ..... p 367 N95-12451
YAMADA, D. ..... p 367 N95-12450
YAMAMOTO, K. ..... p 366 N95-12438
YAMAMOTO, KAZUHIRO ..... p 365 N95-12431
p 365 N95-12432
YAMAMOTO, T. ..... p 366 N95-12443
YAMANAKA, CHIYOE ..... p 365 N95-12431
p 365 N95-12432
YAMAUCHI, GLORIA K. ..... p 232 N95-12360
YAN, D. ..... p 371 N95-11740
YANAGIDAIRA, TAKESHI ..... p 367 N95-12444
YANG, C.-J. ..... p 274 N95-12407
YANG, H. ..... p 237 N95-12582
YANG, X.-Q. ..... p 371 N95-11740
YAO, WEIGUANG ..... p 352 N95-13340
YASUIKE, KAZUHITO ..... p 365 N95-12431
p 365 N95-12432
YATES, LESLIE A. ..... p 295 N95-11971
YATSUI, KIYOSHI ..... p 365 N95-12433
YATSUZUKA, MITSUYASU ..... p 365 N95-12434
p 366 N95-12436
YE, MINYOU ..... p 370 N95-13541
YEE, A. F. ..... p 275 N95-13060
YEE, BENNET ..... p 340 N95-12524
YEH, POCHI ..... p 362 N95-12538
YEUNG, P. K. ..... p 291 N95-11929
YIE, GAOYING ..... p 297 N95-13537
YODER, MAX N. ..... p 288 N95-13181
YOON, C. O. ..... p 272 N95-11847
YOSHIDA, A. ..... p 367 N95-12445
YOSHIKAWA, M. ..... p 367 N95-12450
YOUNG, J. D. ..... p 282 N95-12493
YOUNGBERG, D. ..... p 318 N95-11784
YOUNGBLOOD, DANIEL L. ..... p 242 N95-12702
YOUNGBLOOD, G. E. ..... p 263 N95-12862
YOUNGBLUT, CHRISTINE ..... p 344 N95-13051
YUAN, CHENGJI ..... p 297 N95-13537
YUAN, XIAOLIN ..... p 253 N95-12661
YUDILEVITCH, GIL ..... p 245 N95-12791
YUN, H. M. ..... p 263 N95-12813
YUNG, YUK L. ..... p 382 N95-12011

Z

ZACHARIA, T. ..... p 346 N95-11734
ZAKRAJSEK, J. J. ..... p 300 N95-12377
p 301 N95-12621
p 303 N95-12843
ZALLEN, D. M. ..... p 234 N95-12499
ZALUZEC, N. J. ..... p 285 N95-13057
ZENG, W. J. ..... p 341 N95-11762
ZERBINI, NEWTON JORDAO ..... p 316 N95-13159
ZHANG, BING ..... p 296 N95-12869
ZHANG, LI ..... p 297 N95-13537
ZHANG, S. N. ..... p 380 N95-12463
p 380 N95-12464
ZHANG, SHUXUN ..... p 297 N95-13537
ZHANG, WANCHANG ..... p 360 N95-13536
ZHANG, XIAOYAN ..... p 260 N95-12613
ZHANG, XIUFENG ..... p 360 N95-13536
ZHENG, Q. ..... p 356 N95-11828
p 315 N95-12527
ZHOU, HAILIN ..... p 369 N95-13107
ZHOU, O. ..... p 372 N95-11862
ZHOU, YE ..... p 291 N95-11929
ZHU, JIANG ..... p 231 N95-11917
p 292 N95-11953
ZHU, MARTIN ..... p 253 N95-12564
ZHU, XIAOLEI ..... p 351 N95-11883
ZIEMER, JOHN ..... p 258 N95-12604
ZIMMERMAN, A. H. ..... p 270 N95-12148
ZUND, J. D. ..... p 315 N95-12426
ZUTAVERN, F. J. ..... p 287 N95-12865

CORPORATE SOURCE INDEX

Typical Corporate Source Index Listing

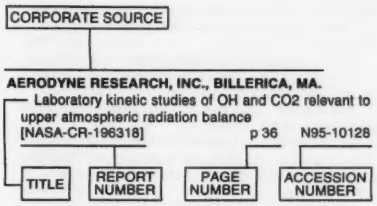

Listings in this index are arranged alphabetically by corporate source. The title of the document provides the user with a brief description of the subject matter. The report number helps to indicate the type of document cited (e.g., NASA report, translation, NASA contractor report). The accession number denotes the number by which the citation is identified. The page number helps you locate the citation in the abstract section. The titles are arranged under each corporate source in ascending accession number order.

A

ACADEMY OF SCIENCES OF THE UKRAINE, KHARKOV.
Radiation amorphization of materials
[DE94-624184] p 374 N95-12948
Stimulated scattering of a slow electromagnetic wave excited by the relativistic electron beam
[DE94-625049] p 285 N95-13343
Structure-phase state of thick amorphous and microcrystalline chromium-carbon films deposited by ion-plasma sputtering
[DE94-624236] p 277 N95-13535
Excitation of fast magneto-acoustic waves in unhomogeneous plasma of a large size tokamak
[DE94-625050] p 370 N95-13540

ACADEMY OF SCIENCES OF THE UKRAINE, KIEV.
On the charged vector particle scattering on a vector particle
[DE94-622787] p 360 N95-13273
The odderon in the deep-inelastic lepton-hadron scattering
[DE94-622791] p 360 N95-13274
Study of the nuclear-coulomb low-energy scattering parameters on the basis of the p-matrix approach
[DE94-622811] p 360 N95-13275
The dissipative mechanism of pinning of a superconducting current
[DE94-623252] p 289 N95-13276
About the structure of the superconducting order parameter of 2 D Fermi system with an arbitrary particle density
[DE94-623268] p 375 N95-13277

ADVANCED MECHANICAL TECHNOLOGY, INC., NEWTON, MA.
Diesel-fired self-pumping water heater
[AD-A283063] p 279 N95-13053

ADVISORY GROUP FOR AEROSPACE RESEARCH AND DEVELOPMENT, NEUILLY-SUR-SEINE (FRANCE).
Psychophysiological assessment methods (including a register of psychophysiologists on microfiches)
[AGARD-AR-324] p 335 N95-12133

AEROJET-GENERAL CORP., AZUSA, CA.
Earth Observing System (EOS)/Advanced Microwave Sounding Unit-A (AMSU-A)
[NASA-CR-189379] p 344 N95-12796

AEROSPACE CORP., EL SEGUNDO, CA.
Screen test for cadmium and nickel plates as developed and used within the Aerospace Corporation
[NASA-CR-196961] p 270 N95-12148
Infrared spectral measurement of Space Shuttle glow
[AD-A282883] p 250 N95-12917

AEROSPACE MEDICAL RESEARCH LABS., BROOKS AFB, TX.
Guided Approach to Instructional Design Advising (GAIDA): How to create GAIDA compatible lessons, volume 2
[AD-A282645] p 343 N95-12500

AIR FORCE INST. OF TECH., WRIGHT-PATTERSON AFB, OH.
Mixed clusters from the coexpansion of C2F6 and n2 in a pulsed, supersonic expansion cluster ion source and beam deflection time-of-flight mass spectrometer: A first application
[AD-A282044] p 361 N95-11910
Mode-locking a longitudinally pumped low pressure atomic iodine laser
[AD-A282363] p 297 N95-11940
Modeling and implementation of a packet routing switch for satellite communications
[AD-A282262] p 282 N95-12412
Fibre optic sensors using adiabatically tapered single mode fibres
[AD-A282306] p 362 N95-12415
Impingement flow heat transfer measurements of turbine blades using a jet array
[AD-A283450] p 375 N95-12512
Measurements of pressure and thermal wakes in a transonic turbine cascade
[AD-A283464] p 232 N95-12548

AIR FORCE OFFICE OF SCIENTIFIC RESEARCH, BOLLING AFB, WASHINGTON, DC.
AFOSR Contractors Meeting in Propulsion
[AD-A282729] p 257 N95-12507

AKRON UNIV., OH.
TLIFE: A program for spur, helical and spiral bevel transmission life and reliability modeling
[NASA-CR-4622] p 300 N95-11889
Brush seal numerical simulation: Concepts and advances p 306 N95-13596

ALABAMA UNIV., HUNTSVILLE, AL.
Ground based research in microgravity materials processing
[NASA-CR-196815] p 278 N95-11759
Convective flow effects on protein crystal growth
[NASA-CR-196790] p 372 N95-11921
FDNS code to predict wall heat fluxes or wall temperatures in rocket nozzles
[NASA-CR-196925] p 292 N95-11999
Advanced computer architecture specification for automated weld systems
[NASA-CR-194006] p 343 N95-12014
Research on Orbital Plasma-Electrodynamics (ROPE)
[NASA-CR-196929] p 361 N95-12147
Optical analysis of crystal growth
[NASA-CR-196514] p 373 N95-12386
Lidar performance analysis
[NASA-CR-196510] p 362 N95-12390
Probability of detection of defects in coatings with electronic shearography
[NASA-CR-196201] p 308 N95-12391
BATSE observations of 3C273
[NASA-CR-196185] p 380 N95-12463
BATSE observations of Nova Muscae 1991
[NASA-CR-196416] p 380 N95-12464
Phase A design study of microgravity fluoride fiber puller
[NASA-CR-196513] p 279 N95-12752
A data and information system for processing, archival, and distribution of data for global change research
[NASA-CR-196770] p 320 N95-12786
Stress relaxation functions: Methods of approximation
[NASA-CR-195830] p 312 N95-12861
Magnetospheric space plasma investigations
[NASA-CR-196793] p 382 N95-12940
FNAS UAH UVSP and complimentary data analysis and modeling
[NASA-CR-194005] p 381 N95-12992
Analysis for Be-7 and Be-10 on LDEF materials and their sources
[NASA-CR-193989] p 268 N95-13084

ALABAMA UNIV., TUSCALOOSA, AL.
Design and application of electromechanical actuators for deep space missions
[NASA-CR-196791] p 299 N95-11701

ALASKA UNIV., FAIRBANKS, AK.
PowerSat: A technology demonstration of a solar power satellite
[NASA-CR-197210] p 253 N95-12661

ALENIA SPAZIO S.P.A., TURIN (ITALY).
STEP: An international collaboration in fundamental physics p 354 N95-12229

ALLIED-SIGNAL AEROSPACE CO., KANSAS CITY, MO.
Trichloroethylene emissions reductions achieved by enclosing solvent spray degreasing operations
[DE94-013741] p 318 N95-11742
Improving the efficiency of high purity water systems
[DE94-013742] p 318 N95-11784
Elimination of internal contamination on semiconductor devices (protective coatings)
[DE94-015868] p 275 N95-12945

ALLISON ENGINE CO., INDIANAPOLIS, IN.
Investigation of advanced counterrotation blade configuration concepts for high speed turboprop systems. Task 8: Cooling flow/heat transfer analysis
[NASA-CR-195359] p 244 N95-11901
Investigation of advanced counterrotation blade configuration concepts for high speed turboprop systems. Task 8: Cooling flow/heat transfer analysis user's manual
[NASA-CR-195360] p 244 N95-11951

AMERICAN ASSOCIATION FOR ARTIFICIAL INTELLIGENCE, MENLO PARK, CA.
The Second Workshop on Principles and Practice of Constraint Programming
[AD-A281731] p 229 N95-13166

AMPTEK, INC., BEDFORD, MA.
Detailed component design for a Compact Environmental Anomaly Sensor (CEASE)
[AD-A283144] p 256 N95-13138

ANALYTICAL SERVICES AND MATERIALS, INC., HAMPTON, VA.
Failure analysis of woven and braided fabric reinforced composites
[NASA-CR-194981] p 262 N95-11926

ARGONNE NATIONAL LAB., IL.
Parallel methods for the flight simulation model
[DE94-013330] p 245 N95-11752
Sloshing analysis of tanks containing multiple fluid layers
[DE94-013333] p 290 N95-11753
A hitchhiker's guide to microscopy and microanalysis using telecommunications, Email and The Internet
[DE94-013299] p 285 N95-13057
Energy dissipation by a longitudinal Raman process
[DE94-015027] p 359 N95-13173
A simplified thermohydrodynamic model for fluid film bearings
[DE94-015011] p 304 N95-13183
Magnetic response of ultrathin Fe on MgO: A polarised neutron reflectometry study
[DE94-013192] p 375 N95-13272
MHD pressure drops and thermal hydraulic analysis for the ITER breeding blanket design
[DE94-015085] p 369 N95-13280
Quenched QCD at finite density
[DE94-011522] p 375 N95-13337
A brightness comparison of thermionic electron sources in a TEM
[DE94-013300] p 360 N95-13338

An informal introduction to parallel processors
[DE94-016347] p 348 N95-13556

ARIZONA STATE UNIV., TEMPE, AZ.
The potential of genetic algorithms for conceptual design of rotor systems
[NASA-CR-196813] p 237 N95-11699
UV extinction and IR emission in diffuse H2 regions
[NASA-CR-196939] p 323 N95-12244

ARMY AEROMEDICAL RESEARCH LAB., FORT RUCKER, AL.
Biomedical imaging
[AD-A282221] p 333 N95-12405
Dynamic sine wave response measurements of CRT displays using sinusoidal counterphase modulation
[AD-A282222] p 333 N95-12406
Semiautomated methodology for measurement of field-of-view, magnification, and distortion of night vision devices as defined in MIL-A-49425(CR)
[AD-A282210] p 362 N95-12427
Aviation epidemiology data register: Cardiovascular disease screening outcomes in the North Dakota Army National Guard aviator cohort
[AD-A283064] p 334 N95-13054
Standards relevant to a NATO anthropometry survey using 3D imaging tools
[AD-A283065] p 339 N95-13055

ARMY ARMAMENT RESEARCH, DEVELOPMENT AND ENGINEERING CENTER, WATERVLIET, NY.
Yield-before-break fracture mechanics analysis of high strength steel pressure vehicles
[AD-A282518] p 270 N95-12401

ARMY COLD REGIONS RESEARCH AND ENGINEERING LAB., HANOVER, NH.
Bibliography on cold regions science and technology, volume 47, part 1
[AD-A281879] p 378 N95-13167

ARMY ENGINEER WATERWAYS EXPERIMENT STATION, VICKSBURG, MS.
Additives in bituminous materials and fuel-resistant sealers
[DOT/FAA/CT-94/78] p 273 N95-12131
Marginal aggregates in flexible pavements: Background survey and experimental plan
[DOT/FAA/CT-94/58] p 246 N95-12216

ARMY RESEARCH LAB., ADELPHI, MD.
Two-tone test method for determining frequency-domain transfer functions
[AD-A283452] p 282 N95-12513
Target recognition in ultra-wideband SAR imagery
[AD-A283462] p 282 N95-12547

ARMY RESEARCH LAB., CLEVELAND, OH.
Analysis of the effects of surface pitting and wear on the vibrations of a gear transmission system
[NASA-TM-106678] p 301 N95-12621
Computerized design and generation of low-noise helical gears with modified surface topology
[NASA-TM-106696] p 303 N95-13083

ARMY RESEARCH LAB., FORT MONMOUTH, NJ.
Frequency doubler (from 4.7 to 9.4 GHz) using a diode
[AD-A282784] p 287 N95-12525
Proceedings of the 36th Power Sources Conference
[AD-A281443] p 288 N95-13164

ARMY RESEARCH LAB., WHITE SANDS MISSLE RANGE, NM.
SuperMariah: A similarity-based method for determining wind, temperature, and humidity profile structure in the surface boundary layer
[AD-A283058] p 327 N95-12997

ATOMIC ENERGY OF CANADA LTD., CHALK RIVER (ONTARIO).
CRYOCOL: A computer program to calculate the cryogenic distillation of hydrogen isotopes
[DE94-622012] p 268 N95-13531

AUBURN UNIV., AL.
Development of nonintrusive, scatter-independent techniques for measurement of liquid density inside dense sprays
[NASA-CR-196413] p 293 N95-12387
Design of a ZVS PWM inverter for a brushless DC motor in an EMA application
[NASA-CR-195808] p 312 N95-12620

AUSTRALIAN GEOLOGICAL SURVEY ORGANISATION, CANBERRA, AUSTRALIAN CAPITAL TERRITORY (AUSTRALIA).
AGSO 1993: Yearbook of the Australian Geological Survey Organisation. Geoscientific research and database development for the year 1 July 1992 to 30 June 1993
p 324 N95-12686

AUTOMATED PRECISION, INC., GAITHERSBURG, MD.
Development of a spindle thermal error characterization and compensation sensor system for machining center accuracy enhancement
[AD-A280891] p 300 N95-11729

B

BABCOCK AND WILCOX CO., LYNCHBURG, VA.
Guideway structural design and power/propulsion/braking in relation to guideways. Volume 3: Appendix B: Maglev guideway structural design
[PB93-169910] p 304 N95-13128

BALL AEROSPACE SYSTEMS DIV., BOULDER, CO.
Feasibility study for a Cryogenic On-Orbit Liquid Depot-Storage, Acquisition and Transfer (COLD-SAT) satellite
[NASA-CR-185248] p 294 N95-13233

BALL CORP., BOULDER, CO.
Feasibility study for the Cryogenic Orbital Nitrogen Experiment (CONE)
[NASA-CR-187231] p 294 N95-13234

BATTELLE COLUMBUS LABS., RESEARCH TRIANGLE PARK, NC.
Methods of modeling radiant energy exchange in radiation fog and clouds
[AD-A283509] p 326 N95-12624

BENSON (ROBERT H.), SPRINGFIELD, VA.
Life Sciences Centrifuge Facility assessment
[NASA-CR-196848] p 332 N95-13423

BENTLEY ENGINEERING, MOFFETT FIELD, CA.
Architectural design of the science complex at Elizabeth City State University p 247 N95-11960

BOEING DEFENSE AND SPACE GROUP, PHILADELPHIA, PA.
Test methods for textile composites
[NASA-CR-4609] p 262 N95-12793

BRANDEIS UNIV., WALTHAM, MA.
Conformation of membrane proteins: Bacteriorhodopsin
[AD-A281282] p 331 N95-13373

BROOKHAVEN NATIONAL LAB., UPTON, NY.
The magnetic structure of holmium-erbium superlattices
[DE94-013728] p 371 N95-11739
Atomic structure modifications of diamond-like nanocomposite films: Observation by Raman spectroscopy, FTIR and STM
[DE94-013732] p 371 N95-11740
Review of electron beam microinstabilities and their relevance to EBIS devices
[DE94-013755] p 364 N95-11746
Fabrication of large area Si cylindrical drift detectors
[DE94-013534] p 295 N95-11780
Strange hadronic matter
[DE94-001493] p 357 N95-12012
Resonant x-ray scattering in 5f magnetism
[DE94-013753] p 358 N95-12829
Neural networks and orbit control in accelerators
[DE94-014877] p 350 N95-13124
Role of implantation-induced defects in surface-oriented diffusion of fluorine in silicon
[DE94-014905] p 374 N95-13125

BROWN UNIV., PROVIDENCE, RI.
Dynamical systems and oceanography
[AD-A282635] p 329 N95-12540
Stochastic control and nonlinear estimation
[AD-A281219] p 350 N95-13369

C

CALIFORNIA INST. OF TECH., PASADENA, CA.
Quantitative understanding of the cycles of oxidized and reduced sulfur on Venus
[NASA-CR-196924] p 382 N95-12011
On the strain and strain-rate dependence of the fraction of plastic work converted to heat: An experimental study using high speed infrared detectors and the Kolsky bar
[SM-92-33] p 354 N95-12728

CALIFORNIA POLYTECHNIC STATE UNIV., SAN LUIS OBISPO, CA.
The FC-1D: The profitable alternative Flying Circus Commercial Aviation Group
[NASA-CR-197152] p 240 N95-12628
The OFP-6M transport jet
[NASA-CR-197159] p 240 N95-12637
Central coast designs: The Eightball Express. Taking off with convention, cruising with improvements and landing with absolute success
[NASA-CR-197181] p 241 N95-12643

CALIFORNIA STATE POLYTECHNIC UNIV., POMONA, CA.
Periglacial and glacial analogs for Martian landforms
[NASA-CR-196772] p 383 N95-12952

CALIFORNIA STATE UNIV., FULLERTON, CA.
Reliability and cost analysis methods
[NASA-CR-196326] p 308 N95-12381

CALIFORNIA UNIV., BERKELEY, CA.
Fire propagation in concurrent flows
[PB94-193844] p 267 N95-12778
Backdraft phenomena
[PB94-193927] p 267 N95-12852

CALIFORNIA UNIV., BERKELEY. LAWRENCE BERKELEY LAB, CA.
Proceedings of the Eighteenth DOE Solar Photochemistry Research Conference
[DE94-014926] p 318 N95-13126
An investigation of the vortex method
[DE94-014931] p 294 N95-13156
Advances in SPARK
[DE94-014935] p 345 N95-13157
Simulating the energy performance of holographic glazings
[DE94-014969] p 296 N95-13158

CALIFORNIA UNIV., DAVIS, CA.
Triaxial and torsional shear test results for sand
[AD-A282725] p 323 N95-12506
Consequences of prolonged inhalation of ozone on Fischer-344/N rats: Collaborative studies. Part 1: Content and cross-linking of lung collagen
[PB94-182748] p 331 N95-13176

CALIFORNIA UNIV., IRVINE, CA.
Self assembly of n-alkanethiolate monolayers on silver nano-structures: Determination of the apparent thickness of the monolayer by scanning tunneling microscopy
[AD-A282322] p 274 N95-12417
Advanced cryogenic propellants
[AD-A282451] p 277 N95-12729
Electrochemical deposition of metal nano-disk structures using the scanning tunneling microscope
[AD-A282464] p 268 N95-13288

CALIFORNIA UNIV., LOS ANGELES, CA.
Aeroelastic simulation of higher harmonic control
[NASA-CR-4623] p 230 N95-11911
Space hardware designs, volume 1
[NASA-CR-197209] p 253 N95-12663
Ion engine propelled Earth-Mars cycler with nuclear thermal propelled transfer vehicle, volume 2
[NASA-CR-197208] p 361 N95-12665
Neotectonics of Asia: Thin-shell finite-element models with faults
[NASA-CR-196436] p 324 N95-12949

CALIFORNIA UNIV., RIVERSIDE, CA.
Spectral analysis, estimation, and prediction of multiple harmonizable random fields and time series
[AD-A283042] p 354 N95-12994

CALIFORNIA UNIV., SANTA BARBARA, CA.
Studies of low temperature, low flux radiation embrittlement of nuclear reactor structural materials
[DE94-013710] p 269 N95-11738
Tuning through the critical regime of the metal-insulator-transition in conducting polymers by pressure and magnetic field
[PB94-179165] p 272 N95-11847
Viscosity solutions of fully nonlinear equations
[AD-A281725] p 351 N95-11861
Studies of optical phase conjugators and applications
[AD-A282626] p 362 N95-12538

CALSPAN CORP., TULLAHOMA, TN.
Environmental process improvement feasibility study and demonstration program
[NASA-CR-196789] p 319 N95-12110

CAMBRIDGE UNIV., CAMBRIDGE (ENGLAND).
Concentration fluctuation models: A comparative study
[CUED/A-AERO/TR-24] p 292 N95-11939

CARNEGIE-MELLON INST. OF RESEARCH, PITTSBURGH, PA.
Development of an Automated Nondestructive Inspection (ANDI) system for commercial aircraft, phase 1
[AD-A283500] p 234 N95-12623

CARNEGIE-MELLON UNIV., PITTSBURGH, PA.
Essential kinematics for autonomous vehicles
[AD-A282456] p 300 N95-12394
B* probability based search
[AD-A282551] p 343 N95-12497
An empirical study of a highly available file system
[AD-A282655] p 378 N95-12502
Performance measurements of the multimedia testbed on real-time Mach
[AD-A282658] p 343 N95-12504
Minimal fixturing of frictionless assemblies: Complexity and algorithms
[AD-A282724] p 300 N95-12505
On-line data reconstruction in redundant disk arrays
[AD-A282709] p 340 N95-12516
Using secure coprocessors
[AD-A281255] p 340 N95-12524
Actuability of underactuated manipulators
[AD-A282788] p 300 N95-12526
A practical approach to drawing undirected graphs
[AD-A282641] p 343 N95-12541

Robust control of underactuated manipulators: Analysis and implementation
[AD-A282836] p 301 N95-12587
Thermal polymerization of styrene in the presence of stable radicals and inhibitors
[AD-A280926] p 275 N95-12773
Population-based incremental learning. A method for integrating genetic search based function optimization and competitive learning
[AD-A282654] p 350 N95-12835
Second Dependable Software Technology Exchange
[AD-A283367] p 344 N95-12922

CASE WESTERN RESERVE UNIV., CLEVELAND, OH.
Chiral recognition in molecular and macromolecular pairs of (S)- and (R)-1-cyano-2-methylpropyl 4'(4-(8-vinyloxyoctyloxy)benzoyl) biphenyl-4-carboxylate enantiomers
[AD-A281438] p 356 N95-11828
Polymer effect on heterochiral molecular recognition in molecular and macromolecular pairs of liquid crystals of (R)- and (S)-2-chloro-4-methylpentyl 4'-((8-(vinyloxy)octyl)oxy)biphenyl-4-caroxylate rs
[AD-A281193] p 358 N95-12522
Intelligent control systems research
[NASA-CR-195380] p 349 N95-12811

CENTRE NATIONAL D'ETUDES SPATIALES, PARIS (FRANCE).
STEP: An international collaboration in fundamental physics p 354 N95-12229

CFD RESEARCH CORP., HUNTSVILLE, AL.
SCISEAL: A CFD code for analysis of fluid dynamic forces in seals p 305 N95-13586

COASTEC, BATON ROUGE, LA.
New York bight study. Report 4: Geographic information systems and relational database management system development
[AD-A281716] p 327 N95-11787

CHINA NUCLEAR INFORMATION CENTRE, BEIJING (CHINA).
A numerical calculation method for the kinetic ballooning mode eigen-equation with three components
[DE94-625048] p 369 N95-13107
Inverse operator theory method mathematics-mechanization for the solutions of nonlinear equations and some typical applications in nonlinear physics
[DE94-624804] p 352 N95-13340
Improvements of HCN laser heterodyne interferometer for measuring plasma density
[DE94-625037] p 370 N95-13341
Response of high T(sub c) superconducting Josephson junction to nuclear radiation
[DE94-624705] p 360 N95-13536
Alignment and experiment of the HL-1 x ray bent-crystal spectrometer
[DE94-624719] p 297 N95-13537
Effect of stochastic damping resonance wave packet on energetic alpha particle transport
[DE94-625041] p 370 N95-13538
Density gradient effects in the tokamak edge turbulence with temperature gradient driving
[DE94-625042] p 370 N95-13539
The experiment and analysis of tailoring V(sub L) and I(sub P) with ZnO voltage-sensitive resistor on HT-6M
[DE94-625074] p 370 N95-13541

CINCINNATI UNIV., OH.
Design of an unmanned Martian polar exploration system
[NASA-CR-197160] p 383 N95-12529

CITADEL COLL., CHARLESTON, SC.
Photographic region elemental abundance analyses of Dr. David S. Leckrone's GTO HST stars 2
[NASA-CR-196756] p 381 N95-12788

CITY COLL. OF THE CITY UNIV. OF NEW YORK, NY.
Tetravalent chromium (Cr(4+)) as laser-active ion for tunable solid-state lasers
[NASA-CR-196481] p 298 N95-12951

CIVIL AEROMEDICAL INST., OKLAHOMA CITY, OK.
Elimination of quinine in two subjects after ingestion of tonic water: An exploratory study
[DOT/FAA/AM-94/16] p 332 N95-11702
The performance of child restraint devices in transport airplane passenger seats
[DOT/FAA/AM-94/19] p 234 N95-12146
Age 60 Rule research. Part 1: Bibliographic database
[DOT/FAA/AM-94/20-PT-1] p 336 N95-13019
Age 60 Rule. Part 2: Airline pilot age and performance. A review of the scientific literature
[DOT/FAA/AM-94/21-PT-2] p 336 N95-13020

CLARK UNIV., WORCESTER, MA.
Adherend surface effects on epoxy cure by NMR
[AD-A282165] p 274 N95-12420

CLEMSON UNIV., SC.
Intelligent processing of ferroelectric thin films
[AD-A282833] p 275 N95-12586
Nonlinear structural response using adaptive dynamic relaxation on a massively-parallel-processing system
[NASA-CR-196491] p 313 N95-13162
Improved assumed-stress hybrid shell element with drilling degrees of freedom for linear stress, buckling, and free vibration analyses
[NASA-CR-192816] p 313 N95-13163

COHERENT TECHNOLOGIES, INC., BOULDER, CO.
Airport surveillance using a solid state coherent lidar p 235 N95-13207
Wake vortex detection at Denver Stapleton Airport with a pulsed 2-micron coherent lidar p 236 N95-13211

COLORADO SCHOOL OF MINES, GOLDEN, CO.
In-situ x-ray analysis of the electrolyte-solid interface
[AD-A282203] p 373 N95-12425
Novel concepts in weld science: Role of gradients and composite structure
[DE94-015482] p 271 N95-12895

COLORADO STATE UNIV., FORT COLLINS, CO.
Dynamical studies in hurricane intensity change
[AD-A282406] p 326 N95-12392

COLORADO UNIV., BOULDER, CO.
Parameterization and scaling of Arctic ice conditions in the context of ice-atmosphere processes
[NASA-CR-196831] p 327 N95-11706
Numerical simulation of particle-wave interaction on boundary layers
[AD-A282184] p 293 N95-12422
Reactions of atmospheric cluster ions
[AD-A282598] p 324 N95-12534
Nonlinear problems in fluid dynamics and inverse scattering: Langmuir circulations in ocean surface layers
[AD-A282934] p 329 N95-12590
Satellite laser ranging and gravity field modeling accuracy
[NASA-CR-196057] p 248 N95-12837
Gravity wave forcing and influences nea. the mesopause
[AD-A282482] p 325 N95-13293
An investigation of the channel crosstalk in optical heterodyne controlled phased array radars
[AD-A281227] p 285 N95-13371

COLUMBIA UNIV., NEW YORK, NY.
Research in astrophysical processes
[NASA-CR-196773] p 382 N95-12939
Algorithms for mathematical programming
[DE94-013544] p 345 N95-13339

CONNECTICUT UNIV., STORRS, CT.
UV and fluorescence studies for vinyl polymerization
[AD-A281187] p 274 N95-12520
Characterization of the one step polyimide synthesis
[AD-A281216] p 276 N95-13367

CORNELL UNIV., ITHACA, NY.
Amine catalyzed intramolecular imidization of alkyl and aryl phthalamates, kinetics and mechanism in deuterated chloroform
[AD-A281741] p 259 N95-11844
Progress on resonance ionization detection of combustion radicals
[DE94-015339] p 267 N95-12762

CRANE (JOHN), INC., MORTON GROVE, IL.
Computer tools for face seal analyses developed at John Crane p 306 N95-13598

D

DEFENCE METALLURGICAL RESEARCH LAB., HYDERABAD (INDIA).
Symposium on Structural Intermetallics: Perspectives on Science and Technology, volume 1
[AD-A283378] p 271 N95-12925

DEFENCE RESEARCH ESTABLISHMENT OTTAWA, OTTAWA (ONTARIO).
Novel activated carbon impregnants consisting of transition metal complexes. Part 1: Background, syntheses and characterizations
[AD-A282583] p 259 N95-12551

DELAB, TRONDHEIM (NORWAY).
Norwegian contribution to the SWG on APSE programme
[PB94-202397] p 341 N95-13557
Provoking and measuring cell losses in ATM systems by importance sampling, control variables and load cycles
[PB94-202520] p 285 N95-13558
200 MHz channel sounder, open description
[PB94-202538] p 285 N95-13559
SURRENDER user's manual, second edition
[PB94-206950] p 346 N95-13571
Fiber-optic sensors and the application to conditional monitoring for mechanical structures
[PB94-207057] p 363 N95-13574
Response to noise around Vaernes and Bodoe airports
[PB94-207065] p 356 N95-13575
Active vibration control using a distributed controller
[PB94-207073] p 313 N95-13576
Linear approximations of delays in buffers receiving correlated ATM cell streams
[PB94-207099] p 286 N95-13577

DEPARTMENT OF THE NAVY, WASHINGTON, DC.
Apparatus and method for forming textured bulk high temperature superconducting materials
[AD-D016394] p 373 N95-12635
Method of phased magnitude correlation using binary sequences
[AD-D016397] p 284 N95-12646
Method for laser-assisted etching of III-V and II-VI semiconductor compounds using chlorofluorocarbon ambients
[AD-D016385] p 298 N95-12779
Method of laser processing ferroelectric materials
[AD-D016386] p 298 N95-12780
Substrate temperature control apparatus and technique for CVD reactors
[AD-D016387] p 374 N95-13150
Synthetic method for ethynylation of aromatic compounds
[AD-D016398] p 261 N95-13151
5-volt low level serial transceiver
[AD-D016399] p 288 N95-13153
Weld acoustic monitor
[AD-D016400] p 356 N95-13154
Modular hydraulic control system
[AD-D016401] p 304 N95-13155
Semiconductor photodetector device
[AD-D016314] p 288 N95-13174
Ceramic composites with ceramic fibers
[AD-D016315] p 275 N95-13175
Phosphazene-containing amine as curing agent for phthalonitrile-base polymer
[AD-D016375] p 276 N95-13179
Silicon carbide and sicaln heterojunction bipolar transistor structures
[AD-D016403] p 288 N95-13181
Duplex rolling element bearing mounting for ensuring preload control
[AD-D016402] p 304 N95-13189

DETROIT DIESEL ALLISON, INDIANAPOLIS, IN.
Compressor discharge film riding face seals p 306 N95-13599

DEUTSCHE AEROSPACE A.G., MUNICH (GERMANY).
STEP: An international collaboration in fundamental physics p 354 N95-12229

DIRECTION DES RECHERCHES, ETUDES ET TECHNIQUES, PARIS (FRANCE).
Polyatomic ion impact on solid surfaces and related phenomena
[PB94-201258] p 360 N95-13242

DISPLAYTECH, INC., BOULDER, CO.
Design and synthesis of tight pitch FLCs for analog voltage-limited electro-optic modulators
[AD-A281472] p 371 N95-11855

DUKE UNIV., DURHAM, NC.
A magnetic shield/dual purpose mission
[NASA-CR-197192] p 255 N95-13006

E

EAST TENNESSEE STATE UNIV., JOHNSON CITY, TN.
Real world software engineering
[AD-A282365] p 342 N95-11941

EDGERTON, GERMESHAUSEN AND GRIER, INC., IDAHO FALLS, ID.
Vacuum system operating experience review for fusion applications
[DE94-015267] p 368 N95-12759

EDGEWOOD ARSENAL, ABERDEEN PROVING GROUND, MD.
Comparison of submaximal cycling and treadmill exercise at similar work rates
[AD-A283430] p 334 N95-12593
Effects of sample formulation on the analysis of heavy metals by x-ray fluorescence
[AD-A282733] p 267 N95-12836
Vapor detection sensitivity as a function of optical resolution for a single Lorentzian band
[AD-A283444] p 316 N95-13142

EDGEWOOD RESEARCH DEVELOPMENT AND ENGINEERING CENTER, ABERDEEN PROVING GROUND, MD.
Phenoxythiocarbonylation and deoxygenation of aryl trifluoromethyl carbinols
[AD-A280519] p 260 N95-12613
Acute inhalation of explosively disseminated carbon fibers in rats
[AD-A280556] p 330 N95-12614

EG AND G SEALOL, CRANSTON, RI.
EG and G and NASA face seal codes comparison p 305 N95-13590

Current developments in brush seals
p 306 N95-13597

ELECTRONICS AND TELECOMMUNICATIONS RESEARCH INST., DAEJON (REPUBLIC OF KOREA).
ETRI brochure: History, mission, and activity highlights
p 389 N95-12697

ELORET CORP., PALO ALTO, CA.
Computational flow predictions for hypersonic drag devices
p 233 N95-11967
Interferograms, schlieren, and shadowgraphs constructed from real- and ideal-gas, two- and three-dimensional computed flowfields
p 295 N95-11971

EMBRY-RIDDLE AERONAUTICAL UNIV., DAYTONA BEACH, FL.
Viper cabin-fuselage structural design concept with engine installation and wing structural design
[NASA-CR-197162] p 239 N95-12305
Triton 2 (1B)
[NASA-CR-197188] p 240 N95-12636
Cabin fuselage structural design with engine installation and control system
[NASA-CR-197173] p 240 N95-12639

EMORY UNIV., ATLANTA, GA.
Magneto-optical properties of quantum structures with reduced dimensionality
[AD-A282597] p 376 N95-12553
Effect of decreased gravity on circulation in the rat
[NASA-CR-196946] p 331 N95-12627
Laser spectroscopy of GdO: Ligand field assignments of 4f7(8S)6p reversing 4f7(8)6s transitions
[AD-A282627] p 268 N95-13180

ENVIRONMENTAL PROTECTION AGENCY, ANN ARBOR, MI.
Regulatory impact analysis and regulatory support document: Control of air pollution; determination of significance for nonroad sources and emission standards for new nonroad compression-ignition engines at or above 37 kilowatts (50 horsepower)
[PB94-194594] p 321 N95-12855

ENVIRONMENTAL PROTECTION AGENCY, RESEARCH TRIANGLE PARK, NC.
Directory of OAQPS information services, May 1994
[PB94-181310] p 318 N95-11848
SO2 guideline document
[PB94-181393] p 319 N95-11893

ENVIRONMENTAL PROTECTION AGENCY, WASHINGTON, DC.
Implementation strategy for the Clean Air Act Ammendments of 1990. Update, May 1994
[PB94-180700] p 319 N95-11849
Access EPA
[PB93-170041] p 319 N95-12356

ESDU INTERNATIONAL LTD., LONDON (ENGLAND).
Pipeline vibrations. Computer program for the prediction of fluid transients in flexible, unbranched three-dimensional piping systems
[ESDU-93031] p 309 N95-11768
Stiffnesses of laminated flat plates
[ESDU-94003] p 309 N95-11769
Stress analysis of laminated flat plates
[ESDU-94004] p 309 N95-11770
Buckling of flat rectangular orthotropic plates
[ESDU-94005] p 310 N95-11771
Elastic buckling of unbalanced laminated fibre reinforced composite plates (rectangular plates of AsBtDs type, all edges simply-supported under biaxial loading)
[ESDU-94006] p 310 N95-11772
Elastic buckling of cylindrically curved laminated fibre reinforced composite panels with all edges simply-supported under biaxial loading
[ESDU-94007] p 310 N95-11773
Symmetric steady manoeuvre loads on rigid aircraft of classical configuration at subsonic speeds
[ESDU-94009] p 238 N95-11774
Thermophysical properties of MtBE (methyl tertbutyl ether)
[ESDU-94010] p 265 N95-11775
Application of multivariate optimisation techniques to determination of optimum flight path trajectories
[ESDU-94012] p 238 N95-11793
Examples of flight path optimisation using a multivariate gradient-search method. Addendum A: Variation of optimum flight profile parameters with range
[ESDU-94016-ADD-A] p 238 N95-11794
Thermal conductivity of gaseous oxygenated aliphatic hydrocarbons. Alcohols, aldehydes, ketones and ethers
[ESDU-94018] p 265 N95-11795
Vapour pressures and critical points of liquids. Polycyclic phenyl and cyclohexyl compounds
[ESDU-94001] p 266 N95-12128
Orthobaric densities and molar volumes of liquids. Polycyclic phenyl and cyclohexyl compounds
[ESDU-94002] p 266 N95-12129

EUROPEAN OFFICE OF AEROSPACE RESEARCH AND DEVELOPMENT, FPO NEW YORK, NY.
Effects of Noise on Hearing 5th International Symposium
[AD-A281439] p 335 N95-13177

F

FAIRFAX MATERIALS RESEARCH, INC., ALEXANDRIA, VA.
Computer modelling of cyclic deformation of high-temperature materials
[AD-A282457] p 263 N95-12833

FEDERAL AVIATION ADMINISTRATION, ATLANTIC CITY, NJ.
Terminal Doppler Weather Radar Build 5A Operational Test and Evaluation (OT/E) integration and OT/E operational test plan
[AD-A283052] p 327 N95-12996

FEDERAL AVIATION ADMINISTRATION, OKLAHOMA CITY, OK.
Simultaneous gas-chromatographic determination of four toxic gases generally present in combustion atmospheres
[DOT/FAA/AM-94/18] p 338 N95-12354

FEDERAL AVIATION ADMINISTRATION, WASHINGTON, DC.
Airborne Windshear Detection and Warning Systems. Fifth and Final Combined Manufacturers' and Technologists' Conference, part 2
[NASA-CP-10139-PT-2] p 234 N95-13203

FERMI NATIONAL ACCELERATOR LAB., BATAVIA, IL.
Search for supersymmetry at CDF
[DE94-014264] p 357 N95-12369
Measurement of the polarization in the decay B(exp 0) yields J/psi K(exp *0) in (bar p)p collisions at the square root of s = 1.8 TeV
[DE94-014265] p 357 N95-12370
Scintillating fiber detector performance, detector geometries, trigger, and electronics issues for scintillating fiber tracking
[DE94-015525] p 358 N95-12905
Inclusive jet and two-jet differential cross sections at CDF
[DE94-015543] p 358 N95-12943
Photon production at CDF and D0
[DE94-014985] p 359 N95-13160
A search for a heavy neutral gauge boson decaying into dielectrons in (-p)p collisions at the squere root of s = 1.8 TeV
[DE94-014987] p 359 N95-13161
Multi-jet analysis for the top search at the Fermilab Collider
[DE94-014988] p 359 N95-13169
A precision measurement of the prompt photon cross section in p(-p) collisions at the square root of s = 1.8 TeV
[DE94-014989] p 359 N95-13170
Gaseous detectors of ultraviolet and visible photons
[DE94-014990] p 296 N95-13171
Analyzing terabytes of data at Fermilab
[DE94-013149] p 347 N95-13269
Development of radiation hard scintillators
[DE94-013204] p 296 N95-13287

FINNISH CENTRE FOR RADIATION AND NUCLEAR SAFETY, HELSINKI (FINLAND).
Validity of fracture toughness determined with small bend specimens
[DE94-624157] p 313 N95-12947

FLORIDA UNIV., GAINESVILLE, FL.
Proceedings of US-Latin American Workshop on Molecular and Materials Sciences: Theoretical and Computational Aspects
[AD-A283359] p 358 N95-12882
US-Latin American Workshop on Molecular and Materials Sciences: Theoretical and Computational Aspects
[AD-A283428] p 359 N95-13141

FOOD AND AGROSYSTEMS, INC., SUNNYVALE, CA.
Methodologies for processing plant material into acceptable food on a small scale
[NASA-CR-177647] p 338 N95-12132

G

GENERAL ACCOUNTING OFFICE, WASHINGTON, DC.
Space Shuttle: NASA's plans for repairing or replacing a damaged or destroyed orbiter. Report to the Chairman, Subcommittee on Investigations and Oversight, Committee on Science, Space, and Technology, House of Representatives
[GAO/NSIAD-94-197] p 249 N95-12851

GENERAL ATOMIC CO., SAN DIEGO, CA.
Fusion programs in applied plasma physics
[DE94-015853] p 369 N95-12944

GENERAL DYNAMICS CORP., SAN DIEGO, CA.
Cryogenic On-Orbit Liquid Depot Storage, Acquisition, and Transfer Satellite (COLD-SAT)
[NASA-CR-185249] p 259 N95-13237

GENERAL ELECTRIC CO., CINCINNATI, OH.
Engine structures analysis software: Component Specific Modeling (COSMO)
[NASA-CR-195378] p 309 N95-11711

GENERAL ELECTRIC CO., LYNN, MA.
Brush seals for turbine engine fuel conservation
p 306 N95-13595

GENERAL ELECTRIC CO., SCHENECTADY, NY.
Evaluation of the improvement in the figure of merit of Bi2Te3 - based alloys with addition of ultrafine scattering centers
[DE94-015363] p 374 N95-13059

GENERAL MOTORS CORP., LAGRANGE, IL.
High-speed seal and bearing test facility
p 247 N95-13601

GEODETIC INST., HELSINKI (FINLAND).
The program for the 1993 adjustment of the Finnish first-order terrestrial triangulation
[REPT-94:3] p 314 N95-11880
Final results of the Baltic Sea Level 1990 GPS Campaign. Research works of the SSG 5.147 of the International Association of Geodesy
[REPT-94:2] p 314 N95-11881
Observation results: Angle measurements in 1964-1965, 1971, 1984 and 1986-1987
[REPT-118] p 314 N95-11950

GEOLOGICAL SURVEY, DENVER, CO.
Preliminary seismicity and focal mechanisms for the Southern Great Basin of Nevada and California, January 1992 - September 1992
[DE94-013589] p 321 N95-11730

GEOPHYSICAL SURVEY SYSTEMS, INC., NORTH SALEM, NH.
Development of ground-penetrating radar equipment for detecting pavement condition for preventive maintenance
[PB94-189537] p 280 N95-11904

GEORGIA INST. OF TECH., ATLANTA, GA.
An acoustic charge transport imager for high definition television applications
[NASA-CR-196806] p 280 N95-11760
Mars Equipment Transport System
[NASA-CR-197158] p 301 N95-12554
External Device to Incrementally Skid the Habitat (E-DISH)
[NASA-CR-197147] p 301 N95-12625
Integrated design and manufacturing for the high speed civil transport
[NASA-CR-197183] p 241 N95-12700
Parallelization and visual analysis of multidimensional fields: Application to ozone production, destruction, and transport in three dimensions
[NASA-CR-195971] p 320 N95-12798
Search for extraterrestrial intelligence/High Resolution Microwave Survey team member
[NASA-CR-196478] p 339 N95-13026
Lunar vertical-shaft mining system
[NASA-CR-197154] p 384 N95-13497
Glass microsphere lubrication
[NASA-CR-197157] p 277 N95-13508

GEORGIA TECH RESEARCH INST., ATLANTA, GA.
Evaluation of candidate millimeter wave sensors for synthetic vision p 236 N95-13214

GEORGIA UNIV., ATHENS.
Electrochemical epitaxy
[AD-A282403] p 373 N95-11993
A deep x-ray survey of the Pleiades cluster and the B6-A3 main sequence stars in Orion
[NASA-CR-196190] p 380 N95-12373
An x-ray search for PMS stars in translucent molecular clouds
[NASA-CR-196151] p 380 N95-12388

GRUMMAN AEROSPACE CORP., BETHPAGE, NY.
Selection process for trade study: Graphite Composite Primary Structure (GCPS)
[NASA-CR-196866] p 261 N95-11803
Trade study plan for Graphite Composite Primary Structure (GCPS)
[NASA-CR-196868] p 261 N95-11834

GUNMA UNIV., KIRYU (JAPAN).
Monochromatic x ray imaging in plasma focus experiment p 366 N95-12443
Hot spots observation in a dense plasma focus
p 367 N95-12444
Observation of a soft x ray emitting core in a dense plasma focus p 367 N95-12445

H

HAMPTON UNIV., VA.
Performance analysis of three dimensional integral equation computations on a massively parallel computer
[NASA-CR-196747] p 346 N95-11863
Spaceborne Photonics Institute
[NASA-CR-196784] p 362 N95-12659

HARVARD UNIV., CAMBRIDGE, MA.
Optical and magnetic resonance investigations of 3D ions in single crystal hosts: Candidates for tunable solid-state lasers
[AD-A281726] p 371 N95-11842
Development of techniques for the in situ observation of OH and HO2 for studies of the impact of high-altitude supersonic aircraft on the stratosphere
[NASA-CR-196759] p 321 N95-12832

HELSINKI UNIV. OF TECHNOLOGY, ESPOO (FINLAND).
TKKMOD: A computer simulation program for an integrated wind diesel system. Version 1.0: Document and user guide
[PB94-179090] p 317 N95-11798
Data acquisition system of the NANOSAW-2 stand alone wind diesel plant. Document and user's guide
[PB94-179108] p 317 N95-11799
AIRSAR software: Computer programs for preprocessing of JPL compressed polarimetric SAR data
[PB94-179116] p 280 N95-11800
Design of systolic algorithms and architectures for digital signal processing
[PB94-179256] p 346 N95-11838
Constructing combinatorial designs by local search
[PB94-179272] p 351 N95-11839
Validation results of wind diesel simulation model TKKMOD
[PB94-179157] p 317 N95-11846
Tuning through the critical regime of the metal-insulator-transition in conducting polymers by pressure and magnetic field
[PB94-179165] p 272 N95-11847
Efficient detection of deadlocks in Petri nets
[PB94-179405] p 343 N95-12366
Scheduling in an input and output queuing three-stage packet switch by using neural networks
[PB94-179413] p 349 N95-12367
Buffer size and switching capacity study in packet switches of broadband ISDN
[PB94-179421] p 281 N95-12368
Plane-wave reflection from uniaxial chiral interface and its application to polarization transformation
[PB94-184496] p 283 N95-12580
Singularity of the Green dyadics for bi-isotropic
[PB94-184504] p 283 N95-12581
Using landmarks for the vehicle location measurement
[PB94-184512] p 237 N95-12582
Chemical Engineering Seminar 1993
[PB94-184538] p 266 N95-12584
Microemulsions as reaction media: Literature review
[PB94-184553] p 267 N95-12585
Proceedings of Bianisotropics 1993: Seminar on Electrodynamics of Chiral and Bianisotropic Media
[PB94-179314] p 283 N95-12595
Development of UV irradiance standards
[PB94-181005] p 320 N95-12771
Gaussian paired comparison models
[PB94-179025] p 352 N95-12820

HELSINKI UNIV. OF TECHNOLOGY, OTANIEMI (FINLAND).
Activities of the Helsinski University of Technology, Applied Electronics Laboratory
[PB94-179074] p 385 N95-11797

HERCULES, INC., WILMINGTON, DE.
Test plan. Task 5, subtask 5.2: Early on-orbit TPSdebris impact tests
[NASA-CR-196873] p 251 N95-11802
Selection process for trade study: Reusable Hydrogen Composite Tank System (RHCTS)
[NASA-CR-196874] p 251 N95-11809
Trade study plan for Reusable Hydrogen Composite Tank System (RHCTS)
[NASA-CR-196871] p 252 N95-11945

HERCULES AEROSPACE CO., WILMINGTON, DE.
Requirements report for SSTO vertical take-off/horizontal landing vehicle
[NASA-CR-196875] p 251 N95-11777

HIGH TECHNOLOGY CORP., HAMPTON, VA.
Effect of nonzero surface admittance on receptivity and stability of compressible boundary layer
[NASA-CR-4621] p 292 N95-12105

HILTON SYSTEMS, INC., CHERRY HILL, NJ.
Age 60 Rule research. Part 1: Bibliographic database
[DOT/FAA/AM-94/20-PT-1] p 336 N95-13019
Age 60 study. Part 4: Experimental evaluation of pilot performance
[REPT-8025-4B] p 336 N95-13199

HIMEJI INST. OF TECH. (JAPAN).
A study on successive generation of intense pulsed ion beams by the inverse pinch ion diode
p 365 N95-12434
Plasma effects on electron beam dynamics in a virtual cathode oscillator p 366 N95-12436

HOWARD UNIV., WASHINGTON, DC.
Systems engineering technology for networks
[NASA-CR-196853] p 280 N95-11804

HUGHES STX, INC., LEXINGTON, MA.
Stochastic indexing
[AD-A283143] p 327 N95-13137

I

IBIS ASSOCIATES, INC., WELLESLEY, MA.
Analysis of cost: Combustion flame CVD diamond deposition
[AD-A282527] p 273 N95-12403

IDAHO UNIV., MOSCOW, ID.
A lunar/Martian anchor emplacement system
[NASA-CR-197193] p 302 N95-12690

ILLINOIS UNIV., CHAMPAIGN, IL.
The terrestrial gravitational wave environment from known sources
[NASA-CR-196167] p 323 N95-12468

ILLINOIS UNIV., URBANA, IL.
A catalogue of potentially bright close binary gravitational wave sources
[NASA-CR-196934] p 379 N95-12234
A framework for exploiting data and functional parallelism on distributed memory multicomputers
[AD-A281194] p 347 N95-12523
The x-ray structure of the supernova remnant W49B
[NASA-CR-196482] p 382 N95-12950

INHALATION TOXICOLOGY RESEARCH INST., ALBUQUERQUE, NM.
Consequences of prolonged inhalation of ozone on Fischer-344/N rats: Collaborative studies. Part 1: Content and cross-linking of lung collagen
[PB94-182748] p 331 N95-13176

INSTITUT DES HAUTES ETUDES SCIENTIFIQUES, BURES-SUR-YVETTE (FRANCE).
Extension of a theorem of Gehring and Pommerenke
[PB94-180858] p 352 N95-12577
Extensions and contractions of the Lie algebra of q-pseudodifferential symbols
[PB94-192374] p 352 N95-12603
Aspects of long time behaviour of solutions of nonlinear Hamiltonian evolution equations
[PB94-192382] p 352 N95-12808

INSTITUT FRANCO-ALLEMAND DE RECHERCHES, SAINT-LOUIS (FRANCE).
Shock tube investigations of combustion phenomena in supersonic flows
[PB94-175262] p 265 N95-11796
Supersonic base flow investigation over axisymmetric afterbodies
[PB94-180957] p 232 N95-12578

INSTITUTE FOR COMPUTER APPLICATIONS IN SCIENCE AND ENGINEERING, HAMPTON, VA.
On the interaction of jet noise with a nearby flexible structure
[NASA-CR-194934] p 290 N95-11812
Microwave heating and joining of ceramic cylinders: A mathematical model
[NASA-CR-194962] p 351 N95-11922
Scale disparity and spectral transfer in anisotropic numerical turbulence
[NASA-CR-194956] p 291 N95-11929
Modeling jets in cross flow
[NASA-CR-194965] p 291 N95-11930
Research in progress in applied mathematics, numerical analysis, fluid mechanics, and computer science
[NASA-CR-194942] p 340 N95-11932
On bottleneck partitioning k-ary n-cubes
[NASA-CR-194966] p 342 N95-12005
Design consideration for parallel graphics libraries
[NASA-CR-194935] p 340 N95-12828
Adaptive relaxation for the steady-state analysis of Markov chains
[NASA-CR-194944] p 345 N95-13420

INSTITUTE FOR DEFENSE ANALYSES, ALEXANDRIA, VA.
An examination of selected software testing tools: 1993 supplement
[AD-A283060] p 344 N95-13051

INSTITUTE OF ELECTRICAL AND ELECTRONICS ENGINEERS, NEW YORK, NY.
Proceedings: The Eleventh IEEE Workshop on Real-Time Operating Systems and Software
[AD-A281738] p 342 N95-11843

INSTITUTE OF PLASMA PHYSICS, PRAGUE (CZECHOSLOVAKIA).
Velocity spread of REB generated by high current diode
[IPPCZ-339] p 364 N95-11886
The reflection of relativistic electron beam by virtual cathode
[IPPCZ-338] p 364 N95-11916

INSTITUTO DE PESQUISAS ESPACIAIS, SAO JOSE DOS CAMPOS (BRAZIL).
Proposal of a methodology to evaluate urban quality of life using conventional and remote sensing data, geographic information system, and a database
[INPE-5552-TDI/536] p 315 N95-12297
An experimental environment for software engineering
[INPE-5540-TDI/528] p 343 N95-12300
Digital image processing techniques for image-mapping applications
[INPE-5546-TDI/532] p 315 N95-12301
Study of a vortical/axial type flameholders with variable angle blades
[INPE-5558-TDI/538] p 266 N95-12302
Estimation of above-ground phytomass in a tropical forest using TM-LANDSAT 5 E HRV-SPOT 1 data
[INPE-5500-TDI/515] p 316 N95-13159
CeO2-ZrO2 powder synthesis by way of alcohol dehydration of aqueous salt solutions
[INPE-5484-PRE/1783] p 276 N95-13191
CESIUM-137 and natural radionuclides in soils from Southern Brazil and in soils and others environmental samples from Antarctic
[INPE-5505-TDI-517] p 321 N95-13192
AVHRR/NOAA images to detect and quantify deforestation in Amazon Forest: Relations with TM/LANDSAT data
[INPE-5501-TDI/516] p 316 N95-13350
Use of remote sensing and geographic information system techniques in integrated studies of watersheds
[INPE-5494-TDI/511] p 316 N95-13352

INSTITUTO DE PESQUISAS ESPACIAIS, SAO PAULO (BRAZIL).
Review of pulse ignition
[INPE-5569-PUD/063] p 265 N95-11885

INTERNATIONAL CENTRE FOR RELATIVISTIC ASTROPHYSICS, ROME (ITALY).
STEP: An international collaboration in fundamental physics p 354 N95-12229

IOWA UNIV., IOWA CITY, IA.
Waves in Space Plasmas (WISP)
[NASA-CR-196432] p 369 N95-13024

J

JAPAN STEEL WORKS LTD., TAKANODAI, CHIBA (JAPAN).
Present status of ohmic ignition chemical launcher experiment p 366 N95-12438

JET PROPULSION LAB., CALIFORNIA INST. OF TECH., PASADENA, CA.
STEP: An international collaboration in fundamental physics p 354 N95-12229

JOHNS HOPKINS UNIV., BALTIMORE, MD.
Visual psychophysics of egomotion
[AD-A282547] p 335 N95-12495
A study of a multi-pinned phase CCD detector for use as a star tracker
[NASA-CR-196287] p 381 N95-13056

JOHNS HOPKINS UNIV., LAUREL, MD.
Studies of electromagnetic ion cyclotron waves using AMPTE/CCE and dynamics explorer
[NASA-CR-196437] p 361 N95-12102

JOINT INST. FOR ADVANCEMENT OF FLIGHT SCIENCES, HAMPTON, VA.
Computation of turbulent boundary layers employing the defect wall-function method
[NASA-CR-4629] p 293 N95-12859

JOINT INST. FOR LAB. ASTROPHYSICS, BOULDER, CO.
Gamma-ray burst constraints on the galactic frequency of extra-solar Oort clouds
[NASA-CR-196197] p 385 N95-12886

JOINT INST. FOR NUCLEAR RESEARCH, DUBNA (USSR).
Measurement of synchrotron radiation transmission of infrared range by YBa2Cu3O(7-delta) film in superconducting state
[DE94-623270] p 372 N95-11899

JOINT PUBLICATIONS RESEARCH SERVICE, ARLINGTON, VA.
JPRS report: Science and technology. Central Eurasia: Life sciences
[JPRS-ULS-93-014] p 318 N95-11743
JPRS report: Science and technology. Central Eurasia: Life sciences
[JPRS-ULS-93-012] p 332 N95-11744

JPRS report: Science and technology. Central Eurasia: Space
[JPRS-USP-94-006] p 247 N95-12000
JPRS report: Science and technology. Central Eurasia
[JPRS-UST-94-017] p 247 N95-12001
JPRS report: Science and technology. Central Eurasia
[JPRS-UST-94-020] p 389 N95-12002
JPRS report: Science and technology. Central Eurasia
[JPRS-UST-94-019] p 389 N95-12003

K

KANAZAWA UNIV. (JAPAN).
Strong beam-plasma turbulence p 367 N95-12450
KANSAS STATE UNIV., MANHATTAN, KS.
Scanning tunneling microscopy/atomic force microscopy for study of nanoscale metal oxide particles (destructive adsorbents)
[AD-A281417] p 357 N95-11851
Human-like robots for space and hazardous environments
[NASA-CR-197171] p 301 N95-12532
KANSAS UNIV., LAWRENCE, KS.
The design and development of signal-processing algorithms for an airborne x-band Doppler weather radar
[NASA-CR-196888] p 281 N95-12374
Gemini: A long-range cargo transport
[NASA-CR-197149] p 239 N95-12626
A preliminary design proposal for a maritime patrol strike aircraft: MPS-2000 Condor
[NASA-CR-197182] p 241 N95-12689
KANSAS UNIV. CENTER FOR RESEARCH, INC., LAWRENCE, KS.
Part A: A data acquisition/controller system. Part B: Supplement to a data acquisition/controller system
[AD-A283373] p 285 N95-12924
KIEV UNIV. (USSR).
Small angle neutron scattering in surface-active agents mixtures
[DE94-624057] p 356 N95-11747
An investigation of Mn Si by the SR-technique
[DE94-624058] p 371 N95-11748
Relativistic theory of superfluidity with two condensates
[DE94-624073] p 290 N95-11749
KUMAMOTO UNIV. (JAPAN).
Gas-puff Z-pinch driven by inductive energy storage pulsed power generator ASO-2 p 366 N95-12439
Behaviors of plasma armature in the augmented railgun using a permanent magnet p 367 N95-12449
KYOTO UNIV., KUMATORI (JAPAN).
Summary reports of activities under visiting research program, 1993
[DE94-753222] p 360 N95-11750
Radiation-induced structural changes, 4
[DE94-753223] p 356 N95-11817
Radiation-induced structural changes, 3
[DE94-753401] p 371 N95-11819
KYOTO UNIV., UJI (JAPAN).
Contribution of hadronic intermediate states in nonleptonic weak decays of K, charm and B mesons
[DE94-753399] p 356 N95-11818

L

LAWRENCE LIVERMORE NATIONAL LAB., LIVERMORE, CA.
High performance climate system modeling using a domain and task decomposition message-passing approach
[DE94-013739] p 322 N95-11741
High average power parametric frequency conversion-new concepts and new pump sources
[DE94-013652] p 314 N95-11783
A 250 GHz microwave interferometer for divertor experiments on D3-D
[DE94-014056] p 364 N95-11786
MSW to hydrogen
[DE94-014741] p 265 N95-11790
Structure and performance of carbon aerogel electrodes
[DE94-014746] p 356 N95-11791
Experimental and theoretical study of neon-like selenium x-ray laser spectral line profiles
[DE94-015327] p 298 N95-12761
The future of diode pumped solid state lasers and their applicability to the automotive industry
[DE94-014736] p 298 N95-12868
Study of magnetic recording media on glass substrates
[DE94-014740] p 296 N95-12869
Interpolation of scattered temperature data measurements onto a worldwide regular grid using radial basis functions with applications to global warming
[DE94-014745] p 321 N95-12926
The impact of elevation data representation on nocturnal drainage wind simulations
[DE94-014752] p 326 N95-12927
Thermodynamic constants for actinide oxides and oxyhydroxides relevant to actinide volatility calculations for thermal oxidation processes
[DE94-007762] p 376 N95-13074
Absorption of intense microwaves and ion acoustic turbulence due to heat transport
[DE94-015140] p 369 N95-13285
An adaptive optics package designed for astronomical use with a laser guide star tuned to an absorption line of atomic sodium
[DE94-012391] p 363 N95-13532
Numerical simulations of creep in ductile-phase toughened intermetallic matrix composites
[DE94-014744] p 264 N95-13533
Laser physics of Nd(exp 3+)-doped phosphate glasses
[DE94-015141] p 299 N95-13534
Time-resolved electron thermal conduction by probing of plasma formation in transparent solids with high power subpicosecond laser pulses
[DE94-015170] p 370 N95-13555
LEHIGH UNIV., BETHLEHEM, PA.
Activities of Lehigh University
[AD-A282098] p 375 N95-13168
LIGHTWAVE ATMOSPHERICS, INC., MARBLEHEAD, MA.
Remote sensing of turbulence in the clear atmosphere with 2-micron lidars p 236 N95-13213
LOCKHEED ENGINEERING AND SCIENCES CO., HAMPTON, VA.
Determining the accuracy of maximum likelihood parameter estimates with colored residuals
[NASA-CR-194893] p 244 N95-11869
An implementation of a chemical and thermal nonequilibrium flow solver on unstructured meshes and application to blunt bodies
[NASA-CR-194967] p 293 N95-12619
LOCKHEED ENGINEERING AND SCIENCES CO., HOUSTON, TX.
An avionics scenario and command model description for Space Generic Open Avionics Architecture (SGOAA)
[NASA-CR-188330] p 242 N95-11913
An axisymmetric analog two-layer convective heating procedure with application to the evaluation of Space Shuttle Orbiter wing leading edge and windward surface heating
[NASA-CR-188343] p 251 N95-11937
LOCKHEED MISSILES AND SPACE CO., PALO ALTO, CA.
Investigation of physical parameters in stellar flares observed by GINGA
[NASA-CR-196823] p 381 N95-11928
STEP: An international collaboration in fundamental physics p 354 N95-12229
LOCKHEED MISSILES AND SPACE CO., SUNNYVALE, CA.
Development of the CSI phase-3 evolutionary model testbed
[NASA-CR-4630] p 256 N95-13195
LOS ALAMOS NATIONAL LAB., NM.
Micromorphology, mineralogy, and genesis of soils and fracture fills and the Pajarito Plateau, New Mexico
[DE94-013612] p 322 N95-11732
Autonomous power system for remote locations
[DE94-013244] p 361 N95-11779
Nuclear rockets: High-performance propulsion for Mars
[DE94-013642] p 257 N95-11782
The cascade-deuteron system
[DE94-011650] p 357 N95-11894
Plasma and ion beam processing at Los Alamos
[DE94-014293] p 365 N95-12371
An observational test of magnetospheric magnetic field mapping
[DE94-014461] p 324 N95-12649
Effect of operating parameters and anode gas impurities upon polymer electrolyte fuel cells
[DE94-014464] p 317 N95-12650
Hypersonic Gas-Surface Energy Accommodation Test Facility
[DE94-014468] p 232 N95-12652
Generation of ultra-high magnetic fields for AGEX
[DE94-015171] p 368 N95-12757
Mechanical behavior of (238)UO2, (238)PuO2, and (239)PuO2 as a function of strain rate and temperature
[DE94-015718] p 312 N95-12784
Mean importance measures for groups of events in fault trees
[DE94-015416] p 353 N95-13061
Polycrystal models to fit experiments
[DE94-014419] p 374 N95-13078
Loads for pulsed power cylindrical implosion experiments
[DE94-014429] p 299 N95-13080
Be-9 and B-11 NMR study of superconductivity in boron doped UBe13
[DE94-014432] p 374 N95-13081
Mass conservation in grain growth
[DE94-014456] p 374 N95-13086
Particle-production mechanism in relativistic heavy-ion collisions
[DE94-014427] p 359 N95-13104
Visible/infrared radiometric calibration station
[DE94-014459] p 363 N95-13106
Shifting our focus: Communicating science to a new, nontechnical culture
[DE94-014258] p 378 N95-13123
Tests of a new cloud treatment in an atmospheric general circulation model
[DE94-013138] p 327 N95-13268
LOUISVILLE UNIV., KY.
Spaceflight and immune responses of Rhesus monkeys
[NASA-CR-196846] p 331 N95-12941
LOVELACE BIOMEDICAL AND ENVIRONMENTAL RESEARCH INST., ALBUQUERQUE, NM.
Consequences of prolonged inhalation of ozone on Fischer-344/N rats: Collaborative studies. Part 1: Content and cross-linking of lung collagen
[PB94-182748] p 331 N95-13176

M

MARCI (J. M.) SPECTROSCOPIC SOCIETY, PRAGUE, STREDOCESKY (CZECHOSLOVAKIA).
Abstracts from the International Conference on Nuclear Analytical Methods in the Life Sciences
[DE94-621923] p 329 N95-11728
MARTIN MARIETTA CORP., DENVER, CO.
Space Station Module Power Management and Distribution System (SSM/PMAD)
[NASA-CR-193991] p 258 N95-12819
Experimental evaluation of shape memory alloy actuation technique in adaptive antenna design concepts
[NASA-CR-194983] p 284 N95-12896
MARTIN MARIETTA CORP., MOORESTOWN, NJ.
Doppler radar detection of vortex hazard indicators p 236 N95-13212
MARTIN MARIETTA LABS., BALTIMORE, MD.
Thin-film model studies of interfacial reactions in intermetallic matrix composites
[AD-A283360] p 263 N95-12883
MARTIN MARIETTA SPACE SYSTEMS, INC., DENVER, CO.
Cryogenic On-Orbit Liquid Depot Storage, Acquisition, and Transfer satellite (COLD-SAT) feasibility study
[NASA-CR-185247] p 256 N95-13232
MARYLAND UNIV., COLLEGE PARK, MD.
Beams 92: Proceedings
[DE94-014783] p 361 N95-11792
Site model based image registration and change detection, RADIUS
[AD-A282796] p 315 N95-12527
Is the pollution effect of the FEM avoidable for the Helmholtz equation considering high wave numbers?
[AD-A282585] p 352 N95-12552
Orion: Design of a system for assured low-cost human access to space
[NASA-CR-197185] p 253 N95-12564
Wavelength-encoded processing in semiconductor lasers
[AD-A282649] p 297 N95-12751
MOOSE: Manned On-Orbit Servicing Equipment
[NASA-CR-197151] p 254 N95-12790
Techniques for designing rotorcraft control systems
[NASA-CR-196192] p 245 N95-12791
Coordinated action in 3-D space
[AD-A281284] p 336 N95-13375
MASSACHUSETTS GENERAL HOSPITAL, BOSTON, MA.
Ultrashort laser pulse effects in ocular and related media: Laser-induced shock wave propagation and retinal damage
[AD-A282599] p 334 N95-12535
MASSACHUSETTS INST. OF TECH., CAMBRIDGE.
The Research Laboratory of Electronics
[AD-A281445] p 386 N95-11830
How are three-dimensional objects represented in the brain?
[AD-A282367] p 335 N95-11942
The quadric reference surface: Theory and applications
[AD-A282379] p 351 N95-12007

Design of passive piezoelectric damping for space structures
[NASA-CR-4625] p 252 N95-12165
An analysis of the effect of Gaussian error in object recognition
[AD-A282260] p 349 N95-12411
Exploring the parallelism exposed by partial evaluation
[AD-A282284] p 347 N95-12414
Project Freebird: An orbital transfer vehicle
[NASA-CR-197201] p 254 N95-12737
Robust control design with real parameter uncertainty using absolute stability theory
[NASA-CR-196971] p 349 N95-12782

MASSACHUSETTS INST. OF TECH., LEXINGTON.
Ground-based wake vortex monitoring, prediction, and ATC interface p 235 N95-13209
Aircraft wake RCS measurement p 235 N95-13210

MASSACHUSETTS UNIV., AMHERST, MA.
Synthesis, structure and properties of segmented polymers containing mesogens
[AD-A281419] p 272 N95-11852
The Two Micron All Sky Survey: Survey rationale and initial testing
[AD-A283514] p 380 N95-12633
Near-infrared imaging of selected areas
[AD-A283519] p 316 N95-12634

MASSACHUSETTS UNIV., LOWELL, MA.
Design, synthesis and characterization of novel nonlinear optical polymers
[AD-A282201] p 274 N95-12424
Short term weather forecasting in real time in a base weather station setting
[AD-A283141] p 327 N95-13134

MATERIALS RESEARCH SOCIETY, PITTSBURG, PA.
Diagnostic techniques for semiconductor materials processing
[AD-A282810] p 373 N95-12602

MATRA MARCONI SPACE, TOULOUSE (FRANCE).
STEP: An international collaboration in fundamental physics p 354 N95-12229

MCAT INST., MOFFETT FIELD, CA.
Parallel aeroelastic computations for wing and wing-body configurations
[NASA-CR-196835] p 230 N95-11766

MCAT INST., SAN JOSE, CA.
A high-performance constant-temperature hot-wire anemometer
[NASA-CR-177645] p 295 N95-11896
Shock-tunnel combustor testing for hypersonic vehicles
[NASA-CR-196836] p 246 N95-11938
High speed civil transport aerodynamic optimization
[NASA-CR-196960] p 232 N95-12389
Design and testing of an oblique all-wing supersonic transport
[NASA-CR-196394] p 242 N95-12785

MCDONNELL-DOUGLAS AEROSPACE, SAINT LOUIS, MO.
Impact of agility requirements on configuration synthesis
[NASA-CR-4627] p 238 N95-11952

MECHANICAL TECHNOLOGY, INC., LATHAM, NY.
Code GFACE: Gas lubricated face seals in laminar regime p 305 N95-13585
User interface development p 305 N95-13587
Incompressible face seals: Computer code IFACE p 307 N95-13606

MICHIGAN TECHNOLOGICAL UNIV., HOUGHTON, MI.
Raman structural studies of the nickel electrode
[NASA-CR-196331] p 289 N95-13344

MICHIGAN UNIV., ANN ARBOR, MI.
Investigation of finite element: ABC methods for electromagnetic field simulation
[NASA-CR-196837] p 279 N95-11707
Pioneer Venus orbiter electron temperature probe
[NASA-CR-196844] p 257 N95-11805
Conceptual design of the AE481 Demon Remotely Piloted Vehicle (RPV)
[NASA-CR-197164] p 238 N95-12294
Analysis of cylindrical wrap-around and doubly conformal patch antennas by way of the finite element-artificial absorber method
[NASA-CR-195211] p 281 N95-12382
Athena: Advanced air launched space booster
[NASA-CR-197148] p 258 N95-12604
The structural basis for fatigue failure initiation in glassy polymers
[DE94-015415] p 275 N95-13060
Synchrotron studies of narrow band materials
[DE94-013698] p 271 N95-13554

MICRO CRAFT, INC., MOFFETT FIELD, CA.
Education: A second career p 377 N95-11956

MINNESOTA UNIV., MINNEAPOLIS, MN.
An interpolation theoretic approach to control
[AD-A281465] p 348 N95-11853
Development of nanostructure fabrication technology and new electron-quantum wave devices
[AD-A281724] p 286 N95-11860

MISSISSIPPI STATE UNIV., BAY SAINT LOUIS, MS.
Design of an intelligent support system for scientific databases
[AD-A283043] p 378 N95-12995

MISSISSIPPI STATE UNIV., MISSISSIPPI STATE, MS.
An investigation of the use of temporal decomposition in space mission scheduling
[NASA-CR-196420] p 377 N95-12618

MITRE CORP., BEDFORD, MA.
Exploitation of virtual reality architectures
[AD-A282263] p 340 N95-12413
GASCAN 2 payload integration
[NASA-CR-197200] p 278 N95-12701
Thunderstorm hypothesis reasoner
[AD-A282664] p 326 N95-12805

MOSCOW PHYSICAL-ENGINEERING INST. (RUSSIA).
The results of the study of compact gas-puff and vacuum spark plasma sources of SXR with Glass-Capillary Converters (GCC) p 367 N95-12446

MOUNT SINAI SCHOOL OF MEDICINE, NEW YORK, NY.
Reduction of ocular counter-rolling by adaptation to space
[NASA-CR-196279] p 333 N95-12376

N

NAGOYA INST. OF TECH. (JAPAN).
Evaluation of dynamic pressure of ablation plasma produced by intense, pulsed, ion beam p 365 N95-12433

NAGOYA UNIV., AICHI (JAPAN).
Solar-Terrestrial Environment Laboratory, Nagoya University p 389 N95-12610

NATIONAL ACADEMY OF SCIENCES - NATIONAL RESEARCH COUNCIL, WASHINGTON, DC.
Aeronautics and space technology, past, present, and future p 229 N95-11892
Meeting the nation's needs for biomedical and behavioral scientists
[LC-94-66477] p 330 N95-12310
Free electron lasers and other advanced sources of light: Scientific research opportunities p 297 N95-12375
Solar influences on global change
[NASA-CR-196966] p 319 N95-12384
Toward infrastructure improvement: An agenda for research
[LC-94-67335] p 376 N95-12385
Space facilities: Meeting future needs for research, development, and operations
[NASA-CR-194821] p 248 N95-12474
Spacecraft maximum allowable concentrations for selected airborne contaminants, volume 1
[NASA-CR-196446] p 255 N95-12879
Activities of the Space Studies Board of the National Research Council
[NASA-CR-195738] p 247 N95-12880

NATIONAL AERONAUTICAL LAB., BANGALORE (INDIA).
A study of naturally initiating notch root fatigue cracks under spectrum loading
[NAL-PD-SN-9406] p 311 N95-11924

NATIONAL AERONAUTICS AND SPACE ADMINISTRATION, WASHINGTON, DC.
Present state of knowledge of the upper atmosphere1993: An assessment report, part 2
[NASA-RP-1337] p 322 N95-12103
X-ray and gamma ray astronomy detectors
[NASA-SP-517] p 379 N95-12304
CENDI Indexing Workshop
[NASA-CP-10160] p 378 N95-12358
NASA STI Program Seminar: Electronic documents
[NASA-TM-109928] p 378 N95-12383
Aeronautical engineering: A continuing bibliography with indexes (supplement 309)
[NASA-SP-7037(309)] p 229 N95-12894
Aerospace medicine and biology: A continuing bibliography with indexes (supplement 394)
[NASA-SP-7011(394)] p 335 N95-13230

NATIONAL AERONAUTICS AND SPACE ADMINISTRATION. AMES RESEARCH CENTER, MOFFETT FIELD, CA.
Effects of oral glucose on exercise thermoregulation in men after water immersion
[NASA-TM-108825] p 329 N95-11810
Interviews with the Apollo lunar surface astronauts in support of planning for EVA systems design
[NASA-TM-108846] p 337 N95-11905
Numerical analysis of tangential slot blowing on a generic chined forebody
[NASA-TM-108845] p 231 N95-11927
Technical paper contest for women 1992. Space challenges: Earth and beyond
[NASA-TM-109953] p 386 N95-11955
The development and application of the self-adaptive grid code, SAGE p 295 N95-11957
Engineering the future with America's high school students p 377 N95-11958
Using emergent order to shape a space society p 377 N95-11959
The Biological Flight Research Facility p 247 N95-11961
Techniques for optimal crop selection in a controlled ecological life support system p 339 N95-11962
Training for life science experiments in space at the NASA Ames Research Center p 339 N95-11964
The rhesus measurement system: A new instrument for space research p 247 N95-11965
On the isolation of halophilic microorganisms from salt deposits of great geological age p 332 N95-11966
Test model designs for advanced refractory ceramic materials p 277 N95-11968
The crop growth research chamber p 248 N95-11969
Meeting the challenge of manned lunar and Martian exploration p 339 N95-11970
Vestibular afferent responses to linear accelerations in the alert squirrel monkey
[NASA-TM-4581] p 330 N95-12006
Science objectives and performance of a radiometer and window design for atmospheric entry experiments
[NASA-TM-4637] p 382 N95-12190
Flight investigation of the use of a nose gear jump strut to reduce takeoff ground roll distance of STOL aircraft
[NASA-TM-108819] p 238 N95-12225
The selective use of functional optical variables in the control of forward speed
[NASA-TM-108849] p 229 N95-12227
Measurements of atmospheric turbulence effects on tail rotor acoustics
[NASA-TM-108843] p 232 N95-12360
Crew factors in flight operations 9: Effects of planned cockpit rest on crew performance and alertness in long-haul operations
[NASA-TM-108839] p 334 N95-12792

NATIONAL AERONAUTICS AND SPACE ADMINISTRATION. GODDARD SPACE FLIGHT CENTER, ALBUQUERQUE, NM.
SeaWiFS technical report series. Volume 19: Case studies for SeaWiFS calibration and validation, part 2
[NASA-TM-104566-VOL-19-PT-2] p 328 N95-11920
SeaWiFS technical report series. Volume 22: Prelaunch acceptance report for the SeaWiFS radiometer
[NASA-TM-104556-VOL-22] p 328 N95-12151

NATIONAL AERONAUTICS AND SPACE ADMINISTRATION. GODDARD SPACE FLIGHT CENTER, GREENBELT, MD.
Greenhouse Effect Detection Experiment (GEDEX). Selected data sets
[NASA-TM-109952] p 318 N95-11845
Differential absorption lidar measurements of atmospheric water vapor using a pseudonoise code modulated AlGaAs laser
[NASA-TM-104610] p 314 N95-11997
FORTRAN programs to process Magsat data for lithospheric, external field, and residual core components
[NASA-TM-104612] p 323 N95-12130
Technical report series on global modeling and data assimilation. Volume 2: Direct solution of the implicit formulation of fourth order horizontal diffusion for gridpoint models on the sphere
[NASA-TM-10406] p 323 N95-12226
SeaWiFS technical report series. Volume 23: SeaWiFS prelaunch radiometric calibration and spectral characterization
[NASA-TM-104566-VOL-23] p 328 N95-12359
Nimbus-7 Earth Radiation Budjet compact solar data set user's guide
[NASA-RP-1346] p 384 N95-12667
Spacecraft attitude determination accuracy from mission experience
[NASA-TM-104613] p 255 N95-12858

NATIONAL AERONAUTICS AND SPACE ADMINISTRATION. HUGH L. DRYDEN FLIGHT RESEARCH CENTER, EDWARDS, CA.
Effects of mass on aircraft sidearm controller characteristics
[NASA-TM-104277] p 244 N95-11868
Dynamic ground effects flight test of an F-15 aircraft
[NASA-TM-4604] p 231 N95-12191

NATIONAL AERONAUTICS AND SPACE ADMINISTRATION. HUGH L. DRYDEN FLIGHT RESEARCH FACILITY, EDWARDS, CA.
Water tunnel flow visualization study of a 4.4 percent scale X-31 forebody
[NASA-TM-104276] p 230 N95-11898

NATIONAL AERONAUTICS AND SPACE ADMINISTRATION. JOHN F. KENNEDY SPACE CENTER, COCOA BEACH, FL.

Debris/ice/TPS assessment and integrated photographic analysis of Shuttle Mission STS-65
[NASA-TM-109205] p 249 N95-12224

NATIONAL AERONAUTICS AND SPACE ADMINISTRATION. LYNDON B. JOHNSON SPACE CENTER, HOUSTON, TX.

Carbon dioxide and water vapor production at rest and during exercise. A report on data collection for the Crew and Thermal Systems Division
[NASA-TP-3500] p 337 N95-11811

Human factors assesaments of the STS-57 SpaceHab-1 mission
[NASA-TM-104802] p 337 N95-11878

Evaluation of COSTAR mass handling characteristics in an environment. A simulation of the Hubble Space Telescope service mission
[NASA-TP-3489] p 333 N95-11887

Software analysis handbook: Software complexity analysis and software reliability estimation and prediction
[NASA-TM-104799] p 339 N95-11914

Liquid flyback booster pre-phase: A study assessment
[NASA-TM-104801] p 248 N95-11934

From undersea to outer space: The STS-40 jellyfish experiment
[NASA-TM-109958] p 250 N95-13122

White Sands Test Facility
[NASA-TM-109901] p 249 N95-13129

STS-65 mission highlights resource tape
[NASA-TM-108589] p 250 N95-13130

STS-68 post flight presentation
[NASA-TM-109959] p 250 N95-13131

STS-61 mission highlights resource tape
[NASA-TM-109963] p 250 N95-13132

Memorial service for the mission 51-L crew (edited)
[NASA-TM-109900] p 250 N95-13133

NATIONAL AERONAUTICS AND SPACE ADMINISTRATION. LANGLEY RESEARCH CENTER, HAMPTON, VA.

Linear Proof Mass Actuator
[NASA-TM-109143] p 310 N95-11814

Accurate interlaminar stress recovery from finite element analysis
[NASA-TM-109149] p 310 N95-11815

Modeling and life prediction methodology for Titanium Matrix Composites subjected to mission profiles
[NASA-TM-109148] p 269 N95-11915

Predicting radiative heat transfer in thermochemical nonequilibrium flow fields. Theory and user's manual for the LORAN code
[NASA-TM-4564] p 291 N95-11936

Modelling and simulation of Space Station Freedom berthing dynamics and control
[NASA-TM-109151] p 252 N95-11947

Computer code for determination of thermally perfect gas properties
[NASA-TP-3447] p 231 N95-11995

Application of two procedures for dual-point design of transonic airfoils
[NASA-TP-3466] p 231 N95-12176

En route noise levels from propfan test assessment airplane
[NASA-TP-3451] p 355 N95-12341

Ten-year ground exposure of composite materials used on the Bell Model 206L helicopter flight service program
[NASA-TP-3468] p 262 N95-12357

Design studies of large aperture, high-resolution Earth science microwave radiometers compatible with small launch vehicles
[NASA-TP-3469] p 315 N95-12379

Flight test of takeoff performance monitoring system
[NASA-TP-3403] p 245 N95-12664

Experimental aerodynamic characteristics of a generic hypersonic accelerator configuration at Mach numbers 1.5 and 2.0
[NASA-TM-4413] p 233 N95-12770

Hypersonic vehicle model and control law development using H(infinity) and micron synthesis
[NASA-TM-4562] p 255 N95-12838

Satellite estimates of shortwave surface radiation and atmospheric meteorology for the BOREAS experiment region
[NASA-TM-109132] p 326 N95-12839

NASA's Hypersonic Research Engine Project: A review
[NASA-TM-107759] p 244 N95-12860

Planar Rayleigh scattering and laser-induced fluorescence for visualization of a hot, Mach 2 annular air jet
[NASA-TM-4576] p 247 N95-13196

World wide web implementation of the Langley technical report server
[NASA-TM-109162] p 345 N95-13198

Airborne Windshear Detection and Warning Systems. Fifth and Final Combined Manufacturers' and Technologists' Conference, part 2
[NASA-CP-10139-PT-2] p 234 N95-13203

Windshear certification data base for forward-look detection systems p 234 N95-13204

Certification methodology applied to the NASA experimental radar system p 235 N95-13205

Simultaneous three-dimensional velocity and mixing measurements by use of laser Doppler velocimetry and fluorescence probes in a water tunnel
[NASA-TP-3454] p 246 N95-13553

NATIONAL AERONAUTICS AND SPACE ADMINISTRATION. LEWIS RESEARCH CENTER, CLEVELAND, OH.

A revolutionary lunar space transportation system architecture using extraterrestrial LOX-augmented NTR propulsion
[NASA-TM-106726] p 249 N95-11703

Object-oriented technology for compressor simulation
[NASA-TM-106723] p 243 N95-11864

The role of crack formation in chevron-notched four-point bend specimens
[NASA-TM-106631] p 310 N95-11865

Intellectual property rights at the National Aeronautics and Space Administration, Lewis Research Center
[NASA-TM-106731] p 379 N95-11866

The development of a highly reliable power management and distribution system for civil transport aircraft
[NASA-TM-106697] p 243 N95-11867

Radiative performance of rare earth garnet thin film selective emitters
[NASA-TM-106722] p 372 N95-11876

Determination of a transient heat transfer property of acrylic using thermochromic liquid crystals
[NASA-TM-106541] p 372 N95-11882

Structure of a swirl-stabilized, combusting spray
[NASA-TM-106724] p 243 N95-11890

Emittance theory for thin film selective emitter
[NASA-TM-106727] p 317 N95-11903

Modification of the two-equation turbulence model in NPARC to a Chien low Reynolds number k-epsilon formulation
[NASA-TM-106710] p 231 N95-11917

Methods of ensuring realizability for non-realizable second order closures
[NASA-TM-106681] p 291 N95-11935

A new Reynolds stress algebraic equation model
[NASA-TM-106644] p 292 N95-11953

Probabilistic simulation of the human factor in structural reliability
[NASA-TM-106498] p 311 N95-11954

Growth of Au on Ni(110): A BFS modelling of surface alloy phases
[NASA-TM-106732] p 270 N95-12104

Analytical and experimental vibration analysis of a faulty gear system
[NASA-TM-106689] p 300 N95-12377

A new algorithm for five-hole probe calibration, data reduction, and uncertainty analysis
[NASA-TM-106458] p 232 N95-12378

Boundary conditions for unsteady compressible flows
[NASA-TM-106737] p 293 N95-12380

Analysis of the effects of surface pitting and wear on the vibrations of a gear transmission system
[NASA-TM-106678] p 301 N95-12621

Room-temperature synthesis of CuInQ2 (Q = S or Se) in non-aqueous solution using an organoindium reagent
[NASA-TM-106557] p 260 N95-12662

Microfabricated hydrogen sensor technology for aerospace and commercial applications
[NASA-TM-106703] p 284 N95-12674

One-step synthesis of dithiocarbamates from metal powders
[NASA-TM-106558] p 260 N95-12692

Synthesis and decomposition of a novel carboxylate precursor to indium oxide
[NASA-TM-106555] p 260 N95-12693

An examination of anticipated g-jitter on Space Station and its effects on materials processes
[NASA-TM-103775] p 278 N95-12703

Defocus measurement using a liquid crystal point diffraction interferometer
[NASA-TM-106687] p 296 N95-12748

Recycle requirements for Nasa's 30 cm xenon ion thruster
[NASA-TM-106668] p 258 N95-12750

Piloted evaluation of an integrated methodology for propulsion and airframe control design
[NASA-TM-106741] p 245 N95-12763

High temperature solid lubricant materials for heavy duty and advanced heat engines
[NASA-TM-106570] p 260 N95-12764

Ferric chloride graphite intercalation compounds prepared from graphite fluoride
[NASA-TM-106447] p 261 N95-12783

Tensile creep and stress-rupture behavior of polymer derived SiC fibers
[NASA-TM-106692] p 263 N95-12813

Large-displacement structural durability analyses of simple bend specimen emulating rocket nozzle liners
[NASA-TM-106521] p 312 N95-12818

Analytical and experimental vibration analysis of a faulty gear system
[NASA-TM-106689] p 303 N95-12843

Validation of the RPLUS3D code for supersonic inlet applications involving three-dimensional shock wave-boundary layer interactions
[NASA-TM-106579] p 233 N95-13058

Computerized design and generation of low-noise helical gears with modified surface topology
[NASA-TM-106696] p 303 N95-13083

Micromechanics Analysis Code (MAC). User guide: Version 1.0
[NASA-TM-106706] p 264 N95-13193

Evaluation of wiring constructions for space applications
[NASA-TM-106735] p 256 N95-13194

Role of wind tunnels and computer codes in the certification and qualification of rotorcraft for flight in forecast icing
[NASA-TM-106747] p 233 N95-13197

Activities of the Structures Division, Lewis Research Center
[NASA-TM-108081] p 313 N95-13235

Space Station Freedom propulsion activities
[NASA-TM-108604] p 256 N95-13236

A low-erosion starting technique for high-performance arcjets
[NASA-TM-106627] p 259 N95-13347

Numerical simulations of drop collisions
[NASA-TM-106751] p 295 N95-13550

Seals Flow Code Development 1993
[NASA-CP-10136] p 304 N95-13583

Environmental and customer-driven seal requirements p 305 N95-13588

Development of a brush seals program leading to ceramic brush seals p 305 N95-13591

Brush seals for cryogenic applications p 305 N95-13592

High temperature seal test rig p 247 N95-13593

Hypersonic engine seal development at NASA Lewis Research Center p 307 N95-13602

Pressure measurements of a three wave journal air bearing p 307 N95-13605

Relative performance comparison between baseline labyrinth and dual-brush compressor discharge seals in a T-700 engine test p 307 N95-13607

Some metallographic results for brush bristles and brush segments of a shroud ring brush seal tested in a T-700 engine p 307 N95-13608

NATIONAL AERONAUTICS AND SPACE ADMINISTRATION. MARSHALL SPACE FLIGHT CENTER, HUNTSVILLE, AL.

A shadowgraph study of the National Launch System's 1 1/2 stage vehicle configuration and Heavy Lift Launch Vehicle configuration
[NASA-RP-1347] p 229 N95-11710

Damage tolerance of candidate thermoset composites for use on single stage to orbit vehicles
[NASA-TP-3506] p 261 N95-11816

Illustrated structural application of universal first-order reliability method
[NASA-TP-3501] p 248 N95-11870

Development of homotopy algorithms for fixed-order mixed H2/H(infinity) controller synthesis
[NASA-TP-3507] p 342 N95-11923

Inner Magnetosphere Imager (IMI) solar terrestrial probe class mission preliminary design study report
[NASA-TM-108464] p 252 N95-11948

STS propellant densification feasibility study data book
[NASA-TM-108467] p 278 N95-12857

NATIONAL AEROSPACE LAB., AMSTERDAM (NETHERLANDS).

Mach number control in the High Speed Wind Tunnel of NLR
[PB94-201670] p 246 N95-13243

NATIONAL AEROSPACE LAB., BANGALORE (INDIA).

A study of fatigue crack growth in lugs under spectrum loading
[NAL-PD-SN-9407] p 311 N95-11879

Experimental Aerodynamics Division
[NAL-SP-9404] p 229 N95-12166

NATIONAL DEFENCE RESEARCH ESTABLISHMENT, LINKOEPING (SWEDEN).

Object-oriented incremental map-generation for mobile robot navigation
[PB94-190717] p 314 N95-11820

Burst transmission in the HF band: A system analysis and proposal for improvement
[PB94-190733] p 280 N95-11821

NATIONAL DEFENCE RESEARCH ESTABLISHMENT, STOCKHOLM (SWEDEN).
Contributions to CD Space Committee, 1993. Summary and comments
[PB94-190618] p 379 N95-11871
Tank crew performance related to cognitive ability and motivation of the tank crew members
[PB94-190642] p 335 N95-11872
Visit to UDRI and USAF, Armstrong Lab., Williams AFB, Phoenix, USA, February 8-11, 1993
[PB94-190659] p 337 N95-11873
Study of adaptive high resolution frequency estimation techniques with hydroacoustical applications
[PB94-179512] p 355 N95-12597

NATIONAL INST. FOR FUSION SCIENCE, NAGOYA (JAPAN).
Physics of High Energy Density Plasmas Produced by Pulsed Power
[NIFS-PROC-18] p 365 N95-12429

NATIONAL INST. OF STANDARDS AND TECHNOLOGY, GAITHERSBURG, MD.
Optical metrology and more. Programs and services of the Radiometric Physics Division, Physics Laboratory
[PB94-191707] p 362 N95-11841
NIST calibration of ASTM E127-type ultrasonic reference blocks
[PB94-191640] p 355 N95-11906
Federal metric progress in 1993
[PB94-196029] p 279 N95-11907
Body dimensions for apparel
[PB94-187739] p 338 N95-11908
Prediction of geometric-thermal machine tool errors by artificial neural networks
[PB94-186673] p 348 N95-11909
Fire propagation in concurrent flows
[PB94-193844] p 267 N95-12778
Backdraft phenomena
[PB94-193927] p 267 N95-12852
Overview of NASREM: The NASA/NBS standard reference model for telerobot control system architecture re
[PB94-194560] p 303 N95-12854
Evaluation of alternative in-flight fire suppressants for full-scale testing in simulated aircraft engine nacelles and dry bays
[PB94-203403] p 236 N95-13247
Equipment for investigation of cryogenic compaction of nanosize silicon nitride powders
[DE94-013593] p 277 N95-13530

NATIONAL OCEANIC AND ATMOSPHERIC ADMINISTRATION, MIAMI, FL.
Hydrographic, carbon dioxide, nutrient and productivity measurements from the south Atlantic during July and August of 1991
[PB94-180668] p 328 N95-11900

NATIONAL OCEANIC AND ATMOSPHERIC ADMINISTRATION, WASHINGTON, DC.
TOVS operational sounding upgrades: 1990-1992
[NOAA-TR-NESDIS-76] p 322 N95-11836
Catalogue of heavy rainfall cases of six inches or more over the continental US during 1993
[NOAA-TR-NESDIS-80] p 327 N95-13095

NATIONAL RENEWABLE ENERGY LAB., GOLDEN, CO.
Solar radiation data manual for flat-plate and concentrating collectors
[DE93-018229] p 317 N95-12647
Effects of piston surface treatments on performance and emissions of a methanol-fueled, direct injection, stratified charge engine
[DE94-011851] p 302 N95-12648

NATIONAL SCIENCE FOUNDATION, ARLINGTON, VA.
Extensions and contractions of the Lie algebra of q-pseudodifferential symbols
[PB94-192374] p 352 N95-12603

NATIONAL TECHNICAL INFORMATION SERVICE, SPRINGFIELD, VA.
Directory of Federal laboratory and technology resources
[PB93-100097] p 389 N95-12223
Catalog of government inventions available for licensing, 1991
[PB92-100171] p 389 N95-12303
Catalog of government inventions available for licensing, 1992
[PB93-128205] p 389 N95-12342

NAVAL AIR WARFARE CENTER, WARMINSTER, PA.
POSIX delta document for the Next-Generation Computer Resources (NGCR) operating systems interface standard baseline, version 4
[AD-A282324] p 347 N95-12418
Hydrogen desulfurization of nickel: Thermodynamics and kinetics
[AD-A282561] p 266 N95-12549

NAVAL COMMAND, CONTROL AND OCEAN SURVEILLANCE CENTER, SAN DIEGO, CA.
Ultrawideband shipboard electrooptic electromagnetic environment monitoring
[AD-A282369] p 280 N95-11943

NAVAL FACILITIES ENGINEERING SERVICE CENTER, PORT HUENEME, CA.
Moisture induced pressures in concrete airfield pavements
[AD-A281974] p 245 N95-11789

NAVAL OCEANOGRAPHIC OFFICE, BAY SAINT LOUIS, MS.
A unified approach to geopotential field modeling
[AD-A283453] p 324 N95-12544
Initial analysis and modeling results from the Polar Orbiting Geomagnetic Survey (POGS) satellite
[AD-A283454] p 253 N95-12545

NAVAL POSTGRADUATE SCHOOL, MONTEREY, CA.
Anode sheath contributions in plasma thrusters
[AD-A280395] p 364 N95-11837
Magnetic field generation in shock waves
[AD-A282234] p 261 N95-12408
Flight dynamics of an unmanned aerial vehicle
[AD-A282259] p 239 N95-12410
Tropical cyclone development and intensification under moderate to strong vertical wind shear
[AD-A282185] p 326 N95-12423
Measures of change and the determination of equivalent change
[AD-A282647] p 351 N95-12501
NPS state vector analysis and relative motion plotting software for STS-51
[AD-A282909] p 249 N95-12510
A study of the deformation of helical springs under eccentric loading
[AD-A283448] p 312 N95-12511
Preliminary digital control system design for the petite amateur Navy satellite (PANSAT)
[AD-A282804] p 253 N95-12528
Investigation of spectral-based techniques for classification of wideband transient signals in additive white Gaussian noise
[AD-A282954] p 283 N95-12592
The effect of Rician fading and partial-band interference on noise-normalized fast frequency-hopped MFSK receivers
[AD-A282805] p 283 N95-12601
Efficient parabolic equation solution of radiowave propagation in an inhomogeneous atmosphere and over irregular terrain: Formulation
[AD-A282648] p 284 N95-12834
Investigation of the effects of solid rocket motor propellant composition on plume signature
[AD-A283365] p 258 N95-12885
Lessons learned from experiments conducted on radar data management systems
[AD-A282896] p 284 N95-12920
Lifetime and reentry prediction for the Petite Amateur Navy Satellite (PANSAT)
[AD-A283366] p 255 N95-12921
Enhancement of EMAG: A 2-D electrostatic and magnetostatic solver for MATLAB
[AD-A283446] p 354 N95-13143
A calibration of the Naval Postgraduate School middle ultraviolet spectrograph and an analysis of the OII 2470 A emission obtained by the middle ultraviolet spectrograph
[AD-A283449] p 354 N95-13144

NAVAL RESEARCH LAB., WASHINGTON, DC.
Uniform spectral amplitude windowing for hyperbolic frequency modulated waveforms
[AD-A282508] p 355 N95-12396
Millimeter-wave radiometric utility study
[AD-A282524] p 281 N95-12402
Information Technology Division's technical paper abstracts
[AD-A282882] p 378 N95-12916
A comparison of two sites for the purpose of satellite laser ranging
[AD-A283149] p 299 N95-13139
Origin of optical anisotropy in strained In(x)Ga(1-x)As/InP and In(y)Al(1-y)As/InP heterostructures
[AD-A283152] p 271 N95-13140

NAVAL SURFACE WARFARE CENTER, BETHESDA, MD.
Laws of infrared similitude
[AD-A282209] p 354 N95-12426

NAVAL SURFACE WARFARE CENTER, SILVER SPRING, MD.
Numerical computations with ABAQUS/Explicit, DYNA3D, and DYSMAS/L
[AD-A282249] p 293 N95-12409

NAVAL UNDERSEA WARFARE CENTER, NEW LONDON, CT.
Modeling of split-core transformers for power transmission
[AD-A282782] p 287 N95-12509

NEW ENGLAND DEACONESS HOSPITAL, BOSTON, MA.
Morphological differentiation of colon carcinoma cell lines in rotating wall vessels
[NASA-CR-196780] p 333 N95-11808

NEW MEXICO STATE UNIV., LAS CRUCES, NM.
Advanced S-Band studies using the TDRSS communications satellite
[NASA-CR-196831] p 281 N95-12010
The differential geodesy of the spherical representation
[AD-A282212] p 315 N95-12428

NEW MEXICO UNIV., ALBUQUERQUE, NM.
Light beam and pulse propagation in nonlinear dielectrics
[AD-A282548] p 282 N95-12496
Hydrolysis and condensation of tin (4) alkoxide compounds: The control of structural evolution
[AD-A282789] p 267 N95-12807
Factors influencing the rates, processes and magnitude of accumulation of carbon in desert soils
[NASA-CR-196820] p 325 N95-13025

NEW ORLEANS UNIV., LA.
Army Research Office Workshop on Dynamic Response of Composite Structures
[AD-A281471] p 262 N95-11854

NEW SOUTH WALES UNIV., KENSINGTON (AUSTRALIA).
Principles of GPS one-way data processing for high precision positioning applications: Algorithms and software issues p 237 N95-12177
Efficient and effective handling of cycle slips in global positioning system data p 237 N95-12230

NEWCASTLE-UPON-TYNE UNIV., NEWCASTLE (ENGLAND).
Parallel preconditioners for the conjugate gradient method
[PB94-201605] p 347 N95-13404
Reliability allocation for a system using Markov analysis
[PB94-205051] p 309 N95-13406
Uniformisation techniques for integral recurrence equations
[PB94-205069] p 347 N95-13407
Recovery blocks
[PB94-205077] p 345 N95-13432
Scene analysis: A brief survey
[PB94-205085] p 336 N95-13433
Delta-4: An open architecture for dependable systems
[PB94-195641] p 341 N95-13436
Visualizing parallel numerical software performance on a shared memory multiprocessor
[PB94-195658] p 352 N95-13437
Some very compositional temporal properties
[PB94-195666] p 345 N95-13438
Category theory: The mathematics for the humanities
[PB94-205044] p 353 N95-13560

NIHON UNIV., TOKYO (JAPAN).
Contraction phase of a gas-puff z-pinch p 366 N95-12440
Common understandings of phenomena in z-pinches p 367 N95-12447

NIIGATA UNIV. (JAPAN).
Measurements of 20 GHz high-power microwaves output from a large diameter plasma filled backward wave oscillator p 365 N95-12435

NISSIN ELECTRIC MFG. CO. LTD., TOKYO, TOKYO (JAPAN).
Study on surface treatment by pulsed electron beams p 366 N95-12437

NORTH CAROLINA AGRICULTURAL AND TECHNICAL STATE UNIV., GREENSBORO, NC.
Self-checking state machine realizations in CMOS
[AD-A282177] p 286 N95-12421

NORTH CAROLINA STATE UNIV., RALEIGH, NC.
Outdoor landmark recognition using hybrid fractal vision system and neural networks
[AD-A282506] p 349 N95-12395

NORTH CAROLINA UNIV., RALEIGH, NC.
Pseudomorphic semiconducting heterostructures from combinations of AlN, GaN and selected SiC polytypes: Theoretical advancement and its coordination with experimental studies of nucleation, growth, characterization and device development
[AD-A281218] p 289 N95-13368

NORTHROP CORP., LOS ANGELES, CA.
Test plan. GCPS task 7, subtask 7.1: IHM development
[NASA-CR-106876] p 250 N95-11767

Requirements report for SSTO vertical take-off/horizontal landing vehicle
[NASA-CR-196875] p 251 N95-11777
Test Plan. GCPS Task 4, subtask 4.2 thrust structure development
[NASA-CR-196869] p 251 N95-11833

NORTHUMBRIA UNIV., NEWCASTLE-UPON-TYNE (ENGLAND).
Category theory: The mathematics for the humanities
[PB94-205044] p 353 N95-13560

NORTHWESTERN UNIV., EVANSTON, IL.
Rational design, construction, and processing of high-performance nonlinear, optical materials
[AD-A281283] p 363 N95-13374
Atomic structures and compositions of internal interfaces
[DE94-013594] p 271 N95-13543

NOTRE DAME UNIV., IN.
Improved image decompression for reduced transform coding artifacts
[NASA-CR-196805] p 341 N95-11761
Vector quantization for efficient coding of upper subbands
[NASA-CR-196804] p 341 N95-11762
Achieving unequal error protection with convolutional codes
[NASA-CR-196803] p 341 N95-11763
An efficient system for reliably transmitting image and video data over low bit rate noisy channels
[NASA-CR-196802] p 341 N95-11764
The Elite: A high speed, low-cost general aviation aircraft for Aeroworld
[NASA-CR-197161] p 239 N95-12530
Icarus Rewaxed: A high speed, low-cost general aviation aircraft for Aeroworld
[NASA-CR-197155] p 239 N95-12609
The Balsa bullet: A high speed, low-cost general aviation aircraft for Aeroworld
[NASA-CR-197165] p 240 N95-12638
Quantum cellular automata
[AD-A283351] p 287 N95-12881

NYMA, INC., BROOK PARK, OH.
A model-based expert system for space power distribution diagnostics
[NASA-CR-195336] p 342 N95-11918
Stationary plasma thruster ion velocity distribution
[NASA-CR-195379] p 257 N95-11919
Status of hollow cathode heater development for the Space Station plasma contactor
[NASA-CR-195364] p 258 N95-12622
Thermomechanical fatigue damage/failure mechanisms in SCS-6/Timetal 21S (0/90)s composite
[NASA-CR-191115] p 263 N95-13082

O

OAK RIDGE NATIONAL LAB., TN.
Design and construction of the astronautics refrigerator magnet
[DE94-013599] p 353 N95-11731
Studies of positron induced luminescence from polymers
[DE94-013622] p 272 N95-11733
Impact analysis on a massively parallel computer
[DE94-013624] p 346 N95-11734
Triple sorbent thermal desorption/gas chromatography/mass spectrometry determination of vapor phase organic contaminants
[DE94-013634] p 264 N95-11735
Surface roughness characterization of various ceramic fibers using AFM and low voltage SEM
[DE94-013635] p 272 N95-11736
Vulnerability assessment of a space based weapon platform electronics system exposed to a thermonuclear weapon detonation
[DE94-013415] p 250 N95-11755
Certain aspects of the melting, casting and welding of Ni3Al alloys
[DE94-013628] p 269 N95-11897
Feedback control and stabilization experiments on the Texas Experimental Tokamak (TEXT)
[DE94-015214] p 368 N95-12758
Parallel algorithms for the spectral transform method
[DE94-015458] p 344 N95-12893
Advanced Industrial Materials Program
[DE94-015528] p 279 N95-12942
The laser and its applications on environment and biotechnology research
[DE94-013831] p 299 N95-13076
Computer-aided design-verification vector generation
[DE94-014022] p 345 N95-13077
Eye-gaze determination of user intent at the computer interface
[DE94-012337] p 363 N95-13421
L-H transition in tokamaks and stellarators
[DE94-013257] p 370 N95-13422

OFFICE OF NAVAL RESEARCH, ARLINGTON, VA.
Naval research reviews, volume 46, February 1994
[AD-A281435] p 265 N95-11827

OHIO AEROSPACE INST., BROOK PARK.
NASA/OAI Research Associates program
[NASA-CR-196824] p 376 N95-11765
Optimization of aerospace structures
[NASA-CR-196763] p 242 N95-12787

OHIO STATE UNIV., COLUMBUS.
Wideband electromagnetic scattering program. Fourier-based radar imaging techniques
[AD-A282540] p 282 N95-12493
Electromagnetic on-aircraft antenna radiation in the presence of composite plates
[NASA-CR-196126] p 284 N95-12856
Regulation of alternative CO2 fixation pathways in prokaryotic and eukaryotic photosynthetic organisms
[DE94-013180] p 331 N95-13271

OHIO UNIV., ATHENS.
Oscillating-flow regenerator test rig
[NASA-CR-196982] p 246 N95-13200

OKLAHOMA UNIV., NORMAN, OK.
A decision support system for tolerance allocation
[NASA-CR-195817] p 308 N95-11994

OLD DOMINION UNIV., NORFOLK, VA.
Annular suspension and pointing system with controlled DC electromagnets
[NASA-CR-197206] p 302 N95-12666
Methodology for sensitivity analysis, approximate analysis, and design optimization in CFD for multidisciplinary applications
[NASA-CR-196981] p 294 N95-13201

OPTICAL SOCIETY OF AMERICA, WASHINGTON, DC.
Optical Remote Sensing of the Atmosphere. Technical digest 1993. Volume 5: Postconference edition
[AD-A281446] p 314 N95-11831
Summaries of papers presented at the High Resolution Spectroscopy Topical Meeting. Technical digest series. Volume 1: Post conference edition
[AD-A281261] p 268 N95-13372

OREGON STATE UNIV., CORVALLIS, OR.
Communications plan
[NASA-CR-196435] p 314 N95-12231
Matter-wave interferometry with laser cooled atoms
[AD-A282484] p 360 N95-13178

OSAKA UNIV., OSAKA (JAPAN).
Beam divergence characteristic of two-stage ion diode p 365 N95-12431
New multi-dimensional diagnostics method for intense ion beams p 365 N95-12432

OSLO UNIV. (NORWAY).
Chaotic time series. Part 1: Estimation of invariant properties in state space
[PB94-206968] p 376 N95-13572

P

PACIFIC NORTHWEST LAB., RICHLAND, WA.
Global ice sheet modeling
[DE94-013744] p 318 N95-11745
Power system applications for PASC converter systems
[DE94-013329] p 286 N95-11751
Effect of pre-welding heat-treatments on welding a two-phase Ni3Al alloy
[DE94-014409] p 270 N95-12372
Rational enzyme redesign
[DE94-014565] p 331 N95-12677
The effect of irradiation on the stability and properties of monolithic silicon carbide and SiC(f)/SiC composites up to 25 dpa
[DE94-014568] p 263 N95-12862
Scaling fluid content-pressure relations of different fluid systems in porous media
[DE94-013349] p 294 N95-13075
The effect of passive damping on feedback control performance of flexible manipulators
[DE94-015000] p 304 N95-13182

PENNSYLVANIA STATE UNIV., UNIVERSITY PARK, PA.
The influence of finite-size sources in acousto-ultrasonics
[NASA-CR-195374] p 308 N95-11813
The synthesis and structure of polyphosphazenes
[AD-A281723] p 272 N95-11832
Hypersonic turbulent boundary-layer and free shear database
[NASA-CR-177610] p 292 N95-11992
Nanometer scale phase separation in mixed composition self-assembled monolayers
[AD-A282671] p 266 N95-12514
Atomic scale dynamics of a two-dimensional gas-solid interface
[AD-A282646] p 358 N95-12617
Project ECHO: Electronic Communications from Halo Orbit
[NASA-CR-197190] p 283 N95-12644
Search for inverse Compton x-rays from the lobes of Fornax A x-rays from radio galaxies straddling the Fanaroff-Riley transition
[NASA-CR-196433] p 385 N95-13023
Weighted Parzen windows for pattern classification
[AD-A281222] p 345 N95-13370

PHILLIPS LAB., HANSCOM AFB, MA.
Determination of the auroral oval Q index from the air weather service K index
[AD-A282764] p 324 N95-12508

PHYSITRON, INC., HUNTSVILLE, AL.
Large area soft x-ray collimator to facilitate x-ray optics testing
[NASA-CR-196923] p 362 N95-12736

PLANNING RESEARCH CORP., EDWARDS, CA.
Strain gage selection in loads equations using a genetic algorithm
[NASA-CR-4597] p 242 N95-12831

POLISH ACADEMY OF SCIENCES, WARSAW (POLAND).
A stochastic model of fatigue crack growth p 309 N95-11698
A numerical analysis of the distribution of stresses in lung parenchyma which accounts for the interactions between the tissue skeleton and flowing air p 332 N95-11806
Sound emission in materials and construction element testing p 355 N95-12013
The field emission of electrons in vacuum insulation systems p 357 N95-12101
The use of an acoustic emission method to estimate the effect of manufacturing process and service factors on the failure of concrete p 311 N95-12108
The use of neuron nets to stabilize dynamic systems p 348 N95-12109
A laboratory vacuum apparatus for magnetron sputtering of thin Z ZnO piezoelectric films, magnetron sputtering p 296 N95-12111
An estimate of the evolution of the acoustic emission spectrum of rocks on the basis of changes in its average frequency in the process of deformation p 323 N95-12112
A model of the density of solar radiation energy on an arbitrary plane identification for Warsaw p 384 N95-12243
An analysis of the load-bearing capacity of members of square cross section with a series of perpendicular notches p 312 N95-12631

PRAGUE AGRICULTURAL UNIV., PRAGUE, STREDOCESKY (CZECHOSLOVAKIA).
Abstracts from the International Conference on Nuclear Analytical Methods in the Life Sciences
[DE94-621923] p 329 N95-11728

PRATT AND WHITNEY AIRCRAFT, WEST PALM BEACH, FL.
High temperature strain gage technology for gas turbine engines
[NASA-CR-191177] p 295 N95-11996
Fatigue in single crystal nickel superalloys
[AD-A283459] p 270 N95-12546

PUERTO RICO UNIV., SAN JUAN.
Neural networks: Structure and repair. Part 1: Ground squirrel visual system. Part 2: Formation, maintenance and plasticity of synaptic connections
[AD-A282420] p 330 N95-12393

PURDUE UNIV., WEST LAFAYETTE, IN.
Design of a high capacity long range cargo aircraft
[NASA-CR-197176] p 239 N95-12363
Theory of complex defects on DNA polymer chain
[AD-A282619] p 275 N95-12536

R

RADIOPHYSICS, INC., BOULDER, CO.
Non-dipolar magnetic field models and patterns of radio emission: Uranus and Neptune compared
[NASA-CR-196412] p 385 N95-12469

RAND CORP., SANTA MONICA, CA.
Case study of risk management in the USAF B-1B bomber program
[AD-A282371] p 377 N95-11944
Tactical satellite orbital simulation and requirements study
[AD-A282314] p 282 N95-12416
The development of the F100-PW-220 and F110-GE-100 engines: A case study of risk assessment and risk management
[AD-A282467] p 244 N95-13289
MapView user's guide
[AD-A282469] p 316 N95-13290

Military applications of microelectromechanical systems
[AD-A282470] p 289 N95-13291

RENSSELAER POLYTECHNIC INST., TROY, NY.
Microbial communities in subsurface environments: Diversity, origin, and evolution
[DE94-013699] p 329 N95-11737
Workshop on Adaptive Methods for Partial Differential Equations
[AD-A281416] p 351 N95-11850

RESEARCH INST. FOR ADVANCED COMPUTER SCIENCE, MOFFETT FIELD, CA.
Analysis and design of numerical schemes for gas dynamics. 2: Artificial diffusion and discrete shock structure
[NASA-CR-196476] p 290 N95-11874
Analysis and design of numerical schemes for gas dynamics 1: Artificial diffusion, upwind biasing, limiters and their effect on accuracy and multigrid convergence
[NASA-CR-196477] p 290 N95-11875
Optimum aerodynamic design via boundary control
[NASA-CR-195882] p 230 N95-11877
Stability and error estimation for Component Adaptive Grid methods
[NASA-CR-196492] p 351 N95-11883
Control theory based airfoil design using the Euler equations
[NASA-CR-196360] p 230 N95-11884

RESEARCH MANAGEMENT CONSULTANTS, INC., WASHINGTON, DC.
Composites (CFCCs) for low cost energy and cleaner environment
[DE94-013601] p 272 N95-11781

RESEARCH TRIANGLE INST., HAMPTON, VA.
Characteristics of civil aviation atmospheric hazards
p 235 N95-13208

RHODE ISLAND UNIV., KINGSTON, RI.
Active Nodal Task Seeking for high-performance, ultra-dependable computing
[AD-A282924] p 344 N95-12588

RICE UNIV., HOUSTON, TX.
Radiative properties of strongly magnetized plasmas
[DE94-015487] p 369 N95-12897

RIJKSINSTITUUT VOOR DE VOLKSGEZONDHEID, BILTHOVEN (NETHERLANDS).
The Additional Programme on Ammonia
[PB94-193075] p 320 N95-12777

RIJKSINSTITUUT VOOR VOLKSGEZONDHEID EN MILIEUHYGIEENE, BILTHOVEN (NETHERLANDS).
Allocating CO2-emissions by using equity rules and optimization
[PB94-192861] p 320 N95-12776

ROCHESTER UNIV., NY.
Eager combining: A coherency protocol for increasing effective network and memory bandwidth in shared-memory multiprocessors
[AD-A281501] p 346 N95-11857
A preliminary evaluation of cache-miss-initiated prefetching techniques in scalable multiprocessors
[AD-A281502] p 346 N95-11858
Enhancement of luminescence in polymer nanocomposites
[AD-A282539] p 262 N95-12404
Electronic energy transfer in new polymer nanocomposite assemblies
[AD-A282233] p 274 N95-12407
Photogeneration of charge carriers in bilayer assemblies of conjugated rigid-rod polymers
[AD-A282625] p 275 N95-12537

ROCKWELL INTERNATIONAL CORP., DOWNEY, CA.
Test plan. GCPS task 7, subtask 7.1: IHM development
[NASA-CR-106876] p 250 N95-11767
Requirements report for SSTO vertical take-off/horizontal landing vehicle
[NASA-CR-196875] p 251 N95-11777
Test plan. Task 5, subtask 5.2: Early on-orbit TPSdebris impact tests
[NASA-CR-196873] p 251 N95-11802
Selection process for trade study: Graphite Composite Primary Structure (GCPS)
[NASA-CR-196866] p 261 N95-11803
Selection process for trade study: Reusable Hydrogen Composite Tank System (RHCTS)
[NASA-CR-196874] p 251 N95-11809
Integrated propulsion technology demonstrator. Program plan
[NASA-CR-196870] p 257 N95-11823
Test Plan. GCPS Task 4, subtask 4.2 thrust structure development
[NASA-CR-196869] p 251 N95-11833
Trade study plan for Graphite Composite Primary Structure (GCPS)
[NASA-CR-196868] p 261 N95-11834
Test Plans. Lightweight Durable TPS: Tasks 1,2,4,5, and 6
[NASA-CR-196867] p 262 N95-11835
Trade study plan for Reusable Hydrogen Composite Tank System (RHCTS)
[NASA-CR-196871] p 252 N95-11945

ROCKWELL INTERNATIONAL CORP., HUNTSVILLE, AL.
High frequency flow/structural interaction in dense subsonic fluids handbook
[NASA-CR-194007] p 230 N95-11807

ROCKY RESEARCH CORP., BOULDER CITY, NV.
Heat transfer additives for adsorption cooling system fluids, phase 2
[PB94-187135] p 290 N95-11840

ROME LAB., GRIFFISS AFB, NY.
Monopulse tracker operating characteristics measurement error performance for azimuth tracking
[AD-A281188] p 262 N95-12521
Digital filter designs that are free of limit cycles
[AD-A282885] p 287 N95-12918
Radiofrequency/microwave radiation biological effects and safety standards: A review
[AD-A282886] p 334 N95-12919

ROTORDYNAMICS-SEAL RESEARCH, INC., NORTH HIGHLANDS, CA.
Beta testing of MTI seal codes p 305 N95-13589

RUTHERFORD APPLETON LAB., CHILTON (ENGLAND).
STEP: An international collaboration in fundamental physics p 354 N95-12229
Hall conductance as a topological invariant
[PB94-179330] p 353 N95-12364
Muon sites and electronic structure
[PB94-179348] p 357 N95-12365
Implementing a linear equation solver in the CFD code PHOENICS
[PB94-195757] p 353 N95-13439

S

SAGA UNIV. (JAPAN).
Plasma opening switch by laser-produced plasma with different kinds of ion species p 367 N95-12451

SANDIA NATIONAL LABS., ALBUQUERQUE, NM.
Target area chamber system design for the National Ignition Facility
[DE94-013347] p 364 N95-11754
Comparison of the KAMELEON fire model to large-scale open pool fire data
[DE94-013441] p 264 N95-11756
Basic mechanisms of radiation effects in the natural space radiation environment
[DE94-013445] p 384 N95-11757
A novel lead-free solder replacement
[DE94-013782] p 269 N95-11785
Pressure studies of alkali, alkaline earth and rare earth doped C60 superconductors
[DE94-013345] p 372 N95-11862
Modeling of transformers using circuit simulators
[DE94-014656] p 287 N95-12863
Learning one-dimensional geometric patterns under one-sided random misclassification noise
[DE94-014659] p 350 N95-12864
Influence of electrode geometry on the high-field characteristics of photoconductive silicon wafers
[DE94-014660] p 287 N95-12865
Learning unions of boxes with membership and equivalence queries
[DE94-014662] p 350 N95-12866
Magnetic field induced minigap in double quantum wells
[DE94-015013] p 376 N95-13172
Ceramic manufacturing: Optimizing a multivariable system
[DE94-015016] p 276 N95-13184
Description of a high temperature quenching furnace for the study of the directional solidification of nickel-base superalloys
[DE94-013812] p 271 N95-13544

SCIENCE APPLICATIONS, INC., SAN DIEGO, CA.
Structure and dynamics of the solar corona
[NASA-CR-196978] p 384 N95-13582

SCRIPPS INSTITUTION OF OCEANOGRAPHY, LA JOLLA, CA.
Trace gas emissions to the atmosphere by biomass burning in the west African savannas
[NASA-CR-196758] p 319 N95-11931
Nonlinear hysteresis in an endochronic solid
[AD-A283142] p 325 N95-13136

SELSKAPET FOR INDUSTRIELL OG TEKNISK FORSKNING, OSLO (NORWAY).
Chaotic time series. Part 1: Estimation of invariant properties in state space
[PB94-206968] p 376 N95-13572
Approximation of scattered data using smooth grid functions
[PB94-207016] p 353 N95-13573

SELSKAPET FOR INDUSTRIELL OG TEKNISK FORSKNING, TRONDHEIM (NORWAY).
Accelerated testing of coatings for protection against atmospheric corrosion
[PB94-202579] p 276 N95-13244
Toolkits for construction and manipulation of geographical data
[PB94-202587] p 378 N95-13245
Laser based combustion laboratory at NTH/SINTEF applied thermodynamics
[PB94-202603] p 299 N95-13248

SHOCK SOCIETY, AUGUSTA, GA.
Summary of the Sixteenth Annual Conference on Shock
[AD-A282643] p 334 N95-12542

SMITH ADVANCED TECHNOLOGY, INC., HUNTSVILLE, AL.
HLLV avionics requirements study and electronic filing system database development
[NASA-CR-193993] p 243 N95-13027

SMITHSONIAN ASTROPHYSICAL OBSERVATORY, CAMBRIDGE, MA.
Analytical investigation of the dynamics of tethered constellations in Earth orbit, phase 2
[NASA-CR-196509] p 252 N95-12106

SOUTH CAROLINA UNIV., COLUMBIA, SC.
Potential molecular wires by an iterative divergent/convergent approach. Doubling of molecular length at each iteration
[AD-A281292] p 360 N95-13376

SOUTHERN RESEARCH INST., BIRMINGHAM, AL.
CGF cartridge development, volume 1
[NASA-CR-196508] p 270 N95-12830

SOUTHWEST RESEARCH INST., SAN ANTONIO, TX.
A study of aircraft post-crash fuel fire mitigation
[AD-A282208] p 234 N95-12499
Open-chamber combustion study
[PB94-184090] p 301 N95-12579
The detectability of extrasolar terrestrial and giant planets during their luminous final accretion
[NASA-CR-196147] p 381 N95-13012

SPACE TELESCOPE SCIENCE INST., BALTIMORE, MD.
Hot absorbers and the x-ray spectra of BL Lac objects
[NASA-CR-196196] p 380 N95-12465
X-ray temporal and spectral studies of blazars with the Ginga satellite
[NASA-CR-196330] p 380 N95-12466
FOC SV support and science data analysis
[NASA-CR-196764] p 381 N95-12821

SPECTRA DIODE LABS., SAN JOSE, CA.
Diode-pumped micro-laser arrays
[AD-A282494] p 299 N95-13294

SPECTROLAB, INC., SYLMAR, CA.
RINGSAT
[NASA-CR-197167] p 253 N95-12632

SPIRE CORP., BEDFORD, MA.
Silicon-based blue light emitting diode
[AD-A282382] p 286 N95-12009

SRI INTERNATIONAL CORP., MENLO PARK, CA.
Magnetospheric-ionospheric Poynting flux
[NASA-CR-196856] p 322 N95-11801
PASP PLUS Transient Pulse Monitor (TPM): Preflight characterization report
[AD-A282582] p 283 N95-12550
Guest investigator program study: Physics of equatorial plasma bubbles
[NASA-CR-196150] p 368 N95-12853
Representation, modeling and recognition of outdoor scenes
[AD-A283361] p 350 N95-12884

STANFORD UNIV., CA.
STEP: An international collaboration in fundamental physics p 354 N95-12229
Precision tethered satellite attitude control
[NASA-CR-196950] p 254 N95-12766
Protein crystal growth in low gravity
[NASA-CR-196980] p 279 N95-13202

STATE UNIV. OF NEW YORK, BUFFALO, NY.
LES, DNS and RANS for the analysis of high-speed turbulent reacting flows
[NASA-CR-196822] p 289 N95-11705
Low oxidation state gallium compounds. Synthesis and characterization of Ga(CH2CMe3)n
[AD-A283369] p 373 N95-12923

STERLING SOFTWARE, INC., MOFFETT FIELD, CA.
Development of a change management system
p 377 N95-11963

SWALES AND ASSOCIATES, BELTSVILLE, MD.
Stepper motor
[NASA-CR-189373] p 287 N95-12795

SWEDISH INST. FOR MATERIALS TESTING, BORAS (SWEDEN).
Calibration of optical wavelength at 1300 nm and 1550 nm using molecular absorption lines
[PB94-180080] p 362 N95-12598
VAMAS round robin on fractography of ceramics. Swedish results
[PB94-180155] p 275 N95-12600

T

TECHNETICS, INC., DELAND, FL.
Ceramic brush seals development
p 306 N95-13594
TECHNICAL RESEARCH CENTRE OF FINLAND, ESPOO (FINLAND).
Gaussian paired comparison models
[PB94-179025] p 352 N95-12820
TECHNICAL UNIV. OF PRAGUE (CZECHOSLOVAKIA).
Proceedings of the CTU Seminar 1994, Part C
[DE94-624078] p 390 N95-12946
TECHNISCHE UNIV., BRUNSWICK (GERMANY).
Non-contacting gas lubricated face seals for high p x v-values
p 308 N95-13609
TECHNISCHE UNIV., DELFT (NETHERLANDS).
Design issues of human operator support systems
[PB94-191376] p 337 N95-11778
Revealing hidden defects: A hybrid evaluation strategy for steel structures
[PB94-191236] p 308 N95-11822
Validating medical knowledge based systems
[PB94-191301] p 377 N95-11824
Autonomous motion on wheels
[PB94-191327] p 348 N95-11825
Environmental lichenology: Biomonitoring trace-element air pollution
[PB94-191335] p 318 N95-11826
Copper metabolism in rats fed ascorbic acid or restricted amounts of copper
[PB94-191343] p 330 N95-11902
Experiments with formal methods in software engineering
[PB94-192416] p 344 N95-12774
Effect of shear lips, loading transitions and test frequency on constant delta K and constant load amplitude fatigue tests
[PB94-192440] p 312 N95-12775
Object recognition for flexible assembly using stereo vision
[PB94-204427] p 363 N95-13248
Numerical time dependent sheet cavitation simulations using a higher order panel method
[PB94-204435] p 294 N95-13249
Studies on the flow induced by an oscillating airfoil in a uniform stream
[PB94-204450] p 233 N95-13250
Integrated sensor bus
[PB94-206810] p 288 N95-13252
CVD techniques for the synthesis or modification of porous ceramics
[PB94-206836] p 276 N95-13284
Trellis-based source and channel coding
[PB94-204443] p 285 N95-13405
Modelling of biopotential recordings and its implications for instrumentation design
[PB94-206844] p 332 N95-13408
Fractional suspension crystallization of organic compounds
[PB94-206851] p 375 N95-13409
Study of in-plane dynamics of tires
[PB94-206893] p 304 N95-13410
Kinetics and characterization of tungsten CVD processes
[PB94-206901] p 271 N95-13411
Finite element methods in resistivity logging
[PB94-206919] p 325 N95-13434
Influence of additives on structure and thermal stability of ammonium nitrate
[PB94-206943] p 278 N95-13435
TECHNOSOFT, INC., CINCINNATI, OH.
Intelligent knowledge-based engineering
[AD-A281906] p 377 N95-11788
TENNESSEE UNIV., TULLAHOMA, TN.
Environmental process improvement feasibility study and demonstration program
[NASA-CR-196789] p 319 N95-12110
TENNESSEE UNIV. SPACE INST., TULLAHOMA, TN.
A wall interference assessment and correction system
[NASA-CR-196940] p 292 N95-12226
TEXAS A&M UNIV., COLLEGE STATION, TX.
Development of ground-penetrating radar equipment for detecting pavement condition for preventive maintenance
[PB94-189537] p 280 N95-11904
Self calibrating autoTRAC
[NASA-CR-196930] p 348 N95-11998
Comparison of symbolic and numerical integration methods for an assumed-stress hybrid shell element
[NASA-CR-195945] p 313 N95-13096
Theoretical versus experimental results for the rotordynamic coefficients of eccentric, smooth, gas annular seal annular gas seals
p 307 N95-13603
Turbomachinery Laboratory Texas A and M University research progress on annular gas seals
p 307 N95-13604
TEXAS INSTRUMENTS, INC., DALLAS.
Ku-band high efficiency GaAs MMIC power amplifiers
[NASA-CR-182156] p 288 N95-13231
TEXAS TECHNOLOGICAL UNIV., LUBBOCK, TX.
Locally connected adaptive Gabor filter for real-time motion compensation
[AD-A282544] p 286 N95-12494
TEXAS UNIV., AUSTIN, TX.
Preconditioning electromyographic data for an upper extremity model using neural networks
[NASA-CR-196877] p 332 N95-11708
Application of scanning tunneling microscopy to studies of electrode surfaces
[AD-A282383] p 373 N95-12004
A robotic exploration mission to Mars and Phobos
[NASA-CR-197168] p 382 N95-12307
Converting the Minuteman missile into a small satellite launch system
[NASA-CR-197169] p 249 N95-12531
First principles investigation of the Ir-Zr-Nb ternary system
[AD-A282644] p 270 N95-12543
Proposal for the design of a zero gravity tool storage device
[NASA-CR-197150] p 302 N95-12627
Minuteman 2 launched small satellite
[NASA-CR-197203] p 254 N95-12765
Helical temperature perturbations associated with tearing modes in tokamak plasmas
[DE94-014708] p 369 N95-12867
Comprehensive and critical literature review on insitu micro-sensors for application in tribology
[AD-A281646] p 296 N95-13165
A musculoskeletal model of the elbow joint complex
[NASA-CR-195812] p 335 N95-13270
Locked modes in TEXT-U tokamak
[DE94-011595] p 370 N95-13529
TEXAS UNIV., DALLAS, TX.
Ionospheric dynamics instrument investigation for the Timed Mission
[NASA-CR-196198] p 325 N95-13190
TOKUSHIMA UNIV. (JAPAN).
Resistivity variation of fuse as an opening switch
p 365 N95-12430
TOKYO INST. OF TECH. (JAPAN).
Control of initial mass on metal vapor puff z-pinch
p 366 N95-12441
Z-pinch plasma by solid fine particle injection
p 366 N95-12442
TOKYO INST. OF TECH., YOKAHAMA (JAPAN).
High resolution diagnostics of intense ion diodes and key issues for bright light ion beam generation
p 367 N95-12448
TOLEDO UNIV., OH.
User's manual for the NASA Lewis ice accretion/heat transfer prediction code with electrothermal deicer input
[NASA-CR-4530] p 291 N95-11888
TORONTO UNIV. (ONTARIO).
Activities of the Institute for Aerospace Studies of Toronto University p 390 N95-12699
An iterative approach to multibody simulation dynamics suitable for parallel implementation
[UTIAS-TN-276] p 347 N95-13353
TRW, INC., REDONDO BEACH, CA.
Passive MMW camera for low visibility landings
p 236 N95-13215

U

UNIVERSITIES SPACE RESEARCH ASSOCIATION, COLUMBIA, MD.
M.E.366-J embodiment design project: Portable foot restraint
[NASA-CR-197163] p 338 N95-12361
Lunar Lander project: A study on future manned missions to the Moon
[NASA-CR-197177] p 383 N95-12362
The Elite: A high speed, low-cost general aviation aircraft for Aeroworld
[NASA-CR-197161] p 239 N95-12530
Human-like robots for space and hazardous environments
[NASA-CR-197171] p 301 N95-12532
Mars Equipment Transport System
[NASA-CR-197158] p 301 N95-12554
The embodiment design of the heat rejection system for the portable life support system
[NASA-CR-197178] p 338 N95-12555
Orion: Design of a system for assured low-cost human access to space
[NASA-CR-197185] p 253 N95-12564
Athena: Advanced air launched space booster
[NASA-CR-197148] p 258 N95-12604
Icarus Rewaxed: A high speed, low-cost general aviation aircraft for Aeroworld
[NASA-CR-197155] p 239 N95-12609
External Device to Incrementally Skid the Habitat (E-DISH)
[NASA-CR-197147] p 301 N95-12625
Proposal for the design of a zero gravity tool storage device
[NASA-CR-197150] p 302 N95-12627
The FC-1D: The profitable alternative Flying Circus Commercial Aviation Group
[NASA-CR-197152] p 240 N95-12628
Integral habitat transport system
[NASA-CR-197156] p 339 N95-12629
Various advanced design projects promoting engineering education
[NASA-CR-197170] p 258 N95-12630
Triton 2 (1B)
[NASA-CR-197188] p 240 N95-12636
The OFP-6M transport jet
[NASA-CR-197159] p 240 N95-12637
The Balsa bullet: A high speed, low-cost general aviation aircraft for Aeroworld
[NASA-CR-197165] p 240 N95-12638
Cabin fuselage structural design with engine installation and control system
[NASA-CR-197173] p 240 N95-12639
Introduction to magnetic bearings
[NASA-CR-197187] p 302 N95-12640
Fusion powered human transport to Mars (UWFR94)
[NASA-CR-197184] p 368 N95-12641
Central coast designs: The Eightball Express. Taking off with convention, cruising with improvements and landing with absolute success
[NASA-CR-197181] p 241 N95-12643
Project ECHO: Electronic Communications from Halo Orbit
[NASA-CR-197190] p 283 N95-12644
LCX: Proposal for a low-cost commercial transport
[NASA-CR-197186] p 241 N95-12645
PowerSat: A technology demonstration of a solar power satellite
[NASA-CR-197210] p 253 N95-12661
Space hardware designs, volume 1
[NASA-CR-197209] p 253 N95-12663
Ion engine propelled Earth-Mars cycler with nuclear thermal propelled transfer vehicle, volume 2
[NASA-CR-197208] p 361 N95-12665
Annular suspension and pointing system with controlled DC electromagnets
[NASA-CR-197206] p 302 N95-12666
Mars methane engine
[NASA-CR-197205] p 302 N95-12668
A preliminary design proposal for a maritime patrol strike aircraft: MPS-2000 Condor
[NASA-CR-197182] p 241 N95-12689
A lunar/Martian anchor emplacement system
[NASA-CR-197193] p 302 N95-12690
Design and testing of a model CELSS chamber robot
[NASA-CR-197196] p 303 N95-12694
Design and construction of a remote piloted flying wing
[NASA-CR-197195] p 241 N95-12695
Conceptual design of an Orbital Debris Defense System
[NASA-CR-197211] p 254 N95-12696
ASPOD modifications of 1993-1994
[NASA-CR-197204] p 254 N95-12698
Integrated design and manufacturing for the high speed civil transport
[NASA-CR-197183] p 241 N95-12700
GASCAN 2 payload integration
[NASA-CR-197200] p 278 N95-12701
Design of a vehicle based system to prevent ozone loss
[NASA-CR-197199] p 242 N95-12702
Project Freebird: An orbital transfer vehicle
[NASA-CR-197201] p 254 N95-12737
Minuteman 2 launched small satellite
[NASA-CR-197203] p 254 N95-12765
Project Genesis: Mars in situ propellant technology demonstrator mission
[NASA-CR-197166] p 277 N95-12822
Project Hyreus: Mars sample return mission utilizing in situ propellant production
[NASA-CR-197189] p 383 N95-12826

Cabin-fuselage-wing structural design concept with engine installation
[NASA-CR-197172] p 242 N95-12993
A magnetic shield/dual purpose mission
[NASA-CR-197192] p 255 N95-13006
Glass microsphere lubrication
[NASA-CR-197157] p 277 N95-13508
SolSTUS: Solar Source Thermal Upper Stage
[NASA-CR-197179] p 257 N95-13581

UNIVERSITIES SPACE RESEARCH ASSOCIATION, HOUSTON, TX.
Gemini: A long-range cargo transport
[NASA-CR-197149] p 239 N95-12626

UNIVERSITY COLL., CORK (IRELAND).
WOCSDICE 1994: European Workshop on Compound Semiconductor Devices and Integrated Circuits
[AD-A283062] p 288 N95-13052

UNIVERSITY CORP. FOR ATMOSPHERIC RESEARCH, BOULDER, CO.
Reports to the Nation on our changing planet. El Nino and climate prediction, no. 3, spring 1994
p 320 N95-12462

UNIVERSITY OF CENTRAL FLORIDA, ORLANDO, FL.
Laser Doppler velocimeter measurements of boundary layer velocity and turbulent intensities in Mach 2.5 flow
[NASA-CR-196861] p 289 N95-11709
Design and testing of a model CELSS chamber robot
[NASA-CR-197196] p 303 N95-12694

UNIVERSITY OF SOUTHERN MISSISSIPPI, HATTIESBURG, MS.
Novel thermooxidatively stable poly(ether-imide-benzoxazole) and poly(ester-imide-benzoxazole)
[AD-A282381] p 273 N95-12008
Synthesis and solid-state NMR characterization of 13C- and 15N-labelled n-methylphthalimide: A model compound for studying polyimides
[AD-A282510] p 273 N95-12397
Towards tailored interphase formation utilizing surface-active benzylsulfonium salts as cationic initiators
[AD-A282511] p 262 N95-12398
Synthesis and characterization of thianthrene-based polyamides
[AD-A282512] p 273 N95-12399
Multifunctional acrylic ether monomers, their polymers, and polymerizable epoxide derivatives from simple alpha-substitution of alkyl acrylates
[AD-A282513] p 273 N95-12400
Thianthrene-based poly(benzoxazole)s
[AD-A282326] p 274 N95-12419
All-hydrocarbon composite resins based on cyclopentadiene
[AD-A282495] p 276 N95-13296
Glass reinforced-diallylbisphenol/maleimide composites with modified interphases
[AD-A282496] p 264 N95-13298
A CRAMPS and 13C CP/MAS NMR examination of solid-solid transitions in n-Hexatriacontane (C36H74)
[AD-A282497] p 375 N95-13299

UTAH STATE UNIV., LOGAN, UT.
SolSTUS: Solar Source Thermal Upper Stage
[NASA-CR-197179] p 257 N95-13581

UTAH UNIV., SALT LAKE CITY, UT.
High frequency thermoacoustic refrigerator
[AD-A280925] p 279 N95-12772

V

VANDERBILT UNIV., NASHVILLE, TN.
Research activities of the Center for the Space Processing of Engineering Materials
[NASA-CR-196484] p 259 N95-11891
Development of ROBOSIM for academic/industrial use
[NASA-CR-196148] p 349 N95-12470
Various advanced design projects promoting engineering education
[NASA-CR-197170] p 258 N95-12630

VEXCEL CORP., BOULDER, CO.
Venus surface roughness and Magellan stereo data
[NASA-CR-196821] p 382 N95-11704

VIGYAN RESEARCH ASSOCIATES, INC., HAMPTON, VA.
A simple analytical aerodynamic model of Langley Winged-Cone Aerospace Plane concept
[NASA-CR-194987] p 252 N95-12175

VIRGINIA POLYTECHNIC INST., BLACKSBURG, VA.
Systems engineering technology for networks
[NASA-CR-196853] p 280 N95-11804

VIRGINIA POLYTECHNIC INST. AND STATE UNIV., BLACKSBURG, VA.
Optimal experimental designs for the estimation of thermal properties of composite materials
[NASA-CR-196792] p 261 N95-11700
Interlaminar stress analysis of dropped-ply laminated plates and shells by a mixed method
[NASA-CR-196851] p 311 N95-11946
Design of a vehicle based system to prevent ozone loss
[NASA-CR-197199] p 242 N95-12702

VIRGINIA UNIV., CHARLOTTESVILLE, VA.
Computer modeling the fatigue crack growth rate behavior of metals in corrosive environments
[NASA-CR-194982] p 269 N95-11933

W

WAKE FOREST UNIV., WINSTON-SALEM, NC.
Quantum chemical study of methane oxidation species
[NASA-CR-196158] p 265 N95-12107

WALOWIT (JED A.), INC., CLIFTON PARK, NY.
Presentation of computer code SPIRALI for incompressible, turbulent, plane and spiral grooved cylindrical and face seals p 305 N95-13584

WASHINGTON UNIV., SEATTLE, WA.
Synchronous picosecond sonoluminescence
[AD-A281498] p 355 N95-11856
Project Genesis: Mars in situ propellant technology demonstrator mission
[NASA-CR-197166] p 277 N95-12822
Project Hyreus: Mars sample return mission utilizing in situ propellant production
[NASA-CR-197189] p 383 N95-12826
Ocean acoustic tomography: Single slice and moving ship experiments
[AD-A283059] p 329 N95-12998
Hydrogen bonding and molecular orientation in water/fluorine adlayers on silver(110)
[AD-A282652] p 268 N95-13549

WEST VIRGINIA UNIV., MORGANTOWN, VA.
Conceptual design of an Orbital Debris Defense System
[NASA-CR-197211] p 254 N95-12696

WESTERN COMMERCIAL SPACE CENTER, INC., LOMPOC, CA.
Environmental process improvement feasibility study and demonstration program
[NASA-CR-196789] p 319 N95-12110

WESTINGHOUSE ELECTRIC CORP., BALTIMORE, MD.
Certification of windshear performance with RTCA class D radomes p 235 N95-13206

WESTINGHOUSE ELECTRIC CORP., PITTSBURGH, PA.
Processing, fabrication, and demonstration of HTS integrated microwave circuits
[AD-A282505] p 289 N95-13300

WESTON (ROY F.), INC., WEST CHESTER, PA.
Supercritical fluid (SCF) technologies: Assessment of applicability to installation restoration processes
[AD-A281504] p 290 N95-11859

WHEELING COLL., WV.
Directory of Federal laboratory and technology resources
[PB93-100097] p 389 N95-12223

WISCONSIN UNIV., MADISON, WI.
Implementation of a state of the art automated system for the production of cloud/water vapor motion winds from geostationary satellites
[NASA-CR-196817] p 325 N95-11758
Growth of potatoes for CELSS
[NASA-CR-177646] p 338 N95-11949
Venus cloud bobber mission: A long term survey of the Venusian surface
[NASA-CR-197174] p 383 N95-12533

WOODS HOLE OCEANOGRAPHIC INST., MA.
Acquisition of a gas source mass spectrometer for paleoclimatology and paleoceanography research
[AD-A282634] p 266 N95-12539

WORCESTER POLYTECHNIC INST., MA.
Design and construction of a remote piloted flying wing
[NASA-CR-197195] p 241 N95-12695

WRIGHT LAB., WRIGHT-PATTERSON AFB, OH.
Pressure measurements on an F/A-18 twin vertical tail in buffeting flow. Volume 3: Buffet power spectral densities
[AD-A281444] p 230 N95-11829
Draft standard for color active matrix liquid crystal displays (AMLCDs) in US Military aircraft. Recommended best practices
[AD-A282950] p 243 N95-12591
Air Force seal activities p 306 N95-13600

Y

YALE UNIV., NEW HAVEN, CT.
Fundamental and experimental studies on the catalytic combustion of methane
[PB94-205895] p 268 N95-13251

Typical Contract Number Index Listing

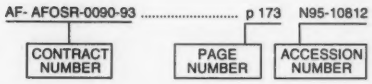

Listings in this index are arranged alphanumerically by contract number. Under each contract number the accession numbers denoting documents that have been produced as a result of research done under that contract are arranged in ascending order. The page number helps to locate the citation in the abstract section. The accession number denotes the number by which the citation is identified.

AF PROJ. 1121 ..... p 343 N95-12500
AF PROJ. 2003 ..... p 243 N95-12591
AF PROJ. 2303 ..... p 268 N95-13180
AF PROJ. 2308 ..... p 257 N95-12507
AF PROJ. 2401 ..... p 230 N95-11829
AF PROJ. 4506 ..... p 282 N95-12521
p 287 N95-12918
p 334 N95-12919
AF PROJ. 9310 ..... p 319 N95-12110
AF-AFOSR-0009-91 ..... p 282 N95-12496
AF-AFOSR-0056-91 ..... p 376 N95-12553
AF-AFOSR-0113-90 ..... p 291 N95-11929
AF-AFOSR-0124-91 ..... p 336 N95-13375
AF-AFOSR-0132-91 ..... p 297 N95-12751
AF-AFOSR-0154-91 ..... p 335 N95-12495
AF-AFOSR-0252-91 ..... p 351 N95-11922
AF-AFOSR-0299-91 ..... p 362 N95-12538
AF-AFOSR-0391-91 ..... p 290 N95-11874
p 290 N95-11875
p 230 N95-11877
p 230 N95-11884
AIF-7089 ..... p 308 N95-13609
AIF-8084 ..... p 308 N95-13609
ARPA ORDER 7597 ..... p 378 N95-12502
ARPA ORDER 8778 ..... p 299 N95-13294
ARPA ORDER 8930 ..... p 346 N95-11857
p 346 N95-11858
DA PROJ. RJ1-4-B-87 ..... p 355 N95-12396
DA PROJ. 1C4-63627-DE-79 ..... p 330 N95-12614
DA PROJ. 1L1-61102-AH-45 ..... p 349 N95-12811
DA PROJ. 1L1-62211-A-47-AB ..... p 262 N95-12357
DA PROJ. 1L1-62211-A-47-A ..... p 300 N95-11889
p 300 N95-12377
p 301 N95-12621
p 303 N95-12843
p 303 N95-13083
DA PROJ. 1O1-61102-A-71-A ..... p 260 N95-12613
DA PROJ. 101-62622-A-553 ..... p 334 N95-12593
p 316 N95-13142
DA PROJ. 301-62787-A-878 ..... p 334 N95-13054
p 339 N95-13055
DAAE07-90-C-RO59 ..... p 300 N95-12394
DAAH01-92-C-R097 ..... p 236 N95-13213
DAAH04-93-G-0007 ..... p 331 N95-13373
DAAH04-93-G-0041 ..... p 314 N95-11831
DAAH04-93-G-0052 ..... p 262 N95-11854
DAAH04-93-G-0056 ..... p 268 N95-13372
DAAH04-93-G-0457 ..... p 357 N95-11851
DAAK60-93-C-0035 ..... p 279 N95-13053
DAAK70-87-C-0043 ..... p 234 N95-12499
DAAK70-92-C-0059 ..... p 234 N95-12499
DAAL03-90-G-0058 ..... p 286 N95-11860
DAAL03-90-G-0102 ..... p 351 N95-11861
DAAL03-90-G-0113 ..... p 371 N95-11842
DAAL03-91-C-0034 ..... p 326 N95-12624
p 267 N95-12836
DAAL03-91-C-0051 ..... p 371 N95-11855
DAAL03-91-G-0019 ..... p 348 N95-11853
DAAL03-91-G-0124 ..... p 272 N95-11832
DAAL03-91-G-0127 ..... p 272 N95-11852
DAAL03-91-G-0333 ..... p 274 N95-12420
DAAL03-92-C-0001 ..... p 386 N95-11830
DAAL03-92-G-0009 ..... p 351 N95-11850
DAAL03-92-G-0117 ..... p 291 N95-11929
DAAL03-92-G-0411 ..... p 342 N95-11941
DACA31-91-D-0079 ..... p 290 N95-11859
DACA76-89-C-0014 ..... p 300 N95-12394
DACA76-92-C-0008 ..... p 350 N95-12884
DACA76-92-C-0024 ..... p 315 N95-12527
DACW39-93-C-0066 ..... p 327 N95-11787
DE-AC01-91CE-40956 ..... p 272 N95-11781
DE-AC02-76CH-00016 ..... p 371 N95-11739
p 371 N95-11740
p 364 N95-11746
p 295 N95-11780
p 357 N95-12012
p 358 N95-12829
p 350 N95-13124
p 374 N95-13125
DE-AC02-76CH-03000 ..... p 357 N95-12369
p 357 N95-12370
p 358 N95-12905
p 358 N95-12943
p 359 N95-13160
p 359 N95-13161
p 359 N95-13169
p 359 N95-13170
p 296 N95-13171
p 347 N95-13269
p 296 N95-13287
DE-AC03-76SF-00098 ..... p 318 N95-13126
p 294 N95-13156
p 345 N95-13157
p 296 N95-13158
DE-AC04-76DP-00613 ..... p 318 N95-11742
p 318 N95-11784
p 275 N95-12945
DE-AC04-94AL-85000 ..... p 364 N95-11754
p 264 N95-11756
p 384 N95-11757
p 269 N95-11785
p 372 N95-11862
p 287 N95-12863
p 350 N95-12864
p 287 N95-12865
p 350 N95-12866
p 376 N95-13172
p 276 N95-13184
p 271 N95-13544
DE-AC05-84OR-21400 ..... p 353 N95-11731
p 272 N95-11733
p 346 N95-11734
p 264 N95-11735
p 272 N95-11736
p 250 N95-11755
p 272 N95-11781
p 269 N95-11897
p 368 N95-12758
p 344 N95-12893
p 279 N95-12942
p 299 N95-13076
p 345 N95-13077
p 363 N95-13421
p 370 N95-13422
DE-AC06-76RL-01830 ..... p 318 N95-11745
p 286 N95-11751
p 270 N95-12372
p 331 N95-12677
p 263 N95-12862
p 294 N95-13075
p 304 N95-13182
DE-AC07-76ID-01570 ..... p 368 N95-12759
DE-AC12-76SN-00052 ..... p 374 N95-13059
DE-AC36-83CH-10093 ..... p 317 N95-12647
p 302 N95-12648
DE-AI01-91CE-50306 ..... p 260 N95-12764
DE-AI05-92OR-22041 ..... p 277 N95-13530
DE-AI08-92NV-10874 ..... p 321 N95-11730
DE-FG02-86ER-13508 ..... p 267 N95-12762
DE-FG02-87ER-45308 ..... p 271 N95-12895
DE-FG02-88ER-45366 ..... p 275 N95-13060
DE-FG02-89ER-12895 ..... p 269 N95-11738
DE-FG02-89ER-45403 ..... p 271 N95-13543
DE-FG02-90ER-45416 ..... p 271 N95-13554
DE-FG02-90ER-60989 ..... p 329 N95-11737
DE-FG02-91ER-20033 ..... p 331 N95-13271
DE-FG02-92ER-25126 ..... p 345 N95-13339
DE-FG02-94ER-25196 ..... p 351 N95-11922
DE-FG03-92ER-54150 ..... p 369 N95-12944
DE-FG03-94ER-54241 ..... p 370 N95-13529
DE-FG05-80ET-53088 ..... p 369 N95-12867
DE-FG05-89ER-14032 ..... p 297 N95-12375
DE-FG05-91ER-14213 ..... p 369 N95-12897
DE-FG05-92ER-54160 ..... p 361 N95-11792
DOT-SHRP-H-104A ..... p 280 N95-11904
DTFA01-90-Z-02069 ..... p 273 N95-12131
p 246 N95-12216
DTFA02-90-C-90125 ..... p 336 N95-13019
p 336 N95-13020
p 336 N95-13199
DTFR53-91-C-00065 ..... p 304 N95-13128
FAA TASK AM-A-91-HRR-138 ..... p 336 N95-13020
FAA TASK AM-A-94-HRR-138 ..... p 336 N95-13019
FAPESP-94/4845-7 ..... p 341 N95-11763
F04701-88-C-0089 ..... p 250 N95-12917
F19628-88-K-0039 ..... p 325 N95-13136
F19628-89-K-0044 ..... p 315 N95-12428
F19628-90-C-0003 ..... p 344 N95-12922
F19628-90-C-002 ..... p 235 N95-13209
F19628-90-C-0159 ..... p 256 N95-13138
F19628-91-K-0021 ..... p 316 N95-12634
F19628-91-K-0040 ..... p 327 N95-13134
F19628-93-C-0051 ..... p 327 N95-13137
F19628-93-C-0193 ..... p 340 N95-12524
F19628-93-K-0014 ..... p 283 N95-12550
F19628-94-C-0001 ..... p 340 N95-12413
p 326 N95-12805
F33615-90-C-1465 ..... p 378 N95-12502
p 340 N95-12524
F33615-91-C-1729 ..... p 282 N95-12493
F33615-91-C-5709 ..... p 300 N95-11729
F33615-93-C-5360 ..... p 377 N95-11788
F49620-91-C-0003 ..... p 377 N95-11944
F49620-92-J-0081 ..... p 350 N95-13369
F49620-93-1-0114 ..... p 363 N95-13374
F49620-93-1-0197 ..... p 267 N95-12807
F49620-93-1-0251 ..... p 277 N95-12729
F49620-93-1-0290 ..... p 334 N95-12535
F49620-93-1-0372 ..... p 324 N95-12534
GRI-5086-293-1848 ..... p 301 N95-12579
GRI-5089-260-1908 ..... p 290 N95-11840
GRI-5091-260-2206 ..... p 268 N95-13251
MDA903-89-C-0003 ..... p 344 N95-13051
MDA903-91-C-0006 ..... p 282 N95-12416
MDA972-90-C-0035 ..... p 340 N95-12516
MDA972-92-C-0047 ..... p 299 N95-13294
NAGW-0715 ..... p 383 N95-12952
NAGW-1195 ..... p 319 N95-12110
NAGW-1335 ..... p 349 N95-12782
NAGW-2014 ..... p 349 N95-12782
NAGW-2239 ..... p 255 N95-12879
NAGW-2598 ..... p 327 N95-11706
NAGW-2727 ..... p 319 N95-11931
NAGW-2753 ..... p 280 N95-11760
NAGW-2996 ..... p 379 N95-12234
p 323 N95-12468
NAGW-3023 ..... p 385 N95-12886
p 381 N95-13012
NAGW-3042 ..... p 324 N95-12949
NAGW-3886 ..... p 320 N95-12798
NAGW-766 ..... p 385 N95-12886
NAGW-810 ..... p 259 N95-11891
NAGW-973 ..... p 323 N95-12130
NAG1-1058 ..... p 284 N95-12856
NAG1-1091 ..... p 362 N95-12659
NAG1-1122 ..... p 289 N95-11705
NAG1-1170 ..... p 346 N95-11863
NAG1-1265 ..... p 294 N95-13201
NAG1-1346 ..... p 298 N95-12951
NAG1-1374 ..... p 313 N95-13096
p 313 N95-13163
NAG1-1402 ..... p 289 N95-11709
NAG1-1505 ..... p 313 N95-13096
p 313 N95-13162
p 313 N95-13163
NAG1-1507 ..... p 261 N95-11700
NAG1-343 ..... p 311 N95-11946

NAG1-745 ..... p 269 N95-11933
NAG2-477 ..... p 230 N95-11911
NAG2-565 ..... p 292 N95-11992
NAG2-573 ..... p 333 N95-12376
NAG2-624 ..... p 331 N95-12941
NAG2-644 ..... p 257 N95-11805
NAG2-700 ..... p 339 N95-13026
NAG2-703 ..... p 333 N95-12376
NAG2-733 ..... p 292 N95-12228
NAG2-764 ..... p 382 N95-12011
NAG2-794 ..... p 245 N95-12791
NAG2-866 ..... p 279 N95-11707
NAG2-87 ..... p 331 N95-12827
NAG2-882 ..... p 237 N95-11699
NAG3-1047 ..... p 300 N95-11889
NAG3-1100 ..... p 308 N95-12381
NAG3-1149 ..... p 284 N95-12674
NAG3-1203 ..... p 242 N95-12787
NAG3-1269 ..... p 246 N95-13200
NAG3-1365 ..... p 308 N95-11813
NAG3-1549 ..... p 341 N95-11761
p 341 N95-11762
p 341 N95-11763
p 341 N95-11764
NAG3-519 ..... p 289 N95-13344
NAG3-72 ..... p 291 N95-11888
NAG3-788 ..... p 349 N95-12811
NAG5-1119 ..... p 381 N95-13056
NAG5-1551 ..... p 381 N95-12788
NAG5-160-1 ..... p 361 N95-12102
NAG5-1608 ..... p 380 N95-12373
NAG5-1610 ..... p 380 N95-12388
NAG5-1671 ..... p 380 N95-12465
NAG5-1733 ..... p 381 N95-12821
NAG5-1743 ..... p 323 N95-12244
NAG5-1828 ..... p 325 N95-13025
NAG5-1926 ..... p 369 N95-13024
NAG5-1959 ..... p 385 N95-13023
NAG5-2018 ..... p 382 N95-12950
NAG5-2141 ..... p 281 N95-12010
NAG5-2142 ..... p 281 N95-12010
NAG5-557 ..... p 341 N95-11763
NAG5-760 ..... p 248 N95-12837
NAG5-995 ..... p 280 N95-11804
NAG8-1012 ..... p 377 N95-12618
NAG8-1017 ..... p 293 N95-12387
NAG8-116 ..... p 349 N95-12470
NAG8-137 ..... p 308 N95-11994
NAG8-212 ..... p 292 N95-11999
NAG8-239 ..... p 382 N95-12940
NAG8-240 ..... p 299 N95-11701
NAG8-697 ..... p 380 N95-12466
NAG8-850 ..... p 312 N95-12861
NAG8-904 ..... p 320 N95-12786
NAG8-920 ..... p 279 N95-13202
NAG8-950 ..... p 372 N95-11921
NAG8-974 ..... p 325 N95-11758
NAG9-520 ..... p 333 N95-11808
NAG9-588 ..... p 335 N95-13270
NAG9-629 ..... p 348 N95-11998
NAL PROJ. EA-9-000 ..... p 229 N95-12166
NAL PROJ. T-0-107 ..... p 311 N95-11924
NAL PROJ. T0-177 ..... p 311 N95-11879
NASA ORDER H-19648-D ..... p 362 N95-12736
NASA ORDER H-22787-D ..... p 332 N95-13423
NASW-4003 ..... p 248 N95-12474
NASW-4435 ..... p 238 N95-12294
p 239 N95-12305
p 382 N95-12307
p 338 N95-12361
p 383 N95-12362
p 239 N95-12363
p 383 N95-12529
p 239 N95-12530
p 249 N95-12531
p 301 N95-12532
p 383 N95-12533
p 301 N95-12554
p 338 N95-12555
p 253 N95-12564
p 258 N95-12604
p 239 N95-12609
p 301 N95-12625
p 239 N95-12626
p 302 N95-12627
p 240 N95-12628
p 339 N95-12629
p 258 N95-12630
p 253 N95-12632
p 240 N95-12636
p 240 N95-12637
p 240 N95-12638
p 240 N95-12639
p 302 N95-12640
p 368 N95-12641
p 241 N95-12643
NASW-4579 ..... p 283 N95-12644
NASW-4627 ..... p 241 N95-12645
NASW-4801 ..... p 253 N95-12661
NASW-4854 ..... p 253 N95-12663
NAS1-14101 ..... p 361 N95-12665
NAS1-14472 ..... p 302 N95-12666
NAS1-15610 ..... p 302 N95-12668
NAS1-16394 ..... p 241 N95-12689
NAS1-17070 ..... p 302 N95-12690
NAS1-17130 ..... p 303 N95-12694
NAS1-18107 ..... p 241 N95-12695
NAS1-18455 ..... p 254 N95-12696
NAS1-18580 ..... p 254 N95-12698
NAS1-18605 ..... p 241 N95-12700
p 278 N95-12701
NAS1-18763 ..... p 242 N95-12702
NAS1-19000 ..... p 254 N95-12737
p 254 N95-12765
NAS1-19241 ..... p 254 N95-12790
NAS1-19247 ..... p 277 N95-12822
NAS1-19317 ..... p 383 N95-12826
p 242 N95-12993
NAS1-19341 ..... p 255 N95-13006
NAS1-19381 ..... p 384 N95-13497
NAS1-19480 ..... p 277 N95-13508
p 257 N95-13581
p 384 N95-13582
p 247 N95-12880
NAS1-19708 ..... p 385 N95-12469
NAS1-20059 ..... p 382 N95-11704
NAS2-13404 ..... p 340 N95-11932
NAS2-13445 ..... p 340 N95-11932
NAS2-13721 ..... p 340 N95-11932
p 340 N95-11932
p 340 N95-11932
p 340 N95-11932
p 340 N95-11932
p 284 N95-12896
p 256 N95-13194
p 340 N95-11932
p 340 N95-12828
p 238 N95-11952
p 244 N95-11869
p 293 N95-12619
p 256 N95-13195
p 262 N95-12793
p 313 N95-13096
p 313 N95-13163
p 252 N95-12175
p 252 N95-12165
p 290 N95-11812
p 351 N95-11922
p 291 N95-11929
p 291 N95-11930
p 340 N95-11932
p 342 N95-12005
p 340 N95-12828
p 345 N95-13420
NAS3-25054 ..... p 262 N95-11926
p 292 N95-12105
NAS3-25062 ..... p 338 N95-12132
NAS3-25063 ..... p 242 N95-12831
NAS3-25076 ..... p 290 N95-11874
NAS3-25266 ..... p 290 N95-11875
p 230 N95-11877
p 351 N95-11883
p 230 N95-11884
NAS3-25270 ..... p 294 N95-13233
p 294 N95-13234
p 259 N95-13237
p 256 N95-13232
p 288 N95-13231
p 311 N95-11954
p 258 N95-12622
NAS3-25517 ..... p 260 N95-12693
NAS3-25776 ..... p 256 N95-13194
NAS3-25952 ..... p 244 N95-11901
NAS3-26617 ..... p 244 N95-11951
NAS3-27186 ..... p 291 N95-11888
p 270 N95-12104
p 295 N95-11996
p 309 N95-11711
p 243 N95-11867
p 342 N95-11918
p 257 N95-11919
p 245 N95-12763
p 263 N95-13082
p 256 N95-13194
p 233 N95-13197
NAS5-31214 ..... p 322 N95-11801
NAS5-31215 ..... p 368 N95-12853
NAS5-31331 ..... p 384 N95-12667
NAS5-32314 ..... p 344 N95-12796
NAS5-32332 ..... p 323 N95-12226
NAS5-32571 ..... p 325 N95-13190
NAS5-32650 ..... p 287 N95-12795
NAS8-36433 ..... p 258 N95-12819
NAS8-36606 ..... p 252 N95-12106
NAS8-37107 ..... p 361 N95-12147
NAS8-38187 ..... p 230 N95-11807
NAS8-38609 ..... p 343 N95-12014
p 373 N95-12386
p 362 N95-12390
p 308 N95-12391
p 380 N95-12463
p 380 N95-12464
p 279 N95-12752
p 381 N95-12992
p 268 N95-13084
NAS8-39026 ..... p 270 N95-12830
NAS8-39029 ..... p 284 N95-12674
NAS8-39131 ..... p 312 N95-12620
NAS8-39215 ..... p 243 N95-13027
NAS8-39936 ..... p 381 N95-11928
NAS9-17900 ..... p 337 N95-11878
p 251 N95-11937
NAS9-18773 ..... p 332 N95-11708
NAS9-18800 ..... p 337 N95-11878
NAS9-19100 ..... p 242 N95-11913
NCA2-839 ..... p 281 N95-12382
NCC1-193 ..... p 250 N95-11767
p 251 N95-11777
p 261 N95-11803
p 257 N95-11823
p 251 N95-11833
p 261 N95-11834
NCC1-24 ..... p 293 N95-12859
NCC1-29 ..... p 244 N95-11869
NCC1-55 ..... p 265 N95-12107
NCC2-301 ..... p 338 N95-11949
NCC2-389 ..... p 254 N95-12766
NCC2-583 ..... p 295 N95-11971
NCC2-617 ..... p 242 N95-12785
NCC2-693 ..... p 321 N95-12832
NCC2-698 ..... p 295 N95-11896
NCC2-738 ..... p 246 N95-11938
NCC2-740 ..... p 230 N95-11766
NCC2-796 ..... p 232 N95-12389
NCC2-9003 ..... p 251 N95-11777
p 262 N95-11835
NCC3-104 ..... p 293 N95-12380
NCC3-120 ..... p 312 N95-12818
NCC3-162 ..... p 260 N95-12692
p 260 N95-12693
NCC3-169 ..... p 376 N95-11765
NCC3-233 ..... p 231 N95-11917
p 291 N95-11935
p 292 N95-11953
p 293 N95-12380
p 295 N95-13550
NCC3-246 ..... p 260 N95-12692
p 260 N95-12693
NCC3-318 ..... p 260 N95-12692
p 260 N95-12693
NCC3-331 ..... p 310 N95-11865
NCC5-37 ..... p 382 N95-12939
NCC8-19 ..... p 278 N95-11759
NCC8-21 ..... p 320 N95-12786
NCC8-39 ..... p 251 N95-11777
p 251 N95-11802
p 251 N95-11809
p 252 N95-11945
NGT-30202 ..... p 281 N95-12374
NGT-50942 ..... p 260 N95-12662
NIST-60NANB0D1042 ..... p 267 N95-12852
NIST-60NANB1D1174 ..... p 267 N95-12778
NOAA-27GP0232-1 ..... p 320 N95-12462
NOAA-50-DGNE-1-00138 ..... p 247 N95-12880
NSF CTS-93-07973 ..... p 291 N95-11929
NSF DMS-89-21189 ..... p 293 N95-12380
NSF DMS-93-05828 ..... p 351 N95-11922
NSF DMS-93-07086 ..... p 352 N95-12603
NSF DMS-93-18166 ..... p 351 N95-11883
NSF EID-90-17558 ..... p 341 N95-11763
NSF IRI-89-00267 ..... p 349 N95-12411
NSF IRI-91-05202 ..... p 343 N95-12497
NSF MIP-90-01651 ..... p 347 N95-12414
NSF MIP-93-08085 ..... p 344 N95-12588
NSF MSS-91-16411 ..... p 376 N95-12385
NSF OCE-93-13563 ..... p 319 N95-12384
N00014-19-J-1919 ..... p 373 N95-11963
N00014-89-J-0185 ..... p 351 N95-11883
N00014-89-J-1145 ..... p 274 N95-12520
p 276 N95-13367
N00014-89-J-1225 ..... p 273 N95-12008
p 273 N95-12397
p 262 N95-12398
p 273 N95-12399
p 273 N95-12400
p 274 N95-12419
p 276 N95-13296
p 264 N95-13298

N00014-89-J-1728 ..... p 375 N95-13299
N00014-89-J-1828 ..... p 297 N95-12375
p 356 N95-11828
p 358 N95-12522
N00014-89-J-3062 ..... p 360 N95-13376
N00014-89-J-3070 ..... p 330 N95-12393
N00014-89-J-3221 ..... p 285 N95-12924
N00014-90-J-1148 ..... p 274 N95-12424
N00014-90-J-1185 ..... p 270 N95-12543
N00014-90-J-1326 ..... p 373 N95-12425
N00014-90-J-1340 ..... p 354 N95-12728
N00014-90-J-1344 ..... p 351 N95-11883
N00014-90-J-1365 ..... p 345 N95-13370
N00014-90-J-1427 ..... p 289 N95-13368
N00014-90-J-1530 ..... p 373 N95-12923
N00014-90-J-1705 ..... p 354 N95-12994
N00014-91-C-0067 ..... p 263 N95-12833
N00014-91-C-0112 ..... p 289 N95-13300
N00014-91-C-0124 ..... p 270 N95-12546
N00014-91-C-0168 ..... p 263 N95-12883
N00014-91-J-1086 ..... p 293 N95-12422
N00014-91-J-1338 ..... p 259 N95-11844
N00014-91-J-1508 ..... p 275 N95-12586
N00014-91-J-1630 ..... p 266 N95-12514
p 358 N95-12617
N00014-91-J-1752 ..... p 373 N95-12004
N00014-91-J-1909 ..... p 268 N95-13549
N00014-91-J-4038 ..... p 349 N95-12411
N00014-91-J-4055 ..... p 329 N95-12998
N00014-91-J-4117 ..... p 329 N95-12998
N00014-91-S-1703 ..... p 275 N95-12536
N00014-91-1-0199 ..... p 358 N95-12882
N00014-92-J-1190 ..... p 285 N95-13371
N00014-92-J-1301 ..... p 266 N95-12539
N00014-92-J-1308 ..... p 375 N95-13168
N00014-92-J-1417 ..... p 291 N95-11929
N00014-92-J-1796 ..... p 290 N95-11874
p 290 N95-11875
N00014-92-J-1801 ..... p 346 N95-11857
p 346 N95-11858
N00014-92-J-1879 ..... p 335 N95-11942
p 351 N95-12007
N00014-92-J-1976 ..... p 230 N95-11877
N00014-92-J-2005 ..... p 325 N95-13293
N00014-92-J-4097 ..... p 347 N95-12414
N00014-92-J-4109 ..... p 378 N95-12995
N00014-93-C-0176 ..... p 286 N95-12009
N00014-93-C-2044 ..... p 273 N95-12403
N00014-93-I-1031 ..... p 352 N95-12552
N00014-93-J-1126 ..... p 279 N95-12772
N00014-93-1-0199 ..... p 359 N95-13141
N00014-93-1-0322 ..... p 355 N95-11856
N00014-93-1-0385 ..... p 335 N95-11942
p 351 N95-12007
N00014-93-1-0456 ..... p 326 N95-12392
N00014-93-1-0674 ..... p 296 N95-13165
N00014-93-1-0675 ..... p 329 N95-12540
N00014-93-1-0757 ..... p 274 N95-12417
p 268 N95-13288
N00014-93-1-0951 ..... p 334 N95-12542
N00014-93-1-1084 ..... p 287 N95-12881
N00014-93-1200 ..... p 349 N95-12395
N00014-94-1-0077 ..... p 286 N95-12494
N00014-94-1-0101 ..... p 275 N95-12773
N00014-94-1-0194 ..... p 329 N95-12590
N00014-94-1-0462 ..... p 286 N95-12421
N00014-94-1-0479 ..... p 344 N95-12588
N00014-94-1-0540 ..... p 262 N95-12404
p 274 N95-12407
p 275 N95-12537
N00039-91-C-0072 ..... p 329 N95-12998
N00173-93-P-6207 ..... p 247 N95-12880
N47408-89-C-1058 ..... p 323 N95-12506
N68171-94-M-5608 ..... p 288 N95-13052
RFA-90-1 ..... p 331 N95-13176
RTOP 199-06-12 ..... p 337 N95-11905
RTOP 199-16-12 ..... p 330 N95-12006
RTOP 199-18-12-07 ..... p 329 N95-11810
RTOP 232-01-0B ..... p 284 N95-12674
RTOP 232-01-04-05 ..... p 252 N95-12175
RTOP 232-01-04-06 ..... p 293 N95-12619
RTOP 232-01-04 ..... p 382 N95-12190
RTOP 232-02-02 ..... p 258 N95-12750
RTOP 233-01-0A ..... p 372 N95-11876
p 317 N95-11903
p 260 N95-12662
p 260 N95-12692
p 260 N95-12693
RTOP 233-01-01-01 ..... p 252 N95-11947
RTOP 233-01-01-06 ..... p 310 N95-11814
RTOP 233-01-01-07 ..... p 256 N95-13195
RTOP 233-01-03-22 ..... p 284 N95-12896
RTOP 233-03-04 ..... p 342 N95-11916
RTOP 323-57-4A ..... p 256 N95-13194
RTOP 412-00-00 ..... p 278 N95-12703
RTOP 422-00-00 ..... p 344 N95-12796
RTOP 474-46-10 ..... p 258 N95-12622
RTOP 505-59-36 ..... p 232 N95-12360
RTOP 505-59-37 ..... p 238 N95-12225
RTOP 505-59-40-10 ..... p 233 N95-12770
RTOP 505-59-50-01 ..... p 292 N95-12105
RTOP 505-59-54-17 ..... p 231 N95-12176
RTOP 505-62-0E ..... p 349 N95-12811
RTOP 505-62-10 ..... p 372 N95-11882
RTOP 505-62-12 ..... p 243 N95-11890
RTOP 505-62-30-01 ..... p 246 N95-13553
RTOP 505-62-36 ..... p 300 N95-11889
p 300 N95-12377
p 301 N95-12621
p 303 N95-12843
p 303 N95-13083
RTOP 505-62-50 ..... p 296 N95-12748
p 245 N95-12763
RTOP 505-62-52 ..... p 232 N95-12378
RTOP 505-63-12 ..... p 264 N95-13193
RTOP 505-63-5A ..... p 260 N95-12764
RTOP 505-63-5B ..... p 309 N95-11711
p 312 N95-12818
RTOP 505-63-50-04 ..... p 269 N95-11915
RTOP 505-63-52 ..... p 310 N95-11865
RTOP 505-63-53-01 ..... p 310 N95-11815
RTOP 505-64-12-01 ..... p 234 N95-13203
RTOP 505-64-13-04 ..... p 245 N95-12664
RTOP 505-64-30-01 ..... p 244 N95-11869
RTOP 505-64-36 ..... p 229 N95-12227
RTOP 505-64-53 ..... p 334 N95-12792
RTOP 505-68-00 ..... p 231 N95-11927
RTOP 505-68-10 ..... p 291 N95-11888
p 233 N95-13197
RTOP 505-68-20 ..... p 244 N95-11868
RTOP 505-68-32 ..... p 243 N95-11864
RTOP 505-68-70-09 ..... p 238 N95-11952
RTOP 505-70-59-03 ..... p 231 N95-11995
RTOP 505-70-62-01 ..... p 293 N95-12859
RTOP 505-70-62-03 ..... p 244 N95-12860
RTOP 505-70-64-01 ..... p 255 N95-12838
RTOP 505-70-91-01 ..... p 247 N95-13196
RTOP 505-90-5K ..... p 291 N95-11935
p 292 N95-11953
p 293 N95-12380
p 295 N95-13550
RTOP 505-90-51 ..... p 308 N95-11813
RTOP 505-90-52-01 ..... p 290 N95-11812
p 351 N95-11922
p 291 N95-11929
p 291 N95-11930
p 340 N95-11932
p 342 N95-12005
p 340 N95-12828
p 345 N95-13420
RTOP 505-90-53-02 ..... p 345 N95-13198
RTOP 505-90-53 ..... p 270 N95-12104
RTOP 506-40-91-01 ..... p 291 N95-11936
RTOP 506-41-41 ..... p 261 N95-12783
RTOP 506-42-31 ..... p 257 N95-11919
p 259 N95-13347
RTOP 506-44-20 ..... p 288 N95-13231
RTOP 506-48-21 ..... p 256 N95-13232
RTOP 506-59-64-01 ..... p 315 N95-12379
RTOP 510-02-12-09 ..... p 262 N95-11926
p 262 N95-12793
RTOP 532-05-37-03 ..... p 262 N95-12357
RTOP 533-02-00 ..... p 230 N95-11898
RTOP 533-02-31 ..... p 231 N95-12191
RTOP 535-03-11-02 ..... p 355 N95-12341
RTOP 537-02-23 ..... p 231 N95-11917
p 233 N95-13058
RTOP 537-04-20 ..... p 263 N95-12813
RTOP 538-01-11 ..... p 243 N95-11867
RTOP 538-02-10-01 ..... p 269 N95-11933
RTOP 538-03-11 ..... p 244 N95-11901
p 244 N95-11951
RTOP 550-00-00 ..... p 255 N95-12858
RTOP 578-12-23-70 ..... p 326 N95-12839
RTOP 584-03-11 ..... p 311 N95-11954
RTOP 590-14-91-52 ..... p 252 N95-12165
RTOP 590-21-11 ..... p 304 N95-13583
RTOP 593-21-21 ..... p 294 N95-13234
RTOP 665-10-70 ..... p 384 N95-12667
RTOP 722-20-00 ..... p 287 N95-12795
RTOP 763-21-31 ..... p 292 N95-11992
RTOP 763-22-41 ..... p 263 N95-13082
RTOP 778-34-2A ..... p 260 N95-12764
RTOP 910-00-00 ..... p 323 N95-12226
RTOP 921-00-00 ..... p 323 N95-12130
RTOP 924-00-00 ..... p 314 N95-11997
SBIR-12.04-8450B ..... p 338 N95-12132
SRI PROJ. 2431 ..... p 368 N95-12853
SRI PROJ. 2432 ..... p 322 N95-11801
W-31-109-ENG-38 ..... p 245 N95-11752
p 290 N95-11753
p 359 N95-13173
p 304 N95-13183
p 375 N95-13272
p 369 N95-13280
p 375 N95-13337
p 360 N95-13338
p 348 N95-13556
W-7405-ENG-36 ..... p 322 N95-11732
p 361 N95-11779
p 257 N95-11782
p 357 N95-11894
p 365 N95-12371
p 324 N95-12649
p 317 N95-12650
p 232 N95-12652
p 368 N95-12757
p 312 N95-12784
p 353 N95-13061
p 374 N95-13078
p 299 N95-13080
p 374 N95-13081
p 374 N95-13086
p 359 N95-13104
p 363 N95-13106
p 378 N95-13123
p 327 N95-13268
W-7405-ENG-48 ..... p 322 N95-11741
p 314 N95-11783
p 364 N95-11786
p 265 N95-11790
p 356 N95-11791
p 298 N95-12761
p 298 N95-12868
p 296 N95-12869
p 321 N95-12926
p 326 N95-12927
p 376 N95-13074
p 369 N95-13285
p 363 N95-13532
p 264 N95-13533
p 299 N95-13534
p 370 N95-13555
2-31-109-ENG-38 ..... p 285 N95-13057

Typical Report Number Index Listing

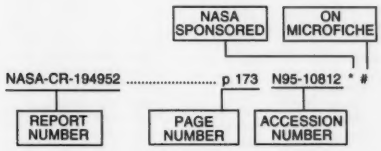

Listings in this index are arranged alphanumerically by report number. The accession number denotes the number by which the citation is identified. The page number helps to locate the citation in the abstract section. An asterisk (*) indicates that the item is a NASA report. A pound sign (#) indicates that the item is available on microfiche.

A-93065 ..... p 292 N95-11992 * #
A-94058 ..... p 330 N95-12006 * #
A-94069 ..... p 382 N95-12190 * #
A-94076 ..... p 238 N95-12225 * #
A-94085 ..... p 329 N95-11810 * #
A-94118 ..... p 230 N95-11911 * #
A-94122 ..... p 232 N95-12360 * #
A-94125 ..... p 231 N95-11927 * #
A-94126 ..... p 295 N95-11896 * #
A-94129 ..... p 338 N95-11949 * #
A-94130 ..... p 338 N95-12132 * #
A-94131 ..... p 337 N95-11905 * #
A-94134 ..... p 334 N95-12792 * #
A-94139 ..... p 229 N95-12227 * #

AD-A280395 ..... p 364 N95-11837
AD-A280519 ..... p 260 N95-12613
AD-A280556 ..... p 330 N95-12614
AD-A280891 ..... p 300 N95-11729
AD-A280925 ..... p 279 N95-12772
AD-A280926 ..... p 275 N95-12773
AD-A281187 ..... p 274 N95-12520 #
AD-A281188 ..... p 282 N95-12521 #
AD-A281193 ..... p 358 N95-12522 #
AD-A281194 ..... p 347 N95-12523 #
AD-A281216 ..... p 276 N95-13367 #
AD-A281218 ..... p 289 N95-13368 #
AD-A281219 ..... p 350 N95-13369 #
AD-A281222 ..... p 345 N95-13370 #
AD-A281227 ..... p 285 N95-13371 #
AD-A281255 ..... p 340 N95-12524 #
AD-A281261 ..... p 268 N95-13372 #
AD-A281282 ..... p 331 N95-13373 #
AD-A281283 ..... p 363 N95-13374
AD-A281284 ..... p 336 N95-13375 #
AD-A281292 ..... p 360 N95-13376 #
AD-A281416 ..... p 351 N95-11850
AD-A281417 ..... p 357 N95-11851 #
AD-A281419 ..... p 272 N95-11852 #
AD-A281435 ..... p 265 N95-11827
AD-A281438 ..... p 356 N95-11828
AD-A281439 ..... p 335 N95-13177
AD-A281443 ..... p 288 N95-13164
AD-A281444 ..... p 230 N95-11829
AD-A281445 ..... p 386 N95-11830
AD-A281446 ..... p 314 N95-11831
AD-A281465 ..... p 348 N95-11853 #
AD-A281471 ..... p 262 N95-11854 #
AD-A281472 ..... p 371 N95-11855 #
AD-A281498 ..... p 355 N95-11856 #
AD-A281501 ..... p 346 N95-11857 #
AD-A281502 ..... p 346 N95-11858 #
AD-A281504 ..... p 290 N95-11859 #
AD-A281646 ..... p 296 N95-13165 #
AD-A281716 ..... p 327 N95-11787
AD-A281723 ..... p 272 N95-11832
AD-A281724 ..... p 286 N95-11860
AD-A281725 ..... p 351 N95-11861
AD-A281726 ..... p 371 N95-11842
AD-A281731 ..... p 229 N95-13166 #
AD-A281738 ..... p 342 N95-11843
AD-A281741 ..... p 259 N95-11844
AD-A281879 ..... p 378 N95-13167 #
AD-A281906 ..... p 377 N95-11788 #
AD-A281974 ..... p 245 N95-11789
AD-A282044 ..... p 361 N95-11910 #
AD-A282098 ..... p 375 N95-13168 #
AD-A282165 ..... p 274 N95-12420 #
AD-A282177 ..... p 286 N95-12421
AD-A282184 ..... p 293 N95-12422
AD-A282185 ..... p 326 N95-12423
AD-A282201 ..... p 274 N95-12424 #
AD-A282203 ..... p 373 N95-12425 #
AD-A282208 ..... p 234 N95-12499 #
AD-A282209 ..... p 354 N95-12426 #
AD-A282210 ..... p 362 N95-12427 #
AD-A282212 ..... p 315 N95-12428 #
AD-A282221 ..... p 333 N95-12405 #
AD-A282222 ..... p 333 N95-12406 #
AD-A282233 ..... p 274 N95-12407 #
AD-A282234 ..... p 281 N95-12408 #
AD-A282249 ..... p 293 N95-12409 #
AD-A282259 ..... p 239 N95-12410
AD-A282260 ..... p 349 N95-12411
AD-A282262 ..... p 282 N95-12412
AD-A282263 ..... p 340 N95-12413 #
AD-A282284 ..... p 347 N95-12414 #
AD-A282306 ..... p 362 N95-12415 #
AD-A282314 ..... p 282 N95-12416 #
AD-A282322 ..... p 274 N95-12417 #
AD-A282324 ..... p 347 N95-12418 #
AD-A282326 ..... p 274 N95-12419 #
AD-A282363 ..... p 297 N95-11940
AD-A282365 ..... p 342 N95-11941
AD-A282367 ..... p 335 N95-11942
AD-A282369 ..... p 280 N95-11943
AD-A282371 ..... p 377 N95-11944
AD-A282379 ..... p 351 N95-12007
AD-A282381 ..... p 273 N95-12008
AD-A282382 ..... p 286 N95-12009
AD-A282383 ..... p 373 N95-12004
AD-A282403 ..... p 373 N95-11993
AD-A282406 ..... p 326 N95-12392 #
AD-A282420 ..... p 330 N95-12393 #
AD-A282451 ..... p 277 N95-12729
AD-A282456 ..... p 300 N95-12394 #
AD-A282457 ..... p 263 N95-12833
AD-A282464 ..... p 268 N95-13288
AD-A282467 ..... p 244 N95-13289
AD-A282469 ..... p 316 N95-13290
AD-A282470 ..... p 289 N95-13291
AD-A282482 ..... p 325 N95-13293
AD-A282484 ..... p 360 N95-13178
AD-A282494 ..... p 299 N95-13294
AD-A282495 ..... p 276 N95-13296
AD-A282496 ..... p 264 N95-13298
AD-A282497 ..... p 375 N95-13299
AD-A282505 ..... p 289 N95-13300
AD-A282506 ..... p 349 N95-12395
AD-A282508 ..... p 355 N95-12396
AD-A282510 ..... p 273 N95-12397
AD-A282511 ..... p 262 N95-12398
AD-A282512 ..... p 273 N95-12399
AD-A282513 ..... p 273 N95-12400
AD-A282518 ..... p 270 N95-12401
AD-A282524 ..... p 281 N95-12402
AD-A282527 ..... p 273 N95-12403
AD-A282539 ..... p 262 N95-12404
AD-A282540 ..... p 282 N95-12493
AD-A282544 ..... p 286 N95-12494
AD-A282547 ..... p 335 N95-12495 #
AD-A282548 ..... p 282 N95-12496 #
AD-A282551 ..... p 343 N95-12497 #
AD-A282581 ..... p 266 N95-12549 #
AD-A282582 ..... p 283 N95-12550
AD-A282583 ..... p 259 N95-12551
AD-A282585 ..... p 352 N95-12552 #
AD-A282597 ..... p 376 N95-12553
AD-A282598 ..... p 324 N95-12534
AD-A282599 ..... p 334 N95-12535
AD-A282619 ..... p 275 N95-12536 #
AD-A282625 ..... p 275 N95-12537
AD-A282626 ..... p 362 N95-12538
AD-A282634 ..... p 266 N95-12539 #
AD-A282635 ..... p 329 N95-12540
AD-A282641 ..... p 343 N95-12541 #
AD-A282643 ..... p 334 N95-12542
AD-A282644 ..... p 270 N95-12543
AD-A282645 ..... p 343 N95-12500
AD-A282646 ..... p 358 N95-12617
AD-A282647 ..... p 351 N95-12501
AD-A282648 ..... p 284 N95-12834
AD-A282649 ..... p 297 N95-12751
AD-A282652 ..... p 268 N95-13549
AD-A282654 ..... p 350 N95-12835 #
AD-A282655 ..... p 378 N95-12502
AD-A282658 ..... p 343 N95-12504
AD-A282664 ..... p 326 N95-12805
AD-A282671 ..... p 266 N95-12514 #
AD-A282709 ..... p 340 N95-12516 #
AD-A282724 ..... p 300 N95-12505 #
AD-A282725 ..... p 323 N95-12506 #
AD-A282729 ..... p 257 N95-12507 #
AD-A282733 ..... p 267 N95-12836 #
AD-A282764 ..... p 324 N95-12508 #
AD-A282782 ..... p 287 N95-12509 #
AD-A282784 ..... p 287 N95-12525 #
AD-A282788 ..... p 300 N95-12526 #
AD-A282789 ..... p 267 N95-12807 #
AD-A282796 ..... p 315 N95-12527 #
AD-A282804 ..... p 253 N95-12528 #
AD-A282805 ..... p 283 N95-12601 #
AD-A282810 ..... p 373 N95-12602 #
AD-A282827 ..... p 268 N95-13180
AD-A282833 ..... p 275 N95-12586 #
AD-A282836 ..... p 301 N95-12587 #
AD-A282882 ..... p 378 N95-12916
AD-A282883 ..... p 250 N95-12917
AD-A282885 ..... p 287 N95-12918
AD-A282886 ..... p 334 N95-12919
AD-A282896 ..... p 284 N95-12920
AD-A282909 ..... p 249 N95-12510
AD-A282924 ..... p 344 N95-12588 #
AD-A282934 ..... p 329 N95-12590 #
AD-A282950 ..... p 243 N95-12591 #
AD-A282954 ..... p 283 N95-12592 #
AD-A283042 ..... p 354 N95-12994 #
AD-A283043 ..... p 378 N95-12995 #
AD-A283052 ..... p 327 N95-12996 #
AD-A283058 ..... p 327 N95-12997 #
AD-A283059 ..... p 329 N95-12998 #
AD-A283060 ..... p 344 N95-13051
AD-A283062 ..... p 288 N95-13052 #
AD-A283063 ..... p 279 N95-13053 #
AD-A283064 ..... p 334 N95-13054
AD-A283065 ..... p 339 N95-13055
AD-A283141 ..... p 327 N95-13134 #
AD-A283142 ..... p 325 N95-13136 #
AD-A283143 ..... p 327 N95-13137 #
AD-A283144 ..... p 256 N95-13138 #
AD-A283149 ..... p 299 N95-13139 #
AD-A283152 ..... p 271 N95-13140 #
AD-A283351 ..... p 287 N95-12881
AD-A283359 ..... p 358 N95-12882
AD-A283360 ..... p 263 N95-12883
AD-A283361 ..... p 350 N95-12884
AD-A283365 ..... p 258 N95-12885
AD-A283366 ..... p 255 N95-12921
AD-A283367 ..... p 344 N95-12922
AD-A283369 ..... p 373 N95-12923
AD-A283373 ..... p 285 N95-12924
AD-A283378 ..... p 271 N95-12925
AD-A283428 ..... p 359 N95-13141 #
AD-A283430 ..... p 334 N95-12593
AD-A283444 ..... p 316 N95-13142 #
AD-A283446 ..... p 354 N95-13143 #
AD-A283448 ..... p 312 N95-12511
AD-A283449 ..... p 354 N95-13144 #
AD-A283450 ..... p 375 N95-12512
AD-A283452 ..... p 262 N95-12513
AD-A283453 ..... p 324 N95-12544

AD-A283454 ..... p 253 N95-12545
AD-A283459 ..... p 270 N95-12546
AD-A283462 ..... p 282 N95-12547
AD-A283464 ..... p 232 N95-12548
AD-A283500 ..... p 234 N95-12623
AD-A283509 ..... p 326 N95-12624
AD-A283514 ..... p 380 N95-12633
AD-A283519 ..... p 316 N95-12634

AD-D016314 ..... p 288 N95-13174
AD-D016315 ..... p 275 N95-13175
AD-D016375 ..... p 276 N95-13179
AD-D016385 ..... p 298 N95-12779
AD-D016386 ..... p 298 N95-12780
AD-D016387 ..... p 374 N95-13150
AD-D016394 ..... p 373 N95-12635
AD-D016397 ..... p 284 N95-12646
AD-D016398 ..... p 261 N95-13151
AD-D016399 ..... p 288 N95-13153
AD-D016400 ..... p 356 N95-13154
AD-D016401 ..... p 304 N95-13155
AD-D016402 ..... p 304 N95-13189
AD-D016403 ..... p 288 N95-13181

AD-E202000 ..... p 324 N95-12508 #
AD-E202062 ..... p 325 N95-13136 #
AD-E202070 ..... p 315 N95-12428 #
AD-E202111 ..... p 327 N95-13137 #
AD-E202116 ..... p 256 N95-13138 #
AD-E202122 ..... p 327 N95-13134 #
AD-E501812 ..... p 344 N95-13051

AECL-10830 ..... p 268 N95-13531 #

AFIT/CI/CIA-94-011D ..... p 362 N95-12415 #
AFIT/CI/CIA-94-012D ..... p 361 N95-11910 #
AFIT/CI/CIA-94-022 ..... p 282 N95-12412
AFIT/CI/CIA-94-030D ..... p 375 N95-12512
AFIT/CI/CIA-94-052 ..... p 297 N95-11940
AFIT/CI/CIA-94-118 ..... p 232 N95-12548

AFOSR-TR-94-0463 ..... p 257 N95-12507 #

AFOSR-94-0393TR ..... p 350 N95-13369 #
AFOSR-94-0401TR ..... p 336 N95-13375 #
AFOSR-94-0416TR ..... p 363 N95-13374
AFOSR-94-0419TR ..... p 362 N95-12538
AFOSR-94-0430TR ..... p 277 N95-12729
AFOSR-94-0434TR ..... p 376 N95-12553
AFOSR-94-0438TR ..... p 268 N95-13180
AFOSR-94-0447TR ..... p 267 N95-12807 #
AFOSR-94-0450TR ..... p 335 N95-12495 #
AFOSR-94-0457TR ..... p 297 N95-12751
AFOSR-94-0459TR ..... p 324 N95-12534
AFOSR-94-0464TR ..... p 334 N95-12535
AFOSR-94-0465TR ..... p 282 N95-12496 #

AGARD-AR-324 ..... p 335 N95-12133 #

AI-M-1414A ..... p 347 N95-12414 #
AI-M-1448 ..... p 351 N95-12007
AI-M-1479 ..... p 335 N95-11942

AIAA PAPER 94-0635 ..... p 295 N95-13550 * #
AIAA PAPER 94-3095 ..... p 243 N95-11864 * #
AIAA PAPER 94-3141 ..... p 257 N95-11919 * #
AIAA PAPER 94-3309 ..... p 258 N95-12622 * #
AIAA PAPER 94-3343 ..... p 249 N95-11703 * #
AIAA PAPER 94-3612-CP ..... p 245 N95-12763 * #
AIAA PAPER 94-4107 ..... p 243 N95-11867 * #
AIAA PAPER 94-4262 ..... p 294 N95-13201 * #

AL/HR-TP-1994-0013-VOL-2 ..... p 343 N95-12500

ANL-HEP-TR-93-115 ..... p 375 N95-13337 #

ANL/DIS/CP-81788 ..... p 245 N95-11752 #

ANL/ER/PP-78774 ..... p 359 N95-13173 #

ANL/IPNS/CP-83050 ..... p 375 N95-13272 #

ANL/MCS/PP-77112 ..... p 348 N95-13556 #

ANL/MSD/CP-82370 ..... p 360 N95-13338 #
ANL/MSD/CP-82371 ..... p 285 N95-13057 #

ANL/OTM/CR-7 ..... p 304 N95-13183 #

ANL/RE/CP-80865 ..... p 290 N95-11753 #

ANL/TD/CP-81660 ..... p 369 N95-13280 #

APL-UW-TR-9308 ..... p 329 N95-12998 #

ARCCB-TR-94017 ..... p 270 N95-12401

ARL-CR-103 ..... p 326 N95-12624
ARL-CR-187 ..... p 349 N95-12811 * #

ARL-TR-264 ..... p 327 N95-12997 #
ARL-TR-378 ..... p 282 N95-12547
ARL-TR-461 ..... p 282 N95-12513
ARL-TR-480 ..... p 262 N95-12357 * #
ARL-TR-506 ..... p 300 N95-11889 * #
ARL-TR-519 ..... p 245 N95-12763 * #
ARL-TR-520 ..... p 301 N95-12621 * #
ARL-TR-573 ..... p 303 N95-13083 * #
ARL-TR-574 ..... p 300 N95-12377 * #
ARL-TR-574 ..... p 303 N95-12843 * #
ARL-TR-72 ..... p 287 N95-12525 #

ARO-27365.15-MA ..... p 348 N95-11853 #
ARO-27425.5-PH ..... p 371 N95-11842
ARO-27578.7-EL ..... p 286 N95-11860
ARO-27869.4-MA ..... p 351 N95-11861
ARO-28314.10-CH ..... p 272 N95-11852 #
ARO-28711.21-CH ..... p 272 N95-11832
ARO-28795.1-CH ..... p 274 N95-12420 #
ARO-28925.90-EL-JSEP ..... p 386 N95-11830
ARO-29079.1-MA-CF ..... p 351 N95-11850
ARO-29367.2-EL-SB2 ..... p 371 N95-11855 #
ARO-29714.1-LS ..... p 331 N95-13373 #
ARO-30904.1-EG-CF ..... p 262 N95-11854 #
ARO-30996.4-MA ..... p 342 N95-11941
ARO-31110.1-GS-CF-VOL-5 ..... p 314 N95-11831
ARO-31111.1-PH-CF ..... p 268 N95-13372 #
ARO-32398.1-CH-DPS ..... p 357 N95-11851 #

ASIPP-0034 ..... p 370 N95-13541 #

ATR-94(8010)-3 ..... p 270 N95-12148 * #

B-257409 ..... p 249 N95-12851 #

BER-612-163 ..... p 299 N95-11701 * #

BFLRF-292 ..... p 234 N95-12499 #

BN-1172 ..... p 352 N95-12552 #

BNL-49016-REV ..... p 295 N95-11780 #
BNL-49500 ..... p 357 N95-12012 #
BNL-60451 ..... p 358 N95-12829 #
BNL-60467 ..... p 371 N95-11740 #
BNL-60489 ..... p 371 N95-11739 #
BNL-60497 ..... p 364 N95-11746 #
BNL-60537 ..... p 374 N95-13125 #
BNL-60586 ..... p 350 N95-13124 #

CARDIVNSWC-TR-94/002 ..... p 354 N95-12426 #

CAST-TR-94-2 ..... p 378 N95-12995 #

CBCL-85 ..... p 351 N95-12007

CCMS-94-04 ..... p 311 N95-11946 * #

CDRL-529 ..... p 344 N95-12796 * #

CERC-TR-94-4 ..... p 327 N95-11787

CMOTT-94-5 ..... p 231 N95-11917 * #
CMOTT-94-7 ..... p 291 N95-11935 * #
CMOTT-94-8 ..... p 292 N95-11953 * #

CMR-94-4 ..... p 279 N95-13202 * #

CMU-CS-94-120 ..... p 378 N95-12502
CMU-CS-94-141 ..... p 343 N95-12504
CMU-CS-94-149 ..... p 340 N95-12524 #
CMU-CS-94-161 ..... p 343 N95-12541 #
CMU-CS-94-163 ..... p 350 N95-12835 #
CMU-CS-94-164 ..... p 340 N95-12516 #
CMU-CS-94-168 ..... p 343 N95-12497 #

CMU-RI-TR-94-08 ..... p 300 N95-12505 #
CMU-RI-TR-94-12 ..... p 301 N95-12587 #
CMU-RI-TR-94-13 ..... p 300 N95-12526 #
CMU-RI-TR-94-14 ..... p 300 N95-12394 #

CMU/SEI-94-SR-06 ..... p 344 N95-12922

CNIC-00641 ..... p 370 N95-13541 #
CNIC-00655 ..... p 370 N95-13538 #
CNIC-00659 ..... p 370 N95-13539 #
CNIC-00679 ..... p 370 N95-13341 #
CNIC-00682 ..... p 360 N95-13536 #
CNIC-00691 ..... p 369 N95-13107 #
CNIC-00700 ..... p 352 N95-13340 #
CNIC-00709 ..... p 297 N95-13537 #

CONF-901295-2-REV-1 ..... p 345 N95-13157 #

CONF-920515-VOL-1 ..... p 361 N95-11792 #
CONF-9305289-3 ..... p 327 N95-13268 #
CONF-930637-8 ..... p 357 N95-12012 #
CONF-9308226-1 ..... p 363 N95-13421 #
CONF-930954 ..... p 329 N95-11728 #
CONF-931048-15 ..... p 369 N95-13285 #
CONF-931107-1 ..... p 295 N95-11780 #
CONF-9311147-8 ..... p 370 N95-13422 #
CONF-940142-40 ..... p 314 N95-11783 #
CONF-940184-PT-C ..... p 390 N95-12946 #
CONF-9403138-1 ..... p 298 N95-12868 #
CONF-940327-6 ..... p 359 N95-13160 #
CONF-940367-3 ..... p 269 N95-11897 #
CONF-940391-7 ..... p 363 N95-13532 #
CONF-940411-34 ..... p 371 N95-11740 #
CONF-940411-39 ..... p 356 N95-11791 #
CONF-940411-40 ..... p 374 N95-13086 #
CONF-940416-19 ..... p 263 N95-12862 #
CONF-940416-20 ..... p 276 N95-13184 #
CONF-9404167-1-REV ..... p 296 N95-13158 #
CONF-9404170-2 ..... p 265 N95-11790 #
CONF-9404175-1 ..... p 286 N95-11751 #
CONF-9404180-1 ..... p 294 N95-13075 #
CONF-9404182-1 ..... p 264 N95-13533 #
CONF-940492-4 ..... p 347 N95-13269 #
CONF-9405100-9 ..... p 322 N95-11741 #
CONF-9405109-9 ..... p 346 N95-11734 #
CONF-9405167-1 ..... p 264 N95-11735 #
CONF-9405168-4 ..... p 358 N95-12905 #
CONF-9405170-2 ..... p 272 N95-11733 #
CONF-9405170-5 ..... p 374 N95-13125 #
CONF-9405174-1 ..... p 318 N95-11784 #
CONF-9405190-1 ..... p 331 N95-12677 #
CONF-940524-12 ..... p 296 N95-13171 #
CONF-940529-14 ..... p 372 N95-11862 #
CONF-940552-11 ..... p 364 N95-11786 #
CONF-940578-8 ..... p 318 N95-11742 #
CONF-940598-2 ..... p 270 N95-12372 #
CONF-9406133-2 ..... p 304 N95-13182 #
CONF-9406158 ..... p 318 N95-13126 #
CONF-940618-9 ..... p 350 N95-13124 #
CONF-9406180-2 ..... p 364 N95-11746 #
CONF-9406185-1 ..... p 299 N95-13076 #
CONF-9406192-3 ..... p 324 N95-12649 #
CONF-9406197-1 ..... p 299 N95-13080 #
CONF-9406200-1 ..... p 359 N95-13104 #
CONF-940625-7 ..... p 232 N95-12652 #
CONF-940629-6 ..... p 375 N95-13272 #
CONF-940629-8 ..... p 296 N95-12869 #
CONF-940630-10 ..... p 364 N95-11754 #
CONF-940634-7 ..... p 365 N95-12371 #
CONF-940664-19 ..... p 369 N95-13280 #
CONF-940668-3 ..... p 264 N95-11756 #
CONF-940678-2 ..... p 287 N95-12865 #
CONF-940719-5 ..... p 321 N95-12926 #
CONF-940722-10 ..... p 359 N95-13170 #
CONF-940722-16 ..... p 358 N95-12943 #
CONF-940722-3 ..... p 357 N95-12370 #
CONF-940722-6 ..... p 357 N95-12369 #
CONF-940722-8 ..... p 359 N95-13169 #
CONF-940722-9 ..... p 359 N95-13161 #
CONF-940723-3 ..... p 363 N95-13106 #
CONF-940725-1 ..... p 357 N95-11894
CONF-940726-12 ..... p 384 N95-11757 #
CONF-940752-3 ..... p 290 N95-11753 #
CONF-940753-14 ..... p 360 N95-13338 #
CONF-940753-20 ..... p 285 N95-13057 #
CONF-940753-21 ..... p 272 N95-11736 #
CONF-940769-5 ..... p 326 N95-12927 #
CONF-940784-1 ..... p 245 N95-11752 #
CONF-940794-1 ..... p 350 N95-12864 #
CONF-940794-2 ..... p 350 N95-12866 #
CONF-9408109-1 ..... p 269 N95-11785 #
CONF-9408113-1 ..... p 374 N95-13081 #
CONF-940812-12 ..... p 317 N95-12650 #
CONF-940812-5 ..... p 361 N95-11779 #
CONF-940819-1 ..... p 358 N95-12829 #
CONF-940819-3 ..... p 371 N95-11739 #
CONF-940847-1 ..... p 376 N95-13172 #
CONF-940871-2 ..... p 299 N95-13534 #
CONF-9409161-1 ..... p 345 N95-13077 #
CONF-9409164-1 ..... p 378 N95-13123 #
CONF-9409166-1 ..... p 287 N95-12863 #
CONF-9409173-1 ..... p 374 N95-13078 #

CRD-1277-VOL-3-APP-B ..... p 304 N95-13128 #

CRHC-94-10 ..... p 347 N95-12523 #

CUED/A-AERO/TR-24 ..... p 292 N95-11939 #

DAAP-LEW-137682 ..... p 313 N95-13235 * #
DAAP-LEW-146939 ..... p 256 N95-13236 * #

DE93-016229 ..... p 317 N95-12647 #
DE94-001493 ..... p 357 N95-12012 #

DE94-007762 ..... p 376 N95-13074 #
DE94-011522 ..... p 375 N95-13337 #
DE94-011595 ..... p 370 N95-13529 #
DE94-011650 ..... p 357 N95-11894
DE94-011851 ..... p 302 N95-12648 #
DE94-012337 ..... p 363 N95-13421 #
DE94-012391 ..... p 363 N95-13532 #
DE94-013138 ..... p 327 N95-13268 #
DE94-013149 ..... p 347 N95-13269 #
DE94-013180 ..... p 331 N95-13271 #
DE94-013192 ..... p 375 N95-13272 #
DE94-013204 ..... p 296 N95-13287 #
DE94-013244 ..... p 361 N95-11779 #
DE94-013257 ..... p 370 N95-13422 #
DE94-013299 ..... p 285 N95-13057 #
DE94-013300 ..... p 360 N95-13338 #
DE94-013329 ..... p 286 N95-11751 #
DE94-013330 ..... p 245 N95-11752 #
DE94-013333 ..... p 290 N95-11753 #
DE94-013345 ..... p 372 N95-11862 #
DE94-013347 ..... p 364 N95-11754 #
DE94-013349 ..... p 294 N95-13075 #
DE94-013415 ..... p 250 N95-11755 #
DE94-013441 ..... p 264 N95-11756 #
DE94-013445 ..... p 384 N95-11757 #
DE94-013534 ..... p 295 N95-11780 #
DE94-013544 ..... p 345 N95-13339 #
DE94-013589 ..... p 321 N95-11730 #
DE94-013593 ..... p 277 N95-13530 #
DE94-013594 ..... p 271 N95-13543 #
DE94-013599 ..... p 353 N95-11731 #
DE94-013601 ..... p 272 N95-11781 #
DE94-013612 ..... p 322 N95-11732 #
DE94-013622 ..... p 272 N95-11733 #
DE94-013624 ..... p 346 N95-11734 #
DE94-013628 ..... p 269 N95-11897 #
DE94-013634 ..... p 264 N95-11735 #
DE94-013635 ..... p 272 N95-11736 #
DE94-013642 ..... p 257 N95-11782 #
DE94-013652 ..... p 314 N95-11783 #
DE94-013698 ..... p 271 N95-13554 #
DE94-013699 ..... p 329 N95-11737 #
DE94-013710 ..... p 269 N95-11738 #
DE94-013728 ..... p 371 N95-11739 #
DE94-013732 ..... p 371 N95-11740 #
DE94-013739 ..... p 322 N95-11741 #
DE94-013741 ..... p 318 N95-11742 #
DE94-013742 ..... p 318 N95-11784 #
DE94-013744 ..... p 318 N95-11745 #
DE94-013753 ..... p 358 N95-12829 #
DE94-013755 ..... p 364 N95-11746 #
DE94-013782 ..... p 269 N95-11785 #
DE94-013812 ..... p 271 N95-13544 #
DE94-013831 ..... p 299 N95-13076 #
DE94-014022 ..... p 345 N95-13077 #
DE94-014056 ..... p 364 N95-11786 #
DE94-014258 ..... p 378 N95-13123 #
DE94-014264 ..... p 357 N95-12369 #
DE94-014265 ..... p 357 N95-12370 #
DE94-014293 ..... p 365 N95-12371 #
DE94-014409 ..... p 270 N95-12372 #
DE94-014419 ..... p 374 N95-13078 #
DE94-014427 ..... p 359 N95-13104 #
DE94-014429 ..... p 299 N95-13080 #
DE94-014432 ..... p 374 N95-13081 #
DE94-014456 ..... p 374 N95-13086 #
DE94-014459 ..... p 363 N95-13106 #
DE94-014461 ..... p 324 N95-12649 #
DE94-014464 ..... p 317 N95-12650 #
DE94-014468 ..... p 232 N95-12652 #
DE94-014565 ..... p 331 N95-12677 #
DE94-014568 ..... p 263 N95-12862 #
DE94-014656 ..... p 287 N95-12863 #
DE94-014659 ..... p 350 N95-12864 #
DE94-014660 ..... p 287 N95-12865 #
DE94-014662 ..... p 350 N95-12866 #
DE94-014708 ..... p 369 N95-12867
DE94-014736 ..... p 298 N95-12868 #
DE94-014740 ..... p 296 N95-12869 #
DE94-014741 ..... p 265 N95-11790 #
DE94-014744 ..... p 264 N95-13533 #
DE94-014745 ..... p 321 N95-12926 #
DE94-014746 ..... p 356 N95-11791 #
DE94-014752 ..... p 326 N95-12927 #
DE94-014783 ..... p 361 N95-11792 #
DE94-014877 ..... p 350 N95-13124 #
DE94-014905 ..... p 374 N95-13125 #
DE94-014926 ..... p 318 N95-13126 #
DE94-014931 ..... p 294 N95-13156 #
DE94-014935 ..... p 345 N95-13157 #
DE94-014969 ..... p 296 N95-13158 #
DE94-014985 ..... p 359 N95-13160 #
DE94-014987 ..... p 359 N95-13161 #
DE94-014988 ..... p 359 N95-13169 #
DE94-014989 ..... p 359 N95-13170 #
DE94-014990 ..... p 296 N95-13171 #

DE94-015000 ..... p 304 N95-13182 #
DE94-015011 ..... p 304 N95-13183 #
DE94-015013 ..... p 376 N95-13172 #
DE94-015016 ..... p 276 N95-13184 #
DE94-015027 ..... p 359 N95-13173 #
DE94-015085 ..... p 369 N95-13280 #
DE94-015140 ..... p 369 N95-13285 #
DE94-015141 ..... p 299 N95-13534 #
DE94-015170 ..... p 370 N95-13555 #
DE94-015171 ..... p 368 N95-12757 #
DE94-015214 ..... p 368 N95-12758
DE94-015267 ..... p 368 N95-12759 #
DE94-015327 ..... p 298 N95-12761 #
DE94-015339 ..... p 267 N95-12762 #
DE94-015363 ..... p 374 N95-13059 #
DE94-015415 ..... p 275 N95-13060 #
DE94-015416 ..... p 353 N95-13061 #
DE94-015458 ..... p 344 N95-12893 #
DE94-015482 ..... p 271 N95-12895 #
DE94-015487 ..... p 369 N95-12897 #
DE94-015525 ..... p 358 N95-12905 #
DE94-015528 ..... p 279 N95-12942 #
DE94-015543 ..... p 358 N95-12943 #
DE94-015718 ..... p 312 N95-12784 #
DE94-015853 ..... p 369 N95-12944 #
DE94-015868 ..... p 275 N95-12945 #
DE94-016347 ..... p 348 N95-13556 #
DE94-621923 ..... p 329 N95-11728 #
DE94-622012 ..... p 268 N95-13531 #
DE94-622787 ..... p 360 N95-13273 #
DE94-622791 ..... p 360 N95-13274 #
DE94-622811 ..... p 360 N95-13275 #
DE94-623252 ..... p 289 N95-13276 #
DE94-623268 ..... p 375 N95-13277 #
DE94-623270 ..... p 372 N95-11899 #
DE94-624057 ..... p 356 N95-11747 #
DE94-624058 ..... p 371 N95-11748 #
DE94-624073 ..... p 290 N95-11749 #
DE94-624078 ..... p 390 N95-12946 #
DE94-624157 ..... p 313 N95-12947 #
DE94-624184 ..... p 374 N95-12948 #
DE94-624236 ..... p 277 N95-13535 #
DE94-624705 ..... p 360 N95-13536 #
DE94-624719 ..... p 297 N95-13537 #
DE94-624804 ..... p 352 N95-13340 #
DE94-625037 ..... p 370 N95-13341 #
DE94-625041 ..... p 370 N95-13538 #
DE94-625042 ..... p 370 N95-13539 #
DE94-625048 ..... p 369 N95-13107 #
DE94-625049 ..... p 285 N95-13343 #
DE94-625050 ..... p 370 N95-13540 #
DE94-625074 ..... p 370 N95-13541 #
DE94-753222 ..... p 360 N95-11750 #
DE94-753223 ..... p 356 N95-11817 #
DE94-753399 ..... p 356 N95-11818 #
DE94-753401 ..... p 371 N95-11819 #

DOE/ER-12895/T1 ..... p 269 N95-11738 #
DOE/ER-13508/8 ..... p 267 N95-12762 #
DOE/ER-14213/4 ..... p 369 N95-12897 #
DOE/ER-20033/2 ..... p 331 N95-13271 #
DOE/ER-25126/1 ..... p 345 N95-13339 #
DOE/ER-45308/7 ..... p 271 N95-12895 #
DOE/ER-45366/6 ..... p 275 N95-13060 #
DOE/ER-45403/5 ..... p 271 N95-13543 #
DOE/ER-45416/4 ..... p 271 N95-13554 #
DOE/ER-54160/1-VOL-1 ..... p 361 N95-11792 #
DOE/ER-54241/130 ..... p 370 N95-13529 #
DOE/ER-60989/4 ..... p 329 N95-11737 #

DOE/ET-53088/663 ..... p 369 N95-12867

DOE/NASA/50306-5 ..... p 260 N95-12764 * #

DOE/OR-2002 ..... p 272 N95-11781 #
DOE/OR-22041/T1 ..... p 277 N95-13530 #

DOT/FAA/AM-94/16 ..... p 332 N95-11702 #
DOT/FAA/AM-94/18 ..... p 338 N95-12354 #
DOT/FAA/AM-94/19 ..... p 234 N95-12146 #
DOT/FAA/AM-94/20-PT-1 ..... p 336 N95-13019 #
DOT/FAA/AM-94/21-PT-2 ..... p 336 N95-13020 #
DOT/FAA/AM-94/23 ..... p 336 N95-13199 #

DOT/FAA/CT-TN92/33 ..... p 291 N95-11888 * #
DOT/FAA/CT-TN94-19 ..... p 327 N95-12996 #

DOT/FAA/CT-94/23-PHASE-1 ..... p 234 N95-12623
DOT/FAA/CT-94/58 ..... p 246 N95-12216 #
DOT/FAA/CT-94/78 ..... p 273 N95-12131 #

DOT/FAA/RD-93/30 ..... p 273 N95-12131 #
DOT/FAA/RD-93/34 ..... p 246 N95-12216 #
DOT/FAA/RD-94/14-PT-2 ..... p 234 N95-13203 * #

DOT/FAA/92/24 ..... p 334 N95-12792 * #

DOT/FRA/NMI-92/25-VOL-3-APP-B ..... p 304 N95-13128 #

DREO-1197-PT-1 ..... p 259 N95-12551

DTI-144F ..... p 371 N95-11855 #

E-6042 ..... p 278 N95-12703 * #
E-7680 ..... p 291 N95-11888 * #
E-8299-1 ..... p 261 N95-12783 * #
E-8319 ..... p 232 N95-12378 * #
E-8489 ..... p 311 N95-11954 * #
E-8643 ..... p 304 N95-13583 * #
E-8644 ..... p 312 N95-12818 * #
E-8684 ..... p 372 N95-11882 * #
E-8715 ..... p 260 N95-12693 * #
E-8717 ..... p 260 N95-12662 * #
E-8718 ..... p 260 N95-12692 * #
E-8798 ..... p 260 N95-12764 * #
E-8839 ..... p 233 N95-13058 * #
E-8879 ..... p 342 N95-11918 * #
E-8921 ..... p 259 N95-13347 * #
E-8940 ..... p 263 N95-13082 * #
E-8948 ..... p 310 N95-11865 * #
E-8949 ..... p 292 N95-11953 * #
E-9014 ..... p 301 N95-12621 * #
E-9024 ..... p 244 N95-11901 * #
E-9025 ..... p 244 N95-11951 * #
E-9028 ..... p 291 N95-11935 * #
E-9030 ..... p 258 N95-12622 * #
E-9043 ..... p 296 N95-12748 * #
E-9045 ..... p 300 N95-12377 * #
E-9045 ..... p 303 N95-12843 * #
E-9047 ..... p 263 N95-12813 * #
E-9056 ..... p 303 N95-13083 * #
E-9058 ..... p 243 N95-11867 * #
E-9061 ..... p 308 N95-11813 * #
E-9065 ..... p 284 N95-12674 * #
E-9068 ..... p 264 N95-13193 * #
E-9072 ..... p 231 N95-11917 * #
E-9073 ..... p 300 N95-11889 * #
E-9088 ..... p 372 N95-11876 * #
E-9089 ..... p 243 N95-11864 * #
E-9091 ..... p 243 N95-11890 * #
E-9093 ..... p 309 N95-11711 * #
E-9094 ..... p 257 N95-11919 * #
E-9096 ..... p 249 N95-11703 * #
E-9097 ..... p 317 N95-11903 * #
E-9107 ..... p 379 N95-11868 * #
E-9108 ..... p 270 N95-12104 * #
E-9113 ..... p 349 N95-12811 * #
E-9129 ..... p 256 N95-13194 * #
E-9138 ..... p 293 N95-12380 * #
E-9149 ..... p 245 N95-12763 * #
E-9151 ..... p 258 N95-12750 * #
E-9159 ..... p 233 N95-13197 * #
E-9167 ..... p 295 N95-13550 * #

EGG-FSP-11037 ..... p 368 N95-12759 #

EPA-220/B-93-008 ..... p 319 N95-12356 #

EPA/410/K-94/001 ..... p 319 N95-11849
EPA/452/B-94/010 ..... p 318 N95-11848
EPA/452/R-94/008 ..... p 319 N95-11893

ERDEC-TR-084 ..... p 330 N95-12614
ERDEC-TR-153 ..... p 260 N95-12613
ERDEC-TR-162 ..... p 267 N95-12836 #
ERDEC-TR-173 ..... p 316 N95-13142 #
ERDEC-TR-175 ..... p 334 N95-12593

ERP-1136 ..... p 324 N95-12508 #

ESDU-73003 ..... p 310 N95-11771
ESDU-74039 ..... p 309 N95-11770
ESDU-75002 ..... p 309 N95-11769
ESDU-86020 ..... p 310 N95-11772
ESDU-87025 ..... p 310 N95-11773
ESDU-93031 ..... p 309 N95-11768
ESDU-94001 ..... p 266 N95-12128
ESDU-94002 ..... p 266 N95-12129
ESDU-94003 ..... p 309 N95-11769
ESDU-94004 ..... p 309 N95-11770
ESDU-94005 ..... p 310 N95-11771
ESDU-94006 ..... p 310 N95-11772
ESDU-94007 ..... p 310 N95-11773
ESDU-94009 ..... p 238 N95-11774
ESDU-94010 ..... p 265 N95-11775
ESDU-94012 ..... p 238 N95-11793
ESDU-94016-ADD-A ..... p 238 N95-11794
ESDU-94018 ..... p 265 N95-11795

ESL-724733-2 ..... p 282 N95-12493

FNAL-TM-1867 ..... p 296 N95-13287 #

FNAL/C-94/101-E ..... p 359 N95-13160 #
FNAL/C-94/112 ..... p 347 N95-13269 #
FNAL/C-94/127-E ..... p 357 N95-12370 #
FNAL/C-94/140 ..... p 296 N95-13171 #
FNAL/C-94/148-E ..... p 359 N95-13170 #
FNAL/C-94/149-E ..... p 357 N95-12369 #
FNAL/C-94/152-E ..... p 359 N95-13169 #
FNAL/C-94/156-E ..... p 359 N95-13161 #
FNAL/C-94/159-E ..... p 358 N95-12943 #
FNAL/C-94/183 ..... p 358 N95-12905 #

FOA-A-30087-9.4 ..... p 379 N95-11871
FOA-A-50020-5.2 ..... p 337 N95-11873

FOA-C-20970-2.2 ..... p 355 N95-12597 #
FOA-C-30729-3.4 ..... p 314 N95-11820 #
FOA-C-30742-3.5 ..... p 280 N95-11821
FOA-C-50103-5.3 ..... p 335 N95-11872

FRCR-4454241/130 ..... p 370 N95-13529 #

GA-A-21347 ..... p 369 N95-12944 #

GAO/NSIAD-94-197 ..... p 249 N95-12851 #

GCPS-TSP-1 ..... p 261 N95-11834 * #

GRI-93/0133 ..... p 301 N95-12579 #
GRI-94/0052-PHASE-2 ..... p 290 N95-11840 #
GRI-94/0118 ..... p 268 N95-13251 #

H-1962 ..... p 242 N95-12831 * #
H-1997 ..... p 230 N95-11898 * #
H-1999 ..... p 231 N95-12191 * #
H-2014 ..... p 244 N95-11868 * #

HEI/RR-65-1/94-PT-1 ..... p 331 N95-13176 #

IAE-0114 ..... p 360 N95-13536 #
IAE-0115 ..... p 352 N95-13340 #

ICASE-94-48 ..... p 290 N95-11812 * #
ICASE-94-49 ..... p 340 N95-12828 * #
ICASE-94-55 ..... p 345 N95-13420 * #
ICASE-94-64 ..... p 291 N95-11929 * #
ICASE-94-69 ..... p 351 N95-11922 * #
ICASE-94-71 ..... p 291 N95-11930 * #
ICASE-94-72 ..... p 342 N95-12005 * #

ICOMP-94-14 ..... p 291 N95-11935 * #
ICOMP-94-15 ..... p 292 N95-11953 * #
ICOMP-94-20 ..... p 231 N95-11917 * #
ICOMP-94-22 ..... p 293 N95-12380 * #
ICOMP-94-23 ..... p 295 N95-13550 * #

IDA-P-2925 ..... p 344 N95-13051

IDA/HQ-93-044715 ..... p 344 N95-13051

IHES/M/93/45 ..... p 352 N95-12577 #
IHES/M/94/13 ..... p 352 N95-12603 #
IHES/M/94/18 ..... p 352 N95-12808 #

INIS-MF-13811 ..... p 329 N95-11728 #
INIS-MF-13872-PT-C ..... p 390 N95-12946 #

INPE-5484-PRE/1783 ..... p 276 N95-13191 #
INPE-5494-TDI/511 ..... p 316 N95-13352 #
INPE-5500-TDI/515 ..... p 316 N95-13159 #
INPE-5501-TDI/516 ..... p 316 N95-13350 #
INPE-5505-TDI-517 ..... p 321 N95-13192 #
INPE-5540-TDI/526 ..... p 343 N95-12300 #
INPE-5546-TDI/532 ..... p 315 N95-12301 #
INPE-5552-TDI/536 ..... p 315 N95-12297 #
INPE-5558-TDI/536 ..... p 266 N95-12302 #
INPE-5569-PUD/063 ..... p 265 N95-11885 #

IPPCZ-338 ..... p 364 N95-11916 #
IPPCZ-339 ..... p 364 N95-11886 #

ISBN-0-16-041867-4 ..... p 319 N95-12356 #
ISBN-0-309-05086-3 ..... p 330 N95-12310
ISBN-0-309-05144-4 ..... p 376 N95-12385
ISBN-0-309-05148-7 ..... p 319 N95-12384 * #
ISBN-0-85679-884-3 ..... p 309 N95-11768
ISBN-0-85679-888-6 ..... p 266 N95-12128
ISBN-0-85679-889-4 ..... p 266 N95-12129
ISBN-0-85679-890-8 ..... p 309 N95-11769
ISBN-0-85679-891-6 ..... p 309 N95-11770
ISBN-0-85679-892-4 ..... p 310 N95-11771
ISBN-0-85679-893-2 ..... p 310 N95-11772
ISBN-0-85679-894-0 ..... p 310 N95-11773
ISBN-0-85679-896-7 ..... p 238 N95-11774
ISBN-0-85679-897-5 ..... p 265 N95-11775
ISBN-0-85679-899-1 ..... p 238 N95-11793
ISBN-0-85679-903-3 ..... p 238 N95-11794
ISBN-0-85679-905-X ..... p 265 N95-11795
ISBN-0-934213-35-6 ..... p 389 N95-12303 #
ISBN-0-934213-38-0 ..... p 389 N95-12342 #
ISBN-0-934213-40-2 ..... p 389 N95-12223 #
ISBN-90-370-0089-4 ..... p 377 N95-11824 #
ISBN-90-370-0090-8 ..... p 337 N95-11778 #
ISBN-90-370-0092-4 ..... p 304 N95-13410
ISBN-90-370-0097-5 ..... p 375 N95-13409
ISBN-90-5326-008-0 ..... p 325 N95-13434
ISBN-90-5326-013-7 ..... p 285 N95-13405
ISBN-90-6275-892-4 ..... p 308 N95-11822 #
ISBN-90-6275-938-6 ..... p 363 N95-13248
ISBN-90-6275-961-0 ..... p 271 N95-13411
ISBN-90-6275-963-7 ..... p 233 N95-13250
ISBN-90-6275-965-3 ..... p 294 N95-13249
ISBN-90-6275-966-1 ..... p 288 N95-13252
ISBN-90-73861-12-8 ..... p 318 N95-11826
ISBN-90-73861-18-7 ..... p 330 N95-11902 #
ISBN-90-9006392-7 ..... p 344 N95-12774 #
ISBN-90-9006530-X ..... p 348 N95-11825 #
ISBN-90-9006833-3 ..... p 278 N95-13435 #
ISBN-92-835-0747-9 ..... p 335 N95-12133 #
ISBN-951-22-1724-4 ..... p 385 N95-11797 #
ISBN-951-22-1775-9 ..... p 343 N95-12366 #
ISBN-951-22-1777-5 ..... p 266 N95-12584 #
ISBN-951-22-1782-1 ..... p 280 N95-11800 #
ISBN-951-22-1849-6 ..... p 349 N95-12367 #
ISBN-951-22-1850-X ..... p 281 N95-12368 #
ISBN-951-22-1855-0 ..... p 346 N95-11838 #
ISBN-951-22-1857-7 ..... p 351 N95-11839 #
ISBN-951-22-1889-5 ..... p 352 N95-12820 #
ISBN-951-22-1892-5 ..... p 283 N95-12595
ISBN-951-22-1910-7 ..... p 317 N95-11798 #
ISBN-951-22-1911-5 ..... p 317 N95-11846 #
ISBN-951-22-1912-3 ..... p 317 N95-11799 #
ISBN-951-22-1994-8 ..... p 237 N95-12582 #
ISBN-951-22-2005-9 ..... p 283 N95-12580 #
ISBN-951-22-2020-2 ..... p 283 N95-12581 #
ISBN-951-22-2069-5 ..... p 320 N95-12771
ISBN-951-711-171-1 ..... p 314 N95-11950 #
ISBN-951-711-172-X ..... p 314 N95-11881 #
ISBN-951-711-174-6 ..... p 314 N95-11880 #

ISL-PU-347/93 ..... p 232 N95-12578

ITER/US-93/TE/SA-18 ..... p 368 N95-12759 #

ITF-93-24 ..... p 290 N95-11749 #
ITF-93-26 ..... p 360 N95-13273 #
ITF-93-29 ..... p 360 N95-13274 #

ITP-93-42 ..... p 375 N95-13277 #
ITP-93-60 ..... p 360 N95-13275 #
ITP-93-67 ..... p 289 N95-13276 #

JINR-R-14-93-411 ..... p 372 N95-11899 #

JPRS-ULS-93-012 ..... p 332 N95-11744 #
JPRS-ULS-93-014 ..... p 318 N95-11743 #

JPRS-USP-94-006 ..... p 247 N95-12000

JPRS-UST-94-017 ..... p 247 N95-12001
JPRS-UST-94-019 ..... p 389 N95-12003
JPRS-UST-94-020 ..... p 389 N95-12002

KAPL-4767 ..... p 374 N95-13059 #

KCP-613-5290 ..... p 318 N95-11784 #
KCP-613-5378 ..... p 318 N95-11742 #
KCP-613-5433 ..... p 275 N95-12945 #

KFTI-93-02-REV ..... p 374 N95-12948 #
KFTI-93-34 ..... p 285 N95-13343 #
KFTI-93-35 ..... p 277 N95-13535 #
KFTI-93-9 ..... p 370 N95-13540 #

KIYAI-93-3 ..... p 356 N95-11747 #
KIYAI-93-9 ..... p 371 N95-11748 #

KURRI-TR-376 ..... p 371 N95-11819 #
KURRI-TR-381 ..... p 360 N95-11750 #
KURRI-TR-383 ..... p 356 N95-11817 #

L-17105 ..... p 233 N95-12770 *
L-17217 ..... p 255 N95-12838 * #
L-17268 ..... p 231 N95-12176 * #
L-17274 ..... p 245 N95-12664 * #
L-17327 ..... p 231 N95-11995 * #
L-17328 ..... p 246 N95-13553 * #
L-17339 ..... p 355 N95-12341 * #
L-17341 ..... p 262 N95-12357 * #
L-17359 ..... p 315 N95-12379 * #
L-17372 ..... p 291 N95-11936 * #
L-17374 ..... p 247 N95-13196 * #
LA-SUB-94-82 ..... p 353 N95-13061 #
LA-SUB-94-84 ..... p 322 N95-11732 #

LA-UR-94-1175 ..... p 357 N95-11894
LA-UR-94-1555 ..... p 361 N95-11779 #
LA-UR-94-1791 ..... p 378 N95-13123 #
LA-UR-94-1848 ..... p 327 N95-13268 #
LA-UR-94-1876 ..... p 317 N95-12650 #
LA-UR-94-1918 ..... p 374 N95-13086 #
LA-UR-94-1984 ..... p 374 N95-13081 #
LA-UR-94-2032 ..... p 365 N95-12371 #
LA-UR-94-2080 ..... p 232 N95-12652 #
LA-UR-94-2107 ..... p 299 N95-13080 #
LA-UR-94-2127 ..... p 363 N95-13106 #
LA-UR-94-2129 ..... p 324 N95-12649 #
LA-UR-94-2141 ..... p 374 N95-13078 #
LA-UR-94-2179 ..... p 359 N95-13104 #

LA-12773 ..... p 368 N95-12757 #
LA-12784-MS ..... p 257 N95-11782 #
LA-12811-MS ..... p 312 N95-12784 #

LBL-29419-REV-1 ..... p 345 N95-13157 #
LBL-35382-REV ..... p 296 N95-13158 #
LBL-35647 ..... p 318 N95-13126 #
LBL-35707 ..... p 294 N95-13156 #

LC-94-66477 ..... p 330 N95-12310
LC-94-67335 ..... p 376 N95-12385
LC-94-67788 ..... p 319 N95-12384 * #
LC-94-92211 ..... p 379 N95-12304 * #

LDTPS-TP-1 ..... p 262 N95-11835 * #

LESC-31195 ..... p 242 N95-11913 * #

LMSC/P086632 ..... p 256 N95-13195 * #

M-755 ..... p 229 N95-11710 * #
M-756 ..... p 248 N95-11870 * #
M-758 ..... p 261 N95-11816 * #
M-759 ..... p 342 N95-11923 * #

MCAT-94-07 ..... p 246 N95-11938 * #
MCAT-94-08 ..... p 230 N95-11766 * #
MCAT-94-09 ..... p 242 N95-12785 * #

MCR-90-1307 ..... p 256 N95-13232 #
MCR-94-1315 ..... p 258 N95-12819 * #

MML-TR-94-12 ..... p 263 N95-12883

MSFC-1 ..... p 332 N95-13423 * #

MT-CWR-094-013 ..... p 271 N95-12895 #

MTR-94B0000071 ..... p 326 N95-12805

MTR93-B-0000191 ..... p 340 N95-12413 #

NAL-PD-SN-9406 ..... p 311 N95-11924 #
NAL-PD-SN-9407 ..... p 311 N95-11879 #

NAL-SP-9404 ..... p 229 N95-12166 #

NAS 1.15: 10406 ..... p 323 N95-12226 * #
NAS 1.15:103775 ..... p 278 N95-12703 * #
NAS 1.15:104276 ..... p 230 N95-11898 * #
NAS 1.15:104277 ..... p 244 N95-11868 * #
NAS 1.15:104556-VOL-22 ..... p 328 N95-12151 * #
NAS 1.15:104566-VOL-19-PT-2 ... p 328 N95-11920 * #
NAS 1.15:104566-VOL-23 ..... p 328 N95-12359 * #
NAS 1.15:104610 ..... p 314 N95-11997 * #
NAS 1.15:104612 ..... p 323 N95-12130 * #
NAS 1.15:104613 ..... p 255 N95-12858 * #
NAS 1.15:104799 ..... p 339 N95-11914 * #
NAS 1.15:104801 ..... p 248 N95-11934 * #
NAS 1.15:104802 ..... p 337 N95-11878 * #
NAS 1.15:106447 ..... p 261 N95-12783 * #
NAS 1.15:106458 ..... p 232 N95-12378 * #
NAS 1.15:106498 ..... p 311 N95-11954 * #
NAS 1.15:106521 ..... p 312 N95-12818 * #
NAS 1.15:106541 ..... p 372 N95-11882 * #
NAS 1.15:106555 ..... p 260 N95-12693 * #
NAS 1.15:106557 ..... p 260 N95-12662 * #
NAS 1.15:106558 ..... p 260 N95-12692 * #
NAS 1.15:106570 ..... p 260 N95-12764 * #
NAS 1.15:106579 ..... p 233 N95-13058 * #
NAS 1.15:106627 ..... p 259 N95-13347 * #
NAS 1.15:106631 ..... p 310 N95-11865 * #
NAS 1.15:106644 ..... p 292 N95-11953 * #
NAS 1.15:106668 ..... p 258 N95-12750 * #
NAS 1.15:106678 ..... p 301 N95-12621 * #
NAS 1.15:106681 ..... p 291 N95-11935 * #
NAS 1.15:106687 ..... p 296 N95-12748 * #
NAS 1.15:106689 ..... p 300 N95-12377 * #

NAS 1.15:106689 ..... p 303 N95-12843 * #
NAS 1.15:106692 ..... p 263 N95-12813 * #
NAS 1.15:106696 ..... p 303 N95-13083 * #
NAS 1.15:106697 ..... p 243 N95-11867 * #
NAS 1.15:106703 ..... p 284 N95-12674 * #
NAS 1.15:106706 ..... p 264 N95-13193 * #
NAS 1.15:106710 ..... p 231 N95-11917 * #
NAS 1.15:106722 ..... p 372 N95-11876 * #
NAS 1.15:106723 ..... p 243 N95-11864 * #
NAS 1.15:106724 ..... p 243 N95-11890 * #
NAS 1.15:106726 ..... p 249 N95-11703 * #
NAS 1.15:106727 ..... p 317 N95-11903 * #
NAS 1.15:106731 ..... p 379 N95-11866 * #
NAS 1.15:106732 ..... p 270 N95-12104 * #
NAS 1.15:106735 ..... p 256 N95-13194 * #
NAS 1.15:106737 ..... p 293 N95-12380 * #
NAS 1.15:106741 ..... p 245 N95-12763 * #
NAS 1.15:106747 ..... p 233 N95-13197 * #
NAS 1.15:106751 ..... p 295 N95-13550 * #
NAS 1.15:107759 ..... p 244 N95-12860 * #
NAS 1.15:108081 ..... p 313 N95-13235 * #
NAS 1.15:108464 ..... p 252 N95-11948 * #
NAS 1.15:108467 ..... p 278 N95-12857 * #
NAS 1.15:108604 ..... p 256 N95-13236 * #
NAS 1.15:108819 ..... p 238 N95-12225 * #
NAS 1.15:108825 ..... p 329 N95-11810 * #
NAS 1.15:108839 ..... p 334 N95-12792 * #
NAS 1.15:108843 ..... p 232 N95-12360 * #
NAS 1.15:108845 ..... p 231 N95-11927 * #
NAS 1.15:108846 ..... p 337 N95-11905 * #
NAS 1.15:108849 ..... p 229 N95-12227 * #
NAS 1.15:109132 ..... p 326 N95-12839 * #
NAS 1.15:109143 ..... p 310 N95-11814 * #
NAS 1.15:109148 ..... p 269 N95-11915 * #
NAS 1.15:109149 ..... p 310 N95-11815 * #
NAS 1.15:109151 ..... p 252 N95-11947 * #
NAS 1.15:109162 ..... p 345 N95-13198 * #
NAS 1.15:109205 ..... p 249 N95-12224 * #
NAS 1.15:109928 ..... p 378 N95-12383 * #
NAS 1.15:109952 ..... p 318 N95-11845 *
NAS 1.15:109953 ..... p 386 N95-11955 * #
NAS 1.15:4413 ..... p 233 N95-12770 *
NAS 1.15:4562 ..... p 255 N95-12838 * #
NAS 1.15:4564 ..... p 291 N95-11936 * #
NAS 1.15:4576 ..... p 247 N95-13196 * #
NAS 1.15:4581 ..... p 330 N95-12006 * #
NAS 1.15:4604 ..... p 231 N95-12191 * #
NAS 1.15:4637 ..... p 382 N95-12190 * #
NAS 1.21:517 ..... p 379 N95-12304 * #
NAS 1.21:7011(394) ..... p 335 N95-13230 *
NAS 1.21:7037(309) ..... p 229 N95-12894 *
NAS 1.26:177610 ..... p 292 N95-11992 * #
NAS 1.26:177645 ..... p 295 N95-11896 * #
NAS 1.26:177646 ..... p 338 N95-11949 * #
NAS 1.26:177647 ..... p 338 N95-12132 * #
NAS 1.26:182156 ..... p 288 N95-13231 * #
NAS 1.26:185247 ..... p 256 N95-13232 * #
NAS 1.26:185248 ..... p 294 N95-13233 * #
NAS 1.26:185249 ..... p 259 N95-13237 * #
NAS 1.26:187231 ..... p 294 N95-13234 * #
NAS 1.26:188330 ..... p 242 N95-11913 * #
NAS 1.26:188343 ..... p 251 N95-11937 * #
NAS 1.26:189373 ..... p 287 N95-12795 * #
NAS 1.26:189379 ..... p 344 N95-12796 * #
NAS 1.26:191115 ..... p 263 N95-13082 * #
NAS 1.26:191177 ..... p 295 N95-11996 * #
NAS 1.26:192816 ..... p 313 N95-13163 * #
NAS 1.26:193989 ..... p 268 N95-13084 * #
NAS 1.26:193991 ..... p 258 N95-12819 * #
NAS 1.26:193993 ..... p 243 N95-13027 * #
NAS 1.26:194005 ..... p 381 N95-12992 * #
NAS 1.26:194006 ..... p 343 N95-12014 * #
NAS 1.26:194007 ..... p 230 N95-11807 * #
NAS 1.26:194821 ..... p 248 N95-12474 * #
NAS 1.26:194893 ..... p 244 N95-11869 * #
NAS 1.26:194934 ..... p 290 N95-11812 * #
NAS 1.26:194935 ..... p 340 N95-12828 * #
NAS 1.26:194942 ..... p 340 N95-11932 * #
NAS 1.26:194944 ..... p 345 N95-13420 * #
NAS 1.26:194956 ..... p 291 N95-11929 * #
NAS 1.26:194962 ..... p 351 N95-11922 * #
NAS 1.26:194965 ..... p 291 N95-11930 * #
NAS 1.26:194966 ..... p 342 N95-12005 * #
NAS 1.26:194967 ..... p 293 N95-12619 * #
NAS 1.26:194981 ..... p 262 N95-11926 * #
NAS 1.26:194982 ..... p 269 N95-11933 * #
NAS 1.26:194983 ..... p 284 N95-12896 * #
NAS 1.26:194987 ..... p 252 N95-12175 * #
NAS 1.26:195211 ..... p 261 N95-12382 * #
NAS 1.26:195336 ..... p 342 N95-11918 * #
NAS 1.26:195359 ..... p 244 N95-11901 * #
NAS 1.26:195360 ..... p 244 N95-11951 * #
NAS 1.26:195364 ..... p 258 N95-12622 * #
NAS 1.26:195374 ..... p 308 N95-11813 * #
NAS 1.26:195378 ..... p 309 N95-11711 * #
NAS 1.26:195379 ..... p 257 N95-11919 * #
NAS 1.26:195380 ..... p 349 N95-12811 * #
NAS 1.26:195738 ..... p 247 N95-12880 * #
NAS 1.26:195808 ..... p 312 N95-12620 * #
NAS 1.26:195812 ..... p 335 N95-13270 * #
NAS 1.26:195817 ..... p 308 N95-11994 *
NAS 1.26:195830 ..... p 312 N95-12861 * #
NAS 1.26:195882 ..... p 230 N95-11877 * #
NAS 1.26:195945 ..... p 313 N95-13096 * #
NAS 1.26:195971 ..... p 320 N95-12798 * #
NAS 1.26:196057 ..... p 248 N95-12837 * #
NAS 1.26:196126 ..... p 284 N95-12856 * #
NAS 1.26:196147 ..... p 381 N95-13012 * #
NAS 1.26:196148 ..... p 349 N95-12470 * #
NAS 1.26:196150 ..... p 368 N95-12853 * #
NAS 1.26:196151 ..... p 380 N95-12388 * #
NAS 1.26:196158 ..... p 265 N95-12107 * #
NAS 1.26:196167 ..... p 323 N95-12468 * #
NAS 1.26:196185 ..... p 380 N95-12463 * #
NAS 1.26:196190 ..... p 380 N95-12373 * #
NAS 1.26:196192 ..... p 245 N95-12791 * #
NAS 1.26:196196 ..... p 380 N95-12465 * #
NAS 1.26:196197 ..... p 385 N95-12886 * #
NAS 1.26:196198 ..... p 325 N95-13190 * #
NAS 1.26:196201 ..... p 308 N95-12391 * #
NAS 1.26:196279 ..... p 333 N95-12376 * #
NAS 1.26:196287 ..... p 381 N95-13056 * #
NAS 1.26:196326 ..... p 308 N95-12381 * #
NAS 1.26:196330 ..... p 380 N95-12466 * #
NAS 1.26:196331 ..... p 289 N95-13344 * #
NAS 1.26:196360 ..... p 230 N95-11884 * #
NAS 1.26:196394 ..... p 242 N95-12785 * #
NAS 1.26:196412 ..... p 385 N95-12469 * #
NAS 1.26:196413 ..... p 293 N95-12387 * #
NAS 1.26:196416 ..... p 380 N95-12464 * #
NAS 1.26:196420 ..... p 377 N95-12618 * #
NAS 1.26:196432 ..... p 369 N95-13024 * #
NAS 1.26:196433 ..... p 385 N95-13023 * #
NAS 1.26:196435 ..... p 314 N95-12231 *
NAS 1.26:196436 ..... p 324 N95-12949 * #
NAS 1.26:196437 ..... p 361 N95-12102 * #
NAS 1.26:196446 ..... p 255 N95-12879 * #
NAS 1.26:196476 ..... p 290 N95-11874 * #
NAS 1.26:196477 ..... p 290 N95-11875 * #
NAS 1.26:196478 ..... p 339 N95-13026 * #
NAS 1.26:196481 ..... p 298 N95-12951 * #
NAS 1.26:196482 ..... p 382 N95-12950 * #
NAS 1.26:196484 ..... p 259 N95-11891 * #
NAS 1.26:196491 ..... p 313 N95-13162 * #
NAS 1.26:196492 ..... p 351 N95-11883 * #
NAS 1.26:196508 ..... p 270 N95-12830 * #
NAS 1.26:196509 ..... p 252 N95-12106 * #
NAS 1.26:196510 ..... p 362 N95-12390 * #
NAS 1.26:196513 ..... p 279 N95-12752 * #
NAS 1.26:196514 ..... p 373 N95-12386 * #
NAS 1.26:196747 ..... p 346 N95-11863 * #
NAS 1.26:196756 ..... p 381 N95-12788 * #
NAS 1.26:196758 ..... p 319 N95-11931 * #
NAS 1.26:196759 ..... p 321 N95-12832 * #
NAS 1.26:196763 ..... p 242 N95-12787 * #
NAS 1.26:196764 ..... p 381 N95-12821 * #
NAS 1.26:196770 ..... p 320 N95-12786 * #
NAS 1.26:196772 ..... p 383 N95-12952 * #
NAS 1.26:196773 ..... p 382 N95-12939 * #
NAS 1.26:196780 ..... p 333 N95-11808 * #
NAS 1.26:196784 ..... p 362 N95-12659 * #
NAS 1.26:196789 ..... p 319 N95-12110 * #
NAS 1.26:196790 ..... p 372 N95-11921 * #
NAS 1.26:196791 ..... p 299 N95-11701 * #
NAS 1.26:196792 ..... p 261 N95-11700 * #
NAS 1.26:196793 ..... p 382 N95-12940 * #
NAS 1.26:196802 ..... p 341 N95-11764 * #
NAS 1.26:196803 ..... p 341 N95-11763 * #
NAS 1.26:196804 ..... p 341 N95-11762 * #
NAS 1.26:196805 ..... p 341 N95-11761 * #
NAS 1.26:196806 ..... p 280 N95-11760 * #
NAS 1.26:196813 ..... p 237 N95-11699 * #
NAS 1.26:196815 ..... p 278 N95-11759 * #
NAS 1.26:196817 ..... p 325 N95-11758 * #
NAS 1.26:196820 ..... p 325 N95-13025 * #
NAS 1.26:196821 ..... p 382 N95-11704 * #
NAS 1.26:196822 ..... p 289 N95-11705 * #
NAS 1.26:196823 ..... p 381 N95-11928 * #
NAS 1.26:196824 ..... p 376 N95-11765 * #
NAS 1.26:196831 ..... p 327 N95-11706 * #
NAS 1.26:196835 ..... p 230 N95-11766 * #
NAS 1.26:196836 ..... p 246 N95-11938 * #
NAS 1.26:196837 ..... p 279 N95-11707 * #
NAS 1.26:196844 ..... p 257 N95-11805 * #
NAS 1.26:196846 ..... p 331 N95-12941 * #
NAS 1.26:196848 ..... p 332 N95-13423 * #
NAS 1.26:196851 ..... p 311 N95-11946 * #
NAS 1.26:196853 ..... p 280 N95-11804 * #
NAS 1.26:196856 ..... p 322 N95-11801 * #
NAS 1.26:196861 ..... p 289 N95-11709 * #
NAS 1.26:196866 ..... p 261 N95-11803 * #
NAS 1.26:196867 ..... p 262 N95-11835 * #
NAS 1.26:196868 ..... p 261 N95-11834 * #
NAS 1.26:196869 ..... p 251 N95-11833 * #
NAS 1.26:196870 ..... p 257 N95-11823 * #
NAS 1.26:196871 ..... p 252 N95-11945 * #
NAS 1.26:196873 ..... p 251 N95-11802 * #
NAS 1.26:196874 ..... p 251 N95-11809 * #
NAS 1.26:196875 ..... p 251 N95-11777 * #
NAS 1.26:196876 ..... p 250 N95-11767 * #
NAS 1.26:196877 ..... p 332 N95-11708 * #
NAS 1.26:196888 ..... p 281 N95-12374 * #
NAS 1.26:196923 ..... p 362 N95-12736 * #
NAS 1.26:196924 ..... p 382 N95-12011 * #
NAS 1.26:196925 ..... p 292 N95-11999 * #
NAS 1.26:196929 ..... p 361 N95-12147 * #
NAS 1.26:196930 ..... p 348 N95-11998 * #
NAS 1.26:196931 ..... p 281 N95-12010 * #
NAS 1.26:196934 ..... p 379 N95-12234 * #
NAS 1.26:196939 ..... p 323 N95-12244 * #
NAS 1.26:196940 ..... p 292 N95-12228 * #
NAS 1.26:196946 ..... p 331 N95-12827 * #
NAS 1.26:196950 ..... p 254 N95-12766 * #
NAS 1.26:196960 ..... p 232 N95-12389 * #
NAS 1.26:196961 ..... p 270 N95-12148 * #
NAS 1.26:196966 ..... p 319 N95-12384 * #
NAS 1.26:196971 ..... p 349 N95-12782 * #
NAS 1.26:196978 ..... p 384 N95-13582 * #
NAS 1.26:196980 ..... p 279 N95-13202 * #
NAS 1.26:196981 ..... p 294 N95-13201 * #
NAS 1.26:196982 ..... p 246 N95-13200 * #
NAS 1.26:197147 ..... p 301 N95-12625 * #
NAS 1.26:197148 ..... p 258 N95-12604 * #
NAS 1.26:197149 ..... p 239 N95-12626 * #
NAS 1.26:197150 ..... p 302 N95-12627 * #
NAS 1.26:197151 ..... p 254 N95-12790 * #
NAS 1.26:197152 ..... p 240 N95-12628 * #
NAS 1.26:197154 ..... p 384 N95-13497 * #
NAS 1.26:197155 ..... p 239 N95-12609 * #
NAS 1.26:197156 ..... p 339 N95-12629 * #
NAS 1.26:197157 ..... p 277 N95-13508 * #
NAS 1.26:197158 ..... p 301 N95-12554 * #
NAS 1.26:197159 ..... p 240 N95-12637 * #
NAS 1.26:197160 ..... p 383 N95-12529 * #
NAS 1.26:197161 ..... p 239 N95-12530 * #
NAS 1.26:197162 ..... p 239 N95-12305 * #
NAS 1.26:197163 ..... p 338 N95-12361 * #
NAS 1.26:197164 ..... p 238 N95-12294 * #
NAS 1.26:197165 ..... p 240 N95-12638 * #
NAS 1.26:197166 ..... p 277 N95-12822 * #
NAS 1.26:197167 ..... p 253 N95-12632 * #
NAS 1.26:197168 ..... p 382 N95-12307 * #
NAS 1.26:197169 ..... p 249 N95-12531 * #
NAS 1.26:197170 ..... p 258 N95-12630 * #
NAS 1.26:197171 ..... p 301 N95-12532 * #
NAS 1.26:197172 ..... p 242 N95-12993 * #
NAS 1.26:197173 ..... p 240 N95-12639 * #
NAS 1.26:197174 ..... p 383 N95-12533 * #
NAS 1.26:197176 ..... p 239 N95-12363 * #
NAS 1.26:197177 ..... p 383 N95-12362 * #
NAS 1.26:197178 ..... p 338 N95-12555 * #
NAS 1.26:197179 ..... p 257 N95-13581 * #
NAS 1.26:197181 ..... p 241 N95-12643 * #
NAS 1.26:197182 ..... p 241 N95-12689 * #
NAS 1.26:197183 ..... p 241 N95-12700 * #
NAS 1.26:197184 ..... p 368 N95-12641 * #
NAS 1.26:197185 ..... p 253 N95-12564 * #
NAS 1.26:197186 ..... p 241 N95-12645 * #
NAS 1.26:197187 ..... p 302 N95-12640 * #
NAS 1.26:197188 ..... p 240 N95-12636 * #
NAS 1.26:197189 ..... p 383 N95-12826 * #
NAS 1.26:197190 ..... p 283 N95-12644 * #
NAS 1.26:197192 ..... p 255 N95-13006 * #
NAS 1.26:197193 ..... p 302 N95-12690 * #
NAS 1.26:197195 ..... p 241 N95-12695 * #
NAS 1.26:197196 ..... p 303 N95-12694 * #
NAS 1.26:197199 ..... p 242 N95-12702 * #
NAS 1.26:197200 ..... p 278 N95-12701 * #
NAS 1.26:197201 ..... p 254 N95-12737 * #
NAS 1.26:197203 ..... p 254 N95-12765 * #
NAS 1.26:197204 ..... p 254 N95-12698 * #
NAS 1.26:197205 ..... p 302 N95-12668 * #
NAS 1.26:197206 ..... p 302 N95-12666 * #
NAS 1.26:197208 ..... p 361 N95-12665 * #
NAS 1.26:197209 ..... p 253 N95-12663 * #
NAS 1.26:197210 ..... p 253 N95-12661 * #
NAS 1.26:197211 ..... p 254 N95-12696 * #
NAS 1.26:4530 ..... p 291 N95-11888 * #
NAS 1.26:4597 ..... p 242 N95-12831 * #
NAS 1.26:4609 ..... p 262 N95-12793 * #
NAS 1.26:4621 ..... p 292 N95-12105 * #
NAS 1.26:4622 ..... p 300 N95-11889 * #
NAS 1.26:4623 ..... p 230 N95-11911 * #
NAS 1.26:4625 ..... p 252 N95-12165 * #
NAS 1.26:4627 ..... p 238 N95-11952 *
NAS 1.26:4629 ..... p 293 N95-12859 * #
NAS 1.26:4630 ..... p 256 N95-13195 * #
NAS 1.55:10136 ..... p 304 N95-13583 * #

NAS 1.55:10139-PT-2 ..... p 234 N95-13203 * #
NAS 1.55:10160 ..... p 378 N95-12358 * #
NAS 1.60-3451 ..... p 355 N95-12341 * #
NAS 1.60:3403 ..... p 245 N95-12664 * #
NAS 1.60:3447 ..... p 231 N95-11995 * #
NAS 1.60:3454 ..... p 246 N95-13553 * #
NAS 1.60:3466 ..... p 231 N95-12176 * #
NAS 1.60:3468 ..... p 262 N95-12357 * #
NAS 1.60:3469 ..... p 315 N95-12379 * #
NAS 1.60:3489 ..... p 333 N95-11887 * #
NAS 1.60:3500 ..... p 337 N95-11811 * #
NAS 1.60:3501 ..... p 248 N95-11870 * #
NAS 1.60:3506 ..... p 261 N95-11816 * #
NAS 1.60:3507 ..... p 342 N95-11923 * #
NAS 1.61:1337 ..... p 322 N95-12103 * #
NAS 1.61:1346 ..... p 384 N95-12667 * #
NAS 1.61:1347 ..... p 229 N95-11710 * #

NASA-CP-10136 ..... p 304 N95-13583 * #
NASA-CP-10139-PT-2 ..... p 234 N95-13203 * #
NASA-CP-10160 ..... p 378 N95-12358 * #

NASA-CR-106876 ..... p 250 N95-11767 * #
NASA-CR-177610 ..... p 292 N95-11992 * #
NASA-CR-177645 ..... p 295 N95-11896 * #
NASA-CR-177646 ..... p 338 N95-11949 * #
NASA-CR-177647 ..... p 338 N95-12132 * #
NASA-CR-182156 ..... p 288 N95-13231 * #
NASA-CR-185247 ..... p 256 N95-13232 * #
NASA-CR-185248 ..... p 294 N95-13233 * #
NASA-CR-185249 ..... p 259 N95-13237 * #
NASA-CR-187231 ..... p 294 N95-13234 * #
NASA-CR-188330 ..... p 242 N95-11913 * #
NASA-CR-188343 ..... p 251 N95-11937 * #
NASA-CR-189373 ..... p 287 N95-12795 * #
NASA-CR-189379 ..... p 344 N95-12796 * #
NASA-CR-191115 ..... p 263 N95-13082 * #
NASA-CR-191177 ..... p 295 N95-11996 * #
NASA-CR-192816 ..... p 313 N95-13163 * #
NASA-CR-193989 ..... p 268 N95-13084 * #
NASA-CR-193991 ..... p 258 N95-12819 * #
NASA-CR-193993 ..... p 243 N95-13027 * #
NASA-CR-194005 ..... p 381 N95-12992 * #
NASA-CR-194006 ..... p 343 N95-12014 * #
NASA-CR-194007 ..... p 230 N95-11807 * #
NASA-CR-194821 ..... p 248 N95-12474 * #
NASA-CR-194893 ..... p 244 N95-11869 * #
NASA-CR-194934 ..... p 290 N95-11812 * #
NASA-CR-194935 ..... p 340 N95-12828 * #
NASA-CR-194942 ..... p 340 N95-11932 * #
NASA-CR-194944 ..... p 345 N95-13420 * #
NASA-CR-194956 ..... p 291 N95-11929 * #
NASA-CR-194962 ..... p 351 N95-11922 * #
NASA-CR-194965 ..... p 291 N95-11930 * #
NASA-CR-194966 ..... p 342 N95-12005 * #
NASA-CR-194967 ..... p 293 N95-12619 * #
NASA-CR-194981 ..... p 262 N95-11926 * #
NASA-CR-194982 ..... p 269 N95-11933 * #
NASA-CR-194983 ..... p 284 N95-12896 * #
NASA-CR-194987 ..... p 252 N95-12175 * #
NASA-CR-195211 ..... p 281 N95-12382 * #
NASA-CR-195336 ..... p 342 N95-11918 * #
NASA-CR-195359 ..... p 244 N95-11901 * #
NASA-CR-195360 ..... p 244 N95-11951 * #
NASA-CR-195364 ..... p 258 N95-12622 * #
NASA-CR-195374 ..... p 308 N95-11813 * #
NASA-CR-195378 ..... p 309 N95-11711 * #
NASA-CR-195379 ..... p 257 N95-11919 * #
NASA-CR-195380 ..... p 349 N95-12811 * #
NASA-CR-195738 ..... p 247 N95-12880 * #
NASA-CR-195808 ..... p 312 N95-12620 * #
NASA-CR-195812 ..... p 335 N95-13270 * #
NASA-CR-195817 ..... p 308 N95-11994 *
NASA-CR-195830 ..... p 312 N95-12861 * #
NASA-CR-195882 ..... p 230 N95-11877 * #
NASA-CR-195945 ..... p 313 N95-13096 * #
NASA-CR-195971 ..... p 320 N95-12798 * #
NASA-CR-196057 ..... p 248 N95-12837 * #
NASA-CR-196126 ..... p 284 N95-12856 * #
NASA-CR-196147 ..... p 381 N95-13012 * #
NASA-CR-196148 ..... p 349 N95-12470 * #
NASA-CR-196150 ..... p 368 N95-12853 * #
NASA-CR-196151 ..... p 380 N95-12388 * #
NASA-CR-196158 ..... p 265 N95-12107 * #
NASA-CR-196167 ..... p 323 N95-12468 * #
NASA-CR-196185 ..... p 380 N95-12463 * #
NASA-CR-196190 ..... p 380 N95-12373 * #
NASA-CR-196192 ..... p 245 N95-12791 * #
NASA-CR-196196 ..... p 380 N95-12465 * #
NASA-CR-196197 ..... p 385 N95-12886 * #
NASA-CR-196198 ..... p 325 N95-13190 * #
NASA-CR-196201 ..... p 308 N95-12391 * #
NASA-CR-196279 ..... p 333 N95-12376 * #
NASA-CR-196287 ..... p 381 N95-13056 * #
NASA-CR-196326 ..... p 308 N95-12381 * #
NASA-CR-196330 ..... p 380 N95-12466 * #
NASA-CR-196331 ..... p 289 N95-13344 * #
NASA-CR-196360 ..... p 230 N95-11884 * #
NASA-CR-196394 ..... p 242 N95-12785 * #
NASA-CR-196412 ..... p 385 N95-12469 * #
NASA-CR-196413 ..... p 293 N95-12387 * #
NASA-CR-196416 ..... p 380 N95-12464 * #
NASA-CR-196420 ..... p 377 N95-12618 * #
NASA-CR-196432 ..... p 369 N95-13024 * #
NASA-CR-196433 ..... p 385 N95-13023 * #
NASA-CR-196435 ..... p 314 N95-12231 *
NASA-CR-196436 ..... p 324 N95-12949 * #
NASA-CR-196437 ..... p 361 N95-12102 * #
NASA-CR-196446 ..... p 255 N95-12879 * #
NASA-CR-196476 ..... p 290 N95-11874 * #
NASA-CR-196477 ..... p 290 N95-11875 * #
NASA-CR-196478 ..... p 339 N95-13026 * #
NASA-CR-196481 ..... p 298 N95-12951 * #
NASA-CR-196482 ..... p 382 N95-12950 * #
NASA-CR-196484 ..... p 259 N95-11891 * #
NASA-CR-196491 ..... p 313 N95-13162 * #
NASA-CR-196492 ..... p 351 N95-11883 * #
NASA-CR-196508 ..... p 270 N95-12830 * #
NASA-CR-196509 ..... p 252 N95-12106 * #
NASA-CR-196510 ..... p 362 N95-12390 * #
NASA-CR-196513 ..... p 279 N95-12752 * #
NASA-CR-196514 ..... p 373 N95-12386 * #
NASA-CR-196747 ..... p 346 N95-11863 * #
NASA-CR-196756 ..... p 381 N95-12788 * #
NASA-CR-196758 ..... p 319 N95-11931 * #
NASA-CR-196759 ..... p 321 N95-12832 * #
NASA-CR-196763 ..... p 242 N95-12787 * #
NASA-CR-196764 ..... p 381 N95-12821 * #
NASA-CR-196770 ..... p 320 N95-12786 * #
NASA-CR-196772 ..... p 383 N95-12952 * #
NASA-CR-196773 ..... p 382 N95-12939 * #
NASA-CR-196780 ..... p 333 N95-11808 * #
NASA-CR-196784 ..... p 362 N95-12659 * #
NASA-CR-196789 ..... p 319 N95-12110 * #
NASA-CR-196790 ..... p 372 N95-11921 * #
NASA-CR-196791 ..... p 299 N95-11701 * #
NASA-CR-196792 ..... p 261 N95-11700 * #
NASA-CR-196793 ..... p 382 N95-12940 * #
NASA-CR-196802 ..... p 341 N95-11764 * #
NASA-CR-196803 ..... p 341 N95-11763 * #
NASA-CR-196804 ..... p 341 N95-11762 * #
NASA-CR-196805 ..... p 341 N95-11761 * #
NASA-CR-196806 ..... p 280 N95-11760 * #
NASA-CR-196813 ..... p 237 N95-11699 * #
NASA-CR-196815 ..... p 278 N95-11759 * #
NASA-CR-196817 ..... p 325 N95-11758 * #
NASA-CR-196820 ..... p 325 N95-13025 * #
NASA-CR-196821 ..... p 382 N95-11704 * #
NASA-CR-196822 ..... p 289 N95-11705 * #
NASA-CR-196823 ..... p 381 N95-11928 * #
NASA-CR-196824 ..... p 376 N95-11765 * #
NASA-CR-196831 ..... p 327 N95-11706 * #
NASA-CR-196835 ..... p 230 N95-11766 * #
NASA-CR-196836 ..... p 246 N95-11338 * #
NASA-CR-196837 ..... p 279 N95-11707 * #
NASA-CR-196844 ..... p 257 N95-11805 * #
NASA-CR-196846 ..... p 331 N95-12941 * #
NASA-CR-196848 ..... p 332 N95-13423 * #
NASA-CR-196851 ..... p 311 N95-11946 * #
NASA-CR-196853 ..... p 280 N95-11804 * #
NASA-CR-196856 ..... p 322 N95-11801 * #
NASA-CR-196861 ..... p 289 N95-11709 * #
NASA-CR-196866 ..... p 261 N95-11803 * #
NASA-CR-196867 ..... p 262 N95-11835 * #
NASA-CR-196868 ..... p 261 N95-11834 * #
NASA-CR-196869 ..... p 251 N95-11833 * #
NASA-CR-196870 ..... p 257 N95-11823 * #
NASA-CR-196871 ..... p 252 N95-11945 * #
NASA-CR-196873 ..... p 251 N95-11802 * #
NASA-CR-196874 ..... p 251 N95-11809 * #
NASA-CR-196875 ..... p 251 N95-11777 * #
NASA-CR-196877 ..... p 332 N95-11708 * #
NASA-CR-196888 ..... p 281 N95-12374 * #
NASA-CR-196923 ..... p 362 N95-12736 * #
NASA-CR-196924 ..... p 382 N95-12011 * #
NASA-CR-196925 ..... p 292 N95-11999 * #
NASA-CR-196929 ..... p 361 N95-12147 * #
NASA-CR-196930 ..... p 348 N95-11998 * #
NASA-CR-196931 ..... p 281 N95-12010 * #
NASA-CR-196934 ..... p 379 N95-12234 * #
NASA-CR-196939 ..... p 323 N95-12244 * #
NASA-CR-196940 ..... p 292 N95-12228 * #
NASA-CR-196946 ..... p 331 N95-12827 * #
NASA-CR-196950 ..... p 254 N95-12766 * #
NASA-CR-196960 ..... p 232 N95-12389 * #
NASA-CR-196961 ..... p 270 N95-12148 * #
NASA-CR-196966 ..... p 319 N95-12384 * #
NASA-CR-196971 ..... p 349 N95-12782 * #
NASA-CR-196978 ..... p 384 N95-13582 * #
NASA-CR-196980 ..... p 279 N95-13202 * #
NASA-CR-196981 ..... p 294 N95-13201 * #
NASA-CR-196982 ..... p 246 N95-13200 * #
NASA-CR-197147 ..... p 301 N95-12625 * #
NASA-CR-197148 ..... p 258 N95-12604 * #
NASA-CR-197149 ..... p 239 N95-12626 * #
NASA-CR-197150 ..... p 302 N95-12627 * #
NASA-CR-197151 ..... p 254 N95-12790 * #
NASA-CR-197152 ..... p 240 N95-12628 * #
NASA-CR-197154 ..... p 384 N95-13497 * #
NASA-CR-197155 ..... p 239 N95-12609 * #
NASA-CR-197156 ..... p 339 N95-12629 * #
NASA-CR-197157 ..... p 277 N95-13508 * #
NASA-CR-197158 ..... p 301 N95-12554 * #
NASA-CR-197159 ..... p 240 N95-12637 * #
NASA-CR-197160 ..... p 383 N95-12529 * #
NASA-CR-197161 ..... p 239 N95-12530 * #
NASA-CR-197162 ..... p 239 N95-12305 * #
NASA-CR-197163 ..... p 338 N95-12361 * #
NASA-CR-197164 ..... p 238 N95-12294 * #
NASA-CR-197165 ..... p 240 N95-12638 * #
NASA-CR-197166 ..... p 277 N95-12822 * #
NASA-CR-197167 ..... p 253 N95-12632 * #
NASA-CR-197168 ..... p 382 N95-12307 * #
NASA-CR-197169 ..... p 249 N95-12531 * #
NASA-CR-197170 ..... p 258 N95-12630 * #
NASA-CR-197171 ..... p 301 N95-12532 * #
NASA-CR-197172 ..... p 242 N95-12993 * #
NASA-CR-197173 ..... p 240 N95-12639 * #
NASA-CR-197174 ..... p 383 N95-12533 * #
NASA-CR-197176 ..... p 239 N95-12363 * #
NASA-CR-197177 ..... p 383 N95-12362 * #
NASA-CR-197178 ..... p 338 N95-12555 * #
NASA-CR-197179 ..... p 257 N95-13581 * #
NASA-CR-197181 ..... p 241 N95-12643 * #
NASA-CR-197182 ..... p 241 N95-12689 * #
NASA-CR-197183 ..... p 241 N95-12700 * #
NASA-CR-197184 ..... p 368 N95-12641 * #
NASA-CR-197185 ..... p 253 N95-12564 * #
NASA-CR-197186 ..... p 241 N95-12645 * #
NASA-CR-197187 ..... p 302 N95-12640 * #
NASA-CR-197188 ..... p 240 N95-12636 * #
NASA-CR-197189 ..... p 383 N95-12826 * #
NASA-CR-197190 ..... p 283 N95-12644 * #
NASA-CR-197192 ..... p 255 N95-13006 * #
NASA-CR-197193 ..... p 302 N95-12690 * #
NASA-CR-197195 ..... p 241 N95-12695 * #
NASA-CR-197196 ..... p 303 N95-12694 * #
NASA-CR-197199 ..... p 242 N95-12702 * #
NASA-CR-197200 ..... p 278 N95-12701 * #
NASA-CR-197201 ..... p 254 N95-12737 * #
NASA-CR-197203 ..... p 254 N95-12765 * #
NASA-CR-197204 ..... p 254 N95-12698 * #
NASA-CR-197205 ..... p 302 N95-12668 * #
NASA-CR-197206 ..... p 302 N95-12666 * #
NASA-CR-197208 ..... p 361 N95-12665 * #
NASA-CR-197209 ..... p 253 N95-12663 * #
NASA-CR-197210 ..... p 253 N95-12661 * #
NASA-CR-197211 ..... p 254 N95-12696 * #
NASA-CR-4530 ..... p 291 N95-11888 * #
NASA-CR-4597 ..... p 242 N95-12831 * #
NASA-CR-4609 ..... p 262 N95-12793 * #
NASA-CR-4621 ..... p 292 N95-12105 * #
NASA-CR-4622 ..... p 300 N95-11889 * #
NASA-CR-4623 ..... p 230 N95-11911 * #
NASA-CR-4625 ..... p 252 N95-12165 * #
NASA-CR-4627 ..... p 238 N95-11952 *
NASA-CR-4629 ..... p 293 N95-12859 * #
NASA-CR-4630 ..... p 256 N95-13195 * #

NASA-RP-1337 ..... p 322 N95-12103 * #
NASA-RP-1346 ..... p 384 N95-12667 * #
NASA-RP-1347 ..... p 229 N95-11710 * #

NASA-SP-517 ..... p 379 N95-12304 * #
NASA-SP-7011(394) ..... p 335 N95-13230 *
NASA-SP-7037(309) ..... p 229 N95-12894 *

NASA-TM-103775 ..... p 278 N95-12703 * #
NASA-TM-10406 ..... p 323 N95-12226 * #
NASA-TM-104276 ..... p 230 N95-11898 * #
NASA-TM-104277 ..... p 244 N95-11868 * #
NASA-TM-104556-VOL-22 ..... p 328 N95-12151 * #
NASA-TM-104566-VOL-19-PT-2 ..... p 328 N95-11920 * #
NASA-TM-104566-VOL-23 ..... p 328 N95-12359 * #
NASA-TM-104610 ..... p 314 N95-11997 * #
NASA-TM-104612 ..... p 323 N95-12130 * #
NASA-TM-104613 ..... p 255 N95-12858 * #
NASA-TM-104799 ..... p 339 N95-11914 * #
NASA-TM-104801 ..... p 248 N95-11934 * #
NASA-TM-104802 ..... p 337 N95-11878 * #
NASA-TM-106447 ..... p 261 N95-12783 * #
NASA-TM-106458 ..... p 232 N95-12378 * #
NASA-TM-106498 ..... p 311 N95-11954 * #
NASA-TM-106521 ..... p 312 N95-12818 * #
NASA-TM-106541 ..... p 372 N95-11882 * #
NASA-TM-106555 ..... p 260 N95-12693 * #
NASA-TM-106557 ..... p 260 N95-12662 * #
NASA-TM-106558 ..... p 260 N95-12692 * #

NASA-TM-106570 ..... p 260 N95-12764 * #
NASA-TM-106579 ..... p 233 N95-13058 * #
NASA-TM-106627 ..... p 259 N95-13347 * #
NASA-TM-106631 ..... p 310 N95-11865 * #
NASA-TM-106644 ..... p 292 N95-11953 * #
NASA-TM-106668 ..... p 258 N95-12750 * #
NASA-TM-106678 ..... p 301 N95-12621 * #
NASA-TM-106681 ..... p 291 N95-11935 * #
NASA-TM-106687 ..... p 296 N95-12748 * #
NASA-TM-106689 ..... p 300 N95-12377 * #
NASA-TM-106689 ..... p 303 N95-12843 * #
NASA-TM-106692 ..... p 263 N95-12813 * #
NASA-TM-106696 ..... p 303 N95-13083 * #
NASA-TM-106697 ..... p 243 N95-11867 * #
NASA-TM-106703 ..... p 284 N95-12674 * #
NASA-TM-106706 ..... p 264 N95-13193 * #
NASA-TM-106710 ..... p 231 N95-11917 * #
NASA-TM-106722 ..... p 372 N95-11876 * #
NASA-TM-106723 ..... p 243 N95-11864 * #
NASA-TM-106724 ..... p 243 N95-11890 * #
NASA-TM-106726 ..... p 249 N95-11703 * #
NASA-TM-106727 ..... p 317 N95-11903 * #
NASA-TM-106731 ..... p 379 N95-11866 * #
NASA-TM-106732 ..... p 270 N95-12104 * #
NASA-TM-106735 ..... p 256 N95-13194 * #
NASA-TM-106737 ..... p 293 N95-12380 * #
NASA-TM-106741 ..... p 245 N95-12763 * #
NASA-TM-106747 ..... p 233 N95-13197 * #
NASA-TM-106751 ..... p 295 N95-13550 * #
NASA-TM-107759 ..... p 244 N95-12860 * #
NASA-TM-108081 ..... p 313 N95-13235 * #
NASA-TM-108464 ..... p 252 N95-11948 * #
NASA-TM-108467 ..... p 278 N95-12857 * #
NASA-TM-108589 ..... p 250 N95-13130 *
NASA-TM-108604 ..... p 256 N95-13236 * #
NASA-TM-108819 ..... p 238 N95-12225 * #
NASA-TM-108825 ..... p 329 N95-11810 * #
NASA-TM-108839 ..... p 334 N95-12792 * #
NASA-TM-108843 ..... p 232 N95-12360 * #
NASA-TM-108845 ..... p 231 N95-11927 * #
NASA-TM-108846 ..... p 337 N95-11905 * #
NASA-TM-108849 ..... p 229 N95-12227 * #
NASA-TM-109132 ..... p 326 N95-12839 * #
NASA-TM-109143 ..... p 310 N95-11814 * #
NASA-TM-109148 ..... p 269 N95-11915 * #
NASA-TM-109149 ..... p 310 N95-11815 * #
NASA-TM-109151 ..... p 252 N95-11947 * #
NASA-TM-109162 ..... p 345 N95-13198 * #
NASA-TM-109205 ..... p 249 N95-12224 * #
NASA-TM-109900 ..... p 250 N95-13133 *
NASA-TM-109901 ..... p 249 N95-13129 *
NASA-TM-109928 ..... p 378 N95-12383 * #
NASA-TM-109952 ..... p 318 N95-11845 *
NASA-TM-109953 ..... p 386 N95-11955 * #
NASA-TM-109958 ..... p 250 N95-13122 *
NASA-TM-109959 ..... p 250 N95-13131 *
NASA-TM-109963 ..... p 250 N95-13132 *
NASA-TM-4413 ..... p 233 N95-12770 *
NASA-TM-4562 ..... p 255 N95-12838 * #
NASA-TM-4564 ..... p 291 N95-11936 * #
NASA-TM-4576 ..... p 247 N95-13196 * #
NASA-TM-4581 ..... p 330 N95-12006 * #
NASA-TM-4604 ..... p 231 N95-12191 * #
NASA-TM-4637 ..... p 382 N95-12190 * #

NASA-TP-3403 ..... p 245 N95-12664 * #
NASA-TP-3447 ..... p 231 N95-11995 * #
NASA-TP-3451 ..... p 355 N95-12341 * #
NASA-TP-3454 ..... p 246 N95-13553 * #
NASA-TP-3466 ..... p 231 N95-12176 * #
NASA-TP-3468 ..... p 262 N95-12357 * #
NASA-TP-3469 ..... p 315 N95-12379 * #
NASA-TP-3489 ..... p 333 N95-11887 * #
NASA-TP-3500 ..... p 337 N95-11811 * #
NASA-TP-3501 ..... p 248 N95-11870 * #
NASA-TP-3506 ..... p 261 N95-11816 * #
NASA-TP-3507 ..... p 342 N95-11923 * #

NATICK-TR-94/025 ..... p 279 N95-13053 #

NAVY-CASE-74809 ..... p 288 N95-13174
NAVY-CASE-75639 ..... p 275 N95-13175

NAWCADWAR-93074-60 ..... p 266 N95-12549 #
NAWCADWAR-94109-70 ..... p 347 N95-12418 #

NFESC-CR-94.003-SHR ..... p 323 N95-12506 #

NFESC-TR-2019-ENV ..... p 245 N95-11789

NIFS-PROC-18 ..... p 365 N95-12429 #

NIST/GCR-94/644 ..... p 267 N95-12778 #
NIST/GCR-94/646 ..... p 267 N95-12852 #

NIST/SP-861 ..... p 236 N95-13247

NISTIR-5367 ..... p 348 N95-11909 #
NISTIR-5411 ..... p 338 N95-11908 #
NISTIR-5412 ..... p 303 N95-12854 #
NISTIR-5413 ..... p 279 N95-11907 #
NISTIR-5429 ..... p 362 N95-11841 #
NISTIR-5430 ..... p 355 N95-11906 #

NLR-TP-92371-U ..... p 246 N95-13243

NOAA-DR-ERL-AOML-24 ..... p 328 N95-11900

NOAA-TR-NESDIS-76 ..... p 322 N95-11836 #
NOAA-TR-NESDIS-80 ..... p 327 N95-13095 #

NONP-NASA-CD-94-24404 ..... p 318 N95-11845 *

NONP-NASA-DK-94-5869 ..... p 308 N95-11994 *

NONP-NASA-SUPPL-DK-94-16044 p 349 N95-12470 * #
NONP-NASA-SUPPL-DK-94-28025 p 312 N95-12861 * #
NONP-NASA-SUPPL-DK-94-5100 p 292 N95-11992 * #

NONP-NASA-VT-94-28236 ..... p 250 N95-13122 *
NONP-NASA-VT-94-28237 ..... p 249 N95-13129 *
NONP-NASA-VT-94-28238 ..... p 250 N95-13130 *
NONP-NASA-VT-94-28239 ..... p 250 N95-13131 *
NONP-NASA-VT-94-28240 ..... p 250 N95-13132 *
NONP-NASA-VT-94-28241 ..... p 250 N95-13133 *

NONP-NTIS-SUPPL-DK-94-28026 p 304 N95-13128 #

NOO-TR-308 ..... p 324 N95-12544
NOO-TR-311 ..... p 253 N95-12545

NPS-EC-94-004 ..... p 284 N95-12834

NPS-MA-94-002 ..... p 351 N95-12501

NRAD-TR-1646 ..... p 280 N95-11943

NREL/TP-425-6161 ..... p 302 N95-12648 #
NREL/TP-463-5607 ..... p 317 N95-12647 #

NRL/FR/7140-94-9713 ..... p 355 N95-12396
NRL/FR/7210-94-9727 ..... p 281 N95-12402

NRL/MR/5510-94-7497 ..... p 378 N95-12916
NRL/MR/8120-94-7604 ..... p 299 N95-13139 #

NSWCDD/TR-93/272 ..... p 293 N95-12409 #

NUWC-NPT-TD-10557 ..... p 287 N95-12509 #

ORNL/M-3326 ..... p 272 N95-11781 #

ORNL/TM-12487 ..... p 250 N95-11755 #
ORNL/TM-12507 ..... p 344 N95-12893 #
ORNL/TM-12730 ..... p 353 N95-11731 #
ORNL/TM-12757 ..... p 368 N95-12758
ORNL/TM-12763 ..... p 279 N95-12942 #

PB92-100171 ..... p 389 N95-12303 #
PB93-100097 ..... p 389 N95-12223 #
PB93-128205 ..... p 389 N95-12342 #
PB93-169910 ..... p 304 N95-13128 #
PB93-170041 ..... p 319 N95-12356 #
PB94-175262 ..... p 265 N95-11796
PB94-179025 ..... p 352 N95-12820 #
PB94-179074 ..... p 385 N95-11797 #
PB94-179090 ..... p 317 N95-11798 #
PB94-179108 ..... p 317 N95-11799 #
PB94-179116 ..... p 280 N95-11800 #
PB94-179157 ..... p 317 N95-11846 #
PB94-179165 ..... p 272 N95-11847
PB94-179256 ..... p 346 N95-11838 #
PB94-179272 ..... p 351 N95-11839 #
PB94-179314 ..... p 283 N95-12595
PB94-179330 ..... p 353 N95-12364
PB94-179348 ..... p 357 N95-12365
PB94-179405 ..... p 343 N95-12366 #
PB94-179413 ..... p 349 N95-12367 #
PB94-179421 ..... p 281 N95-12368 #
PB94-179512 ..... p 355 N95-12597 #
PB94-180060 ..... p 362 N95-12598
PB94-180155 ..... p 275 N95-12600 #
PB94-180668 ..... p 328 N95-11900
PB94-180700 ..... p 319 N95-11849
PB94-180858 ..... p 352 N95-12577 #
PB94-180957 ..... p 232 N95-12578
PB94-181005 ..... p 320 N95-12771
PB94-181310 ..... p 318 N95-11848
PB94-181393 ..... p 319 N95-11893
PB94-182748 ..... p 331 N95-13176 #
PB94-184090 ..... p 301 N95-12579 #
PB94-184496 ..... p 283 N95-12580 #
PB94-184504 ..... p 283 N95-12581 #
PB94-184512 ..... p 237 N95-12582 #
PB94-184538 ..... p 266 N95-12584 #
PB94-184553 ..... p 267 N95-12585 #
PB94-186673 ..... p 348 N95-11909 #
PB94-187135 ..... p 290 N95-11840 #
PB94-187739 ..... p 338 N95-11908 #
PB94-189537 ..... p 280 N95-11904
PB94-190618 ..... p 379 N95-11871
PB94-190642 ..... p 335 N95-11872
PB94-190659 ..... p 337 N95-11873
PB94-190717 ..... p 314 N95-11820 #
PB94-190733 ..... p 280 N95-11821
PB94-191236 ..... p 308 N95-11822 #
PB94-191301 ..... p 377 N95-11824 #
PB94-191327 ..... p 348 N95-11825 #
PB94-191335 ..... p 318 N95-11826
PB94-191343 ..... p 330 N95-11902 #
PB94-191376 ..... p 337 N95-11778 #
PB94-191640 ..... p 355 N95-11906 #
PB94-191707 ..... p 382 N95-11841 #
PB94-192374 ..... p 352 N95-12603 #
PB94-192382 ..... p 352 N95-12808 #
PB94-192416 ..... p 344 N95-12774 #
PB94-192440 ..... p 312 N95-12775 #
PB94-192861 ..... p 320 N95-12776 #
PB94-193075 ..... p 320 N95-12777 #
PB94-193844 ..... p 267 N95-12778 #
PB94-193927 ..... p 267 N95-12652 #
PB94-194560 ..... p 303 N95-12854 #
PB94-194594 ..... p 321 N95-12855 #
PB94-195641 ..... p 341 N95-13436
PB94-195658 ..... p 352 N95-13437
PB94-195666 ..... p 345 N95-13438
PB94-195757 ..... p 353 N95-13439
PB94-196029 ..... p 279 N95-11907 #
PB94-201258 ..... p 360 N95-13242
PB94-201605 ..... p 347 N95-13404
PB94-201670 ..... p 246 N95-13243
PB94-202397 ..... p 341 N95-13557
PB94-202520 ..... p 285 N95-13558
PB94-202538 ..... p 285 N95-13559
PB94-202579 ..... p 276 N95-13244
PB94-202587 ..... p 378 N95-13245
PB94-202603 ..... p 299 N95-13246
PB94-203403 ..... p 236 N95-13247
PB94-204427 ..... p 363 N95-13248
PB94-204435 ..... p 294 N95-13249
PB94-204443 ..... p 285 N95-13405
PB94-204450 ..... p 233 N95-13250
PB94-205044 ..... p 353 N95-13560
PB94-205051 ..... p 309 N95-13406
PB94-205069 ..... p 347 N95-13407
PB94-205077 ..... p 345 N95-13432
PB94-205085 ..... p 336 N95-13433
PB94-205895 ..... p 268 N95-13251 #
PB94-206810 ..... p 268 N95-13252
PB94-206836 ..... p 276 N95-13284 #
PB94-206844 ..... p 332 N95-13408 #
PB94-206851 ..... p 375 N95-13409
PB94-206893 ..... p 304 N95-13410
PB94-206901 ..... p 271 N95-13411
PB94-206919 ..... p 325 N95-13434
PB94-206943 ..... p 278 N95-13435 #
PB94-206950 ..... p 346 N95-13571
PB94-206968 ..... p 376 N95-13572
PB94-207016 ..... p 353 N95-13573
PB94-207057 ..... p 363 N95-13574
PB94-207065 ..... p 356 N95-13575
PB94-207073 ..... p 313 N95-13576
PB94-207099 ..... p 286 N95-13577

PHY-94R028 ..... p 362 N95-12736 * #

PL-TR-93-2267 ..... p 324 N95-12508 #
PL-TR-94-2005 ..... p 325 N95-13136 #
PL-TR-94-2012 ..... p 327 N95-13137 #
PL-TR-94-2048 ..... p 327 N95-13134 #
PL-TR-94-2131 ..... p 283 N95-12550
PL-TR-94-2132 ..... p 256 N95-13138 #
PL-TR-94-2143 ..... p 315 N95-12428 #

PNL-SA-22934 ..... p 270 N95-12372 #
PNL-SA-23330 ..... p 304 N95-13182 #
PNL-SA-23362 ..... p 286 N95-11751 #
PNL-SA-23607 ..... p 263 N95-12862 #
PNL-SA-23878 ..... p 294 N95-13075 #
PNL-SA-24337 ..... p 331 N95-12677 #

PNL-9414 ..... p 318 N95-11745 #

PSU/ARL-TR-94-10 ..... p 345 N95-13370 #

PW/GESP-FR21998-23 ..... p 270 N95-12546

R/D-7290-EE-02 ..... p 288 N95-13052 #

RAL-93-102 ..... p 353 N95-13439
RAL-94-030 ..... p 353 N95-12364
RAL-94-034 ..... p 357 N95-12365

RAND/N-3568-A ..... p 282 N95-12416 #
RAND/N-3616-AF ..... p 377 N95-11944
RAND/N-3616-AF ..... p 244 N95-13289

REPT-01 ..... p 279 N95-12772
REPT-10300-12 ..... p 344 N95-12796 * #
REPT-115-38-8515 ..... p 333 N95-11808 * #
REPT-118 ..... p 314 N95-11950 #
REPT-722792-5 ..... p 284 N95-12856 * #
REPT-8025-1A-PT-2 ..... p 336 N95-13020 #
REPT-8025-4B ..... p 336 N95-13199 #
REPT-94:2 ..... p 314 N95-11881 #
REPT-94:3 ..... p 314 N95-11880 #
REPT-94B00103 ..... p 314 N95-11997 * #
REPT-94B00108 ..... p 384 N95-12667 * #
REPT-94B00115 ..... p 328 N95-11920 * #
REPT-94B00126-VOL-22 ..... p 328 N95-12151 * #
REPT-94B00142 ..... p 323 N95-12130 * #
REPT-94B00143 ..... p 323 N95-12226 * #
REPT-94B00144-VOL-23 ..... p 328 N95-12359 * #
REPT-95B00001 ..... p 255 N95-12858 * #

RFP-ASE274L-0893 ..... p 382 N95-12307 * #

RHCTS-TP-1 ..... p 251 N95-11802 * #

RHCTS-TSP-1 ..... p 252 N95-11945 * #

RIACS-TR-94-14 ..... p 351 N95-11883 * #
RIACS-TR-94-15 ..... p 290 N95-11875 * #
RIACS-TR-94-16 ..... p 290 N95-11874 * #
RIACS-TR-94-17 ..... p 230 N95-11877 * #
RIACS-TR-94-18 ..... p 230 N95-11884 * #

RIVM-222105002 ..... p 320 N95-12777 #
RIVM-222901012 ..... p 320 N95-12776 #

RL-TR-94-52 ..... p 282 N95-12521 #
RL-TR-94-53 ..... p 334 N95-12919
RL-TR-94-54 ..... p 287 N95-12918
RL-TR-94-79 ..... p 340 N95-12413 #

RSL-TR-10540-1 ..... p 281 N95-12374 * #

S-774 ..... p 339 N95-11914 * #
S-775 ..... p 333 N95-11887 * #
S-778 ..... p 248 N95-11934 * #
S-779 ..... p 337 N95-11878 * #
S-781 ..... p 337 N95-11811 * #

SAI-026 ..... p 287 N95-12795 * #

SAIC-94/1151 ..... p 384 N95-13582 * #

SAND-93-2416C ..... p 264 N95-11756 #
SAND-94-0063C ..... p 372 N95-11862 #
SAND-94-0663 ..... p 271 N95-13544 #
SAND-94-1227C ..... p 287 N95-12865 #
SAND-94-1305C ..... p 276 N95-13184 #
SAND-94-1383C ..... p 350 N95-12864 #
SAND-94-1384C ..... p 350 N95-12866 #
SAND-94-1542C ..... p 269 N95-11785 #
SAND-94-1580C ..... p 384 N95-11757 #
SAND-94-1603C ..... p 364 N95-11754 #
SAND-94-1715C ..... p 287 N95-12863 #
SAND-94-1748C ..... p 376 N95-13172 #

SERC-1-93 ..... p 349 N95-12782 * #

SFIM-AEC-TS-CR-93127 ..... p 290 N95-11859 #

SHRP-H-672 ..... p 280 N95-11904

SIP-0049 ..... p 370 N95-13538 #
SIP-0051 ..... p 370 N95-13539 #
SIP-0054 ..... p 370 N95-13341 #
SIP-0056 ..... p 369 N95-13107 #
SIP-0057 ..... p 297 N95-13537 #

SM-92-33 ..... p 354 N95-12728 #

SMC-TR-93-53 ..... p 250 N95-12917

SP-RAPP-1993:38 ..... p 275 N95-12600 #
SP-RAPP-1994:07 ..... p 362 N95-12598

SPO-10544 ..... p 279 N95-13202 * #

SR-1 ..... p 327 N95-13137 #
SR-2 ..... p 327 N95-13134 #
SR-3 ..... p 256 N95-13138 #
SR-6 ..... p 315 N95-12428 #

SRI-MME-93-261-7244.02-VOL-1 p 270 N95-12830 * #

SRI-4651 ..... p 283 N95-12550

SSD94D0207 ..... p 257 N95-11823 * #
SSD94D0209 ..... p 251 N95-11809 * #
SSD94D0210 ..... p 261 N95-11803 * #
SSD94D0211 ..... p 251 N95-11833 * #
SSD94D0217 ..... p 251 N95-11777 * #
SSD94D0218 ..... p 262 N95-11835 * #
SSD94D0219 ..... p 252 N95-11945 * #
SSD94D0221 ..... p 251 N95-11802 * #
SSD94D0222 ..... p 261 N95-11834 * #
SSD940212 ..... p 250 N95-11767 * #

SSTO-REQ-1 ..... p 251 N95-11777 * #

STF15-A93105 ..... p 299 N95-13246
STF24-A94508 ..... p 276 N95-13244
STF31-A93045-PT-1 ..... p 376 N95-13572
STF33-A93044 ..... p 378 N95-13245
STF33-A94003 ..... p 353 N95-13573
STF40-A93136 ..... p 356 N95-13575
STF40-A93148 ..... p 285 N95-13558
STF40-A93158 ..... p 286 N95-13577
STF40-A93169 ..... p 346 N95-13571
STF40-A94015 ..... p 285 N95-13559
STF40-A94027 ..... p 341 N95-13557
STF40-A94035 ..... p 363 N95-13574
STF40-A94048 ..... p 313 N95-13576

STUK-YTO-TR-63 ..... p 313 N95-12947 #

SWRI-3178-4.3 ..... p 301 N95-12579 #

TEC-0055 ..... p 315 N95-12527 #
TEC-0057 ..... p 350 N95-12884

TIMED-IDI ..... p 325 N95-13190 * #

TKK-F-A716 ..... p 272 N95-11847

TKK-F-C155 ..... p 317 N95-11798 #
TKK-F-C156 ..... p 317 N95-11846 #
TKK-F-C157 ..... p 317 N95-11799 #

TR-0091(6940-03)-2 ..... p 250 N95-12917
TR-1469 ..... p 349 N95-12411
TR-14 ..... p 373 N95-11993
TR-18 ..... p 259 N95-11844
TR-18 ..... p 266 N95-12514 #
TR-1 ..... p 358 N95-12882
TR-1 ..... p 268 N95-13288
TR-20 ..... p 275 N95-12773
TR-2 ..... p 274 N95-12417 #
TR-2 ..... p 275 N95-12537
TR-2 ..... p 359 N95-13141 #
TR-35-ONR ..... p 276 N95-13367 #
TR-37-ONR ..... p 360 N95-13376 #
TR-3 ..... p 262 N95-12404
TR-3 ..... p 268 N95-13549
TR-41 ..... p 274 N95-12520 #
TR-485 ..... p 346 N95-11857 #
TR-4 ..... p 274 N95-12407 #
TR-515 ..... p 346 N95-11858 #
TR-65 ..... p 274 N95-12419 #
TR-66 ..... p 264 N95-13298
TR-67 ..... p 273 N95-12400
TR-68 ..... p 273 N95-12397
TR-69 ..... p 262 N95-12398
TR-70 ..... p 276 N95-13296
TR-71 ..... p 375 N95-13299
TR-72 ..... p 273 N95-12008
TR-73 ..... p 273 N95-12399

TRS-457 ..... p 341 N95-13436
TRS-458 ..... p 352 N95-13437
TRS-466 ..... p 345 N95-13438
TRS-467 ..... p 347 N95-13404
TRS-476 ..... p 353 N95-13560
TRS-477 ..... p 309 N95-13406
TRS-478 ..... p 347 N95-13407
TRS-479 ..... p 345 N95-13432
TRS-480 ..... p 336 N95-13433

UAH-5-33267 ..... p 308 N95-12391 * #

UCRL-ID-115386 ..... p 376 N95-13074 #

UCRL-JC-114939 ..... p 363 N95-13532 #
UCRL-JC-115610 ..... p 322 N95-11741 #
UCRL-JC-115986 ..... p 326 N95-12927 #
UCRL-JC-116212 ..... p 369 N95-13285 #
UCRL-JC-116276 ..... p 364 N95-11786 #
UCRL-JC-116421 ..... p 265 N95-11790 #
UCRL-JC-116422 ..... p 356 N95-11791 #

UCRL-JC-116424 ..... p 296 N95-12869 #
UCRL-JC-116440 ..... p 264 N95-13533 #
UCRL-JC-116742 ..... p 299 N95-13534 #
UCRL-JC-116760 ..... p 314 N95-11783 #
UCRL-JC-116773 ..... p 298 N95-12868 #
UCRL-JC-117247 ..... p 321 N95-12926 #

UCRL-LR-116938 ..... p 298 N95-12761 #
UCRL-LR-117409 ..... p 370 N95-13555 #

UILU-ENG-94-2224 ..... p 347 N95-12523 #

UMICH-031155-2-T ..... p 279 N95-11707 * #
UMICH-031173-3-T ..... p 281 N95-12382 * #

US-PATENT-APPL-SN-019956 ..... p 276 N95-13179
US-PATENT-APPL-SN-023440 ..... p 284 N95-12646
US-PATENT-APPL-SN-062689 ..... p 374 N95-13150
US-PATENT-APPL-SN-075933 ..... p 261 N95-13151
US-PATENT-APPL-SN-179013 ..... p 275 N95-13175
US-PATENT-APPL-SN-221330 ..... p 288 N95-13174
US-PATENT-APPL-SN-709671 ..... p 298 N95-12780
US-PATENT-APPL-SN-831830 ..... p 298 N95-12779
US-PATENT-APPL-SN-858363 ..... p 373 N95-12635
US-PATENT-APPL-SN-861411 ..... p 288 N95-13153
US-PATENT-APPL-SN-921151 ..... p 288 N95-13181
US-PATENT-APPL-SN-922425 ..... p 356 N95-13154
US-PATENT-APPL-SN-953339 ..... p 304 N95-13189
US-PATENT-APPL-SN-953342 ..... p 304 N95-13155

US-PATENT-CLASS-219-121.68 .. p 298 N95-12779
US-PATENT-CLASS-219-121.69 .. p 298 N95-12780
US-PATENT-CLASS-219-130 ..... p 356 N95-13154
US-PATENT-CLASS-257-77 ..... p 288 N95-13181
US-PATENT-CLASS-342-189 ..... p 284 N95-12646
US-PATENT-CLASS-375-7 ..... p 288 N95-13153
US-PATENT-CLASS-384-517 ..... p 304 N95-13189
US-PATENT-CLASS-427-248.1 .... p 374 N95-13150
US-PATENT-CLASS-505-400 ..... p 373 N95-12635
US-PATENT-CLASS-528-168 ..... p 276 N95-13179
US-PATENT-CLASS-568/437 ..... p 261 N95-13151
US-PATENT-CLASS-91-363 ..... p 304 N95-13155

US-PATENT-5,283,586 ..... p 284 N95-12646
US-PATENT-5,304,625 ..... p 276 N95-13179
US-PATENT-5,306,893 ..... p 356 N95-13154
US-PATENT-5,308,800 ..... p 373 N95-12635
US-PATENT-5,310,989 ..... p 298 N95-12779
US-PATENT-5,310,990 ..... p 298 N95-12780
US-PATENT-5,316,393 ..... p 304 N95-13189
US-PATENT-5,318,801 ..... p 374 N95-13150
US-PATENT-5,321,165 ..... p 261 N95-13151
US-PATENT-5,322,003 ..... p 304 N95-13155
US-PATENT-5,325,395 ..... p 288 N95-13153
US-PATENT-5,326,992 ..... p 288 N95-13181

USAARL-94-22 ..... p 333 N95-12406 #
USAARL-94-25 ..... p 362 N95-12427 #
USAARL-94-30 ..... p 339 N95-13055
USAARL-94-31 ..... p 334 N95-13054

USGS-OFR-93-369 ..... p 321 N95-11730 #

UTIAS-TN-276 ..... p 347 N95-13353

VDAP-R1 ..... p 382 N95-11704 * #

VPI-E-94-04 ..... p 311 N95-11946 * #

WL-TM-94-3066-VOL-3 ..... p 230 N95-11829

WL-TR-93-1133 ..... p 282 N95-12493
WL-TR-93-1177 ..... p 243 N95-12591 #
WL-TR-93-8034 ..... p 300 N95-11729
WL-TR-94-4065 ..... p 377 N95-11788 #

YITP/U-93-16 ..... p 356 N95-11818 #

APPENDIX

NASA SCIENTIFIC AND TECHNICAL INFORMATION OFFICE PRODUCTS AND SERVICES

The NASA Scientific and Technical Information (STI) Office provides for the collection and announcement of aerospace-related reports and literature obtained worldwide through agreements and exchanges. The result of the collection is the comprehensive NASA STI Database that covers aeronautics, space, and supporting disciplines.

The STI Database, documents generated or obtained by NASA, and products and services derived from or supporting the database are made available to the NASA research community and to the public. Descriptions and sources of these items are presented in the following pages.

Scientific and Technical Aerospace Reports (STAR) is an abstract journal, listing citations with abstracts for aerospace-related reports obtained from worldwide sources. *STAR* is issued on the first of each month, and announces current documents that have been entered into the NASA STI Database during the previous month. The reports are of the following types:

- NASA, NASA contractor, and NASA grantee reports;
- Reports issued by other U.S. Government agencies, domestic and foreign institutions, universities, and private firms;
- Translations in report form;
- NASA-owned patents and patent applications
- Other U.S. Government agency and foreign patents and patent applications
- Domestic and foreign dissertations and theses.

Journal, book, and conference literature, journal translations, and certain foreign dissertations having the same subject scope as *STAR* are announced in a companion journal, *NASA Open Volumes on Aerospace (NOVA). NOVA* is issued on the 15th of each month and is available from the NASA Center for AeroSpace Information, at the address below.

ELIGIBILITY AND REGISTRATION FOR NASA STI PRODUCTS AND SERVICES

Organizations of the type listed below that have registered with NASA can receive products and services.

- NASA offices and installations, contractors, subcontractors, grantees, and consultants;
- Other U.S. Government agencies and their contractors;
- Libraries in the United States that have arrangements with NASA to maintain collections of NASA documents for public reference;
- Other organizations in the United States having a need for NASA documents in work related to aeronautics and space research;
- Organizations abroad that have established reciprocal documents exchange arrangements with NASA.

The central service points—central points of document acquisition and control within qualified organizations—or individuals are eligible to register for NASA STI products and services. Domestic organizations or individuals may be eligible to receive various classes of NASA publications and services and should address their requests for registration or further information to:

ATTN: Registration Services
NASA Center for AeroSpace Information
800 Elkridge Landing Road
Linthicum Heights, MD 21090-2934
301-621-0390

Organizations abroad should direct requests to:

National Aeronautics and Space Administration
Scientific and Technical Information Office (JTT)
International STI Office
Washington, DC 20546-0001
USA
703-271-5640

SUBJECT SCOPE

The subject scope of *STAR* and *NOVA* includes all aspects of aeronautics and space research and development, supporting basic and applied research, and applications. Aerospace aspects of Earth resources, energy development, conservation, oceanography, environmental protection, urban transportation, and other topics of high national priority are also covered.

HOW TO USE *STAR* SUBJECT CATEGORIES

Abstracts in *STAR* are categorized by 10 major subject divisions that are divided further into 76 specific subject categories. The subject divisions and categories are listed in the Table of Contents together with a note for each that defines its scope and provides any cross-references. For example:

16 SPACE TRANSPORTATION

Includes passenger and cargo space transportation, e.g., shuttle operations; and space rescue techniques. For related information see also *03 Air Transportation and Safety* and *18 Spacecraft Design, Testing and Performance*. For space suits see *54 Man/System Technology and Life Support*.

CROSS-REFERENCES

Individual *STAR* abstracts are not ordinarily cross-referenced, except for certain conference reports or book translations that have had separate abstracts written for their component papers or chapters. Citations and abstracts of the components follow immediately after those of the parent document. When the subject content of a component differs sufficiently from the general content of the parent, a cross-reference citation also is printed at the end of the category to which it normally would have been assigned if it were independent.

DOCUMENTS ON MICROFICHE

Documents available on microfiche are designated by a pound sign (#) following the accession number.

LIMITED REPRODUCIBILITY

A note of limited reproducibility appears in the citation, if there are factors affecting the reproducibility of more than 20% of the document. These factors include faint or broken type, color photographs, black and white photographs, foldouts, dot matrix print, or some other factor that limits the reproducibility of the document. This notation also appears on the microfiche header.

NASA PATENTS AND PATENT APPLICATIONS

Patents and patent applications owned by NASA are announced in *STAR* under appropriate subject categories and are referenced in the *STAR* indexes. In the Report Number Index, patents are indexed by the NASA Case Number, and the U.S. Patent Class. Patent applications are indexed by the NASA Case Number and the U.S. Patent Application Serial Number.

Printed copies of patents (which are not microfiched) are available for purchase from the U.S. Patent and Trademark Office.

When ordering patents, the U.S. Patent Number should be used, and payment must be remitted in advance, by money order or check payable to the Commissioner of Patents and Trademarks. Prepaid purchase coupons for ordering are also available from the U.S. Patent and Trademark Office.

NASA patent application specifications are sold in both paper copy and microfiche by the NASA Center for AeroSpace Information (CASI). The N accession number should be used in ordering either paper copy or microfiche from CASI.

The patents and patent applications announced in *STAR* are owned by NASA and are available for royalty-free licensing. Requests for licensing terms and further information should be addressed to:

National Aeronautics and Space Administration
Associate General Counsel for Intellectual Property
Code GP
Washington, DC 20546-0001

SOURCES FOR DOCUMENTS

One or more sources from which a document announced in *STAR* is available to the public is ordinarily given on the last line of the citation. The most commonly indicated sources and their acronyms or abbreviations are listed below, and their addresses are listed on page A-6. If the publication is available from a source other than those listed, the publisher and his address will be displayed on the availability line or in combination with the corporate source line.

Avail: CASI. Sold by the NASA Center for AeroSpace Information. Prices for hard copy (HC) and microfiche (MF) are indicated by a price code following the letters HC or MF in the *STAR* citation. Current values for the price codes are given in the tables on page A-7.

NOTE ON ORDERING DOCUMENTS: When ordering publications from CASI, use the N accession number or other report number. It is also advisable to cite the title and other bibliographic identification.

Avail: SOD (or GPO). Sold by the Superintendent of Documents, U.S. Government Printing Office, in hard copy.

Avail: BLL (formerly NLL): British Library Lending Division, Boston Spa, Wetherby, Yorkshire, England. Photocopies available from this organization at the price shown. (If none is given, inquiry should be addressed to the BLL.)

Avail: DOE Depository Libraries. Organizations in U.S. cities and abroad that maintain collections of Department of Energy reports, usually in microfiche form, are listed in *Energy Research Abstracts*. Services available from the DOE and its depositories are described in a booklet, *DOE Technical Information Center - Its Functions and Services* (TID-4660), which may be obtained without charge from the DOE Technical Information Center.

Avail: ESDU. Pricing information on specific data, computer programs, and details on Engineering Sciences Data Unit (ESDU) topic categories can be obtained from ESDU International Ltd. Requesters in North America should use the Virginia address while all other requesters should use the London address, both of which are on page A-6.

Avail: Fachinformationszentrum Karlsruhe. Gesellschaft für wissenschaftlich-technische Information mbH 76344 Eggenstein-Leopoldshafen, Germany.

Avail: HMSO. Publications of Her Majesty's Stationery Office are sold in the U.S. by Pendragon House, Inc. (PHI), Redwood City, CA. The U.S. price (including a service and mailing charge) is given, or a conversion table may be obtained from PHI.

Avail: Issuing Activity, or Corporate Author, or no indication of availability. Inquiries as to the availability of these documents should be addressed to the organization shown in the citation as the corporate author of the document.

Avail: NASA Public Document Rooms. Documents so indicated may be examined at or purchased from the National Aeronautics and Space Administration (JBD-4), Public Documents Room (Room 1H23), Washington, DC 20546-0001, or public document rooms located at NASA installations, and the NASA Pasadena Office at the Jet Propulsion Laboratory.

Avail: NTIS. Sold by the National Technical Information Service. Initially distributed microfiche under the NTIS SRIM (Selected Research in Microfiche) are available. For information concerning this service, consult the NTIS Subscription Section, Springfield, VA 22161.

Avail: Univ. Microfilms. Documents so indicated are dissertations selected from *Dissertation Abstracts* and are sold by University Microfilms as xerographic copy (HC) and microfilm. All requests should cite the author and the Order Number as they appear in the citation.

Avail: US Patent and Trademark Office. Sold by Commissioner of Patents and Trademarks, U.S. Patent and Trademark Office, at the standard price of $1.50 each, postage free. (See discussion of NASA patents and patent applications on page A-3.)

Avail: (US Sales Only). These foreign documents are available to users within the United States from the National Technical Information Service (NTIS). They are available to users outside the United States through the International Nuclear Information Service (INIS) representative in their country, or by applying directly to the issuing organization.

Avail: USGS. Originals of many reports from the U.S. Geological Survey, which may contain color illustrations, or otherwise may not have the quality of illustrations preserved in the microfiche or facsimile reproduction, may be examined by the public at the libraries of the USGS field offices whose addresses are listed on page A-6. The libraries may be queried concerning the availability of specific documents and the possible utilization of local copying services, such as color reproduction.

FEDERAL DEPOSITORY LIBRARY PROGRAM

In order to provide the general public with greater access to U.S. Government publications, Congress established the Federal Depository Library Program under the Government Printing Office (GPO), with 53 regional depositories responsible for permanent retention of material, inter-library loan, and reference services. At least one copy of nearly every NASA and NASA-sponsored publication, either in printed or microfiche format, is received and retained by the 53 regional depositories. A list of the regional GPO libraries, arranged alphabetically by state, appears on page A-8. These libraries are *not* sales outlets. A local library can contact a regional depository to help locate specific reports, or direct contact may be made by an individual.

PUBLIC COLLECTION OF NASA DOCUMENTS

An extensive collection of NASA and NASA-sponsored publications is maintained by the British Library Lending Division, Boston Spa, Wetherby, Yorkshire, England for public access. The British Library Lending Division also has available many of the non-NASA publications cited in *STAR.* European requesters may purchase facsimile copy or microfiche of NASA and NASA-sponsored documents, those identified by both the symbols # and * from ESA — Information Retrieval Service European Space Agency, 8-10 rue Mario-Nikis, 75738 CEDEX 15, France.

SUBMITTING DOCUMENTS

All users of this abstract service are urged to forward reports to be considered for announcement in *STAR.* This will aid NASA in its efforts to provide the fullest possible coverage of all scientific and technical publications that might support aeronautics and space research and development. If you have prepared relevant reports (other than those you will transmit to NASA, DOD, or DOE through the

usual contract- or grant-reporting channels), please send them for consideration to the NASA Center for AeroSpace Information, 800 Elkridge Landing Road, Linthicum Heights, MD 21090-2934.

Reprints of journal articles, book chapters, and conference papers are also welcome. These will be considered for announcement in *STAR's* companion journal, *NOVA*.

You may specify a particular source to be included in a report announcement if you wish; otherwise the report will be placed on a public sale at the NASA Center for AeroSpace Information. Copyrighted publications will be announced but not distributed or sold.

PURCHASE OF *STAR*

STAR is publicly available on annual subscription from the NASA Center for AeroSpace Information (CASI). 1995 *STAR* subscription prices are $100.00/domestic and $125.00/foreign. Single copy prices: $33.00/domestic, $41.00/foreign.

An annual, cumulative *STAR Index* is also available at $70.00/domestic and foreign.

STAR is available to registered users on annual subscription from the NASA Center for AeroSpace Information, ATTN: Registration Services, 800 Elkridge Landing Road, Linthicum Heights, MD 21090-2934.

ADDRESSES OF ORGANIZATIONS

British Library Lending Division
Boston Spa, Wetherby, Yorkshire
England

Commissioner of Patents and Trademarks
U.S. Patent and Trademark Office
Washington, DC 20231

Department of Energy
Technical Information Center
P.O. Box 62
Oak Ridge, TN 37830

European Space Agency-
Information Retrieval Service ESRIN
Via Galileo Galilei
00044 Frascati (Rome) Italy

Engineering Sciences Data Unit International
P.O. Box 1633
Manassas, VA 22110

Engineering Sciences Data Unit
International, Ltd.
251-259 Regent Street
London, W1R 7AD, England

Fachinformationszentrum Karlsruhe
Gesellschaft für wissenschaftlich-technische
Information mbH
76344 Eggenstein-Leopoldshafen, Germany

Her Majesty's Stationery Office
P.O. Box 569, S.E. 1
London, England

NASA Center for AeroSpace Information
800 Elkridge Landing Road
Linthicum Heights, MD 21090-2934

National Aeronautics and Space Administration
Scientific and Technical Information Office
(JTT)
Washington, DC 20546-0001

National Technical Information Service
5285 Port Royal Road
Springfield, VA 22161

Pendragon House, Inc.
899 Broadway Avenue
Redwood City, CA 94063

Superintendent of Documents
U.S. Government Printing Office
Washington, DC 20402

University Microfilms
A Xerox Company
300 North Zeeb Road
Ann Arbor, MI 48106

University Microfilms, Ltd.
Tylers Green
London, England

U.S. Geological Survey Library National Center
MS 950
12201 Sunrise Valley Drive
Reston, VA 22092

U.S. Geological Survey Library
2255 North Gemini Drive
Flagstaff, AZ 86001

U.S. Geological Survey
345 Middlefield Road
Menlo Park, CA 94025

U.S. Geological Survey Library
Box 25046
Denver Federal Center, MS914
Denver, CO 80225

CASI PRICE TABLES

(Effective November 1, 1994)

STANDARD PRICE DOCUMENTS

PRICE CODE	NORTH AMERICAN PRICE	FOREIGN PRICE
A01	$ 6.00	$ 12.00
A02	9.00	18.00
A03	17.50	35.00
A04-A05	19.50	39.00
A06-A09	27.00	54.00
A10-A13	36.50	73.00
A14-A17	44.50	89.00
A18-A21	52.00	104.00
A22-A25	61.00	122.00
A99	Call For Price	Call For Price

MICROFICHE

PRICE CODE	NORTH AMERICAN PRICE	FOREIGN PRICE
A01	$ 9.00	$ 18.00
A02	12.50	25.00
A03	17.50	35.00
A04	19.50	39.00
A06	27.00	54.00
A10	36.50	73.00

IMPORTANT NOTICE

CASI Shipping and Handling Charges
ADD $1.00 for each document ordered

Does NOT apply to orders
requesting CASI RUSH HANDLING.
CASI accepts most credit/charge cards.

NASA Center for AeroSpace Information
800 Elkridge Landing Road
Linthicum Heights, MD 21090-2934
Telephone: (301) 621-0390
E-mail: help@sti.nasa.gov
Fax: (301) 621-0134

FEDERAL REGIONAL DEPOSITORY LIBRARIES

ALABAMA

AUBURN UNIV. AT MONTGOMERY LIBRARY
Documents Dept.
7300 University Dr.
Montgomery, AL 36117-3596
(205) 244-3650 Fax: (205) 244-0678

UNIV. OF ALABAMA
Amelia Gayle Gorgas Library
Govt. Documents
P.O. Box 870266
Tuscaloosa, AL 35487-0266
(205) 348-6046 Fax: (205) 348-0760

ARIZONA

DEPT. OF LIBRARY, ARCHIVES, AND PUBLIC RECORDS
Research Division
Third Floor, State Capitol
1700 West Washington
Phoenix, AZ 85007
(602) 542-3701 Fax: (602) 542-4400

ARKANSAS

ARKANSAS STATE LIBRARY
State Library Service Section
Documents Service Section
One Capitol Mall
Little Rock, AR 72201-1014
(501) 682-2053 Fax: (501) 682-1529

CALIFORNIA

CALIFORNIA STATE LIBRARY
Govt. Publications Section
P.O. Box 942837 - 914 Capitol Mall
Sacramento, CA 94337-0091
(916) 654-0069 Fax: (916) 654-0241

COLORADO

UNIV. OF COLORADO - BOULDER
Libraries - Govt. Publications
Campus Box 184
Boulder, CO 80309-0184
(303) 492-8834 Fax: (303) 492-1881

DENVER PUBLIC LIBRARY
Govt. Publications Dept. BSG
1357 Broadway
Denver, CO 80203-2165
(303) 640-8846 Fax: (303) 640-8817

CONNECTICUT

CONNECTICUT STATE LIBRARY
231 Capitol Avenue
Hartford, CT 06106
(203) 566-4971 Fax: (203) 566-3322

FLORIDA

UNIV. OF FLORIDA LIBRARIES
Documents Dept.
240 Library West
Gainesville, FL 32611-2048
(904) 392-0366 Fax: (904) 392-7251

GEORGIA

UNIV. OF GEORGIA LIBRARIES
Govt. Documents Dept.
Jackson Street
Athens, GA 30602-1645
(706) 542-8949 Fax: (706) 542-4144

HAWAII

UNIV. OF HAWAII
Hamilton Library
Govt. Documents Collection
2550 The Mall
Honolulu, HI 96822
(808) 948-8230 Fax: (808) 956-5968

IDAHO

UNIV. OF IDAHO LIBRARY
Documents Section
Rayburn Street
Moscow, ID 83844-2353
(208) 885-6344 Fax: (208) 885-6817

ILLINOIS

ILLINOIS STATE LIBRARY
Federal Documents Dept.
300 South Second Street
Springfield, IL 62701-1796
(217) 782-7596 Fax: (217) 782-6437

INDIANA

INDIANA STATE LIBRARY
Serials/Documents Section
140 North Senate Avenue
Indianapolis, IN 46204-2296
(317) 232-3679 Fax: (317) 232-3728

IOWA

UNIV. OF IOWA LIBRARIES
Govt. Publications
Washington & Madison Streets
Iowa City, IA 52242-1166
(319) 335-5926 Fax: (319) 335-5900

KANSAS

UNIV. OF KANSAS
Govt. Documents & Maps Library
6001 Malott Hall
Lawrence, KS 66045-2800
(913) 864-4660 Fax: (913) 864-3855

KENTUCKY

UNIV. OF KENTUCKY
King Library South
Govt. Publications/Maps Dept.
Patterson Drive
Lexington, KY 40506-0039
(606) 257-3139 Fax: (606) 257-3139

LOUISIANA

LOUISIANA STATE UNIV.
Middleton Library
Govt. Documents Dept.
Baton Rouge, LA 70803-3312
(504) 388-2570 Fax: (504) 388-6992

LOUISIANA TECHNICAL UNIV.
Prescott Memorial Library
Govt. Documents Dept.
Ruston, LA 71272-0046
(318) 257-4962 Fax: (318) 257-2447

MAINE

UNIV. OF MAINE
Raymond H. Fogler Library
Govt. Documents Dept.
Orono, ME 04469-5729
(207) 581-1673 Fax: (207) 581-1653

MARYLAND

UNIV. OF MARYLAND - COLLEGE PARK
McKeldin Library
Govt. Documents/Maps Unit
College Park, MD 20742
(301) 405-9165 Fax: (301) 314-9416

MASSACHUSETTS

BOSTON PUBLIC LIBRARY
Govt. Documents
666 Boylston Street
Boston, MA 02117-0286
(617) 536-5400, ext. 226
Fax: (617) 536-7758

MICHIGAN

DETROIT PUBLIC LIBRARY
5201 Woodward Avenue
Detroit, MI 48202-4093
(313) 833-1025 Fax: (313) 833-0156

LIBRARY OF MICHIGAN
Govt. Documents Unit
P.O. Box 30007
717 West Allegan Street
Lansing, MI 48909
(517) 373-1300 Fax: (517) 373-3381

MINNESOTA

UNIV. OF MINNESOTA
Govt. Publications
409 Wilson Library
309 19th Avenue South
Minneapolis, MN 55455
(612) 624-5073 Fax: (612) 626-9353

MISSISSIPPI

UNIV. OF MISSISSIPPI
J.D. Williams Library
106 Old Gym Bldg.
University, MS 38677
(601) 232-5857 Fax: (601) 232-7465

MISSOURI

UNIV. OF MISSOURI - COLUMBIA
106B Ellis Library
Govt. Documents Sect.
Columbia, MO 65201-5149
(314) 882-6733 Fax: (314) 882-8044

MONTANA

UNIV. OF MONTANA
Mansfield Library
Documents Division
Missoula, MT 59812-1195
(406) 243-6700 Fax: (406) 243-2060

NEBRASKA

UNIV. OF NEBRASKA - LINCOLN
D.L. Love Memorial Library
Lincoln, NE 68588-0410
(402) 472-2562 Fax: (402) 472-5131

NEVADA

THE UNIV. OF NEVADA LIBRARIES
Business and Govt. Information Center
Reno, NV 89557-0044
(702) 784-6579 Fax: (702) 784-1751

NEW JERSEY

NEWARK PUBLIC LIBRARY
Science Div. - Public Access
P.O. Box 630
Five Washington Street
Newark, NJ 07101-7812
(201) 733-7782 Fax: (201) 733-5648

NEW MEXICO

UNIV. OF NEW MEXICO
General Library
Govt. Information Dept.
Albuquerque, NM 87131-1466
(505) 277-5441 Fax: (505) 277-6019

NEW MEXICO STATE LIBRARY
325 Don Gaspar Avenue
Santa Fe, NM 87503
(505) 827-3824 Fax: (505) 827-3888

NEW YORK

NEW YORK STATE LIBRARY
Cultural Education Center
Documents/Gift & Exchange Section
Empire State Plaza
Albany, NY 12230-0001
(518) 474-5355 Fax: (518) 474-5786

NORTH CAROLINA

UNIV. OF NORTH CAROLINA - CHAPEL HILL
Walter Royal Davis Library
CB 3912, Reference Dept.
Chapel Hill, NC 27514-8890
(919) 962-1151 Fax: (919) 962-4451

NORTH DAKOTA

NORTH DAKOTA STATE UNIV. LIB.
Documents
P.O. Box 5599
Fargo, ND 58105-5599
(701) 237-8886 Fax: (701) 237-7138

UNIV. OF NORTH DAKOTA
Chester Fritz Library
University Station
P.O. Box 9000 - Centennial and University Avenue
Grand Forks, ND 58202-9000
(701) 777-4632 Fax: (701) 777-3319

OHIO

STATE LIBRARY OF OHIO
Documents Dept.
65 South Front Street
Columbus, OH 43215-4163
(614) 644-7051 Fax: (614) 752-9178

OKLAHOMA

OKLAHOMA DEPT. OF LIBRARIES
U.S. Govt. Information Division
200 Northeast 18th Street
Oklahoma City, OK 73105-3298
(405) 521-2502, ext. 253
Fax: (405) 525-7804

OKLAHOMA STATE UNIV.
Edmon Low Library
Stillwater, OK 74078-0375
(405) 744-6546 Fax: (405) 744-5183

OREGON

PORTLAND STATE UNIV.
Branford P. Millar Library
934 Southwest Harrison
Portland, OR 97207-1151
(503) 725-4123 Fax: (503) 725-4524

PENNSYLVANIA

STATE LIBRARY OF PENN.
Govt. Publications Section
116 Walnut & Commonwealth Ave.
Harrisburg, PA 17105-1601
(717) 787-3752 Fax: (717) 783-2070

SOUTH CAROLINA

CLEMSON UNIV.
Robert Muldrow Cooper Library
Public Documents Unit
P.O. Box 343001
Clemson, SC 29634-3001
(803) 656-5174 Fax: (803) 656-3025

UNIV. OF SOUTH CAROLINA
Thomas Cooper Library
Green and Sumter Streets
Columbia, SC 29208
(803) 777-4841 Fax: (803) 777-9503

TENNESSEE

UNIV. OF MEMPHIS LIBRARIES
Govt. Publications Dept.
Memphis, TN 38152-0001
(901) 678-2206 Fax: (901) 678-2511

TEXAS

TEXAS STATE LIBRARY
United States Documents
P.O. Box 12927 - 1201 Brazos
Austin, TX 78701-0001
(512) 463-5455 Fax: (512) 463-5436

TEXAS TECH. UNIV. LIBRARIES
Documents Dept.
Lubbock, TX 79409-0002
(806) 742-2282 Fax: (806) 742-1920

UTAH

UTAH STATE UNIV.
Merrill Library Documents Dept.
Logan, UT 84322-3000
(801) 797-2678 Fax: (801) 797-2677

VIRGINIA

UNIV. OF VIRGINIA
Alderman Library
Govt. Documents
University Ave. & McCormick Rd.
Charlottesville, VA 22903-2498
(804) 824-3133 Fax: (804) 924-4337

WASHINGTON

WASHINGTON STATE LIBRARY
Govt. Publications
P.O. Box 42478
16th and Water Streets
Olympia, WA 98504-2478
(206) 753-4027 Fax: (206) 586-7575

WEST VIRGINIA

WEST VIRGINIA UNIV. LIBRARY
Govt. Documents Section
P.O. Box 6069 - 1549 University Ave.
Morgantown, WV 26506-6069
(304) 293-3051 Fax: (304) 293-6638

WISCONSIN

ST. HIST. SOC. OF WISCONSIN LIBRARY
Govt. Publication Section
816 State Street
Madison, WI 53706
(608) 264-6525 Fax: (608) 264-6520

MILWAUKEE PUBLIC LIBRARY
Documents Division
814 West Wisconsin Avenue
Milwaukee, WI 53233
(414) 286-3073 Fax: (414) 286-8074

•U.S. GOVERNMENT PRINTING OFFICE: 1995-387-253/00013

National Aeronautics and
Space Administration
Code JTT
Washington, DC 20546-0001